Yucca Mountain Science and Engineering Report

Technical Information Supporting Site Recommendation Consideration

Revision 1

U.S. Department of Energy
Office of Civilian Radioactive Waste Management
February 2002

CONTENTS

CONTENTS (Continued)

Page

CONTENTS (Continued)

CONTENTS (Continued)

CONTENTS (Continued)

CONTENTS (Continued)

Page

CONTENTS (Continued)

CONTENTS (Continued)

Page

FIGURES

Page

FIGURES (Continued)

Page

FIGURES (Continued)

Page

FIGURES (Continued)

Page

FIGURES (Continued)

FIGURES (Continued)

Page

FIGURES (Continued)

Page

FIGURES (Continued)

Page

FIGURES (Continued)

FIGURES (Continued)

Page

FIGURES (Continued)

Page

INTENTIONALLY LEFT BLANK

TABLES

Page

TABLES (Continued)

TABLES (Continued)

Page

INTENTIONALLY LEFT BLANK

EXECUTIVE SUMMARY

I.   INTRODUCTION

Commercial electric power generation, nuclear weapons production, the operation of naval reactors, and research and development activities produce spent nuclear fuel and high-level radioactive waste. These radioactive materials have accumulated since the mid-1940s at sites now managed by the U.S. Department of Energy (DOE) and since 1957 at commercial reactors and storage facilities across the country. The responsible management and disposal of these materials is a critical part of the DOE mission to dispose of high-level radioactive waste and spent nuclear fuel from federal facilities, including the nuclear weapons program, as well as commercially generated spent nuclear fuel.

The U.S. has evaluated methods for the safe storage and disposal of radioactive waste for more than 40 years. Many organizations and government agencies have participated in these studies. At the request of the U.S. Atomic Energy Commission, the National Academy of Sciences evaluated options for land disposal of radioactive waste in the 1950s. The U.S. Atomic Energy Commission and its successor agencies, the U.S. Energy Research and Development Administration and the DOE, continued to analyze nuclear waste management options throughout the 1960s and 1970s. In 1979, an Interagency Review Group that included representatives of 14 federal government entities provided findings and recommendations to the President. After analyzing a range of options, disposal in mined geologic repositories emerged as the preferred long-term environmental solution for the management of spent nuclear fuel and high-level radioactive waste. This consensus was reflected in the Nuclear Waste Policy Act of 1982 (NWPA), which established the U.S. responsibility and policy for the disposal of spent nuclear fuel and high-level radioactive waste.

Congress established the framework for addressing the issues of nuclear waste disposal in the NWPA and related statutes and designated the roles and responsibilities of the federal government and the owners and generators of the waste. Congress assigned responsibility to:

- The DOE to site, construct, operate, and close a repository for the disposal of spent nuclear fuel and high-level radioactive waste

- The U.S. Environmental Protection Agency (EPA) to set public health and safety standards for releases of radioactive materials from a repository

- The U.S. Nuclear Regulatory Commission (NRC) to promulgate regulations governing the construction, operation, and closure of a repository

- The generators and owners of spent nuclear fuel and high-level radioactive waste to pay the costs of disposal of such radioactive materials.

Congress amended the NWPA in 1987 and directed the DOE to investigate Yucca Mountain, Nevada, exclusively, to determine whether it is a suitable site for the first geologic repository for the nation's spent nuclear fuel and high-level radioactive waste. The DOE has studied Yucca Mountain for more than 20 years to characterize the site and assess the future performance of a potential repository. Preliminary engineering specifications have been developed for surface and subsurface facilities and the waste package. Analyses that integrate design- and site-specific data and models have been conducted to assess how a repository at Yucca Mountain might perform.

Yucca Mountain Science and Engineering Report describes the results of scientific and engineering studies of the Yucca Mountain site, the waste forms to be disposed, the repository and waste package designs, and the results of the most recent assessments of the long-term performance of the potential repository. The scientific investigations include site characterization studies of the geologic, hydrologic, and geochemical environment, and evaluation of how conditions might evolve over time. These analyses considered a

range of processes that would operate in and around the potential repository. Since projections of performance for 10,000 years are inherently uncertain, the uncertainties associated with analyses and models of long-term performance are also described, along with the likely impact of these uncertainties on performance assessment.

The NWPA specifies a process for the recommendation and approval of a site for development of a repository, and it requires that the Secretary of Energy provide a comprehensive statement of the basis for any site recommendation. *Yucca Mountain Science and Engineering Report* contains information that would be included in any site recommendation from the Secretary to the President, consistent with Sections 114(a)(1)(A), (B), and (C) of the NWPA (42 U.S.C. 10134(a)(1)(A), (B), and (C)). The NWPA requires that the DOE hold public hearings in the vicinity of the site before the Secretary makes a decision whether or not to recommend the Yucca Mountain site. The DOE has held numerous public hearings to inform residents of the area, including all 17 counties in Nevada and Inyo County, California, that the site is being considered for possible recommendation and to receive their comments. In May 2001, concurrent with the release of the initial version of this report, the DOE opened a public comment period on the Secretary's consideration of the possible recommendation of the Yucca Mountain site. This initial version and its references provided information for public review and comment in advance of public hearings. These reports also supported the process of informing the public, elected officials, affected units of government, Indian tribes, regulatory agencies, review groups, and other interested parties of the Secretary's consideration of a possible recommendation of the Yucca Mountain site. Since the beginning of the public comment period, the DOE has also made available for public review several supplemental analyses that are being considered as part of the basis for any site recommendation decision.

The DOE's scientific and technical understanding of the Yucca Mountain site continues to evolve and improve as the DOE proceeds through completion of site characterization activities, the site recommendation process, and any license application process. If the site is recommended by the Secretary and the site designation becomes effective, the DOE anticipates that this evolution in understanding of the site and repository design will continue through construction and operation of the repository if the repository is licensed.

II.   SOURCES OF MATERIALS CONSIDERED FOR DISPOSAL

By statute, the DOE is responsible for the safe, permanent disposal of spent nuclear fuel from commercial nuclear power plants. The DOE must also dispose of large quantities of DOE-owned high-level radioactive waste from the production of nuclear weapons and smaller quantities of spent nuclear fuel from weapons production reactors, research reactors, and naval reactors.

The NWPA limits the amount of spent nuclear fuel and high-level radioactive waste that can be emplaced in the nation's first geologic repository to 70,000 MTHM until a second repository is in operation. The materials that may be disposed at Yucca Mountain include about 63,000 MTHM of commercial spent nuclear fuel; about 2,333 MTHM of DOE spent nuclear fuel; and about 4,667 MTHM of DOE high-level radioactive waste. All the waste forms transported to and received at a repository would be solid materials. No liquid waste forms would be accepted for disposal. Figure 1 shows the current locations and types of waste that would be emplaced at a repository.

As of December 1999, the United States had generated about 40,000 MTHM of spent nuclear fuel from commercial nuclear power plants. This amount could more than double by 2035 if all currently operating plants complete their initial 40-year license period. By 2035, the United States will also have about 2,500 MTHM of spent nuclear fuel from research reactors, naval reactors, reactor prototypes, and reactors that produced nuclear weapons materials. The majority of this spent nuclear fuel is stored at DOE sites in Idaho, South Carolina, and Washington. In addition, liquid waste from nuclear weapons production programs is stored in underground tanks at the same DOE sites. This high-level radioactive waste will be mixed
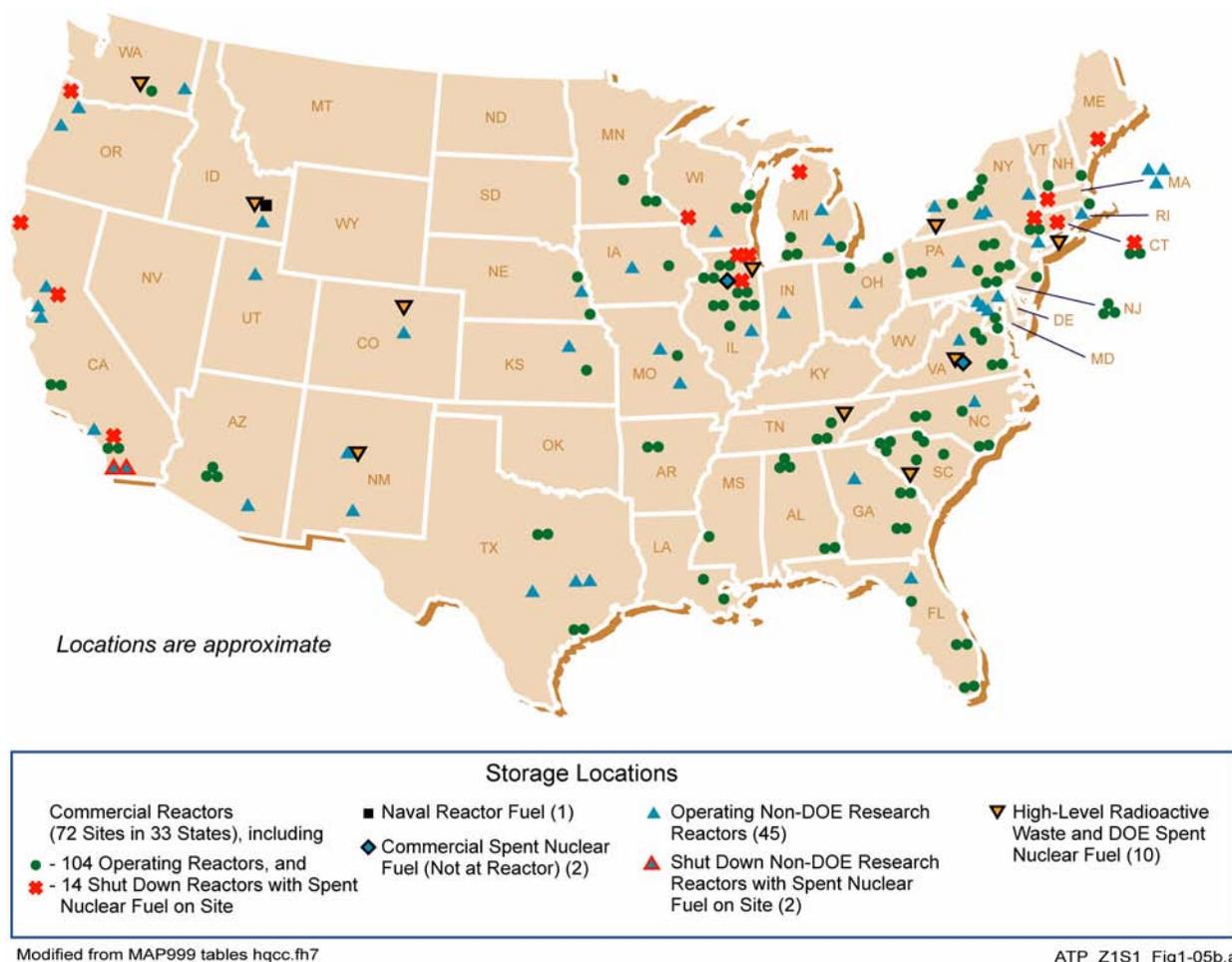
Figure 1. **Map Showing Current Locations of Waste Destined for Geologic Disposal**
Commercial waste may include West Valley vitrified waste if an agreement is reached between the DOE and the state of New York for disposal of this waste.

with silica sand and other constituents, melted together, and poured into stainless steel canisters. Once the glass solidifies (vitrifies), the canister would be sealed, loaded into a transport cask, and shipped to a repository. Vitrified waste is resistant to dissolution and would stay intact for thousands of years.

Some of the material that would be disposed in a repository would come from surplus plutonium resulting from the production and decommissioning of nuclear weapons. A nominal 50 metric tons of surplus plutonium must be safely dispositioned. Current plans call for some of the surplus plutonium to be combined with uranium to form fuel that would be used in commercial reactors.

The resulting spent nuclear fuel would be disposed as commercial spent nuclear fuel. Some of the surplus plutonium would be immobilized in ceramic and placed in canisters for repository disposal. These canisters will be filled with molten high-level radioactive waste glass, which will vitrify into a glass waste form.

III. GEOLOGY OF THE YUCCA MOUNTAIN SITE

The Yucca Mountain site is located on federal land adjacent to the Nevada Test Site in Nye County, Nevada, about 160 km (100 mi) northwest of Las Vegas. The mountain consists of a series of ridges extending 40 km (25 mi) from Timber Mountain in

the north to the Amargosa Desert in the south. The water table at Yucca Mountain is approximately 500 to 800 m (1,600 to 2,600 ft) below the surface of the mountain at the potential repository location. The zone of soil or rock below the ground surface and above the water table is called the unsaturated zone. The underground facility would be located in the unsaturated zone, about 200 to 500 m (660 to 1,600 ft) below the surface and, on average, about 300 m (1,000 ft) above the water table. The deep water table and thick unsaturated zone at Yucca Mountain result from the low infiltration rate of surface water due to low annual rainfall and high rates of evaporation and transpiration (the process by which water vapor passes from soil into plants, then into the air).

The potential repository would be located in volcanic rock, called tuff, that was deposited by a series of eruptions between approximately 11 and 14 million years ago. The characteristics of the volcanic rock have been studied in underground excavations and boreholes, and by geologic mapping of the surface. Mapping and other studies show that faults are present in the vicinity of Yucca Mountain. The location, timing, and amount of movement on these faults have been characterized as part of the DOE's seismic hazard analysis.

The location of the underground facility was identified using several factors, including the thickness of overlying rock and soil, the characteristics of the rock that would host the repository, the location of faults, and the depth to groundwater. The facility would be sited deep enough underground to prevent waste from being exposed to the environment and to discourage human intrusion. The host rock for a geologic repository must be stable enough to sustain excavated openings during repository operations. The rock must also be able to absorb heat generated by the spent nuclear fuel. The Topopah Spring Tuff rock unit, in which the underground facility would be constructed, exhibits these characteristics.

IV.   REPOSITORY DESIGN

The DOE has developed a design for a Yucca Mountain disposal system that could give future generations the choice of either closing and sealing

the underground facility as early as allowable under NRC regulations or keeping it open and monitoring it for a longer time period. The design for the potential repository would not preclude the option for future generations to make societal decisions to monitor the repository for up to 300 years before making decisions to close the underground facility.

Figure 2 is a conceptual illustration of the proposed facilities and structures that would make up a potential repository. It shows the facilities as they would appear after construction. In general, the operations that would be performed include:

- Receiving spent nuclear fuel and high-level radioactive waste in shipping casks certified by the NRC from rail and truck transporters

- Unloading, handling, and packaging spent nuclear fuel and high-level radioactive waste into waste packages suitable for underground emplacement

- Transporting waste packages from the surface to the underground facility

- Emplacing waste packages in underground drifts

- Monitoring operations and repository system performance to ensure the safety of workers and the public

- Decommissioning and closure.

The design that has been developed is intended to fulfill the functional requirements defined for the facilities while maintaining the flexibility to adapt to various construction and operational conditions and requirements. Four key aspects of design flexibility are:

1. The ability of the repository design to support a range of construction approaches (e.g., change in emplacement drift spacing, modular or sequential construction of surface and subsurface facilities)
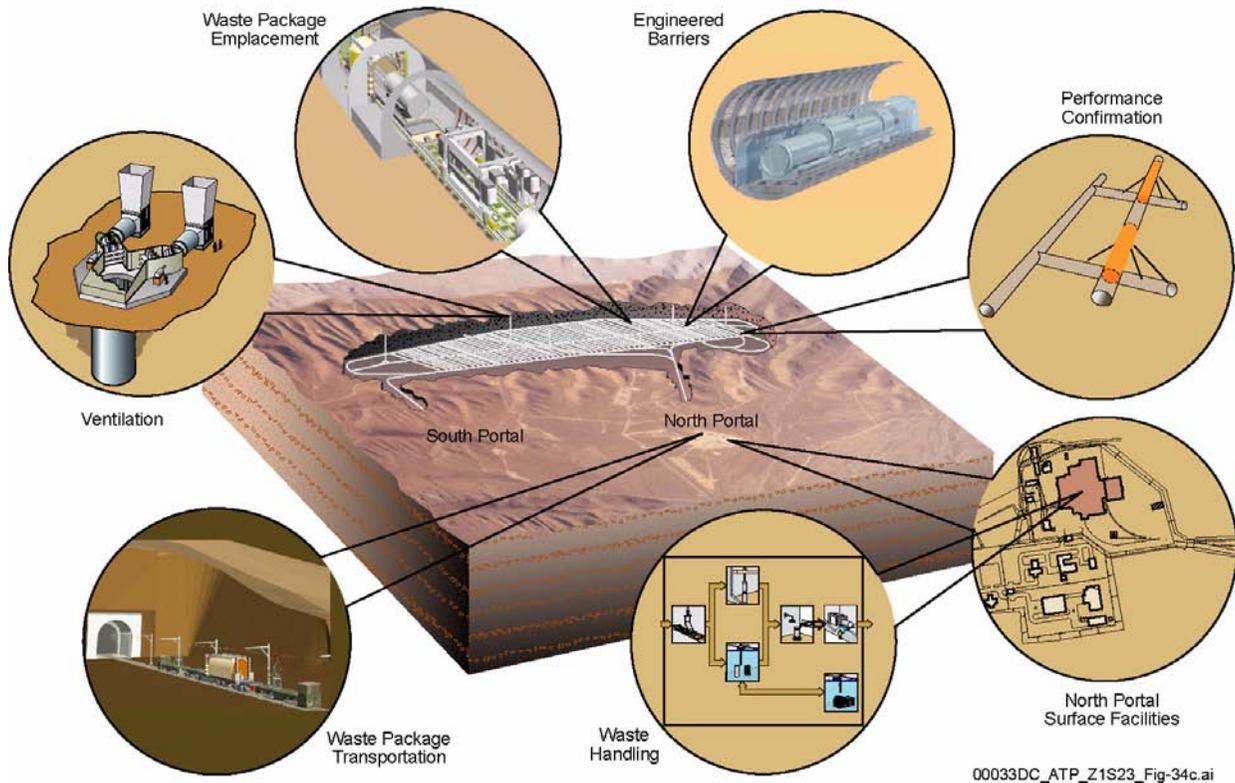
Figure 2.   Proposed Repository Facilities

2. The capability to dispose of a wide range of radioactive waste container sizes

3. The ability to support a range of thermal operating modes (e.g., defining a larger waste emplacement area or varying ventilation duration and rates to reduce the temperature in the underground facility)

4. The ability to continue to enhance the design to best achieve performance-related benefits identified through ongoing analyses.

Thermal Management Strategy—Radioactive elements in spent nuclear fuel and high-level radioactive waste become less radioactive over time. As part of this process, energy is released in the form of heat. In the potential repository, this heat could affect thermal, hydrologic, chemical, and mechanical processes in the emplacement drifts and surrounding rock. The DOE plans to manage the thermal environment of the repository to take advantage of potentially beneficial characteristics that might be associated with alternative operational modes. For example, a repository operated at higher temperatures (i.e., above the boiling point of water) would dry out the emplacement drifts, thereby limiting the amount of water available to contact waste packages. A repository operated at lower temperatures would cause less disturbance of the local environment near the emplaced waste and hydrologic and geochemical processes in the rock would be less complex than in a higher-temperature operating mode. For this reason, models of the performance of a repository operated at lower temperature may be less complex and possibly less uncertain than the models of the performance of a higher-temperature repository.

The general repository design concept provides flexibility for operation over a range of thermal operating modes. This range has been and continues to be examined to identify the potential

benefits of different environmental conditions (higher or lower temperatures and associated humidity conditions) in the emplacement drifts. The temperatures at the drift wall and waste package surfaces can be varied, along with the relative humidity, by modifying operational parameters such as the thermal output of the waste packages, the spacing of waste packages in emplacement drifts, and the duration and rate of ventilation (e.g., active ventilation that uses fans or passive ventilation that relies on natural air flow).

Surface Facilities—The potential repository's surface facilities would be located in the North Portal Repository Operations Area, the South Portal Development Area, and the Surface Shaft Areas. All waste receipt and handling operations would be conducted at the North Portal area in the Waste Handling Building.

The Waste Handling Building would receive, prepare, and package the waste for emplacement underground in the repository. All waste handling operations would be conducted using remotely operated equipment. Thick concrete walls, air locks, and controlled area access techniques would be used to protect workers from radiation exposure. The Waste Handling Building and its equipment would also be designed to withstand the effects of ground motion from potential earthquakes on repository operations. The Waste Handling Building would house all systems necessary to prepare waste for emplacement. These include:

- The carrier/cask handling system, which would receive and unload transportation casks from rail and truck carriers

- The assembly transfer system, which would receive transportation casks containing spent nuclear fuel assemblies from commercial reactors, unload the assemblies from the casks, and load the assemblies into disposal containers

- The canister transfer system, which would receive transportation casks containing canisters of DOE high-level radioactive waste or spent nuclear fuel, unload the canisters from the casks, and load the canisters into disposal containers

- The disposal container handling system, which would receive loaded disposal containers from the assembly and canister transfer systems and install and weld closure lids onto the disposal containers (referred to as waste packages after they have been loaded, sealed, and inspected)

- The waste package remediation system, which would receive waste packages that are damaged, have failed the inspection process, or have been selected for retrieval from the repository to examine their performance. Waste packages that are damaged or fail inspection would be repaired or repackaged into another container.

Underground Facility—The potential repository's underground facility would be designed to contribute to the isolation of waste. Waste packages would be disposed in dedicated drifts, supported on emplacement pallets, and aligned end-to-end on the drift floor. For the higher-temperature operating mode, the packages would be spaced about 10 cm (4 in.) apart. The base design includes 58 horizontal emplacement drifts excavated to a 5.5-m (18-ft) diameter at a center-to-center drift spacing of 81 m (266 ft). The total subsurface area required to accommodate 70,000 MTHM is about 1,150 acres. For the lower-temperature operating mode, several alternative waste package and emplacement drift spacings and configurations have been and continue to be evaluated. A final determination of the waste package and drift configuration has not been made. However, a larger area (up to about 2,500 acres) may be required for a lower-temperature operating mode. In the present design, the underground facility would be constructed over a period of about 23 years.

Waste packages would be moved, one at a time, from the surface to the emplacement drifts by way of a connecting rail system. Equipment in the Waste Handling Building would place a waste package into a shielded transporter. Two electric locomotives, one on each end of the transporter,

would move the transporter down the North Ramp, through the repository's main access drift, to an emplacement drift. Once the transporter arrives at the assigned emplacement drift and the drift's isolation doors are opened, the transporter's shielded doors would be opened and the waste package would be moved out of the transporter using a retractable deck. An in-drift gantry would lift the waste package and its supporting pallet off the deck and deposit them in their designated position inside the drift. Before the repository is permanently closed, overlapping and interlocking drip shields would be placed over the waste packages to divert any water that might drip from the top of the emplacement drifts.

Emplacement operations would take place in finished emplacement drifts at the same time as future emplacement drifts are being constructed. During construction, separate ventilation systems operating on the development side and the waste emplacement side would allow separate regulation of airflow to accommodate different needs. During emplacement, ventilation would maintain temperatures within the range for equipment operation. Before closure, ventilation would remove most of the heat generated by the waste packages and keep the relative humidity low.

V. NATURAL BARRIERS

The barriers important to waste isolation are broadly characterized as natural barriers, associated with the geologic and hydrologic setting, and engineered barriers, discussed in the following section. The engineered barriers are designed specifically to complement the natural system in prolonging radionuclide isolation within the disposal system and limiting their potential release. The natural barriers at Yucca Mountain include:

- Surface soils and topography
- Unsaturated rock layers above the repository
- Unsaturated rock layers below the repository
- Volcanic tuff and alluvial deposits below the water table.

Natural barriers would contribute to waste isolation by (1) limiting the amount of water entering emplacement drifts and (2) limiting the transport of

radionuclides through the natural system. In addition, the natural system would provide an environment that would contribute to the long lives of the waste packages and drip shields.

The location, elevation, and configuration of the underground facility was based on several factors that take advantage of the natural barriers, including the thickness of overlying rock and soil, the extent and geomechanical characteristics of the host rock, the location of faults, and the depth to groundwater. The host rock for a potential repository should be able to sustain the excavation of stable openings that can be maintained during repository operations and that would isolate the waste for an extended period after closure. In addition, the rock should be able to absorb any heat generated by the waste without undergoing changes that could threaten the site's ability to safely isolate the waste. The host rock should be of sufficient thickness and lateral extent to construct an underground facility large enough to support the design's intended disposal capacity. Moreover, the amount of suitable host rock should provide adequate flexibility in selecting the depth, configuration, and location of the facility.

The Topopah Spring Tuff, which would be the host rock for the potential repository, has a maximum thickness of about 375 m (1,230 ft) near Yucca Mountain. Site characterization studies to date have shown that the Topopah Spring Tuff has the features and characteristics listed above. The results of laboratory and underground testing to date show that the heat added by the emplaced waste would not adversely affect the stability of the geologic repository operations area. Design analyses and experience in the Exploratory Studies Facility indicate that stable openings can be constructed and maintained in the Topopah Spring Tuff.

The distribution and characteristics of fractures in the rock units at Yucca Mountain are important because in many of the hydrogeologic units, particularly the welded tuffs, fractures are the dominant pathways for water flow in both the unsaturated and saturated zones. By controlling where, and at what rates, water is likely to flow under various conditions, the fracture systems are expected to

play a major role in the performance of the disposal system. The underground facility has been designed to take advantage of the free-draining nature of the repository host rock, which would promote the flow of water past the emplaced waste and limit the amount of water available to contact the waste packages.

Fractures are common in the Topopah Spring Tuff. These fractures provide the main pathways for water to flow through the rock unit that would host emplaced waste. The water table below the Yucca Mountain site is located within the rock units called the Calico Hills Formation and the Crater Flat Group which are less fractured, which may result in fewer fracture flow pathways and slower flow through these units. Another important feature of the tuffs of the Calico Hills Formation is the abundance of zeolite minerals in the rock

matrix and fractures. Zeolites are silicate minerals that have the ability to sorb (take up on their mineral surface and hold) many types of radionuclides and other ions that might be transported in solution in water.

VI.   ENGINEERED BARRIERS

The components of the engineered barrier system are designed to complement the natural barriers in isolating waste from the environment. The repository design includes the following engineered barriers: the waste package, the waste form, the drip shield, and the emplacement drift invert. Figure 3 depicts waste packages within an emplacement drift.

The engineered barriers would contribute to waste isolation by (1) using long-lived waste packages
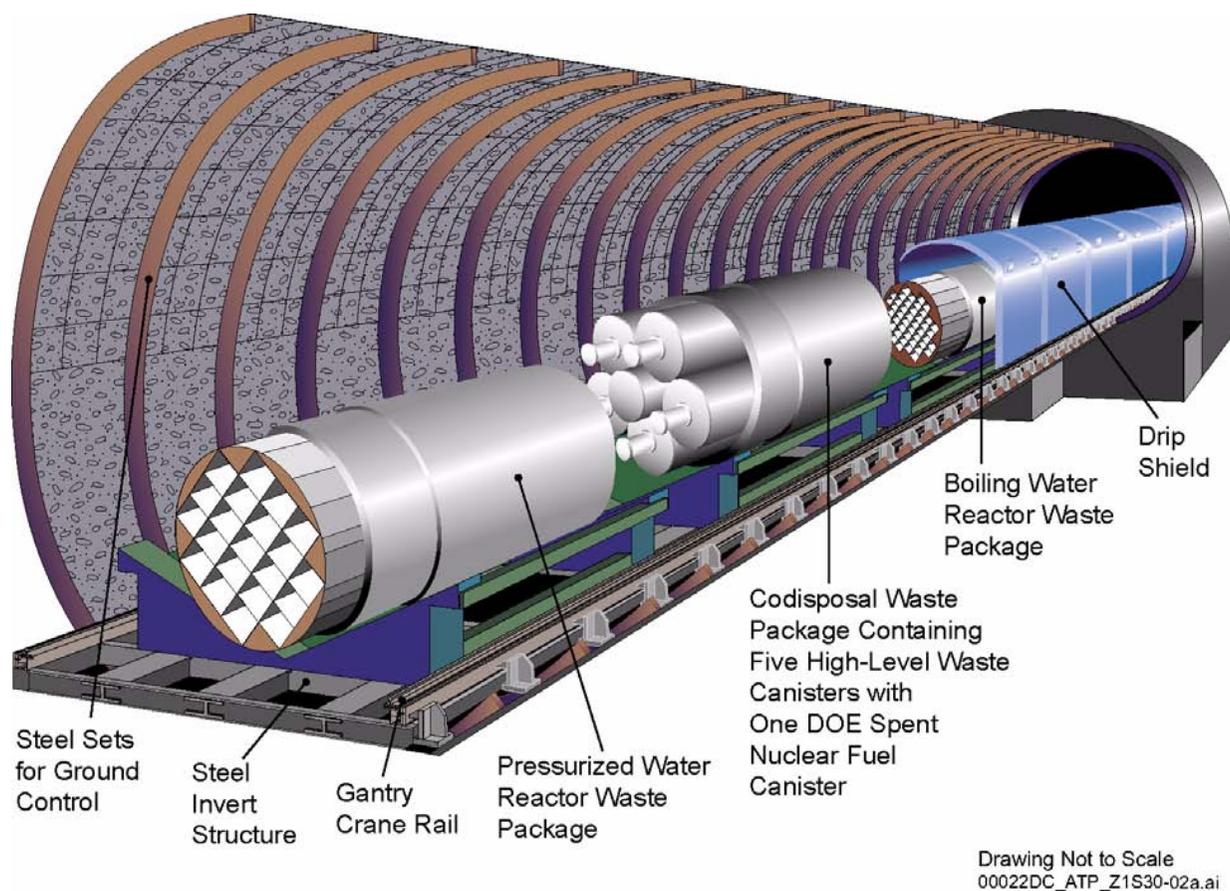
Figure 3.   Schematic Illustration of the Emplacement Drift, with Cutaway Views of Different Waste Packages

and drip shields to keep water away from the waste forms and (2) limiting release of radionuclides from the engineered barriers through components engineered for optimum performance in the expected environment.

Waste Packages—Waste packages would have a dual-metal design containing two concentric cylinders. The inner cylinder would be made of Stainless Steel Type 316NG. The outer cylinder would be made of a corrosion-resistant, nickel-based alloy (Alloy 22). Alloy 22 would protect the stainless steel inner cylinder from corrosion, and Stainless Steel Type 316NG would provide structural support for the thinner Alloy 22 cylinder. Corrosion tests have been performed and are continuing in a variety of thermal and chemical environments to provide additional information on the corrosion rate of Alloy 22. Numerous analyses of the expected performance of the waste package and associated uncertainties have been performed. Tests and analyses indicate that Alloy 22 would last considerably longer than 10,000 years in the range of expected repository environments at Yucca Mountain.

Each waste package would have outer and inner lids at each end of the cylinder. The outer (closure) lids would be made of Alloy 22, and the inner lids would be made of Stainless Steel Type 316NG. The loading end of the waste package has a third flat closure lid made of Alloy 22, which would be placed between the inner lid of stainless steel and the outer lid of Alloy 22. The flat closure lid provides an extra barrier against a potential release caused by cracks and corrosion in the closure weld areas.

The basic waste package design is the same for all the waste forms. However, the sizes and internal configurations vary to accommodate the different waste forms. Figure 3 illustrates several common internal designs, including two for different types of commercial spent nuclear fuel and one for high-level radioactive waste and DOE spent nuclear fuel (a codisposal package).

Waste Form—The materials that would be disposed at Yucca Mountain include spent nuclear fuel and vitrified high-level radioactive waste. Both of these waste forms are solid materials that will degrade very slowly in the unsaturated environment of the repository. Spent nuclear fuel primarily consists of heavy metal oxides of uranium, plutonium, and other radionuclides. High-level waste consists of a vitrified borosilicate glass containing radionuclides. The release of radionuclides from the waste form will further be limited by the low solubilities of most radionuclides in the oxidizing environment of the unsaturated repository.

Drip Shields—Drip shields would be installed over the waste packages prior to repository closure. The drip shields would divert any moisture that might drip from the drift walls, as well as condensed water vapor, around the waste packages to the drift floor. All the drip shields would be the same size, so one design could be used with all the waste packages. The drip shields would be made of titanium, which would provide corrosion resistance and structural strength. They are designed to divert moisture around waste packages for thousands of years. Tests continue on drip shield materials to assess how well current data and models can be extrapolated over long periods of time. The drip shields would also maintain their function in the event of expected rockfalls, as the emplacement drifts degrade over time.

Drift Invert—The invert includes the structures and materials that would support the pallet and waste package, the drift rail system, and the drip shield. It is composed of two parts: the steel invert structure and the ballast (or fill) that consists of granular material.

Following closure, one function of the granular material in the invert would be to provide a layer of material below the waste packages that would slow the movement of radionuclides into the host rock. Water is not expected to accumulate and flow beneath the drip shields, so the most likely way radionuclides could move is by diffusion (where dissolved or suspended particles migrate slowly from zones of high concentration to zones of low concentration) through thin films of water on the granular material.

VII. SITE CHARACTERIZATION DATA AND ANALYSES

During the site characterization program, the DOE has performed extensive surface-based tests and investigations, underground tests, laboratory studies, and modeling activities designed to provide the technical information necessary for the evaluation of long-term repository performance. The site characterization program has evolved in response to advancements in scientific understanding, changes in regulatory requirements, and changes in program requirements, such as changes in design requirements for the potential repository.

Yucca Mountain Science and Engineering Report describes the data collected during site characterization and explains the DOE's understanding of the processes that could affect the ability of the potential repository system to isolate waste. Computer models of the hydrologic, geochemical, thermal, and mechanical processes that would operate in the repository system over time have been developed from the data collected. These process models have been used to develop an overall total system performance assessment (TSPA) model that evaluates how the potential repository may behave for 10,000 years. Analyses have also considered uncertainty in model results, and have evaluated alternative conceptual models to assess the extent to which the results of performance assessment depend on the details of the underlying process models.

VIII. PROCESSES IMPORTANT TO LONG-TERM REPOSITORY PERFORMANCE

The processes important to the repository's performance after it is closed (postclosure) include those that control the movement of water through the geologic setting. These processes begin with precipitation, as rain and snow, at the surface, a fraction of which infiltrates into the mountain. This net infiltration would move through the unsaturated zone to the level of the emplacement drifts, then downward through the unsaturated zone to the saturated zone. Within the saturated zone, water would move laterally away, where it could eventually reach the accessible environment. Within the underground facility, water moving past the engi-

neered barriers would be affected by the physical and chemical processes associated with heat from the emplaced waste. These processes could eventually corrode waste packages, degrade the waste form, and dissolve some of the waste. Only after all of these processes have occurred could radionuclides move out of the repository.

To analyze the possible future performance of the repository, the DOE has studied many of the physical and chemical processes that would act on the repository system's barriers. The results of these studies are provided in *Yucca Mountain Science and Engineering Report*, along with an analysis of how the parts of the system would work together to isolate waste. The following subsections present a summary of the interdependent processes that may affect the repository's ability to isolate waste. Figure 4 illustrates the processes that were considered and modeled for the TSPA. Certain disruptive events that could affect these processes are also considered in the following discussion. The treatment of uncertainties associated with these processes is addressed in a later section.

Unsaturated Zone Flow—Because of the present-day arid climate at Yucca Mountain and the surface processes of runoff, evaporation, and transpiration, the amount of water available to contact and transport radionuclides is expected to be small. However, the availability of water may increase as a result of wetter climates that may occur in the future. The higher-temperature operating mode described in this report uses the heat produced by the waste to effectively limit the potential for contact between water and waste packages for hundreds to thousands of years. The pillar area between the emplacement drifts would be maintained below the boiling point of water to promote water drainage through the cooler portions of the rock pillars. Both the higher-temperature and lower-temperature operating modes would also take advantage of natural processes that would divert water around drift openings. Most water moving in the unsaturated zone flows through fractures. Water flowing in narrow fractures will usually remain in them rather than flow into large openings, such as drifts, because of capillary pressure in the fractures. Thus, capillary forces and water flow in unsaturated zone fractures would
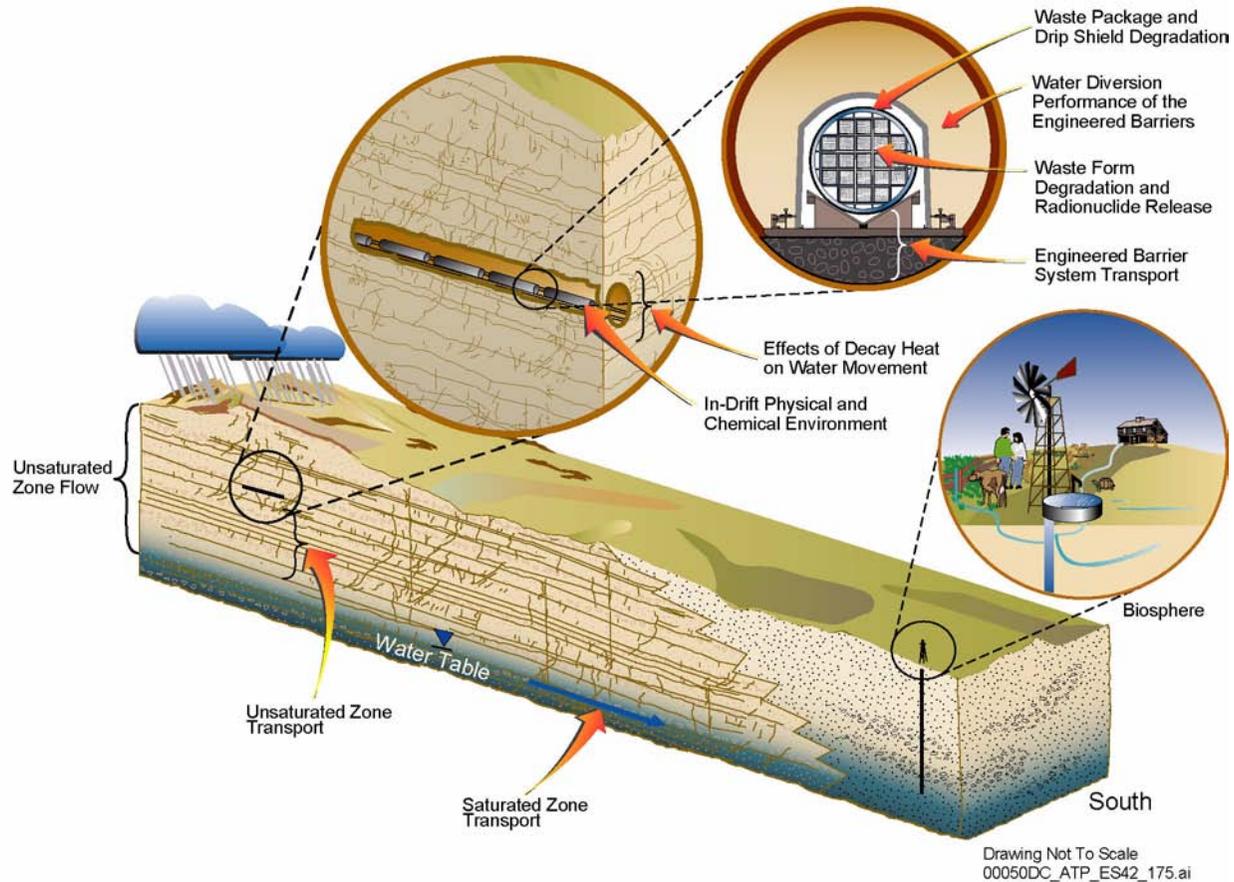
Figure 4. **Schematic Illustration of the Processes Modeled for Total System Performance Assessment**

limit seepage into openings, allowing most water to move past (not into) the emplacement drifts. If water does seep into an emplacement drift, most of it would flow down the drift wall to the floor and drain without contacting either the drip shields or the waste packages. Models of repository performance have evaluated both higher- and lower-temperature operating modes.

Many processes have been studied during the evaluation of the Yucca Mountain site. Important processes considered in the unsaturated zone flow models include:

- Climate and infiltration

- Fracture flow or matrix flow within major rock units

- Flow above the underground facility

- Flow below the underground facility, including the formation and significance of perched water (a zone of saturation separated from the water table by an intervening unsaturated zone)

- Fracture–matrix interaction

- Effects of major faults

- Seepage into drifts.

Effects of Heat on Water Movement—In the higher-temperature operating mode, no liquid water can remain in the emplacement drifts, and very little can remain in the nearby rock as long as the drift wall remains at temperatures above the boiling point of water. Even after hundreds to a few thousand years, when the waste packages have cooled below the boiling point of water, their

continued, but reduced heat production will still cause evaporation in and near emplacement drifts, thereby limiting the amount of water in the rock near the waste packages. The heat from emplaced waste may change the flow properties of the rock, as well as the chemical composition of the water and minerals in the engineered barrier system and surrounding rock. The nature and extent of these effects, however, would depend on thermal loading, ventilation rates and durations, and thermal operating properties.

Because the repository would be ventilated during operations, the major effects of heat on water movement would take place during the postclosure period. Thermal-hydrologic processes in the repository environment will determine the conditions in the drift, including temperature, relative humidity, and seepage at the drift wall.

In the lower-temperature operating modes that the DOE has evaluated, the heat from emplaced waste would still increase evaporation rates and, to some extent, dry out the rock near the emplacement drifts. Although liquid water could enter drifts, it is likely that only limited amounts of water would be available because of fracture flow and processes related to seepage.

Physical and Chemical Environment—The lifetimes of the drip shields and waste packages would depend on the conditions to which they are exposed: the in-drift physical and chemical environment. Once water enters a degraded waste package, the transport of radionuclides released from the waste form inside also depends on the drift environment. For the higher-temperature operating mode described in this report, the repository environment would be warm, with temperatures at the surface of the waste package initially increasing above the boiling point of water. The expected duration of temperatures above the boiling point of water on the surfaces of the waste packages would be hundreds to thousands of years. The precise time period varies for three main reasons: (1) location within the repository layout, (2) spatial variation in the infiltration of water at the ground surface, and (3) variability in the heat output of individual waste packages. The repository edges would cool first because they

would lose heat to the cooler rock outside the perimeter. Water percolating downward through the host rock in response to infiltration at the ground surface would hasten cooling of the repository; locations with greater percolation cool faster. The heat output of individual waste packages will vary, depending on the type and age of the waste they contain; however, this variability can be managed. Except for the first few hundred years, the environment of the repository would be similar for both higher- and lower-temperature operating modes.

The chemical environment is expected to be at near-neutral pH (mildly acidic to mildly alkaline) and mildly oxidizing. Under such conditions, Alloy 22 will form a thin, stable oxide layer that is extremely corrosion resistant. Important processes affecting the chemical environment include the evaporation and condensation of water, the formation of salts, and the effects of gas composition. While the repository environment is warm, relative humidity will probably control the water chemistry.

Waste Package and Drip Shield Degradation— The lifetimes of the drip shields and waste packages will depend on the environment to which they are exposed and the degradation processes that occur. Corrosion is the most important degradation process considered in selecting the materials for the waste package and drip shield. A number of corrosion processes have been investigated in detail. The results have been used to support the selection of materials and the design of components.

Because most corrosion occurs only in the presence of water, and because highly corrosive chemical conditions are not expected in the repository environment, both the titanium drip shield and the Alloy 22 outer layer of the waste package are expected to have long lifetimes. Analyses based on laboratory tests and other evaluations indicate that, in the absence of a disruptive event or human intrusion, no waste packages are expected to be breached by corrosion for more than 10,000 years. The DOE has also evaluated the possibility that waste packages could be breached by processes other than corrosion such as stress corrosion cracking. These analyses indicate that improper

heat treatment of welds could cause cracks in a small number of packages (approximately zero to three) over 10,000 years. The small number of breaches would not have a significant impact on repository performance.

Analyses to date indicate that the drip shields and waste packages will be long-lived for both higher- and lower-temperature operating modes. The DOE has evaluated and will continue to evaluate whether keeping waste package surface temperatures cooler would improve performance or reduce the uncertainty in the models used. Water could contact waste packages sooner in lower-temperature operating modes. However, the physical environment of lower-temperature operating modes may reduce the potential for corrosion susceptibility of Alloy 22. Analyses to date have not demonstrated a significant difference in waste package and drip shield performance between higher- and lower-temperature operating modes. The DOE continues to perform materials tests and evaluate corrosion data to provide a stronger technical basis for the projections of waste package and drip shield lifetimes.

Water Diversion Performance of the Engineered Barriers—The water diversion function of the engineered barrier system is to limit the amount of water contacting waste packages for the 10,000-year performance period and to limit the transport of released radionuclides from breached waste packages to the host rock at the drift wall. The engineered barrier system components that will perform these functions principally include the drip shield and the drift invert (consisting of a steel support structure with crushed rock ballast).

Water that enters the emplacement drifts as seepage can flow along three types of pathways: (1) water flow that bypasses the drip shield and moves down drift walls or drips directly to the invert; (2) water droplets that contact the drip shield but are diverted by it to the invert; and (3) water droplets that contact the drip shield and migrate through breaches to the waste package. Water diversion models used for TSPA are used to estimate the fraction of seepage water that penetrates the drip shield and the fraction of resulting leakage that penetrates the waste package.

Models of the movement of water within emplacement drifts focus on the process of seepage. For water to contact a drip shield or waste package, water droplets must form from seepage above the waste package and fall. Other modes of flow, such as film flow on the drift wall, may divert some or all of the seepage around the drift. Most seepage would probably occur at or near faults or fractures that could focus percolation into a drift. Analyses indicate that the emplacement drifts have enough drainage capacity to ensure that water would not rise above the level of the invert even under extreme seepage conditions.

Supplemental studies of the lower-temperature operating mode suggest that flow processes are similar to those modeled for higher-temperature operating modes, except for the period when temperatures are above the boiling point of water. The composition of seepage at early times (for the lower-temperature operating mode) is within the range of aqueous compositions used in laboratory corrosion testing. For this reason, the modeled performance of the engineered barrier system is similar regardless of the choice of thermal operating modes.

Waste Form Degradation and Radionuclide Release—Because of the characteristics of the natural system and the engineered barriers, the DOE does not expect water to penetrate intact waste packages and contact waste for over 10,000 years. Even if water were to penetrate a breached waste package before 10,000 years, several characteristics of the waste form and the other natural and engineered barriers would limit radionuclide releases. First, because of elevated temperatures associated with both higher- and lower-temperature operating modes, much of the water that penetrates the waste package will evaporate before it can dissolve or transport radionuclides. Both spent nuclear fuel and glass high-level radioactive waste forms will degrade slowly in the waste package environment. Further, data and analyses indicate that most of the radionuclides in the waste are not very soluble in the warm, near-neutral pH conditions that are expected. To dissolve radionuclides that may be soluble (technetium-99, iodine-129, neptunium-237, and all isotopes of uranium), water must also penetrate the metal cladding of the

spent nuclear fuel assemblies. Although the performance of the cladding as a barrier may vary because of possible degradation, it is expected to limit contact between water and the waste.

Release of radionuclides from the waste forms is a three-step process requiring (1) degradation of the waste forms, (2) mobilization of the radionuclides from the degraded waste forms, and (3) transport of the radionuclides away from the waste forms. Radionuclides can be released only after the waste package is breached and air and water begin to enter. The rates of water flow and evaporation will determine when and if water accumulates in a waste package. Even if water is available to dissolve radionuclides, the chemistry inside the waste package would influence the rate at which the waste forms degrade and the mobility of radionuclides from the degraded waste forms.

The waste form solubility model is not significantly affected by the temperature of the operating mode because radionuclides can only dissolve after the drip shield and waste package have degraded and water has reached the waste form inside. The subsequent transport processes could occur only after temperatures have cooled below boiling, thereby allowing water to be available as a transport mechanism.

Engineered Barrier System Transport—The invert below the waste package would contain crushed tuff that would limit the transport of radionuclides from breached waste packages into the unsaturated zone. Transport could occur either through advection, which is the flow of liquid water, or by diffusion. The scarcity of water makes advective transport unlikely, but diffusive transport through thin films on the waste form, on the waste package, and in the invert ballast is possible.

Unsaturated Zone Transport—Eventually, components of the repository's engineered barrier system will degrade and small amounts of water will contact the waste. Even after the engineered barriers have degraded, however, features of the geologic setting and underground facility would limit releases to the accessible environment and slow migration for hundreds to thousands of years. Processes that could be important to the movement

of radionuclides include sorption, matrix diffusion, dispersion, and dilution.

Sorption is a process in which minerals in the rock or soil along flow paths attract and hold (adsorb) constituents dissolved in water. Rocks in the unsaturated zone at Yucca Mountain contain minerals that can adsorb many types of radionuclides. Matrix diffusion is a process in which dissolved radionuclides diffuse into and out of the rock pores as water flows in the rock fractures. This process would increase both the time it takes for radionuclides to move out of the repository and the likelihood that they would be exposed to sorbing minerals. Dispersion is a process in which radionuclides contained in water spread out as the water flows, resulting in lower concentrations of contaminants. Dilution occurs naturally as contaminated groundwater flows and mixes with noncontaminated groundwater, which reduces the concentration of contaminants.

Process models of transport in the unsaturated zone have incorporated the processes described above. The results of these models indicate that the movement of radionuclides from a breached waste package down to the water table would require hundreds to thousands of years, depending on the mobility of specific radionuclides. Many radionuclides would not move over much longer time spans because of their particular chemical properties.

Saturated Zone Flow and Transport—The same basic processes that apply to the movement of radionuclides in the unsaturated zone (sorption, matrix diffusion, dispersion, and dilution) also apply to transport in the saturated zone. Flowing groundwater transports radionuclides either in solution (dissolved) or in suspension (bound to very small particles called colloids). Any radionuclides released by water contacting breached waste packages would have to migrate through the unsaturated zone down to the water table and then travel through the saturated zone to reach the accessible environment. Groundwater in the saturated zone below the underground facility generally moves southeast before flowing south out of the volcanic rocks and into the thick alluvium deposits of the Amargosa Desert. Figure 5
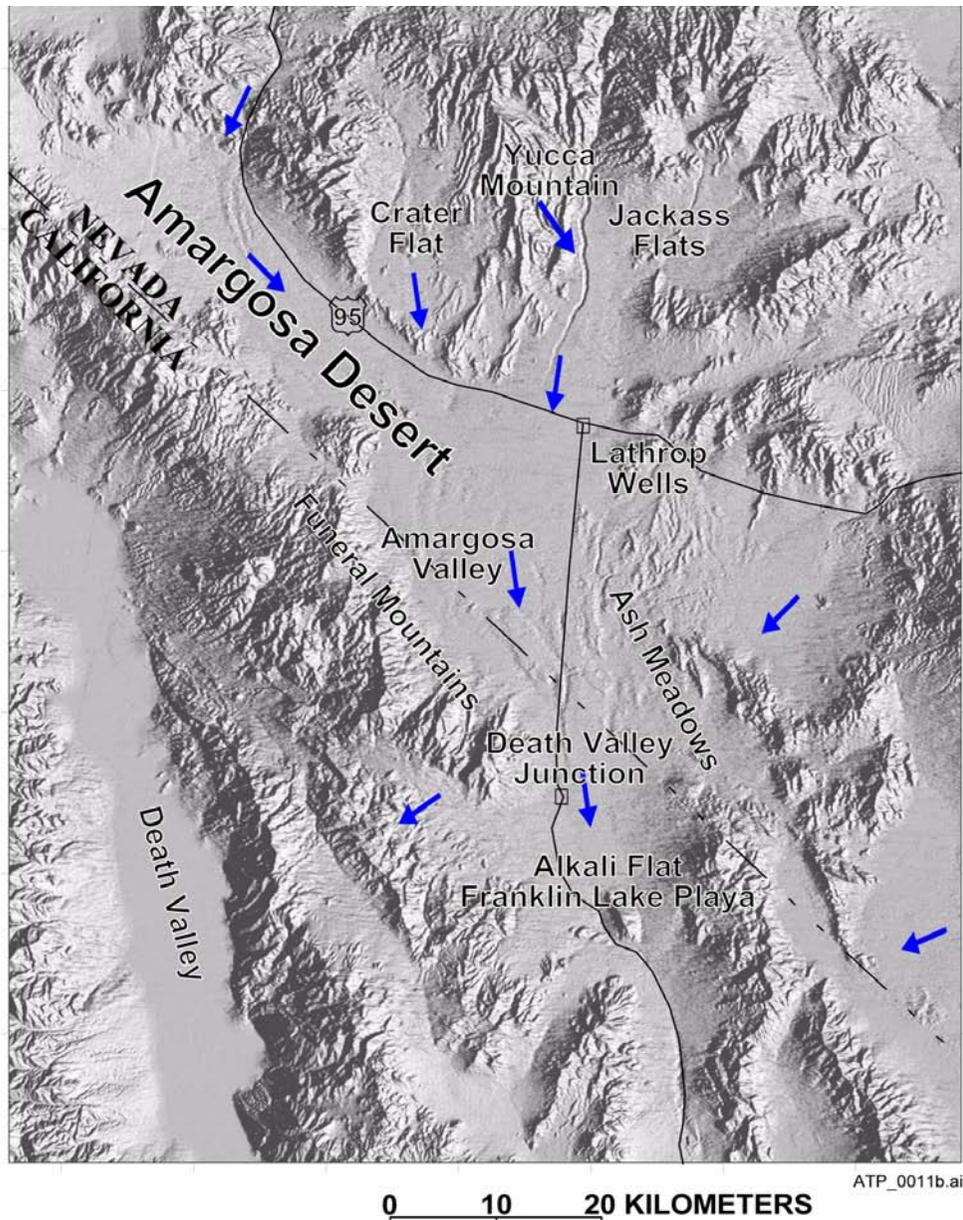
Figure 5.   Regional Map of the Saturated Zone Flow System

shows the general directions of groundwater flow in the saturated zone on a regional scale. Analyses show that it would take thousands of years or longer (depending on the mobility of specific radionuclides) for radionuclides to move down through the unsaturated zone, into the saturated zone, and then to the accessible environment.

Biosphere—The biosphere is the ecosystem of the earth and the organisms inhabiting it, including the soil, surface water, air, and all living organisms.

Biosphere analyses of the Yucca Mountain site have been performed to develop conversion factors that enable analysts to estimate doses to a receptor from the transport and retention of radionuclides within the biosphere.

The biosphere analyses scrutinize processes and pathways that could either disperse or concentrate radionuclides released from the Yucca Mountain disposal system. In calculating radiation exposure, biosphere analyses consider the environment

around and the lifestyle (including diet and activity) of individuals who would be exposed. The terms "accessible environment" and "reasonably maximally exposed individual" are EPA and NRC regulatory terms that define where radioactive releases from Yucca Mountain must be evaluated and the characteristics of the hypothetical individual who would be exposed to the radiation. All postclosure releases are evaluated within the accessible environment at a point whose latitude is specified and which is above the highest radionuclide concentration in the contaminated groundwater plume. This point lies about 18 km (11 mi) from the southern edge of the currently designed Geologic Repository Operations Area. The reasonably maximally exposed individual who is exposed to releases from the Yucca Mountain disposal system is assumed to have a diet and living style that represents the current residents of Amargosa Valley, Nevada. The radionuclide concentrations that reach this individual are calculated using factors that are unique to the biosphere in which the individual lives.

Disruptive Processes and Events Scenarios— Analyses of disposal system performance must also consider events that could occur in the future that have the potential to compromise the system's ability to protect public health and safety. Analysts have evaluated a wide variety of potentially disruptive processes and events that could affect performance. These range from extremely unlikely events to processes that are likely to occur and that could affect long-term repository performance. The potential for igneous (volcanic) activity in or near the Yucca Mountain site has been specifically included in performance assessments in the disruptive scenario case, and the effects of seismic activity (i.e., vibratory ground motion that might damage the cladding on spent nuclear fuel) have been considered in the nominal scenario case.

A stylized inadvertent human intrusion into the repository was analyzed in a separate performance assessment. NRC licensing regulations at 10 CFR Part 63 would require the DOE to determine the earliest time after disposal when the waste packages would degrade sufficiently that a human intrusion could occur without recognition by the drillers. Analyses indicate that the earliest time

after disposal at which a driller would not recognize that a waste package or drip shield has been penetrated would be after about 30,000 years, even if a few waste packages failed (i.e., developed cracks) at earlier times due to improper heat treatment of welds. The DOE also analyzed an inadvertent intrusion occurrence 100 years after closure, based on proposed NRC regulations. This analysis showed that the doses from a 100-year intrusion would be less than about 0.01 mrem/yr.

IX. THE ATTRIBUTES OF SAFE DISPOSAL

The Yucca Mountain disposal system can be described in terms of five key attributes that would be important to long-term performance: (1) limited water entering waste emplacement drifts; (2) long-lived waste package and drip shield; (3) limited release of radionuclides from the engineered barriers; (4) delay and dilution of radionuclide concentrations by the natural barriers; and (5) low mean annual dose considering potentially disruptive events. These attributes are summarized below. The first four reflect the interactions of natural barriers and the engineered barriers in prolonging the containment of radionuclides within the repository and limiting their release. The fifth attribute reflects the likelihood that disruptive events would not affect repository performance over 10,000 years.

Limited Water Entering Emplacement Drifts— The climate at the Yucca Mountain site is dry and arid with precipitation averaging about 190 mm (7.5 in.) per year. Little of this precipitation percolates into the mountain; nearly all of it (above 95 percent) either runs off or is lost to evaporation or transpiration, thereby limiting the amount of water available to seep into the underground facility. For the higher-temperature operating mode described in *Yucca Mountain Science and Engineering Report*, a thermal management strategy was developed that would take advantage of the heat of the emplaced wastes to drive the limited water that exists away from the emplacement drifts. The heat generated by the waste would dry out the rock surrounding the drift and decrease the amount of water available to contact the waste packages until the wastes have cooled substan-

tially. Drainage of water in the rock pillars between drifts would be encouraged by keeping much of the pillar rock between the drifts below the boiling temperature of water. As long as emplacement drift walls remain at temperatures above the boiling point of water, no liquid water can remain in the underground facility, and very little can remain in the underground structure. For the lower-temperature operating modes (and for higher-temperature operating modes after the waste packages have cooled below the boiling point of water), the heat associated with waste will still cause evaporation in and near the emplacement drifts. This process would limit the amount of water in the rock near the waste packages. In lower-temperature operating modes, the waste packages would be exposed to water sooner. Because the rock would eventually cool in any operating mode, there does not appear to be a significant difference in the amount of water to which the waste packages would eventually be exposed.

The repository design also takes advantage of the mechanical and hydrologic processes that divert water around emplacement drift openings in the unsaturated zone. Because of capillary forces, water flowing in narrow fractures tends to remain in the fractures rather than flow into large openings, such as drifts. If any water reached an emplacement drift, it could flow down the drift wall to the floor and drain without contacting the drip shields or waste packages. Thus, the natural and engineered features of a Yucca Mountain disposal system will combine to limit the potential for water to enter the emplacement drifts.

Long-Lived Waste Package and Drip Shield—To further reduce the possibility of water contacting waste, the DOE has designed a robust, dual-wall waste package with an outer cylinder of corrosion-resistant nickel-based metal, Alloy 22. Alloy 22 was selected because it will remain stable in the geochemical environment expected in the potential repository. In the higher-temperature operating mode, the repository environment would be warm, with temperatures at the waste package surface initially rising above the boiling point of water. Waste package surface temperatures are expected to gradually decrease to below boiling after a period of hundreds to thousands of years,

depending on the waste package's location in the repository and other factors discussed previously. In lower-temperature operating modes, the waste packages would be exposed to water earlier.

Chemically, the environment is expected to be at near-neutral pH (mildly acidic to mildly alkaline) and mildly oxidizing. Because most corrosion would occur only in the presence of water, and because highly corrosive chemical conditions are not expected, both the titanium drip shield and the Alloy 22 outer barrier of the waste package are expected to have long lifetimes.

Limited Release of Radionuclides from the Engineered Barrier System—Because of the characteristics of the natural system, the drip shields, and the waste packages, the DOE does not expect water to come into contact with the waste forms for more than 10,000 years. Even if water were to penetrate a breached waste package before 10,000 years, several characteristics of the waste form and the repository would limit radionuclide releases. First, because of the warm temperatures, much of the water that penetrates the waste package would evaporate before it could dissolve or transport radionuclides. Neither spent nuclear fuel nor glass waste forms will dissolve rapidly in the expected repository environment. Although the performance of the cladding as a barrier may vary because of possible degradation, it is expected to limit contact between water and the waste. The component of the engineered barrier system below the waste package, called the invert, contains crushed tuff that would also limit the transport of radionuclides into the host rock, as discussed under Engineered Barrier System Transport.

Delay and Dilution of Radionuclide Concentrations by the Natural Barriers—Eventually, components of the engineered barrier system will degrade, and small amounts of water will contact waste. Analyses indicate that this is not likely to occur within the first 10,000 years following repository closure. Even then, features of the geologic environment and the repository would limit radionuclide migration to the accessible environment and slow it by hundreds to thousands of years. Processes that could be important to the movement of radionuclides include sorption, matrix diffusion,

dispersion, and dilution. Rock units in both the unsaturated zone and the saturated zone contain minerals that can adsorb many types of radionuclides (i.e., radionuclides would attach to and collect on the mineral surfaces). As water flows through fractures, dissolved radionuclides can diffuse into and out of the pores of the rock matrix, increasing both the time it takes for radionuclides to move through the geologic setting and the likelihood that radionuclides will be exposed to sorbing minerals. Dispersion and dilution will occur naturally as potentially contaminated groundwater flows and mixes with other groundwater and reduces the concentration of contaminants.

Low Mean Annual Dose Considering Potentially Disruptive Events—Yucca Mountain provides an environment in which hydrologic and geologic conditions important to waste isolation (e.g., a thick unsaturated zone with low rates of water movement) have changed little for millions of years. Analysts have identified and evaluated a wide variety of potentially disruptive processes and events that could affect the performance of the Yucca Mountain disposal system. These range from extremely unlikely events, such as meteor impacts, to events that are likely to occur, such as regional climate change. Although the probability of volcanic activity in or near the Yucca Mountain site is low, volcanic activity was a consideration in TSPA in the disruptive scenario case. Performance assessment results to date show that potentially disruptive events are not likely to compromise the system performance.

X.   UNCERTAINTIES IN DATA AND MODELS

Quantitative assessments of the long-term performance of the disposal system consider a comprehensive set of features, events, and processes that may have an effect on that performance. The features and characteristics of the site and geologic setting are incorporated into conceptual and numerical models. The likelihood of occurrence and consequences of processes and events that may affect repository performance are evaluated, then incorporated, as appropriate, into the numerical models. Although the DOE continues to evaluate ways to reduce uncertainties in repository performance models, uncertainties will always remain because of the long time frames over which the system performance must be assessed, the natural variability in features and processes at the site, and limitations on the amount of data that can be collected. Features, events, and processes are generally represented probabilistically in a performance assessment to address this inherent uncertainty and variability.

Numerous analyses have been performed to help the DOE understand the extent to which the results of total system performance assessments are robust (not likely to change significantly as new information is gathered in the future). These include analyses to assess the degree of realism in current process models, to quantify key uncertainties, and to improve the understanding of conservatism in the models and in performance assessment results. The DOE has also evaluated whether uncertainties (especially modeling uncertainties that are not easily quantified) can be reduced further by operating the repository at lower temperatures.

Because uncertainty cannot be eliminated, the DOE's approach to building confidence in analyses of repository performance relies on multiple lines of evidence. Collectively, these multiple lines of evidence are known as the postclosure safety case. Elements of the safety case include:

- Quantitative assessments of long-term performance (i.e., TSPA).

- Selection of a site and design of a repository that provides defense in depth—a system of multiple, independent, and redundant barriers designed to ensure that failure of one barrier does not result in failure of the entire system. The system would also provide a margin of safety against radionuclide releases and a margin of safety compared to applicable radiation protection standards.

- Qualitative insights gained from the study of natural and man-made analogues to the repository or to processes that may affect system performance.

- Long-term management to ensure the integrity and security of the repository and long-term monitoring (a performance confirmation program) to evaluate the behavior of the repository and enable sound scientific and engineering bases for a later repository closure decision.

Quantitative analyses indicate that the repository design and operating modes described in *Yucca Mountain Science and Engineering Report* offer both defense in depth and a significant safety margin. Analogue studies have provided several lines of evidence that suggest most current models are representative and, in some cases, may be overly conservative.

XI. PERFORMANCE ASSESSMENT RESULTS

The numerical (quantitative) evaluation of postclosure repository performance is an important part of demonstrating that a Yucca Mountain disposal system can be constructed that would protect public health and safety. The DOE has completed a TSPA to evaluate the system performance. TSPA is a numerical calculation, based on the process models described above, that forecasts when and to what extent radionuclides released from a Yucca Mountain disposal system might reach the accessible environment and expose human beings. The results are typically displayed as a graph of dose rate plotted in millirem per year against time (10,000 years).

The total system analyses are presented in three scenarios: nominal (the scenario that uses the features, events, and processes expected to occur), disruptive (the scenario that uses possible but unlikely events with potentially harmful consequences), and stylized human intrusion (the scenario proposed by the NRC in which someone drills through a waste package 100 years after the repository had been permanently closed). As noted earlier, the DOE does not expect a human intrusion during the compliance period. The analysis is included, however, to illustrate the disposal system's resilience. Analyses were completed to evaluate the potential importance of each feature, event, or process at the site to system performance

and included or excluded each from TSPA analyses, as appropriate.

Performance assessments for the initial 10,000-year period after closure have been completed in a manner consistent with the EPA radiation protection standards and NRC licensing regulations. In addition to these assessments, the peak mean annual dose to the reasonably maximally exposed individual beyond the 10,000-year time period was also calculated to see if dramatic changes in the performance of the disposal system could be anticipated beyond 10,000 years. These results are described in Section 4.4.

Nominal Scenario—The DOE has assessed the repository's performance for the nominal case. The TSPA-SR model projected no dose over a 10,000-year period. A supplemental TSPA model projected a dose to the reasonably maximally exposed individual of 2×10^{-4} mrem/yr, while a revised supplemental TSPA model projected a dose of 1.7×10^{-5} mrem/yr over a 10,000-year period. Both doses were calculated based on the higher-temperature operating mode. The doses calculated by the supplemental and revised supplemental TSPA models would be reduced by approximately one-third if an annual water demand of 3,000 acre-ft was used, consistent with final NRC regulations (10 CFR 63.312).

Disruptive Scenario—The primary disruptive event considered in these analyses is igneous activity. The TSPA models evaluated two igneous disruptions: a volcanic eruption that intersects drifts and brings waste to the surface; and an igneous disruption that damages waste packages and exposes radionuclides for groundwater transport. The probability of igneous disruption is extremely low (the mean annual probability is about one chance in 60 million per year of occurring). The TSPA-SR model projected a probability-weighted mean dose from igneous activity of 0.08 mrem/yr over a 10,000-year period, and both the supplemental TSPA model and the revised supplemental TSPA model projected a dose to the receptor of 0.1 mrem/yr over 10,000 years.

Human Intrusion Scenario—The DOE has assessed the consequences of a stylized human

intrusion into the repository at 100 years after closure, pursuant to the proposed NRC regulation. The results of this analysis show that the peak mean dose is approximately 0.01 mrem/yr over a 10,000-year period. Consistent with final NRC regulations at 10 CFR 63.321, the DOE analyzed the period of time that would be necessary for waste packages to degrade sufficiently that a human intrusion could occur without recognition by a driller. The DOE subsequently found that human intrusion would not occur for more than about 30,000 years. Therefore, no doses related to human intrusion would occur within 10,000 years. The dose from a human intrusion at 30,000 years is analyzed and presented in the final environmental impact statement (EIS).

XII. EVALUATION OF THERMAL OPERATING MODES

The performance assessment presented in *Yucca Mountain Science and Engineering Report* considers both lower- and higher-temperature operating modes. The repository design is flexible: it can be operated in a range of modes that would allow the temperature and humidity in the underground environment to be varied. Analyses of the effects of the higher-temperature operating mode indicate that higher temperatures would effectively limit the potential for contact between water and waste packages for time periods of hundreds to thousands of years. However, during that period, the interaction of rock, water, and heat in and near emplacement drifts may affect rock properties and water chemistry in complex ways that cannot be fully captured in the models.

The complexity of these processes introduces uncertainty into the analyses. For this reason, the DOE has completed extensive analyses to determine whether the complexity of the associated process models could be reduced. As part of these investigations, the DOE has analyzed the performance of the repository over a range of thermal operating modes. The results indicate that the repository's performance is similar over range of operating modes, encompassing above- and below-boiling conditions.

The DOE expects the repository design and operating mode to be refined as the project evolves. This design evolution will be based on a process that includes (1) refining specific design requirements and performance goals to recognize performance-related benefits that could be realized through design and (2) enhancing components of the design to best achieve the performance-related benefits.

XIII. PRECLOSURE SAFETY ASSESSMENT

A potential repository at Yucca Mountain would be designed and operated in a manner that would limit worker and public exposures to radiation. A preclosure safety evaluation has been conducted to evaluate the performance of the Geologic Repository Operations Area during the preclosure period. The safety evaluation plays a key role in identifying design features and controls that are important to safety, and is a primary input to the quality assurance classification process. Results indicate that a repository could be operated such that radiation doses to the public and workers would be below EPA and NRC regulatory limits.

To begin the safety evaluation, the DOE systematically identified and examined a range of potential hazards and the event sequences such hazards could cause, as well as their likelihood and consequences. From this examination, the DOE identified structures, systems, and components important to safety that would be relied upon to protect the public and workers. These structures, systems, and components are those engineered features of the repository whose function is to (1) reasonably ensure that spent nuclear fuel and high-level radioactive waste can be received, handled, staged, emplaced, and retrieved without exceeding regulatory limits; or (2) prevent or reduce the impact of Category 1 and Category 2 event sequences (events the repository would be designed to withstand) that could potentially lead to exposure of individuals to radiation. The structures, systems, and components were then classified in grades according to their importance to safety to ensure that appropriate quality assurance controls are implemented during the repository's operational lifetime. The DOE has developed a preclosure safety test and evaluation

program to verify that structures, systems, and components are designed as specified and perform as required.

XIV. PERFORMANCE CONFIRMATION AND MONITORING

A performance confirmation program established to monitor and confirm that the Yucca Mountain disposal system is performing as expected was initiated during site characterization and will continue to permanent closure. The focus of the performance confirmation program is to gather and analyze data on natural processes and engineered barriers performance that will affect repository performance after closure and to evaluate their impacts. Subsurface facilities, including performance confirmation drifts and alcoves, would be constructed to facilitate monitoring of the underground facility and the performance of the engineered barrier system. Primary testing and monitoring activities will include seepage monitoring to evaluate flow of water into excavations and confirm expected waste package environment; in situ waste package surface temperature monitoring to infer cladding temperatures; rock mass monitoring to confirm the conceptual understandings and numerical simulations of coupled processes considered in performance assessments; and other activities that focus on providing an increased understanding of processes important to repository postclosure safety. Performance confirmation and monitoring activities would continue throughout the preclosure period, which could be extended up to 300 years.

INTENTIONALLY LEFT BLANK

ACRONYMS AND ABBREVIATIONS

Acronyms

AEC	U.S. Atomic Energy Commission
ALARA	as low as is reasonably achievable
CQ	conventional quality
DOE	U.S. Department of Energy
ECRB	Enhanced Characterization of the Repository Block
EIS	environmental impact statement
EPA	U.S. Environmental Protection Agency
ERDA	U.S. Energy Research and Development Administration
FEP	feature, event, and process
NRC	U.S. Nuclear Regulatory Commission
NWPA	Nuclear Waste Policy Act of 1982
NWTRB	Nuclear Waste Technical Review Board
QL	quality level
TSPA	total system performance assessment
TSPA–SR	total system performance assessment for site recommendation
USGS	U.S. Geological Survey
VA	Viability Assessment

Abbreviations

atm	atmosphere
BHN	Brinnel hardness number
cm	centimeter
Eh	redox potential
ft	foot
g	gram
gal	gallon
GWd	gigawatt day
hp	horsepower
Hz	Hertz

in.	inch
kg	kilogram
km	kilometer
kPa	kilopascal
kW	kilowatt
MTHM	metric tons of heavy metal
MTU	metric tons of uranium
L	liter
lb	pound
m	meter
M	molar
mg	milligram
mi	mile
min	minute
mL	milliliter
mm	millimeter
MPa	megapascal
mV	millivolt
MW	megawatt
M_w	moment magnitude
μm	micrometer (micron)
nm	nanometer
Pa	pascal
pCi	picocurie
pH	scale of acidity and alkalinity (hydrogen-ion concentration notation)
ppm	parts per million
psi	pounds per square inch
rem	roentgen equivalent man
s	second
W	watt
wt	weight
yr	year

1. INTRODUCTION

Spent nuclear fuel and high-level radioactive wastes are the result of commercial power generation, nuclear weapons production, and other research and development activities. They have accumulated since the mid-1940s at sites now managed by the U.S. Department of Energy (DOE) and since 1957 at commercial reactors and storage facilities across the country. The responsible management and disposal of these materials is a critical part of the DOE mission to dispose of high-level radioactive waste and spent nuclear fuel from federal facilities, including the nuclear weapons program, as well as commercially generated spent nuclear fuel.

The U.S. has evaluated methods for the safe storage and disposal of radioactive waste for more than 40 years. Many organizations and government agencies have participated in these studies: at the request of the U.S. Atomic Energy Commission (AEC), the National Academy of Sciences evaluated options for the disposal of radioactive waste on land in the 1950s (National Academy of Sciences Committee on Waste Disposal 1957). The AEC and its successor agencies, the U.S. Energy Research and Development Administration (ERDA) and the DOE, continued to analyze nuclear waste management options throughout the 1960s and 1970s. In cooperation with the U.S. Geological Survey (USGS), nationwide surveys were performed to identify potentially acceptable locations for disposal sites. During the late 1970s and early 1980s, the U.S. Nuclear Regulatory Commission (NRC) and the U.S. Environmental Protection Agency (EPA) performed numerous studies of disposal options and safety and began developing regulatory standards. An Interagency Review Group that included representatives of 14 federal government entities provided findings and recommendations on nuclear waste management to President Carter in 1979 (Interagency Review Group on Nuclear Waste Management 1979). After analyzing a wide variety of options, disposal in mined geologic repositories emerged as the preferred long-term environmental solution for the management of spent nuclear fuel and high-level radioactive waste. This consensus is reflected

in the Nuclear Waste Policy Act of 1982 (NWPA) (42 U.S.C. 10101 et seq.), which established U.S. policy when it was enacted by Congress in 1982 (Public Law No. 97-425) and amended in 1987 (Public Law No. 100-203).

Congressional Findings

Section 111(a) of the NWPA (42 U.S.C. 10131(a)) contains seven Congressional findings for the repository program:

(1) Radioactive waste creates potential risks and requires safe and environmentally acceptable methods of disposal;

(2) A national problem has been created by the accumulation of (A) spent nuclear fuel …; and (B) radioactive waste …

(3) Federal efforts during the past 30 years to devise a permanent solution … have not been adequate;

(4) While the Federal government has the responsibility to provide for … permanent disposal … , the costs … should be the responsibility of the generators and owners…

(5) The generators and owners of high-level radioactive waste and spent nuclear fuel … have the primary responsibility to provide for, and … pay the costs of, the interim storage of such waste and spent fuel until … accepted by the Secretary of Energy …

(6) State and public participation … is essential in order to promote public confidence in the safety of disposal …

(7) High-level radioactive waste and spent nuclear fuel have become major subjects of public concern, and appropriate precautions must be taken to ensure that [they] do not adversely affect public health and safety or the environment for this or future generations.

In the NWPA, Congress described the technical and policy issues that make nuclear waste disposal so difficult. Congress assigned the responsibility for paying the costs of disposal to the generators and owners of high-level radioactive waste and spent nuclear fuel and recognized that a solution could only be achieved through a process that included public and state involvement. The national policy reflected in the NWPA is that geologic disposal should be accomplished by the generation that created the waste, not deferred to future generations.

The NWPA required the EPA to establish standards for the protection of public health and safety; directed the DOE to site, design, construct, operate, and close a repository; and assigned to the NRC the responsibility to regulate and license a repository and ensure compliance with applicable standards. The Nuclear Waste Policy Amendments Act of 1987 (Public Law No. 100-203) directed the DOE to characterize only Yucca Mountain, Nevada, for a repository. It also created the Nuclear Waste Technical Review Board (NWTRB), an independent organization within the executive branch, and charged it with evaluating the technical and scientific validity of the program and reporting its findings, conclusions, and recommendations to Congress and the Secretary not less than twice a year.

The DOE (including the national laboratories) and the USGS began studying Yucca Mountain (Figure 1-1) in the late 1970s. Detailed investigations of the geology, hydrology, geochemistry, and other characteristics of the site have been performed since 1986 to determine whether it is a suitable place to build a geologic repository. As part of this effort, the DOE has developed preliminary designs for surface and subsurface facilities and for waste packages. Analyses that integrate design- and site-specific data and models have been conducted to assess how a repository at Yucca Mountain might perform.

The NWPA specifies a process for the recommendation and approval of a site for development of a repository, and it requires that the Secretary of Energy provide a comprehensive statement of the

ATP_Z1S1_Fig. 1-1a.ai

Figure 1-1.   Aerial View of Yucca Mountain, Looking South, Showing the Desert Environment and the Remote Location
The potential repository would be located about 300 m (1,000 ft) below the eastern slope of the mountain.

basis for a recommendation if the site is recommended. This report is being issued to describe the results of site characterization studies, the waste forms to be disposed, a repository and waste package design, and the updated results of assessments of long-term performance of the potential repository.

Studies of Yucca Mountain will not end if the site is recommended. NRC regulations specify that testing and monitoring of Yucca Mountain would continue during licensing and, if the site is licensed, throughout construction, operation, and after permanent closure of the repository.

1.1 PURPOSE AND SCOPE

If the DOE decides to recommend the development of the Yucca Mountain site to the President, it is required by the NWPA to provide a comprehensive statement of the basis for the recommendation. This report is one part of a comprehensive suite of analyses and documents that the DOE is considering with respect to the possible recommendation. It describes the results of scientific and technical studies that have been performed to determine whether the Yucca Mountain site should be recommended for development as a geologic repository. It contains information that would be included in any site recommendation from the Secretary to the President, consistent with Sections 114(a)(1)(A), (B), and (C) of the NWPA (42 U.S.C. 10134(a)(1)(A), (B), and (C)). Section 1 introduces the report and provides background information on both the Yucca Mountain site and the site recommendation decision process set forth in the NWPA. Section 2 describes a preliminary design for a potential repository at Yucca Mountain, and Section 3 describes the proposed waste package designs and the waste forms to be disposed. Section 4 discusses data related to the safety of the Yucca Mountain site and describes how natural and engineered repository systems would work together to protect public health and limit the release of radionuclides to the environment. It explains the relationship between the waste form, the waste package, and the geologic medium at Yucca Mountain. It also describes analyses of the future long-term performance of a repository at Yucca Mountain. Section 5 describes analyses that

evaluate the safety of the potential repository during operation and before final closure.

The DOE has actively sought public involvement and participation in the consideration of the Yucca Mountain site. In May 2001, the DOE released an initial version of this report (DOE 2001a) to facilitate public comments on the consideration of the possible recommendation of Yucca Mountain. It was based on the technical information, and the draft regulations, available at the time of its preparation. Comments regarding the possible recommendation of the site were solicited during initial and supplemental public comment periods announced in the Federal Register, and at numerous public hearings conducted throughout the State of Nevada. Since the beginning of the public comment period, the EPA, NRC, and DOE have also released final versions of regulations relevant to Yucca Mountain. Therefore, this report has been updated to:

1. Identify and incorporate analyses consistent with final regulations, as necessary

2. Reflect public comments received by the DOE

3. Identify and consider the results of supplemental scientific and engineering analyses that have been completed by the DOE and its contractor since May 2001.

This *Yucca Mountain Science and Engineering Report* is based on an extensive foundation of scientific, engineering, regulatory, and programmatic research that analyzed the Yucca Mountain site, the potential repository and waste package designs, and other information. This report is supported by a comprehensive set of scientific and technical integrating documents that explain in detail the basis for the results presented. The major integrating documents include:

- *Total System Performance Assessment for the Site Recommendation* (CRWMS M&O 2000a). This document describes in detail the results of the quantitative analysis of the long-term performance of a potential repository at Yucca Mountain.

- *Yucca Mountain Site Description* (CRWMS M&O 2000b). This document contains a thorough description of the natural system at Yucca Mountain, including the geology and hydrology, on both a regional and a site-specific scale.

- *Monitored Geologic Repository Project Description Document* (Curry 2001). This report presents a summary of the design and operational concepts for the potential Yucca Mountain repository, including facilities at the surface for receiving, handling, and packaging waste; facilities underground for waste disposal; and engineered barriers that would contribute to the ability of the repository system to safely isolate waste.

Key technical references include nine process model reports that describe how the natural and engineered systems at a potential repository would perform. In addition, hundreds of reports summarizing scientific and engineering studies on a wide variety of topics have been prepared, including:

- Analysis and model reports describing the detailed scientific models of how the potential repository might behave in the future

- Scientific reports of the results of site characterization investigations, regional studies, and studies of natural analogues that are used to help understand the behavior of a potential repository

- Descriptions of performance objectives, design requirements, design analyses (over a range of thermal operating modes), and design alternative studies for the repository surface and subsurface facilities, engineered barrier systems, and waste packages.

Several supplemental analyses relevant to the site recommendation have been released for public comment since May 2001. These supplemental analyses include:

- *FY01 Supplemental Science and Performance Analyses* (BSC 2001a; BSC 2001b). Volume 1 of this report (BSC 2001a)

describes (1) supplemental analyses performed to quantify uncertainties, (2) updated process models based on recent scientific information, and (3) analyses of the effects of a lower-temperature repository operating mode on process model results. Volume 2 of this report (BSC 2001b) documents revised performance analyses based on a supplemental TSPA model, incorporating information from Volume 1.

- *Total System Performance Assessment— Analyses for Disposal of Commercial and DOE Waste Inventories at Yucca Mountain— Input to Final Environmental Impact Statement and Site Suitability Evaluation* (Williams 2001a). This report documents revised TSPA results based on a supplemental TSPA model revised to conform to final 40 CFR Part 197.

- *Total System Performance Assessment Sensitivity Analyses for Final Nuclear Regulatory Commission Regulations* (Williams 2001b). This report documents additional TSPA sensitivity analyses to address final 10 CFR Part 63 (66 FR 55732) provisions. These analyses are also discussed in the site suitability evaluation.

- *Technical Update Impact Letter Report* (BSC 2001c). This report reviews additional technical information collected since the models and analyses described in this report and *FY01 Supplemental Science and Performance Analyses* (BSC 2001a; BSC 2001b) were completed. The report also includes an assessment of the impact of the new information on the TSPA analyses.

1.2   BACKGROUND INFORMATION

This section briefly describes the materials planned for disposal at Yucca Mountain. It also summarizes the evolution of and the rationale for the U.S. nuclear waste disposal program.

All of the waste forms that would be transported to and received at the potential repository would be solid materials that would be stable in a deep, dry

geologic repository. These waste forms fall into two categories: spent nuclear fuel and high-level radioactive waste. Some elements of this waste decay in only a few years; others are radioactive for hundreds of thousands of years (see Section 4.4.1.4). This waste must be safely contained and isolated to protect human health and the environment.

1.2.1 Sources of Materials Considered for Disposal

Commercial nuclear power plants, which supply about 20 percent of the nation's electricity, produce spent nuclear fuel. The DOE manages several facilities that manufactured materials for nuclear weapons and, in doing so, produced spent nuclear fuel and high-level radioactive waste. The DOE also operates research reactors that produce spent nuclear fuel and has operated reprocessing facilities that produce high-level radioactive waste. Most of the waste from reprocessing was generated before 1982. Small quantities of high-level radioactive waste are produced in medical research that uses nuclear materials. In addition, the DOE owns small quantities of spent nuclear fuel from research reactors in foreign countries. This spent nuclear fuel will be returned to the U.S. for disposal to support nonproliferation goals.

The total inventory of spent nuclear fuel and high-level radioactive waste in the U.S. could eventually exceed 100,000 MTHM or MTU, depending on the number of reactors that receive operating license extensions. MTHM and MTU are approximately equivalent terms for the once-through nuclear fuel cycle and can be used interchangeably for most of the material to be emplaced in the repository. The first repository is limited by the NWPA to 70,000 MTHM until a second repository is in operation. Section 3 of this report and Appendix A of the draft environmental impact statement (EIS) (DOE 1999a) describe the materials planned for disposal in a repository. The repository design summarized in Section 2 and analyzed in Section 4 is based on an inventory allocation that includes 63,000 MTHM of commercial spent nuclear fuel; 2,333 MTHM of DOE spent nuclear fuel; and 4,667 MTHM of DOE high-level radioactive waste.

1.2.1.1 Commercial Spent Nuclear Fuel

As of December 1999, the U.S. had accumulated about 40,000 MTHM of spent nuclear fuel from commercial nuclear power plants (CRWMS M&O 1999a, Tables B-11 and B-12) This amount could more than double by 2035 if all currently operating plants complete their initial 40-year license period. Commercial spent nuclear fuel makes up most of the spent nuclear fuel that requires disposal. Spent nuclear fuel contains uranium-235 and uranium-238, relatively short-lived fission products such as strontium-90 and cesium-137, and relatively long-lived transuranic isotopes (i.e., isotopes with atomic numbers greater than 92) such as pluto-nium-239 and americium-243. Commercial spent nuclear fuel is now stored at 72 commercial nuclear sites in 33 states, where it will remain until a permanent repository, or an NRC-licensed storage facility, is in operation. These sites can only be decommissioned and used for other purposes after the spent nuclear fuel and other radioactive materials have been removed.

1.2.1.2 U.S. Department of Energy Spent Nuclear Fuel

By 2035, the U.S. will have accumulated about 2,500 MTHM of spent nuclear fuel from reactors that produced materials for the nation's nuclear weapons program, from research reactors, from reactors on nuclear-powered naval vessels, and from reactor prototypes. These materials include commercial spent nuclear fuel that has been trans-ferred to the DOE for research, project demonstration, or other purposes. An example is the core debris from the Three Mile Island-2 reactor. All of this spent nuclear fuel is the respon-sibility of the DOE. The majority is currently stored at sites in Idaho, South Carolina, and Wash-ington (DOE 1999a, Appendix A, Tables A-16 and A-17). Under a negotiated agreement that involved the State of Idaho, the U.S. Navy, and the DOE, the DOE must remove all spent nuclear fuel from Idaho by the year 2035 (*Public Service Co. of Colorado v. Batt*, settlement agreement).

In addition to the sites already mentioned, about 55 other facilities have small quantities of spent nuclear fuel and high-level radioactive waste.

These sites include research reactors at universities, commercial research reactors, DOE laboratories, and commercial fuel fabrication plants. In most cases, DOE spent nuclear fuel and/or DOE waste stored at these facilities will be shipped to one of the larger DOE sites for drying, packaging or other treatment, and storage prior to transport to the repository for disposal.

1.2.1.3 High-Level Radioactive Waste

Large volumes of high-level radioactive waste were created in the past when spent nuclear fuel was treated chemically (i.e., reprocessed) to separate uranium or plutonium isotopes that could be reused from the other elements in the fuel. The high-level radioactive waste left over from this process exists in both liquid and solid form; liquid wastes are stored in underground tanks at DOE sites near Hanford, Washington; Savannah River, South Carolina; Idaho Falls, Idaho; and West Valley, New York (DOE 1997a, p. 34). Liquid high-level radioactive waste will be vitrified (turned into glass) prior to shipment for disposal. In this process, the waste materials are mixed with other components of glass, melted, and poured into stainless steel canisters. The vitrified waste, typically in a form known as borosilicate glass, is leach-resistant and long-lived. Where there are agreements between the DOE and the states where the waste is stored, this high-level radioactive waste will be solidified and placed in about 22,000 canisters for future disposal in any permanent geologic repository for the disposal of high-level radioactive waste (DOE 1997b, Section 1.5.4). No liquid wastes will be received at or disposed in a geologic repository.

1.2.1.4 Surplus Plutonium

The end of the Cold War has reduced the need for nuclear materials for weapons, which has resulted in the closure and cleanup of several weapons plants and the identification of a nominal 50 metric tons of surplus plutonium. The surplus plutonium associated with weapons production are no longer needed and must be safely disposed. Current plans call for some of the surplus plutonium, up to 33 metric tons, to be combined with uranium-238 to form a mixed-oxide fuel that would be used in commercial reactors, with later disposal of the commercial spent nuclear fuel at the potential Yucca Mountain repository. Up to approximately 17 metric tons would be immobilized in ceramic, placed inside stainless steel cans, and placed in canisters. These canisters will be filled with molten high-level radioactive waste glass, which will vitrify into a glass waste form around the stainless steel cans, as described above.

1.2.1.5 Present Location of Spent Nuclear Fuel and High-Level Radioactive Waste

Spent nuclear fuel and high-level radioactive waste are presently stored in 39 states, as shown in Figure 1-2. During repository operations, waste would be consolidated for transport to the repository from 77 storage sites (72 commercial and 5 DOE [DOE 1999a, Section 1]). These storage sites are located in a mixture of urban, suburban, and rural environments.

1.2.2 U.S. Policy: The Rationale for Geologic Disposal

U.S. policy on nuclear waste management has been developed by Congress through legislation and implemented by a succession of agencies, beginning immediately after World War II. The Atomic Energy Act of 1954 (42 U.S.C. 2011 et seq.) placed management of all aspects of the nation's nuclear programs under the jurisdiction of the AEC. Although the AEC initially focused on military applications, Congress soon realized it needed a broader mandate. Congress assigned the AEC major roles, which included continuing the nuclear weapons program, promoting the private use of atomic energy for peaceful applications, and protecting public health and safety from the hazards of nuclear power (Walker 2000).

The AEC recognized that the nation needed a long-term strategy for managing and disposing of radioactive waste. On February 28, 1955, it reached an agreement with the National Academy of Sciences/National Research Council to establish a committee of leading scientists to evaluate methods of disposal and report their findings. The committee was also asked to recommend areas
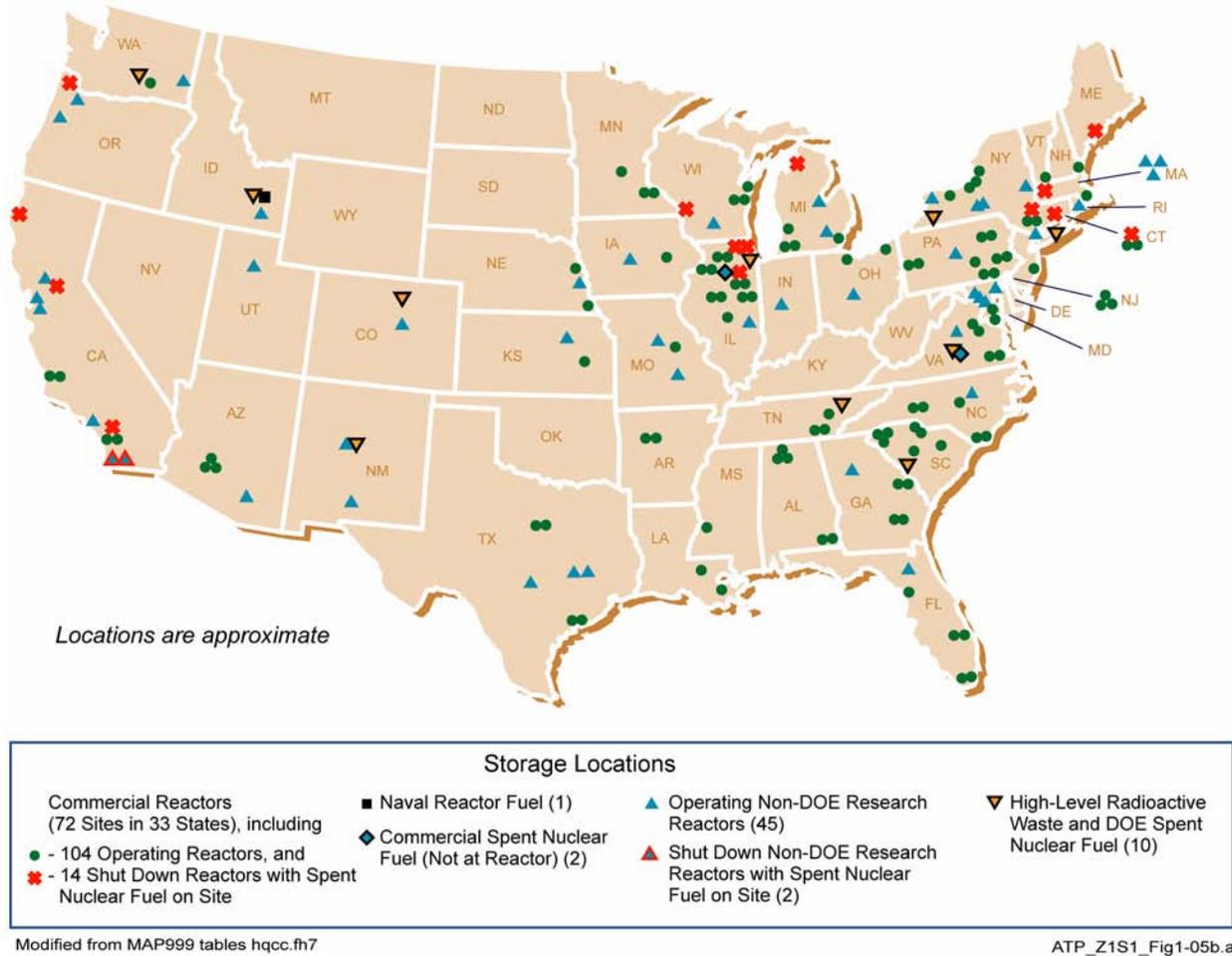
Figure 1-2.   Map Showing Locations of Spent Nuclear Fuel and High-Level Radioactive Waste Destined for Geologic Disposal
Commercial waste may include West Valley vitrified waste if an agreement is reached between the DOE and the state of New York for the disposal of this waste. Source: Modified from DOE 1999a, Figure 1-1.

where research was needed (National Academy of Sciences Committee on Waste Disposal 1957, p. 8).

The hazards posed by radioactive waste decline over time because of radioactive decay. Some radionuclides decay quickly and do not present a significant risk after a few decades, whereas others remain radioactive for thousands of years. Therefore, early studies of disposal options sought the most effective way to isolate waste long enough for the hazard to decline to levels that do not pose a significant risk to public health or the environment. The search led to geologic environments that have remained stable and are likely to remain so in the future.

The committee evaluated a wide range of options and reached several conclusions and recommendations (National Academy of Sciences Committee on Waste Disposal 1957). One important conclusion was that a safe disposal facility for radioactive waste could be constructed at many sites in the U.S. However, the committee warned that many areas do not contain any likely disposal sites. The committee specifically noted that favorable conditions for disposal were not found along the Atlantic seaboard.

The committee examined the best means for disposing of the liquid high-level radioactive waste that was already accumulating at sites in Hanford, Washington, and Savannah River, South Carolina.

The scientists explored a variety of options and concluded that storage in tanks was, at the time, the safest short-term method (National Academy of Sciences Committee on Waste Disposal 1957, p. 6). However, tank storage of large volumes of liquid waste was not viewed as a permanent solution; deep disposal in cavities mined in salt deposits was suggested as the most promising possibility for a long-term solution.

The committee noted that disposal would be much simpler if liquid waste could be converted to a solid form of "relatively insoluble character" (National Academy of Sciences Committee on Waste Disposal 1957, p. 1). A variety of options were considered feasible for disposal of solid wastes, including salt or dry mines or excavations in other geologic environments. The committee cautioned that the deep geologic disposal of waste would be a "special problem for each particular installation" (National Academy of Sciences Committee on Waste Disposal 1957, p. 77), and that "the education of a considerable number of geologists and hydrologists … is going to be necessary" (National Academy of Sciences Committee on Waste Disposal 1957, p. 7).

Between 1957 and the early 1970s, the need to find a safe method for waste disposal grew more urgent as the commercial nuclear utility industry expanded dramatically. However, little progress was made on a long-term solution. In 1970, the AEC tentatively selected a site for a repository in salt deposits near Lyons, Kansas. Under considerable political and technical fire, the Lyons site was abandoned two years later because of concern that nearby salt mine drilling had compromised the integrity of the geologic formation (The League of Women Voters 1993, p. 49).

As the commercial nuclear utility industry continued to grow in the 1960s, the AEC was increasingly criticized because of the conflict between its roles of promoting peaceful uses of atomic energy and regulating the industry to protect public health and safety. Congress passed the Energy Reorganization Act in 1974 (42 U.S.C. 5801 et seq.), which divided the AEC into the ERDA and NRC. The NRC was assigned the regulatory role, with the responsibility to protect public health and safety, both for reactor operations and for the management and disposal of spent nuclear fuel and high-level radioactive waste.

The energy crisis of the 1970s prompted Congress to pass the Department of Energy Organization Act in 1977 (42 U.S.C. 7101 et seq.), which combined the ERDA with other energy-related agencies to form the DOE. The act assigned to the DOE the responsibility for managing the nation's nuclear weapons programs and for managing the program for disposing the nation's nuclear waste. Since the middle of the 1980s, the environmental cleanup of the nuclear weapons complex has been a major focus of DOE efforts nationwide.

After Congress created the DOE, waste management activities accelerated. The DOE initiated the National Waste Terminal Storage Program in 1977 to identify suitable sites and develop the technology to license, construct, operate, and close a repository. Site screening focused on areas with salt deposits and federal lands where radioactive materials were already present, specifically Hanford, Washington, and the Nevada Test Site. The Carter administration initiated an Interagency Review Group in 1978 to review national nuclear waste policy. The group recommended that the U.S. proceed with geologic disposal and proposed that the DOE study geologic settings other than salt deposits. The DOE decided to proceed with a strategy that relied on mined geologic disposal in 1980, as documented in *Final Environmental Impact Statement Management of Commercially Generated Radioactive Waste* (DOE 1980). The report evaluated many options, including disposal in deep boreholes, ice sheets, subseabeds, and space. Geologic disposal in different host rocks was also evaluated. The DOE's decision to move forward with geologic disposal was consistent with the original recommendation of the committee formed by the National Academy of Sciences/ National Research Council and was later affirmed by numerous other evaluations, both in the U.S. and abroad. In a 1984 rulemaking known as the Waste Confidence Decision (49 FR 34658), the NRC found that mined geologic disposal was feasible and that spent nuclear fuel and high-level radioactive waste could be safely managed in a geologic repository. The NRC revisited the deci-

sion in 1990 (55 FR 38474) and again in 1999 (64 FR 68005), with similar conclusions.

Congress enacted the NWPA in 1982 (it became law on January 7, 1983), which established a comprehensive policy for the disposal of the nation's commercial spent nuclear fuel and high-level radioactive waste. The NWPA directed the DOE to develop guidelines for site characterization. The Secretary considered various geologic media in which repositories could be located, including salt, volcanic rock (such as basalt and tuff), and crystalline rock (such as granite). The site selection process developed by the DOE is described in 10 CFR Part 960 (Energy: General Guidelines for the Recommendation of Sites for Nuclear Waste Repositories). In 1983, the DOE selected nine locations in six states to study as potential repository sites and performed preliminary environmental assessments of each. In 1986, the DOE published the results of these assessments, which documented the selection of five candidate sites from the original nine (DOE 1986a). The Secretary then recommended to the President that site characterization programs be undertaken at three sites: Yucca Mountain, Nevada; Hanford, Washington; and Deaf Smith County, Texas (DOE 1986b).

The DOE began developing site characterization plans for each site and was preparing to begin site studies when Congress amended the NWPA in 1987. Concerned with rising cost projections for the simultaneous characterization of three sites, Congress directed the DOE to study only Yucca Mountain, to determine whether it was suitable for a repository, and to discontinue repository-related activities at the other sites and the work on the second repository program unless there is Congressional authorization.

The concept of disposing of waste in the desert regions of the Southwest was first proposed by the USGS in the 1970s. In 1976, the director of the USGS identified a number of positive attributes in and around the Nevada Test Site that would make positive contributions to geologic disposal, including multiple natural barriers, remoteness, and an arid climate (McKelvey 1976). In 1981, a USGS scientist documented that water tables in the

desert Southwest are among the deepest in the world, and the geologic setting includes multiple natural barriers that could isolate waste for "tens of thousands to perhaps hundreds of thousands of years" (Winograd 1981). In contrast to the strategy for isolating waste in salt or deep sites below the water table, waste could be disposed near the Nevada Test Site at relatively shallow depths, well above the water table. Following the initial USGS recommendation, the DOE sponsored investigations of the feasibility of disposal above the water table. Formal site characterization at Yucca Mountain began in 1986 and continues today.

Recent experience in the U.S. has demonstrated that it is feasible to site and construct a repository for radioactive waste. In 1975, the ERDA selected a site in salt deposits near Carlsbad, New Mexico, to develop the Waste Isolation Pilot Plant for the disposal of transuranic waste. Transuranic waste contains radionuclides that are heavier than uranium; it emits less radiation and generates less heat than spent nuclear fuel. It is a by-product of the reprocessing of spent nuclear fuel and the use of plutonium in manufacturing nuclear weapons. Like high-level radioactive waste, transuranic waste remains hazardous for centuries and requires long-term isolation. In 1998, after more than 20 years of study, design, and analysis, the Waste Isolation Pilot Plant received the required permits from the EPA to receive and dispose transuranic waste. The plant opened in 1999 and has begun receiving waste from several DOE sites.

With the end of the Cold War, many nuclear weapons have been disassembled and removed from the nation's stockpile, which has resulted in the accumulation of surplus nuclear materials. A repository is part of the strategy for managing and disposing these materials.

Since the first scientific study in 1957, professional organizations that have looked at the nuclear waste problem have agreed that a geologic repository is the best approach for disposal. Scientists have widely agreed that waste encased in robust, long-lived waste packages and placed deep in stable geologic environments could be isolated from the biosphere for the long time periods necessary. As stated in a 1990 report from the National Academy

of Sciences, there is "a worldwide scientific consensus that deep geological disposal, the approach being followed by the U.S., is the best option for disposing of high-level radioactive waste" (National Research Council 1990, p. vii). An international group of scientists issued a similar opinion in 1995 that affirmed the consensus for geologic disposal in a document entitled *The Environmental and Ethical Basis of Geological Disposal of Long-Lived Radioactive Wastes: A Collective Opinion of the Radioactive Waste Management Committee of the OECD Nuclear Energy Agency* (NEA 1995).

The DOE published *Viability Assessment of a Repository at Yucca Mountain* (DOE 1998) in December 1998. This assessment summarized the results of site characterization, described preliminary repository and waste package designs, and presented the DOE analysis of the future performance of a potential repository located at Yucca Mountain. It concluded that Yucca Mountain remained a promising site for development as a repository. The Viability Assessment also described a program of studies to address remaining uncertainties before the Secretary would decide whether to recommend the site.

Although there is a general scientific consensus in favor of geologic disposal, views differ on when to dispose of the waste and whether to dispose of it permanently. Many believe that the recoverable uranium-235 and other fissionable isotopes in spent nuclear fuel could be a future energy resource and should not be irreversibly disposed until their potential economic value is certain. Reprocessing spent nuclear fuel to reclaim the unused material is technically feasible but currently uneconomical in the U.S. Also, U.S. policy is to not encourage the civilian use of plutonium. Accordingly, the U.S. does not engage in plutonium reprocessing. Although reprocessing would reduce the amount of radioactive waste that requires disposal, it would not eliminate the need for disposal because reprocessing would generate additional waste materials that must be treated and disposed.

Some experts advocate alternative technologies that might make geologic disposal easier. For example, accelerator transmutation of waste—bombarding waste with nuclear particles to convert it into material that is less radioactive or shorter-lived—has been proposed as an alternative waste management strategy. A National Research Council study found that transmutation is "technically feasible," but as a method to treat spent nuclear fuel it "would require many tens to hundreds of billions of dollars and require several decades to implement" (National Research Council 1996a, p. 81). Although transmutation would reduce the total radionuclide inventory to be disposed, disposal of large quantities of high-level radioactive waste would still be necessary.

It has been suggested that a monitored retrievable storage facility, constructed at Yucca Mountain or elsewhere, would be preferable to geologic disposal at present. Although a monitored facility could safely isolate wastes for as long as it was properly maintained, this strategy has several disadvantages compared to a repository. It would not close the fuel cycle, and geologic disposal would still be required eventually. If the monitored facility were constructed at a location other than the same location as a repository, waste forms would have to be transported twice before final disposal, increasing the risk to workers and the public. Total program costs would be increased because of the need to construct, operate, and maintain two facilities.

One way to accommodate these different views and still provide a permanent solution is to dispose waste in a manner that permits, but does not require, its retrieval. The NWPA (42 U.S.C. 10101 et seq.) requires that the DOE design a repository so that waste can be retrieved for any reason. NRC licensing regulations require that the DOE design a repository so that waste can be retrieved on a reasonable schedule starting at any time up to 50 years after waste emplacement begins, unless a different period is approved or specified by the NRC (10 CFR 63.111(e) [66 FR 55732]).

Future generations would decide whether to keep the repository open and monitored or close it. To ensure that future decision-makers have some flexibility, the DOE will design the potential repository

so it can be closed as early as 50 years or as late as 300 years after emplacement starts.

1.3 DESCRIPTION OF THE SITE CHARACTERIZATION PROGRAM AND THE YUCCA MOUNTAIN SITE

In 1986, the DOE began a formal program of site characterization, as required by Section 113 of the NWPA (42 U.S.C. 10133). This program is described in *Site Characterization Plan Yucca Mountain Site, Nevada Research and Development Area, Nevada* (DOE 1988). The plan established a comprehensive set of studies to gather the information needed to evaluate the suitability of the site against EPA, NRC, and DOE regulations in effect at the time. After releasing the plan in draft form in January 1988 for review by the NRC, the State of Nevada, Congress, and other interested parties, the DOE issued the final plan in December 1988. Progress reports (e.g., DOE 1999b) describing ongoing site characterization activities and plans are issued semiannually.

This report draws on numerous references that describe the investigations and results of the site characterization program in detail. *Yucca Mountain Site Description* (CRWMS M&O 2000b) is the most comprehensive.

1.3.1 Site Characterization Investigations

The site characterization program has performed extensive surface-based tests and investigations, underground tests, laboratory studies, and modeling activities designed to provide the technical basis for an evaluation of repository performance. Figure 1-3 shows the location of the surface-based and underground test facilities at Yucca Mountain, including boreholes and underground excavations. The single largest effort of the site characterization program was the Exploratory Studies Facility, which provided access to the subsurface environment for exploration and testing along the entire north–south extent and at the proposed depth of the potential repository. Work on the Exploratory Studies Facility started in late 1992, and excavation with a tunnel boring machine began in September 1994 (Figure 1-4). The 8-km (5-mi) underground tunnel that is the main part of

the Exploratory Studies Facility was completed in April 1997. A drift across the entire planned width of the potential repository, the Enhanced Characterization of the Repository Block (ECRB) Cross-Drift, was completed in October 1998. Additional subsurface niches and alcoves have been excavated to support specific tests.

The suite of site characterization testing and analysis includes the following components:

- Surface-based mapping, sampling, and testing of geologic and hydrologic features and properties

- Surface-based and borehole geophysical testing at both regional and site-specific scales

- Geologic, hydrologic, and geochemical sampling and testing in the Exploratory Studies Facility and the ECRB Cross-Drift

- Studies of hydrologic processes and investigations of coupled thermal-hydrologic-geochemical-mechanical processes in the Exploratory Studies Facility and the ECRB Cross-Drift

- Characterization of geologic and hydrologic properties from borehole studies and long-term borehole monitoring of hydrologic properties

- Surface-based, borehole, and Exploratory Studies Facility studies of hydrologic and geologic properties of faults and fractures, as well as their distribution

- Hydrologic testing in the Calico Hills hydrogeologic unit at the Busted Butte test facility

- Regional geologic studies and trenching for seismic and volcanic hazard studies

- Meteorological monitoring and modeling

- Surface environmental studies, including biological and ecological investigations

Figure 1-3.   Site Investigation Area Showing Location of the Surface-Based and Underground Test Facilities at Yucca Mountain, Including Boreholes and Underground Excavations

Additional investigation locations, including the Nye County Early Warning Program wells, are not shown because they are located outside the boundaries of the area depicted.

ATP_Z1S1_Fig.1-07.cdr

Figure 1-4.   Photograph Showing the Tunnel Boring Machine Operating at Yucca Mountain
Work on the Exploratory Studies Facility started in late 1992, tunnel boring machine operations commenced in September 1994, and the Exploratory Studies Facility ramps and main drift were completed in the spring of 1997.

- Geotechnical investigations, including in situ and laboratory testing of soil properties

- Seismic monitoring and seismic hazard studies to address the potential for, and characteristics of, earthquakes that could affect the potential repository

- Laboratory geochemical tests and analyses of the transport characteristics of water and rocks under ambient and potential repository conditions

- Laboratory chemical tests and analyses of the dissolution properties of waste materials under ambient and potential repository conditions

- Laboratory physical tests of the mechanical properties and behavior of rocks under potential repository conditions

- Laboratory testing of materials planned for use in the repository under potential repository conditions

- Development of conceptual and numerical models, and verification and validation of hydrologic, transport, and coupled process models

- Performance assessment modeling of repository behavior

- Analogue studies of hydrologic and geologic processes.

The results of site investigations have been reported regularly since 1990 in semiannual progress reports (e.g., DOE 1999b). The progress reports also demonstrate the evolution of the scientific and engineering program from the *Site Characterization Plan Yucca Mountain Site, Nevada Research and Development Area, Nevada* (DOE 1988). The technical program has evolved in response to advancements in scientific understanding and proposed changes in regulatory and program requirements, such as the design of the repository. These changes are summarized in appendices to the 1997 and 1998 progress reports (e.g., DOE 1997c), and have been documented in a separate report since 1998 (e.g., CRWMS M&O 1999b). For example, EPA regulations in place in 1988 would have required the DOE to assess compliance with the radiation protection standards at a point 5 km (3 mi) from the repository boundary. Currently, NRC and EPA regulations would require the DOE to assess potential doses to humans from the transport of radionuclides at the accessible environment specified by 40 CFR Part 197 and 10 CFR Part 63 (66 FR 55732). This regulatory change created a need to understand the hydrologic flow and transport characteristics of the region between 5 km (3 mi) and the accessible environment (approximately 18 km [11 mi] south of the potential repository) from Yucca Mountain. The DOE has addressed this need by supporting and incorporating the results of the Nye County Early Warning Drilling Program and other information into the analyses and models used to assess the performance of the potential repository.

The program has also changed because of information learned during site characterization. One example is the seepage tests in the Exploratory Studies Facility that were added to evaluate how much water flow is likely to be diverted around underground openings.

Scientific and engineering activities are documented in the key technical references supporting this report, which include nine process model reports describing the DOE's understanding of the current and future behavior of a potential repository. These reports address the following topics:

- Integrated site model
- Unsaturated zone flow and transport
- Near-field environment
- Biosphere
- Waste package degradation
- Waste form degradation
- Engineered barrier system degradation, flow and transport
- Saturated zone flow and transport
- Disruptive events (volcanic/seismic hazards).

1.3.2   Description of the Yucca Mountain Site

This section provides an overview of the location, geography, current population, and key geologic characteristics of the Yucca Mountain site. This description is provided as background information for Sections 2 and 3, which present a description of the proposed repository design (including information related to repository performance over a range of operating mode temperatures) and descriptions of the waste forms and waste packages. This section also provides a framework for the descriptions of hydrologic, geochemical, thermal, and other processes related to the performance of the potential repository contained in Sections 4.2, 4.3, and 4.4.

Yucca Mountain is located on federal land in a remote area of Nye County in southern Nevada, approximately 160 km (100 mi) northwest of Las Vegas (Figure 1-5). If the site is recommended for repository development, sufficient land may be withdrawn to consolidate the control of the facilities and land needed to operate the repository. The draft EIS describes the potential withdrawal area (DOE 1999a, Section 3.1.1.3).

1.3.2.1   Geography, Land Use, and Population

Yucca Mountain consists of a series of ridges extending approximately 40 km (25 mi) from Timber Mountain in the north to the Amargosa Desert in the south. The elevation at the crest of the
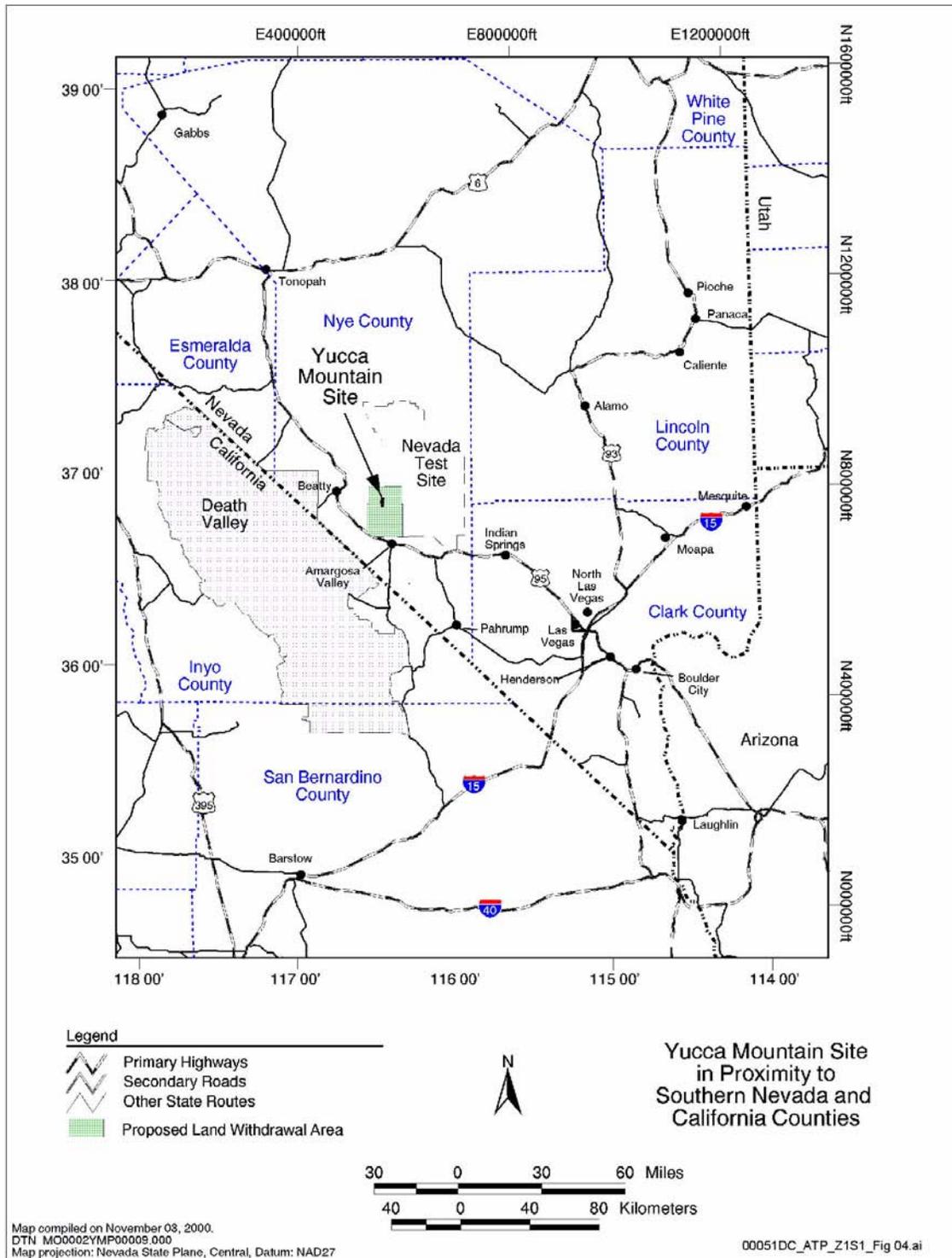
Figure 1-5.   Map Showing the Location of Yucca Mountain in Relation to Major Highways; Surrounding Counties, Cities, and Towns in Nevada and California; the Nevada Test Site; and Death Valley National Park

Yucca Mountain is located on federal land in Nye County in southern Nevada, approximately 160 km (100 mi) northwest of Las Vegas.

ridges varies from approximately 1,800 m (5,900 ft) to 900 m (3,000 ft) above sea level. At the potential repository site, the crest of Yucca Mountain is 1,400 to 1,500 m (4,600 to 4,900 ft) above sea level. The western part of the potential repository site is a steep slope that rises approximately 300 m (1,000 ft) above the base of Solitario Canyon. On the eastern side, the mountain slopes gently to the east and is incised by a series of east- to southeast-trending stream channels. The elevation at the base of the eastern slope is approximately 350 to 450 m (1,100 to 1,500 ft) below the ridge crest.

The site is in Nye County, which is bordered by Clark, Lincoln, White Pine, Eureka, Lander, Churchill, Mineral, and Esmeralda counties in Nevada and Inyo County in California. The federal government controls nearly all of the land in the region. The area needed for the potential repository encompasses land controlled by three federal agencies: the U.S. Air Force (Nellis Air Force Range), the DOE (Nevada Test Site), and the U.S. Bureau of Land Management (Figure 1-6). Except for a few scattered facilities constructed on the Nevada Test Site to support former U.S. nuclear propulsion and defense programs, there has been no development at the site. The land around Yucca Mountain will remain federally owned and, should the site be recommended, will be withdrawn from public use.

The tracts of private land nearest to Yucca Mountain are to the south, in the Amargosa Desert. The closest year-round housing is at the intersection of U.S. Highway 95 and Nevada State Route 373, approximately 22 km (14 mi) south of the site. Active agricultural operations can be found approximately 30 km (19 mi) south of Yucca Mountain, in Amargosa Valley. There is one patented mining claim about 16 km (10 mi) south of the potential repository site. Scattered private lands are also present near the town of Beatty, 24 to 32 km (15 to 20 mi) west of the site.

Because groundwater in the Yucca Mountain region flows toward the south, the potential for future exposure to radionuclides would be highest for populations living south of the site. EPA and NRC regulations (40 CFR 197.21(b) and 10 CFR 63.312 [66 FR 55732], respectively) for Yucca Mountain would direct the DOE to assume that the receptor is a person, known as the reasonably maximally exposed individual, with a diet and living style similar to the current residents of the Town of Amargosa Valley.

The population density near Yucca Mountain is very low (CRWMS M&O 2000b, Section 2.3). There are no permanent residents within 22 km (14 mi), and Nye County as a whole averages only 0.6 persons per square kilometer (1.5 persons per square mile). Of the total population of 29,730 in Nye County, 68 percent live in the unincorporated town of Pahrump, 70 to 80 km (43 to 50 mi) southsoutheast of Yucca Mountain. The major economic activities in the towns of Amargosa Valley and Beatty include agricultural and mining operations. Most of the other counties surrounding Yucca Mountain, including Lincoln and Esmeralda counties in Nevada and Inyo County in California, also have low population densities. The nearest large populations reside in Clark County, approximately 130 km (80 mi) southeast of Yucca Mountain.

1.3.2.2   Geology

The Yucca Mountain site is located on the western boundary of the Nevada Test Site, where scientists have conducted geologic investigations since the 1950s. Studies related to nuclear waste disposal have focused on Yucca Mountain since the late 1970s and have included careful mapping of the rocks at the surface and in more than 10 km (6 mi) of tunnels below Yucca Mountain, along with the drilling and logging of numerous wells and boreholes. The characterization of the geology of Yucca Mountain provides a framework for understanding the future behavior of the potential repository. Section 4 describes data and analyses related to postclosure safety, including a discussion of processes such as water flow and thermal effects and how they would affect both the natural and engineered parts of the repository system. The following overview of the geology of the site describes the physical environment of the repository. It is based on the comprehensive description contained in *Yucca Mountain Site Description* (CRWMS M&O 2000b).
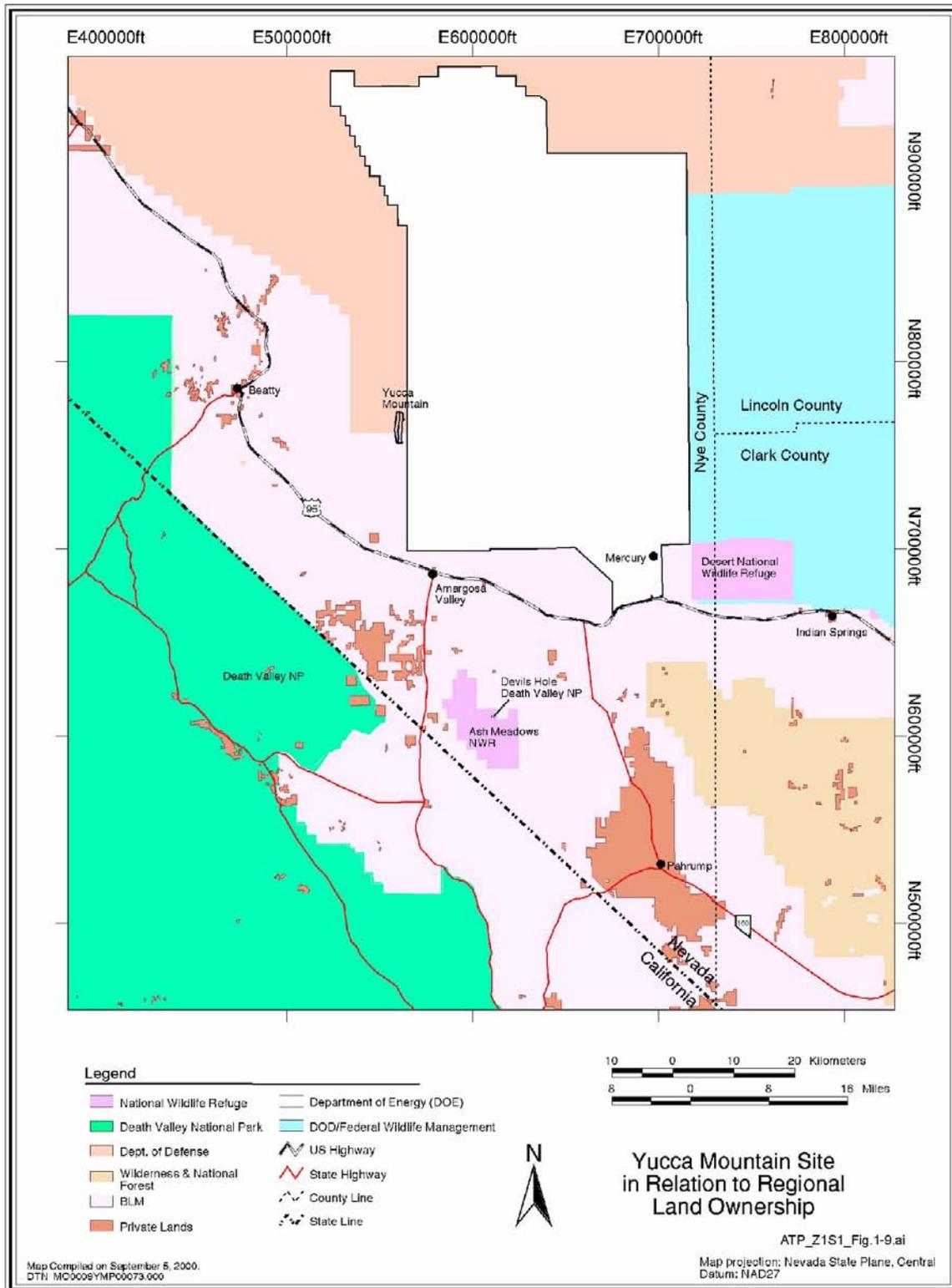
Figure 1-6.   Map Showing the Location of Yucca Mountain and Land Status in the Region
The potential repository straddles land controlled by three federal agencies: the U.S. Air Force (Nellis Air Force Range), the DOE (Nevada Test Site), and the U.S. Bureau of Land Management (BLM).

1.3.2.2.1   Regional Geology

As shown in Figure 1-7, Yucca Mountain is located in the Basin and Range province of the western U.S., within the region known as the Great Basin. The Great Basin encompasses nearly all of Nevada and parts of Utah, Idaho, Oregon, and California. The Basin and Range, which extends into northern Mexico, draws its name from its characteristic, generally north–south aligned mountain ranges. These ranges are separated by basins containing thick deposits of sediment (mostly sand and gravel) derived from erosion of the adjacent ranges over millions of years. The structure of the Basin and Range has developed over a period of more than 30 million years. In the region of southern Nevada that includes Yucca Mountain, the pattern of mountains and valleys has formed over the past 15 million years from faults moving on one or both sides of the ranges (Fridrich 1999). The tilted, fault-bounded mountain ranges may extend more than 80 km (50 mi) in length and are generally 8 to 24 km (5 to 15 mi) wide. Relief between valley floors and mountain ridges is typically 300 to 1,500 m (1,000 to 5,000 ft), and valleys occupy between 50 and 60 percent of the total land area.

Most modern tectonic activity (i.e., active faulting and volcanism) in the southwestern Great Basin occurs to the south, west, and northwest of Yucca Mountain. Among the most active areas in the region are the Furnace Creek–Death Valley fault zone, the Sierra Nevada front (i.e., the Owens Valley and Mammoth Lakes area), and the area north of the Garlock fault in the Mojave Desert. This domain includes modern basins and ranges with great structural relief, such as the Death Valley basin and the Panamint Range. The modern faulting and volcanic activity is caused by the continuation of the same tectonic extension that resulted in the formation of the entire Basin and Range. The crust on the western edge of the Great Basin (the Sierra Nevada) is gradually moving to the west relative to the eastern edge of the basin (the Wasatch Front in Utah).

Regional Stratigraphy—Rocks and sedimentary deposits exposed in the region surrounding Yucca Mountain range in age from geologically old (Precambrian, or more than 570 million years old)

in the mountains to geologically recent (Holocene, or less than about 10,000 years old) in the valleys. Understanding the distribution of rock types enables geologists to understand the geologic history of the area, which is fundamental to analyses of geologic hazards. Also, the characteristics of rock types below and around Yucca Mountain influence the regional flow of groundwater and would control where any potential releases of radionuclides from the repository system might migrate.

Most of the Precambrian (older than about 570 million years) and Paleozoic (570 to 240 million years old) rocks in the Yucca Mountain region are sedimentary or metamorphic rocks that are not very permeable. The oldest Precambrian "basement" rocks are highly metamorphosed gneisses and schists that have been dated at about 1.7 billion years. These rocks are overlain by less metamorphosed sedimentary layers composed primarily of quartzite, siltstone, shale, and carbonate (CRWMS M&O 2000b, Section 4.2.2). Except for the carbonates described below, all of the Precambrian and Paleozoic units that underlie the volcanic rocks in the Yucca Mountain region are aquitards (i.e., rocks of low permeability that do not readily transmit water). In these units, water flow generally occurs only in strongly fractured zones.

In contrast, there are several Paleozoic carbonate (limestone or dolomite) units that form important aquifers throughout southern Nevada (Winograd and Thordarson 1975). For example, the Spring Mountains, between Yucca Mountain and the Las Vegas Valley, are composed largely of carbonate rocks, which are a major source of recharge (i.e., rainfall that enters the flow system) to the regional groundwater system. Near Yucca Mountain, the most significant groundwater discharge occurs in carbonate rocks throughout the Ash Meadows area, which is about 50 km (30 mi) south-southeast of the potential repository. The aquifer from which this flow originates lies below the aquifers in the tuff units at Yucca Mountain. Knowledge of the location of groundwater recharge and discharge points, the direction of flow, and the relationship between the rock units and the groundwater system is important to analyses of potential future releases of radionuclides to the environment.

DTN MO0009YMP00093.000

00051DC_ATP_Z1S1_Fig 06.ai
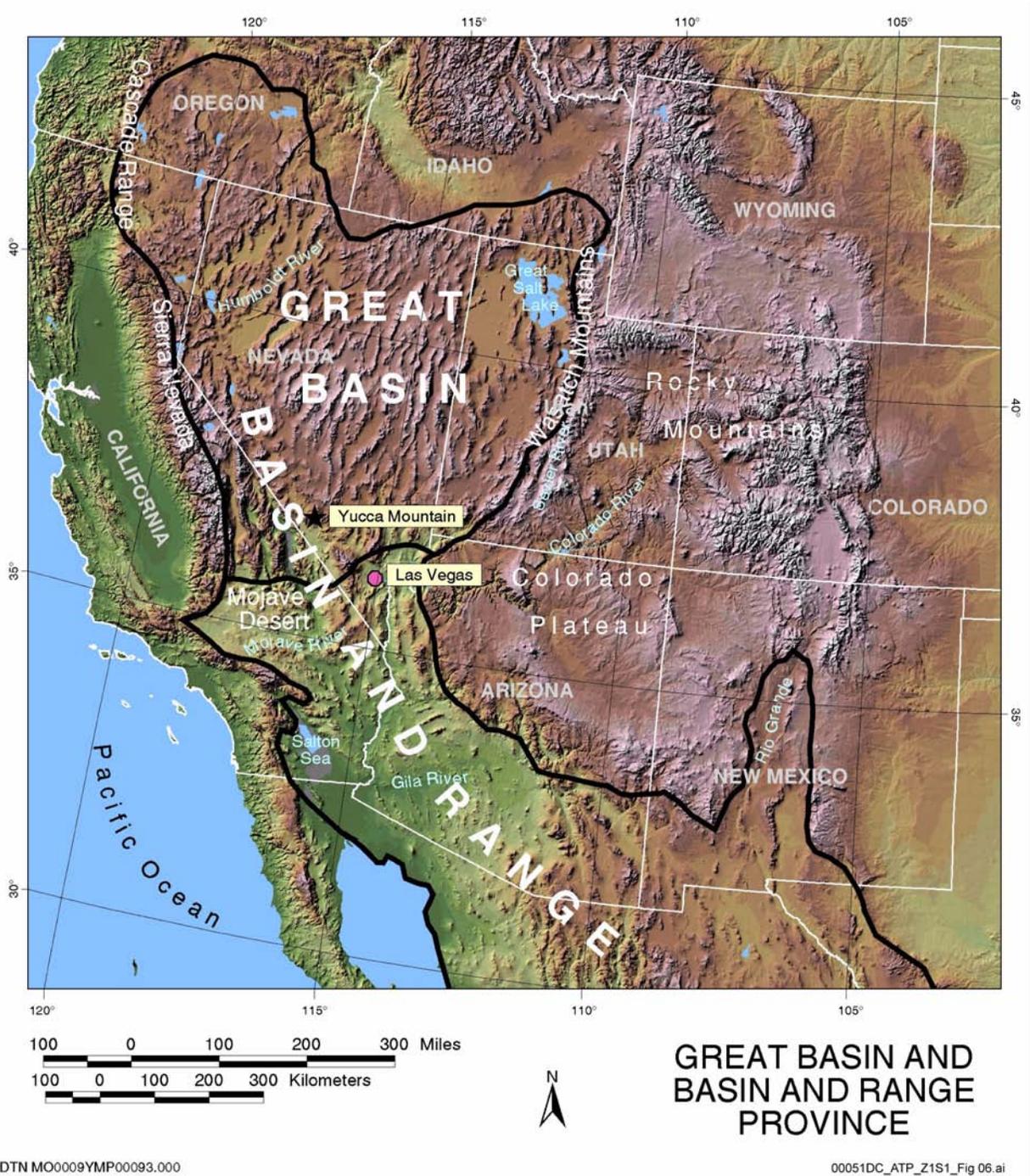
Figure 1-7.   Map Showing the Location of Yucca Mountain and Major Physiographic Provinces of the Southwest

Yucca Mountain is located in the southern Great Basin, within the Basin and Range province of the western U.S. The Great Basin is bounded on the east by the Rocky Mountains and the Colorado Plateau, and on the west by the Sierra Nevada Range.

Between about 14 and 7.5 million years ago (during the Miocene Epoch of the Cenozoic Era), a series of large-scale volcanic eruptions resulted in the formation of Yucca Mountain and the south-western Nevada volcanic field (Sawyer et al. 1994), which consists of six major volcanic centers, or calderas (Figure 1-8). The Claim Canyon Caldera, just north of Yucca Mountain, was the eruptive source of the approximately 13-million-year-old rock units, known as the Paint-brush Group, that now form the mountain ridges at the potential repository site. Eruptions from the southwest Nevada volcanic field ended about 7 million years ago. More recently, small volume volcanoes (known as cinder cones) have erupted lava flows and volcanic ash to the west and south of Yucca Mountain (Crowe, Perry et al. 1995). Four cinder cones formed between about 1.3 and 0.7 million years ago in Crater Flat, west of Yucca Mountain. The latest volcanic episode created the Lathrop Wells Cone, about 16 km (10 mi) south of the potential repository site, about 80,000 years ago. This most recent volcanic activity in Crater Flat and at Lathrop Wells is described in *Yucca Mountain Site Description* (CRWMS M&O 2000b, Section 12.2), which provides the basis for the assessment of volcanic hazards in Section 4.3.2.1.

Surficial deposits in the Yucca Mountain region provide a record of the evolution of surface processes and climate conditions over the past several hundred thousand years. Most surficial deposits in the region are composed of sands and gravels that are called alluvium if they are depos-ited by flowing surface water or colluvium if they originate from hill slopes as flows of debris. Eolian (wind-blown) deposits, such as sand dunes, are generally a minor component of the surficial deposits, except for a massive dune at Big Dune and sand ramps like those that flank Busted Butte southeast of Yucca Mountain. Southwest and south of Yucca Mountain, scientists have mapped minor spring and marsh deposits reflecting past, wetter climates. The ages of surficial deposits range from less than 1,000 years to more than 760,000 years, but most deposits exposed at the surface were deposited during the last 100,000 years. Deter-mining the ages and distributions of these deposits is important to understanding the age and move-ment of faults in the area. A complete description

of the results of studies of surficial deposits can be found in *Yucca Mountain Site Description* (CRWMS M&O 2000b, Section 4.4).

The characteristics of surface deposits indicate that erosion in the Yucca Mountain region generally has proceeded slowly. Volcanic features are well preserved, and basic geologic relationships indi-cate that modern landforms (e.g., ridges and valleys) were already established by the time of eruption of the Rainier Mesa Tuff, approximately 11.6 million years ago.

Near-surface carbonate deposits (sometimes called caliche or calcrete) occur in soils at shallow depths parallel to the surface and as fracture fillings. Evidence indicates that these deposits are pedogenic (i.e., related to the formation of soil) in origin, supporting the conclusion that past climate in the region has generally been similar to the modern semiarid to arid conditions, although some periods have been wetter. These types of deposits form in arid environments when downward infil-trating rainwater dissolves minerals present at the surface. Calcium carbonate is then precipitated in the soils when the infiltrating water evaporates or is taken up by plant roots.

1.3.2.2.2 Site Bedrock Geology

The rocks that might host the potential repository are important to all aspects of repository design and performance. Figures 1-9 and 1-10 are a simplified geologic map and cross section modi-fied from Day, Dickerson et al. (1998) that show geologic relations at a repository scale. In addition, stratigraphic, structural, and rock property data have been combined to form an integrated site geologic model (CRWMS M&O 1997a). This geologic model provides a common framework for developing the repository design and assessing the performance of the repository system.

Measurements of the water level in boreholes at Yucca Mountain indicate that the water table is approximately 500 to 800 m (1,600 to 2,600 ft) below the ground surface. The potential repository would be located above the water table in the unsaturated zone. The ash-flow tuff layers

EXPLANATION

00051DC_ATP_Z1S1_Fig-07a.cdr

—⊥—⊥—⊥— Caldera topographic walls

———— Caldera structural margins

•••••••• Inferred caldera margins

———----- Contacts between geologic units, dashed where approximate

0   15 km

0   10 mi

| Qa | Quaternary (less than 2 million years old) deposits of alluvium and other sedimentary deposits |

| Qby | Late Quaternary basaltic volcanic rocks, less than about 770,000 years in age |

| Qbo | Early Quaternary basaltic volcanic rocks, ranging from about 1.6 to 0.77 million years in age |

| Typ | Late Tertiary (Pliocene) basaltic volcanic rocks, ranging from about 5.0 to 1.6 million years in age |

| Tyb | Tertiary (Miocene) basaltic volcanic rocks, greater than 5 million years in age |

| Tv | Tertiary volcanic rocks of Miocene age (ranging from about 15 to 7.5 million years in age), including welded and nonwelded silicic ash-flow tuff deposited outside of the caldera margins |

| Tvc | Tertiary volcanic rocks of Miocene age (ranging from about 15 to 7.5 million years in age), including welded and nonwelded silicic ash-flow tuff deposited within the caldera margins |

| | Older pre-Tertiary bedrock. Rock types include mostly Paleozoic (approximately 225 to 570 million year old) quartzite, limestone, dolomite, shale, siltstone, and sandstone. |

Figure 1-8. Simplified Geologic Map Showing the Location of Yucca Mountain in Relation to the Southwestern Nevada Volcanic Field

The map shows the location of (1) pre-Tertiary basement rocks (mostly Paleozoic sedimentary rocks ranging from 225 to 570 million years in age); (2) Tertiary volcanic rocks of Miocene age (i.e., 15 to 7.5 million years old) deposited during very large, caldera-forming eruptions; (3) Tertiary and Quaternary basaltic rocks of the southwestern Nevada volcanic field formed during much smaller volcanic eruptions, with ages ranging from more than 5 million years to about 77,000 years; and (4) Quaternary deposits of alluvium and other sedimentary deposits less than 2 million years old. Source: modified from Sawyer et al. 1994; Stewart 1997.
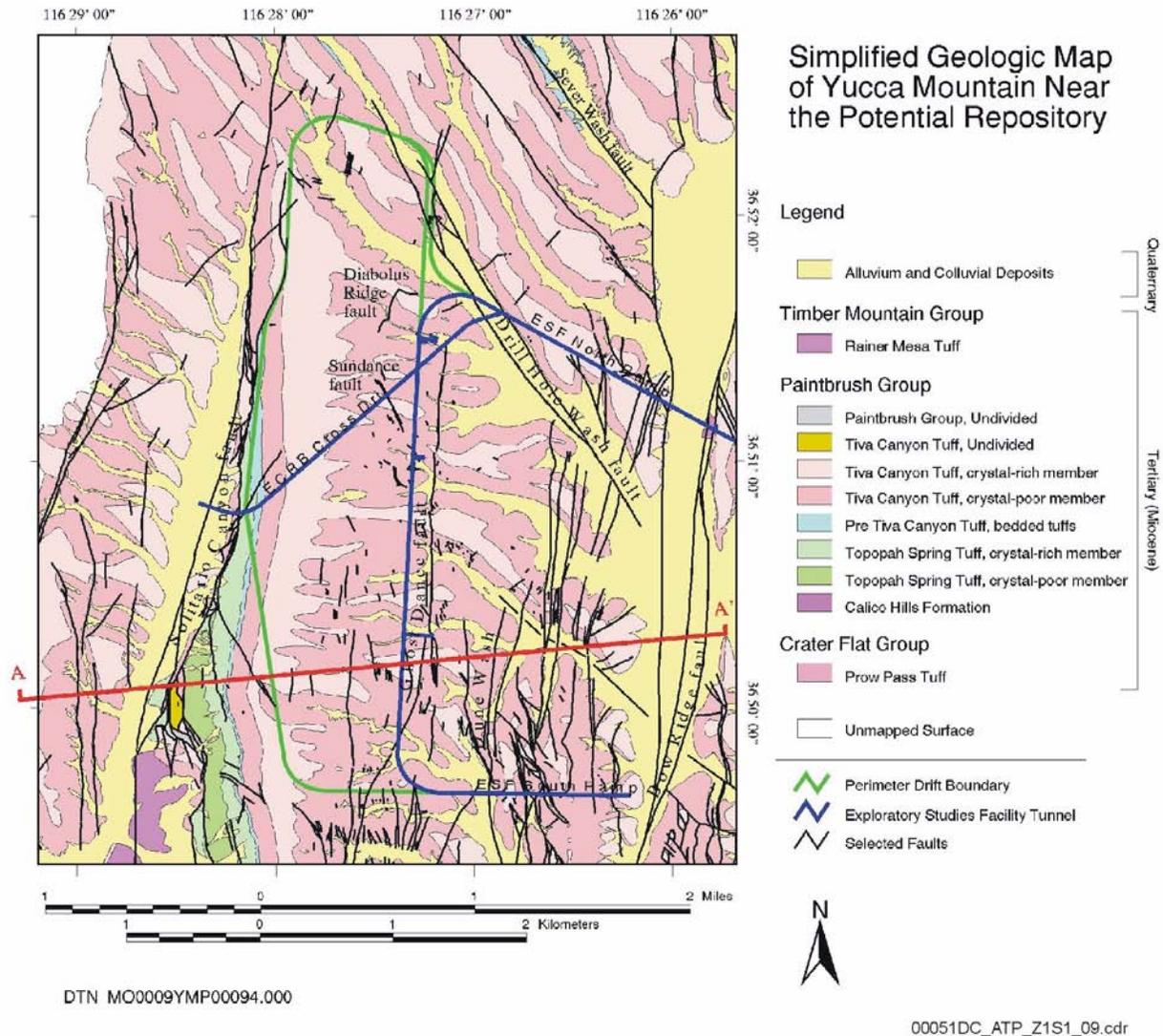
Figure 1-9.   Simplified Geologic Map of Yucca Mountain Near the Potential Repository
The geologic map shows the distribution of the eastward dipping volcanic rocks that form Yucca Mountain and the locations of selected faults. The line A–A' indicates the plane of the cross section shown in Figure 1-10. ESF = Exploratory Studies Facility. Source: Modified from Day, Dickerson et al. 1998.

discussed in this section lie mostly within the unsaturated zone.

Site Stratigraphy—Yucca Mountain consists of successive layers of volcanic rocks (called tuffs), approximately 14 to 11.6 million years old, formed by eruptions of volcanic ash from calderas to the north. Individual layers of tuff thin from north to south. Most of these volcanic rocks are ash-flow tuffs of two types, welded and nonwelded, that formed when hot volcanic gas and ash erupted violently and flowed quickly over the landscape.

As the ash settled, it was subjected to various degrees of compaction and fusion, depending on temperature and pressure. When the temperature was high enough, the ash was compressed and fused to produce a welded tuff—a hard, brick-like rock with very little open pore space in the rock matrix. Nonwelded tuffs, which occur between welded layers, are compacted and consolidated at lower temperatures, are less dense and brittle, and have a higher porosity (more open pore space in the rock). The composition of the rocks at Yucca Mountain ranges from rhyolite (a volcanic rock

Simplified Cross Section of Yucca Mountain Near the Potential Repository

DTN MO0009YMP00095.000

00051DC_ATP_Z1S1_10.cdr
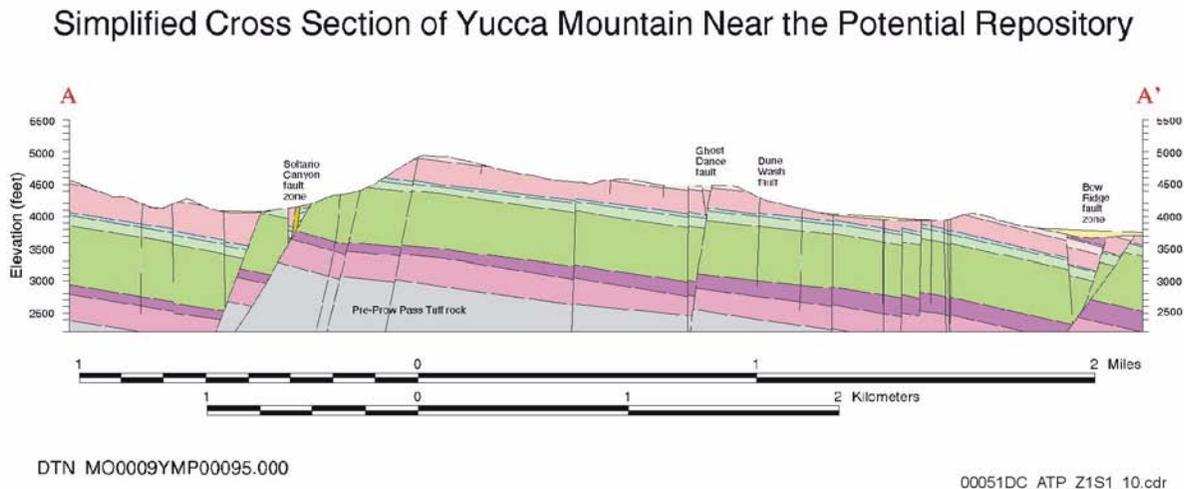
Figure 1-10.   Simplified Cross Section of Yucca Mountain Near the Potential Repository
The cross section shows the distribution of the eastward dipping volcanic rocks that form Yucca Mountain and the locations of selected faults. The location of this cross section, A–A', is indicated in Figure 1-9, and the legend in Figure 1-9 corresponds to this geologic cross section. Source: Modified from Day, Dickerson et al. 1998.

type with a chemical composition similar to granite) to dacite or latite. Dacite and latite are volcanic rock types with chemical compositions characterized by silica contents that are intermediate between rhyolite (high silica) and basalt (low silica).

In the immediate vicinity of the potential repository, the stratigraphically highest volcanic unit present is the Rainier Mesa Tuff of the Timber Mountain Group. As shown in Figures 1-9 and 1-10, the Rainier Mesa Tuff, which is approximately 11.6 million years old, is found in only a few locations in the faulted valleys east and west of the crest of Yucca Mountain. It consists of nonwelded to partially welded rhyolitic ash flows that are up to about 30 m (100 ft) thick in this area. Beneath the Rainier Mesa Tuff, other volcanic rocks (known as pre-Rainier Mesa bedded tuffs) are also locally present. These tuffs are also nonwelded ash-flow deposits, and they range in thickness from 0 to approximately 60 m (200 ft).

Most of the surface of Yucca Mountain above the potential repository location is composed of the volcanic rocks of the Paintbrush Group. The Paint-

brush Group is composed of three distinct volcanic tuff layers that occur between the surface and the location of the potential repository: the Tiva Canyon welded tuff at the surface, the Topopah Spring welded tuff at the level of the potential repository, and an intervening layer of nonwelded tuffs. As a result of faulting over the last 13 million years, these layers are all tilted to the east about 10° (Figure 1-10). The Tiva Canyon Tuff is a large-volume, regionally extensive ash-flow tuff (Sawyer et al. 1994, Table 1) that has been dated at approximately 12.7 million years old. The thickness of the Tiva Canyon Tuff ranges from 50 to 175 m (165 to 575 ft); it is approximately 100 m (330 ft) thick near the potential repository site.

A layer of nonwelded tuff underlies the Tiva Canyon Tuff near the site of the potential repository. This nonwelded layer includes two separate ash flows, the Yucca Mountain Tuff and the Pah Canyon Tuff. In the vicinity of the potential repository, the total thickness of the nonwelded units ranges from 30 to 50 m (100 to 165 ft). These nonwelded units contain few fractures, so they delay the downward flow of water below the surface.

The lowermost unit in the Paintbrush Group is the Topopah Spring Tuff, which would be the host rock for the potential repository. The Topopah Spring Tuff was formed by an eruption about 12.8 million years ago and has a maximum thickness of about 375 m (1,230 ft) near Yucca Mountain. Based on surface mapping and studies of boreholes and underground exposures, the Topopah Spring Tuff has been subdivided into several layers according to chemical composition, mineral content, the size and abundance of pumice and rock fragments, and other variations in texture and appearance. An important characteristic of the layers is the presence and abundance of lithophysae, which are small, bubble-like holes in the rock caused by volcanic gases that were trapped in the rock matrix as the ash-flow tuff cooled. The average lithophysae range from about 1 to 50 cm (0.3 to 20 in.) in size, with a maximum size of about 1 m (3.3 ft) (CRWMS M&O 2000b, Section 4.5.3.1). Their nature, size, and abundance may affect the tuff's thermal, mechanical, and hydrologic properties.

The lower and middle portions of the Topopah Spring Tuff have been divided into four layers according to the amount of lithophysae they contain. Because these layers are tilted, and the drifts in the potential repository would be approximately horizontal, the potential repository horizon crosses the lithophysal zones. Like the Tiva Canyon Tuff, the Topopah Spring Tuff is fractured throughout; these fractures provide the main pathway for water to flow through the rock unit (see Section 4.2.1).

Beneath the Paintbrush Group, the Calico Hills Formation is a series of mostly nonwelded rhyolite tuffs and lavas that were erupted approximately 12.9 million years ago (Sawyer et al. 1994, Table 1). The formation thins southward, from a total thickness of about 290 m (950 ft) north of the repository block to 40 m (135 ft) south of it. Several characteristics of the Calico Hills Formation are important to repository performance. None of the tuffs of the Calico Hills are densely welded; therefore, they generally have higher matrix porosities than the Topopah Spring Tuff. Because the rock has higher ductility, the fractures that are common in welded tuffs are less common in the Calico Hills Formation. Surface, borehole, and

Exploratory Studies Facility observations indicate that the highly fractured Topopah Spring Tuff may overlie tuffs of the Calico Hills Formation that have a lower fracture density (CRWMS M&O 2000b, Section 4.6.6.3).

Analyses of surface and borehole samples (e.g., Bish and Chipera 1986, Table 2; Broxton et al. 1993, p. 1) show another important feature of the tuffs of the Calico Hills Formation: an abundance of zeolite minerals in the rock matrix and fractures. Zeolites are silicate minerals that have the ability to sorb (take up on their mineral surface and hold) radionuclides and other ions that might be transported in solution in water. The DOE's approach to ion exchange sorption is to quantify the extent of radionuclide-sorbent interaction, which does not require identifying the specific underlying processes of sorption (see Section 4.2.8.1). The zeolite minerals may also affect transport properties in another way: tuffs with high zeolite content have reduced matrix permeability, which will tend to focus water flow into any fractures that are present (CRWMS M&O 2000c, Section 3.6.3.1).

The geologic units below the water table contain older volcanic rocks composed mainly of welded and nonwelded ash-flow tuffs. These older units can be up to 1,000 m (3,300 ft) thick below Yucca Mountain (CRWMS M&O 2000b, Section 4.5.4). The volcanic rocks are underlain by the Paleozoic limestones and dolomites described in Section 1.3.2.2.1. Near Yucca Mountain, the older volcanic rocks and the Paleozoic rocks lie deep beneath the surface, but they are found at much shallower depths (and even at the surface) to the south, where they are an important component of the hydrologic flow system.

Selection of the Repository Location and Host Rock—The identification of a subsurface location for a potential repository was based on several factors, including the thickness of overlying rock and soil, the extent and geomechanical characteristics of the host rock, the location of faults, and the depth to groundwater (CRWMS M&O 2000d). Figure 1-11 shows the key features of the site that have controlled the siting of the repository, as described below.
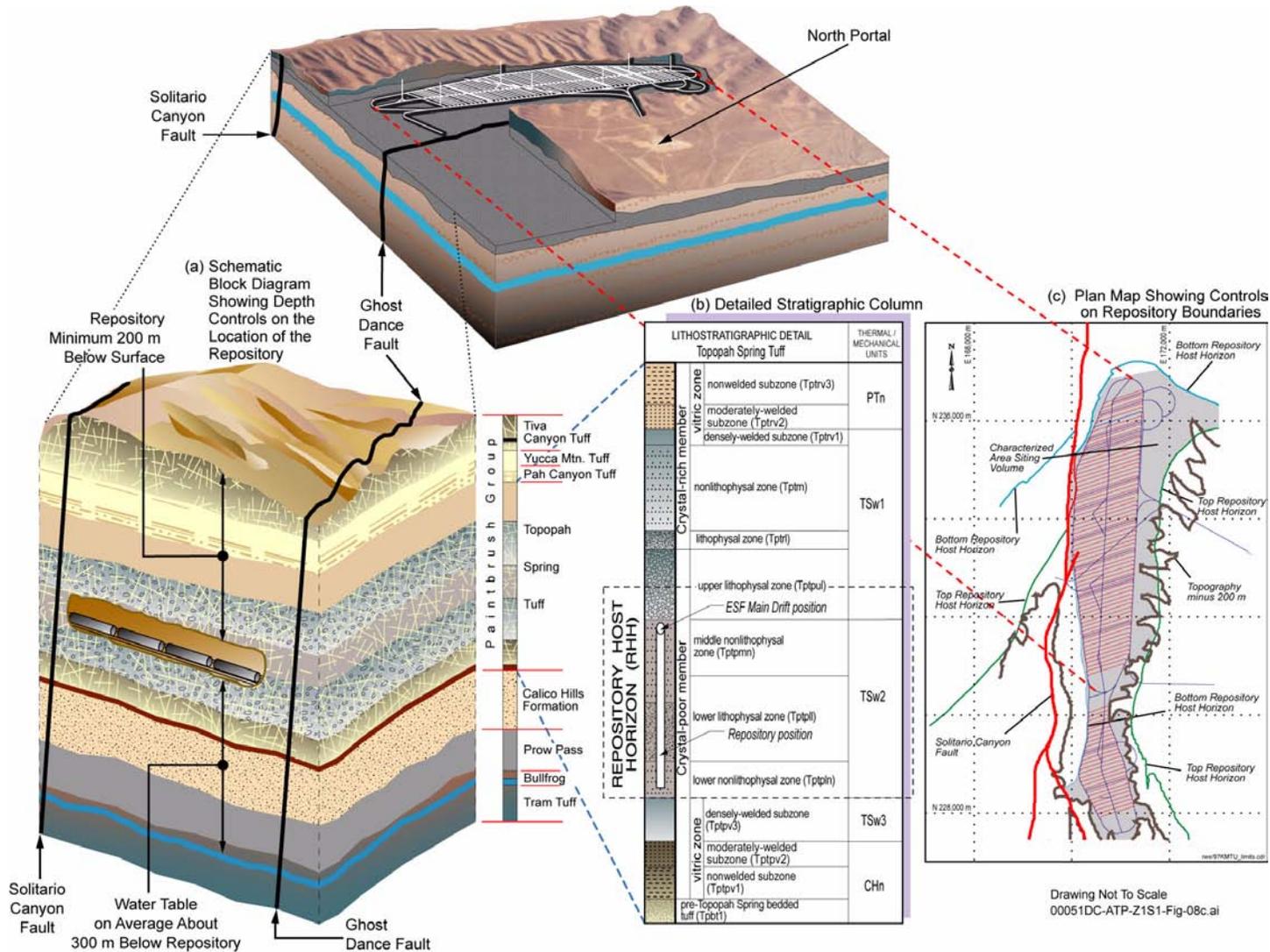
Figure 1-11. Layout and Boundaries of the Potential Repository

(a) Block diagram showing the location of the potential repository with respect to depth below the surface, the water table, and nearby faults. The scale of the emplacement drifts is exaggerated to show schematic waste packages. (b) Stratigraphic section showing the rock units in the Topopah Spring welded tuff that could host emplacement drifts. (c) Plan map showing how the lateral boundaries of the potential repository were identified based on the combined constraints of all of the factors. ESF = Exploratory Studies Facility.

A repository would be sited deep enough to protect waste from exposure to the environment and discourage intentional or inadvertent human intrusion into the facility. Designers have specified a minimum overburden thickness of 200 m (650 ft) to ensure adequate protection from surface events.

The host rock for a repository should be able to sustain the excavation of stable openings that can be maintained during repository operations and that will isolate the waste for an extended period after closure. In addition, the rock should be able to absorb any heat generated without undergoing changes that could threaten the site's ability to safely isolate the waste. The host rock should be of sufficient thickness and lateral extent to construct a repository large enough to support the design's intended disposal capacity. Moreover, the amount of suitable host rock should provide adequate flexibility in selecting the depth, configuration, and location of the repository. Studies to date have shown that the Topopah Spring Tuff has these features and characteristics. Experience gained from excavating the Exploratory Studies Facility demonstrates that openings can be excavated and maintained in the unit (Figure 1-12). The dense welding of the tuff originally occurred at temperatures of approximately 800°C (1,500°F); the results of laboratory and underground testing to date show that the heat added by the emplaced waste would

ATP_Z1S1_Fig1-15.ai

Figure 1-12.   View Looking Down Exploratory Studies Facility
The photo of the Exploratory Studies Facility at the potential repository level shows that stable openings can be excavated and maintained in the Topopah Spring welded tuff with standard ground support measures. The inset shows a representative sample of lithophysae in the repository host rock. The lithophysae appear as flattened white voids within the rock. The white color is derived from mineral precipitation (primarily silica polymorphs or calcite) in the lithophysae.

not adversely affect the stability of the underground repository (CRWMS M&O 2000e).

Faults could impact repository performance by affecting the stability of underground openings or by acting as pathways for water flow that could decrease waste package lifetimes and eventually lead to radionuclide release. No faults with significant displacement (i.e., movement of more than a few meters) occur within the area defined for emplacement. Detailed studies of the faults within the emplacement area indicate that they are not active; thus, they are considered to have an extremely low probability of being active in the future (CRWMS M&O 2000f, Section 2.1.1.3). The main potential repository emplacement area is bounded on the west by the Solitario Canyon fault, and on the east by the Ghost Dance fault. To mitigate any possible effects from fractures near faults (e.g., higher potential for water flow in fractures or less stable openings), emplacement drifts will be set back from faults.

Because the potential repository is designed to take advantage of the performance characteristics of the unsaturated zone, separation from the saturated zone is an important component in selecting the repository elevation. The repository would be isolated not only from present-day groundwater levels but also from future fluctuations of the water table. Geologic evidence (CRWMS M&O 2000b, Section 9.4) shows that the water table has not been more than about 120 m (390 ft) higher than its present level over the past several million years, even during cooler and wetter climates. Figure 1-13 illustrates a conceptual repository layout that addresses the design and range of operating modes described in this document, superposed on a contour map of the known water table elevations in the vicinity of the potential repository. Details A through D of the figure indicate the elevations of the northernmost emplacement drifts of the upper and lower blocks. The northernmost emplacement drift in the upper block would be approximately 210 m (690 ft) above the present water table elevation at that location; the northernmost emplacement drift in the upper block is the closest emplacement drift in this layout to the present water table. The water table elevation in Borehole WT-24 can be used as a check on this observation.

As indicated in Figure 1-13, WT-24 is located approximately 120 m (390 ft) in a northerly direction from the location of Detail A; the elevation of the water table at WT-24 was reported as 840 m (2,750 ft) (CRWMS M&O 2000g, Table 3). The northernmost emplacement drift in the lower block is approximately 265 m (870 ft) above the present elevation of the water table at that location.

Even at the higher levels associated with a water table rise, the emplacement drifts would still be more than about 90 m (290 ft) above the highest projected water table elevation. Analyses of the potential for variation in the elevation of the water table have also considered the possibility that water table variations could be caused by tectonic, volcanic, or hydrothermal processes. In addition to the DOE (CRWMS M&O 2000b, Section 4.4.5), both the National Academy of Sciences/National Research Council (National Research Council 1992) and the NWTRB (1999a, pp. 19 to 21) have reviewed evidence regarding the hypothesis that tectonic or hydrothermal processes could cause large-scale variations in the water table, possibly compromising the performance of the potential repository. Each review found that the available evidence did not support the hypothesis that large-scale fluctuations in the water table (to the level of the potential repository) had occurred in the past. The National Research Council also evaluated the theoretical possibility that the water table could rise significantly in the future and concluded that large variations were unlikely. More recently, the NWTRB found that a review of information developed and presented after the National Research Council review did not significantly affect their conclusions (NWTRB 1999a, p. 20).

The combination of factors described above resulted in the selection of the middle to lower portion of the Topopah Spring welded tuff as the potential repository horizon (Figure 1-11) (BSC 2001d). This section is densely welded, with variable fracture density and lithophysal content. Experience in the Exploratory Studies Facility (e.g., monitoring of excavation characteristics, rock bolt loads, deformation of portal girders, and strain magnitudes of steel sets) and design analyses indicate that stable openings can be constructed in the Topopah Spring Tuff (Figure 1-12). Also, the
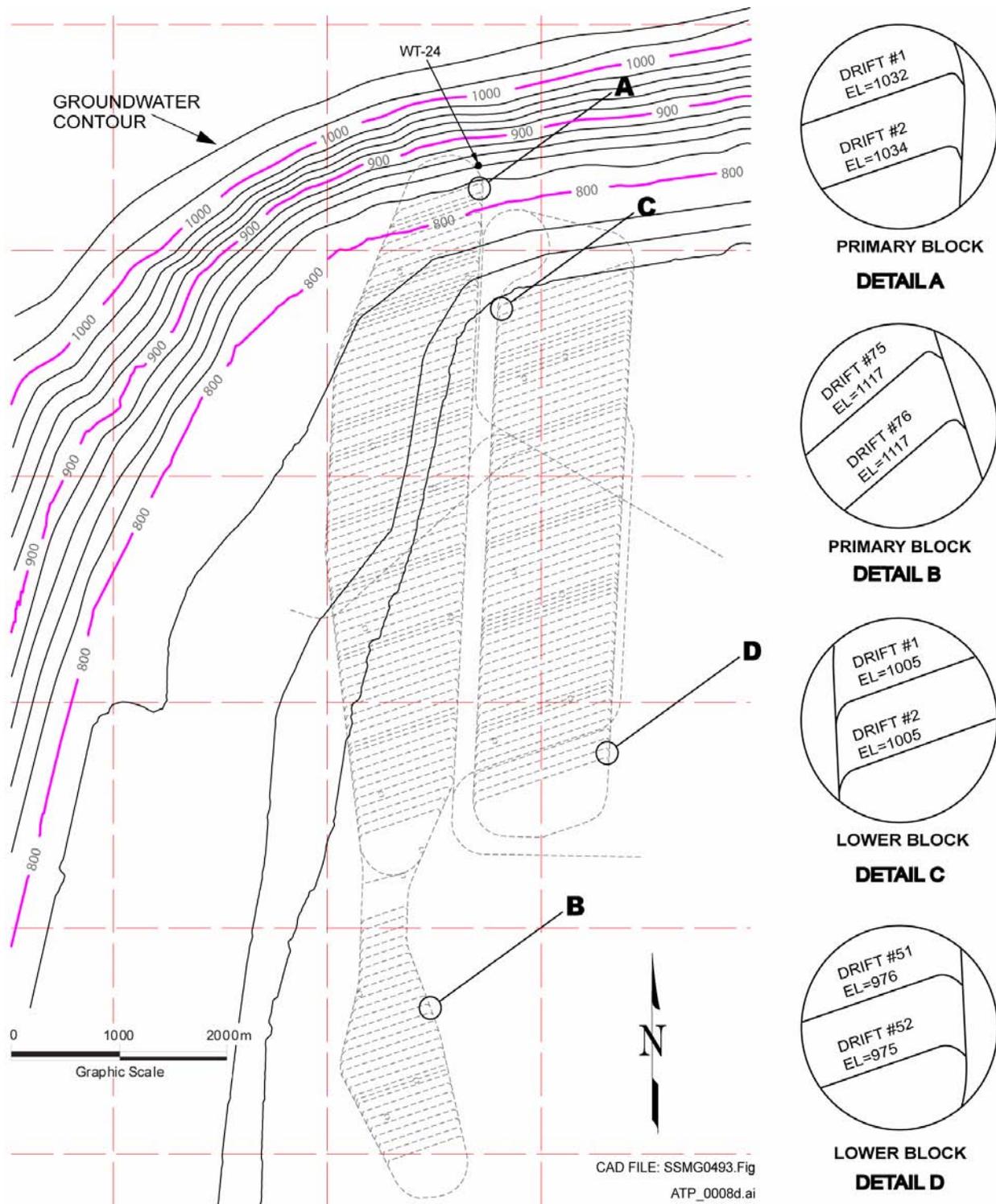
Figure 1-13. Groundwater Elevation Contours, with Their Relationship to a Conceptual Repository Layout
The water table in the vicinity of Yucca Mountain shows a steeper gradient toward the north and northwest. The northernmost emplacement drifts in the primary block area would be closest to the water table, the closest emplacement drift being approximately 210 m (690 ft) above it. The areas where the emplacement drifts in the primary and lower blocks would be closest to (locations A and C, respectively) or farthest from (locations B and D, respectively) the water table have been identified in the figure. EL = elevation. Elevations are given in meters above sea level. Groundwater contours are shown at intervals of 20 m (66 ft). Source: BSC 2001e.

thermal and mechanical properties of the rock should enable it to accommodate the range of temperatures expected during repository construction and operation. The selected horizon is well below the surface and well above the water table. Finally, the potential repository development area is located between major faults, with setbacks to mitigate any potential effects.

Faulting and Local Structural Geology—The distribution and properties of faults and fractures in the volcanic bedrock are important elements of the structural geology of a potential repository at Yucca Mountain. They control the hydrologic and rock-mechanical properties of the system and therefore may affect postclosure performance and design. The distribution and recurrence history of the faults also controls estimates of seismic hazard for the repository. Ground motion from earthquakes is one factor to be considered during the preclosure operation of surface facilities. Studies show that the effects of fault displacement in the repository after closure will not significantly affect performance (see Section 4.3.2.2). The evaluations of seismic hazard, and its potential effects on the preclosure and postclosure performance of the repository, are described in *Probabilistic Seismic Hazard Analyses for Fault Displacement and Vibratory Ground Motion at Yucca Mountain, Nevada* (Wong and Stepp 1998), Section 3 of the *Disruptive Events Process Model Report* (CRWMS M&O 2000f), and *Preliminary Preclosure Safety Assessment for Monitored Geologic Repository Site Recommendation* (BSC 2001f). As described in the *Subsurface Facility System Description Document*, repository emplacement drifts will be set back from known faults (CRWMS M&O 2000h, Section 1.2.2.1.5).

The structural geology of Yucca Mountain is controlled by block-bounding faults spaced 1 to 4 km (0.6 to 2.5 mi) apart. These faults include (from west to east) the Windy Wash, Fatigue Wash, Solitario Canyon, Bow Ridge, and Paintbrush Canyon faults (Figure 1-14). The Dune Wash and Midway Valley faults are also block-bounding faults but differ from the others in that they have no evidence of Quaternary movement (within the past 2 million years). The block-bounding faults commonly dip 50° to 80° to the west, with scat-

tered dips of 40° to 50° and 80° to 90°. Some left-lateral displacement is commonly associated with these faults (Simonds et al. 1995; Day, Dickerson et al. 1998, p. 8).

In some fault zones, several Paintbrush Group rock types have been mixed within the most intensely deformed parts of the fault, indicating that faulting has structurally juxtaposed various subunits as displacement of the bedrock has occurred. This is most apparent in the Solitario Canyon fault system. Individual fault strands within these zones are highly brecciated (i.e., composed of angular, broken fragments of rock).

Displacement between the block-bounding faults occurs along multiple smaller faults, which may intersect block-bounding faults at oblique angles. The Ghost Dance and Sundance faults are examples of smaller "intrablock" faults near the potential repository. The Ghost Dance fault trends in a north–south direction, and can be followed on the surface for 3.7 km (2.3 mi). The fault plane dips steeply to the west (75° to 85°). The displacement and amount of brecciation (the degree to which rocks adjacent to the fault are broken and deformed) varies considerably along its length (Day, Dickerson et al. 1998). The fault zone has a maximum displacement of approximately 27 m (89 ft) down-to-the-west offset. There is no demonstrable Quaternary displacement (movement in the last 2 million years). Mapping in the Exploratory Studies Facility has shown that the zone of brecciation near the fault at the depth of the potential repository is very narrow.

The northwest-trending Sundance fault is the only named fault within the boundaries of the potential repository (Spengler et al. 1994; Potter et al. 1999). It can be traced for approximately 750 m (2,460 ft), and shows no evidence of activity during the past 2 million years. The northeast-side-down vertical displacement across the fault zone does not exceed 11 m (36 ft).

Fracture Characteristics—The distribution and characteristics of fractures at Yucca Mountain are important because in many of the hydrogeologic units at the site, particularly the welded tuffs, fractures are the dominant pathways for water flow in
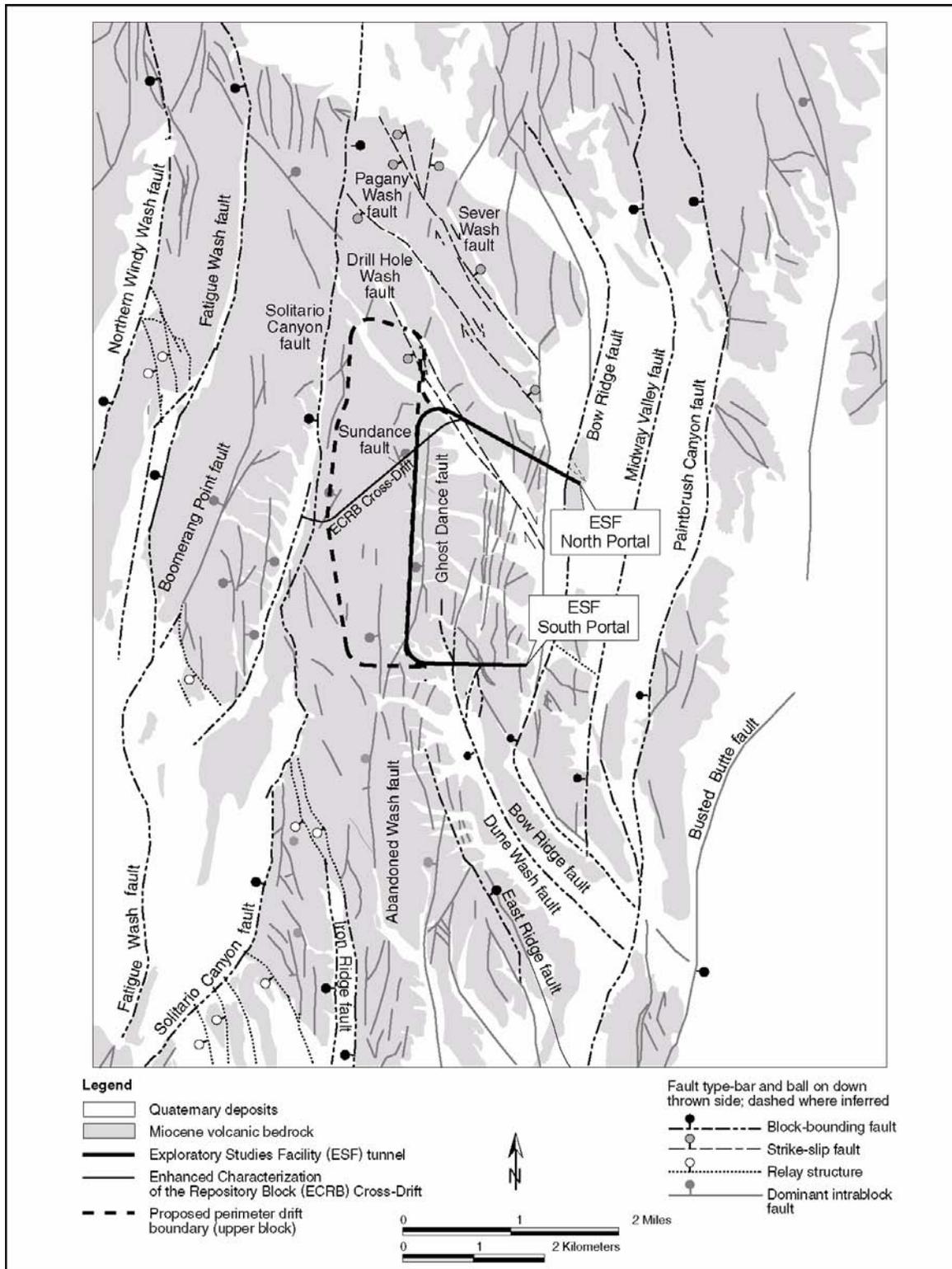
ATP_Z1S1_Fig. 1-16.ai

Figure 1-14.   Mapped Faults at Yucca Mountain and in the Yucca Mountain Vicinity
This map shows the location of various types of faults, as described in Section 4.6.4 of the *Yucca Mountain Site Description* (CRWMS M&O 2000b).

both the unsaturated and saturated zones. By controlling where, and at what rates, water is likely to flow under various conditions, the fracture systems play a major role in the performance of the repository. The potential repository has been designed to capitalize on the free-draining nature of the repository host rock, which would promote the flow of water past the emplaced waste and limit the amount of possible contact between waste and water. This feature was one of the attributes originally recognized by geologists studying Yucca Mountain (Roseboom 1983).

Fractures at Yucca Mountain are generally of three types: early cooling joints formed during the original cooling of the rock mass, later tectonic joints caused by faulting and rock stress, and joints due to erosional unloading. Cooling and tectonic joints have similar orientations, but cooling joints are smoother. Cooling joints form two orthogonal (at 90° angles to each other) sets of steeply dipping fractures and, in some areas, a set of approximately horizontal fractures. Four steeply dipping sets and one nearly horizontal set of tectonic joints have been identified.

Fracture density (the number of fractures in a given volume of rock), connectivity (the number of fractures that intersect each other), and fracture hydraulic conductivity (the capacity of the rock to transmit water in fractures) are highest in the densely welded tuffs and lowest in the nonwelded tuff units. The Tiva Canyon and Topopah Spring welded units are characterized by well-connected fracture networks, whereas the Paintbrush nonwelded units and the Calico Hills tuffs generally do not exhibit connected fractures. In the lithophysal zones of welded tuffs, the degree of connectivity is intermediate because fractures may end in the void spaces rather than propagate through them. In all the geologic units, fracture density varies both vertically and laterally because of variations in tuff properties.

Fractures related to faults may affect the hydraulic properties near fault zones and provide flow paths through hydrologic units that are otherwise not prone to fracture flow. Even nonwelded units, such as the Pah Canyon and Calico Hills tuffs, may allow water to move in fractured zones adjacent to

faults. Based on observations at the surface and in the Exploratory Studies Facility, the zone of influence around faults in which fracture properties are modified may range from approximately 1 to 7 m (3 to 23 ft) (Sweetkind et al. 1997, p. 67). The width of the zone with increased numbers of fractures generally correlates with the amount of movement on the fault (i.e., faults with larger displacements have larger fractured zones). The amount of fracturing also depends on the rock type involved: nonwelded or partially welded tuffs can accommodate a greater amount of fault movement without fracturing than densely welded rocks.

Integrated Site Model—A repository site would support stable excavations that can be safely maintained during the operating life of the facility, and it should have geochemical and hydrologic properties that contribute to waste isolation after closure. The welded tuffs in the unsaturated zone at Yucca Mountain were originally identified as potential candidates for hosting a repository (Roseboom 1983) because of their geologic, hydrologic, and geochemical characteristics. Site characterization has confirmed the basic assumptions about how a repository in the unsaturated zone would likely perform.

The stratigraphic and structural data from the site have been combined with rock property and mineralogical results to build a three-dimensional integrated site model (CRWMS M&O 2000i). Data from boreholes, surface geological mapping, and geophysical surveys form the basis for the conceptual understanding of the geologic framework of the site. This framework was used to develop spatial models of the distribution of geological, geotechnical, hydrologic, mineralogic, and geochemical parameters. The integrated site model thus provides technical input to the design of the potential repository and to the models used to assess its future performance.

1.3.2.2.3 Geomorphology and Erosion

Any potential geologic repository site would be selected and designed so that natural geologic and hydrologic processes do not compromise the integrity of the repository (DOE 1986c, Section 6.3.1.5). Because erosion of the rock overlying the

potential repository could, in theory, threaten waste isolation, an evaluation of erosion rates over time and an assessment of the potential for future erosion have been performed. A wide variety of geologic evidence indicates that erosion at Yucca Mountain has occurred at very slow rates for millions of years and would not adversely affect the waste isolation capability of the site in the future (CRWMS M&O 2000b, Section 7.4).

Geologic evidence indicates that the basic morphology (or shape) of Yucca Mountain was already formed about 10 million years ago. Studies of the tectonic evolution of the area (Day, Dickerson et al. 1998, pp. 17 to 19; CRWMS M&O 2000b, Section 4.6.3.3) demonstrate that most of the faulting occurred shortly before, during, and soon after the eruption of the tuffs that comprise Yucca Mountain. This period of intense tectonic activity began about 16 million years ago with faulting related to the extension of the Basin and Range, followed by eruption of the volcanic units below Yucca Mountain onto the Paleozoic and Precambrian basement. About 12.8 to 12.7 million years ago, the thick tuff units of the Paintbrush Group (including the Topopah Spring and Tiva Canyon tuffs) were erupted from calderas to the north and deposited in approximately horizontal layers. Movement along block-bounding faults then tilted the volcanic rocks 10° to 20° to the east and formed major topographic features, such as Solitario Canyon and Midway Valley. The Rainier Mesa Tuff of the Timber Mountain Group was erupted about 11.6 million years ago onto an irregular land surface that was already similar to modern Yucca Mountain (i.e., major ridges and valleys created by faulting already existed). Faulting continued after deposition of the Rainier Mesa Tuff but at greatly reduced rates: displacement on the block-bounding faults was up to several hundred meters before 11.6 million years but has been only a few meters in the last 10 million years.

Over the past several million years, erosion in the Yucca Mountain region has been slow, with only minor effects on major landforms. Several lines of evidence have been considered in the analysis of potential erosion at or near Yucca Mountain. These include evidence related to:

- The rate of degradation of the slopes and stream channels on Yucca Mountain at the potential repository site

- The rate of erosion in stream channels in the Yucca Mountain region, such as Fortymile Wash (to the west of Yucca Mountain)

- The rate of degradation of landforms in the Yucca Mountain region, such as the Lathrop Wells cinder cone (approximately 16 km [10 mi] south of the potential repository site).

Several techniques have been used to assess the stability of the slopes and stream channels at Yucca Mountain. By studying the geochemical and isotopic characteristics of the surfaces of boulders exposed on hillslopes, it is possible to determine how long they have been exposed to the sun and the atmosphere and to calculate erosion rates. Also, by studying the age and composition of sediments in the stream channels, it is possible to analyze how fast sediments have accumulated or eroded in various streams. The studies indicate that long-term average erosion rates at and near Yucca Mountain are low (CRWMS M&O 2000b, Section 7.4.2.2). Rates of bedrock and hillslope erosion range from less than 0.1 cm to 0.5 cm (0.04 to 0.24 in.) per thousand years in the Yucca Mountain area. These low erosion rates are consistent with the surface exposure ages of hillslope boulder deposits found near Yucca Mountain, which range in age from several hundred thousand to over a million years. The boulders have thick deposits of rock varnish and show no signs of significant movement by hillslope erosion since they were formed.

Stream incision rates have also been calculated for the Yucca Mountain area. In local areas, some downcutting in stream channels can be observed. However, regional studies indicate that Fortymile Wash has apparently reached a state of near equilibrium (CRWMS M&O 2000b, Section 7.4.2.5). The rates of sediment accumulation and erosion are approximately equal, with little aggradation (sediment accumulation) or degradation (erosion) at present and with the entire Fortymile drainage system adjusted to the base level of the main channel. This system-wide, long-term equilibrium

in the Fortymile drainage system indicates that episodic pulses of erosion are unlikely to significantly incise stream channels on Yucca Mountain.

Bedrock channel incision rates have also been evaluated at Yucca Mountain and in Fortymile Canyon. Several small canyons on Yucca Mountain are cut 60 to 100 m (200 to 330 ft) into 12.7-million-year-old volcanic tuff. Thus, the long-term incision rate for the first-order streams is 0.8 cm (0.3 in.) per thousand years or less. The drainage system of Fortymile Wash and its tributaries was established more than 10 million years ago and has changed little in basic plan since then.

Studies of the Lathrop Wells cinder cone at the south end of Yucca Mountain indicate that only minor degradation has occurred over approximately the past 80,000 years (Wells et al. 1990). The lack of degradation indicates that severe erosional processes have not occurred in the Yucca Mountain area, even during a time period that includes substantial climate change from the last glacial period.

1.3.2.2.4 Natural Resource Potential

A repository must isolate the spent nuclear fuel and high-level radioactive waste it contains from both people and the environment. In order to reduce the chance that future individuals or groups might inadvertently encounter waste while searching for other exploitable resources, sites with high potential for natural resources have typically been excluded from consideration. As part of the characterization of the Yucca Mountain site, therefore, the potential for economically valuable resources has been carefully evaluated. This section summarizes the results of that assessment.

Resource potential is difficult to predict because it depends on many factors, including economics (i.e., supply, demand, and cost of production), the potential discovery of new uses for resources, and the discovery of synthetic materials to replace natural resources. Therefore, this evaluation is based on the present-day use and economic value of resources; it does not predict future market trends or undiscovered uses for resources. All common types of natural resources—including

metallic minerals, industrial rocks and minerals, hydrocarbons (i.e, petroleum, natural gas, oil shale, tar sands, and coal), and geothermal energy—have been considered.

In a general sense, Nevada contains abundant resources, ranking second in the U.S. in the value of nonfuel (i.e., excluding oil, gas, coal, and geothermal) mineral production in 1996 (Nevada Bureau of Mines and Geology 1997, Summary). Nevada leads the nation in the production of gold, silver, mercury, and barite. Additional metals, including copper, lead, zinc, iron, and such industrial materials as brucite, magnesite, clays, gemstones, gypsum, sand, gravel, and crushed stone are being or have been produced in Nevada. Small but economic oil deposits occur in Railroad Valley in east-central Nevada, and geothermal resources occur in California and northern Nevada within the Great Basin.

Although economic gold mineralization is present in the region (most notably near Beatty), Yucca Mountain contains no identified metallic mineral or uranium resources (CRWMS M&O 2000b, Section 4.9). On the basis of detailed studies of geology, geochemistry, mineralogy, mineral alteration, and geophysical data and remote sensing, the Yucca Mountain site is considered to have little or no potential for deposits of metallic minerals or uranium resources that could be mined economically now or in the foreseeable future. Geological and geochemical comparisons between Yucca Mountain and metal mining districts in the region indicate substantial differences in the geologic and geochemical patterns observed for precious metals, base metals, and pathfinder elements (Castor et al. 1999, Section 6).

Many industrial rock and mineral commodities occur in the Great Basin but not at Yucca Mountain. Although barite, clay minerals, fluorite, limestone, perlite, and zeolites have been identified in samples from Yucca Mountain, these occurrences are minor and at depths too great to be mined economically (Castor and Lock 1995, Section 7).

It is possible that alluvial deposits at the site could be used as concrete aggregate for local construc-

tion and that some of the Tertiary tuff could be used as building stone. However, neither the alluvial deposits nor the tuff have any properties or features that would make them more marketable than other deposits readily available and closer to processing plants and end users (Castor and Lock 1995, Section 6.4.3.1).

Nevada is not a large producer of oil or natural gas, although a few producing fields exist north of the Yucca Mountain region. Some of the conditions of source, reservoir, trap, and seal that characterize petroleum accumulations of the Great Basin are present to some degree in the Yucca Mountain area (French 2000, p. 39). Most evidence, however, indicates that the accumulation of oil or natural gas near the potential repository site is unlikely.

It is extremely unlikely that tar sands, oil shale, or coal occur as economic resources at the Yucca Mountain site. If any of these resources were associated with Paleozoic marine rocks underlying the Tertiary volcanic rocks at Yucca Mountain, they would occur at depths greater than 1,800 m (5,900 ft). Extraction at these depths would not be economically feasible in the foreseeable future.

There are no geothermal discoveries near Yucca Mountain, and there are no potential users located at or near the site. Chemical analyses of fluids throughout the area indicate that most waters are nonthermal in origin. Geophysical data, including gravity, magnetic, seismic, and heat flow data, failed to delineate any systematic structural evidence for a thermal anomaly. Compared with the physical attributes of geothermal systems that have developed in other parts of the Great Basin, no economically viable resources were identified within the Yucca Mountain area (Flynn et al. 1996).

1.4 POSTCLOSURE PERFORMANCE

Since the National Academy of Sciences concluded that geologic disposal was feasible in 1957 (National Academy of Sciences Committee on Waste Disposal 1957), many scientists (e.g., de Marsily et al. 1977; Konikow and Ewing 1999) and reviewers of the U.S. repository program (NWTRB 1999b; NWTRB 2000; Budnitz et al.

1999) have recognized the difficulty associated with assessing repository performance over the long time frames necessary to protect public health and safety.

Developing confidence in the long-term performance of a geologic repository is one of the greatest challenges faced by the DOE. Because of the uncertainty associated with assessments of performance for 10,000 years, there is no simple way to guarantee that the facility will function as modeled throughout the period of performance. In NRC's licensing rule, 10 CFR Part 63 (66 FR 55732), the NRC recognizes this irreducible uncertainty and clearly states that "proof" of performance cannot be produced in the ordinary sense of the word. Rather, the NRC, like the EPA, would require in licensing a "reasonable expectation" that the postclosure performance standards will be met.

The DOE's approach to developing confidence in the safety of geologic disposal, known as the postclosure safety case, relies on multiple, independent lines of evidence. The first element of the safety case is a thorough and quantitative evaluation of the future performance of the repository, based on a comprehensive testing program that has evolved to address identified uncertainties and a repository design developed to complement the natural setting of the site. EPA and NRC regulations specify the method by which the DOE will analyze and demonstrate in licensing that a repository can safely isolate spent nuclear fuel and high-level radioactive waste (i.e., a total system performance assessment [TSPA]). The process used to develop the total system performance assessment for site recommendation (TSPA-SR), which is described briefly in Section 4.4 and in more detail in *Total System Performance Assessment for the Site Recommendation* (CRWMS M&O 2000a), includes analyses of all the processes expected to operate at the repository that could affect its ability to isolate waste. The supplemental TSPA described in *FY01 Supplemental Science and Performance Analyses* (BSC 2001a; BSC 2001b) and the revised supplemental TSPA models described in *Total System Performance Assessment—Analyses for Disposal of Commercial and DOE Waste Inventories at Yucca Mountain—Input to Final*

Environmental Impact Statement and Site Suitability Evaluation (Williams 2001a) and *Total System Performance Assessment Sensitivity Analyses for Final Nuclear Regulatory Commission Regulations* (Williams 2001b) all use the same TSPA approach and method. All of these models and analyses also explicitly consider both disruptive events and alternative models that could result in unanticipated behavior (i.e., identify what could go wrong). The evaluation directly addresses uncertainty in both the DOE's knowledge of the site and in future conditions, and it includes numerical sensitivity analyses to test how the repository might perform if current or future conditions differ from those expected.

Because the DOE recognizes that uncertainty about the future performance of the repository cannot be completely quantified or eliminated (i.e., models alone cannot capture all the uncertainties in natural systems), the safety case includes several additional measures designed to provide confidence and assurance that the repository will meet applicable radiation protection standards after it is permanently closed. These measures include:

- Studies of natural and man-made analogues to the repository or to processes that may affect repository performance, which can further the understanding of natural processes related to repository performance that operate over long time frames (thousands of years) or large spatial distances (tens of kilometers) that cannot easily be tested.

- Selection and design of a repository system that provides defense in depth and a margin of safety compared to health and safety requirements. The DOE has implemented this approach through the characterization of the Yucca Mountain site and the development of a repository system with multiple natural and engineered barriers to the migration of radionuclides. The engineered components of the system are designed specifically to complement the natural attributes of the site. This multiple barrier repository system provides defense in depth, so that the safety of the repository does not depend on only one or two barriers. Also, investigations of

performance over a range of thermal operating modes provides insight into the best ways to address the treatment of uncertainty inherent in thermally coupled processes.

- Long-term management and monitoring (a performance confirmation program) to ensure the integrity and security of the repository and to ensure that the scientific and engineering bases for the disposal decision are well founded. The NRC regulation, 10 CFR Part 63 (66 FR 55732) establishes a period of 50 years after the start of emplacement in which retrieval must be possible, unless a different period is specified by the NRC. DOE design requirements provide for an extended monitoring period of up to 300 years to provide the ability to retrieve the spent nuclear fuel and high-level radioactive waste for any reason before closure, if future generations decide that doing so is appropriate.

This approach is similar to that recommended by many national and international organizations that have investigated the technical and social problems of nuclear waste disposal. As a panel of the National Academy of Sciences observed, "Confidence in the disposal techniques must come from a combination of remoteness, engineering design, mathematical modeling, performance assessment, natural analogues, and the possibility of remedial action in the event of unforeseen events" (National Research Council 1990, pp. 5 to 6). Such an approach has also been recommended and adopted by most nations with nuclear waste programs (see, for example, *Confidence in the Long-Term Safety of Deep Geological Repositories—Its Development and Communication* [NEA 1999a]). The postclosure safety case is described in more detail in Section 4.1. The rest of this section briefly describes how the DOE has used a performance-assessment-based approach to deal with uncertainty, to guide testing and repository design programs, and to evaluate the likely performance of a repository at the Yucca Mountain site. Taken in total, the approach provides a strong engineering and scientific basis supporting the DOE's evaluation of the performance of the potential Yucca Mountain repository system.

1.4.1   Performance Assessment

As noted above, the regulatory requirements for a potential repository are based on quantitative assessments of the system's performance. For Yucca Mountain, performance assessment provides not only a means for estimating relative performance but also a framework for organizing and describing the site and the repository design. Performance assessment has been used as a management tool to integrate the scientific and engineering programs and to assess the importance and priority of various program activities, consistent with the overall goal of determining whether Yucca Mountain can safely host a repository facility.

Performance assessment is a systematic method for evaluating repository system behavior over an extended time. Analysts build detailed mathematical models of the features, events, and processes that could affect performance. Then they incorporate the results of these detailed models into an overall model of the repository system, called the "total system performance assessment model." This integrated model is used to assess how the natural and engineered elements of a waste disposal system would work together over the long period required to isolate wastes. Sections 4.2, 4.3, and 4.4 present the results of these analyses, which are more fully described in *Total System Performance Assessment for the Site Recommendation* (CRWMS M&O 2000a). Supplemental analyses are described in *FY01 Supplemental Science and Performance Analyses* (BSC 2001a; BSC 2001b), and *Total System Performance Assessment—Analyses for Disposal of Commercial and DOE Waste Inventories at Yucca Mountain—Input to Final Environmental Impact Statement and Site Suitability Evaluation* (Williams 2001a), and *Total System Performance Assessment Sensitivity Analyses for Final Nuclear Regulatory Commission Regulations* (Williams 2001b).

Performance assessment models are probabilistic (i.e., they consider the likelihood that the system will behave in a certain way) because of the nature of the processes and systems being analyzed. The natural system is heterogeneous both in space and time; the processes simulated in the models are also variable in space and time. For these reasons, performance assessment uses a probabilistic approach that directly incorporates evaluations of the variability of site properties and a range of possible process behaviors that could occur into the estimates of the future performance of the repository. Performance assessments provide one means to identify which uncertainties about the behavior of a disposal system are significant and which are not, and which elements of the repository design are most important to performance. This helps focus efforts to improve the design and the defensibility of performance analyses. Performance assessments are refined iteratively during the course of developing, evaluating, and improving a repository design.

The DOE has also conducted analyses of potential barriers to radionuclide migration to identify and evaluate the performance contribution of natural features of the geologic setting and design features of the engineered barrier system (see Section 4.5). At Yucca Mountain, these multiple barriers may contribute to confidence in the performance of the repository by providing defense in depth: several elements of the natural and engineered systems contribute to the isolation of waste by functioning independently to limit possible releases.

Section 4.4 presents a summary of the results of the performance assessment calculations performed for the Yucca Mountain site and found in *Total System Performance Assessment for the Site Recommendation* (CRWMS M&O 2000a) and subsequent analyses (BSC 2001a; BSC 2001b; Williams 2001a; Williams 2001b). The TSPA-SR results show that for a 10,000-year period, the calculated dose in the nominal scenario is zero (CRWMS M&O 2000a). A supplemental TSPA model yielded a calculated dose of approximately 2×10^{-4} mrem/yr (BSC 2001b, Section 5.1). A revised supplemental TSPA model calculates a dose of 1.7×10^{-5} mrem/yr (Williams 2001a). The small doses in the supplemental TSPA model result from the inclusion of a few early failures of waste packages due to improper heat treatment. The supplemental TSPA model projected a peak mean dose of 2×10^{-4} mrem/yr for the higher-temperature operating mode and 6×10^{-5} mrem/yr for the lower-temperature operating mode over a 10,000-

year period. Over this same period, the revised supplemental TSPA model projected a peak mean dose to the reasonably maximally exposed individual of 1.7×10^{-5} mrem/yr for the higher-temperature operating mode and 1.1×10^{-5} mrem/yr for the lower-temperature operating mode for the nominal scenario (BSC 2001b, Section 4.1.3; Williams 2001a, Section 6, Table 6).

1.4.2 Importance of Repository System Components to Long-Term Performance

The various components of the repository system contribute to performance in different ways. Certain components of the system are more important to performance than others, as shown by performance assessment sensitivity studies (e.g., Section 4.4.5). Considerations of safety margin, defense in depth, insights from analogues, and expert judgments also help identify the importance of repository components to performance (see Section 4.1). Knowledge of how components of the system affect performance can provide insights on how design or operating mode features could be developed in a manner that could contribute to long-term performance or mitigate potentially adverse conditions. Ongoing evaluations over the range of operating modes could lead to enhanced understanding of how the repository system components could contribute to long-term performance.

1.4.3 Addressing Uncertainty in Total System Performance Assessment

Even though the Yucca Mountain site represents a fairly simple geologic/hydrologic system conceptually—a relatively dry site consisting of fractured volcanic rock hundreds of meters above the water table—it has complexities that are difficult to model but could be important over long periods of time. Uncertainties exist in the understanding of both natural processes (e.g., infiltration of water at the surface, percolation in fractures and rock matrix, disruptive processes of earthquakes and volcanism) and the ways in which the engineered system will perform when exposed to the environment (e.g., seepage into drifts, thermal processes

related to the heat generated by the waste, corrosion of waste packages).

Capturing those uncertainties and understanding their impacts is critical to understanding how a repository might behave in the future. Accommodating uncertainties in the assessment of the performance of a potential repository at Yucca Mountain means recognizing that uncertainties exist and explicitly identifying those that may be important to performance. The DOE's approach to dealing with uncertainties is described in Sections 4.1.1.2 and 4.4.1.2. Some, but not all, of those uncertainties can be quantified; that is, scientists can and have collected data that allow them to estimate the probability that a variable will assume different values over the spatial and temporal scales of an operating repository. Those uncertainties that can be quantified can be incorporated directly into performance assessment results. Approaches to address design-related uncertainty concerns through consideration of a range of thermal operating modes and the effects on performance across the range of temperatures are described in Sections 2.1.5 and 4.4.5.1.2.

Studies have been performed to enhance the understanding of the environmental conditions associated with the lower-temperature ranges of the operating modes. Supplemental performance assessment analyses and sensitivity studies have been conducted to evaluate the performance of lower-temperature operating modes. The analyses incorporate the results of other efforts to quantify uncertainties and extend the applicable range of the process models. Of particular interest are analyses that address performance-related responses of the design and operating mode, considering temperature-sensitive parameters and coupled thermal-mechanical-chemical-hydrologic processes. This approach is intended to ensure that the performance evaluations appropriately consider the potentially detrimental and potentially beneficial aspects of the repository's performance over a range of operating modes encompassing temperatures above and below the boiling point of water. Results of these evaluations are described in *FY01 Supplemental Science and Performance Analyses* (BSC 2001a; BSC 2001b).

There are also uncertainties that cannot readily be quantified (e.g., the possibility that the models used for compliance analyses do not include, or accurately simulate, processes that may be important to performance). The DOE has made a substantial effort to identify, characterize, and mitigate the potential impacts of these unquantified uncertainties. They have been identified and characterized through detailed consideration of the features, events, and processes that might affect repository performance. The principal mechanism for mitigating unquantified uncertainties is the multiple lines of evidence provided by the postclosure safety case, as described in Section 4.1. In particular, design (safety) margin and defense in depth provide a degree of confidence independent of the results of TSPA analyses.

1.4.4 Time Frame for Performance Analyses

EPA standards and NRC licensing regulations relevant to the Yucca Mountain disposal system contain postclosure performance standards that would apply during the first 10,000 years after repository closure.

For this reason, performance assessment results have been presented on plots that extend for 10,000 years, as shown in Section 4.4. The EPA's 40 CFR 197.35 and NRC's 10 CFR 63.341 (66 FR 55732) also specify that the DOE should calculate the peak dose that would occur after 10,000 years but within the period of geologic stability, and present the results in the EIS. Although no regulatory standard applies to the results of this analysis, the EPA and NRC noted that the peak dose calculations would complement the 10,000-year performance assessment results as an indicator of long-term performance. These analyses, which have been performed out to 100,000 years and 1 million years (see Sections 4.4.2.2 and 4.4.2.4, respectively), provide additional confidence in the 10,000-year results.

2. DESCRIPTION OF THE POTENTIAL REPOSITORY

Section 114(a)(1)(A) of the Nuclear Waste Policy Act of 1982 (NWPA), as amended (42 U.S.C. 10134(a)(1)(A)), requires "a description of the proposed repository, including preliminary engineering specifications for the facility." Refining the design and the choice of operating mode for the potential repository is an ongoing, iterative process involving scientists, engineers, and decision-makers. The goal of this process is to develop a design that works with the natural system to enhance containment and isolation of spent nuclear fuel and high-level radioactive waste.

The U.S. Department of Energy (DOE) completed a major milestone in December 1998 with the publication of *Viability Assessment of a Repository at Yucca Mountain* (DOE 1998). That report included a repository design referred to as the Viability Assessment (VA) design. Based on an improved understanding of the interactions of potential repository features with the natural environment and the addition of engineered features for enhanced waste containment and isolation, the VA design has evolved into the design described in this report. As the program moves forward, the design will continue to evolve.

Figure 2-1 depicts a cutaway view of a proposed layout for the repository facilities. Construction of the emplacement drifts and subsurface facilities would be accomplished in phases. In the current plan, about 10 percent of the emplacement drifts
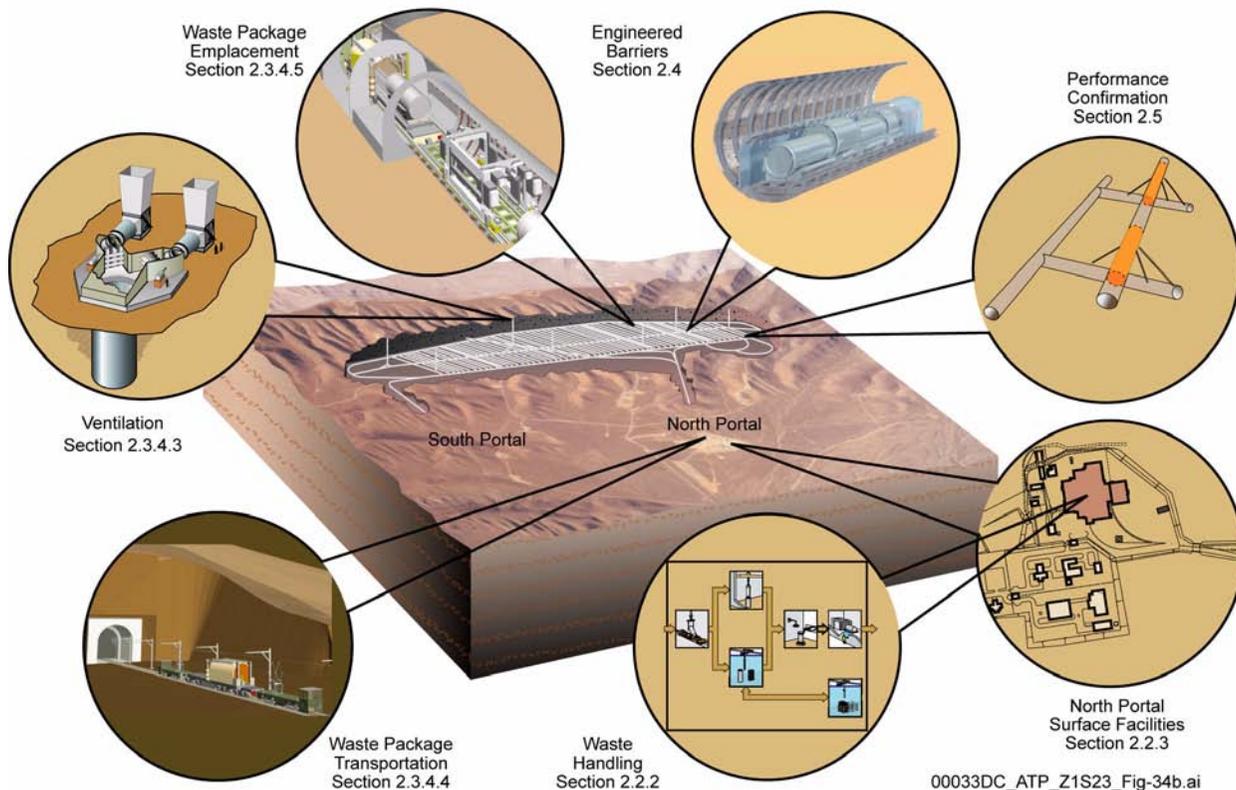
Figure 2-1.   Proposed Monitored Geologic Repository Facilities at Yucca Mountain
This figure shows the proposed surface and subsurface facilities for the repository. Waste handling and packaging would take place at the surface facilities, from which the sealed waste packages would be transported to the underground emplacement drifts via the north ramp. The repository subsurface area is divided in two zones, the development side and the emplacement side, each zone having separate ventilation systems. The South Portal would be used mainly for access to the development side of the repository and for transportation of construction materials. The south ramp would also be used as the conveyor route for removal of excavation waste, or muck.

would be completed during the initial construction phase (prior to initiation of waste emplacement), with the remainder of the emplacement drifts being completed during the operation phases. This phased construction would allow the DOE flexibility to develop the repository based on future deliveries of spent nuclear fuel.

The potential repository facilities have been designed to be fully integrated, using a systems engineering approach to identify and then fulfill requirements by providing adequate design solutions. This systems engineering approach to design and development is explained in Section 2.1.1. An important aspect of the design solutions is that they provide the flexibility to accommodate developing operational scenarios, including associated thermal environment characteristics. They provide a basis to refine the design as it evolves in response to increased understanding of the performance of its components. They can also accommodate unanticipated underground conditions that may be encountered during construction with minimal interruptions and no need for expensive retrofits.

The description of the potential geologic repository at Yucca Mountain is organized into five parts. Section 2.1 presents a general overview of the engineering and design process common to all design disciplines in the Yucca Mountain project. It also discusses the evolution of the design, design and operating flexibility, and an assessment of a broader range of thermal operating modes. Design descriptions for the surface and subsurface facilities are covered in Sections 2.2 and 2.3, respectively. Section 2.4 describes the emplacement drift design features that are part of the engineered barriers. Although the definition of engineered barriers includes the waste package, the descriptions of waste package designs and the different waste forms that would be contained within waste packages are provided separately in Section 3. Section 2.5 describes the surface and subsurface facilities that support the performance confirmation program for the potential repository.

The design and operating mode that was analyzed to assess long-term performance of the repository

system presented in *Total System Performance Assessment for the Site Recommendation* (CRWMS M&O 2000a) was based on a higher-temperature operating mode. Subsequent analyses that considered the performance of lower-temperature operating modes are described in *FY01 Supplemental Science and Performance Analyses* (BSC 2001a; BSC 2001b).

2.1 ENGINEERING AND DESIGN ANALYSIS

Design development for the potential repository follows a structured approach that links statutory, regulatory, and derived requirements to the final design products. Design work has been performed in accordance with a quality assurance program (DOE 2000a). This program has been reviewed and accepted by the U.S. Nuclear Regulatory Commission (NRC). Figures 2-2, 2-3, and 2-4 discussed in the following section, illustrate the steps in the design process.

2.1.1 Design Process

This section describes the design process, including how requirements are identified and passed down to individual systems through an established document hierarchical system and how systems are analyzed and then classified according to their importance to preclosure radiological safety.

2.1.1.1 Allocation of Yucca Mountain Site Characterization Project Requirements

The framework for the design of the major repository structures, systems, and components is consistent with the following:

- The Nuclear Waste Policy Act of 1982 (42 U.S.C. 10101 et seq.)

- 10 CFR Part 63 (Disposal of High-Level Radioactive Wastes in a Proposed Geologic Repository at Yucca Mountain, NV) (66 FR 55732)

Legend

CRWMS RD	Civilian Radioactive Waste Management System Requirements Document
MGR RD	Monitored Geologic Repository Requirements Document
MGR PDD	Monitored Geologic Repository Project Description Document
SDDs	System Description Documents
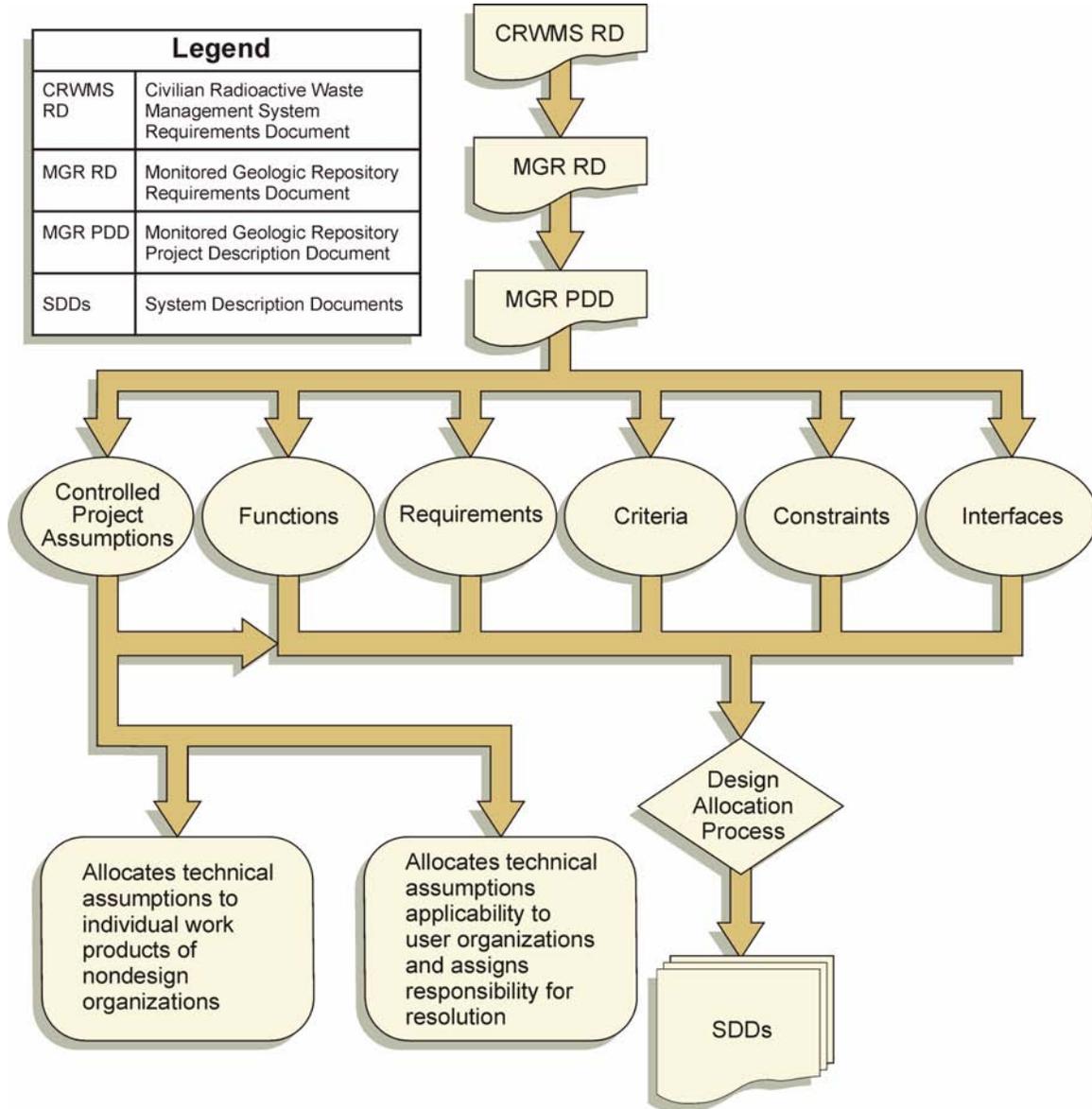
00033DC_ATP_Z1S21_Fig-02d.cdr

Figure 2-2.   Allocation of Functions, Criteria, and Requirements
Design activities for the repository follow a hierarchical system of allocation of functions from the high-level requirements documents to the individual systems. The functions, requirements, and criteria for each individual system are described in the System Description Document for that system. Source: Curry 2001, Section 1.7.
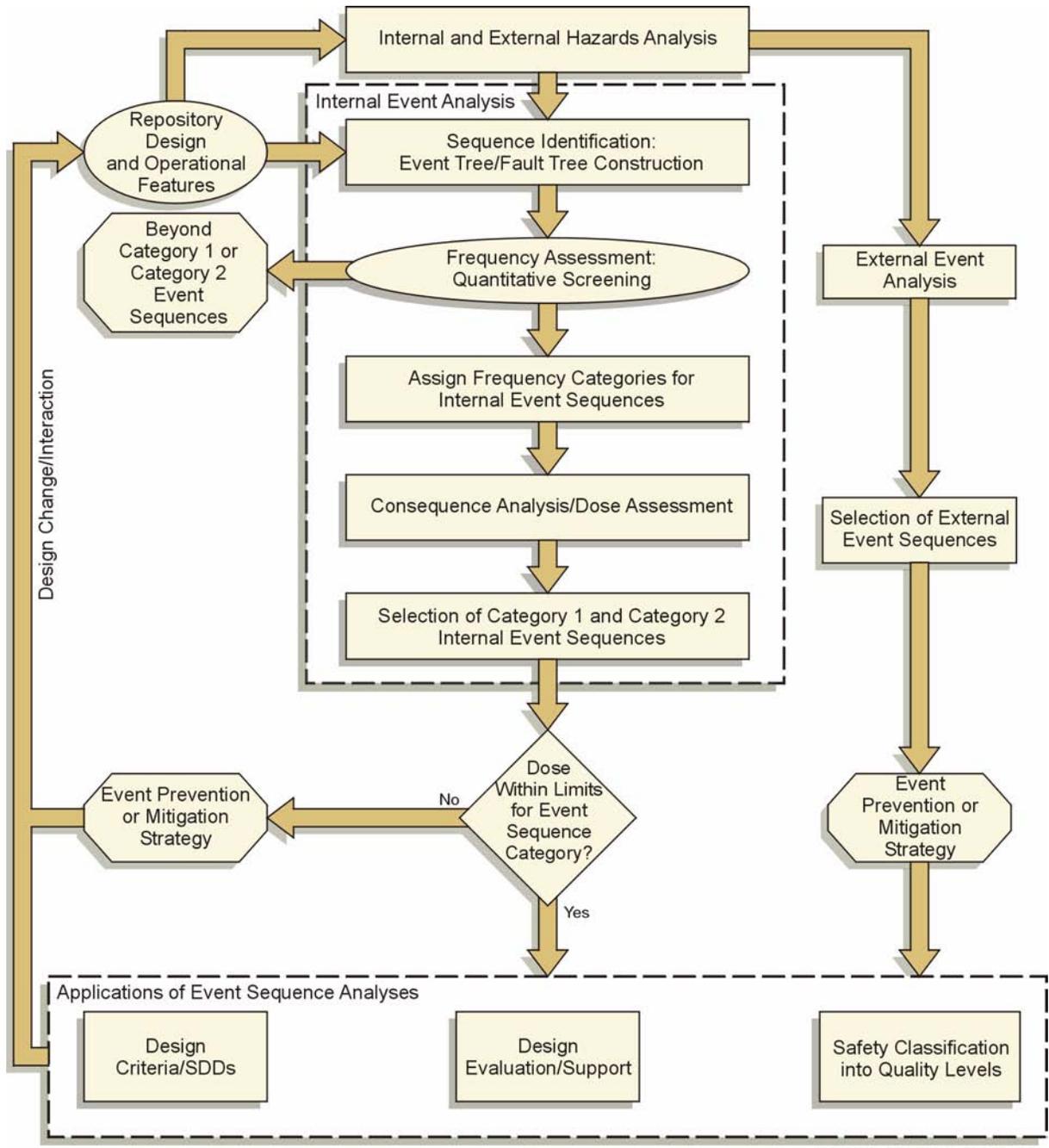
Figure 2-3.   Preclosure Safety Analysis Process
Each repository structure, system, and component is subjected to a preclosure safety analysis process that identifies events that are important to radiological safety. The analysis determines the probability of those events, whether they would result in a release of radiation, and the potential consequence of events that would. Structures, systems, and components are then classified into quality levels. SDD = System Description Document. Source: BSC 2001f, Section 5.2.

00033DC_ATP_Z1S21_Fig-04d.cdr
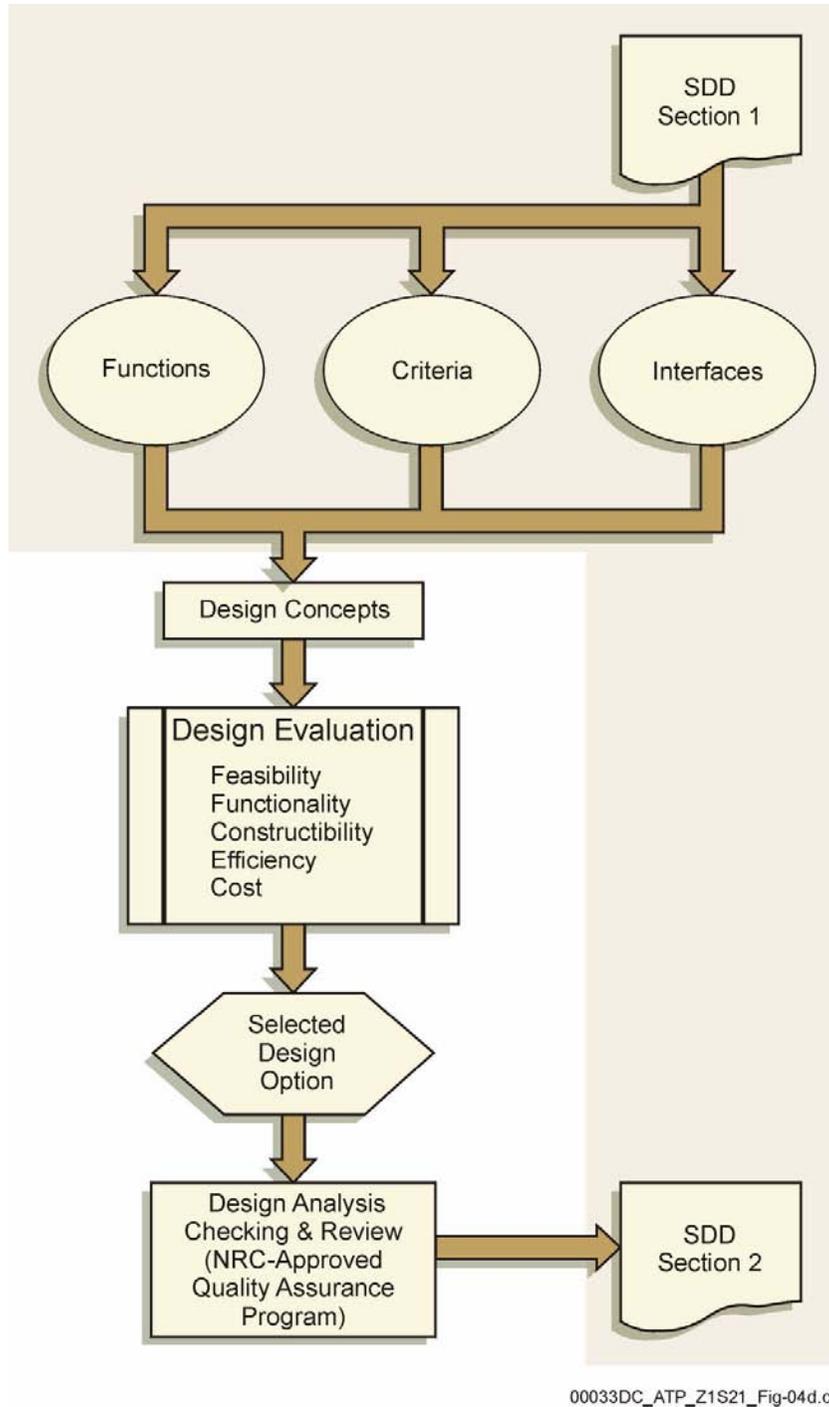
Figure 2-4.   Design Documents Development
This figure illustrates the relationship between the system description document and the design analysis, as described in the *Monitored Geologic Repository Project Description Document* (Curry 2001). There is a somewhat parallel development of these two activities, with Section 1 of the System Description Document dictating design requirements to the design analysis. Once the design analysis is completed, the results are rolled into Section 2 of the System Description Document as a design description and requirements compliance section. At the end of the process, the System Description Document contains a complete set of design information for its system. SDD = System Description Document.

- 10 CFR Part 20 (Energy: Standards for Protection Against Radiation)

- 10 CFR Part 73 (Energy: Physical Protection of Plants and Materials)

- 10 CFR Part 71 (Energy: Packaging and Transportation of Radioactive Material)

- 40 CFR Part 197 (Protection of Environment: Public Health and Environmental Radiation Protection Standards for Yucca Mountain, Nevada).

The DOE has published a comprehensive hierarchy of design documents for a monitored geologic repository. The primary document is the *Civilian Radioactive Waste Management System Requirements Document* (DOE 2000b). Requirements in that document applicable to the repository site are allocated to the *Monitored Geologic Repository Requirements Document* (YMP 2000a). The hierarchy then branches into specific areas of scope, becoming more detailed with each level of document, from the *Monitored Geologic Repository Project Description Document* (Curry 2001) to a set of System Description Documents. The *Monitored Geologic Repository Requirements Document* (YMP 2000a) captures top-level functions and requirements. *Monitored Geologic Repository Project Description Document* (Curry 2001) documents the functions, requirements, criteria, and assumptions for a potential repository while allocating each to the appropriate systems, as detailed in the System Description Documents. For instance, the guidance for blending spent nuclear fuel assemblies to achieve a maximum thermal output of 11.8 kW per waste package at the time of emplacement is contained in the *Monitored Geologic Repository Project Description Document* (Curry 2001). This document also includes controlled assumptions and captures performance criteria and design constraints. In this way, it supplements the higher-level approach of the *Monitored Geologic Repository Requirements Document* (YMP 2000a). Figure 2-2 illustrates this transfer of requirements from higher-level to lower-level documents, as well as the allocation of functions, requirements, and criteria by the *Moni-*

tored Geologic Repository Project Description Document (Curry 2001) to individual systems.

The requirements documents also include references to codes and standards applicable to specific structures, systems, and components. These codes and standards are generally developed by professional organizations, such as the American Society of Mechanical Engineers or the American Nuclear Society, in cooperation with the American National Standards Institute.

2.1.1.2 Safety Classification of Structures, Systems, and Components

The design components of the repository system would contribute to performance in varying degrees. Certain design components of the system are more important to safety of preclosure operations, as described in *Preliminary Preclosure Safety Assessment for Monitored Geologic Repository Site Recommendation* (BSC 2001f). Other design components are more important to postclosure performance, as shown by performance assessment sensitivity studies (e.g., Section 4.4.5). Considerations of safety margin and defense in depth, insights from analogues, and expert judgments also help identify the importance of repository components to performance (see Section 4.1). Knowledge of how components of the system affect performance can provide insights on how design or operating mode features could be developed in a manner that could contribute to long-term performance or mitigate potentially adverse conditions.

The definitions of design criteria and requirements are influenced by a consideration of the importance of each system, its structures, and its components in the overall safety strategy for the potential repository. That safety strategy has been developed over the years based on determinations of critical factors in design with respect to preclosure safety and postclosure performance. The structures, systems, and components important to preclosure safety are identified through engineering analyses and relate directly to the health and safety of facility workers, the health and safety of the public, and the environment. The factors important to postclosure performance are determined through

evaluations of the importance of the components to overall system performance. These evaluations include total system performance assessment (TSPA), considerations of safety margin and defense in depth, and independent, multiple lines of evidence. These evaluations integrate the performance of natural barriers (i.e., the geologic environment) and man-made barriers (e.g., the drip shield and waste package outer barrier) with respect to their complementary attributes in containing and isolating radioactive waste over long periods of time.

For the preclosure period, the importance of design features is defined in terms of their role in preventing or controlling radiological exposure to repository workers and the public. The design of these features must address the health and safety requirements associated with radiological work. The more important a design feature is to ensuring radiological safety, the more process controls are imposed on that design. To the maximum extent practicable, the design of potential repository structures, systems, and components has been developed from the design of structures, systems, and components already in use at other licensed nuclear facilities. The standards used in the designs of such facilities are well developed.

Following the process summarized in Figure 2-3, structures, systems, and components are classified to define their importance to preclosure safety. Event sequences form the basis of these safety classifications. This process is integrated in the sense that all structures, systems, and components important to safety are analyzed for event sequences that represent a complete set of bounding conditions. This set of events results from scenario analysis and grouping of the internal and external hazards. The preclosure safety assessment integrates safety evaluations through a joint consideration of safety measures that otherwise might conflict, including but not limited to integration of fire protection, radiation safety, criticality safety, and chemical safety measures. Event sequences include natural or human-induced events that are reasonably likely to occur and that could lead to exposure of individuals to radiation. Event sequences also include other natural or human-induced events that are unlikely but suffi-

ciently probable to warrant consideration (i.e., that have at least 1 chance in 10,000 of occurring before permanent closure of the repository).

Event sequences could be internal (e.g., collision, loss of power, or fire) or external (e.g., earthquake, tornado, or flood). A potential bounding event sequence (i.e., the one resulting in the worst failure) is identified for analysis of a particular structure, system, or component. The frequency of occurrence of that event sequence determines its event credibility (probability) and category. An engineering analysis is then performed to determine whether a radiological release could result from the failure of a structure, system, or component because of a credible event. These analyses are performed with mathematical and analytical models of processes and events. The consequences of the release are evaluated to determine whether the resulting doses are within regulatory limits and, if not, what preventive or mitigating measures are required to bring the radiological consequences within compliance limits. Structures, systems, and components required to meet regulatory limits are classified as important to safety. Once the safety classifications are defined, individual systems are ranked based on the importance to safety of the performance of their structures and components. The process depicted in Figure 2-3 is iterative in nature and results in a safety analysis that is integrally tied to the facility design (BSC 2001f, Section 5.2).

This report focuses on the most important systems, those that could adversely affect worker and public safety if they failed. To this end, potential systems have been evaluated for their importance to safety and classified into four groups of quality levels, as defined in the *Preliminary Preclosure Safety Assessment for Monitored Geologic Repository Site Recommendation* (BSC 2001f, Section 4.4.1):

- **Quality Level (QL)-1:** Those structures, systems, and components whose failure could directly result in a condition adversely affecting public safety. These items have a high safety or waste isolation significance.

- **QL-2:** Those structures, systems, and components whose failure or malfunction could

indirectly result in a condition adversely affecting public safety, or whose direct failure would result in consequences in excess of normal operational limits. These items have a low safety or waste isolation significance.

- **QL-3:** Those structures, systems, and components whose failure or malfunction would not significantly impact public or worker safety, including those defense in depth design features intended to keep possible radiation doses as low as is reasonably achievable (ALARA). These items have a minor impact on public and worker safety and waste isolation.

- **Conventional Quality (CQ):** Those structures, systems, and components not meeting any of the criteria for QL-1, QL-2, or QL-3. CQ items are not subject to the requirements of *Quality Assurance Requirements and Description* (DOE 2000a).

The preclosure safety analysis process is shown in Figure 2-3. Event sequences are classified as Category 1 or Category 2, based on the frequency of the entire event sequence (also known as the scenario frequency). The frequency ranges for each event sequence category, given in Table 2-1, correlate with the probability-based definitions from 10 CFR 63.2 (66 FR 55732), assuming for the purpose of analysis a period of 100 years before repository closure (BSC 2001f, Section 5.2).

2.1.1.3   System Description Documents

Monitored Geologic Repository Project Description Document (Curry 2001, Section 4) captures, by logical groupings, the hierarchical arrangement of the repository design documents. In that hierarchy, the repository is divided into three major systems, each with several secondary systems, as follows:

- Waste Handling System
  – Carrier/cask shipping and receiving systems
  – Waste preparation systems
  – Waste treatment systems
  – Waste emplacement and retrieval systems

- Waste Isolation System
  – Engineered barrier system
  – Natural barrier system
  – Performance confirmation system

- Operational Support System
  – Underground development system
  – Management and administrative systems
  – Safety and security systems
  – Nonradiological waste systems
  – Utility systems
  – Transportation systems (onsite).

The secondary systems are discussed further in this section, since they relate to the surface and subsurface design descriptions. The complete arrangement for all the potential repository systems is described in Section 4 of *Monitored Geologic*

Table 2-1. Event Sequence Frequency Categories

Event Sequence Category	Frequency of Occurrence	10 CFR 63.2 Definition
1	One or more times before permanent closure	A series of actions and/or occurrences within the natural and engineered components of a geologic repository operations area that could potentially lead to exposure of individuals to radiation and that are expected to occur one or more times before permanent closure of the geologic repository operations area.
2	At least 1 chance in 10,000 of occurring before permanent closure.	Other event sequences that have at least 1 chance in 10,000 of occurring before permanent closure of the geologic repository.

Source: BSC 2001f, Section 5.2.1.

Repository Project Description Document (Curry 2001).

Each repository system would eventually have a complete System Description Document. Figure 2-4 illustrates the relationship of a System Description Document to the design process. Section 1 of a System Description Document defines the system functions, criteria, requirements, constraints, and interface requirements with other systems, as applicable to that system's structures and components.

Given this set of information, the design engineer develops design concepts that fulfill the system needs; those concepts are subjected to additional evaluations, including technical feasibility, functionality, constructibility, cost, and operations and maintenance efficiency analyses. These analyses identify the selected design option. Selected design options may be subjected to further scrutiny such as ALARA evaluations for radiological exposures.

The design work is documented in calculations, technical reports, and design analyses that are submitted for independent reviewers to check and for impacted organizations to review, following a rigorous NRC-approved quality assurance program. Design documents are revised to incorporate checking and review comments, then rechecked for conformance to checking and design review comment resolutions before approval.

Section 2 of a System Description Document summarizes the design information contained in the approved design documents with a description of the system, its structures, and its components. Section 2 of each System Description Document also includes a demonstration of how the system criteria and requirements are fulfilled by the selected design for systems important to radiological safety.

2.1.2 Design and Operational Mode Evolution

Refining the design for the potential repository and the mode in which the design is operated has been an ongoing, iterative process involving scientists, engineers, and decision-makers. The design and

mode of operations of a potential Yucca Mountain repository has evolved as more has been learned about the site and the performance contribution of design attributes and operational objectives.

Previous studies have investigated repository operating modes, layout, and performance considerations for a range of thermal conditions. Mansure and Ortiz (1984) developed evaluations of areas that could be used for expansion of the repository conceptual design footprint based on uncertainty of rock characteristics. This information was used in *Environmental Assessment Yucca Mountain Site, Nevada Research and Development Area, Nevada* (DOE 1986c) and the *Site Characterization Plan Yucca Mountain Site, Nevada Research and Development Area, Nevada* (DOE 1988). Building on this information, alternative design concepts were presented in *Viability Assessment of a Repository at Yucca Mountain* (DOE 1998, Volume 2, Section 8.3.2). *Viability Assessment of a Repository at Yucca Mountain* (DOE 1998) described the evolution of the repository design from the *Site Characterization Plan Conceptual Design Report* (SNL 1987) to the publication of the Viability Assessment. This section briefly discusses the evolution of the repository design and the range of thermal operations, from the publication of the Viability Assessment in December 1998 to the present. Descriptions of the design and mode of operations used in performance evaluations are covered in more detail in Sections 2.2 through 2.5 and in Section 3 to assist in understanding the design.

The DOE initiated an effort to evaluate a range of alternative design concepts and operational performance objectives during the License Application Design Selection process. This process culminated with the selection of what was referred to as the "license application design" (CRWMS M&O 1999c) and the subsequent analyses and designs for the selected design alternative, Enhanced Design Alternative II (CRWMS M&O 1999d). The Enhanced Design Alternative II concept was modified to remove backfill from the emplacement drifts and add operational performance objectives for thermal loading and ventilation (Wilkins and Heath 1999; Stroupe 2000). This design selection process considered a range of thermal conditions.

The Enhanced Design Alternative II design concept and mode of operations provide a moderate repository environment compared to the design described in the Viability Assessment. The Enhanced Design Alternative II design would keep the spent nuclear fuel cladding temperature below 350°C (662°F), a design requirement established to maintain the integrity of the cladding, and keep the boiling fronts from coalescing in the rock pillars between the emplacement drifts. To achieve the operational objective of keeping the boiling fronts from coalescing in the rock pillars, the ventilation rate in the emplacement drifts was increased, which allowed the spacing between waste packages to be reduced.

The design of structures, systems, and components and the methods used to operate and maintain these structures, systems, and components are distinct but interrelated in their developmental and evolutionary processes. Sensitivity analyses have been performed to identify design features and operational objectives that contribute to the isolation of waste or reduce uncertainty in performance analyses. In the design evaluation process described above, the design features and operational objectives were evaluated together to identify the combination of design features and the range of operational objectives that might enhance the performance of the potential repository system.

The draft environmental impact statement (EIS) for the potential Yucca Mountain repository recognized the potential for operating modes spanning a range of lower temperatures and presented results of analyses of the impacts associated with the range of thermal loadings (DOE 1999a, Appendix I, Section I.4.2). The conceptual layouts analyzed for the draft EIS for the different thermal load scenarios and inventories were developed considering the TSPA model domains and a number of rock areas within which the emplacement drifts would be located. The repository and emplacement areas for the higher- and lower-temperature operating modes with a 70,000-MTHM inventory are illustrated in Figures 2-5 and 2-6. Repository layouts for the draft EIS high, intermediate, and low thermal load scenarios are illustrated in Figure 2-7. The figure also illustrates, for comparative purposes, the layout for the higher-temperature operating mode described in this report.

A more detailed analysis of the lower-temperature operating modes resulted in a repository layout (see Figure 2-10) capable of accommodating the 70,000 MTHM and 97,000 MTHM inventories within the primary and lower blocks (BSC 2001g). This analysis also included parametric studies and layout sensitivity analyses for a wide range of repository thermal operating modes. The postclosure performance assessment for this new layout was discussed in Volume 2 of *FY01 Supplemental Science and Performance Analyses* (BSC 2001b). The layout is also described in the final EIS.

The various components of the repository system would contribute to performance in different ways. Certain components of the system are more important to performance than others, as shown by performance assessment sensitivity studies (e.g., Section 4.4.5). Considerations of safety margin and defense in depth, insights from analogues, and expert judgments also help identify the importance of repository components to performance. Knowledge of how components of the system affect performance can provide insights on how design features or the operating mode could be developed in a manner that contributes to long-term performance or could mitigate potentially adverse conditions.

2.1.2.1 Summary of Evolution of Design Features

From the issuance of *Viability Assessment of a Repository at Yucca Mountain* (DOE 1998) to the present, some design features in surface, subsurface, and engineered barrier systems and in the waste package have evolved. This section summarizes the evolution of these features.

Surface Facilities—The design of the surface facilities has evolved in two areas since the publication of the Viability Assessment (DOE 1998). The design of the Waste Handling Building has evolved to include an expanded-capacity spent nuclear fuel blending pool. The number of assembly and canister transfer lines was reduced to two assembly transfer lines and one canister
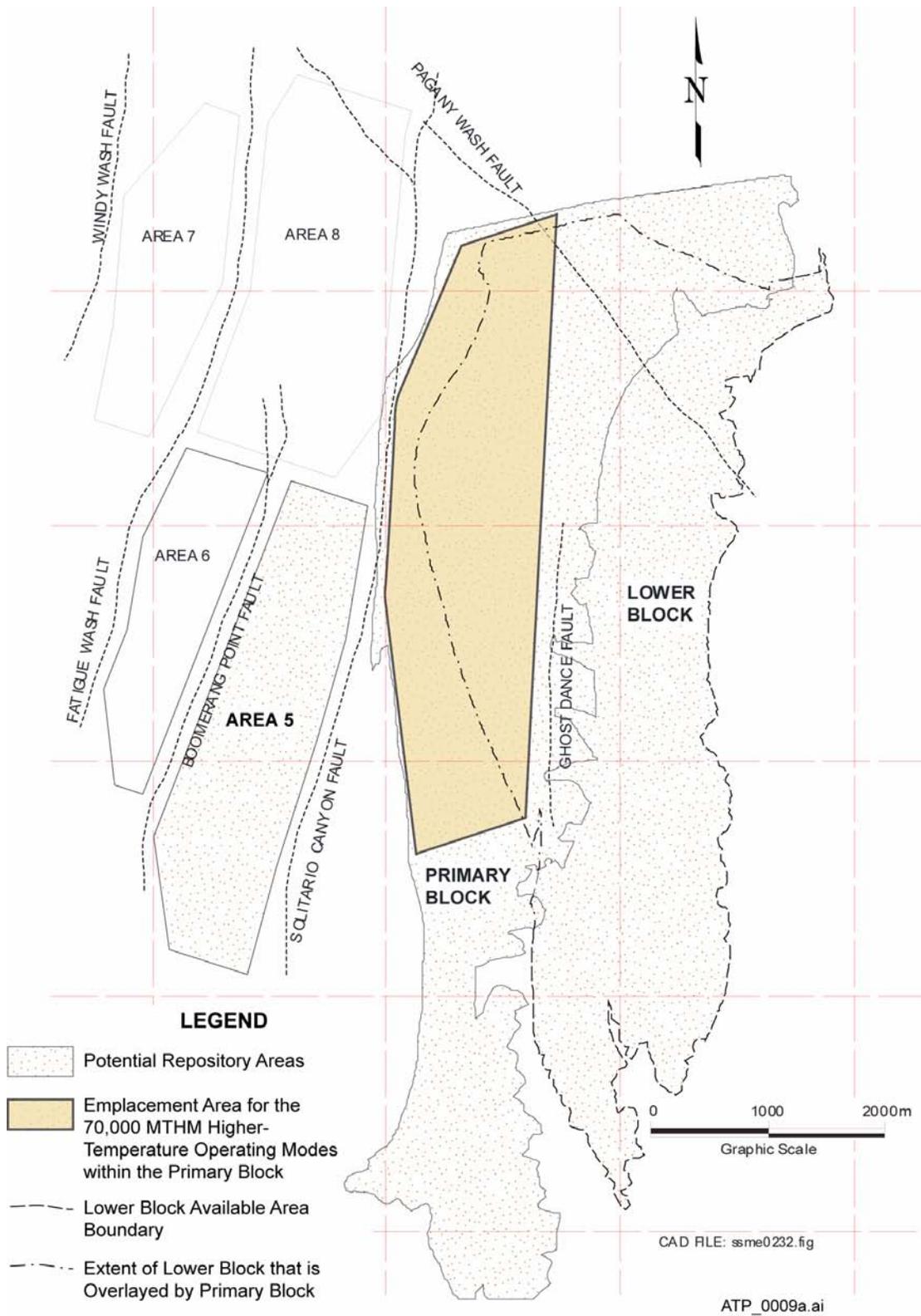
Figure 2-5.   Potential Repository Areas and Emplacement Area for the Higher-Temperature Operating Modes

The emplacement area shown within the primary block would accommodate 70,000 MTHM in higher-temperature operating modes. Source: Modified from BSC 2001d; CRWMS M&O 2000d; and CRWMS M&O 2000j.
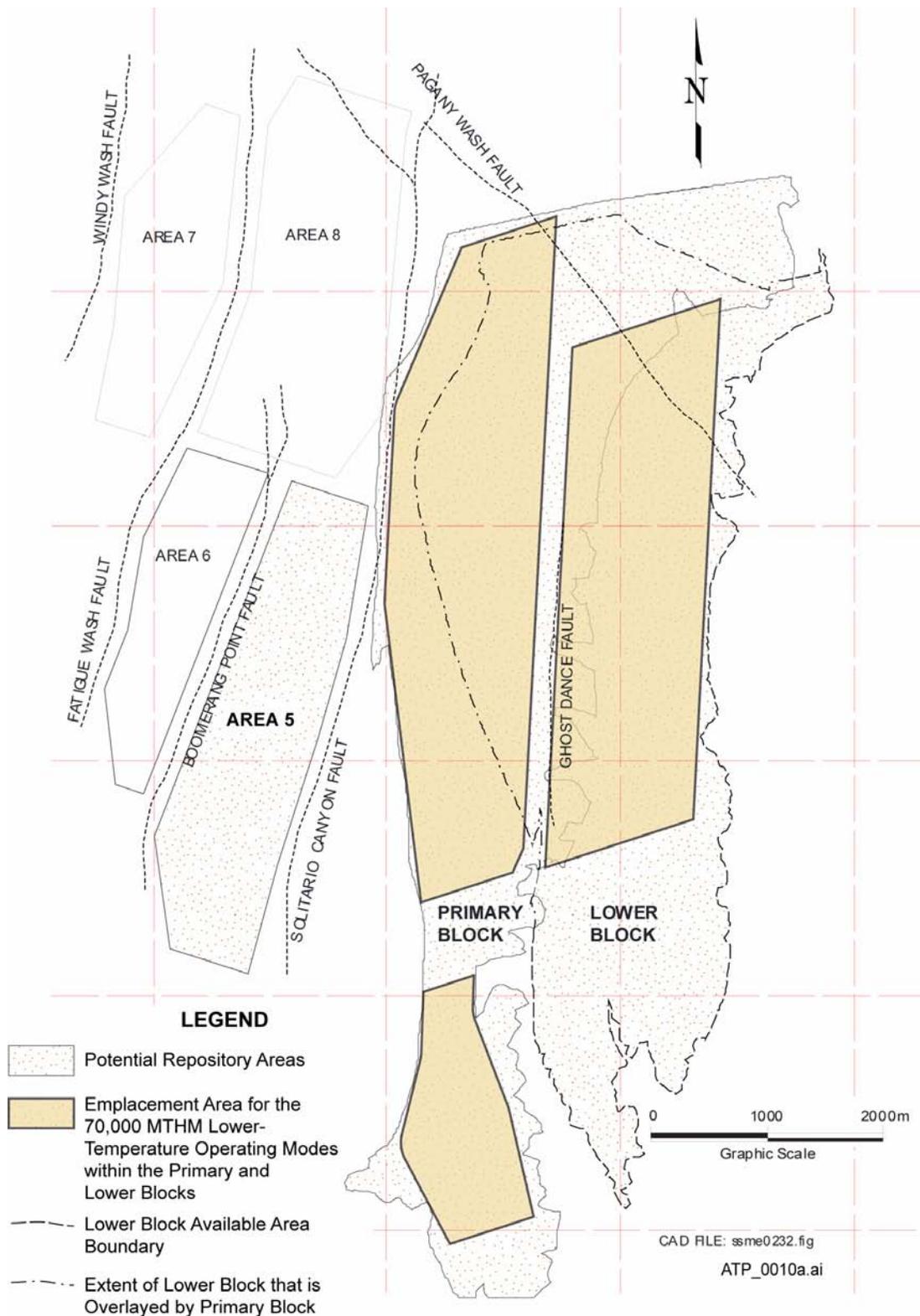
Figure 2-6. Potential Repository Areas and Emplacement Area for the Lower-Temperature Operating Modes

The emplacement areas shown within the primary and lower blocks would accommodate 70,000 MTHM in lower-temperature operating modes. Source: Modified from BSC 2001d; CRWMS M&O 2000d; and CRWMS M&O 2000j.
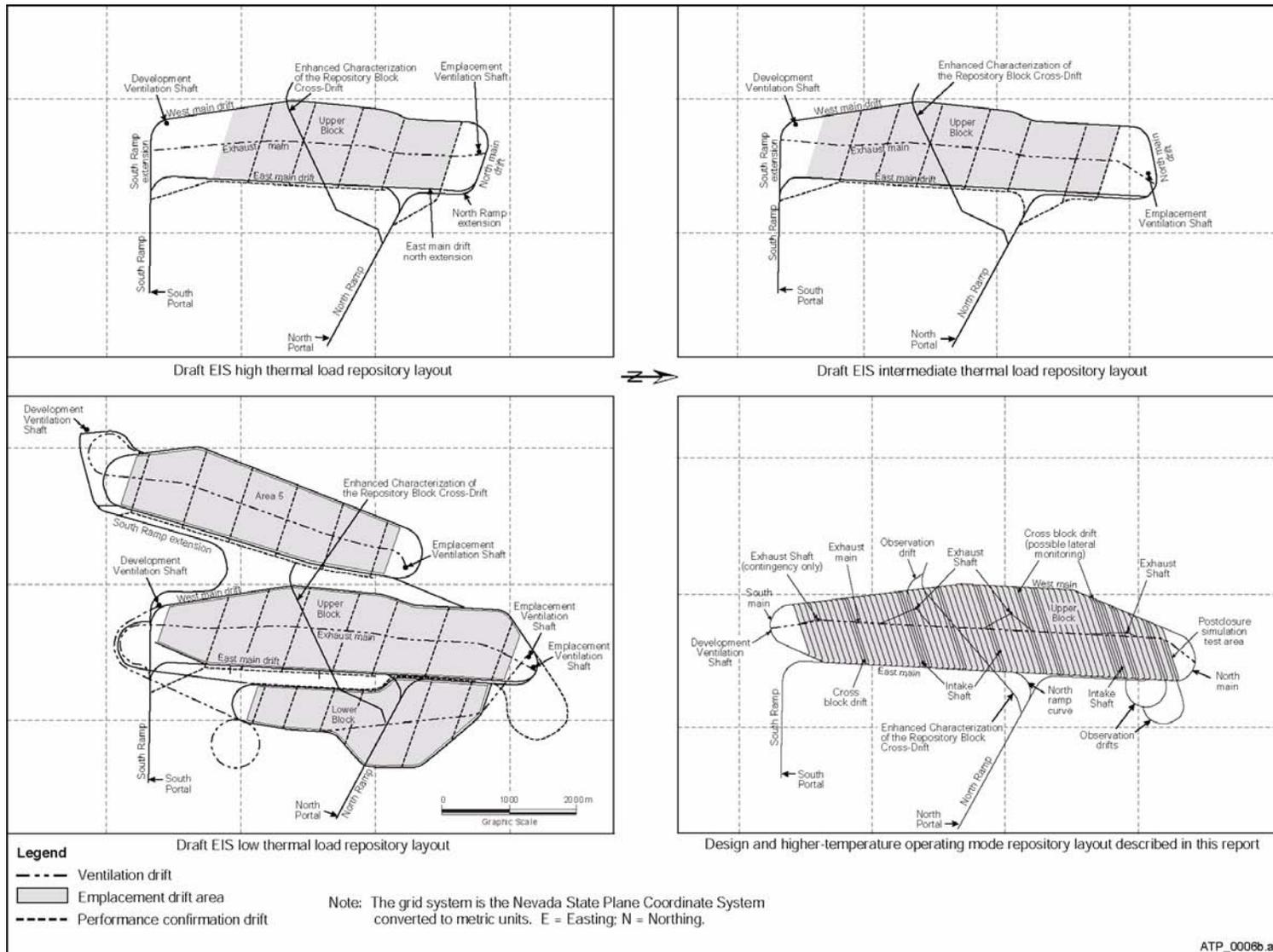
Figure 2-7.   Repository Layouts for the Draft Environmental Impact Statement for High, Intermediate, and Low Thermal Load Scenarios and the Design for the Higher-Temperature Operating Mode

Source: High, intermediate, and low thermal load scenario repository layouts for the draft EIS modified from DOE 1999a, Figures 2-14, 2-15, and 2-16.

transfer line; the design described in the Viability Assessment included three assembly transfer lines and two canister transfer lines. The fuel blending strategy is presented in Section 2.2.1. Also, a solar power generating facility was added to supplement power from the site, which gets its power from the southern Nevada grid.

Subsurface Facilities and the Emplacement Drift Portion of the Engineered Barriers—The evolution of the subsurface facilities design has introduced several changes since the VA design, mainly to permit operating the repository to accommodate a range of thermal conditions. The most significant design change relates to thermal loading (the allowable amount of introduced heat per unit of subsurface emplacement area). The higher-temperature operating mode design described in this report uses a spacing between emplacement drifts of approximately 81 m (266 ft), compared to a spacing of approximately 28 m (92 ft) in the VA design (DOE 1998). Operational parameters, such as waste package spacing and ventilation, can be varied to support flexible thermal goals (see Section 2.1.2). In addition, the design and operating mode used in the performance analyses achieves a more uniform distribution of rock temperatures along the drift, limiting potentially complex thermal-mechanical effects resulting from a varying thermal gradient along the drift axis.

The emplacement drifts were reoriented to increase drift stability. Based on the dominant rock mass joint orientation and a minimum offset criterion of 30° between the joint strike and drift orientation, a reorientation of the emplacement drifts to an azimuth of 252° was established for the design described in this report (BSC 2001d, Section 6.2.2.2).

Emplacement drift backfill and drip shields were added to further limit the possibility of water contacting the waste packages. The backfill concept also offers the waste package protection against rockfall (CRWMS M&O 1999c, Section 4.4.2). The backfill concept was later eliminated because of its potential adverse impact on spent nuclear fuel cladding temperatures. The backfill inhibits heat dissipation into the rock, resulting in

higher waste package temperatures. Granular back-fill placed around the waste packages as a layered system could divert moisture away from the waste package by capillary action (CRWMS M&O 1999c, Section 4.4.2). The drip shield is a metal structure placed over the waste package that serves as a diversion shield for water entering the drift from the rock strata above. The drip shield design concept is described in Section 2.4.

The ground control design concept for emplacement drifts was changed from precast concrete liners with a concrete invert to a combination of steel or ballast invert with steel sets and welded wire fabric, with and without grouted rock bolts. Concerns with the long-term impact of concrete on the alkalinity of the drift environment, along with its implications for corrosion of the engineered barrier and waste package components and for the possible enhancement of colloidal radionuclide transport, motivated this change in the design for ground control in the emplacement drifts. Section 2.3.4.1 describes the ground support system.

The evolution to line-loading of waste packages resulted in modifications in the design and function of the waste package support assembly, from two independent post supports in the VA design to a more substantial emplacement pallet for the entire waste package. This necessitated a change in transporter and emplacement gantry design. The support design simplifies and enhances the reliability of transporting and emplacing waste packages.

Waste Package—Two waste package design attributes have evolved since the publication of the Viability Assessment. The first involves the metallurgy of the inner and outer shells of the waste package. The design described in the Viability Assessment utilized a corrosion-resistant Alloy 22 inner shell and a structurally strong, carbon-steel outer shell. The design described in this report utilizes a corrosion-resistant Alloy 22 outer shell and a structurally strong, stainless steel inner shell. In addition to the enhanced shell design, the waste package has a modified top lid design. A third lid has been added and the lid design has been modified to accommodate stress mitigation techniques in the closure weld area.

2.1.2.2 Summary of Evolution of Operational Parameters

This section presents a summary of the evolution of the operational mode from issuance of *Viability Assessment of a Repository at Yucca Mountain* (DOE 1998) to this report for a range of thermal conditions.

Emplacement Drift Ventilation—The TSPA described in *Viability Assessment of a Repository at Yucca Mountain* (DOE 1998, Volume 3) utilized a mode of operations where the emplacement drift ventilation rate was 0.1 m^3/s (3.5 ft^3/s) after waste package emplacement. This low ventilation rate was not designed to remove heat from the emplacement drifts. This operating mode had temperatures in the host rock throughout the emplacement area above the boiling temperature of water. This zone of above-boiling temperatures extended into the host rock up to approximately 100 m (330 ft) from the emplacement drifts.

To keep the boiling fronts from coalescing in the rock pillars between the emplacement drifts, the ventilation system has to remove approximately 70 percent of the heat generated by the waste packages. Meeting this requirement demands ventilation of the emplacement drifts at an estimated rate of 15 m^3/s (530 ft^3/s) (see Section 2.3.4.3).

Waste Package Spacing—The spacing between the waste packages that was used in the VA evaluations varied depending on both the thermal environment in the emplacement drift and the time-dependent heat output for each individual waste package. The concept behind the spacing was to maintain a fairly uniform linear thermal loading along the length of the emplacement drifts. Since the thermal output of the waste packages varied with the waste form and the age of the waste enclosed, the spacing between the waste packages varied from approximately 1.3 to 9.3 m (4.3 to 30.5 ft). With this spacing, the waste packages could act as point sources for heat in the emplacement drifts.

With the requirement for the ventilation system to remove approximately 70 percent of the heat

generated by the waste packages, the concept of uniform linear thermal loading evolved into a line-loading concept for waste package emplacement. Line loading, that is, placing the waste packages end to end, with a separation of 10 cm (4 in.), achieves a more uniform thermal profile along the length of the emplacement drifts with the ventilation conditions described. The concentration of heat sources resulting from line loading required that the emplacement drifts be spaced farther apart to distribute the thermal load over a larger area.

2.1.2.3 Design and Operating Mode Evolution

The repository design concept described in this document is a flexible design that can be operated over a range of thermal conditions. The future evolution of the design and operating mode will follow a process that includes (1) refining specific design requirements and performance goals to recognize performance-related benefits that could be realized through design and (2) enhancing components of the design to best achieve the performance-related benefits. The iterative design process has focused on improving the understanding of the contribution of design features to the performance of a potential repository. The emphasis of the approach using a flexible design and modes of operation for a potential repository at Yucca Mountain is to understand the impact that a design attribute or operational performance objective has on the performance of the site across a range of environmental conditions. This approach examines the sensitivity of a design parameter to a range of operating temperatures and environmental conditions, and it evaluates the performance and uncertainties associated with the temperature variation. If a design attribute is shown to have a significant impact on the performance of the repository, then the attribute undergoes further evaluation to fully develop the positive contribution or minimize the negative contribution to the performance of the repository.

Sensitivity analyses that consider the performance of a design over a range of thermal operating modes provide information that will guide the future development of the repository design. The evolution of the design will take advantage of

insights gained through the performance analyses. Furthermore, if the performance evaluations indicate benefits to be gained by refinement of the basic design concept on which the performance analyses over the range of operating modes were based, the evolution of the design will take advantage of those insights as well. This flexible design, which will continue to evolve for license application if the site is recommended, will complement a set of operational parameters that can be managed to accommodate thermal characteristics of a waste stream with potentially evolving characteristics. Adjustments can continue based on updated information on waste stream and other repository variables during the very long emplacement period.

The DOE has expanded the assessment of performance of the repository design to better understand how to use reductions in uncertainty to improve the design. The DOE is further expanding the range of thermal operating modes by assessing the performance of a potential repository operated to achieve lower temperatures. The TSPA described in Section 4 of this report utilizes an operating mode where the walls of the emplacement drifts are above the boiling temperature of water. Results of preliminary engineering evaluations show that the design can also be operated in a lower-temperature mode (CRWMS M&O 2000k). The results of these preliminary evaluations have been further corroborated with more detailed calculations and analyses presented in the following documents:

- *Calculation of Potential Natural Ventilation Airflows and Pressure Differential* (CRWMS M&O 2000l)

- *ANSYS Calculations in Support of Natural Ventilation Parametric Study for SR* (BSC 2001h)

- *Thermal Management Analysis for Lower-Temperature Designs* (BSC 2001i)

- *Lower-Temperature Subsurface Layout and Ventilation Concepts* (BSC 2001g).

- *Thermal Hydrology EBS Design Sensitivity Analysis* (BSC 2001j).

The effect of heat on the performance of the repository and the associated uncertainties are subjects of ongoing studies. These studies are considering ranges of drift wall temperatures from as high as 200°C (390°F) to below the boiling point of water (96°C [205°F] at the elevation of the emplacement horizon). The performance assessment in the Viability Assessment (DOE 1998, Volume 3) was based on a design that allowed drift wall temperatures to exceed 200°C (390°F). An objective of the operating mode described in this report is to maintain temperatures in a portion of the rock between the emplacement drifts below the boiling point of water. More recent design studies include sensitivity analyses that evaluate repository performance limiting all drift wall temperatures below the boiling point of water (BSC 2001g; BSC 2001h; BSC 2001i; BSC 2001j; CRWMS M&O 2000l). Lower-temperature operating modes to reduce uncertainty about corrosion rates associated with waste package performance have been evaluated in *FY01 Supplemental Science and Performance Analyses* (BSC 2001a; BSC 2001b). These evaluations have considered waste package temperatures as low as 85°C (185°F).

The evaluation of the performance characteristics of the proposed repository design over a range of operating conditions is an important step in the evolution of the design of a potential repository at Yucca Mountain. While certain details of design are needed to understand the environmental conditions as input to the performance analyses, future evaluations will recognize and be based on the performance implications of the design and accompanying range of operating modes.

2.1.3 Design Flexibility

The design described in this report is part of an overall waste management system that is flexible, continues to evolve, and can adapt to various construction and operational conditions.

In this report, the phrase "flexibility in design" refers to capabilities inherent in the repository design to accommodate changing conditions, such as unanticipated underground conditions and new design requirements. The need for flexibility in the

repository design evolves from operational requirements, such as:

- Disposal of a wide range of radioactive waste forms and container sizes, with the understanding that not all details are yet known on waste receipt and delivery schedules (see Sections 2.4 and 3)

- Maintaining a capability to retrieve one or all of the waste packages (see Section 2.3.4.6)

- Maintaining the ability to monitor the facilities and surrounding environment over many years before committing to closure (see Sections 2.3.4.7, 2.5.2, and 4.6.1)

- Maintaining a fuel blending capability to achieve the selected repository thermal goal (see Section 2.2.1)

- Designing a subsurface ventilation system that can be adapted to achieve the selected repository thermal conditions and to adapt to concurrent and continually advancing drift construction and waste emplacement (see Sections 2.1.5 and 2.3.5)

- Defining a larger emplacement area than is expected to be needed to provide flexibility in achieving the selected repository thermal goals (see Section 2.1.4).

Flexibility in the design allows this evolutionary process to continue and to take advantage of the interrelationship between the design and operating mode. Because the specific thermal criteria (e.g., the waste package and drift wall temperature limits) that will be imposed on future design enhancements have not been selected, the repository design must be sufficiently flexible to allow operation under a wide range of thermal conditions. Assessment of performance over a range of thermal conditions will support the definition of specific thermal criteria upon which future design enhancements will be based. There is a possibility that spent nuclear fuel with higher burnup than presently projected would be received. This could lead to a higher integrated heat over the first 1,000 years of emplacement and could change the

predicted temperature profile. The repository would have the flexibility to accept spent nuclear fuel with higher burnup rates.

Key aspects of design flexibility are (1) the ability of the repository design to support a range of construction approaches; (2) the capability to dispose of a wide range of waste container sizes; (3) the ability to support a range of thermal operating modes; and (4) the ability to continue to enhance the design to best achieve performance-related benefits identified through ongoing analyses. The following discussion describes the design's flexibility to accommodate sequential and modular construction of surface and subsurface facilities. Section 2.1.4 describes the design's flexibility to support a range of thermal operating modes.

Sequential and Modular Repository Development—The design of the repository can accommodate modular or sequential construction of surface and subsurface facilities. The phrase "modular or sequential implementation" describes a process in which decisions concerning repository development are made in a stepwise manner: at each step in the process, a decision whether to proceed would be made based on the licensing and regulatory requirements, the funding profile, and operating experience. The next stage of construction would proceed informed by the experience gained from the previous stage.

The DOE has assessed possible benefits of a modular or stepwise approach, which range from the incorporation of lessons learned after each stage of construction to the leveling of annual construction costs (CRWMS M&O 1998a). However, the potential benefits and impacts from modular and sequential construction have not been fully assessed. The DOE has requested that the National Research Council continue the study of possible repository development strategies (Itkin 2000). A report on the results of this study will be provided at a later date, and the DOE will continue to assess this concept for construction activities.

Sequential and modular construction would not be expected to change the design or operational

concepts of a potential repository at Yucca Mountain and would not, therefore, impact an evaluation of repository performance.

2.1.4 Operating Flexibility to Achieve a Range of Thermal Operating Modes

Preliminary engineering evaluations, including *Operating a Below-Boiling Repository: Demonstration of Concept* (CRWMS M&O 2000k) and *Natural Ventilation Study: Demonstration of Concept* (CRWMS M&O 2000m), show that the design described in this report can be operated to support a range of thermal operating modes. For example, the potential repository could be operated in a mode that keeps temperatures below the boiling point of water (96°C [205°F] at the repository elevation); or the potential repository could be operated such that the host rock reaches a temperature that is above the boiling point of water. Drift wall and waste package temperatures and relative humidity can be managed by altering several operational features of the design: (1) varying the thermal load to the repository by managing the thermal output of the waste packages; (2) managing the period and rate of drift ventilation prior to repository closure; and (3) varying the distance between waste packages in emplacement drifts (CRWMS M&O 2000k, Section 3.2). These factors are described in the following paragraphs. Other parameters, such as postemplacement natural ventilation, could also be used to reduce long-term repository temperatures (CRWMS M&O 2000m). Altering design features, such as emplacement drift spacing, could also be used in conjunction with variations in operational parameters to achieve a lower-temperature repository environment.

Recently completed calculations and analyses (BSC 2001j; CRWMS M&O 2000l; BSC 2001h; BSC 2001i; BSC 2001g) support the preliminary findings on the feasibility of operating the repository to meet varying thermal goals by adjusting the three operational features listed above (i.e., controlling the thermal output of the waste packages, adjusting the period of ventilation, or varying the emplacement distance between waste packages).

Since completion of the TSPA-SR analyses, the DOE has performed additional analyses supporting the effects of a range of thermal operating modes on projected system performance. These analyses were described in *FY01 Supplemental Science and Performance Analyses* (BSC 2001a; BSC 2001b). Evaluations of higher- and lower-temperature operating modes in the supplemental TSPA model have provided insight into system performance at the subsystem level over a range of thermal operating modes. While some subsystem models indicated significant differences, results from changing the thermal operating mode showed only a minor impact on overall repository performance. The supplemental model also showed that the repository could be operated at either a higher- or lower-temperature operating mode with a low probability of the development of aggressive chemistries on the waste package and the subsequent potential for localized corrosion.

If the site is recommended for development of a repository, the DOE will utilize the enhanced understanding of repository performance to further improve the repository design for any license application.

Thermal Output of the Waste Packages—The major contributor of heat in the repository would be commercial spent nuclear fuel, which would likely have a wide range of thermal outputs. The thermal load of a repository is directly related to the amount of thermal energy contained in the fuel emplaced in it. The thermal energy contained in the fuel, in turn, is directly related to its age. The age and burnup rate of spent nuclear fuel received for emplacement in a repository would vary considerably, so the current operational plan for the potential repository specifies that the DOE will manage the fuel inventory by one or more of the following features: (1) fuel blending (i.e., placing low heat output fuel with high heat output fuel within a waste package); (2) de-rating (i.e., limiting the number of spent fuel assemblies to less than the waste package design capacity); (3) placing high heat output fuel in smaller waste packages; or (4) aging (i.e., placing hotter fuel into the fuel blending inventory to be emplaced later). Managing the average thermal output of the waste packages through any of these means can control

drift wall temperatures of the repository (CRWMS M&O 2000k, Section 3.2; BSC 2001a; BSC 2001b).

Duration and Rate of Forced Ventilation—During active repository operations, some of the heat generated by the waste and the moisture in the surrounding rock would be removed from the repository by forced ventilation of the loaded emplacement drifts. The amount of energy transferred from the waste to the host rock can be managed by varying the duration and the rate of emplacement drift ventilation (CRWMS M&O 2000k, Section 3.2.3).

Distance Between Waste Packages—The distance between waste packages in emplacement drifts is another design feature that can be modified to manage the temperature in the potential repository. As waste packages are spaced farther apart, the linear thermal density in the drift (measured in kilowatts of heat output per meter of drift length) decreases, delivering less heat per unit volume of the host rock when the drift-to-drift spacing remains fixed (CRWMS M&O 2000k, Section 3.2.2).

Natural Ventilation—Postemplacement natural ventilation could be employed in several lower-temperature operating scenarios. The subsurface ventilation system described in Section 2.3 could support both forced and natural ventilation. To facilitate natural ventilation, the ventilation system would be enhanced through a combination of air balancing techniques, such as adjusting the size of the openings, location and number of intake/exhaust openings, and flow controls (CRWMS M&O 2000m).

2.1.5 Assessing The Performance of a Lower-Temperature Operating Mode

The basic operational features to achieve a lower-temperature repository were described in *Operating a Below-Boiling Repository: Demonstration of Concept* (CRWMS M&O 2000k). That report outlines the relationships between operational parameters such as ventilation and linear thermal load. In subsequent design evaluations (BSC 2001j; CRWMS M&O 2000l; BSC 2001h; BSC

2001i; BSC 2001g), the DOE has used a range of lower-temperature operating mode characteristics to investigate the performance attributes of possible alternative lower-temperature designs and operating modes.

This section describes features of some of these lower-temperature operating modes. These features have been used to assess the performance of a potential lower-temperature repository and the sensitivities of projected performance to different parameters and design features (BSC 2001b). Evaluations of a range of operating temperatures will support the development of a design and operating mode to support any license application. Features of lower-temperature operating modes have also been assessed to support the development of the ranges of design-related environmental conditions required as input to the TSPA analyses.

Design and performance evaluations could include varying the separation between the emplacement drifts (drift-to-drift spacing) to adjust the areal mass loading; increasing the number and diameter of ventilation shafts to improve efficiency; or zone emplacement, which tailors ventilation and design attributes to the thermal output of waste packages emplaced in specific drifts (or zones). The DOE will also examine strategies to reduce ventilation times and meet thermal goals for a lower-temperature operating mode. This could involve lengthening the time to emplace all of the wastes, further reducing areal thermal densities, rearranging emplaced fuel, or combining the aging of fuel with enhanced fuel blending inventory strategies.

Lower-temperature operating modes are being considered for mitigating some of the potential uncertainties in assessing long-term repository performance. There are many ways of combining operational parameters to achieve lower repository temperatures. Figure 2-8 illustrates the variables affecting the thermal performance of the repository, from waste forms to emplacement drifts. Within the constraints imposed by the physical system, the potential repository can be operated in lower-temperature modes while also meeting other technical, policy, regulatory, schedule, and opera-
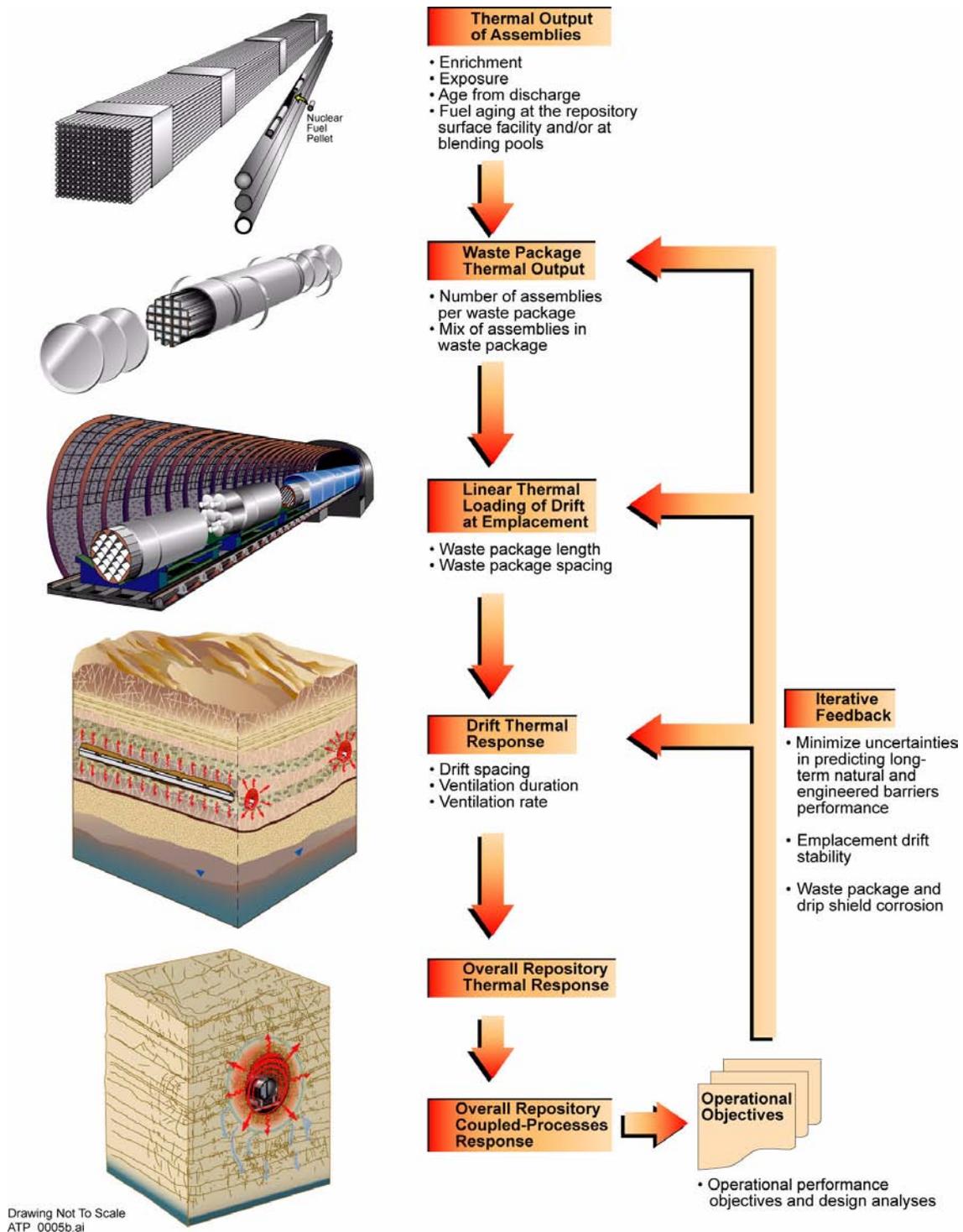
Figure 2-8.   Variables Affecting the Thermal Performance of the Repository
This figure illustrates the variables associated with spent nuclear fuel assemblies, waste packages, and in-drift emplacement, and which affect repository thermal performance. Changing these variables through design modifications or operations directly impacts the repository thermal regime and indirectly impacts the host rock chemical, mechanical, and hydrologic regimes. These impacts, in turn, affect performance of the repository engineered barriers. Evolution of optimal designs and operating modes must include assessments of these changes and impacts on an iterative basis for continuous improvement of repository components. This iterative feedback would continue through the licensing process and into the construction and operational phases of the repository.

tional objectives. Some of these objectives are described in the following paragraphs.

Reduced Uncertainty in Corrosion Rates—The corrosion susceptibility of Alloy 22 may be reduced by either keeping waste package surface temperatures at or below 85°C (185°F) or maintaining in-drift relative humidity below 50 percent (see Figure 2-9) (Dunn et al. 1999, p. xvi; CRWMS M&O 2000n, Section 3.1.3.1). Operating the repository such that the combination of in-drift temperature and relative humidity does not enter the window of corrosion susceptibility of Alloy 22 may result in better overall performance.

Keeping Drift Wall Temperatures Below Boiling—In the higher-temperature operating mode, the rock temperatures within the first several meters around the emplacement drifts exceed the boiling point of water. A possible lower-temperature objective would be to keep all the rock in the repository below the boiling point of water to reduce uncertainties associated with thermal-hydrologic and thermal-mechanical processes.

Capacity for Waste Inventory—Potential objectives are (1) to ensure that 70,000 MTHM can be emplaced within the characterized area and (2) to maintain the flexibility to accommodate up to 119,000 MTHM within the repository area.
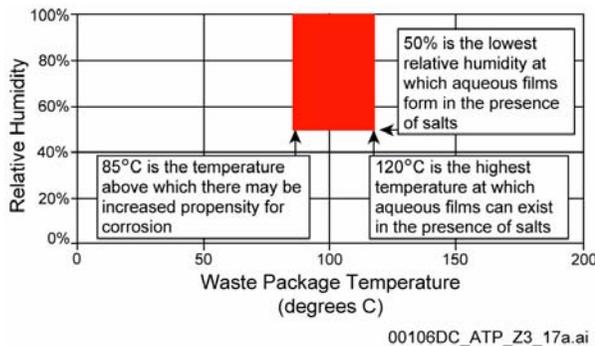
Figure 2-9. **Window of Potentially Increased Susceptibility of Localized Corrosion for Alloy 22**
The temperature–humidity corrosion susceptibility ranges are preliminary and under evaluation and are subject to the results of ongoing testing. Source: Dunn et al. 1999, p. xvi; CRWMS M&O 2000n, Section 3.1.3.1.

However, the smaller the space that is used for inventory, the more reliance must be placed on other means of meeting lower-temperature goals.

Duration of the Ventilation Period—Potential objectives are (1) to provide for closure and sealing of the repository within a prescribed time limit determined by the Secretary of Energy or (2) to allow for natural ventilation to continue after permanent closure of the repository. Allowing some dependence on extended ventilation reduces the area required for disposal of a given amount of waste. However, a design based on centuries of ventilation through air passages connecting the repository to the surface could involve technical issues that would have to be explored.

Thermal Output of the Waste Package—The thermal output of the waste packages can be managed by combining one or more of the following features: (1) fuel blending to produce a thermal loading at or below 11.8 kW per waste package; (2) de-rating the waste packages to produce a thermal loading below 11.8 kW per waste package; (3) placing high heat output fuel in smaller waste packages to produce a thermal loading below 11.8 kW per waste package; or (4) aging spent nuclear fuel assemblies to reduce their heat output.

2.1.5.1 Lower-Temperature Operating Mode—Coupled Operational Parameters

Figure 2-10 illustrates a layout of potential development areas (or blocks) within the characterized area of Yucca Mountain that may be utilized for the emplacement of waste. The shaded areas denote portions of the upper and lower blocks that could be utilized for the emplacement of waste under different operating modes, ranging from higher-temperature to lower-temperature cases corresponding to the examples given in Table 2-2.

The TSPA-SR evaluated the performance of a higher-temperature operating mode. In this mode, as rock temperatures increase above the boiling point of water, moisture around the emplacement drifts evaporates and is driven away from the drifts as water vapor. As described in Section 4.2.2, this
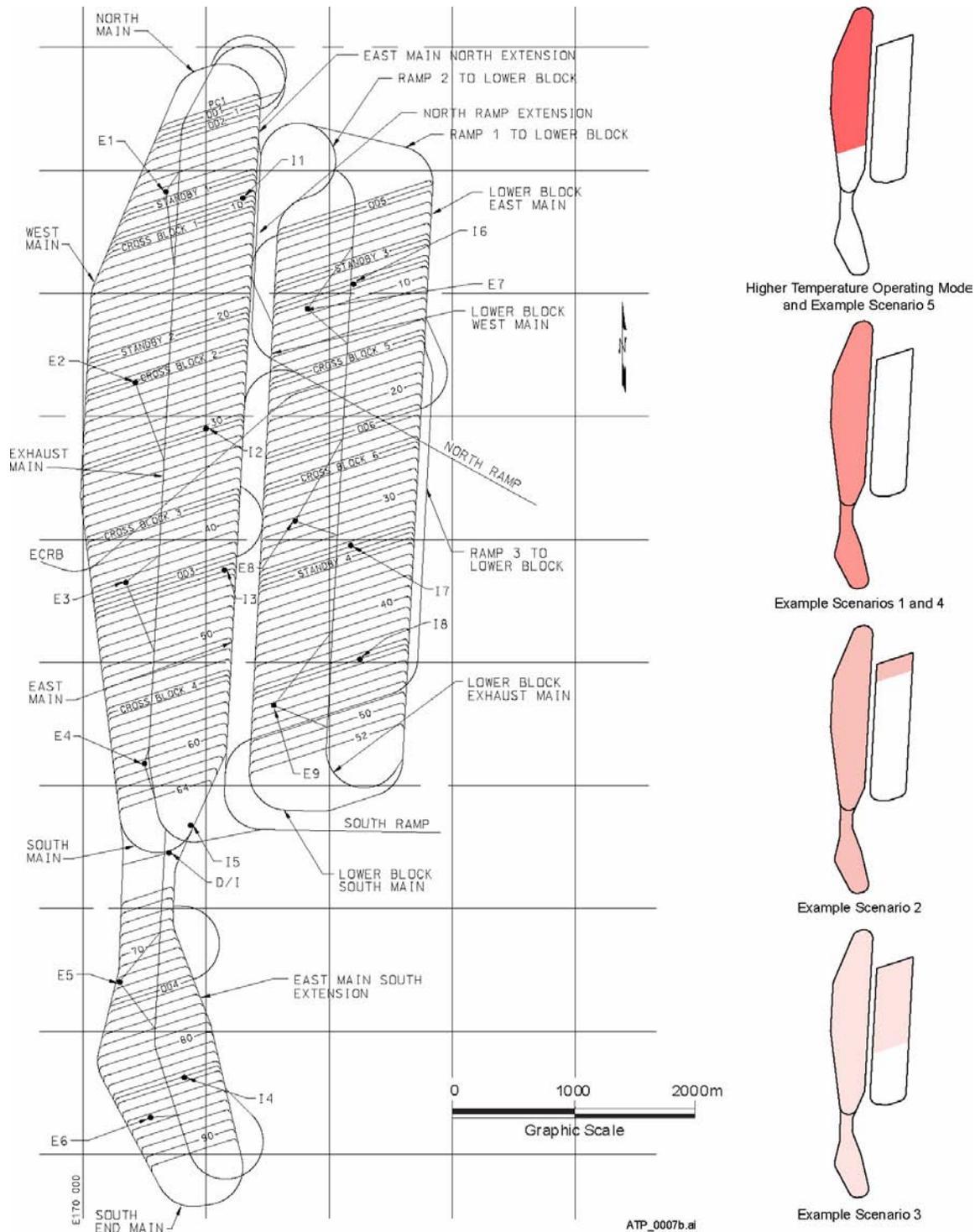
Figure 2-10. Layout of Potential Repository Development Areas, Showing Areas Utilized in Example Operating Mode Scenarios for a Repository Capacity of 70,000 MTHM

The shaded areas on the right denote the portions of the upper and lower blocks that would be utilized for emplacement of waste under different operating modes, ranging from higher-temperature to lower-temperature cases. These five cases are the example scenarios defined in Table 2-2. Dimensions, coordinates, and elevations are given in meters. PC = postclosure test drift; OD = observation drift; I1 = intake shaft; E1 = exhaust shaft; D/I = development/intake shaft; ECRB = Enhanced Characterization of the Repository Block Cross-Drift. Source: Modified from BSC 2001d.

Table 2-2. **Comparison of Estimates of Operational Parameters for Example Lower-Temperature Operating Modes**

Parameters	TSPA-SR Higher-Temperature Operating Mode	Example Scenarios				
		1 Increased Waste Package Spacing and Extended Ventilation	2 De-Rated or Smaller Waste Packages	3 Increased Spacing and Duration of Forced Ventilation	4 Extended Surface Aging with Forced Ventilation	5 Extended Natural Ventilation
Variable Parameters						
Waste package spacing (m)	0.1	2	0.1	6	2	0.1
Maximum waste package thermal loading	11.8 kW	11.8 kW	<11.8 kW	11.8 kW	<11.8 kW	11.8 kW
Linear thermal loading objective (kW/m) at emplacement	1.45	1	1	0.7	0.5	1.45
Years of forced ventilation after start of the emplacement	50	75	75	125	125	75
Years of natural ventilation after forced ventilation period	0	250	250	0	0	>300
Dependent Parameters						
Size of pressurized water reactor waste packages	21 PWR	21 PWR	<21 PWR	21 PWR	21 PWR	21 PWR
Total excavated drift length (km)	~60	~80	~90	~130	~80	~60
Required emplacement area (acres)	~1,150	~1,600	~1,800	~2,500	~1,600	~1,150
Average waste package maximum temperature (°C)	>96	<85	<85	<85	<85	<96

NOTE: PWR = pressurized water reactor.

may have performance benefits because it would delay the time at which liquid water could begin to seep into the emplacement drifts. However, there are heat-related uncertainties about the long-term impact of thermal, chemical, and mechanical effects on the hydrologic properties of the potential repository host rock. Maintaining the repository at lower temperatures (below the boiling point of water) may reduce these uncertainties. Additional analyses of lower-temperature operating modes were performed and are presented in *FY01 Supplemental Science and Performance Analyses* (BSC 2001a; BSC 2001b).

To demonstrate how the DOE can vary operational parameters of the design to manage the thermal load of the repository, a set of preliminary calculations was performed to assess the effects on repository temperatures of the parameters described in the previous section: (1) the age of the spent fuel emplaced; (2) the duration of ventilation;

and (3) the distance between waste packages (CRWMS M&O 2000k; CRWMS M&O 2000m).

The family of operational parameters that would produce average maximum drift wall temperatures below the boiling temperature of water (96°C [205°F]) is shown in Figure 2-11. This figure plots these parametric curves using postloading ventilation duration as the horizontal axis and distance between waste packages as the vertical axis. Each of the labeled curves in this plot represents a different duration of additional aging beyond the average age of the waste stream in the year it is received. The curve with 0 years of aging corresponds to the case where the fuel is emplaced at the rate it is received, without additional aging. The curve for 5 years of aging corresponds to the case where the waste is allowed, on average, an additional 5 years of aging.

An example of how these curves are used can be shown by examining the point on the 10-year aging
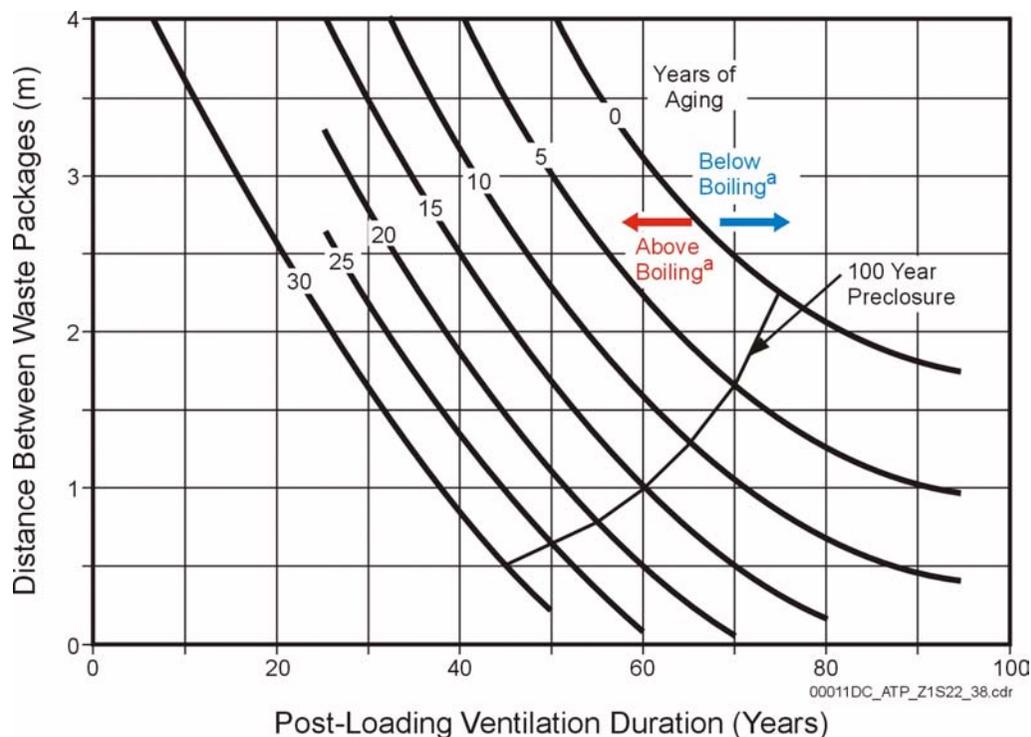
Figure 2-11.   Below-Boiling Repository Operating Curves
[a]The above-boiling and below-boiling arrows are associated with the particular curve indicated and reflect conditions that lie to the left and right of that curve. The arrows may be reproduced for each curve in the figure to reflect where the associated above and below-boiling conditions lie.
This figure illustrates the relationship between two design variables: (1) end-to-end spacing between waste packages in the emplacement drift and (2) average years of aging of the waste prior to emplacement—and how these two variables relate to the duration in years of forced (mechanical) ventilation required to maintain the average maximum host rock temperature below the boiling point of water during preclosure and after closure of the repository. The "years of aging" (bold curved lines) mark the boundary at which the average maximum host rock temperature would exceed the boiling temperature of water at a given increment of waste package spacing, for a given duration of ventilation. For example, for a 1-m (3.3-ft) spacing between waste packages whose waste has been aged for 15 additional years, 60 years of forced ventilation would be required to maintain average maximum rock temperatures below 96°C (205°F) during preclosure and after closure. This figure uses a 100-year preclosure duration as an example to illustrate the combinations of aging and ventilation. Source: CRWMS M&O 2000k, Figure 3-4.

curve for 50 years of ventilation and a waste package spacing of about 2.3 m (7.5 ft). For a drift operated this way, the postclosure emplacement drift wall would reach a peak temperature of just at or below 96°C (205°F). If the drift were to receive fewer years of ventilation, keeping the age of the fuel loaded in the drift and the waste package spacing constant (to the left of the point in question), then the average maximum temperature of the host rock walls would increase above the boiling point of water during the postclosure period. On the other hand, if an emplacement drift were ventilated longer (to the right of the point in question), then the peak temperatures in the emplacement drift rock would be farther below the boiling point of water.

The trade-offs between the operational parameters that can be changed to achieve a below-boiling repository operating mode can be determined from Figure 2-11. For example, if an emplacement drift is loaded with waste packages spaced around 2.3 m (7.5 ft) apart without fuel aging, 75 years of post-loading ventilation is required. If the age of the waste stream is increased by 10 years, a waste package spacing of 2.3 m (7.5 ft) can be used with only 50 years of ventilation. For this case, aging the waste for 10 years saves 25 years of ventilation.

Increasing the duration of aging, however, yields diminishing benefits. As the waste ages appreciably, the rate of decay in heat generation diminishes greatly. Consequently, whether the waste is aged further on the surface or underground in the potential repository makes less and less difference in keeping the drift wall below boiling. The flattening shape of the curves in Figure 2-11 beyond 75 years of ventilation also shows that increasingly longer ventilation periods would be required to remove the same quantity of decay heat from the repository.

2.1.5.2 Example Lower-Temperature Operating Scenarios

Lower-temperature operating modes have been developed to provide options for mitigating some of the potential uncertainties in assessing long-term repository performance. Analyses of the potential performance of lower-temperature operating modes are described in *FY01 Supplemental Science and Performance Analyses* (BSC 2001a; BSC 2001b).

This section describes several possible operating scenarios, each of which meets the primary goals for lower-temperature operating modes described in Section 2.1.5 while achieving one set of possible operating objectives. Table 2-2 compares operational parameters used in the TSPA-SR with operational parameters that could be used to achieve a lower-temperature operating mode.

The following sections compare five examples of lower-temperature operating scenarios. These examples provide a basis for understanding the technical issues associated with developing a lower-temperature operating mode.

2.1.5.2.1 Lower Waste Package Temperature Achieved through Extended Ventilation and Minimal Increase in Disposal Area

By extending the time during which loaded emplacement drifts are ventilated, the repository could be operated at lower temperatures with minimal increase in the disposal area. This section describes two example lower-temperature oper-

ating mode scenarios that are likely to satisfy the following three objectives:

1. Maintain average waste package surface temperatures below 85°C (185°F)

2. Ensure that 70,000 MTHM of waste fits mostly within the upper block, as shown in Figure 2-10

3. Close and seal the repository within approximately 300 years.

Example scenarios 1 and 2 could achieve a lower-temperature operating mode through extended forced and natural ventilation. Example scenario 2 also includes a de-rated waste package.

Example Scenario 1: Increased Waste Package Spacing and Extended Ventilation—In this example, loaded waste packages would be emplaced an average of about 2 m (6.6 ft) apart to create a 1-kW/m drift thermal load at emplacement. The drift-to-drift spacing would remain at 81 m (266 ft), as specified in the design described in this report. For the first 75 years after the start of emplacement, fans would actively ventilate the drifts with an airflow rate of 15 m^3/s per drift. Because of the time required for emplacement, the drifts loaded last would be actively ventilated for 50 years. The repository would be allowed to ventilate naturally for 250 years. Other operational parameters would be unchanged.

Figure 2-12 contains plots of waste package surface and drift wall temperatures over time for the drifts loaded in the final year of emplacement operations under this scenario, as projected by two-dimensional models (BSC 2001h). In the plots shown in Figure 2-12 (also in Figures 2-13, 2-14, and 2-15), the time axis begins after the last emplacement drift is loaded; this results in bounding projections of the maximum waste package and drift wall temperatures in drifts that are loaded earlier in the emplacement period. Descriptions of the repository layout and the changes to the ventilation system that would be required to implement this scenario are discussed later in this section.
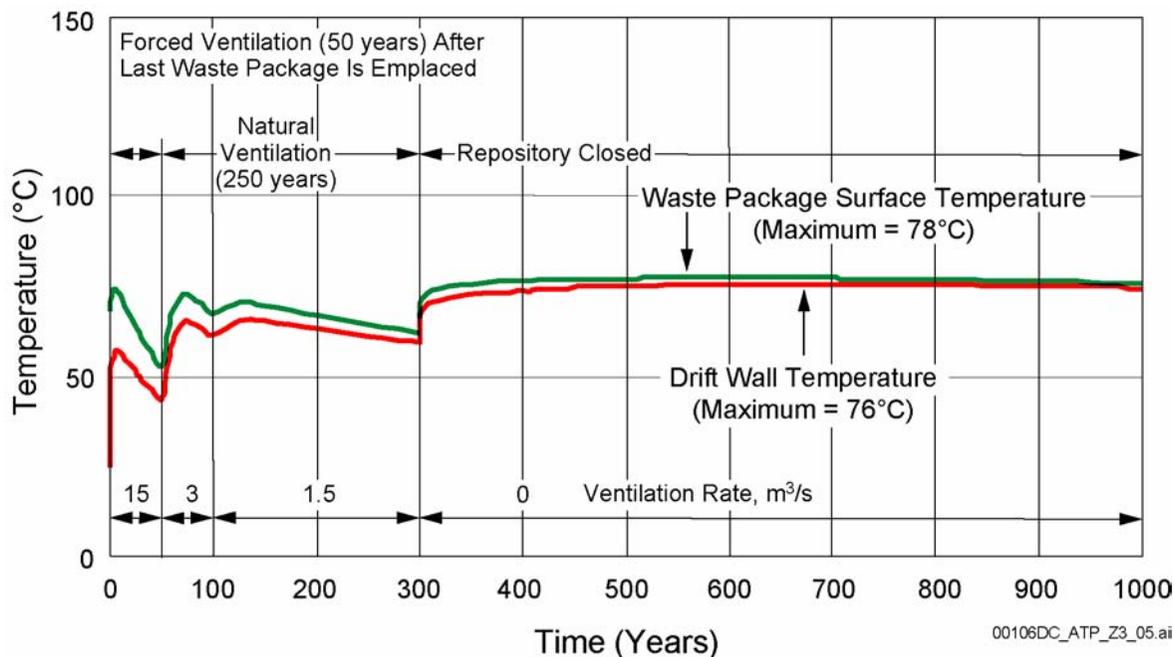
Figure 2-12. Waste Package Surface and Drift Wall Temperatures for an Operational Scenario in Which Drifts Loaded at 1 kW/m in the Last Year of Emplacement Operations are Actively Ventilated for 50 Years and Naturally Ventilated for Another 250 Years
Source: Modified from BSC 2001h, Figure XVII-4.

Some of the implications of this scenario are (1) the flexibility to readily adjust to a higher-temperature operating mode in drifts loaded later by moving waste packages closer together; (2) a requirement for additional drift excavation to accommodate more widely spaced waste packages; (3) increased complexities in projecting the thermal-hydrologic response of the repository because the widely spaced waste packages would act more like point heat sources within drifts; and (4) the programmatic uncertainty associated with the protracted period of natural ventilation.

Example Scenario 2: De-Rated or Smaller Waste Packages—In this scenario, the thermal output of the waste packages is reduced by limiting waste package loading. This can be achieved by limiting the number of spent nuclear fuel assemblies to less than the waste package design capacity (de-rating) or replacing the large waste packages (e.g., ones containing 21 pressurized water reactor fuel assemblies) with smaller waste packages (e.g., ones that would contain 12 pressurized water

reactor fuel assemblies) that have a lower thermal output.

All waste packages would be placed approximately end-to-end within the drifts to create a 1-kW/m linear thermal load at emplacement. Other operational parameters of this scenario are identical to those in Scenario 1. Two-dimensional projections of waste package surface and drift wall temperatures over time are the same as those shown in Figure 2-12.

Figures 2-12 through 2-15 show variations in the waste package and drift wall temperature responses with time. Figure 2-12 illustrates a representative process, as follows.

1. During the forced ventilation period (0 to 50 years), the heating effect of the waste is steadily reduced until the fans are turned off in year 50.

2. From that point, natural ventilation flow continues to remove heat; however, the reduced flow rate (3 m³/s) takes several

years to turn the temperature response to a downward trend (approximately years 70 to 100).

3. The natural ventilation flow rate gradually decreases over time as the waste decays, since the heat from the waste is the main driver in inducing convective currents in airflow. The simplified calculation methods used could not simulate a steady decline in the natural ventilation rate, so this decline was simulated by stepping down the rate in years 100 to 300 from 3 m^3/s to 1.5 m^3/s.

4. The temperature rises from years 100 to approximately 130 due to this abrupt reduction in the natural ventilation flow rate. After year 130, the reduced flow rate starts reducing temperatures until year 300, when the repository would be sealed and closed.

5. At that point, the lack of ventilation induces a steep rise in the drift temperatures until the host rock's capacity to transfer heat away from the waste packages starts to have a regulating effect on drift temperatures and establishes a very slow downward trend in thermal response over a period of 1,000 years or longer.

Note that in the more natural situation of a steady decrease in the natural ventilation flow rate, the calculated thermal response curves would actually show a steady decrease in drift temperatures across most of the natural ventilation period, rather than the variations shown around the 100-year period.

The primary difference between this scenario and Scenario 1 is a potential reduction in the complexity of modeling the thermal-hydrologic response of the repository because the thermal loading would more closely resemble a line load. A second difference is the increase in the number of waste packages needed, which could result in an increase in the total excavated drift length and the total area required for emplacement.

2.1.5.2.2 Lower Waste Package Temperature Achieved through Increased Disposal Area and Limited Ventilation Period

Lower-temperature operating goals can also be achieved with a limited increase in the ventilation period by increasing the area used for emplacement. The three objectives for this set of examples are:

1. Maintain average waste package surface temperatures below 85°C (185°F)

2. Ensure that 70,000 MTHM of waste fits within the upper and lower blocks (Figure 2-10)

3. Close and seal the repository within approximately 125 years.

Example scenarios 3 and 4 could achieve lower temperatures through extended forced ventilation. Example scenario 4 also includes extended surface aging of spent nuclear fuel.

Example Scenario 3: Increased Spacing and Duration of Forced Ventilation—Lower temperatures could be achieved with a limited increase in the preclosure period by emplacing waste packages an average of about 6 m (20 ft) apart. This would create a drift thermal load at emplacement of approximately 0.7 kW/m. The drift-to-drift spacing would remain at 81 m (266 ft). The loaded drifts would be actively ventilated for 125 years from the start of waste emplacement, with the drifts that are loaded in the last year of emplacement operations receiving 100 years of forced ventilation. Figure 2-13 displays preliminary projections of waste package surface and drift wall temperatures over time for this scenario.

The implications of this approach include: (1) a preclosure period comparable to the current preclosure period of approximately 100 years; (2) an increase in waste package spacing, which would likely result in point thermal loading of drifts and may give rise to increased complexities in modeling the thermal-hydrologic response of the host rock; (3) increases in the total excavated drift
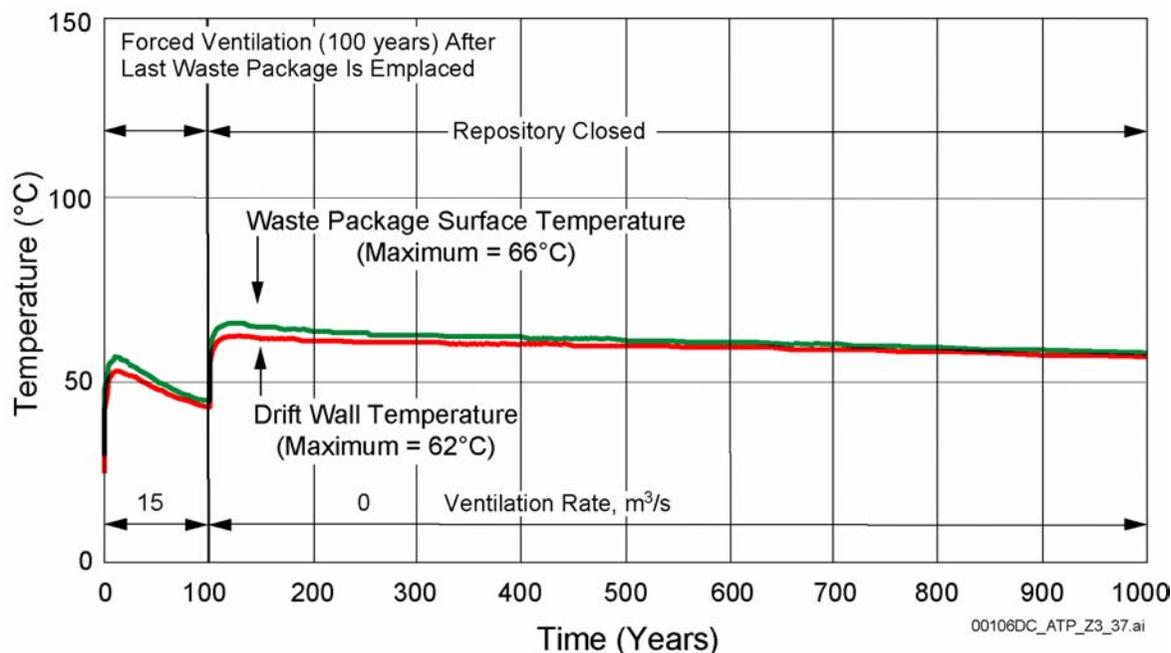
Figure 2-13. **Waste Package Surface and Drift Wall Temperatures for an Operational Scenario in Which Drifts Loaded at 0.7 kW/m in the Last Year of Emplacement Operations are Actively Ventilated for 100 Years**
Source: CRWMS M&O 2000o, Figure 3.

length and the total area required for emplacement; and (4) requirements for additional years of forced ventilation, maintenance, and other site and operations support.

Example Scenario 4: Extended Surface Aging with Forced Ventilation—In this example, surface aging of the hotter portion of the commercial spent nuclear fuel inventory, combined with the spacing of waste packages approximately 2 m (6.6 ft) apart within the drifts, reduces the linear thermal load to about 0.5 kW/m at emplacement. Surface aging of the hottest wastes would extend the total emplacement period from approximately 24 years to 50. However, initiation of repository operations would not be delayed because the cooler commercial spent nuclear fuel, along with the generally cooler DOE waste forms, could be emplaced immediately while the hotter commercial spent nuclear fuel cools through aging.

To meet the goal of a maximum waste package surface temperature of 85°C (185°F), forced drift ventilation would continue for approximately

125 years from the start of waste emplacement, with the last drifts loaded receiving 75 years of forced ventilation. At the end of the operating period, the repository would be closed and sealed, with no provision for extended natural ventilation. Figure 2-14 shows preliminary projections of waste package surface and drift wall temperatures over time for this scenario.

The implications of this scenario include: (1) the ability to accommodate the waste packages, with drift-to-drift spacing of 81 m (266 ft), in the areas currently characterized for a repository; (2) a preclosure period comparable to that of the higher-temperature operating mode; (3) a smaller increase in total drift length and disposal area than in Scenario 3; (4) an increase in the spacing of waste packages, which may result in thermal point loading that introduces additional complexities in modeling the thermal-hydrologic response of the potential repository; and (5) a longer emplacement period and additional fuel handling activities, which could increase the preclosure safety risk.
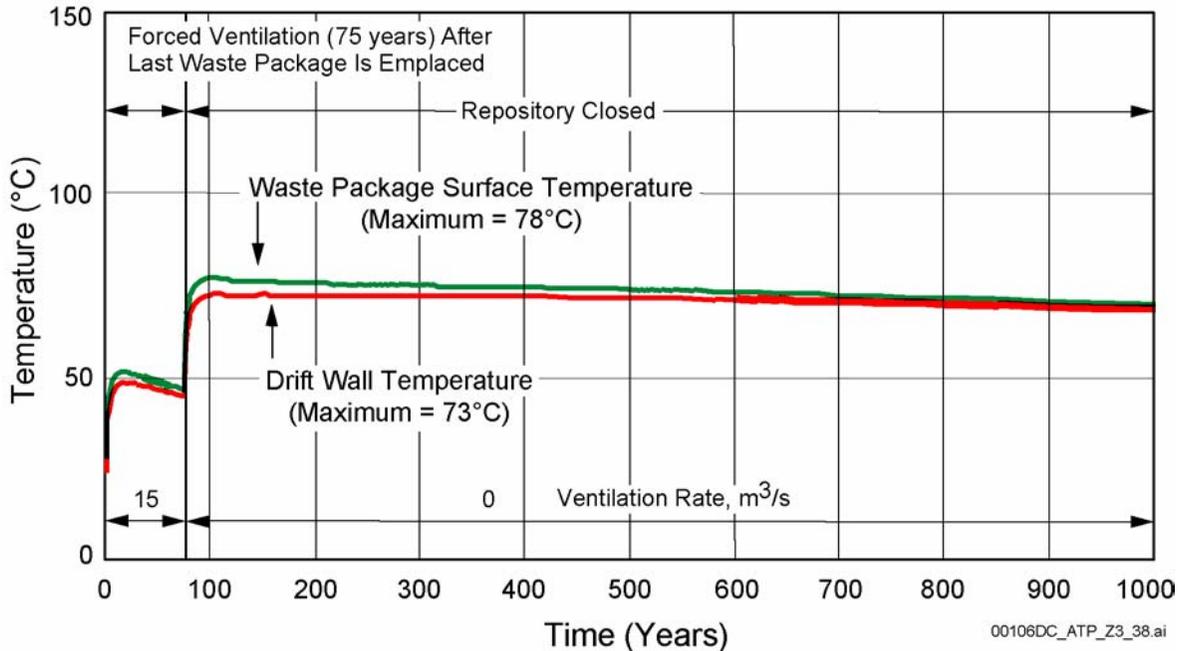
Figure 2-14. **Waste Package Surface and Drift Wall Temperatures for an Operational Scenario in which Drifts Loaded at 0.5 kW/m in the Last Year of Emplacement Operations are Actively Ventilated for 75 Years**

Source: CRWMS M&O 2000o, Figure 2.

2.1.5.2.3 Lower Rock Temperature and In-Drift Relative Humidity through Indefinite Natural (Passive) Ventilation

A third approach for meeting the goals of lower-temperature operating modes is to keep the temperature of the host rock below the boiling point of water and maintain in-drift relative humidity below 50 percent by incorporating passive natural ventilation into repository operations. A repository that maintains a low relative humidity is possible because of the natural characteristics of the Yucca Mountain site, including the arid environment and thick unsaturated zone.

An example lower-temperature scenario using this approach is framed around the following objectives:

1. Maintain in-drift relative humidity below 50 percent

2. Maintain the host rock temperature below the boiling point of water

3. Ensure that 70,000 MTHM of waste fits within the upper block (Figure 2-10).

Example Scenario 5: Extended Natural Ventilation—One concept for creating a lower-temperature, dry repository is to increase the ventilation duration of the current operation to approximately 75 years after the start of emplacement or 50 years after the last drift is loaded, followed by an indefinite period of natural ventilation. At the end of the forced ventilation period, the repository would stay open to allow natural ventilation to circulate cooler air for an extended period of time. Figure 2-15 shows projections of waste package surface temperatures, drift wall temperatures, and in-drift relative humidity over time (BSC 2001h).

Implications of this approach include: (1) a total excavated drift length and emplacement area comparable to the high-temperature operating mode layout; (2) the same thermal line loading,
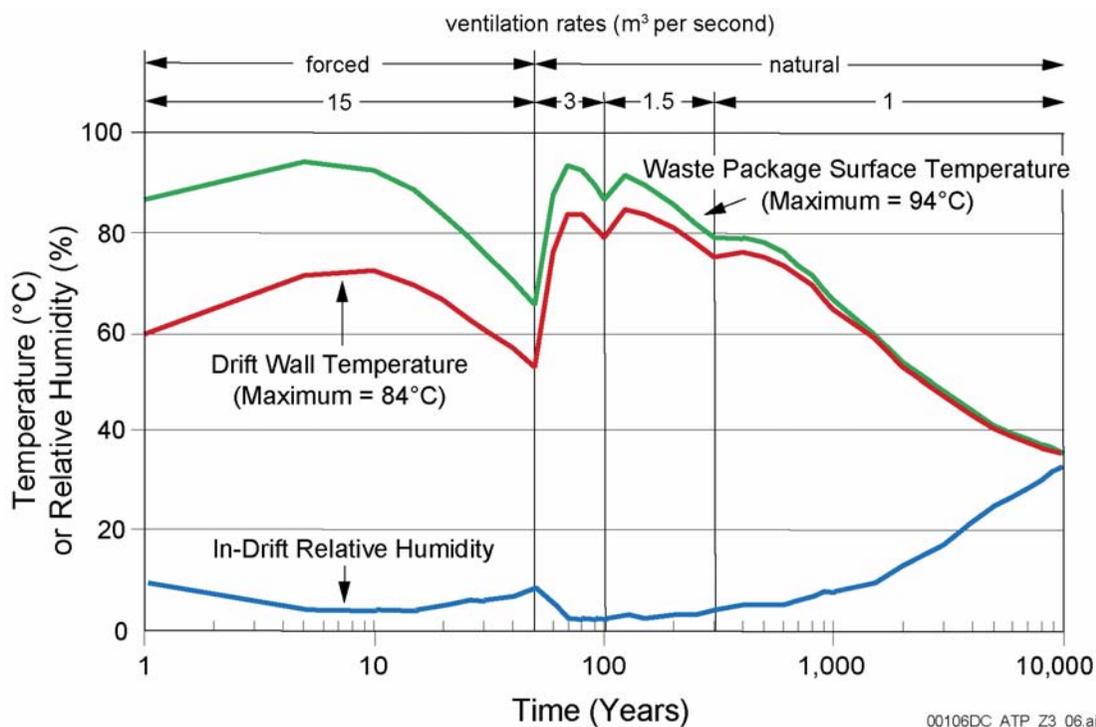
Figure 2-15. **Waste Package Surface Temperature, Drift Wall Temperature, and In-Drift Relative Humidity for an Operational Scenario in Which Drifts Loaded at the End of Emplacement Operations at 1.45 kW/m are Actively Ventilated for 50 Years and then Naturally Ventilated Indefinitely**
After 100 years, the relative humidity increases as the temperature declines, and moisture returns to the host rock around the drift. Source: Modified from BSC 2001k.

waste package spacing, and drift-to-drift spacing as the higher-temperature operating mode; and (3) the programmatic uncertainty associated with the indefinite period of natural ventilation.

2.1.5.3 Comparative Analysis of Alternative Lower-Temperature Operating Scenarios

Thermal management involves the consideration of complex, nonlinear relationships among many parameters of the repository system. The major determinants of peak temperatures are the age of the fuel at emplacement, the linear heat load along each drift, and the ventilation period after emplacement. Figure 2-11 shows the relationships among preemplacement aging, ventilation period, and waste package spacing for an average thermal goal of 96°C (205°F) at the drift wall (BSC 2001h). For

this case, the thermal goal can be achieved with a total preclosure period of about 100 years. The results change as the temperature goal is lowered to 85°C (185°F) or below on the waste package surface; in particular, the preclosure period might be extended. With longer periods of ventilation after waste emplacement, aging spent nuclear fuel before emplacement has less impact, and the key parameters become the ventilation period and the overall areal mass loading. The areal mass loading can be varied by changing the linear thermal load in each drift, the drift spacing, or both.

The examples in Section 2.1.5.2 were selected for discussion because they illustrate the effects that varying parameters can have in achieving the objectives of lower temperature and humidity. This section summarizes the main issues associated with the principal trade-offs in the example scenarios.

2.1.5.3.1 Reducing Peak Temperatures through Extended Ventilation Period or Reduced Linear Thermal Load

Analyses of ways to achieve a below-boiling repository indicate that reducing peak temperatures even further, so that waste package surface temperature does not exceed 85°C (185°F), would require a significant reduction in the linear thermal load in each drift when the total preclosure period is about 100 years, which is the period now contemplated for open operation of a repository. Scenarios 1, 2, 3, and 4 would require a substantially larger repository area. If ventilation can be extended well beyond 100 years, meeting the goal of temperatures at or below 85°C (185°F) would not require as much expansion of the disposal area. This extended ventilation period also adds flexibility in choosing between reduced waste package loading or increased waste package spacing. The added flexibility results because, with extended ventilation, the most important factor is total areal mass loading. Scenarios 1 and 2 in Section 2.1.5.2 assume that the ventilation period is extended to approximately 325 years after the start of emplacement. Scenarios 3 and 4 assume that forced ventilation continues for about 125 years after the start of emplacement; they rely primarily on reducing the linear thermal load. These two cases represent different ways of reducing the linear load at emplacement: increasing waste package spacing and aging waste. The following paragraphs focus on the broad trade-offs between extended ventilation and reduced linear thermal load.

2.1.5.3.2 Reducing Linear Heat Load by Using Widely Spaced Large Waste Packages or Closely Spaced Small Waste Packages

The total heat load over the entire emplacement area determines the repository temperature in the long term. However, in the short term, the amount of heat per unit length of drift is more important in determining the peak temperatures of both the rock and the waste package surface. Heat per unit length of drift is the dominant factor before the heat from each drift has time to move through the rock and influence temperatures in the adjacent drifts, and

before the heat-producing radionuclides with a short half-life (e.g., strontium-90 and cesium-137) have had time to decay to comparatively low levels. As illustrated by Scenarios 1 and 2 in Section 2.1.5.2, there are two ways of reducing the linear thermal load at emplacement: moving larger waste packages farther apart or using de-rated or smaller waste packages without increasing the spacing.

2.1.5.3.3 Aging Hotter Waste or Reducing the Linear Heat Load to Allow a Short Ventilation Period

To achieve a maximum waste package temperature of 85°C (185°F) with ventilation and closure periods of 100 years or less, the linear thermal load at emplacement must be reduced substantially, requiring an increase in drift length. Preemplacement aging can have a significant effect on the magnitude of the increase needed by allowing the heat-generating radionuclides with an intermediate half-life to decay before emplacement. Scenarios 3 and 4 in Section 2.1.5.2, which use roughly the same preclosure ventilation period, show the effects of using aging to reduce drift length requirements.

2.1.5.4 Other Considerations of Lower-Temperature and Lower-Humidity Operating Modes

Additional considerations associated with the various operating modes that reduce drift temperatures and relative humidity are discussed in this section.

Drip Shields—The drip shield is intended to protect the waste package from seeping water. This aspect of corrosion protection is effective early in the postclosure period and is a component of the DOE defense-in-depth strategy. In a lower-temperature design specifically engineered to remain outside the window of corrosion susceptibility, such protection may be less important or unnecessary. The benefits of drip shields in deflecting seepage and the time of their emplacement will be evaluated in light of the environments associated with the range of thermal operating modes.

Another related design issue is that some of the lower-temperature options include waste package spacing of several meters. In such cases, it may be more cost effective to have individually placed drip shields for each waste package rather than a continuously interlocked set of drip shields (BSC 2001l). The impact of these individually placed drip shields on repository performance will be the subject of future evaluations.

Repository Layout—Changes in such variables as waste package spacing or emplacement drift spacing to achieve lower-temperature operating conditions may alter the layout of the potential repository, including the total size of the repository footprint, as identified in Table 2-2. Layouts have been developed for both the primary (upper) and lower blocks characterized as areas for a potential higher-temperature operating mode, as described in *Site Recommendation Subsurface Layout* (BSC 2001d), and for a lower-temperature operating mode as presented in *Lower-Temperature Subsurface Layout and Ventilation Concepts* (BSC 2001g). The latter analysis developed layout configurations that support lower-temperature operating modes for the 70,000 MTHM and 97,000 MTHM cases, utilizing the primary and lower blocks. The analysis also presented results of parametric studies to evaluate the sensitivity of the layout configurations against operational and design options including waste package spacing, smaller waste package sizes, waste package heat output, and emplacement drift spacing.

Nonuniform Temperatures within the Drift—When the thermal loading within drifts is adjusted by increasing the distance between waste packages, the thermal load to the rock environment becomes more discretized along the drift axis, more like point loads than a continuous line load. This could result in a nonuniform temperature distribution along the axis of the drift after the repository is sealed. A significant nonuniform temperature distribution in the drift walls or within the emplacement drift could cause water or steam to move from the high heat region toward the low heat region, resulting in water dripping from the walls onto the drip shields, or water condensing on drip shields or low heat output waste packages.

The rate of moisture transport decreases with a decrease in the thermal gradient.

Natural Ventilation—Another possibility for mitigating uncertainties associated with corrosion is to keep in-drift relative humidity below 50 percent by allowing longer-term natural ventilation of the repository. By taking advantage of natural ventilation, a repository can be operated so the temperature of the host rock remains below the boiling point of water while relative humidity stays below 50 percent, the value bounding the conservatively defined window of susceptibility for localized corrosion of Alloy 22.

It is illustrative to examine a scenario in which the period of natural ventilation is extended indefinitely. In example scenario 5, the repository is operated through the periods of emplacement and for 75 years after emplacement, during which the emplacement drifts are actively ventilated, after which the repository is allowed to ventilate naturally for an extended period of time. Figure 2-15 depicts nominal waste package surface temperature, emplacement drift wall temperature, and in-drift humidity as a function of time for this scenario, as predicted by two-dimensional models (BSC 2001h). In this case, the natural ventilation period was allowed to extend indefinitely. Natural ventilation flow rates were modeled at 3 m^3/s per drift for the first 50 years, at 1.5 m^3/s per drift for the next 200 years, and at 1 m^3/s per drift thereafter. In calculating relative humidity, an infiltration flux of 60 mm/yr (2.4 in./yr) was assumed over the emplacement drifts. (This infiltration flux is ten times greater than the present-day mean infiltration rate over the repository footprint.) As Figure 2-15 shows, the peak drift wall temperature for this scenario is projected to stay below 90°C (194°F). Because of the ample carrying capacity of the dry desert air, the average relative humidity in the drifts does not exceed 30 percent until waste package temperatures drop below 40°C (104°F).

Natural Analogues—Natural analogues support the concept that a deep geologic repository in the unsaturated zone would keep waste dry and isolated, particularly through natural ventilation. Dry environments, in which fragile cultural arti-

facts have been preserved for millennia, could provide a hospitable environment for more robust materials. Prehistoric paintings, for example, survive in numerous caves that are analogous to a deep geologic repository. Water tends to flow around caves and tunnels in the unsaturated zone, depending partly on the size of the openings: the smaller the size of the cave, the more likely water will flow around it. Most unsaturated zone caves with highly preserved artwork have openings larger than the 5.5-m (18-ft) diameter proposed for emplacement drifts. This suggests the drifts may remain even drier than caves, which have stayed dry enough to preserve ancient paintings (Stuckless 2000, pp. 2 to 4). A cooler repository would be more closely related to these natural analogues than a higher-temperature repository.

The oldest authenticated examples of Paleolithic (older than 10,000 years) human cave paintings are the Chauvet paintings in southeastern France. These recently discovered cave paintings include images of the mammoth, long extinct, and the rhinoceros, long absent from Europe. The intact Chauvet paintings are more than 30,000 years old and still survive in a subhumid climate with annual precipitation ranging up to roughly 80 cm (31 in.); average annual precipitation at Yucca Mountain is less than 20 cm (8 in.). On the cave's ceiling, even the soot from later human use of oil lamps has remained, despite having been deposited some 26,000 years ago (Stuckless 2000, pp. 2 to 4).

Spirit Cave, about 75 miles east of Reno, Nevada, is another example of a natural analogue to a repository. Several small burial pits were discovered in this cave; in one of these pits, archaeologists found an almost completely intact human body, mummified by the dryness of the climate. Subsequent analyses, including carbon-14 testing, have shown the body to be that of a 45- to 55-year-old male who died around 9,400 years ago. His scalp was completely intact, including a small tuft of hair. He wore a breechcloth of fiber and was wrapped in mats woven of fibers from tule leaves, all highly preserved (Barker et al. 2000, Section 4).

2.2 REPOSITORY SURFACE FACILITIES

The design described in this report focuses on protecting the health and safety of both repository workers and the public. To meet these requirements, an integrated set of surface facilities is being designed. Operation of a repository would involve a number of distinct but interrelated waste activities and functions; the major ones include receiving, handling, and packaging. The following design description discusses the surface facilities for a potential repository for spent nuclear fuel and high-level radioactive waste, based on current concepts documented in *Engineering Files for Site Recommendation* (CRWMS M&O 2000p) and *WHB/WTB Space Program Analysis for Site Recommendation* (CRWMS M&O 2000q).

The surface facilities would be located in the North Portal Repository Operations Area, the South Portal Development Area, and the Surface Shaft Areas. Figure 2-16 shows the general surface layout of the North Portal Repository Operations Area and South Portal Development Area. The Surface Shaft Areas, where the ventilation shafts and fans would be located, would be on the crest of Yucca Mountain. Together (but excluding the area for the solar power arrays), these areas would cover more than 105 acres of land, on which at least 30 structures would be built to house the operations and services needed for safe and effective repository operations (CRWMS M&O 2000p, Attachment II, Section 2.11.1).

The North Portal Repository Operations Area is logically segregated into the Radiologically Controlled Area, the balance-of-plant area, and the site services area. The Radiologically Controlled Area comprises all facilities necessary to receive, package, and emplace waste in the repository. The balance-of-plant area comprises general infrastructure facilities, such as administration, emergency management (medical and fire), and motor pool and fleet services. The site services area comprises general parking and the visitor center.

The South Portal Development Area would support continuing construction of a repository, even as the North Portal Repository Operations Area accepts and prepares waste for underground emplacement
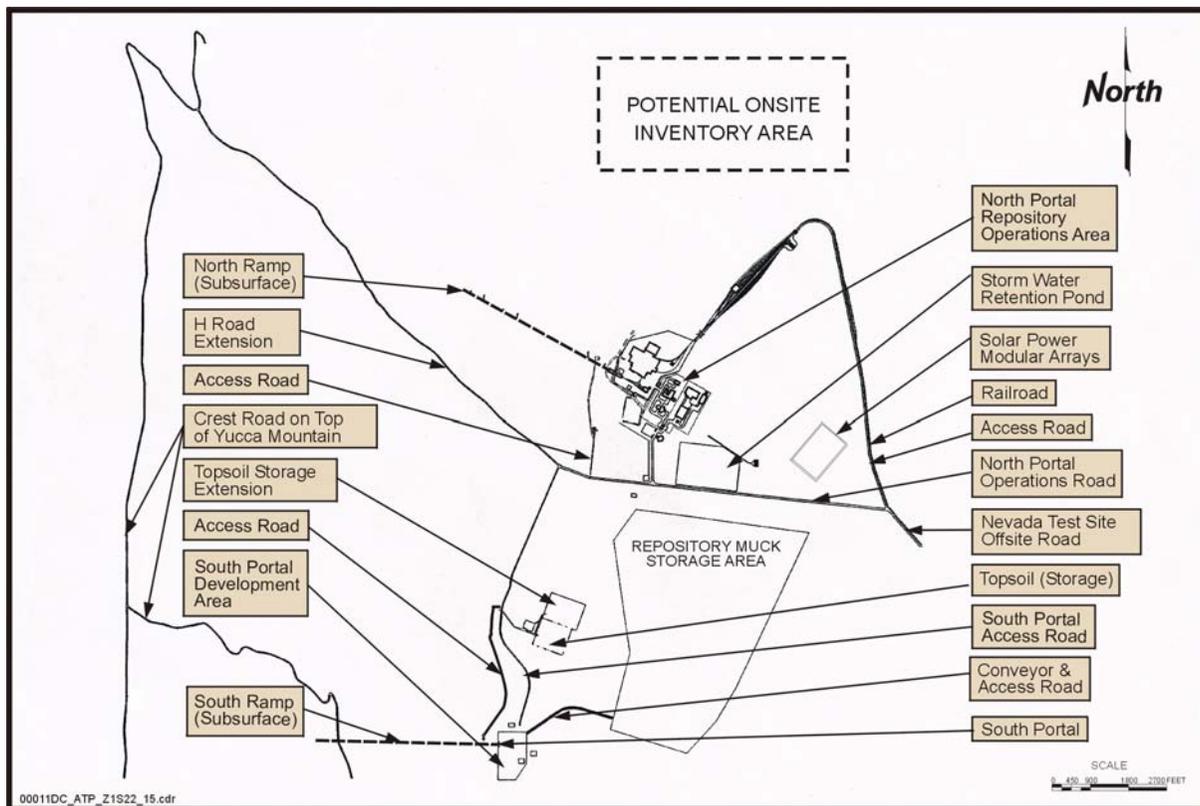
Figure 2-16.   Repository Overall Site Plan
Surface facilities would be developed to support operations and construction activities at the North and South Portals, respectively. Roadways would be constructed to link these areas with supporting surface areas. Source: Modified from CRWMS M&O 2000p, Figure I-19.

in the first emplacement drifts. This section focuses on the proposed design and development of three primary structures at the North Portal surface facility. Section 2.3 addresses other areas more closely associated with subsurface development and emplacement activities.

Consistent with 10 CFR Part 63 (66 FR 55732), a set of monuments extending at least 6.2 m (20 ft) above the surface would be constructed prior to the beginning of postclosure to identify the geologic repository area.

In addition to the design requirements driven by the fuel blending inventory strategy (described in Section 2.2.1), continual emphasis on environmental, industrial, and radiological health and safety criteria will be designed into all of the surface facilities and systems. The ALARA radio-

logical health and safety design and operational criteria are discussed in Section 2.2.5. Operations at the North Portal Repository Operations Area are described in Section 2.2.2. Details of these surface facilities and systems, and the designers' emphasis on health and safety, are presented in Section 2.2.4.

2.2.1   Fuel Blending Inventory Strategy

Spent nuclear fuel and high-level radioactive waste arriving at the repository would be in solid form but in a variety of types and sizes. Hence, the materials would arrive in a variety of transportation casks, all certified for use by the NRC.

Commercial spent nuclear fuel would arrive as individual fuel assemblies placed directly into transportation casks, or in dual-purpose canisters, which would have to be opened to remove the fuel

assemblies. DOE spent nuclear fuel would arrive in disposable canisters. Because of the variety of waste forms, a number of different designs for disposal containers (called waste packages once they are loaded, sealed, and certified) would be needed. Figure 2-17 depicts the anticipated types of transportation casks, waste forms, and disposal containers (CRWMS M&O 2000p, Attachment II, Section 1.1.3.1).

The radioactive decay process generates heat. The concentration of the particular isotopes present vary among the different waste forms, so different waste forms generate different amounts of heat. The design and operating mode described in this report were developed to meet established temperature limits for the higher-temperature operating mode (i.e., a maximum heat output of 11.8 kW for

all waste packages) (CRWMS M&O 2000p, Attachment II, Section 1.1.1.4).

The limit on heat output from individual waste packages imposes special considerations for operations. The strategy for controlling heat output for the waste packages is to load low heat output waste with high heat output waste to balance total waste package heat output. This process, called "fuel blending," applies only to commercial spent nuclear fuel.

Some fuel assemblies must be placed into fuel blending inventory until they generate less heat from radioactive decay, or until additional low heat output fuel assemblies arrive for blending. Fuel assemblies would stay in inventory until they are selected for blending. By carefully planning and implementing a fuel-blending procedure, the heat
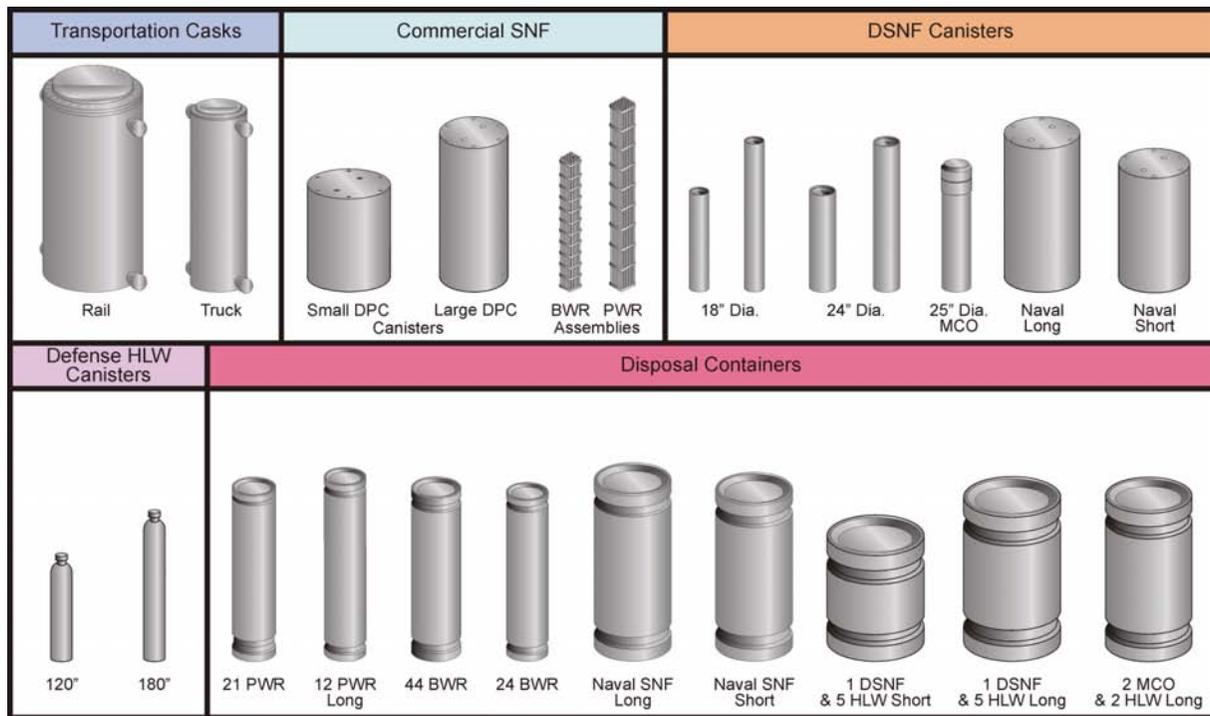
Figure 2-17. Casks, Containers, and Waste Forms Handled at the Surface Facility
Items handled at the surface facility include large and small transportation casks containing the waste forms and disposal containers. Dimensions for all waste forms and containers (except the transportation casks) are provided in Section 3. SNF = spent nuclear fuel; DSNF = DOE spent nuclear fuel; DPC = dual-purpose canister; HLW = high-level radioactive waste; PWR = pressurized water reactor; BWR = boiling water reactor; MCO = multi-canister overpack. Source: Modified from CRWMS M&O 2000p, Figure I-2.

output of the waste packages can be limited and optimized without increasing the number of waste packages and the amount of fuel blending inventory unnecessarily. The tracking, recording, and archiving of waste forms would be handled by the operations monitoring and control system (Section 2.2.4.2.12).

Engineers developed a computer model to estimate the design amount of fuel blending inventory space needed. Computer model simulations helped form the present configuration of the Waste Handling Building (CRWMS M&O 2000p, Attachment II, Section 1.1.1.3). Results indicate that, for the 11.8-kW heat output limit for the waste package, a fuel blending inventory capacity of approximately 5,000 MTHM, or 12,000 spent nuclear fuel assemblies, will be needed. This simulation also showed the surface facilities will need an inventory of approximately 40 small canisters (containing DOE spent nuclear fuel or high-level radioactive waste) for the canister transfer system. This small canister inventory is needed to ensure that a waste package containing five high-level radioactive canisters and one DOE spent nuclear fuel canister can be loaded using the canister inventory on hand. The inventory size accounts for the fact that these canisters will not always arrive at a ratio of five high-level waste canisters to one spent nuclear fuel canister. Additionally, the simulations established the need for two assembly transfer lines and one canister transfer line (CRWMS M&O 2000p, Attachment II, Section 1.1.4.1). The use of fuel blending inventory in the assembly transfer system ensures that any disposal container loaded with commercial spent nuclear fuel will not exceed a thermal output of 11.8 kW for the design and operating mode described in this report.

2.2.2   Operations in the North Portal Repository Operations Area

This section describes the movement of spent nuclear fuel and high-level radioactive waste forms through the North Portal Repository Operations Area. It presents the interrelationship of the systems, equipment, and facilities for receiving, preparing, packaging, and transporting these waste forms. It also provides information on how the waste would arrive at the repository, how the

systems for handling the different waste forms would operate, and how secondary low-level radioactive waste would be handled.

2.2.2.1   Waste Receiving Operations

Spent nuclear fuel and vitrified high-level radioactive waste would be transported to the repository in NRC-certified transportation casks by U.S. Department of Transportation-licensed cask transportation contractors. The waste would be transported by rail and/or road to the North Portal security station, where personnel will verify the shipping manifests, then inspect and survey the cask and its carrier. After the cask and its carrier enter the Radiologically Controlled Area, they would be stationed in parking areas designated for either truck carriers or rail carriers. When the cask is scheduled for processing, a site prime mover (transporter) would move the cask and carrier to the Carrier Preparation Building. Figure 2-18 presents a simplified flow diagram of waste receiving operations.

Inside this building, workers:

- Retract or remove personnel barriers
- Retract or remove impact limiters
- Survey the cask surface for radiation
- Decontaminate cask surfaces (if necessary)
- Measure the cask's temperature
- Install any required special tools or devices (e.g., cask-lifting attachments).

The casks would be taken on the carrier to a parking area to await movement to the Waste Handling Building carrier bay according to operations scheduling requirements.

2.2.2.2   Waste Handling Operations

At the carrier bay, the carrier/cask handling system would lift the transportation cask to a vertical position and place it on a cask transfer cart. Depending on the cask's contents, the cart would move to one of two transfer systems. Casks that contain disposable containers (e.g., DOE canisters that would not be opened but transferred, as is, directly into a disposal container) would go to the canister transfer system. Casks that contain commercial
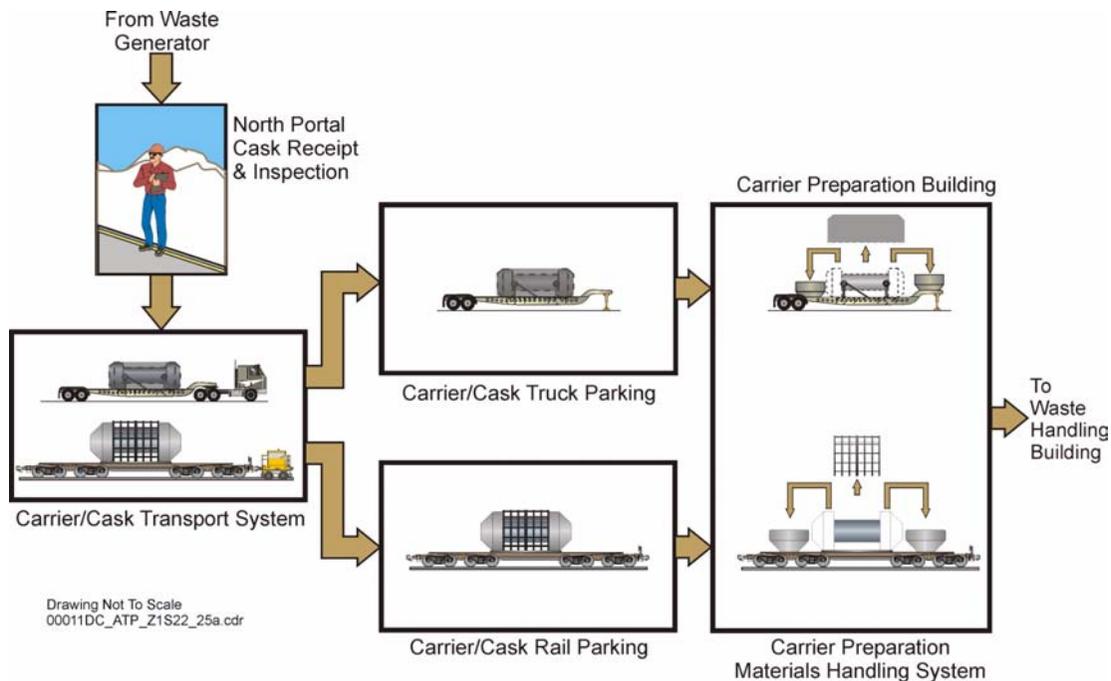
Figure 2-18. Waste Receiving Operations
Waste shipments by road and rail would be stopped at the security gate for inspection. Offsite prime movers would be decoupled from the carriers, and site prime movers would be attached. Carriers may be staged temporarily within the controlled security area until ready for processing in the Carrier Preparation Building, where the transportation casks would be made ready for transfer to the Waste Handling Building. Source: Modified from CRWMS M&O 2000p, Figure I-18.

spent nuclear fuel in dual-purpose canisters or individual fuel assemblies would go to the assembly transfer system. Figure 2-19 is a flow diagram of Waste Handling Building operations (CRWMS M&O 2000p, Attachment II, Sections 1.1.1 through 1.1.5).

The Waste Handling Building would have one canister transfer line that moves the disposable fuel canisters through the building to prepare the waste for emplacement in the repository. The system would move arriving casks through an air lock on a transfer cart into a cask preparation area. Once a cask arrives inside the cask preparation area, workers would use remotely operated equipment to vent and sample gases from the cask, remove the lid bolts, and open the cask. An overhead crane would move the cask to a transfer cart, which would take the cask to a shielded transfer area. Inside the transfer area, machines would remove the canister from the cask. The canister may go directly into a disposal container for repository emplacement or to a holding rack for later place-

ment in a disposal container. Another transfer cart would move loaded disposal containers to the disposal container handling system. A transfer cart would move the empty transportation casks back to the cask decontamination area, where they would be surveyed and decontaminated, if required, before return shipment. From the decontamination area, casks would be moved to the carrier/cask handling system, which would place them back on a transporter. The empty cask and cask transporter would return to the Carrier Preparation Building to be readied for offsite shipment.

The Waste Handling Building would have two assembly transfer lines. Each line would operate independently to handle waste throughput and support maintenance operations. The assembly transfer process begins by moving the cask on a transfer cart through the air lock into the cask preparation area. Once inside the cask preparation area, workers would use remotely operated equipment to inspect, vent, and cool the cask and remove the cask lid bolts. A large overhead crane would lift the
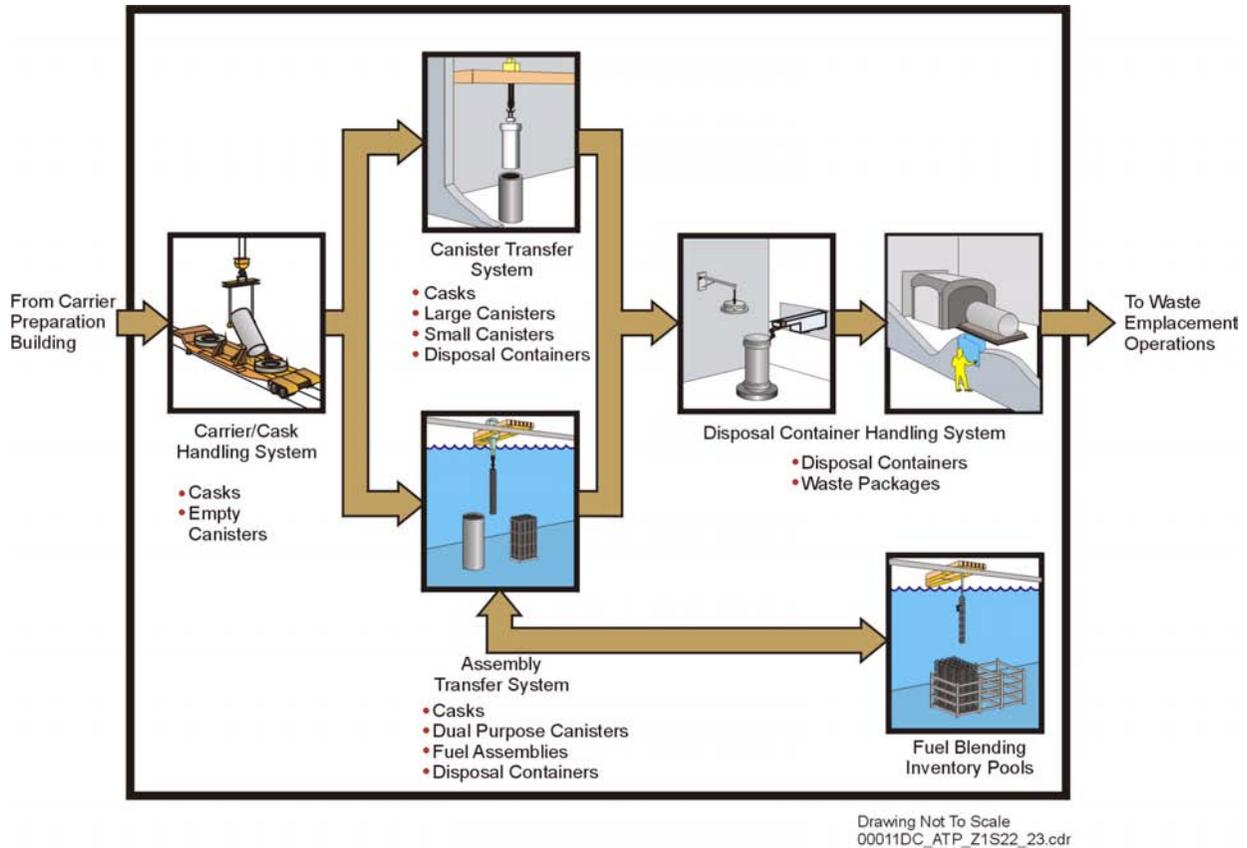
Figure 2-19.   Waste Handling Operations
In the Waste Handling Building, transportation casks would be transferred from their carriers to one of two transfer systems: the canister transfer system for spent nuclear fuel and high-level radioactive waste already packaged in canisters suitable for direct insertion into disposal containers; or the assembly transfer system for spent fuel not packaged in containers suitable for direct insertion into disposal containers. After loading, the disposal containers would be welded closed and the welds inspected. After acceptance of the welds, the disposal container is referred to as a waste package. Source: CRWMS M&O 2000p, Figure I-1.

casks and place them in a cask unloading pool, where fuel-handling machines would open the casks and unload the fuel assemblies. If the cask contains dual-purpose canisters, they would be removed and placed in an overpack, where the top of the canister would be cut off. The system would move the empty casks and dual-purpose containers back out through the cask decontamination area. The fuel-handling machines would transfer the fuel assemblies, one at a time, to a holding pool, where they would be placed in assembly baskets. A transfer cart would move the baskets containing the fuel assemblies underwater from the assembly holding pool through a transfer canal to a fuel-blending inventory pool. When a fuel assembly is selected from the fuel inventory pool for pack-aging, a transfer cart would move it underwater

back through the fuel blending pool to an inclined transfer canal and onto a cart that connects to the assembly drying area.

After fuel assemblies arrive at the assembly drying area, a fuel-handling machine would transfer them into one of two drying vessels. After drying, the system would retrieve the assemblies and transfer them, one at a time, to a disposal container. The empty assembly baskets would be returned to the pool area for reuse. After loading, workers would purge the disposal container with inert gas and temporarily seal it for transfer to the disposal container handling system.

The disposal container handling system would receive loaded disposal containers from both the

canister transfer system and the assembly transfer system. Each disposal container would again be purged with inert gas, after which the container's lids would be welded and the welds inspected. If the welds meet inspection criteria, the sealed disposal container would be reclassified as a waste package. A crane would transfer the waste package to the transporter loading area, where it would be decontaminated and placed on a pallet, then on a transporter for emplacement in the subsurface repository. Table 2-3 gives the preliminary performance specifications for this equipment.

2.2.2.3 Treatment of Low-Level Radioactive Waste from Repository Operations

Operations at a repository—receiving, handling, and repackaging commercial and DOE spent nuclear fuel and high-level radioactive waste— would generate secondary low-level radioactive waste. Some of this waste may be defense-related

transuranic waste. In this report, any transuranic and low-level waste is referred to collectively as low-level waste. The majority would be generated in the Waste Handling Building; smaller quantities may be produced in the Waste Treatment Building, where secondary low-level waste is processed. Operations in the Carrier Preparation Building are not expected to generate any significant waste quantity. All secondary waste would be monitored at the point of generation, and administrative controls would direct its disposition. The design of the repository would include a processing system, which would minimize the volume of liquid and solid waste. To the extent applicable, it would be properly treated and packaged for shipping and disposal off the repository site.

Some hazardous wastes may also be generated during repository operations. The use of hazardous constituents will be reviewed and controlled so that the generation of hazardous wastes is minimized. When hazardous wastes are commingled with

Table 2-3. Preliminary Crane and Lifting Machine Performance Specifications

Equipment Description	Quantity	Capacity	Span meters (ft)
Carrier Preparation Building Bridge Crane	2	10 tons	17.68 (58)
Carrier Bay Bridge Crane	1	160 tons	23.77 (78)
Cask Unloading Area Bridge Crane	2	160 tons Aux. Hoist: 25 tons	13.11 (43)
Assembly Handling Cell Bridge Crane	2	15 tons Aux. Hoist: 5 tons	10.85 (35.6)
Nonstandard Fuel Pool Overhead Crane	1	30 tons	10.97 (36)
Fuel Basket Storage Pool Overhead Service Crane	4	20 tons	15.24 (50)
Canister Transfer Cell Bridge Crane	1	65 tons	10.67 (35)
Offnormal Canister Handling Cell Bridge Crane	1	15 tons	9.14 (30)
Disposal Container Handling Cell Bridge Crane	2	150 tons Aux. Hoist: 10 tons	22.56 (74)
Empty Disposal Container Preparation Bridge Crane	1	60 tons Aux. Hoist: 10 tons	25.6 (84)
Welder Maintenance Bridge Crane	1	20 tons	10.97 (36)
Waste Package Horizontal Lifting Machine	1	100 tons	6.71 (22)
Waste Package Transporter Load Cell Bridge Crane	1	10 tons	10.36 (34)
Waste Package Remediation System Cutting Machine	1	4 tons	10.67 (35)
Waste Package Remediation System Manipulator and Hoist	1	4 tons	10.67 (35)
Assembly Transfer System and Canister Transfer System Equipment Transfer Corridor Bridge Crane	1	50 tons	14.63 (48)
Disposal Container Handling and Waste Package Remediation System Equipment Transfer Corridor Bridge Crane	1	50 tons	17.37 (57)

Source: CRWMS M&O 2000r.

radioactive wastes, the result is mixed waste. The generation of hazardous and mixed wastes will be minimized at the repository. However, if it is generated, it would be collected and repackaged for shipment to an approved offsite location for treatment and disposal. The packaged mixed waste would then be staged in the Waste Treatment Building for transport offsite to an approved facility. No low-level or hazardous waste would be disposed in the potential repository. Hazardous wastes that are not mixed wastes would also be packaged for shipment offsite to an approved treatment disposal facility. Wet solid low-level waste (e.g., spent ion exchange resins and filtration materials) generated in the Waste Handling Building would be collected and packaged for disposal. Then it would be transferred in containers to the Waste Handling Building for shipment off the site for disposal. Any other solid low-level waste generated in the Waste Handling Building that does not exceed the radioactivity limit for the Waste Treatment Building would be collected at its point of origin and transferred to the Waste Treatment Building to be processed and packaged for shipping and disposal at an approved low-level radioactive waste facility. Solid waste that exceeds Waste Treatment Building administrative activity limits would be packaged at the source of generation for shipment and disposal off the repository site. Spent dual-purpose containers would be volume-reduced and disposed at a suitable low-level radioactive waste disposal site. Recycling of spent disposal containers for recovery of metal content will be examined in future design activities. The Waste Treatment Building would be large enough to hold all the necessary equipment for processing the proposed maximum annual secondary-waste generation rate on a regular operating schedule (CRWMS M&O 2000p, Attachment II, Section 1.2).

2.2.3 North Portal Repository Operations Area Layout

This section describes the overall orientation, configuration, and general construction features of the repository surface facilities.

The North Portal Repository Operations Area would include a Radiologically Controlled Area

and a balance-of-plant area (Figure 2-20). The Radiologically Controlled Area, also known as the protected area, is where the waste would be received from offsite transportation carriers and placed in waste packages for disposal. The balance-of-plant area includes all structures and systems supporting repository operations that are not encompassed by the Radiologically Controlled Area. An additional area of 350 acres is available to stage retrieved waste, should the need arise; this area should be sufficient to stage all the waste that may be emplaced in the potential repository (CRWMS M&O 2000p, Attachment II, Section 2.11.3.3).

A buried storm drainage collection system would contain water runoff from the Radiologically Controlled Area. The drainage system would also prevent spillage over the fill slopes and runoff from the balance-of-plant area. A retention pond would be built to prevent storm water pollution (CRWMS M&O 2000p, Attachment II, Section 2.11.3.1).

Except for its north edge, the North Portal pad would be above the flood-prone area of the probable maximum flood. Two open channels around the perimeter of the pad would protect the North Portal from water flow. The operating floor of the Waste Handling Building is 0.5 m (1.5 ft) above the maximum elevation of the flood stage that intersects the building to allow for freeboard (CRWMS M&O 2000p, Attachment II, Section 2.11.3.1).

2.2.4 Surface Systems and Structures

This section includes detailed descriptions of the layout, support structures, systems, and utilities of each major surface facility. Design objectives and criteria are derived from NRC regulations, industry standards for nuclear facilities, and DOE policy. For example, NRC regulatory guides were used in preparing the System Description Document design requirements. NRC guides used in developing the System Description Document for the Waste Handling Building included:

- Regulatory Guide 3.49, *Design of an Independent Spent Fuel Storage Installation (Water-Basin Type)*
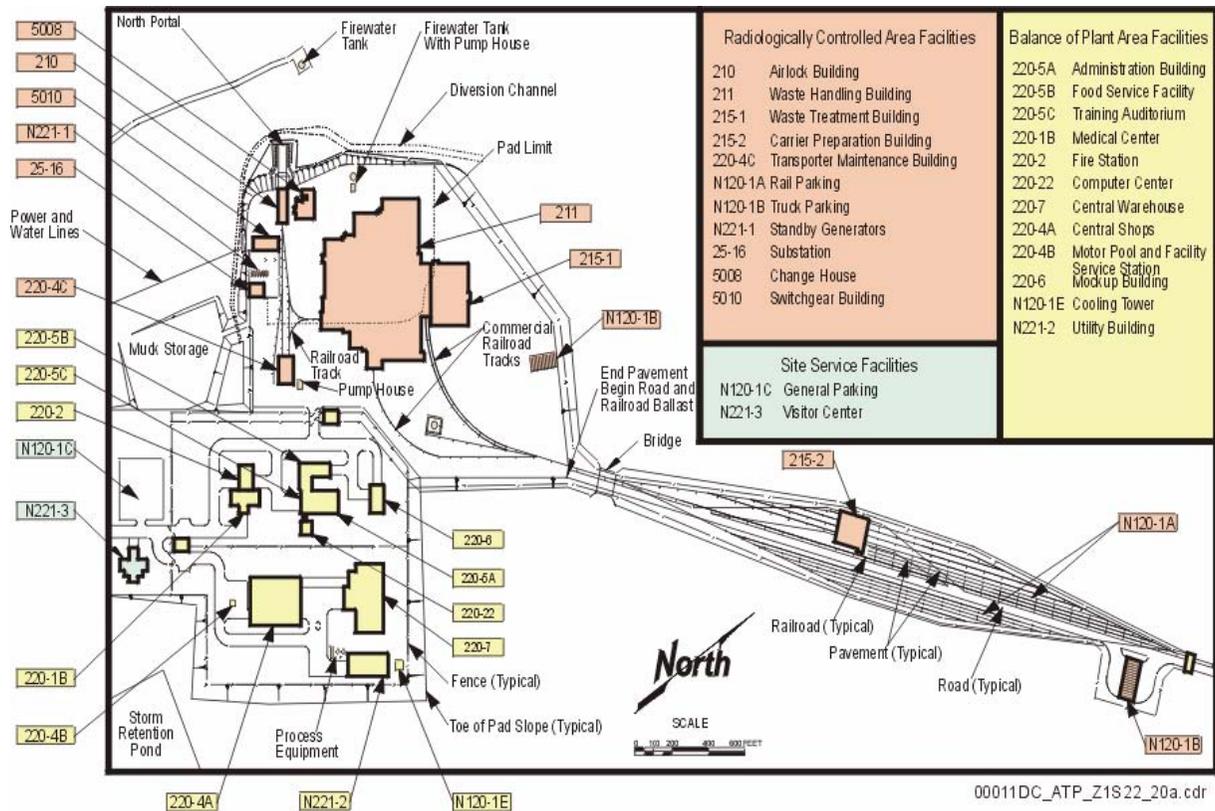
Figure 2-20. North Portal Repository Operations Area Site Plan
The North Portal Repository Operations Area is defined by three distinct use areas: the Radiologically Controlled Area, the balance-of-plant area, and site service facilities. All radiologic materials would be handled only in the Radiologically Controlled Area. RCA = Radiologically Controlled Area; BOP = balance-of-plant. Source: Modified from CRWMS M&O 2000p, Figure I-20.

- Regulatory Guide 1.13, *Spent Fuel Storage Facility Design Basis*

- Regulatory Guide 1.102, *Flood Protection for Nuclear Power Plants*

- Regulatory Guide 8.8, *Information Relevant to Ensuring that Occupational Radiation Exposures at Nuclear Power Stations will be as Low as is Reasonably Achievable*

- *Human–System Interface Design Review Guideline* (NUREG-0700) (NRC 1996).

System Description Documents for the surface facilities would be maintained and updated as required over the life of the facility or system. Codes and standards were chosen based on a review of relevant federal laws and regulations, as well as applicable industry codes, standards, and good engineering practices. Three structures and systems in the surface facilities have been classified as QL-1 (YMP 2000b):

- The Waste Handling Building structure
- The assembly transfer system
- The canister transfer system.

QL-1 systems include those structures, systems, and components whose failure could directly result in a condition adversely affecting public safety. These items have a high safety or waste isolation significance. For this reason, QL-1 systems are discussed in greater detail than systems that are not classified as QL-1. Systems that are not classified as QL-1 are defined in Section 5.2.5, where their functions important to safety are likewise described.

The Carrier Preparation Building, Waste Handling Building, and Waste Treatment Building are described in this section, as are the processes that would occur within each and the equipment that would support such activities. Some of the operations discussed, along with the equipment needed to perform them, are:

- Removing the waste forms from their transportation casks

- Cleaning and decontaminating the casks for reuse

- Loading the waste forms into disposal containers

- Sealing the disposal containers

- Repairing defective disposal containers and waste packages

- Controlling radiation exposures to personnel

- Processing, cleaning, recycling, and solidifying low-level radioactive waste for shipment and disposal off the repository site.

2.2.4.1   Carrier Preparation Building

The Carrier Preparation Building, to be located at the North Portal pad, would support preparation of the waste transportation casks before they enter the Waste Handling Building. Planned as a steel-framed structure, the building would be approximately 58 m (190 ft) long, 37 m (120 ft) wide, and 14 m (46 ft) high. The operations area, divided into two identical carrier operations bays, would accommodate four parallel rail tracks/roadways for passage of both rail and truck carriers. Each bay would have two rail/truck lines, separated by a dual-function work platform and equipment laydown area, a bridge crane, and a bridge-mounted manipulator. The transportation carriers would enter and exit the building through one of eight remotely operated roll-up doors (CRWMS M&O 2000p, Attachment II, Section 1.3).

2.2.4.1.1   Carrier Preparation Building: Architectural and Structural Features

The Carrier Preparation Building would be an on-grade, one-story, high-bay, steel-framed structure, enclosed with insulated steel roof and wall panels. The interior framing would be of light-gauge steel and easily decontaminated panels. The foundations would consist of reinforced concrete spread footings, to support the building's columns, and continuous reinforced concrete mat foundations, to support the railroad tracks. To mitigate vibrations from carrier movement, the spread footings would be separated from the mat foundations. The building's columns would support two bridge cranes running the length of the building, each of which would span a gantry crane for servicing the tracks (CRWMS M&O 2000p, Attachment II, Section 1.3.1.3.1).

2.2.4.1.2   Carrier Preparation Building: Material Handling System

The material handling system in the Carrier Preparation Building would receive and inspect shipping casks from the carrier/cask transport system, then prepare the casks for unloading in the Waste Handling Building (Figure 2-21). Four parallel tracks/roadways would permit the passage of both truck and rail carriers. The two outer tracks/roadways would serve incoming carriers from the rail yard or truck-parking area, and the two inner tracks/roadways would serve outgoing carriers (CRWMS M&O 2000p, Attachment II, Sections 1.3.2.1, 1.3.1.3.1).

Receiving operations include:

- Performing a radiation survey of the carrier and the transportation cask
- Removing or retracting the personnel barrier(s)
- Sampling the cask exterior for contamination
- Measuring the cask's temperature
- Removing or retracting the cask impact limiters
- Installing the cask's lifting attachments (if any).
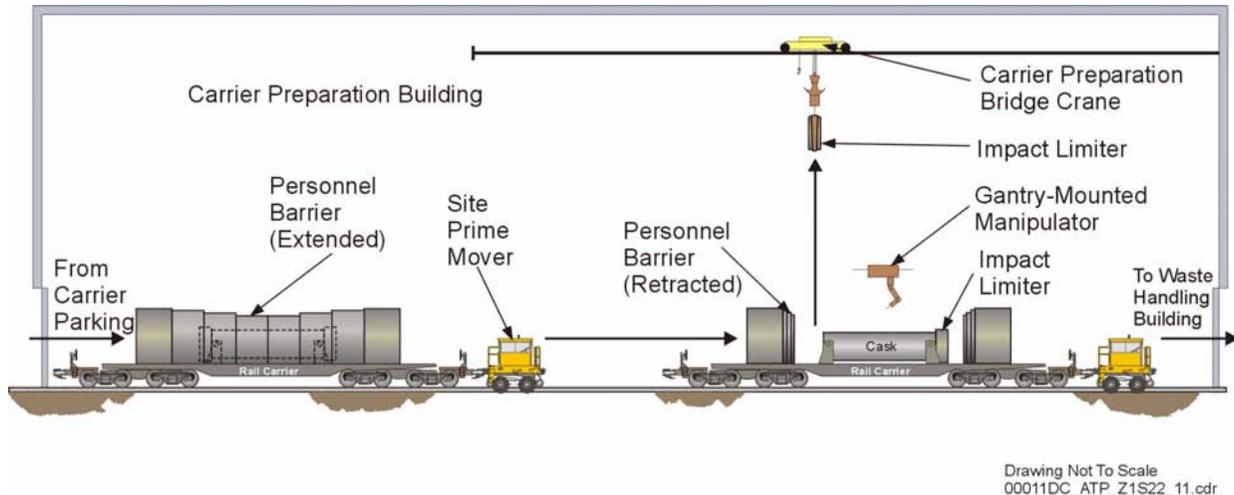
Figure 2-21.   Carrier Preparation Building Materials Handling System
The materials handling system uses manual and remote equipment to prepare incoming road and rail transportation casks for offloading in the Waste Handling Building. The system removes/retracts personnel barriers which prevent inadvertent touching of the thermally hot casks, removes the impact limiters from both ends of the casks, and adjusts any tie-down bolts for easy removal so the casks can be offloaded in the Waste Handling Building. Source: Modified from CRWMS M&O 2000p, Figure I-16.

Shipping operations for carriers/casks leaving the repository would include:

- Removing the cask's trunnions (if required)
- Checking the cask's tie-downs
- Installing the cask's impact limiters
- Performing another radiation survey of the cask
- Installing the personnel barriers.

Unloaded casks would undergo the same series of operations as loaded casks, except in reverse (CRWMS M&O 2000p, Attachment II, Section 1.3.2.1).

One 10-ton capacity, remotely operated overhead bridge crane spanning 17.7 m (58 ft) and one remotely operated manipulator would serve each pair of preparation lines. Operations would support both manual and remote handling of carrier/cask materials. Having both manual and remote handling options would improve the maintenance of facilities and equipment, permit the replacement of interchangeable components, and lower radiation doses to workers. The building's support equipment would include tools and fixtures for removing and installing personnel barriers, impact

limiters, cask lifting attachments, and cask tie-downs (CRWMS M&O 2000p, Attachment II, Section 1.3).

The material handling system would interface with the cask/carrier transport system to move carriers to and from the building. The Carrier Preparation Building would house all necessary equipment and systems (e.g., facility, utility, safety, auxiliary) to support its operations and protect personnel (CRWMS M&O 2000p, Attachment II, Section 1.3.2.1). No spent nuclear fuel or high-level radioactive waste casks would be lifted in the Carrier Preparation Building. The waste forms would be protected by the transportation casks.

2.2.4.2   Waste Handling Building

The Waste Handling Building would provide the space, layout, structures, and built-in systems to support waste handling operations, loading and holding of waste packages, and inventory of unused disposal containers (CRWMS M&O 2000s). This complex would also provide a safe environment for personnel and equipment involved in waste handling operations. Figures 2-22 and 2-23 show the Waste Handling Building in plan
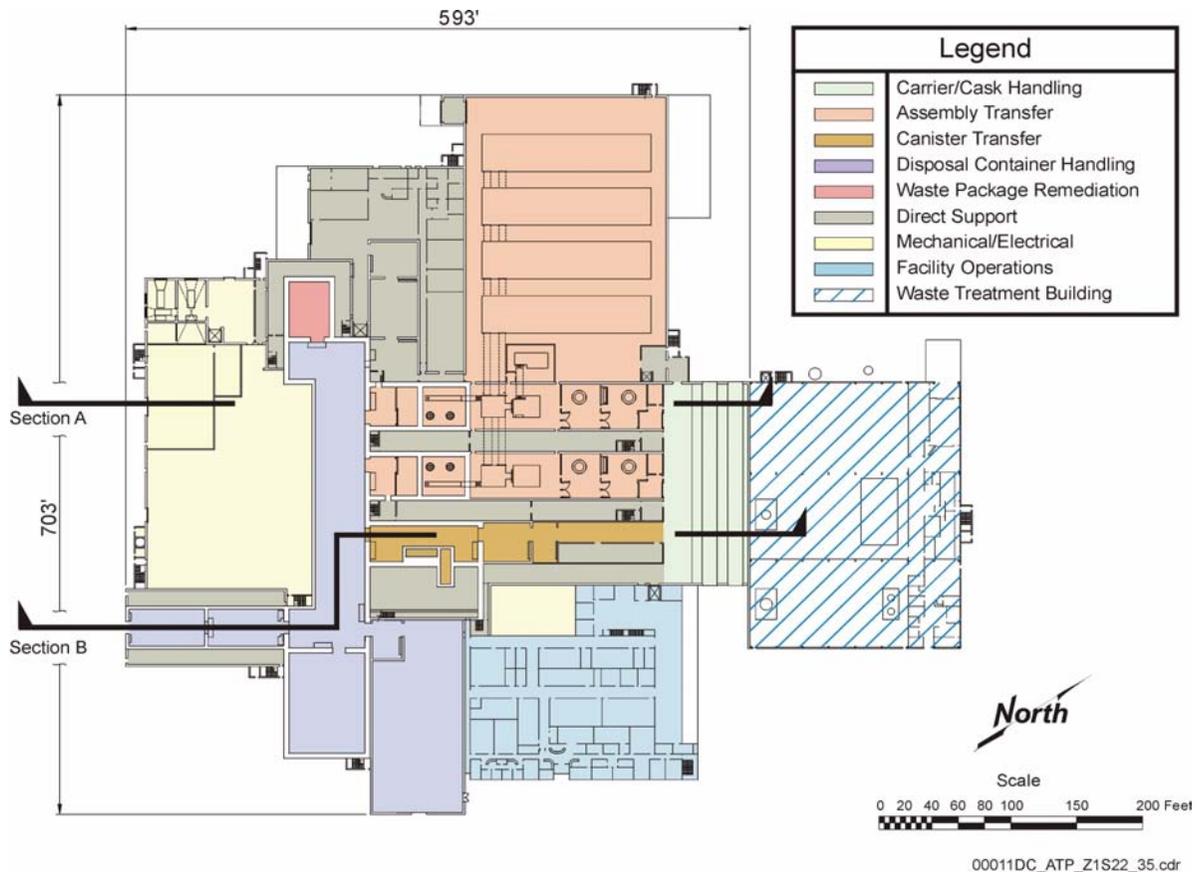
Figure 2-22.   Waste Handling Building Systems Layout
Spent nuclear fuel and high-level radioactive waste in transportation casks would be removed from their carriers in the carrier/cask handling area and sent to one of two systems, depending upon how they are packaged, for further processing: either the assembly transfer system or the canister transfer system. After the transportation contents have been transferred into a disposal container, the disposal container would be moved to the disposal container handling system, where the lids would be welded onto the container and then inspected. A waste package remediation area would be provided to address any mechanical problems with the waste package. The Waste Treatment Building would collect and process solid, liquid, and gaseous low-level radioactive waste. Solid waste would be packaged for shipment and offsite disposal. Sections A and B are shown in Figure 2-23. Elevation: 100 ft. Source: Modified from CRWMS M&O 2000q, Figures I-1 and I-4.

view and sections, respectively. A 30.5-m (100-ft) elevation designation has been assigned to the finished grade elevation of the Waste Treatment Building; all other references to building elevation are measured from this assigned designation. Table 2-4 gives the preliminary performance specifications for the Waste Handling Building.

The Waste Handling Building would contain different systems to:

- Confine potential contaminants
- Enhance industrial safety
- Control and monitor operations

- Provide general safeguards and security
- Supply necessary fire protection, ventilation, and utilities.

The building would also provide the needed space and layout for maintenance, administration, and other support operations associated with waste handling activities. It would have designed-in means of protecting its systems and subsystems from the adverse effects of any natural or man-made environment. The complex will also be designed to ensure that radiation exposure levels to workers are kept ALARA.
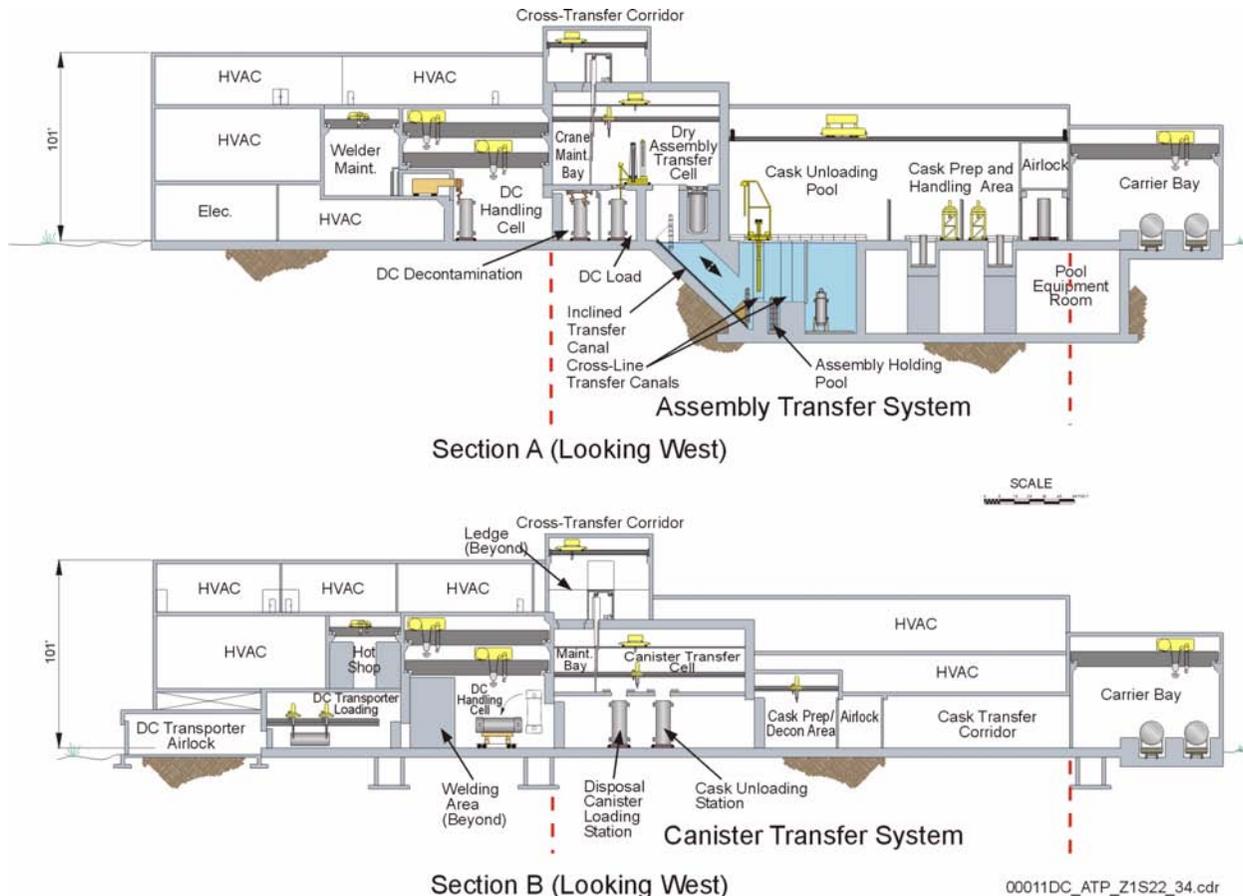
Figure 2-23.   Waste Handling Building Sections
The top figure, Section A, depicts the assembly transfer system (two lines), where individual spent nuclear fuel assemblies would be loaded into disposal containers. The bottom figure, Section B, depicts the canister transfer system (one line), where canisters already loaded with spent nuclear fuel or high-level radioactive waste and suitable for direct insertion would be transferred into disposal containers. Various electrical and heating, ventilation, and air conditioning equipment support waste handling operations. Locations of these two sections are shown in the plan view in Figure 2-22. More detailed figures follow. HVAC = heating, ventilation, and air conditioning; DC = disposal container. Source: Modified from CRWMS M&O 2000q, Figure I-9.

2.2.4.2.1   Waste Handling Building: Architectural Features

The Waste Handling Building would be located in the North Portal area. Built adjacent to the south wall of the Waste Treatment Building, the Waste Handling Building would be a multilevel, concrete and steel structure made of noncombustible materials. The exterior walls would be mainly concrete; walls that do not provide shielding for radiation protection would be constructed of metal siding panels with insulation. The building would be approximately 180 m (600 ft) wide by 210 m (700 ft) long (CRWMS M&O 2000q, Figure I-4).

Figure 2-23 shows section views of the building. All personnel would enter the building through a security portal. Staff who work in contaminated or potentially contaminated areas would change into protective clothing in the change rooms before proceeding to workstations through entrance/exit corridors. All operations levels would be accessible by corridors and stairwells. To meet function and safety requirements, the operating galleries would be located outside the transfer cells. Operating galleries are shielded areas where operators can safely and remotely observe and control operations. Shielding walls, windows, and doors would

Table 2-4. Preliminary Waste Handling Building Performance Specifications

Source of Requirement	Performance Specification
Performance Criteria	Support and optimize dry handling of high-level radioactive waste for the expected waste throughput
	Support and optimize wet handling of high-level radioactive waste for the expected waste throughput
	Provide space for staging, layout, and storage of equipment and tools
	Provide space for preparation of canisters, waste packages, and empty disposal containers
	Facilitate the collection and transfer of solid and liquid low-level waste (no mixing with noncontaminated systems) for processing in the Waste Treatment Building
Nuclear Safety Criteria	Structure shall be designed to withstand a Frequency Category 2 design basis earthquake
	Provide suitable barriers to impede the spread of fires to systems and equipment that are important to confinement
	System design shall provide that during and after a design basis events and off-normal environmental conditions, operation of QL-1 systems important to safety is not affected by failure of other structures, systems, and components
	Building shall maintain control of radioactive waste and radioactive effluents
	Building shall limit radioactive contamination by creating confinement zones based on isolating activities that have a potential for emissions
	Building shall be designed for the design basis flood in accordance with guidelines in Regulatory Guide 1.102, *Flood Protection for Nuclear Power Plants*
	Building design shall limit the accumulation of radioactive contamination and facilitate decontamination of components and surfaces
Nonnuclear Safety Criteria	Floor surfaces upon which transportation casks are loaded and unloaded shall be flat and at the same level as the top of any railroad track rails
	Building shall be designed to permit prompt termination of operations and evacuation of personnel during an emergency
Environmental Criteria	Building shall be designed such that components susceptible to radiation will not deteriorate excessively when exposed to the radiation environment in which it is located
	Building shall be designed for an outside temperature of 5° to 117°F (-15° to 47°C)
	Building shall be designed for a maximum daily snowfall of 10 in. (25.4 cm) and a maximum snowfall accumulation of 17 in. (43.18 cm)
	Building shall be designed for a maximum annual precipitation of 10 in. (25.4 cm) and a maximum daily precipitation of 5 in. (12.7 cm)
	Building shall be designed to withstand a frost line depth of 15 in. (38.1 cm) below the undisturbed ground surface.

Source: CRWMS M&O 2000s.

protect staff operating and maintaining the five primary waste handling systems.

The Waste Handling Building would integrate the five primary systems (CRWMS M&O 2000q, Section 6.2.1) that receive, lift, unload, handle, reload, package, and deliver high-level radioactive waste to subsurface waste handling systems. Table 2-5 summarizes these preliminary engineering specifications. The primary systems in the building would be:

- Carrier/cask handling system
- Assembly transfer system
- Canister transfer system
- Disposal container handling system
- Waste package remediation system.

Carriers would move transportation casks into and out of the Waste Handling Building through vertical lift doors at the carrier bay. The casks would then be transferred through air locks to one of two assembly transfer system lines or to the one canister transfer system line. Each assembly transfer line would contain:

- A cask preparation and decontamination area
- A pool area for holding and unloading the cask
- An inclined transfer canal to an assembly handling cell
- A disposal container loading cell
- A disposal container decontamination cell.

Table 2-5. Preliminary Facility Space Specifications for the Waste Handling Building

Facility Space/System	Floor Area m² (ft²)
Cask/carrier handling system	1,456 (15,680)
Assembly transfer system	7,645 (82,300)
Canister transfer system	1,374 (14,800)
Disposal container system	4,751 (51,140)
Waste package remediation system	185 (2,000)
Primary support areas	6,791 (73,100)
Heating, ventilation, and air conditioning equipment areas	22,413 (241,260)
Other building areas not listed above	15,358 (165,320)
TOTAL	59,978 (645,600)

Source: CRWMS M&O 2000q, Table 6-2.

The assembly transfer pools would be connected, via fuel basket transfer canals, to four compartmentalized fuel blending inventory pools. The canister transfer line would consist of a cask preparation and decontamination area, a cask unloading area, and a station for loading the disposal containers with the waste. After being loaded, the disposal containers from the three transfer lines would be staged in the disposal container handling cell, where their lids would be robotically welded on. Finally, the loaded, sealed, inspected, and accepted disposal containers, now referred to as waste packages, would be transferred into the waste package transporter cell and loaded onto a transporter for subsurface emplacement.

A number of systems and structural features would support these waste handling operations. An area would be designated for preparing empty disposal containers, and a holding area would provide room for loaded and sealed waste packages waiting for emplacement. A maintenance bay would be available to maintain the handling cranes. The building would also have shops to repair and maintain instruments, robotic welders, and other equipment, along with storage areas for all necessary tools, maintenance materials, high-efficiency air particulate filters, and gas bottles.

2.2.4.2.2 Waste Handling Building: Structural System

The building's foundation would be a reinforced concrete mat (CRWMS M&O 2000p, Attachment II, Section 1.1.6.4). Before construction of the foundation, the undocumented fill of the existing North Portal pad would be improved by the DOE. The building would be designed to withstand (CRWMS M&O 1999e):

- Tornado winds of up to 302 km/hr (189 mi/hr)
- Tornado-generated missiles
- A pressure drop of 0.81 psi
- A rate of pressure drop of 0.3 psi/s.

Although unlikely, ground motion from earthquakes of significant magnitude may occur at the site of the Waste Handling Building (for a discussion of site earthquake ground motion, see Section 4.3.2.2). The best way to provide confidence that the Waste Handling Building can be safely constructed and operated is to determine the response of the building to ground motion. To this end, the DOE has performed a preliminary soil–structure interaction analysis, using a simplified conceptual design of the Waste Handling Building. This analysis demonstrates that a Waste Handling Building can be designed so that its response to large earthquakes would be within acceptable levels and its structural members would not be overstressed (CRWMS M&O 2000t). The final detailed design of the Waste Handling Building will be in accordance with NRC regulations, which require the building to safely survive a site-specific earthquake with a probability of occurring once in 10,000 years.

The design of the Waste Handling Building would include features to limit worker radiation exposure to levels that are ALARA (CRWMS M&O 2000p, Attachment II, Section 1.1.6.3.4). Various areas in the Waste Handling Building have been designated to have radiation levels that either preclude human occupancy or in which occupancy would be controlled. These areas are designated as radiation access zones, which are defined as areas with radiation levels that potentially fall within boundaries that correlate to the limits in 10 CFR Part 20 and

10 CFR Part 835 if the facility were to be licensed. The object of the radiation access zones is to provide a design framework that realistically limits radiation exposures to the lowest levels that are reasonable, given the state of technology, economics, and benefits to public health and safety. Figure 2-24 shows the radiation access zones that are currently designated in the Waste Handling Building. The slab thicknesses for missile protection will be validated during detailed design. Radiological areas would have 1.5-m (5-ft) thick concrete floors that can support loads of up to 126 metric tons (140 tons) of heavy equipment that would handle casks and waste packages (CRWMS M&O 2000p, Attachment II, Section 1.1.6.4). The walls would also be concrete, with stepped

decreases in thickness at the ceiling. The roof would be a concrete slab supported by steel beams and concrete walls (CRWMS M&O 2000q, Section 6.2.7). The roof structure would also be designed to withstand tornado-force winds and wind-generated missiles.

Underwater waste handling operations would be conducted in the assembly transfer system pool area, which would consist of several pools for holding and unloading casks and one nonstandard fuel pool. Fuel would be stored in the Pool Fuel Blending Inventory Building, near the assembly transfer system line unloading pools. The Pool Fuel Blending Inventory Building would be a steel-framed structure measuring approximately 85 m
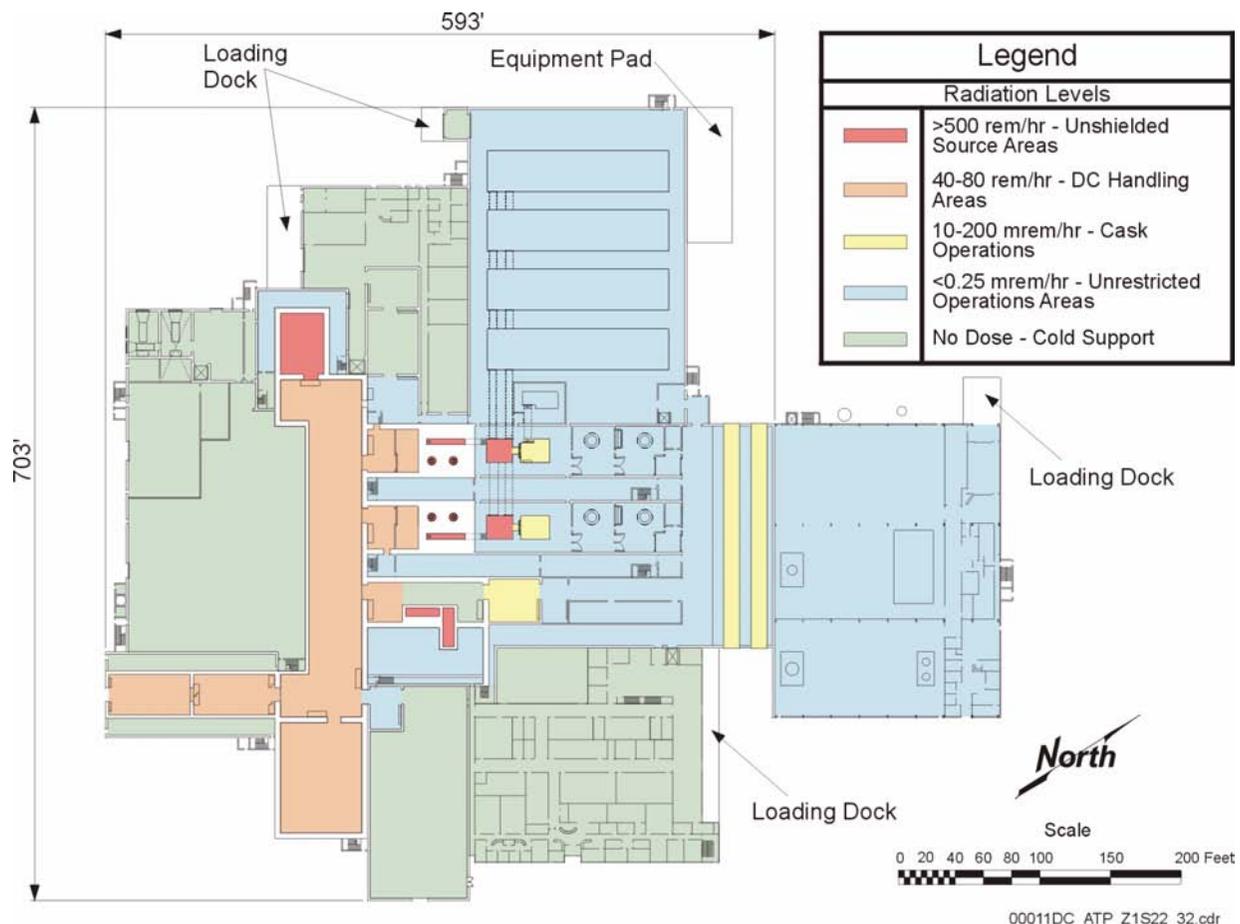
Figure 2-24. Waste Handling Building Radiation Levels
All waste handling operations would be conducted behind shielded concrete walls using remotely operated equipment. Personnel access to such areas would be prohibited during operations, and the doors to the cells would be locked to prevent accidental entry. Radiation areas would be marked in accordance with the requirements of the NRC, which places an upper limit on annual worker radiation exposures of 5,000 mrem. Elevation: 100 ft. DC = disposal container. Source: Modified from CRWMS M&O 2000p, Figure I-28.

(280 ft) long, 59 m (194 ft) wide, and 21 m (70 ft) high. It would house four inventory pools measuring 48 m (160 ft) long, 11 m (37 ft) wide, and 15 m (50 ft) deep. The inventory pools would be connected to the assembly transfer system unloading pools by two transfer canals. The pools would be designed to withstand earthquakes and other anticipated design basis events. They would meet radiation shielding requirements through construction of reinforced concrete floors and walls lined with stainless steel plate, which would also keep pool water from coming into contact with the concrete pool, floor, and walls, and leaking out (CRWMS M&O 2000p, Section II, Attachment 1.1.6.4). The stainless steel liners would contain leak detection systems.

The Waste Handling Building complex would contain several nonradiological facilities that would be separated from the main building to avoid possible interactions during an earthquake (CRWMS M&O 2000p, Attachment II, Section 1.1.6). The facility support area would include administrative offices and laboratories. It would be a two-story, steel-framed structure with sheet metal siding and a metal deck roof. The structure would consist of steel beams, columns, and bracing, with metal-clad siding and insulated roofing (CRWMS M&O 2000p, Attachment II, Section 1.1.6.4). The first floor would be concrete slab on grade; the second floor would be concrete slab on metal decking. The columns would have combined spread footings to avoid settlement.

The other nonradiological facilities would be used for cleaning transport equipment and storing and preparing new waste packages. The structure for these facilities would be light steel framing with sheet metal siding. The floors would support the loads from rail and truck transporters bringing waste packages into the buildings and from storing prepared, empty disposal containers.

2.2.4.2.3   Waste Handling Building: Carrier/Cask Handling System

The Waste Handling Building carrier/cask handling system would receive rail and truck carriers containing transportation casks from the carrier/cask transport system, unload the casks, and reload the empty casks back onto the carriers for shipment off the repository site. Loaded casks would be transferred to the assembly transfer system or the canister transfer system.

The carrier/cask handling system would also receive dual-purpose canister overpacks from the carrier/cask transport system, unload them, transfer them to the assembly transfer system, receive the overpacks with the empty dual-purpose canisters back from the assembly transfer system, and reload the empty dual-purpose canisters onto carriers for shipment off the repository site. The carrier/cask handling system would be configured to accommodate the waste transportation and processing schedules established for the repository (CRWMS M&O 2000p, Attachment II, Section 1.1.3.1).

The carrier/cask handling system would be housed in the carrier bay of the Waste Handling Building. Figure 2-25 provides a mechanical flow diagram that is based on the waste handling system operations documented in the *Engineering Files for Site Recommendation* (CRWMS M&O 2000p, Attachment II, Section 1.1.3.1).

A site prime mover would tow the truck carrier or railcar into the carrier bay's loading area. After removal of the cask tie-downs, a 160-ton capacity bridge crane would lift the cask off the carrier and place it onto a cask transfer cart for delivery to the assembly transfer system or the canister transfer system, as appropriate. After the cask is unloaded and decontaminated, it would be returned to the carrier/cask handling system for shipment offsite.

The Waste Handling Building, which would house the carrier/cask handling system, would provide the necessary utility and safety systems (CRWMS M&O 2000p, Attachment II, Section 1.1.3.1). No spent nuclear fuel or high-level radioactive waste would be directly handled by the carrier/cask handling system. The waste forms would be protected by the transportation casks.

2.2.4.2.4   Waste Handling Building: Canister Transfer System

The Waste Handling Building would house the canister transfer system, which would receive rail
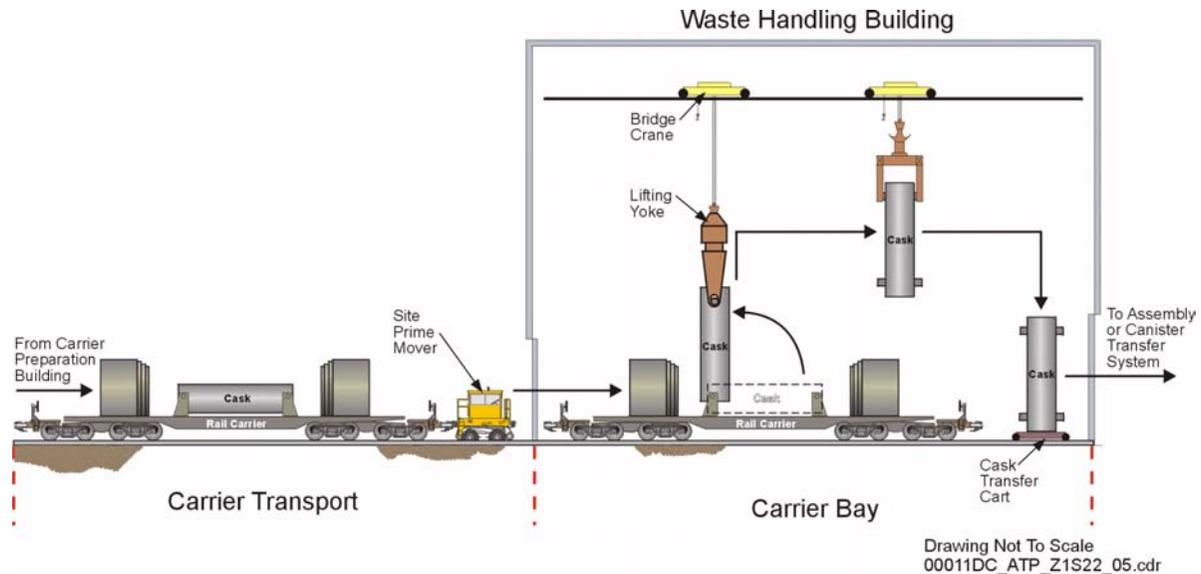
Figure 2-25. Carrier/Cask Handling System
Transportation casks containing spent nuclear fuel and high-level radioactive waste would be offloaded from road/rail carriers in the carrier bay of the Waste Handling Building. The cask would be placed on a seismically restrained cask transfer cart that sits on rails and is powered by electric motors. The cart is the means by which loaded and emptied transportation casks would be moved about within the Waste Handling Building. The transportation casks would remain closed while in the carrier bay. Source: CRWMS M&O 2000p, Figure I-11.

and truck transportation casks from the carrier/cask handling system and empty disposal containers from the disposal container handling system. Figure 2-26 provides a mechanical flow diagram for the operations of the canister transfer system. One canister transfer line would handle canister waste and support maintenance of the system. The line would be configured to handle disposable canisters of DOE high-level radioactive waste or spent nuclear fuel, ultimately loading them into disposal containers. The canister transfer line would also have:

- An air lock

- A cask preparation and decontamination area

- A canister transfer cell

- An off-normal canister handling cell

- A transfer tunnel connecting the canister transfer and off-normal canister handling cells.

WHB/WTB Space Program Analysis for Site Recommendation (CRWMS M&O 2000q, Section

6.2.1.3) documents the physical arrangement of the canister transfer system. Preliminary engineering specifications are given in Table 2-6.

A transportation cask containing canisters of DOE high-level radioactive waste or spent nuclear fuel would be unloaded in the Waste Handling Building's carrier bay, then transferred to a cask transfer cart and secured against overturning. The cask transfer cart would move through a transfer corridor into a canister transfer system air lock, which would have isolation doors at both ends to maintain a lower air pressure in the canister transfer work areas than in the carrier bay. The cart would take the cask through the air lock to the cask preparation area (CRWMS M&O 2000p, Attachment II, Section 1.1.2.1).

The cask preparation area would include a preparation station and a decontamination station. Remote handling equipment would consist of a cask transfer cart, cask preparation manipulator, and the tools required to perform cask unbolting, venting,
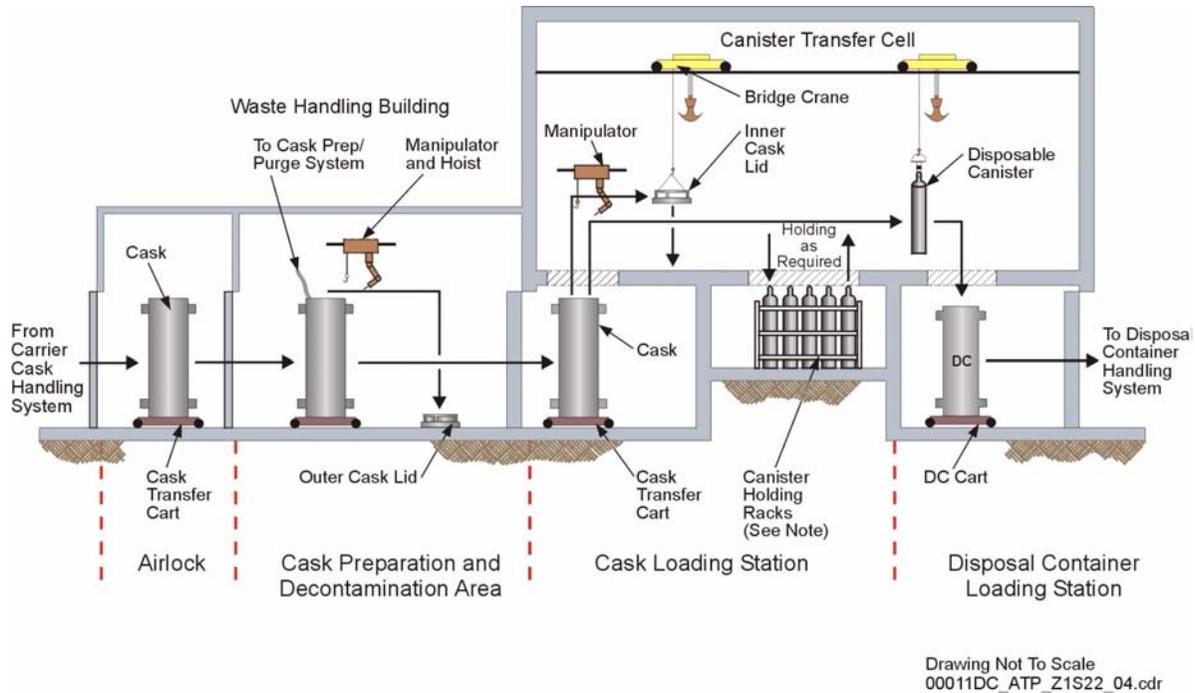
Figure 2-26.   Canister Transfer System
The transportation cask outer lid would be removed and the internal gas sampled using a purge system and remote manipulator. If necessary, the gas would be filtered prior to release. The cask transfer cart would move the cask into the canister transfer cell, where the inner cask lid would be removed and the canister removed from the transportation cask and inserted directly into a disposal container. Canister holding racks are not in the direct transfer path from the loading station to the disposal station; they are provided to facilitate efficient operations. Such inventory allows the creation of precise thermal loads for each waste package. The disposal container would be moved and positioned using a seismically restrained transfer cart similar to the one used for moving the transportation cask. DC = disposal container. Source: Modified from CRWMS M&O 2000p, Figure I-6.

lid removal, and decontamination. Workers preparing a cask would:

- Sample the cask's vent ports

- Vent the cask and purge the cavity gas, if required, to the atmosphere through a high-efficiency particulate air filtration system

- Loosen the outer lid bolts

- Secure a lifting fixture to the outer lid

- Remove the outer lid and stage it in the cask preparation area.

Casks containing disposable canisters are not required to have outer and inner lids; for example, the naval spent nuclear fuel canister would have only one closure lid. A special lifting fixture would be installed on naval spent nuclear fuel canisters, using the hoist and the manipulator. The cask transfer cart would then move the cask to the canister transfer cell, where the canister would be loaded directly into a disposal container (CRWMS M&O 2000p, Attachment II, Section 1.1.2.1).

Once the canisters are removed from the transportation cask, the empty cask would be prepared for shipment back to a transportation contractor for reuse. The cask transfer cart would move the cask to the decontamination area, where workers would:

- Remove the inner lid lifting fixture
- Install and tighten the inner lid bolts
- Install and tighten the outer lid bolts
- Remove the outer lid lifting fixture
- Perform a radiation survey on the empty cask
- Decontaminate the cask (if required).

Table 2-6. Preliminary Canister Transfer System Performance Specifications

Source of Requirement	Performance Specification
Performance Criteria	System shall transfer required canister waste types
	System shall support required average transportation cask turnaround times to the Regional Servicing Contractor
	System shall provide for canister inventory
	Provide features to sample, measure, and monitor the transportation cask parameters prior to opening
	System shall limit canister temperatures while in inventory racks
	Provide capability for off-normal canister handling
Nuclear Safety Criteria	System shall be designed to ensure that canisters cannot be breached from any credible drop, considering each type of canister handled[a]
	Canister racks shall be designed to maintain their geometry during and following a Category 2 design basis earthquake
	System design shall prevent the drop of suspended canisters during and following a Category 1 design basis earthquake
	Cranes and hoists shall be designed to remain on their rails during and following a Category 2 design basis earthquake
	System shall be designed to retain suspended loads during and after a loss of electrical power
	System shall be designed for criticality safety under normal and accident conditions
	Maintain control of canistered waste and permit prompt termination of operations during an emergency
	System design shall define safe load paths for the movement of heavy loads to minimize the potential for drops on canister waste
Nonnuclear Safety Criteria	System shall be designed to incorporate the use of noncombustible and heat resistant materials to the extent practicable
	System design shall include provisions for decommissioning and decontamination

[a]The exception is the naval canister, which is not certified to withstand all credible handling impacts.
Source: CRWMS M&O 2000u; BSC 2001f, Section 5.4.

After the cask has been prepared, it would be moved to the carrier bay for loading onto a rail or truck carrier (CRWMS M&O 2000p, Attachment II, Section 1.1.2.1).

All canister transfer operations would be performed remotely in shielded canister transfer or off-normal canister handling cells. The canister transfer cell would consist of:

- Upper and lower transfer rooms
- A cask unloading port
- A disposal container loading port where canisters would be loaded
- An off-normal canister transfer port
- A small canister holding area
- A crane maintenance area.

Small canisters would either be loaded directly into a disposal container or staged in the canister transfer cell until enough canisters are available to fill a disposal container. Large canisters of naval spent nuclear fuel would be loaded directly into a disposal container. The canister transfer system would then deliver the loaded disposal containers to the disposal container handling system. Any canisters that are damaged during handling or received in a condition that does not meet acceptance criteria would be considered off-normal. Off-normal canisters would be transferred to the off-normal canister handling cell for corrective action (CRWMS M&O 2000p, Attachment II, Section 1.1.2.1).

The canister transfer cell would be divided into lower and upper rooms, as previously described, with transfer ports between the rooms to allow vertical lifting of a canister from its transportation cask to its disposal container, to the holding area, or to the off-normal transfer tunnel. The upper

room would include a maintenance bay and ports for:

- Unloading transportation casks
- Loading disposal containers
- Transferring off-normal canisters
- Moving the canisters to the holding area.

The lower room would include:

- A station for unloading casks
- A station for loading disposal containers
- The canister holding area
- A transfer tunnel and cart for off-normal canisters.

A rack would accommodate temporary holding of 20 small canisters in a shielded area. This arrangement would reduce the height of any potential canister drop during transfers (CRWMS M&O 2000p, Attachment II, Section 1.1.2.3).

The canisters would be removed from a transportation cask one at a time by remote equipment and placed in a disposal container, taken to the holding area, or moved through the port for off-normal canisters to the off-normal canister handling cell. Remote handling equipment in the transfer cell would include a 65-ton overhead bridge crane (sized to handle large naval canisters), an electromechanical manipulator, and a suite of small canister-lifting fixtures. The remote equipment would be designed to facilitate in-cell operations, maintenance, and recovery from off-normal events. A maintenance bay inside the cell would facilitate in-cell maintenance. Interchangeable components would facilitate maintenance, repair, and replacement of equipment. Lay-down areas would be provided, as required, for fixtures, tooling, and canister grapples. If in-cell equipment fails, the crane and manipulator can be remotely withdrawn to the maintenance bay by using off-normal and recovery operations. Once a disposal container has been loaded, it would be moved to the disposal container handling system (CRWMS M&O 2000p, Attachment II, Section 1.1.2.1).

A separate off-normal handling cell would be located next to the canister transfer cell, connected by the off-normal canister transfer tunnel. Special equipment would receive, handle and, if necessary, repackage off-normal canisters before final disposal in the repository. The cell's equipment would include a small overhead crane, a bridge-mounted electromechanical manipulator, and two overpack loading and welding stations (for canisters with different diameters and heights). The loading and welding stations would be located in a pit to reduce the height above the floor that a canister must be lifted for placement into an overpack. At both the loading and welding stations, special fixtures would be used to properly position, load, and weld the overpacks. A robotic welding machine, positioned between the pits, would remotely weld a loaded overpack in either station. The off-normal canister handling cell would also contain the following (CRWMS M&O 2000p, Attachment II, Section 1.1.2.3):

- A canister transfer cart
- Racks for holding 20 small canisters
- A canister repair station
- Canister overpacks
- Remote-handling fixtures
- A decontamination station
- Closed-circuit television systems
- Shield windows.

2.2.4.2.5 Waste Handling Building: Assembly Transfer System

The assembly transfer system would include the equipment, facilities, workers, and processes for preparing individual spent nuclear fuel assemblies for disposal in the potential repository. Preliminary engineering specifications are given in Table 2-7.

Two assembly transfer system lines would be housed in the Waste Handling Building. Each would operate independently to handle waste throughput and support maintenance operations. Each would include a cask unloading area and a transfer cell area. The cask unloading area would contain an air lock, a cask preparation and decontamination area, and a pool area. The pool area would contain a cask unloading pool and an assembly holding pool. A single transfer canal would connect the two pools. An inclined transfer canal would be used for moving the spent nuclear fuel assemblies from the holding pool to the

Table 2-7. Preliminary Assembly Transfer System Performance Specifications

Source of Requirement	Performance Specification
Performance Criteria	Transfer intact fuel assemblies from specified assembly classes
	Remove spent nuclear fuel assemblies from the dual-purpose canisters
	System shall support average specified transportation times to the regional servicing contractor
	Provide for inventory of 5,000 MTHM of spent nuclear fuel assemblies
	Provide temporary seals, evacuate gases, and backfill disposal containers with inert gas to preclude oxidation of the spent nuclear fuel assemblies
	Provide capability for nonstandard canister handling
Nuclear Safety Criteria	System design shall reduce the probability of a spent fuel assembly drop onto another spent fuel basket during dry handling to less than a Category 1 design basis event
	Spent fuel assembly transfer baskets and basket staging racks shall be designed for a Category 2 design basis event
	Overhead cranes and fuel transfer machines shall be designed for a Category 2 design basis earthquake and not be dislodged from their rails
	System shall be designed to retain suspended loads during and after a loss of electrical power
	System shall be designed for criticality safety under normal and accident conditions
	System design shall define safe load paths for the movement of heavy loads to minimize the potential for drops on spent nuclear fuel
	System shall provide overhead limit sensing and alarming capabilities to automatically stop handling operations and warn operators of unsafe conditions
Nonnuclear Safety Criteria	System shall be designed to incorporate the use of noncombustible and heat resistant materials to the extent practicable
	System design shall include provisions for decommissioning and decontamination

Source: CRWMS M&O 2000v.

assembly handling cell. The assembly transfer system would include an assembly handling cell, a disposal container loading cell, and a disposal container decontamination cell. The assembly transfer system would also include fuel blending inventory pools and a special pool for nonstandard fuel, which would be located in an annex to the Waste Handling Building. The physical arrangement of the assembly transfer system is documented in the *WHB/WTB Space Program Analysis for Site Recommendation* (CRWMS M&O 2000q, Section 6.2.1.2).

Figures 2-27, 2-28, and 2-29 depict mechanical flow diagrams that illustrate assembly transfer system operations. The process begins with the receipt of transportation casks from the carrier/cask handling system and the receipt of empty disposal containers from the disposal container handling system. The casks are prepared for unloading, cooled, and filled with water. The system would then transfer the rail and truck transportation casks to the cask unloading pools. In the pool, the system would remove the inner cask lid and unload indi-vidual spent nuclear fuel assemblies, single-element canisters, and dual-purpose canisters from the transportation casks. Dual-purpose canisters would be opened in the pool using remote under-water tools. Other assembly transfer system operations include (see also Table 2-7):

- Holding assemblies in pools

- Transferring assemblies to transfer cells

- Drying assemblies

- Loading assemblies into disposal containers

- Filling the containers with inert gas

- Installing lid sealing devices

- Decontaminating the lid areas

- Transferring loaded disposal containers from the cell area to the disposal container handling system
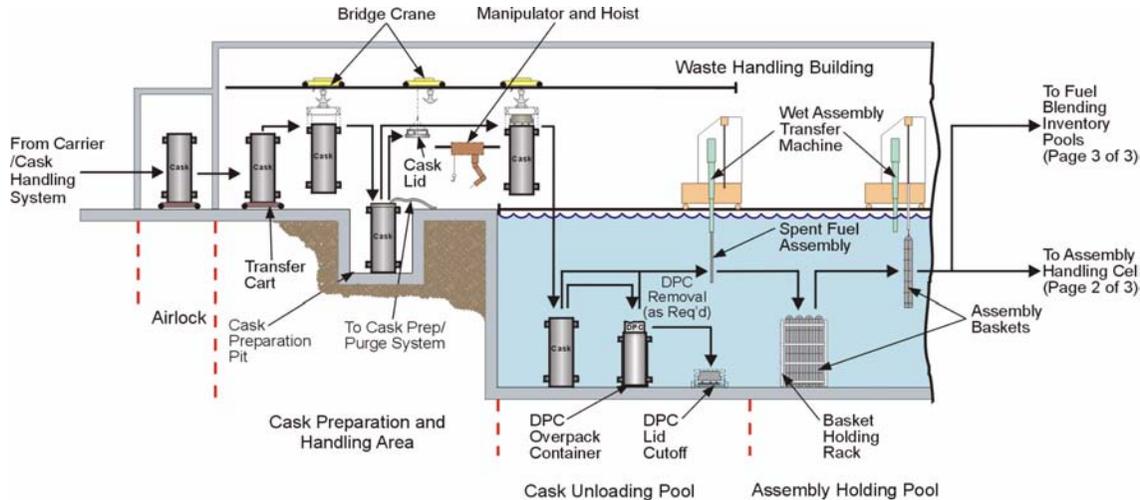
Figure 2-27.   Assembly Transfer System (1 of 3)
An overhead building crane would lift the cask from the cask transfer cart and place it in one of two cask preparation/purge pits, where the outer lid would be removed and the interior gas sampled and, if necessary, filtered prior to release. The crane would then move the cask from the pit into the pool, where the inner lid would be removed. Individual spent nuclear fuel assemblies would be removed from the cask one at a time and placed into basket staging racks for transfer to the assembly handling cell or the fuel pool blending inventory area. Spent fuel assemblies contained in dual-purpose canisters, which are not approved for insertion into disposal containers, would be removed after the lid has been cut off. Use of a fuel blending inventory allows precise thermal loads to be created for each waste package. DPC = dual purpose canister. Source: CRWMS M&O 2000p, Figure I-3.

- Repackaging nonstandard fuel assemblies to meet waste package criteria

- Preparing empty transportation casks and dual-purpose canister overpacks for offsite shipment.

Cask Preparation and Handling—A transportation cask would enter a cask preparation area on a cask transfer cart (CRWMS M&O 2000p). The cask preparation and decontamination area would include two cask preparation and decontamination rooms. Each room would contain a station for unloading and loading transportation casks from the cask transfer cart to a cask preparation pit. These stations would also be used to transfer empty transportation casks and dual-purpose container overpacks (on transfer carts) to the decontamination area. Each cask preparation pit would contain access platforms that can be adjusted for various cask sizes. The pit would also include a cask preparation manipulator and hoist that would be operated remotely. The manipulator and hoist would mount on a gantry and straddle the pit and access platforms. The system would contain a variety of remotely operated tools and accessories for preparing and decontaminating casks using the cask preparation manipulator and hoist. Each assembly transfer system line would include a large overhead bridge crane. The cask preparation area would also include a maintenance bay where workers can perform maintenance on the bridge crane.

The cask preparation and handling area (Figure 2-27) equipment would include:

- A cask transfer cart
- A bridge crane that serves the cask unloading area
- Two cask preparation manipulators with hoists mounted on gantries
- Yokes for lifting casks and dual-purpose canister overpacks
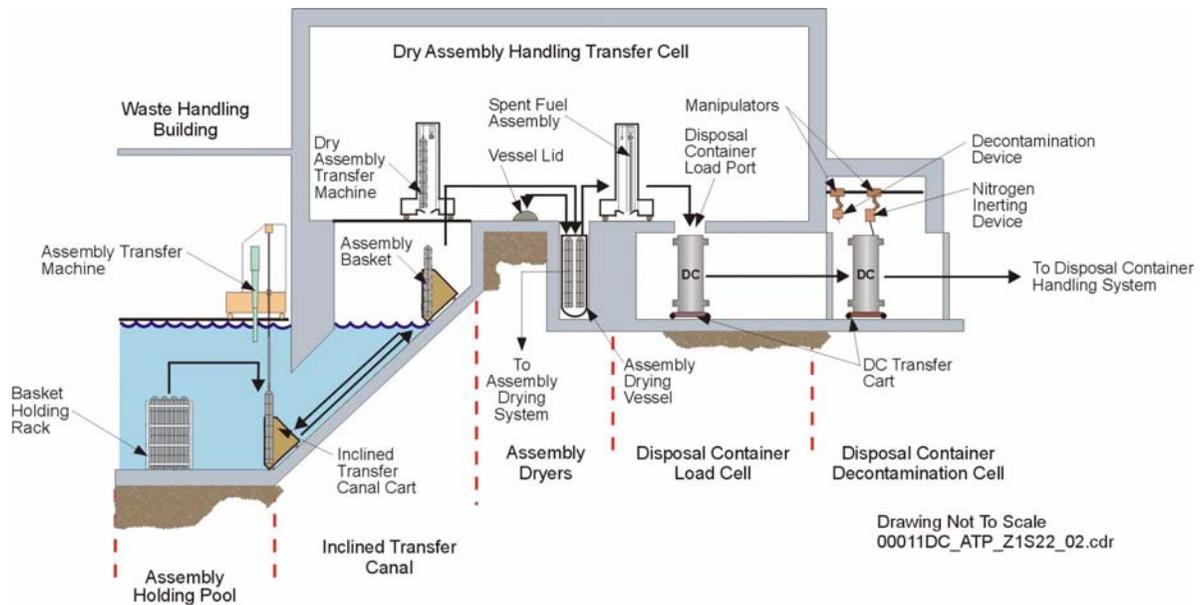
Figure 2-28. Assembly Transfer System (2 of 3)

Individual baskets containing four to nine spent nuclear fuel assemblies would be removed from the staging racks and transferred to an assembly handling cell. Baskets would be transferred from the pool to the assembly handling cell via the inclined transfer canal cart. The baskets would then be placed into one of two drying vessels, where water would be removed to ensure that the interior of the disposal container is exposed to little moisture. After drying, the assemblies would be removed from the dryer one at a time and loaded into the disposal container through the load port in the floor of the cell. After loading, the disposal container would be temporarily sealed and inerted using nitrogen in preparation for later inerting with helium and permanent closure in the disposal container handling system. The disposal container would be moved and positioned using a seismically restrained transfer cart similar to the one used for moving the transportation cask. DC = disposal container. Source: CRWMS M&O 2000p, Figure I-4.
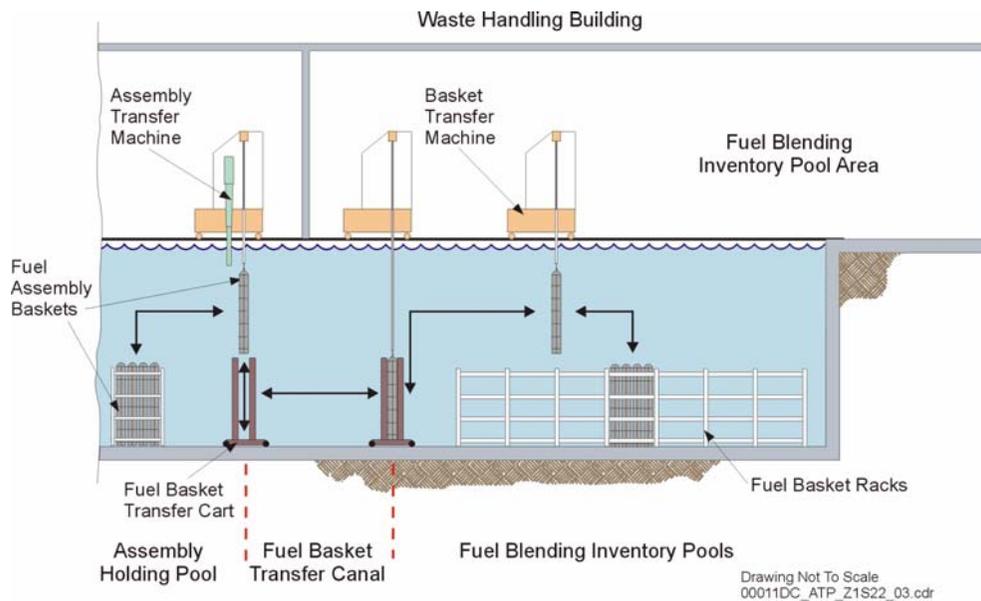
Figure 2-29. Assembly Transfer System (3 of 3)

Each waste package must meet precise thermal load limits. To facilitate meeting such limits, an inventory is established. In that inventory would be older, and therefore cooler, spent nuclear fuel, as well as younger, and therefore hotter, fuel. With an adequate inventory, specific thermal loads can be created for each waste package. Source: CRWMS M&O 2000p, Figure I-5.

- Handling fixtures
- Remotely operated tools and accessories.

The cask unloading and holding pools would be equipped with:

- Remotely operated assembly transfer machines mounted on the pool deck
- Grapples for lifting fuel assemblies
- Cutting tools for removing lids from dual-purpose canisters
- Dual-purpose canister overpacks
- Assembly baskets
- Basket holding racks
- Transfer carts.

The assembly transfer process begins when the carrier/cask handling system unloads a transportation cask from a truck or rail carrier. A crane would lift the cask vertically and transfer it to a cart at the entrance to an assembly transfer system line. The cask would be secured against overturning. The transfer cart would move the cask into an air lock, which would control air movement between the carrier bay and the cask preparation and decontamination area for contamination protection. The air lock would have isolation doors at both ends to maintain a slightly lower air pressure in the radiation work areas than in the carrier bay. The transfer cart would then move the cask to one of two rooms for preparing and decontaminating casks.

The cask preparation and decontamination rooms would have equipment for both remote and manual operations. The large bridge crane in the unloading area and a dry cask lifting yoke would be used to lift the cask from the transfer cart, move it, and lower it into a cask preparation pit. Access platforms would adjust to the size of the cask.

Cask preparation activities would require both remote and manual operations using the crane, manipulator, and associated tools. All cask preparation activities would be performed in a dry environment, but the casks must be prepared for direct transfer to the cask unloading pools. Cask preparation would involve casks with and without dual-purpose canisters. Casks without canisters would have an outer lid or lids, and an inner lid with a built-in shield plug to provide radiation

protection for manual operations. Casks with dual-purpose canisters would have a shield plug built inside the top of the canister.

Remote or manual cask preparation operations consist of:

- Sampling and venting gas from the cask
- Unbolting and removing the cask lid
- Cooling the cask with gas and/or water
- Unbolting the shield plug
- Attaching the shield-plug lifting fixture.

Gas sampling and venting operations would be performed by the cask prep/purge system, which vents to the atmosphere through a high-efficiency particulate air filtration system. If the cask contains individual spent nuclear fuel assemblies with no dual-purpose canister, it would be filled with water in the preparation pit and transferred to the cask unloading pool.

If the cask contains a dual-purpose canister, workers would remove the outer lid while the cask is in the preparation pit. Using remotely operated and manual tools, workers would then open the vent valves on the dual purpose canister; sample, vent, and cool the interior cavity; attach a lifting fixture to the canister; and fill the canister with water. The bridge crane and lifting yoke would transfer the cask containing the dual-purpose canister to the cask unloading pool.

Cask Unloading Pool—The pool area would contain a cask unloading pool and an assembly holding pool (see Figure 2-27), connected by a transfer canal. As shown in Figure 2-28, another inclined transfer canal would connect the assembly holding pool to a handling area. Transfer canals that contain transfer carts for fuel baskets would connect both holding pools to fuel blending inventory pools. Another transfer canal would connect the cask unloading pool and the nonstandard fuel pool.

If a cask contains individual spent nuclear fuel assemblies, then the bridge crane, cask shield plug fixture, and wet lifting yoke would be used to remove its shield plug underwater in the cask unloading pool. If the cask contains a dual-purpose

canister, then the bridge crane, canister lifting fixture, and wet lifting yoke would be used to lift the canister from the cask and place it in a dual-purpose canister overpack. Two 160-ton bridge cranes, each with a 25-ton auxiliary hoist, would be provided to facilitate these operations. Using remote cutting tools, workers would then sever and remove the dual-purpose canister lid. All of these activities would take place underwater in the cask unloading pool (CRWMS M&O 2000r).

A wet assembly transfer machine would remove the individual fuel assemblies from the opened shipping casks and dual-purpose canisters, then load them into assembly baskets in the holding pool. The fuel would remain in these baskets until it is dried and placed in inspected and approved disposal containers. The fuel baskets would contain either four fuel assemblies from pressurized water reactors or eight fuel assemblies from boiling water reactors. The holding pool can hold a maximum of 16 fuel baskets at any one time. When the assembly baskets in the holding pool are full, the wet assembly transfer machine would move the baskets to a transfer cart, which, in turn, would move the loaded fuel baskets to a fuel blending inventory pool or the assembly handling transfer cell for disposal container loading.

The pool area bridge crane and wet handling tools would return the empty transportation casks, and the canister overpacks containing empty dual-purpose canisters and lids, to the cask preparation and decontamination area. The cask preparation and decontamination process would include replacing and bolting down the lids on the empty transportation casks and dual-purpose container overpacks. Workers would decontaminate and dry the casks and containers and then survey them for remaining contamination. After decontamination, workers would transfer empty casks and containers to the carrier/cask handling system for shipment off the repository site and reuse or disposal.

Fuel Blending Inventory—The fuel blending inventory area (shown in Figure 2-29), located in an annex to the Waste Handling Building, would contain four modular inventory pools for spent nuclear fuel and one pool for nonstandard fuel. Each modular pool would have a maximum inven-

tory of 750 fuel baskets loaded with spent nuclear fuel and would be equipped with a 20-ton capacity overhead crane. Transfer canals from the assembly holding pool in each assembly transfer line would connect the modular fuel-blending inventory pools. The pools would have isolation gates so that, if necessary, one pool can be isolated from the other pools. The fuel inventory area would also have a separate pool for handling nonstandard and defective fuel in single-element canisters. All spent fuel and basket-handling operations would be conducted underwater.

The fuel assemblies would stay in the inventory pools until they are selected, according to their heat output, for placement in a disposal container. For the design and operating mode described in this report, the maximum heat generation limit for a waste package is 11.8 kW (CRWMS M&O 2000p, Attachment II, Section 1.1.1). Any higher heat-generating fuel loaded into the disposal container must be thermally blended with lower-heat-generating fuel to meet this limit, a procedure called "fuel blending." Some fuel assemblies would remain in the inventory pool until they generate less heat from radioactive decay, or until lower-heat fuel assemblies become available for blending. Approximately 12,000 spent fuel assemblies in 2,800 assembly baskets would accumulate in the inventory pools during the emplacement period to satisfy the 11.8-kW waste package limit. The inventory pools would be large enough to accommodate 5,000 MTHM of spent nuclear fuel; each pool would have a capacity of 1,250 MTHM, or 750 fuel baskets.

Dry Assembly Handling—A fuel assembly is selected for a disposal container according to the heat generation of the assemblies planned for placement in the disposal container. Assembly baskets and fuel would be transferred from the fuel blending inventory pools. The basket transfer machine would lift and place the fuel basket on a transfer cart, which would take the basket back to the assembly holding pool. The wet assembly transfer machine would move the assembly basket to another transfer cart for the inclined transfer canal. This cart would transport the assembly basket up the inclined canal, out of the pool water, and into the dry assembly handling transfer cell.

The dry assembly handling transfer cell (shown in Figure 2-28) would contain:

- A disposal container loading port
- An assembly transfer machine
- An in-cell manipulator
- Two drying vessels
- An in-cell service crane
- A maintenance bay.

A dry assembly transfer machine would move the assembly basket into one of two drying vessels. It will be necessary to dry the fuel assemblies to meet repository waste package performance criteria. After drying the assemblies, the machine would remove them from the drying vessel and load them into a disposal container. The disposal container would be joined to the disposal container loading port below the assembly transfer cell. The dry assembly transfer machine would install the sealing device and the disposal container's inner lid. The transfer cart would then transfer the disposal container to the decontamination cell, where the top lid area and the inner-lid sealing device would be decontaminated. The system would then evacuate the disposal container internal cavity and fill it with nitrogen gas to exclude oxygen and prevent oxidation. Finally, the transfer cart would transfer the disposal container to the disposal container handling system for lid welding and inspection.

Disposal Container Loading—An empty disposal container equipped with a lifting collar, a base collar, and an inner-lid sealing device would be transferred (Figure 2-28) into the disposal container loading cell and mated with the disposal container loading port. The dry assembly transfer machine would remove the disposal container loading port lid and the inner-lid sealing device. After the fuel assemblies are dry, the dry assembly transfer machine would remove fuel assemblies, one at a time, from the baskets in the drying vessel and load them into the disposal container, positioned below the disposal container loading port. When the disposal container is loaded, the inner-lid sealing device and the loading port lid would be reinstalled using the assembly transfer machine. The disposal container would be disengaged from the loading port and transferred to the decontami-

nation cell, using the transfer cart. The empty assembly baskets would be returned to the pools.

Disposal Container Decontamination and Inerting—In the decontamination cell, the lid of the disposal container and the inner-lid sealing device would be decontaminated. The disposal container would be evacuated and filled with nitrogen gas using an inerting manipulator. The disposal container would then be transferred to the disposal container handling system on the transfer cart for lid welding, inspection, and emplacement in the repository.

A transfer cart would transfer disposal containers between the disposal container handling cell, the decontamination cell, and the loading cell. An isolation door would separate the loading cell and the decontamination cell, and a shield door would separate the decontamination cell and the handling cell. A loading port mating device in the loading cell would provide a contamination barrier between the assembly handling cell, the disposal container loading port, and the disposal container during transfer of spent nuclear fuel. The decontamination cell (Figure 2-28) would be equipped with:

- A bridge-mounted inerting manipulator

- A bridge-mounted decontamination manipulator

- A decontamination tool

- A contamination sample pass-through glove box (this would be used to transfer contamination survey samples into an adjacent operating gallery for counting).

All assembly transfer system remote operations would be controlled from operating galleries next to each assembly transfer cell. Strategically located closed-circuit television systems and shield windows would monitor remote operations. All transfer cell area equipment would be designed to facilitate remote operations and removal for contact decontamination and maintenance. Interchangeable components would be provided where appropriate. The assembly transfer system would

also be designed to provide safe and efficient recovery from equipment failures and malfunctions.

Handling Nonstandard Fuel—One assembly transfer system line would be specifically designed and equipped for processing spent nuclear fuel that does not meet the standard loading criteria for disposal containers. This nonstandard fuel might not meet the loading criteria because, for example, it is in an irregular size single or multiple-element canister, it is not intact, or it contains failed fuel (for a definition of nonstandard fuel, see the glossary). The Waste Handling Building would include a handling room for nonstandard fuel in the fuel blending inventory pool annex. The assembly transfer system line cask unloading pool would connect to the fuel handling room through an underwater transfer canal equipped with isolation gates and a transfer cart. To meet disposal container loading criteria, the nonstandard fuel canister may undergo cutting, unloading, and repackaging operations. These operations would take place underwater in the nonstandard fuel pool.

Any cask containing nonstandard spent nuclear fuel would be directed to the appropriate transfer line. After the cask has been prepared, it would be placed in the cask unloading pool. The cask would be opened and the isolation gates between the cask unloading pool and the nonstandard fuel pool opened. The wet assembly transfer machine would unload the fuel assemblies or canisters from the cask and place them in assembly baskets in the nonstandard assembly basket transfer cart. The transfer cart would then be moved to the nonstandard fuel pool. Once the fuel has been unloaded and transferred, the isolation gates between the two pools would be closed. Using a 30-ton capacity overhead bridge crane, the assembly baskets would be removed from the transfer cart and placed into the nonstandard fuel pool basket holding rack. After the fuel has been repackaged, it would be loaded into the assembly basket again and sent back to the cask unloading pool by reversing the above steps. Once in the cask unloading pool, the loaded fuel baskets would be directed either to the fuel blending inventory pools or to the assembly handling transfer cell.

2.2.4.2.6 Waste Handling Building: Disposal Container Handling System

The disposal container would consist of two concentric metal cylinders: an inner cylinder made from stainless steel and an outer cylinder made of a high-nickel alloy (Alloy 22). The bottom end of each cylinder would be closed with inner and outer lids made of the same materials used to make the cylinder itself. The upper end of each cylinder would be used for final closure lid welds, one for the inner cylinder and two for the outer cylinder. Refer to Section 3 for information on the design, fabrication, and welding of the disposal container. The disposal container would arrive without any waste forms inside. After the radioactive waste is loaded, the disposal container design provides some radiation shielding for operating personnel but not enough to keep occupational exposures within allowable limits. Therefore, all loaded disposal container operations would be done remotely in hot cells. Operations on disposal containers and waste packages containing waste would be performed in dedicated, shielded cells.

The lids for the upper end of the disposal container would be fabricated, but they would not be welded and inspected until after waste is loaded into the container. The three top lids would be installed and welded inside the Waste Handling Building. Once the disposal container is loaded, and its inner and outer top lids are welded, inspected, and accepted, the disposal container is called a waste package.

Figure 2-30 provides a mechanical flow diagram for the operations of the disposal container handling system. The system would receive loaded disposal containers from the canister and assembly transfer systems (Sections 2.2.4.2.4 and 2.2.4.2.5), as well as empty disposal containers from the carrier/cask transport system (Section 2.2.4.2.3). The system, located in the Waste Handling Building, would include areas for:

- Preparing empty disposal containers
- Welding disposal container lids
- Holding loaded disposal containers
- Docking and loading the waste package transporter
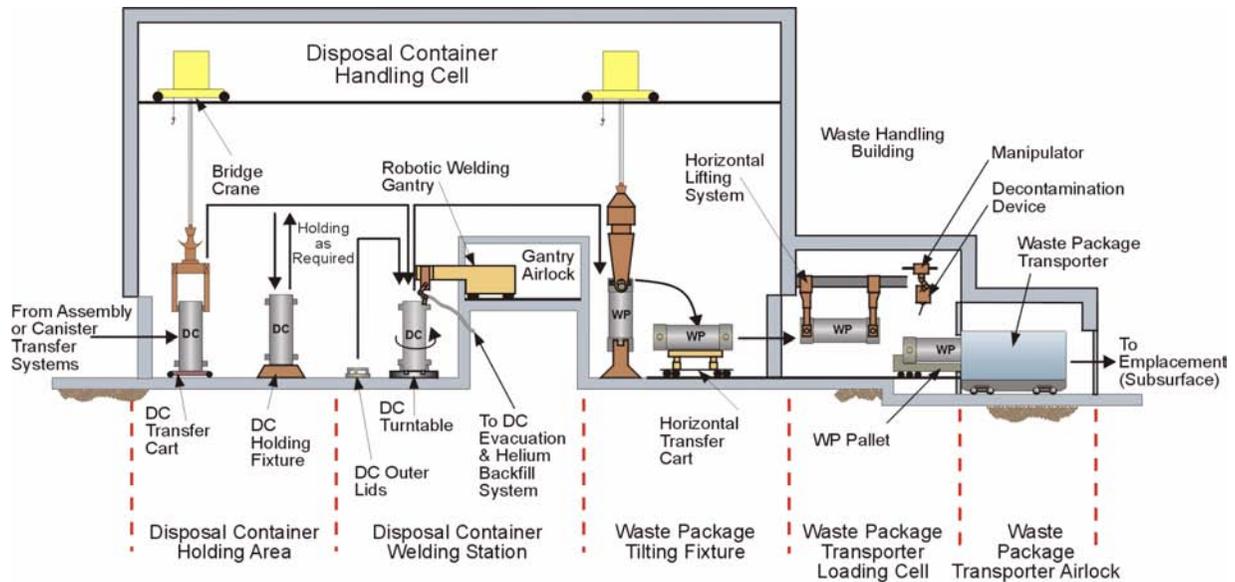
Figure 2-30.   Disposal Container Handling System
Loaded disposal containers would be received from the assembly or canister transfer systems. An overhead bridge crane would lift the disposal container from the transfer cart and place it onto the disposal container turntable, where the disposal container is permanently sealed (inner lid is welded) and the interior backfilled with helium to promote efficient heat transfer from the inner portion of the container to the outer walls. Next, the two outer lids would each be welded on. The welds of each of the three welded lids would be checked after each weld. After remote inspection and acceptance of the welds, the disposal container is termed a waste package. The waste package would be moved to a horizontal position in preparation for loading into the waste package transporter, which would be used in moving the waste package underground to the emplacement drifts. DC = disposal container; WP = waste package. Source: CRWMS M&O 2000p, Figure I-13.

- Maintaining equipment used in handling the disposal containers/waste packages.

To adequately accommodate the throughput rates for disposal containers/waste packages, these areas would operate concurrently for 120 hours per week, 50 weeks per year (CRWMS M&O 2000p, Attachment II, Section 1.1.5). The Waste Handling Building's physical arrangement for the disposal container handling system is documented in the *WHB/WTB Space Program Analysis for Site Recommendation* (CRWMS M&O 2000q, Section 6.2.1.4).

The empty disposal container would be fabricated at a commercial supplier's facility and shipped, with the inner and outer closure lids, to the Waste Handling Building for loading. The disposal container handling system would receive and prepare the empty container for loading, then

deliver it to either the assembly or canister transfer systems for loading.

Once loaded, the container would be returned to the disposal container handling cell for welding. A number of welding stations would be provided to receive loaded containers from the assembly or canister transfer system lines. The welding operations include:

- Mounting the container on a turntable
- Removing temporary lid sealing devices
- Installing and welding the lids
- Conducting nondestructive examination
- Performing in-process weld stress relief.

Following nondestructive examination and acceptance of the weld, the container would be certified as a waste package and either staged or transferred to a tilting station for transport to the underground

repository. Any disposal container that does not meet the weld examination criteria would be transferred to the waste package remediation system for repair or corrective action. A suite of handling fixtures, including yokes, lift beams, collars, grapples, and attachments, would support the operations of the disposal container handling system. The remote equipment will be designed to facilitate decontamination, maintenance, and use of interchangeable components, where appropriate. Setaside areas would be included, as required, for fixtures and tooling to support off-normal and recovery operations. Semiautomatic, remote, manual, and backup control methods would be used to support normal, maintenance, and recovery operations. The interfaces of the Waste Handling Building would provide the facility, utility, maintenance, safety, and auxiliary systems required to support operations and radiation protection activities.

Disposal Container Handling—The disposal container handling cell would be a large, shielded structure containing areas for several welding and inspection stations, holding of loaded containers, transfer cart operations, tilting of the waste package to a horizontal position, and maintenance of the overhead cranes. Handling operations for disposal containers would involve two remotely operated, 150-ton capacity bridge cranes (spanning 22.6 m [74 ft]) and hoists, as well as peripheral equipment. An empty disposal container would be lifted by one of the cranes. The container would either be staged or directly transferred to a transfer cart servicing one of the two assembly transfer system lines or the canister transfer system line for loading. The outer lids for the disposal container would be staged near the welding stations for sealing after the container is loaded. The empty container would be taken into either the assembly transfer system or the canister transfer system for loading. When loaded, the disposal container would be returned to either the holding area or to one of eight welding stations. Each welding station would be equipped with a robotic gantry, a turntable, and multiple sealing tools.

Following examination and certification of the welds, the waste package would be prepared for transport underground to the repository. A completed waste package would be moved to the holding area for loaded disposal containers or to the waste package tilting area, where the waste package would be rotated to a horizontal position resting on a horizontal transfer cart. This cart would transfer the waste package to the transporter loading cell.

Equipment for the disposal container handling system (shown in Figure 2-30) is designed to facilitate remote retrieval for manual decontamination, maintenance, and component replacement, as required. All handling operations would be supported by a variety of remote handling fixtures, including:

- Disposal container lifting and base collars
- Lifting trunnions
- Lifting yokes
- Lifting beams
- Tilting fixtures
- Holding fixtures
- Lid sealing devices.

A crane maintenance bay at the far end of the handling cell would allow for contact maintenance and testing of the cranes in the cell.

Disposal Container Sealing and Closure—The disposal container handling system shown in Figure 2-30 would receive a loaded and temporarily sealed disposal container from the assembly transfer system or the canister transfer system, then transfer it to a holding area or a welding station. Sealing and closure would include a number of steps and remote equipment operations. Additional steps and remote equipment would also be required to conduct weld inspections and postweld heat-treatment operations. Following weld inspection and weld certification, the container would either be staged or prepared for transfer to the subsurface of the repository.

The cranes in the disposal container handling cell would be used to lift and transfer a loaded container to one of several independent lid-welding stations. A remotely controlled robotic gantry would set up, prepare, weld, and backfill the container with inert gas. The gantry would also

serve as the remote handling platform to inspect the sealing operations, which would include:

- Securing the disposal container to the welding station's turntable
- Removing temporary sealing devices
- Purging the lid with inert gases for welding
- Backfilling the container with helium prior to closure
- Turning the container
- Welding the inner lid
- Installing the outer lids
- Welding the outer lids.

Welding would be performed using automatic welders deployed from the robotic gantry platform such that they can be remotely removed from the cell for retooling, testing, adjustments, and maintenance. This feature eliminates the need for personnel to enter the radiation environment in the handling cell. Laser peening and annealing processes may be used to relieve stresses in the weld area.

One air lock would be provided for each of the eight welders. The welder air locks would provide access to the robotic gantry, remote welder, nondestructive examining equipment, and postweld heat-treating equipment (CRWMS M&O 2000p, Attachment II, Section 1.1.5.4). Access and service work on the equipment would be possible in these rooms without exposing the workers to the atmosphere and radiation sources in the disposal container handling cell.

Waste Package Holding—The holding area for loaded disposal containers would be used to stow loaded disposal containers or waste packages awaiting transfer to the waste package transporter loading cell. Waste handling simulations have shown that holding 20 loaded disposal containers in the disposal container handling cell can accommodate a 2-week interruption in repository emplacement operations (CRWMS M&O 2000p, Attachment II, Section 1.1.5.4).

To reduce radiation levels in the crane maintenance bay, loaded disposal containers would be staged in a separate area inside the disposal container handling cell. This area would have partial walls

and an access door to facilitate transfers of disposal containers to and from holding locations. The partial walls would provide shielding for the main portions of the cell and the maintenance bay, where protection of equipment and personnel is required. The design configuration incorporates both distance and shielding by isolating radiation sources to one area of the transfer cell and adding a wall separating the staged disposal containers from the welding, handling, and crane maintenance areas. This would significantly reduce radiation doses to equipment during normal operations, while also reducing radiation levels during manned entry into the cell for periodic maintenance and test operations.

Waste Package Transporter Loading—As shown in Figure 2-30, the final handling sequence for the surface facilities involves:

- Repositioning the waste package to a horizontal position

- Transferring the waste package to a decontamination and transporter loading cell

- Loading the emplacement pallet onto the waste package transporter and the waste package onto the emplacement pallet

- Decontaminating the waste packages (final)

- Inspecting the waste packages (final)

- Certifying and tagging waste packages.

These operations would be performed using:

- A remotely operated horizontal transfer cart
- A waste package horizontal lifting machine
- Decontamination and inspection manipulators
- The waste package transporter.

Only one transporter loading line would be available for the final decontamination, inspection, transfer, and loading of waste packages onto a transporter. The waste package, once it is moved into the transporter loading cell from the disposal container handling cell, would be lifted off the

horizontal transfer cart by the lifting collar, the base collar, and the horizontal lifting machine. While suspended, the waste package would be decontaminated, inspected, and certified. Important data needed for repository record keeping would be recorded. The mobile pallet of the transporter would then move into the cell, and the waste package would be lowered onto the pallet. The handling collars would be remotely removed and taken out of the waste package transporter loading cell for reuse. Any contamination picked up during disposal container sealing would be manually removed in rooms for equipment contamination before the collars are transferred to the empty disposal container preparation area for reuse.

A transporter air lock would be provided at the Waste Handling Building exit of the transporter loading line so the waste package transporter vehicle may enter and be docked for loading. The air lock would prevent movement of air between the transporter loading cell and the outside atmo-sphere. In the final surface waste handling steps, the waste package pallet and rolling bed plate would be pulled into the shielded waste package transporter, the transporter shield doors would be closed, and the waste package transporter would be disengaged from the loading cell dock. Then the waste package would be transported to the subsur-face of the repository.

2.2.4.2.7 Waste Package Remediation System

A waste package found to be out of specification would be transferred from the disposal container handling system to the waste package remediation system. This system would be housed in a multi-purpose cell inside the Waste Handling Building. Figure 2-31 provides a mechanical flow diagram for the system's operations. The diagram is based on the waste handling system operations docu-mented in the *Engineering Files for Site Recommendation* (CRWMS M&O 2000p, Attach-ment II, Section 1.1.4.1).
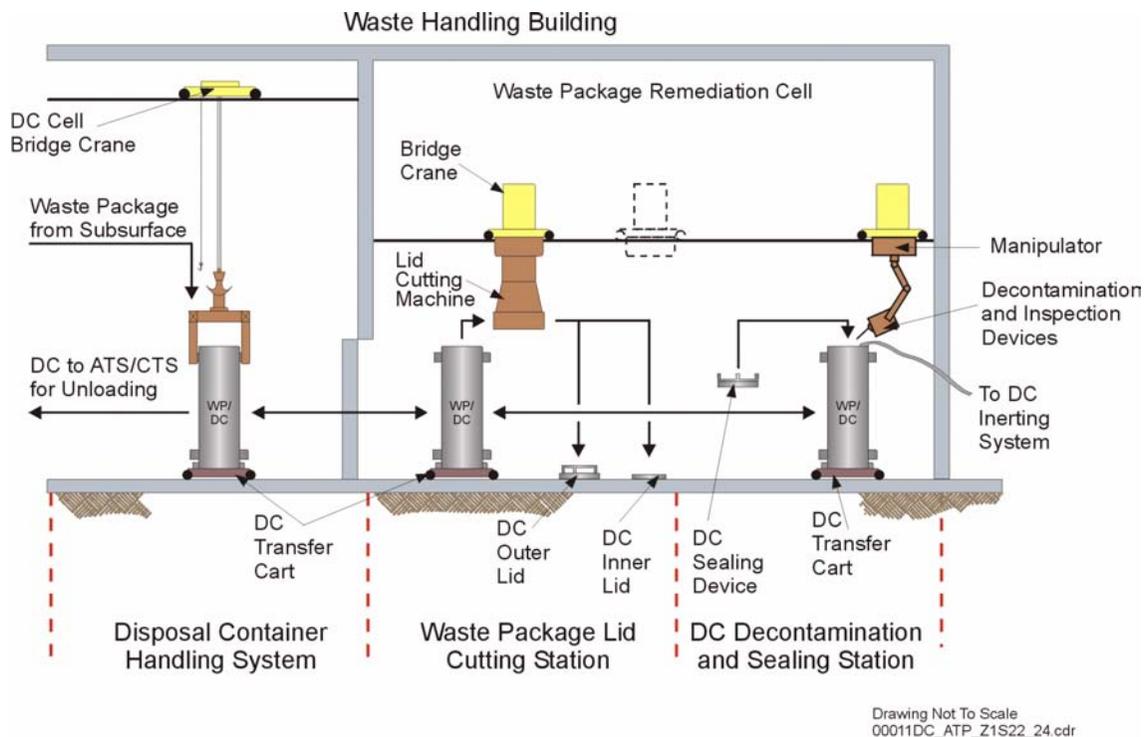
Figure 2-31.   Waste Package Remediation System
The waste package remediation system can be used to repair minor defects in disposal containers and waste packages. The system will be used to remedy weld defects and unload waste packages. A lid cutting machine would be used to open the waste packages. DC = disposal container; WP = waste package; ATS = assembly transfer system; CTS = canister transfer system. Source: CRWMS M&O 2000p, Figure I-12.

The waste package remediation system would receive disposal containers and waste packages that:

- Are damaged out of specification

- Have failed the weld inspection processes

- Have been selected for retrieval from the repository for examinations.

The out-of-specification waste packages would be repaired. After the waste packages have been examined, repaired or, if necessary, unsealed and repackaged, the remediation system would deliver them back to the disposal container handling system (CRWMS M&O 2000p, Attachment II, Section 1.1.4.1).

If inspections of the closure weld reveal an unacceptable but repairable welding defect, the disposal container would be prepared for rewelding, which may include partial or complete weld removal. Correction of rejected closure welds would require removal of the defect in such a way that the disposal container can be returned to the disposal container handling system to complete the closure welding process. If examination of the closure weld shows the defect or damage to be irreparable, the container would be opened. If a waste package is retrieved from the repository for any reason—suspected damage, known failure, or planned performance confirmation examinations—it would be opened in the waste package remediation system (CRWMS M&O 2000p, Attachment II, Section 1.1.4.1).

The processes for opening a waste package or disposal container would include remotely cutting the closure weld, collecting and processing the cutting fines, removing and disposing of the cutting waste, and installing a temporary seal to confine contamination to the inside of the container.

All remediation operations on radioactive waste packages or disposal containers would be performed remotely in a dedicated, shielded cell accessible directly from the large handling cell inside the disposal container handling system. The remediation cell would accommodate one waste package or disposal container at a time. A shield door would open to allow the transfer cart to enter. After the transfer cart enters the remediation cell, the damaged container would be positioned at one of two workstations in the remediation cell and would exit the cell without being removed from the cart. The two remotely operated workstations would accommodate different repair tasks. One workstation would facilitate the cutting, removal, and holding of the container lids. The other would allow remote inspection, examination, and purging of the container, as well as backfilling it with inert gas, temporarily sealing it, and decontaminating it (CRWMS M&O 2000p, Attachment II, Section 1.1.4.2.4).

The remediation system would use a variety of remotely operated equipment, including an overhead bridge crane, an in-cell multipurpose manipulator, a lid-cutting machine, and closed-circuit television viewing systems. System operations would all be performed remotely, using equipment designed to facilitate decontamination, maintenance, and replacement of interchangeable components, as required (CRWMS M&O 2000p, Attachment II, Section 1.1.4.2.4).

If examination of the closure weld indicates an irreparable welding defect, or if a waste package has been retrieved because of suspected failure or damage, the package would be opened. Opening waste packages and disposal containers should be infrequent but would require the capability to unseal the container, vent it, measure the temperature and pressure, and sample the composition of the gas inside. Opening a sealed container would require:

- Cutting the closure welds of the outer and inner lids
- Removing and holding the lids
- Collecting and processing cutting fines
- Removing and disposing of cutting waste
- Installing a temporary seal to confine contamination to the inside of the container.

Following remediation, the container would be inspected for contamination and remotely decontaminated, as required. The container would then

be returned to the disposal container handling system for rewelding, transferred to the assembly transfer system for unloading of fuel assemblies, or transferred to the canister transfer system for unloading of canisters (CRWMS M&O 2000p, Attachment II, Section 1.1.4.2.4).

The remediation system would also interface with the performance confirmation data acquisition/ monitoring system to gather data needed to support the performance confirmation program.

2.2.4.2.8   Waste Handling Building: Ventilation System

The ventilation system for the Waste Handling Building would provide heating, ventilation, and air conditioning for worker health, safety, and comfort and would maintain the appropriate environmental conditions for waste handling operations. It would protect the environment, the public, and workers by preventing airborne emissions of radioactive particulates (CRWMS M&O 2000p, Attachment II, Section 1.1.7.3.1); mechanical equipment selection will consider the application of alternative technology to minimize the use of toxic refrigerants and lubricants.

The Waste Handling Building would have uncontaminated and potentially radiologically contaminated areas. Separate ventilation systems would be installed in these areas to limit the spread of airborne particulates by controlling the air pressure between the areas and directing the airflow from the uncontaminated areas to the potentially contaminated areas (Figure 2-32) (CRWMS M&O 2000p, Attachment II, Section 1.1.7.3.1).

The potentially contaminated area would be divided into three confinement zones: primary, secondary, and tertiary (Figure 2-33). These zones would be classified according to the type, quantity, and packaging of waste to be handled and the potential for contamination from airborne radioactive material or other hazardous materials. The primary zone would normally have some contamination, the secondary zone would have a high potential for contamination, and the tertiary zone would have a low potential for contamination. Each zone would have an independent ventilation

system to prevent cross-contamination. The primary and secondary zones would have once-through ventilation; the tertiary zone would use some recycled air. A secondary contamination confinement zone designation is assigned to the various pool water areas and their associated pool water cooling and treatment systems. Ventilation confinement in pool water areas is assigned a tertiary ventilation contamination confinement zone designation. The ventilation system in the confinement zones would remain operational during normal and off-normal operating modes and during and after any design basis event (CRWMS M&O 2000p, Attachment II, Section 1.1.7.3.1).

The air supply equipment for each ventilation system would contain multiple air-handling units, supply-air fans, and associated distribution duct-work. Each air-handling unit would contain a prefilter, final filters, heating coils, cooling coils, and a humidifier. The exhaust air equipment would contain high-efficiency particulate air filtration units, exhaust-air fans, and associated ductwork. Each filtration unit would contain prefilters (moisture eliminators) and high-efficiency particulate air filters. Final exhaust air (after filtration) from all the confinement zones would discharge to the outside environment through a common exhaust air stack with contamination monitoring sensors. The exhaust air stack is located on the south side of the Waste Handling Building; it is designed to be taller than the adjacent structure and is located away from all outside air intakes to preclude reentrainment of any potentially emitted radiological contaminant (CRWMS M&O 2000q, Section 6.2).

The uncontaminated areas of the Waste Handling Building would have a separate ventilation system, configured to maintain proper air quality standards (CRWMS M&O 2000p, Attachment II, Section 1.1.7.3).

The ventilation equipment for the uncontaminated area would consist of air-handling units, supply-air and exhaust-air fans, and associated distribution ductwork (CRWMS M&O 2000q, Section 6.2.5). This separate ventilation system would maintain higher air pressure than the potentially contaminated area to prevent airborne contamination from
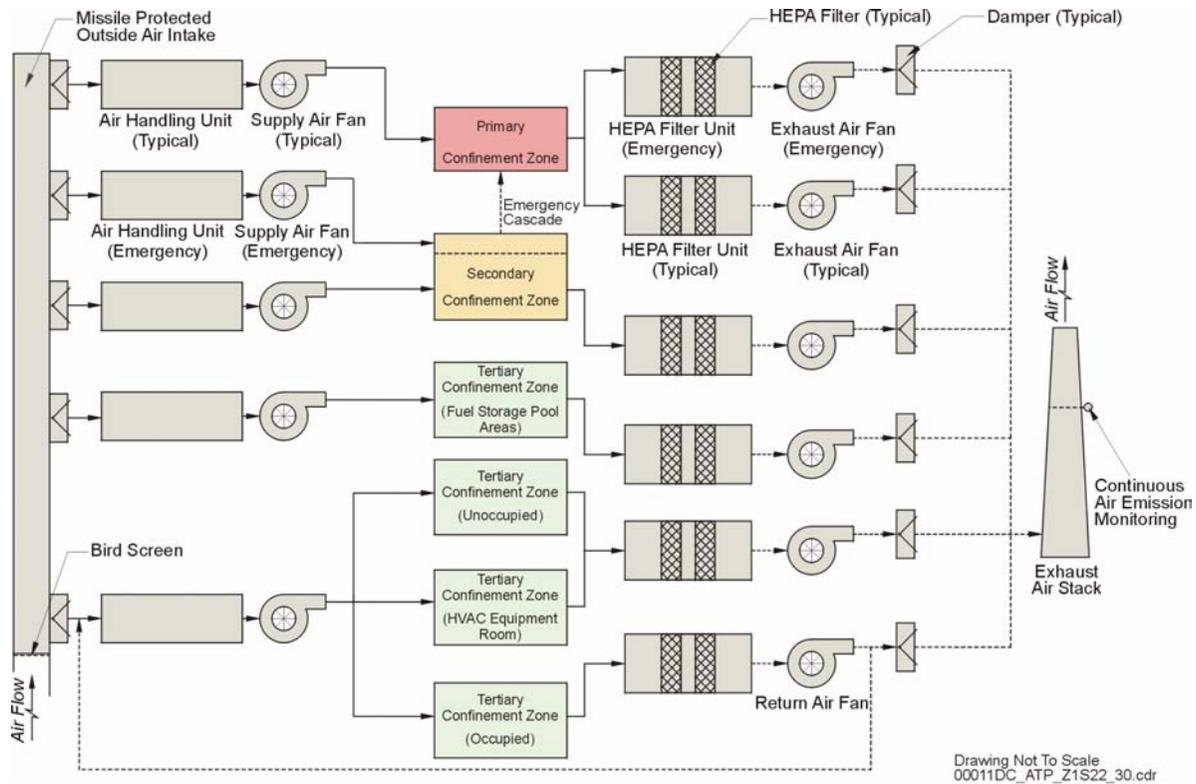
Figure 2-32. Waste Handling Building Heating, Ventilation, and Air Conditioning Confinement Flow Diagram
The heating, ventilating, and air conditioning systems are segmented to control air flow. High-efficiency particulate air filters would be used to trap particulates. The pressure drop across each filter would be measured and the filters would be replaced, as necessary. Tornado dampers would be provided to isolate the systems in case of a tornado and prevent depressurization of the confinement zones. All air flows would be radiologically monitored prior to release from the exhaust air stack, and the systems would shut down automatically in case of an alarm. HEPA = high-efficiency particulate air; HVAC = heating, ventilation, and air conditioning. Source: CRWMS M&O 2000p, Figure I-25.

entering (CRWMS M&O 2000p, Attachment II, Section 1.1.7.3).

2.2.4.2.9 Waste Handling Building: Treatment and Cooling System for Pool Water

The Waste Handling Building would contain nine pools and several transfer canals for underwater waste handling operations. The nine pools consist of two cask unloading pools, two holding pools, one nonstandard pool, and four blending inventory pools. The water treatment and cooling system would:

• Control water temperatures
• Control water quality and radioactive contamination

• Operate the pool's leak detection systems
• Control pool water levels.

Water Cooling System—Spent nuclear fuel assemblies would emit heat, which, if not properly removed, could cause pool water temperatures to increase to unacceptable levels. Therefore, each assembly transfer pool, fuel inventory pool, and associated transfer canal would be connected to a water cooling system to maintain the water temperature at approximately 15°C (60°F). This low temperature would reduce water evaporation and retard the growth of algae, which would improve water clarity (CRWMS M&O 2000p, Attachment II, Section 1.1.8).

The water cooling systems would continually monitor and control the temperature of water in the
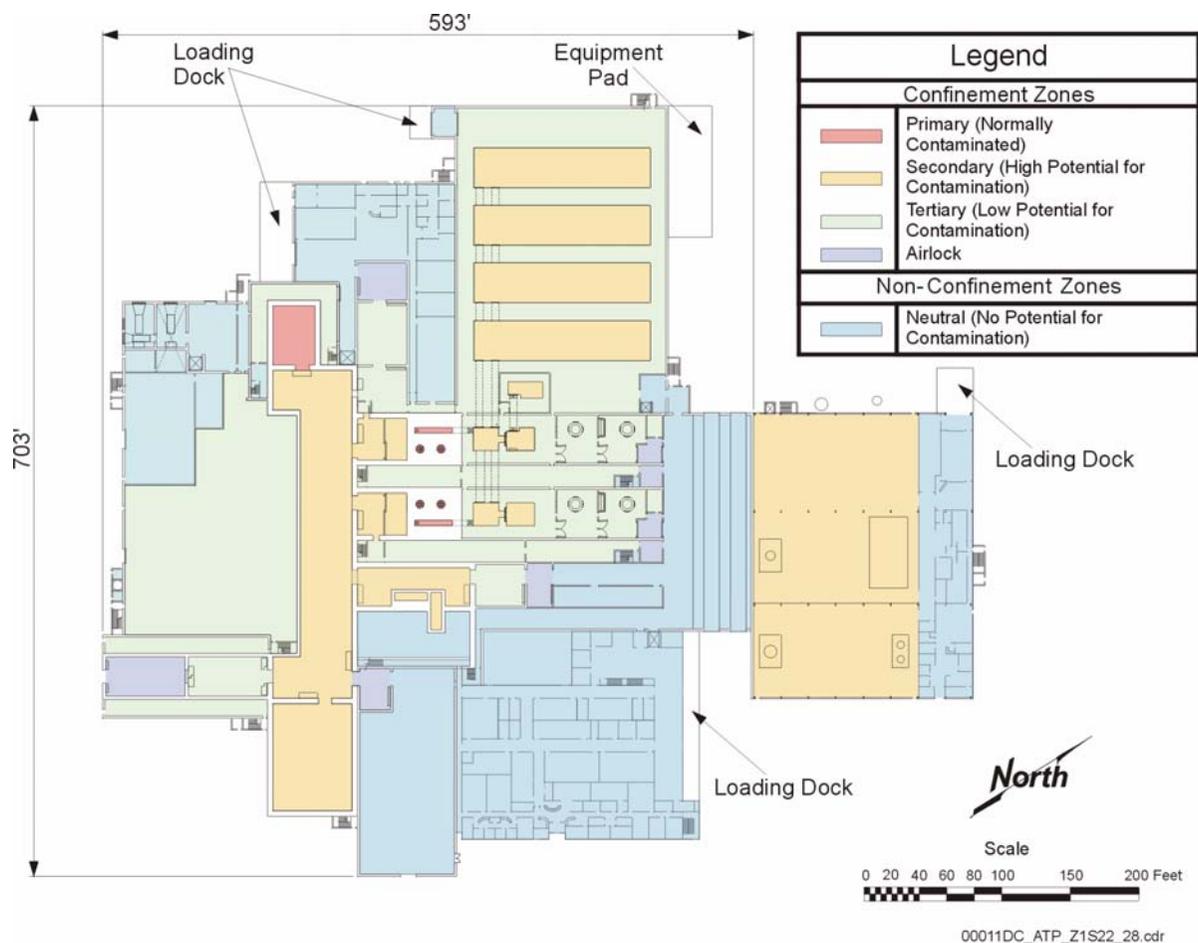
Figure 2-33.   Waste Handling Building Confinement Zone Configuration
Multiple heating, ventilating, and air conditioning systems would be used to control air flow from areas of lower potential contamination to areas of greater potential contamination. Elevation: 100 ft. Source: Modified from CRWMS M&O 2000p, Figure I-23.

pool and transfer canal. When the temperature rises to a set point, the system would pump water from the pool through a heat exchanger to cool the pool water and return it to the source. The heat exchanger would transfer heat from the water to an independent chilled-water loop. The chilled-water loop, in turn, would transfer the heat to a refrigerant system, which would discharge it to the environment through air-cooled heat exchangers. The refrigerant system would use an environmentally acceptable refrigeration agent. The water cooling systems would maintain higher pressure on the chilled-water side of the heat exchangers than on the pool side to prevent the chilled water from becoming contaminated if a heat exchanger fails (CRWMS M&O 2000p, Attachment II, Section 1.1.8).

Water Treatment System—The water in the waste handling pools and transfer canals would be subject to continuous radioactive contamination from underwater waste handling operations. Therefore, all assembly transfer pools, assembly holding pools, and associated transfer canals would be connected to a water treatment system that would continuously filter radioactive material and purify the water to keep worker radiation exposures ALARA and maintain pool water clarity (CRWMS M&O 2000p, Attachment II, Section 1.1.8.2.2.1).

The treatment system would continually pump the water in the pools and treatment canals through the system. It would process all water in the pools at least once every 72 hours. The water in the treatment system would first pass through filters to

remove particulates. After filtration, the water would pass through a mixed-bed ion-exchange system to remove residual radionuclides. The deionized water would pass through an organic-material-capturing filter to remove trace organic materials and any ion-exchange resin carried out of the mixed-bed system. Finally, the water would pass through an ultraviolet sterilization system to destroy algae. The system would then return the water back to the pool system (CRWMS M&O 2000p, Attachment II, Section 1.1.8.2.2.1).

The treatment system would also remove floating debris from the surfaces of the pools. Workers would use vacuums to remove particles from pool walls and floors. Water from these cleaning operations would pass through roughing filters to remove large particles before passing through the water treatment system. Workers would process and package the radioactive materials collected in the water-treatment process (the source of generation) and transfer them to the Waste Treatment Building for shipping and disposal off the repository site (CRWMS M&O 2000p, Attachment II, Section 1.1.8.2.2.1).

Leak Detection System—Each waste handling pool would have a leak detection system to identify, locate, contain, and quantify any leakage between pool liners and the surrounding concrete walls and alert personnel if a leak occurs. Any leaking water would collect in sumps below the pools. The sumps would be able to pump accumulated water back to the pools. Personnel would analyze this water and take the appropriate remedial actions (CRWMS M&O 2000p, Attachment II, Section 1.1.8.3).

Water Level Management System—Each waste handling pool would have a water level management system to maintain water levels within design parameters. This would ensure that the pool water provides sufficient shielding to keep worker radiation exposures ALARA (CRWMS M&O 2000p, Attachment II, Section 1.1.8.4). Return water lines would be designed such that a break in the line would not allow the pool to siphon below an acceptable level above the assemblies.

Assembly transfer pools would be equipped with overflow weirs to control the maximum water level during cask handling and unloading operations. Overflow water from the weirs would collect in a sump. The system would reuse this water to supplement the water level when it is too low. If the water level drops below a set point, an automatic system would pump more water into the pools from the sump or from a supplemental water system (CRWMS M&O 2000p, Attachment II, Section 1.1.8.4).

Supplemental Water System—If necessary, a supplemental water system would provide water from the site's deionized water system to increase the water level in a waste handling pool. This supplemental system can provide enough water to compensate for evaporation and other water loss. The supplemental water system would connect to backup power, or a gravity feed system would be used to provide make-up water to the pools in the event of a power outage (CRWMS M&O 2000p, Attachment II, Section 1.1.8.5).

2.2.4.2.10 Waste Handling Building: Fire Protection System

The fire protection system in the Waste Handling Building would provide active and passive features to protect life and property against fire (CRWMS M&O 2000p, Attachment II, Section 2.14.1).

Automatic fire suppression systems would be used in selected areas of the Waste Handling Building. These system would provide the capability to extinguish potential fires in the building (CRWMS M&O 2000p, Attachment II, Section 1.1.9.1).

Sensors would monitor the building for fires and early combustion byproducts. The fire protection system would warn occupants of a fire, alert fire response personnel, and transmit an alarm when the automatic sprinkler system is activated. It would include manual pull stations and detection equipment to initiate alarms. In the event of a fire, the system would automatically transmit an alarm to the Yucca Mountain fire station via radio or dedicated telecommunications lines (CRWMS M&O 2000p, Attachment II, Section 1.1.9.1). Where required for control of fire suppression

system runoff or accumulation, features would be provided to prevent the spread of radiological contamination and criticality.

2.2.4.2.11 Waste Handling Building: Electrical Power System

The Waste Handling Building electrical power system would receive electrical power from the site electrical power system. If the site electrical power supply becomes unavailable, the Waste Handling Building's emergency power supply system would provide electricity to equipment and systems that are important to radiological safety. This system would include a single diesel generator and battery system with enough capacity to supply necessary electrical loads (CRWMS M&O 2000p, Attachment II, Section 1.1.10.1). Workers can test the system during facility operations or while the facility is shut down.

The electrical system for supporting equipment important to safety would be separate from the electrical system supporting equipment not important to safety, and would be able to function during and after any unexpected adverse event (CRWMS M&O 2000p, Attachment II, Section 1.1.10.1). The electrical system important to safety would have redundant load groups, so each group can receive power either from the normal electrical system or from the emergency system.

The DOE would install a grounding system for the Waste Handling Building that would connect to the switchyard substation ground. All major electrical equipment in the Waste Handling Building, including power panel boards, lighting panel boards, and motors, would connect to the grounding system. The building's lightning arresters (i.e., lightning rods) would also connect to the grounding system (CRWMS M&O 2000p, Attachment II, Section 1.1.10.3).

2.2.4.2.12 Repository Operations Monitoring and Control System

Two central control centers would be established in the Geologic Repository Operations Area to monitor and control repository surface operations and perform emergency command functions. The control centers would be located in the Waste Handling Building and the Administration Building.

Operators in the Waste Handling Building control center would monitor and control specific operations in the Waste Handling Building and throughout the plant: for example, track all radioactive material in the building, operate building utilities, and control radiation containment doors. The control system would have local consoles at various locations, including the operating galleries, where workers would control remote waste handling operations while watching the mechanical operations. Operators at the main control center would monitor gallery console operations and respond to emergency and off-normal events. If a gallery console malfunctions or a gallery becomes uninhabitable, the main control center would perform any necessary emergency response functions. Gallery console operators would communicate with main control center operators via secured communication lines (CRWMS M&O 2000p, Attachment II, Section 1.1.11.3). A separate emergency control panel would serve as a backup to the main control center system. If the main system fails, this panel would be able to bring waste handling systems and other systems that are important to safety to a safe operating or shutdown condition (CRWMS M&O 2000p, Attachment II, Section 1.1.11.3).

2.2.4.3 Waste Treatment Building

The Waste Treatment Building would be located on the North Portal pad, north of the carrier bay in the Waste Handling Building. It would house structures, systems, and components that support the collection, segregation, and disposal of both liquid and solid low-level radioactive waste generated during operations. Table 2-8 summarizes these preliminary engineering specifications. It would contain areas for processing nonrecyclable low-level waste, solid low-level waste, and recyclable liquid low-level waste. The building would also contain the equipment, tanks, and piping needed to recycle water in waste handling and waste preparation pools (CRWMS M&O 2000p, Attachment II, Section 1.2.1.4).

Table 2-8. Preliminary Facility Space Specifications for the Waste Treatment Building

Facility Space	Floor Area m² (ft²)
Process area (low-level waste)	3,244 (34,920)
Mixed and hazardous waste	351 (3,780)
Other areas not listed above	3,363 (36,200)
TOTAL	6,958 (74,900)

Source: CRWMS M&O 2000q, Table 6-4.

The activities conducted in the Waste Treatment Building would include:

- Sorting dry waste resulting from repository operations

- Super-compacting and grouting waste resulting from repository operations

- Cleaning liquid waste resulting from repository operations.

The systems for performing these tasks would be located in a limited access area and would be designed to limit worker radiation doses to ALARA levels (CRWMS M&O 2000p, Attachment II, Section 1.2.1.1).

2.2.4.3.1 Waste Treatment Building: Architectural and Structural Features

The Waste Treatment Building would be one story with a mezzanine, approximately 60 m (200 ft) wide and 80 m (260 ft) long. It would be an open, high-bay industrial structure. The main operating floor would consist of a reinforced concrete slab at grade level. The superstructure would be a braced frame of structured steel, with metal siding and a metal deck roof. The Waste Treatment Building would be a lightly loaded building. It would not contain overhead cranes, and the major equipment would be anchored to the ground floor slab. The foundation would consist of individual spread footings of reinforced concrete, which would support the building columns (CRWMS M&O 2000p, Attachment II, Section 1.2.1.5). The Waste Treatment Building would be separated from the Waste Handling Building by a seismic joint to prevent structural interaction during an earthquake

(CRWMS M&O 2000p, Attachment II, Section 1.2.1.4). As a safety-related nuclear facility, the Waste Handling Building would be designed to withstand a potential collapse of the Waste Treatment Building.

2.2.4.3.2 Management System for Liquid Low-Level Radioactive Waste

A number of operations at the repository would produce liquid low-level radioactive waste, that is, liquids containing low-level radioactive materials. These liquids would be generated in the processes of handling the transportation casks, the canisters containing DOE high-level radioactive waste or spent nuclear fuel, commercial spent nuclear fuel assemblies, and the waste packages. The main source of this low-level waste would come from decontamination of casks placed into the wet unloading pools, where these casks would be exposed to the contamination that has washed off of the individual spent nuclear fuel assemblies. Depending on the characteristics of the waste and the materials used in processing it, the low-level radioactive liquid waste generated may or may not be recyclable. Therefore, surface facilities would be available to prepare liquid low-level radioactive waste for recycling and reuse, if possible, or for disposal off the repository site in a dry form. There would be two separate systems in the Waste Treatment Building for collecting and treating recyclable and nonrecyclable liquids (CRWMS M&O 2000p, Attachment II, Section 1.5.2).

After decommissioning, or if a pool has to be emptied for pool liner repairs or other reasons, there are several options for treatment of the water in the fuel pools prior to disposal. The water in the pools would be circulated through the pool water treatment system to reduce the radionuclide content to the maximum extent possible. This might involve multiple change-outs of the ion-exchange resin beds in the treatment system. Following this treatment, the water could be routed to the recyclable water treatment system, which uses ion-exchange beds and an evaporator/condenser to treat recyclable water for reuse. The evaporator could be used to evaporate excess water to the atmosphere using the high-efficiency particulate air filtration system and discharge stack.

If ion-exchange and evaporation prove to be unsuitable, the water from the nonrecyclable low-level radioactive waste treatment system could be mixed with grout and disposed at a suitable low-level waste disposal site.

2.2.4.3.3 Management System for Recyclable Liquid Low-Level Radioactive Waste

Recyclable liquid low-level radioactive waste from all repository operations would be collected and treated. Treating and recycling conserves water and reduces the volume of waste to be disposed. Treated liquids would also be recycled to provide water for decontamination activities in radiologically controlled areas of the repository. Any residual liquid from the recycling treatment process would be routed to the system for managing nonrecyclable liquid low-level radioactive waste, solidified into waste materials, packaged, and shipped off the repository site for disposal. There would be no liquid effluents from the recyclable liquid treatment system (CRWMS M&O 2000p, Attachment II, Section 1.5.2).

Recyclable liquid low-level radioactive waste would be segregated from nonrecyclable liquid waste at the point of generation. The recyclable liquid would then be pumped through a piping system to the Waste Treatment Building for processing.

Once in the Waste Treatment Building, the recyclable liquids would be filtered to remove particulates. After filtration, the liquid waste would be transferred to a batch evaporator, where water would be evaporated. The evaporated water would then be condensed and passed through a mixed-bed ion-exchange unit, which would remove any residual radionuclides. The deionized water would pass through an organic-material-capturing filter to remove trace organic materials and any ion-exchange resin carried out of the mixed-bed system. The final recycled water would then be transferred to a recycled-water storage tank, where it would be pumped to the Waste Handling and Waste Treatment Buildings for reuse. During the entire process, specially implemented administrative controls would limit and direct all activities

involving liquid waste streams. Figure 2-34 depicts the flow of recyclable liquid low-level radioactive waste through the treatment system (CRWMS M&O 2000p, Attachment II, Section 1.5.2.1.3).

2.2.4.3.4 Management System for Nonrecyclable Liquid Low-Level Radioactive Waste

The system for managing nonrecyclable liquid low-level radioactive waste has two functions: (1) collecting nonrecyclable liquids from repository operations and (2) processing them into a solid form suitable for disposal off the repository site. As a result, there would be no liquid low-level radioactive waste effluents from the repository (CRWMS M&O 2000p, Attachment II, Section 1.5.3).

Nonrecyclable liquid low-level radioactive waste would be segregated from recyclable liquid waste at the point of generation. The nonrecyclable waste would then be pumped through a piping system to the Waste Treatment Building for processing (CRWMS M&O 2000p, Attachment II, Section 1.5.3).

Once in the Waste Treatment Building, the pipes would convey the nonrecyclable liquid radioactive waste into a surge tank. Residual liquid from the evaporation step in the recyclable liquid waste processing system would also be collected in this tank. The contents of the tank would then be mixed, sampled, and analyzed to determine the pH of the liquid. If necessary, acid or caustic solution would be added to neutralize the tank's contents (CRWMS M&O 2000p, Attachment II, Section 1.5.3).

The nonrecyclable liquid low-level radioactive waste would then be mixed, in drums, with Portland cement or another solidifying agent to take out all the liquid. The finished drums would be moved to a curing area and later shipped off the repository site for disposal. Figure 2-35 depicts the flow of nonrecyclable liquid low-level radioactive waste through the treatment system (CRWMS M&O 2000p, Attachment II, Section 1.5.3). The design of the repository would include a processing
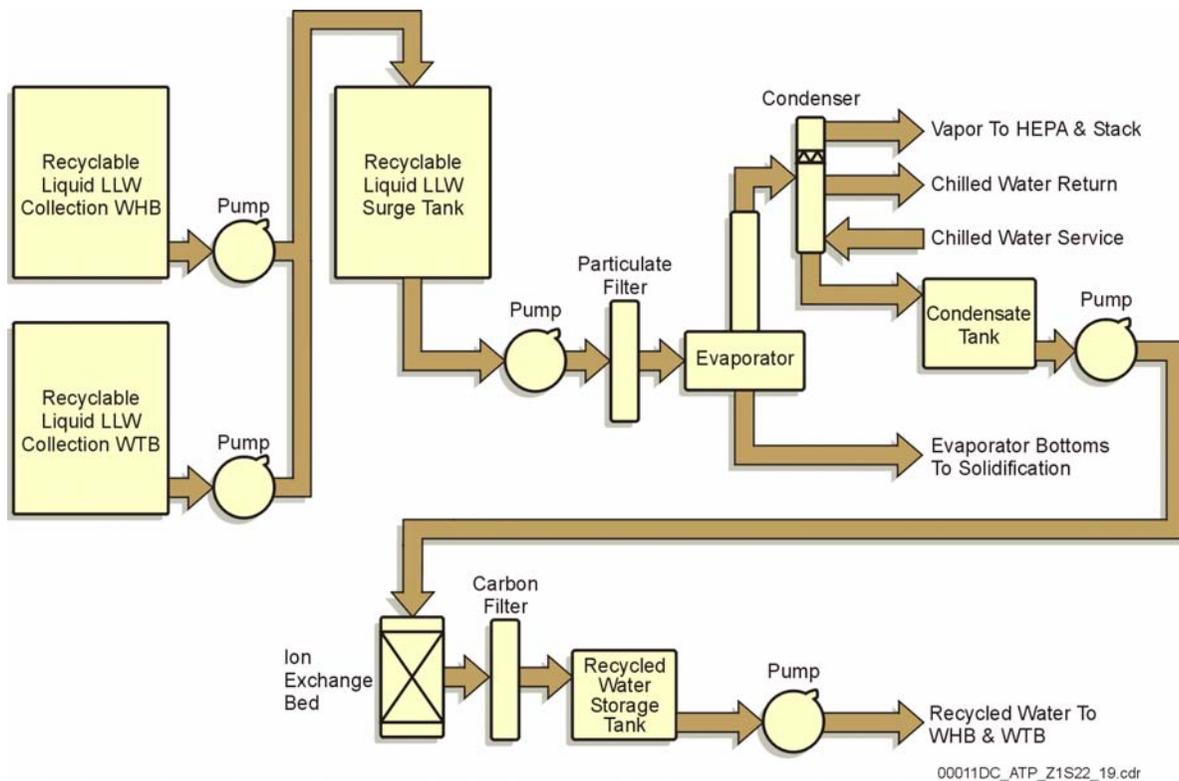
Figure 2-34.   Recyclable Liquid Low-Level Radioactive Waste Collection System Diagram
As part of a resources conservation program, water that becomes contaminated via facility operations will be treated with state-of-the-art technology to recover such water for reuse in facility operations. Precipitated particulates (evaporator bottoms) would be transferred to the nonrecyclable liquid low-level waste treatment system. Water would be treated by particulate filter, ion exchange bed, and carbon filter. LLW = low-level radioactive waste; WHB = Waste Handling Building; WTB = Waste Treatment Building; HEPA = high-efficiency particulate air. Source: Modified from CRWMS M&O 2000p, Figure II-3.

system that would minimize the volume of liquid and solid waste.

2.2.4.3.5   Management System for Solid Low-Level Radioactive Waste

A number of operational processes at the repository would produce what is called "solid low-level waste," meaning solids containing low-level radioactive materials. These materials would be generated in the process of handling the transportation casks, the canisters containing DOE high-level radioactive waste and other vitrified waste, the spent nuclear fuel assemblies, and the waste packages that would be emplaced in the subsurface of the repository.

The solid waste would be collected at its point of generation and then treated, usually in the Waste Treatment Building (CRWMS M&O 2000p, Attachment II, Section 1.5.4). Surface facilities would be able to process this waste into a form suitable for disposal off the repository site. Solid waste is composed of two categories, dry solid waste and wet solid waste, discussed in the following paragraphs.

Dry Solid Waste—The system for managing dry solid waste has several functions:

- Collect the waste
- Segregate the waste according to type
- Reduce the volume of the waste
- Package the waste for shipping and disposal off the repository site.
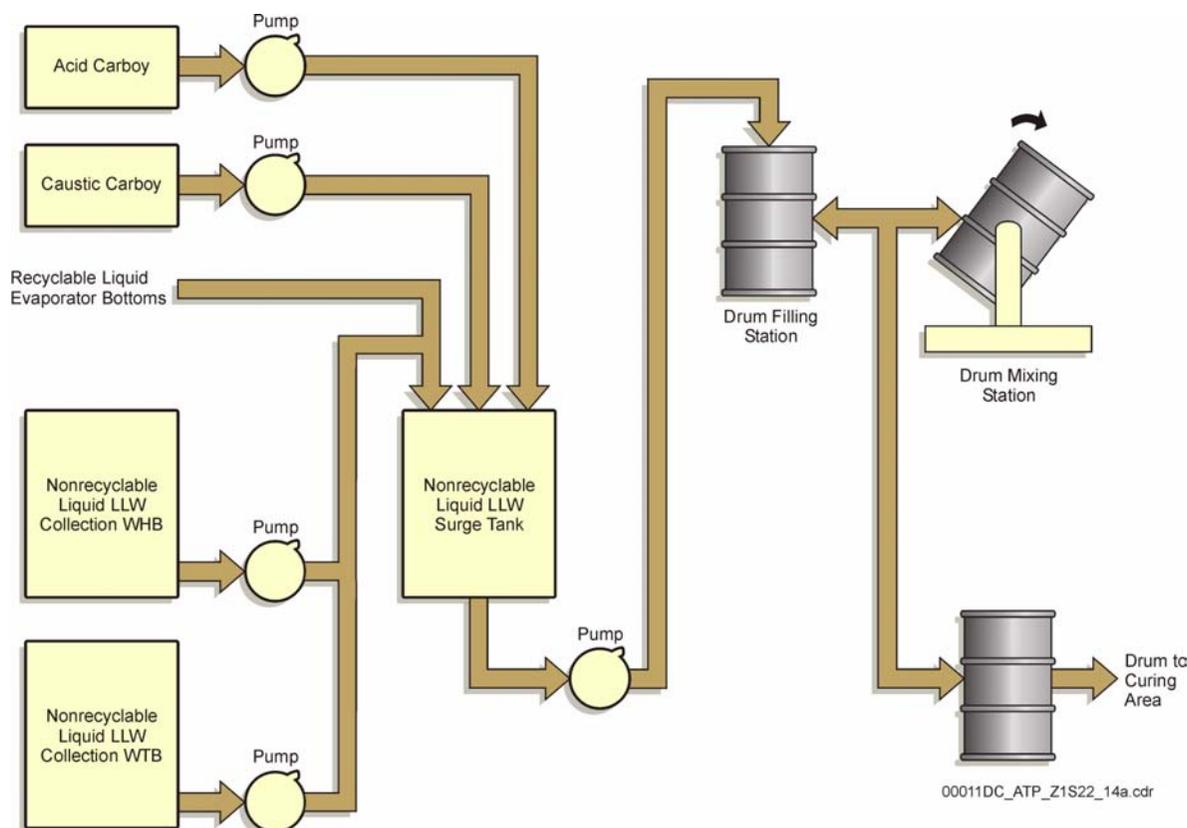
Figure 2-35.   Nonrecyclable Liquid Low-Level Radioactive Waste Treatment System Diagram
Materials that cannot be recycled would be mixed in drums with cement or other solidifying agents to create a solid low-level radioactive waste. Such waste would be staged and subsequently transported offsite for disposal. LLW = low-level waste; WHB = Waste Handling Building; WTB = Waste Treatment Building. Source: Modified from CRWMS M&O 2000p, Figure II-4.

Dry solid waste would be collected at its point of generation and transferred to a special area of the Waste Treatment Building for processing. Once inside the Waste Treatment Building, the dry solid waste would first be sorted to separate noncontaminated waste from contaminated waste. The waste would then be sorted to separate noncompactible waste from compactible waste. Noncompactible waste would be reduced in size by mechanical methods, such as shearing or disassembly, before being packaged for disposal. Compactible waste would be fed into a shredder for size reduction. The shredded dry waste would then be compacted into drums for disposal off the repository site. Figure 2-36 presents a simplified flow sketch of the system in the Waste Treatment Building for processing dry solid low-level radioactive waste (CRWMS M&O 2000p, Attachment II, Section 1.5.4).

Wet Solid Waste—The system for managing wet solid waste also has several functions:

• Collect the waste

• Dewater the waste

• Package the waste for shipping and disposal off the repository site.

Materials generated within the Waste Handling Building may be sufficiently contaminated to be classified as "noncontact handled," which means they should be placed into radiation-shielded containers immediately at their point of origin. Noncontact handling is not anticipated for wet solid wastes produced in the Waste Treatment Building (CRWMS M&O 2000p, Attachment II, Section 1.5.4).
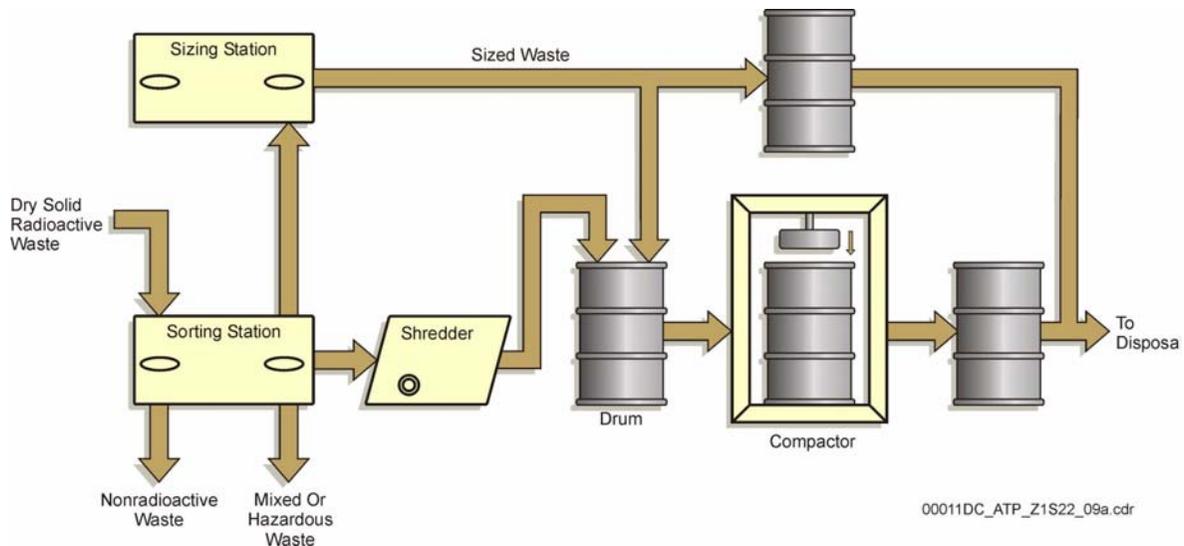
Figure 2-36. Dry Solid Low-Level Radioactive Waste Processing System
Dry waste is of two types. Sized waste consists of such items as contaminated tools and equipment. Such items are not suitable for compaction. The second type of dry waste consists of contaminated clothing, such as overalls and rubber gloves. Such materials are suitable for shredding and subsequent compaction, which reduces the overall volume of such wastes. Drummed wastes would be staged until they are transported offsite for disposal. Source: Modified from CRWMS M&O 2000p, Figure II-5.

Spent Ion-Exchange Resins—Most of the spent ion-exchange resins would be generated in the Waste Handling Building, though a much smaller quantity would be generated in the Waste Treatment Building. Spent ion-exchange resins would be processed at the point of generation. In the Waste Handling Building, ion-exchange resins become waste when they are saturated with radionuclides; likewise, when resin in the Waste Treatment Building's system for processing recyclable liquid low-level radioactive waste becomes saturated with radionuclides, it must be replaced, producing wet solid low-level waste. In both these locations, the waste resins would be transferred directly, via piping systems, to high-integrity disposal containers. Air drying would remove free water from the containers. When the contents are dry, the containers would be loaded into transportation casks for shipping and disposal off the repository site (CRWMS M&O 2000p, Attachment II, Section 1.5.4).

Filter Cartridges—Special filter cartridges would be used in the pool water treatment system of the Waste Handling Building and in the system for treating recyclable liquid low-level waste in the Waste Treatment Building. These cartridges would be changed when they become fully loaded with debris. The cartridge unit would be removed from the system and placed in a 55-gallon drum. The drum's lid would be placed onto the drum remotely. Used filters from the Waste Handling Building that emit more radiation than allowed under the administrative controls for the Waste Treatment Building would be processed at the source of generation. If the filters do not emit more radiation than allowed in the Waste Treatment Building, however, drums containing the used filters would be transferred there for processing. At either location, the drum would be moved to a grouting station, where premixed grout would be added to thoroughly encapsulate the waste filter media. The encapsulated waste would then be shipped for disposal off the repository site (CRWMS M&O 2000p, Attachment II, Section 1.5.4).

2.2.4.3.6 Mixed Waste Management System

Since administrative controls designed into a monitored geologic repository would generally restrict the use of hazardous materials, the DOE does not anticipate that operating a repository would generate a significant amount of mixed waste. If

mixed waste is generated, however, it would be collected and repackaged for disposal at the point of generation. During packaging, samples would be collected for analysis. The packaged mixed waste would then be transferred to the Waste Treatment Building for holding before being transported to a suitable facility (CRWMS M&O 2000p, Attachment II, Section 1.5.5).

2.2.4.3.7   Radiological Safety System

The radiological safety system would ensure that activities associated with operating, monitoring, and closing a repository would limit the exposure of workers and the public to radiation doses. Moreover, the DOE will implement its policy of keeping both occupational doses and possible doses to the public ALARA (CRWMS M&O 2000p, Attachment II, Section 2.7).

The radiological safety system would establish the controls for ensuring that the repository and its operations would have appropriate and sufficient radiation protection features. The system would cover such aspects as facility designs (i.e., shielding and facility layout), operational activities, and facility policies to assure radiation safety. The radiological safety system is part of the overall formal radiation protection program for controlling radiological areas, approving radiological work, and monitoring worker exposures (CRWMS M&O 2000p, Attachment II, Section 2.7).

2.2.4.3.8   Process-Oriented Radiological Monitoring, Sampling, and Analysis Systems

Radiological data is collected and analyzed to:

- Control processes
- Keep doses to workers and the public within applicable regulatory limits and ALARA
- Characterize and classify waste
- Certify compliance with regulations.

Thus, the repository would have a designed-in, process-oriented system for monitoring, sampling, and analyzing radiological data (CRWMS M&O 2000p, Attachment II, Section 1.5.6).

Both online radiological monitoring and direct sample/analysis monitoring would be used in the systems for processing waste generated at the repository. Use of both methods would ensure proper process control and effective quality control of the waste forms. Sampling would be performed with automatic sampling equipment under human control. The analytical equipment would be both computer-controlled and human-controlled (CRWMS M&O 2000p, Attachment II, Section 1.5.6).

Surface dose rates at the ion-exchange beds and filter modules would be continuously monitored to ensure that dose limits are not exceeded. The dose limits would be set to ensure that the radiation protection limits provided by the shielding designs of both the facility and the cask would not be exceeded. Thus, doses to personnel during standard operations would remain within limits, including ALARA goals. Ion-exchange resin beds and filter cartridges would be changed out before their surface dose rates exceed established limits (CRWMS M&O 2000p, Attachment II, Section 1.5.6).

Samples would be analyzed in laboratory areas in the Waste Handling and Waste Treatment Buildings. For quality assurance, samples may also be analyzed at offsite commercial laboratories (CRWMS M&O 2000p, Attachment II, Section 1.5.6). In addition, computer-controlled instruments would perform continuous online monitoring and notify operators if radiation set points are approached (CRWMS M&O 2000p, Attachment II, Section 1.5.6).

2.2.4.3.9   Waste Treatment Building: Ventilation System

The ventilation system would protect the environment and public by preventing airborne effluents and emissions of radioactive or other hazardous contaminants from the Waste Treatment Building. The Waste Treatment Building would have designated uncontaminated and potentially radiologically contaminated areas. Separate ventilation systems would be used in these areas to limit the spread of airborne contaminants by controlling the air pressure between the areas and directing airflow

from the uncontaminated areas to the potentially contaminated areas (CRWMS M&O 2000p, Attachment II, Sections 1.2.5.1 and 1.2.5.3).

The potentially contaminated area may receive airborne contamination from low-level radioactive waste or other hazardous materials during or after an off-normal operating event. Therefore, it would have an independent ventilation system, preventing cross-contamination with the uncontaminated area. The air pressure in the potentially contaminated area would be maintained at a lower pressure than the outside environment to prevent leakage to the outside. The ventilation system in the potentially contaminated area would remain operational at all times (CRWMS M&O 2000p, Attachment II, Section 1.2.5.3.1).

2.2.5 Surface Facilities Radiological Control and Management Systems

This section describes the process involved in designing the repository surface facilities to comply with the site's radiation protection criteria. As for other nuclear facilities, a repository must be designed so that the protected (i.e., radiologically controlled) spaces within its operation areas maintain radiation levels and doses, as well as concentrations of radioactive material in the air, to within specified limits. Nuclear licensees make every reasonable effort to maintain radiation exposures even lower—as far below the dose limits as is reasonably achievable. This goal of ALARA means the DOE will make every reasonable effort to maintain exposures as far below the established dose limits as is practical (CRWMS M&O 2000p, Attachment II, Section 1.9.1).

The DOE plans to continue development of a radiation protection program to ensure consistency with 10 CFR Part 20 criteria and to incorporate ALARA guidelines and training into all phases of the design and operations of the repository (CRWMS M&O 2000p, Attachment II, Section 1.9.1.1).

Radiation protection would be planned and implemented in a multifaceted manner. A sound program of designing for radiation protection must have the following essential elements (CRWMS M&O 2000p, Attachment II, Section 1.9.1):

- Management commitment to the program
- Training in the ALARA approach
- Oversight of the design program by radiation protection specialists
- Radiation protection analysis
- An effective means for monitoring radiation in facilities and during operations
- A plan for implementing the radiation protection program during actual operations.

During design, engineers identify key structures, systems, and components. Radiation protection personnel perform occupational dose assessments based on this identification. Finally, system designs are evaluated against performance criteria to assure compliance. Compliance criteria can include (CRWMS M&O 2000p, Attachment II, Sections 1.9.1.1 and 1.9.1.2):

- Total cumulative occupational dose
- Maximum individual dose
- Average individual dose
- Person-rem reductions.

2.2.5.1 Dose Assessment and Designing for ALARA Goals

Dose assessments combine estimated dose rates in radiologically controlled work areas, the time needed to perform a task, the number of personnel performing a task, the type of personnel performing a task, and how often a task is performed each year. These factors provide the average exposure to an individual in a work group and the total group exposure. These values can then be evaluated to determine how effectively the design protects workers from radiation exposure (CRWMS M&O 2000p, Attachment II, Sections 1.9.1.1 and 1.9.1.2).

The design group would use the dose assessment information to evaluate where the design can be changed to reduce projected doses cost-effectively. As the design progresses, the dose assessments may be modified to incorporate design changes, as well as more complete data on labor, layout, and

equipment requirements (CRWMS M&O 2000p, Attachment II, Sections 1.9.1.1 and 1.9.1.2).

Dose assessments would be performed on all significant work in radiation areas, including normal, abnormal, accident, and recovery events and activities. The dose assessment can also be useful in evaluating decommissioning options (CRWMS M&O 2000p, Attachment II, Sections 1.9.1.1 and 1.9.1.2).

The health safety system would monitor repository workers' exposures to radiation and prevent personnel from receiving doses above applicable regulations and DOE ALARA limits for radiological workers (10 CFR Part 20). The system would include radiation monitors in repository facilities, personal dosimetry equipment, and decontamination facilities and equipment.

The health safety records of all personnel performing waste handling and other radiological work at the repository would be monitored and tracked (CRWMS M&O 2000p, Attachment II, Section 2.12). To enter the radiologically controlled areas, workers would read, sign, and perform work according to the instructions and conditions stated on the radiation work permits or on special work permits (CRWMS M&O 2000p, Attachment II, Section 2.12.1). Monitors would control access to radiologically controlled areas according to each worker's permit status and radiation exposure history. Personnel entering or leaving controlled facilities would pass through radiation detection portals that can detect very low levels of radioactive contamination. Any workers who have detectable contamination on them would undergo a decontamination procedure (CRWMS M&O 2000p, Attachment II, Section 2.12.1).

2.2.5.2 Radiological and Emergency Response Systems

The purpose of the site radiological monitoring system area-radiation and continuous-air monitors would be to keep radiation doses to repository workers ALARA. The site radiological monitoring system would continually monitor the repository surface facilities for general area radiation levels and concentrations of airborne radioactive particu-

lates. Monitors would also test air in the exhaust stacks for radiological effluents and emissions into the ventilation exhausts of the Waste Handling Building and the Waste Treatment Building. If radiation in the exhaust air from these buildings exceeds preset threshold levels, the monitors would trigger alarms (CRWMS M&O 2000p, Attachment II, Sections 1.1.13 and 2.7).

The system would provide continuous local and central displays of all radiation levels. It would audibly warn workers of unsafe radiation levels and trends and would communicate with the central control and radiation protection systems. The range of these monitoring systems would be specified to ensure that the instruments are on scale during both normal operations and potential off-normal occurrences. The site radiological monitoring system as a whole, and its component instruments individually, would be designed to self-test their operating status and calibration, recording results and reporting anomalies and failures (CRWMS M&O 2000p, Attachment II, Section 1.1.13.3).

2.2.6 Site-Wide Support Systems

This section describes the structures, systems, and components that provide common or site-wide support necessary for safe waste handling operations. These systems include emergency response and management, safeguards and security, maintenance and supply, and site power.

2.2.6.1 Emergency Response System

The emergency response system monitors the status of top-level systems such as the operations monitoring and control, security, and emergency response systems. It would provide emergency analysis and dispatch personnel to respond to site off-normal conditions (CRWMS M&O 2000p, Attachment II, Section 2.14). The following provide data to the emergency response system:

- Fire station
- Safeguards and security
- Health and safety
- Radiological monitoring
- Site environmental monitoring

- Meteorological monitoring and forecasts
- Emergency communications
- Site utility systems.

The emergency response system is composed of facilities, equipment, personnel, and instruments that support emergency response, medical emergencies, and underground response (CRWMS M&O 2000p, Attachment II, Section 2.14).

2.2.6.2   Site Fire Protection

The fire protection system for the surface facilities would include alarm systems for detecting explosions and fires and include the appropriate facilities, staff, and equipment for extinguishing fires and responding to emergencies. The design for the fire protection system will comply with applicable DOE requirements (CRWMS M&O 2000p, Attachment II, Section 2.6.3).

Each surface facility would provide fire alarms to warn occupants of a fire, signal activation of automatic fire protection systems, and alert fire response personnel. Surface facilities would connect to the site fire alarm system, so if a fire alarm sounds in a surface facility, a signal would transmit to the site fire station (CRWMS M&O 2000p, Attachment II, Section 2.6.3). The site fire protection system would also include a firewater system with the appropriate flow and pressure for automatic fire sprinklers and hoses to suppress a fire. Water storage and pumping systems would be provided by the DOE to satisfy this requirement.

A central fire annunciator in the fire station would monitor fire alarms throughout the site. This system would also monitor sprinkler systems, deluge fire systems, firewater pumps and tanks, and special fire protection systems (CRWMS M&O 2000p, Attachment II, Section 2.6.4).

2.2.6.3   Surface Environmental Monitoring System

The surface environmental monitoring system would monitor weather, seismic, air quality, and radiological data throughout the plant. The monitoring system would interface with the central

command control system by providing the collected data. The data would be analyzed and appropriate action initiated in the central command control room. The system would help protect the public, the environment, repository personnel, and property from potential radioactive and hazardous material emissions (CRWMS M&O 2000p, Attachment II, Section 2.8.3).

The surface environmental monitoring system would use monitoring and testing instruments located throughout the surface facilities. A complete data management and distribution system would store and distribute the environmental information acquired by the monitors and instruments, as well as the analyses and reports necessary to meet regulatory compliance requirements (CRWMS M&O 2000p, Attachment II, Section 2.8.3).

An additional laboratory-based information management system (CRWMS M&O 2000p, Attachment II, Section 2.8.3) would allow further data acquisition, real-time process control, and analyses of the acquired data to:

- Provide information for managing hazardous materials and reporting hazardous and toxic chemical inventories, as required by the Emergency Planning and Community Right-to-Know Act of 1986 (42 U.S.C. 11001 et seq.)

- Monitor the overall environmental situation at the repository site (for example, the meteorological monitoring system would collect meteorological information about the site and provide weather forecasting and climatological data)

- Support shallow subsurface exploration and analysis of general geologic conditions, including collecting vegetation and soil samples and analyzing their physical and chemical properties

- Provide seismic monitoring and analysis by collecting data for ongoing seismic surveys of the region.

2.2.6.4 Safeguards and Security System

The safeguards and security system would protect the public by safekeeping the physical inventory of radioactive waste at the repository against radiological sabotage. Under the safeguards and security system, workers would record the receipt of all spent nuclear fuel and high-level radioactive waste as it arrives and track it as it is prepared for emplacement. The waste packages would be welded closed and provided with proper identifiers before emplacement. Identifiers would be securely attached on the outside of each waste package.

This record would contain specific information for each waste package, including:

- Identification numbers
- A description of the material in the package
- Shipping manifests and other information on the origin of the materials
- Documentation on any removal of a waste package from the repository.

In addition, the DOE would periodically inventory the radioactive waste onsite and generate nuclear material transfer and other status reports. Physical inventory of nuclear waste would be performed by reviewing emplacement records and, if applicable, removal records (CRWMS M&O 2000p, Attachment II, Section 1.7.1).

The safeguards and security system would provide protection against loss of physical control of radioactive wastes through physical barriers, access controls, continuous surveillance, intrusion detection, and an alarm system. The system would also respond to barrier intrusions and threat assessments, communicate reportable events to required agencies, and provide for evacuation of facility personnel. The safeguards and security system would comply with applicable regulatory requirements (CRWMS M&O 2000p, Attachment II, Section 1.7).

2.2.6.5 Maintenance and Supply System

The primary waste handling systems would be operational about 70 percent of the time (6,000 hours per year) but unavailable for the remaining 30 percent for regular maintenance. Workers would perform scheduled preventive maintenance and periodic repair, replacement, and testing of equipment (CRWMS M&O 2000p, Attachment II, Section 2.10.3).

Equipment failures may cause a system or area to be taken down for corrective maintenance or repair. Preventive maintenance would be scheduled based on the likely failure rate of a piece of equipment, as determined by mean-time-between-failure criteria. These rates would be predicted from models of waste handling systems. Thus, both scheduled and unscheduled maintenance downtimes would be incorporated into the repository design (CRWMS M&O 2000p, Attachment II, Section 2.10.3).

The maintenance and supply system would have a structured maintenance program. The appropriate quantity and type of equipment, spare parts, components, and supplies needed for both scheduled and unscheduled maintenance to support repository operations would be procured, stored, and distributed. The system would use maintenance schedules developed for corrective, preventive, and periodic repair and replacement of surface facility components (CRWMS M&O 2000p, Attachment II, Section 2.10.3).

2.2.6.6 Site Electrical Power

The site electrical power system would receive and distribute utility power to all repository facilities that require electrical service. The electrical system, remotely monitored and controlled from the surface operations monitoring and control system, would be functional during all active phases of the repository's lifetime: construction, operation, monitoring, closure, and decontamination and decommissioning (CRWMS M&O 2000p, Attachment II, Section 2.2.1).

A transmission line from offsite would terminate in the main substation, where it would connect to transformers through substation power circuit breakers and disconnect switches. From the main substation, the system would branch out to four primary electrical distribution points: a North Portal substation, a South Portal substation, and

two shaft substations (CRWMS M&O 2000p, Attachment II, Section 2.2.3.3). Figure 2-37 shows the arrangement of the site electrical power system.

Standby power would be provided for personnel safety items and the subsurface ventilation system, if needed (CRWMS M&O 2000p, Attachment II, Section 2.2.1).

2.2.6.7   Site Solar Power System

Electricity from renewable energy sources would also be used at the repository (Griffith 2000). Solar power would be used in conjunction with commercially available power to meet power requirements. Solar power panels would be added in modular fashion up to 3 MW.

2.2.7   Operational Maintenance

The repository operational maintenance program would keep all facilities and systems important to repository operations and safety in working order. The maintenance program would be based on federal regulations and nuclear industry standards for maintenance on similar facilities and systems at other nuclear sites. It would include the necessary work processes, training, and equipment for inspecting, testing, and maintaining structures, systems, and components important to safety. The system would also maintain operational readiness (CRWMS M&O 2000p, Attachment II, Section 3).

The repository maintenance program would ensure that all maintenance personnel have the necessary qualifications, experience, licenses, and training for specific maintenance tasks (CRWMS M&O 2000p, Attachment II, Section 3). It would require
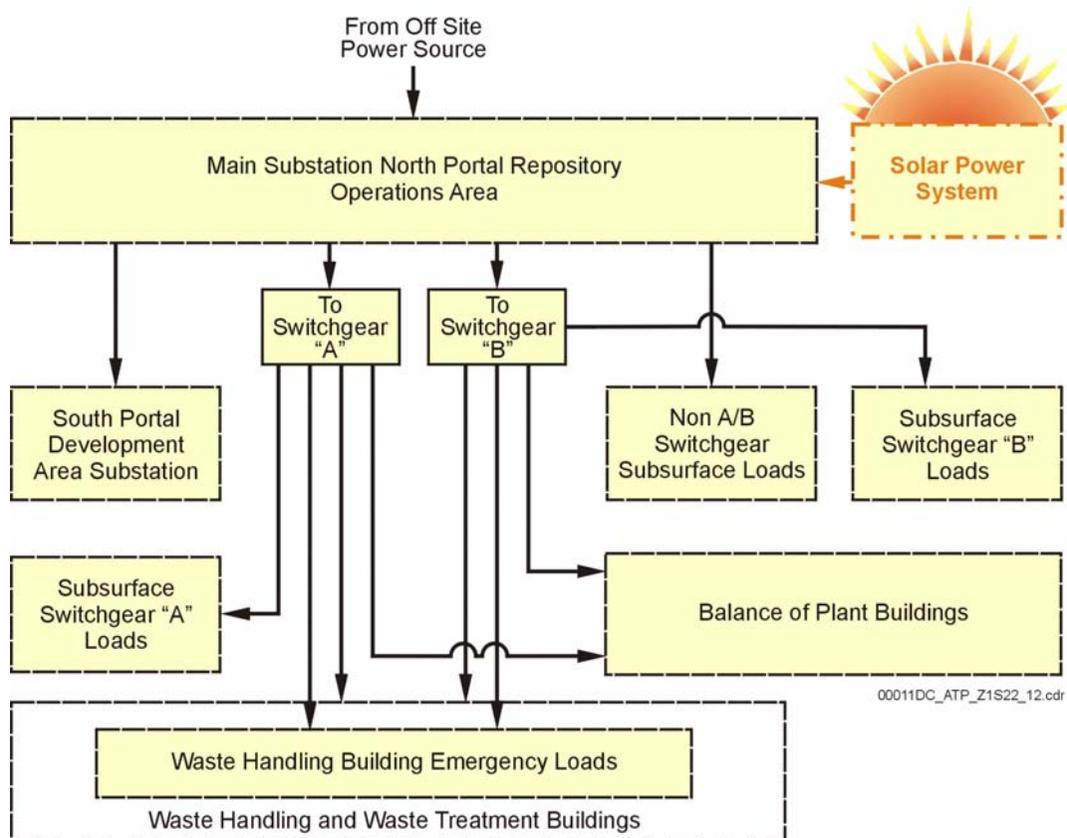
Figure 2-37.   Monitored Geologic Repository Site Electrical Power Distribution Diagram
The facility would rely on a combination of electricity from commercial generating sources, as well as the sun.
Source: CRWMS M&O 2000p, Figure I-32.

personnel to perform all routine and nonroutine maintenance activities under administrative controls and according to established procedures and job-specific safety criteria. Health physics personnel would assist maintenance staff with all work in radiologically controlled areas (CRWMS M&O 2000p, Attachment II, Section 3). The maintenance program would use a maintenance activity database to track information on maintenance actions, system failures, and corrective actions. The database would include detailed information, such as the time and location of every failure, its type and cause, the repairs needed, and descriptions of any parts needed to make the repairs. This information would be valuable for controlling material inventories and establishing trends in equipment failures.

Maintenance program personnel would review all NRC reports on nuclear industry activities and incidents, then incorporate lessons-learned information from other sites into the repository maintenance program (CRWMS M&O 2000p, Attachment II, Section 3).

2.2.8 Decontamination and Decommissioning of Surface Facilities

Any repository surface facilities that could become contaminated are designed to simplify decontamination. Thus, the design of the surface facilities would support three general DOE goals:

- Heath and safety performance objectives that would limit loss of, or damage to, federal property, including losses resulting from an inability to readily decontaminate or decommission facilities for subsequent uses

- Interior corridors of a size and arrangement that would accommodate the facility's ultimate decontamination and decommissioning, including enough room for the equipment required to perform the decontamination

- Dispersion limits on radioactive or other hazardous contaminating materials to simplify periodic decontamination and the ultimate decontamination and decommissioning of the facility for disposal or reuse.

To more directly support these goals, surface facilities would include specific features for future decontamination and decommissioning. For example, items like service piping, conduits, and ductwork would be kept to a minimum in areas of potential contamination; where they are necessary, they would be arranged to ease the job of decontamination. Ventilation system filters would be located to minimize potential contamination of ductwork. Walls, ceilings, and floors would be finished with washable or strippable coverings. Metal liners would be used where needed to ensure a means of decontamination (e.g., pool and transfer cell areas).

Taken together, these and other design features would serve the goals of decontamination and decommissioning of the surface facilities, while permitting reuse or proper disposal of federal property after the repository is sealed and closed (CRWMS M&O 2000p, Attachment II, Section 1.10.3).

2.3 REPOSITORY SUBSURFACE FACILITIES

The design described in this report is focused on protecting the health and safety of both repository workers and the public. To meet these requirements, an integrated set of surface and subsurface facilities is being designed. Operation of a repository would involve a number of distinct but interrelated activities and functions; the major ones include repository development, waste emplacement, retrieval capability, and eventual sealing and closure of the repository. The following design description discusses the subsurface facilities for a potential repository for spent nuclear fuel and high-level radioactive waste, based on current operating concepts.

The subsurface facilities would be located in the South Portal Repository Operations Area and the Subsurface Repository Operations Area. The South Portal Repository Operations Area would support continuing construction of the repository as the North Portal Repository Operations Area accepts and prepares waste for underground emplacement.

This section focuses on the proposed design and development of the potential subsurface repository. A continual emphasis on environmental, industrial, and radiological health and safety criteria would be designed into all of the subsurface facilities and systems.

This section contains design descriptions for the major subsurface facilities, including:

- Access ramps
- Main drifts
- Exhaust mains
- Turnouts
- Emplacement drifts
- Ventilation shafts and ancillary subsurface and surface facilities
- Mechanical and structural support systems
- Underground utilities
- Waste emplacement and retrieval equipment
- Surface-based controls for subsurface operations.

The information provided in this section on the proposed design and development of the potential subsurface repository is summarized from a large set of design descriptions and analyses, including:

- *Site Recommendation Subsurface Layout* (BSC 2001d)
- *Ground Control for Emplacement Drifts for SR* (CRWMS M&O 2000w)
- *Overall Subsurface Ventilation System* (CRWMS M&O 2000x)
- *Subsurface Transporter Safety Systems Analysis* (CRWMS M&O 2000y)
- *Bottom/Side Lift Gantry Conceptual Design* (CRWMS M&O 2000z)
- *Retrieval Equipment and Strategy for WP on Pallet* (CRWMS M&O 2000aa).

2.3.1   Repository Design Capacity

The subsurface repository design considers two cases. The base case, also referred to as the "statutory case," addresses a nuclear waste storage capacity of 70,000 MTHM (63,000 MTHM of commercial spent nuclear fuel and 7,000 MTHM of DOE waste). The NWPA limits the first repository capacity to no more than 70,000 MTHM until

such time as a second repository is in operation. A second case, referred to as the "full inventory" case, would have a capacity of 97,000 MTHM, while not precluding 119,000 MTHM (referred to as "additional repository capacity") for bounding purposes (see Stroupe 2000, Attachment 1).

2.3.1.1   The Base Case Repository Layout

The 70,000-MTHM subsurface repository layout (Figure 2-38) consists of 58 emplacement drifts excavated to a 5.5-m (18-ft) diameter at a center-to-center drift spacing of 81 m (266 ft). The emplacement drifts would be excavated between the east and west mains with an azimuth of 252 degrees. Emplacement drifts 1 through 51 are required for emplacement of the waste package inventory. Emplacement drift 52 would be excavated as an allowance for possible variances in the waste stream. Emplacement drifts 53 through 58 are contingency drifts that would only be excavated in the event that conditions during development of the repository are found to be such that the intended emplacement area cannot be used because of unexpected adverse ground conditions. The required total emplacement drift length to accommodate the 70,000 MTHM is 56,222 m (184,455 ft), which requires an area of approximately 1,150 acres and results in an areal mass loading of approximately 56 MTHM/acre (this rate is calculated based on the tonnage of commercial spent nuclear fuel only, that is, 63,000 MTHM). The repository emplacement drift average thermal load, based on line-loading with 10 cm (4 in.) end-to-end spacing between waste packages, is 1.42 kW/m for the base case layout (CRWMS M&O 2000h, Section 2.3.1; BSC 2001d, Section 6.3.1). Table 2-9 summarizes the preliminary subsurface excavation dimensions for the base case repository layout.

Within the emplacement area, six standby and cross-block drifts with a diameter of 5.5 m (18 ft) would be excavated within the pillars of adjacent emplacement drifts (see Figure 2-38). The two standby drifts would be located within the first half of the emplacement drifts, to be available early for possible relocation of waste packages. The four cross-block drifts would perform possible ventilation, monitoring, emergency egress, and
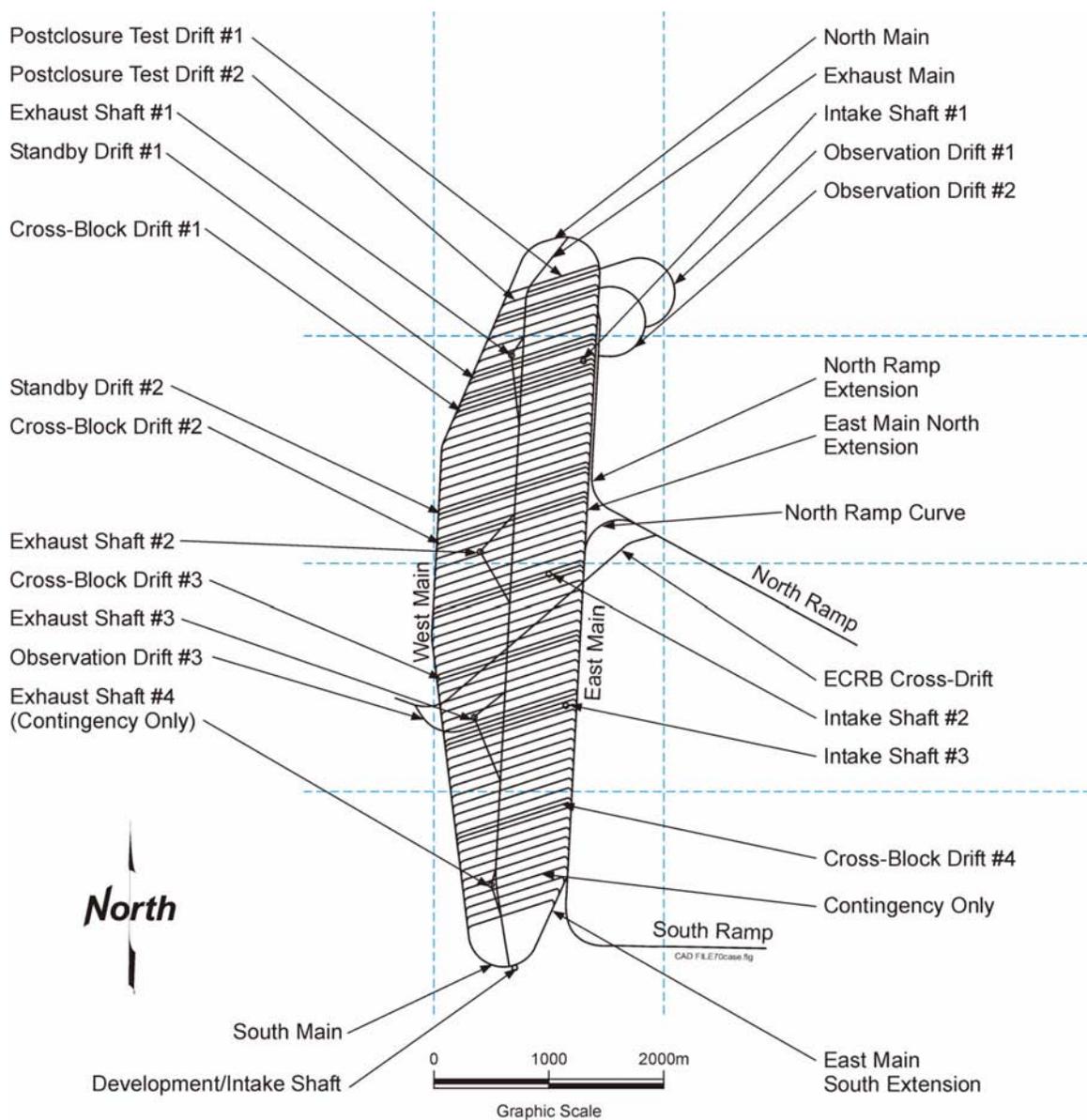
Figure 2-38.   Repository Layout for the 70,000-MTHM Case
The repository layout for the subsurface facilities illustrated in this figure will accommodate 70,000 MTHM of spent nuclear fuel and high-level radioactive waste. This quantity represents the statutory capacity for the repository as mandated by the NWPA and is referred to in this report as the base case. Source: BSC 2001d, Section 6.3.

Table 2-9. Preliminary Subsurface Excavation Dimensions for the Base Case Repository Layout

Designation	Excavated Diameter or Size meters (ft)	Length meters (ft)	Notes
Access Ramps • North Ramp • South Ramp	 7.62 (25.0) 7.62 (25.0)	 2,804 (9,199) 2,223 (7,293)	The access ramps were constructed as part of the Exploratory Studies Facility and will be upgraded for use by the repository
Main Drifts • East Main • North Main • South Main • West Main • North Ramp Extension • North Ramp Curve	7.62 (25.0)	12,988 (42,612)	Typical 300 mm (1 ft) concrete layer over concrete invert segment
Exhaust Main Drift	7.62 (25.0)	6,542 (21,463)	Located below the emplacement horizon
Turnouts	7.0 × 8.0 (23.0 × 26.2)	Varies	7 m (23 ft) high with 4 m (13.1 ft) radius arch; 24 m (78.7 ft) straight section and variable curve lengths
Emplacement Drifts	5.50 (18.0)	56,222 (184,455)	52 each (for base case) on 81-m (266 ft) center-to-center spacings. Typical 908-mm (3-ft) thick circular segment invert fill.
Enhanced Characterization of the Repository Block Cross-Drift	5.0 (16.4)	2,681 (8,796)	This facility is already constructed; measured length from as-built surveys.
Observation Drifts • Observation Drift #1 • Observation Drift #2 • Observation Drift #3	 5.50 (18.0) 5.50 (18.0) 5.50 (18.0)	 1,931 (6,335) 2,103 (6,900) 1,568 (5,144)	
Ventilation Shafts	8.0 (26.2)	Varies	Three intake, three exhaust, one development; variable lengths because of fluctuations in surface terrain
Ventilation Raises	2.0 (6.6)	15 (49.2)	
Alcoves	Varies	Varies	Various configurations, minor excavations

NOTES: Dimensions are approximate unless already constructed. Sources: BSC 2001d, Sections 6.2 and 6.3; for Enhanced Characterization of the Repository Block Cross-Drift dimensions, CRWMS M&O 1999f, Section 4.2.

performance confirmation functions. The 70,000-MTHM layout includes other drifts, such as the postclosure test drifts and the observation drifts, which are used for the performance confirmation program discussed in Sections 2.5 and 4.6.

The access mains to the emplacement area for the 70,000-MTHM layout include the north main, west main, north ramp extension, east main north extension, east main south extension, and south main. These access mains account for approximately 12,988 m (42,612 ft) of excavation. The access mains would be excavated to a diameter of 7.62 m (25 ft). The east and west mains, including the east main north and south extensions, would be used primarily for access to the emplacement drifts during waste emplacement operations. The north and south mains have been configured between the east and west mains to provide access from one side of the repository block to the other. The north ramp extension is provided to the north end of the repository block as a bypass from the north ramp to allow waste emplacement operations concurrent with subsurface facilities development.

The exhaust main, excavated to a diameter of 7.62 m (25 ft), is approximately 6,542 m (21,463 ft) in length and is situated a minimum of 10 m (33 ft) below the emplacement horizon, extending from the north end of the repository block to the extreme south end. The exhaust main is graded upwards in the vicinity of the north and south mains to allow interception for access into the exhaust main from either end of the repository block. The ventilation system uses three intake shafts, excavated to a diameter of 8 m (26.2 ft), in addition to the north and south ramps, for air intake. The development shaft in the south end,

also excavated to a diameter of 8 m (26.2 ft), provides air intake for the construction and development operations for the subsurface facility. Three exhaust shafts, excavated to a diameter of 8 m (26.2 ft), are required to exhaust air from the subsurface facility. Exhaust Shaft #4 would only be required if excavation within the emplacement contingency area is necessary.

2.3.1.2 The Full Inventory Repository Layout

A 97,000-MTHM layout (Figure 2-39) requires 90 emplacement drifts. Drifts 1 through 78 are required for emplacement of the waste package inventory. Drifts 79 and 80 would be excavated as an allowance for possible variances in the waste stream. Drifts 81 through 90 are contingency drifts that would only be excavated in the event that conditions during development of the repository are found to be such that the intended emplacement area cannot be used because of unexpected adverse ground conditions. Emplacement drift orientation is the same as that for the base case layout.

The required emplacement length to accommodate a 97,000-MTHM layout is approximately 74,214 m (243,484 ft), which requires an area of approximately 1,485 acres. This layout results in an areal mass loading of approximately 57 MTHM/acre (this rate is calculated based on the tonnage of commercial spent nuclear fuel only, that is, 83,800 MTHM) and an emplacement drift average thermal load of 1.43 kW/m for the same waste package line-loading condition as the base case (CRWMS M&O 2000h, Section 2.3.2; BSC 2001d, Section 6.4.1).

2.3.1.3 Additional Repository Capacities

In addition to the full inventory design for the repository, the design does not preclude the flexibility to be expanded to accommodate greater quantities (up to 119,000 MTHM). This amount of waste could be generated only if numerous commercial nuclear reactors receive extensions to their initial operating lives from the NRC.

This expanded repository capacity could be used to dispose of both additional commercial spent nuclear fuel and DOE high-level radioactive waste and spent nuclear fuel. As much as 42,000 MTHM of commercial spent nuclear fuel, in addition to 14,250 canisters of DOE high-level radioactive waste and spent nuclear fuel, may require disposal. These amounts are over and above the 70,000 MTHM base case repository layout.

2.3.2 Functional Requirements

The repository facilities have been designed to be fully integrated, using the systems engineering approach to identify functional requirements based on performance objectives and then fulfill these requirements by providing design solutions. This section describes the functional attributes of the systems considered important to preclosure radiological safety.

2.3.2.1 Subsurface Systems Functions

All 17 subsurface systems were evaluated and classified according to their importance to preclosure radiological safety (see Section 2.1). Three systems were classified as QL-1, two as QL-2, one as QL-3, and eleven as CQ. The QL-1 systems are those considered most critical to radiological safety; the CQ systems are those considered to have no impact on radiological safety. Table 2-10 provides the subsurface system safety classifications.

Six principal systems (shaded in Table 2-10) from this set of 17 were prioritized for development of detailed System Description Documents. These systems comprise components that are key to understanding the performance of the potential repository at Yucca Mountain. Preliminary engineering specifications, as required by the NWPA (42 U.S.C. 10101 et seq.), were developed for the selected systems. The six System Description Documents produced were:

- *Subsurface Facility System Description Document* (CRWMS M&O 2000h)

- *Emplacement Drift System Description Document* (CRWMS M&O 2000ab)
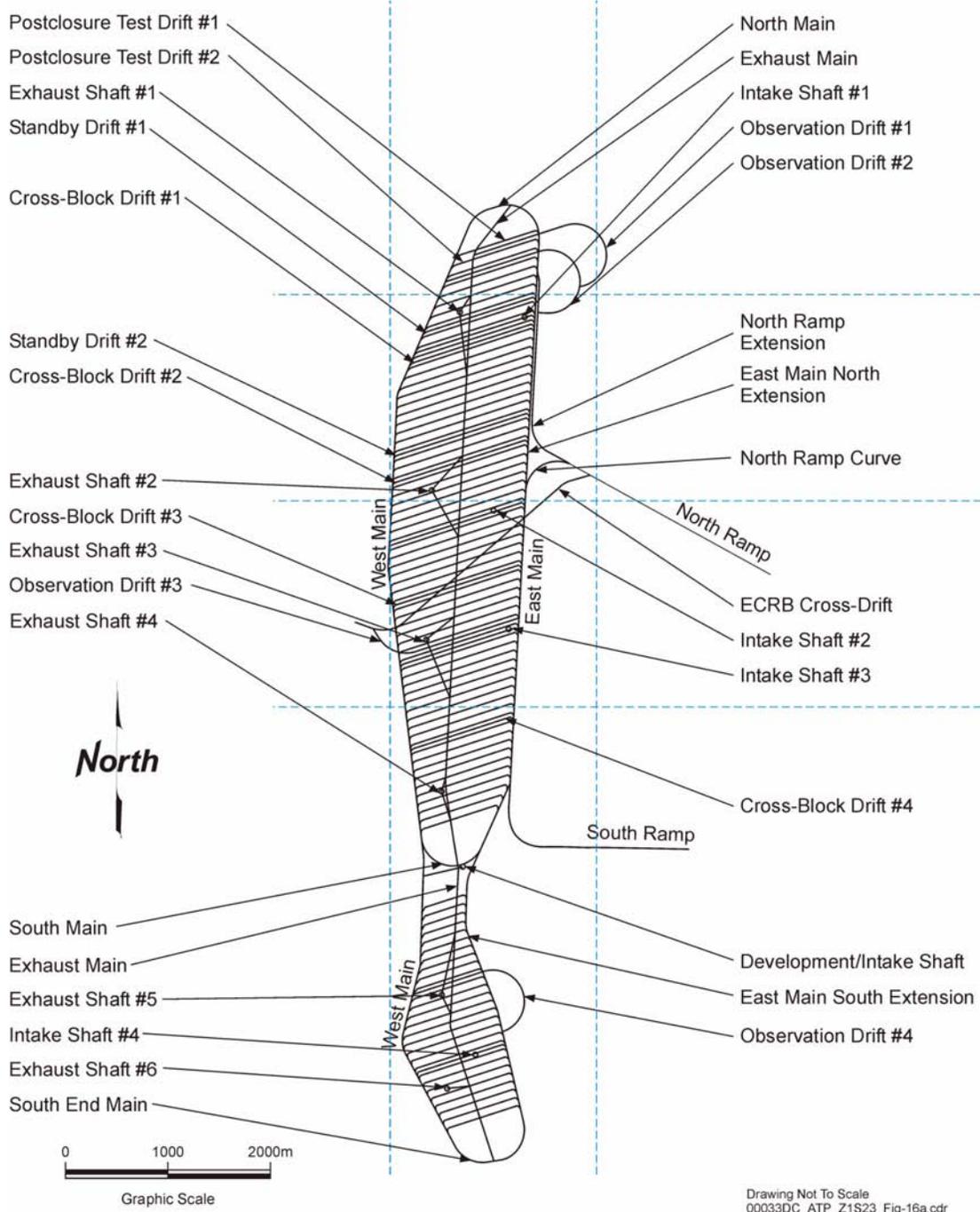
Figure 2-39. Repository Layout for the 97,000-MTHM Case
The subsurface facilities illustrated in this layout represent enough capacity for the storage of 97,000 MTHM of spent nuclear fuel and high-level radioactive waste. This amount is designated in this report as the full inventory case, and it accommodates additional waste resulting from potential extended operation (relicensing) of existing nuclear power plants. Source: BSC 2001d, Section 6.4.

Table 2-10. Safety Classifications for Repository Subsurface Systems

System Designation	System Description	QL Classification
SFS	Subsurface Facility	1
EDS	Emplacement Drift	1
WES	Waste Emplacement/Retrieval	1
GCS	Ground Control	2
BES	Backfill Emplacement	2
PCM	Performance Confirmation Emplacement Drift Monitoring	3
SVS	Subsurface Ventilation	CQ
SED	Subsurface Electrical Distribution	CQ
SCA	Subsurface Compressed Air	CQ
SWD	Subsurface Water Distribution	CQ
MHS	Muck Handling	CQ
SDT	Subsurface Development Transportation	CQ
SCS	Subsurface Closure and Seals	CQ
SWC	Subsurface Water Collection/Removal	CQ
SET	Subsurface Emplacement Transportation	CQ
SES	Subsurface Excavation	CQ
SFR	Subsurface Fire Protection	CQ

Source: YMP 2000b.

- *Waste Emplacement/Retrieval System Description Document* (CRWMS M&O 2000ac)

- *Ground Control System Description Document* (CRWMS M&O 2000ad)

- *Backfill Emplacement System Description Document* (CRWMS M&O 2000ae)

- *Subsurface Ventilation System Description Document* (CRWMS M&O 2000af).

The selected group includes all the QL-1 and QL-2 systems and one CQ system. The subsurface ventilation system, although classified as a CQ system, was included in the selection because of the importance of ventilation to the overall repository design concept. Design descriptions and other information about the remaining 11 systems in Table 2-10 were obtained from a variety of sources. Information on the performance confirmation emplacement drift monitoring system was obtained from the *Performance Confirmation Plan* (CRWMS M&O 2000ag) and from a design analysis, *Instrumentation and Controls for Waste Emplacement* (CRWMS M&O 2000ah). Three separate analysis reports (CRWMS M&O 2000ai; CRWMS M&O

2000aj; CRWMS M&O 2000ak) provided information on the subsurface closure and seals system. Design descriptions provided in subsequent sections explain how the design of subsurface facility components fulfills the functions assigned to them. Functions assigned to other project systems are discussed in Sections 2.2 and 3. The functions of the six principal subsurface systems are summarized below.

Subsurface Facility System—The functions assigned to the subsurface facility system are to:

- Accommodate safe disposal and retrieval of waste packages

- Provide layout, location, and size of underground openings

- Allow personnel and equipment access throughout the repository

- Provide openings for subsurface ventilation

- Provide subsurface refuge areas for subsurface emergencies and exits for emergency evacuation

- Control subsurface flood events and limit subsurface inundation from the surface

- Protect subsurface personnel and equipment from radiation emanating from emplacement drifts

- Locate the repository in an area that would limit radioactive emissions.

Emplacement Drift System—The functions assigned to the emplacement drift system are to:

- Isolate spent nuclear fuel and high-level radioactive waste

- Limit the possibility of a self-sustaining fission reaction in both the near and far fields

- Limit the effect of rockfall on waste packages

- Provide physical support for waste packages

- Influence the environment within the emplacement drift to protect the waste packages and the natural barrier

- Limit the movement of radionuclides to the natural barrier in the event of waste package breach

- Limit microbial activity

- Allow periodic inspection, testing, and maintenance of structures, systems, and components before permanent closure.

Waste Emplacement/Retrieval System—The functions assigned to the waste emplacement/retrieval system are to:

- Receive waste packages at the Waste Handling Building

- Transfer waste packages to the subsurface repository

- Emplace waste packages in their final location within drifts

- Retrieve to the surface some or all emplaced waste packages under normal conditions

- Recover individually selected emplaced waste packages to the surface under normal and off-normal conditions

- Remove rock, ground support, failed equipment, and debris impeding retrieval and recovery operations

- Install ground support to permit safe conduct of retrieval and recovery operations

- Limit or prevent the spread of radioactive contamination

- Support the collection of material control and accounting data

- Operate within the natural and human-induced environmental conditions expected at the surface and subsurface of the repository

- Provide features to minimize radiation exposure to workers

- Provide features and equipment for reducing the risk of, responding to, and recovering from off-normal events and credible design basis events

- Provide features for the inspection, testing, and maintenance of system equipment

- Remediate off-normal events involving the portions of the system supporting waste emplacement, retrieval, and recovery

- Mitigate the effects of a radioactive release in the subsurface repository

- Emplace and recover surrogate (empty) waste packages to support performance confirmation investigations.

Ground Control System—The design functions for the ground control system are intended for the preclosure period; however, they may provide

some benefit during the early part of postclosure. The functions assigned to the ground control system are to:

- Provide structural support for the subsurface repository openings

- Protect waste packages against rockfall, loosening of rock blocks, and fracturing and surface deterioration of the rock mass surrounding each opening

- Maintain adequate subsurface operating envelopes (dimensional clearances)

- Provide for monitoring of ground control performance.

Backfill Emplacement System—The design described in this report does not use backfill in the emplacement drifts; however, there are potential design advantages that warrant maintaining the capability to use it. Design documents include references to emplacement drift backfill and assessments of the effect of backfill on emplacement drift features. Moreover, maintaining this design option provides the flexibility to accommodate future changes, as necessary. Backfill emplacement is required for repository closure operations, which include backfilling ramps, mains, and shafts; however, these closure functions fall under the subsurface closure and seals system. The functions assigned to the backfill emplacement system are to:

- Retrieve and prepare stockpiled material to be used as backfill

- Transport prepared backfill material from the surface to the subsurface

- Install prepared backfill material in the emplacement drifts

- Provide mechanisms and safety features for the protection of operating personnel and equipment.

Subsurface Ventilation System—The functions assigned to the subsurface ventilation system are to:

- Generate and control subsurface airflow

- Maintain air quality standards within established limits

- Contribute to the control of subsurface air temperatures and the rate of air temperature change by removing heat

- Control personnel access to the emplacement drifts

- Monitor the status of system and equipment operation

- Provide operating parameters and air-related environmental data

- Mitigate the spread of a subsurface fire.

2.3.2.2 Containment and Isolation

The subsurface facilities design features contribute to waste containment and radiological shielding during the preclosure period and to the containment and isolation of the waste from the environment during the preclosure and postclosure periods.

The repository design described in this report includes a project design requirement for removal of 70 percent of the heat generated by the waste packages during the preclosure period. Meeting this requirement demands ventilation of the emplacement drifts at an estimated rate of 15 m^3/s (530 ft^3/s) (see Section 2.3.4.3). To accomplish this ventilation rate, the emplacement drift isolation doors would have louvers to permit airflow through the drifts while the doors are closed. Exhaust shafts would draw the drift airflow through the exhaust raise and the exhaust main to the surface. This high ventilation rate would keep emplacement drift wall temperatures below boiling during preclosure and would also contribute to the removal of moisture naturally present in the rock,

as well as water introduced by construction activities.

The continuous preclosure ventilation design contributes to waste isolation by preventing a portion of the rock in the pillars between emplacement drifts from reaching boiling temperatures after closure. Above-boiling temperatures near the emplacement drift walls drive moisture away from the drifts; water will drain through the below-boiling zones of the pillars, rather than into the emplacement drifts. Field tests show that moisture condenses in the pillar area and percolates downward, away from the repository horizon (CRWMS M&O 2000al, Section 3.6.1.3.1). This will reduce the availability of fluid in the matrix of the rock surrounding the emplacement drifts. Lower-temperature operating modes result in lower rock and waste package temperatures. While more water would be available to contact the waste packages, the lower potential for corrosion contributes to containment.

During the preclosure period, engineered subsurface design features (other than movable radiation shields) that can contribute to radiation protection for workers are the emplacement drift isolation doors and the turnouts. The isolation doors, which provide ventilation and access control for the emplacement drift, also contribute to radiation attenuation as well as isolation of potential airborne contaminants. The curved geometry of the turnouts provide protection to workers in the main drifts; direct radiation from the emplacement drifts would be scattered and attenuated by the turnout walls so that only limited radiation reaches the main drifts. After a drift is loaded, the isolation doors would remain closed. The doors cannot be manually operated because of their weight and control mechanisms. Their operation (opening, closing, and louver regulation) would be continuously controlled and monitored by the repository monitoring and control system (see Section 2.3.3). When the doors are open during a waste package transfer operation, the docking area of the turnouts would be under video surveillance by the remote control operators, and personnel access to the area would be denied. Entering the emplacement drifts through a ventilation raise would be difficult, and this mode of entry would not be considered accidental. Other repository design features for prevention of human access during preclosure are described in Section 2.2. The repository preclosure safety test and evaluation program (see Section 5.4) describes the monitoring, testing, and evaluations of repository structures, systems, and components. This program would help ensure safe operation of waste emplacement and other repository functions.

Corrosion-resistant materials have been chosen for waste package supports to aid in maintaining the integrity and stability of waste packages during preclosure and postclosure (see Sections 2.3.4.4.2 and 2.4.3.1).

The emplacement drift engineered barriers (see Section 2.4) and the structures designed for repository closure and sealing (see Section 2.3.4.8) are the two subsurface design features that contribute to waste package containment and isolation during the postclosure period.

2.3.2.3 Thermal Management

The higher-temperature operating mode described in this report ensures that there will be portions of the pillars with temperatures below the boiling point of water (96°C [205°F] at the elevation of the emplacement horizon). This will allow the mobilized water to drain through the pillars, rather than into the emplacement drifts, when the temperature of the adjacent rock is above boiling (see Section 4.2.2). The development of localized boiling fronts around each emplacement drift, rather than a single boiling front encompassing all of the emplacement drifts, ensures that a much smaller amount of water is allowed to build up above any emplacement drift. This substantially decreases the likelihood of any liquid water entering the emplacement drifts. These evaluations resulted in new thermal management criteria for the operating mode analyses presented in this report that seek to keep boiling temperatures from spreading all the way through the rock between drifts during postclosure. Those criteria also introduced the concept of line-loading the waste packages, that is, placing the packages with minimal end-to-end separations to achieve a more uniform thermal profile along the length of the emplacement drifts. The concentration of heat

sources resulting from line-loading required that the emplacement drifts be spaced farther apart to distribute the thermal load over a larger area. Operating modes that result in lower temperatures on the waste package surface and in the rock mass are also relevant to the DOE's thermal management strategies. As discussed in Section 2.1, recent evaluations have investigated performance-related attributes of operating modes of the design described in this report that result in lower waste package surface temperatures, as well as lower rock temperatures. In particular, below-boiling conditions associated with lower-temperature operating conditions could reduce uncertainties in the understanding of corrosion processes for the waste packages.

Given a projected thermal-loading schedule from waste package emplacement, projected nuclear fuel decay, and various rates of ventilation, computer simulations helped define ventilation design concepts that could satisfy the performance objectives related to a range of operating modes for a lower-temperature repository.

2.3.3 Concept of Operations and Maintenance

Current planning calls for the potential repository to be developed and operated in six major phases: (1) site characterization, (2) construction, (3) operations, (4) monitoring, (5) closure, and (6) postclosure (CRWMS M&O 1999g, Section 3.1). This section focuses on two of these phases: construction and operations.

All waste handling activities would be conducted pursuant to approved operations and maintenance procedures to assure safe operations. The project would also have a site-wide centralized instrumentation and controls system to assist in subsurface operations.

2.3.3.1 Subsurface Facilities Construction

The subsurface repository facilities would have concurrent construction and waste emplacement activities; as described in Section 2.3.5, some differentiation is made between initial construction

and construction during emplacement. The construction activities during the first 5 years are called initial construction, and the construction activities that are simultaneous with emplacement are called development.

Examples of the major activities that would take place during the initial construction phase are:

- Transitioning the existing Exploratory Studies Facility to repository facilities

- Refurbishing Exploratory Studies Facility drifts

- Constructing access shafts and ventilation systems

- Excavating at least one exhaust shaft and one intake shaft

- Excavating and finishing portions of the main drifts and exhaust main

- Installing the muck handling system

- Installing utilities, controls, and communication systems

- Constructing the initial set of isolation air locks

- Excavating performance confirmation facilities and installing testing and monitoring equipment.

Development activities would be scheduled so panels of emplacement drifts are completed and commissioned for emplacement at different times throughout the development phase (see Section 2.3.5). These activities would include such work as:

- Continuing excavation, finishing, and equipping of the subsurface facilities, including main and exhaust drift extensions, emplacement drifts, performance confirmation drifts, intake and exhaust shafts, access drifts, and ventilation raises

- Constructing additional air locks and installing additional ventilation equipment

- Commissioning panels of emplacement drifts

- Installing additional monitoring, controls, and communications systems.

In addition to the construction and development activities described above, major subsurface system operations would be performed, including:

- Ground control
- Ventilation
- Waste emplacement.

These major systems would be supported by other subsurface systems (e.g., electrical distribution, compressed air, water distribution, and fire protection) on a regular basis. Routine inspections and maintenance operations activities would be performed as required for each system.

The *Monitored Geologic Repository Concept of Operations* (CRWMS M&O 1999g), as well as applicable NRC nuclear safety requirements, national safety requirements, and DOE Orders (as applicable), would provide the basic guidelines and requirements for operations and maintenance of the subsurface systems.

2.3.3.2 Operations Support Facilities

The repository subsurface facilities would include (1) access facilities, (2) the subsurface Geologic Repository Operations Area, and (3) support areas.

The main access facilities are the north and south ramps, with the development/intake shaft providing additional access throughout the development phase. The north ramp would be the access route for waste emplacement operations; however, during initial construction, it would also be used as a major ventilation air intake. The south ramp would provide primary access for hauling mined rock (muck), personnel, equipment, and construction materials to support repository development operations. The south ramp would also serve as a main ventilation intake and exhaust airway throughout the development phase. The develop-

ment/intake shaft would be available during the development phase for personnel access, muck removal, and introduction of equipment and construction materials, as needed.

The subsurface Geologic Repository Operations Area would consist of all the completed and commissioned subsurface facilities supporting waste emplacement, containment, and isolation. These include the emplacement drift panels, mains, performance confirmation drifts and associated facilities, and subsurface ventilation facilities. This operations area would grow until it reached fully developed dimensions about 25 years after initial construction.

The support facilities for the subsurface operations would include support systems at the surface facilities area, such as:

- Equipment maintenance and repair
- Personnel access control
- Decontamination facilities
- Control and communications centers
- Performance confirmation data processing center
- Security and emergency response systems.

The support facilities at the South Portal would include staging areas for construction equipment and materials, areas for equipment assemblage, muck stockpiles, and construction personnel access and control facilities.

2.3.3.3 Operational Phase

The subsurface operational phase would include the following major activities:

- Transport and emplacement of loaded waste packages
- Performance confirmation
- Completion of drift excavation
- Placement of engineered barriers
- Monitoring and maintenance of structures, systems, and components.

Physical and functional separation of development and emplacement operations would be maintained throughout the operational phase by using engi-

neering controls (e.g., isolation air locks) and administrative controls (e.g., separate access controls). When a predetermined number of newly excavated drifts are ready for waste emplacement, the controls would be moved to include the newly commissioned drifts in the emplacement area.

Waste emplacement operations would include transfer of the waste packages underground, emplacement drift operations, and waste package management. Sections 2.3.4.4 and 2.3.4.5 describe the first two operations. Waste package management operations would include such activities as:

- Monitoring the integrity of the waste packages after emplacement

- Thermal management of the repository block

- Monitoring drift conditions that may affect waste package integrity and implementing mitigation measures

- Periodic removal or relocation of waste packages for testing or mitigation measures, as needed.

Performance confirmation operations include maintaining facilities, equipment, instrumentation, and data communication systems, and constructing new facilities, such as alcoves and boreholes, in support of performance confirmation monitoring. Section 2.5 describes performance confirmation subsurface facilities, and Section 4.6 explains the performance confirmation program.

Operations related to completion of emplacement drifts include calibration of ventilation flow regulators, installation of shielding and local ventilation controls (e.g., turnout air locks), and operational testing of isolation doors.

Section 2.4 discusses the in-drift engineered barriers. The general operational activity in this area is the preparation of the emplacement drifts for installation of the drip shields over the waste packages. Support operations related to this activity would include staging and transportation of the drip shields to the subsurface. Drip shields would be installed during the closure phase.

The repository would be monitored and maintained continually during the emplacement and monitoring phases. Permanently installed sensors would monitor waste packages, drifts, and the surrounding rock from accessible locations. These sensors would provide the data required for performance confirmation activities and for day-to-day monitoring of operational and environmental conditions. System tests and evaluations would also be conducted to ensure functionality and confirm expected performance for the various subsurface systems. Section 5.4 explains the repository test and evaluation program. The following section discusses the repository maintenance approach.

2.3.3.4   Maintenance

To the extent practical, maintenance of equipment and facilities would be conducted by removing and replacing faulty or suspect components. Faulty components would be returned to the shop facilities for repair or for processing for offsite repair or salvaging. Maintenance for nuclear operations requires a specialized workforce certified in the operation of remote handling equipment, containment equipment, and hardware decontamination. A formal maintenance and training program would be implemented, and specialized maintenance procedures would be developed.

In addition to stationary and mobile equipment, the subsurface facilities would have a wide range of monitoring and control systems. To the extent practical, these systems would be designed in a modular fashion. This modular design would allow maintenance personnel to unplug failing units, such as radiation or thermal sensors, programmable logic controllers, input/output circuit boards, and video cameras, and quickly replace them with functioning units. The emplacement drift design philosophy is to minimize in-drift maintenance after the first waste package has been emplaced.

To minimize downtime, a comprehensive scheduled maintenance program would be implemented to ensure that appropriate systems and equipment are given adequate preventive maintenance. Periodic, planned maintenance would preserve the

integrity of the shafts, ramps, and main and access drifts.

Maintenance in response to major system malfunctions would be supported by the surface maintenance facilities at both the North and South Portals. A staff of mechanics, electricians, and supervisors would respond to and repair unplanned equipment outages. Equipment that can be moved would be taken to the surface maintenance facility for evaluation and repair. Some equipment, such as large excavation machinery (e.g., roadheaders or tunnel boring machines), would most likely be repaired in place.

An underground maintenance shop may be added to facilitate repairs and support ongoing drilling or boring operations (CRWMS M&O 1999g, Section 4.6.4).

2.3.4 Design Descriptions and Systems Operations

The following sections describe the design characteristics and concept of operations for the most important subsurface systems of a potential repository at Yucca Mountain.

2.3.4.1 Developing and Maintaining Stable Excavations

2.3.4.1.1 Underground Openings and Excavation Methods

The potential repository excavations were divided into two groups for ground control design analyses: emplacement drifts and nonemplacement areas. The reason for this differentiation is that the emplacement drifts are exposed to higher temperatures than nonemplacement openings (CRWMS M&O 2000w, Sections 5.2 and 6.3.3).

The emplacement drifts would be 5.5-m (18-ft) diameter drifts excavated by a tunnel boring machine, which is a mechanical excavator equipped with a rotating cutting head that chips the rock with hardened disc cutters. Temporary ground control would be installed immediately behind the excavator to provide structural support and worker protection (CRWMS M&O 2000w, Section 6.2.2).

The repository would have several types of nonemplacement excavations (BSC 2001d, Section 6.2):

- Main drifts: The main drifts are large circular tunnels with a diameter of 7.62 m (25 ft), excavated with tunnel boring machines. Examples of main drifts are the existing north ramp and the repository perimeter mains.

- Exhaust main: The exhaust main, also to be excavated with a tunnel boring machine, has a diameter of 7.62 m (25 ft).

- Turnouts: The turnouts are curved sections of tunnel connecting the emplacement drifts to the main drifts. They would be excavated with roadheaders, which are mechanical excavators equipped with a rotating grinding drum mounted at the end of an excavating arm. Drill-and-blast techniques are an alternative option for excavating the turnouts. The turnouts have vertical walls and an arched ceiling. The excavated turnouts are 8 m (26.2 ft) wide, with the ceiling arch reaching a maximum height of 7 m (23 ft) (BSC 2001d, Section 6.2.1.2).

- Performance confirmation test drifts: The performance confirmation test drifts are the same as the emplacement drifts in configuration and construction.

- Performance confirmation observation drifts: These drifts are similar in cross-sectional area to the emplacement drifts and provide access to the monitoring instrumentation stations and alcoves. The observation drifts may be constructed by a combination of tunnel boring machines and roadheaders or by conventional drill-and-blast techniques.

- Alcoves: The alcoves are areas of limited length that would be excavated with roadheaders or by conventional drill-and-blast techniques. Alcoves would serve different purposes, such as refuge chambers and equipment or instrumentation chambers. Mechanical excavation techniques would be used in areas where rock properties being

monitored might be adversely affected by blasting.

- Ventilation shafts and raises: These vertical openings, typically circular, would be excavated by mechanical means (e.g., vertical mole, drilling, and raise boring) or by drill-and-blast techniques. The repository ventilation shafts are large, 8 m (26.2 ft) in diameter. The raises are much smaller, with a diameter of 2 m (6.6 ft). The use of drill-and-blast techniques may be limited near the emplacement horizon because of the potential for disturbing the natural rock conditions.

The Exploratory Studies Facility is a drift 7.62 m (25 ft) in diameter that was excavated with a tunnel boring machine. This facility would become the north ramp–north ramp curve–east main–south ramp loop in the potential repository (see Figure 2-38). The Exploratory Studies Facility uses several types of ground control supports (CRWMS M&O 2000am), including:

- Shotcrete

- Welded wire mesh with rock bolts

- Steel sets with welded wire mesh, steel lagging, or rock bolts, or without additional support.

The Exploratory Studies Facility ground support would be upgraded to cast-in-place concrete lining during the initial construction phase.

Other existing excavations in the repository area significant to ground control are the Enhanced Characterization of the Repository Block Cross-Drift (Figure 2-38) and the Drift Scale Test. The ECRB Cross-Drift is a drift 5 m (16.4 ft) in diameter, excavated with a tunnel boring machine. The drift is equipped with ground control supports similar to those installed in the Exploratory Studies Facility drifts (CRWMS M&O 1998b, Section 7). The ECRB Cross-Drift traverses the repository horizon in a southwesterly direction and intercepts a major fault zone outside the potential repository emplacement area, providing opportunities to characterize the rock environment at the repository

level and in areas of major geological disturbance. Using the ECRB Cross-Drift as a performance confirmation facility is also being proposed.

The Drift Scale Test is located off the north ramp in an alcove loop (CRWMS M&O 1998c). It is a prototype emplacement drift equipped with high-powered electric heater canisters that simulate waste packages. The rock environment and its response to the heat load is being meticulously monitored and documented as part of the characterization phase of the repository program. A portion of the Drift Scale Test facility uses a cast-in-place concrete ground support system. The remainder of the facility uses rock bolts and wire mesh for ground support.

This diversity of excavations in the potential repository area has given engineers firsthand experience with the different levels of support needed and with the effectiveness and reliability of different ground control techniques. This knowledge base is supplemented with rock mechanics information collected from the Drift Scale Test, where the repository rock formation is subjected to thermal stresses equal to or greater than those expected from the thermal load of a higher-temperature operating mode (SNL 1998).

2.3.4.1.2 Proposed Ground Control Structures

Ground control structures are required to ensure that underground openings are stable. The design and construction of an underground high-level radioactive waste repository introduce challenges not ordinarily found at other subsurface facilities. The presence of heat from the spent nuclear fuel and the resulting thermal-mechanical stresses introduce a series of requirements for the overall design and construction of the facility to conform to project performance objectives. In situ loads, construction loads, potential loads from repository operations, and loads from seismic occurrences must also be addressed in the design.

2.3.4.1.2.1 Emplacement Drifts

The initial ground support system for the emplacement drifts also serves as the final support system;

it consists of steel sets with welded-wire fabric and fully grouted rock bolts. Figure 2-40 shows a cross section of a typical emplacement drift with the proposed ground support and a perspective view of the drift with the steel sets and welded-wire fabric detail. This ground support system minimizes routine maintenance, which is not practical once the emplacement drifts are loaded. Project design requirements (CRWMS M&O 2000ad, Section 1.2.2.2.2) state that the ground control system shall also include provisions that support a deferral of closure for up to 300 years. This design satisfies a project design requirement for a service life of not less than 175 years (CRWMS M&O 2000ad, Section 1.2.2.2.4). The steel sets and rock bolt systems are well suited for quick installation with the tunnel boring machine excavation, thereby providing personnel safety during construction. These systems also allow geologic mapping activities in support of the performance confirmation program, since the rock wall remains mostly visible through the support structures.

An all-steel ground support system for emplacement drift support is installed in a single-pass operation. This system consists of W6 × 20 rolled steel ring beams, called steel sets, bolted together to form a full circle, along with welded-wire fabric. Following immediately behind the tunnel boring machine, steel set sections would be bolted together around the drift circumference between the temporary invert sections that support the tunnel boring machine rail. The steel sets would be set in place at 1.5-m (5-ft) intervals along the length of the drift, and tie rods would be inserted between the steel sets. A partial shield, extending from the rear of the tunnel boring machine, would protect the steel set assembly area from rockfall. The welded-wire fabric would be installed behind the shield between the steel set and the rock, with steel pins holding it against the exposed rock to prevent movement of the rock blocks into the drift. Using hydraulic jacks, the steel set would be expanded against the fabric as the tunnel boring machine moves forward (CRWMS M&O 2000w, Sections 6.2.1.1 and 6.5).

A rock bolt system consists of a pattern of steel rock bolts installed through the welded-wire fabric and grouted with cementitious material to hold them in place. The material used for grouting the rock bolts does not present a problem for long-term
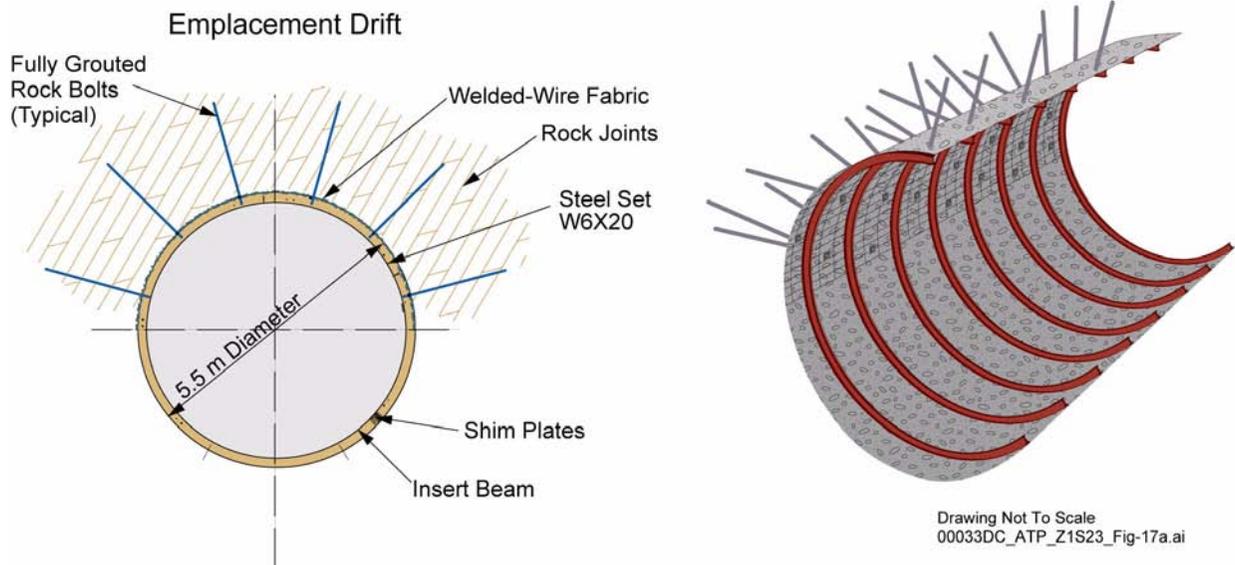
Figure 2-40.   Emplacement Drift Ground Support
Ground support systems for the emplacement drifts consist of a combination of steel sets, rock bolts, and welded-wire fabric. The steel sets would be bolted together to form individual "rings" spaced at 1.5-m centers along the length of the drift. Rock bolts and fabric would be installed in the upper half of the drift. Density of rock bolt installations would vary with degree of fracturing in the rock. The wire fabric would prevent loose blocks of rock from becoming detached from the drift wall. Source: CRWMS M&O 2000w, Section 6.

waste isolation (e.g., the alkalinity issue related to elimination of precast concrete liners in emplacement drifts, as discussed in Section 2.1.2.1) because (1) the amount used for grouting is relatively small compared to the total volume of concrete that it would take to line the emplacement drifts and (2) the high-strength cementitious grout is likely to remain intact and attached to the rock even if the rock collapses. A typical rock bolt for this application is 3 m (10 ft) long. Rock bolts prevent key blocks from loosening. In areas with massively jointed rock, or where key blocks are mobilized by excavation and can fall, rock bolts would be installed in a radial pattern above the drift springline (the level of maximum horizontal width of the drift). These conditions are anticipated primarily in nonlithophysal rock areas, which comprise about 30 percent of the emplacement area (CRWMS M&O 2000w, Sections 6.2 and 6.5).

2.3.4.1.2.2 Nonemplacement Excavations

The main drifts, turnouts, exhaust main, and ventilation shafts will have initial and final ground support systems developed. Initial ground control methods will vary depending on ground conditions and would include a combination of steel sets, welded-wire fabric, rock bolts, and shotcrete (concrete sprayed onto the surface at high pressure). Steel sets would be needed to control more difficult, localized geologic conditions. The preva-

lent initial ground control is expected to be a combination of welded-wire fabric and rock bolts. Occasional use of shotcrete is expected to stabilize areas with extensive fracturing. The final ground support system for these nonemplacement excavation areas would be cast-in-place concrete liners with a nominal thickness of 0.3 m (1 ft). Figure 2-41 shows typical cross sections for a main drift and a turnout (CRWMS M&O 2000w, Sections 6.1, 6.2, and 6.6).

The observation drifts, which support the performance confirmation program, would have a ground support system similar to that for the emplacement drifts if they are excavated with a tunnel boring machine. Otherwise, they would have a combination of support systems, including steel sets, welded-wire fabric, rock bolts, and shotcrete, depending on ground conditions (CRWMS M&O 2000w, Section 6.2.2).

2.3.4.1.3   Determination of Ground Control Design Loads

In designing the repository excavations and their ground support structures, stresses resulting from four sources were considered: (1) in situ stresses, including excavation effects; (2) stresses from construction and operation activities; (3) thermal stresses from the waste packages; and (4) seismic stresses. In situ stresses are present before drift
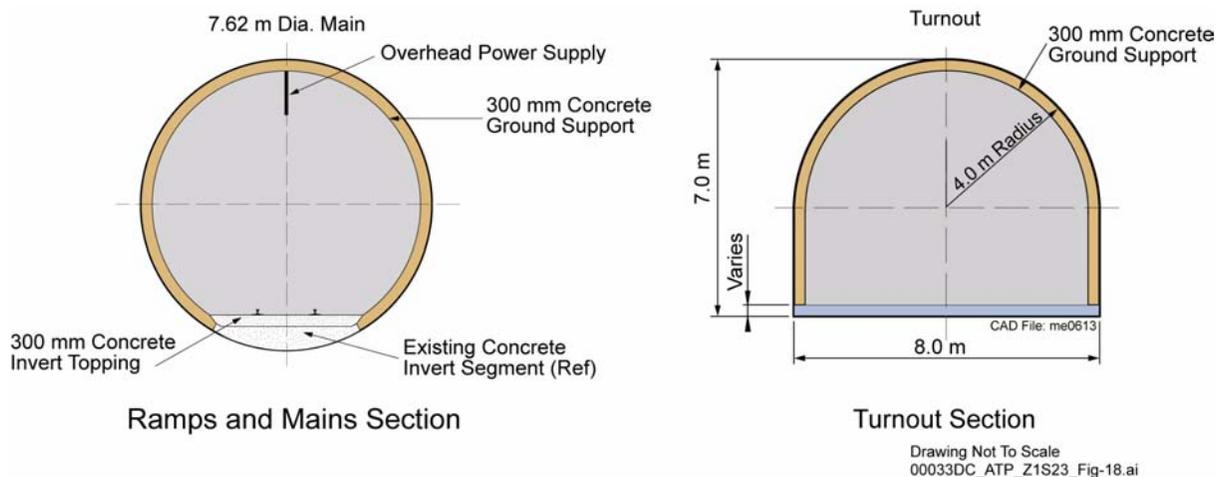
Figure 2-41. Typical Final Ground Support System for Nonemplacement Excavations
Nonemplacement drifts and turnouts use a cast-in-place concrete liner, approximately 300 mm (12 in.) thick, as the final ground support system. Source: CRWMS M&O 2000w, Section 6; BSC 2001d, Section 6.2.

excavation and will be altered during repository excavation. The stresses during construction, including stresses due to installation activities (e.g., jacking process) and equipment movement (e.g., the weight of the tunnel boring machine during excavation), are considered in the design of the ground support systems. The stresses due to repository operations, such as loads caused by gantry or waste package weight, are also considered in the design. Thermal stresses will occur after waste emplacement, and the magnitude of these temperature-induced loads in the rock will depend on the location of the rock relative to the emplaced waste packages, the repository thermal loading, and the time that has passed since emplacement. The magnitude and duration of earthquake-induced stresses are a function of the intensity and duration of the earthquake, the distance of the event from the repository, and the direction and size of the seismic wave relative to the opening (CRWMS M&O 2000w, Section 6.3).

Different techniques were used to estimate stresses and design loads. Analytical techniques used and results obtained are documented in a design analysis report, *Ground Control for Emplacement Drifts for SR* (CRWMS M&O 2000w, Sections 6.3 through 6.6).

Table 2-11 describes the relationship of the lithostratigraphic units in the Topopah Spring Tuff to the thermal-mechanical units within the potential repository emplacement horizon. Table 2-12 summarizes the ground control component preliminary specifications for the subsurface excavations.

Table 2-11. Lithostratigraphic Units and Relationship to Thermal-Mechanical Units of the Topopah Spring Tuff Within the Repository Emplacement Horizon

Formation	Thermal-Mechanical Units	Lithostratigraphic Units
Topopah Spring Tuff	TSw1	Lower part of upper lithophysal zone
	TSw2	Middle nonlithophysal zone
		Lower lithophysal zone
		Lower nonlithophysal zone

Source: CRWMS M&O 1998d, Figure C-2.

Table 2-12. Subsurface Ground Control Components

Excavations	Ground Control Components
Access main drifts, exhaust main drift, turnouts, ventilation shafts	Initial ground control—shotcrete, rock bolts, welded-wire fabric Final ground control—300-mm (12-in.) thick cast-in-place concrete liner
Emplacement drifts	152-mm (6-in.) wide flange beam steel sets, grouted rock bolts, welded-wire fabric
Other subsurface excavations	Various combinations of steel sets, welded-wire fabric, rock bolts, and shotcrete as needed

The emplacement drifts would be essentially contained within the TSw2 unit. This unit includes both lithophysal and nonlithophysal rock, sloping slightly, so that 70 percent of the emplacement drifts would be in the former and 30 percent in the latter. Because the nonlithophysal rock is more jointed and has lower strength and stiffness properties, the emplacement drift ground support design focused on this type of rock. This results in a conservative design. Analyses were also performed on the lithophysal rock for sensitivity effects and completeness. Some initial ground supports for the nonemplacement drifts, such as the east main, were installed during Exploratory Studies Facility construction (CRWMS M&O 2000am). Knowledge acquired and lessons learned during construction of the Exploratory Studies Facility and the ECRB Cross-Drift (CRWMS M&O 1998b) were used in identifying effective initial ground support systems for the proposed main drift extensions.

Results of the analyses for unsupported excavations indicate that the proposed drifts will be inherently stable for the design loads analyzed, including the seismic load. The thermal loads induce minor deformations to which the ground support systems must adapt. Analyses showed that the selected ground support structures for the emplacement drifts could safely handle these anticipated deformations (CRWMS M&O 2000w, Section 7).

Analysis results for the nonemplacement drifts concluded that the maximum combined stress in the concrete lining will be about 50 percent of the

concrete allowable strength. Therefore, the cast-in-place concrete lining would be suitable as the final ground support system for the nonemplacement drifts (CRWMS M&O 2000w, Section 7).

2.3.4.2 Maintaining a Safe Working Environment

The subsurface facilities will be maintained as a safe working environment managed under the *Integrated Safety Management Plan* (DOE 2000c). The facilities have been designed with worker safety as a priority in all phases of development, operations, and closure. The applicable nuclear safety requirements of the Code of Federal Regulations and DOE Orders will be followed. The repository underground environment will be continuously monitored for key environmental quality parameters to alert workers of potential hazards, and dosimetry records for individual workers will be monitored to ensure compliance with radiation dose limits. The facilities would be provided with refuge chambers, evacuation facilities, and emergency response equipment and capabilities. Subsurface communication systems would be available throughout the subsurface facilities for communicating with surface control centers and for broadcasting hazard warnings or emergency communications.

The major potential environmental hazards at the repository, besides waste package radiation, are expected to be: (1) heat; (2) dust from construction activities; (3) dust from other activities containing harmful contaminants or materials, such as silica dust or airborne radioactive particulates; (4) radon progeny (radon gas and its radioactive decay daughter products); (5) fire; and (6) rockfall. Engineering controls are incorporated into the repository design of features and components where these hazards may be encountered. Ventilation and ground control are key subsurface facilities systems where these engineering controls are incorporated into the design.

These engineering controls will be supplemented with frequent monitoring of repository conditions, an aggressive maintenance program and, as needed, administrative controls.

2.3.4.2.1 Ventilation System Monitoring and Operational Safety Requirements

2.3.4.2.1.1 Design Requirements

Ventilation system analyses (CRWMS M&O 2000x, Section 4.2; CRWMS M&O 2000an, Section 4.2) identify criteria for limits on subsurface air temperature, prevention of cross-contamination, radon concentrations, and safety systems.

Temperature Limits—The ventilation system would be designed to limit the maximum dry bulb temperature to 48°C (118°F) in subsurface areas requiring human access (CRWMS M&O 2000af, Section 1.2.1.3). For subsurface areas requiring human access for a full shift (i.e., eight hours or more) without personnel heat stress protection, the ventilation system shall limit the maximum effective temperature to 25°C (77°F) (CRWMS M&O 2000af, Section 1.2.1.3).

Temperature limits would also be imposed on the ventilation system for protection of instrumentation, monitoring equipment, and remote access equipment. For those areas and activities where remote access is required (i.e., activities in emplacement drifts like emplacement, retrieval, recovery, and off-normal modes of operation), the dry bulb temperature must be maintained at or below 50°C (122°F).

Prevention of Cross-Contamination—Engineering controls for prevention of cross-contamination of air supplies are imposed by the requirement that the ventilation systems for the development areas and the emplacement areas be separate and independent systems, with the emplacement system operating under negative pressure and the development system operating under positive pressure. A separate requirement states that the emplacement drift ventilation system be designed to prevent reverse airflow (i.e., airflow from the emplacement drifts into the turnouts).

Radon—The ventilation system must control concentrations of radon progeny in potentially occupied areas to levels that will not result in worker exposure exceeding regulatory limits. The

ventilation system has been designed to satisfy Section 14.5 of ANSI N13.8-1973, *American National Standard Radiation Protection in Uranium Mines*, to control concentrations of radon progeny in potentially occupied areas of the repository.

Preventing the Spread of Surface and Airborne Contamination—The ventilation system will be designed to ensure that occupational doses are ALARA, in accordance with repository program goals, applicable NRC regulations, and NRC Regulatory Guide 8.8.

Safety Systems—The ventilation system has to provide for the following alarm status indicators, as a minimum, from the subsurface safety and monitoring systems: (1) subsurface fire detection, (2) subsurface radiological conditions, and (3) subsurface air quality.

2.3.4.2.1.2 Operational Safety Requirements

The emplacement area ventilation system would be separated from the construction system with isolation barriers, or air locks. The use of these air lock systems is discussed in Section 2.3.5. Operating the emplacement surface fans in an exhaust mode would prevent airflow reversal from the emplacement side to the construction side. Section 2.3.4.3 describes how the surface fans draw air through the exhaust mains at a rate that ensures that air always circulates into emplacement drifts from the main drifts and never allows air to recirculate back to the main drifts (CRWMS M&O 2000x, Section 6.1). Section 2.3.4.3 also discusses the regulation of air temperatures in the emplacement drifts.

Human access to the exhaust main is made possible by dividing the main in halves along its length with an airtight partition. For the operating mode described in this report, rock temperatures around the observation drifts have been estimated to peak at about 46°C (115°F) during the preclosure period. Therefore, during the preclosure period the observation drifts would be exposed to temperatures within the design conditions for human access, even without accounting for any cooling from airflow. Airflow in the observation drifts will vary and can be adjusted to maintain temperatures as

needed for human comfort during the preclosure period. The observation drifts and emplacement drifts will be under the same negative pressure system. The airflow in each drift would be controlled by regulators at the drift entrances or the exhaust raise outlets. The intake air for each drift is supplied via the east or west mains. Airflow and pressures would be monitored electronically to ensure that proper airflow directions and quantities are maintained. Maintaining the airflow direction from the mains into the drifts will prevent airborne radiological contamination from migrating into the mains and observation drifts. The air exiting these drifts would be carried in an air stream, separate from the emplacement air stream, into one half of the exhaust main, designated the "service side." That half of the main would be considered a normal workplace. If maintenance work is needed in the emplacement exhaust side of the exhaust main, temporary openings through the partition could redirect cooler air to the warmer air stream. The exhaust shafts would not be partitioned, so if maintenance or repair work is required in those areas, the emplacement air volume would be temporarily reduced so personnel can work in the shafts (CRWMS M&O 2000x, Section 6.1).

Section 2.3.5 discusses ventilation techniques used during construction and dust control techniques used in the active excavation fronts. The ventilation analysis discusses dust control techniques in use at the site. Those dust control guidelines are expected to be followed during the repository construction and operation phases (CRWMS M&O 2000x, Section 6.4.1).

Radon gas emissions are common in any excavation in igneous rock. Radon gas is liberated in proportion to the exposed area of rock, but dilution can control it. Using blowers in development headings (at the excavation front), filtering the air, and spraying lining materials on the rock surface could also control radon exposure. However, use of spraying foam may not be acceptable at the repository because of the prohibition against the use of organic materials in the subsurface environment. Ongoing characterization work at the Exploratory Studies Facility will determine radon emission rates; once these have been determined, airflow volumes required for dilution can be estimated and

ventilation rates established to limit radon exposures (CRWMS M&O 2000x, Section 6.4.2).

2.3.4.2.1.3 Ventilation and Radiation Monitoring

The subsurface ventilation monitoring system is one of the components of the repository operations monitoring and control system. Figures 2-42 and 2-43 show conceptual locations and monitoring parameters for the ventilation system components (CRWMS M&O 2000x, Section 6.5).

2.3.4.2.2 Fire Protection

A subsurface fire hazards analysis reported in the subsurface ventilation analysis (CRWMS M&O 2000x, Section 6.6.2) concluded that the potential for a toxic, biological, or radiological incident due to a fire is not considered significant for the following reasons:

- Most materials selected for construction are essentially inert.
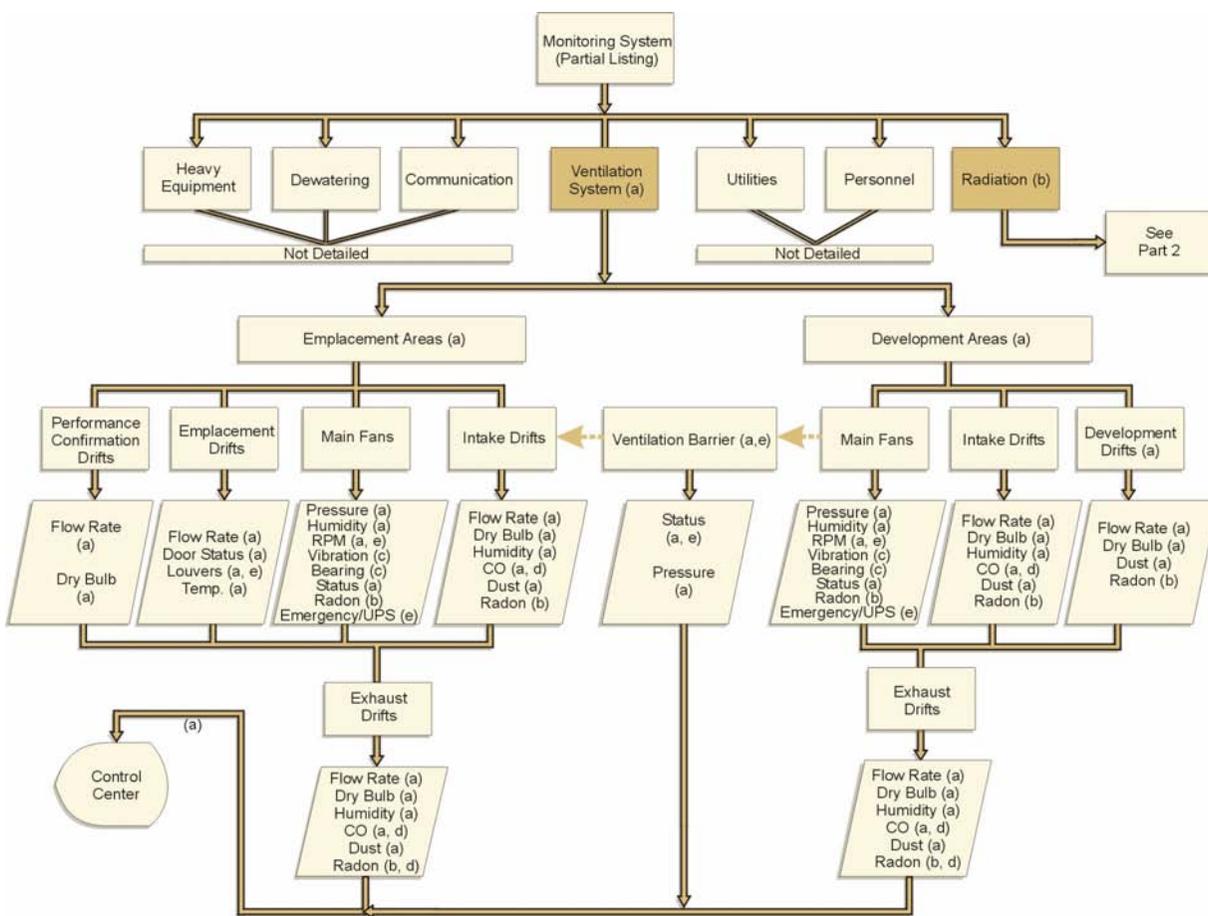
00033DC_ATP_Z1S23_Fig-25.cdr

Figure 2-42. Ventilation and Radiation Monitoring Conceptual Diagram, Part 1
(a) Monitoring operations interface/parameters; (b) Site radiological interface; (c) Motor parameters; (d) Alarm status for fire, radiation, and air quality; (e) Operator control of fans, dampers, and doors. The ventilation system would be continuously monitored for critical component function and performance and for key parameters of airflow at many locations throughout the repository. Only ventilation and monitoring system parameters are sketched; the monitoring system list is partial. Nonradioactive particulate is referred to as "dust" in these diagrams. RPM = revolutions per minute; UPS = uninterruptible power supply. Source: CRWMS M&O 2000x, Section 6.5.
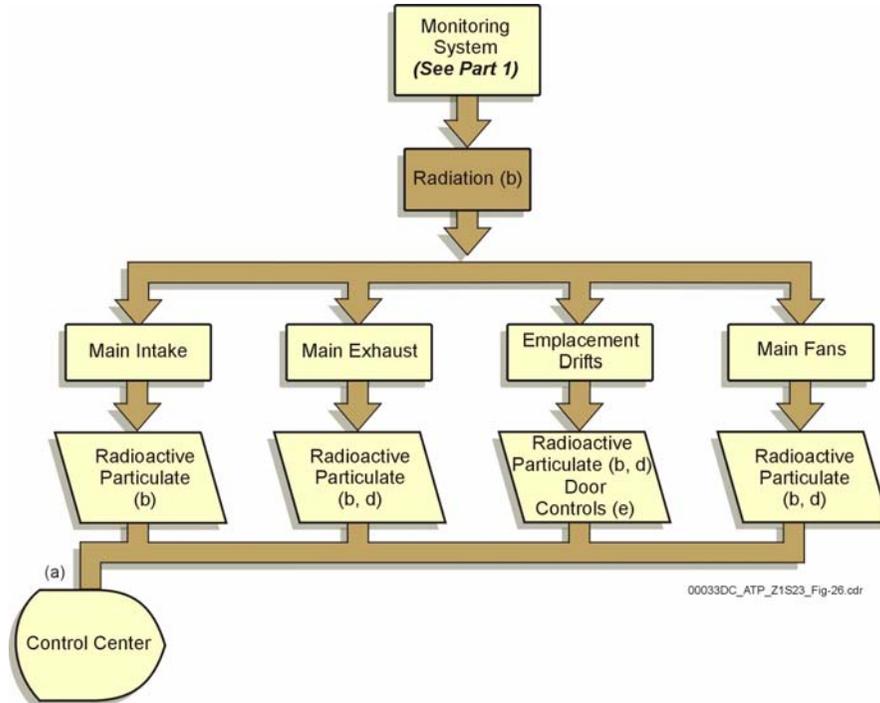
Figure 2-43.   Ventilation and Radiation Monitoring Conceptual Diagram, Part 2
Notes (a) through (e) are given in Part 1 of the conceptual diagram (Figure 2-42). Monitoring of repository ventilation includes measurements of airborne radioactivity at all intake and exhaust points. Nonradioactive particulate is referred to as "dust" in these diagrams. Source: CRWMS M&O 2000x, Section 6.5.

• The risk of combustion due to burning electrical cables is low because of the expected use of special high-temperature and fire-rated cables, and because power cables will be separated from any instrument cables that are not fire-rated.

• Spent nuclear fuel and high-level radioactive waste will not be present in the areas being constructed. During the emplacement phase, radioactive materials, although present, will be contained in the sealed waste packages. A fire in the subsurface large enough to produce heat exceeding the waste package cladding peak temperature tolerance of 570°C (1,060°F) is considered a beyond Category 1 and Category 2 event sequence.

Remotely controlled equipment that may be susceptible to electrical fires would have the same fire detection and suppression systems as the waste package emplacement gantry, as described in Section 2.3.4.5.1. The potential for fire would also

be minimized by administratively controlling the types and amounts of combustible materials brought underground.

2.3.4.2.3   Ground Control Monitoring and Maintenance

Design criteria for emplacement and nonemplacement drifts ground control (CRWMS M&O 2000w, Section 4.2) includes the following requirements directly related to worker safety:

1. The ground support systems must be designed to prevent rockfall that could result in personnel injury.

2. The ground control system must be designed to withstand a Category 1 or Category 2 earthquake, as appropriate to the seismic frequency classification assigned to each particular structure, system, and component.

3. The ground control system must be designed to include provisions which support a deferral of closure for up to 300 years (CRWMS M&O 2000w).

4. The ground support systems must be designed to function without planned maintenance during the operational life of the repository while providing the option to perform unplanned maintenance as needed.

Meeting these design criteria will create solid bases for a safe underground working environment as related to ground control. Even though the necessary maintenance for ground support systems is minimal, the rock face and ground supports would be inspected regularly. Additional supports would be installed as needed, and existing supports would be replaced if found to be inadequate or defective.

The presence of personnel in the emplacement drifts after waste emplacement is not expected unless repair or remedial work is absolutely necessary because of an off-normal event. Nonetheless, the emplacement drifts would be periodically inspected using remotely controlled inspection gantries. These remote inspections would document the conditions of the ground support systems inside the emplacement drifts. If conditions develop that could result in rock or ground support failure, appropriate maintenance and repairs would be scheduled. Preventive maintenance is intended to provide stable and safe subsurface facilities for personnel during preclosure.

2.3.4.3   Thermal Load Requirements

Results from computer simulations were used to analyze the effects of preclosure continuous ventilation in the emplacement drifts (CRWMS M&O 2000x, Section 4.1.1) and to define bounding conditions for the ventilation system design. Estimated temperatures in the emplacement drift exhaust air that would result from waste package linear heat loads of different magnitudes over a period of up to 200 years were considered for various ventilation rates. The results obtained for a ventilation rate of 15 m^3/s (530 ft^3/s) and for initial linear heat loads from waste packages of 1.4 and

1.6 kW/m indicated that peak air temperatures in the emplacement drifts of 58°C (136°F) and 63°C (145°F), respectively, would be reached 10 years after emplacement. The calculations also showed that, at heat loads of 1.4 kW/m and 1.6 kW/m and a ventilation rate of 15 m^3/s (530 ft^3/s), 71 percent of the heat generated would be removed in 50 years. The achieved heat removal percentage agrees favorably with the design requirement for the ventilation system to remove 70 percent of the heat generated by the waste packages during preclosure (CRWMS M&O 2000af, Section 1.2.1.9). The 1.4-kW/m and 1.6-kW/m linear loads provide a lower and upper bound for the average 1.45-kW/m linear heat load. Stroupe (2000, Attachment 1) imposed a maximum linear heat load of 1.5 kW/m on the operating mode described in this report. These linear loads are average loads for an emplacement drift. The waste emplacement requirements document (CRWMS M&O 2000ac, Section 1.2.4.16), however, allows emplacement of individual waste packages with a thermal output as high as 11.8 kW.

To achieve the 71 percent heat removal rate, an emplacement drift has to receive continuous ventilation for 50 years from the start of emplacement with the operating mode described in this report. If an emplacement drift is ventilated for more or less than 50 years, the amount of heat removal will be different (CRWMS M&O 2000x, Section 4.1.1).

For an average line load of 1.45 kW/m, an exhaust air temperature of approximately 60°C (140°F) was calculated as the expected peak (CRWMS M&O 2000x, Section 4.1).

Computer modeling using the program NUFT 3.0 shows that the temperature at the center portion of the rock pillar between emplacement drifts, defined as the quarter-pillar area, remains below 96°C (205°F) for the 1.45-kW/m thermal load. This condition prevails during the preclosure and postclosure periods for the ventilation rate specified for the higher-temperature operating mode (BSC 2001d, Section 6.2.3.7).

The emplacement drift ventilation flow can be varied to allow limited-time personnel or remote equipment access for evaluation and remediation

work for off-normal operation events. Since the emplacement drift exhaust air temperature peaks at 60°C (140°F), additional airflow will be required to lower the temperature below 50°C (120°F). An off-normal ventilation rate of 47 m³/s (1,660 ft³/s) per emplacement drift split, referred to as "blast cooling," will rapidly decrease drift temperatures. After 50 years of emplacement, the drift outlet temperature would fall below 50°C (120°F), and blast cooling would no longer be needed (CRWMS M&O 2000x, Section 6.1.4). Tables 2-13 and 2-14 summarize the characteristics of the ventilation system for the base case repository design and the allowable subsurface working temperatures.

Table 2-13. Design Basis of Ventilation System for Base Case Repository Layout

Item	Detail
Number of exhaust ventilation shafts	3
Number of intake ventilation shafts	3
Number of ventilation fans per exhaust shaft	2
Total electrical power for exhaust fans	10,000 hp
Airflow Quantities • Exhaust shaft airflow rate • Emplacement drift (70% heat removal) • Emplacement drift (blast cooling)	800 to 850 m³/s 15 m³/s 47 m³/s
Airflow Velocities • Minimum • Haulage mains and ramps • Exhaust main • Intake and exhaust shaft accesses • Intake and exhaust shafts	1 m/s 6 m/s 8 m/s 8 m/s 20 m/s
Emplacement drift average heat load (based on 10 cm end-to-end waste package spacing)	1.42 kW/m

Table 2-14. Allowable Subsurface Working Temperatures

Item	Temperature °C (°F)
Human access maximum temperature	48 (118)
Human full shift occupation (8 hours +)	25 (77)
Instruments, monitoring equipment, and remote access equipment limit	50 (122)

2.3.4.3.1 Ventilation System Design

The ventilation system design covers four phases of the repository: (1) construction; (2) waste emplacement; (3) monitoring; and (4) closure. The emphasis of the system description in this section

is thermal load management. Other functions of the ventilation system related to personnel safety are discussed in Section 2.3.4.2. All four phases are relevant to management of thermal loads.

The ventilation design is flexible in terms of repository capacity expansion, if needed. Ventilation designs for two repository sizes were analyzed: the first for the base case, or "statutory case," of a 70,000-MTHM repository, and the second for a hypothetical "full inventory" case of 97,000 MTHM.

2.3.4.3.1.1 Repository Ventilation System Concept

Figure 2-44 shows a general airflow pattern for ventilation of the emplacement drifts, using a representative section of the fully developed repository. Figure 2-45 shows a flow process diagram for the emplacement ventilation. These two figures illustrate the terms and processes described in this section. In the basic ventilation design, fresh air enters through intake shafts and the ramps and is distributed to the east and west mains. From the mains, air enters the emplacement, performance confirmation, or reserve drifts and flows to exhaust raises located near the center of each drift. The exhaust raises direct the airflow down to the exhaust main, where it continues to an exhaust shaft and then to the surface.

Fans located at the surface at the ends of the exhaust shafts would provide the moving force for subsurface repository airflow. The fans are designed with enough power to exhaust the maximum amount of air required during the emplacement, monitoring, and closure phases. The airflow volume that is moved by the fans would be variable, so as the thermal requirements of the repository change with time, the air volume can be adjusted. Air distribution within the repository would be controlled by flow regulators (valves or louvers) at each emplacement drift and in the exhaust main. The surface fan installation would create a higher negative air pressure on the exhaust main level than on the emplacement level, preventing recirculation from the emplacement drifts out to the main drifts. In other words, the surface fans would draw air through the exhaust
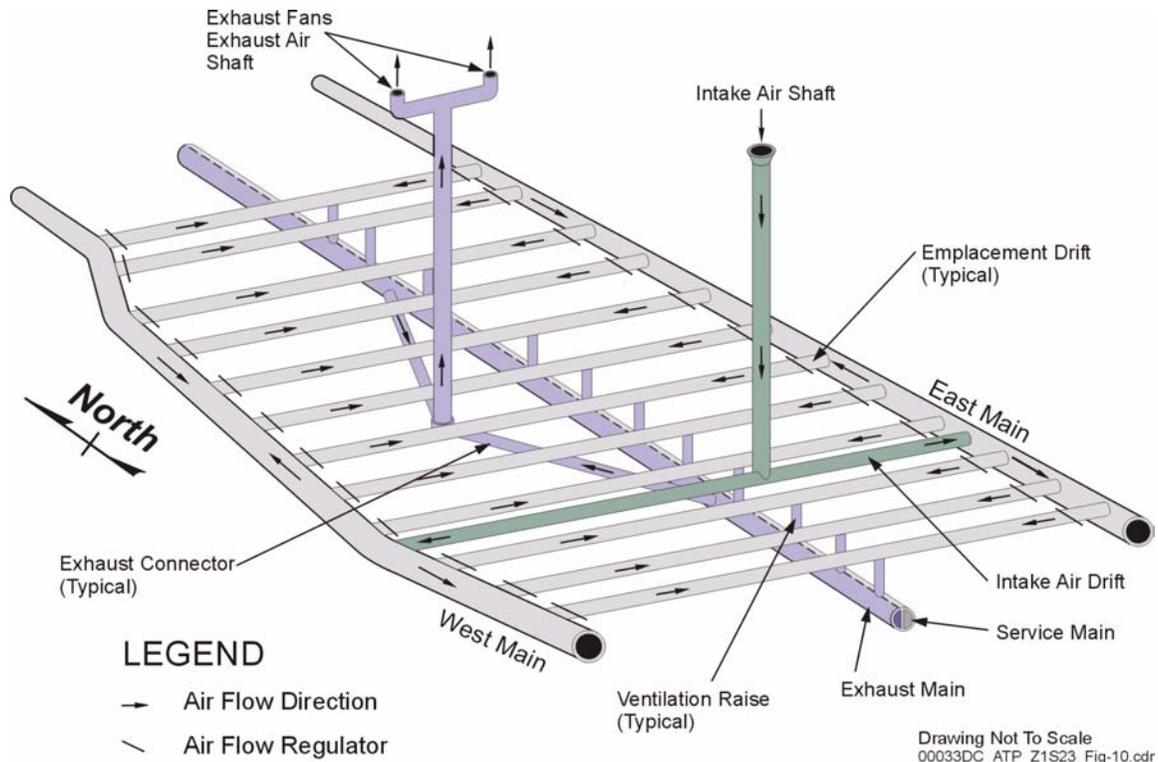
Figure 2-44.   Repository Emplacement Area General Airflow Pattern
This simplified representation of the repository illustrates the emplacement side ventilation airflow patterns. Fresh air would be introduced through the intake air shafts and diverted to the east and west mains via the intake air drifts. Airflow from the mains would be available at both entrances to the emplacement drifts; the airflow rate into each "half" of the emplacement drifts would be controlled by airflow regulators. Heated air exits the emplacement drifts via the ventilation raises and enters the exhaust side of the exhaust main. Air from the exhaust main would be moved through the exhaust connectors to the exhaust air shafts, where it would exit to the surface. Dual exhaust fans at the surface end of each exhaust shaft would provide the moving force for the emplacement side ventilation system, such that the entire emplacement side is always under negative (vacuum) pressure. Source: CRWMS M&O 2000x, Section 6.3.3.

mains at a rate that ensures that air always circulates into the emplacement drifts from the main drifts and that never allows air to recirculate back to the main drifts.

The cross-block and performance confirmation drifts are designed to carry a variable airflow to react to off-normal events, maintenance requirements, waste package retrieval, drip shield installation, or drift repair. These drifts can carry additional airflow to the east or west mains or down the exhaust raises to vary or redirect the airflow on either the emplacement level or the exhaust level (CRWMS M&O 2000x, Section 6.1).

2.3.4.3.1.2 Emplacement Drift Ventilation

Ventilation requirements for emplacement drifts will vary according to the activities conducted in the emplacement drifts. Prior to emplacement, ventilation provides fresh air and controls dust levels to provide an acceptable environment for construction personnel. During emplacement, ventilation maintains drift temperatures within an acceptable range for equipment operation. After emplacement, ventilation will remove 71 percent of the heat generated by the waste packages. Ventilation rates in the emplacement drifts are adjustable to react to other requirements, such as mitigation of off-normal events in emplacement drifts (e.g., repair of collapsed ground supports). These various
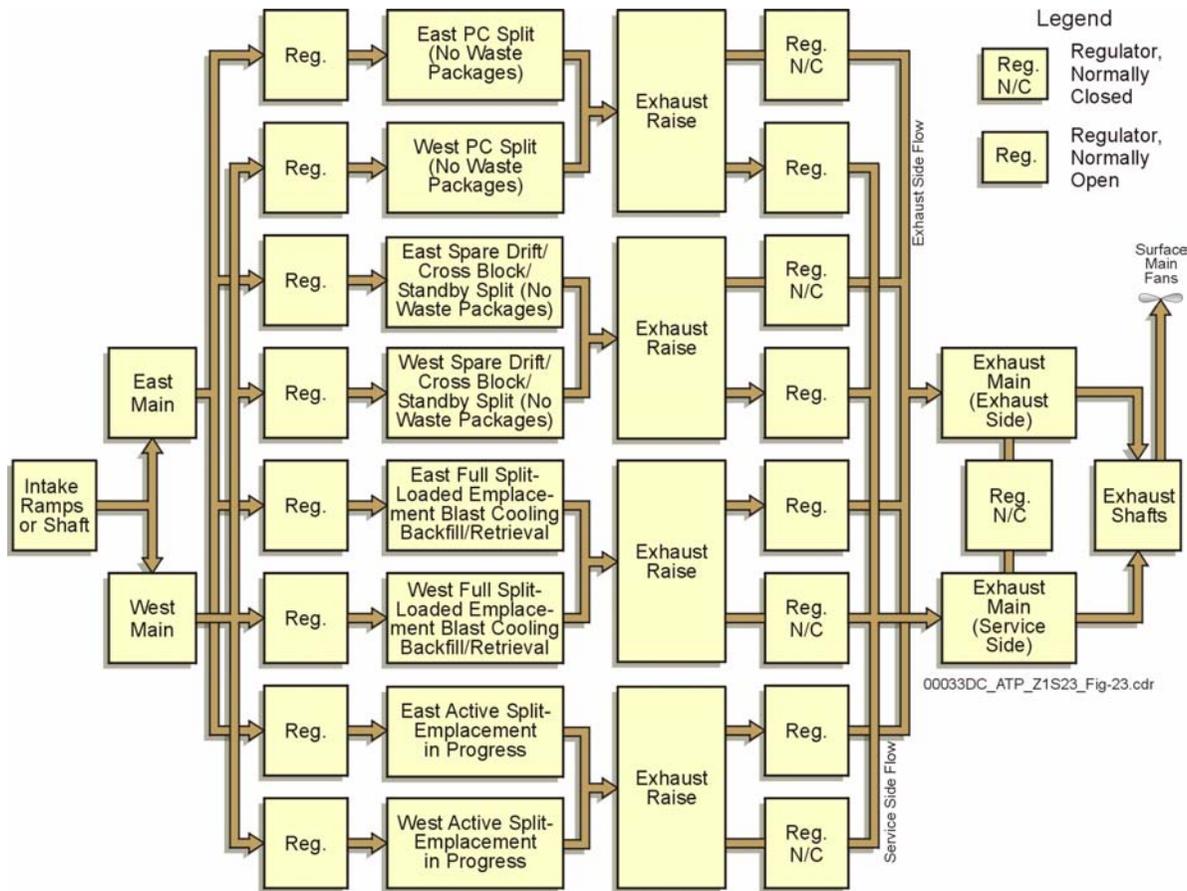
Figure 2-45.   Flow Process Diagram for the Repository Emplacement Ventilation
This flow process diagram shows how the ventilation airflow is distributed and regulated throughout the emplacement side of the repository. Loaded emplacement drifts and drifts with emplacement in process would normally exhaust into the exhaust side. Cross-block and performance confirmation drifts would normally exhaust into the service side. PC = performance confirmation. Source: CRWMS M&O 2000x, Section 6.1.

requirements would be met by providing airflow regulators at the raises and doors of the emplacement drifts, and varying the total air volume at the surface fans.

The emplacement drift design includes two emplacement doors (isolation doors), one in the east turnout and one in the west turnout. Louvers built into these doors would serve as the inlets for the ventilation air, and a gate at the exhaust raise would serve as the outlet. These devices serve as the airflow regulators for the emplacement drifts. Both regulators are needed to control the airflow in emplacement drifts, since emplacement doors would periodically be opened to receive the waste

packages. When the doors are opened, the valve at the exhaust raise would be the sole means of controlling the airflow (CRWMS M&O 2000an, Section 6.3.1).

2.3.4.3.1.3 Flow Rate Requirements for Heat Removal

The calculations described in Section 2.3.4.3 concluded that, with a ventilation flow rate of 15 m^3/s (530 ft^3/s), 71 percent of the heat would be removed after an emplacement drift had been ventilated for 50 years. This meets the requirement for 70 percent heat removal during the preclosure period (CRWMS M&O 2000af, Section 1.2.1.9).

Since each emplacement drift is divided in half (each half is called a "split"), an emplacement drift ventilation rate of 15 m^3/s (530 ft^3/s) per split was used in the ventilation analysis (CRWMS M&O 2000x, Sections 6.1 and 6.2). As air passes over the waste packages, it is heated, and it expands as a result of the heat. The equivalent ventilation rate, adjusted to account for the expansion of the air, is then calculated to be 17 m^3/s (600 ft^3/s) for an exhaust temperature of 60°C (140°F). This expanded ventilation rate is multiplied by two (two splits per emplacement drift) and by the number of emplacement drifts to obtain the total ventilation rate required for emplacement heat removal. The calculated emplacement ventilation rates are 1,870 m^3/s (66,000 ft^3/s) and 2,584 m^3/s (91,250 ft^3/s) for the base and full inventory cases. After adding incremental ventilation rates for nonemplacement drifts and rapid cooling demands for off-normal cases (such as for off-normal retrieval, as described in Section 2.3.4.6), the total repository ventilation rates for the two design cases are estimated as 2,225 m^3/s (78,580 ft^3/s) and 2,901 m^3/s (102,450 ft^3/s), respectively.

In case of ventilation system failure after the waste is emplaced, it would take a period of approximately 2 to 3 weeks for the drift wall maximum temperature limit (96°C [205°F]) to be exceeded. To maintain thermal goals, any required repairs would have to be completed and the ventilation system restarted during this period.

2.3.4.3.1.4 Sizing of Ventilation Facilities

The minimum number of ventilation shafts and fans required to provide these total ventilation rate requirements have been determined in the ventilation analysis (CRWMS M&O 2000x, Sections 6.2 and 6.7). Using two fans per shaft operating in parallel, as shown in Figure 2-46, with a combined exhaust shaft ventilation rate of 800 to 850 m^3/s (28,250 to 30,000 ft^3/s), it is estimated that at least three exhaust shafts are needed to support the 70,000-MTHM repository design. The 97,000-MTHM repository design would require at least four exhaust shafts. Each exhaust shaft is paired with an equivalent intake shaft. Therefore, the two repository design cases would require at least six

and eight ventilation shafts, respectively. The combined electric motor capacity required to operate these ventilation systems has been calculated as at least 10,000 hp and 13,000 hp, respectively.

As explained in Section 2.3.5, when the repository is undergoing concurrent development and emplacement operations, two separate ventilation systems would have to be maintained for each operational area. This separation is accomplished by placing air locks in the main drifts to physically separate the air space between the two areas. On the development side, the ventilation system works under positive pressure, with air being forced in through the development/intake shaft or the south ramp through a duct and exhausted through the south ramp. Exhausting air through the exhaust main is also possible (through the service or "cool" side of the exhaust main) if the required facilities are available. In the early stages of repository construction, the exhaust shafts on the development side are being developed, so they would not be available for exhausting air. On the emplacement side, all the required ventilation facilities for the commissioned emplacement panels are available and operational in their final configuration; the ventilation system works under negative pressure by drawing air out through the exhaust main (through the exhaust or "hot" side of the exhaust main) and from there through the exhaust shafts. This is accomplished by operating the ventilation fans installed at the exhaust shaft surface openings in an exhaust mode. Air in the emplacement side is drawn in through the intake shafts and the north ramp. The air locks prevent air from the emplacement side, which could be contaminated, from migrating to the development side. If the air locks are not completely airtight, airflow is induced from the development side to the emplacement side because of the pressure differential across the air locks (i.e., the negative pressure on the emplacement side acts as a vacuum at this interface).

The overall repository design layouts for the 70,000- and 97,000-MTHM case, as illustrated in Figures 2-38 and 2-39, show proposed locations for the intake and exhaust shafts, emplacement and nonemplacement drifts, mains, and ramps.
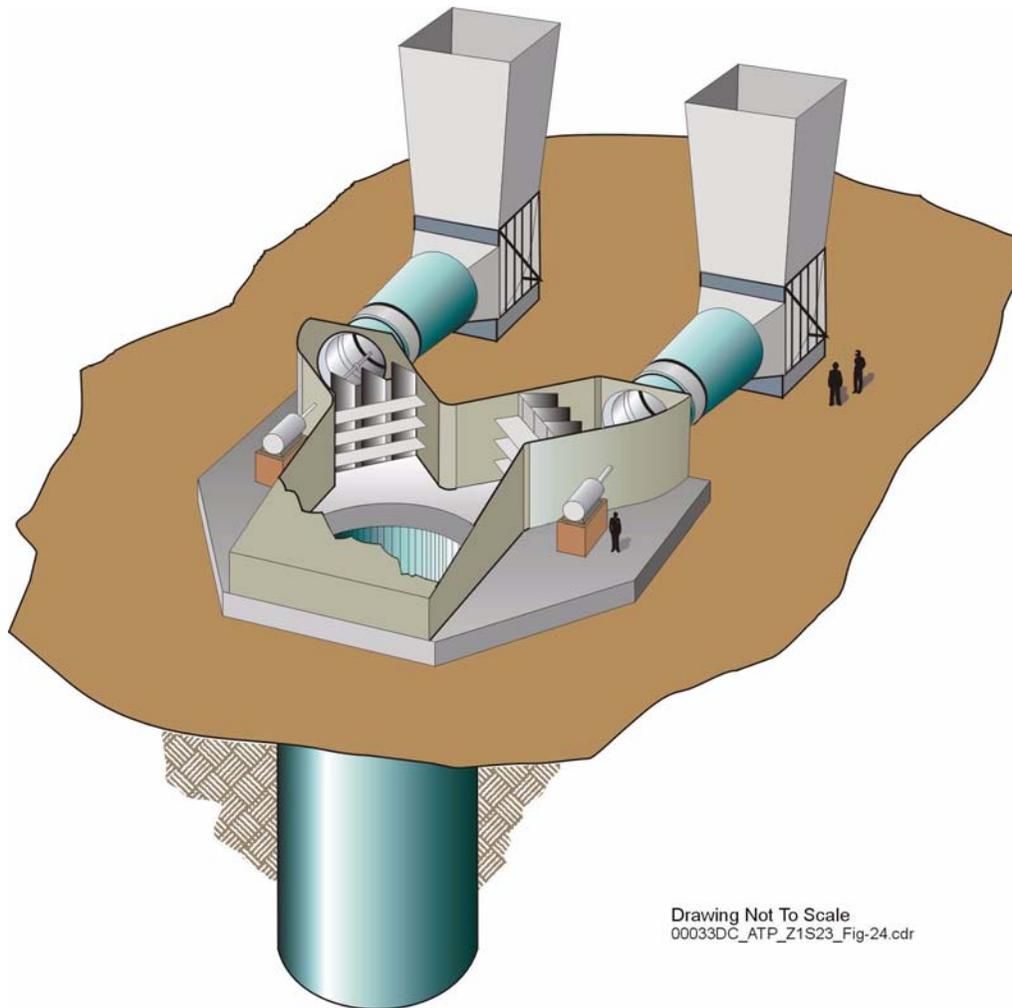
Figure 2-46.   Repository Exhaust Shaft Conceptual Dual Fan Installation
Each repository exhaust shaft would be equipped with dual fans with a combined capacity to remove up to 850 m^3/s of heated air. Source: CRWMS M&O 2000x, Section 6.2.4.

Tables 2-13 and 2-14 summarize the preliminary engineering specifications for the subsurface ventilation system.

2.3.4.4   Waste Transfer and Transport

This section describes the equipment and methods proposed for transferring and transporting waste packages from the repository surface facilities to the emplacement drifts. The equipment and methods for emplacing waste packages into emplacement drifts are discussed in Section 2.3.4.5.

2.3.4.4.1   Onsite Transportation Routes and Waste Package Handling Sequence

The onsite transportation routes from the surface facilities to the underground emplacement area will vary, depending on the emplacement drift selected as the destination for a particular waste package. Selection of the emplacement drift is based on a predefined emplacement plan that considers waste package thermal properties and other operational considerations. Generally, however, waste emplacement will occur from north to south, lagging behind emplacement drift construction, with waste packages emplaced in recently

completed drifts as they become available. Figure 2-47 shows the overall repository subsurface layout (BSC 2001d, Figure 10), to which a portion of the surface facilities and the rail line connecting the surface and subsurface facilities have been added. The repository features pertinent to the transfer of waste package operations and shown in the figure (where they are labeled by the following numbers) are:

1. The Waste Handling Building, which is part of the surface facilities and is where the waste packages would be transferred to the train that transports them underground

2. The rail line from the Waste Handling Building to the North Portal

3. The North Portal, which is one of two entrances to the repository subsurface facilities

4. The north ramp, which is an underground tunnel leading from the North Portal to the east main

5. The north ramp extension, which is the tunnel that extends from the north ramp (above the curve) toward the north to meet the east main

6. The north ramp curve, which is the section of the north ramp that turns toward the south to meet the east main drift

7. The north main, which is the loop that connects the east main to the west main at the north end of the repository block

8. The east and west mains, which are the tunnels that provide access to the ends of the emplacement drifts

9. The south main, which is the loop that connects the east main to the west main at the south end of the repository block

10. Emplacement drift turnouts, which are the curved sections of drift connecting each

end of an emplacement drift to the main drifts. The turnout approach from the main drifts is always from the south, at both the east and west sides of the repository block.

The subsequent sections describe the subsurface system components and equipment. Refer to the following figures for additional illustration of components:

*   Locomotives and the transporter: Figures 2-48, 2-49, and 2-50
*   Emplacement drift turnouts: Figure 2-49
*   Pallets: Figure 2-51
*   Waste packages: Figure 2-52
*   Emplacement gantries: Figures 2-55 and 2-56.

The subsurface facilities listed above would be used at different times during the life of the repository for waste package transfer operations. In the early years of emplacement, a typical route and sequence of events would be:

*   The waste package will be loaded onto the transporter at the Waste Handling Building.

*   The locomotives will move the loaded transporter from the Waste Handling Building to the North Portal, down the north ramp to the north ramp extension, and from there to the preselected emplacement drift turnout. The train (transporter and locomotives, as shown in Figure 2-48) will generally follow the shortest route to the emplacement drift; however, orientation of the transporter is important, depending on whether the emplacement drift is going to be reached from the east or west main. The open deck of the transporter must face the drift docking area for transfer of the waste package. The transporter and locomotives, once they enter the subsurface area in these early emplacement years, cannot rotate or change the orientation of the transporter. Therefore, the transporter must be oriented in the proper direction at the surface facilities using railroad turnouts.
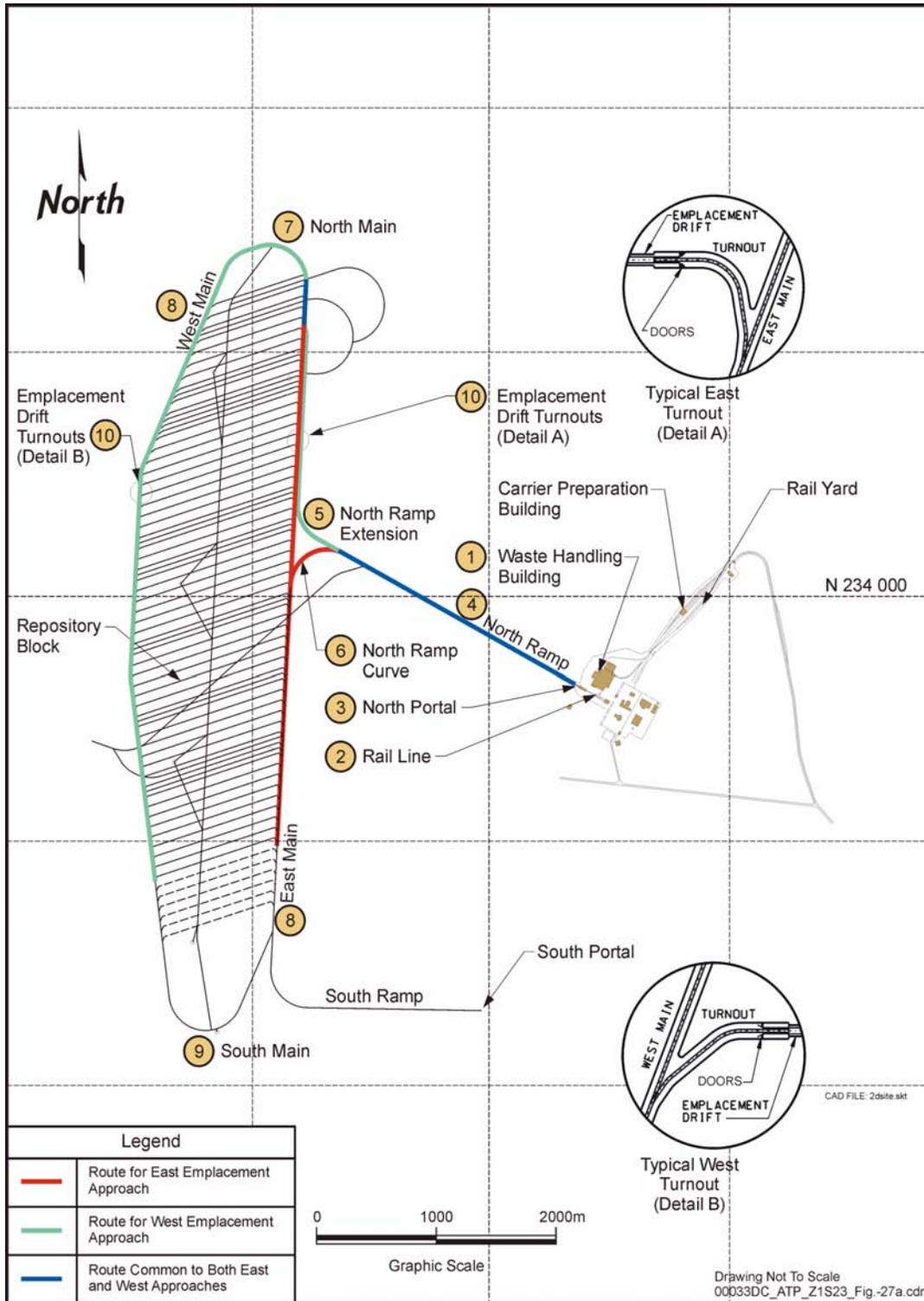
Figure 2-47.   Waste Package Emplacement Route—Key Locations

The waste package transportation train would follow a predetermined route selected according to the destination of the waste package in the underground drifts. The emplacement location of each waste package would be determined based on thermal management procedures and operational considerations, such as emplacement sequencing.

Drawing Not To Scale
00033DC_ATP_Z1S23_Fig-73.ai

Figure 2-48.   Locomotives and Waste Package Transporter Approaching the North Portal
Two electric locomotives, one on each end of the waste package transporter, would be used to move the transporter containing the waste package. This train would travel from the Waste Handling Building at the surface to the emplacement drift entrance. Travel down the gently sloping north ramp would be made safe by using dual operators and locomotives and a transporter equipped with redundant and independent brake systems. Automatic brake controls would monitor the speed of travel to minimize dependency on operators.

- If an emplacement drift will be reached from the west main, the train will get there by going around the north end.

- The return trip to the surface will follow the same route in the reverse sequence. The transporter's open deck must face the Waste Handling Building to accept another waste package. Therefore, the transporter must be properly oriented before docking at the Waste Handling Building.

A typical route from the Waste Handling Building to an emplacement drift would change as construction of the repository and emplacement activities progress. The open deck of the transporter must face the emplacement drift docking area for transfer of the waste package, and it must face the Waste Handling Building to accept another waste package. Therefore, routing takes into account the orientation of the waste package transporter. The proper orientation of the transporter is achieved by making a circular route all the way around the repository perimeter mains, or by switching the direction of the train at the surface turnouts or at locations where the north ramp and the north ramp extension meet the east main.

The waste package handling sequence is simple and would not change throughout the waste emplacement period. Waste package transportation for emplacement is always by rail. The sequence

can be summarized as follows (CRWMS M&O 2000ao, Section 6; CRWMS M&O 2000y, Section 6):

1. The waste package, loaded on an emplacement pallet, is placed on the deck of the transporter waiting at the receiving dock of the Waste Handling Building.

2. A semirigid chain mechanism pulls the pallet and waste package into the shielded enclosure of the transporter via the bed plate, which is supported on rollers.

3. The shielded enclosure doors are closed to protect the operators, and a primary locomotive pulls the loaded transporter away from the Waste Handling Building docking area.

4. During a stop at a track turnout outside the Waste Handling Building, a secondary locomotive joins the train by coupling itself to the transporter. Both locomotives are driven by operators.

5. Both locomotives, one in front and one behind, move the loaded transporter into the subsurface facilities.

6. The train stops at the main drift, near the predetermined emplacement drift turnout.

7. The locomotive at the rear of the transporter is decoupled from the transporter. The locomotive operators leave the locomotives and move to a designated location to protect themselves from radiation while the emplacement drift doors are open.

8. The locomotive controls are turned over to remote control operators in a control center at the surface, and the locomotive in front of the transporter moves the transporter into the turnout and stops before reaching the emplacement drift docking area.

9. The transporter doors are fully opened, and the emplacement drift isolation doors

are also fully opened from the surface control center.

10. The locomotive docks the transporter (see Figures 2-49 and 2-50), pushing the open deck section of the transporter completely inside the emplacement drift.

11. The semirigid chain mechanism pushes the pallet and waste package from inside the shielded transporter enclosure to the open deck area of the transporter via the bed plate, which is supported on rollers.

12. The waste package emplacement gantry, also riding on rails and remotely operated, moves from inside the emplacement drift completely over the waste package and pallet, straddling the transporter's open deck. The gantry lifts the waste package by its pallet and moves back into the drift to the waste package emplacement location.

13. The locomotive moves the transporter away from the emplacement drift docking area and stops. The transporter doors and the drift doors are completely closed.

14. The locomotive moves the transporter from the turnout to the main drift and stops to allow the second locomotive to couple to the train.

15. The operators board the locomotives, the controls are turned back to manual operation, and the train proceeds to the surface for another cycle.

16. Before docking at the Waste Handling Building, the train stops, the locomotive in front of the transporter is decoupled and moved away to a standby location, and the locomotive behind the transporter moves the transporter to the building dock.

Some of the steps in this sequence are illustrated in Figures 2-48, 2-49, and 2-50.
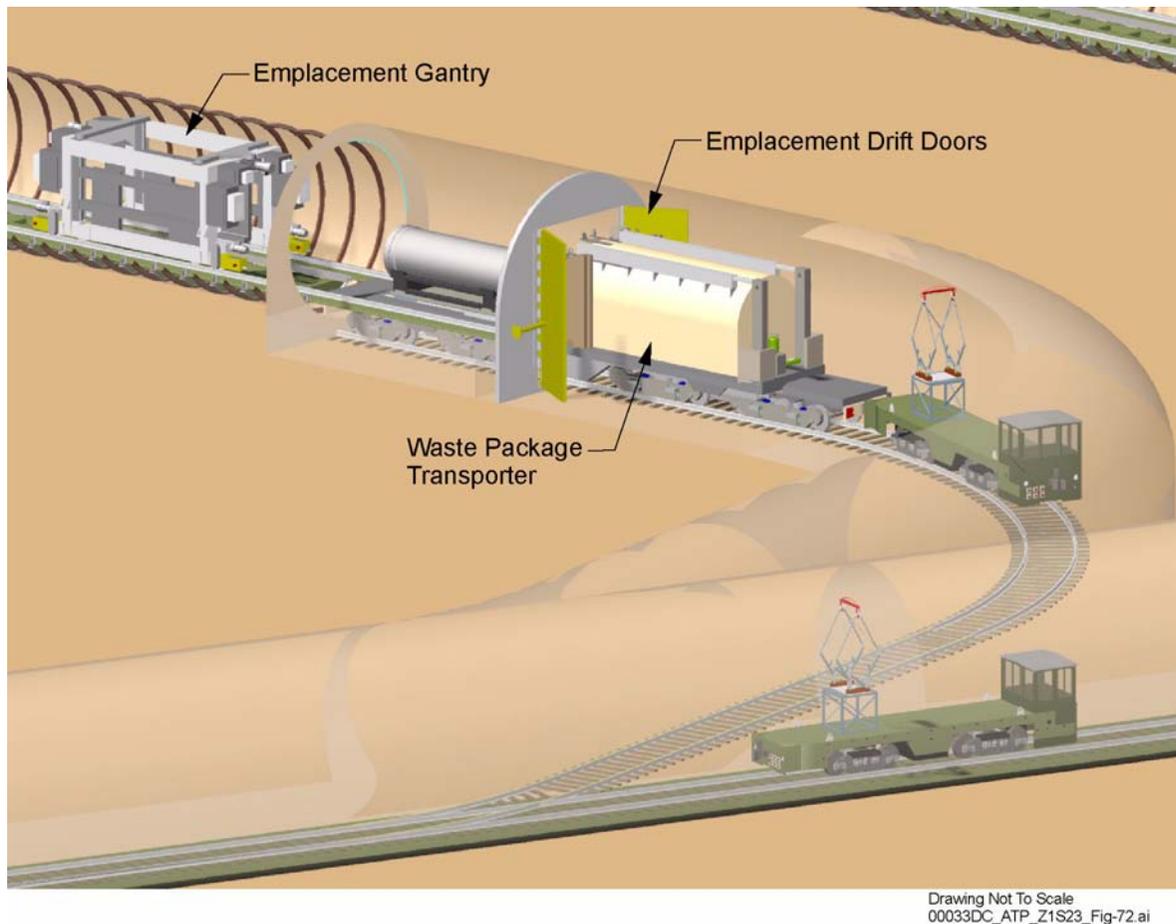
Figure 2-49.   Locomotive Operations at Emplacement Drift Turnout
This figure has been designed with see-through drift rock walls so the maneuvering of the locomotives and transporter at the emplacement drift turnouts can be better appreciated. One locomotive is decoupled from the transporter at the main drift, the operators leave the locomotives and take shelter while the drift doors open, and the other locomotive is then remotely operated for the travel into the turnout area and delivery of the waste package. This figure shows one locomotive on standby while the other locomotive moves the transporter into the turnout.

2.3.4.4.2   Waste Packages and Pallets

Section 3 provides specific information about waste package types and sizes, their characteristics, and the waste forms they contain.

Figure 2-51 provides an isometric view of an emplacement pallet. There would be two sizes of pallets: one that holds most of the waste packages, and a second, shorter version used for the 5-DHLW/DOE SNF waste package (CRWMS M&O 2000ap, Section 6.2). The emplacement pallets would be fabricated from Alloy 22 plates welded together to form the waste package

supports. Two supports would be connected by square stainless steel tubing to form the completed emplacement pallet. The supports would have a V-groove top surface to accept all waste package diameters. Emplacement pallet surfaces that contact the waste package would be Alloy 22, the same material used for the package's outer shell. The pallet would be shorter than the waste packages, so the waste package is supported on the outer package shell between the trunnion collar sleeves (see Figure 2-52). The waste package would not be mechanically attached to the pallet; it would rest on the V-groove surfaces of the pallet. The ends of the waste package extend past the ends
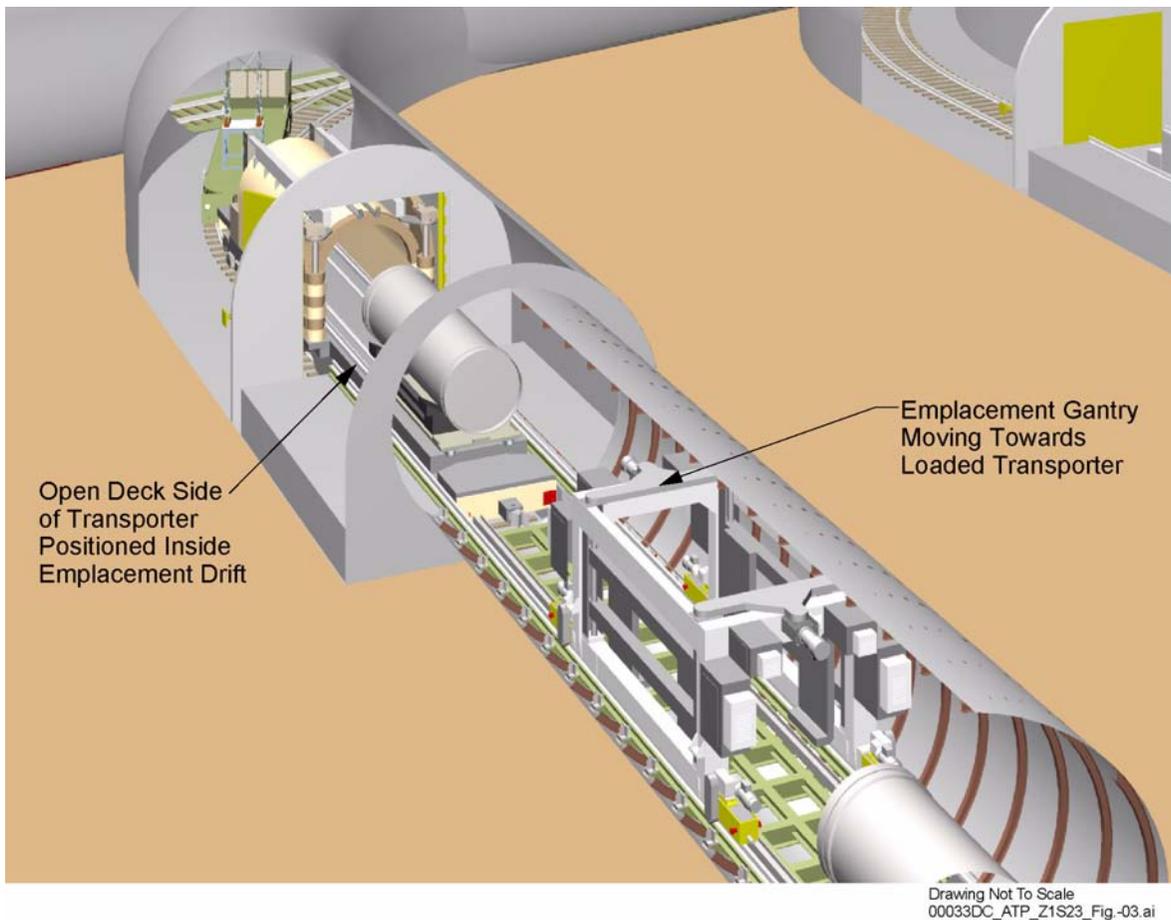
Figure 2-50. Docked Transporter with Pallet and Waste Package on Transporter's Open Deck and Emplacement Gantry Approaching the Docking Area for Pickup

As the transporter is docked into the emplacement drift entrance, the waste package resting on the pallet would be rolled out of the transporter shielded enclosure via a bed plate mounted on rollers. The emplacement gantry, waiting inside the emplacement drift, would be moved over the waste package to straddle and pick up the pallet and the waste package combination. The loaded gantry would then be moved into the drift for emplacement of the waste package and pallet.

of the emplacement pallet, which would allow the waste packages to be placed end to end, within 10 cm (4 in.) of each other, without interference from the pallets.

The emplacement pallet would be moved as one unit with the waste package from the Waste Handling Building to the emplacement drift, and would support the waste package in the drift permanently. While loaded with a waste package, the pallet would be lifted by lifting points at the support, directly under the upper stainless steel tubes, as Figure 2-52 illustrates. The pallet design meets the design requirements for structural

strength (CRWMS M&O 2000ap, Section 6.2) during lifting under the weight of the heaviest waste package, as documented in *Design Analysis for the Ex-Container Components* (CRWMS M&O 2000ap, Section 6.4). Dimensions and dimensional clearances for the pallet/waste package combination are provided in Section 2.3.4.5.

The *Emplacement Drift System Description Document* (CRWMS M&O 2000ab, Section 1.2.1.20) requires that the waste packages be retrievable for a period of up to 300 years. Therefore, the emplacement pallet must remain in a condition that can be lifted even at the end of this period. Neces-
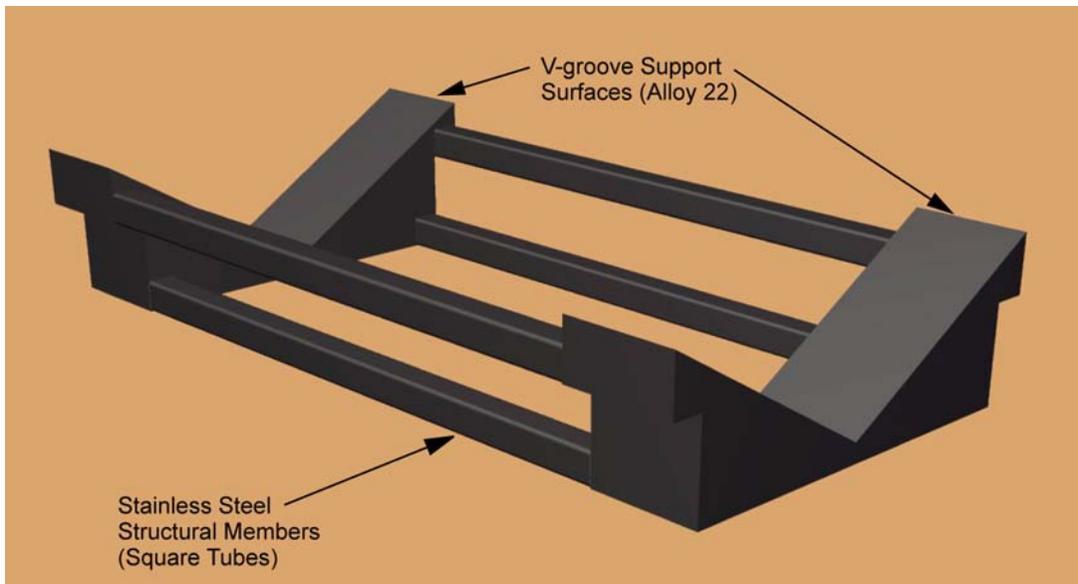
Drawing Not to Scale
00033DC_ATP_Z1S23_Fig-04.ai

Figure 2-51.   Emplacement Pallet Isometric View
This figure illustrates the configuration of the pallet. There would be two sizes, one for long packages and another for short packages. Source: CRWMS M&O 2000ap, Section 6.2.
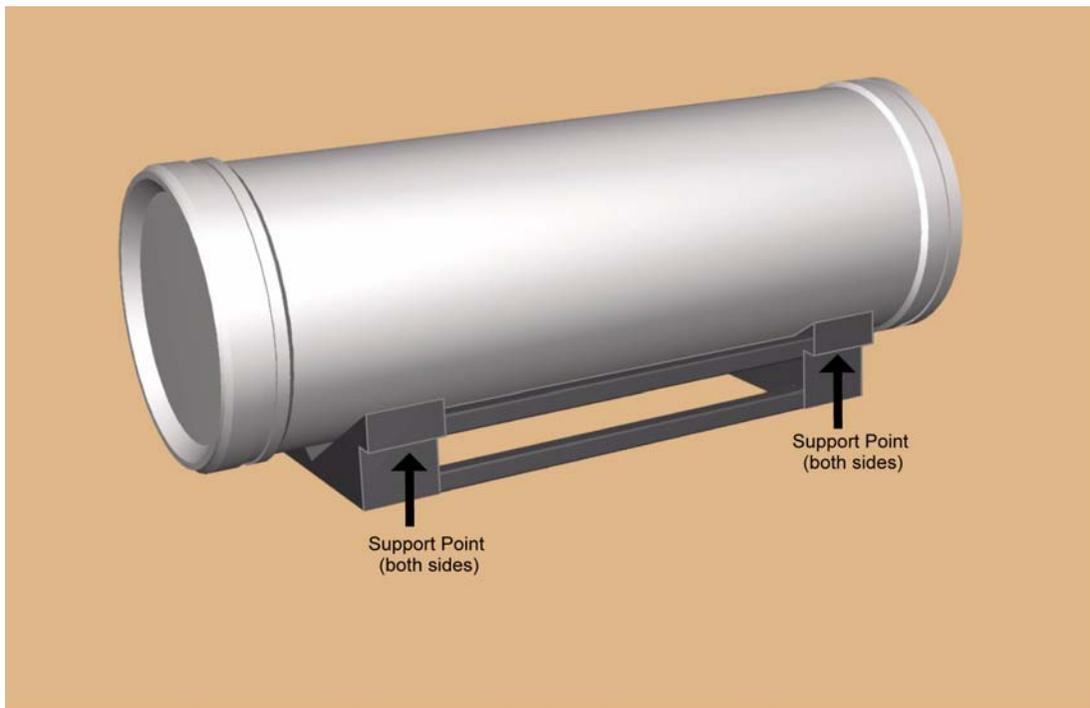
Drawing Not To Scale
00033DC_ATP_Z1S23_Fig-05.ai

Figure 2-52.   Emplacement Pallet Loaded with Waste Package
The emplacement gantry lifting arms engage the pallet at the support points illustrated in the figure, on both sides of the pallet. The gantry during the lifting or emplacement operations does not contact the waste package. The shorter length of the pallet, with respect to the length of the waste package, allows the gantry to emplace one waste package close to another without interference by the pallets. Source: CRWMS M&O 2000ap, Section 6.2.

sary calculations have been done to support this design requirement (CRWMS M&O 2000ap, Section 6.4). Seismic activity could also affect the ability of the pallet to maintain the normal waste package position. Seismic calculations would be incorporated in support of license application (CRWMS M&O 2000ap, Section 6.2).

2.3.4.4.3 Locomotives and Waste Package Transporter

2.3.4.4.3.1 Rail System

The locomotives and waste package transporter use a track gauge of 1.44 m (56.7 in.). An American Institute of Steel Construction standard crane rail of 66.9 kg/m (135 lb/yd) would be used in the north ramp, in all the main drifts and turnouts, and for the rail line leading to the Waste Handling Building (CRWMS M&O 2000ao, Sections 6 and 7). The rail system is designed to support the transportation of waste packages over the life of the system, including retrieval, for the design loads imposed on the rail by the locomotives and transporter. The bounding weight used in the calculations for a loaded transporter is 400 metric tons (CRWMS M&O 2000ao, Section 6.4.3.4). This bounding weight includes component weights listed below, in addition to an adequate design margin:

- The heaviest loaded waste package: 85 metric tons (includes 12.5-metric ton design margin)

- The pallet: 3 metric tons

- The bed plate that rolls in and out of the shielded enclosure: 9 metric tons

- Transporter shielding and fixed equipment: 164 metric tons

- The transporter flat deck car: 136 metric tons.

The trucks and wheels for the locomotives and transporter are designed to negotiate the 20-m (65.6-ft) curve radius that is the design basis of the track system. The curvature of the emplacement drift turnouts imposes this limitation. The north ramp and other main drifts will not have curvatures with less than a 305-m (1,000-ft) radius (CRWMS M&O 2000ao, Section 4.2.3.4). This limitation is not driven by the rail alignment but by the allowable curvature of the muck conveyor system used during excavation to avoid transfer stations.

The steepest railroad grade for the entire waste emplacement and transportation system is found in the north ramp. The grade is only 2.15 percent, which is well within the operational range of the proposed locomotives (CRWMS M&O 2000y, Sections 4 and 5). Rail grades in the south ramp are steeper but are not intended for waste package transportation. The south ramp would be used to support repository development activities, such as transportation of construction materials.

2.3.4.4.3.2 Locomotives

The two waste package transport locomotives would be 50-ton, 4-axle, 8-wheel units, as Figures 2-48 through 2-50 illustrate. The locomotives use electrical power (650-volt nominal direct current) supplied through an overhead catenary wire and a pantograph (a wide contactor supported by a hinged, diamond-shaped structure mounted on the roof). The rails act as the ground, completing the electrical circuit. The overhead catenary wires would be installed in all drifts and turnouts where the locomotives would operate. Each locomotive has dual direct-current electric motors rated at 170 hp each (CRWMS M&O 1998e, Section 7.3). Other functions performed by the waste transport locomotives include:

- Transporting waste packages to the surface in support of retrieval operations, if necessary

- Transporting waste packages between drifts, as needed, to support repository operations and maintenance activities

- Transporting the emplacement gantry carrier from the surface to the emplacement drift turnouts and from drift to drift

- Transporting the inspection gantry carrier from the surface to the emplacement drift turnouts and from drift to drift

- Transporting the drip shields and their emplacement gantry from the surface to the emplacement drifts.

For redundancy and added safety, two locomotives would be used any time the transporter is mobilized (except during docking operations at the Waste Handling Building and at the emplacement drift turnouts, where only one locomotive is used). One locomotive would be in front of and the other behind the transporter. This train configuration provides assurance against the possibility of a runaway transporter or adverse situations created by operator error. Section 2.3.4.4.4 discusses safety analyses of the locomotives and waste package transport operations.

The locomotives and transporter would operate within the space clearances in the north ramp, north ramp extension, and main drifts. The main drifts would be excavated to the same diameter as the ramps, 7.62 m (25 ft). Figure 2-53 is a perspective view of the locomotives and transporter in transit along one of the main drifts. This figure illustrates the size of the equipment relative to the main drift diameter.

The maximum operating speed for the locomotives and transporter has been defined as 8 km/hr (5 mph) (CRWMS M&O 2000ac, Section 1.2.2.1.2). Standard underground industry practice defines 16 km/hr (10 mph) as the maximum standard operating speed for locomotive travel within a mine environment (CRWMS M&O 2000y, Section 6.6). Therefore, the selected train operating speed for the repository is well within safety limits established by the industry.

2.3.4.4.3.3 Waste Package Transporter

The waste package transporter consists of a flat railcar 22 m (72.4 ft) in length, with a waste package shielding structure at one end and an open deck at the other end. Ancillary equipment installed on the transporter includes mechanisms for opening and closing the shielded doors; a bed plate supported on rollers; a semirigid chain mechanism; and tracks for rolling the bed plate in and out of the shielded enclosure. Figure 2-54 illustrates the transporter and its components.

This waste package transporter design with an integrated transfer deck eliminates the complexities of aligning several separate components at the waste
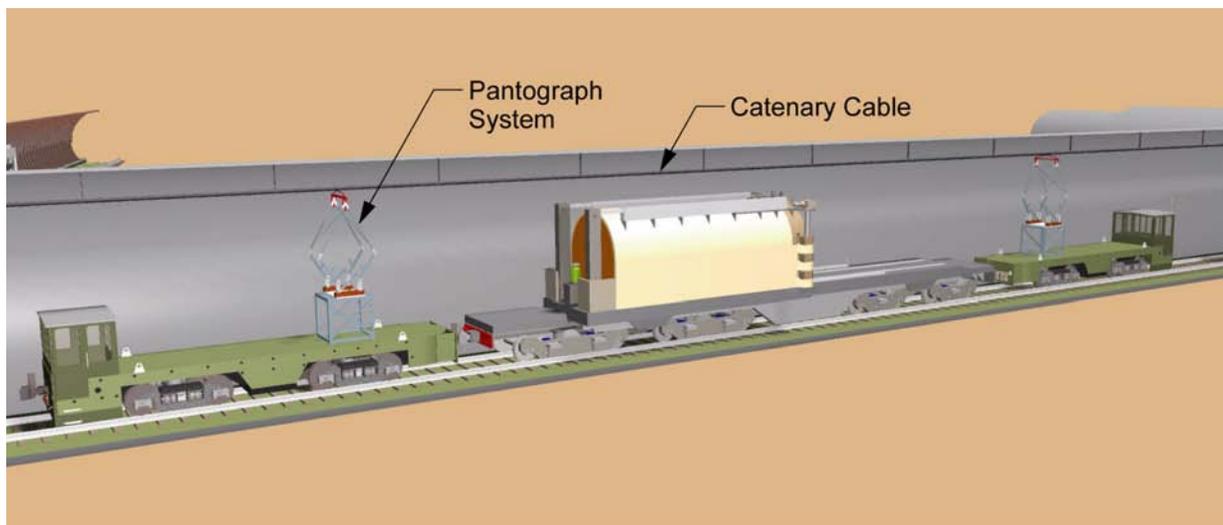
Drawing Not To Scale
00033DC_ATP_Z1S23_Fig-06.ai

Figure 2-53.   Waste Package Transportation Equipment Traveling Along Main Drift
This figure illustrates the size of the waste package transportation equipment relative to the size of the main drift. It also illustrates the catenary cable and pantograph system for continuous power supply to the locomotives.

Drawing Not To Scale
00033DC_ATP_Z1S23_Fig-07.ai
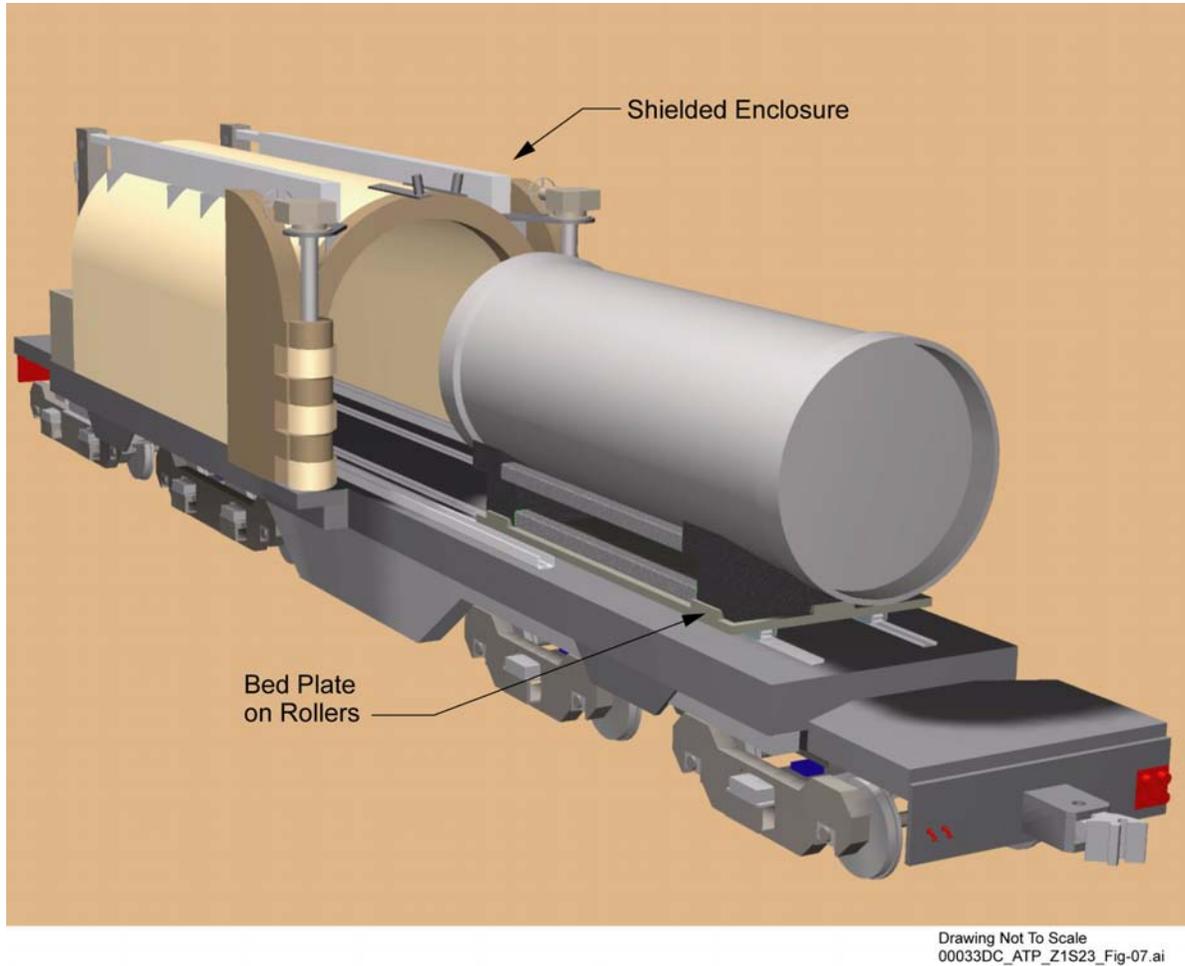
Figure 2-54.   Waste Package Transporter and Its Components
The waste package transporter would be equipped with a radiation shield enclosure and self-contained mechanical systems for opening the enclosure doors and for rolling the bed plate in and out of the enclosure. The open deck portion of the transporter extends into the emplacement drift when docked at the drift entrance. This allows the emplacement gantry to straddle the transporter and be positioned right over the loaded pallet for its pick up. The emplacement drift rail gauge would be wide enough to accommodate the transporter between rails.

package transfer locations. The integrated transporter design, with the shielded enclosure located toward one end of the flat deck car, allows the open deck area to extend adequately beyond the shielding structure, which permits the waste package and pallet to be moved together out of the enclosure and positioned for access by the emplacement gantry. The waste package transporter would be docked between the rails of the emplacement gantry in the emplacement drift, enabling the emplacement gantry to straddle the transfer deck to pick up the waste package and pallet.

A bed plate sized to contain and restrain the pallet has four low-profile, heavy-duty rollers affixed to its underside to aid movement of the waste package out of the shielded enclosure. After the emplacement gantry engages the pallet and raises the loaded pallet high enough to clear the bed plate, the bed plate would be retracted back into the shielded enclosure. This transporter design eliminates the need for precise alignment of tracks between the transporter and the emplacement drift, and it diminishes the possibilities for waste package mishandling and dropping incidents (CRWMS M&O 2000ao, Section 6.4). The gantry lifting

screw limits the maximum height the waste package can be lifted to less than 1 m above the deck of the transporter (CRWMS M&O 2000z, Section 6.3). This maximum lifting height limit is much less than the 2-m (6.6-ft) vertical lift limit specified for protection of the waste package (CRWMS M&O 2000ac, Section 1.2.2.1.3). To eliminate the risk of dropping a waste package in the docking area, the transporter remains in the area until the loaded gantry moves back into the emplacement drift.

Design calculations for the transporter (CRWMS M&O 2000ao, Section 6.4) were done for various static and dynamic loading conditions, which resulted in the selection of industry standard 320 BHN (Brinnel hardness number) wheels and rails. The wheels have a diameter of 762 mm (30 in.). The 320 BHN wheels can be used by equipping the transporter with dual 3-axle trucks for the rear and dual 2-axle trucks for the front.

The bed plate consists of a thick steel plate that distributes the waste package and pallet load through rollers (attached to the bottom of the bed plate) to the transporter. The design uses reliable, low-profile unitary rollers. The roller assembly runs on an inverted channel installed on the deck of the transporter. The channel safely and reliably guides the bed plate rollers to a position centered with the emplacement gantry for pickup. The bed plate would be attached to the ends of two gear-driven semirigid chains that run in floor-mounted guides on each side of and parallel to the bed plate as it rests on the transporter. The chain guides extend from inside the shielded enclosure along the transfer deck. The semirigid chain attached to the bed plate pushes the bed plate out of, and draws it back into, the shielded transporter enclosure. The bed plate incorporates restraints and spacers to immobilize the waste package, pallet, and bed plate inside the transporter for safe transit to the emplacement drift (CRWMS M&O 2000ao, Section 6.4).

The shielded enclosure is designed to meet the radiation dose rate limit of 100 mrem/hr on the transporter surface (CRWMS M&O 2000ao, Section 6.7.3), which is accomplished with a very thick A 516 steel enclosure wall. The steel wall

provides sufficient shielding for nonaccessible areas (i.e., the deck floor below the shielded enclosure) during normal operations. In addition to the A 516 steel, the shielded enclosure has a borated polyethylene layer for neutron shielding (CRWMS M&O 2000ao, Section 6.7).

2.3.4.4.4 Waste Transfer and Transport Safety Analyses

A safety analysis (CRWMS M&O 2000y) was performed for the waste package transport system. The analysis addressed scenarios for a runaway train and derailment, tipover determinations, effectiveness of impact limiters, and mitigation of uncontrolled descents. During the development of the analysis, several safety features were identified and evaluated, resulting in the system components described in the discussions that follow.

2.3.4.4.4.1 Transporter Safety Features

The primary brake system for the transporter consists of an automatic, fail-safe tread-brake system activated by a decrease in air pressure. The application of a brake shoe against the tread of a rail wheel is called tread braking. Although most commercial railcar brake systems are activated by a decrease in air pressure, the actual tread brake application is performed with compressed air. A pneumatic control valve responds to signals sent by the locomotive operator; these signals are in the form of changes in air pressure within the main air line, or trainline. The trainline is the physical air connection from the locomotive to each railcar air brake system. Compressed air is supplied by the air compressor on the locomotive and stored in air reservoirs on each railcar. When the air pressure in the trainline is reduced, the control valve on each railcar mechanically senses the pressure drop and delivers compressed air from the railcar reservoir to the brake cylinder(s). The amount of air sent to the brakes is proportional to the drop in brake pipe pressure.

Although commercial railcar brake systems are fail-safe and proven in the railroad industry, a simpler brake system is envisioned for the transporter. This brake system uses a spring-acting/air-release brake cylinder to provide the stopping

force. Powerful compression springs within the cylinder apply the required brake shoe force against the wheel, rather than using air pressure from the reservoir. With this system, compressed air is used to collapse the springs, thereby releasing the brake shoe from the transporter wheels. As air pressure decreases in the trainline, brake shoe force is proportionally applied by the springs. This brake system eliminates the need for the waste package transporter to have a compressed air reservoir and control valve, resulting in a simpler fail-safe brake system (CRWMS M&O 2000y, Section 6.1).

The secondary, or redundant, brake system for the transporter is a hydraulically applied disk brake system. This brake system comprises a disk and a caliper mounted on each axle of the transporter trucks. The calipers are hydraulically applied and spring released, which is not a fail-safe configuration. Pressure is applied to the brake calipers through a hydraulic connection to the locomotive hydraulic system.

2.3.4.4.4.2 Locomotive Safety Systems

The locomotive braking system consists of four brake systems: tread, disk, parking, and dynamic brakes. The tread and disk brakes can each stop the train independently. The parking brakes hold the train in position once stopped. The dynamic braking systems regulate the train speed as it descends the north ramp but would not be used for a complete stop.

The locomotive tread brakes are automatic, fail-safe air brakes, similar to the transporter tread brakes. Like the transporter brakes, the stopping force of the locomotive tread brakes is provided by powerful compression springs. Air pressure is used to collapse the springs, thereby releasing the brake shoes from the locomotive wheels.

The disk brakes are the backup, redundant brake system installed within the transmissions of the locomotive. The disk brake calipers are hydraulically applied and spring released, which is not a fail-safe configuration.

The locomotive parking brake is a spring-applied, manual-release disk brake. The brake consists of

an independent caliper mounted to operate on the same disk as the redundant disk brake system.

Dynamic braking uses the locomotive direct-current drive motors to typically control train speeds on steep grades. The locomotive wheels are allowed to transfer mechanical power opposite the moving direction by back-driving the transmissions and drive motors. Extended-range dynamic braking may be included on the locomotive, allowing it to be used at speeds as low as 4.8 km/hr (3 mph).

2.3.4.4.4.3 Summary of Results of Safety Evaluations

From the maximum operating speed of 8 km/hr (5 mph), the transporter and the two locomotives will take 13.5 m (44.3 ft) to stop at a 13 percent brake ratio. This is a ratio, expressed as a percentage, of the total net brake shoe force applied at the wheel tread to the rated gross weight of the railcar. From the same maximum operating speed of 8 km/hr (5 mph), a full emergency brake application (60 percent brake ratio) will stop the transporter and the two locomotives in 1.58 m (5.18 ft) (CRWMS M&O 2000y, Section 6.3.3).

The analysis also showed that the impact force resulting from a collision at a maximum transporter operating speed of 8 km/hr (5 mph) is less severe than the impact from a 2-m (6.6-ft) design basis waste package drop.

Calculations of a hypothetical runaway scenario down the north ramp, with the runaway train (locomotives and transporter) reaching a maximum velocity of 31.9 m/s (71.4 mph), concluded that the equivalent stopping distances are 2,518 m (8,260 ft) at a 13 percent brake ratio, and 321 m (1,054 ft) with the emergency brake application (60 percent brake ratio) (CRWMS M&O 2000y, Section 6.3.3).

Calculations of various runaway scenarios show that the runaway velocity is above the tipover speed. Therefore, it is possible for the loaded waste package transporter to partially tip over during the defined runaway scenario (CRWMS M&O 2000y, Section 6.4.3). Impact limiters are devices attached

to the waste package transporter that would help absorb impact energy in the event of a collision. In a worst-case runaway condition, the transporter would most likely tip over on the north ramp curve. Because of the size of the transporter relative to the drift diameter, the transporter would not tip over completely; the transporter would impact the wall above the deck level. Therefore, impact limiters installed at the transporter deck level and on the ends would provide negligible impact protection for the tipover condition (CRWMS M&O 2000y, Section 6.5). The analysis suggests that additional impact protection could be provided by incorporating an energy-absorbing layer on the inside of the radiological shield of the transporter (CRWMS M&O 2000y, Section 6.5), although it would increase the overall size of the shielding. Such an energy-absorbing layer, which would present design and operational complexities, will be evaluated further.

An analysis for derailment showed that a wheel-climb derailment was only possible with severely worn rails under full runaway conditions (CRWMS M&O 2000y, Section 7). This condition would be prevented by inspection and replacement of the rails before they become severely worn. However, other types of derailment, such as those that could result from rail failure, would still be possible. Periodic inspection and maintenance would help prevent rail failure occurrences. Following derailment, the transporter would hit the wall at the north ramp curve on a course almost parallel to the wall. For this lateral impact, the impact protection from an impact limiter installed on the front of the transporter deck would be negligible because the impact limiter would not make contact with the drift wall. The top of the transporter would make contact with the drift wall instead (CRWMS M&O 2000y, Section 6.5).

To limit the potential for a runaway condition, additional controls (i.e., magnetic track brakes and car retarders) are being evaluated to mitigate an uncontrolled descent. In addition, automatic controls are being evaluated. The magnetic track brakes can provide railcar deceleration rates on the order of 2.46 to 3.58 m/s^2 (8.1 to 11.7 ft/s^2). Car retarders, when used, are incorporated into the rail system. The major types of retarders used are the wheel clamp and the hydraulic piston-type retarders. The former produces friction by clamping to both sides of each rail wheel, while the latter are passive energy absorption systems similar in function to a shock absorber.

For the safety classification of structures, systems, and components, an event sequence impact is considered in the design if its estimated frequency of occurrence is 1×10^{-6}/yr or greater. The safety analysis concluded that the occurrence of a runaway transporter event could be reduced to a frequency less than 1×10^{-6}/yr. Therefore, a runaway event could be screened out as a beyond Category 1 or Category 2 event sequence. The event frequency is reduced to less than 1×10^{-6}/yr by enhancing the design features of the brake control and communications system.

A primary reason for enhancing the onboard systems is to reduce the reliance on human operators to respond properly to a runaway event. These design features include an electronic interlock that prevents the operator from starting the train down the north ramp without having dynamic brakes engaged; an alarm to alert the operators when the speed of descent is too high; and an automatic application of tread brakes to maintain speed within the normal operating range (CRWMS M&O 2000y, Section 7.1). These design features imply greater reliance on the brake control and communications system, thus creating the need for redundancy and diversity among brake systems. Additionally, a reliability analysis was performed on a conceptual rail-mounted speed retarder system. Such a system is based on proven technology and appears to be promising as a different means of controlling the train's speed of descent that is redundant with the onboard brake systems (CRWMS M&O 2000y, Sections 6.7 and 6.8.3).

2.3.4.5 Waste Package Emplacement

As described in the previous section, waste package emplacement is a remotely controlled operation directed from a control center at the surface facilities. The environment inside the emplacement drifts, due to high temperatures and radiation, makes it unsafe for a person to enter the drift when waste packages are present. If equip-

ment recovery or drift maintenance becomes necessary, human entry would be possible only after all the waste packages have been temporarily relocated to a different drift and after increased ventilation has lowered the ambient temperature of the drift to below 50°C (122°F).

Emplacement of waste packages for the 70,000-MTHM base case has been estimated to take a total of 24 years (YMP 2000a, Table 3-2). The period of time for emplacement of the 97,000-MTHM full inventory case has not been estimated, and there are different emplacement options. The ultimate emplacement duration will depend on what strategy is adopted for codisposal of DOE spent nuclear fuel and high-level radioactive waste. The maximum emplacement rate is expected to be 605 waste packages per year (CRWMS M&O 2000ac, Section 2.2.2.4); therefore, the capability is available to emplace 97,000 MTHM of full inventory waste in less than 30 years.

Tables 2-15 through 2-19 summarize preliminary engineering specifications for waste package transportation and emplacement system components.

Table 2-15. Summary of Waste Emplacement Track Specifications

Item	Detail
Rail type	AISC Standard Crane Rail of 320 standard BHN
Rail weight	66.9 kg/m (135 lb/yd)
Track gauge	2.95 m
Rail support beam	Two W8x67
Transverse rail and pallet support beam	One W12x65 per 1,500 mm spacing
Longitudinal pallet support beam	Three W12x65
Guide beam	Two W6
Stiffener bracket	Not specified
Design load	400 metric tons
Turn radius of curvature • Emplacement drift turnouts • North ramp and main drifts	 20 m 305 m
Maximum track grade	2.15 percent

NOTE: AISC = American Institute of Steel Construction.

Table 2-16. Summary Description of Waste Package Transporter Components

Item	Detail
Structure	Flat railcar with partial overhead enclosure
Undercarriage	3-axle rear trucks, 2-axle front trucks, 762-mm diameter wheels of 320 standard BHN
Dimensions • Height • Width • Length • Weight	 4.3 m 2.9 m 22 m 400 metric tons maximum when loaded
Waste package pallet	Alloy 22 welded plates for waste package support, Stainless Steel Type 316L stainless steel square tube supports
Shielding	Standard Steel Type A 516 steel enclosure, 171.5 mm radial wall thickness, 196.9 mm axial wall thickness; borated polyethylene layer

Table 2-17. Summary of Waste Emplacement Locomotive Specifications

Item	Detail
Unit weight	50 tons
Maximum speed	8 km/hr (5 mph)
Undercarriage	4 axle, 8 wheel
Drive	Dual electric 170 hp motors
Power	Electric 650 volt direct current
Power supply	Overhead catenary wire, pantograph, and ground rails

Table 2-18. Summary of Bounding Weights of Waste Package Transporter Components

Component	Mass (metric tons)
Loaded transporter maximum weight	400
Transporter shielding	164
Flat car	136
Largest waste package (includes design margin)	85
Bed plate	9
Waste package pallet	3

Table 2-19. Design Basis Summary of Waste Package Transporter Performance

Item	Detail
Waste emplacement period	24 years
Operational period during which retrieval could be initiated	Any time from the start of emplacement up to approximately 100 years, with the potential for retrieval to start during an extended operational period of 300 years
Duration of retrieval planning and operations	Up to 34 years
Number of waste packages	11,750
Maximum emplacement rate of waste packages	605 per year
Maximum gantry speed	2.7 km/hr

Transporter braking
• Deceleration rate
• Stopping distance
  - 8 km/hr speed at 13% braking
  - 8 km/hr speed at 60% braking
	2.46 to 3.58 m/s^2
	
	13.2 m
	1.58 m

Radiation dose limit on transporter surface	100 mrem/hr
Maximum lifting height of waste package	1 m

NOTE: All numbers are for the base case waste package inventory (CRWMS M&O 2000h, Table 1).

2.3.4.5.1   Emplacement Gantry

The gantry designed to handle the waste package and pallet is called the bottom/side lift gantry (CRWMS M&O 2000z). The gantry illustrated in Figure 2-55 rides on 135 lb/yd rails with a rail centerline to rail centerline distance of 2.95 m (8.2 ft). The gantry has been designed so it will not drop a waste package or become inoperable as a result of a Category 1 earthquake event.

The gantry is designed to operate in the high-temperature, high-radiation environment inside the emplacement drifts. Its operation only involves moving forward and backward on the rails and moving the lifting arms up and down. This simple operation reduces the complexity of the gantry's mechanical, electrical, and control systems, which makes the gantry inherently reliable. The incorporation of high-quality hardware and software components further enhances control system reliability. These components mainly include redundant programmable control computers,

instruments, and communications equipment. Fault-tolerant operation is ensured by physically separating the redundant components, providing backup electrical power and data communication systems, and employing diverse technologies that will not be susceptible to similar failures from a single cause. Shielded and insulated cabinets protect the heat- and radiation-sensitive instruments, and solid-state air conditioning units regulate the temperature. Built-in fire detection would automatically activate fire suppression systems if an onboard fire is detected (CRWMS M&O 2000z, Section 6.6.6). At this point, the gantry would be retrieved from the drift for repairs.

The primary source of electrical power for the gantry is an electrified third rail (conductor bar) system. The vehicle would have redundant power pickup mechanisms to ensure a reliable and continuous connection to the source of power. The gantry would have an emergency backup power system (onboard rechargeable storage batteries) with enough power to lower and release the load and return to the drift entrance. The locomotion system would have four independent direct-current drive motors, with one motor at each of the wheel assemblies. The maximum operating speed that the gantry can travel when carrying an 88-metric ton load waste package and pallet is limited to 2.7 km/hr (150 ft/min or 1.7 mph). The gantry would have independent fail-safe braking systems (a primary system and an emergency system). In the event of a power or communication loss, or of a vehicle control system malfunction, the braking systems would engage and bring the gantry to a stop (CRWMS M&O 2000z, Section 6.6.2). At this point, the gantry would be retrieved from the drift for repair.

The video system of the gantry would provide operators at the remote control center with real-time visual information about the operating environment and vehicle performance. This system would consist of several onboard high-resolution, articulated, closed-circuit television cameras and a series of high-intensity lights. Thermal and radiological sensing instruments would provide the remote control center with real-time status on these two environmental conditions in the emplacement drift (CRWMS M&O 2000z, Section 6.6.5).

Electric Motors
(Total of Four)
Provide Power to
Gantry Wheels

Lifting Arms that Engage Pallet
(Right-Side Arms Are Not Visible)

Drawing Not To Scale
00033DC_ATP_Z1S23_Fig-08.ai
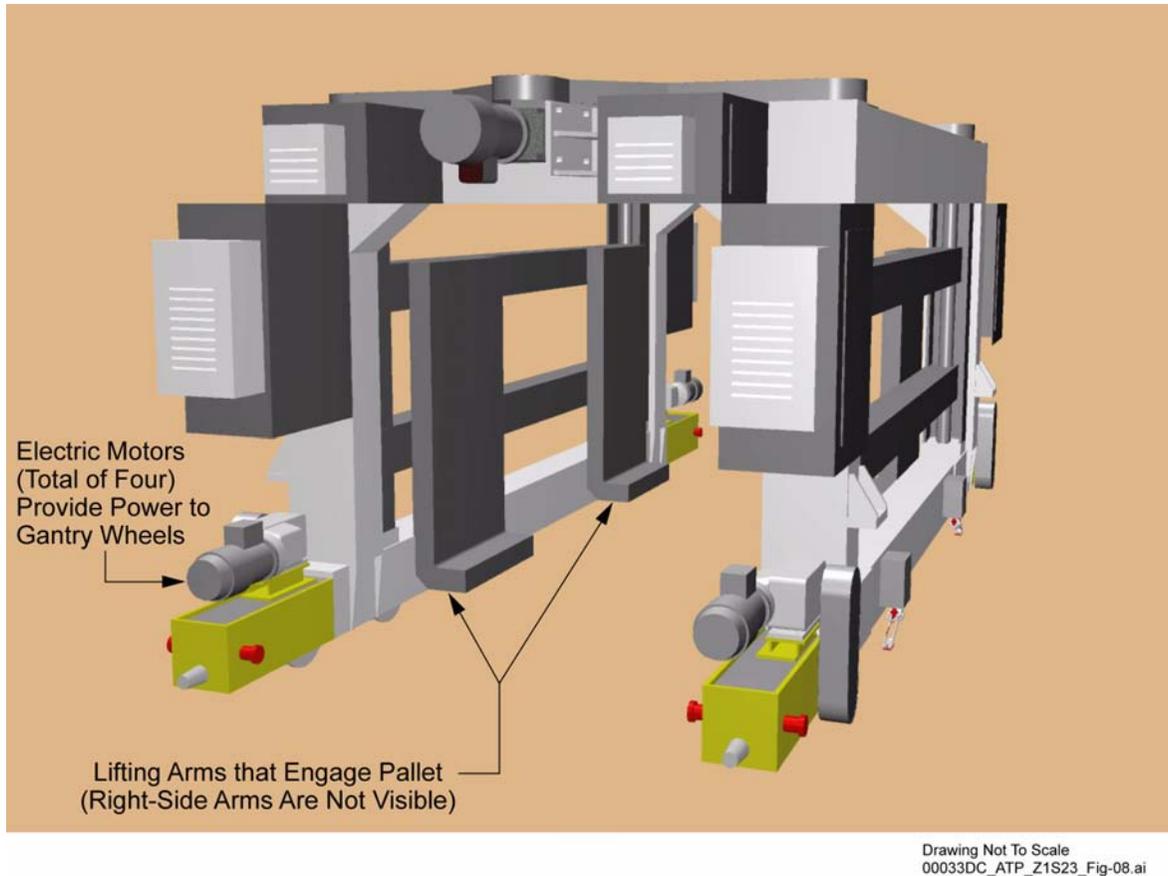
Figure 2-55.   Bottom/Side Lift Emplacement Gantry—Perspective View
The emplacement gantry has four lifting arms that travel only in the vertical directions. Their vertical displacement is limited to one meter. Their sole function is to pick up the loaded pallet and gently place it on the drift floor. The gantry would be electric and remotely operated and equipped with data gathering and transmitting instrumentation, control computers, high-resolution television cameras and lights, and fire detection and suppression systems. Source: Modified from CRWMS M&O 2000z, Figures 7 through 9.

2.3.4.5.2   Gantry Operation

As discussed in Section 2.3.4.4, the emplacement gantry would be inside the drift when the loaded transporter is docked at the drift entrance for delivery of a waste package.

The rail in the emplacement drifts upon which the gantry would travel is not continuous from the east to the west end. A ventilation access (raise), which connects the drift to the exhaust main below, inter-rupts the gantry rail. The raise is located approximately at the midpoint of most drifts (Figure 2-44). Because the gantry cannot lift a pallet and waste package over a previously emplaced waste package, emplacement in each half of the drift starts at the raise, where the rail

ends. Emplacement progresses from the raise toward the drift entrance until that half of the drift is full.

Before moving the gantry, the vertical positions of the lifting arms (Figure 2-55) would be adjusted so that their horizontal extensions can slip underneath the projecting parts of the pallet structure as the gantry moves over the unit. The gantry would then raise its arms to engage the pallet structure such that the pallet and its accompanying waste package are lifted vertically off the transporter (or off the drift invert). During normal operations, the gantry would lift a waste package and pallet unit approxi-mately 20 cm (8 in.) off the floor. The gantry would keep the waste package and pallet at that elevation when moving. After raising the loaded

pallet to the desired elevation, the gantry would move the waste package to its emplacement location in the drift. It would lower the waste package and pallet until the pallet rests directly on the drift invert. The gantry would then move slowly away from the emplaced waste package until the arms are clear. Returning to a normal speed, the gantry would proceed to the drift entrance to await the arrival of another loaded transporter (CRWMS M&O 2000z, Section 6.1).

The bottom/side lift gantry is designed to handle a wide range of waste package sizes without having to adjust the horizontal spacing of the arms. Lack of a need for such adjustments reduces the complexity of mechanical components, thereby increasing their reliability. The lifting arms never contact the waste package, thus eliminating the possibility of waste package damage by contact. This gantry concept also allows waste packages to be emplaced 10 cm (4 in.) apart, end to end (CRWMS M&O 2000z, Sections 4.2.8 and 6.1).

The emplacement gantry is designed to operate within the clearances inside the 5.5-m (18-ft) diameter emplacement drifts. Figure 2-56 shows a perspective view of the gantry inside the emplacement drift.

The emplacement gantry would not be left inside an emplacement drift for extended idle periods because of the potential detrimental effects of heat and radiation on the gantry sensors and instruments. An emplacement gantry carrier, which is a

Drawing Not To Scale
00033DC_ATP_Z1S23_Fig-09.ai
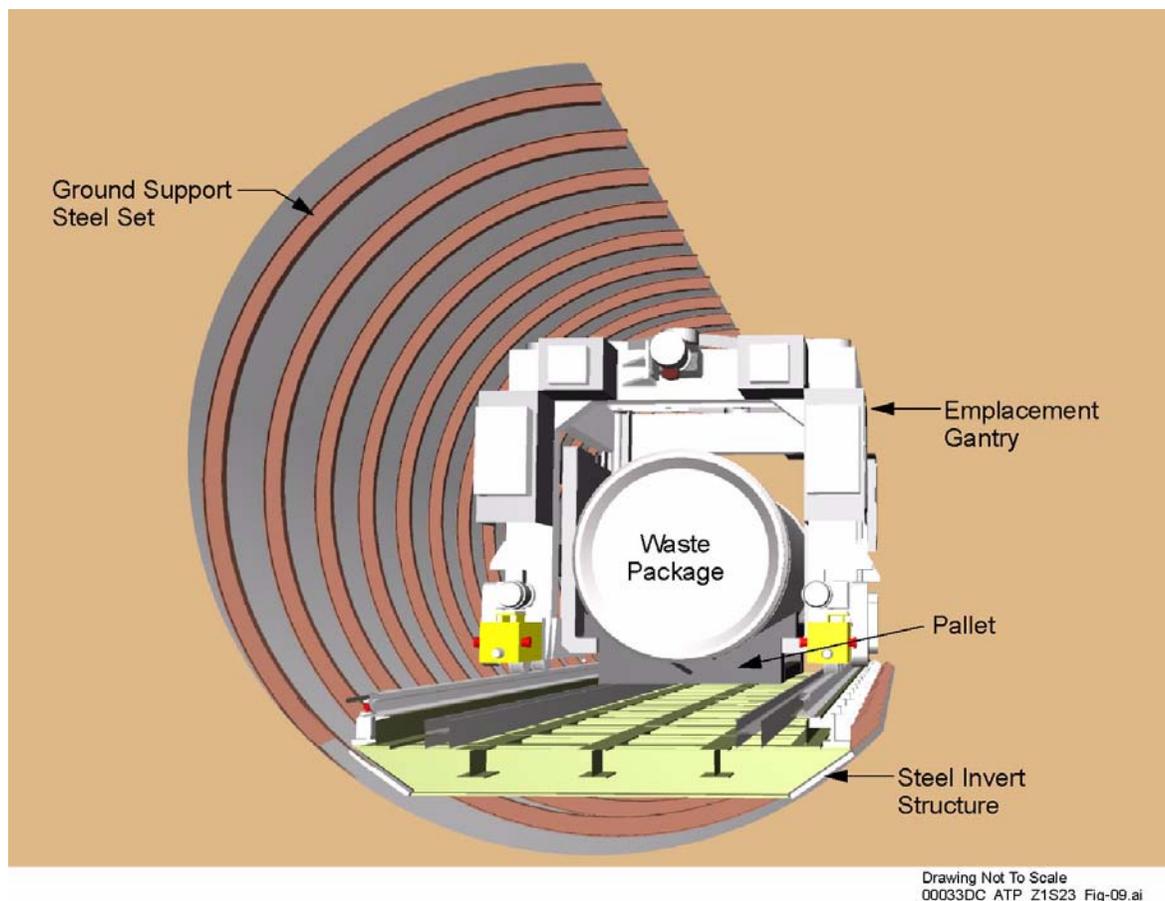
Figure 2-56.   Bottom/Side Lift Emplacement Gantry—End View within Emplacement Drift
This figure illustrates the emplacement gantry transporting a loaded pallet inside an emplacement drift. Also illustrated is the steel invert section that constitutes the "floor" or emplacement surface of the drift. Relative size of the gantry with respect to the emplacement drift diameter can also be appreciated in this figure. Source: Adapted from CRWMS M&O 2000z, Figure 10.

flatbed railcar with on-deck rail tracks that mate the drift tracks, moves the gantry from drift to drift, or to a staging area.

2.3.4.6   Retrieval

2.3.4.6.1   Requirements for Retrievability

Retrievability at a high-level radioactive waste repository is a requirement mandated by the NWPA (42 U.S.C. 10101 et seq.). The NWPA, as amended in 1987, provides the reasons for which retrievability may be exercised. Section 122 of the NWPA (42 U.S.C. 10142) states that any repository to be approved as a result of the NWPA shall be designed and constructed to permit the retrieval of any or all spent nuclear fuel placed in such a repository. It also states that such retrieval should take place during an appropriate period of operation of the facility. Retrievability is justified under the NWPA for reasons that include public health and safety, environmental concerns, and recovery of the economically valuable contents of spent nuclear fuel.

The NRC regulation, 10 CFR Part 63 (66 FR 55732), establishes a minimum period during which retrieval must be possible. Waste must be retrievable on a reasonable schedule, starting anytime up to 50 years after the start of emplacement. The DOE has developed a schedule that would permit retrieval in about the same time taken for construction of the Geologic Repository Operations Area and the emplacement of wastes. The design described in this report allows for a preemplacement construction period of 5 years and a period of repository operations and performance confirmation testing of 50 years, including emplacement. It should be noted that the performance confirmation testing period started during the site characterization and would continue until closure of the repository. Retrieval, if needed, would require up to 34 additional years, which includes 10 years for planning, engineering, and procurement and 24 years for retrieval (CRWMS M&O 1998f).

The regulatory requirements for retrievability help define three basic criteria for the design of the subsurface facilities.

Robust Infrastructure—The preclosure period for the repository would vary, depending on decisions and licensing issues that would evolve with time. Current estimates for closure include scenarios for no retrieval action, exercise of the retrieval option, and an extended preclosure monitoring period.

- If no retrieval is deemed necessary, closure activities could be initiated as early as 60 years after waste emplacement begins. This period includes 50 years for emplacement and monitoring, and 10 years for decommissioning, sealing, and closure.

- If the retrieval option is exercised, and assuming that all waste packages are retrieved, the preclosure period increases to 99 years (rounded to 100). This includes pre-emplacement construction, emplacement, monitoring, planning, retrieval, decommissioning, sealing, and closure.

- The requirements documents reflect criteria for an extended monitoring of the repository that would extend the preclosure period to as long as 300 years after the last waste package is emplaced. The decision to close the repository would be made by future generations, based on considerations that cannot be anticipated at this time, such as the availability of future treatment technology, the reuse of the nuclear fuel, or the realization of a better disposal alternative.

Because the potential repository may remain open for as long as 300 years, its structures must last that long with manageable maintenance in an environment with high radiation and high temperature. This requirement applies to excavations, ground support, permanent mechanical components, transportation, ventilation, and other utilities.

Selective Retrieval—Maintaining the ability to selectively retrieve emplaced waste packages affects the basic repository layout, mechanical equipment, and infrastructure (to allow performance of emplacement functions in reverse order), as well as the flexibility of access to individual waste packages. Section 2.3.4.6.3 discusses the

operation of retrieval equipment to selectively retrieve a single waste package.

Alternate Ingress and Egress Routes— Emplacement drift ground control deterioration and rockfall, progressive or sudden, could block access and ventilation to a particular location of the repository. To maintain the capability to retrieve any spent nuclear fuel from the repository, dual or redundant drift access is important. The design and operating mode described in this report has the ventilation raise coming up in the center of each drift, so the emplacement rails are not continuous through the drift. This does not allow full access to all parts of the drift from either end without temporary modifications. Design improvements are being considered to maintain rail access across the raise, such as a lower-profile raise collar or a ventilation exhaust main above the plane of the repository emplacement drifts, which would allow a different raise configuration. Temporary capping or other means to span the raise if access is needed across it are also being considered.

2.3.4.6.2   Drift Conditions during Retrieval and Impact on Retrievability

After the emplacement drifts have been loaded with waste packages, ventilation would continue throughout the preclosure period. With a sustained ventilation flow rate of 15 m^3/s (530 ft^3/s), air temperatures inside the drift would remain at or below a peak temperature of approximately 60°C (140°F) during the first 100 years (CRWMS M&O 2000x). An increase in the ventilation rate would lower the drift air temperatures below 50°C (120°F), low enough for the monitoring and retrieval gantries to operate reliably in the drift environment. Radiation levels would be too high for unprotected personnel access (CRWMS M&O 2000ao, Section 6.7). In cases where human incursion may be necessary, some or all of the waste packages would probably have to be removed, and extensive preparations would have to be made for radiation control.

Other potential drift conditions would affect retrievability, including:

- The structural integrity of the support pallets

- The conditions of the invert structure and railing

- A large block rockfall

- Conditions related to the containment integrity of the waste packages

- Any major deterioration and collapse of the ground support and drift walls.

The unlikely presence of a potentially breached waste package would require case-specific information and planning before any retrieval attempt, as would any detected adverse condition in the emplacement drift that would force a deviation from normal operating conditions.

2.3.4.6.3   Normal Retrieval Procedure and Equipment

The emplacement drifts would be monitored periodically, with an expected inspection frequency of 10 years. A remotely operated inspection gantry would be used during those inspections. Such monitoring would provide data for a database on drift conditions that would be used to plan maintenance activities. If it were decided that emplaced waste would be retrieved from the repository, this database and additional case-specific monitoring would be available for planning of retrieval activities. If drift conditions were normal, retrieval operations would be executed using the same waste package emplacement equipment in reverse sequence as that used for emplacement. To maintain air temperatures below 50°C (120°F) during retrieval, the ventilation flow rates may have to be adjusted several weeks before the drift incursion.

The normal retrieval sequence of operations is illustrated in Figure 2-57 (CRWMS M&O 2000aa). This sequence has been simplified to show key steps in the process. A more detailed description of the normal retrieval sequence is:

1. The locomotive and gantry carrier travel to the emplacement drift.

2. The emplacement drift isolation doors are opened and the gantry carrier engages the emplacement drift dock.
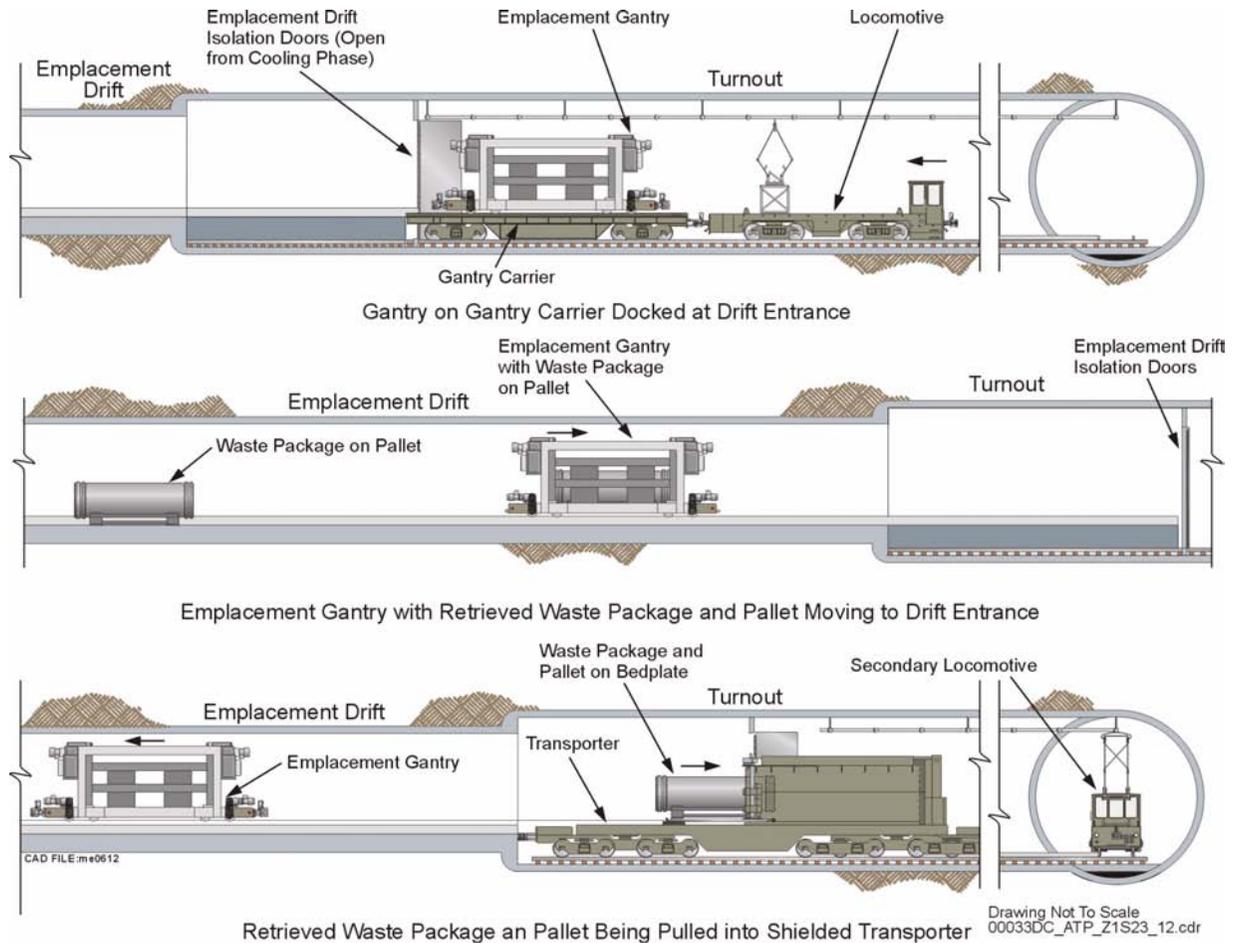
Figure 2-57. Equipment and Sequence of Operations for Normal Retrieval
The normal retrieval process for waste packages uses the same equipment and techniques utilized for emplacement but in the reverse order. The emplacement gantry would be mobilized to the drift where the waste package to be retrieved is located. The gantry would be maneuvered by remote controls over the waste package; the gantry would pick up the pallet with the waste package on it and deliver it to the transporter for transportation to the surface. Source: CRWMS M&O 2000aa, Section 6.

3. The gantry moves off the gantry carrier and the carrier is removed from the drift turnout.

4. The drift isolation doors are closed, and the gantry moves to the location of the first waste package.

5. The gantry picks up the pallet and waste package and moves back to the emplacement drift dock.

6. The transport locomotives and empty waste package transporter move to the main drift adjacent to the emplacement drift. The controls are turned over to remote operation, and the operators leave the locomotives and move to a designated protected area.

7. A secondary locomotive decouples ahead of the drift entrance. The primary locomotive and waste package transporter move from the main drift into the drift turnout.

8. The drift isolation doors open, the waste package transporter doors open, the waste package transporter docks, and the bed plate is extended onto the open deck.

9. The loaded gantry moves over the open deck of the transporter, deposits the pallet and waste package on the transporter bed plate, and moves back into the drift.

10. The pallet and waste package are pulled into the shielded compartment of the transporter via the bed plate, which is supported on rollers.

11. The primary locomotive moves the waste package transporter away from the edge of the emplacement drift, and the transporter doors and drift doors close.

12. The primary locomotive and waste package transporter move from the turnout into the main drift.

13. The secondary locomotive couples to the rear of the waste package transporter, the operators board the locomotives, and the train moves to the surface. (Steps 5 through 13 are repeated for each waste package to be retrieved from the drift.)

14. The locomotive moves the gantry carrier from the main drift to the emplacement drift turnout.

15. The drift doors are opened and the gantry carrier engages the emplacement drift dock.

16. The gantry is moved onto the gantry carrier, the locomotive pulls the carrier away from the emplacement drift dock, and the drift isolation doors close.

17. The locomotive and the gantry carrier move from the turnout to the main drift and return to a standby location.

If the waste package to be retrieved were not readily available from the drift entrance, all waste packages in front of it would have to be temporarily relocated to a standby drift or to another emplacement drift, following a sequence of events similar to that described above. If a condition preventing normal retrieval is encountered, then the sequence is interrupted, and a contingency plan

would be initiated to mitigate the problem. Retrieved waste packages that are in good condition would be taken to the surface and staged in a dedicated area within the surface facilities complex (see the Potential Onsite Inventory Area in Figure 2-16). In the unlikely event that waste packages were damaged, or if waste packages were suspected of being damaged, they would be taken to the surface facilities for detailed inspection, repairs, or repackaging.

The locomotives, gantry, gantry carrier, and waste package transporter used for normal retrieval are the same as those described in Section 2.3.4.4. Therefore, their characteristics and preliminary engineering specifications are not repeated in this section.

2.3.4.6.4 Off-Normal Retrieval Procedures and Equipment

When the equipment and operating sequence described above cannot be used, retrieval conditions are considered off-normal. Off-normal retrieval conditions, most likely due to drift wall deterioration and the resulting blockage of the railing system, prevent the use of the waste package gantry. Under off-normal retrieval conditions, several additional operations would be added to the retrieval sequence. These additional steps would most likely include the following:

- Monitoring and detailed characterization of damage

- Development of a case-specific contingency plan

- Cleanup and removal of debris

- Stabilization of the drift (including ground support repairs or replacement)

- Restoration of the tracks and other damaged structures and utilities

- Repositioning of the pallet and waste package, if necessary

- Establishment of radiation controls and other administrative controls for retrieval, as needed.

Off-normal retrieval procedures and equipment would be used commensurate with the situation. A series of event sequences that could affect normal retrieval conditions were analyzed (CRWMS M&O 2000aa, Section 6.2.2) to determine the operational procedure and type of equipment that could be used to retrieve waste packages. The two event sequences analyzed and of particular relevance to off-normal retrieval conditions in the emplacement drifts were (1) rockfall or ground support collapse onto a waste package from causes other than seismic events and (2) rockfall or ground support collapse onto a waste package caused by a seismic event (a beyond Category 1 or Category 2 event sequence earthquake). Other event sequences analyzed with respect to off-normal retrieval pertained to the mechanical failure of the gantry and the derailment of the gantry at normal speed.

The two pieces of equipment designed for removal of the gantry, the emplacement drift gantry carrier and the multipurpose hauler (Figure 2-58), operate on rollers. Steel plate would have to be installed over the drift invert to deploy this equipment. A multipurpose vehicle (Figure 2-59) can be operated from the multipurpose hauler to clear debris, emplace steel plates, and cut and remove damaged structures. This equipment would be remotely operated.

When a derailed or damaged gantry has to be removed from the drift, the emplacement drift gantry carrier can load and carry the gantry away from the emplacement drift (Figure 2-60). The multipurpose hauler can be used to pull and load the pallet and waste package onto the deck of the hauler to proceed with retrieval operations (Figure 2-58).

2.3.4.6.5   Summary of Retrievability

Waste package retrieval under normal conditions uses the same subsurface equipment and facilities as emplacement, but in reverse order. This provides a built-in capability for retrieval that can be readily implemented. Individual waste package removal for inspection, testing, and maintenance reasons is not considered retrieval; however, waste package removal for these purposes, if needed, would involve the same equipment and operational steps.

Alternative waste package retrieval equipment has been identified for off-normal conditions when normal retrieval procedures may be difficult or impossible to execute. Additionally, support equipment (i.e., equipment to remove obstacles, prepare surfaces, or install temporary ground supports) that can be used in retrieval operations under off-normal conditions has been identified. Various scenarios of off-normal retrieval have been analyzed, and conceptual use of such equipment has been demonstrated (CRWMS M&O 2000aa, Sections 6.2 and 6.3). Proof-of-principle demonstra-tions of waste package retrieval may be conducted following the license application as another step in the series of requirements for successful construction and operation of the repository.

2.3.4.7   Decommissioning

The primary objective of the decommissioning of the subsurface facilities is the removal of any material or equipment that is not part of the perma-nent repository installation. Decommissioning will precede closure activities, or in some cases will be concurrent with them.

Subsurface decommissioning activities would include:

1. Dismantling structures and equipment for removal of components from the under-ground facilities, decontamination if necessary, and transport to the surface for additional decontamination, release, or disposal.

2. Demolition of reinforced concrete struc-tures and steel support structures after the equipment and fixtures have been removed.

3. Transporting the removed materials and equipment to onsite or offsite disposal
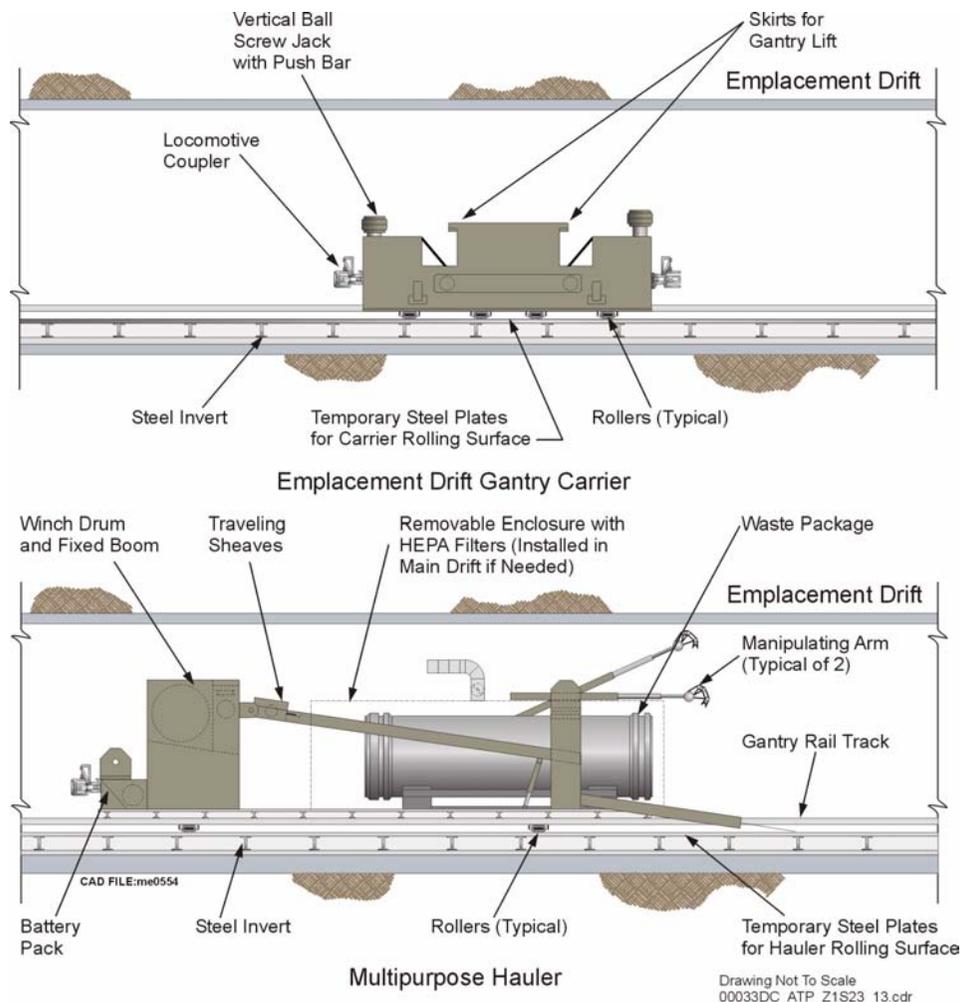
Figure 2-58. Emplacement Drift Gantry Carrier and Multipurpose Hauler
During off-normal retrieval, when emplacement drift conditions do not allow implementation of normal retrieval procedures, alternative retrieval equipment can be utilized. These consist of an assortment of equipment designed for removal of disabled gantries, removal of debris, construction of temporary structures to support retrieval, and retrieval of damaged or undamaged waste packages. HEPA = high-efficiency particulate air. Source: CRWMS M&O 2000aa, Section 6.2.

facilities, depending on type, quantity, and waste characterization, in accordance with a preapproved DOE waste management plan. These materials and equipment will include ventilation system components, railroad track, rolling stock, utilities, concrete and construction materials, instrumentation and communication equipment, pumps, pipelines, and any other materials that may be considered detrimental to repository performance after closure.

4. Identifying and removing equipment and materials for salvage. Some equipment and materials may be targeted for salvage because of their value or because their reuse is anticipated (e.g., for site restoration or other future activities at the repository surface facilities). Such equipment and materials will be protected as needed and staged at the surface facilities.

5. Placement of underground markers, monuments, or any other permanent features deemed necessary before closure activities.
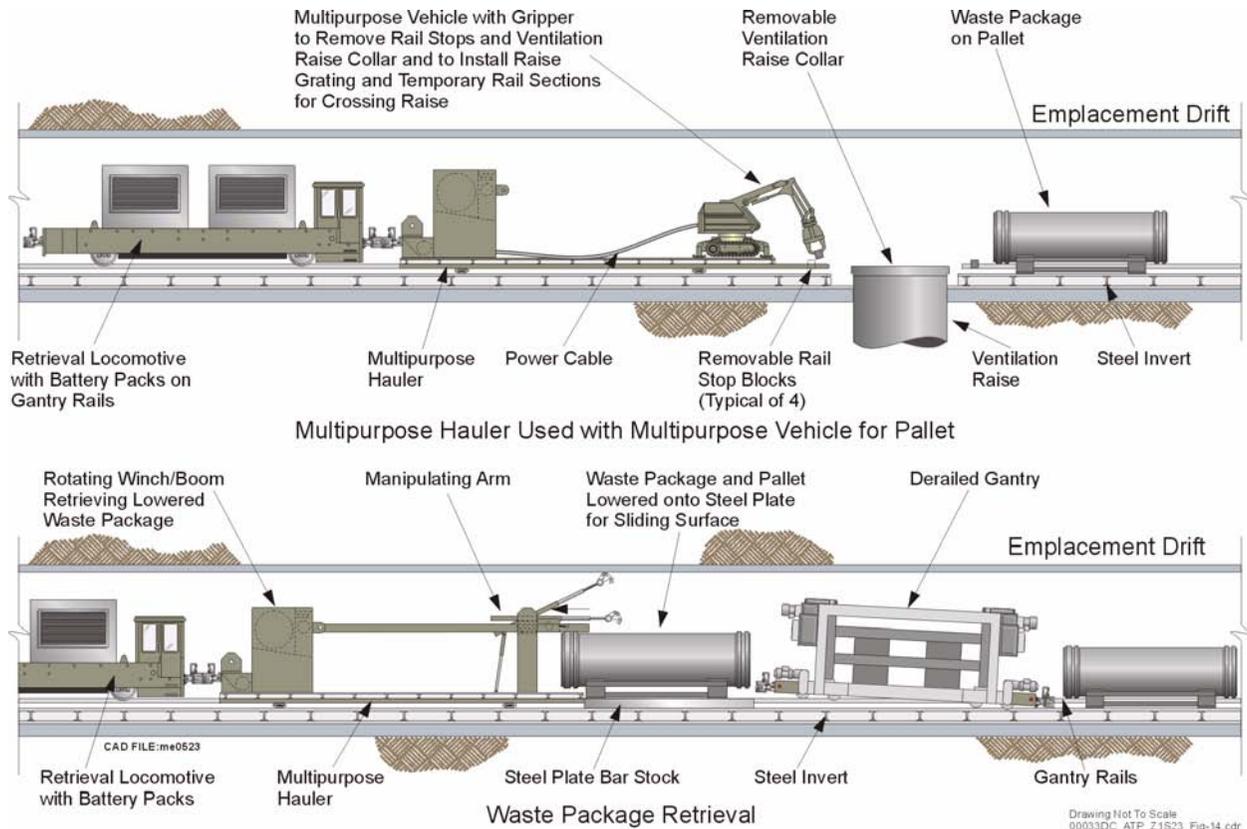
Figure 2-59. Multipurpose Hauler Used with Multipurpose Vehicle for Pallet and Waste Package Retrieval
Remotely controlled equipment can be utilized for different functions during retrieval, thus preventing personnel exposure. Source: CRWMS M&O 2000aa, Section 6.2.

6. Completion of as-built surveys of the subsurface facilities before closure.

7. General cleanup in preparation for closure activities.

It is likely that some of these activities can be performed gradually during the operational phase of the repository.

2.3.4.8 Closure and Sealing Structures

Closure of the repository subsurface facilities requires closing and sealing all openings from the surface to the underground facilities. These openings consist of the north and south access ramps, ventilation shafts, and exploratory boreholes within the repository footprint (the waste emplacement area projected vertically to the surface) and in an area extending 400 m (1,300 ft) from the foot-

print boundaries. If left unsealed, these openings could enhance the movement of moisture from the surface into the waste emplacement area, and the larger openings, such as the ramps and shafts, could allow unauthorized human intrusion. Openings connecting the waste emplacement area to the surface could also serve as conduits for airborne radioactive contamination to migrate into the atmosphere.

Regulatory requirements imposed on the repository design to provide protection against human intrusion, as well as requirements to prevent or minimize release of contamination, create the necessity that these openings be sealed during the closure phase of the repository.

Tables 2-20 and 2-21 summarize the preliminary engineering specifications for closure and sealing components.
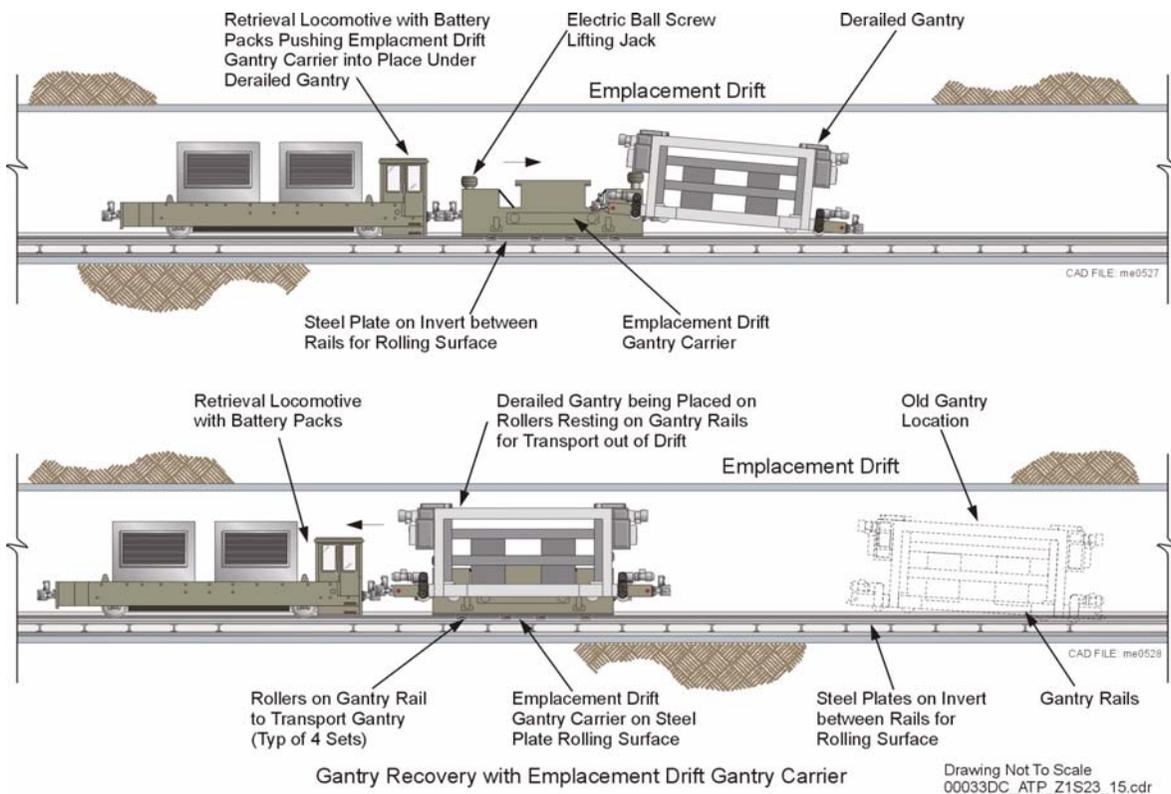
Figure 2-60.   Gantry Recovery with Emplacement Drift Gantry Carrier
This figure illustrates the operation of a gantry carrier used for retrieval gantry recovery, in case of a disabled gantry.
Source: CRWMS M&O 2000aa, Section 6.2.

Table 2-20. Summary of Design Basis of Closure and Sealing Components

Item	Property
Favorable material characteristics	• Low permeability • Chemical stability in thermal-hydrologic environment • Material longevity • Availability • Similar hydraulic conductivity and permeability to host rock mass
Concrete structural loading factors	• Seismic activity • Host rock stress relief • Hydraulic pressure • Backfill material lateral pressure

Table 2-21. Summary of Closure and Sealing Component Materials

Component	Material
Ramp and shaft plugs and bulkheads	Concrete
Seals and backfill	Concrete, grout, crushed tuff, bentonite, bentonite–sand mixture
Boreholes	Bentonitic grout

2.3.4.8.1   Repository Openings

Section 2.3.1 describes the locations of the north and south ramps, and Section 2.3.4.3 describes the ventilation shafts. The specific locations of the boreholes within the repository footprint, including the 400-m (1,300-ft) buffer zone around the perimeter, are not addressed in this report but are well documented in the DOE's scientific database (BSC

2001d, Attachment III). There are approximately 16 deep boreholes in the potential repository area, including a 400-m (1,300-ft) buffer zone around the potential repository perimeter.

2.3.4.8.2 Criteria for Selection of Seal Locations

The geological environment and the rock structure are central considerations in determining the specific locations where seals would be most effective. The constructibility advantages offered by one location over another are also considerations in determining seal locations. For example, seal construction in large openings is preferable in the straightaway rather than in curves or intersections because of such issues as simplicity of design, construction, equipment access, and materials placement.

Two stratigraphic nomenclature systems are used for the classification of the host rock at Yucca Mountain: a thermomechanical nomenclature and a lithostratigraphic nomenclature. The thermomechanical nomenclature is based solely on the thermal and mechanical properties of the rock. The lithostratigraphic nomenclature is based on primary geologic processes (e.g., the depositional character and assemblage of the rock) and secondary geologic processes (e.g., the degree of welding, devitrification, and vapor-phase crystallization). A thermomechanical unit typically contains several lithostratigraphic units. The thermomechanical units are defined by the thermal and mechanical characteristics of the natural rock, and they do not necessarily correspond to lithostratigraphic formation boundaries. The PTn and the TCw thermomechanical units (see Sections 1.3.2.2.2 and 2.3.4.1.3 for geologic unit descriptions) are important in defining the location of closure seals above the emplacement block. The TCw unit has a well-connected fracture system and high permeability. The PTn unit has very low permeability. These contrasting attributes can be used advantageously by locating a seal in the more permeable unit (the TCw) near its boundary with the less permeable unit (the PTn). At this location, the seal would help disperse sporadic infiltration fluxes into the more permeable matrix of the TCw

formation, which otherwise would tend to create a moisture buildup in the less permeable PTn unit.

The condition of the rock immediately surrounding a potential seal location is the most important factor in deciding the locations of closure seals in the ramps and shafts, mainly for reasons of seal structural integrity and stability. Closure seal locations should be selected to avoid ground conditions resulting from geologic disturbances, such as faults and fracture zones. Therefore, developing detailed characterizations of the rock structure at the ramps and ventilation shaft locations is essential. The structural geology of the north and south ramps is well characterized, and several candidate seal locations have been identified (CRWMS M&O 2000aj, Appendices A and B). Detailed characterization of the ventilation shafts, however, would be possible only after their excavation. Therefore, detailed seal design must also be performed after shaft excavation.

Faults create instability in the rock and present potential pathways for inflow of moisture. Major faults along the north and south access ramps are already documented (CRWMS M&O 2000aj, pp. 22 and 23), and they will be avoided in selecting closure seal locations. Similar identification and evaluation of major faults will be performed for the ventilation shafts after their excavation; however, the locations of the shafts have been selected partly by avoiding documented geologic hazards, such as faults or excessively fractured rock zones.

Fractures (structural discontinuities in the rock) and joint sets (groups of fractures with similar orientation) also provide an indication of rock mass stability. Fractures directly affect the strength of the rock. The frequency and orientation of the fractures can affect the short- and long-term stability of the excavation. Five joint sets have been identified in the Exploratory Studies Facility, which includes the north and south ramps (CRWMS M&O 2000aj, Table 6). Within the repository block, the Undifferentiated Overburden and PTn thermomechanical units have the lowest density of fracturing, while the nonlithophysal portions of the other three thermomechanical units (TCw, TSw1, and TSw2) have

the highest fracture density (CRWMS M&O 2000aj, p. 24).

2.3.4.8.3 Selection of Closure Seal Materials

Selection of seal materials must consider material strength and the ability to slow moisture and airflow through the repository block. Seals would be composed of different materials, individually or in combination, that will effectively discourage human intrusion and control moisture inflow.

Seal and closure system components must be mechanically, chemically, geologically, and thermally compatible with the subsurface environment. Materials that can meet these compatibility requirements include concrete, grout, crushed tuff, bentonite, and bentonite–sand mixtures.

Earthen materials have been recommended for use as backfill in ramps and shafts to prevent preferential pathways for moisture movement and discourage human intrusion. Properties considered desirable for backfill materials include low permeability, chemical stability in the thermal and hydrologic environment in the repository, material longevity, and availability. The selected backfill material should have the approximate hydraulic conductivity and permeability of the surrounding rock mass. Earthen materials analyzed for use as closure backfill include crushed tuff, clays (such as bentonite), and combinations of bentonite and sand (CRWMS M&O 2000ak). Crushed tuff would be readily available as a by-product of tunnel excavation; this excavated material is often called muck. The muck material would be screened and crushed to enhance the characteristics useful for closure backfill. It has been determined that a bentonite–sand mixture with 5 to 10 percent bentonite would result in an acceptable hydraulic conductivity range (10^{-4} to 10^{-7} cm/s) for use in closure backfill or seal designs (CRWMS M&O 2000ak, Figure 1).

Several grout types were analyzed as sealing media for rock fractures and for sealing between the rock face and the structural components of the main closure seals. These grouts included chemical, cementitious, and bentonite-based materials. Their advantages and disadvantages are listed in *Closure*

Seal Materials and Configuration (CRWMS M&O 2000ak, pp. 11 to 13).

Concrete is recommended for ramp and shaft plugs and bulkheads. Concrete structures can be designed to withstand loading from seismic activity, host rock stress relief, and hydraulic pressure, and to retain backfill material.

2.3.4.8.4 Closure and Sealing Structures

Conceptual seal designs and closure structure designs have been developed from the recommended materials described in Section 2.3.4.8.3. These concepts may be expanded into preliminary designs during the license application phase; however, detailed designs of the shaft seals may not be feasible until complete geologic mapping of the excavated shafts is finished.

Repository closure operations would include placement of backfill throughout the ramps, shafts, and main drifts. Figures 2-61 and 2-62 illustrate typical backfill placement methods for the ramps and main drifts and for the shafts, respectively. The method illustrated in Figure 2-61 consists of a pneumatic conveyance system. However, more conventional placement methods are available that use standard underground equipment (e.g., load-haul-dump underground haulers). Pneumatic systems provide good placement control, but they require extensive dust control to maintain acceptable working conditions. The shaft backfill placement method illustrated in Figure 2-62 is a conventional and industry-proven practice that produces satisfactory results.

Deep boreholes would be sealed by injecting a bentonite grout from the surface opening. Concrete caps would be installed near the surface, closing all openings, to prevent or discourage human intrusion. These caps would be covered with backfill as part of the surface restoration work. Figure 2-63 illustrates a typical installation for a shaft concrete cap, as well as the water dispersion structure placed in the TCw thermomechanical unit (see Section 2.3.4.8.3).

Seals would be placed in shafts and ramps at several locations, depending on more detailed
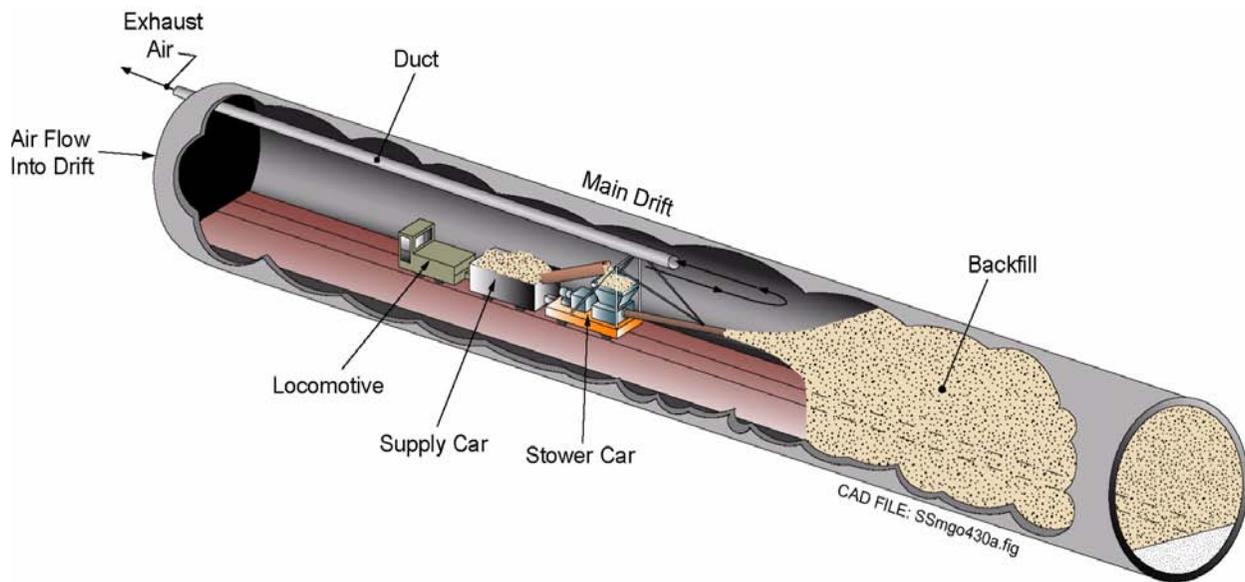
Figure 2-61.   Conceptual Arrangement for Placement of Backfill in Ramps and Main Drifts
Repository closure activities include backfilling of the ramps and main drifts with granular material. This figure portrays a method by which such operation could be accomplished. Source: CRWMS M&O 2000ai, Section 6.1.2.

designs for control of moisture infiltration into the emplacement area. Seals would be located in relation to major faults and highly fractured rock zones to improve performance by attenuating sudden inflows of water and promoting slow percolation back into the rock matrix. Conceptual seal plug designs have been developed for areas of high, moderate, and low water inflow. Figure 2-64 illustrates the seal plug design concept for a high water inflow application. This design concept consists of a combination of dual concrete plugs that "sandwich" a bentonite–sand plug. The concrete plugs would provide structural support, while the bentonite–sand mixture fill would expand, filling voids and fractures. Conceptual designs for moderate and low water inflow applications would be simpler, consisting of single concrete plugs "sandwiched" by backfill material. In all these seal applications, construction of the concrete plugs would be preceded by interface grouting of the rock forma-

tion around the plug perimeter to enhance the watertightness of the seals.

2.3.5 Phased Construction—Development and Emplacement Sequence

The subsurface components of the repository would be built in phases to support waste emplacement. The current design assumes that waste packages would be delivered over a period of 24 years (YMP 2000a, Table 3-2), which allows a phased approach to completion of the emplacement drifts. This phased construction approach is described in the discussions that follow.

The construction phases for the subsurface facilities will be (1) initial construction and (2) development. Subsurface systems operations will vary during these construction phases as emplacement activities begin and continue over a period of several decades.
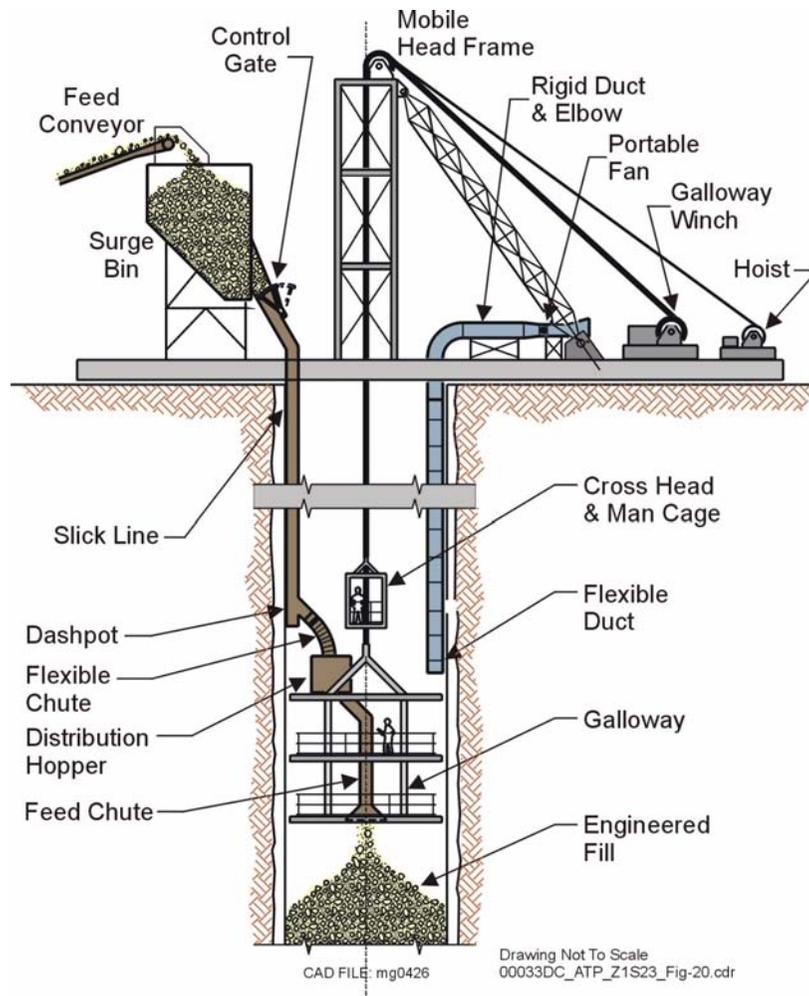
Figure 2-62.   Conceptual Arrangement for Placement of Backfill in Shafts
Intake and exhaust shafts would also be backfilled with granular material as part of the repository closure activities.
Source: CRWMS M&O 2000ai, Section 6.1.2.

2.3.5.1   Initial Construction

2.3.5.1.1   Facilities

In the initial construction phase, activities in the north side of the emplacement block would include excavation of the north ramp extension and excavation of the east main, north of the north ramp curve (Figure 2-65). These two drifts would be 7.62 m (25 ft) in diameter, excavated with tunnel boring machines. After excavation of the north ramp extension, one of the tunnel boring machines would continue with excavation of the north main and part of the west main. The other machine would start excavating the exhaust main from the north, heading south.

The first two drifts in the emplacement block would be excavated with another tunnel boring machine, 5.5 m (18 ft) in diameter. These two drifts, Postclosure Test Drifts #1 and #2, would be dedicated to performance confirmation testing; their construction would be identical to the construction of emplacement drifts. The performance confirmation function of these postclosure test drifts is explained in Section 2.5. After excavating these first two drifts, the smaller-diameter tunnel boring machine would excavate the first set of ten emplacement drifts, progressing from north to south.

A second 5.5-m (18-ft) diameter tunnel boring machine would start excavation of Observation
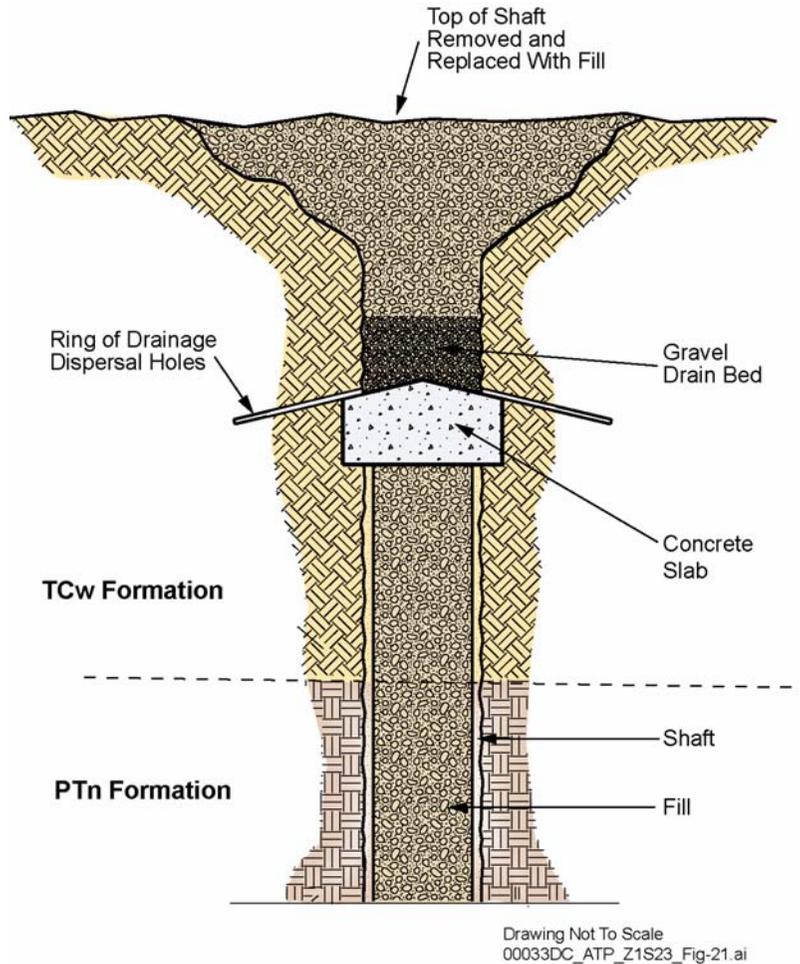
Figure 2-63. Conceptual Arrangement of Shaft Plug
Location of shaft plugs, another repository closure feature, would depend on characteristics of the geologic strata. These seals would be located in fractured rock strata with a higher permeability than the underlying strata, to promote dispersion of surface water inflows into the rock formation. Source: CRWMS M&O 2000ai, Section 6.1.1.

Drifts #1 and #2, in sequence. These two drifts are also part of the performance confirmation facilities; the functions of these drifts are explained in Section 2.5. After completing these two drifts, this tunnel boring machine would be relocated ahead of the other 5.5-m (18-ft) diameter tunnel boring machine. Then it would excavate a cross-drift for Intake Shaft #1 and another standard emplacement drift connecting the southernmost extension of the west main to the east main.

Other subsurface facilities excavated during this phase would include Intake Shaft #1, Exhaust Shaft #1, and two 7.62-m (25-ft) diameter access drifts connecting the exhaust shaft to the exhaust main. Observation Drift #3 (Figure 2-65) would

also be excavated during this period by the second 5.5-m (18-ft) diameter tunnel boring machine, starting from the ECRB Cross-Drift. The intake and exhaust shafts are 8 m (26 ft) in diameter, excavated from the surface down by drill-and-blast techniques (BSC 2001d, Sections 5.2.7.2, 6.3.2.3, and 6.3.2.5).

2.3.5.1.2 Ventilation and Controls

During the initial construction period, air would be taken in from the surface through the north ramp and exhausted out to the surface through the south ramp. This section defines the global ventilation system for this phase of construction. Within the global system, local ventilation systems support
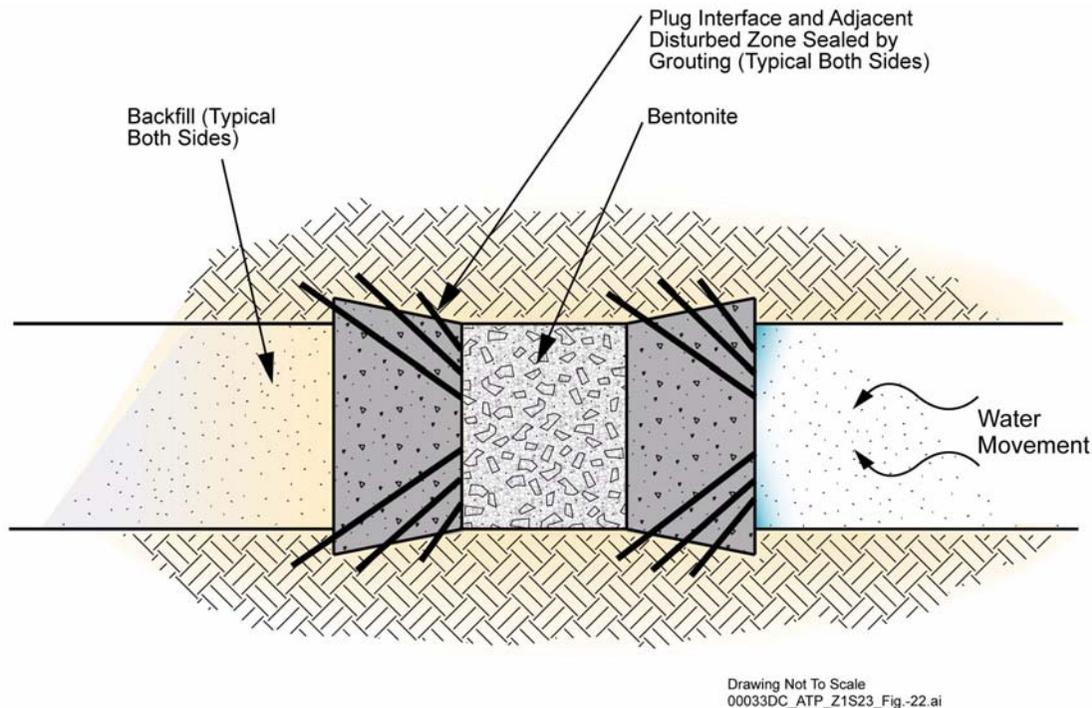
Figure 2-64. Dual Concrete Seal Plug Design Concept
Dual concrete seal plugs are one of the proposed closure and sealing features for the repository ramps. Source:
CRWMS M&O 2000ak, Section 5.

each excavation deadheading. These local systems provide ventilation from the main drift through to the working face, where a mechanical excavator extends the length of a drift that is a dead-end heading. Ventilation at the excavation headings is achieved in three ways: (1) intake through a duct, exhaust through a drift; (2) intake through a drift, exhaust through a duct; and (3) intake through a duct, exhaust through another duct. Figure 2-66 illustrates the global and local ventilation design concepts as they apply to the initial construction phase. For local ventilation, the figure only illustrates the concept described in item 1 above. Local dust scrubbers remove dust from exhausted air before the air is returned to the main drift and exhausted from the underground to the surface. Each shaft excavation would be ventilated by local systems that would take fresh air in from the surface (CRWMS M&O 2000x, Section 6.3.1).

2.3.5.2   Development and Emplacement Phase I

2.3.5.2.1   Facilities Construction

As the first emplacement drifts from the initial construction phase become available for waste emplacement, transportation of waste packages to the subsurface would begin. This event marks the beginning of Phase I of development and emplacement. During Phase I, concurrent with waste emplacement in the first drifts, construction of new emplacement drifts would progress in a southerly direction. Figure 2-67 illustrates the subsurface facilities constructed during Phase I of development and emplacement.

During Phase I, eight emplacement drifts would be excavated. Excavation of the exhaust main and the west main would continue in a southerly direction. After completing the excavation of the west main,
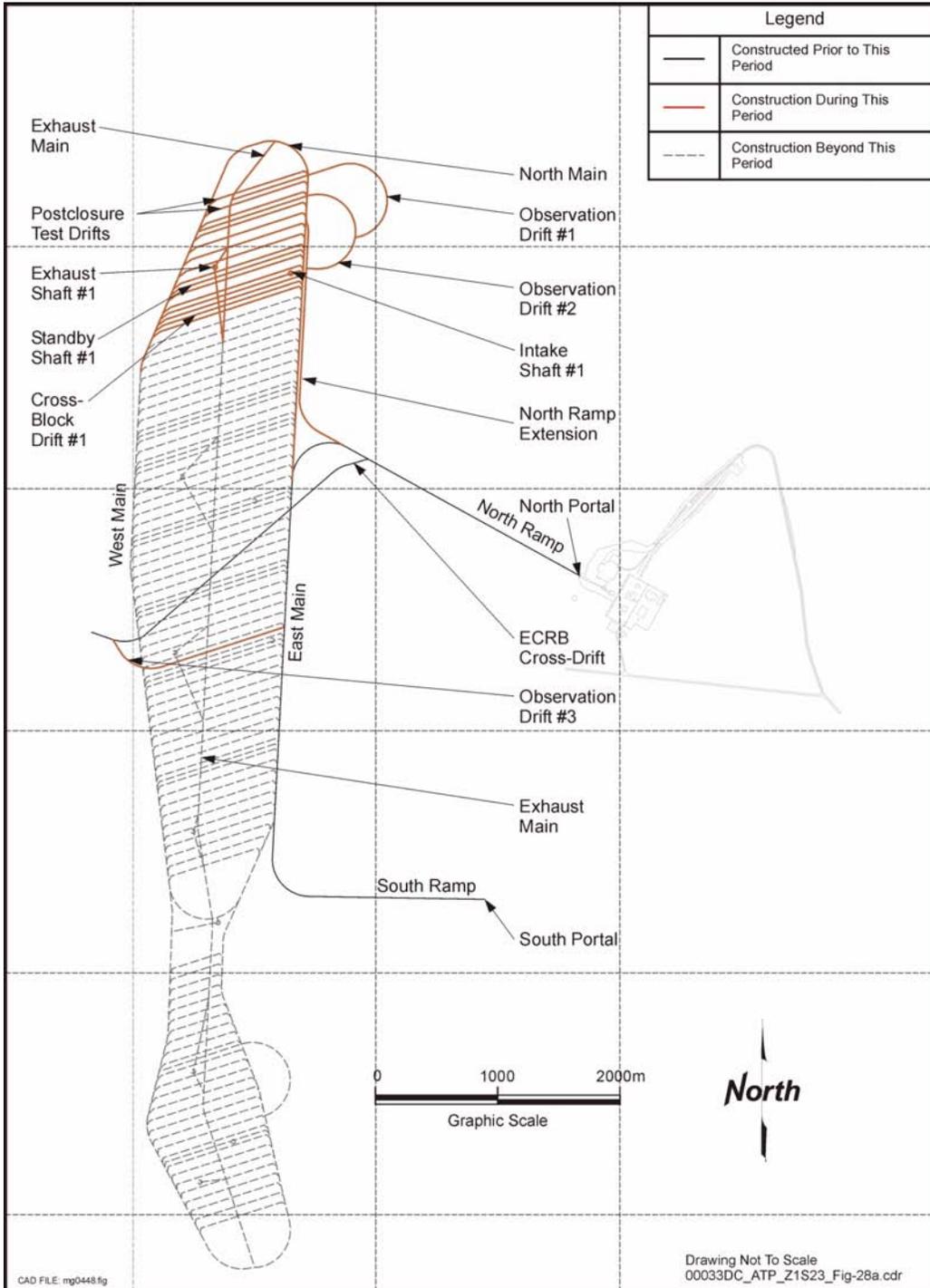
Figure 2-65.   Repository Subsurface Layout—Initial Construction
Initial repository construction includes three observation drifts and ten emplacement drifts.
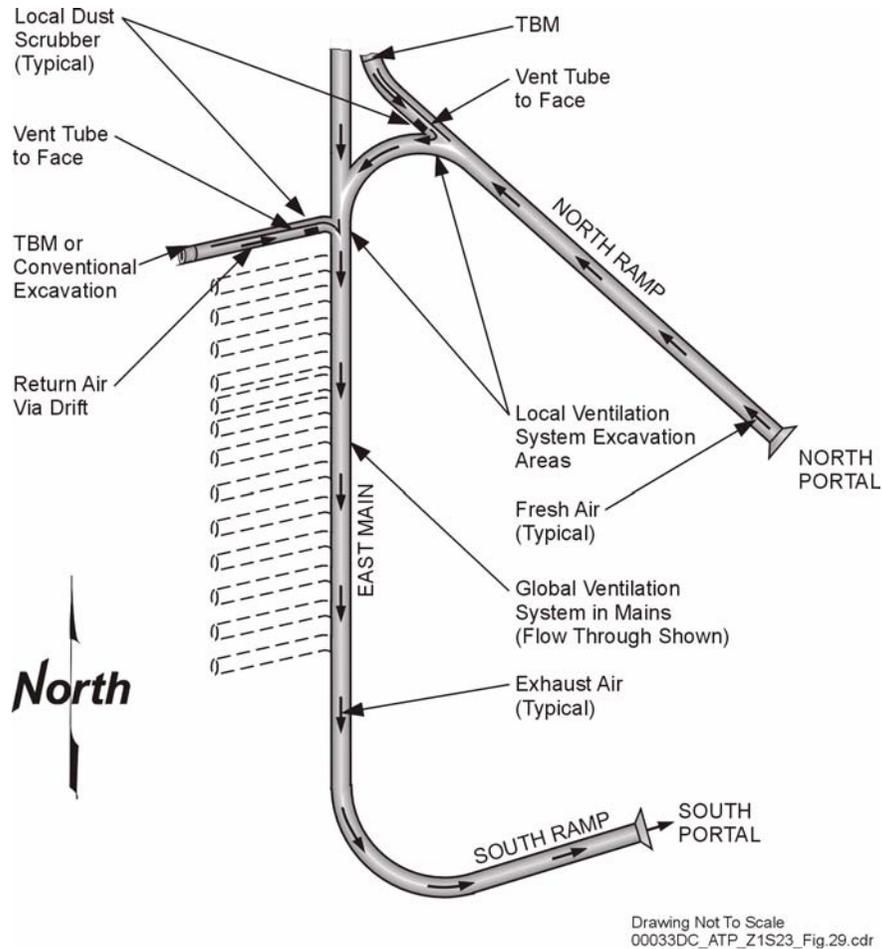
Figure 2-66.   Examples of Global and Local Ventilation
Dust scrubbers would be used at excavation headings to control airborne particulates before air is returned to the main airways. TBM = tunnel boring machine. Source: Modified from CRWMS M&O 2000x, Section 6.3.

the 7.62-m (25-ft) diameter tunnel boring machine would continue excavating to open the south main to its intersection point with the existing east main. During this phase, excavation of the exhaust main by the other 7.62-m (25-ft) tunnel boring machine would continue to the south main. Other excavations during this phase include Exhaust Shaft #2 and the access drifts connecting it to the exhaust main; Intake Shaft #2 and the cross-drift connecting it to the east and west mains; and the development intake shaft.

2.3.5.2.2   Ventilation and Controls

The first ten drifts have a separate ventilation system to support waste emplacement. Air locks in the exhaust main, in the east and west mains north

of the tenth drift turnouts, and on the north ramp curve would isolate the initial panel (the first ten drifts) from the new development area that starts with construction of the thirteenth drift. The emplacement area air intake would be drawn through the north ramp and exhausted through Exhaust Shaft #1. On the development side, air would be blown in through Intake Shaft #1 and exhausted through the south ramp.

2.3.5.3   Development and Emplacement Phase II

2.3.5.3.1   Facilities Construction

Figure 2-68 illustrates Phase II development and emplacement work. Facilities constructed during
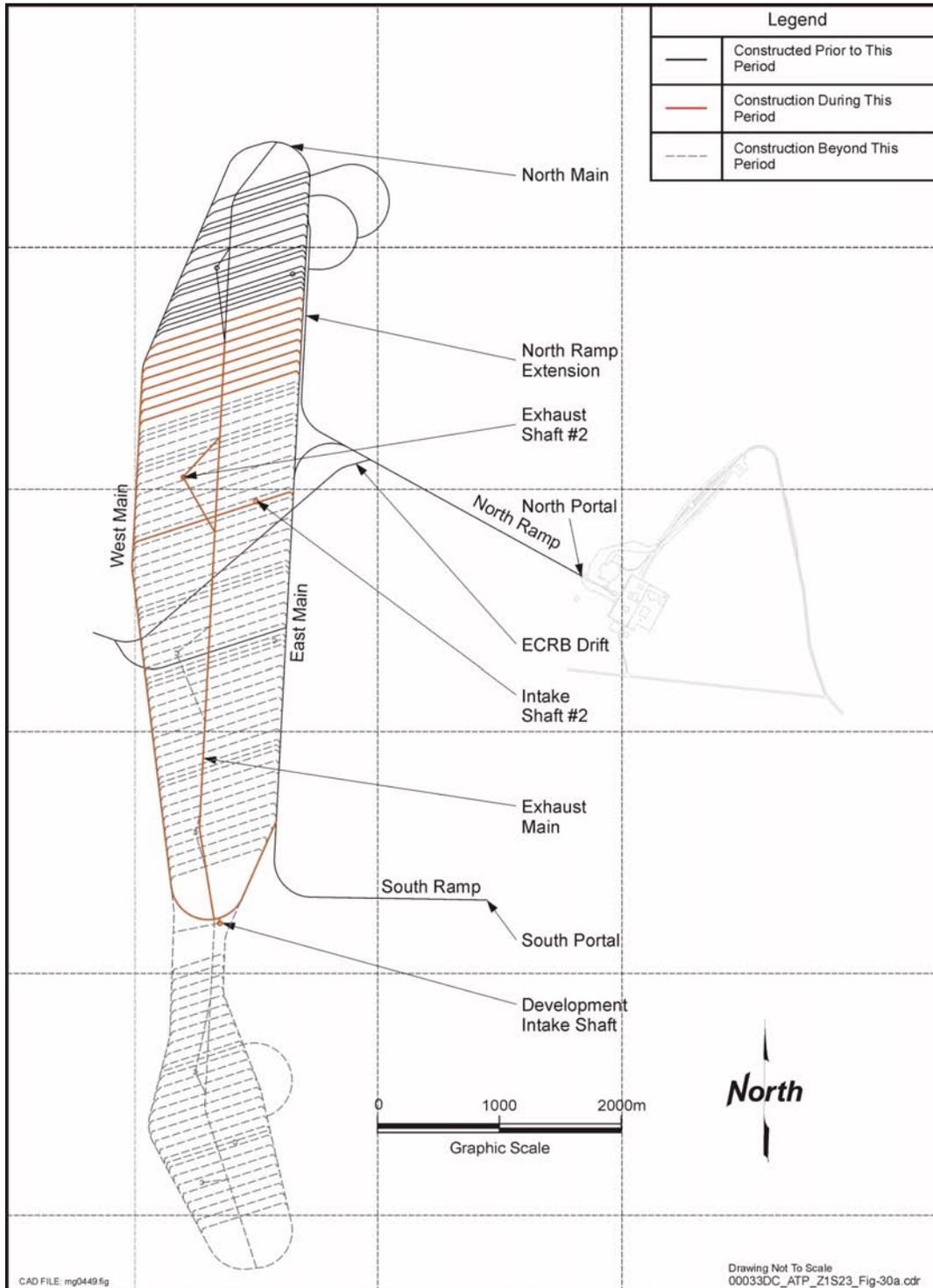
Figure 2-67.   Repository Subsurface Layout—Development and Emplacement for Phase I
Phase I development activities include construction of eight emplacement drifts while waste emplacement in the first ten drifts is initiated.
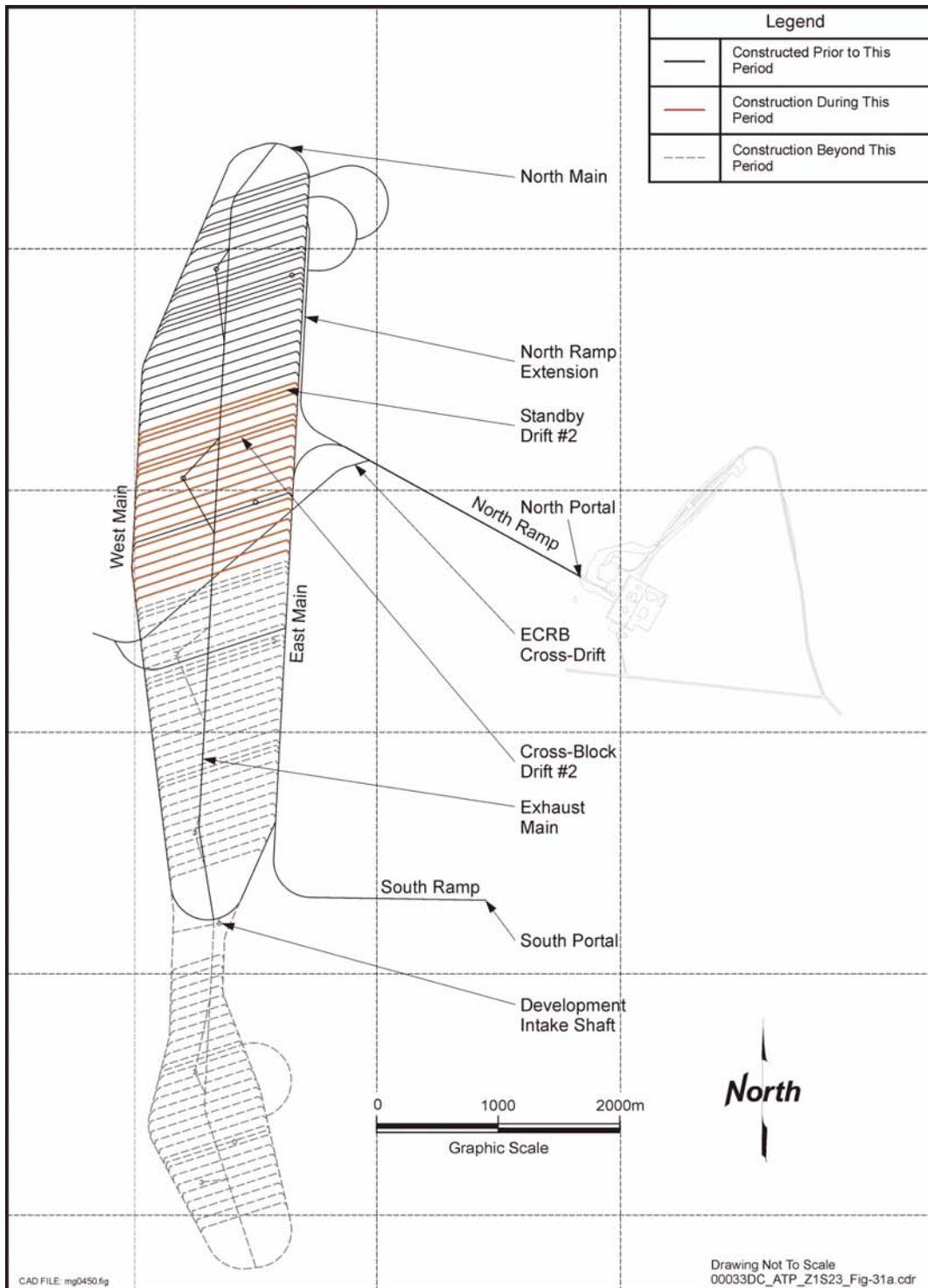
Figure 2-68. Repository Subsurface Layout—Development and Emplacement for Phase II
The second phase of development and emplacement includes the construction of 17 emplacement drifts while waste emplacement operations go on in the previously built 18 drifts.

this phase consist of Standby Drift #2, Cross-Block Drift #2, and 17 emplacement drifts. Emplacement operations would continue in the emplacement drifts completed during Phase I.

2.3.5.3.2   Ventilation and Controls

Air locks used to separate the emplacement area from the development area would be relocated southward along the exhaust main and the east and west mains. During Phase II, intake air for the emplacement area would be drawn in through the north ramp and Intake Shaft #1 and exhausted through Exhaust Shaft #1. Fresh air for the development side would be blown in through the intake development shaft and Intake Shaft #2 and exhausted through Exhaust Shaft #2 and the south ramp.

2.3.5.4   Development and Emplacement Phase III

2.3.5.4.1   Facilities Construction

Figure 2-69 illustrates Phase III of development and emplacement work. Development activities during this phase consist of the following excavations:

- Fourteen emplacement drifts

- Intake Shaft #3 and the cross-drift connecting it to the east and west mains

- Exhaust Shaft #3 and access drifts connecting it to the exhaust main

- Cross-Block Drift #3.

In Phase III, emplacement activities would continue in emplacement drifts completed during Phase II.

2.3.5.4.2   Ventilation and Controls

The ventilation air locks would be relocated along the exhaust main and the east and west mains to isolate the development ventilation system from the emplacement area. Intake air for the emplacement area would be drawn through Intake Shafts

#1 and #2 and the north ramp and exhausted through Exhaust Shafts #1 and #2. On the development side, fresh air would be blown in through Intake Shaft #3 and the intake development shaft and exhausted through Exhaust Shaft #3 and the south ramp.

2.3.5.5   Development and Emplacement Phase IV

2.3.5.5.1   Facilities Construction

The final development and emplacement phase for the 70,000-MTHM repository design, Phase IV, consists of construction of the last three emplacement drifts and one cross-block drift (Cross-Block Drift #4). Emplacement operations during this phase would continue in emplacement drifts excavated during Phase III. Figure 2-70 illustrates the construction activities during Phase IV.

2.3.5.5.2   Ventilation and Controls

The development side ventilation system would be separated from the emplacement side by relocating air locks along the exhaust main and the east and west mains to points immediately north of the construction activity. The air for the emplacement area during this phase would be drawn through Intake Shafts #1, #2, and #3 and the north ramp. Emplacement air would be exhausted through Exhaust Shafts #1, #2, and #3. Air for the development side would be blown in through the intake development shaft and exhausted through the south main.

2.4   ENGINEERED BARRIERS

The engineered barriers include those components within the emplacement drift that contribute to waste containment and isolation. The design and operating mode described in this report includes the following components as engineered barriers: (1) waste package, (2) emplacement drift invert, and (3) drip shield.

Previous designs (DOE 1998, Volume 2; CRWMS M&O 1999c; CRWMS M&O 1999d) included other engineered barriers that were subsequently eliminated. These include emplacement drift back-
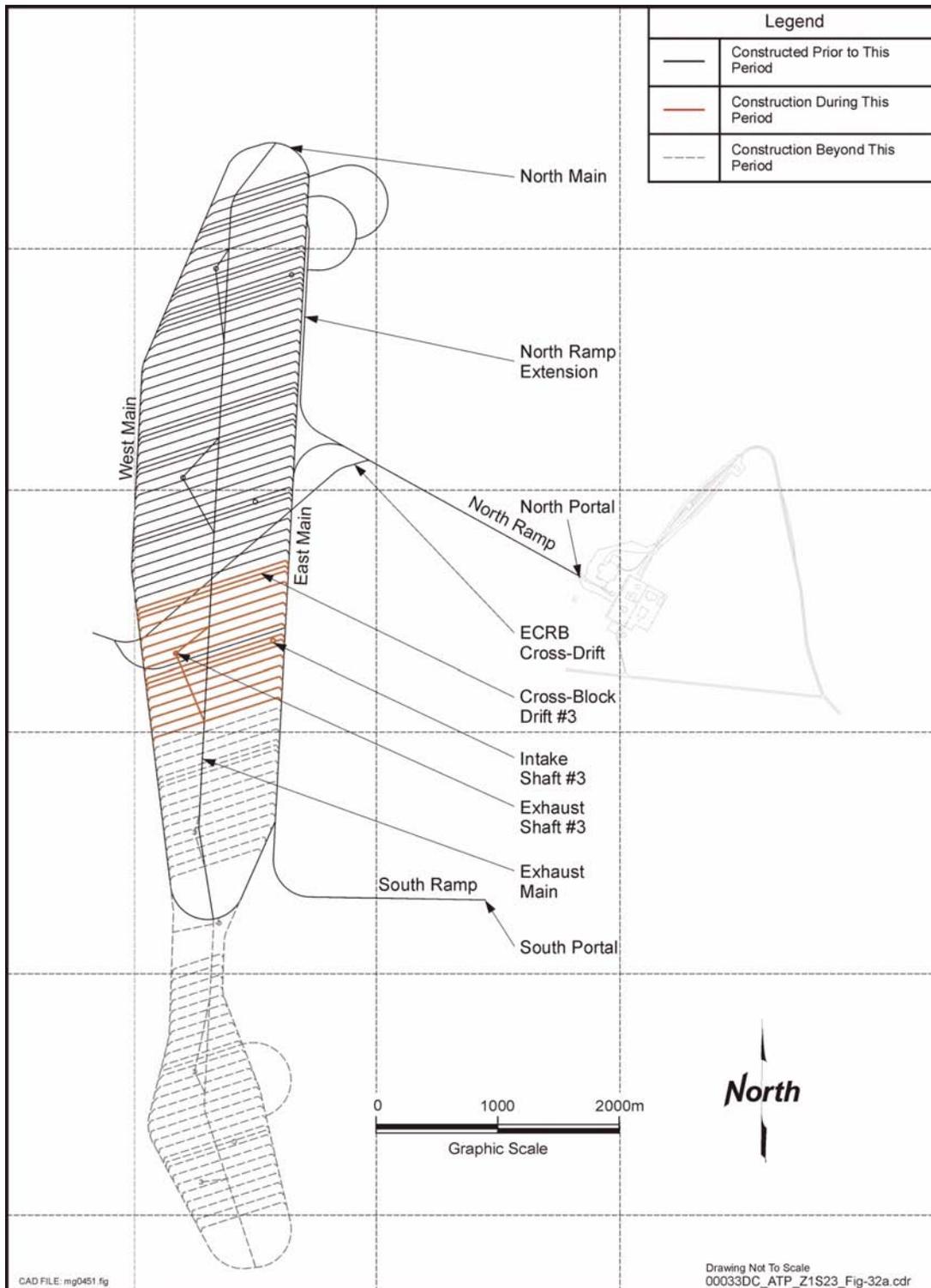
Figure 2-69. Repository Subsurface Layout—Development and Emplacement for Phase III
Construction of emplacement drifts continues during the third phase of development, with completion of 14 more emplacement drifts. Waste emplacement operations continue in previously commissioned drifts.
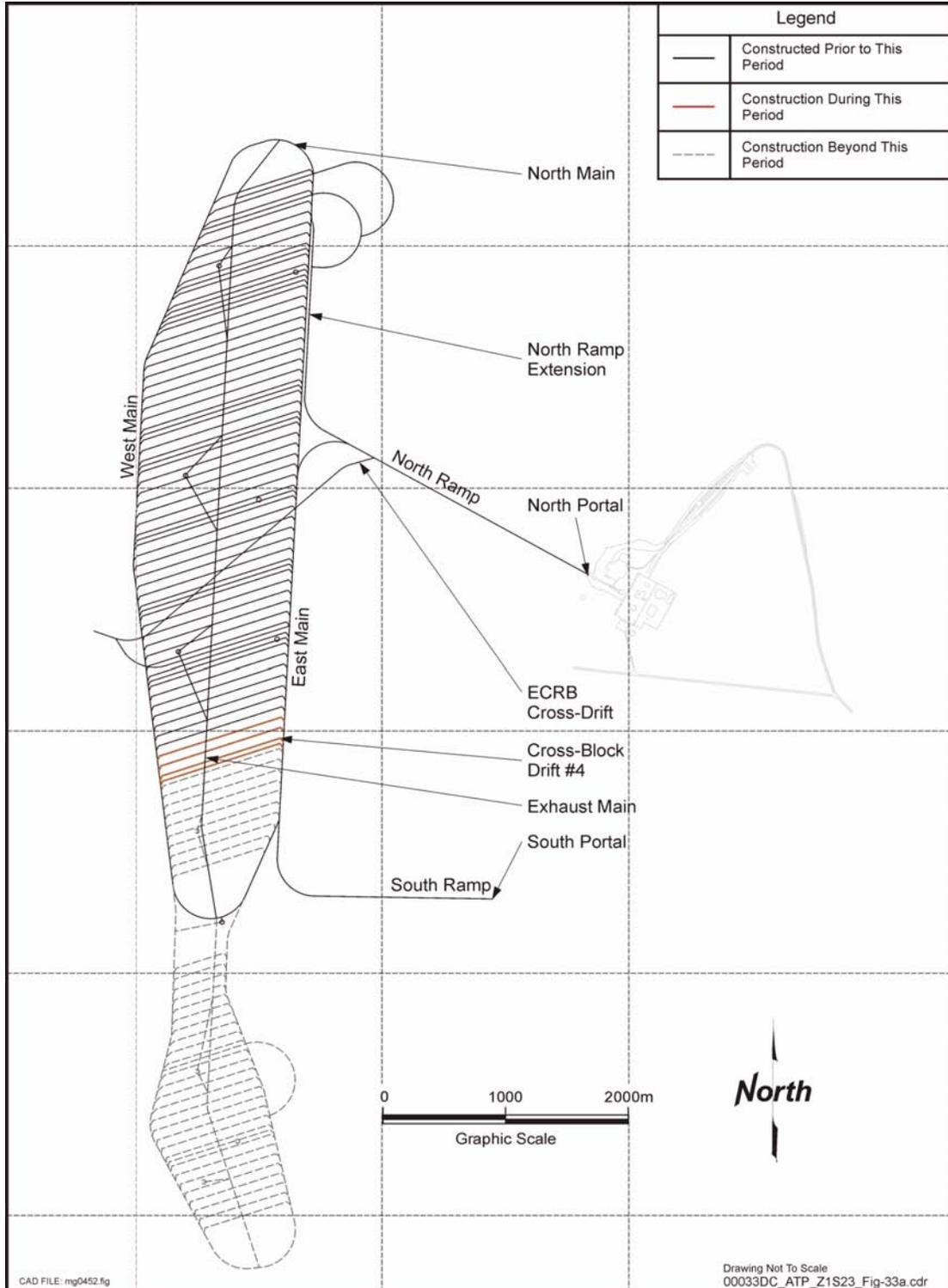
Figure 2-70.   Repository Subsurface Layout—Development and Emplacement for Phase IV
Construction activities are limited in Phase IV of development, with the last three emplacement drifts for the base case layout being completed.

fill material, placed either as a homogeneous fill or as a layered system with flow capillary barrier capabilities; chemical retardation and sorption materials in the invert; and precast concrete emplacement drift lining (a ground support system with limited barrier attributes). Discussion of the design evolution and reasons for the elimination of these other engineered barriers are provided in Section 2.1.2 and documented in design assessments (CRWMS M&O 1999c; CRWMS M&O 1999d; Wilkins and Heath 1999; Dyer 2000). The emplacement drift backfill has been retained as an engineered barrier option (Dyer 2000).

The description of engineered barriers provided in this section is summarized from a large set of design descriptions and analyses, including:

- *Invert Configuration and Drip Shield Interface* (CRWMS M&O 2000aq)
- *Design Analysis for the Ex-Container Components* (CRWMS M&O 2000ap)
- *Drip Shield Emplacement Gantry Concept* (CRWMS M&O 2000ar).

2.4.1 Drift Invert

The term "invert" in this design includes the structures and materials that form a platform that supports the pallet and waste package, the drift rail system, and the drip shield. The invert is composed of two parts: the steel invert structure and the ballast (fill), which is composed of granular material.

2.4.1.1 Steel Invert Structure

The design of the steel invert structure must consider construction loads, waste package emplacement and retrieval loads, drip shield loads, and thermal and seismic loads. In case the backfill design option is used in the future, the invert design also considered any backfill loads and related backfill emplacement loads. The invert configuration has to accommodate the other structures inside the emplacement drifts, namely the ground support structures, waste package pallet, waste package emplacement gantry, inspection gantry, drip shield emplacement gantry, and backfill emplacement equipment (if backfill is used).

The invert structures would support repository preclosure operations for up to 300 years with limited maintenance in the emplacement drift environment. Additionally, the invert design will be coordinated with the pallet design to fulfill the requirement for maintaining the waste packages in a horizontal emplacement position for 10,000 years after closure (CRWMS M&O 2000aq, Section 4.2.1.7).

Steel materials were selected for the inverts to avoid uncertainties associated with the use of cementitious materials in the emplacement drifts (CRWMS M&O 2000aq, Section 6.2). There is some concern with the use of steel products in the emplacement drifts because of potential impacts on radionuclide transport after waste packages have degraded. The concern is rooted in the fact that ferric-based iron colloids can transport radionuclide materials. Although the concern is applicable only after the waste packages have failed, it may affect the peak dose rate at the time beyond 10,000 years, which is the design life for the waste packages. The ferric-based iron colloids will mainly affect solubility-limited radionuclides, such as plutonium and americium, which have a high affinity with iron-oxyhydroxide colloids (CRWMS M&O 2000as, Section 3.1.2). This potential impact has been considered in TSPA evaluations. Figure 2-71 illustrates the proposed steel invert structure in place in the drift. It shows the relationship of the steel invert structure with the invert ballast, drift wall, ground support structure, pallet and waste package, and drip shield. Figure 2-72 provides a perspective view of a section of an emplacement drift, illustrating the location of the invert components with respect to the ground support steel sets. The steel drift invert is not part of the ground control system. The transverse support beams for the invert would be installed between the structural steel ground control components, as shown in Figure 2-72. To maintain the structural independence of the invert, the ground control components would not contact the steel invert components.

The transverse support beams, which are part of the structural steel invert frame, would rest on the drift wall in such a way that they transfer the loads directly to the rock. Installation of the steel invert structure would include shimming, aligning, and
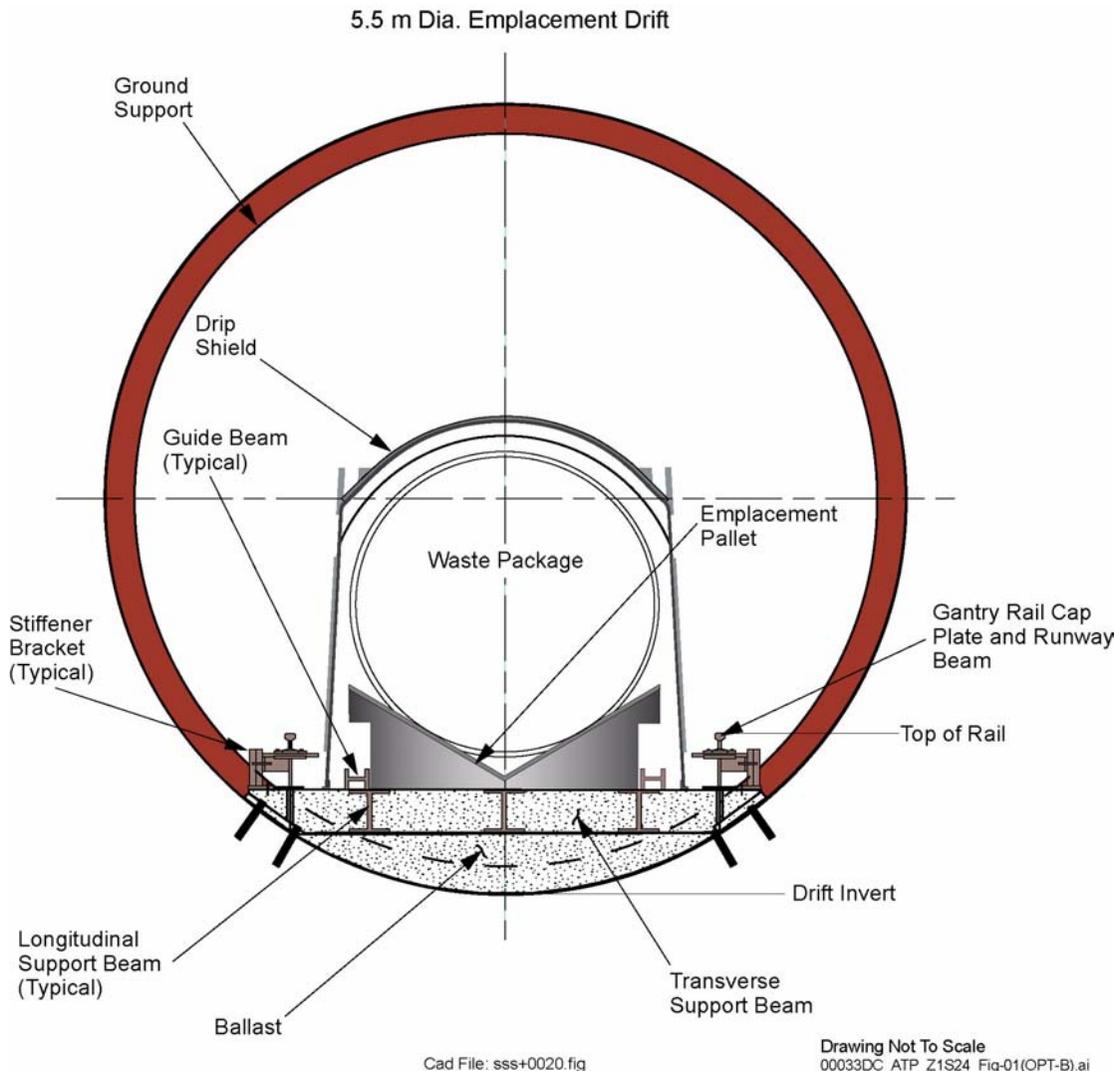
Figure 2-71.   Emplacement Drift Cross Section with Invert Structure in Place
This cross section of an emplacement drift shows the engineered barriers and the invert section structures and components. This figure also illustrates how the invert structure is supported by and attached to the drift wall. Source: CRWMS M&O 2000aq, Figure 5.

anchoring the attached base plates to the drift rock wall. The pallet, loaded with a waste package, would rest directly on the structural steel invert frame. The steel invert frame would also support the drip shield and any backfill material, if used, placed directly above the frame and directly above the drip shield, along with the backfill emplacement equipment, the inspection gantry, and the drip shield emplacement gantry. The drip shield would transmit the weight of backfill placed directly above it to the emplacement drift invert structure.

The emplacement drift rail, as shown in Figures 2-71 and 2-72, is mounted on the steel invert. Therefore, the invert structure would also support the transportation loads from the waste package gantry and the remote inspection gantry (CRWMS M&O 2000aq, Section 6.4). The inspection gantry is described in Section 2.5.

The invert structure has three longitudinal support beams that provide continuous support for the emplacement pallets (Figure 2-72). The spacing of the gantry rail centerlines accommodates the drip shield gantry, used for shield emplacement opera-
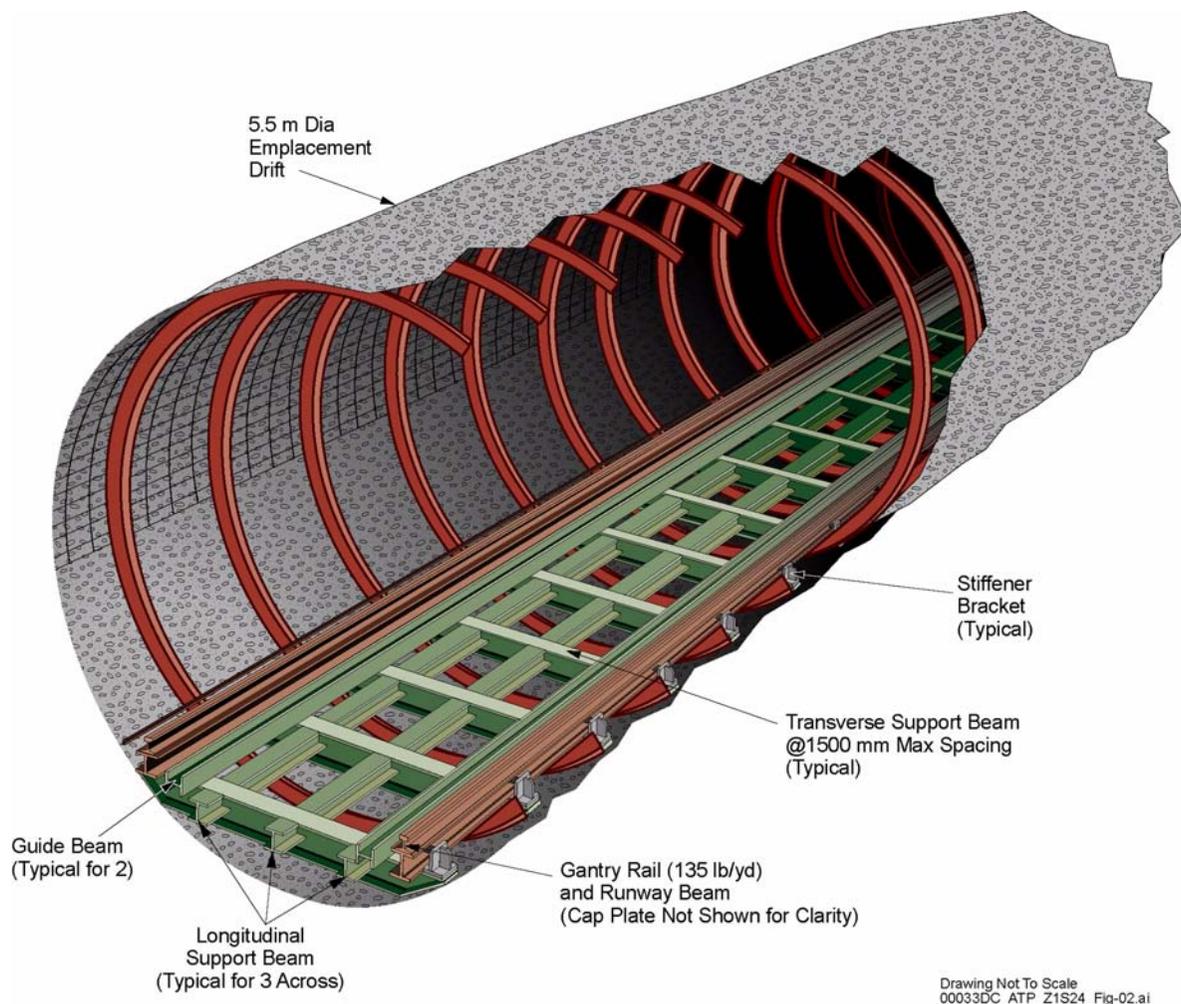
Figure 2-72. Emplacement Drift Perspective View with Steel Invert Structures in Place
This figure shows the transverse and longitudinal beams for the invert structure and how they are positioned with respect to the ground support steel sets. Source: CRWMS M&O 2000aq, Figure 6.

tions. After all the assembly details are specified, the invert design will be checked against dynamic seismic loads to ensure structural integrity and to ensure that the loaded pallet and drip shield do not move significantly from their original locations because of seismic events (CRWMS M&O 2000aq, Section 6.4). Movement of the loaded pallet and drip shield can be mitigated, if necessary, by the installation of guide beams made of structural steel, as shown in Figures 2-71 and 2-72. The emplacement drift invert can be periodically monitored and repaired or replaced as necessary to ensure that the intended emplacement position of each waste package is maintained for a preclosure period of up to 300 years (CRWMS M&O 2000aq, Section 6.4).

Selection of the invert structure materials was based on structural strength properties, compatibility with the emplacement drift environment, and expected longevity. These requirements are contained in the *Emplacement Drift System Description Document* (CRWMS M&O 2000ab, Section 1.2.1). The structural members of the emplacement drift invert would be made of ASTM A 572/A 572M steel. A crane rail of ASTM A 759 carbon steel would be used for the gantry rail. Compatibility of the carbon steel invert materials with the materials forming the drip shield base is being evaluated to determine the potential effects of corrosion. The shield plates for the drip shields would be made with Titanium Grade 7, and the drip shield structural members would be made with

Titanium Grade 24 (CRWMS M&O 2000ap, Section 4.1). A structural angle of Alloy 22 would be used as a base (at the bottom of the side plates of the drip shield) to separate the titanium materials from the carbon steel invert materials (CRWMS M&O 2000aq, Section 6.5).

2.4.1.2   Invert Ballast

The repository subsurface layout is configured so moisture entering the emplacement drifts during preclosure and postclosure periods can drain directly into the surrounding host rock without draining along the drift. A design criterion requires that the invert ballast material be crushed tuff (CRWMS M&O 2000aq, Section 4.3.3). Crushed tuff would be produced by crushing the material removed from Yucca Mountain in the process of excavating the emplacement drifts. Because of the inherent resistance of crushed tuff and carbon steel to the thermal loads expected, these materials will not be affected by the temperatures expected in the emplacement drifts (CRWMS M&O 2000aq, Section 6.5). The principal function for the invert ballast material as an engineered barrier is to provide a layer of material below the waste packages in which the transport of radionuclides from the emplacement drifts into the host rock is dominated by diffusive transport, which is slower than the kind of flow expected to occur in rock fractures. Radionuclides would only be released into the emplacement drifts after deterioration of the waste packages results in the release of radionuclides to the environment. It is expected that crushed tuff ballast materials will provide such a barrier (CRWMS M&O 2000aq, Section 6.4). Materials and their properties are being tested and investigated; the results of those investigations will be incorporated into future design enhancements.

Ballast material would be placed in and around the steel members of the invert structure to an elevation just below the top of the longitudinal and transverse support beams (Figures 2-71 and 2-72). This level of fill will ensure that the pallets and drip shields do not rest on the ballast material, but are fully supported by the steel invert beams. The ballast material would be sufficiently compacted to consolidate it to the point where settlement of the ballast over time would not be significant. The gap

resulting from consolidation would be small enough that the ballast would prevent the backfill material, if used, from migrating under the bottom of the drip shield during placement.

2.4.2   Ground Support

The primary purpose of ground support systems is to maintain the stability and geometry of the emplacement drifts during preclosure. However, some ground support systems (see Section 2.3.4.1 for a description) offer secondary benefits as engineered barriers.

The VA design (DOE 1998, Volume 2) used a precast concrete liner as the ground support for the emplacement drifts. This type of ground support system would offer some additional value as an engineered barrier by serving as a barrier to flow into the drift. The precast concrete liner would not prevent water from entering the drift, but would serve as a diversion barrier by forcing water to follow the path of least resistance. This engineered barrier function, however, would last only while the concrete liner remained intact, and concrete may raise the alkalinity in the drift, adversely impacting the containment of radioactive materials. Consequently, the concrete liner in the emplacement drift was eliminated from the design described in this report.

The concrete liner design for the ground support system for the emplacement drifts was replaced with steel sets with welded-wire fabric and rock bolts. Like the concrete liner, these types of structures support waste isolation by preventing rockfall during preclosure. This report and its supporting documents currently support the use of steel sets, in addition to rock bolts and steel wire fabric, to enhance the reliability of the no-maintenance or low-maintenance design concept for the emplacement drifts. However, concerns about introduction of man-made materials into the emplacement drifts may cause future changes in the design. Deterioration of steel products over time results in iron-oxide by-products that may potentially impact the longevity of waste package materials and the transport of radionuclides away from the drift. This concern, if proven valid and significant, may result in a requirement for minimization of steel products

in the emplacement drifts, which may shift the emphasis to a ground support design that relies mainly on rock bolts and steel wire fabric or other attractive design options.

2.4.3 Support Assembly for the Waste Package

In accordance with project design criteria, the invert and the emplacement pallet must maintain the waste package in its nominal emplacement position for 300 years. This requirement satisfies waste package retrieval needs, if that option is exercised. Another design criterion for the invert and the emplacement pallet is that they shall maintain the nominal horizontal emplacement position of the waste package for 10,000 years after closure (CRWMS M&O 2000ap, Section 4.2). This criterion supports waste isolation by keeping the waste package under the drip shield, where it is less vulnerable to rockfall or degradation from water-induced corrosion.

The design of the emplacement pallet fulfills these requirements by using construction materials that will last 10,000 years, and by providing structurally sound and stable invert and pallet designs. Horizontal movement of the waste package over 10,000 years may be caused by support beam corrosion, ballast settlement, and seismic activity (CRWMS M&O 2000ap, Section 6.2.2). Support beam corrosion and ballast settlement will be evaluated during later design phases, as will the seismic response of the emplacement pallet loaded with a waste package.

2.4.3.1 Pallet Design

The pallet design supports line-loading of waste packages by allowing placement of waste packages end to end within 10 cm (4 in.) of each other. The pallet is shorter than the waste package (Figure 2-52), so it does not interfere with the close placement requirement.

The emplacement pallets would be fabricated from Alloy 22 plates welded together to form the waste package supports. Alloy 22 is highly resistant to corrosion. Two supports, one at each end of the pallet, would be connected by four square stainless

steel tubes to form the completed emplacement pallet assembly (Figure 2-51). These pallet tubes would be fabricated from Stainless Steel Type 316L for corrosion survivability (CRWMS M&O 2000ap, Section 4.1). The Alloy 22 supports have a V-shaped top surface to accept all waste package diameters (CRWMS M&O 2000ap, Section 6.2.1). All surfaces of the emplacement pallet that contact a waste package outer barrier would be Alloy 22, the same material as the outer barrier (CRWMS M&O 2000ap, Section 6.2.2).

Calculations determined the dimensions required of emplacement pallet components to keep stresses within the allowable limits while under static loading. These calculations were performed for an emplacement pallet loaded with the heaviest waste package and resting on the invert (CRWMS M&O 2000ap, Section 6.5). Stress corrosion cracking is not considered an issue for the emplacement pallet because the waste package loads acting on the supporting surfaces are compressive loads. Thus, the emplacement pallet plates would not be susceptible to stress corrosion cracking. Corrosion during the first 300 years would be negligible.

In summary, the prevention of stress corrosion cracking, in conjunction with the corrosion resistance of Alloy 22 and Stainless Steel Type 316L, will contribute to long-term pallet integrity. This, in turn, will ensure that the pallet will maintain the waste package in its normal emplacement position for a preclosure period of up to 300 years (CRWMS M&O 2000ap, Section 6.5). The same factors will contribute to the ability of the pallet to maintain the waste package in its nominal horizontal position for 10,000 years after closure.

2.4.3.2 Pallet Interface with Invert

As explained in Section 2.4.1.1, the steel invert has transverse support beams that rest on the rock wall. Attached to these transverse support beams are three longitudinal support beams that provide continuous support for the emplacement pallets (Figures 2-71 and 2-72). The transverse support beams and longitudinal support beams thus transfer the waste package load to the rock at the points where the transverse beams rest on the rock wall. The steel invert materials would be fabricated in

panels consisting of longitudinal and transverse support beams with attached base plates. Adjacent panels would be attached by bolting or welding.

2.4.4   Drip Shield

Design requirements for the emplacement drift system (CRWMS M&O 2000ab) state that drip shields be installed over the waste packages before closure. After closure, and after the heat produced by the waste packages has dissipated, moisture may enter the emplacement drifts in liquid form or as water vapor. The function of the drip shields is to divert the liquid moisture that drips from the drift walls, as well as the water vapor that condenses on the drip shield surface, around the waste packages and to the drift floor, prolonging the longevity and structural integrity of the waste packages. The drip shields are designed to link together, forming a single, continuous barrier for the entire length of the emplacement drift. Table 2-22 summarizes the preliminary engineering specifications for the drip shield design.

Table 2-22. Drip Shield Design Detail

Item	Detail
Material • 15-mm water diversion surfaces • Structural members • Stands (feet)	Titanium Grade 7 Titanium Grade 24 Alloy 22
Dimensions • Height • Width • Length • Weight	2,586 mm (overlap end) 2,521 mm (butt end) 2,512 mm (overlap end) 2,505 mm (butt end) 6,105 mm 3.087 metric tons

Source: CRWMS M&O 2000at, Attachment II.

The design requirements for drip shields include corrosion resistance as well as structural strength. Corrosion resistance is required so the drip shields can perform their moisture diversion function with high reliability for 10,000 years. Structural strength is required so the drip shield can protect the waste package against damage by rockfalls resulting from degradation of the drift walls, withstanding damage from rocks weighing up to 6 metric tons (CRWMS M&O 2000ab, Sections 1.2.1.14 and 1.2.1.15).

The drip shields must also withstand the static loads from backfill (if used) and rock from the design basis rockfall without exceeding 20 percent of the yield strength of the drip shield materials. This requirement is needed to prevent stress corrosion cracking (CRWMS M&O 2000ap, Section 4.2.3).

2.4.4.1   Drip Shield Design

Figure 2-73 illustrates the drip shield design. The drip shield would be fabricated from Titanium Grade 7 plates for the water diversion surfaces, Titanium Grade 24 for the structural members, and Alloy 22 for the feet. The Alloy 22 feet would be mechanically attached to the titanium drip shield side plates, since the two materials cannot be welded together. The Alloy 22 feet prevent direct contact between the titanium and the carbon steel members in the invert, which could result in hydrogen embrittlement of the titanium (CRWMS M&O 2000ap, Section 6.1.1). All the drip shields would be uniformly sized, so one design will suffice for any waste package size. As Figure 2-74 illustrates, the drip shield sections interlock to prevent separation between sections. The interlocking is accomplished by using pins and holes and also by using an overlapping section with connector guides.

To provide long-term protection against corrosion, the drip shield would be manufactured entirely of Titanium (Grades 7 and 24) and Alloy 22. Calculation results have verified that the long-term static stresses that could lead to stress corrosion cracking will remain below 20 percent of the yield strength of the materials in the drip shield components (CRWMS M&O 2000ap, Section 6.1.2.7). A Titanium Grade 7 thickness of 15 mm (0.6 in.) has been selected for long-term corrosion resistance. Calculations have verified the adequacy of this thickness and material grade. Titanium Grade 24 was selected for the structural components because of its superior strength in comparison with Titanium Grade 7. The required dimensions for the Titanium Grade 24 structural components, shown in Figure 2-75, have been defined by structural calculations (CRWMS M&O 2000ap, Section 6.1.2).
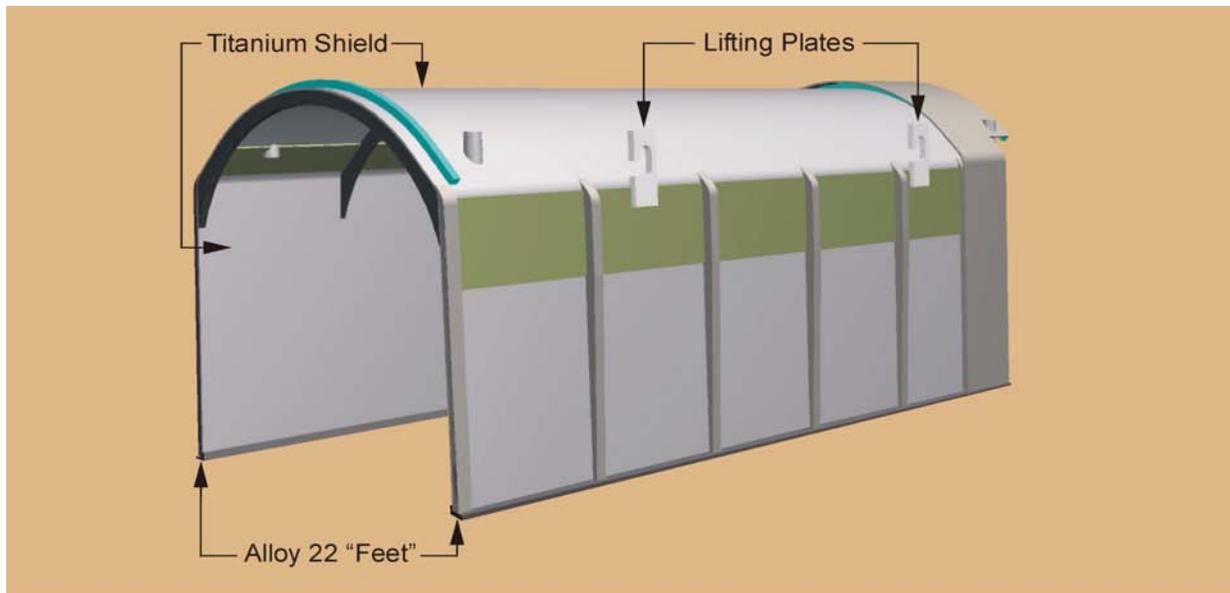
Figure 2-73.   Drip Shield Isometric View
The drip shield is a self-standing structure built from structural grade titanium. Source: Modified from CRWMS M&O 2000ap, Figure 1.
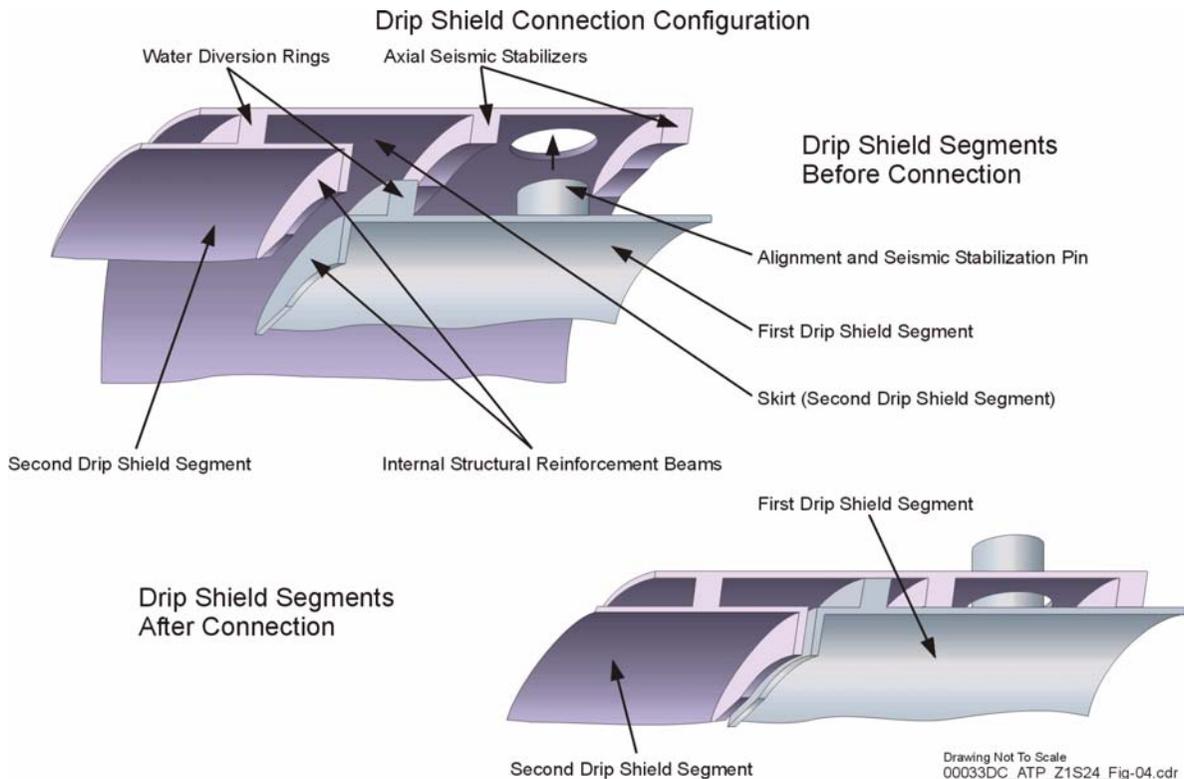
Figure 2-74.   Drip Shield Interlocking Connection
The drip shield has a raised section at one end that overlaps and interlocks with the adjacent drip shield. Built-in water diversion rings keep moisture from penetrating the drip shield interface area. Source: CRWMS M&O 2000ap, Figure 2.

The geometry of the drip shield design will divert dripping water around the waste package and onto the emplacement drift floor. The interlocking mechanisms of the drip shield include water diversion rings to divert dripping water at the seams between drip shield segments and around the waste packages to the emplacement drift floor.

2.4.4.2   Drip Shield Interface with Invert

The drip shield feet would rest on the transverse support beams of the drift invert and alongside the longitudinal guide beams, as Figure 2-71 illustrates. The guide beams are also shown in Figure 2-72. The primary purpose of these longitudinal guide beams is to center the emplacement pallet; however, they also create a separation barrier between the pallet and the drip shield.

2.4.4.3   Drip Shield Emplacement

A drip shield emplacement gantry would emplace the drip shields (CRWMS M&O 2000ar, Section 6.1). The emplacement gantry is designed specifically to emplace drip shields over emplaced waste packages in the 5.5-m (18-ft) diameter emplacement drifts. The drip shield emplacement gantry design is based on the waste package emplacement gantry design, with similar structural and mechanical components. In addition to the drip shield emplacement gantry, other equipment used in drip shield emplacement operations includes:

- A flatbed gantry carrier railcar
- A flatbed railcar for transportation of the drip shields
- A locomotive to move the railcars.

The drip shield emplacement operation is similar to the waste package emplacement operation described in Section 2.3.4.5. The locomotive and the gantry carrier would transport the drip shield emplacement gantry to the emplacement drift turnout. After following the same sequence of events for switching to remote control operation of the locomotive and opening the drift isolation doors, the gantry carrier would dock at the emplacement drift. The remote control operators would then drive the drip shield emplacement gantry into the drift and put the gantry on standby

inside the drift until a drip shield is delivered to the emplacement drift entrance. After a drip shield carrier car docks at the emplacement drift, the drip shield emplacement gantry would move over a drip shield by straddling the railcar. The gantry would engage the drip shield using a set of four lift pins that engage lifting plates on the shield. The gantry would lift the drip shield off the railcar, then carry the shield through the emplacement drift and over the waste packages to emplace the shield (CRWMS M&O 2000ar, Section 6.1). Figure 2-76 shows the drip shield emplacement gantry. An insert on this figure shows the lift plate and lift pin interface.

The weight of each drip shield unit has been estimated at about 3 metric tons (CRWMS M&O 2000ar, Section 5.4), but an upper-limit bounding value of 4 metric tons was used in the design. The lifting mechanism on the gantry uses ball-screw jacks, a common form of screw jack used for lifting heavy loads, to raise the drip shields. This mechanism has longer duty cycles and higher efficiencies than typical machine screw mechanisms. The gantry frame is a steel structure designed to support its own weight, the weight of the drip shield, and any seismic loads. The gantry would be self-propelled, using four two-wheeled trucks, with one truck placed at each corner of the gantry frame. A direct-current, variable-speed electric motor would drive one wheel in each truck through a gear reducer and chain drive. An integral brake within the direct-current electric motor would provide braking. Integral brake motors would work in a fail-safe configuration: if the electric motor loses power, a spring mechanism would automatically apply the brakes. All motors (including the ball-screw jack motors) and any other operating components of the gantry would be electrically operated and controlled (CRWMS M&O 2000ar, Sections 6.2.1 and 6.2.3).

The frame for the drip shield emplacement gantry would be made of ASTM A 36 steel and fabricated following American Welding Society standards. The selection of ASTM A 36 steel, or possibly other high-strength steels, will be reevaluated during final design of the gantry. The gantry frame and lifting mechanism dimensions would be sized to provide sufficient clearance for the drip shield over the rail transporter and emplacement drift

Component Name	Material	Thickness	Mass (KG)	Qty Rod
Drip Shield Plate-1	SB-265 R52400	15	837	1
Drip Shield Plate-2	SB-265 R52400	15	780	2
Base	SB-575 N06022	10	55	2
Bulkhead	SB-265 R56400	38	45	4
Peripheral Bulkhead	SB-265 R56400	48	56	2
Post	SB-265 R56400	100	5.6	2
Internal Support Plate	SB-265 R52400	12.7	16	10
External Support Plate	SB-265 R52400	12.7	27	10
Lifting Plate	SB-265 R56400	50	17	4
Support Beam-Connector	SB-265 R56400	102	27	6
Support Beam-Large	SB-265 R56400	76	37	8
Drip Shield Connector Guide	SB-265 R52400	50	30	2
Drip Shield Connector Plate-1	SB-265 R52400	15	142	1
Drip Shield Connector Plate-2	SB-265 R52400	15	89	2
Drip Shield Connector Guide-A	SB-265 R52400	50	26	1
Drip Shield Connector Guide-B	SB-265 R52400	50	31	1
Drip Shield Assembly	-	-	4203	1

Note: All measurements are in mm.
Do not scale from drawing.

Drawing Not To Scale
00033DC_ATP_Z1S24_Fig-05.cdr

Figure 2-75.   Drip Shield Structural Components
Support beams, bulkheads, and support plates give the drip shield the strength and structural rigidity required to withstand backfill, if used, and rockfall. All measurements are in millimeters. Do not scale from drawing. OD = outside diameter; ID = inside diameter. Source: Modified from CRWMS M&O 2000at, Attachment II.
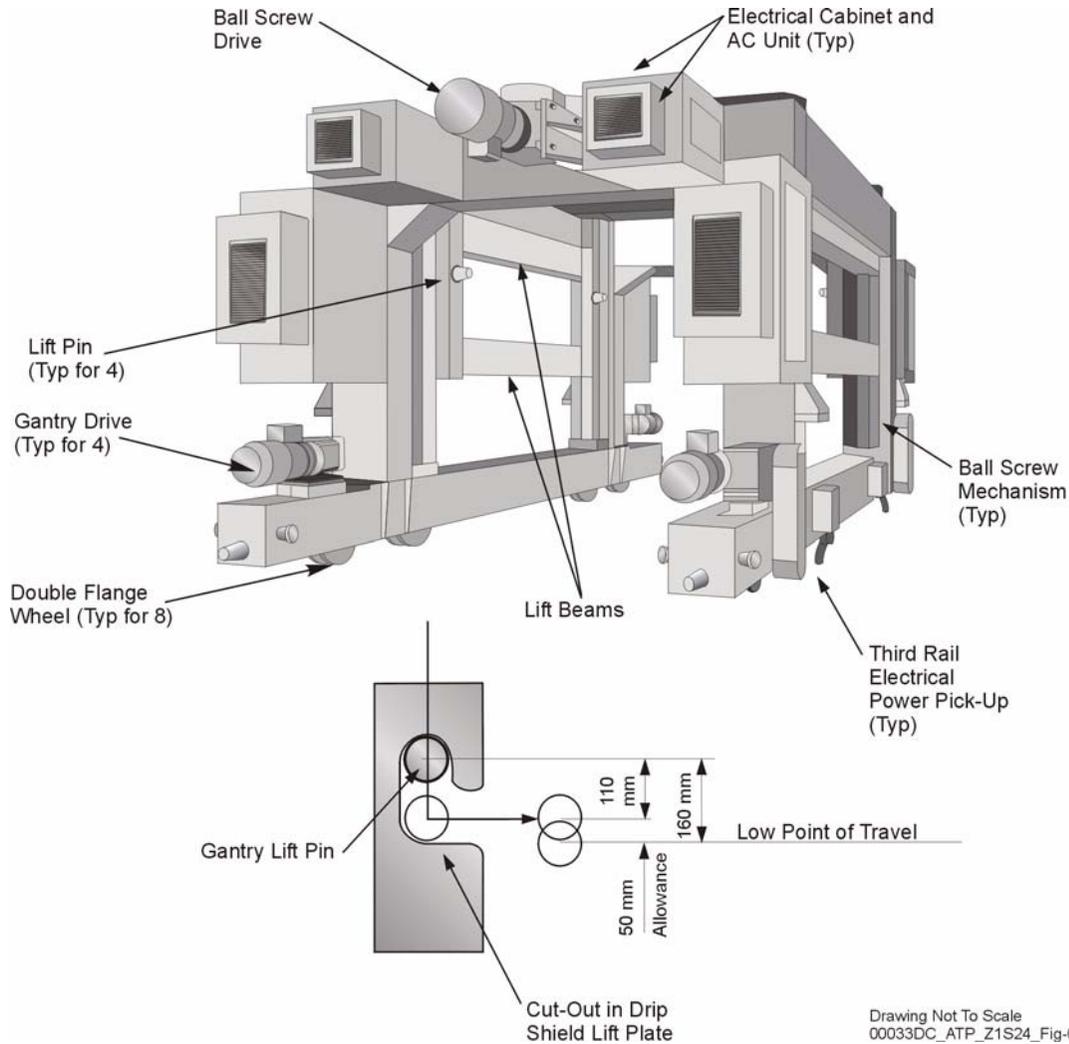
Figure 2-76.   Drip Shield Emplacement Gantry and Lift Pin Mechanism
The drip shield emplacement gantry has a lift pin mechanism to engage the shield, lift it, and safely emplace it over the waste packages. AC = air conditioning. Source: CRWMS M&O 2000ar, Figures 2 and 4.

structural invert. These dimensions also take into account the vertical travel distance required for lifting pin disengagement (CRWMS M&O 2000ar, Section 6.2.3, Figure 3).

The drip shield emplacement gantry is designed to operate in the harsh environment inside the emplacement drifts, taking into account the moderately high temperature of 50°C (122°F), a relative humidity ranging from 10 to 100 percent, and high radiation levels. Operators at a remote control console located at the surface would remotely control the drip shield emplacement gantry (CRWMS M&O 2000ar, Section 6.2.5).

The primary source of electrical power for the drip shield emplacement gantry would be an electrified third rail (conductor bar) system. This is the same electrical supply system that would be used by the waste package emplacement gantry. Like the waste package emplacement gantry, the drip shield emplacement gantry would be supplied with redundant power pickup mechanisms to ensure a reliable and continuous source of power. The gantry would also carry an emergency backup power system that would provide a limited supply of electrical power. This backup system would provide enough power for the gantry to lower and release a drip shield and move to the emplacement drift entrance (CRWMS M&O 2000ar, Section 6.2.5.1).

Instrumentation and controls on the gantry would consist of high-resolution, articulated, closed-circuit television cameras and a series of high-intensity lights. The gantry would be equipped with thermal and radiological sensing instruments. Onboard cabinets and all temperature-sensitive components would be cooled with air-conditioning units mounted on each enclosure. The gantry would also be equipped with a fire protection system that would respond automatically if an onboard fire is detected. The fire detection portion of the system would immediately notify remote operators, through the gantry control computers, of the location and nature of the fire (CRWMS M&O 2000ar, Section 6.2.5.6).

Figure 2-77 illustrates a typical section of an emplacement drift with a series of emplaced waste packages of different sizes and with the drip

shields in place. A portion of the drip shields has been cut out in the illustration for clarity in showing placement of the waste packages and interlocking of the drip shields.

No significant rockfall is anticipated during the preclosure period. It is envisioned that special equipment or attachments to the waste package or drip shield emplacement gantries will be used to "sweep" the mating surface of the emplaced drip shield on which the adjacent drip shield will be coupled. Debris on the invert surface that could interfere with emplacement of the drip shields would be removed or "plowed" aside. These operations would occur before or during drip shield emplacement. The design of such equipment will be developed as needed and as the detailed subsurface equipment designs evolve.
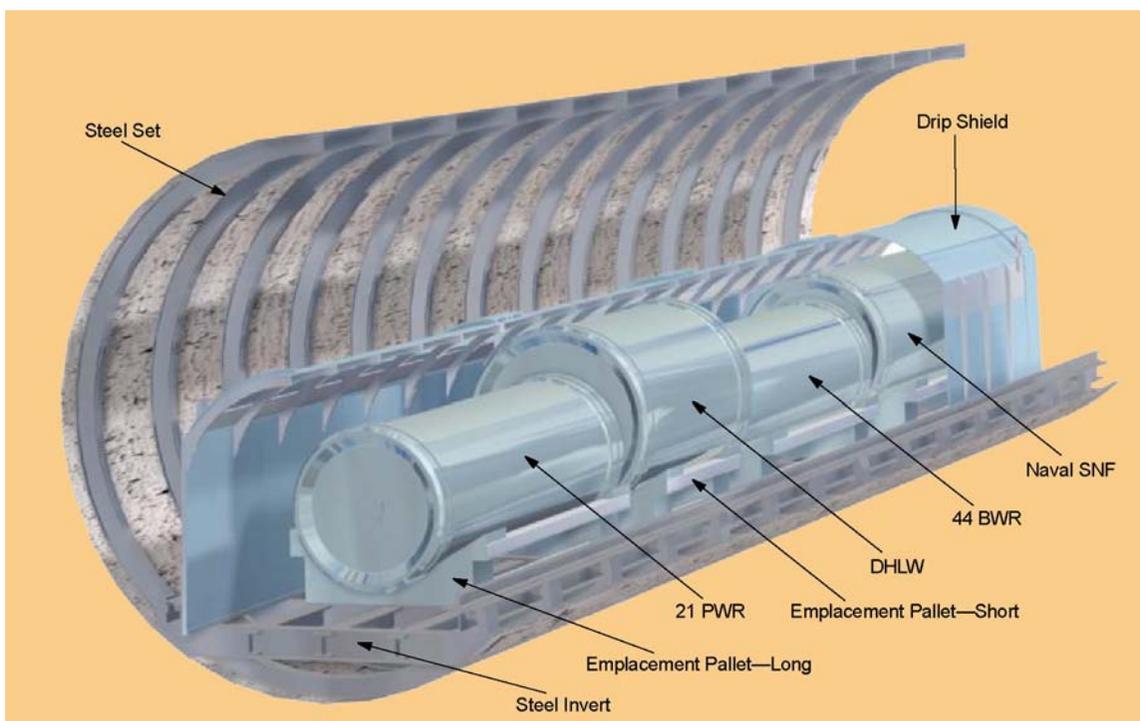
Drawing Not To Scale
00033DC_ATP_Z1S25_Fig-05.ai

Figure 2-77.   Typical Section of Emplacement Drift with Waste Packages and Drip Shields in Place
The final configurations of waste package emplacement and drip shield emplacement are illustrated in this figure. A cutaway view is provided to better illustrate the waste packages. The different types of waste packages are shown for illustration purposes only. One size drip shield accommodates all sizes of waste packages.

2.5 PERFORMANCE CONFIRMATION FACILITIES DESIGN

This section discusses the elements of repository subsurface design that support the *Performance Confirmation Plan* (CRWMS M&O 2000ag). Section 4.6 summarizes the objectives and scope of the plan. Section 5.4 outlines additional testing and evaluation performed during the preclosure years that will support the performance confirmation program. The description of performance confirmation facilities provided in this section is based primarily on *Performance Confirmation Plan* (CRWMS M&O 2000ag).

2.5.1 Facilities Functions and Types

The roles of the subsurface systems in support of performance confirmation are:

- Constructing the subsurface facilities required for performance confirmation program implementation

- Supporting the installation of monitoring equipment, instrumentation, data acquisition systems, and data communication networks

- Providing operations support and system maintenance

- Providing transportation, ventilation, and utilities

- Supporting planning and construction of future facilities, as needed

- Operating and supporting specialized emplacement drift access equipment, such as the remote inspection gantry.

The subsurface systems provide facilities to support monitoring of the natural and engineered barriers, emplacement drift and main drift environments, rock temperature and moisture regimes, water inflow into emplacement drifts, waste package integrity, and seismic activity. The subsurface facilities supporting the performance confirmation program can be grouped into the following types:

- Postclosure test drifts
- Observation drifts
- Alcoves
- Niches
- Boreholes.

A single type or a combination of these types of facilities can constitute a performance confirmation arrangement, depending on the requirements for access to the monitored geologic media and on the objectives of the monitoring. For example, monitoring the rock environment between emplacement drifts would require a combination of an observation drift, alcoves, and boreholes. The observation drift would provide the main access facility for personnel and equipment and would serve as a ventilation airway to maintain ambient temperatures suitable for personnel and instruments. Alcoves extend away from the observation drifts, like fingers, to provide advantageous positioning of monitoring equipment. Alcoves also provide space for installation equipment (e.g., drilling rigs) and monitoring equipment away from the observation drift transportation corridor. The alcoves are designed such that they provide strategic platforms from which instrumentation boreholes can be drilled. Boreholes drilled at different angles and to different lengths can provide monitoring access to the rock media at many locations around the emplacement drifts. The boreholes used in performance confirmation will be small-diameter, precision-drilled holes that allow remote access to monitoring locations within the rock. They offer a less intrusive way to reach areas around the emplacement drifts. Niches are small, excavated areas along the walls of the main drifts or observation drifts that would be used for setting up specialized instruments or monitoring equipment, such as seismometers or data communications equipment.

2.5.2 Proposed Performance Confirmation Facilities

Figure 2-78 illustrates the proposed locations of the performance confirmation facilities. This figure is a layout of the potential repository that shows how
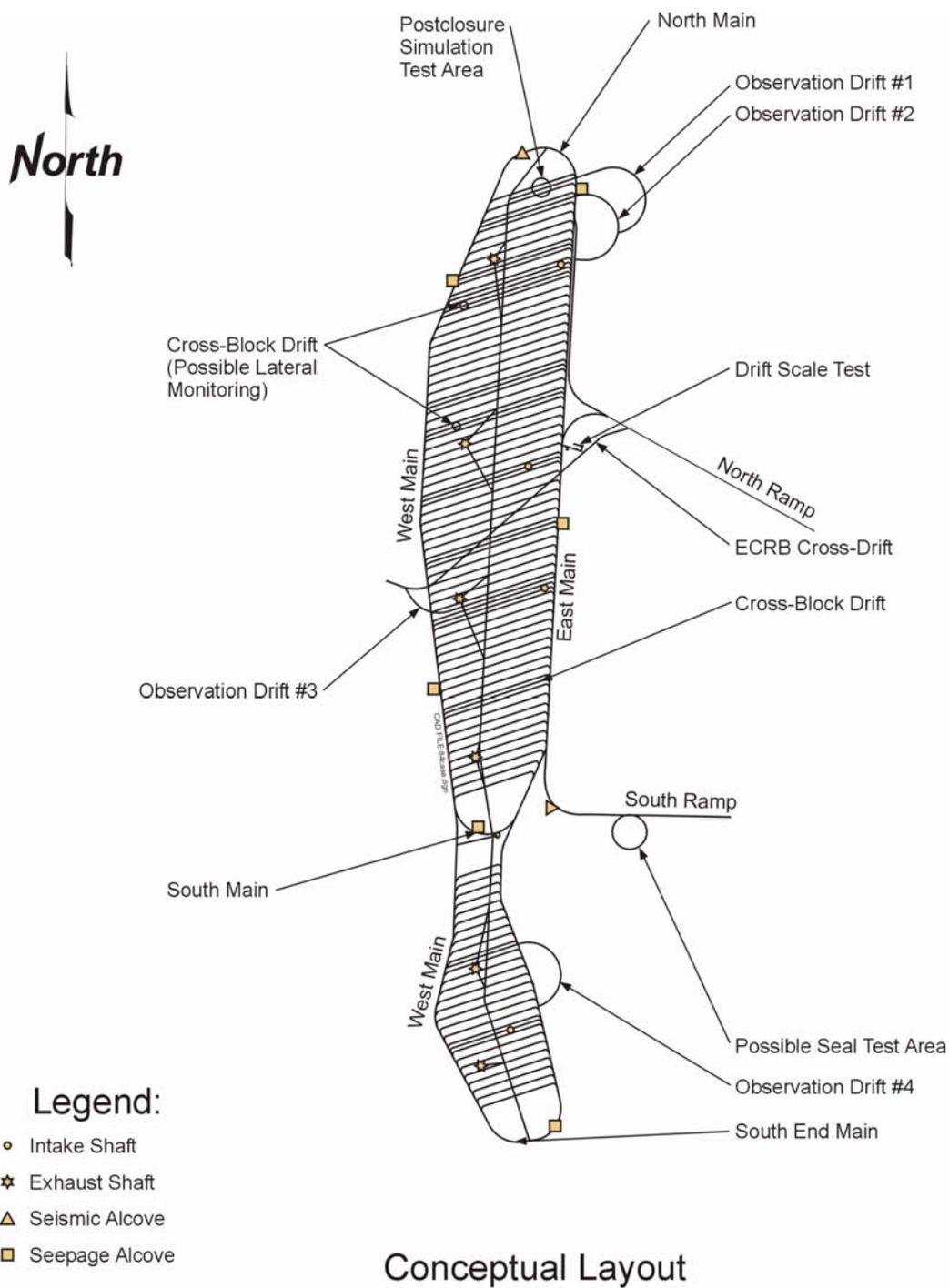
Figure 2-78. Subsurface Performance Confirmation Facilities Layout
This plan view shows the major subsurface facilities that support performance confirmation activities and how those facilities relate to the rest of the subsurface facilities layout. Source: Modified from CRWMS M&O 2000ag, Figure 5-4.

the proposed performance confirmation facilities have been completely integrated into the overall repository design for the best use of access, transportation, and ventilation networks.

2.5.2.1   Postclosure Simulation Test Area

The Postclosure Simulation Test Area consists of a single test drift, located at the edge of the emplacement horizon, with similar physical characteristics to a representative emplacement drift. This test drift would be separated into test sections, which would allow for the simulation of several different test cases. Within a particular test section, heaters

or actual waste packages would be emplaced for a period long enough to allow for heating and drying effects on the adjacent rock mass. After a prescribed time, the postclosure configuration would be constructed in the section with heater-equipped surrogate or actual waste packages, and drip shields, using expected postclosure configurations. Instruments would be placed in the drift from adjacent alcoves associated with an observation drift (Figure 2-79) located below the emplacement level. The alcoves would be located below the postclosure test drift to minimize any potential impact on the moisture flow around the test drift opening (i.e., the near-field geohydrology).
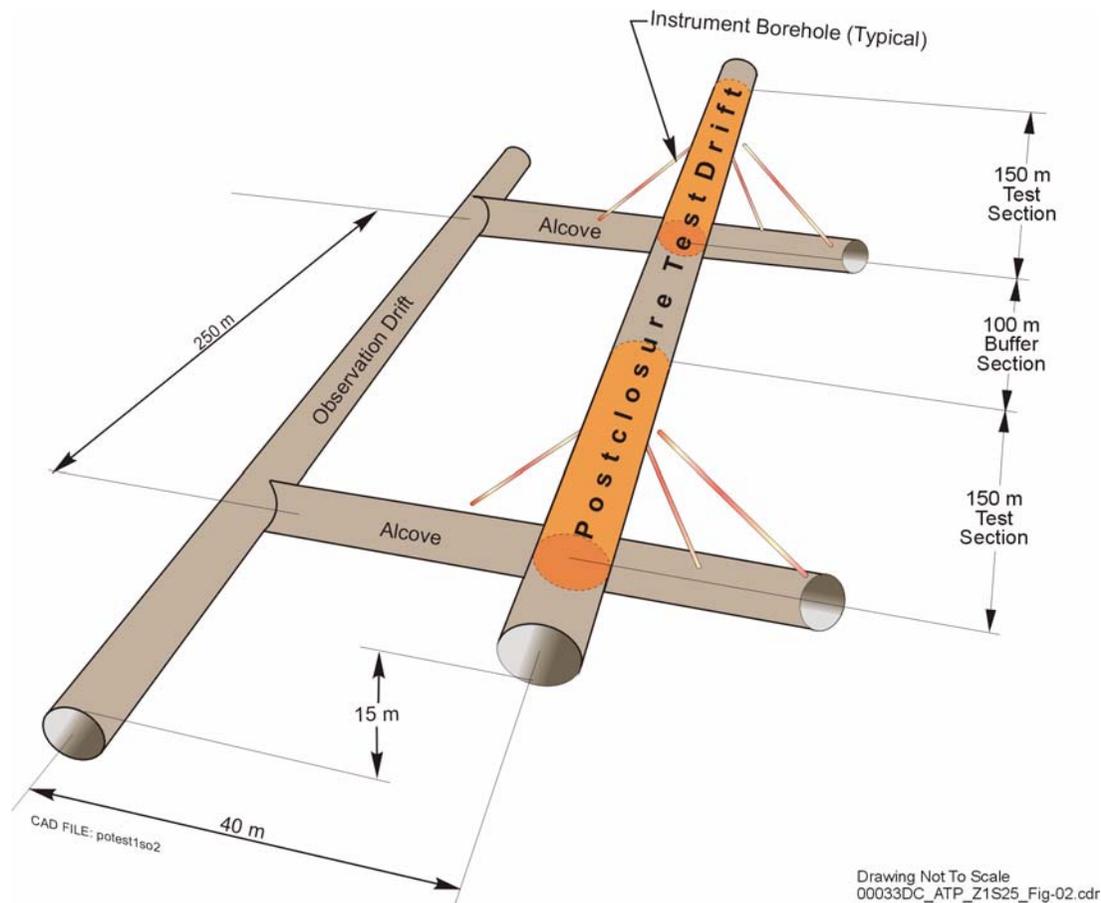
Figure 2-79.   Conceptual Configuration for Postclosure Simulation Test Sections
The initial one or two drifts in the northern section of the repository block would be dedicated to performance confirmation activities, serving as postclosure test drifts. Both real and dummy waste packages would be used in these facilities to collect performance data and natural barrier response during the emplacement and monitoring phases of preclosure to support postclosure performance assessments. For clarity, only a portion of the Postclosure Simulation Test Area is illustrated, and only a few boreholes are shown. Source: Modified from CRWMS M&O 2000ag, Figure 5-3.

Alcoves at this location would also permit monitoring of the rock mass response below the drift, where greater temperature and response may be expected (CRWMS M&O 2000ag, Section 5.3.2).

Figure 2-79 provides a conceptual layout of the Postclosure Simulation Test arrangement, showing the relative locations of the test drift, observation drift, and alcoves. Also shown is a typical pattern of boreholes drilled into the rock from the alcoves and reaching areas in the rock around the test drift.

2.5.2.2 Observation Drifts

Figure 2-78 illustrates the proposed observation drifts. All are aligned parallel to the emplacement drifts and located along the centerline of the rock pillars but at different elevations than the emplacement drifts. Observation Drift #1, located below the emplacement drift horizon, is associated with the Postclosure Simulation Test area discussed in Section 2.5.2.1. Observation Drift #2 would be located above the emplacement drift horizon, within the first panel of emplacement drifts. Observation Drift #3, also located above the emplacement drift horizon, would be at about the midpoint in the repository block. Observation Drift #4, located above the emplacement horizon, would monitor the southern extension of the repository block. The existing ECRB Cross-Drift is also being proposed as an observation drift from which several emplacement drifts in the central area of the repository can be monitored.

These observation drifts and associated alcoves would be used to monitor the thermal-mechanical-hydrologic coupled processes in the rock. Monitoring these processes, along with the changes caused by the heat from emplaced waste and the eventual reduction in heat from spent nuclear fuel decay, is important in demonstrating repository performance (CRWMS M&O 2000ag, Section 5.4.1.2). Sensors to measure process parameters (see Section 4.6) would be installed and grouted into the boreholes. Data acquisition and communication equipment attached to the sensors would be located at the alcoves. The data communication lines would be linked to a central communications network, using fiber-optic cables leading from the alcoves to the performance confirmation control

and data processing center at the repository surface facilities.

Observation Drift #1 would be located approximately 10 to 15 m (35 to 50 ft) below the emplacement drifts, while Observation Drifts #2, #3, and #4 would be located approximately 15 to 30 m (50 to 100 ft) above the emplacement drifts (CRWMS M&O 2000ag, Figure 5.5). These drifts will be thermally affected by the heat of the emplacement horizon; however, the separation will be enough to make the observation drifts accessible to personnel without additional ventilation. Rock temperatures around the observation drifts have been estimated to peak at about 46°C (115°F) during the preclosure period for the design and operating mode presented in this report. Therefore, the observation drifts will be exposed to rock temperatures within the design conditions for human access during the preclosure period without the aid of additional ventilation. Airflow can be maintained and regulated, as needed, to maintain the drift temperatures at a more comfortable level for human access. The pattern for ventilation of the observation drifts would be similar to the pattern for ventilation of the emplacement drifts: fresh air would be supplied at both ends of the observation drifts from the east and west mains and exhausted through a raise connected to the service side of the exhaust main. Figure 2-80 illustrates a typical layout for the ventilation system in an observation drift. The observation drifts would be at a different elevation plane than the east and west mains; therefore, ventilation raises at the ends of the observation drifts would connect the drifts to the main drift airways. Ventilation regulators would control the airflow to the observation drifts, as needed (CRWMS M&O 2000x, Figure 1).

Observation drifts may be equipped with rail for transportation of drilling and other heavy equipment into the drifts.

2.5.2.3 Other Performance Confirmation Facilities

The ventilation cross-drifts excavated parallel to and between emplacement drifts, at the same elevation plane, provide advantageous locations from which to drill boreholes into the rock pillars.
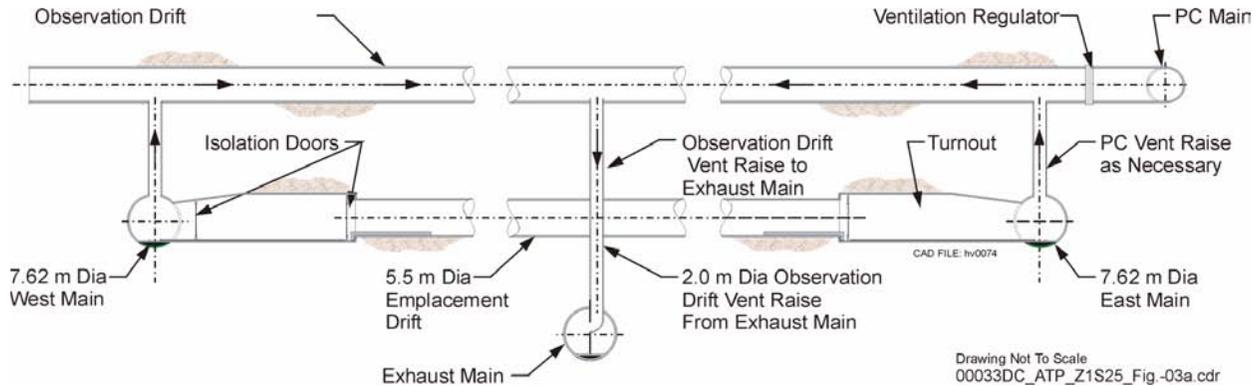
Figure 2-80.   Observation Drift Airflow Concept
As illustrated in this figure, vertical raises are used to connect the observation drifts to the ventilation air supply from the east and west mains; another raise exhausts the air to the service side (unheated air) of the exhaust main. PC = performance confirmation. Source: CRWMS M&O 2000x, Figure 3.

These cross-drifts could therefore be used for additional monitoring installations, as needed.

The ECRB Cross-Drift (Figure 2-78), located approximately 15 to 30 m (49 to 98 ft) above the emplacement drifts, also offers a potentially suitable platform for performance confirmation facilities. With the use of alcoves and instrumentation boreholes, nine emplacement drifts could be monitored from this position.

Figure 2-78 also shows the location of the existing Drift Scale Test near the north ramp curve. After the test is completed, this facility will probably continue to serve performance confirmation functions during the preclosure period. The figure also shows the proposed location for the Seal Test Area, where constructibility and performance testing of the ramp and shaft seals would be performed in support of the performance confirmation program.

Several performance confirmation facilities would be located along the main drifts, in either alcoves or niches. Figure 2-78 shows proposed locations for two seismic alcoves to be equipped with seismometers at opposite ends of the repository block. Seismic facilities would monitor the subsurface response at the repository horizon level to seismic events. This subsurface seismic monitoring would require short alcoves, or niches, to house and protect a data acquisition system installed adjacent to a borehole containing a seismic probe (CRWMS M&O 2000ag, Section 5.4.1.3.4).

Figure 2-78 also shows the proposed locations of six seepage alcoves, where percolation from the rock strata above the emplacement horizon would be monitored around the perimeter of the emplacement block. In situ monitoring of seepage would require short alcoves hermetically sealed from the ventilation system with bulkheads. Inspection or maintenance of instrumentation inside the sealed alcoves would require access through the bulkhead seal (CRWMS M&O 2000ag, Section 5.4.1.3.2).

2.5.3   Subsurface Performance Confirmation Support Facilities

2.5.3.1   Data Acquisition Support Facilities

The subsurface data collection system would consist of groups of instruments reporting to a single local data acquisition system. The data acquisition system would collect data from the integrated instruments at set intervals, using input/output boards. The data acquisition system would store the data locally.

These local data acquisition systems would collect and transmit data from the various repository monitoring areas to a surface-based data control and storage facility. Based on current technology, data acquisition systems would transmit data through controller boards, over fiber-optic trunk lines installed in access ways and along observation drifts, and to the surface data control facility (CRWMS M&O 2000ag, Section 5.4.1.4).

2.5.3.2   Mobile Vehicle Control Systems

In addition to the stationary control system, mobile performance confirmation systems, such as the remote inspection gantry (Figure 2-81), would collect data. Such equipment would also be controlled from the surface facilities during monitoring incursions into the emplacement drifts. A mobile vehicle operations control system and an associated communications transmission system would be required to collect data from both mobile and stationary instruments and to provide real-time data to control these moving observation platforms accurately and safely. Microwave or radio wave transmissions from the gantry would be collected by in-drift wires and transmitted through a subsurface network to an operator control station at the surface. The operator control station would control and monitor a variety of systems throughout the repository, in addition to the mobile equipment (CRWMS M&O 2000ag, Section 5.4.1.5).
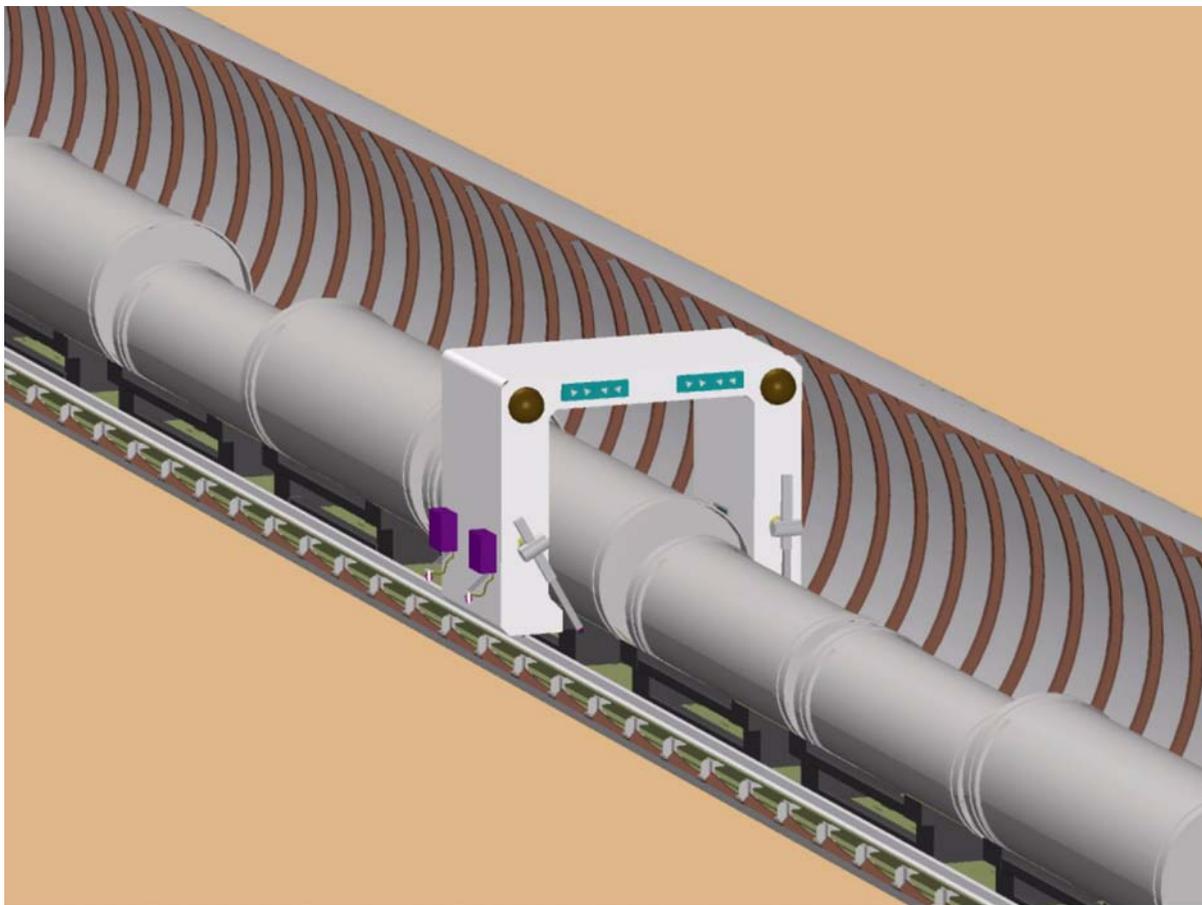
Drawing Not to Scale
00033DC_ATP_Z1S25_Fig-04.ai

Figure 2-81.   Remote Inspection Gantry Used for In-Drift Performance Confirmation Activities
A remotely operated inspection gantry would be used to inspect and collect information in the emplacement drifts during preclosure. Lights, cameras, sensors, on-board computers, and robotic arms would be designed to make this gantry an efficient and safe inspection tool. Source: CRWMS M&O 2000ag, Figure 5-1.

3. DESCRIPTION OF THE WASTE FORM AND PACKAGING

Section 114(a)(1)(B) of the Nuclear Waste Policy Act of 1982 (NWPA), as amended (42 U.S.C. 10134(a)(1)(B)), requires "a description of the waste form or packaging proposed for use at such repository, and an explanation of the relationship between such waste form or packaging and the geologic medium of the site." This section describes the waste forms to be disposed, along with their packaging; Section 4 explains their relationship with the geologic medium of the site. An explanation of the important parameters considered in the design of the waste package is included in this section, as is a summary of the expected performance of the waste package design. This section:

- Presents an overview of the waste forms and the waste package designs

- Describes the waste package, its design bases, and its functions

- Discusses in detail the waste forms, the parameters considered in designing the waste package (and its variations), and the evaluations performed on the designs

- Describes the material selection and fabrication of the waste package

- Presents the results of design evaluations of the waste package.

Waste Form Overview—Waste forms to be received and packaged for disposal include spent nuclear fuel from commercial power reactors, spent nuclear fuel owned by the U.S. Department of Energy (DOE) (including naval fuel), and canisters of solidified high-level radioactive waste from prior commercial and defense fuel reprocessing operations, some of which would contain cans of immobilized plutonium.

Section 114(d) of the NWPA (42 U.S.C. 10134(d)) limits the first repository's capacity to no more than 70,000 MTHM "...until such time as a second repository is in operation." The types of waste that would be accepted at the potential repository have been allocated as follows (DOE 2002, Chapter 2):

- 63,000 MTHM of commercial spent nuclear fuel

- 7,000 MTHM of DOE high-level radioactive waste, commercial high-level radioactive waste, and DOE spent nuclear fuel.

The waste forms received at a potential repository will be in solid form. Materials that could ignite or react chemically at a level that would compromise containment or isolation will not be accepted by the potential repository. Neither the waste forms nor the waste packages will contain free liquids that could compromise waste containment. Materials that are regulated as hazardous waste under the Resource Conservation and Recovery Act of 1976 (42 U.S.C. 6901 et seq.) will not be disposed in the potential repository (DOE 1999c, Section 4.2.3).

Waste Package Overview—The design of a waste package is based on the characteristics of the waste forms that it would hold. Because commercial and DOE high-level radioactive waste forms have similar characteristics, both may be placed into a waste package of the same design. This has allowed the DOE to design waste packages capable of accommodating all the types of spent nuclear fuel and high-level radioactive waste currently generated or anticipated in the United States, whether commercial or governmental.

The waste package has been designed, in conjunction with the natural and other engineered barriers, to ensure compliance with applicable U.S. Nuclear Regulatory Commission (NRC) regulations, to contribute to safe operations during the preclosure phase, to make efficient use of the potential repository area, and to preserve the option of retrieving the waste. To perform its containment and isolation functions, the waste package described in this report has been designed to take advantage of a location in the unsaturated zone.

All the waste package designs consist of two concentric cylinders in which the waste forms would be placed. The inner cylinder would be composed of Stainless Steel Type 316NG. The outer cylinder would be made of a corrosion-resistant nickel-based alloy (Alloy 22). The waste package designs for DOE spent nuclear fuel and high-level radioactive waste are larger in diameter and thicker than those for commercial spent nuclear fuel. The outer layer of corrosion-resistant material protects the underlying layer of structural material from corrosion, and the structural material supports the thinner material of the outer layer.

Each waste package design has outer and inner lids. The outer (closure) lids would be made of Alloy 22. The inner lids would be made of Stain-less Steel Type 316NG, and their thickness will vary, depending on the waste package design. In addition to the inner and outer lids, an Alloy 22 lid on the closure end of the waste package (flat closure lid) would provide additional protection against stress corrosion cracking in the closure weld area.

A titanium drip shield would be placed over the waste package before the repository is closed. This drip shield would protect the waste package against rockfall and dripping water. Figure 3-1 illustrates the waste package and drip shield materials.

Before the double-walled waste package is sealed, helium would be added as a fill gas. The helium will prevent oxidation of the waste form and help
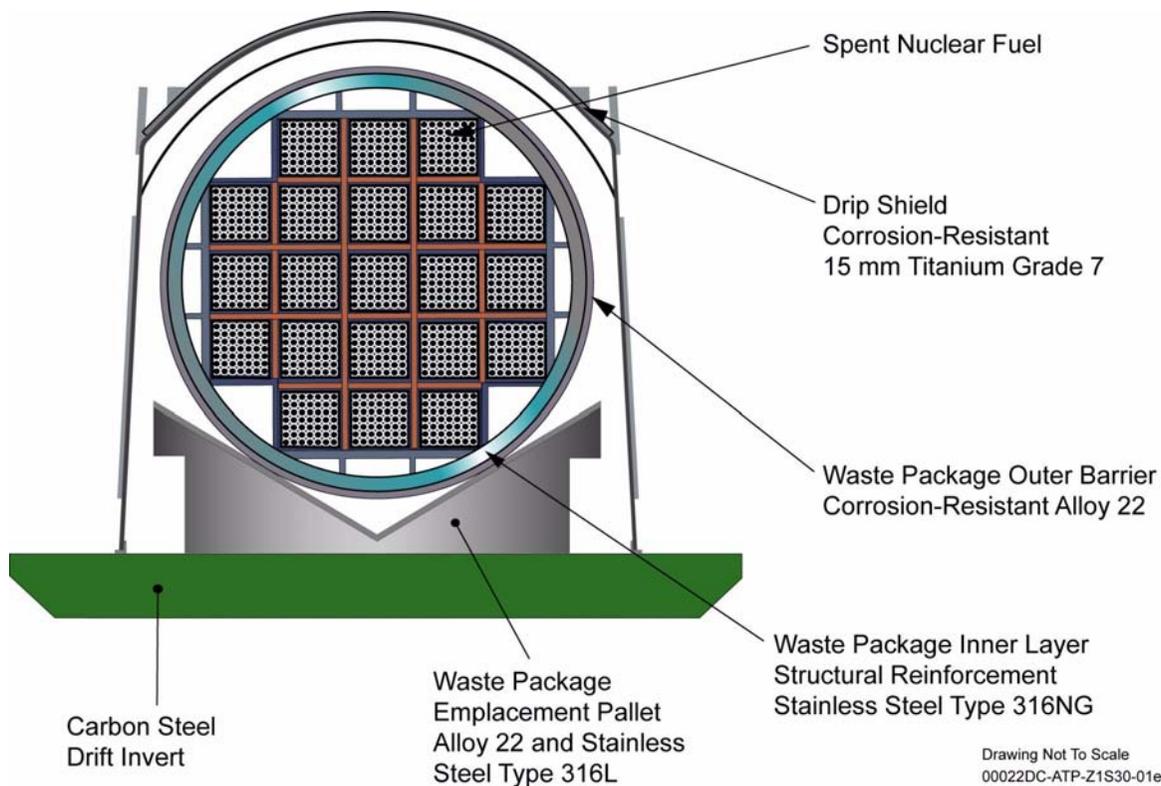
Figure 3-1.   Cross-Sectional Illustration of an Alloy 22 and Stainless Steel Emplaced Dual-Metal Waste Package
The figure illustrates a waste package supported on an emplacement pallet and covered by a titanium drip shield, showing multiple engineered barriers that provide defense in depth. The use of engineered barriers of different materials protects against common mode failures.

transfer heat from the waste form to the wall of the inner shell of the waste package. Transferring heat away from the waste form is an important means of controlling waste form temperatures. This helps preserve the integrity of the metal cladding on the fuel rods, thus extending the life of an existing barrier to water infiltration.

All waste package designs will use a remote lifting-and-handling mechanism. The collar-sleeve-and-trunnion joint apparatus illustrated in Figure 3-2 will allow the necessary handling of the waste package before it is placed on an emplacement pallet and transferred to the designated drift. Each waste package would also have a

unique permanent identifying label (CRWMS M&O 2000au, Section 1.2.1.14).

Although they share the features described previously, the waste package designs have different internal components to accommodate the different waste forms. For example, the waste package for uncanistered commercial spent nuclear fuel has an internal basket assembly to support fuel assemblies. In other waste packages (e.g., the high-level radioactive waste and DOE spent nuclear fuel waste packages), the internal basket has a different design, or, as is the case with naval spent nuclear fuel, the basket is contained inside the canister. Internal components are discussed in more detail in the respective waste package design sections.
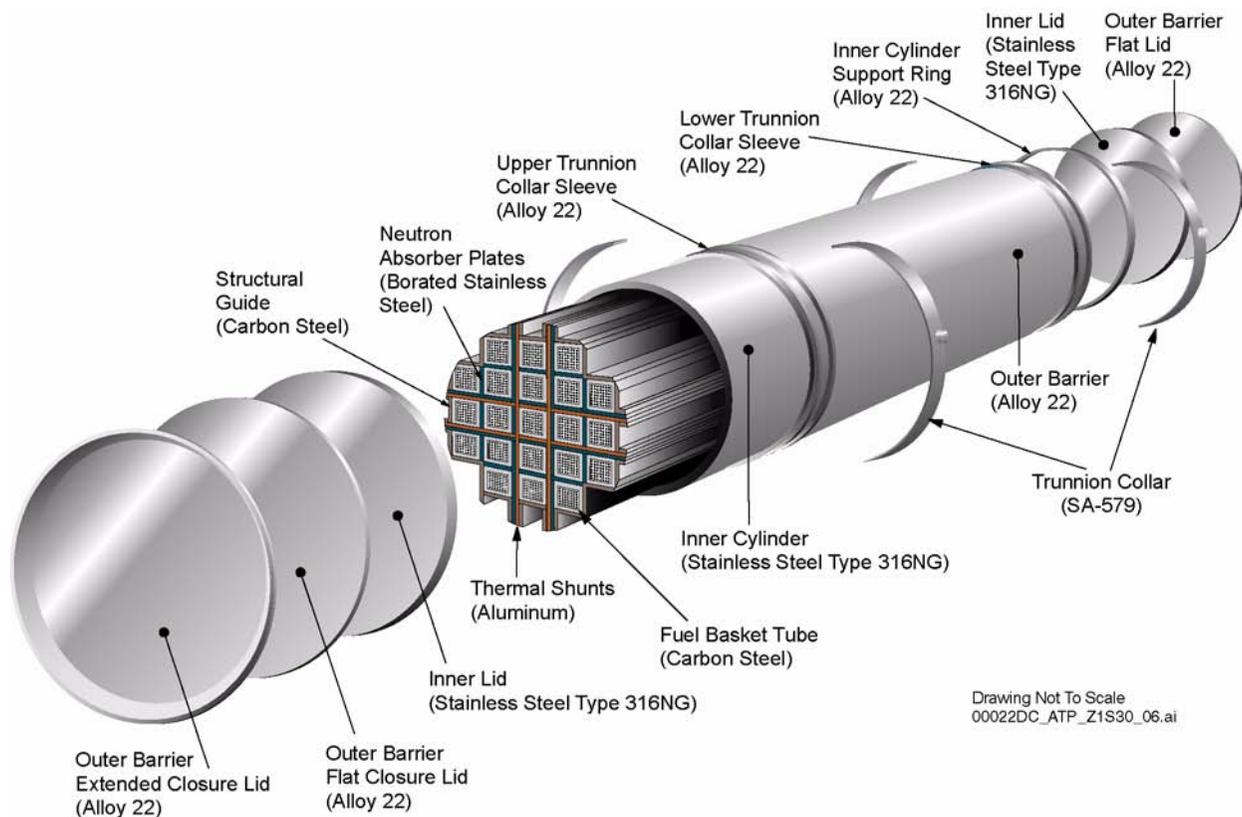
Figure 3-2.   21-PWR Absorber Plate Waste Package Design
Components for the 21-PWR commercial spent nuclear fuel assembly with an absorber plate (to prevent criticality) are illustrated. Internal strength is provided by carbon steel structural guides and fuel basket tubes. Aluminum thermal shunts assist in removing heat, and plates made of a stainless steel and boron alloy assist in preventing criticality by absorbing neutrons. Temporary trunnion collars would be installed on the waste package to facilitate handling operations. The inner cylinder support ring holds the inner cylinder to the outer barrier. All waste package designs have the same concept for lids, trunnions, and a multilayer configuration, although internal components vary among designs.

3.1 GENERAL DESIGN BASIS FOR THE WASTE PACKAGE

The engineered barrier system would be an important element of a potential repository. The primary component of the system would be the waste package. As defined in 10 CFR 63.2 (66 FR 55732), a waste package includes the waste form and any containers, shielding, packing, and other absorbent materials immediately surrounding it. The invert material does not immediately surround the waste package, so it is not considered part of the waste package. Figure 3-3 illustrates the waste package within the emplacement drift of the engineered barrier system.

The waste package has been designed to use materials that perform well under the anticipated conditions at Yucca Mountain. The design analyses performed on the waste package include evaluations of structural integrity, thermal performance, criticality safety, and shielding properties. In addition, data from the material and waste form testing programs have been used to model both the waste package and the cladding on the spent nuclear fuel as part of the total system performance assessment (TSPA) discussed in Section 4.

The waste packages emplaced in repository drifts will be affected by the atmosphere that surrounds them, the water that could come in contact with
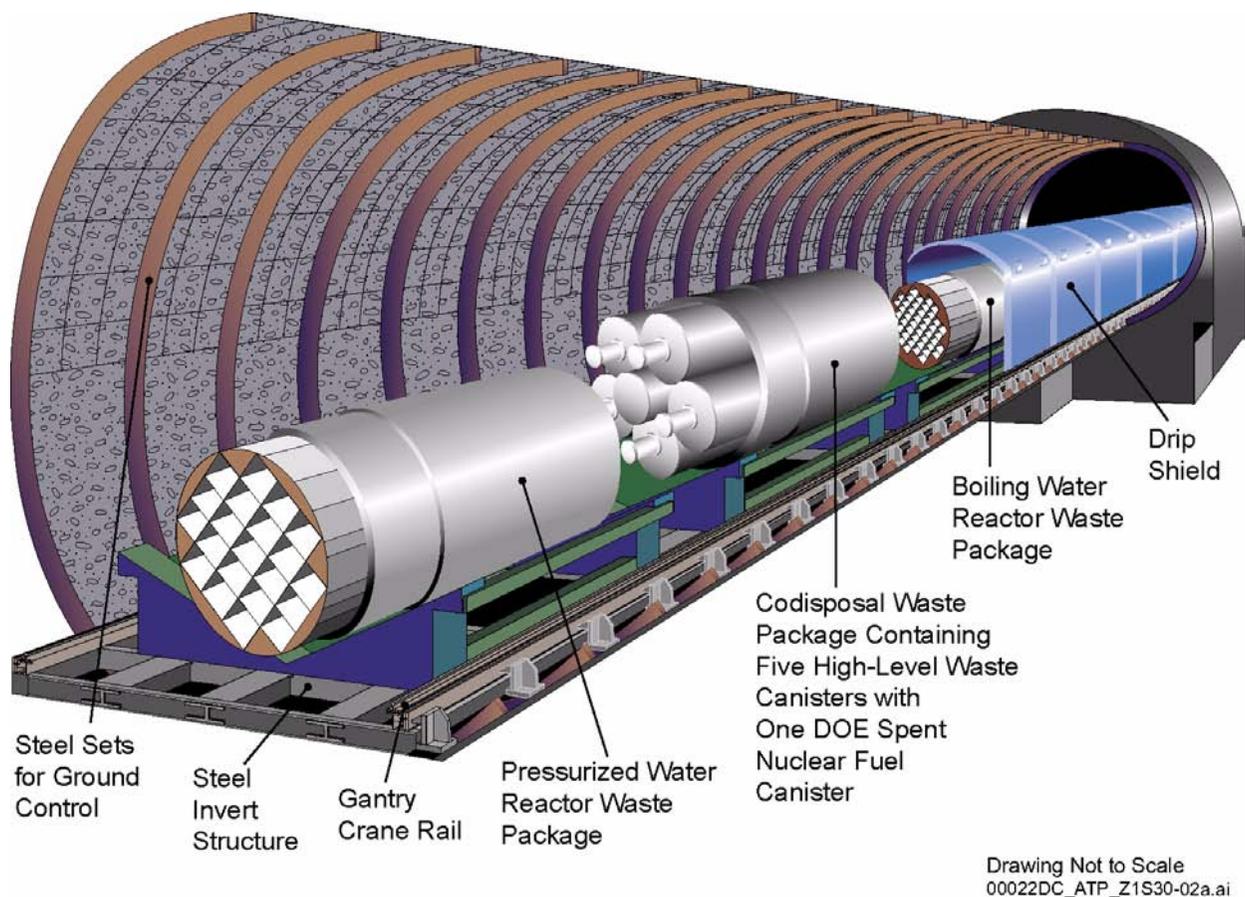
Figure 3-3.   Schematic Illustration of the Emplacement Drift with Cutaway Views of Different Waste Packages
Ground support for emplacement drift walls is illustrated in the figure, which also shows three designs for dual-metal waste packages (representing various waste forms), a protective drip shield, and emplacement pallets supporting the waste package above the drift floor.

them, and the movement of the host rock in which they are emplaced. How the decay heat produced by waste forms is managed impacts the atmosphere surrounding the waste package. In the higher-temperature operating mode described in this report, fuel blending would be used to manage the amount of thermal output from the waste packages (i.e., how much heat they emit) to ensure that temperatures in most of the rock between the emplacement drifts stays below the boiling point of water.

3.1.1   Waste Package Functions

Waste containment begins when the waste form is sealed in the waste package. Once sealed, the waste package ensures a dry and stable physical and chemical environment for as long as it remains intact. Engineers have designed the waste package to work with the natural environment: the material for the outer barrier of the waste package was selected because of its resistance to corrosion in an environment such as the one expected at Yucca Mountain (CRWMS M&O 2000av).

The waste package performs a number of other functions. System Description Documents define each function as the basis for a waste package performance specification (CRWMS M&O 2000au, Section 1.1; CRWMS M&O 2000aw, Section 1.1; CRWMS M&O 2000ax, Section 1.1). The waste package, in conjunction with other systems, has been designed to:

- Restrict the transport of radionuclides

- Provide criticality protection during waste package loading and emplacement

- Manage the decay heat for the potential repository

- Provide identification (i.e., each waste package will be uniquely labeled and its contents identified)

- Enhance the safety of personnel, equipment, and the environment

- Prevent adverse reactions involving the waste form

- Maintain structural integrity during loading, onsite transportation, emplacement, and retrieval

- Resist corrosion in the emplacement drift environment

- Provide physical and chemical stability for the waste form

- Promote heat transfer between the waste form and the outside environment

- Facilitate decontamination of the waste package's outer surface.

The following sections discuss the general performance specifications that apply during repository operations (preclosure phase) and after closure of the repository (postclosure phase).

3.1.2   Preclosure Design Performance Specifications

The performance specifications for the functionality of the waste package during the repository's preclosure phase are consistent with 10 CFR 63.112(b) (66 FR 55732). This regulation provides for the DOE's analysis of the ability of the waste package's structures, systems, and components to perform their intended safety functions during an accident or event sequences. For the waste package, design basis events are determined by identifying the functions of the waste package and evaluating the effects on its performance of given events that could occur during normal handling of the waste package or during a credible accident scenario (i.e., events that have at least 1 chance in 10,000 of occurring before permanent closure of the geologic repository) (CRWMS M&O 2000ay, Section 4.2.1).

These event sequences and their effects on performance were defined by reviewing the *Preliminary MGDS Hazards Analysis* (CRWMS M&O 1996a), studying NRC standard review plans for similar facilities (e.g., the *Standard Review Plan for Dry*

Cask Storage Systems [NRC 1997]), and considering current surface and subsurface design information. This review process led to the classification of two types of event sequences that might affect waste packages during the preclosure period: internal (normal operations, mechanical or other failures, and operator error) and external (natural phenomena and man-made events not initiated by repository operations). The results constituted a bounding list of preclosure event sequences that could affect the waste packages. Using this list, engineers performed structural, thermal, and criticality analyses of the impacts such events could have on waste package performance (CRWMS M&O 2000ay). The event sequences were developed early in the design process and were based on conceptual designs for commercial spent nuclear fuel. The fuel design has evolved, but the event sequences evaluated still represent plausible accident scenarios that can be used to evaluate the adequacy of the waste package designs.

Table 3-1 summarizes the complete list of event sequences (CRWMS M&O 2000au, Section 1.2.2), which constitute the performance specifications for the waste package and support the waste package function specifications. In accordance with NRC guidance, designers considered many other types of events. However, because some events are either very low probability or their consequences are not significant, they were not included in the safety analysis. Section 3.5 presents the results of representative design evaluations for select waste packages.

3.1.3   Postclosure Performance Specification

10 CFR 63.113(b) (66 FR 55732) requires the entire repository system to meet specific dose limits for 10,000 years. The waste package is one of many barriers relied upon to meet this limit. The DOE's objective is to design a waste package that works in concert with the natural environment to meet performance standards while reducing the uncertainty associated with the current understanding of natural processes at the site.

3.1.4   Design Descriptions

An analysis was undertaken to determine the number of designs needed to handle the different waste forms that would constitute the anticipated waste stream in the most economical manner (CRWMS M&O 1997b). The objective of the evaluation was to determine:

- The number of different waste package designs needed

- The capacity of each waste package design (i.e., the amount of waste it would hold)

- The limits on spent nuclear fuel properties (e.g., age, thermal characteristics) that might apply to each waste package design.

The complete system of waste package designs is intended to allow reliable disposal of those waste forms that a repository would accept while still enhancing overall efficiencies.

To determine the most efficient set of waste package designs for commercial spent nuclear fuel, the DOE designed waste packages of various assembly-holding capacities and incorporated into the design methods for removing decay heat and preventing criticality. This resulted in the selection of a set of five waste package designs as the most efficient means of accommodating the anticipated waste stream of commercial spent nuclear fuel. A similar process led to three designs for DOE non-naval spent nuclear fuel and DOE and commercial high-level radioactive waste. Two other designs are specific to naval spent nuclear fuel, which will arrive presealed in canisters (CRWMS M&O 2000az, Sections 4.2 and 4.3). Some DOE non-naval spent nuclear fuel will be loaded into waste packages with high-level radioactive waste; this DOE spent nuclear fuel and high-level radioactive waste will also arrive in presealed canisters. Table 3-2 lists the waste package designs and a description of each. Table 3-3 provides a breakdown of the percentage of waste packages by waste package design and the percentage of MTHM by waste package design. Figures 3-4 and 3-5 illustrate the waste forms and associated waste package designs.

Table 3-1. Bounding Event Sequences for Waste Packages

Analysis Type	Event Group	Event	Performance Specification
Structural	Falling Objects— Side Impact on Waste Package	Rockfall from the drift onto the waste package	Withstand 13-metric ton (14-ton) rock falling 3 m (10 ft). Drop height based on a 5.5-m (18-ft) drift and a distance of 2.4 m (8 ft) between the top of the drift and the top of the waste package (CRWMS M&O 1999h, p. 40)[a]
	Falling Objects— End of Waste Package Impact	Handling equipment drop onto the waste package	Withstand 2.3-metric ton (2.5-ton) object falling 2 m (6.6 ft). Drop height based on the distance between the handling equipment and the top of the waste package
	Waste Package Vertical Drops and Waste Package End Collisions	Waste package vertical drop from the disposal container cell crane	Withstand 2-m (6.6-ft) drop. Drop height based on the maximum crane hook height; the bottom of the waste package cannot be lifted higher than 2 m (6.6 ft) above the floor
	Waste Package Horizontal Drops and Waste Package Side Collisions	Emplacement drift gantry drops waste package	Withstand 2.4-m (8-ft) drop
	Puncture Hazards	Waste package falls onto a sharp object while being transported in a horizontal position	Withstand 2-m (6.6-ft) horizontal drop onto a steel support or 2.4-m (8-ft) horizontal drop onto a concrete pier, whichever is worse
	Tipover	Tipover due to vertical drop or seismic event	Withstand tipover from a vertical position onto a flat surface
	Seismic Activity	Earthquake	Maintain structural integrity and prevent tipover during a design basis earthquake
	Missile	The missile identified was a valve stem being ejected at the surface facility	Withstand impact of a valve stem weighing 0.5 kg (1.1 lb), with a 1-cm (0.39-in.) diameter, inside a valve with 5 cm (2 in.) of packing and under a system pressure of 2.1 MPa (305 psi), which has become a missile with a velocity of 5.7 m/s (19 ft/s)
	Transporter Runaway	Failure to maintain the transporter at or below the maximum speed limit	Withstand maximum impact from a transporter runaway, derailment, and impact at a speed of 63 km/hr (39 mi/hr)
	Fuel Rod Rupture/Internal Pressurization	100% fuel rod rupture and fission gas release	Withstand internal pressure of 1 MPa (146 psi)
Thermal and Structural	Thermal Stresses and Peak Waste Package Temperature	Fire in disposal container cell	Survive a fire, defined as exposure of whole waste package for not less than 30 minutes to a heat flux not less than that of a thermal radiation environment of 800°C (about 1,500°F) with an emissivity coefficient of at least 0.9. Surface absorptivity must be at least 0.8. If significant, convective heat transfer must be considered on the basis of still air at 800°C (about 1,500°F).
Criticality	Criticality Safety	Criticality scenario inside a waste package	The effective multiplication factor (k_{eff}) is less than or equal to 0.95 under assumed accident conditions, considering allowance for the bias in the method of calculation and the uncertainty in the experiments used to validate the method of calculation

NOTE: [a]This rock size requirement was lowered to 6 metric tons (BSC 2001m) since completion of the rock fall analysis in support of a potential site recommendation (CRWMS M&O 2000au, Section 2.5.2.1).

Table 3-2.   Waste Package Design

Waste Package Design	Description
21-PWR Absorber Plate	Capacity: 21 commercial pressurized water reactor assemblies and an absorber plate for preventing criticality.
21-PWR Control Rod	Capacity: 21 commercial pressurized water reactor assemblies with higher reactivity, requiring additional criticality control that is provided by the placement of control rods in all assemblies.
12-PWR Long	Capacity: 12 commercial pressurized water reactor assemblies and an absorber plate for preventing criticality; longer than the fuel assemblies placed in the 21-PWR packages. Because of its smaller capacity, it may also be used for fuel with higher reactivity or thermal output.
44-BWR	Capacity: 44 commercial boiling water reactor assemblies and an absorber plate for preventing criticality.
24-BWR	Capacity: 24 commercial boiling water reactor assemblies with higher reactivity, requiring a thicker absorber plate to prevent criticality than that used in the 44-BWR design.
5-DHLW/DOE SNF Short	Capacity: 5 short high-level radioactive waste canisters and 1 short DOE SNF canister. When high-level radioactive waste includes immobilized plutonium cans, no DOE spent nuclear fuel is placed in the center.[a]
5-DHLW/DOE SNF Long	Capacity: 5 long high-level radioactive waste canisters and 1 long DOE SNF canister.[a]
2-MCO/2-DHLW Long	Capacity: 2 DOE multicanister overpacks and 2 long high-level radioactive waste canisters.
Naval SNF Short	Capacity: 1 short naval SNF canister.
Naval SNF Long	Capacity: 1 long naval SNF canister.

NOTE: [a]DOE non-naval spent nuclear fuel

Table 3-3.   Breakdown of Waste Packages for 70,000 MTHM

Waste Package Design	Approximate Percentage of Waste Packages by Waste Package Design	Approximate Percentage of MTHM by Waste Package Design
21-PWR Absorber Plate	38%	55%
21-PWR Control Rod	1%	1%
12-PWR Long	2%	2%
44-BWR	25%	32%
24-BWR	1%	<1%
5-DHLW/DOE SNF Short[a]	14%	3%
5-DHLW/DOE SNF Long[a]	15%	4%
2-MCO/2-DHLW Long	1%	<1%
Naval SNF Short	2%	<1%
Naval SNF Long	1%	<1%

NOTE: [a]DOE non-naval spent nuclear fuel

3.2   COMMERCIAL SPENT NUCLEAR FUEL

Commercial nuclear fuel rods are arranged in assemblies that range in length from about 2 to 5 m (6.6 to 16 ft). These assemblies are arranged in a square, cross-sectional pattern and customized to meet the size and performance requirements of the reactor they will fuel. The fuel rods are sealed metal tubes, about 6.5 to 12.7 mm (0.26 to 0.50 in.) in diameter, that contain ceramic-like fuel pellets. The fissionable material in the fuel rods is uranium dioxide. Fissionable material has the ability to sustain a controlled nuclear chain reaction and, in so doing, release energy in a controlled manner. Spent nuclear fuel contains uranium-235 and uranium-238, short-lived fission products such as strontium-90 and cesium-137, and long-lived transuranic isotopes (i.e., isotopes with atomic numbers greater than 92) such as plutonium-239 and americium-243.

In most nuclear fuel assemblies, the tubes containing the fuel pellets are made of Zircaloy, a zirconium-based material. The generic name for the metal that the tubes are composed of is "cladding." Zirconium-based cladding is used for
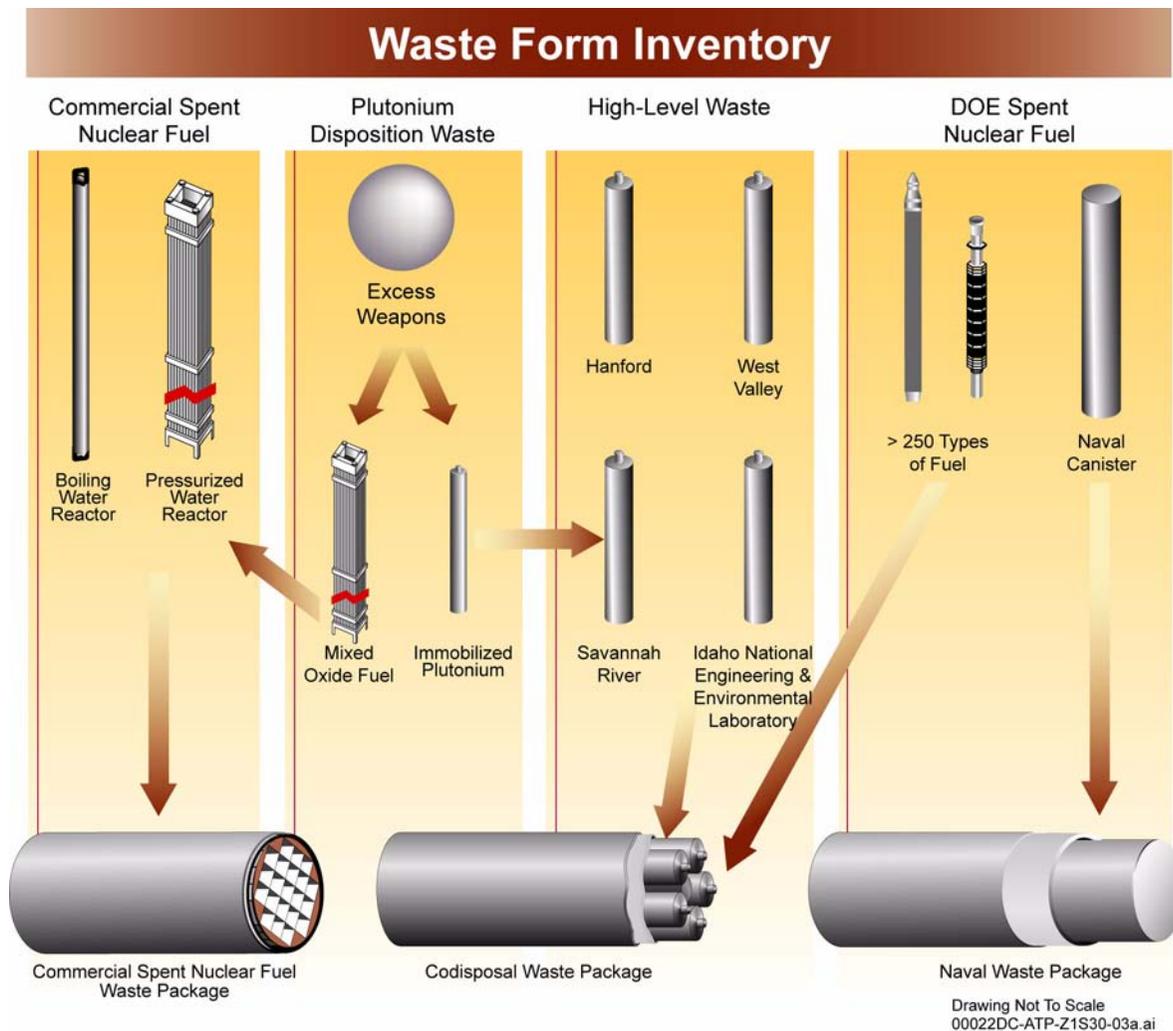
Figure 3-4.   Waste Form Inventory
The figure depicts the types and quantities of waste forms to be disposed in a first repository and their representative waste package designs. Until a second repository is in operation, the Nuclear Waste Policy Act limits inventory in the first repository to 70,000 MTHM. Dispositioning excess plutonium from weapons programs into mixed-oxide fuel for burnup in reactors and disposal in a repository aids in the fight against nuclear proliferation.

98.5 percent of pressurized water reactor fuel assemblies and 99.8 percent of boiling water reactor fuel assemblies. The cladding on the remainder is made of stainless steel. Future fuel designs are not expected to change from mostly zirconium-based cladding (CRWMS M&O 1999a, Section 3.1.1). Figure 3-6 illustrates a typical commercial nuclear fuel assembly for a pressurized water reactor.

Approximately 292,000 commercial spent nuclear fuel assemblies will be generated by 2040: 167,000 from boiling water reactors and 125,000 from pres-

surized water reactors (CRWMS M&O 1999a, Section 3.1, Tables 3 and 4). About 220,000 of these assemblies would be emplaced in the potential repository. Up to 33 metric tons of U.S. surplus weapons-usable plutonium will be fabricated into uranium–plutonium fuel (called mixed-oxide fuel) and irradiated in commercial reactors. Use of mixed-oxide fuel will be limited to only a few specific commercial reactors and would involve, at most, no more than 1,800 assemblies (CRWMS M&O 1999a, Appendix B). Mixed-oxide spent nuclear fuel would become part of the commercial waste stream accepted for disposal at a repository.
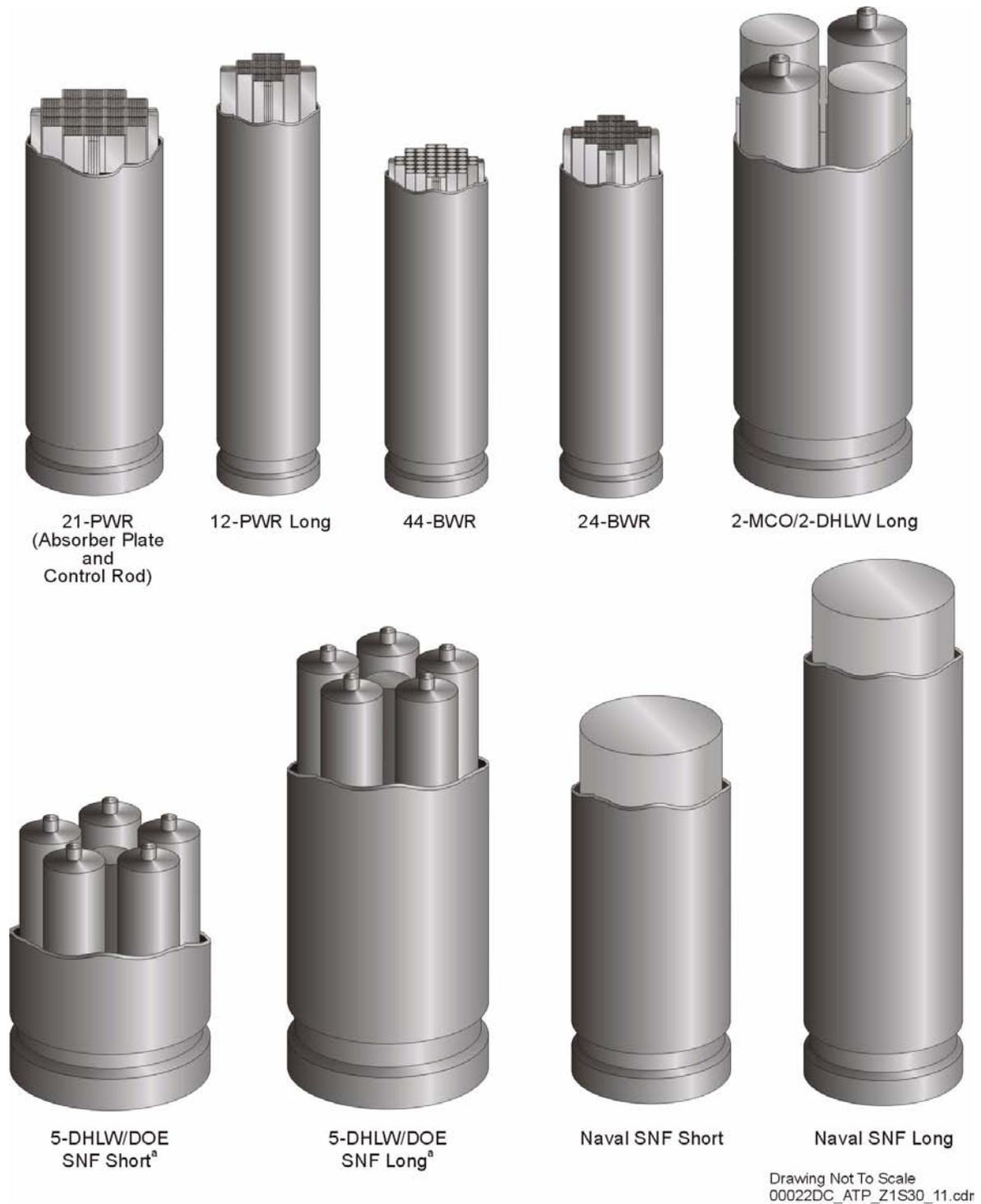
Figure 3-5.   Waste Package Designs with Waste Forms
[a]Basket is excluded from illustration for clarity.
The waste package designs are depicted close to scale, along with the waste form configuration contained in each design. The 21-PWR waste package is representative of both the 21-PWR Absorber Plate and 21-PWR Control Rod designs.
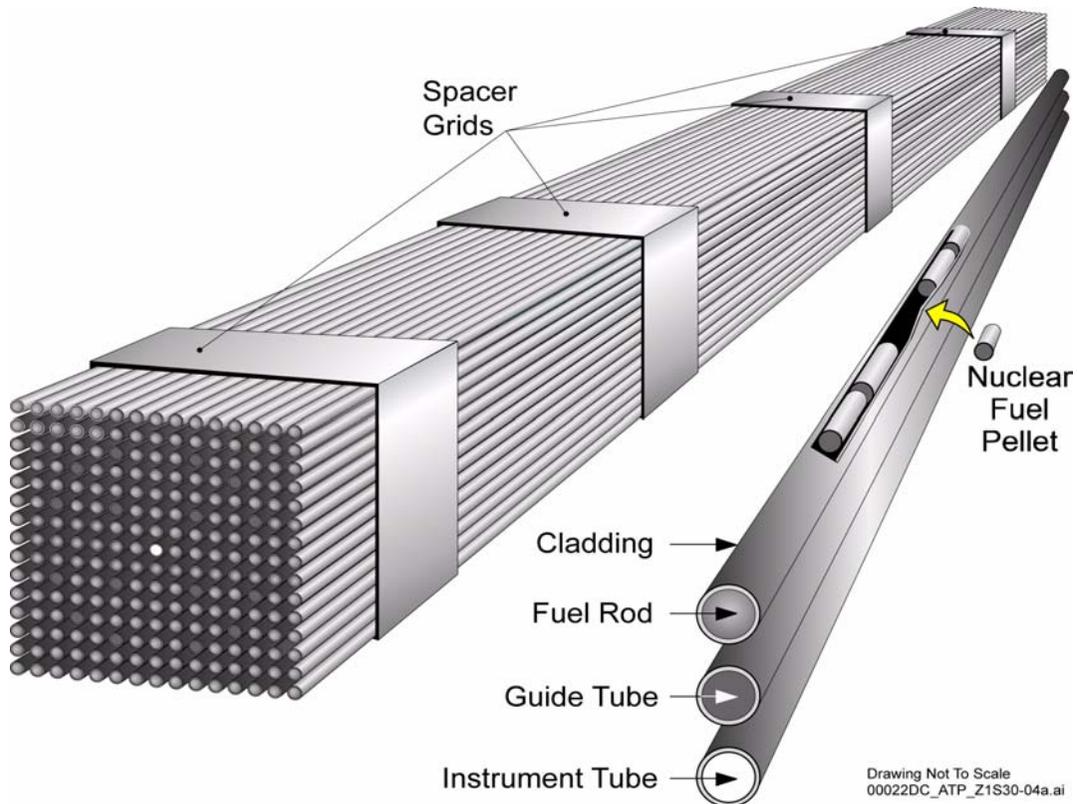
Figure 3-6.   Cross-Sectional Illustration of a Typical Pressurized Water Reactor Fuel Assembly
The figure shows the spacer grids, which provide structural strength and maintain the cross-sectional configuration of the assembly; clad fuel rods, which contain fingertip-sized, ceramic-like fuel pellets that become highly radioactive in a reactor; and guide and instrument tubes. The array depicted contains 208 fuel rods, which would weigh about 550 kg (1,200 lbs), and would be 4.3 m (14 ft) long.

Each mixed-oxide fuel assembly irradiated and disposed would replace an energy-equivalent enriched uranium assembly. Preliminary evaluations indicate that mixed-oxide fuel can be accommodated within the suite of waste package designs (CRWMS M&O 2000ba, p. vii).

In addition to standard commercial fuel assemblies, a small portion (less than 2 percent) of the spent nuclear fuel will arrive in canisters containing individual fuel rods. Utilities repackage fuel rods that have damaged cladding in these canisters to confine radioactive materials during handling and shipment. To ensure that waste package designs have the flexibility to accommodate canistered fuel, the canisters would have sizes within the range of dimensions that qualify as standard fuel. Thus, it will be possible to handle and dispose canistered fuel in the same way as uncanis-

tered spent nuclear fuel assemblies (CRWMS M&O 1999a, Section 3.2).

Most commercial spent nuclear fuel assemblies would arrive at the potential repository undamaged and suitable for immediate disposal. Some of the fuel rods in these assemblies are expected to have minor defects in their cladding (i.e., small cracks or pinholes due to manufacturing defects or corrosion). The initial condition of the cladding is considered in the TSPA analysis (see Section 4.2.6).

Based on prior experience, testing, and the design of the system and equipment, transport will not impact the integrity of spent nuclear fuel. Assemblies, canistered or not, would be placed intact into waste packages. The entire assembly, which may

include nonfuel hardware components (such as control rods), would be packaged for disposal.

3.2.1 Commercial Spent Nuclear Fuel: Assigning the Right Waste Package

The characteristics of spent nuclear fuel assemblies (i.e., size, thermal output, and reactivity) will be used to select the appropriate waste package design. The size of assemblies is used to determine the size and configuration of the fuel within the waste package, and to perform structural analyses to evaluate the integrity of the waste package during normal handling and event sequences. The thermal output and reactivity of the fuel is used to determine which waste package can accommodate each given fuel assembly.

3.2.1.1 Physical Characteristics of Commercial Spent Nuclear Fuel

The physical characteristics of commercial spent nuclear fuel include length, cross section, weight,

and cladding. Table 3-4 summarizes boiling water reactor assembly dimensions and weights by related groups; Table 3-5 provides similar information for pressurized water reactor assemblies (CRWMS M&O 1999a, Section B.1.1). The information provided in Tables 3-4 and 3-5 represents the full inventory of approximately 292,000 assemblies. Operating and shut down reactors are shown in Figure 1-2 of Section 1.

Based on physical dimensions, approximately 95 percent of the fuel assemblies can be emplaced using two waste package designs (the 21-PWR Absorber Plate and the 44-BWR). The 12-PWR Long is designed to accommodate assemblies from Combustion Engineering and the South Texas Project, which are longer than the others. Because the 12-PWR Long holds fewer assemblies, it can also be used to manage thermal load and criticality concerns about fuel with higher thermal output and reactivity.

Table 3-4. Design Basis Dimensions of Assemblies for Boiling Water Reactors

Assembly Group	Length mm (in.)	Width mm (in.)	Weight kg (lb)	Percent of Total BWR Assemblies	Total BWR Assemblies
Big Rock Point	2,071.6 to 2,154.0 (81.6 to 84.8)	165.1 to 183.1 (6.5 to 7.2)	207 to 268 (456 to 591)	<1	524
Humbolt Bay, Dresden 1, and LaCrosse[a]	2,413.0 to 3,591.5 (95.0 to 141.4)	101.6 to 160.0 (4.0 to 6.3)	125 to 218 (276 to 481)	<1	1,615
General Electric BWR (8x8 and 9x9)	4,343.4 to 4,521.2 (171.0 to 178.0)	132.1 to 154.9 (5.2 to 6.1)	252 to 329 (556 to 725)	99	164,800

NOTES: [a]See Figure 1-2 in Section 1 for a map of currently operating and shut down reactors.
BWR = boiling water reactor.

Table 3-5. Design Basis Dimensions of Assemblies for Pressurized Water Reactors

Assembly Group	Length mm (in.)	Width mm (in.)	Weight kg (lb)	Percent of Total PWR Assemblies	Total PWR Assemblies
Haddam Neck, Indian Point 1, San Onofre 1, and Yankee Rowe[a]	2,837.1 to 3,561.1 (111.7 to 140.2)	160.0 to 218.4 (6.2 to 8.6)	198 to 731 (437 to 1,612)	2	2,460
Westinghouse, Babcock & Wilcox, and Others	3,708.4 to 4,406.9 (146.0 to 173.5)	198.1 to 218.4 (7.8 to 8.6)	497 to 773 (1,100 to 1,700)	84	105,500
Combustion Engineering 16x16 and South Texas Project	4,490.7 to 5,110.5 (176.8 to 201.2)	203.2 to 215.9 (8.0 to 8.5)	649 to 882 (1,430 to 1,940)	14	16,900

NOTES: [a]See Figure 1-2 in Section 1 for a map of currently operating and shut down reactors.
PWR = pressurized water reactor.

3.2.1.2 Thermal Output

Commercial spent nuclear fuel arriving at the repository is expected to have a wide range of thermal outputs. The waste package has been designed to ensure that this anticipated range can be accommodated in a way that supports the range of thermal operating modes being considered for the potential repository (see Section 2).

The key factors used to determine the thermal output of spent nuclear fuel are its age (i.e., number of years out of the reactor), burnup (measured in gigawatt-days per metric ton of uranium), and initial enrichment of fissile material (i.e., uranium-235 or plutonium). To cover anticipated thermal outputs, waste package designers considered the average characteristics provided in Table 3-6. Maximum characteristics were also evaluated to ensure that these fuel assemblies could be placed in the waste package.

Determining which waste package design can accommodate a particular spent nuclear fuel assembly thermally will require calculating the assembly's thermal output at the time it is emplaced in the repository. The appropriate waste package is chosen to ensure that the maximum thermal output limit is not violated. In the higher-temperature operating mode, this limit has been set at 11.8 kW.

Of the five commercial waste package designs, the 21-PWR Absorber Plate is the most limiting in thermal output. The characteristics of spent nuclear fuel assemblies loaded into this waste package type will be carefully chosen to ensure that the thermal output limit is not violated.

The thermal output of the waste package can be reduced, if necessary, to accommodate either a range of thermal operating modes or potential changes in the characteristics of the waste stream. Reduction can be achieved by using one or more of the following waste package loading strategies: (1) fuel blending (i.e., combining low heat output fuel and high heat output fuel within a single waste package); (2) de-rating (i.e., loading fewer assemblies than the waste package is designed to hold); or (3) increasing the use of the 12-PWR Long waste package (i.e., placing high heat output fuel in smaller waste packages). For more information on variables that can be modified to accommodate a range of operating modes, see Section 2.1.

3.2.1.3 Criticality Control

Waste package designs will be evaluated to ensure that subcritical limits can be met, as well as the thermal limits described in the previous section. As Section 3.5.2 describes in detail, loading curves will be developed from commercial spent nuclear fuel parameters to determine the method of loading waste packages. This will ensure that the reactivity of the fuel being loaded is below the level at which criticality could occur.

3.2.2 Commercial Spent Nuclear Fuel Waste Package Designs

All the waste package designs for commercial spent nuclear fuel have similar components that perform multiple functions. Figure 3-2 illustrates a representative waste package design. The general features of waste package design were described in Section 3.1; the internal components of commercial spent nuclear fuel waste package design are described in this section, along with their functions.

Table 3-6. Fuel Assembly Characteristics at Arrival

Assembly Type	Average Assembly Age (years)	Average Assembly Burnup (GWd/MTHM)	Average Assembly Initial ^{235}U Enrichment (wt%)	Weight of Heavy Metal (MTHM)
Boiling water reactor	22.7	33.6	3.03	0.200
Pressurized water reactor	23.1	41.2	3.75	0.475

NOTES: GWd = gigawatt day. Source: CRWMS M&O 2000bb, Table 5.

3.2.2.1 Internal Basket Design

Baskets are composed of interlocking plates, fuel tubes, thermal shunts, and structural guides. These elements will displace any water that might be present inside a breached waste package, helping to prevent criticality. All four elements and their functions are described below.

Interlocking Plates—The interlocking plates set the pattern for how the fuel assemblies will be arranged inside the waste package. The basket for each design is customized to meet requirements for the size, type, and number of fuel assemblies it can hold, as well as the specific waste form being packaged. The material composition and thickness of the interlocking plates are tailored to provide enough structural strength to maintain fuel geometry during normal handling and design basis events, and to prevent criticality. However, this extra durability is not considered in the structural analyses (CRWMS M&O 2000au). The interlocking plates are made of either Neutronit A 978 (a stainless steel and boron alloy) or SA 516 Grade 70 carbon steel and range between 5 and 10 mm (0.2 and 0.4 in.) in thickness.

The neutron absorber materials that prevent criticality can be placed directly into the plates using Neutronit A 978 or can take the form of separate control rods. Plates that include neutron absorber material will vary in thickness because of the number of plates in the design. For example, the 44-BWR waste package has more plates than the 21-PWR waste package; therefore, the plates in the 44-BWR can be thinner, but the entire waste package will still have about the same mass of neutron absorber material as the 21-PWR.

The corrosion rate for Neutronit A 978 plates is slow, and the plates tend to corrode by pitting. Because of this, the plates remain in place between the fuel assemblies even as they corrode. To avoid processes that could accelerate stress corrosion cracking, there will be no bends or structural welds on the Neutronit A 978 plates.

Fuel Tubes—The fuel tubes are long, square containers that line the insides of the cavities created by the interlocking plates. They support the internal structure created by the interlocking plates while holding the fuel assemblies in place. The fuel tubes provide structural strength for the internal basket during event sequences they also help conduct heat away from the cladding. The fuel tubes for each waste package design are made of SA 516 Grade 70 carbon steel that is 5 mm (0.2 in.) thick (CRWMS M&O 2000au, Section 2.4.1.2).

Thermal Shunts—All the waste package designs for commercial spent nuclear fuel except the 24-BWR require thermal shunts. These shunts, which are made of 5-mm (0.2-in.) thick SB 209 6061 T4 (an aluminum alloy), are placed alongside the interlocking plates (CRWMS M&O 2000au, Section 2.4.1.3). The shunts are added to help transfer heat from the waste form to the walls of the waste package. Adding thermal shunts is a simple and effective method to improve heat conduction between the center of the waste package and the outer edge of the internal basket, providing a reliable means of keeping the temperature of the cladding within design limits. Limiting cladding temperatures helps protect the waste form by minimizing damage to the fuel cladding (CRWMS M&O 2000au, Section 2.4.1.3).

Structural Guides—The structural guides for each waste package are made of 10-mm (0.4-in.) thick SA 516 Grade 70 carbon steel and are placed inside the inner layer of the waste package to hold the basket structure in place. They help maintain fuel geometry, which can prevent criticality during event sequences. The structural guides also help conduct heat from the waste form to the walls of the waste package, where it is radiated to the surrounding drift walls (CRWMS M&O 2000au, Section 2.4.1.4).

3.2.2.2 Control Rods

Control rods similar to those used in reactors will be placed in waste packages that need additional long-term criticality control, such as those containing highly reactive fuel assemblies from pressurized water reactors. Control rods are made of boron carbide and have Zircaloy cladding. Because this is the same material used in most fuel rod cladding, it will have similar corrosion properties and longevity.

3.2.3 Preliminary Engineering Specifications for the Commercial Spent Nuclear Fuel Waste Package Designs

The preliminary engineering specifications for the waste package design include the waste form characteristics, the physical dimensions of the waste package, and material specifications. Tables 3-7 and 3-8 provide preliminary engineering specifications for the waste package designs for commercial spent nuclear fuel based on the physical dimensions, thermal output, and reactivity of the fuel. Table 3-9 shows the material specifications of the waste package components. These engineering specifications were developed to meet the performance specifications given in Table 3-1.

3.3 U.S. DEPARTMENT OF ENERGY SPENT NUCLEAR FUEL, HIGH-LEVEL RADIOACTIVE WASTE, AND IMMOBILIZED PLUTONIUM

Ten types of canisters of DOE spent nuclear fuel and high-level radioactive waste may be received at the potential repository (CRWMS M&O 2000az, Sections 4.2 and 4.3):

1. Naval spent nuclear fuel canisters, short

2. Naval spent nuclear fuel canisters, long

3. DOE spent nuclear fuel canisters, short

4. DOE spent nuclear fuel canisters, long

Table 3-7. Physical Dimensions of Commercial Waste Package Designs

No.	Waste Package Design	Outer Diameter mm (in.)	Outer Length mm (in.)	Mass of Empty WP kg (lb)	Mass of Loaded WP kg (lb)
1	21-PWR Absorber Plate	1,644 (64.7)	5,165 (203.3)	26,000 (57,300)	42,300 (93,300)
2	21-PWR Control Rod	1,644 (64.7)	5,165 (203.3)	26,000 (57,300)	42,300 (93,300)
3	12-PWR Long	1,330 (52.4)	5,651 (222.5)	19,500 (43,000)	30,100 (66,400)
4	44-BWR	1,674 (65.9)	5,165 (203.3)	28,000 (61,700)	42,500 (93,700)
5	24-BWR	1,318 (51.9)	5,105 (201)	19,400 (42,800)	27,300 (60,200)

NOTES: Control rods do not add any mass to the package because they displace the mass of nonfuel components (e.g., existing control rods, in-core detectors) included in the fuel assembly mass. WP = waste package. Source: CRWMS M&O 2000au; BSC 2001n.

Table 3-8. Commercial Spent Nuclear Fuel Characteristics by Waste Package Design

Waste Package Design	Average Waste Package Heat Generation Rate Based on Assembly Heat at Repository Arrival (kW)	Number of Assemblies	Assembly Average Burnup (GWd/MTHM)	Assembly Average Initial ^{235}U Enrichment (wt)	Average MTHM per Assembly	Average Assembly Age (years)
21-PWR Absorber Plate	11.53	90,262	41.5	3.74	0.430	23.00
21-PWR Control Rod	3.11	1,992	19.6	3.57	0.368	36.14
12-PWR Long	9.55	1,955	46.3	4.01	0.540	18.04
44-BWR	7.38	124,532	34.1	3.04	0.177	22.41
24-BWR	0.52	2,013	8.1	2.63	0.167	40.32

NOTES: Based on 63,000 MTHM. GWd = gigawatt day. Source: CRWMS M&O 2000bb, Table 10.

Table 3-9. Waste Package Design Component Materials

Component	Material

Dual-layer design:
  Inner structural shell
  Outer corrosion-resistant barrier
	
	Stainless Steel Type 316NG
	Alloy 22 (SB 575 N06022)

WP fill gas	Helium
Fuel tubes for commercial SNF WP basket design	Carbon steel (SA 516 Grade 70)
Neutron absorber interlocking plates for commercial SNF WP	Neutronit A 978 (borated 316 stainless steel)
Interlocking plates for 21-PWR Control Rod design	Carbon steel (SA 516 Grade 70)
Structural guides for commercial SNF WP basket design	Carbon steel (SA 516 Grade 70)
Canister guide for 5-DHLW/DOE SNF designs	Carbon steel (SA 516 Grade 70)
Thermal shunts for commercial SNF WP basket design	Aluminum plate (SB 209 6061 T4)

NOTES: SNF = spent nuclear fuel; WP = waste package.

5. Larger-diameter DOE spent nuclear fuel canisters, short

6. Larger-diameter DOE spent nuclear fuel canisters, long

7. Solidified high-level radioactive waste canisters, short

8. Solidified high-level radioactive waste canisters, long

9. Solidified high-level radioactive waste canisters containing immobilized plutonium cans, short

10. Multicanister overpacks containing spent nuclear fuel from the Hanford N Reactor.

The number of canisters of solidified high-level radioactive waste will greatly exceed the number of canisters of DOE spent nuclear fuel. Therefore, the DOE has developed an efficient arrangement for packing them together (CRWMS M&O 2000az, Section 4.2). This mixing of DOE spent nuclear fuel and high-level radioactive waste is called "codisposal." Codisposal also helps maintain criticality control for DOE spent nuclear fuel that contains highly enriched uranium. Naval spent nuclear fuel canisters, which are larger in diameter, will not be placed in codisposal waste packages; they will be placed one canister per waste package. Because the waste package designs being considered will contain both DOE spent nuclear fuel and

high-level radioactive waste, the following section describes both waste forms, as well as the appropriate waste package designs.

3.3.1   U.S. Department of Energy Spent Nuclear Fuel

DOE spent nuclear fuel has a wide variety of physical, chemical, and nuclear characteristics and represents an inventory of approximately 2,500 MTHM; 2,333 MTHM of this is included in the waste allocation for disposal in the first repository (DOE 1999d, Section 8.1). The waste packages designed for DOE spent nuclear fuel will accept fuel irradiated at DOE facilities, naval spent nuclear fuel, and certain types of material irradiated at commercial nuclear reactors, including debris from the Three Mile Island-2 reactor and fuel from the Fort Saint Vrain reactor. All DOE waste canisters will be sealed before they are transported to the potential repository.

The largest single component of the DOE spent nuclear fuel inventory by weight is uranium metal fuel, at approximately 2,130 MTHM (DOE 1999d, Appendix C, Section 5.1, Table 1). Fuel from the N Reactor at Hanford, Washington, accounts for 2,100 MTHM of this inventory. During its 20-year life, the N Reactor produced nuclear isotopes for defense purposes. N Reactor fuel has an initial enrichment of less than 2 percent uranium-235. It will be placed in multicanister overpacks that will both store the waste onsite and transport it to the potential repository. The multicanister overpack is

a stainless steel container that is slightly wider at the top than at the bottom (DOE 1999d, Appendix C, Section 5.1, Table 1). Although N Reactor fuel is the largest portion of the DOE spent nuclear fuel inventory by weight, it will be emplaced in the repository in only one percent of the waste packages (Table 3-3).

Approximately 184 MTHM of the DOE inventory is low-enriched uranium oxide, some of which is standard commercial spent nuclear fuel used for testing. Some is the fuel debris from the damaged reactor core at Three Mile Island-2, which is already stored in small canisters that can be placed inside a standard DOE canister. The DOE canister can then be inserted into a transportation cask and transported to the potential repository (DOE 1999d, Appendix C, Section 5.1, Table 1).

Approximately 125 MTHM of the DOE inventory includes uranium enriched initially to more than 20 percent uranium-235, uranium enriched initially to between 5 and 20 percent uranium-235, and thorium- and plutonium-based fuels (DOE 1999d, Appendix C, Section 5.1, Table 1).

Naval nuclear fuel is designed to operate in a high-temperature, high-pressure environment for many years. Naval fuel is highly enriched. To ensure it can withstand battle-shock loads, naval fuel is surrounded by large amounts of structural material

made of Zircaloy. There are two canister designs for naval fuel; both use similar materials and mechanical arrangements. The DOE plans to emplace about 65 MTHM of naval spent nuclear fuel in the potential repository. This fuel will be contained within about 300 sealed canisters, which will be transferred directly from transport casks into waste packages (DOE 1999d, Appendix C, Section 5.1, Table 1).

3.3.1.1 Physical Characteristics

The canisters for DOE spent nuclear fuel will be standardized to efficiently utilize the waste package design (CRWMS M&O 2000aw). Table 3-10 gives the preliminary canister dimensions.

3.3.1.2 Thermal Output

DOE spent nuclear fuel has a low thermal output, with naval spent nuclear fuel being the hottest. The maximum thermal output of a naval spent nuclear fuel canister is 8.01 kW, which is well below the maximum limit of 11.8 kW (CRWMS M&O 2000ax, Section 2.5.4.2).

3.3.1.3 Criticality Control

The controlling factors in disposal criticality analyses of DOE spent nuclear fuel are fuel matrix,

Table 3-10. U.S. Department of Energy Waste Forms for Disposal, According to Waste Package Design

Waste Package Design	Canister Length mm (in.)		Canister Diameter mm (in.)		Canister Mass kg (lb)		Canisters/ Waste Package
	HLW	SNF	HLW	SNF	HLW	SNF	
5-DHLW/DOE SNF Short[a]	3,000 (118.1)	3,000 (118.1)	610 (24.0)	457 (18.0)	2,500 (5,512)	2,270 (5,004)	5 HLW / 1 SNF
5-DHLW/DOE SNF Long[a]	4,500 (177.2)	4,570 (179.9)	610 (24.0)	457 (18.0)	4,200 (9,259)	2,721 (6,000)	5 HLW / 1 SNF
Naval SNF Short	N/A	4,750 (187)	N/A	1,689.1 (66.5)	N/A	44,452 (98,000)	1
Naval SNF Long	N/A	5,385 (212.0)	N/A	1,689.1 (66.5)	N/A	44,452 (98,000)	1
2-MCO/2-DHLW Long	4,500 (177.2)	4,200 (165.3)	610 (24.0)	643 (25.3)	4,200 (9,259)	8,910 (19,642)	2 HLW / 2 SNF

NOTES: [a]DOE non-naval spent nuclear fuel.
HLW length and diameter are nominal; HLW mass is maximum. DHLW = defense high-level radioactive waste;
MCO = multicanister overpack; SNF = spent nuclear fuel; N/A = not applicable; HLW = high-level radioactive waste.
Sources: DOE 1999c; Naples 1999; DOE 2000d.

primary fissile isotope, geometry, and enrichment (DOE 1999d, Section 5.2). The 250 types of DOE spent nuclear fuel have been divided into groups based on these four factors to perform criticality analyses.

DOE non-naval spent nuclear fuel from each of the four groups will be analyzed in the appropriate configuration, and data important to preventing criticality—such as fissile loading, enrichment, initial configuration of the basket and spent nuclear fuel, and neutron absorber loading in the canister— will be identified. From these results, waste acceptance criteria will be developed for each group. The canister design will also control criticality by limiting the amount of fissile material in each waste package. If required, neutron absorbers would be added into a canister for further criticality control.

A separate analysis will be performed for naval spent nuclear fuel to demonstrate that criticality would be precluded for all credible event sequence conditions during handling at the repository (Mowbray 1999).

3.3.2 High-Level Radioactive Waste and Immobilized Plutonium

About 22,000 canisters of high-level radioactive waste will be generated by 2035 (DOE 1997b, Section 1.5.4). Approximately 1.5 percent will come from reprocessed commercial nuclear fuel; the rest will come from treatment of materials from the defense nuclear program. The estimated number of high-level radioactive waste canisters to be emplaced in the first repository is approximately 8,300, based on the total inventory limit in the NWPA.

Liquid high-level radioactive waste will undergo a process at its current site that yields a solid leach-resistant material, typically a borosilicate glass. While still liquid, the glass is poured into stainless steel canisters. After the glass cools and solidifies, the canisters are sealed. The potential repository would accept solid high-level radioactive waste generated from activities at DOE's Savannah River, South Carolina, and Hanford, Washington, sites, as well as from the Idaho National Environ-

mental and Engineering Laboratory. The waste will arrive in presealed canisters. The potential repository would also receive, subject to the execution of a disposal contract between the DOE and the state of New York, commercial high-level radioactive waste from the West Valley Demonstration Project in New York.

Up to 17 metric tons of surplus plutonium that is excess to national defense needs will be immobilized within ceramic discs that will have neutron absorber material evenly distributed throughout their matrix (65 FR 1608). The ceramic will resist the leaching of plutonium. Section 3.2 describes the additional 33 metric tons of surplus plutonium that will be converted into mixed-oxide fuel.

3.3.2.1 Physical Characteristics

The canisters containing high-level radioactive waste will be standardized to accommodate the waste package design and to reduce manufacturing costs. Table 3-10 gives the canister dimensions.

3.3.2.2 Thermal Output

DOE high-level radioactive waste has a low thermal output. The total heat generation rate will not exceed 1.5 kW per 3-m (9.8-ft) canister or 1.97 kW per 4.5-m (15-ft) canister (DOE 1999c, Section 4.2.3.1). The maximum thermal output of the hottest waste package, the 5-DHLW/DOE short, is 9.16 kW—well below the maximum limit of 11.8 kW (CRWMS M&O 2000aw, Section 2.5.4.2).

3.3.2.3 Criticality Control

With the exception of high-level radioactive waste canisters containing immobilized plutonium, evaluations have indicated that DOE high-level radioactive waste will not contain enough fissile material to pose a criticality risk.

A principal criticality control measure for the immobilized plutonium is the incorporation of neutron absorbing materials (i.e., gadolinium and hafnium) into the waste form. These materials are an effective criticality control measure for both the preclosure and postclosure phases. The planned

loading strategy for immobilized plutonium is to transfer it into a codisposal waste package containing five high-level radioactive waste canisters but no DOE spent nuclear fuel canister in the center. Detailed criticality analyses (CRWMS M&O 2000ba) have shown that preclosure and postclosure criticality for a waste package that contains five plutonium-loaded canisters, but that does not have a center DOE spent nuclear fuel canister, is below the subcritical limit for criticality to occur. See Section 3.5.2.4 for a brief discussion of the criticality potential of the immobilized plutonium waste form.

3.3.3 U.S. Department of Energy Waste Package Designs

Three waste package design configurations have been developed for codisposal of DOE non-naval spent nuclear fuel and high-level radioactive waste. In two designs that differ only in length, the typical arrangement places a DOE spent nuclear fuel canister in the center of a ring of five high-level radioactive waste canisters. The exception occurs for high-level radioactive waste canisters containing immobilized plutonium, which will be packaged without a DOE spent nuclear fuel canister in the center. Structural guides will provide support to ensure that the DOE spent nuclear fuel canister is not damaged by an impact to the waste package. These guides also facilitate waste package loading. Such support is not needed for high-level radioactive waste glass, which maintains its own structural integrity (CRWMS M&O 2000aw).

The third waste package design will accept multicanister overpacks, which will have a diameter larger than those of DOE spent nuclear fuel or high-level radioactive waste canisters. To prevent criticality, no more than two multicanister overpacks will be put into a waste package. To improve packaging efficiency without compromising criticality prevention, two long high-level radioactive waste canisters will be codisposed with the two multicanister overpacks. A DOE study determined that codisposing two multicanister overpacks with two long DOE high-level radioactive waste canisters would be the most efficient arrangement (CRWMS M&O 2000aw).

Naval spent nuclear fuel will arrive at the potential repository in canisters suitable for long-term disposal. The canisters will fit one to a waste package. Because the naval fuel will arrive in canisters of two sizes (one short and one long), the DOE has devised two waste package designs for it. The larger of these two types will be the heaviest and longest of all the waste packages. No additional features would be necessary for structural support, heat transfer, and criticality control, since these are provided by the naval spent nuclear fuel or the canister (CRWMS M&O 2000ax).

3.3.4 Preliminary Engineering Specifications

The preliminary engineering specifications for the waste package include the waste form, the physical dimensions of the waste package, and material specifications. Tables 3-10 and 3-11 present preliminary engineering specifications for waste package designs for DOE spent nuclear fuel and high-level radioactive waste, which are based on the physical dimensions, thermal output, and criticality potential of the fuel. Table 3-9 shows the material specifications of the waste package components. These engineering specifications were developed to meet the performance specifications given in Table 3-1.

3.4 SELECTING MATERIALS AND FABRICATING WASTE PACKAGES

The selection of materials from which reliable waste packages could be fabricated followed a multistep analysis and design process. It began by analyzing the critical functions of a particular waste package and its various components. In selecting a material for a component, the designers considered both the material's availability and the critical functions the component would serve as part of the waste package. They identified eight major components and eight performance criteria for selecting materials to fabricate them (CRWMS M&O 1997c, Section 3). The eight major components are:

- Structural shell
- Corrosion-resistant barrier
- Fill gas
- Interlocking plates for commercial designs

Table 3-11. Physical Dimensions of Waste Packages Designed for U.S. Department of Energy Waste Forms

No.	Waste Package Design	Outer Diameter mm (in.)	Outer Length mm (in.)	Weight of an Empty Waste Package kg (lb)	Weight of a Loaded Waste Package kg (lb)
1	5-DHLW/DOE SNF Short	2,110 (83.0)	3,590 (141.3)	23,400 (51,600)	38,100 (84,000)
2	5-DHLW/DOE SNF Long	2,110 (83.0)	5,217 (205.4)	32,600 (71,900)	56,300 (124,000)
3	Naval SNF Short	1,949 (76.7)	5,430 (213.8)	25,800 (56,900)	70,300 (155,000)
4	Naval SNF Long	1,949 (76.7)	6,065 (238.8)	28,000 (61,700)	72,500 (159,000)
5	2-MCO/2-DHLW Long	1,815 (71.5)	5,217 (205.4)	21,800 (48,100)	48,100 (106,000)

NOTES: DHLW = defense high-level radioactive waste; MCO = multicanister overpack; SNF = spent nuclear fuel. Source: CRWMS M&O 2000bc, Section 4.3.

- Fuel tubes for commercial designs
- Structural guides for commercial designs
- Guide tube for codisposal designs
- Thermal shunts for commercial designs.

Not every waste package design requires all of these components; it varies according to the waste form each will hold. However, all eight of these components cover the major requirements of all ten waste package designs.

The eight criteria that contribute to performance are:

- Mechanical performance (strength)
- Chemical performance (resistance to corrosion and microbial attack)
- Predictability of performance (understanding the behavior of materials)
- Compatibility with materials of the waste package and waste form
- Ease of fabrication using the material
- Previous experience (proven performance record)
- Thermal performance (heat distribution characteristics)
- Neutronic performance (criticality and shielding).

Reasonableness of cost was considered as a discriminator.

3.4.1 Material Selection

The first step in selecting the waste package materials was identifying the functional requirements for each component. Next, the characteristics of materials that would help meet the requirements were selected. Candidate materials were chosen from commonly available materials (or, in the case of fill gas, from common gases). The materials were then analyzed in terms of how they would perform their intended functions. Once the candidate materials and alternates were selected, they were tested; the results of these tests are summarized in Section 4.2.4.

Table 3-9 lists the component materials selected after testing. The following sections explain the material selection process in more detail.

3.4.1.1 Waste Package Materials: Contributing to Containment

Corrosion-Resistant Materials—Corrosion performance has been determined to be the most important criterion for a long waste package lifetime. Essential performance qualities therefore include a material's resistance to general and localized corrosion, stress corrosion cracking, and hydrogen-assisted cracking and embrittlement. The effects of long-term thermal aging are also important. To address recommendations provided by the Nuclear Waste Technical Review Board, the DOE has initiated studies to gain a better understanding of the processes involved in predicting the rate of

waste package material corrosion over the 10,000-year regulatory period.

Combinations and arrangements of materials as containment barriers were carefully considered from several perspectives. In the process, analysts considered such criteria as (1) material compatibility (e.g., galvanic/crevice corrosion effects); (2) the material's ability to contribute to defense in depth (e.g., because it has a different failure mode from other barriers); (3) the material's ease of fabrication; and (4) the potential impact of thin, corrosion-resistant materials used as containment barriers on a repository's essential operations, such as waste package loading, handling, and emplacement.

The major objectives centered on understanding the temperature and humidity conditions that would exist at different times for a range of thermal operating modes in a particular unsaturated zone, then designing the waste packages accordingly. Since the properties of any material selected for a corrosion barrier would inevitably be influenced by the temperature and humidity conditions in a repository of a particular design at a particular site, selecting the right corrosion-resistant material became one of the most important priorities.

After assessing potential materials available for waste package corrosion barriers, analysts selected nickel- and titanium-based alloys as the most promising candidate materials for corrosion resistance in an oxidizing environment such as Yucca Mountain. Using a corrosion-resistant material as the outer barrier of the waste package will significantly lower the risk of waste package failure from corrosion. Alloy 22 was selected as the preferred material for the outer barrier because it has excellent resistance to corrosion in the environment expected at Yucca Mountain; it is easier to weld than titanium; and it has a better thermal expansion coefficient match to Stainless Steel Type 316NG than titanium. A structurally strong material (stainless steel) was chosen for the inner layer of the waste package (CRWMS M&O 2000av, Section 7.6).

Alloy 22 also offers benefits in the areas of program and operating flexibility. It is extremely corrosion-resistant under conditions of high temperature and low humidity, such as those that would prevail for hundreds to thousands of years in a repository designed to allow a relatively high thermal output from the waste packages. At low temperatures, Alloy 22 is extremely corrosion-resistant in either low or high humidity. Thus, the selection of Alloy 22 supports the flexibility to operate the potential repository over a range of thermal modes (CRWMS M&O 2000av). Uncertainty about the waste package corrosion rate may be reduced by avoiding the conservatively defined window of corrosion susceptibility for Alloy 22, which can be accomplished by keeping waste package temperatures below 85°C (185°F) or maintaining the in-drift relative humidity below 50 percent (Dunn et al. 1999, p. xvi; CRWMS M&O 2000n, Section 3.1.3.1). Table 3-12 presents the chemical composition of Alloy 22.

Table 3-12. Chemical Composition of Alloy 22

Element	Composition (wt%)
Carbon (C)	0.015 (max)
Manganese (Mn)	0.50 (max)
Silicon (Si)	0.08 (max)
Chromium (Cr)	20.0 to 22.5
Molybdenum (Mo)	12.5 to 14.5
Cobalt (Co)	2.50 (max)
Tungsten (W)	2.5 to 3.5
Vanadium (V)	0.35 (max)
Iron (Fe)	2.0 to 6.0
Phosphorus (P)	0.02 (max)
Sulfur (S)	0.02 (max)
Nickel (Ni)	Balance

Source: ASTM B 575-97, *Standard Specification for Low-Carbon Nickel-Molybdenum-Chromium, Low-Carbon Nickel-Chromium-Molybdenum, Low-Carbon Nickel-Chromium-Molybdenum-Copper and Low-Carbon Nickel-Chromium-Molybdenum-Tungsten Alloy Plate, Sheet, and Strip.*

Structural Materials—The major functional requirement of the structural material for the inner layer of the waste package is to support the corrosion-resistant outer material. The DOE chose Stainless Steel Type 316NG for the structural layer (CRWMS M&O 2000av, Section 5.2). This material provides the required strength; has a better compatibility with Alloy 22 than carbon steel; and

provides an economical solution to functional requirements. Table 3-13 presents the chemical composition of Stainless Steel Type 316NG.

Table 3-13.   Chemical Composition of Stainless Steel Type 316NG

Element	Composition (wt%)
Carbon (C)	0.020 (max)
Phosphorus (P)	0.030 (max)
Silicon (Si)	0.75 (max)
Copper (Cu)	0.50 (max)
Titanium (Ti)	0.05 (max)
Tantalum (Ta) and Niobium (Nb)	0.05 (max)
Manganese (Mn)	2.00 (max)
Sulfur (S)	0.005 (max)
Nitrogen (N)	0.060 to 0.10
Cobalt (Co)	0.10 (max)
Boron (B)	0.002 (max)
Bismuth (Bi) + Tin (Sn) + Arsenic (As) + Lead (Pb) + Antimony (Sb) + Selenium (Se)	0.02 (max)
Chromium (Cr)	16.00 to 18.00
Molybdenum (Mo)	2.00 to 3.00
Nickel (Ni)	11.00 to 14.00
Vanadium (V)	0.1 (max)
Aluminum (Al)	0.04 (max)
Iron (Fe)	Balance

Sources: For all elements except carbon and nitrogen, values presented are within the ranges and maximum limits provided by ASTM A 276-91a, *Standard Specification for Stainless and Heat-Resisting Steel Bars and Shapes.* Values for carbon and nitrogen are given by Danko (1987, p. 931).

3.4.1.2   Waste Package Materials: Internal Components

The designs for commercial spent nuclear fuel and DOE codisposal waste packages include internal components (i.e., structural guides, interlocking plates, fuel tubes, and thermal shunts) that must be able to sustain the mechanical loads created by handling, emplacement, and, if necessary, retrieval. Thus, mechanical performance was a major selection criterion. Thermal performance was also an important selection criterion because these components provide an additional path for conducting heat from the waste form to the walls of the waste package. The fuel tubes contact both the waste

form and the basket plates. If the material selected for the tubes causes the waste form to degrade, release rates could be increased; if it causes the plates to degrade, criticality control could be compromised. Therefore, compatibility with other materials was an important criterion. The waste package design does not rely on these components for postclosure performance, so corrosion-resistant materials are not needed. Two grades of carbon steel (SA 516 Grades 55 and 70) were found to be the best choices for these internal components, based on the criteria; the designers chose to use Grade 70 (CRWMS M&O 2000bd, Section 4).

Neutron Absorber Interlocking Plates—The most important function of the neutron absorber is to reduce the potential for criticality. The neutron absorber material is typically an additive to a carrier material (e.g., stainless steel alloyed with a boron compound). The neutron absorber is used in the interlocking plates in the internal basket. Corrosion behavior is important in keeping the neutron absorber material in place and effective long after emplacement, so chemical performance in a variety of environments was an important selection criterion. Mechanical performance was an evaluation factor because the interlocking plates must be able to sustain the mechanical loads created by handling, emplacement, and, if necessary, retrieval. Compatibility with other materials was considered, since the plates must not cause the waste form to degrade. The plates also provide an important path for conducting heat from the waste form to the walls of the waste package, so thermal performance was considered. The material of choice was Neutronit A 978. Its selection was based on its corrosion performance compared to the other candidate materials, as well as its available boron concentration. The composition of Neutronit is similar to SA 240 Stainless Steel Type 316 but with 1.6 percent boron added (CRWMS M&O 2000be, Section 3.1.3).

Thermal Shunts—The thermal shunts provide another important path for conducting heat from the waste form (in this case, commercial spent nuclear fuel) to the walls of the waste package. The thermal conductivity of the material is very important. The thermal shunts would be in contact with the waste form, so compatibility with spent nuclear

fuel was an important evaluation criterion. The thermal shunts are only needed during the early period of repository performance, when the decay heat from spent nuclear fuel would be relatively high. The material selected does not need a high degree of corrosion resistance. The thermal shunts must have enough structural strength to withstand handling, emplacement, and possible retrieval operations. However, these service loads are not very large, so mechanical performance was not selected as an evaluation criterion. Aluminum alloys 6061 and 6063 were selected over copper because of concerns that, should a waste package be breached and water enter, copper may react with the chloride ions in the water. This could result in accelerated degradation of the Zircaloy cladding on the spent nuclear fuel, which would eventually release radionuclides from the waste (CRWMS M&O 2000be, Section 3.2.3).

3.4.1.3   Fill Gas

The fill gas can be a significant conductor of heat from the waste form to the internal basket, so thermal performance was deemed one of the most important criteria in choosing a gas. The fill gas should not degrade other components of the waste package, so compatibility with other materials was another important criterion. Helium is routinely used as the fill gas for fuel rods, which indicates that helium would have an excellent compatibility with spent nuclear fuel. Based on a review of data on thermal conductivity and the fact that helium is chemically inert, it was chosen over other candidate gases, such as nitrogen, argon, and krypton (CRWMS M&O 2000be, Sections 3.3.1 through 3.3.3).

3.4.2   Waste Package Fabrication Process

This section describes the fabrication process for the waste package, which is shown schematically in Figures 3-7 and 3-8. The fabrication process was based on both the design criteria and the physical characteristics of the selected materials.

The waste package will be fabricated, welded, and inspected in accordance with those portions of the *ASME Boiler and Pressure Vessel Code,* Section III, Division I, Subsection NB (Class 1 Compo-

nents) (ASME 1995) that will ensure the waste package will perform in accordance with the design basis. Because the largest number of waste packages will be manufactured for commercial spent nuclear fuel, this type will serve to illustrate the basic fabrication process for all waste package types. The other types would be fabricated in a similar way, though some dimensions would vary.

The commercial fuel waste package uses Neutronit A 978 and carbon steel interlocking plates with carbon steel tubes (CRWMS M&O 2000bf, Section 8.1). All waste package fabrication would take place offsite, including the welding of the bottom lids. The top lids, although fabricated offsite, would be welded on in the Waste Handling Building after the waste package had been loaded.

3.4.2.1   Outer Cylinder Fabrication

Forming the outer cylinder of rolled and welded Alloy 22 plate requires two half-length cylinders (see Table 3-7 for completed waste package lengths) because of the limitations of most rolling fabricators. Initially, the plate would be approximately 5,080 mm (200 in.) long by 2,540 mm (100 in.) wide. The thickness would permit machining (for rounding) after welding. After being received by the fabricator, the plate would be inspected, laid out to establish the developed length, and thermally cut to size. The plate would then be rolled (CRWMS M&O 2000bf, Section 8.1.1).

The cylinder would then be adjusted to meet the required diameter and the inner circumference, taking into consideration the subsequent weld shrinkage of the longitudinal seam. The long seam weld preparations would be machined and prepared for welding. The cylinder would be braced to minimize the weld distortion and welded. The braces would be removed, and the weld seam would be prepared for nondestructive examination. One end of the cylinder would be prepared for circumferential seam welding. In parallel, a second cylinder would be prepared the same way (CRWMS M&O 2000bf, Section 8.1.1).

The two cylinders would then be joined and circumferentially welded, with subsequent nonde-
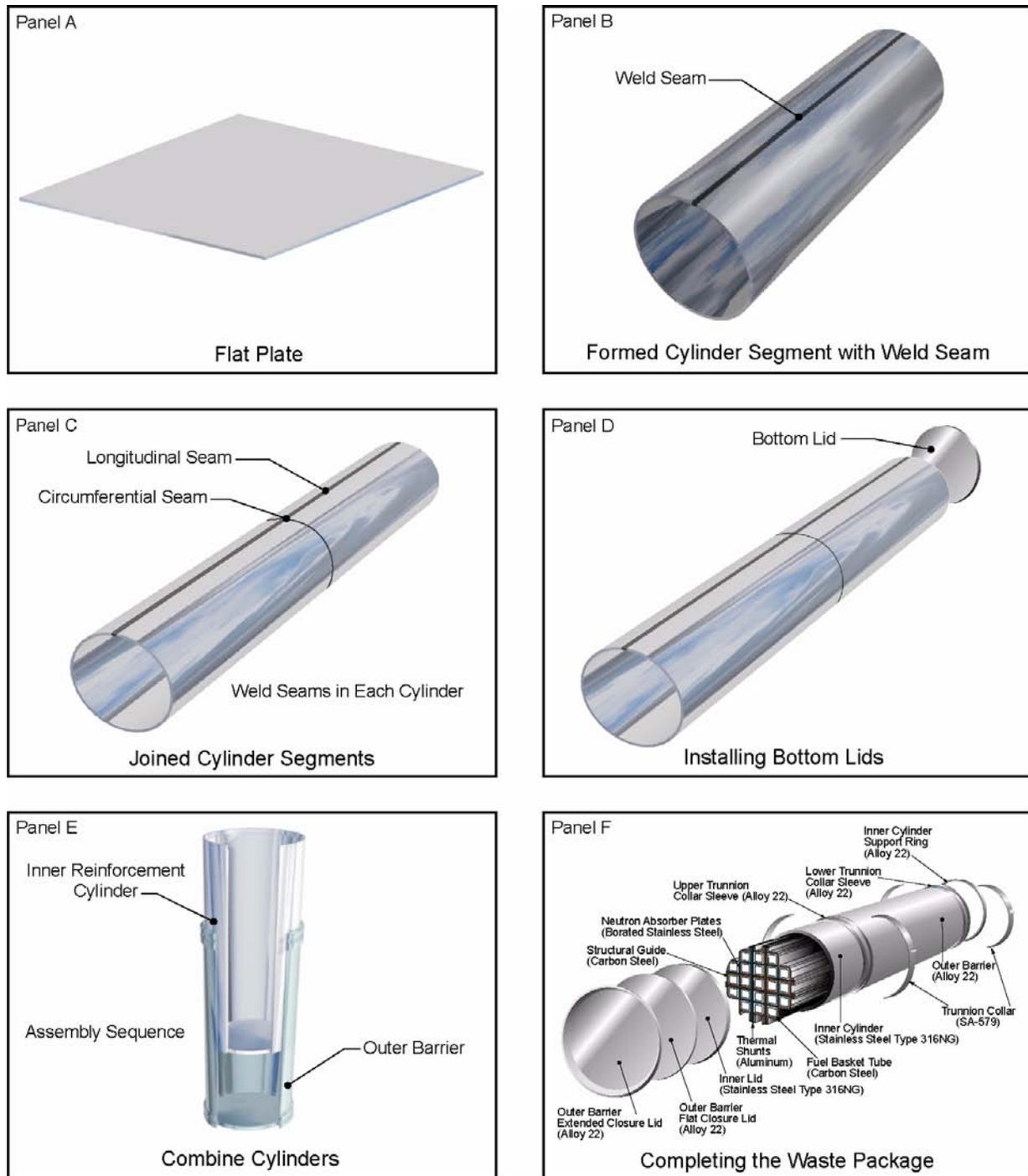
Figure 3-7.   Waste Package Fabrication Process
The waste package fabrication process starts with a flat plate of metal (Alloy 22 for the outer cylinder, Stainless Steel Type 316NG for the inner cylinder) (Panel A). The plate is rolled and welded to form a cylinder segment (Panel B). Two cylinder segments are combined and welded to form a waste package inner or outer cylinder (Panel C). Lids are attached to the inner and outer cylinders (Panel D). The inner cylinder is inserted into the outer cylinder to form the waste package (Panel E). The internal components, waste form, and lids are added to complete the waste package (Panel F).
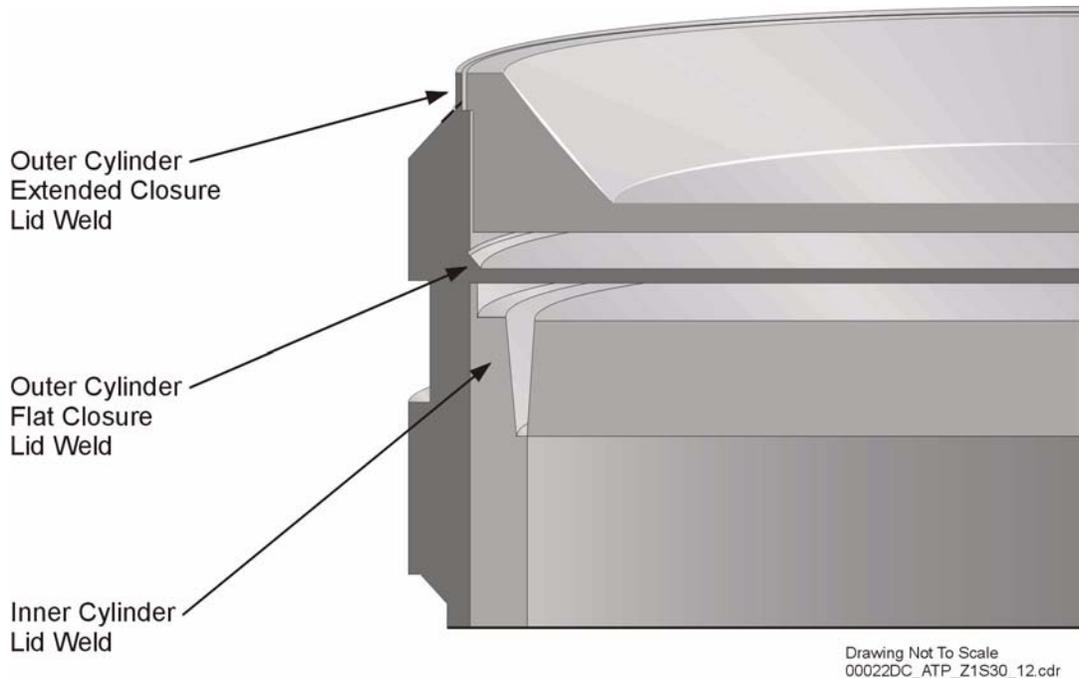
Figure 3-8.   Waste Package Final Closure Welds
The process for the final closure welds on the top lids must be performed remotely in a high-radiation environment to produce high-integrity welds that can be inspected in the "as-welded" condition. Weld joint configurations, process techniques, and procedures have been developed for, and demonstrated on, inner and outer cylinder final closure welds for full-diameter waste package mockups. The narrow-groove, hot-wire, semiautomatic gas tungsten arc weld process can be done remotely, and has proven to produce single-bead layer welds with acceptable weld and corrosion properties.

structive examination testing performed on the circumferential seam. The outer cylinder would be inspected to verify that the inside diameter is within tolerance. The inside of the cylinder would then be machined (CRWMS M&O 2000bf, Section 8.1.1).

3.4.2.2   Inner Cylinder Fabrication

To form the stainless steel inner cylinder, workers would start with two plates of Stainless Steel Type 316NG large enough to make half the inner cylinder length (see Table 3-7 for completed waste package lengths). The full cylinder length would require two plates, each approximately 4,980 mm (196 in.) wide by 2,540 mm (100 in.) long. Each plate would be cut or machined for size and longitudinal weld preparations. The plates would be roll-formed to make two half-cylinders and welded. Inspectors would use nondestructive techniques to examine both the cylinders and the welds. The weld preparations for the circumferen-

tial seam would be machined, then the cylinder would be assembled and circumferentially welded. Nondestructive examination inspections would again be performed on the circumferential weld, and the cylinder would then be machined (CRWMS M&O 2000bf, Section 8.1.2).

3.4.2.3   Lid Fabrication

The outer and flat closure lids would be fabricated from Alloy 22 plates approximately 1,900 mm (75 in.) wide and 3,800 mm (150 in.) long. The plates would then be cut to the correct diameter and the edges machine cleaned to prepare for the weld (CRWMS M&O 2000bf, Section 8.1.3).

The inner lids would be fabricated from a Stainless Steel Type 316NG plate approximately 1,800 mm (71 in.) wide and 3,600 mm (142 in.) long. The plate would be laid out for the cutting of two circles. The plates would then be thermally cut to the correct diameter, and the edges would be

machine cleaned to prepare for the weld (CRWMS M&O 2000bf, Section 8.1.3).

3.4.2.4   Assembly of Support Ring

A support ring attached to the inner diameter of the outer cylinder is required to hold the inner cylinder in place. This ring would be made from 20-mm (0.8-in.) thick Alloy 22 plate. A piece would be cut 100 mm (4 in.) wide and rolled into a ring, then weld preparations would be machined. The ring would be fit to the inside of the outer cylinder near the bottom end, welded, and inspected (CRWMS M&O 2000bf, Section 8.1.4).

3.4.2.5   Assembly of Lid to Cylinder

Once the inner and outer cylinders had been completed, the inner and outer bottom lids would be welded in place. The structures would be set in a vertical position and the lids assembled to each cylinder. The welding could then be done in the flat position. After the welding had been completed, radiographic examination, ultrasonic examination, and liquid penetrant examination would be performed on the inner and outer lid seams. Radiographic and ultrasonic inspection would ensure that all detectable flaws, regardless of their orientation, were identified. Liquid penetrant inspection would ensure that surface indications were identified (CRWMS M&O 2000bf, Section 8.1.5).

3.4.2.6   Annealing of Outer Cylinder

Annealing is a process in which a material is subjected to a controlled heating and cooling cycle to affect material properties, for example, to relieve residual stress. Residual stresses are a common by-product of fabrication processes, such as forming, machining, and welding. Stress mitigation techniques, such as annealing, will be applied to the outer cylinder to minimize the potential for stress corrosion cracking. Since the closure lids will be welded shut after the waste has been loaded, different mitigation techniques may be employed. The parameters for the annealing operation are still being developed, but the DOE expects that the cylinder assembly will be heated in a furnace and then quenched by water (CRWMS M&O 2000bf, Section 8.1.7).

3.4.2.7   Assembly of Commercial Spent Nuclear Fuel Waste Package

The objective of machining is to produce a gap ranging from 0 to 4 mm (0 to 0.16 in.) between the inner and outer cylinders. Over time, the stainless steel inner cylinder will expand in response to the heat emitted by the radioactive decay of its contents. Even with the cylinders touching, there is enough allowance for the inner cylinder to heat up and expand without putting excessive stress on the Alloy 22 outer cylinder. Static loads in the outer barrier shell will not produce tensile stresses above 10 percent of the yield strength of the outer barrier material (CRWMS M&O 2000au, Section 1.2.1.23).

After both the outer and inner reinforcement cylinders had been machined, they would be fitted together. The outer cylinder would be heated to about 370°C (700°F) to allow the inner cylinder to be lowered inside. The heat would then be removed and the cylinders allowed to cool (CRWMS M&O 2000bf, Section 8.1.8).

3.4.2.8   Basket and Internal Components

Once the inner and outer cylinders and the bottom lids had been assembled, the container would be ready for the addition of the internal components. The cylinder would be laid out to establish the location of the internal corner guide assemblies and the internal side guides. The corner guide assemblies and the side guides would be put in place and welded, using manual gas tungsten arc welding.

The bottom set of plates would be installed in an interlocking fashion, followed by three additional sets. The tubes would be inserted and the tube tops stitch-welded together, if required.

The waste package would then be cleaned, wrapped, and protected for shipment to the repository surface facility and storage until it was ready to be loaded and sealed (CRWMS M&O 2000bf, Section 8.1.10). The final fabrication step, performed at the repository surface facility, would be the annealing of the closure weld area to mitigate the stresses that may have been induced during the welding of the outer closure lid. For

more details on the process of loading the waste package, refer to Section 2.2.4.

3.5 WASTE PACKAGE DESIGN EVALUATIONS

The waste package must satisfy defined performance specifications to protect the public and workers and to meet the performance objectives of a repository. An example of a performance specification is the ability of a waste package to withstand a tipover event without breaching. Performance specifications are discussed in the following sections, where they are categorized by relevant engineering discipline (i.e., thermal, criticality, structural, and shielding). Detailed discussions of performance specifications are available in System Description Documents (e.g., CRWMS M&O 2000au).

Some of the performance specifications and supporting evaluations depend on temperature. In these cases, the evaluation is based on the higher-temperature operating mode. Further evaluations of lower-temperature operating modes are part of ongoing engineering studies.

To show that waste packages can be successfully developed for the various waste forms expected to be received at the repository, a sensitivity analysis was performed to determine which waste package designs best represent the widest array of design configurations and waste forms (CRWMS M&O 2000az). This selection was based on the number of waste package types expected to be needed for the repository—for instance, the two commercial spent nuclear fuel waste package designs chosen for analysis represent over 95 percent of the total required—and the relationship of a waste package type to a limiting performance specification (e.g., a heavier waste package would be more susceptible to a drop event). Detailed design work was performed for four waste package types:

- 21-PWR Absorber Plate
- 44-BWR
- 5-DHLW/DOE SNF Short
- Naval SNF Long.

3.5.1 Thermal Evaluations Performed on the Waste Package Design

Thermal analyses have been performed to demonstrate that waste form temperatures will not exceed levels established to maintain waste form integrity. The thermal specification for commercial spent nuclear fuel ensures that the cladding temperature will not compromise the integrity of the cladding, a barrier to radionuclide release. A specification for DOE high-level radioactive waste ensures that the glass does not reach a transition temperature that would cause significant changes in its phase structure or composition. Such an alteration would increase the solubility of the glass and reduce the time required for movement of the radionuclides embedded inside.

With respect to these thermal functions, two performance specifications were selected for evaluation: (1) Zircaloy commercial spent nuclear fuel cladding must be maintained below 350°C (660°F) under normal conditions (CRWMS M&O 2000au, Section 1.2.1.6), and (2) the temperature of DOE high-level radioactive waste must be maintained below 400°C (750°F) under normal conditions (CRWMS M&O 2000aw, Section 1.2.1.6).

3.5.1.1 Spent Nuclear Fuel Cladding Temperature

To calculate the cladding temperature for commercial spent nuclear fuel, time-dependent heat generation rates of the waste packages were adjusted to ensure that the average heat generation rate of an emplacement drift segment was the same as that for the repository as a whole, as discussed in Section 2.3.1. The calculation used a representative section of a drift containing one 21-PWR Absorber Plate, one 44-BWR, and one 5-DHLW/DOE SNF waste package, arranged as shown in Figure 3-3. The 21-PWR Absorber Plate serves as the design basis waste package, with a maximum heat generation rate of 11.8 kW. The second waste package, the 44-BWR, is based on an average heat generation rate of 7.0 kW. The 5-DHLW/DOE SNF waste package serves as a balancing package in which the heat generation rate is varied to ensure the average in the drift segment is the same as that

in the repository as a whole. The time-dependent waste package surface temperatures calculated were used to perform a two-dimensional analysis of the internal components of the waste package. This calculation gives the peak cladding temperature for the design basis waste package (CRWMS M&O 2000au). The peak cladding temperature for commercial spent nuclear fuel was calculated to be 282°C (542°F), with the peak occurring 35 years after emplacement. The waste package spacing for the calculation was modeled as 0.1 m (0.3 ft), with a 25-year ventilation period (CRWMS M&O 2000au, Section 2.5.1.6). Active ventilation for 25 years would provide heat removal, limiting the heat-up of the waste package during preclosure.

Peak cladding temperature is not an issue for DOE spent nuclear fuel because no credit is taken for the fuel cladding in performance assessment. A canister of naval spent nuclear fuel will have lower heat generation than a waste package containing commercial spent nuclear fuel. Thermal analysis indicates that thermal limits associated with naval spent nuclear fuel will not be exceeded in the repository (CRWMS M&O 2000ax, Section 2.5.4.2).

3.5.1.2 High-Level Radioactive Waste Canister Temperatures

The vitrified high-level radioactive waste form could undergo devitrification at temperatures above 400°C (750°F). A maximum peak value of 214.5°C (418°F) occurs in the glass under normal conditions, which is well below the 400°C (750°F) threshold (CRWMS M&O 2000aw).

3.5.2 Criticality Evaluations Performed on Waste Package Designs

3.5.2.1 Preclosure Evaluations— Commercial Spent Nuclear Fuel

This section describes the performance specifications for criticality of commercial spent nuclear fuel. Further details on preclosure criticality analysis are available in the *Preclosure Criticality Analysis Process Report* (CRWMS M&O 1999i).

Each specific fuel assembly or material received by the repository has an associated fuel reactivity, or capability of contributing to a self-sustained nuclear fissioning process (criticality). The major properties of fuel reactivity in available commercial spent nuclear fuel are the initial enrichment and the burnup of the fuel when it was discharged from the reactor. Enrichment is the weight percentage of a fissile isotope compared to the total amount of uranium in the fuel assembly. Burnup is a measure of the amount of energy produced by the assembly while it was in operation. The higher the initial enrichment of the fuel, the more it can contribute to a critical system. The higher the burnup, for domestic commercial nuclear fuel, the less it can contribute to a critical system. A detailed description of the physics of criticality is provided in Section 4.3.3.2.1.

During the preclosure period, criticality is prevented in waste packages by ensuring, before loading, that the reactivity for each fuel assembly is below the level required for criticality. This is accomplished through the use of loading curves. Loading curves show the minimum allowed burnup as a function of initial enrichment and provide a simple go/no-go check, using the available information, on whether a fuel assembly can be loaded unaltered into a standard waste package without any concern for criticality. The presence of a moderator will be controlled as necessary to ensure subcriticality.

There are two main aspects to loading curve development: the determination of the value of reactivity considered limiting and the determination of the burnup/enrichment pairs that correspond to this value.

The loading curve methodology summarized below is described in detail in the *Preclosure Criticality Analysis Process Report* (CRWMS M&O 1999i, Section A.1). The effective neutron multiplication factor (k_{eff}) of a system is the measure of criticality; when k_{eff} is greater than or equal to 1.0, criticality occurs. If the effective neutron multiplication is less than 1.0, the system is considered subcritical. When designing a system (e.g., a waste package) to be subcritical, there must be a means for ensuring that a k_{eff} value conservatively repre-

sents the true k_{eff} of the system. This is accomplished by choosing a value below 1.0 at which nuclear criticality is assumed to occur. This value is known as the critical limit. The critical limit is determined by accounting for and bounding the bias in the calculational method used, and the uncertainty in the experiments used, to validate the method of calculation. For the calculations performed thus far, the critical limit for k_{eff} is 0.98. Because ensuring subcriticality is important to the health and safety of the repository workers, the calculations add an administrative safety margin of 5 percent for preclosure to provide additional conservatism. The loading curve is therefore based on a k_{eff} value of 0.93, referred to as the administrative limit. Any criticality calculation that uses the same tools on which the critical limit was based and shows a k_{eff} less than or equal to 0.93 provides high confidence that the system will not become critical (CRWMS M&O 2000bg, Section 6.2.1).

Once the criticality limit is established, many calculations are performed to determine, for a specific value of initial enrichment, what burnup results in a k_{eff} that equals the administrative limit (Figure 3-9). These calculations are performed for a point where the waste package is fully loaded with the same fuel assembly. Criticality calculations are performed in increments over the range of initial enrichments and burnups for each commercial fuel type to be received at the repository. The points where the different burnup/enrichment pairs equal the administrative limit can then be represented as a single curve of initial enrichment versus burnup, referred to as a loading curve.

Figure 3-9 shows an example of a loading curve. Loading curves will be developed for each waste package type containing commercial spent nuclear fuel. Any fuel that has a burnup/enrichment pair equal to or above the loading curve line can be loaded unaltered into that waste package type, and criticality will not occur in that waste package during preclosure. Some assemblies that fall below the curve will have to be loaded into the waste package with additional neutron absorber material so they will be above the line. Another option is to load the fuel assembly into a type of waste package that contains fewer fuel assemblies (e.g., the
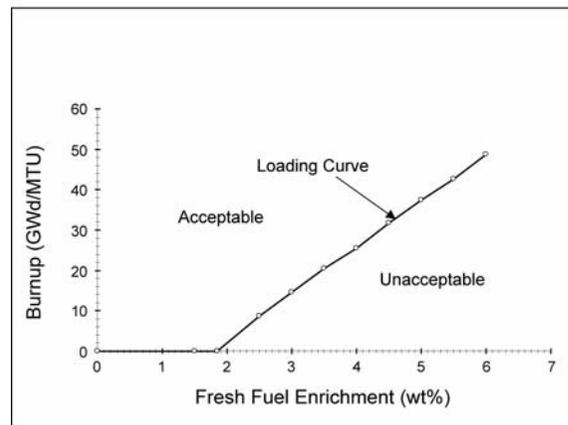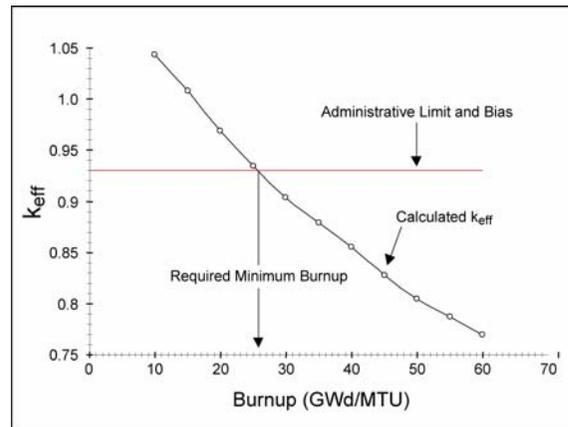
00022DC_ATP_Z1S3-05.ai

Figure 3-9. Administrative Limit for Calculated k_{eff} and Typical Loading Curve

Criticality calculations are performed in increments over the range of initial enrichments and burnups for each commercial spent nuclear fuel type to be received at the repository. The points where the different burnup/ enrichment pairs equal the administrative limit can then be represented as a single curve of initial enrichment versus burnup. This representation is a typical criticality loading curve. Fuel that meets the initial enrichment (in this case, the 4 percent initial enrichment is shown) and has the minimum required burnup (shown in the area noted as "acceptable") may be placed in the waste package for which the evaluation is being performed. GWd = gigawatt day.

12-PWR and 24-BWR), making the waste packages subcritical.

In the loading curve evaluation, margin to criticality is shown assuming the highly unlikely (beyond design basis), but essential to criticality, event of a waste package that is completely filled with water. A loading curve evaluation has been performed for the 21-PWR Absorber Plate model, as documented in the *21 PWR Waste Package Loading Curve Evaluation* (CRWMS M&O 2000bg, Section 6). The 21-PWR waste package design was chosen because more information is available about it than about the other designs. The 21-PWR waste package is also considered to be the design with the highest inherent reactivity (CRWMS M&O 2000az, Table 8). The 21-PWR loading curve evaluation is representative of calculations that will be performed for the other waste package types.

The waste package will be designed so that during preclosure, nuclear criticality cannot be possible unless at least two unlikely, independent, and concurrent or sequential changes occur in the conditions essential to nuclear criticality safety.

3.5.2.2 Postclosure Criticality Evaluation: Commercial Spent Nuclear Fuel

The methodology that has been developed to evaluate potential for criticality and to ensure that significant impacts are prevented during the postclosure period is described in detail in *Disposal Criticality Analysis Methodology Topical Report* (YMP 2000c, Section 3). Section 4.3.3.2 summarizes this methodology and the analyses conducted using it.

Evaluations show that there is a very small probability that a potential critical configuration might result under the repository and fuel conditions described in this report, but that if a postclosure criticality were to occur, the effects would not compromise the ability of the repository to protect public health or meet design objectives or regulatory limits. The evaluations were performed assuming the most reactive combinations of such factors as the amount of fissile uranium and plutonium, the physical arrangement of the fuel, and the presence and amount of moderator in the waste package. The results indicate that all applicable limits can be met and public health protected using the current waste package designs.

3.5.2.3 Evaluations of Criticality Potential of U.S. Department of Energy Spent Nuclear Fuel

Analyses to demonstrate the viability of disposal have been performed or are in process for seven groups of DOE non-naval spent nuclear fuel. A separate analysis is being performed for naval spent nuclear fuel to demonstrate that criticality will be prevented for all credible event sequence conditions in the repository (Mowbray 1999).

In general, the amount of DOE spent nuclear fuel allowed per canister is a function of the physical size and weight limitations of the canister. The limitation on the amount of fissile material per canister provides criticality control. However, insoluble neutron absorbers (gadolinium compounds and alloys) are required for criticality control within the canister for some DOE spent nuclear fuel groups. To date, several items have been identified as important to criticality (DOE 1999d, Section 5.2). The performance and distribution of the neutron absorber material is important in preventing criticality.

The canister shell is also important in preventing criticality because it initially confines the fissile elements and neutron absorber material so they cannot be separated. The canister baskets developed for the representative fuel types are particularly important in cases where they provide the distribution mechanism for neutron absorber material.

The configurations evaluated for each fuel type include varying degrees of degradation, resulting in many different geometric configurations and fissile distributions. These degraded configurations also bound the other types of fuels in a group as long as the limits on fissile mass, linear fissile loading, and enrichment are not exceeded (DOE 1999d, Section 5.2). Further details on DOE spent nuclear fuel criticality analysis are available in completed viability evaluations (CRWMS M&O

2000bh; CRWMS M&O 2000bi; CRWMS M&O 1999j; CRWMS M&O 2000bj; CRWMS M&O 2000bk).

3.5.2.4 Evaluation of Criticality Potential of the Immobilized Plutonium Waste Package

The criticality potential of the immobilized plutonium ceramic discs is effectively controlled by neutron absorbers (i.e., gadolinium and hafnium), which are fabricated into the waste form itself. These materials are an effective criticality control measure. During postclosure, about 50 percent of the hafnium and about 1 percent of the gadolinium is needed to maintain subcriticality under all dilution situations. The DOE has exhaustively examined the physical and chemical processes that might be able to cause a separation, or removal of the neutron absorbers from the waste package entirely, and concluded they are insufficient to warrant further consideration. Detailed criticality analyses (CRWMS M&O 2000ba, p. xii) have shown that five plutonium-loaded canisters, without a center DOE spent nuclear fuel canister, can be placed in the same waste package.

3.5.3 Structural Evaluations Performed on Waste Package Designs

A performance specification for the waste package requires that it not breach during normal operations and event sequences. To address the term "breach" in a quantified manner, threshold limits for failure from the American Society of Mechanical Engineers code will be used. The waste package is designed to meet American Society of Mechanical Engineers code requirements. For event sequences, breach is assumed to have occurred when 90 percent of the ultimate tensile strength has been exceeded. To demonstrate the design adequacy of the waste package with respect to these structural functions, several performance specifications were selected, as documented in the *Waste Package Design Sensitivity Report* (CRWMS M&O 2000az, Section 7). These include:

- Internal pressurization
- Retrieval
- Rockfall

- Vertical drop
- Tipover
- Missile impact (i.e., from an accidental airborne projectile).

3.5.3.1 Internal Pressurization

Pressurization of a commercial spent nuclear fuel waste package could be caused by the rupture of all the fuel rods. Evaluations have been performed over uniform waste package temperatures, ranging from 20° to 600°C (68° to 1,100°F). The peak stresses at the junction of the waste package shell and lid were then compared to the ultimate tensile stress of the waste package materials.

The 21-PWR Absorber Plate waste package was evaluated because it would have the maximum internal pressure due to fuel rod failure. Detailed calculations show that the resulting stresses for all components of the waste package are less than 90 percent of the ultimate tensile strength of the materials; therefore, the waste package will not breach as a result of pressurization, and the criterion is met (CRWMS M&O 2000au, Section 2.5.2.10).

3.5.3.2 Retrieval

The waste package is being designed to allow retrieval up to 300 years after emplacement. The Naval SNF Long waste package is the heaviest waste package for retrieval. The ability of the waste package and pallet to be lifted together as a single unit was calculated. The results show that the maximum stress intensities from lifting among the emplacement pallet Alloy 22 and Stainless Steel Type 316L components are 96 MPa (14,000 psi) and 39 MPa (5,700 psi), respectively. These stress intensity magnitudes are less than one-third of the yield strength and one-fifth of the tensile strength for each of the corresponding materials.

Atmospheric corrosion penetration rates for Alloy 22 and Stainless Steel Type 316 are 0.0093 µm/yr and 0.025 µm/yr, respectively. The calculated cumulative decrease of thickness of the structural members of the emplacement pallet over 300 years of preclosure emplacement is 2.8 µm for Alloy 22 and 7.5 µm for Stainless Steel Type 316.

This negligible level of corrosion renders the waste package retrieval calculation unnecessary, since the consequential change of the results presented in this calculation would be insignificant (CRWMS M&O 2000ax, Section 2).

3.5.3.3   Rockfall

The 21-PWR Absorber Plate waste package design was selected for this evaluation because it would be the most vulnerable to rockfall. Its thinner walls in the outer barrier and its greater sensitivity to internal basket deformation cause greater vulnerability. It is also the most common waste package, and hence the most likely to actually suffer a rockfall impact. This calculation modeled a representative rockfall from the roof of the drift onto the unprotected waste package during preclosure. A height of 3.1 m (10 ft) and a rock size of 13 metric tons (14 tons), which were determined in the event sequence hazards analysis, were modeled (CRWMS M&O 2000au, Section 2.5.2.1). The calculated results, presented in Table 3-14, indicate the survivability of a 21-PWR Absorber Plate waste package in a rockfall event (CRWMS M&O 2000au, Section 2.5.2.1). For event sequences such as rockfall, breach has occurred analytically when 90 percent of the ultimate tensile strength has been exceeded.

Table 3-14.   Summary of Results for Rockfall Calculation

Shell Composition	Calculated Maximum Stress Intensity MPa (psi)	Ultimate Tensile Stress MPa (psi)	Percent of Ultimate Stress
Alloy 22	563 (81,600)	690 (100,000)	82
Stainless Steel	291 (42,200)	517 (75,000)	60

3.5.3.4   Vertical Drop

The vertical drop evaluation was performed using the Naval SNF Long waste package because it is the heaviest design and has the highest internal load; therefore, it will have the highest stresses in the lids during a vertical drop. This calculation modeled a waste package being dropped from a distance of 2 m (6.6 ft).

Detailed calculations demonstrate the survivability of a Naval SNF Long waste package in a vertical drop. The results show that the maximum stresses among the waste package (made of Alloy 22, except for the lower trunnion collar sleeve) and Stainless Steel Type 316NG components are 433 MPa (63,000 psi) and 275 MPa (40,000 psi), respectively. Since these stress intensities are less than 90 percent of the ultimate tensile strength for each of the corresponding materials, the performance specifications are met. The maximum stress in the lower trunnion collar sleeve contacting the unyielding surface is 799 MPa (116,000 psi), which exceeds the tensile strength of Alloy 22. However, this does not constitute failure because the collar sleeve is designed to protect the waste package by acting as a crush zone at the point of impact (CRWMS M&O 2000ax, Section 2.5.2.3).

3.5.3.5   Tipover

A waste package might tip over because of a vertical drop or a seismic event. The 21-PWR Absorber Plate waste package was selected for the preclosure tipover evaluation because of its thinner walls in the outer barrier (made of Alloy 22) and its greater sensitivity to internal basket deformation. It is also the most common waste package. The tipover analysis was simulated in a detailed calculation. Table 3-15 shows the results. The stresses for all components that make up the waste package are less than 90 percent of the ultimate tensile strength of those materials (CRWMS M&O 2000au, Section 2.5.2.6).

Table 3-15.   Summary of Results of Tipover Calculation for 21-PWR Absorber Plate Waste Package

Waste Package Component	Calculated Maximum Stress MPa (psi)	Ultimate Tensile Stress MPa (psi)
Outer Shell and Lids	553 (80,000)	690 (100,000)
Inner Shell and Lids	327 (47,000)	517 (75,000)

3.5.3.6   Missile Impact

A potential internal missile event sequence could take the form of a valve stem being ejected from equipment operating at high pressures. The valve

was estimated to have a mass of 0.5 kg (1.1 lb), a diameter of 1.0 cm (0.39 in.), and a velocity of 5.7 m/s (19 ft/s). The missile impact evaluation was performed for the 21-PWR, 44-BWR, 5-DHLW/DOE SNF, and Naval SNF waste package designs.

The calculated minimum velocity is significantly less that would be required to compromise the integrity of the waste package (CRWMS M&O 2000au, Section 2.5.2.8).

3.5.4 Shielding Evaluations Performed on the Waste Package Design

Shielding analyses evaluate the effects of ionizing radiation on personnel, equipment, and materials. The primary sources for waste package radiation are gamma rays and neutrons emitted from spent nuclear fuel and high-level radioactive waste. Loading, handling, and transporting of waste packages would be carried out remotely to keep personnel exposure as low as is reasonably achievable (e.g., having the human operators behind radiation shield walls, using remote manipulators, viewing operations with video cameras). Shielding analyses were performed for waste package designs to assess the effects of radiation on material and equipment. These analyses provide information used by both the subsurface and surface design programs to determine shielding requirements in the surface facility, on the waste package transporter, and in the subsurface facility.

Because they were designed to contain the waste forms for thousands of years, the waste packages must reduce radiation levels at their surfaces so that radiolytically enhanced corrosion under aqueous conditions is negligible. The shielding analyses determined radiation exposure rates on the surface of the waste package and evaluated whether radiolytically induced corrosion would be a contributing factor to the overall degradation of the waste package.

Shielding analyses were also performed on equipment to determine radiation exposure during the welding of the waste package closure lids. Various pieces of monitoring and control equipment, such as the welding heads and camera, would be close to radiation sources. The results of the shielding analyses will be used to quantify the shielding necessary for a piece of equipment to function properly at a given location for a required period of time.

In emergency situations, which could occur during the transport of waste packages from the surface facilities to the emplacement drifts or during the emplacement of waste packages in the drifts, personnel may have to enter areas near waste packages. Shielding analyses provide an evaluation of the radiation environment surrounding the waste packages so that worker safety can be ensured.

3.5.4.1 Source Term

Engineering calculations were performed to generate source terms, which are used to evaluate an upper limit for the surface dose rate of waste package. The source terms calculated for both pressurized water reactor and boiling water reactor spent nuclear fuel have the following characteristics: 5.5 percent (by weight) initial uranium-235, 75.0 GWd/MTU, and a 5-year decay time for the active fuel region; and 0.711 percent (by weight) initial uranium-235, 75.0 GWd/MTU burnup, and a 5-year decay time for the hardware regions of the assembly. The rationale for these assumptions is discussed in *PWR Source Term Generation and Evaluation* (CRWMS M&O 1999k) and *BWR Source Term Generation and Evaluation* (CRWMS M&O 1999l).

3.5.4.2 Results

The calculated maximum dose rate at the external surface of a 21-PWR Absorber Plate waste package is 1,130 rem/hr (+/-60 rem/hr) (CRWMS M&O 2000bl). The calculated maximum dose rate at the external surface of a 44-BWR waste package is 1,409 rem/hr (+/-32 rem/hr) (CRWMS M&O 2000bl, Section 6.2.3). Radiolytically enhanced corrosion is expected to be insignificant because the gamma dose on the surface of the waste package will not affect the corrosion properties of the waste package (see Sections 4.2.3.1.4 and 4.2.4.3.3).

INTENTIONALLY LEFT BLANK

4. DISCUSSION OF DATA RELATING TO THE POSTCLOSURE SAFETY OF THE SITE

Section 114(a)(1)(C) of the Nuclear Waste Policy Act of 1982 (NWPA), as amended (42 U.S.C. 10134(a)(1)(C)), requires "a discussion of data, obtained in site characterization activities, relating to the safety of such site." This report presents a summary of the results of site investigations, design studies, and analyses of the performance of a potential repository at Yucca Mountain that began in 1978. Since 1986, the U.S. Department of Energy (DOE) has performed these studies as part of a formal program of site characterization that addresses regulations of the U.S. Nuclear Regulatory Commission (NRC). The program is also reviewed by the Nuclear Waste Technical Review Board, the State of Nevada, affected units of local government, and others. This section presents a summary of the data collected during site characterization as they relate to analyses of the postclosure safety of the site. The discussion is divided into six major parts:

- Section 4.1 presents an overview of the postclosure safety assessment approach used by the DOE to evaluate whether Yucca Mountain can safely isolate nuclear waste. It describes the methods the DOE has used to qualitatively and quantitatively assess the safety of the system. The information presented in this section provides a context for understanding how the data collected are related to safety. The discussion includes explicit recognition of the inherent uncertainty in analyses of future performance, and the potential consequences of alternative conceptual models or unexpected events. Methods to accommodate or mitigate uncertainty are summarized. The regulatory requirements for the performance assessment are also explained.

- Section 4.2 describes the data collected during site characterization and explains the DOE's conceptual understanding of the possible future behavior of the potential repository system, based on the data collected. The description is focused on processes important to safety (i.e., those that could affect a radionuclide release). The dis-

cussion is organized around the hydrologic and geologic processes that would operate in the repository system over time. For each component of the system, the text describes the data and information that form the basis of the DOE's understanding, and how the physical processes have been captured, or "abstracted," in the performance assessment. The processes affecting system components described in Section 4.2 include, for example, flow in the unsaturated zone, coupled thermal-hydrologic-geochemical processes near the repository, degradation of drip shields and waste packages, flow into and out of the waste packages, dissolution of the waste form, and transport of radionuclides away from the repository.

- Section 4.3 describes features, events, and processes (FEPs) that, if they occurred at Yucca Mountain, could affect repository performance. The discussion explains how scenarios (i.e., combinations of FEPs used to represent possible future conditions) have been defined that represent possible future conditions and behavior in the potential repository. These scenarios are the basis for the numerical analyses captured in the total system performance assessment (TSPA) and include all of the conditions and processes expected to operate at the repository, as well as disruptive events that could affect performance. Specific potentially disruptive events relevant to Yucca Mountain are described in detail.

- Section 4.4 explains the methods used to quantitatively assess the performance of the potential Yucca Mountain repository and presents the quantitative results of the TSPA for a nominal scenario (i.e., for the 70,000-MTHM base-case layout and higher-temperature mode of operations) and disruptive scenario (i.e., igneous activity), as well as a human intrusion scenario. The purpose of the TSPA analysis is to determine whether a Yucca Mountain repository could adequately protect public health and safety where the

safety standard is defined by regulations that specify limits on allowable radiation doses to the public over the next 10,000 years. The effectiveness of the potential repository system is assessed by probabilistically analyzing performance (i.e., calculating dose rates, expressed as mrem per year) for a wide variety of possible future behaviors. Sensitivity analyses for the various scenarios of environmental conditions are presented to provide insight to the processes and model parameters that most influence TSPA results.

- Section 4.5 describes and explains qualitatively and quantitatively the performance capability of the natural and engineered barriers at Yucca Mountain.

- Section 4.6 describes the proposed program of performance monitoring, testing, and site stewardship that would be conducted at the potential repository. This program has been designed to provide additional confidence that a repository could be safely constructed and operated. It would include a performance confirmation program designed to monitor repository performance during and after its operation to verify that the technical basis for the program is sound. It would also include measures to maintain the ability to retrieve any or all of the waste at any time prior to closure.

This section emphasizes the scientific and engineering data and analyses related to the safety of the Yucca Mountain site. Most of the detailed scientific and engineering data is presented in Sections 4.2 and 4.3, which describe in detail the subsystem processes and the possible disruptive events that would control the performance of the potential repository. Although many of the concepts and descriptions presented are technically complex, the discussion is, to the extent possible, presented in nontechnical terms, so the information is accessible to non-technical readers.

4.1 THE POSTCLOSURE SAFETY ASSESSMENT METHOD

Assessing how a repository will perform over the next 10,000 years and beyond is a challenge for both the DOE and regulators. The limitations to the analyses and the uncertainties inherent in future system behavior cannot be completely eliminated by further testing or modeling. For this reason, the DOE has adopted an approach that relies on multiple lines of evidence to evaluate whether or not a repository at Yucca Mountain could adequately isolate and contain waste during the compliance period. This approach is documented in the *Repository Safety Strategy: Plan to Prepare the Safety Case to Support Yucca Mountain Site Recommendation and Licensing Considerations* (CRWMS M&O 2001a, Volume 2). The postclosure safety case depends on combining sound science and engineering practice with informed judgment and planning. The postclosure safety case is described here because it provides a context for understanding how data and analyses presented throughout the rest of this section are related to safety.

The first element of the postclosure safety case is a thorough and quantitative evaluation of the possible future performance of the repository. This element is based on a comprehensive testing program that has evolved to address identified uncertainties, and an engineered barrier design developed specifically to work in combination with the natural barriers of the site. U.S. Environmental Protection Agency (EPA) and NRC regulations specify the method by which the DOE will analyze whether a repository can safely isolate spent nuclear fuel and high-level radioactive waste (i.e., a TSPA). The TSPA is described briefly in Section 4.4 but in more detail in *Total System Performance Assessment for the Site Recommendation* (CRWMS M&O 2000a) and several subsequent documents including *FY01 Supplemental Science and Performance Analyses* (BSC 2001a; BSC 2001b) and *Total System Performance Assessment—Analyses for Disposal of Commercial and DOE Waste Inventories at Yucca Mountain—Input to Final Environmental Impact Statement and Site Suitability Evaluation* (Williams 2001a). These reports include analyses of all the processes

expected to operate at the repository that could affect its ability to isolate waste. They also explicitly consider both disruptive events and alternative process models that could result in unanticipated behavior (i.e., identifies what could go wrong). These evaluations directly address uncertainty in both the DOE's knowledge of the site and in future conditions and include numerical sensitivity analyses to test how the repository might perform if current or future conditions differ from those expected.

To capture the technical inputs used in developing the overall TSPA system level model, a set of analysis model reports have been prepared. These reports contain the detailed technical information regarding data, analyses, models, software, and supporting documentation that is used in the development of the process models. The analysis model reports provide the direct input into the TSPA analyses, as well as document the abstraction of the process level models for use in the overall TSPA system level model.

Using the analysis model reports as a basis, the descriptions of these process level models are documented in a suite of process model reports that cover the following areas:

- Integrated site model (CRWMS M&O 2000i)

- Unsaturated zone flow and transport (CRWMS M&O 2000c)

- Near-field environment (CRWMS M&O 2000al)

- Engineered barrier system degradation, flow, and transport (CRWMS M&O 2000as)

- Waste package degradation (CRWMS M&O 2000n)

- Waste form degradation (CRWMS M&O 2000bm)

- Saturated zone flow and transport (CRWMS M&O 2000bn)

- Biosphere (CRWMS M&O 2000bo)

- Disruptive events (i.e., seismicity and volcanism) (CRWMS M&O 2000f).

The process model reports synthesize the information contained in the individual analysis model reports and provide an integrated perspective for understanding each of the process level models. This hierarchical process of documentation was used to ensure the traceability of supporting information from its source through the analysis model reports and process model reports to its eventual use in the TSPA. Supplemental analyses at both the process model level, and the total system level, are presented in *FY01 Supplemental Science and Performance Analyses* (BSC 2001a; BSC 2001b).

Because the DOE recognizes that uncertainty about the future performance of the repository cannot be completely eliminated, the postclosure safety case includes several additional measures designed to provide confidence and assurance that the repository will meet postclosure performance standards. These measures include:

- Qualitative (and sometimes quantitative) insights gained from the study of natural and man-made analogues to the repository or to processes that may affect repository performance. Analogue observations are especially useful in the analysis of processes related to repository performance that operate over long time frames (thousands of years) or large spatial distances (tens of kilometers) that cannot easily be tested.

- Selection and design of a repository system that provides defense in depth and a margin of safety compared to postclosure health and safety requirements. The DOE has implemented this approach through the selection of a specific location in the unsaturated zone at Yucca Mountain and the development of a design with multiple natural and engineered barriers to the migration of radionuclides. The engineered components of the site are designed specifically to complement the natural attributes of the potential repository host rock. This multiple barrier repository system provides defense in depth, so that the

safety of the repository does not depend on only one or two barriers.

- A commitment to a performance confirmation program and long-term management and monitoring to ensure the integrity and security of the repository and to ensure that the scientific and engineering bases for the disposal decision are well founded. This commitment includes maintaining, for a period of up to 300 years, the ability to retrieve the spent nuclear fuel and high-level radioactive waste before closure for any reason, if future generations decide that doing so would be desirable.

This approach is similar to that recommended by many national and international professional organizations that have studied nuclear waste disposal. As a panel of the National Academy of Sciences observed, "Confidence in the disposal techniques must come from a combination of remoteness, engineering design, mathematical modeling, performance assessment, natural analogues, and the possibility of remedial action in the event of unforeseen events" (National Research Council 1990, pp. 5 to 6).

The various elements of the postclosure safety case contribute in different ways to building confidence in analyses of the long-term performance of the repository. Quantitative numerical models permit scientists to test their understanding of the site and assess the consequences of uncertainty or assumptions in their models. Observations of natural or man-made analogues can help scientists determine whether the results of repository models are consistent with the behavior of actual systems. They can also be used to qualitatively evaluate the reliability and uncertainties associated with modeling. Safety margin and defense in depth provide one way to compensate for uncertainty in analyses. Long-term monitoring can help scientists verify that the uncertainties in site and design performance have been appropriately characterized. In total, the elements documented in the *Repository Safety Strategy: Plan to Prepare the Safety Case to Support Yucca Mountain Site Recommendation and Licensing Considerations* (CRWMS M&O 2001a, Volume 2)

support the postclosure safety case for the Yucca Mountain site. The sections that follow contain additional descriptions of each element of the safety case.

4.1.1   Total System Performance Assessment

Analysis of the future performance of the potential repository is fundamental to the DOE's understanding of the Yucca Mountain site. Therefore, the first element of the safety case is a thorough analysis of how a repository at Yucca Mountain would behave in the future. As noted previously, the methods used and the results of the TSPA for Yucca Mountain are described in Sections 4.3 and 4.4.

Performance assessment is a method or tool defined and provided by the EPA and the NRC (in 40 CFR Part 197 and 10 CFR Part 63 [66 FR 55732], respectively) for the evaluation of a Yucca Mountain repository. The objective of the total system performance assessment for site recommendation (TSPA-SR) for Yucca Mountain is to provide a basis for evaluating whether the safety of the general public will be protected. However, the DOE has also used the performance assessment for broader purposes during site characterization of Yucca Mountain. For instance, it has been used as a tool to evaluate the effects of uncertainty on total system performance and to identify areas where further work is needed. This has been accomplished in an iterative manner. For this updated *Yucca Mountain Science and Engineering Report*, TSPA results are presented and discussed in one comprehensive report, summarizing several additional supplemental documents that describe analyses performed to address specific technical and/or regulatory issues. The key TSPA references include:

- *Total System Performance Assessment for the Site Recommendation* (CRWMS M&O 2000a). This report describes a comprehensive analysis of the performance of a repository at Yucca Mountain. It documents the TSPA methodology and explains how process models have been incorporated in the TSPA-SR analysis.

- *FY01 Supplemental Science and Performance Analyses* (BSC 2001a; BSC 2001b). This two-volume report describes additional analyses performed to examine the uncertainty in TSPA analyses of Yucca Mountain. Volume 1 (BSC 2001a) describes new technical information and models of processes that may be important to performance; it provides additional quantitative analysis of uncertainties and investigates the effect of the thermal operating mode of the repository on the uncertainty associated with process models. Volume 2 (BSC 2001b) documents supplemental total system analyses based on an updated TSPA model (referred to in this report as the supplemental TSPA model), based on information in Volume 1.

- *Total System Performance Assessment—Analyses for Disposal of Commercial and DOE Waste Inventories at Yucca Mountain—Input to Final Environmental Impact Statement and Site Suitability Evaluation* (Williams 2001a). This document describes revised TSPA analyses (referred to in this report as the revised supplemental TSPA model) consistent with EPA's final 40 CFR Part 197 rule, including distance to the accessible environment, and calculation of radionuclide concentrations in groundwater at approximately 18 km (11 mi) from the repository.

- *Total System Performance Assessment Sensitivity Analyses for Final Nuclear Regulatory Commission Regulations* (Williams 2001b). This report describes additional TSPA sensitivity analyses to address final 10 CFR Part 63 (66 FR 55732) provisions, including the possible treatment of unlikely events (igneous intrusion) in assessing groundwater protection and human intrusion, and the effects of a change to 3,000 acre-ft/yr water demand for evaluation against the individual protection standard.

Figure 4-1 schematically presents the information flow within an iterative TSPA approach. Informa-

00052DC_ATP_Z1S40_Fig-01.ai
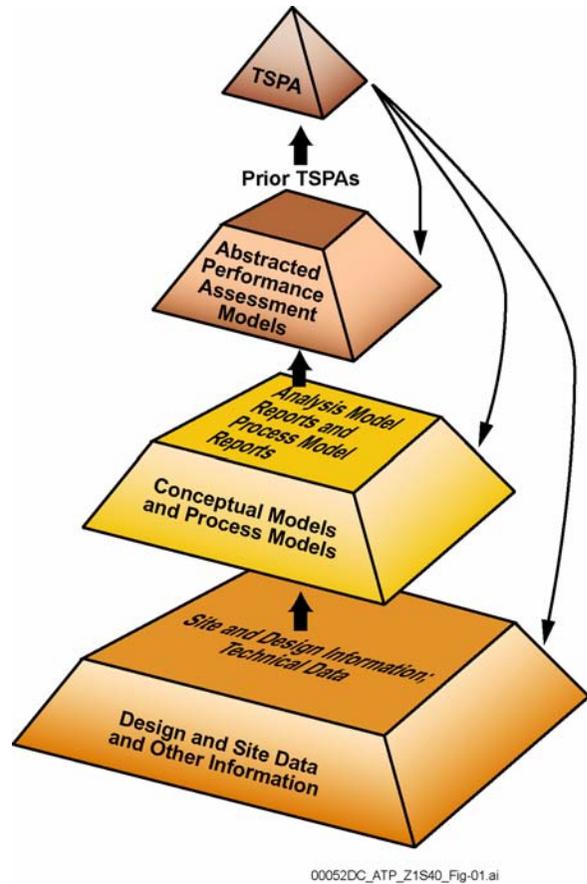
Figure 4-1. Total System Performance Assessment Pyramid Illustrating the Progressive and Iterative Process of Synthesizing Design Information, Site Data, Process Models, and Total System Performance Assessment Expertise

tion gained during studies and testing flows upward through the development of conceptual and numerical models that provide the basis for the TSPA. Information gained through analysis flows downward in the form of specific information needs for the next iteration of the TSPA.

The foundations of the TSPA are site characterization and engineering design data. Project scientists and engineers use this information to formulate conceptual models of the FEPs that could affect the performance of the natural and engineered barriers at the site. An important step in the formulation of these conceptual models is the identification of uncertainties in the current state of knowledge.

These conceptual models, the level of uncertainty associated with each, and the essential assumptions used in their formulation are documented in Sections 4.2 and 4.3, as well as supporting documents describing the DOE's understanding of the Yucca Mountain repository system.

The conceptual models are next cast into process-level models. These are typically numerical computer models that range from simple to quite complex representations designed to capture and simulate the fundamental physical phenomena that influence the process being modeled. The process models, together with important uncertainties and assumptions, are also described in Sections 4.2 and 4.3, as well as in supporting references.

Many process level models are needed to analyze the various subsystems that could affect the performance of the potential repository. Some of the individual models are so complex that it is not possible or desirable to include them in a single linked total system model, due to computing limits or because simplified models of certain processes may be equally defensible. A total system model that depended on a single representation of a process might overlook credible alternative models. Therefore, the total system model is generally based on simplified (abstracted) models that enable assessment of the effects of alternative representations of potentially important processes.

The process level models described in Sections 4.2 and 4.3 provide the foundation for the abstracted models contained in the TSPA described in Section 4.4. These abstracted models include the important details of the process level models, so they can be used to simulate or bound the results of the process level models. Scientists and engineers evaluate the output of the detailed process level models to identify key results, uncertainties, and assumptions that must be captured by the abstracted models. For example, it may be determined that, of the many processes and parameters contained within a process level model, only a few have a significant effect on overall behavior. Analysts use test results, comparisons with alternative process level models, and judgment to determine how best to incorporate the uncertainty associated with each specific

process in the abstracted models. The complexity of an abstracted model is governed by how sensitive total system performance is to the specific process and by how well the model incorporates uncertainty. The abstracted TSPA models, associated uncertainties, and important assumptions are described in Section 4.4 and in *Total System Performance Assessment for the Site Recommendation* (CRWMS M&O 2000a). More recent analyses are described in *FY01 Supplemental Science and Performance Analyses* (BSC 2001a; BSC 2001b) and *Total System Performance Assessment—Analyses for Disposal of Commercial and DOE Waste Inventories at Yucca Mountain—Input to Final Environmental Impact Statement and Site Suitability Evaluation* (Williams 2001a).

The abstracted models are combined into a total system model, which is used both to assess the potential future performance of the repository and to evaluate how uncertainty in the understanding of FEPs might affect performance. Throughout site characterization, the DOE has used this information to identify and prioritize future work activities. In this manner, the testing program has been updated and the repository design modified to continually improve the DOE's confidence in assessments of future performance. In the past decade, the DOE completed comprehensive analyses of total system performance in 1991, 1993, 1995 and 1998 (Barnard et al. 1992; Eslinger et al. 1993; Wilson, M.L. et al. 1994; CRWMS M&O 1995; DOE 1998, Volume 3). Each of these represented a significant advance in the DOE's understanding of how the potential Yucca Mountain repository might perform, and each resulted in modifications to the site testing program or the repository design to address key uncertainties. This report and the *Total System Performance Assessment for the Site Recommendation* (CRWMS M&O 2000a) reflect the knowledge and insights gained through this process. Additional analyses and insight are presented in *FY01 Supplemental Science and Performance Analyses* (BSC 2001a; BSC 2001b) and *Total System Performance Assessment—Analyses for Disposal of Commercial and DOE Waste Inventories at Yucca Mountain—Input to Final Environmental Impact Statement and Site Suitability Evaluation* (Williams 2001a).

4.1.1.1 Total System Performance Assessment Methods and Objectives

TSPA is a systematic analysis that synthesizes information (data, analyses, and expert judgment) about the site and region with the design attributes of the engineered barriers of the repository system. As defined in 10 CFR 63.2 (66 FR 55732),

> Performance assessment means an analysis that:
>
> (1) Identifies the features, events and processes (except human intrusion) and sequences of events and processes (except human intrusion) that might affect the Yucca Mountain disposal system and their probabilities of occurring during 10,000 years after disposal;
>
> (2) Examines the effects of those features, events, and processes and sequence of events and processes upon the performance of the Yucca Mountain disposal system; and
>
> (3) Estimates the dose incurred by the reasonably maximally exposed individual, including the associated uncertainties, as a result of releases caused by all significant features, events, and processes, and sequences of events and processes weighted by their probability of occurrence.

Features are the physical components of the total repository system, including both the natural system (e.g., the geologic setting) and the engineered system (e.g., the waste package). Processes typically act more or less continuously on the features; for example, moisture flow through the geologic materials and corrosion of the waste package. Events also act on the features but at discrete times. Examples include seismic and volcanic events.

The TSPA approach and models are designed to address the processes that could lead to release and migration of radionuclides, and the radiological consequences to potential human receptors. The approach is intended to provide a transparent analysis of the geologic repository in terms of the performance of the natural and engineered barriers over long periods of time.

40 CFR Part 197 provides that the DOE and NRC should determine compliance with the radiation protection standard of 40 CFR 197.20 based on the mean of the distribution of the highest doses resulting from the performance assessment. In the background information accompanying their final rule (66 FR 32074, p. 32125), the EPA noted that they believe that a thorough assessment of repository performance should examine the full range of reasonably foreseeable conditions and processes. However, they also stated that quantitative estimates of repository performance should not be dominated by unrealistic or extreme situations or assumptions. Therefore, the EPA believed the use of the mean was reasonable but still conservative. They further noted that the use of the mean was consistent with the literal mathematical interpretation of the term "reasonable expectation" and with the approach used to certify Waste Isolation Pilot Plant.

During their consideration of the appropriate performance measure, the EPA evaluated other possible measures, such as the median value of the distribution, or more extreme measures, such as the 95th or 99th percentile. Their analysis showed that the use of either the mean or the median was reasonably conservative because both are influenced by the high exposure estimates, without reflecting only the high dose results.

Although the EPA selected the mean for the compliance determination, both the EPA and NRC provide that the DOE consider the uncertainties inherent in performance assessment results. One way that the DOE's method addresses this concern is by presenting and analyzing the full range of doses resulting from the performance assessment. In addition, the DOE has performed numerous sensitivity and uncertainty analyses to characterize

the properties and processes that are particularly important to dose calculations.

The TSPA described briefly in Section 4.4 and in more detail in *Total System Performance Assessment for the Site Recommendation* (CRWMS M&O 2000a), Volume 2 of *FY01 Supplemental Science and Performance Analyses* (BSC 2001b), and *Total System Performance Assessment—Analyses for Disposal of Commercial and DOE Waste Inventories at Yucca Mountain—Input to Final Environmental Impact Statement and Site Suitability Evaluation* (Williams 2001a) examines the performance of the potential repository for a broad range of potential subsurface and surface conditions (e.g., hydrologic, geologic, climatic, and biosphere) and evaluates potential radiation doses to future generations. The radiation protection standards that would apply to the postclosure performance of a Yucca Mountain repository are found in regulations promulgated by the EPA (40 CFR 197.20, 197.25, and 197.30) and the NRC (10 CFR 63.113(b), (c), and (d) [66 FR 55732]). Specific technical requirements for a comprehensive TSPA are prescribed in the NRC regulation, 10 CFR Part 63.

The TSPA method requires evaluation of postclosure performance of the Yucca Mountain disposal system where there is no human intrusion into the repository. The final regulations also require evaluation of the performance of the system where there is human intrusion, in accordance with NRC regulations. The TSPA evaluation method in both cases is the same, except that the TSPA method for human intrusion provides prescribed assumptions about the human intrusion scenario (10 CFR 63.322 [66 FR 55732]).

Human intrusion refers to inadvertent intrusion into the repository as a result of exploratory drilling for groundwater. Limited intrusion means a single borehole that penetrates the repository and the underlying groundwater aquifer.

To present the assessment results transparently, the first case (without human intrusion) is further subdivided into:

- A nominal scenario composed of the likely FEPs representing the most plausible evolution of the repository system, without the occurrence of unlikely disruptive FEPs

- Disruptive scenarios that include unlikely FEPs that could diminish the waste isolation capability of the repository system (e.g., igneous activity).

The result of a TSPA analysis is a distribution (range) of possible outcomes of future performance. Because of the probabilistic nature of the method, TSPA results can capture and display much of the uncertainty associated with complex models and unknown future conditions. For this reason, however, the results should be regarded as indicative of future performance, not as predictive in a precise way.

The TSPA methodology (i.e., approach and models) described in this report is the culmination of research and development conducted over more than a decade. Moreover, reviews of previous TSPAs by internal and external professional organizations have been invaluable in enhancing the rigor of the approach and guiding the improvements of the models. Most notably, important advances in the TSPA methodology have been made in response to review comments from:

- Nuclear Waste Technical Review Board (NWTRB 1998; NWTRB 1999a; NWTRB 2000)

- Total System Performance Assessment Peer Review Panel (Budnitz et al. 1999)

- NRC staff (Paperiello 1999)

- State of Nevada consultants and other independent expert review groups.

The TSPA methodology used for this report is very similar to that used in the compliance certification application for the Waste Isolation Pilot Plant

(DOE 1996a, Section 6.1; Helton, Anderson et al. 1999), a bedded salt repository in southern New Mexico. The Waste Isolation Pilot Plant was certified by the EPA in 1998 and began receiving and disposing of transuranic nuclear waste in March 1999. The TSPA approach is also similar to approaches adopted by other countries currently conducting detailed siting studies for potential geologic repositories (NEA 1991; Thompson 1999). In addition, the computer techniques used in TSPAs to address uncertainties are rooted in the probabilistic risk assessment method applied in the safety assessments for commercial nuclear reactors (Rechard 1999).

4.1.1.2 Treatment of Uncertainty in the Performance Assessment

Inherent uncertainties will exist in any projections of the future performance of a deep geologic repository. These uncertainties must be addressed in a way that is both clear and understandable to ensure technical credibility and sound decision-making and must be reduced or eliminated if important. Most, but not all, of those uncertainties can be quantified and addressed in the TSPA; examples include:

- Potential changes in climate, seismicity, and other processes, such as coupled thermal-hydrologic-chemical processes, over the compliance period for geologic disposal (i.e., 10,000 years)

- Variability and lack of knowledge of the properties of geologic media over large spatial scales of the hydrogeologic setting (e.g., the flow path from the repository to a point of compliance)

- Incomplete knowledge about the long-term material behavior of engineered components (e.g., corrosion of metals over many thousands of years).

Both the EPA and the NRC have recognized that uncertainty about the future performance of the repository will remain even after site characterization is complete. In the licensing context, both EPA

regulations at 40 CFR 197.14 and NRC regulations at 10 CFR 63.304 (66 FR 55732) have incorporated "reasonable expectation" as the standard for the NRC to determine whether the DOE complies with EPA and NRC regulations. Characteristics of reasonable expectation include that it:

- Requires less than absolute proof because absolute proof is impossible to attain for disposal due to the uncertainty of projecting long-term performance

- Accounts for the inherently greater uncertainties in making long-term projections of the performance of the Yucca Mountain disposal system

- Does not exclude important parameters from assessments and analyses simply because they are difficult to precisely quantify to a high degree of confidence

- Focuses performance assessments and analyses upon the full range of defensible and reasonable parameter distributions rather than only upon extreme physical situations and parameter values.

There are a number of ways to accommodate or address uncertainty in analyses of performance. The methods employed for the TSPA models include:

- Definition of parameter probability distributions

- Representation of spatial and temporal variability

- Definition of data bounds or conservative estimates

- Formulation and evaluation of alternative models permitted by current state of knowledge

- FEPs screening (screening out certain aspects from consideration because of low probability or consequence).

Whether uncertainties are incorporated quantitatively through probabilistic distributions, or by developing "conservative" or "bounding" estimates, it is important to define and document assumptions on how uncertainties are treated in performance analyses. Clear documentation of the rationale for the assumptions in the models will enable others to understand and evaluate their adequacy. For the total system model to be transparent and defensible, the selection of each probability distribution must also be defensible. In some instances, the insufficient information that exists on the subsystem model is so complex that a probability distribution cannot be defined defensibly. In these instances, conservative or bounding approaches are taken.

Individual sources of uncertainties may be either quantified or unquantified. Quantified uncertainty consists of those sources of uncertainties that can be and have been explicitly (i.e., mathematically) represented and evaluated through a probabilistic performance analysis. Unquantified uncertainties are those that are recognized but are not well suited for direct evaluation through a probabilistic analysis.

As described in Section 4.4.1.2, many uncertainties have been quantified and incorporated directly into the TSPA models. The analyses done to address quantified uncertainties in the TSPA-SR model include a variety of sensitivity studies that address how total system performance might be affected if individual or groups of processes or parameters differed significantly from the way they were represented in the TSPA-SR model. These are described further in Section 4.4.5 and in *Total System Performance Assessment for the Site Recommendation* (CRWMS M&O 2000a). Additional uncertainties have been identified, analyzed, and quantified in *FY01 Supplemental Science and Performance Analyses* (BSC 2001a; BSC 2001b). These analyses are described, as appropriate, throughout Section 4.

As noted by the National Research Council (1990, p. 13) and others, there are residual uncertainties with deep geologic disposal that cannot easily be quantified and incorporated into performance analyses. Nevertheless, their potential impact must be,

to the extent practicable, addressed and, if important, mitigated to provide confidence in postclosure performance. Examples of residual uncertainties associated with geologic disposal that are difficult to quantify include:

- The potential for currently unknown processes to affect performance

- The possibility that incompletely characterized processes have been incorporated in the TSPA in a manner that results in the underestimation of radionuclide releases; examples of incompletely characterized processes include thermal, chemical, hydrologic, and mechanical processes that are coupled in complex ways that cannot be completely tested at the scale of a repository, as well as processes that are difficult to observe and test, such as colloidal transport of radionuclides

- Uncertainty associated with the projections of engineered barrier performance over 10,000 years based on data from short-term (e.g., several years) laboratory testing

- Uncertainty associated with the large spatial scale of the three-dimensional groundwater flow system, which makes it difficult to characterize flow paths and processes.

The DOE has made a substantial effort to identify, characterize, and mitigate the potential impacts of residual uncertainties that could significantly affect long-term performance. Where practicable, additional tests have been conducted to collect information that would provide insight to analysts. For example, the DOE, along with Nye County and the National Park Service, is continuing research on the regional groundwater system. The program includes cooperative and joint analysis of soil, rock, and water samples provided by Nye County, which is drilling additional boreholes to characterize the saturated zone as part of its review of the project.

To address uncertainties associated with coupled thermal-hydrologic-geochemical processes, the DOE has performed numerous tests that were not

envisioned when site characterization began. Where additional testing was not feasible (e.g., it is not possible to run tests over the same time period as the repository must perform) or of limited benefit (e.g., no amount of excavation or drilling could completely characterize the natural system), modelers used conservative assumptions to "bound" their analyses of uncertain processes. To do this, they have incorporated assumptions in their models that represent the observed range of properties and processes and that also include parameter values or processes likely to result in calculated dose assessments that are greater than actual dose. The DOE has also used empirical observations and qualitative lines of evidence from natural analogues to address uncertainties (see Section 4.1.2).

In some cases, more than one conceptual model may be consistent with available data and observations; if so, the analysis of uncertainty includes the identification of the basis for model selection. In the absence of definitive data sets or compelling technical arguments for any specific conceptual model, analyses or sensitivity studies may be performed to test whether the selection of a given model is likely to substantially affect analyses of system performance. When model uncertainty is unavoidable, analysts may develop simplified performance models for use in TSPA that reflect the range of outcomes predicted by more detailed and specific conceptual models. The selection of models, model parameters, and scenarios of potential future behavior are described in *Total System Performance Assessment for the Site Recommendation* (CRWMS M&O 2000a) and its supporting documents, as well as in *FY01 Supplemental Science and Performance Analyses* (BSC 2001a; BSC 2001b) and *Total System Performance Assessment—Analyses for Disposal of Commercial and DOE Waste Inventories at Yucca Mountain—Input to Final Environmental Impact Statement and Site Suitability Evaluation* (Williams 2001a).

In addition, consistent with the postclosure safety case described in Section 4.1.3, the DOE has implemented a safety margin/defense-in-depth approach to the design of repository facilities. This approach mitigates some of the residual uncertainties by providing additional confidence in the performance of the total system. The iterative approach to characterization and testing, design, and performance analysis remains a fundamental part of the DOE approach in evaluating whether Yucca Mountain is a safe site to host a repository.

One disadvantage of an approach that combines both conservative and representative parameter distributions is that it is difficult to assess the extent to which the total system results are conservative or realistic. More realistic representations may be drawn from literature data, analogue systems or processes, and the technical judgment of the broader scientific and engineering community. In addition, the DOE initiated several activities to improve the treatment of uncertainty in current models. These are described in *FY01 Supplemental Science and Performance Analyses* (BSC 2001a; BSC 2001b). These activities:

- Identified and evaluated the degree of conservatism introduced by current approaches, quantified key unquantified uncertainties, and characterized the effect of explicitly quantifying ranges of possible parameters

- Developed alternative representations of key unquantified uncertainties and evaluated the impact on TSPA results

- Considered the uncertainties associated with alternative models into which assumptions or conservatisms were introduced when they were abstracted for use in the TSPA, in addition to assumptions and conservatisms in the process model

- Developed more realistic representations of models and parameters, based on all available information and the scientific judgment of individuals who are experts in the appropriate disciplines

- Developed, for each model in the TSPA, alternate lines of evidence, such as additional analogues and defense in depth, that are less dependent on the TSPA computational tool than those given in *Repository Safety Strategy: Plan to Prepare the Safety Case to Support Yucca Mountain Site Recommenda-*

tion and Licensing Considerations (CRWMS M&O 2001a).

This approach provides recommendations for consistent treatment of uncertainties, which will lead to a more rigorous treatment of the different types of uncertainty. It will also lead to a more transparent description of uncertainties in the process models and in the overall system models.

4.1.1.3 Explicit Consideration of Disruptive Processes and Events that Could Affect Repository Performance

Most of this report, as well as the *Total System Performance Assessment for the Site Recommendation* (CRWMS M&O 2000a), the *FY01 Supplemental Science and Performance Analyses* (BSC 2001a; BSC 2001b), the *Total System Performance Assessment—Analyses for Disposal of Commercial and DOE Waste Inventories at Yucca Mountain—Input to Final Environmental Impact Statement and Site Suitability Evaluation* (Williams 2001a), and associated documentation, focuses on the processes that are expected to operate in and near the repository over time (e.g., water flow, the effects of heat on conditions near waste packages, and the slow degradation of the engineered barrier system). Because of the time frames involved, however, it is also important for analysts to understand the safety consequences of unexpected events or behavior. Consequently, the performance analysis also describes explicitly how disruptive events (i.e., possible but unlikely events that could negatively affect performance) and alternative models of processes could affect the performance of the total system. This thorough consideration of what could go wrong, how wrong the models could be, and what the effect of inaccuracy in the models would be is a key element of the postclosure safety case.

A comprehensive set of potentially disruptive events, ranging from meteor or comet impacts to unexpected flooding of the repository, has been identified and evaluated. Similarly, a wide variety of potentially harmful processes, such as unanticipated failure of the waste packages and damage to repository systems by seismic activity, have been identified and evaluated. Section 4.3 describes the

identification and screening of these potentially adverse processes and events. Depending on the results of this analysis, the events and processes have been treated in one of three ways:

1. Events or processes with very low probabilities (e.g., less than 1 chance in 10,000 of occurring in 10,000 years, such as meteor impacts) or very small consequences (e.g., potential radionuclide releases much lower than regulatory standards) have been screened out and not analyzed further.

2. Events or processes that have probabilities greater than 1 chance in 10,000 of occurring in 10,000 years (e.g., intrusive igneous activity), have been included in the performance assessment probabilistically—that is, the consequence of each event is weighted by its probability of occurrence.

3. Events or processes expected to occur during the period of regulatory compliance, such as climate change or ground shaking associated with earthquakes, are included directly in models of the performance of the repository.

The potential consequences of each event and process considered in the performance assessment models are analyzed. These analyses are summarized in Section 4.2, which considers alternative models of subsystem processes that could affect performance, and Section 4.3, which considers specific events or processes that are not part of nominal site behavior. Section 4.4.5 also describes a number of sensitivity studies that enable analysts to assess the importance of alternative models or unexpected events on total system performance.

Many different events and processes have been considered to assess whether they might have the potential to disrupt repository performance. Examples of potential events considered include:

- The potential for future volcanism near the repository

- The potential for future seismic activity near the repository

- The potential for future human intrusion into the repository

- The potential for climate change in the region of the repository

- The potential for criticality to occur during the postclosure period.

Climate change and cladding damage caused by earthquake ground motion is directly incorporated into the nominal case performance analyses (CRWMS M&O 2000c) because climate change and seismic activity are expected to occur during the period of regulatory compliance.

Many other events and processes have been considered but screened out because their impacts are so inconsequential that inclusion in the TSPA-SR is not warranted. Examples include the potential for future rises in the water table that could inundate the repository and the potential for nuclear criticality in spent nuclear fuel after repository closure. These examples are discussed in Section 4.3.

It is not possible to foresee every event or process that could affect the potential repository. However, by recognizing and explicitly analyzing all identified events and processes that could affect repository performance, the DOE has provided a sound basis for evaluating the performance of the repository system.

4.1.2 Observations from Natural and Man-Made Analogues

An alternative means of analyzing the reliability of repository performance models is by comparing them with natural or anthropogenic (man-made) analogues. As defined in this report, analogues are systems in which processes similar to those that could occur in a nuclear waste repository have occurred over long time periods (decades to millennia) and large spatial scales (up to tens of kilometers) not suited to laboratory or field experiments. The concept of geologic disposal is based

on an analogue observation that certain geologic environments have intrinsic properties that contribute to the isolation of waste and will continue to do so for a long time. Analogue studies can also help scientists understand how specific repository systems might behave by allowing them to compare possible future behavior with the known past behavior of an analogue system. A variety of specific analogue sites are described throughout Section 4.2, including several in settings that provide insight into the flow of water in the unsaturated zone, as described in Section 4.2.1.2.13.

For example, observations of the hydrologic behavior of ancient man-made tunnels and natural caves can provide relevant information about water seepage into mined openings in an unsaturated zone over thousands of years. Similarly, observations of the past migration of radioactive contaminants in groundwater in similar environments can provide insight into the possible future transport of radionuclides away from a repository. Such information can be obtained from both natural analogues (e.g., natural deposits of uranium and other minerals) or from anthropogenic analogues (e.g., the Nevada Test Site, Hanford, or the Idaho National Engineering and Environmental Laboratory), where the movement of radionuclides in groundwater caused by past releases is currently being monitored. The archaeological and historical record can also provide qualitative information on the degradation of materials that may be relevant to the performance of the repository (e.g., the preservation of materials in Egyptian pyramids and tombs more than 5,000 years old).

The value of natural analogues is not restricted to locations that may mimic aspects of repository behavior. The study of natural analogues is an intrinsic part of scientific studies, particularly in the earth sciences. For example, in order to undertake studies of basaltic volcanism in the vicinity of the Yucca Mountain site, an investigator must be versed in basaltic volcanism and especially in basaltic volcanism in the southern Great Basin. All other known occurrences of basaltic volcanism become, to some degree, natural analogues for volcanism near Yucca Mountain. Each occurrence can tell the investigator something about the mech-

anisms and controls on volcanic episodes. The overall understanding of volcanic processes gained from regional studies provides a basis for analyzing trends and patterns in the Yucca Mountain area that are essential to evaluating the possibility that future volcanic events could occur and affect a repository. In fact, it would be impossible to understand basaltic volcanism as a site characterization issue without recourse to natural analogues. One of the fundamental tasks for the investigator is to recognize and appreciate the value of the information offered by this kind of analogue study.

The scientific community has endorsed the use of analogues as a means of assessing the potential future performance of systems, components, and processes related to nuclear waste disposal (Chapman and Smellie 1986). The National Academy of Sciences/National Research Council (National Research Council 1990) and the NRC (10 CFR 63.101(a)(2) [66 FR 55732]) have also encouraged analogue studies.

There are no close analogues to a total repository system at Yucca Mountain. Nevertheless, studies of a variety of analogues can and have been used to assess how well repository models represent processes known to be important to performance, as well as the magnitude and duration of the phenomena. Analogue information has also been used (1) to evaluate the validity of extrapolating from short-term field-scale experiments to longer time scales in which field-scale experiments are impractical and (2) to add confidence when spatially extrapolating processes studied at laboratory and intermediate-scale experiments to tests at larger spatial scales. Knowledge gained from natural analogues has helped refine performance assessment model assumptions and parameter ranges and has improved the robustness and consistency of process models.

Given the imprecise nature of the information gained from investigations of similar, but not identical, processes and sites, analogue studies alone cannot prove that process or total system performance models are valid in a strict sense. However, natural analogue observations can confirm that a model takes into account the relevant processes in

appropriate ways. In this way, the analogues can build confidence in models of future behavior. This is consistent with the expectations of NRC regulations in 10 CFR 63.101(a)(2) (66 FR 55732), which state: "Demonstrating compliance will involve the use of complex predictive models that are supported by limited data from field and laboratory tests, site-specific monitoring, and natural analog studies that may be supplemented by prevalent expert judgment."

Throughout this report and its supporting documents, numerous analogues are analyzed to provide information on processes that may affect both engineered and natural system features of a geologic repository at Yucca Mountain. Specific examples of relevant analogues are presented in Table 4-1. Additional discussion of analogues is provided as appropriate throughout Sections 4.2 and 4.3, which discuss in greater detail the understanding of the Yucca Mountain site. Although the direct applicability of the analogues for each process model varies, the analogue observations generally suggest that the conceptual and numerical models that form the basis for analyses of repository performance are reasonable to conservative. For many of the analogues, a large body of literature exists.

4.1.3 Use of Defense in Depth and Safety Margin to Increase Confidence in System Performance

The extensive testing program at Yucca Mountain and the thorough assessments of the future performance of the potential repository do not "prove," in the usual sense of the word, that the potential repository will be safe. To provide additional assurance of long-term safety, the third major element of the postclosure safety case relies on a complementary, but less analytical, approach that is based on engineering principles that have a proven track record for safety. These principles are known as "safety margin" (or design margin) and "defense in depth."

Safety margin refers to the standard engineering practice of including safety factors on the performance of engineered components to account for uncertainty and variability in material, fabrication,

Table 4-1. Process Models and Natural Analogues

Process Model	Feature, Event, or Process	Model Parameter	Information from Analogues
UZ Flow and Transport	Climate	Range of climate conditions	Paleoclimate studies in Great Basin provide bounds on precipitation and temperature expected under wetter future climate scenarios.
	Infiltration	Range of infiltration values	Infiltration at Yucca Mountain, determined by models, is within range of measured infiltration rates in Negev Desert, Israel.
	Seepage into drifts	Drift seepage model; effect of discrete fractures	Excavations worldwide in arid environments (e.g., Altamira, Spain; Amman, Jordan) show high seepage thresholds. At Rainier Mesa, Nevada, tunnel in welded tuff above perched water zone shows no seepage. Tunnel in zeolites below perched water experiences seepage. Very limited seepage occurs at Hell's Half Acre, Idaho, 1 m below a monitored overhang in fractured tuff.
	Coupled processes: effects on UZ flow	UZ flow and transport, THC processes	Magma intrusions, such as sill at Paiute Ridge, Nevada, and Grants Ridge, New Mexico, as well as lava flow contact at Banco Bonito, New Mexico, show extent of alteration effects at temperatures greater than 100°C is less than 1 m from contact; fracture sealing has occurred in welded rhyolitic tuff in Yellowstone geothermal field.
	Coupled processes: thermal-mechanical effects	Rockfall size distributions and thermal-mechanical effects	Measured thermal-mechanical stress at Krasnoyarsk-26, Russia, is small over 50-year operation period of underground nuclear reactor (temperatures less than 100°C).
	Moisture, temperature, and chemistry on drip shield	Mineral reaction rates and assemblages in near-field	Geothermal fields (e.g., Wairakei, New Zealand; Yellowstone, Wyoming), and Yucca Mountain as self-analogue, predict mineral assemblage similar to syngenetic alteration at Yucca Mountain; mineral precipitation kinetics is faster in field than in laboratory tests.
	Moisture, temperature, and chemistry on waste package	Same as for drip shield, with addition of drip shield for protection	Potential drip shield analogue at Japanese archaeological site.
	UZ flow and transport: advective pathways	(1) UZ flow; effects of transient flow	(1) Box Canyon (Idaho National Engineering and Environmental Laboratory) analogue in fractured basalt shows little effect from transient flow.
		(2) Effect of water table rise	(2) Records associated with historical earthquakes in Nevada show water table rise is limited to about 5 m and is transient.
	UZ flow and transport: sorption and matrix diffusion	UZ flow and transport	Sorption of uranium takes place in fracture-coating minerals in rhyolitic tuff at Peña Blanca, Mexico, where matrix diffusion is minor; Peña Blanca has experienced only minor transport of uranium daughter products over 300,000 years. Trace metals at Santorini, Greece, were transported less than 5 m in rhyolitic tuff over 3,000 years.
	UZ flow and transport: colloid-facilitated transport	UZ flow and transport	Idaho National Engineering and Environmental Laboratory may be an analogue for colloid transport.
	Coupled processes: effects on UZ transport	UZ flow and transport; THC processes	Clay mineral alteration assemblages produced by THC processes in high-silica rocks at Oklo, Gabon, and Cigar Lake, Canada, are effective in sequestering radionuclides.
Waste Package, Waste Form, and Engineered Barrier Processes	Performance of waste package barriers	Degradation of steel alloys and cladding	Meteorites with high nickel/iron content have higher rate of preservation than those with low nickel/iron ratio; meteorites, iron nails, and other iron artifacts are better preserved in the presence of a corrosion crust; eskolaite for chromate (Cr_2O_3); rare earth phosphates as analogue to gadolinium phosphate ($GdPO_4$) (neutron absorber); stability of the mineral josephinite, a natural iron-nickel alloy.
	Commercial spent nuclear fuel waste form performance	Chemical alteration of uranium dioxide and secondary mineral formation	Uraninite alteration at Nopal I in Peña Blanca, Mexico, produces the same mineral assemblage as in laboratory tests of spent fuel degradation.

Table 4-1. Process Models and Natural Analogues (Continued)

Process Model	Feature, Event, or Process	Model Parameter	Information from Analogues
Waste Package, Waste Form, and Engineered Barrier Processes (continued)	DOE spent nuclear fuel, plutonium disposition waste form performance	Chemical alteration of uranium and secondary mineral formation	Natural plutonium has remained unfractionated from uranium at Poços de Caldas, Brazil, for more than 100,000 years.
	High-level waste glass waste form performance	Stability of glasses	In the absence of radiation, devitrification of volcanic glasses (basaltic and rhyolitic) and manufactured uranium-bearing glasses is too slow to be significant to a repository.
	Dissolved radionuclide concentration limits	Solubility of waste form	(Solubility limiting conditions not usually observed through analogues.)
	In-package radionuclide transport	Radiolysis, sequestration in secondary minerals	At Oklo, Gabon, radiolysis caused reduction of iron and oxidation of uranium, followed by sequestration of uranium and fission products in clays and iron oxides.
	Performance of cements	Effects of materials on performance	Maqarin, Jordan, provides data on thermodynamic stability of natural cement minerals and interaction with groundwater. Krasnoyarsk, Russia, provides data on stability of cement minerals under THC conditions. Microbes are instrumental in attacking cement at New Zealand geothermal sites. Roman concretes varied in stability with dependence on composition of contact material.
	Performance of getter (sorptive materials in backfill)	Effects of materials on performance	Clay minerals are instrumental in sequestering radionuclides at Cigar Lake, Canada, and have preserved ancient wood fiber at Dunarobba Forest, Italy.
SZ Flow and Transport	SZ flow and transport—advective pathways	Transverse and longitudinal dispersion	Contaminant plumes at DOE and EPA sites (e.g., Hanford) can be used to determine the limits of dispersion in a particular substrate.
	SZ flow and transport—sorption and matrix diffusion	Sorption coefficient in alluvium, importance of matrix diffusion	Sorption coefficient tested at Nevada Test Site. Matrix diffusion plays strong role at Poços de Caldas, Brazil; Alligator Rivers, Australia; Oklo, Gabon; Palmottu, Finland; Cigar Lake, Canada. Fracture pathways play a role in transport at Palmottu; Poços de Caldas; and Alligator Rivers.
	SZ flow and transport—colloid-facilitated transport	Colloidal transport in SZ	Filtration of colloids is effective at El Berrocal, Spain; Poços de Caldas, Brazil; Alligator Rivers, Australia; and Cigar Lake, Canada.
Biosphere	Biosphere transport and uptake	Plant uptake of radionuclides	High uranium concentrations found in green plants near ore bodies at Poços de Caldas, Brazil, and Peña Blanca, Mexico.
Potentially Disruptive Events	Volcanism	Eruptive frequency, location, and intensity	Nevada–California–Arizona provide eruptive histories of similar basalt fields.
	Seismicity	Frequency of event, extent and location of fault rupture, intensity of ground motion	Nevada–California historic earthquakes provide database for predictions.
	Criticality	Probability and consequence of criticality	Occurred at Oklo 2 billion years ago and lasted several hundred thousand years; studies have determined which radionuclides remained in the ore body, which ones were transported, and to what distances.
	Water table rise	Probability and consequence of water table rise	Travertine Point calcite and silica deposits provide insight into the origin of surficial deposits at Yucca Mountain.

NOTES: THC = thermal-hydrologic-chemical; UZ = unsaturated zone; SZ = saturated zone. Sources: CRWMS M&O 2000bp; Stuckless 2000; CRWMS M&O 2000b, Section 13.

and use. These safety factors are typically expressed as a ratio of the calculated level of performance to an allowable or laboratory measured level of performance. They are developed to ensure that the component or system has ample reserve performance capability. A simple example of a safety factor would be the limiting of the stress in a component to a fraction of what would cause failure. The safety margin is then the reserve strength over and above what would actually be applied. A Yucca Mountain-specific example of safety margin is the design and selection of the waste package material. The assumed corrosion resistance of Alloy 22, used in the outer shell of the waste packages, was decreased (or the corrosion rate was increased) over the laboratory values to account for potential environmental conditions. The corrosion rate of Alloy 22 was increased by 2.5 times to address potential heat-accelerated corrosion and an additional 2.0 times to address potential microbial corrosion.

The defense-in-depth approach (or reliance on multiple system attributes) complements design margin in that it provides a method of ensuring overall performance if one or more components of the repository system fail to perform as expected. Defense in depth is provided by having safety components that do not share common failure modes. In other words, the processes or conditions (such as the geochemical environment) that might cause a degradation of performance of one component of the design will not similarly affect other components. In a repository, defense in depth is provided by the attributes of both the natural barriers and the engineered barrier system.

The safety margin/defense-in-depth approach is not specifically required by the regulations for a repository. However, the NRC regulation (10 CFR Part 63 [66 FR 55732]) does contain statements that are based on a similar philosophy, adapted to the long-term requirements for postclosure safety. 10 CFR 63.113(a) provides that a repository include multiple barriers, consisting of both natural barriers and an engineered barrier system.

At Yucca Mountain, the potential geologic repository system would contain several different barriers. As defined in 10 CFR 63.2 (66 FR 55732), a barrier is any material, structure, or feature that prevents or substantially reduces the rate of movement of water or radioactive material from the Yucca Mountain repository to the accessible environment. Table 4-2 presents a summary

Table 4-2. Identification of Natural and Engineered Barriers at Yucca Mountain

Barrier	Barrier Function
Surficial soils and topography	Reduce the amount of water entering the unsaturated zone by surficial processes (e.g., precipitation lost to runoff, evaporation, and plant transpiration).
Unsaturated rock layers overlying the repository and host unit	Reduce the amount of water reaching the repository by subsurface processes (e.g., lateral diversion and flow around emplacement drifts).
Drip shield above the waste packages	Prevent water contacting the waste package and waste form by diverting water flow around the waste package.
Waste package	Prevent water from contacting the waste form for thousands of years.
Spent fuel cladding	Delay and/or limit liquid water contacting spent nuclear fuel after waste packages have degraded.
Waste form	Prevent liquid water from contacting waste as a result of elevated temperatures in the commercial spent nuclear fuel waste package; limit radionuclide release rates as a result of intrinsic low leach rates of DOE high-level radioactive waste glass form.
Drift invert below the waste package	Limit transport into the host rock.
Unsaturated rock layers below the repository	Delay radionuclide movement to the groundwater aquifer because of water residence time, matrix diffusion, and/or sorption.
Volcanic tuff and alluvial deposits below the water table (flow path extending from below the repository to point of compliance)	Delay radionuclide movement to the receptor location because of water residence time, matrix diffusion, and/or sorption; decrease radionuclide concentrations by passive mixing.

of the natural and engineered barriers present at Yucca Mountain, along with a brief description of their intrinsic and intended functions for the design analyzed in this section. An analysis of each barrier's contribution to performance is presented in Section 4.5.

Implementation of the safety margin/defense-in-depth approach has resulted in several improvements in the repository design since the design described in 1998 in the Viability Assessment (VA) (DOE 1998). Examples include:

- Modification of the waste package design to place the corrosion-resistant Alloy 22 layer on the outside. Having the corrosion-resistant layer outside provides sufficient margin that performance assessments indicate complete containment (in the absence of unlikely disruptive processes) of nuclear wastes throughout the period of regulatory compliance.

- Evaluating thermal loading strategies that may reduce the complexity of coupled processes in the near-field zone and simultaneously maximizes the redirection of water away from the repository drifts.

- Adding drip shields to the engineered barrier design to minimize the potential for dripping water to contact the waste packages (and waste form).

More detailed descriptions of the barriers and their performance functions are summarized in Section 4.5. Additional information is available in Volume 2 of *Repository Safety Strategy: Plan to Prepare the Safety Case to Support Yucca Mountain Site Recommendation and Licensing Considerations* (CRWMS M&O 2001a) and *Total System Performance Assessment for the Site Recommendation* (CRWMS M&O 2000a) as well as *FY01 Supplemental Science and Performance Analyses* (BSC 2001a; BSC 2001b) and *Total System Performance Assessment—Analyses for Disposal of Commercial and DOE Waste Inventories at Yucca Mountain—Input to Final Environmental Impact Statement and Site Suitability Evaluation* (Williams 2001a).

4.1.4 Mitigation of Uncertainties by Selection of a Thermal Operating Mode

One way of mitigating the uncertainties in modeling long-term repository performance is to operate the repository so the temperature of the host rock stays below the boiling point of water. Uncertainties in thermally driven processes are of special interest because of their complexity and because the current modeling approach may mask the importance of thermal effects on performance. Two key uncertainties about thermal effects on potential repository performance are (1) the way coupled processes in the mountain will respond to the heat generated by emplaced waste and (2) the long-term performance of waste package materials in the potential repository environment.

In the models and design described in this report, uncertainties related to the higher-temperature operating mode have been recognized and addressed. Since the VA, the design has evolved to include a thermal management strategy that limits the region of rock with temperatures above the boiling point of water, along with other features (such as drip shields) that mitigates uncertainty. Current models attempt to capture the remaining uncertainties well enough to understand their impacts; however, the DOE has considered additional options for mitigation. In particular, the performance characteristics of lower-temperature operating mode concepts such as those described in Section 2.1 have been investigated in *FY01 Supplemental Science and Performance Analyses* (BSC 2001a; BSC 2001b) and *Total System Performance Assessment—Analyses for Disposal of Commercial and DOE Waste Inventories at Yucca Mountain—Input to Final Environmental Impact Statement and Site Suitability Evaluation* (Williams 2001a).

Because uncertainties due to thermally induced coupled processes cannot be eliminated through additional testing, the DOE's approach is to consider options for mitigating thermal uncertainties by lowering temperatures in the emplacement drifts and on the waste package surface. Keeping the host rock temperature below boiling may reduce uncertainties associated with coupled processes (Anderson et al. 1998, p. 18; Cohon

1999). In addition, uncertainties in localized corrosion rates may be mitigated by avoiding the conservatively defined window of increased susceptibility by keeping the temperature of the waste package below 85°C (185°F) or the relative humidity in the emplacement drifts below 50 percent. Section 2.1 provides additional discussions of lower-temperature operating modes.

4.1.5 Performance Confirmation, Postclosure Monitoring, and Site Stewardship

The EPA, NRC, and DOE have recognized that some uncertainty about repository performance cannot be eliminated. Furthermore, the DOE understands that ensuring public safety requires continued site stewardship, including a program for evaluating new information discovered during the construction and operation phases. Therefore, the final component of the postclosure safety case is a program of performance confirmation, monitoring, and site stewardship that accomplishes several goals related to the DOE's obligation to protect public health and safety and the environment. The program addresses 10 CFR Part 63 (66 FR 55732) Subpart F provisions for performance confirmation to ensure consistency with license specifications after waste emplacement and before permanent closure. The program also includes activities necessary for the DOE to provide postclosure oversight, as specified by Section 801(c) of the Energy Policy Act of 1992 (Public Law No. 102-486), and post-permanent closure monitoring, consistent with 10 CFR 63.51(a)(2). Specifically, the DOE will continue to observe and test the performance of the repository during and after waste emplacement and will maintain the integrity and security of the repository through a variety of institutional controls. The DOE will also continue to participate in research on geologic disposal, in cooperation with other international programs. These activities will ensure that any new information discovered at Yucca Mountain (or elsewhere) that is relevant to future repository decisions is considered appropriately.

The performance confirmation program is the most important monitoring activity. NRC regulations provide for performance confirmation to continue for at least 50 years after the initiation of waste emplacement. The DOE will continue its performance confirmation program until the repository is permanently closed. The amount of information collected during this period may be more relevant for long-term analyses of the repository than any experiment or test that could be conducted now or in the near future. Any decision to close the repository would be based on the increased understanding and confidence derived from decades of testing and observation.

The performance confirmation program will provide data on the actual performance of the key natural and engineered systems and components of the repository as conditions evolve. The program will also provide data to confirm (after repository construction and operation) that subsurface conditions encountered, and any changes in those conditions during repository construction and waste emplacement, are consistent with the expected performance of the repository. A primary goal of the program will be to confirm, through observation, monitoring, and analysis, that the repository is performing in a manner that will contain and isolate waste.

As described in Section 4.6, the performance confirmation program will monitor the processes important to future waste isolation in the repository. Examples include the flow of water past and near the repository, the geochemical environment in and near emplaced waste, coupled thermal-hydrologic-chemical-mechanical processes, and the performance characteristics of engineered materials in the repository environment (e.g., drip shield and waste package degradation). In addition to technical monitoring of the performance of the site, the DOE will maintain the security and integrity of the site throughout the performance confirmation period and beyond as required by the Energy Policy Act of 1992, Section 801(c) (Public Law No. 102-486). A program will be developed to prevent any human activity, including deliberate or inadvertent human intrusion, that could affect engineered or geologic barriers.

Section 122 of the NWPA (42 U.S.C. 10142) requires the DOE to maintain the ability to retrieve any and all emplaced wastes "for any reason

pertaining to the public health and safety, or the environment, or for the purpose of permitting the recovery of the economically valuable contents of such spent fuel" prior to closure. For example, if it were learned from the monitoring program that an engineered barrier had been damaged, the waste packages could be removed and repairs could be made, as necessary.

NRC regulations (10 CFR Part 63 [66 FR 55732]) anticipate that the repository could be closed as early as 50 years after initial waste receipt. Closing the repository would involve the sealing of shafts, ramps, exploratory boreholes, and other underground openings. These actions would discourage any human intrusion into the repository and prevent water from entering through these openings. If a decision to close the repository were made, the DOE would still be responsible for a program of site stewardship under the Energy Policy Act of 1992 (Public Law No. 102-486).

At the surface, all radiological areas would be decontaminated, all structures removed, and all wastes and debris disposed at approved sites. All disturbed areas would be restored as close as practicable to their preconstruction condition.

NRC regulations (10 CFR Part 63 [66 FR 55732]) require the DOE to submit a plan for postclosure monitoring with any application to close the repository. The DOE has also committed to maintain security and continue monitoring at the Nevada Test Site for the foreseeable future. A network of permanent monuments and markers would be erected around the site to warn future generations of the presence and nature of the buried waste. Detailed records of the repository would be placed in the archives and land records of local, state, and federal government agencies and archives elsewhere in the world that future generations would be likely to consult. These records would identify the location and layout of the repository and the nature and hazard of the waste it contains.

4.2 DESCRIPTION OF SITE CHARACTERIZATION DATA AND ANALYSES RELATED TO POSTCLOSURE SAFETY

This section discusses the data obtained during site characterization activities, as well as analyses of the safety of a potential Yucca Mountain repository. The DOE planned and conducted its site characterization program to collect data about the site and about those physical and chemical processes that would affect the ability of the repository system to isolate waste.

Section 1.3 presented a brief summary of the geology of Yucca Mountain based on the results of site investigations. It provided a framework for the descriptions of the repository and waste package designs contained in Sections 2 and 3. In this section, the results of studies focused on the characteristics and potential future behavior of the repository system are presented in additional detail. The discussion is organized to provide a description of the major processes that control the waste isolation capability of the potential repository. As shown schematically in Figure 4-2, Section 4.2 describes in sequence the data and analyses relevant to the processes that affect the movement of water through Yucca Mountain and relevant to the potential for that water to contact and mobilize radionuclides. Disruptive events could potentially affect these processes and, therefore, also need to be considered. The data and analyses related to potential disruptive events are presented in Section 4.3, and the combined analysis of the potential performance of the repository is summarized in Section 4.4.

The processes pertinent to performance include those physical processes that control the movement of water, beginning with precipitation as rain and snow at the surface, followed by infiltration into the mountain, flow through the unsaturated zone to the potential repository level, flow from the repository level to the saturated zone, and from there to the accessible environment. At the repository level, water moving past the engineered barriers would be affected by the physical and chemical processes associated with the decay heat and could interact with waste packages and waste forms. These
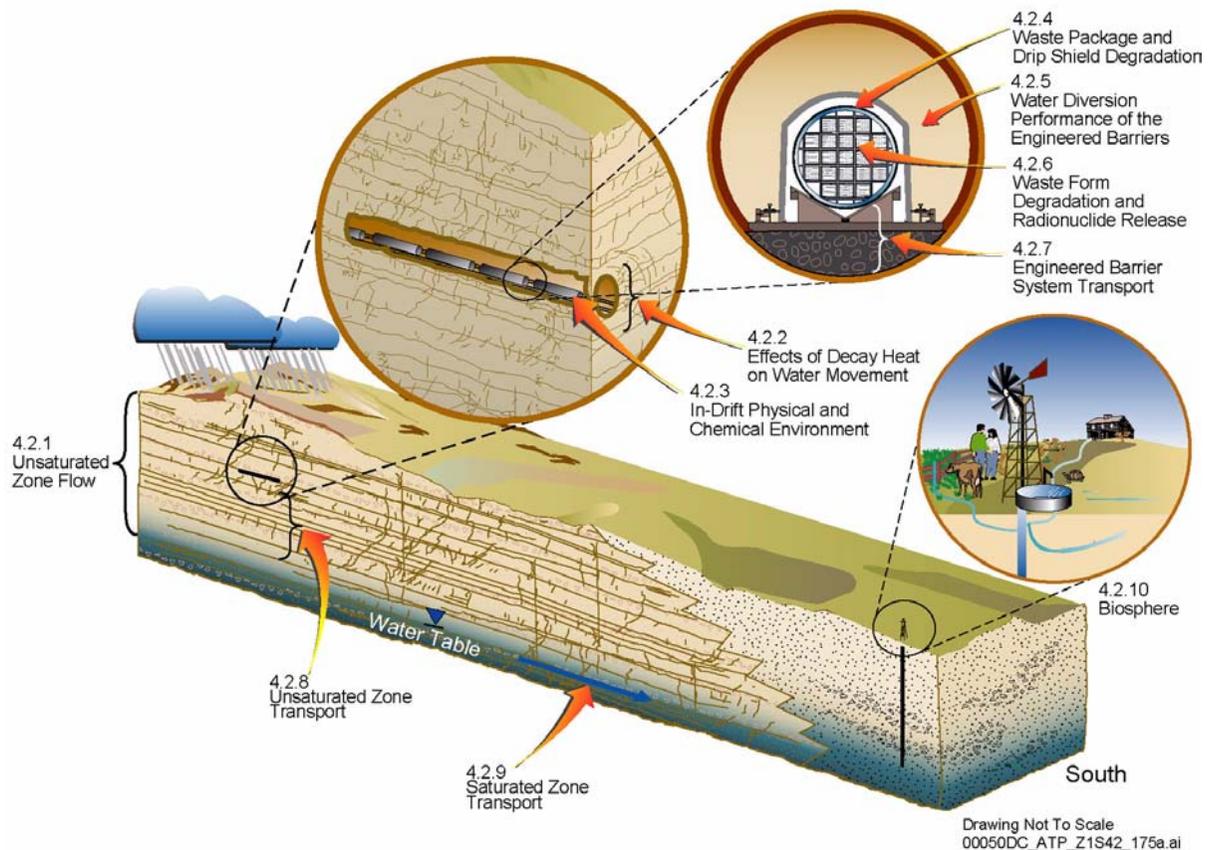
Figure 4-2.   Schematic Illustration of the Ten General Processes Considered and Modeled for Total System Performance Assessment
These ten highlighted processes roughly correspond to the ten sections in Section 4.2, as indicated.

processes could lead to the mobilization of radio-nuclides. Eventually, the water could move out of the repository horizon and further downward through the unsaturated zone. Subsequently, it could move into the saturated zone, where it could be transported to the accessible environment where humans could be exposed.

The data collected during site characterization have been used to develop conceptual and numerical models of the hydrologic, geochemical, thermal, and mechanical processes that will determine how a repository at Yucca Mountain may behave over the next 10,000 years. These process models have, in turn, been used to develop a TSPA model that has been used to assess quantitatively the potential for radionuclide releases to the public and, conse-quently, the safety of the Yucca Mountain site.

Attributes Important to Long-Term Perfor-mance—The potential repository system can be described in terms of five key attributes that would be important to long-term performance: (1) limited water entering waste emplacement drifts; (2) long-lived waste package and drip shield; (3) limited release of radionuclides from the engineered barriers; (4) delay and dilution of radionuclide concentrations by the natural barriers; and (5) low peak mean annual dose considering potentially disruptive events. These attributes are summarized below. The first four reflect the interactions of natural barriers and the engineered barriers in prolonging the containment of radionuclides within the repository and limiting their release. The fifth attribute reflects the likelihood that disruptive events would not affect repository performance over 10,000 years.

1. **Limited Water Entering Emplacement Drifts**—The climate at Yucca Mountain is dry and arid, with precipitation averaging about 190 mm (7.5 in.) per year. Little of this precipitation percolates into the mountain; nearly all of it (above 95 percent) either runs off or is lost to evaporation, limiting the amount of water available to seep into emplacement drifts. For the higher-temperature operating mode described in this report, a thermal management strategy was developed that would take advantage of the heat of the emplaced wastes to drive water away from the emplacement drifts. The heat generated by the waste would dry out the rock surrounding the drift and decrease the amount of water available to contact the waste packages until the wastes have cooled substantially. Drainage of water in the rock pillars between drifts would be encouraged by keeping much of the pillar rock between the drifts below the boiling temperature of water. As long as the drift walls remained at temperatures above the boiling point of water, there would no liquid water in the emplacement drifts and very little in the nearby rock. Even after the drift walls cooled below the boiling point of water, the residual heat would increase evaporation in and near emplacement drifts, thereby continuing to limit the amount of water present in the rocks adjacent to waste packages. In lower-temperature operating modes, the waste packages would be exposed to water earlier. Because the rock would eventually cool in any operating mode, there does not appear to be a significant difference in the amount of water to which the waste packages would eventually be exposed.

   Over the range of operating modes, the design also takes advantage of the mechanical and hydrologic processes that divert water around emplacement drift openings in the unsaturated zone. Because of capillary forces, water flowing in narrow fractures tends to remain in the fractures rather than flow into large openings, such as drifts. If any water reaches an emplacement drift, it could flow down the drift wall to the floor and drain without contacting the drip shield or the waste packages (however, in taking a more conservative approach in modeling, this potential process is not included in the models). Thus, the natural and engineered features of a repository in the unsaturated zone will combine to limit the potential for water to enter the emplacement drifts.

2. **Long-Lived Waste Package and Drip Shield**—To further reduce the possibility of water contacting waste, the DOE has designed a robust, dual-wall waste package with an outer cylinder of corrosion-resistant material, Alloy 22. Alloy 22 was selected because it will remain stable in the geochemical environment that would be expected in a repository at Yucca Mountain. In the operating mode described in this report, the repository environment would be warm, with temperatures at the waste package surface initially rising above the boiling point of water. Waste package surface temperatures are expected to gradually decrease to below boiling after a period of hundreds to thousands of years, depending on the waste package's location within the repository layout, spatial variation in the infiltration of water at the ground surface, and variability in the heat output of individual waste packages.

   Chemically, the environment is expected to be near-neutral pH (mildly acidic to mildly alkaline) and mildly oxidizing. Because most corrosion would occur only in the presence of water and because highly corrosive chemical conditions are not expected, both the titanium drip shield and the Alloy 22 outer barrier of the waste package are expected to have long lifetimes in an unsaturated zone repository. In lower-temperature operating modes, the waste packages would be exposed to water earlier.

3. **Limited Release of Radionuclides from the Engineered Barriers**—Because of the characteristics of the natural system, the drip shields, and the waste packages, scientists do not expect water to come into contact with the waste forms for over 10,000 years. Even if water were to penetrate a breached waste package before 10,000 years, several characteristics of the waste form and the repository would limit radionuclide releases. First, because of the warm temperatures, much of the water that penetrates the waste package will evaporate before it can dissolve or transport radionuclides. Neither spent nuclear fuel nor glass waste forms will dissolve rapidly in the expected repository environment. Further, a large majority of the radionuclide inventory is insoluble in the geochemical environment expected within the repository. Although the performance of the cladding (metallic outer sheath of a fuel element) as a barrier may vary because of possible degradation, it is expected to limit contact between water and waste. The component of the engineered barrier system below the waste package, called the invert, contains crushed tuff that would also limit the transport of radionuclides into the host rock.

4. **Delay and Dilution of Radionuclide Concentrations by the Natural Barriers**—Eventually, the engineered barrier systems in the repository are expected to degrade, and small amounts of water may contact waste. Even then, features of the geologic environment and the repository system will help decrease radionuclide migration to the accessible environment and slow it by hundreds to thousands of years. Processes that could be important to the movement of radionuclides include sorption, matrix diffusion, dispersion, and dilution. Rock units in both the unsaturated zone and the saturated zone at Yucca Mountain contain minerals that can adsorb many types of radionuclides (i.e., radionuclides would attach to and collect on the mineral surfaces). As water flows through fractures, dissolved radionuclides can diffuse into and out of the pores of the rock matrix, increasing both the time it takes for radionuclides to move from the repository and the likelihood that radionuclides will be exposed to sorbing minerals. Dispersion and dilution will occur naturally as potentially contaminated groundwater flows and mixes with other groundwater and lowers the concentration of contaminants.

5. **Low Mean Annual Dose Considering Potentially Disruptive Events**—Yucca Mountain provides an environment in which hydrogeologic conditions important to waste isolation (e.g., a thick unsaturated zone with low rates of water movement) have not changed very much for at least hundreds of thousands of years. Analysts have identified and evaluated a wide variety of potentially disruptive processes and events that could affect the performance of the design and operating mode described in this report. These range from extremely unlikely events, such as meteor impacts, to events that are likely to occur, such as regional climate change. Although the probability of volcanic activity in or near the potential repository is low, volcanic activity was a consideration in TSPA in the disruptive scenario case. Performance assessment results to date show that potentially disruptive events are not likely to compromise the performance of the repository, and the probability-weighted mean dose for an igneous disruption is low.

Table 4-3 shows the relationship between the key attributes of the site and the physical barriers that comprise the repository system, the processes important to waste isolation, and the descriptions presented in Sections 4.2.1 through 4.2.10 and in Section 4.3. The table is based on similar information developed and presented in *Repository Safety Strategy: Plan to Prepare the Safety Case to Support Yucca Mountain Site Recommendation and Licensing Considerations* (CRWMS M&O 2001a)

Table 4-3. **Correlation of Key Attributes of Yucca Mountain, Barriers to Radionuclide Release, and Processes Important to Performance, with Reference to Where Descriptions of the Processes can be Found in this Report and Process Model Reports**

Key Attributes of System	Barrier: Function	Processes Affecting Repository Performance	S&ER Section	PMR
Limited Water Entering Emplacement Drifts	**Surficial soils and topography:** Reduce the amount of water entering the unsaturated zone by surficial processes	Climate	Section 4.2.1	UZ Flow and Transport (CRWMS M&O 2000c)
		Net infiltration		
	Unsaturated rock layers overlying the repository: Reduce the amount of water reaching the repository by subsurface processes	Unsaturated zone flow	Section 4.2.1	UZ Flow and Transport (CRWMS M&O 2000c)
		Seepage into emplacement drifts		
		Coupled thermal effects on unsaturated zone flow and seepage	Section 4.2.2	Near-Field Environment (CRWMS M&O 2000al); UZ Flow and Transport (CRWMS M&O 2000c)
Long-Lived Waste Package and Drip Shield	**Drip shield above the waste packages:** Prevent water from contacting the waste package and waste form by diverting water flow. **Waste package:** Prevent water from contacting the waste form for thousands of years	In-drift physical and chemical environments	Section 4.2.3	Near-Field Environment (CRWMS M&O 2000al); EBS Degradation, Flow and Transport (CRWMS M&O 2000as)
		Drip shield degradation and performance	Section 4.2.4	Waste Package Degradation (CRWMS M&O 2000n)
		Waste package degradation and performance		
		In-drift water movement and moisture distribution	Section 4.2.5	EBS Degradation, Flow and Transport (CRWMS M&O 2000as)
Limited Release of Radionuclides from the Engineered Barriers	**Spent fuel cladding:** Delay and/or limit liquid water contacting spent nuclear fuel after waste packages have degraded	Cladding degradation and performance	Section 4.2.6	Waste Form Degradation (CRWMS M&O 2000bm)
	Waste form: Limit liquid water contacting waste during the period when temperatures are elevated and limit radionuclide release rates as a result of low solubilities and leach rates	Radionuclide inventory	Section 4.2.6	Waste Form Degradation (CRWMS M&O 2000bm)
		In-package environments		
		Commercial SNF and DOE SNF degradation and performance		
		DOE HLW degradation and performance		
		Dissolved radionuclide concentrations		
		Colloid-associated radionuclide concentrations		
		In-package radionuclide transport		
	Invert below the waste packages: Limit transport of radionuclides out of the engineered barrier system	Engineered barrier system transport, inverts, degradation and performance	Section 4.2.7	EBS Degradation, Flow and Transport (CRWMS M&O 2000as)
Delay and Dilution of Radionuclide Concentrations by the Natural Barriers	**Unsaturated rock layers below the repository:** Delay and reduce the concentration of radionuclides in the groundwater aquifer because of water residence time, matrix diffusion, and/or sorption	Unsaturated zone radionuclide transport (advective pathways; colloid transport and retardation; dispersion)	Section 4.2.8	UZ Flow and Transport (CRWMS M&O 2000c)
	Volcanic tuff and alluvial deposits below the water table: Delay radionuclide movement to the receptor location by water residence time, matrix diffusion, and/or sorption	Saturated zone radionuclide transport (advective pathways; colloid transport and retardation; dispersion; dilution)	Section 4.2.9	SZ Flow and Transport (CRWMS M&O 2000bn)
		Dilution	Section 4.2.10	Biosphere (CRWMS M&O 2000bo)
Low Mean Annual Dose Considering Potentially Disruptive Events	N/A (Disruptive processes and events act on the barriers listed above)	Probability and consequences of volcanic eruption (characteristics and effects of eruption, atmospheric transport); Probability and consequences of igneous intrusion (characteristics and effects of igneous intrusion); Probability and consequences of seismic events; Probability and consequences of other disruptive events; Biosphere dose conversion factors	Section 4.3	Disruptive Events (CRWMS M&O 2000f)

NOTES: EBS = engineered barrier system; HLW = high-level radioactive waste; N/A = not applicable; PMR = process model report; S&ER = *Yucca Mountain Science and Engineering Report*; SNF = spent nuclear fuel; SZ = saturated zone; UZ = unsaturated zone.

and the *Total System Performance Assessment for the Site Recommendation* (CRWMS M&O 2000a). The table incorporates the results of lower-temperature operating mode evaluations (BSC 2001b). In addition to the information presented in these sources, Table 4-3 relates the key attributes and processes to the natural and engineered barriers that would contribute to waste isolation at Yucca Mountain. The last column of the table also lists process model reports that contain more detailed descriptions of the processes summarized here and included in the TSPA. The column showing the processes important to repository performance is not intended to be comprehensive: it is presented at a summary level. More detailed definitions of the proposed repository system and relevant specific processes are included in the individual sections that follow.

Organization of Section 4.2—As organized below, and shown in Figure 4-2, the total system consists of numerous interdependent subsystems that are described in ten subsections, as follows:

- Section 4.2.1 describes the data and analyses relevant to the movement of water in the unsaturated zone and describes the development of process models related to the potential movement of water into the repository.

- Section 4.2.2 describes the data and analyses related to the effects of decay heat on the movement of water through the unsaturated zone.

- Section 4.2.3 describes information that provides the basis for the DOE's understanding of the physical and chemical environment within the repository drifts, which influences the expected lifetimes of the drip shields and waste packages.

- Section 4.2.4 summarizes the data and evaluations that support models of the degradation of drip shields and waste packages, which will affect the lifetimes of the engineered barrier system.

- Section 4.2.5 describes the information that supports the analysis of the performance of engineered barriers in diverting water away from the waste package. After the eventual degradation of the waste packages, and in the presence of liquid water, it would be possible for chemical reactions to occur to mobilize radionuclides within the waste packages.

- Section 4.2.6 describes the experimental data and analyses of the chemical and hydrologic processes within the breached waste packages that would result in the release of radionuclides from the waste form.

- Section 4.2.7 describes information related to the potential transport of mobilized radionuclides through the engineered barriers.

- Section 4.2.8 describes the data and analyses related to the potential flow and transport of radionuclides through the unsaturated zone.

- Section 4.2.9 describes potential flow and transport in the saturated zone.

- Section 4.2.10 describes the biosphere model used to model the uptake and biological consequences of released radionuclides that eventually reach the human environment.

Within each of these sections, a similar internal organization is used to present the DOE's understanding of the key processes and to present the data and analyses that provide the basis for that understanding. Each discussion includes:

1. A summary description of how each process would operate in a potential repository

2. A description of the investigations, tests, and other data (including analogue information) that provide the technical basis for the DOE's understanding

3. A description of the conceptual and numerical models that have been developed to allow the DOE to assess potential future performance, including specific

information about the sources and treatment of uncertainties, alternative models, and model calibration and validation

4. A description of how the conceptual and numerical models have been abstracted (or represented) in the TSPA-SR (CRWMS M&O 2000a).

4.2.1 Unsaturated Zone Flow

This section summarizes the current understanding of water movement (i.e., percolation flux) through the unsaturated zone and into a repository (i.e., seepage into drifts) at Yucca Mountain. Fluid flow through the unsaturated zone at Yucca Mountain is described at length in *Unsaturated Zone Flow and Transport Model Process Model Report* (CRWMS M&O 2000c, Sections 3.2 to 3.4 and 3.6 to 3.9), which is supported by 24 detailed analysis model reports. *Yucca Mountain Site Description* (CRWMS M&O 2000b, Sections 8.2 to 8.10) also provides a comprehensive summary of investigations performed to characterize flow and seepage in the unsaturated zone. Figure 4-3 shows the relationships between the main unsaturated zone processes, with those relevant to unsaturated zone flow highlighted.

The primary purpose of *Unsaturated Zone Flow and Transport Model Process Model Report* (CRWMS M&O 2000c) is to develop models for the TSPA that evaluate the postclosure performance of the unsaturated zone. *Unsaturated Zone Flow and Transport Model Process Model Report* supplies to the TSPA (1) ambient and predicted (i.e., future) three-dimensional flow fields based on different climate states and infiltration scenarios and (2) seepage rates into potential waste emplacement drifts. The flow fields are used directly in TSPA calculations of transport, while the seepage rates are used to calculate distributions of the fraction of waste packages in contact with seepage water and the volumetric flow rate to a waste package segment, taking into account possible flow focusing effects from site scale to drift scale (see Section 4.2.1.4).

As noted in Section 4.1.4, the DOE is evaluating the possibility of mitigating uncertainties in

modeling long-term repository performance by operating the design described in this report at lower temperatures. Some analyses described in this section have been updated and expanded to capture the features and processes relevant to operating the design at lower temperatures. The updated analyses are described in Volume 2, Section 4 of *FY01 Supplemental Science and Performance Analyses* (BSC 2001b).

4.2.1.1 Conceptual Basis

On the most fundamental level, the important factors affecting unsaturated groundwater flow at Yucca Mountain are climate and rock hydrologic properties. Derived from these two basic components are estimates of percolation flux and seepage into potential waste emplacement drifts, both of which are key unsaturated zone processes.

Located in southern Nevada, one of the most arid regions of the United States, Yucca Mountain is underlain by a thick unsaturated zone (CRWMS M&O 2000c, Section 3.2.1). A dry climate and a deep water table are considered favorable characteristics for waste isolation. In a desert environment, the total amount of available water is small. The potential repository would be designed to complement the hydrologic environment by diverting the small flow of water that does occur away from the waste packages. Multiple natural and engineered barriers are expected to limit contact between water and waste forms, and retard radionuclide migration. The climate data and unsaturated zone characteristics are discussed in Sections 4.2.1.2.1 and 4.2.1.2.2, respectively.

The major components of the unsaturated zone and the emplacement drifts that affect water movement are illustrated in Figure 4-4. Water movement starts with rainfall in the arid environment, which is subject to runoff, evaporation, and plant uptake, such that much of the rainfall never reaches the potential repository host rock units. The infiltration of water that penetrates into the rock units of the unsaturated zone is redistributed by flow processes in the fractured and faulted, welded and nonwelded tuff layers. When percolating water encounters an underground drift, much of it will be diverted by

00050DC_ATP_Z1S42_122.ai
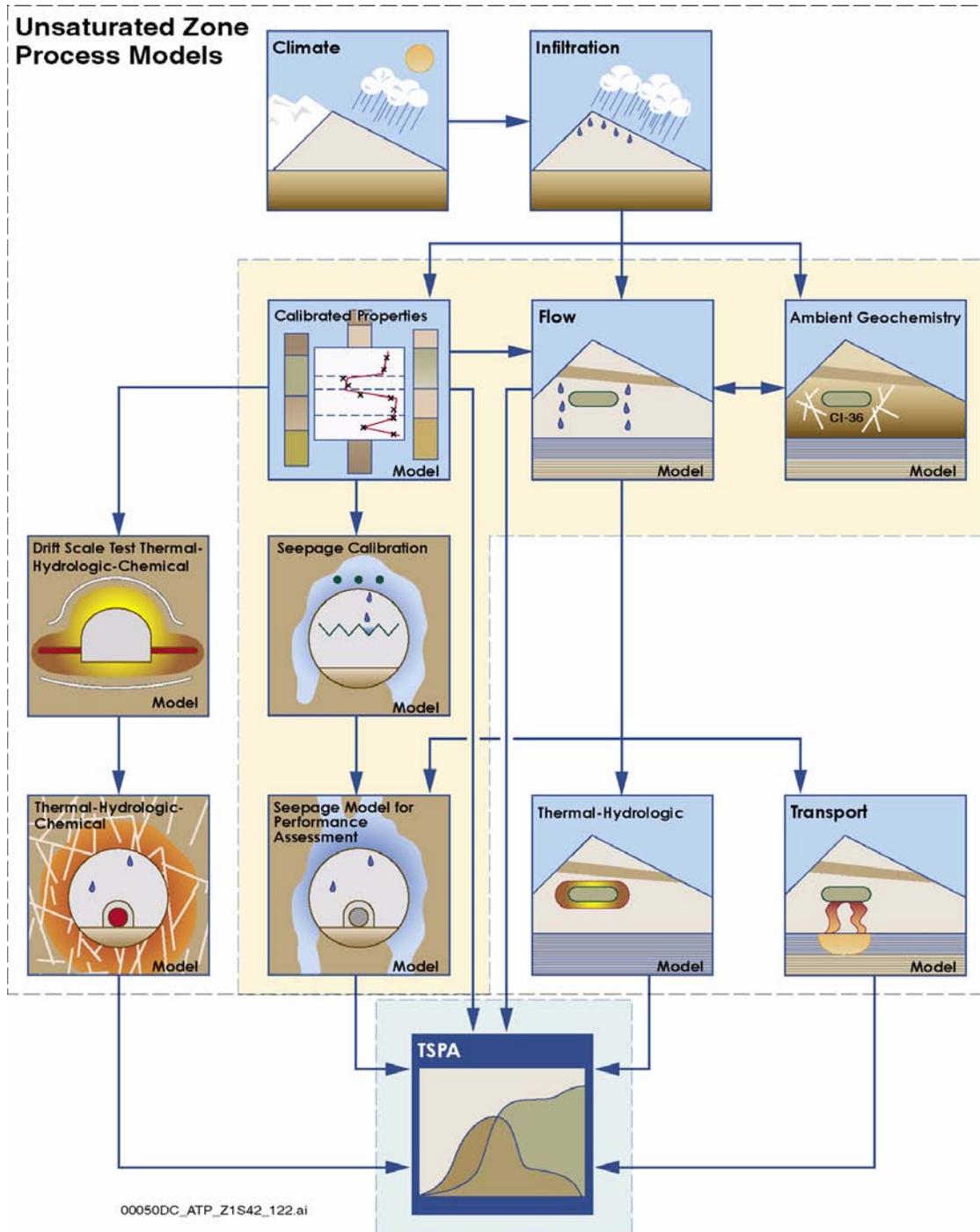
Figure 4-3.   Main Models Included in the Unsaturated Zone Process Model Report, Their Interrelations, and Their Connections to Total System Performance Assessment

Models relevant to this section are highlighted with a cream-colored background. Source: CRWMS M&O 2000c, Figure 1-2.
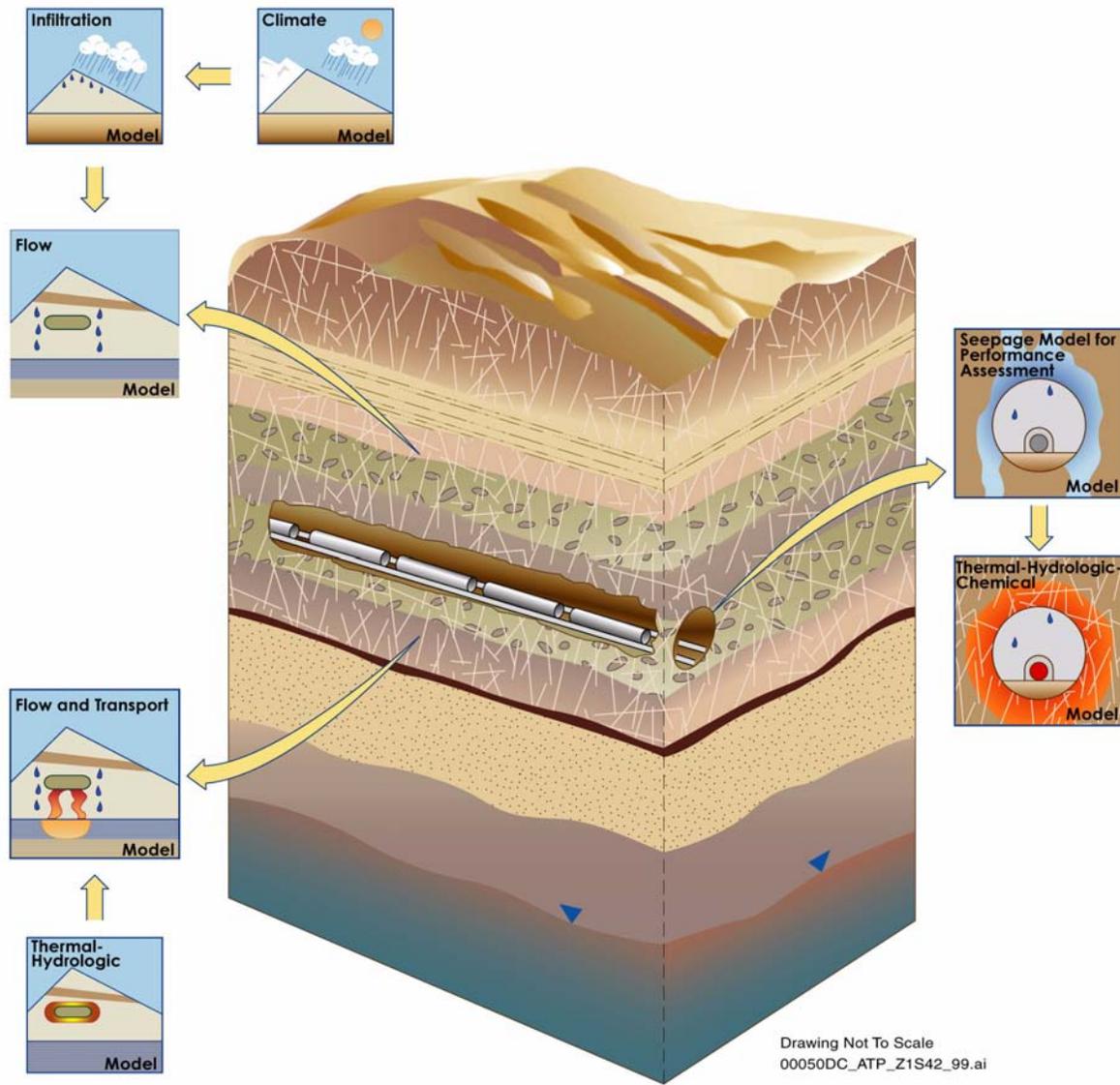
Figure 4-4. **Schematic Block Diagram Showing Major Unsaturated Zone Flow Processes Above, Within, and Below Repository Emplacement Drifts**

capillary barrier mechanisms around the opening and never contact the engineered barriers within.

Major issues related to unsaturated zone flow processes include:

- Climate and infiltration

- Fracture flow versus matrix flow within major hydrogeologic units

    – Flow above the potential repository

    – Flow below the potential repository, including the formation and hydrologic significance of perched water

- Fracture–matrix interaction

- Effects of major faults

- Seepage into drifts.

Using these major issues as subheadings, a summary of the current conceptual understanding of unsaturated zone flow beneath Yucca Mountain

is first presented. Following this summary are subsections that describe the data supporting the conceptual understanding of flow in the unsaturated zone (Section 4.2.1.2), the development and integration of numerical process models based on the conceptual interpretation of the available data (Section 4.2.1.3), and how the results of unsaturated zone numerical modeling studies have been abstracted for the TSPA (Section 4.2.1.4).

4.2.1.1.1   Climate and Infiltration

Climate is defined by the variation of meteorological conditions (such as temperature, pressure, humidity, precipitation rate and prevailing winds) over time. At Yucca Mountain, climate is important because it provides the boundary conditions for the hydrologic system—specifically, the amount of water available at the surface. Estimates of the precipitation rate and temperature taken from climate models have been used as information to determine the net infiltration of water into Yucca Mountain and the percolation flux at the repository horizon. Percolation flux within the unsaturated zone, governed by climate and rock hydrogeologic properties, is a key process affecting seepage in waste emplacement drifts and transport of radioactive particles below the repository. Three representative climates are forecast to occur within the next 10,000 years (i.e., the period of regulatory compliance): the modern (present-day) climate, a monsoon climate, and a glacial-transition climate (USGS 2000a, Section 6.6). Beyond 10,000 years, the TSPA-SR extends the glacial-transition climate for base-case simulations and includes a revised long-term climate model in a sensitivity study, as discussed in Section 4.4.2.4 (CRWMS M&O 2000a, Section 3.2.1.2) and Volume 1, Section 3.3.1 of *FY01 Supplemental Science and Performance Analyses* (BSC 2001a).

Net infiltration refers to the penetration of liquid water through the ground surface and to a depth where it can no longer be removed by evaporation or transpiration by plants. Net infiltration is the source of groundwater recharge and water percolation at the potential repository horizon; it provides the water for flow and transport mechanisms that could move radionuclides from the potential repository to the water table. The overall framework of

the conceptual model for net infiltration is based on the hydrologic cycle. Important processes that affect net infiltration include precipitation (rain and snow), runoff and run-on (flow of surface water off one place and onto another), evaporation, transpiration, and moisture redistribution by flow in the shallow subsurface (USGS 2000b, Section 6.1.3). Infiltration is temporally and spatially variable because of the nature of the storm events that supply precipitation and because of variation in soil cover and topography (CRWMS M&O 2000bq, Section 6.1.1). Surficial soils and topography are considered part of the natural barrier system because they reduce the amount of water entering the unsaturated zone by surficial processes (e.g., precipitation lost to runoff, evaporation, and plant transpiration) (Table 4-2). Net infiltration rates are believed to be high on sideslopes and ridge tops where bedrock is exposed and fracture flow in the bedrock is able to move liquid water away from zones of active evaporation (Flint, L.E. and Flint 1995, p. 15).

Within the limits of extant monitoring data, significant net infiltration occurs only every few years under the present climate (CRWMS M&O 2000bq, Section 6.1.1). In these years, the amount of net infiltration still varies greatly, depending on storm amplitude, duration, and frequency. In very wet years, net infiltration pulses into Yucca Mountain may occur over a period of a few hours to a few days. A detailed discussion of net infiltration processes can be found in *Simulation of Net Infiltration for Modern and Potential Future Climates* (USGS 2000b) and in Volume 1, Section 3.3.1 of *FY01 Supplemental Science and Performance Analyses* (BSC 2001a).

4.2.1.1.2   Fracture Flow and Matrix Flow within Major Hydrogeologic Units

An early conceptual hydrologic model of unsaturated flow at Yucca Mountain, developed by Montazer and Wilson (1984), identified five major hydrogeologic units within the unsaturated zone. From the land surface to the water table, these units are the Tiva Canyon welded (TCw), the Paintbrush nonwelded (PTn), the Topopah Spring welded (TSw), the Calico Hills nonwelded (CHn), and the Crater Flat undifferentiated (CFu) units. Table 4-4

Table 4-4. **Major Hydrogeologic Unit, Lithostratigraphic Unit, Detailed Hydrogeologic Unit, and Unsaturated Zone Model Layer Nomenclatures**

Major Hydrogeologic Unit	Lithostratigraphic Unit		Detailed Hydrogeologic Unit	Unsaturated Zone Model Layer
Tiva Canyon welded (TCw)	Tiva Canyon Tuff	Topic	CCR, CUC	tcw11
		Tpcp	CUL, CW	tcw12
		Tpcpv3	CMW	tcw13
		Tpcpv2		
Paintbrush nonwelded (PTn)		Tpcpv1	CNW	ptn21
	Bedded Tuff	Tpbt4	BT4	ptn22
	Yucca Mountain Tuff	Tpy	TPY	ptn23
			BT3	ptn24
	Bedded Tuff	Tpbt3		
	Pah Canyon Tuff	Tpp	TPP	ptn25
	Bedded Tuff	Tpbt2	BT2	ptn26
	Topopah Spring Tuff	Tptrv3		
		Tptrv2		
Topopah Spring welded (TSw)		Tptrv1	TC	tsw31
		Tptrn	TR	tsw32
		Tptrl	TUL	tsw33
		Tptpul		
		Tptpmn	TMN	tsw34
		Tptpll	TLL	tsw35
		Tptpln	TM2 (upper 2/3)	tsw36
			TM1 (lower 1/3)	tsw37
		Tptpv3	PV3	tsw38
		Tptpv2	PV2	tsw39
Calico Hills nonwelded (CHn)		Tptpv1	BT1 or BT1 (altered)	ch1 (vit, zeo)
	Bedded Tuff	Tpbt1		
	Calico Hills Formation	Tac	CHV (vitric) or CHZ (zeolitic)	ch2 (vit, zeo)
				ch3 (vit, zeo)
				ch4 (vit, zeo)
				ch5 (vit, zeo)
	Bedded Tuff	Tacbt	BT	ch6
	Prow Pass Tuff	Tcpuv	PP4 (zeolitic)	pp4
		Tcpuc	PP3 (devitrified)	pp3
		Tcpmd	PP2 (devitrified)	pp2
		Tcplc		
		Tcplv	PP1 (zeolitic)	pp1
	Bedded Tuff	Tcpbt		
Crater Flat undifferentiated (CFu)	Bullfrog Tuff	Tcbuv		
		Tcbuc		
		Tcbmd	BF3 (welded)	bf3
		Tcblc		
		Tcblv	BF2 (nonwelded)	bf2
	Bedded Tuff	Tcbbt		
	Tram Tuff	Tctuv		
		Tctuc		
		Tctmd	Not Available	tr3
		Tctlc		
		Tctlv & below	Not Available	tr2

Source: CRWMS M&O 2000c, Table 3.2-2.

correlates major hydrogeologic, lithostratigraphic, and detailed hydrogeologic units with the layering scheme used in unsaturated zone modeling activities. These units are described in greater detail in the *Development of Numerical Grids for UZ Flow and Transport Modeling* (CRWMS M&O 2000br, Section 6.4.1), in the *Geologic Framework Model (GFM3.1)* (CRWMS M&O 2000bs, Section 6.4.1), and by Flint, L.E. (1998).

The texture of Yucca Mountain tuffs ranges from nonwelded to densely welded (CRWMS M&O 2000c, Section 3.2.1). Typically, the porosity and permeability of the rock mass are inversely proportional to the degree of welding, and the degree of fracturing is directly proportional to the degree of welding. The degree of welding observed in the individual tuff units is primarily controlled by their cooling history. Generally speaking, the slower a rock cools, the more densely welded the material becomes. This densely welded material (matrix) is usually quite brittle in nature and develops well-connected fracture networks. These extensive, well-connected fracture networks, in turn, provide numerous pathways for the flow of liquids and gases. Conversely, the nonwelded rocks, which experienced rapid heat dissipation, display high matrix porosity and possess few fractures. Flow through these rocks is dominated by matrix flow processes (CRWMS M&O 2000c, Section 3.3.3).

The partitioning of total flux between the fracture flow component and the matrix flow component is one of the most important processes to determine in the unsaturated zone. Percolation distribution determines the amount of water that could potentially contact the waste packages and other components of the engineered barrier system. Determination of the flow components is also important for chemical transport processes. Water flow in fractures is typically much faster than flow in the matrix, leading to much faster movements for radionuclides and other chemicals in fractures compared to the matrix (CRWMS M&O 2000c, Section 3.3.3). The characteristic flow behavior in each of the major hydrogeologic units is described in the following paragraphs.

Flow Above the Potential Repository—The TCw is the most prevalent hydrogeologic unit exposed at the land surface (CRWMS M&O 2000c, Section 3.2.2.1). The unit is of variable thickness because of erosion and is composed of moderately to densely welded, highly fractured pyroclastic flow deposits of the Tiva Canyon Tuff. The high density of interconnected fractures and low matrix permeability of the unit (CRWMS M&O 2000bt, Sections 6.1 and 6.2) are considered to give rise to significant water flow in fractures and limited matrix imbibition (water flow from fractures to the matrix). Therefore, episodic infiltration pulses are expected to move rapidly through the fracture system into the underlying PTn unit with little attenuation by the matrix.

At the interface between hydrogeologic units TCw and PTn, tuffs grade downward over a few tens of centimeters from densely welded to nonwelded, accompanied by an increase in matrix porosity and a decrease in fracture frequency (Figure 4-5a) (CRWMS M&O 2000c, Section 3.2.2.1). The relatively high matrix permeabilities and porosities, and low fracture densities, of the PTn (CRWMS M&O 2000bt, Sections 6.1 and 6.2) should convert the predominant fracture flow in the TCw to dominant matrix flow within the PTn unit (CRWMS M&O 2000bq, Section 6.1). This, along with the relatively large storage capacity of the matrix resulting from its high porosity and low saturation, is expected to give the PTn significant capability to attenuate infiltration pulses and smooth areal differences in infiltration from the overlying welded unit and result in approximately steady-state water flow below the PTn. Through-going fracture networks within the PTn unit are rare and typically associated with faults (Rousseau, Kwicklis et al. 1999, pp. 53 to 54), so only a small amount of water is expected to pass through the PTn by way of fast flow paths. Recent analyses indicates that some lateral diversion on the PTn is probable (BSC 2001a, Section 3.3.3).

Conceptualization of the character of flow at the interface between the PTn and the overlying TCw for the TSPA-SR model was based on findings from estimates of flux rates in the PTn from geochemistry (Yang and Peterman 1999) and on hydrogeological properties described by Flint, L.E. (1998). The implication of that characterization was that little or no lateral flow diversion of down-
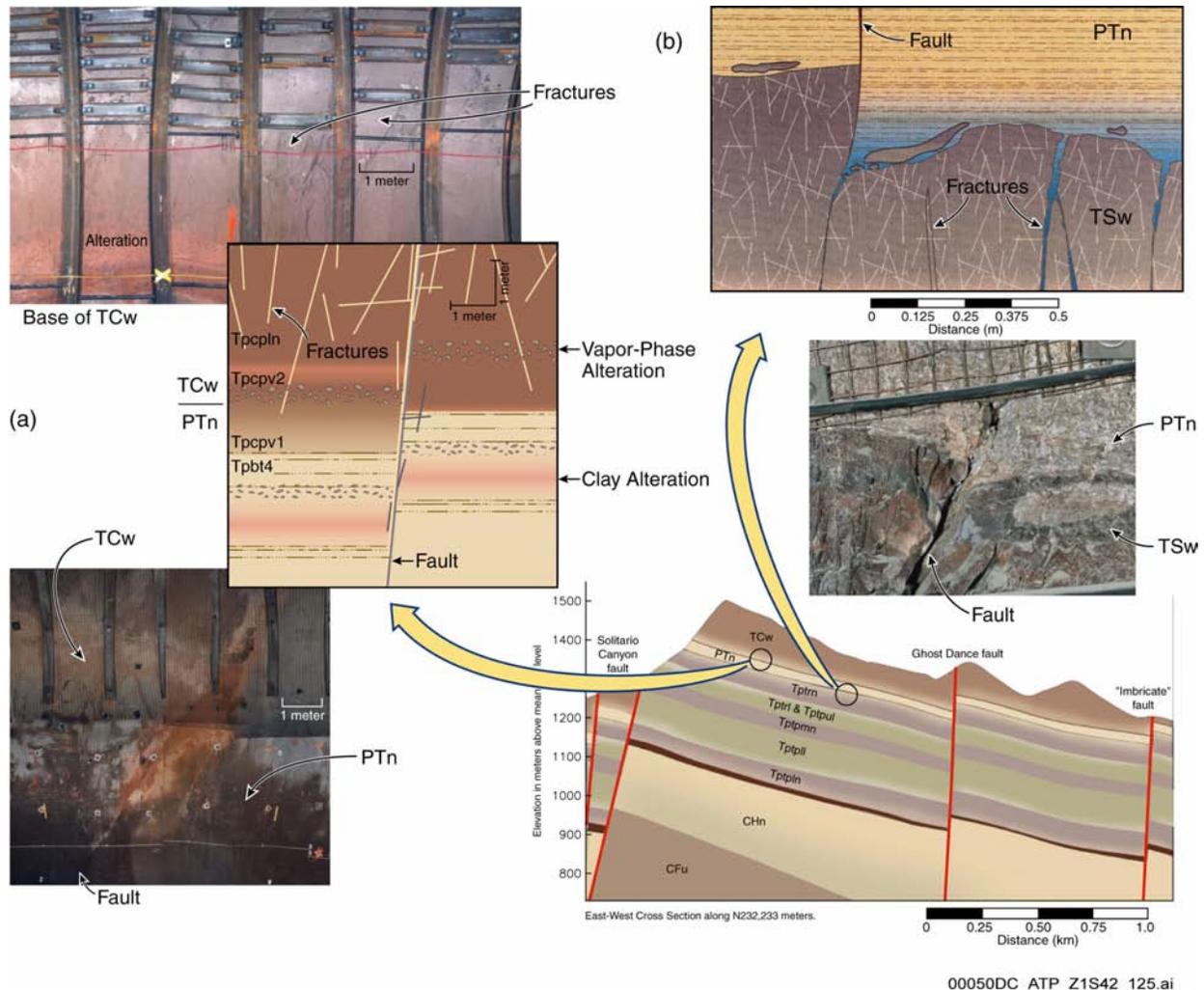
Figure 4-5. **Lithostratigraphic Transitions at the Upper and Lower Margins of the PTn Hydrogeologic Unit** (a) Photos and schematic at the TCw–PTn interface, where tuffs grade downward from densely welded to nonwelded, accompanied by an increase in matrix porosity and a decrease in fracture frequency. (b) Photo and schematic at the PTn–TSw interface, where tuffs grade downward from nonwelded to densely welded, accompanied by a decrease in matrix porosity and an increase in fracture frequency. Source: Adapted from CRWMS M&O 2000c, Figures 3.2-2 and 3.3-3.

ward percolating unsaturated zone water could be expected as a result of a contrast of hydrologic properties across this surface and its gentle dip to the east. If diversion of downward percolating water to permeable fault zones outside the potential repository footprint at that elevation occurs, it implies that water might be diverted around a repository, thus benefiting repository performance. Earlier work by Montazer and Wilson (1984) supported the conceptual model of lateral diversion on the PTn. The TSPA-SR model did not include lateral diversion on the PTn on the assumption that

if any such diversion exists, it is small and that to leave it out of the model is conservative.

Geochemical evidence collected since the conceptualization of the original TSPA-SR modeling appears to support the existence of lateral diversion in the PTn based on chloride abundance (BSC 2001a, Section 3.2.3). Recent modeling approaches that combine pneumatic data from above, below, and within the PTn, saturation and water potential data, and geochemical data were used to calibrate unsaturated characteristic parameters and to differ-

entiate alternative conceptual models (BSC 2001a, Section 3.2.3). Using a fine grid spacing, calibrated to match the chloride distributions and the estimated percolation flux data in the unsaturated zone below the PTn, supports the lateral diversion of water around a potential repository and the relatively uniform distribution of percolation flux in the deep unsaturated zone (BSC 2001a, Section 3.3.3). The PTn exhibits inhomogeneous lithologic character and distribution and some evidence, in the form of inferred occurrences of bomb-pulse chlorine-36 at depth, that fast flow paths for relatively small volumes of water may exist along faults and perhaps in zones of fracture flow focusing. In most of the region of the potential repository footprint, the PTn is expected to damp flow surges in the percolation flux rate and smooths areal differences in flow, which originate in the temporal and spatial patterns of infiltration at the surface (CRWMS M&O 2000c, Section 3.3.3.2). Smoothing of flow is supported by evenly distributed chloride mass balance data (BSC 2001a, Section 3.3.3).

Although the PTn is predominantly nonwelded, rock-hydrologic properties are highly heterogeneous because of differing depositional environments, lateral variations in welding, and the variable distribution of mineralogically altered (e.g., smectitic and zeolitic) intervals within the individual PTn subunits (CRWMS M&O 2000c, Section 3.2.2.2).

The transition from the lower PTn into the upper TSw is marked by a decrease in matrix porosity and an increase in fracture frequency (Figure 4-5b) (CRWMS M&O 2000c, Section 3.2.2.2) as the tuffs grade sharply downward from nonwelded to densely welded. These changes in porosity and fracture characteristics may create saturated conditions above this contact that could initiate fracture flow into the TSw.

Lithostratigraphic units within the TSw (including the middle nonlithophysal, lower lithophysal, and lower nonlithophysal potential repository host units) are moderately to densely welded and are primarily distinguished by the relative abundance of lithophysae (cavities formed by bubbles of volcanic gases trapped in the tuff matrix during

cooling), crystal content, mineral composition, pumice and rock fragment abundance, and fracture characteristics (CRWMS M&O 2000c, Section 3.2.2.3). Differences in lithophysal abundance and fracture characteristics are shown in Figure 4-6.

Unsaturated flow in the TSw is primarily through the fractures because of the magnitude of matrix hydraulic conductivity of the TSw relative to the estimated average infiltration rate. If the hydraulic gradient is assumed to be one (i.e., flow is vertically downward and gravity driven), the maximum matrix percolation rate is the same as the matrix hydraulic conductivity. Because the estimated matrix hydraulic conductivity of some TSw subunits is much lower than the average estimated infiltration rate (CRWMS M&O 2000bq, Section 6.1.2), the remainder of the flow must be distributed in the fracture network.

Flow Below the Potential Repository—Flow behavior below the TSw is important for modeling radionuclide transport from the repository horizon to the water table because transport paths follow the water flow pattern. The main hydrogeologic units below the TSw are the CHn and CFu (CRWMS M&O 2000c, Sections 3.2.2.4 and 3.2.2.5). The CHn contains primarily nonwelded layers whose initial vitric composition has been variably transformed by high and low temperature alteration to clays and zeolites. A portion of the lower half of the CHn (corresponding to the interior of the Prow Pass Tuff) is characterized by moderately welded to densely welded layers that have undergone devitrification (high-temperature conversion of glass to crystalline material). Devitrified, welded rocks show greater fracture intensity than the nonwelded layers and typically do not contain alteration minerals (Flint, L.E. 1998, p. 9). In the southern half of the potential repository footprint and to the south, a portion of the upper CHn (corresponding principally to the Calico Hills Formation, Tac) is largely unaltered (i.e., vitric). This volume of vitric material is believed to represent the part of the CHn that remained above past elevated saturated zone water levels (CRWMS M&O 2000c, Section 3.2.4).

The CFu unit (consisting of portions of the Bullfrog and Tram tuffs that occur above the water
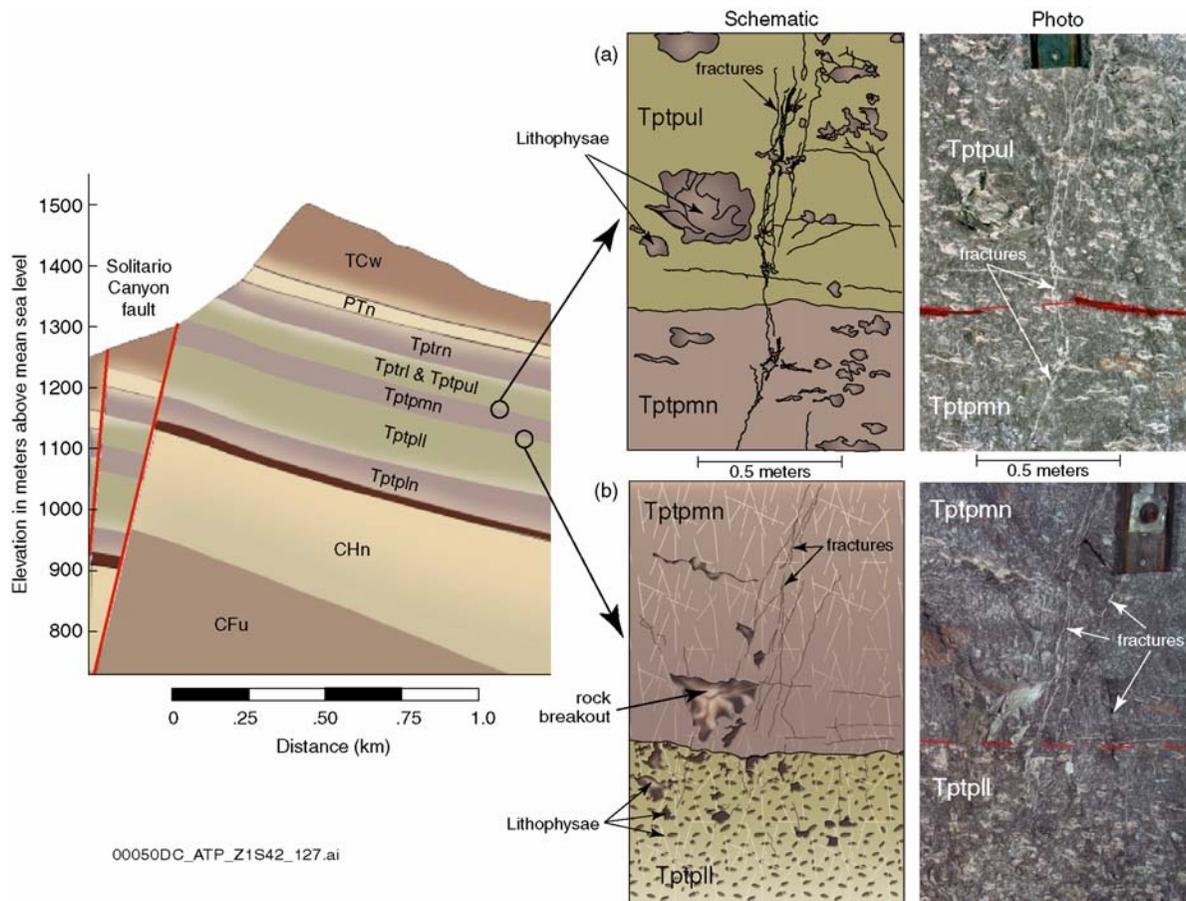
Figure 4-6.   Lithophysal Transitions within the TSw Unit
(a) Photo and schematic of the contact between the upper nonlithophysal (Tptpul) and the middle nonlithophysal (Tptpmn) zones showing a downward decrease in lithophysal volume. (b) Photo and schematic of the contact between the middle nonlithophysal (Tptpmn) and lower lithophysal (Tptpll) zones showing a downward increase in lithophysal volume. Fractures in the nonlithophysal units are generally smoother, more planar, and more continuous than fractures in the lithophysal units. Source: CRWMS M&O 2000c, Figure 3.2-4.

table) is a subset of the Crater Flat Group, which contains the Prow Pass, Bullfrog, and Tram tuffs (CRWMS M&O 2000b, Section 4.5.4.5). Lithostratigraphic units within the CFu are nonwelded to densely welded, with the nonwelded tuffs being pervasively altered to zeolites. The Prow Pass, Bullfrog, and Tram tuffs are all similar in that they each contain devitrified, densely welded interiors that grade above and below into nonwelded, zeolitically altered tuffs.

The nonwelded vitric, nonwelded zeolitic, and welded devitrified tuffs have significantly different properties and flow characteristics. The zeolitic rocks have very low matrix permeability and slightly greater fracture permeability; therefore, a relatively small amount of water may flow through the zeolitic units (primarily through fractures), while most of the water is diverted around these low-permeability bodies (Figure 4-7b) (CRWMS M&O 2000c, Section 3.3.3.4). Conversely, vitric portions of the CHn have relatively high matrix porosity and permeability and are characterized by low fracture frequencies (similar to layers within the PTn); therefore, matrix flow dominates, and fracture flow is believed to be limited in the vitric units. Devitrified tuffs have slightly lower matrix porosities than the nonwelded tuffs and increased
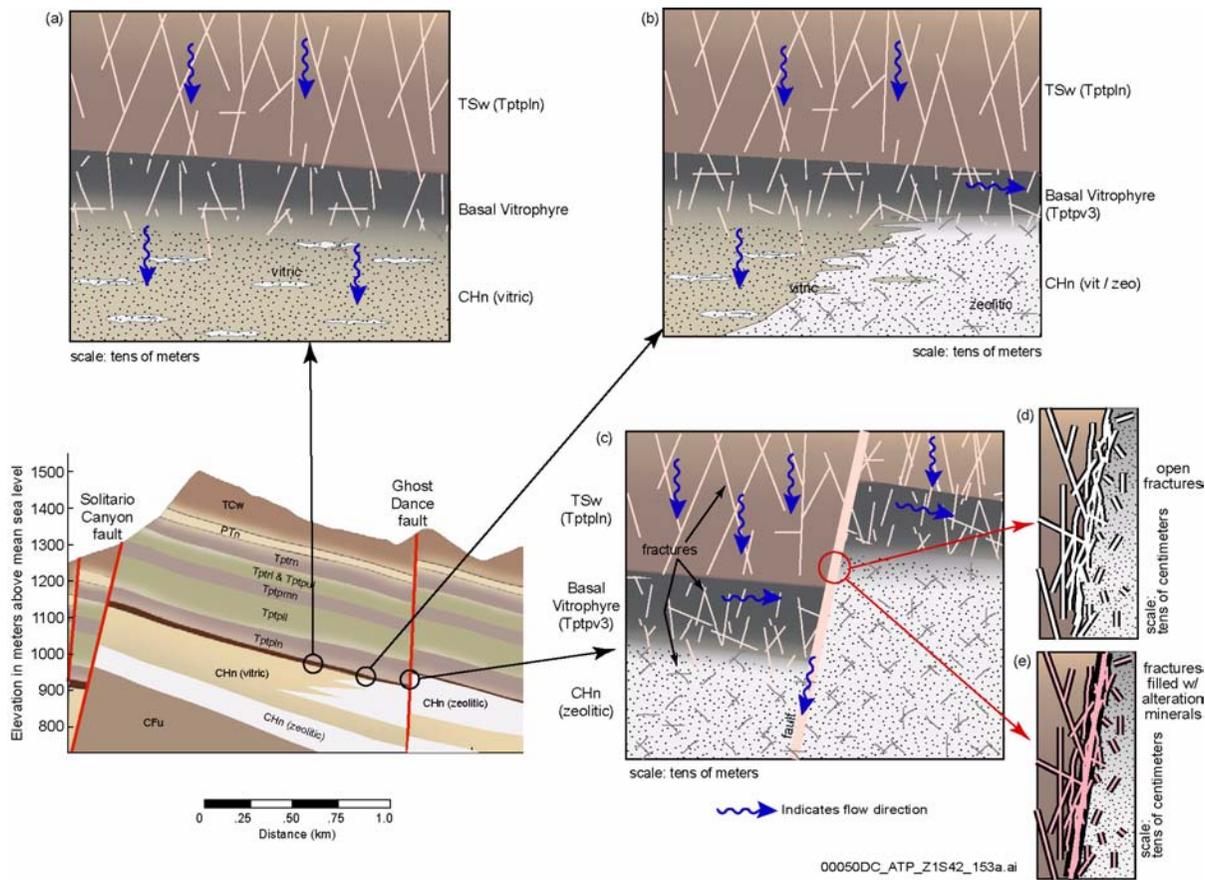
Figure 4-7.   Lithostratigraphic Transitions and Flow Patterns at the TSw–CHn Interface
(a) Schematic with minimal alteration at the TSw–CHn contact showing a transition from fracture-dominated to matrix-dominated flow. (b) Schematic with variable alteration at the TSw–CHn contact showing flow diversion around zeolites. (c) Schematic with prevalent alteration at the TSw–CHn contact showing lateral flow within the perched-water body, followed by fault-dominated flow. (d) Schematic detail of open fractures, which may represent a fast flow pathway. (e) Schematic detail illustrating fractures filled by deposits of alteration minerals, which could create a flow barrier. Source: CRWMS M&O 2000c, Figure 3.2-5.

fracturing (because of increased welding), yet little or no alteration, giving them relatively higher permeabilities than the zeolitic tuffs (Flint, L.E. 1998, pp. 29 and 32).

The high storage capacity of the vitric (unaltered) CHn matrix will attenuate the rate of water movement through the unsaturated zone (Figure 4-7a). Where extensive mineralogic alteration has occurred—for example, at the TSw–CHn contact—the downward flux of water may exceed the rock's transmissive capacity, leading to ponding above the flow barrier and the formation

of perched water (Figure 4-7c). The presence of a low-permeability barrier to vertical flow can lead to lateral flow diversion, especially if the flow barrier is dipping and saturated moisture conditions (i.e., perched water bodies) exist above the barrier. Therefore, not all flow paths below the potential repository horizon are expected to be vertical. Lateral diversion of water at perching horizons may lead to flow focusing if the vertical flow barrier is intersected by a high-permeability feature, such as a fault, that could channel flow to the water table (CRWMS M&O 2000c, Sections 3.3.3.4 and 3.3.5).

4.2.1.1.3   Effects of Major Faults

Different kinds of faults with varying amounts of displacement exist at Yucca Mountain (CRWMS M&O 2000c, Section 3.3.5). Fault hydrologic properties are variable and generally controlled by rock type and stratigraphic displacement. Because major faults have the potential to significantly affect the flow processes at Yucca Mountain, they are important features of the unsaturated zone.

A fault can act as a fast flow conduit for liquid water (Figure 4-7d). In this case, transient water flow may occur within a fault as a result of temporally variable infiltration. Major faults cut through the PTn unit, possibly reducing the attenuating effect of the PTn on transient water flow. However, fast flow along major faults is expected to carry only a small amount of water and may not contribute significantly to the flow of water above the potential repository horizon in the unsaturated zone (see Section 4.2.1.3.1.1). Faults intercepting the perched water bodies, however, can correspond to significant vertical water flow if fault permeability is relatively high because of the locally saturated conditions existing in the surrounding rock (see Figure 4-7c) (CRWMS M&O 2000c, Sections 3.3.5 and 3.7.3.2).

If faults within the CHn are relatively permeable features, they may provide a direct flow pathway to the water table. This is particularly significant because radionuclides released from the potential repository could bypass zeolitic or vitric layers within the CHn unit, where they could be retarded by sorption. Conversely, faults might be considered a positive feature of the site if they divert water around waste emplacement drifts or prevent laterally flowing water from focusing at the area of waste emplacement.

Alternatively, a fault can act as a barrier for water flow (CRWMS M&O 2000c, Section 3.3.5). Where a fault zone is highly fractured, the corresponding coarse openings will create a capillary barrier for lateral flow. On the other hand, a fault can displace the surrounding geologic units such that a unit with low permeability abuts one with relatively high permeability within the fault zone. In this case, the fault will act as a permeability barrier to lateral flow within the units with relatively high permeability. Montazer and Wilson (1984, p. 20) hypothesized that permeability would vary along faults, with higher permeability in the brittle, welded units and lower permeability in the nonwelded units where gouge or sealing material may be produced. While a fault sealed with gouge or other fine-grained material has much higher capillary suction (i.e., driving imbibition), it also has low permeability, retarding the movement of water.

Large lateral flow to the faults and/or focusing of infiltration near the fault zone on the ground surface are required to generate significant water flow in faults. Below the repository, low-permeability (zeolitic) layers in the CHn may channel some flow to faults that act as pathways to the water table. However, it is also possible that alteration of faulted rocks in the CHn and CFu causes the faults to be of low permeability (Figure 4-7e), slowing water movement from the TSw to the water table.

4.2.1.1.4   Fracture–Matrix Interaction

Fracture–matrix interaction refers to flow and transport between fractures and the rock matrix (CRWMS M&O 2000c, Section 3.3.4). Owing to their different hydrologic properties, distinct flow and transport behavior occurs in each hydrogeologic unit. The extent of fracture–matrix interaction is therefore a key factor in assessing flow and transport processes in the unsaturated zone (BSC 2001a, Section 4.2.1).

4.2.1.1.5   Seepage into Drifts

Potential seepage of water into waste emplacement drifts is important to the overall performance of the potential repository system. The corrosion of drip shields and waste packages, the mobilization of radioactive contaminants from breached waste packages, and the migration of radionuclides to a receptor location all depend on the distribution of water seepage into the emplacement drifts.

Seepage is defined as flow of liquid water into an underground opening, such as a waste emplacement drift or exploratory tunnel (CRWMS M&O

2000c, Section 3.9.1). Seepage does not include water vapor movement into openings or condensation of water vapor within openings. Seepage flux is the rate of seepage flow per unit area. The seepage percentage is the ratio of seepage flux to percolation flux in the surrounding host rock unit. Seepage threshold is defined as a critical percolation flux below which seepage into the opening is unlikely to occur. The seepage fraction is the proportion of waste packages that are located where drift seepage occurs. The drift shadow zone is a zone of reduced water saturation beneath the emplacement drift as a result of diversion of seepage around the drift opening by capillary forces.

Estimating seepage into underground openings excavated from an unsaturated fractured formation requires an understanding of processes on a wide range of scales (CRWMS M&O 2000c, Section 3.9.1). These scales range from the mountain-scale distribution of percolation flux, to the intermediate-scale channeling or dispersion of flow in an unsaturated fracture network, to the small-scale capillary-barrier effect, to the microscale phenomena within fractures, and specifically at the drift wall. Moreover, the thermodynamic environment in the drift (temperature, relative humidity, ventilation regime, etc.) must be considered. Figure 4-8 illustrates and summarizes seepage-related processes. The factors affecting drift seepage highlighted in Figure 4-8 are outlined below.

Capillary-Barrier Effect, Flow Diversion, and Seepage Threshold—For unsaturated conditions, the seepage flux is expected to be less than the percolation flux because the drift opening acts as a capillary barrier (Philip et al. 1989). When percolating water encounters the opening, capillary forces retain the water in the rock, preventing it from seeping into the drift. Water accumulates in the rock around the opening, and if the rock permeability is sufficient, the water flows around the drift opening. If the incident percolation flux is very high or the rock permeability is insufficient,
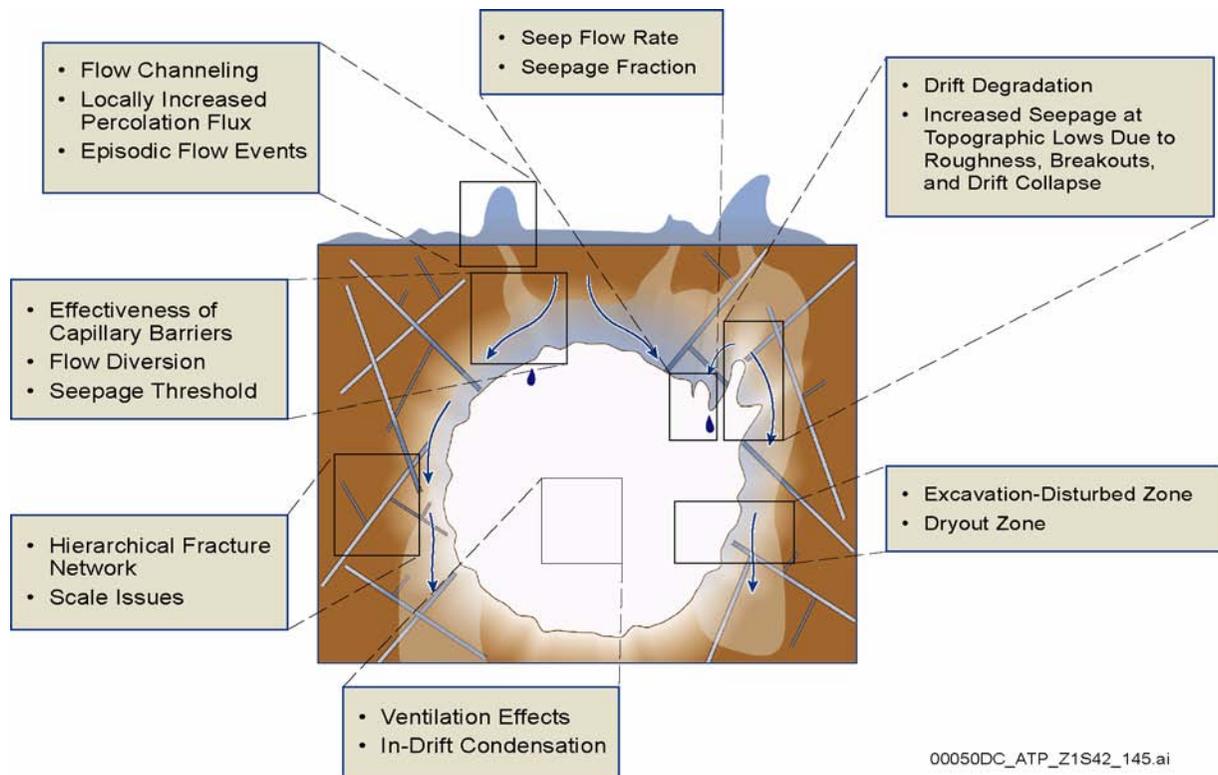
Figure 4-8. **Schematic of Phenomena and Processes Affecting Drift Seepage**
Source: Adapted from CRWMS M&O 2000c, Figures 3.9-1 and 3.9-3.

complete water saturation occurs in the rock above the opening, and seepage occurs. The effectiveness of the capillary barrier to seepage is determined by the capillarity of fractures surrounding the drift and by the permeability and connectivity of the fracture network in the horizontal direction (BSC 2001a, Section 4.2.2). Note that even if seepage occurs, the seepage flux is generally less than the percolation flux unless flow is focused by fractures or other features. The seepage threshold indicates whether or not water seeps into the opening for a given average percolation flux in the surrounding rock. Seepage threshold behavior is controlled by drift geometry, fracture geometry, capillary properties of fractures, and the hydrologic properties of the fracture network (BSC 2001a, Section 4.2.2).

Distribution of Percolation Flux, Flow Channeling, and Episodic Flow—The magnitude and spatial distribution of percolating water in the potential repository host rock is the most important factor affecting seepage. The distribution of flow channels in the fracture network and the hydrologic properties of individual flowing fractures determine how seepage occurs (CRWMS M&O 2000c, Section 3.9.1). Depending on the flow of water within an individual channel, the seepage threshold may or may not be exceeded locally. This is important because seepage is sensitive to the magnitude of the percolation flux, which is moderated by flow processes between the ground surface and the potential repository horizon. For repository thermal loading conditions, the percolation flux will include downward flow of condensed water, in addition to water that infiltrates at the ground surface.

Hierarchal Fracture Network—The characteristics of the fracture network affect seepage because they determine the spatial distribution of percolation flux and the effectiveness of the capillary barrier (CRWMS M&O 2000c, Section 3.9.1). Intermediate-scale characteristics (between mountain-scale and drift-scale) of the fracture network control the potential focusing of flux in the unsaturated zone. Heterogeneity of the fracture network affects local percolation flux and, therefore, seepage. The capillary-barrier effect depends on the connectivity of the fracture network near drift openings and the capillary properties of individual

fractures. Small fractures and microfractures, if interconnected, can decrease seepage because they have sufficient capillarity to hold water, but (unlike the rock matrix) sufficient permeability for flow diversion around the openings.

Drift Opening Geometry and Rock Surface Characteristics—The shape and size of underground openings also affects the likelihood of seepage. Partial collapse of the opening because of rockfall can affect seepage. Analytical solutions demonstrating the impact of drift geometry on seepage were developed by Philip et al. (1989). In addition, the geometry of the rock roof in drift openings and the characteristics of the rock surface control processes that could lead to dripping of seepage onto the engineered barriers below.

Ventilation, Evaporation, and Condensation—Until permanent closure of the potential repository, the emplacement drifts will be ventilated. The resulting temperature and humidity conditions in the drift will determine evaporation and condensation effects. Evaporation at the drift wall will generally decrease droplet formation and dripping (Ho 1997a) and create a dryout zone around the drift. When relative humidity in the drift is kept well below 100 percent by ventilation, seepage of liquid water will decrease, while water vapor movement into the drift will increase. Seepage flux and the moisture from increased vapor influx will be effectively removed by ventilation. After the thermal period, the relative humidity in emplacement drifts may be high enough to support condensation within the drift and engineered barrier system whose thermal properties are such that their temperature may be below the dew point. This would mostly occur after the diminution of all or most of the waste heat and the cessation of drift ventilation.

Excavation-Disturbed Zone and Dryout Zone Effects—The capillary-barrier effect that produces seepage diversion around openings occurs within a limited region around the opening (CRWMS M&O 2000c, Section 3.9.1). The extent of this zone is approximately given by the height to which water rises on account of capillarity. It is probably smaller than the zone affected by the mechanical effects of excavation; therefore, these effects may

modify seepage behavior. Thermally induced stress changes may also cause changes in fracture permeability. These stress changes are currently under investigation in field-scale thermal testing at Yucca Mountain (BSC 2001a, Section 4.3.1.5). In addition, drift ventilation and heating will produce a dryout zone with associated dissolution and precipitation of minerals (CRWMS M&O 2000c, Section 3.9.1). The consequent alteration of hydrologic properties and its extent are also under investigation (BSC 2001a, Section 4.3.5).

Design—The layout and design of the potential repository and the engineered barrier system affect the probability of seepage water contacting waste packages. Orientation of the emplacement drifts with respect to natural fracturing and in situ stress directions affects the hydrologic behavior of the fracture network around the openings and the potential for rockfall that changes the drift geometry (see Section 2.3.4.1). Thermal loading controls temperatures, the duration and extent of dryout associated with heating, and the potential for coupled mechanical and chemical processes that can impact hydrologic properties of the host rock.

4.2.1.2   Summary State of Knowledge

Site data characterizing the ambient unsaturated system at Yucca Mountain have been collected since the early 1980s (CRWMS M&O 2000c, Section 2.1). The data are of numerous types (e.g., lithology, rock hydrologic properties, mineralogy, temperature, geochemistry, climate/infiltration) collected from surface-based activities (e.g., geologic mapping, installation of vertical boreholes) as well as subsurface mapping, sampling, and in situ testing in excavated tunnels.

Data collection has focused mainly on near-surface units down to the potential repository horizon. Site characterization data gathered from surface-based studies (including vertical boreholes and mapped pavements) represent the upper hydrogeologic units (i.e., TCw, PTn, and TSw), which are more readily accessible than the deeper units (i.e., the CHn and CFu) in the unsaturated zone. Exploratory tunnels excavated within Yucca Mountain, allowing scientists to collect large amounts of many different types of data, transect those layers

above the lowest lithostratigraphic unit within which a repository would be constructed (i.e., the lower nonlithophysal unit of the TSw).

The discussion that follows summarizes the results of studies that collected many different types of data, including:

- Climate and infiltration data
- Geologic data
- Pneumatic data
- Matrix properties
- Fracture properties
- Fault properties
- Evidence for fracture flow
- Evidence for flow attenuation in the matrix
- Field observation of fracture–matrix interaction
- Mineralogic and perched water data
- Geochemical and isotopic field measurements
- Seepage data information from studies of natural analogues to Yucca Mountain.

4.2.1.2.1   Climate and Infiltration Data

The southwestern United States is characterized by dry climates with evaporation exceeding annual precipitation. The dry climates are divided into an arid (or desert) type and a semiarid (or steppe) type from annual temperature and precipitation considerations (Moran et al. 1997, pp. 438 to 443; Trewartha and Horn 1980, pp. 221 to 229). For Yucca Mountain's mean annual air temperature of approximately 17°C (63°F) (USGS 2000b, Section 6.4.2), the climate is arid if the precipitation is less than 243 mm (9.6 in.) per year and is semiarid if the precipitation is between 243 mm (9.6 in.) and 486 mm (19.1 in.) per year, based on a modified Köppen climate classification scheme (Trewartha and Horn 1980, p. 228). Seasonal variations and atmospheric conditions can be used to further modify and refine the classifications. The climate boundary definition depends on the classification scheme used and is best viewed as convenient approximation only (Trewartha and Horn 1980, p. 223).

Present day climate data have been collected in and around Yucca Mountain since 1988. The climate is

dry and arid. The average annual potential evapo-transpiration rate is approximately six times greater than the average precipitation rate (USGS 2000b, Section 6.1.4). On average over the unsaturated zone flow and transport model area, Yucca Mountain receives about 190 mm (7.5 in.) of rain and snow per year; nearly all the precipitation (above 95 percent) either runs off or is lost to evaporation (USGS 2000b, Table 6-9; CRWMS M&O 2000c, Table 3.5-2). The precipitation increases with elevation, so the higher portions of the mountain receive more precipitation than adjacent valleys. Over a larger area that includes valleys and flat lands around the Yucca Mountain model area, the average precipitation value can be lower (Hevesi et al. 1994, p. 2520, Figure 1).

Yucca Mountain is located in the rain shadow caused by the Sierra Nevada and other mountain ranges, which limits the number of storms that can generate precipitation throughout the Great Basin (USGS 2000a, Section 6.1). During the winter, regional precipitation comes from the occasional intrusion of frontal storms associated with polar fronts; during the summer, precipitation comes from the regular intrusion of hot, dry, subtropical high-pressure weather systems. Local vegetation on all but the highest mountains is limited by the poor soils and the amount of available water. The vegetation that grows there typically uses most of the available precipitation that is not removed by evaporation or runoff. Therefore, infiltration of precipitation from the surface into the underlying rock is modest and commonly associated with wet years that may be linked to El Niño cycles.

The climate study also evaluated the long-term records of analogue sites, such as calcite dating data from Devils Hole (Winograd et al. 1992) and microfossil records from Owens Lake (Forester et al. 1999, pp. 14 to 18). Geological information indicates that the regional climate has changed over the past million years and that long-term average precipitation (which reflects wetter glacial and monsoonal cycles in the past) is greater than modern conditions. Future climate scenarios use available climate data from wetter analogue sites in western states (CRWMS M&O 2000b, Section 6.4; USGS 2000a, Section 6.6.2).

Studies of past climates indicate that the climate oscillates between glacial and interglacial periods. The current climate is typical of interglacial periods, although paleoclimate records suggest that the present interglacial period is hotter and drier than some earlier interglacial periods. In contrast with the current climate, periods of more extensive glaciation have dominated the long-term climate for most of the past 500,000 years. Glacial periods characterized by wetter and colder conditions than now exist have prevailed during approximately 80 percent of that time (USGS 2000a, Section 6.2).

No glaciation has occurred in the Yucca Mountain region during these glacial periods; instead, the region has experienced climates characterized by increased rainfall and cooler temperatures (USGS 2000a). During glacial periods, winter storm activity is more common because the polar front moves far south of its average present-day position. Subtropical high-pressure systems in the summer are less frequent to nonexistent. Local vegetation receives more water from the atmosphere and average air temperatures are colder, leading to lower plant uptake rates and higher soil infiltration rates than today. The primary form of annual precipitation shifts from summer rain to winter precipitation (often snow). Wetlands are common on the valley floors, and local streams are active during all or most of the year. Large closed basins, such as Owens Valley and Death Valley, contain lakes. Although glacial climates are generally characterized by cooler temperatures and higher precipitation, particular glacial periods vary. Some are relatively warm and wet, whereas others are cold and may be either wet or dry.

In *Future Climate Analysis* (USGS 2000a, Section 6.6), three climatic states are forecast: (1) the current arid climate, (2) an interglacial monsoon climate of warm but wetter conditions, and (3) a cooler, wetter, glacial-transition climate typical of glacial conditions over much of the past several hundred thousand years. Within each of these general categories, conditions may vary from year to year and over decades and centuries. Monsoon climates would vary from climates like present-day Yucca Mountain to somewhat wetter climates like Nogales, Arizona, or Hobbs, New Mexico. Glacial-transition climates would likely range from condi-

tions like the present-day central Great Basin (in central Nevada) to cooler conditions like the climate near Spokane, Washington. None of the likely future climates for Yucca Mountain is characterized by much larger annual precipitation rates at least for times on the order of 10,000 years. However, the cooler temperatures and decreased plant uptake of water would allow more water to infiltrate into Yucca Mountain during a glacial-transition climate.

The infiltration study at Yucca Mountain was initiated in 1984. To date, the infiltration study has used nearly 100 shallow boreholes located on ridgetops, on sideslopes, on stream terraces, and in/across stream channels to measure the changes in water-content profiles in response to precipitation and snowmelt events (Flint, L.E. and Flint 1995; Flint, A.L. et al. 1996, pp. 60 to 63; USGS 2000b, Sections 6.3.4 and 7.1). Weekly or monthly measurements were collected from 1984 through 1995. Four washes were instrumented for run-on and runoff measurements. Water-balance calculations from precipitation, evapotranspiration, run-on, and runoff along washes are used to derive the infiltration flux values over the ridge top, side slopes, and stream channels. Areas with exposed bedrock and no soil cover promote greater infiltration compared to areas with soil covers that have substantial storage capacity for excess water.

Deep soils and vegetation inhibit infiltration by allowing evaporation and plant transpiration to remove water. Steep slopes encourage rapid runoff, also limiting infiltration (USGS 2000b, Section 6.1.2). For these reasons, most infiltration probably occurs in areas with low slopes and relatively shallow soil cover, as is common at the higher elevations on the northern part of Yucca Mountain. Analyses of groundwater chemistry (especially oxygen and hydrogen isotopic compositions) indicate that much of the infiltration at Yucca Mountain occurs during the winter. During the cool rainy season, evaporation rates are low because of low temperatures, and low-intensity but sustained precipitation can saturate shallow soil or cover the soil with snow. Summer storms are more intense than winter rains, but higher runoff and evaporation combine to limit summer infiltration.

The infiltration distributions for different climate states are used as upper boundary conditions for the unsaturated zone flow model and TSPA models. A numerical, water-balance, infiltration model was developed for the Yucca Mountain area, including the area of the three-dimensional, site-scale unsaturated zone flow model. The infiltration model uses physiographic and hydrologic information and a daily precipitation record to calculate daily values of infiltration using a water-balance approach. The infiltration model was calibrated first by comparison to the total water-content change in the soil profile in neutron boreholes during 1984 to 1995 and then by comparison of model-simulated streamflow to discharge measures at stream-gauging sites on Yucca Mountain during 1994 to 1995 (USGS 2000b, Section 6.8.2).

The numerical infiltration model was used to simulate lower-bound, mean, and upper-bound infiltration associated with three climate scenarios determined to be pertinent to performance of the potential repository: modern, monsoon, and glacial-transition (USGS 2000b, Section 6.9). The modern, or present-day, climate conditions are expected to prevail for about the next 400 to 600 years. Monsoon climate conditions, with wetter summers than the modern climate, are expected to prevail for the following 900 to 1,400 years. Glacial-transition climate conditions, with cooler air temperatures and higher annual precipitation than the modern climate, are expected to begin in about 2,000 years and continue throughout the remainder of the 10,000-year period specified for performance analyses.

Average precipitation and average infiltration rates over the unsaturated zone flow model area are presented in Section 4.2.1.3.3. The distributions of mean present-day, monsoon, and glacial-transition infiltration are also shown in Section 4.2.1.3.1.3 in Figure 4-25.

4.2.1.2.2   Geologic Data

Depth below ground surface to the water table ranges from approximately 500 to 800 m (1,600 to 2,600 ft) within the potential repository area. The higher-temperature repository layout has the waste emplacement drifts at a depth ranging from about

200 to 500 m (660 to 1,600 ft) below ground surface and between about 210 and 390 m (690 and 1,300 ft) above the water table. These distances were estimated using the *Site Recommendation Subsurface Layout* (BSC 2001d, Table V-1), topographic data from the *Geologic Framework Model (GFM 3.1)* (CRWMS M&O 2000bs, Section 4.1), and water table elevations (USGS 2000c, Table I-1; CRWMS M&O 2000g, Table 3).

Some of the most important site characterization data come from surface-based vertical boreholes. The first deep boreholes at Yucca Mountain were used to define site lithostratigraphy, to locate the water table, to collect core for rock-property analyses, and to test in situ borehole monitoring techniques. The lithostratigraphic description of the tuff units has been refined with coring, mapping, and geophysical logging data from additional surface-based boreholes and confirmed by data collected in the underground drifts (i.e., the Exploratory Studies Facility and Cross-Drift tunnels). Figure 4-9 illustrates the locations of selected deep boreholes, the underground Exploratory Studies Facility, and the Enhanced Characterization of the Repository Block (ECRB) Cross-Drift. A summary of the geology of Yucca Mountain is presented in Section 1.3.

The division of tuff units into members, zones, and subzones is based on variations in degree of welding (compaction and fusion at high temperatures), abundance of lithophysae (cavities formed by bubbles of volcanic gases trapped in the tuff matrix during cooling), depositional features, crystal content, mineral composition, pumice and rock fragment abundance, and fracture characteristics. These features of site lithostratigraphy are described by Moyer et al. (1996, pp. 7 to 54) and Buesch et al. (1996, pp. 4 to 16) and in the *Unsaturated Zone Flow and Transport Model Process Model Report* (CRWMS M&O 2000c, Section 3.2).

Early geologic mapping of Yucca Mountain was done by Scott and Bonk (1984) and was later updated and refined by Day, Potter et al. (1998) to include additional small faults at the land surface (such as the Sundance fault in the potential repository block) (Spengler et al. 1994, pp. 9 to 11). The fracture patterns in the bedrock were also mapped in pavement studies (i.e., with thin soil covers removed) and in shallow-pit studies of fractures exposed on the pit walls. Mapping and sampling data along transects, especially along washes and valleys, together with logs and core samples from deep boreholes and regional geophysical surveys, were used to construct early stratigraphic and structural models. Current three-dimensional geologic models rely heavily on surface-based vertical boreholes, as well as the Day, Potter et al. (1998) geologic map (CRWMS M&O 2000bs, Section 4). These geologic models are used as a framework for development of numerical models for simulating unsaturated zone flow and transport processes (CRWMS M&O 2000br).

4.2.1.2.3 Pneumatic Data

Several deep boreholes at Yucca Mountain have been instrumented in the unsaturated zone and continuously monitored to record changes in pneumatic pressure and gas flow with depth in response to changes in barometric pressure of the atmosphere (CRWMS M&O 2000b, Section 8.4.2). Changes in atmospheric pressure are transmitted very rapidly throughout the TCw because of its high fracture permeability. In contrast, the PTn significantly attenuates the atmospheric-pressure signal and imposes a time delay to signal arrival because of higher porosity and water content and much lower fracture density and bulk permeability than the TCw. In general, attenuation of the atmospheric-pressure signal across the TSw is negligible and pressure signals are transmitted nearly instantaneously throughout most of the entire vertical section of the TSw. Nearly all the pressure data from the TSw indicate that the fractures within the TSw apparently are very permeable and highly interconnected within both the lithophysal and nonlithophysal units. In situ pressure records indicate that essentially all of the remaining barometric signal is attenuated by the CHn, primarily due to low permeability and the presence of perched-water zones.

When the Exploratory Studies Facility was excavated, the effects on in situ pneumatic pressure were carefully monitored to determine how the overall gaseous-phase system in the unsaturated
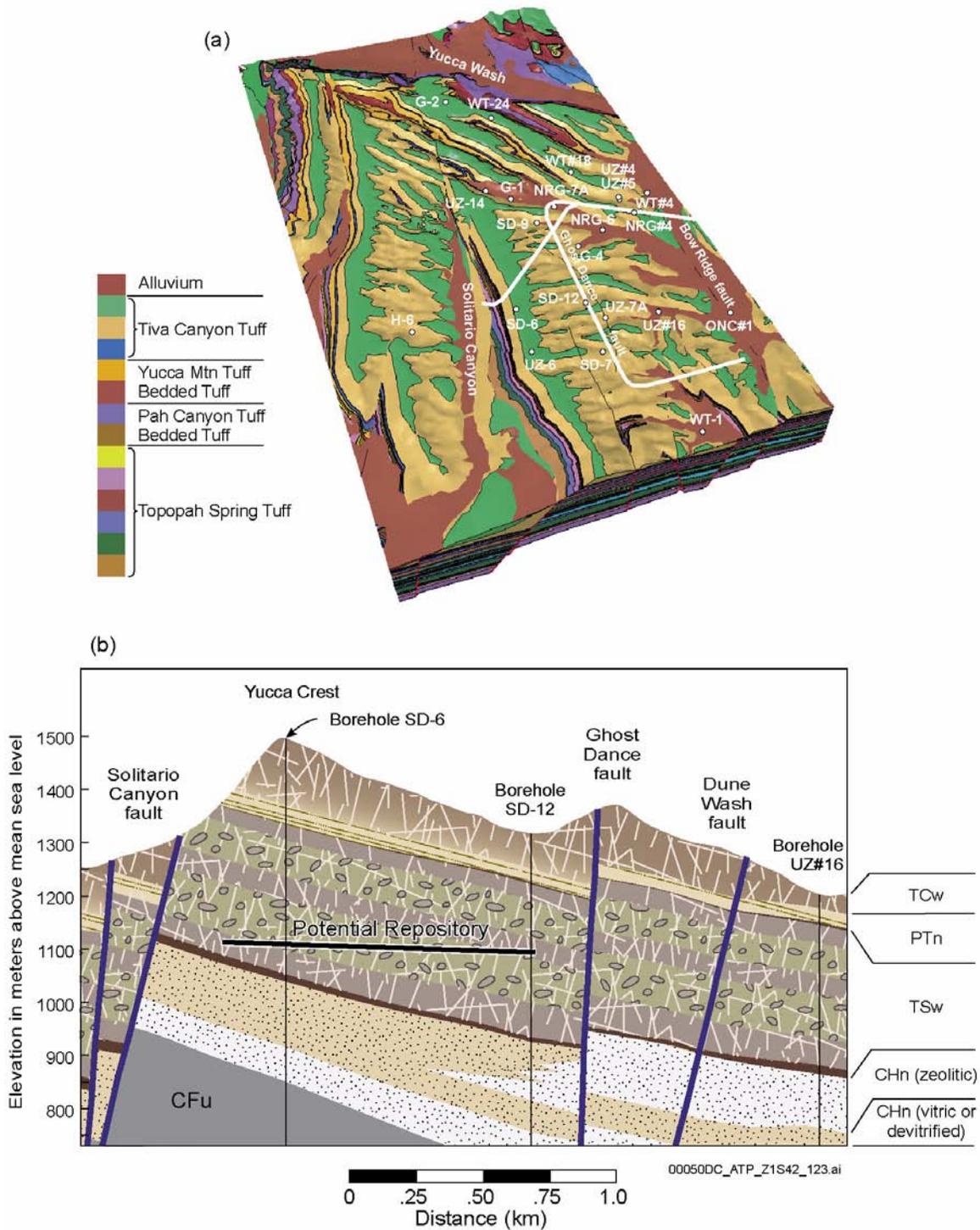
Figure 4-9.   Yucca Mountain Site-Scale Geology
(a) Three-dimensional perspective with borehole, Exploratory Studies Facility, and ECRB Cross-Drift locations.
(b) View along an east–west cross section, showing locations of boreholes SD-6, SD-12, and UZ#16. Source:
Adapted from CRWMS M&O 2000c, Figures 2.1-2 and 3.2-1.

zone was affected by direct exposure of deeply buried rock units to atmospheric pressure by way of the tunnel. Pneumatic monitoring data indicate that some faults, such as the Drill Hole Wash fault, transmit pneumatic-pressure signals over distances of several hundred meters nearly instantaneously. The data also indicate that gas-phase flow from the atmosphere into the TSw was essentially short-circuited when the Exploratory Studies Facility penetrated the PTn, locally removing this pneumatic barrier (CRWMS M&O 2000b, Section 8.4.2).

4.2.1.2.4   Matrix Properties

Rock matrix hydrogeologic properties (including porosity, bulk density, particle density, water content, saturated hydraulic conductivity, moisture retention characteristics, and saturation) have been measured for several thousand core samples recovered from 8 deep boreholes and over 30 relatively shallow boreholes. The deep boreholes penetrate to at least the bottom of the TSw, while the shallow boreholes penetrate only to the top of the TSw. Collection, processing, and preliminary analyses of the core data are described by Flint, L.E. (1998). Results show that nonwelded tuffs (i.e., PTn and CHn) usually have large matrix porosities (typically 30 to 50 percent), while the densely welded tuffs (i.e., TCw and TSw) tend to have greatly reduced pore space (generally less than 15 percent matrix porosity). Because of variations in capillary strength, liquid saturations are usually lower in the nonwelded tuffs than in the welded tuffs, unless the nonwelded tuffs contain significant amounts of clay or zeolite. Mean matrix permeability ranges from about 10^{-15} to 10^{-12} m^2 (10^{-14} to 10^{-11} ft^2) for the unaltered nonwelded tuffs and from about 10^{-18} to 10^{-15} m^2 (10^{-17} to 10^{-14} ft^2) for the welded and altered (i.e., zeolitized) nonwelded tuffs.

Numerical models of flow and transport use matrix property data to estimate effective hydrogeologic properties for each layer within the model. Upscaling of rock properties (particularly permeability) from core scale to mountain scale is required for the larger, three-dimensional numerical models. Upscaling is an adjustment to the estimate of the effective property when the property data are collected on one scale but the estimate

is intended for use in simulations and predictions on a much larger scale. Additional data from in situ water potential measurements are used to estimate moisture-retention characteristics. Collection and preliminary analysis of these data are described by Rousseau, Loskot et al. (1997, Section 4.2) and Rousseau, Kwicklis et al. (1999, pp. 143 to 151).

4.2.1.2.5   Fracture Properties

Fracture data are very important to the characterization of unsaturated flow at Yucca Mountain. Fracture hydrologic properties are estimated using (1) permeability data from in situ air-injection tests conducted in four surface-based boreholes and boreholes in alcoves of the Exploratory Studies Facility; (2) porosity data from gas tracer tests in boreholes in Alcove 5 of the Exploratory Studies Facility; and (3) fracture mapping from the Exploratory Studies Facility, ECRB Cross-Drift, and surface-based boreholes.

Air-injection testing is described by LeCain (1997, pp. 2 to 9; 1998, pp. 5 to 11) and Rousseau, Kwicklis et al. (1999, pp. 63 to 67) and in *In Situ Field Testing of Processes* (CRWMS M&O 2000bu, Section 6.1). The data show the TCw unit as having the highest mean fracture permeabilities (as high as 10^{-10} m^2 or 10^{-9} ft^2) and the CHn as having the lowest mean fracture permeabilities (on the order of 10^{-14} m^2 or 10^{-13} ft^2). Mean values of fracture permeability within PTn and TSw layers are approximately 10^{-13} and 10^{-11} m^2 (10^{-12} and 10^{-10} ft^2), respectively. As stated previously in this section, most data available is from testing at the upper hydrogeologic units. There are limited air-permeability data for units below the TSw. Air-permeability data for the CHn are available from a single sampled interval in borehole UE-25 UZ#16. This interval lies within a zeolitically altered portion of the upper CHn.

Detailed line surveys and full peripheral mapping of fracture networks have been conducted along the Exploratory Studies Facility and ECRB Cross-Drift by Barr et al. (1996, pp. 133 to 135) and Albin et al. (1997, Appendix 1) (also see data sources listed in CRWMS M&O 2000c, Attachment I, Table I-4). Additional features have been mapped, including the observations of an intensely

fractured zone in the southern part of the Exploratory Studies Facility main drift (Buesch and Spengler 1998, p. 19) and several recently discovered faults that show no surface expression in the western part of the ECRB Cross-Drift (see data sources listed in CRWMS M&O 2000c, Attachment I, Table I-4). The fracture density distributions from geologic mapping and geophysical imaging are illustrated in Figure 4-10. Nonwelded tuffs typically have few fractures (less than 1 per meter), while the densely welded tuffs generally have abundant fractures (approximately 1 to 4 per meter) (CRWMS M&O 2000bt, Section 6.1.2.3). Each lithostratigraphic unit generally has its own fracture network characteristics (fracture spacing, intensity, and connectivity) that are controlled by variations in lithology and degree of welding (Rousseau, Kwicklis et al. 1999, p. 23). Fracture characteristic data are used to estimate the potential for, and distribution and amount of, fracture flow within the welded and nonwelded layers in the unsaturated zone. It is important to reiterate that the exploratory tunnels do not penetrate units below the TSw; therefore, fracture characteristics below the TSw are available only from deep boreholes. There are limited fracture data from units below the TSw. For the CHn, vitric and zeolitic fracture frequencies are available from two boreholes (USW SD-12 and USW NRG-7a). Fracture frequencies and properties have not been determined for the CFu unit, which underlies the CHn and is present in the unsaturated zone only along the western margin and in the southwestern part of the repository area (CRWMS M&O 2000c, Section 3.2.2.5, Figure 3.2-3).

Some fracture property data were considered but not used in unsaturated zone flow modeling (CRWMS M&O 2000c, Section 3.6.3.2). In particular, fracture frequency data from the surface of the mountain, measured on outcrops and at the Large Block Test area, are not considered representative of fracture frequencies in the deep subsurface because unloading, or the absence of overburden at the surface, is likely to produce enhanced fracturing. Permeability data from air-injection testing in four Exploratory Studies Facility niches were not used because the scale on which the measurements were made was 0.3 m (1 ft); thus, the data may not be representative of the fracture perme-

ability at the scale of interest. The scale of the air-injection test data that are used for flow modeling is from 1 to 12 m (3 to 40 ft) (CRWMS M&O 2000bt, Section 6.1.1.1).

4.2.1.2.6 Fault Properties

Fault permeability measurements are described by LeCain (1998, pp. 19 to 22). Direct measurements of fault-specific properties have been conducted using air-injection tests in Exploratory Studies Facility Alcoves 2 and 6 (the Bow Ridge Fault Alcove and the North Ghost Dance Fault Access Drift, respectively). Analyses of cross-hole tests run in the Bow Ridge Fault Alcove (LeCain 1998, p. 21) and the North Ghost Dance Fault Access Drift (LeCain et al. 2000, Table 8) give estimates of fracture permeability in the TCw and TSw fault layers, respectively. These data indicate that, within the welded units, the fractures in the faults are more permeable and porous than the fractures in the formation (or nonfaulted rock).

4.2.1.2.7 Evidence for Fracture Flow

Currently, the estimates of percolation flux at Yucca Mountain range from 1 to 10 mm/yr (0.04 to 0.4 in./yr). Given the low matrix permeabilities of the welded tuffs (i.e., TCw and TSw), a large fraction of the percolation flux in the welded units must travel through fracture networks. This conceptual model is supported by the presence of relatively high fractional abundances of chlorine-36 measured in TCw samples from boreholes (CRWMS M&O 2000bv, Section 6.6.3). The source of the elevated (bomb-pulse) chlorine-36 has been attributed primarily to nuclear testing in the Pacific Ocean conducted in the 1950s, and its occurrence in the TCw indicates the presence of fast pathways for water flow within the unit (CRWMS M&O 2000bq, Section 6.1.2).

Episodic infiltration pulses are expected to move rapidly through the fracture system of the TCw unit with little attenuation by the rock matrix. This conceptual model of minimal flow attenuation by the densely welded matrix is partially supported by pneumatic data for the TCw unit (CRWMS M&O 2000bq, Section 6.1.2), which show little attenuation of the barometric signal in monitoring

(a) Drilling of Borehole SD-6 on the Crest of Yucca Mountain

(b) Pavement Cleared for Ghost Dance Fault Mapping

Objectives:
- Determine lithology and structural features of tuff units.
- Evaluate distribution of fractures and faults.

Approaches:
- Map features on bedrock, in trenches, and along Exploratory Studies Facility drifts.
- Conduct geophysical logging along boreholes.
- Deploy geophysical tomographic imaging techniques on the surface and in underground drifts.

Results:
- Refined geological maps of bedrock, washes, and faults.
- Improved geological framework of tuff layers and fault offsets.
- Detailed line surveys and full peripheral maps along drifts.
- Interpreted fracture density distributions between surface and underground drifts.
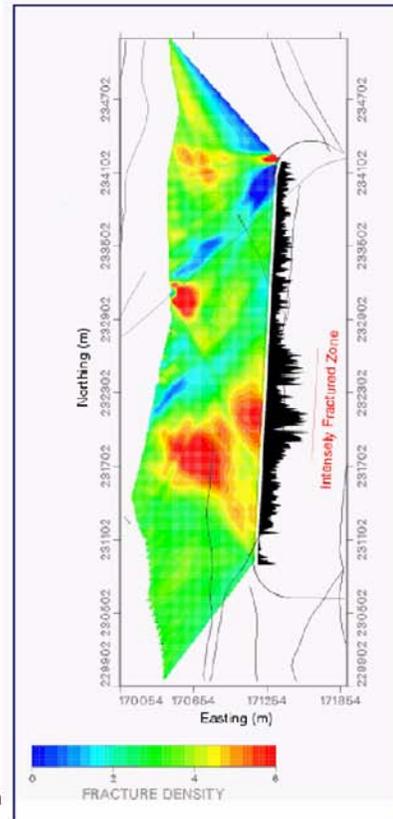
(c) Fracture Density Distributions by Detailed Line Survey and Seismic Tomograph

00050DC_ATP_Z1S42_Fig-124b.ai

Figure 4-10.   Geological and Geophysical Studies on the Surface and along the Exploratory Studies Facility
Source: CRWMS M&O 2000c, Figure 2.2-1.

boreholes relative to the barometric signal observed at the land surface (Rousseau, Kwicklis et al. 1999, p. 89).

Other evidence for fracture flow comes from calcite-coating data, which are signatures of water flow history and indicate that most of the deposition is found within the fractures in the welded units (Paces, Neymark, Marshall et al. 1998, p. 37). As discussed in *Conceptual and Numerical Models for UZ Flow and Transport* (CRWMS M&O 2000bq, Section 6.1.2), carbon-14 ages of the perched water bodies below the TSw unit also suggest fracture-dominant flow within the TSw. These ages range from approximately 3,500 to 11,000 years (Yang, Rattray et al. 1996, p. 34), which is much younger than if the major path for water flow within the TSw was through the matrix (CRWMS M&O 2000bq, Section 6.1.2).

Field testing within Exploratory Studies Facility alcoves and niches also supports prevailing fracture flow within welded units. Figure 4-11, for example, summarizes the results of liquid release testing in Alcove 6, located within the fractured, densely welded, middle nonlithophysal unit of the TSw.

4.2.1.2.8   Evidence for Flow Attenuation in the Matrix

Liquid release tests conducted in Alcove 4 of the Exploratory Studies Facility, situated in nonwelded tuffs of the lower PTn, support the matrix flow-damping conceptual model of the PTn (CRWMS M&O 2000bu, Section 6.7). The Alcove 4 test bed includes a small fault within which tracer-tagged water was released, as illustrated in Figure 4-12. A mass-balance approach involving recovery of outflow in a slot was adopted. The matrix of the PTn effectively damped flow pulses along the fault. The data in Figure 4-12 show a slow decline in water intake rates with time. One explanation for the slow decline is the possible swelling of clays in the PTn layers and subsequent reduction of fault permeability. Another observation made during liquid release testing was that, with sequential wetting, detection of downgradient increases in saturation occurred faster (i.e., the wetting front moved faster with each liquid release test).

Geochemical data from the Exploratory Studies Facility also support the conceptual model of predominantly matrix flow through the PTn by showing a lack of widespread, elevated (bomb-pulse) chlorine-36 signatures at the base of the PTn (Fabryka-Martin, Wolfsberg, Levy et al. 1998).

4.2.1.2.9   Fracture–Matrix Interaction

Field observations show limited fracture–matrix interaction within welded units at Yucca Mountain. The chloride concentration data indicate that perched water is recharged mainly from fracture water, with a small degree of interaction with matrix water (CRWMS M&O 2000bq, Section 6.1.3). The small degree of interaction between fractures and the matrix at locations associated with geologic features is also suggested by the presence of bomb-pulse chlorine-36 (CRWMS M&O 2000bv, Section 6.6.3) at the potential repository level in the Exploratory Studies Facility. Studies by Ho (1997b, pp. 407 and 409) show that the match between simulations and observed matrix saturation data is improved by reducing the fracture–matrix interaction significantly.

The concept of limited fracture–matrix interaction in welded tuff at the Yucca Mountain site is also supported by many other independent laboratory tests, as well as theoretical and numerical studies (CRWMS M&O 2000bq, Section 6.1.3). In a number of laboratory experiments without considering matrix imbibition, Glass et al. (1996, pp. 6 and 7) and Nicholl et al. (1994) demonstrated that gravity-driven fingering flow is a common flow mechanism in individual fractures. This can reduce the wetted area in a single fracture to fractions as low as 0.01 to 0.001 of the total fracture area (Glass et al. 1996, pp. 6 and 7), although the matrix imbibition can increase wetted areas of fingering flow patterns in individual fractures (Abdel-Salam and Chrysikopoulos 1996, pp. 1537 to 1538). A theoretical study by Wang and Narasimhan (1993, pp. 329 to 335) indicated that the wetted area in a fracture under unsaturated flow conditions is generally smaller than the geometric interface area between fractures and the matrix, even in the absence of fingering flow. This results from the consideration that liquid water in an unsaturated fracture occurs as saturated segments that cover

(a) Photograph of Alcove 6 Test Bed

(c) Schematic of Liquid Release Test

(b) Closeup of Trays on the Slot

Objectives:
- Quantify fracture–matrix interaction and the fraction of fracture flow.

Approaches:
- Use a slot below boreholes to capture fracture flows.
- Estimate the fracture–matrix flow partioning by mass balance.
- Use borehole sensors to detect wetting front arrivals.

Results:
- A maximum of 80% of injected water was recovered for high-rate injection tests (i.e., 80% fracture flow).
- Out flows occurred in step increments which could be related to water stored in fracture flow paths.

(d) Water Collected in the Slot

00050DC_ATP_Z1S42_Fig-128.ai

Figure 4-11.   Fracture–Matrix Interaction Test at Alcove 6
Sources: CRWMS M&O 2000c, Figure 2.2-6; CRWMS M&O 2000bu, Section 6.6.

(a) Photograph of Alcove 4 Test Bed

(b) Closeup of Tray on the Left-Hand Side of the Slot

(c) Schematic of Boreholes at Alcove 4

(d) Water Intake Rate at PTn Fault
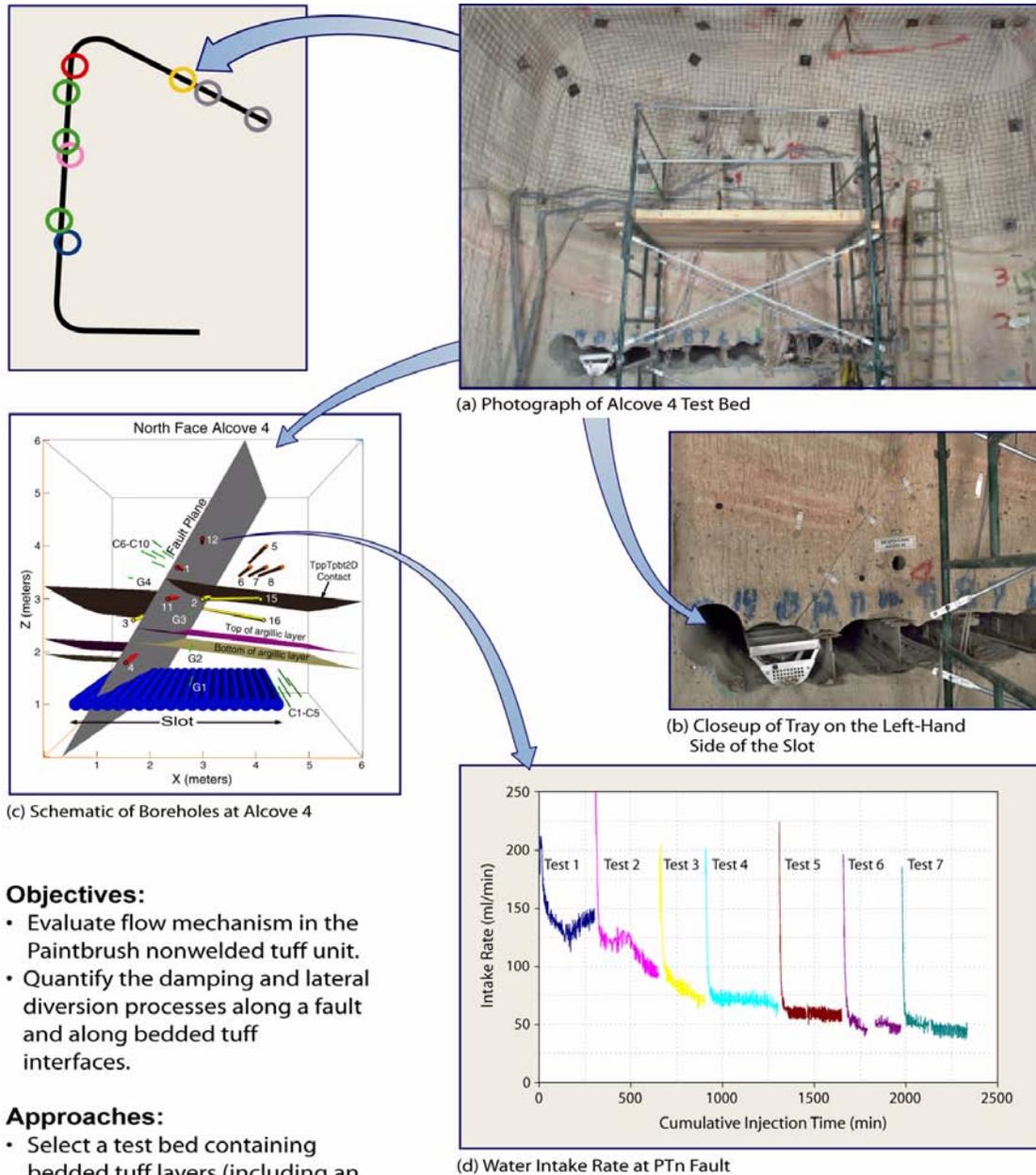
Objectives:
- Evaluate flow mechanism in the Paintbrush nonwelded tuff unit.
- Quantify the damping and lateral diversion processes along a fault and along bedded tuff interfaces.

Approaches:
- Select a test bed containing bedded tuff layers (including an argillic layer), a fault, and a fracture.
- Release water under constant-head conditions to determine the intake rates.
- Monitor wetting front arrivals and measure potential changes in boreholes.

Results:
- Water intake rate in the fault decreased as more water was introduced into the release zone.
- Clay swelling is one mechanism proposed to interpret the field data.
- Detection of downgradient increases in saturation occurred over shorter time intervals with each liquid release test.

00050DC_ATP_Z1S42_126a.ai

Figure 4-12.   Paintbrush Fault and Porous Matrix Test at Alcove 4
Sources: CRWMS M&O 2000c, Figure 2.2-7; CRWMS M&O 2000bu, Section 6.7.

only a portion of the fracture–matrix interface area. Liu et al. (1998, p. 2645) suggested that in unsaturated, fractured rocks, fingering flow occurs at both a single fracture scale and a connected fracture-network scale, which is supported by the field observations from the Rainier Mesa site (see Section 4.2.1.2.13) and by a numerical study of Kwicklis and Healy (1993). They found that a large portion of the connected fracture network played no role in conducting the flow. Studies have also shown that fracture coatings can either reduce or increase the extent of fracture–matrix interaction. Thoma et al. (1992) performed experiments on coated and uncoated tuff fractures and observed that the low-permeability coatings inhibited matrix imbibition considerably. In contrast, fracture coatings may in some cases increase the fracture–matrix interaction when microfractures develop in the coatings (Sharp et al. 1996, p. 1331).

4.2.1.2.10 Mineralogic and Perched Water Data

The spatial distributions of vitric and zeolitic material within the CHn, along with the characterization of the basal vitrophyre (Tptpv3) of the TSw, are important for understanding the distribution of perched water and for determining potential flow paths for radionuclides.

Perched water has been encountered in a number of boreholes (e.g., USW UZ-14, USW NRG-7a, USW SD-7, USW SD-9, USW SD-12, and USW G-2) at the base of the TSw and above units of zeolitic tuff within the CHn (CRWMS M&O 2000bw, Sections 6.2.1 and 6.2.2).

The spatial distribution of low-permeability zeolites has been modeled using mineralogic and petrologic data from several boreholes and is presented in the Integrated Site Model (ISM3.1) of Yucca Mountain (CRWMS M&O 2000i, Section 3.4). Figure 4-13 shows the modeled distribution of zeolites for layers within the lower TSw (Tptpv3 and Tptpv2) and the upper CHn (Tptpv1 through Tcpuv). Areas with less than or equal to 3 percent zeolite by weight are considered vitric, or unaltered. The figure shows that zeolites within the CHn are prevalent in the northern and eastern portion of the model domain. The areal extent of

the vitric region diminishes with depth and is considered to be largely confined to the fault block bounded in the north and east by the Sundance and Ghost Dance faults, respectively, and in the west by the Solitario Canyon fault. The northern half of the potential repository area is underlain by predominantly zeolitic CHn, while the southern half is underlain by the predominantly vitric upper portion of the CHn. However, below the vitric CHn (yet occurring above the water table) are nonwelded portions of the Prow Pass, Bullfrog, and Tram tuffs that are pervasively altered to zeolites. Thus, there is no evidence to support a model that includes a direct vertical pathway from the potential repository horizon to the water table that does not intersect zeolitic units, except, perhaps, within fault zones.

4.2.1.2.11 Geochemical and Isotopic Field Measurements

Samples have been collected in boreholes and along the Exploratory Studies Facility for geochemical and isotopic measurements. Pore water is obtained by physical extraction from samples of tuff and used for chemical analyses and age dating. Measurements of total dissolved solids and chloride concentration in pore waters are mainly available for nonwelded tuff samples, which generally yield sufficient amounts of water by compression for chemical analyses (Yang, Yu et al. 1998, pp. 6 to 7). These pore waters tend to be more concentrated in dissolved solids than water flowing in fractures, which indicate that the percolation flux in the rock matrix is limited.

Chemical composition, including the total dissolved carbon dioxide concentration, is measured in pore water samples to determine the origin of calcite and amorphous silica solids found in the unsaturated zone and to characterize the evolution of carbonate as waters percolated downward. Ion-exchange reactions along flow paths generally increase the abundance of cations like calcium and strontium with depth in the tuff units. Deviation from the general trend of geochemical evolution with depth provides information about the effects of faults and other structural features. Strontium participates in ion-exchange with zeolites, and concentrations can be significantly
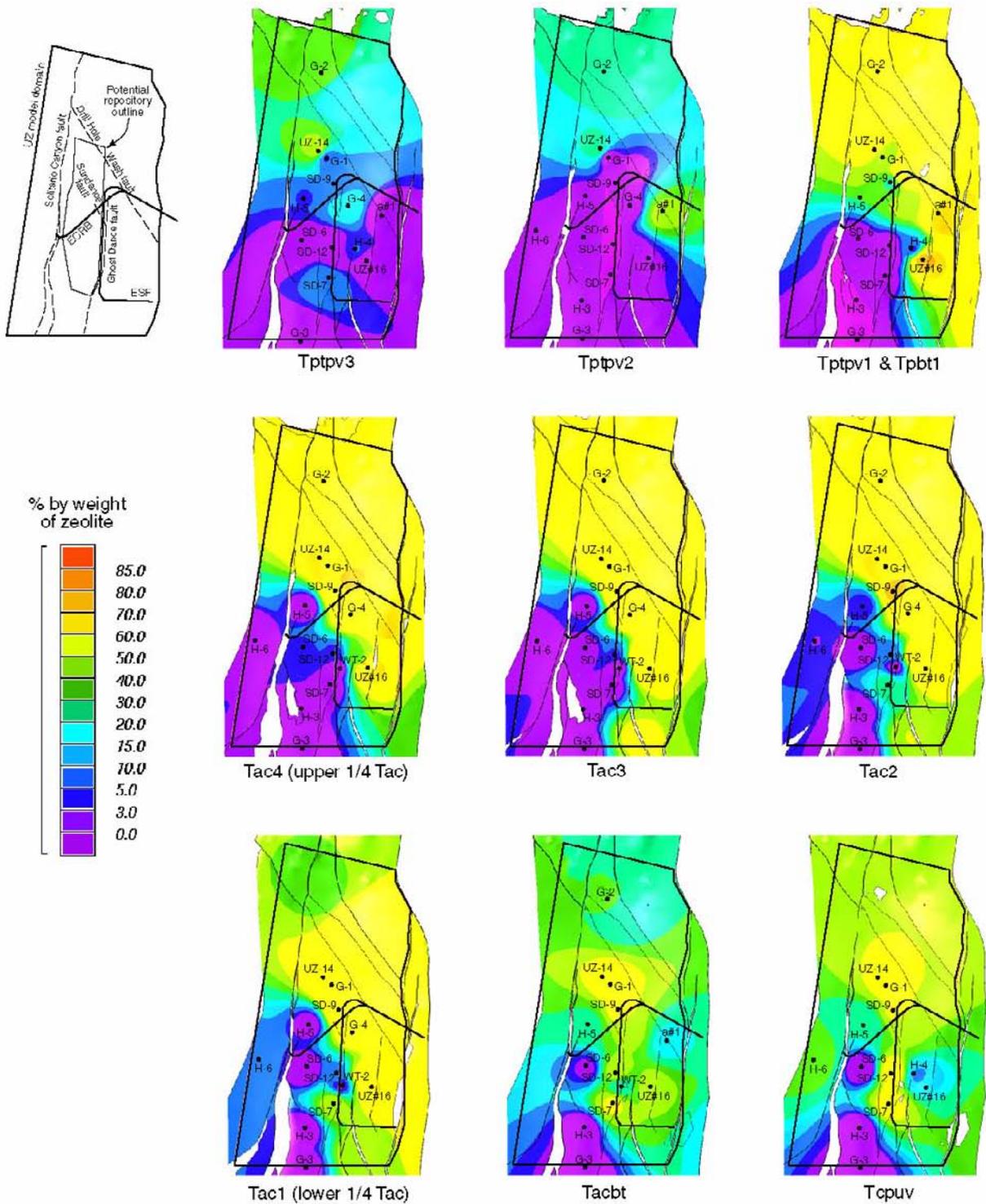
Figure 4-13. Distribution of Zeolites in Certain Layers below the Potential Repository Horizon
Areas of less than or equal to 3 percent zeolite are considered vitric, or unaltered. Source: CRWMS M&O 2000c, Figure 3.2-7.

depleted in the zeolitically altered CHn unit, signifying effectiveness of hydrogeochemical processes (Sonnenthal and Bodvarsson 1999, pp. 143 to 147). The calcite and opal deposits found on fracture surfaces (Paces, Neymark, Marshall et al. 1998) and within lithophysal cavities (CRWMS M&O 2000bv, Section 6.10.1.1; CRWMS M&O 2000c, Section 3.9.7.1) are analyzed to evaluate flow in fractures and seepage into cavities over millions of years. Figure 4-14 shows examples of geochemical studies of tuff samples.

Environmental isotope data are used to infer the presence of fast flows from the ground surface through the unsaturated zone. Elevated chlorine-36 isotopic ratios well above background levels are related to global fallout from thermonuclear tests conducted in the Pacific Ocean within the last 50 years. The presence of such elevated concentrations (referred to as "bomb-pulse") of chlorine-36 in the unsaturated zone therefore suggests transport from the ground surface in 50 years or less. The bomb-pulse chlorine-36 signals, first observed in surface-based boreholes and later in the Exploratory Studies Facility at faults and other features, have received much attention and continue to be analyzed (Fabryka-Martin, Wightman et al. 1993; Fabryka-Martin, Wolfsberg, Dixon et al. 1996, Section 5.3; CRWMS M&O 2000bv, Section 6.6.3).

Other environmental isotopes have also been analyzed (CRWMS M&O 2000c, Section 3.8.1). Bomb-pulse tritium concentrations are present at depth in several locations and are associated with pathways for liquid and gas flow. The carbon-14 apparent age of the gas phase in the unsaturated zone increases with depth in borehole USW UZ-1, with less obvious trends in other boreholes. Deuterium and oxygen-18 data reflect climatic conditions at the time of groundwater recharge. Based on the analysis of these two isotopes, pore water in the CHn unit is inferred to have originated either during winter precipitation or during a time of colder climate. Perched water appears to be up to 11,000 years old, based on apparent carbon-14 and chlorine-36 ages. The perched water does not appear to have equilibrated with matrix water, based on major constituent concentrations and uranium isotope data (Paces, Ludwig et al. 1998;

CRWMS M&O 2000bv, Section 6.6). Figure 4-15 illustrates examples of isotopic studies of tuff samples.

4.2.1.2.12   Seepage Data

Diversion of flow around underground openings in the potential repository host rock units at Yucca Mountain has been investigated through a series of tests conducted in "niche" openings constructed off the exploratory tunnels. More detailed descriptions of these tests and the associated modeling are provided in supporting documentation (Wang, Trautz et al. 1999; CRWMS M&O 2000bu, Section 6.2; CRWMS M&O 2000c, Sections 2.2.2 and 3.9).

Four niches were excavated along the Exploratory Studies Facility main drift to test drift seepage processes. The seepage tests were motivated by the observed absence of continuous seepage in the Exploratory Studies Facility drifts following their excavation. For each niche test, pretest characterization of the rock was performed and the openings were excavated using a boom-cutter excavating machine (Figure 4-16). The use of water during excavation was controlled so that it did not spread into the rock above the openings. Seepage into the niche openings was monitored while pulses of water were infused at very low injection pressure into the rock above. Staining dyes were used to monitor the presence of seepage and the extent of seepage water movement within fractures and openings.

Pre- and Post-Excavation Permeability Distribution—Air-injection tests were performed in horizontal boreholes drilled at niches, and air-permeability values were determined before and after excavations (CRWMS M&O 2000bu, Section 6.1). The average excavation-induced increases in permeability are in the range of one to two orders of magnitude (i.e., increases by factors of ten to a hundred). The permeability enhancements could be interpreted as the opening of preexisting fractures induced by stress releases associated with niche excavation (Wang and Elsworth 1999; Bidaux and Tsang 1991). A geostatistical analysis of these postexcavation air permeabilities provided a measure of statistical variability and spatial corre-
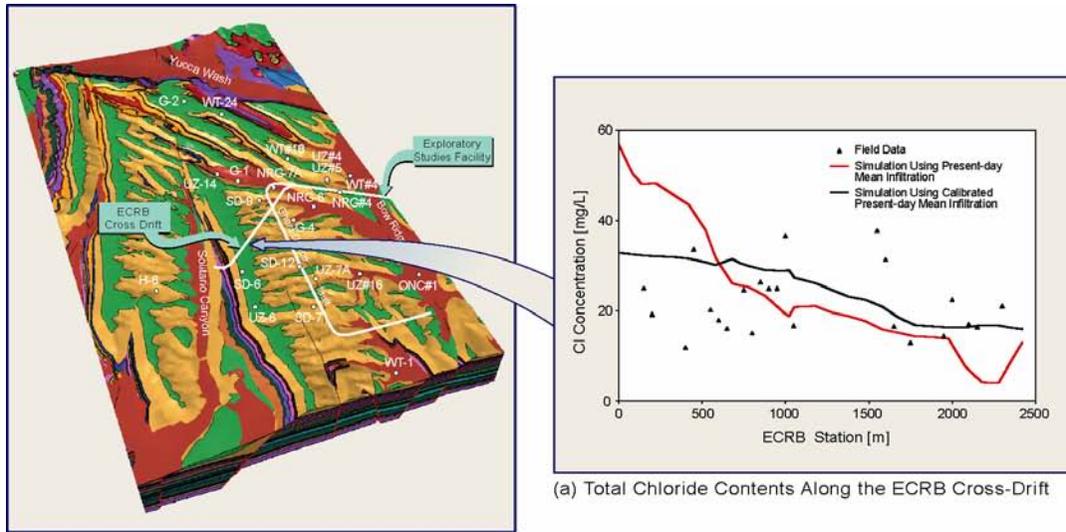
(a) Total Chloride Contents Along the ECRB Cross-Drift

Objectives:
- Provide data to define geochemical evolution of water in the unsaturated zone.
- Provide data to estimate percolation flux at depth.

Approaches:
- Collect gas and perched water samples by pumping.
- Extract pore water by compression, ultracentrifuge, or vacuum distillation.
- Determine major ion concentrations by chemical analyses.

Results:
- Total dissolved solid and chloride are used to estimate infiltration rates and percolation fluxes.
- Pore waters are related to soil-zone processes: evapotranspiration, dissolution, and precipation of pedogenic calcite and amorphous silica.
- Deep pore waters are used to evaluate restricted water—rock interactions and significant lateral movement within Calico Hills unit.
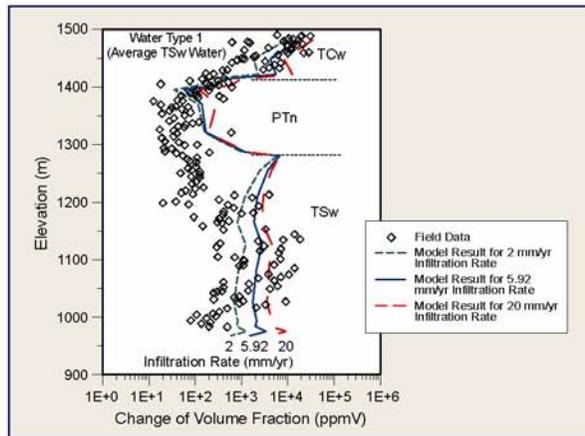
(b) Calcite Distributions Used for Infiltration and Percolation Evaluations
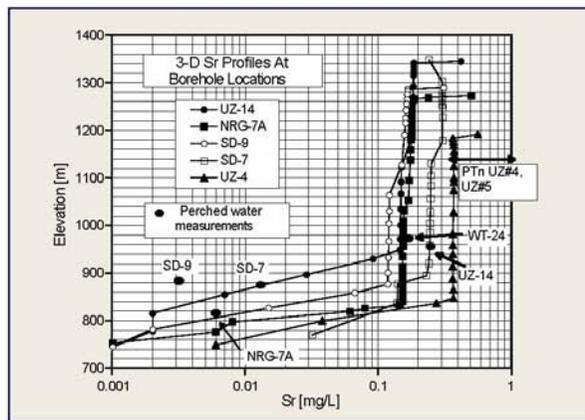
(c) Strontium Profiles Used for Zeolite Quantification

00050DC_ATP_Z1S42_140a.ai

Figure 4-14. Geochemical Studies of Tuff Samples
Sources: CRWMS M&O 2000c, Figure 2.2-10; CRWMS M&O 2000bw, Section 6.5; Sonnenthal and Bodvarsson 1999, p. 146.
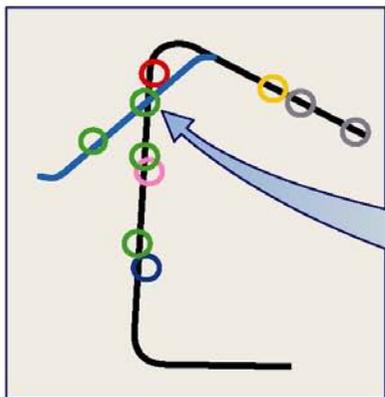
(a) Photograph of a Fracture with Calcite Infill

(b) Ages of Opal Indicate Long Term Flow in Fractures

(c) Perched Water Ages Determined by ^{14}C and ^{36}Cl/Cl Data

00050DC_ATP_Z1S42_141b.ai

Objectives:

- Provide isotopic data to define age evolution of water in the unsaturated zone.
- Provide data to delineate flow paths over geological time scales.

Approaches:

- Leach salts from unsaturated zone cores or cutting for ^{36}Cl and Sr isotopic analyses.
- Extract water for tritium, hydrogen and oxygen stable isotopes, and carbon isotopic analyses.
- Digest mineral samples for analyses of Sr isotope ratios and of U series nuclides.

Results:

- Bomb-pulse ^{36}Cl/Cl signals are present in the vicinity of some fault zones in the Exploratory Studies Facility
- Detectable levels of tritium are present in ~6% of pore water samples.
- Bomb-pulse ^{36}Cl/Cl and tritium signals are not present in perched waters.
- Age of perched waters, mixing between fast and slow flows, climate of recharge are estimated by carbon and stable isotope analyses.
- ^{234}U/^{238}U activity ratios indicate recharge through fractures and minimal exchange between pore water and fracture water.

Figure 4-15.   Isotopic Studies of Tuff Samples
pmc = percent modern carbon. Sources: CRWMS M&O 2000c, Figure 2.2-11; CRWMS M&O 2000bv, Section 6.6.
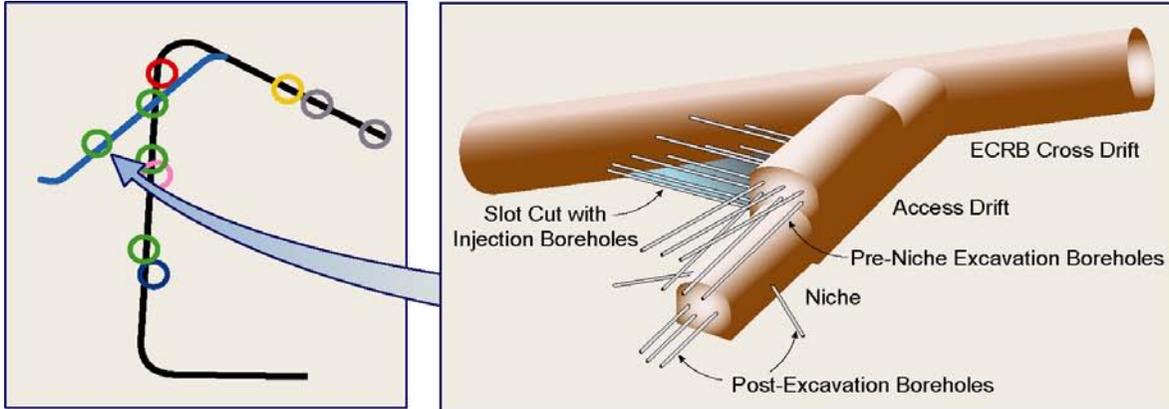
(a) Schematic of Niche 3

Objectives:

- Quantify seepage into drift in the lower lithophysal unit at a cavity-rich zone.
- Characterize the pneumatic and liquid flows in the presence of lithophysal cavities and porous tuff.
- Determine the differences between lower lithophysal unit and middle nonlithophysal unit of the potential repository rock.
- Quantify fracture—matrix interaction at lower lithophysal unit.

Approaches:

- Observe flow paths during dry excavation, use air-injection tests to characterize liquid release intervals, and conduct drift seepage tests with liquid releases at different rates.
- Adopt, improve, and extend the methodologies used in tests conducted in the middle nonlithophysal niches and test beds.

Results:

- Pre-excavation air-injection test results suggest that lower lithophysal unit has higher permeability than middle nonlithophysal unit.
- Access drift has been excavated with an Alpine Miner.
- Seepage tests are prepared to be conducted after niche excavations.

00050DC_ATP_Z1S42_151c.ai

(b) Alpine Miner Excavating the Access Drift
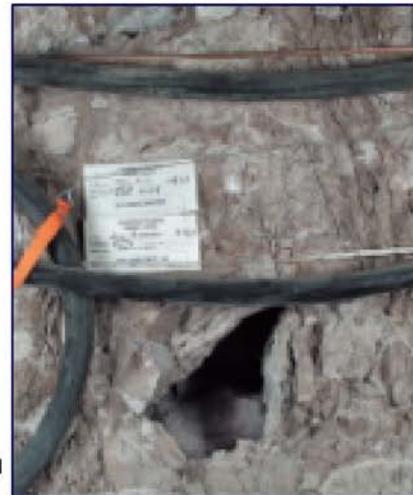
(c) Example of a Cavity in the Lower Lithophysal Tuff Unit

(d) Scanner Image along Borehole AK-1 at Niche 5

Figure 4-16.   Lower Lithophysal Seepage Test at Cross-Drift Niche 5
Source: Adapted from CRWMS M&O 2000c, Figure 2.2-5.

lation. The air-permeability field at Niche 2 (located at Station 36+50) was found to be largely random, with fairly weak spatial correlation.

Seepage Threshold Tests—A series of short-duration liquid release tests was performed at Niche 2 (Wang, Trautz et al. 1999; CRWMS M&O 2000bu, Section 6.2). Any water that migrated from the injection boreholes and dripped into the niche opening was captured and weighed. The seepage percentage, defined as the mass of water that dripped into the capture system divided by the total mass of water injected, was used to quantify seepage into the drift from a localized water source of known duration and flow rate. The seepage threshold was estimated for each location from a series of injection tests with decreasing flow rates, continuing until no seepage occurred.

Dye tracers were injected as pulses designed to represent repeated, episodic percolation events, as illustrated in Figure 4-17, for the seepage tests at Niche 2. Seepage flow paths indicated by dye tracers were used to observe wetting-front movement through the fractures. Seepage threshold data and wetting-front movement data were used to estimate the unsaturated hydrologic properties for the fractures (Wang, Trautz et al. 1999; CRWMS M&O 2000bu, Section 6.2).

Drift seepage tests were also conducted at Niche 3 (located at Station 31+07), near the crossover point between the Exploratory Studies Facility Main Drift and the ECRB Cross-Drift, and at Niche 4 (located at Station 47+88), which is in an intensely fractured zone. All the niche studies were conducted behind bulkheads to isolate them from ventilation, so that high-humidity conditions were maintained.

Flow Path Associated with Fault—In the excavation of Niche 1 (located at Station 35+66) in the vicinity of the Sundance fault (Figure 4-18a), a damp feature was observed, as illustrated in Figure 4-18b (Wang, Trautz et al. 1999, pp. 331 to 332). The feature was nearly vertical and approximately 0.3 m (1 ft) wide by over 3 m (10 ft) long. It dried out before the bulkhead could be installed to prevent contact by ventilation air. Full rewetting of this feature was not observed after more than

2 years of observation with the bulkhead closed. Figure 4-18c shows that the Sundance fault is one of several faults and features with bomb-pulse signals detected from chlorine-36 isotopic measurements along the Exploratory Studies Facility, as discussed previously.

Moisture Monitoring—Ventilation needed for underground operations and construction activities may explain the lack of observed seepage in the exploratory tunnels. Ventilation can remove a large amount of moisture, producing a dryout zone around the openings, thereby suppressing seepage. Ventilation would be used during repository operations to remove heat during thermal periods (CRWMS M&O 2000c, Section 2.2.2.2.1). To further investigate seepage processes without the influence of ventilation, two additional bulkhead sealing studies are ongoing. The first is at Alcove 7 in an over 100-m (330-ft) long drift segment that intersects the Ghost Dance fault. The second is at the furthest extent of the ECRB Cross-Drift, in an over 1,000-m (3,300-ft) long drift segment that intersects the Solitario Canyon fault. Both studies use double bulkheads for isolation from ventilation effects. To date, no continuous seeps have been observed in either of these two drift segments (CRWMS M&O 2000c, Section 2.2.2). Results will be documented following the completion of the tests. There have, however, been as yet undocumented reports of observations of the effects of liquid water, including organic growths, in the closed section. The closed sections were selected based on inferences from the unsaturated zone models of areas most likely to show seepage under ambient conditions. The lack of observable seepage could be due to incomplete rewetting of the rock following the period of ventilation. The observed effects of liquid water could be due to processes other than seepage. Condensation related to the effects of heat sources or leakage of moist air through fractured rock around the bulkheads could also lead to these effects. Studies to address this issue are continuing, and results will be documented following the completion of these studies.

4.2.1.2.13 Natural Analogues

Natural and man-made analogues with geological or archaeological records can be used to support
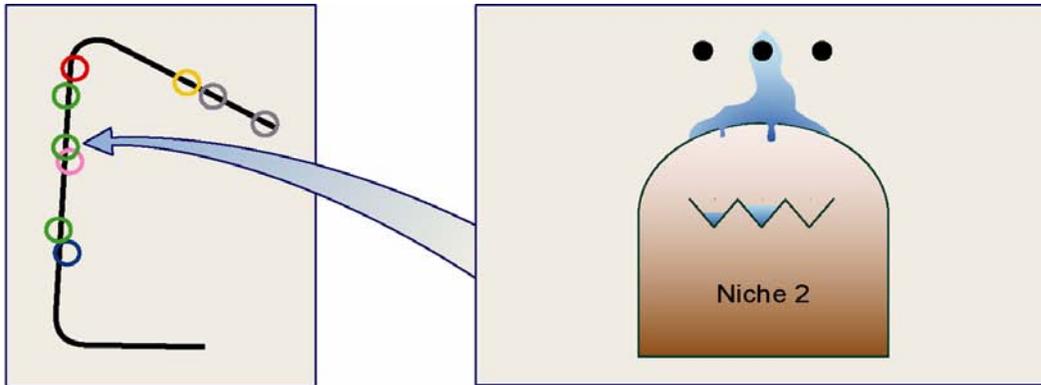
(a) Schematic of Niche 2 in the Exploratory Studies Facility

Objectives:
- Quantify seepage threshold below which no seepage occurs.
- Evaluate capillary barrier mechanism and measure drift-scale parameters.

Approaches:
- Use air injection tests to characterize the niche site with resolution of 0.3-m scale (one tenth of drift dimensions).
- Use pulse releases to represent episodic percolation events.
- Determine seepage thresholds by sequences of liquid releases with reducing rates.
- Derive in situ fracture characteristic curves with wetting front arrival analyses.

Results:
- Measured seepage threshold ranges from 200 mm/yr to 136,000 mm/yr at localized release intervals.
- Six out of sixteen tested intervals did not seep.
- Observed both flow along high-angle fractures and flow through fracture network.
- Derived fracture capillary parameters and characteristic curves, with equivalent fracture porosity as high as 2.4%.

(b) Water Collection During a Drift Seepage Test

FD&C Blue Number 1 Pre-excavation

Pyranine Post-excavation

FD&C Red Number 40
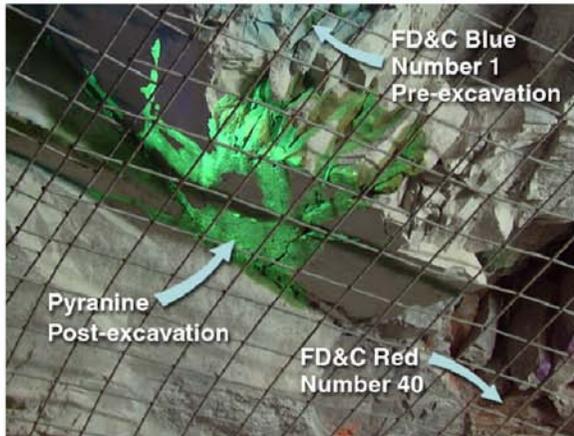
(c) Flow Paths Indicated by Dye Tracers on Niche Ceiling

00050DC_ATP_Z1S42_148b.ai

Figure 4-17.   Drift Seepage Test at Niche 2
Sources: CRWMS M&O 2000c, Figure 2.2-3; CRWMS M&O 2000bu, Section 6.2.

(a) Schematic of Sealed Niche 1 in the Exploratory Studies Facility

Objectives:

- Characterize the hydrologic setting of a site with bomb-pulse ^{36}Cl signals, the Sundance fault and its first cooling joint.
- Quantify seepage processes.

Approaches:

- Mine the niche without spreading water to the ceiling during excavation.
- Close the bulkhead to prevent moisture removal by ventilation.
- Monitor the rock and drift over long time periods.

Results:

- One damp feature observed after dry excavation at end of the niche. It dried up before bulkhead installation and did not rewet after long-term monitoring over two years.

00050DC_ATP_Z1S42_149a.ai

(b) Photograph of a Damp Feature in the Brecciated Zone at the Back of Niche 1

(c) Distribution of $^{36}Cl/Cl$ in the Exploratory Studies Facility

Figure 4-18.   Damp Feature Observed during Dry Excavation of Niche 1 and Bomb-Pulse Chlorine-36 Isotopic Signals along the Exploratory Studies Facility

ESF = Exploratory Studies Facility. Sources: CRWMS M&O 2000c, Figure 2.2-4; Wang, Trautz et al. 1999, pp. 331 to 332; CRWMS M&O 2000bv, Section 6.6.

long-term predictions of future performance of a repository at Yucca Mountain. Short-term field experiments cannot predict long-term performance, but many examples from the geologic record can be used qualitatively to evaluate aspects of repository performance for tens of thousands of years or more. The Yucca Mountain Site Characterization Project has used analogue studies for testing conceptual models and evaluating coupled processes as both quantitative and qualitative tools. An analogue relates a process or set of properties to a similar process or set of properties, either in another place or another time. Natural and man-made analogues offer direct comparisons for some of the actual long-term processes and functions of a repository. The confidence in the safe emplacement of nuclear wastes in the unsaturated zone may be greatly enhanced with natural analogue studies to supplement field testing and modeling (CRWMS M&O 2000bp; CRWMS M&O 2000b, Section 13; Stuckless 2000). Figure 4-19 illustrates examples of analogue sites for unsaturated flow, transport, and seepage process evaluations.

Climate and Infiltration—A set of natural analogues related to climate and infiltration is listed in Table 4-5. The current climate and paleo-climate records of several sites in the southwestern and western United States were used to derive the climate and infiltration fluxes for future periods. Infiltration at Yucca Mountain under wetter conditions cannot be measured directly, but infiltration under wetter conditions at a geologically similar location can be measured, and the results can be used quantitatively. Monsoonal climates have been studied at Nogales, Arizona, and Hobbs, New Mexico. Beowawe, Nevada currently has a climate

similar to that expected at Yucca Mountain during a glacial-transition period (USGS 2000a, Section 6.6.2).

Future climates can be modeled based on determinations of past climates because climates worldwide have been cyclical for the past 2 million years and are expected to remain cyclical in response to astronomical cycles. There is a calcite deposit at Devils Hole, Nevada, that has been precipitated continuously for the last 500,000 years (Winograd et al. 1992). Minute changes in the composition of this calcite provide an accurate record of the climate in southern Nevada for that time. In a similar fashion, sedimentary deposits at Owens Lake, California (Forester et al. 1999) provide a nearly 425,000-year record of past climates in the region (USGS 2000a, Section 6.5.1). These two records can be used to model likely future climates at Yucca Mountain.

Unsaturated Flow and Fracture–Matrix Interaction—The series of natural analogues for unsaturated flow and seepage processes is listed in Table 4-6. The conceptual and numerical modeling methodologies for the unsaturated zone at Yucca Mountain are applicable to other sites, including Rainier Mesa, Apache Leap, Box Canyon, and other arid and semiarid sites where there is fractured rock. The Peña Blanca site evaluation of uranium migration and the Box Canyon, Idaho, infiltration test modeling are two examples of analogue studies presented in *Natural Analogs for the Unsaturated Zone* (CRWMS M&O 2000bp). Field sampling of borehole cores, evaluation of migration from veins, and assessment of seepage into mine adits was conducted at the Nopal I mine

Table 4-5. Natural Analogues for Climate and Infiltration Process Evaluation

Analogue	Data and/or Process
Devils Hole, Nevada	Paleoclimate, calcite deposit (Winograd et al. 1992)
Beowawe, Nevada	Climate-glacial-transition period lower bound analogue (USGS 2000a)
Spokane, Rosalia, and St. John, Washington	Climate-glacial-transition period upper bound analogue (USGS 2000a)
Nogales, Arizona	Climate-monsoon period upper bound analogue (USGS 2000a)
Owens Lake, California	Paleoclimate (Forester et al. 1999)
Hobbs, New Mexico	Climate-monsoon period upper bound analogue (USGS 2000a)

Source: Adapted from CRWMS M&O 2000c, Table 2.3-1.

Objectives:
- Enhance understanding of unsaturated zone flow and transport processes.
- Demonstrate the feasibility of long-term waste isolation in underground drifts.

Approaches:
- Evaluate analogue site information and review available data.
- Apply methodologies used at Yucca Mountain to selected analogue sites for comparison.

Examples:

(a) Rainier Mesa, Nevada Test Site
- Nuclear testing tunnel complex within similar tuff units in semiarid climate.
- No seepage in dry drifts in nonwelded Paintbrush tuff and heterogeneous seeps along drifts in and below perched water bodies.

(b) Peña Blanca, Mexico
- Uranium deposits and mine galleries in arid climate.
- Radionuclide migration over only a few meters and along a few major fractures under oxidizing conditions.

(c) Box Canyon, Idaho
- Fractured basalt with heterogeneous flow structures exposed on canyon wall.
- Infiltration tests analyzed with the same modeling approach used at Yucca Mountain.

00050DC_ATP_Z1S42_179b.ai

(d) Altamira, Spain
- 14,000-year-old iron oxide and charcoal painting on the ceiling with no apparent water damage.
- <1% of 400 mm/yr infiltration seeps into a limestone/mudstone cave 7 m below surface.

(e) Chauvet Cave, France
- Over 32,000-year-old charcoal painting in large caves (>5 m wide) in subhumid region.
- Evidence of the process of water flow down the wall over otherwise well-preserved painting.

(f) Underground City of Kaymakli, Turkey
- Eight levels of ancient (second to eleventh centuries A.D.) habitation in partially welded, rhyolite ash-flow tuff.
- No evidence yet observed of active seeps and minerals deposited by seeps.

Figure 4-19.   Analogue Studies for Unsaturated Zone Flow, Transport, and Seepage

Table 4-6. Natural Analogues for Unsaturated Flow and Seepage Process Evaluation

Analogue	Data and/or Process
Rainier Mesa, Nevada Test Site, Nevada	Seepage into drifts, discrete fractures, percolation, perched water (Thordarson 1965; Russell et al. 1987; Wang, Cook et al. 1993)
Caves and rock shelters, Nevada Test Site and vicinity	Packrat midden preservation (Spaulding 1985)
Archaeological finds: preservation of cave arts in France and Germany; preserved seeds and Dead Sea scrolls in Israel; wood, textiles, and plants in Peruvian cave; mummies in Chilean pits; manuscripts in Gobi desert; Chinese cave temples, etc.	Demonstrating the efficacy of an unsaturated environment in isolating nuclear wastes (Winograd 1986)
Caves, western North America	Biotic remains preservation (Davis 1990)
Apache Leap, Arizona	Seepage into drifts, discrete fractures, transient flow (Bassett et al. 1997)
Mitchell Caverns, California	Infiltration, dripping water deposits (CRWMS M&O 2000b, Section 13.4.2.2.3)
Idaho National Engineering and Environmental Laboratory, Box Canyon, Idaho	Seepage, discrete fractures, transient flow, colloid-facilitated transport (Faybishenko et al. 1998; CRWMS M&O 2000bp)
Negev Desert, Israel	Infiltration (Nativ et al. 1995)
Cappadocia, Turkey	Drift stability and insulation (Aydan et al. 1999)
Altamira, Spain	Cave seepage (Villar et al. 1985)
Chauvet, Cosquer, and Lascaux, France	Cave painting preservation (Stuckless 2000)
Angola	Rock shelter painting preservation (Stuckless 2000)

Source: Adapted from CRWMS M&O 2000c, Table 2.3-1.

at Peña Blanca, Mexico (Figure 4-19b). For the Box Canyon site, the modeling approach used in the unsaturated zone model for Yucca Mountain is used to interpret ponded-infiltration results through fractured rock (Figure 4-19c).

The calculated rate and amount of radionuclides that could be transported away from a repository is, in part, dependent upon the interaction between fracture flow and pore water in the matrix. The amount of naturally occurring fracture water at Yucca Mountain has been too small to allow direct observations of these important processes. However, Rainier Mesa (Figure 4-19a), located about 40 km (25 mi) northeast of Yucca Mountain, is also composed of alternating welded and nonwelded tuffs, and both pore and fracture water can be collected due to the higher moisture content. With the matrix close to saturation at Rainier Mesa, there should be limited fracture–matrix interaction. Thordarson (1965, pp. 6, 7, and 75 to 80) noted that typically only portions of fractures carried water, and that the chemical composition of water obtained from fractures was substantially different from that of water samples extracted from the nearby rock matrix at that site, which supports the concept of limited fracture–matrix interaction

under conditions of near saturation. Further support for this concept can be found at a field site in the Negev Desert, Israel, where man-made tracers were observed to migrate with velocities of several meters per year across a 20- to 60-m (66- to 200-ft) thick unsaturated zone of fractured chalk (Nativ et al. 1995). Such high velocities could only occur for conditions of limited fracture–matrix interaction.

Seepage—Hydrologic models indicate that much of the water moving through the unsaturated zone will preferentially move around openings such as waste emplacement drifts. This modeling result is supported by the natural preservation of paintings, artifacts, and other remains in caves, man-made openings, and rock shelters (Stuckless 2000). Well known examples of this phenomenon include the Paleolithic caves of France and Spain, which contain paintings as old as 30,000 years in an environment 3 to 4 times wetter than that of Yucca Mountain. Figure 4-19e shows a painting made with charcoal from Chauvet cave in southern France that has been dated by the carbon-14 method to be approximately 32,000 years old (Stuckless 2000, p. 4). In addition to the remarkable preservation of these fragile paintings, the

figure shows a common phenomenon for seepage in underground openings: much of the seepage flows down the walls. Current models do not take credit for seepage that would be diverted around waste canisters by this mechanism, and the models are, therefore, conservative in their estimates of the effects of seepage.

Spirit Cave, about 75 miles east of Reno, Nevada, is another example of a natural analogue to a repository. In this cave, several small burial pits were discovered. In one of these pits was found an almost completely intact human body, mummified by the dryness of the climate. Subsequent analyses, including carbon-14 testing, have shown the body to be that of a 45- to 55-year-old male who died around 9,400 years ago. His scalp was complete with a small tuft of hair. He wore a breechcloth of fiber and was wrapped in mats woven of fibers from tule leaves, all highly preserved (Barker et al. 2000).

Spirit Cave Man is not alone in being preserved by the dry air that circulates in the caves and rock shelters of the desert Southwest. Among other preserved biologic remains are numerous packrat middens. These middens consist of twigs, fecal droppings, and other debris cemented together by dried urine. Some of the packrat middens analyzed have been preserved for over 50,000 years (Stuckless 2000, pp. 2 to 4).

Elsewhere, in the western United States, caves and rock shelters have preserved fragile biologic remains for tens of thousands of years (Spaulding 1985; Davis 1990). These examples of natural preservation, plus archaeological artifact preservation (Winograd 1986; Stuckless 2000), support the results of mathematical models that predict waste isolation at Yucca Mountain over similar time periods. In addition to flow and transport data and geological records from analogue sites, archaeological records can be more comprehensible to the public than hydrologic-geochemical data and mathematical-numerical models. Paintings and tools preserved in caves, man-made openings and rock shelters (partial openings), structure integrity of underground dwellings (Figure 4-19f), and artifacts found in underground chambers can be used to demonstrate the possibility of preserving man-

made materials surrounded by dry air over geological time scales.

Man-made structures include the subterranean tombs of Egypt that are 3 to 4 thousand years old and contain perfectly preserved wood, fabric, and murals. Although this example is from a drier climate than that of Southern Nevada, similar preservations of murals carved into volcanic rock as much as 2,200 years ago can be found in Buddhist temples carved into volcanic rock in India. In this area of India, the climate is monsoonal, with over four times as much precipitation in just four months as occurs annually in the Yucca Mountain region (Stuckless 2000, p. 19).

A particularly well-studied analogue is the paleolithic cave near Altamira, Spain, which is located in the unsaturated zone of a fractured limestone formation that contains clay-rich layers (Villar et al. 1985). Annual precipitation at this site is approximately six times greater than at Yucca Mountain. Nevertheless, seepage rates into the caves are observed to be a small fraction—about 1 percent—of the calculated percolation flux (Stuckless 2000, p. 6). Also, there is virtually no fluctuation in the observed seepage rate despite monthly changes in the amount of precipitation, even though the unsaturated zone is only about 7 m (23 ft) thick (CRWMS M&O 2000c, Section 3.9.7.3), which supports the hydrologic modeling prediction of the buffering effect of the unsaturated zone.

Seepage was also measured in the tunnels at Rainier Mesa. Most of the tunnels excavated for nuclear testing are in a sequence of zeolitized and fractured tunnel bed units within or below perched water zones. When intersected by tunnels or boreholes, a fraction of fractures and faults yielded significant amounts of water, with the total discharge from one tunnel complex equal to 8 percent of the measured precipitation (320 mm or 12.6 in. per year) (Russell et al. 1987; Wang, Cook et al. 1993). In a tunnel excavated above the perched water bodies in the Paintbrush nonwelded unit, no measurable seepage was observed. While this analogue is not ideal because of the near-saturation of the tuffs and because most of the tunnel penetrations are through the lower nonwelded

zeolitic tuff with perched water bodies, it provides a conservative example because of the high precipitation relative to that at Yucca Mountain. The potential waste emplacement drifts would be located in welded tuff above the perched water bodies.

4.2.1.3 Process Model Development and Integration

4.2.1.3.1 Unsaturated Zone Flow Model

The unsaturated zone flow model simulates present and future hydrologic conditions between the ground surface and the water table (CRWMS M&O 2000c, Section 3.7). The flow model integrates site characterization data into a single, calibrated three-dimensional model. It captures infiltration at the ground surface and estimates the distribution of percolating water in the unsaturated zone. It quantifies the movement of water through fractures and through the porous tuff matrix at the site. The model includes the occurrence of perched water, which has implications for lateral diversion of flow along interfaces between rock layers. The flow model incorporates the damping of infiltration pulses from the surface as water percolates downward through the rock layers and also includes the effects of faults on water movement.

The unsaturated zone flow model is a tool used to (1) quantify the movement of moisture as liquid and vapor through the unsaturated zone for present-day and future climate scenarios; (2) develop hydrologic properties and other model inputs for predicting seepage into drifts and radionuclide transport; and (3) provide the scientific basis for representing unsaturated zone flow processes in TSPA. Output from the unsaturated zone flow model that is used by other models consists primarily of infiltration and percolation flux distributions and hydrologic properties for hydrogeologic units and fault zones. The flow model supports these outputs with extensive analysis and interpretation of the flow regime, perched-water occurrence, and chemical and isotopic data from the site.

Input to the flow model includes Yucca Mountain geologic and rock properties data in addition to site characterization data from surface hydrology investigations, borehole testing, field tests performed underground in exploratory tunnels, geochemical sampling, and isotopic sampling of the unsaturated zone. These inputs are among the input data represented in Figure 4-20. Section 3.7.2 of *Unsaturated Zone Flow and Transport Model Process Model Report* (CRWMS M&O 2000c) describes the development of the component models shown in the figure based on site characterization data. Modeling changes associated with such issues as ventilation and transportation in the drift shadow, thermally coupled processes, with a change of the proposed repository footprint for analysis of a lower-temperature operating mode case are discussed in Volume 1, Section 11.3.4 of *FY01 Supplemental Science and Performance Analyses* (BSC 2001a). Output from the flow model directly feeds the assessments of drift seepage, thermal-hydrology, and radionuclide transport, which ultimately support the TSPA.

4.2.1.3.1.1 Modeling Assumptions

Numerous methods exist for mathematically representing the unsaturated flow processes occurring at Yucca Mountain. These representations range from the relatively simple to the extremely complex. The existing site characterization data for Yucca Mountain suggest that flow between the land surface and the water table is complex. Even though large amounts of site characterization data exist for certain areas of the mountain, for other areas information is based on natural analogues and other sources. Therefore, any mathematical representation of the unsaturated zone at Yucca Mountain must avoid any unjustified complexity, as well as oversimplifications of the flow behavior beneath the mountain.

Mathematical representations of complex, actual phenomena will always require some simplification. Assumptions are made, with justification provided to lend confidence to the model. Some of the important assumptions made in the development of the unsaturated zone flow model of Yucca Mountain are summarized below.

Selection of Continuum Models—Estimates of the number of potentially water-conducting frac-
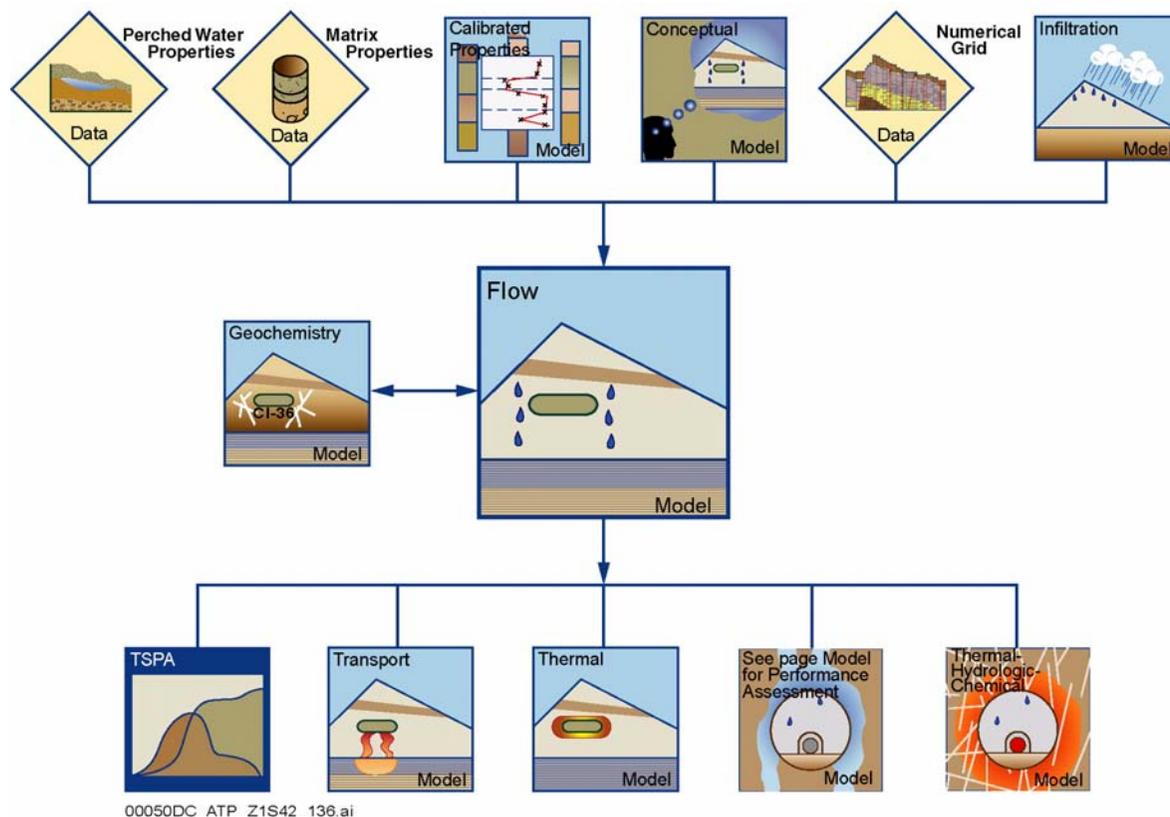
Figure 4-20.   Schematic of the Major Input Data to the Unsaturated Zone Flow Model and Models that Use Its Output
Source: CRWMS M&O 2000c, Figure 3.7-5.

tures at Yucca Mountain are on the order of one billion (Doughty 1999, p. 77). It is not feasible to model discrete fractures at this scale, so a continuum modeling approach is used. This is justified by considering two important aspects of flow and transport behavior that are expected to occur in the unsaturated zone. The first, as further discussed in this section, is that where fast flow occurs, it will do so along a few flow pathways that carry relatively small amounts of water. There are numerous slower flow paths dispersed throughout the unsaturated zone, so the continuum model is a reasonable choice for simulating flow and trans-port. The second aspect is the coexistence of matrix-dominated flow in nonwelded units and fracture-dominated flow in welded units. This is readily accommodated by continuum models but not by other approaches, such as fracture-network modeling. Because continuum models are rela-tively simple and straightforward to implement,

they are preferred for most practical applications (National Research Council 1996b, p. 331).

Dual-Permeability Models—Flow processes in fractured rock have been studied intensively. In order to make continuum models represent observed flow behavior more accurately, dual-permeability models have been developed that represent the rock matrix and the fracture network by different continua. The two continua are coupled together to represent flow interaction between the fractures and the rock matrix (National Research Council 1996b, p. 380). Darcy's law is used to represent flow in each continuum. The van Genuchten model (van Genuchten 1980), which is widely used to relate capillary pressure and satura-tion in porous media, is employed for both the fracture and matrix continua. Fracture flow in unsaturated media is believed to occur only in a subset of all fractures (called active fractures),

depending on the flux of water moving through the fracture network. For such media, the active fracture model describes the relationship between fracture saturation and the flow interaction between the fracture and matrix continua (Liu et al. 1998; CRWMS M&O 2000bq, Section 6.4.5).

Using the dual-permeability approach, one-, two-, and three-dimensional numerical grids of the unsaturated zone were developed. Figure 4-21 illustrates the flow of information associated with the gridding process, summarizing key input and output. Hydrogeologic data, mainly from the Integrated Site Model (ISM3.1) of Yucca Mountain (CRWMS M&O 2000i), are used to develop numerical grids of the unsaturated zone mountain-scale domain. These grids include layering of hydrogeologic rock units, faults, and different types of rock where the geology is laterally heterogeneous. Fracture properties (CRWMS M&O 2000br, Table 5) are used to formulate the dual-permeability grids. Figure 4-22 illustrates the structural and stratigraphic framework established in the numerical grids of the unsaturated zone domain.

Fracture–Matrix Interaction—An active fracture model was developed by Liu et al. (1998) to account for the portion of fracture surfaces interacting with the matrix. Limited fracture–matrix interaction occurs for a variety of reasons, such as fingering flow (gravity-dominated, nonequilibrium, flow channeling within fractures) and fracture surface coatings. The active fracture model is documented in *Conceptual and Numerical Models for UZ Flow and Transport* (CRWMS M&O 2000bq, Section 6.4.5). In the model, only a portion of connected fractures are considered to actively conduct liquid water at a fracture network scale.

Transient Versus Steady-State Flow—Temporal variation in the infiltration rate drives the time-dependent or transient nature of flow in the unsaturated zone. The temporal variation of infiltration may be short-term due to weather fluctuations that drive episodic flow or occur over much longer time periods corresponding to climate change. As discussed previously, the PTn is believed to greatly attenuate episodic infiltration pulses such that

water flow below the PTn is approximately steady. However, water flow in a relatively small area near the Solitario Canyon fault may be transient because the PTn is not present in that area. Some transience is also expected for liquid flow through isolated fast flow paths that cut through the PTn because of the lack of a significant attenuation mechanism. However, these isolated flow paths are believed to carry only a small amount of water because (1) inferred bomb-pulse chlorine-36 isotopic ratios have been found in only a few locations in the Exploratory Studies Facility; (2) no significant correlation between high matrix saturation and elevated chlorine-36 isotopic ratios has been reported; (3) these discrete fast paths are not associated with large catchment areas involving large volumes of infiltrating water; (4) bomb-pulse signatures of chlorine-36 were not found in the perched water bodies (CRWMS M&O 2000bv, Section 6.6.3); and (5) post-bomb tritium was detected only in one sample from the perched water (in Borehole NRG-7a) but not in any of the other samples (CRWMS M&O 2000bv, Section 6.6.2).

The PTn is expected to damp episodic flow in the unsaturated zone resulting from the temporally occasional nature of storms in the site area and the local nature and wide scattering of storm tracks. Individual locations may receive significant rainfall only once in several years, even in the case of focused runoff along arroyos. Geomorphic character, such as conditions of soil cover and slope, further contribute to the variability of infiltration from storms. Larger-scale variation in infiltration is the result of altitude, which controls seasonal rainfall quantity by influencing storm frequency. In general, the northernmost part of the site area is highest, the central part is intermediate in elevation, and the southern part is lowest. The site-scale pattern of infiltration magnitude as well as that of percolation flux at the proposed repository level reflects the site altitude (Figure 4-23). The percolation flux patterns in the unsaturated zone below the PTn (Figure 4-24) do not reflect differences in infiltration magnitude resulting from local storm tracks or surface conditions in regions of the site that are about at equal altitude because of the damping influence of the PTn.
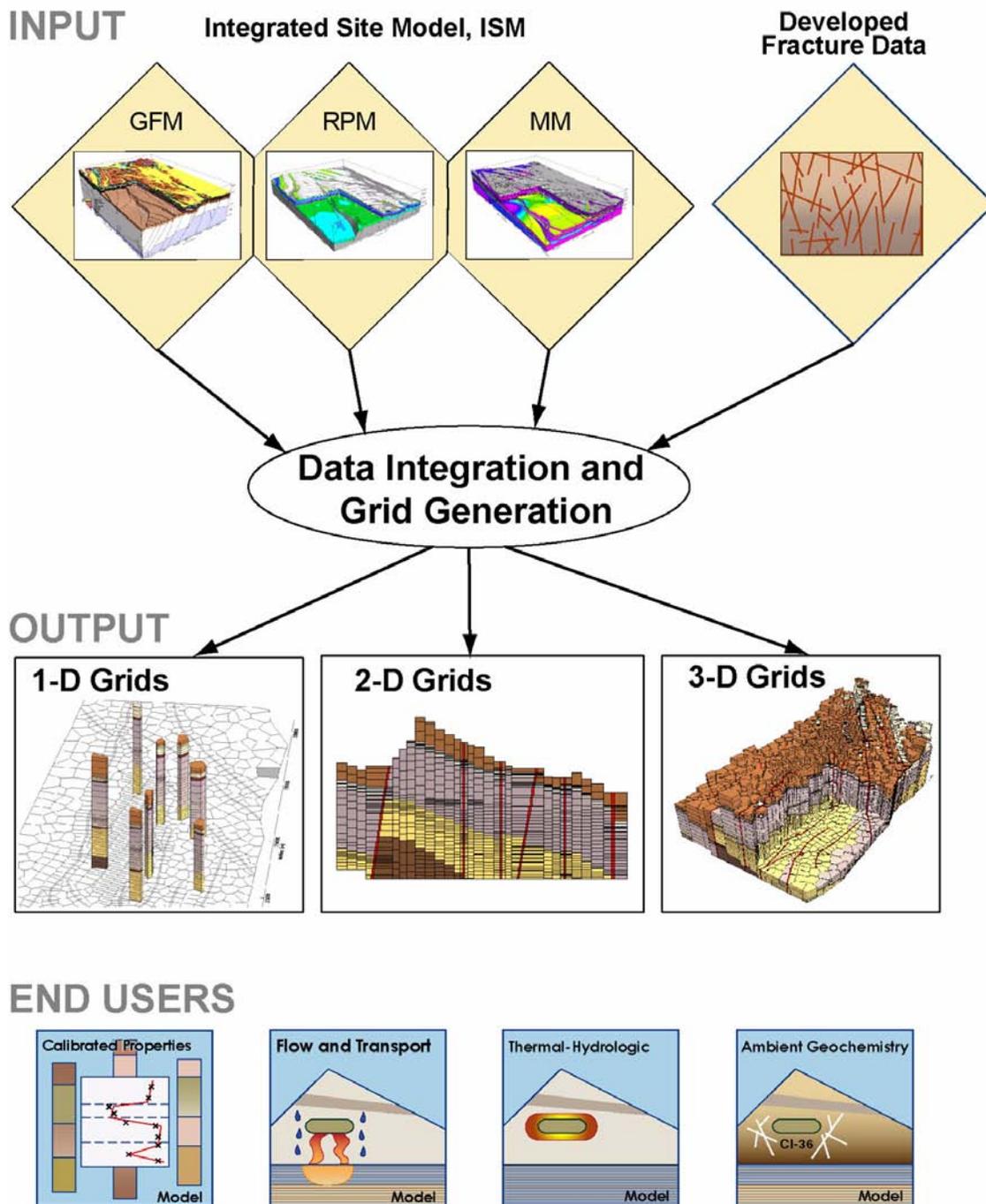
00050DC_ATP_Z1S42_Fig-129.ai

Figure 4-21. Flow Diagram Showing Key Input Data Used in Numerical Grid Development, the Types of Grids Generated, and the End Users

GFM = geologic framework model; RPM = rock properties model; MM = mineralogic model. Source: CRWMS M&O 2000c, Figure 3.4-2.
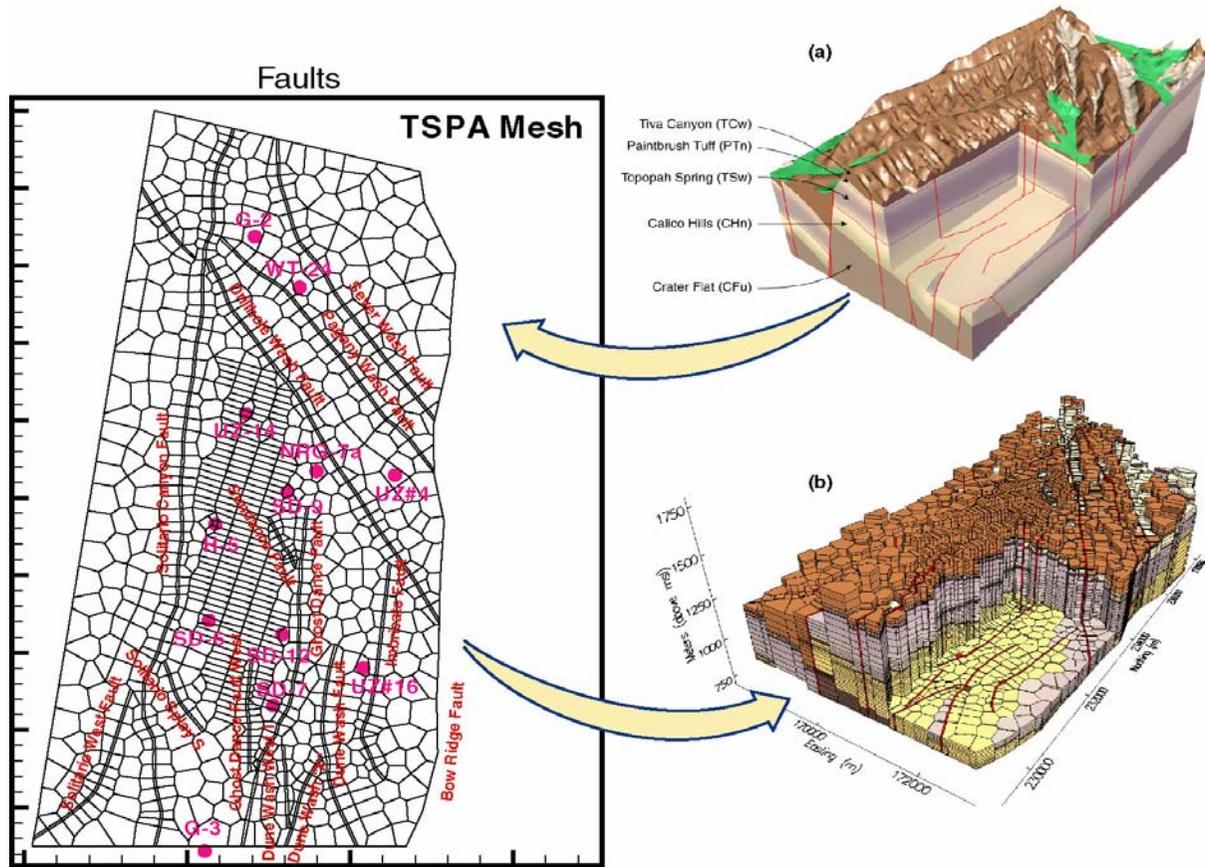
Figure 4-22. Perspective View of the Unsaturated Zone Model Domain of Yucca Mountain, Showing Hydrogeologic Units, Layers, and Major Faults
(a) Geologic model. (b) Numerical grid. Source: CRWMS M&O 2000c, Figure 3.7-2.

Percolation flux in the unsaturated zone is expected to be episodic on the scale of seconds, minutes, hours, or days. Percolation is periodic flow especially in unsaturated, interconnected fracture systems because water must accumulate to gravitationally overcome capillary and frictional resistance to flow at tight asperities. The rate of episodic pulses of water movement in such a system is regulated by the overall flux rate, by evaporation, and by imbibition of water flowing in the fractures by the matrix, which together limit the storage necessary to push flow episodes. The volume and period of episodic flow events, therefore, is limited by ambient conditions. No large, long-period episodic flow surge has been observed at Yucca Mountain (BSC 2001a, Section 4.3.5.6.2). Geologic evidence at Yucca Mountain (Whelan,

Roedder, and Paces 2001), based on the distribution of secondary minerals deposited in the unsaturated zone, clearly supports a flow regime in which most flow is film flow and void spaces along fracture networks are never filled. Such a flow environment is not conducive to larger-scale, long-period episodic flow. Episodic flow severe enough to impact seepage fractions into drifts and transport rates from the repository to the saturated zone has been proposed as a tentative alternative conceptual model based only on numerical simulation of thermally influenced flux (BSC 2001a, Section 4.2.2). The existence of episodic flow of sufficient magnitude to cause such impact in the nonthermal ambient environment in the unsaturated zone remains very improbable (BSC 2001a, Section 4.3.5.6.2).
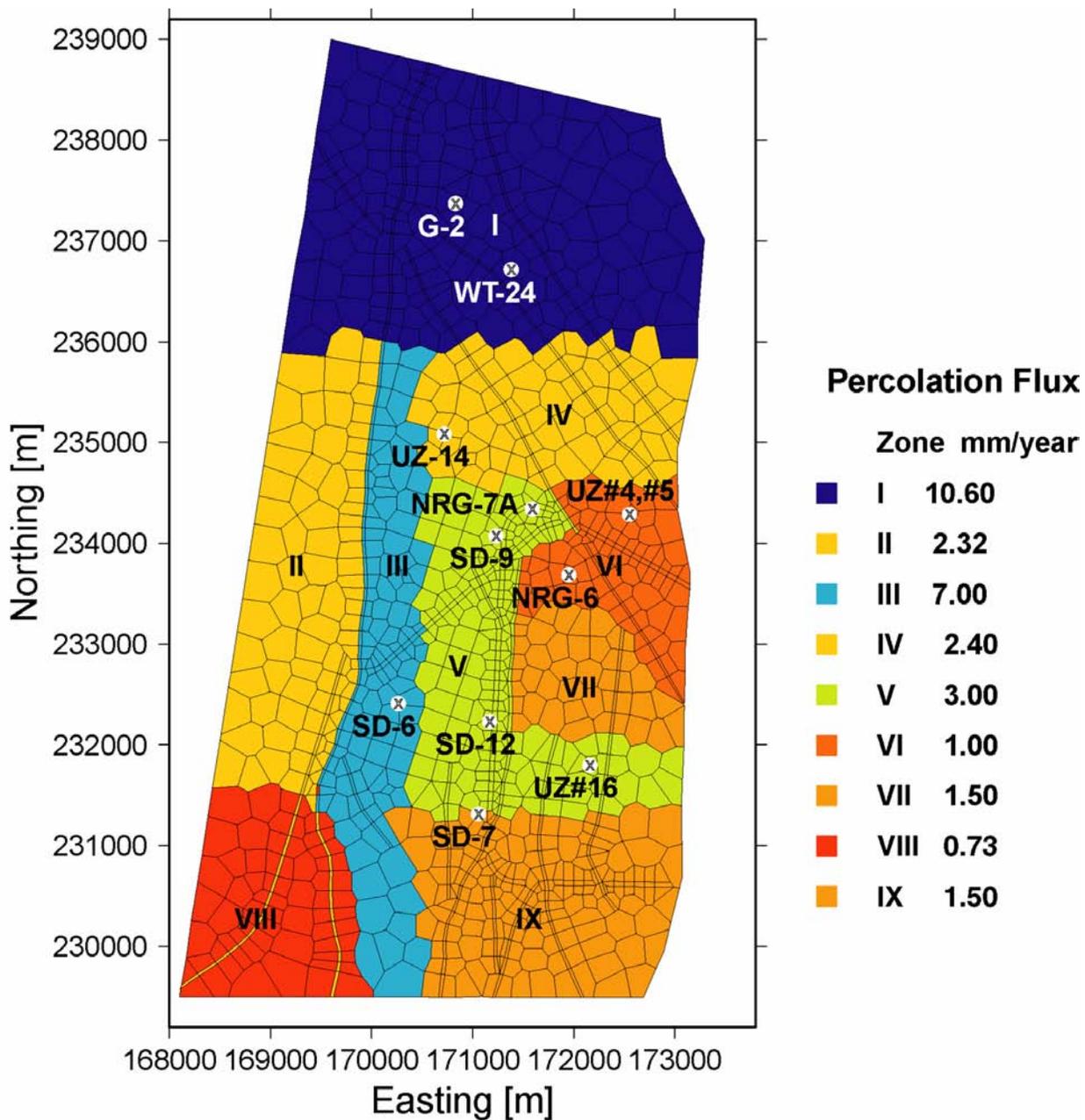
00050DC_ATP_Z1S42_142.ai

Figure 4-23.   Percolation Flux Map for Three-Dimensional Calibration Grid
Sources: Adapted from CRWMS M&O 2000bw, Figure 6-24; CRWMS M&O 2000c, Figure 3.8-4.
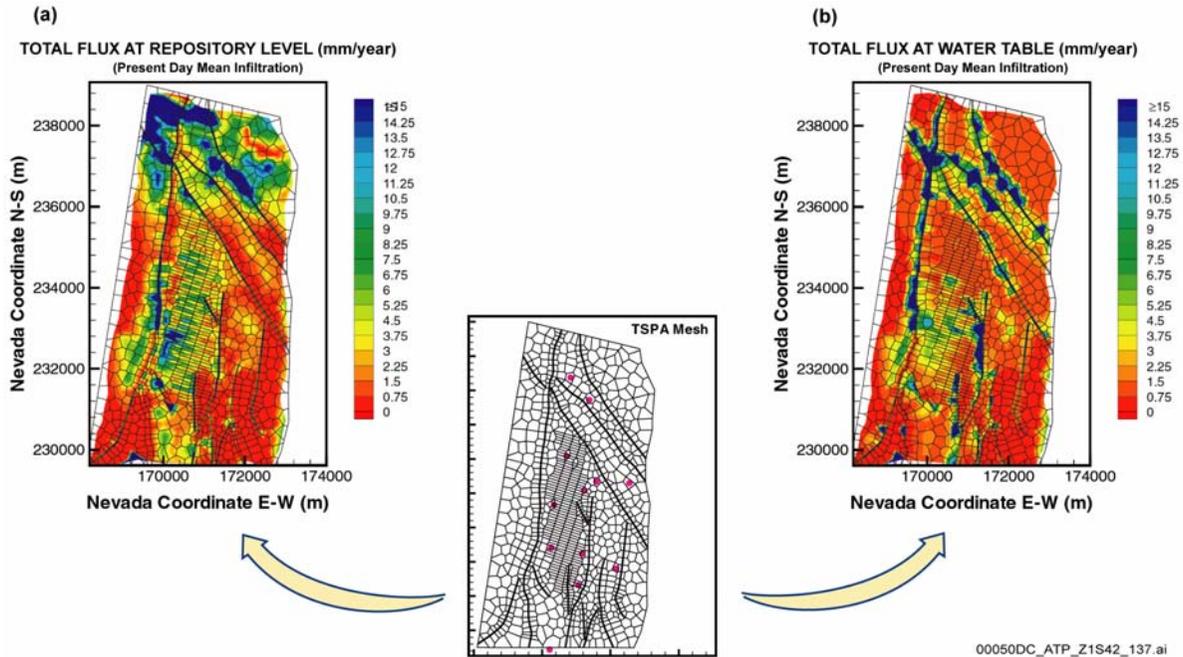
Figure 4-24.   Comparison between Simulated Percolation Flux (mm/yr) Contours at the Potential Repository Horizon and at the Water Table Under the Present-Day Mean Infiltration Rate
(a) Total flux at the potential repository horizon. (b) Total flux at the water table. For labeled details of the TSPA mesh, see Figure 4-23. Sources: Adapted from CRWMS M&O 2000c, Figure 3.7-10; data from CRWMS M&O 2000bw, Section 6.6.3.

Inferred occurrences of bomb-pulse chlorine-36 may exist in the deep unsaturated zone only in association with small volumes of water that flowed rapidly down permeable fault zones. The representation of ambient percolation flux in the unfaulted regions of the deep unsaturated zone in the unsaturated zone flow model and the seepage model as steady flow is appropriate.

The principal variable contributing to the regulation of episodic fracture flow volume and period resulting from capillary resistance is the overall flux rate. Condensation resulting from evaporation due to waste heat may locally cause accelerated percolation flux above the potential emplacement drifts. This local acceleration of percolation flux has the potential to impact seepage flux by generating enhanced episodic flow pulses near the potential emplacement drifts (BSC 2001a, Section 4.3.5). In the cases of higher-temperature operating modes, the boiling front may provide some protection of the emplacement drifts from episodic flow

surges. In both the higher- and lower-temperature operating modes, the enhanced episodic flow may impact the seepage fraction in the emplacement drifts during the heating and cooldown periods (BSC 2001a, Section 4.3.5). No impact is expected after cooldown is complete. Sensitivity studies indicate that variability in seepage flow rates has only minimal impact on performance.

Based on these considerations, flow and transport in the unsaturated zone from episodic infiltration is believed to have low consequence; therefore, transient flow behavior is not considered in the unsaturated zone process model.

4.2.1.3.1.2   Unsaturated Zone Flow Submodels

A number of applications of the flow model have been developed for detailed study of the effects of specific hydrogeologic features on flow in the unsaturated zone. These include (1) flow through the PTn unit (CRWMS M&O 2000c, Section

3.7.3.1); (2) the occurrence of perched water and the effect of alteration within the CHn unit on flow (CRWMS M&O 2000c, Section 3.7.3.3); and (3) the role of major faults as potential conduits or as barriers to flow (CRWMS M&O 2000c, Section 3.7.3.2). Each of these topics is summarized below.

Flow through the PTn and at the Potential Repository Horizon—Flow behavior within the predominantly nonwelded PTn unit was evaluated using the mountain-scale flow model with the three climate states (i.e., present day, monsoonal, and glacial-transition). Table 4-7 compares the proportions of vertical fracture flow and matrix flow at the middle of the PTn unit and at the potential repository horizon. The model results support the hypothesis that matrix flow is dominant in the PTn, taking nearly 90 percent of the total flow, with little variation among the three climate scenarios. This is consistent with observed pneumatic responses to barometric pressure fluctuations, which showed attenuated response within the PTn unit (Ahlers et al. 1999). As indicated in Table 4-7, the conditions change to fracture-dominated flow at the interface between the PTn and the underlying TSw unit (potential repository host rock).

Table 4-7. Comparison of the Water Flux through Matrix and Fractures as a Percentage of the Total Flux at the Middle PTn and at the Potential Repository Horizon

Climate	Flux at middle PTn (%)		Flux at Potential Repository (%)	
	Fracture	**Matrix**	**Fracture**	**Matrix**
Present-Day	11.6	88.4	88.3	16.3
Monsoonal	12.1	87.9	89.5	10.5
Glacial-Transition	11.8	88.2	91.4	8.6

Sources: CRWMS M&O 2000bw, Section 6.6.3; CRWMS M&O 2000c, Table 3.7-2.

More recent studies with new geochemical field data (BSC 2001a, Section 3.3.3) showed that the PTn acted as a buffer, damping out variations in the transient net infiltration, so that flow beneath the PTn was essentially steady-state. Lateral flow diverted net infiltration above the potential repository area eastward to the Ghost Dance and Drill Hole Wash faults. Flow thus diverted bypassed the potential repository block.

Effects of Major Faults—The effect of faults is important for site characterization because faults could provide direct flow pathways from the potential repository to the water table, which could bypass sorptive layers within the CHn unit that have the capacity to retard migration of radionuclides. Consequently, radionuclides could enter the saturated zone where such faults intersect the water table. Alternatively, faults could benefit potential repository performance if they cause water to be diverted away from emplacement drifts.

Based on the representation of faults in the unsaturated zone flow model, the model simulations indicate that the fraction of flow occurring through the modeled faults, as a percentage of the total flow (through fractures, matrix, and faults), increases with depth. Table 4-8 lists these predicted percentages at four different depth horizons for the three climate scenarios and for the northern and southern parts of the model domain. A recent analysis with a refined model indicates that flow through faults at the PTn–TSw interface may be slightly higher than shown here (BSC 2001a, Section 3.3.3.4.2). The table shows that flow percentages through faults at the water table would be very different in the southern part (where the CHn unit is thinner and highly porous) than in the northern part (where the CHn unit is thicker and altered to zeolites). This indicates that more lateral flow diversion on or within the CHn unit would occur in the northern part of the site area.

The simulations predict that percolation flow in the unsaturated zone will converge into the faults as water flows downward through the geologic units, and that lateral diversion of water into faults occurs mainly in the CHn unit below the potential repository horizon. Some lateral diversion into faults is also predicted to occur in the PTn unit above the potential repository horizon, as indicated in Table 4-8. In addition, although the percentage of fault flow at the water table below the potential repository is predicted to increase as the average infiltration increases, the percentage of fault flow above and at the level of the potential repository horizon is predicted to decrease as infiltration increases.

Table 4-8. Comparison of Water Flux through Faults as a Percentage of the Total Flux at Four Different Horizons for the Three Mean Infiltration Scenarios

Climate Scenarios	Fraction of Total Flow through Faults (%)											
Average Infiltration (mm/yr)	Ground Surface			PTn–TSw Interface			Potential Repository Level			Water Table		
	Total	South	North	Total	South	North	Total	South	North	Total	South	North
Present-Day (4.6)	3.8	3.6	3.9	14.3	18.9	12.7	14.6	19.8	12.7	34.9	15.9	42.0
Monsoonal (12.2)	4.1	3.8	4.2	10.5	13.0	9.6	10.5	13.3	9.5	42.4	21.9	51.3
Glacial-Transition (17.8)	4.0	3.7	4.1	9.1	10.8	8.4	9.1	11.0	8.2	44.4	24.3	54.2

NOTES: "Total" denotes flow over the entire model domain, "South" denotes flow over the southern part/half of the model domain, and "North" denotes flow over the northern part/half of the model domain. Sources: CRWMS M&O 2000c, Tables 3.7-3 and 3.5-4; data from CRWMS M&O 2000bw, Section 6.6.3.

Studies of the CHn and Perched Water Occurrence—The CHn unit lies between the potential repository horizon and the saturated zone; thus, for groundwater flow and radionuclide transport from the potential repository, the CHn unit has an important role in site performance. Prolonged rock–water interaction in the geologic past has produced low-permeability clays and zeolites within the CHn, particularly in the northern part of the site area. This alteration has important implications for occurrence of perched water, for groundwater flow paths, and for radionuclide transport.

Model simulations have been performed using the three climate states (i.e., modern, monsoonal, and glacial transition) (CRWMS M&O 2000c, Section 3.7). The results generally match the observed perched water table elevations from Yucca Mountain boreholes, provided that percolation flux greater than 1 mm/yr (0.04 in./yr) exists at the site. All modeling results indicate significant lateral flow diversion (40 to 50 percent of the total flow) just above or within the CHn where low-permeability zeolites occur.

The effect of perched water zones on flow through the CHn is best explained by comparing percolation fluxes simulated at the repository level and the water table. Figure 4-24 presents map views of the simulated vertical percolation flux distributions at the potential repository horizon and at the water table. Comparison of these views shows large differences in the percolation flux distributions at the potential repository horizon and at the water table, a result that is consistent with the expectation of significant lateral flow diversion occurring just above or within the CHn unit. Simulated results for the northern part of the site area show that percolation flux at the water table tends to be focused along faults. Simulated results for the southern part of the site area show that percolation tends to flow vertically through the CHn unit as matrix-dominated flow in relatively high-permeability vitric zones. Below these vitric zones, however, are zeolitic layers (above the water table) that laterally divert some of the flow eastward, where it is intercepted by faults (Figure 4-24).

4.2.1.3.1.3 Percolation Flux at the Potential Repository Horizon

Percolation flux through the unsaturated zone is important to performance of the potential repository because it directly controls drift seepage and radionuclide transport and also influences the evolution of temperature and humidity in the emplacement drifts (CRWMS M&O 2000c, Section 3.7.4.1). Because the low percolation flux through the unsaturated zone at Yucca Mountain cannot be readily measured, results from the unsaturated zone flow model are used to estimate the flux.

At the mountain scale, percolation flux at the potential repository horizon is mainly a reflection of the infiltration distribution at the ground surface. Areas with greater infiltration (i.e., the northern part of the site area and the crest of Yucca Mountain) have greater percolation flux, while areas with less infiltration have correspondingly less percolation flux. Percolation throughout the unsaturated zone reflects the redistribution of infiltration below the ground surface because of lateral flow, fracture–matrix flow partitioning, flow into faults, and other flow processes. Over an infinite area, the average infiltration flux would be equal to the average percolation flux. Over a limited area, such as within the repository footprint, percolation flux may be either greater or less than infiltration because of flow redistribution over a larger area.

Figure 4-25 shows the simulated distribution of vertical percolation flux at the repository level for the three climate states (i.e., present-day, monsoonal, and glacial-transition). Areas of higher percolation (shown in blue) are located principally in the northern part of the site area and along the Solitario Canyon fault. The distribution of percolation flux at the potential repository horizon closely matches the distribution of the infiltration at the ground surface (Figure 4-26) because of the limited lateral flow diversion between the surface and the potential repository level, as discussed previously.
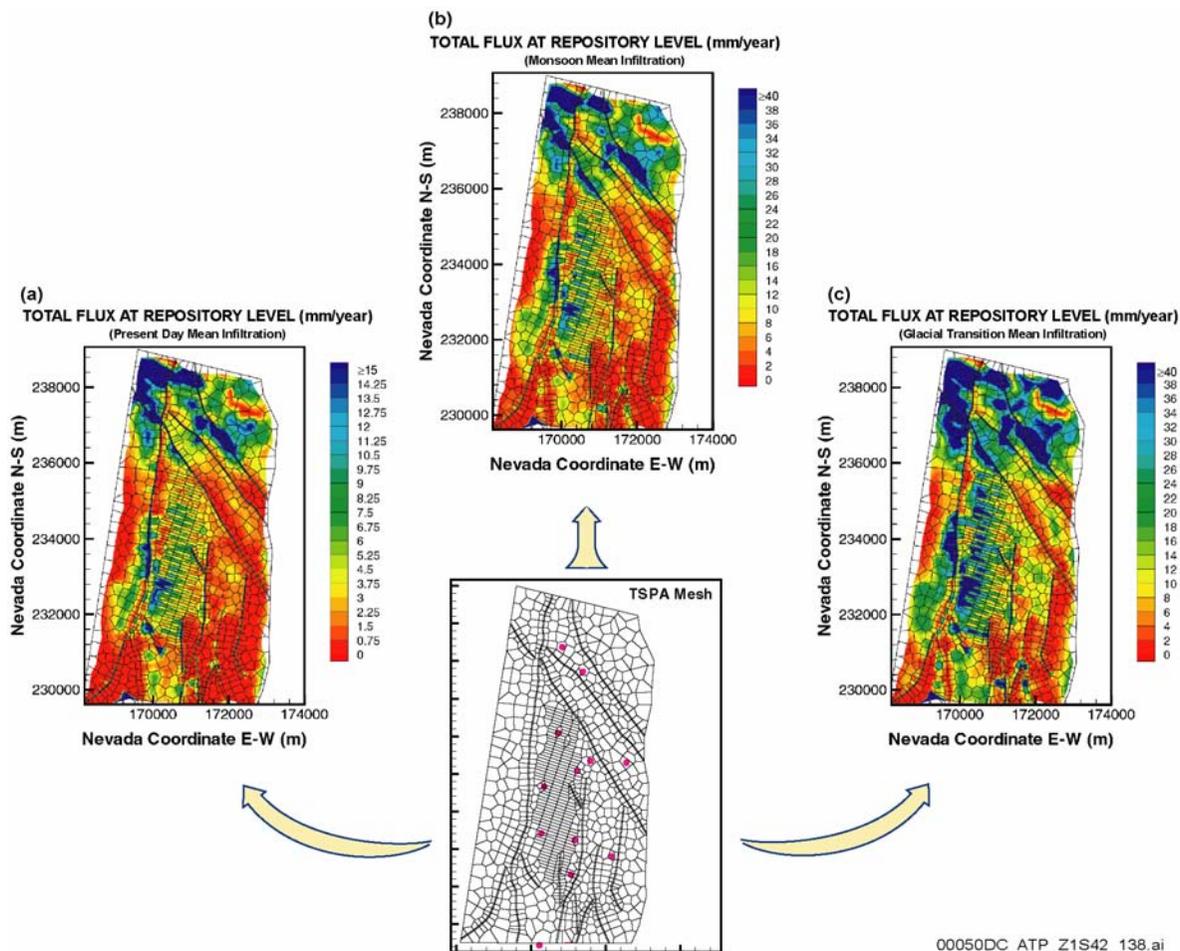
Figure 4-25. **Simulated Percolation Fluxes at the Potential Repository Horizon Under the Mean Infiltration Scenarios**

(a) Present-day infiltration scenario. (b) Monsoon scenario. (c) Glacial-transition scenario. For labeled details of the TSPA mesh, see Figure 4-23. Source: Adapted from CRWMS M&O 2000c, Figure 3.7-11.

Table 4-9 lists summary statistics for the averaged percolation fluxes within the potential repository footprint. The table indicates that the average percolation within the potential repository horizon is similar to the average infiltration over the entire model domain.

4.2.1.3.1.4 Fracture and Matrix Flow Components

Fracture flow has important implications for seepage flow into emplacement drifts and radionuclide transport and will directly influence the performance of a repository (CRWMS M&O 2000c, Section 3.7.4.3). The partitioning of flow between fractures and matrix is inferred from model results. Figure 4-27 shows the simulated

steady-state distribution of the total percolation flux through both the matrix and fractures at the potential repository horizon for the present-day climate state. In the potential repository host rock, fracture flow controls percolation wherever the total flux exceeds the hydraulic conductivity of the matrix.

Table 4-10 lists the proportion of fracture flux at the potential repository horizon and at the water table as a percentage of the total flux. Calculated results are shown for nine scenarios (i.e., present-day, monsoonal, and glacial-transition climate states, each with upper bound, mean, and lower bound infiltration). Fracture flow dominates both at the potential repository horizon and at the water table. As expected, the percentage of fracture flow
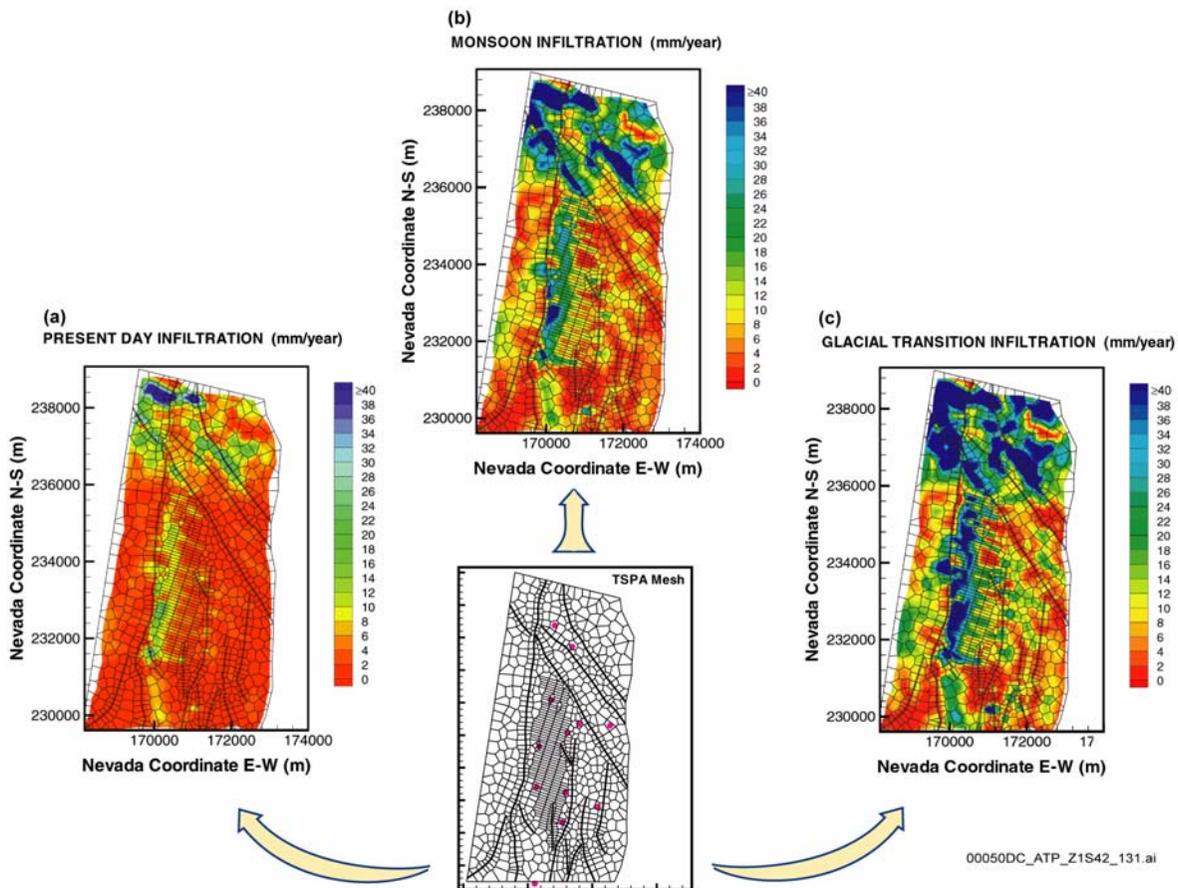
Figure 4-26. Infiltration Distribution over the Flow Model Domain for the Mean Infiltration Scenarios
(a) Present-day climate scenario. (b) Monsoon climate scenario. (c) Glacial-transition climate scenario. For labeled details of the TSPA mesh, see Figure 4-23. Source: Adapted from CRWMS M&O 2000c, Figure 3.7-4.
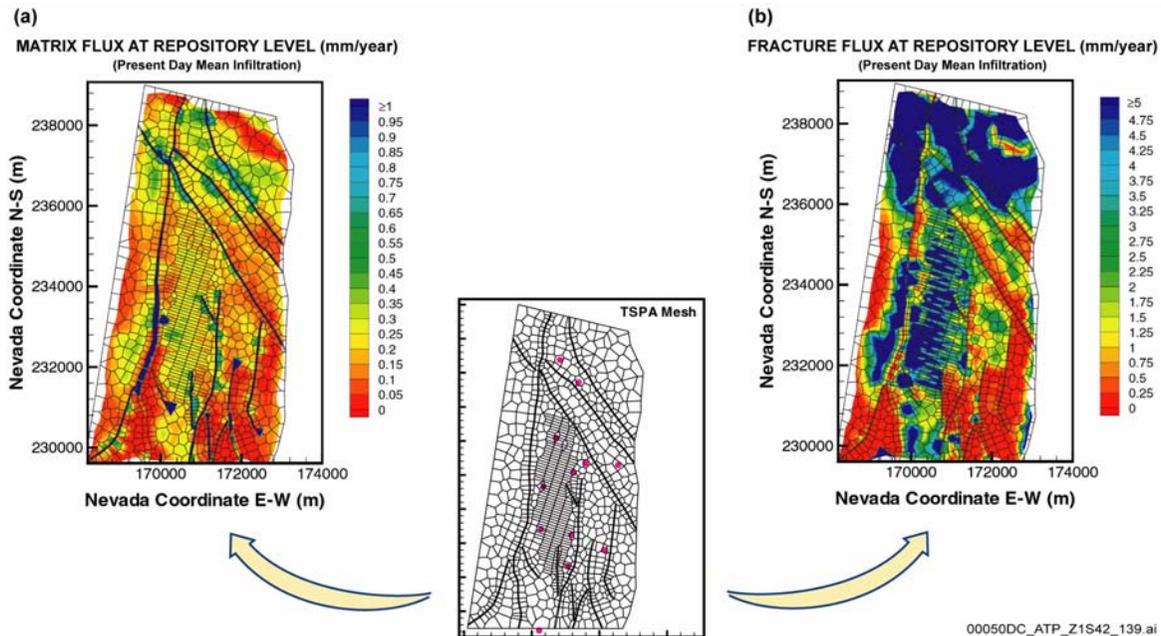
Figure 4-27. **Simulated Percolation Flux in the Matrix and in Fractures at the Potential Repository Horizon, Using Present-Day Mean Infiltration Rate**
(a) Matrix percolation flux. (b) Fracture percolation flux. For labeled details of the TSPA mesh, see Figure 4-23.
Source: CRWMS M&O 2000c, Figure 3.7-13.

Table 4-9. **Average Percolation Fluxes Simulated within the Potential Repository Footprint for the Three Mean Infiltration Scenarios**

Climate Scenario	Average Infiltration over Model Domain mm/yr (in./yr)	Average Percolation Flux within Potential Repository mm/yr (in./yr)		
		Fracture	Matrix	Total
Present-Day	4.6 (0.18)	4.0 (0.16)	0.5 (0.02)	4.5 (0.18)
Monsoonal	12.4 (0.49)	12.1 (0.48)	0.8 (0.03)	12.9 (0.51)
Glacial-Transition	18.0 (0.71)	19.5 (0.77)	0.9 (0.04)	20.5 (0.81)

NOTES: The average percolation flux values in mm/yr have been rounded to one decimal place. Sources: CRWMS M&O 2000c, Table 3.7-4; data from CRWMS M&O 2000bw, Section 6.6.3.

Table 4-10. **Comparison of Water Flux through Fractures as a Percentage of the Total Flux at the Potential Repository and at the Water Table, Using the Nine Infiltration Scenarios**

Climate	Present-Day		Monsoonal		Glacial-Transition	
Infiltration	Potential Repository (%)	Water Table (%)	Potential Repository (%)	Water Table (%)	Potential Repository (%)	Water Table (%)
Lower Bound	86.6	84.7	90.0	90.1	86.9	87.2
Mean	83.7	86.7	89.5	90.2	91.4	90.5
Upper Bound	94.5	95.4	95.6	96.5	96.5	96.9

Sources: CRWMS M&O 2000c, Table 3.7-5; data from CRWMS M&O 2000bw, Section 6.6.3.

is somewhat higher for the future climate scenarios compared to the present-day climate scenario because the total flux is greater. The results from fracture–matrix interaction tests at Alcove 6 in the Exploratory Studies Facility (shown in Figure 4-11) illustrate the dominance of fracture flow for high fluxes.

4.2.1.3.1.5 Supporting Geochemical Analysis

Geochemical processes are useful for estimating and bounding infiltration rates and percolation flux in the potential repository host rock (CRWMS M&O 2000bv, Section 6.9). Upper-bound limits on infiltration rates and percolation flux at the potential repository horizon have been estimated from geochemical data, using several analyses and models (CRWMS M&O 2000c, Section 3.8). Collectively, these conceptual models and analyses are referred to in supporting documentation as the ambient geochemistry model. The primary data used for calibration and validation in this overview are pore water chloride concentrations, relative abundance of chlorine-36 in pore water (or extracted salts), and calcite abundance.

Calcite Deposition Analysis—Calcite and carbon-14 ages in the unsaturated zone have been used as a tool for estimating percolation fluxes (CRWMS M&O 2000bv, Sections 6.6.4.3, 6.7.2.2, 6.10.1.1, and 6.10.3.9). Modeling studies incorporating reactive transport in unsaturated zone flow simulations were used to investigate the relationship of calcite deposition to infiltration rate, water and gas compositions, and reactive surface area (CRWMS M&O 2000bw, Section 6.5). Model results for borehole USW WT-24 indicated that the infiltration rate ranges from about 2 mm/yr to 20 mm/yr (0.08 to 0.8 in./yr), which bounds the observed range of calcite abundance. An infiltration rate of approximately 6 mm/yr (0.2 in./yr) can account for the average abundance of calcite in the TSw unit (Figure 4-14b).

Chloride Mass Balance—Small concentrations of chloride occur in rainfall at Yucca Mountain, averaging approximately 1 mg/L (CRWMS M&O 2000bv, Section 6.3.2). The chloride becomes more concentrated as evaporation occurs. The water that does not run off or evaporate infiltrates into the unsaturated zone, carrying the dissolved chloride. The resulting concentration of chloride in unsaturated zone pore waters indicates the extent of evaporative concentration relative to rainwater, and the infiltration flux is inferred using the average annual precipitation and runoff.

Chloride concentrations in unsaturated zone pore waters can be used to evaluate the unsaturated zone flow model. The comparison of concentrations for the present-day climate state and mean infiltration (CRWMS M&O 2000c, Section 3.8) are shown in Figure 4-14. The modeled concentrations were higher than measured concentrations toward the northeast end (left side of Figure 4-14a) and lower at the southwest end of the Exploratory Studies Facility (right side). The northeast end of the drift corresponds to an area of very low infiltration rates, whereas the southwest end is beneath the crest of Yucca Mountain, where infiltration is greater. Measured chloride concentrations exhibit a smaller range of variation than is predicted using the present-day, steady-state infiltration rates. The general agreement among these results indicates that the average of present-day infiltration over the model domain for the mean infiltration distribution, 4.6 mm/yr (0.18 in./yr), is accurate.

As an alternative interpretation of the observed chloride data, infiltration rates were adjusted in the UZ flow and transport models to match with the measured pore water chloride concentration data. The match can be achieved by adjusting infiltration rates in those areas where the match can be improved, while maintaining the average infiltration the same as the current model (USGS 2000b, Section 6.11; CRWMS M&O 2000bw, Section 6.4.3.1). The modified percolation flux map is shown in Figure 4-23. The domain was divided into 9 regions, and for those regions where pore water chloride data were unavailable (Regions I, II, and VIII), the map was filled in using average infiltration values from the unsaturated zone flow model.

The modified model has a more uniform spatial distribution of infiltration rates. However, it is possible to have an alternative interpretation if the PTn, between the shallow infiltration zone in TCw and the potential repository unit in TSw, has strong

damping capacity and the large lateral diversion of flow occurs in the PTn. The spatial variation of infiltration can remain the same as the current model while flow redistribution occurs in the PTn. Significant damping and lateral diversion of flow by the PTn is strongly supported by the recent analyses (Section 4.2.1.1.2). It is therefore demonstrated that alternative models can be formulated to maintain both the heterogeneous distribution of infiltration near the surface and more uniform distribution of chloride content along the underground drifts in the potential repository unit.

Applying the chloride mass balance approach to estimating percolation (using measured pore water chloride concentration data), a modified percolation flux map was developed (Figure 4-23). The domain was divided into 9 regions, and for those regions where pore water chloride data were unavailable (Regions I, II, and VIII), the map was filled in using average infiltration values from the unsaturated zone flow model. The percolation flux values estimated in this manner were then evaluated as estimates of the infiltration rates (USGS 2000b, Section 6.11). The infiltration rates estimated by chloride mass balance are similar to the mean infiltration rates obtained by averaging the rates over the same area (CRWMS M&O 2000bw, Section 6.4.3.1). This provides confirmation that the infiltration data used in the unsaturated zone flow model represent the present-day climate state.

As an alternative interpretation of these data, chloride concentrations modeled from the mean infiltration rates were compared to the measured chloride concentrations (Figure 4-14). The modeled concentrations were higher toward the northeast end (left side of Figure 4-14a) and lower at the southwest end of the exploratory drift (right side). The northeast end of the drift corresponds to an area of very low infiltration rates, whereas the southwest end is beneath the crest of Yucca Mountain, where infiltration is greater. Measured chloride concentrations exhibit a smaller range of variation than is predicted using the present-day, steady-state infiltration rates. However, the general agreement among these results indicates that the average of present-day infiltration over the model domain for the mean infiltration distribution, 4.6 mm/yr (0.18 in./yr), is accurate.

Chlorine-36 Isotopic Analysis—Measured background chlorine-36 isotopic ratios in extracted pore waters, while highly variable, are uniformly lower over much of the south ramp compared to the north ramp of the Exploratory Studies Facility. Modeled results indicate that chlorine-36 isotopic ratios in the south ramp should be much lower than in the north ramp, even though the PTn unit is thinner, because the infiltration flux is less. The greater background chlorine-36 isotopic ratios in the north ramp could also be the result of mixing of bomb-pulse water with older matrix pore water. Bomb-pulse chlorine-36 isotopic ratios, indicating fast flow paths, are found in several locations in the vicinity of some fault zones in the exploratory tunnels. Elevated chlorine-36 signatures are confined to the immediate vicinity of faults and other structural features, fast flow zones are localized, and large areas of the potential repository appear to be unaffected by fast-path flow (CRWMS M&O 2000bv, Section 6.6). With regard to perched water, the lack of bomb-pulse chlorine-36 is difficult to interpret because of potential mixing with older water. However, low tritium signatures in perched waters below the potential repository horizon are consistent with the interpretation of limited fast flow at this depth.

Because of the important implications of the occurrence of bomb-pulse chlorine-36 to the site-scale unsaturated zone flow and transport model, the project has undertaken a study to confirm the occurrence of bomb-pulse chlorine-36 at two locations in the Exploratory Studies Facility (the Drill Hole Wash fault zone and the Sundance fault zone). Preliminary results from this ongoing study have not confirmed the presence of chlorine-36, and the analyses of the validation samples at two different laboratories are not consistent. The project has defined a path forward to understand the reasons for the differences: a common set of protocols will be developed, and analyses of the validation samples will continue. However, the unsaturated zone flow and transport model and the TSPA are based on the original data set used in the conceptualization of unsaturated zone behavior. Hence, the project approach conservatively bases the model on the presence of bomb-pulse chlorine-36.

4.2.1.3.1.6 Summary and Conclusions from Unsaturated Zone Mountain-Scale Modeling

Results from the unsaturated zone flow model and from analysis of supporting geochemical data are summarized in Figures 4-28 and 4-29, respectively. In summary, available site data have been used to construct an unsaturated zone flow model that has provided infiltration and percolation flux distributions and hydrologic properties, as intended. The model accounts for the occurrence of perched water and enhances the understanding of the effects of the PTn unit and fault zones on flow in the unsaturated zone at the site. The flow model has been interpreted for comparison with chemical and isotopic data, confirming the flow model results in an average sense.

Upper-bound limits on infiltration rates and percolation fluxes at Yucca Mountain are estimated based on multiple approaches (CRWMS M&O 2000bw, Sections 6.2, 6.4, 6.5, and 6.6). These include analyses of chloride and chlorine-36 isotopic ratios, calcite deposition, and the occurrence of perched water. The analysis of chloride data indicates that the average percolation rate over the model domain at Yucca Mountain is about 4.6 mm/yr (0.18 in./yr). Analysis of calcite deposition gives infiltration estimates of 2 to 20 mm/yr (0.08 to 0.8 in./yr) in the vicinity of borehole USW WT-24. To match perched water occurrences, three-dimensional model calibrations require that the present-day average infiltration rate be greater than 1 mm/yr (0.04 in./yr), with an upper limit of about 15 mm/yr (0.6 in./yr).
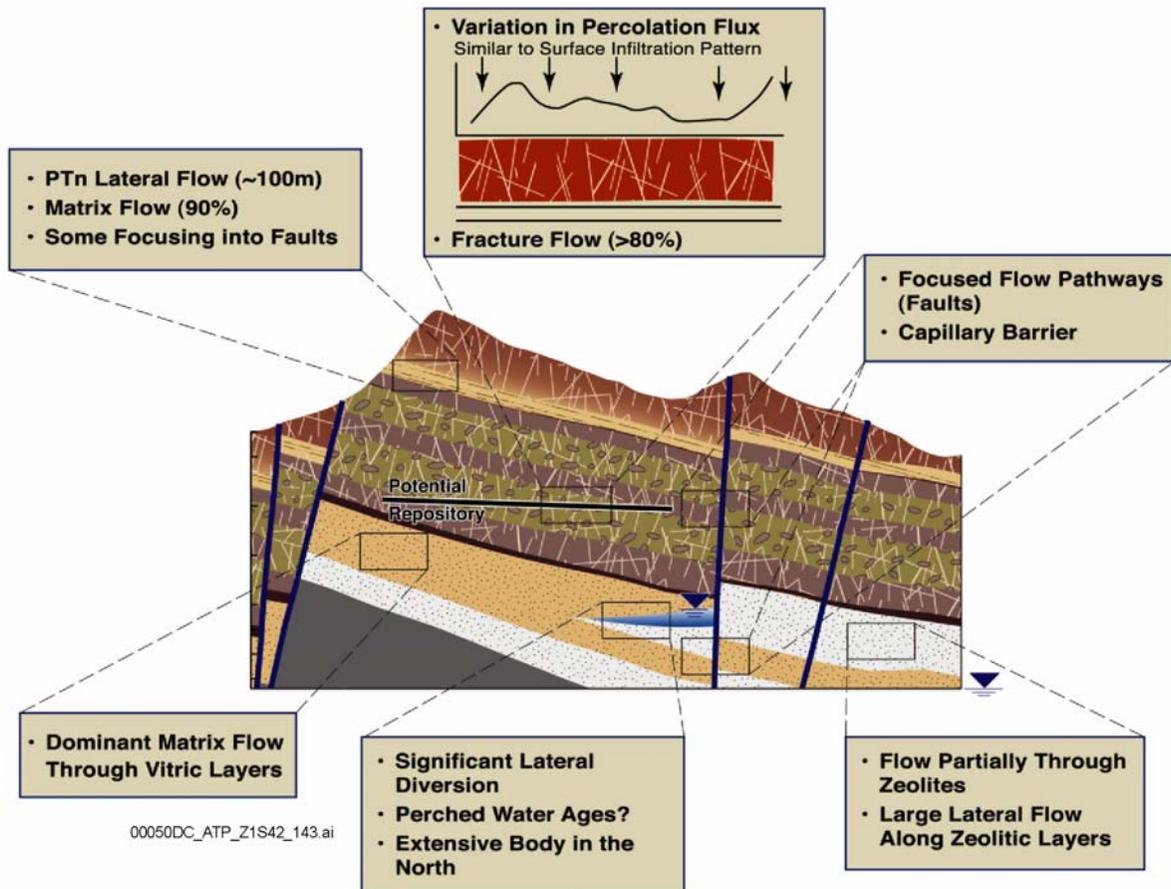
Figure 4-28.   Summary of the Unsaturated Zone Flow Model Results
Source: CRWMS M&O 2000c, Figure 3.7-19.

Cl concentrations lower under repository than in north and south ramps, as indicated by infiltration maps
- Percolation fluxes more uniform than those predicted by infiltration maps and calibrated hydrologic properties

Predicted chloride concentrations in the ECRB are close to measured values, without calibration

Fast-Flow Path:
- Bomb-pulse ^{3}H, ^{36}Cl/Cl found near faults, and not in other areas, indicating only localized fast flow zones

^{36}Cl/Cl may indicate longer travel times to repository where PTn is thicker

Proportion of matrix flow in zeolitic units still unresolved

Perched Water:
- Lack of ^{3}H and bomb-pulse ^{36}Cl, indicating no more than a small component of recent fast-flow water

00050DC_ATP_Z1S42_Fig-144.ai

Figure 4-29. Conceptual Model of Unsaturated Zone Flow and Transport at Yucca Mountain Showing Results from Analysis of Geochemical Data
Source: CRWMS M&O 2000c, Figure 3.8-8.

4.2.1.3.2   Drift Seepage Model

A qualitative description of drift seepage processes was provided in Section 4.2.1.1.5. The characterization and modeling approach presented here for the seepage calibration model focuses on obtaining effective hydrologic properties based on relevant seepage test data (CRWMS M&O 2000c, Section 3.9.1). Figure 4-30 schematically shows the relationships between the different seepage models, as well as data input and the exchange of information. Seepage test data, such as those from the niche studies, are used for developing the seepage calibration model. The modeling approach and parameters are then used in the seepage model for performance assessment. This model supports the abstraction of drift seepage for use directly in TSPA calculations.

The seepage calibration model is a porous-medium model of the fracture continuum that has spatially variable permeability based on air-permeability data (CRWMS M&O 2000c, Section 3.9.4.4) and is calibrated to the test data from Niche 2 in the Exploratory Studies Facility (CRWMS M&O 2000c, Section 3.9.4.5). Model calibration was used to determine effective hydrologic properties that represent the potential effects of individual fractures and microfractures on drift seepage. Simulations with multiple realizations of the heterogeneous property field were performed to account for the random nature of the fracture network (CRWMS M&O 2000bx, Section 6.3). The steps involved in development of the seepage calibration model are shown schematically in Figure 4-31.

Model Assumptions—All seepage models presented in this section are single-continuum models, explicitly representing only the fracture network (not the rock matrix). The justification for this approach is based on the conceptual framework that the fracture network is extensive and well connected, and that flow conditions are steady-state or very slowly varying throughout
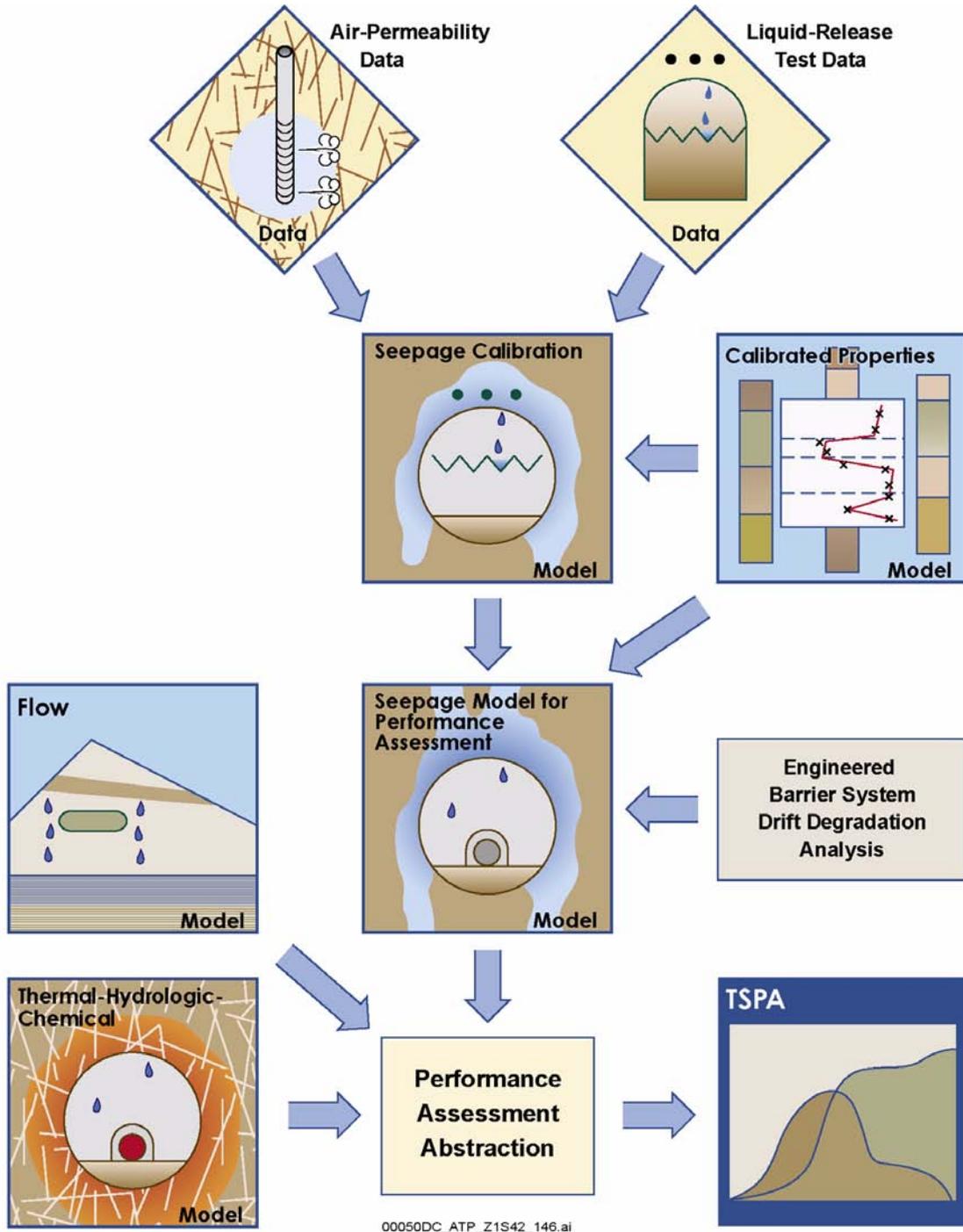
Figure 4-30.   Schematic Showing Data Flow and Series of Models Supporting Evaluation of Drift Seepage
Source: CRWMS M&O 2000c, Figure 3.9-2.
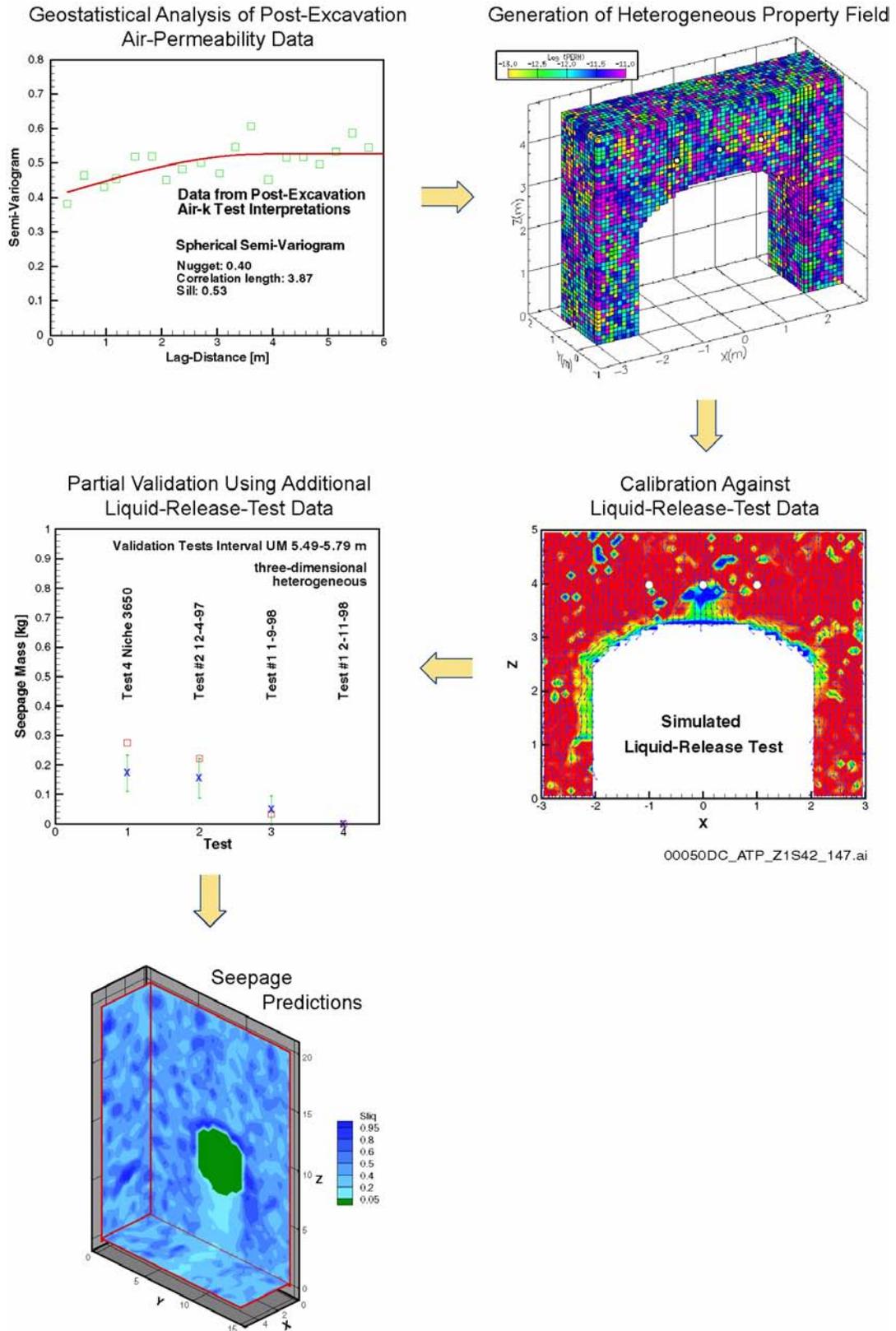
Figure 4-31.   Schematic Showing General Approach for the Development of the Seepage Calibration Model
Source: Adapted from CRWMS M&O 2000c, Figure 3.9-4.

much of the potential repository host rock because of the moderating influence of the overlying PTn unit. Under steady flow conditions, the flow interaction between the fractures and the matrix in the vicinity of the emplacement drifts will be negligible because of the low permeability of the rock matrix relative to that of the fractures (CRWMS M&O 2000c, Sections 3.3.13 and 3.6.3.2).

The continuum approach is valid for simulating drift seepage, as well as percolation flux, based on the observation that the fracture network in the middle nonlithophysal unit of the Topopah Spring Tuff is well connected (CRWMS M&O 2000bx, Section 6.7). The appropriateness of using the continuum approach to simulate flow through fractured rock was also studied by Jackson et al. (2000) using synthetic and actual field data. They concluded that heterogeneous continuum representations of fractured media are self-consistent (i.e., appropriately estimated effective-continuum parameters can represent the underlying fracture network characteristics).

Adopting the continuum approach, unsaturated flow of liquid water is governed by Richards' equation, the governing equation of water content or capillary pressure based on mass conservation law (Richards 1931). Relative permeability and capillary pressure are described according to the van Genuchten–Mualem model (Luckner et al. 1989, pp. 2191 to 2192). Within the heterogeneous property distribution, capillarity of the effective medium is correlated to absolute permeability according to the Leverett scaling rule, with capillary strength inversely proportional to the square root of permeability (Leverett 1941, p. 159).

Since percolation flux cannot be directly measured in the field, the average percolation flux in the host rock is estimated by the unsaturated zone flow model and multiplied by flow-focusing factors derived using the active-fracture concept (CRWMS M&O 2000by, Section 6.3.3).

In-drift evaporation and ventilation effects are not included in the current seepage model, but neglecting them is conservative because it produces greater estimates of predicted seepage. The evaporation reduces drop formation and drip-ping (Ho 1997a) and enhances the vapor diffusion into the drift. Neglecting evaporation effects increases predicted seepage of liquid water (CRWMS M&O 2000c, Section 3.9.3.3).

Seepage Threshold Prediction—Steady-state seepage simulations were performed with the seepage calibration model (CRWMS M&O 2000bz, Section 6.6). In this application, percolation flux was applied at the top of the model, instead of from a borehole as in the niche tests. The ambient percolation flux was varied over a wide range, starting from a small value yielding zero seepage, increasing stepwise until seepage was predicted to occur, and increasing further to estimate seepage percentage. Using this procedure, a seepage threshold of approximately 200 mm/yr (7.8 in./yr) was obtained for the middle nonlithophysal unit of the Topopah Spring Tuff. The seepage-threshold prediction obtained for Niche 2 suggests that diversion of flow around the emplacement drift openings is an effective barrier to water that could otherwise contact waste packages (BSC 2001a, Sections 4.2.2 and 11.3.1.1.1).

4.2.1.3.3 Model Calibration and Validation

An important objective for the unsaturated zone flow model is to produce a model consistent with the available site characterization data. This is accomplished through an iterative process of model calibration to the data, adjusting the hydrologic properties that represent the rock units (CRWMS M&O 2000c, Section 3.9.4.5). A combination of one-, two-, and three-dimensional numerical models is used to represent the lateral variation of hydrologic conditions in the unsaturated zone, for example, from the northern to the southern ends of the potential repository layout area. The data that constrain the calibration process include borehole-measured matrix saturation, water potential, temperature, the presence of perched water, pneumatic-pressure measurements, and geochemical data. The model calibrations require specification of the water infiltration at the ground surface and its variation throughout the site area (USGS 2000b, Section 6.11). To represent uncertainty in the infiltration estimates, separate infiltration distributions are used, representing upper-bound, mean, and lower-bound conditions.

Separate model calibrations (i.e., hydrologic property sets) are developed for the three infiltration distributions. The distributions of infiltration for future monsoonal and glacial-transition climate conditions were developed using the infiltration model (CRWMS M&O 2000c, Section 3.5.2), which was calibrated using data for present-day infiltration rates. Table 4-11 summarizes average precipitation and infiltration rates. Figure 4-25 shows mean infiltration distributions over the model domain for each climate state.

Model calibrations were performed using one-dimensional numerical grids to estimate mountain-scale hydrologic properties for the hydrogeologic units. The one-dimensional calibration model consists of 11 vertical columns, shown schematically in Figure 4-32, representing the hydrostratigraphy at 11 boreholes for which suitable site characterization data are available. The use of a one-dimensional vertical model implicitly assumes that flow is adequately approximated as one-dimensional and vertical (i.e., that lateral flow is not important). In the TCw, PTn, and TSw rock units, this assumption is supported by the absence of perched water (CRWMS M&O 2000c, Sections 3.6.4.1). At the bottom of the TSw unit and below, perched water does exist in some areas, especially to the north. Perched water is investigated using the three-dimensional model (CRWMS M&O 2000c, Section 3.7.3.3).

The one-dimensional calibrated mountain-scale formation properties are then used as input to a two-dimensional model, which is used to calibrate the fault properties. The two-dimensional model consists of an east–west cross section, shown schematically in Figure 4-33. This cross section is located where there are borehole data available for the ambient hydrologic conditions in a fault at Yucca Mountain. Use of a two-dimensional model implies that flow constrained to the vertical and east–west directions adequately represents ambient conditions. The dip of the bedding and the strike of the fault are approximately parallel to the cross section; therefore, the assumption is reasonable. The same types of properties calibrated for the mountain-scale formation properties are calibrated for the faults. Figure 4-33 also shows the match between the calibrated simulation and the saturation, water potential, and pneumatic data for present-day ambient conditions (mean infiltration).

The resulting calibrated hydrologic properties (including fracture and matrix permeability, fracture and matrix van Genuchten parameters, and active-fracture parameters) are then used as input to mountain-scale and drift-scale hydrologic models. Calibration activities in three dimensions (involving hydrologic measurements, perched water, temperature, and ambient geochemical data) are carried out for additional refinement of mountain-scale properties. Figure 4-34 shows an example of the results from the three-dimensional calibration. This figure compares the observed and simulated matrix saturation and perched water

Table 4-11. Average Precipitation and Average Infiltration Rates over the Unsaturated Zone Flow Model and Transport Model Domain

	Present-Day Climate (to 600 years)			Monsoon Climate (600 to 2,000 years)			Glacial-Transition Climate (beyond 2,000 years)		
	Upper bound	Mean	Lower bound	Upper bound	Mean	Lower bound	Upper bound	Mean	Lower bound
Average Precipitation Rate,[a] mm/yr (in./yr)	268.6 (10.58)	190.6 (7.50)	186.8 (7.35)	414.8 (16.33)	302.7 (11.92)	190.6 (7.50)	433.5 (17.07)	317.8 (12.51)	202.2 (7.96)
Average Infiltration Rate,[b] mm/yr (in./yr)	11.1 (0.44)	4.6 (0.18)	1.3 (0.05)	19.8 (0.78)	12.2 (0.48)	4.6 (0.18)	33.0 (1.30)	17.8 (0.70)	2.5 (0.10)

Source: [a]CRWMS M&O 2000c, Table 3.5-2.
[b]CRWMS M&O 2000c, Table 3.5-4.
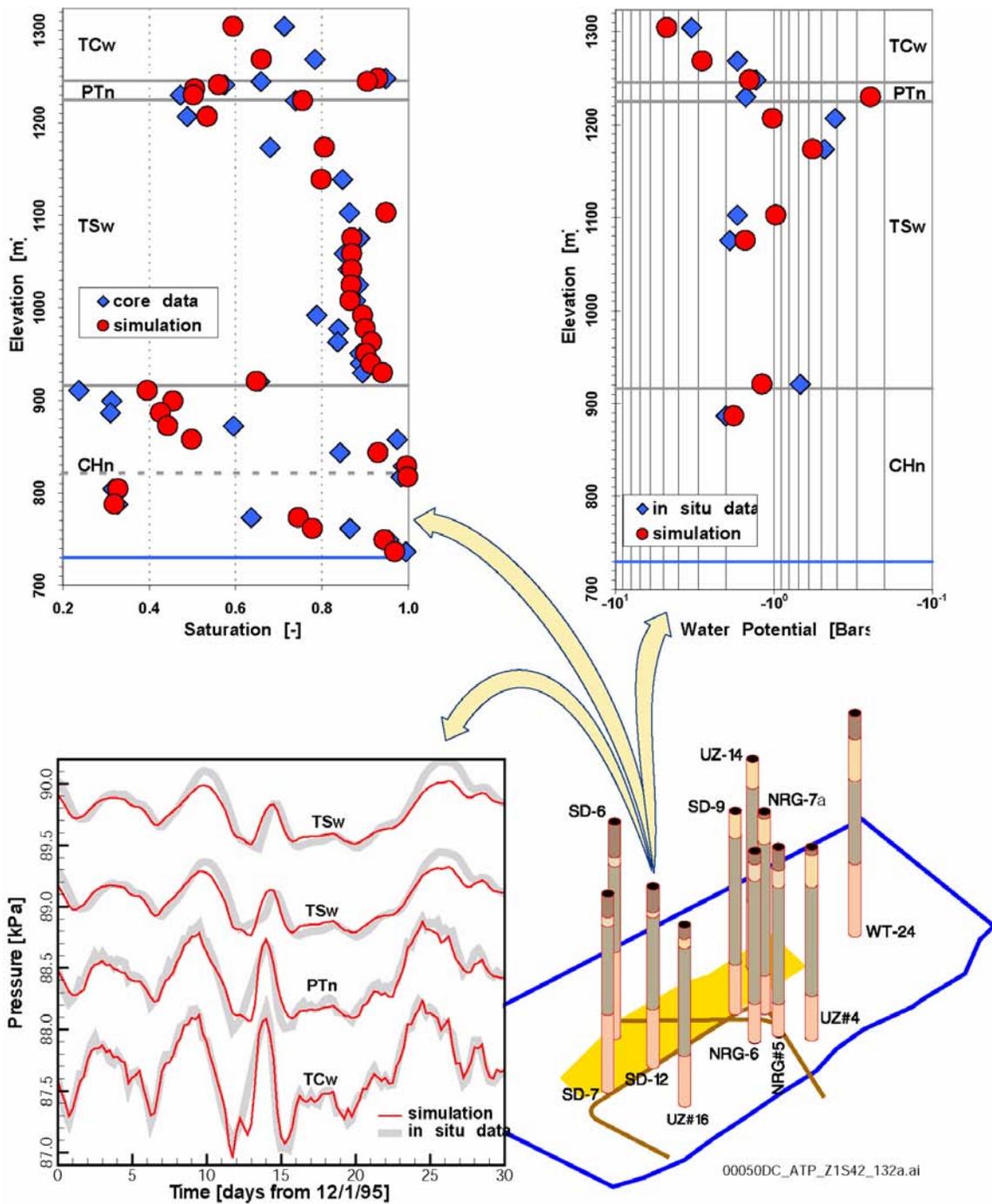
Figure 4-32.   Calibrated One-Dimensional Simulation Match to Saturation, Water Potential, and Pneumatic Data

Data from Borehole USW SD-12 and simulation results for the present-day mean infiltration rate. Source: CRWMS M&O 2000c, Figure 3.6-4.
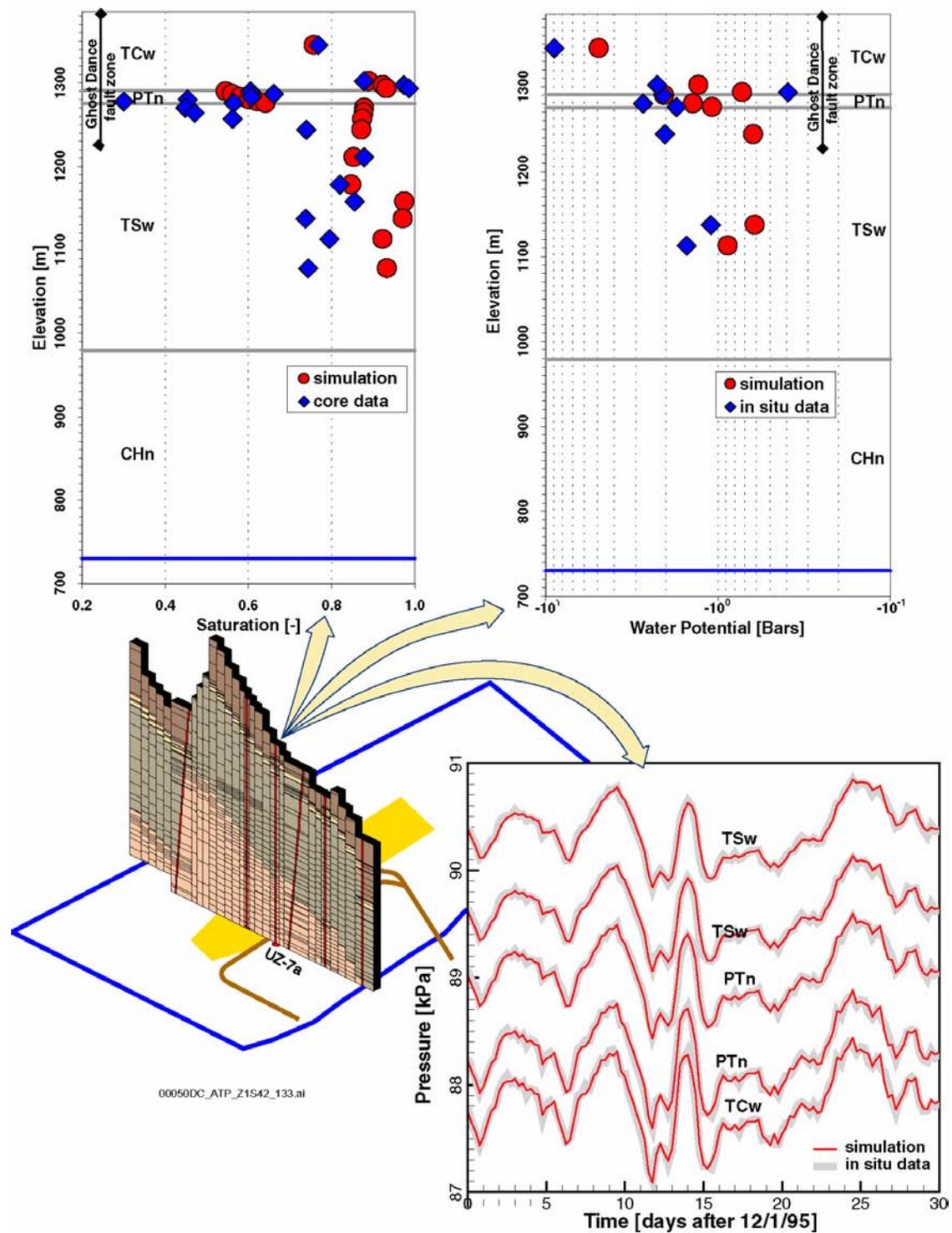
Figure 4-33. Calibrated Two-Dimensional Simulation Match to Saturation, Water Potential, and Pneumatic Data

Data from Borehole USW UZ-7a and simulation results for the present-day mean infiltration rate. Source: CRWMS M&O 2000c, Figure 3.6-5.
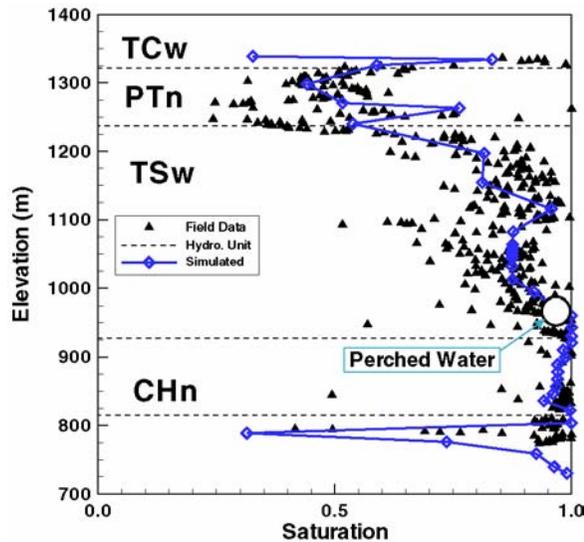
00050DC_ATP_Z1S42_134.ai

Figure 4-34. Comparison of Simulated and Observed Matrix Liquid Saturations, Showing Perched Water Elevations
Data from Borehole USW UZ-14 and simulation results for the present-day mean infiltration rate. Source: Data from CRWMS M&O 2000bw, Section 6.6.3, Figure 6-41; figure adapted from CRWMS M&O 2000c, Figure 3.7-14.

elevation at borehole USW UZ-14, using the present-day ambient conditions (mean infiltration). Overall, the simulation results for this borehole (and others used in the calibration activity) are generally consistent with the observed saturation and perched water data.

Model Validation and Confidence Building— Validation of the calibrated hydrologic property sets constituting the calibrated properties model was performed using the three-dimensional model (CRWMS M&O 2000bw, Section 6.8). In situ water potential data measured from the ECRB Cross-Drift compare well with predicted water potentials, as shown in Figure 4-35. Although the predicted water potentials are generally lower, the difference is only a few tenths of a bar (1 bar = 10^5 Pa). Pneumatic pressure data also compare well to the predicted pneumatic pressures shown in Figure 4-35. These and other results presented in *Unsaturated Zone Flow and Transport Model Process Model Report* (CRWMS M&O 2000c, Section 3.6.5.3) show that the calibrated properties are

valid for predicting ambient conditions, and that the assumptions of one-dimensional and two-dimensional flow are suitable for use in the calibration process.

Pore water chemical composition data have been used to validate the unsaturated zone flow model to bound the infiltration flux, flow pathways, and transport time through the unsaturated zone. Infiltration rate calibrations are performed using the pore water chloride concentration data. Agreement between the predicted chloride distributions and observed data are improved when the calibrated infiltration rates are used. Similar analyses have been performed using calcite deposition to further constrain hydrologic parameters, such as infiltration flux. These geochemical studies provide additional support for validation of flow and transport models (CRWMS M&O 2000bw, Sections 6.4 and 6.5; CRWMS M&O 2000c, Sections 3.7 and 3.8).

Seepage Model Calibration—Data from five tests (CRWMS M&O 2000bz, Table 6) were selected for calibration of the seepage model. The five tests were conducted in a 0.3-m (1-ft) long borehole interval at various injection rates to sample the dependence of seepage on flux. Approximately 1 liter of water was injected in each test. Seepage percentages from the test series demonstrate storage effects and seepage rates above and below a seepage threshold. Analysis of all five tests provided a match between model results and observed seepage. As shown in Figure 4-36, the heterogeneous three-dimensional seepage calibration model matches the observed seepage data better than the two-dimensional or homogeneous alternatives.

Seepage Model Validation—The seepage calibration model was used to make predictions of observed seepage percentages from liquid injection tests that were performed in a different borehole interval using different injection rates and varying other test conditions. The uncertainty of the model predictions was evaluated using linear error propagation analysis and Monte Carlo simulation. (This approach reflects the intended use of the resulting seepage models, in which seepage is treated statistically.) Observed seepage percentages lay within
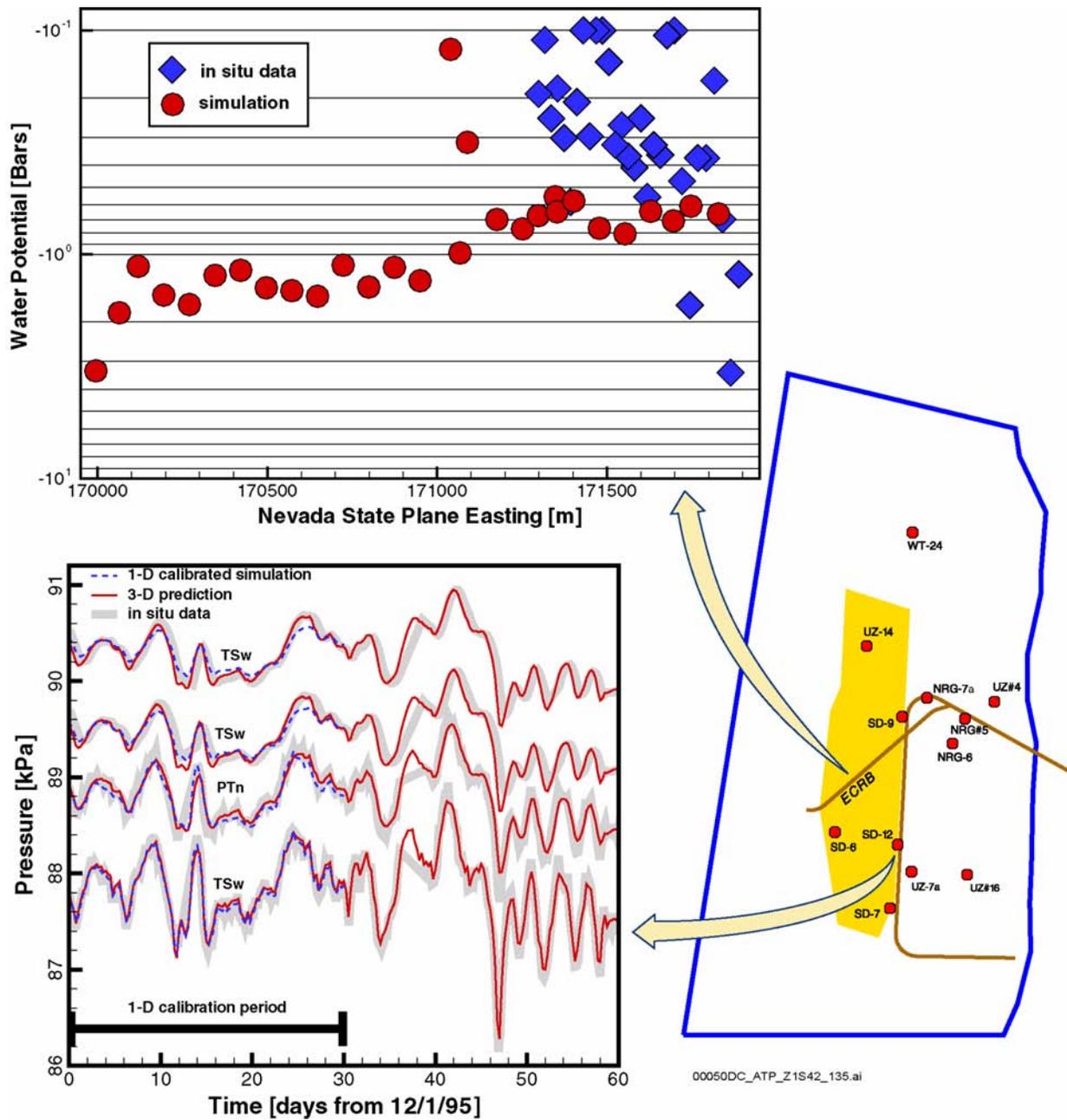
Figure 4-35. Comparison of Predictions from the Three-Dimensional Model with In Situ Water Potential Data and Pneumatic Pressure Data

Water potential data from the ECRB Cross-Drift and pneumatic pressure data from Borehole USW SD-12. Source: CRWMS M&O 2000c, Figure 3.6-8.
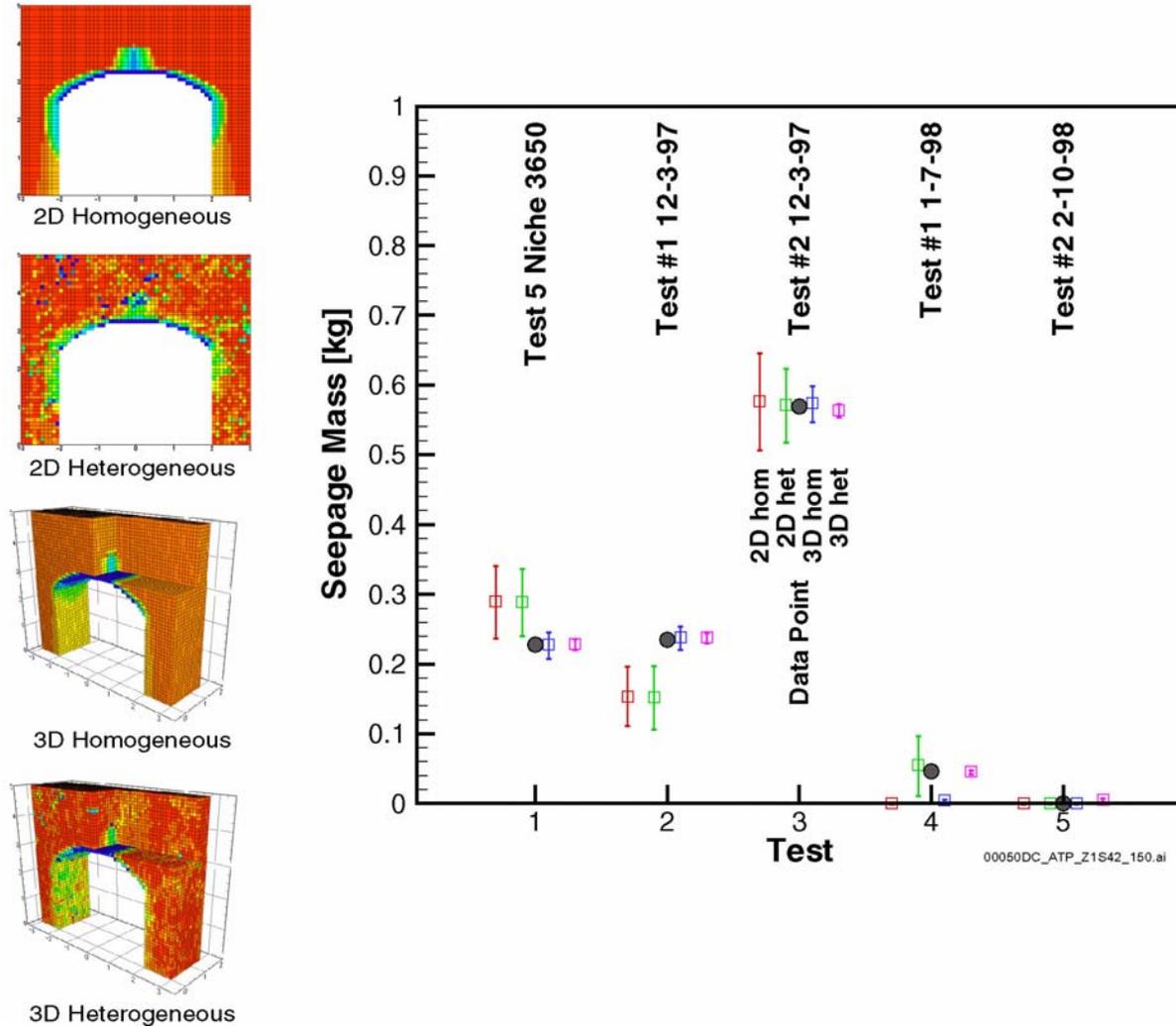
Figure 4-36.   Comparison between the Measured Seepage Mass and Seepage Mass Calculated with Two-Dimensional and Three-Dimensional Homogeneous and Heterogeneous Models
Measured seepage mass is plotted with black dots. The model predictions are plotted with squares. The four models are visualized on the left and labeled by color, as indicated inside the plot. The uncertainty of the model predictions is shown as error bars on the 95 percent confidence level. The three-dimensional heterogeneous seepage calibration model matches the data best. Source: CRWMS M&O 2000c, Figure 3.9-6.

the uncertainty range of the model predictions. This favorable result provides confidence in the validity of the seepage model. More details about the seepage calibration model can be found in *Seepage Calibration Model and Seepage Testing Data* (CRWMS M&O 2000bz).

4.2.1.3.4   Alternative Conceptual Processes

In developing models of water movement through the unsaturated zone at Yucca Mountain, alterna-

tive conceptual processes were identified and considered (CRWMS M&O 2000c, Section 1.2.4). This section summarizes some key alternative concepts for processes governing water movement through the unsaturated zone.

PTn Lateral Flow—In an early conceptual model of Yucca Mountain, Montazer and Wilson (1984, pp. 45 to 47) hypothesized that significant lateral flow occurs within and above the PTn unit because of the contrast in hydraulic properties at the contact

between the TCw and PTn units. They also showed that vertical heterogeneities within the PTn may result in a much larger effective permeability of the unit in the direction of dip, compared with the effective permeability in the direction normal to the bedding plane. Montazer and Wilson (1984, p. 47) argued that the combination of this factor and capillary barrier effects might introduce considerable lateral flow within the unit. Recent modeling of the potential for diversion on or in the PTn supports the Montazer and Wilson conceptual model of lateral flow and diversion. Pneumatic measurement of permeability on, in, and below the PTn, geochemical data, and saturation and water potential data were used to calibrate unsaturated zone parameters and to differentiate alternative conceptual models. Modeling based on the capillary barrier effect using a fine grid spacing supports the concept of diversion of flow above the potential repository horizon (BSC 2001a, Section 3.3.3.4.2). Diversion of flow above the repository would be beneficial to the performance of the repository. It is not necessary for diversion large enough to result in diversion to faults to occur for the PTn to damp episodic flow in the unsaturated zone, but diversion might be an additional mechanism for uniformly distributing the areal variation of infiltration.

PTn Fracture Flow—An alternative conceptual model for water flow through the PTn is one that assumes pervasive fracture flow through this unit (CRWMS M&O 2000c, Section 3.3.3). However, the available data, which show high matrix porosity and storage capacity combined with relatively high matrix permeability and limited fracturing (see to Sections 4.2.1.2.3 through 4.2.1.2.5)—in addition to geochemical data that indicate a lack of widespread bomb-pulse chlorine-36 signatures in the PTn (see Section 4.2.1.2.8)—support the preferred conceptual model of predominantly matrix flow through the PTn.

Episodic Flow Within the TSw—In the prevailing conceptual model, episodic flow into the TSw unit is considered to be damped by the PTn to the extent that flow can be regarded as steady-state when it enters the TSw. The exception is that at or near major faults, episodic flow may still persist through the PTn, though these isolated fast flow

paths are considered to carry only a small amount of water. An alternative view to this conceptual process is one in which episodic flow is pervasive through the TSw unit (CRWMS M&O 2000c, Section 3.7.3.1). This alternative may be a more conservative conceptualization because a greater amount of episodic flow could lead to greater seepage into potential waste emplacement drifts. However, for the reasons presented in Section 4.2.1.3.1.1 (in the discussion of transient versus steady-state flow), flow and transport in the unsaturated zone has been found to have low consequence; thus, the approach that is regarded as more plausible has been taken.

Flow Through Faults—As discussed in Section 4.2.1.2.6, limited fault permeability measurements are only available for the welded units, TCw and TSw. From these data, it is inferred that faults within the PTn and CHn/CFu units have relatively higher permeabilities than the adjacent nonfaulted rock. An alternative view is one in which faults within the PTn and CHn/CFu units have low permeabilities and retard the movement of water because of the occurrence of low-permeability alteration minerals within the fault zones (CRWMS M&O 2000c, Section 3.3.5). This conceptual model would result in slow transport from the TSw to the water table. Available measured data are insufficient to confirm either conceptual model. However, the conceptualization of faults as higher-permeability structures in the PTn and CHn/CFu units is adopted because it is the conservative approach, providing fast flow pathways to the water table and allowing discharge from perched water bodies.

Discrete Fracture Network Model for Seepage—A discrete fracture network model is an alternative conceptual model to the heterogeneous fracture continuum model (CRWMS M&O 2000bz, Section 6.7). A high-resolution discrete fracture network model, in principle, should be capable of simulating channelized flow and discrete seepage events. However, the development of a defensible discrete fracture network model for the unsaturated zone at Yucca Mountain would require the collection of geometric and hydrologic property data on billions of fractures. While some of the required geometric information could be

obtained from fracture mappings, the detailed description of the fracture network would be incomplete and highly uncertain. Moreover, measurement of unsaturated hydrologic parameters on the scale of individual fractures would be required, which would be largely impractical. The development of a discrete fracture network model at the mountain scale is therefore impractical (CRWMS M&O 2000bz, Section 6.7), so an equivalent fracture continuum model is used to represent the fracture system for the prediction of effective seepage quantities. The appropriateness of this model is demonstrated by Finsterle (2000).

4.2.1.3.5 Limitations and Uncertainties

The assessment of the current understanding of flow through the unsaturated zone needs to take into account the limitations and uncertainties in the unsaturated zone flow model. The model is limited mainly by the current characterization of the unsaturated zone flow system within Yucca Mountain, including geologic and conceptual models; by the applicability of the volume-averaging modeling approach; by the assumption of steady-state moisture flow; and by the available field and laboratory data (CRWMS M&O 2000c, Section 3.7.4.5). Remaining uncertainties in the model parameters include (1) accuracy in the estimated present-day, past, and future net infiltration rates over the mountain; (2) quantitative descriptions of heterogeneity within the welded and nonwelded tuff units, the flow properties associated with these units, and the detailed spatial distribution of these units within the mountain, especially below the potential repository horizon; (3) sufficiency of field studies and data, especially for characterizing hydrologic properties of faults and fractures within the zeolitic units; (4) alternative conceptual models quantifying the fluid transmissive properties of faults; and (5) evidence for lateral diversion above or within the zeolitic portions of the Calico Hills nonwelded hydrogeologic unit beneath the potential repository horizon (CRWMS M&O 2000c, Section 3.7.4.5).

As noted in Section 4.1.1.2, the DOE has initiated several activities to improve the treatment of uncertainty in current models (BSC 2001a, Section 2.1). Some of the unsaturated zone models will be updated as a result of those activities. Those updates will be documented in future reports.

The identification and propagation of uncertainties is important for the appropriate treatment of the models used in TSPA-SR calculations. Uncertainties associated with the major unsaturated zone model components are described in detail in the *Unsaturated Zone Flow and Transport Model Process Model Report* (CRWMS M&O 2000c, Section 3.13).

The uncertainty and variability in the model parameters are due, in part, to the natural variability and heterogeneity in the geological, hydrologic, chemical, and mechanical systems that are difficult to characterize in situ, such as the precise fracture network in the unsaturated zone. Uncertainties in models may also be due to conditions that are difficult to predict, such as future climate states.

Uncertainties Associated with Climate—As described in *Future Climate Analysis* (USGS 2000a, Section 6.5), future climates cannot be predicted in any precise way. Uncertainty arises because of the complexity of global climate systems and because climate changes can be triggered by unforeseen circumstances, such as major tectonic events (e.g., volcanic eruptions) or human activity. However, studies of past climates (paleoclimate studies) demonstrate that changes can be correlated with cyclical variations in the earth's orbit and the tilt of the earth's axis of rotation, both of which affect the amount of solar radiation the atmosphere receives. The earth's orbit changes in a regular and predictable manner over a cycle of about 400,000 years. Paleoclimate studies, which include geochemical analyses of sediments deposited in lakes, minerals deposited in springs, fossils of microorganisms that lived in both lakes and springs, and plant and animal remains preserved in caves, suggest that the sequence of climate changes in the 400,000-year cycle is not random, and that future climate conditions will evolve systematically. The variability of the glacial-transition period has large impacts to the model predictions as the results of long duration and high precipitation values. In the TSPA-SR, a conservative approach is adopted, with the glacial-transition

climate extending beyond 10,000 years and the shorter and drier interim periods not taken into account (CRWMS M&O 2000a, Section 3.2.1.2).

Although future climate conditions cannot be precisely predicted and climate varies considerably even within glacial and interglacial periods, studies provide a reasonable basis for forecasting the range of climates Yucca Mountain will probably experience in the future (USGS 2000a). This forecast, which incorporates the variability observed in studies of the past climate, has been used as input to models that assess the future performance of a repository at Yucca Mountain. The present warm, dry interglacial period will probably end in the next 400 to 600 years, and may be followed by a transition to a warm, wet monsoon climate for approximately 900 to 1,400 years. The climate would then shift to a glacial-transition period. The variability of the climate conditions is quantified by upper bounds for wetter climates and lower bounds for drier climates, as presented in Section 4.2.1.3.1.

Uncertainties Associated with Lower Tuff Units—The relatively high density of data in the potential repository area, particularly within and above the TSw, helps to reduce uncertainty in the understanding of flow behavior between the land surface and potential repository horizon. Greater uncertainty exists, however, below the TSw (i.e., within the CHn and CFu) because rock hydrologic properties are highly variable and few data are available to capture the spatial variability. Modeling uncertainties also increase rapidly with lateral distance away from the potential repository area as the density of data points is greatly reduced.

As a result, many of the hydrologic properties used in unsaturated zone modeling studies of Yucca Mountain for layers within the CHn and CFu have been estimated using analogue data from the PTn, the TSw, and portions of the CHn for which data are available. Despite similar welding characteristics, the PTn data (specifically, fracture permeability) used as an analogue to the CHn tend to be conservative because of many inherent differences in the depositional and postdepositional history of these tuffs. Fault properties were esti-

mated for the CHn/CFu, derived from in situ fault testing in the TSw; however, there are different welding textures associated with each major unit. For example, faults may be more permeable within the TSw because the brittle nature of the densely welded tuffs can lead to the development of well-connected fracture networks. Within the CHn, however, the predominantly nonwelded tuffs are likely to exhibit more plastic deformation (producing fewer well-connected fractures) and are much more susceptible to alteration (producing low-permeability clays and zeolites that hinder vertical flow) when exposed to percolating water.

Uncertainties Associated with Calibrated Property Values—Calibrated rock hydrologic property values derived from core-sample measurements, fracture mapping, and in situ field data provide important input to the unsaturated zone model in that they define the hydrologic characteristics of each cell within the numerical grid. Uncertainties related to calibrated hydrologic properties include (1) variability in measured properties of rock core samples and uncertainty in cross-correlations between measured properties; (2) spatial variability in rock properties; (3) uncertainty in the initial estimates of rock properties and in upscaling of measured data to model grid blocks; and (4) nonuniqueness of results generated by the estimation procedure (CRWMS M&O 2000c, Table 3.13-1). With a total of 194 calibrated properties (all the calibrated hydrogeologic unit and fault properties), the quantitative estimation of uncertainty is complex. Cross correlations between some of the properties tend to compound the uncertainties assigned to individual properties. Furthermore, the statistical assumptions that underlie the uncertainty analysis implemented in the estimation procedure are not justified if the estimation uncertainties become very large because of cross correlations. However, the calibrated property values generally do not vary much from the initial values input to the estimation procedure, and the initial values are chosen to be plausible. Because the initial and calibrated properties are generally similar, the uncertainties of the initial property estimates can be used as surrogates for the uncertainties of the calibrated property values (CRWMS M&O 2000c, Section 3.6.5.2).

Where the calibrated properties change significantly with respect to the initial values, the numerical model produces results that differ from the initial interpretation. For example, the transitions between matrix-dominated and fracture-dominated flow, at interfaces between nonwelded and welded tuff, depend on processes that occur at scales smaller than the numerical grid spacing. Consequently, the calibrated property values at these interfaces reflect the response of the numerical model, which uses coarser spacing.

Uncertainties Associated with the Numerical Approach—An additional uncertainty in unsaturated zone modeling is the mathematical representation of complex flow phenomena. The volume-averaging approach used, and the model assumption of steady-state moisture flow (used in interpreting ambient conditions), simplify the representation of water flow through the site, adding uncertainty to the model results.

Uncertainties Associated with Geochemical Analyses—The amount of calcite precipitated over time is sensitive to the water and gas composition, the reactive surface area, and the thermodynamic and kinetic parameters used in the model (CRWMS M&O 2000bw, Section 6.5). Because calcite abundances are highly variable at the different locations sampled (CRWMS M&O 2000bv, Section 6.10.1.1; see also Figure 4-14 in Section 4.2.1.2.12), the calcite analysis approach is suitable for estimating a range of percolation fluxes, as discussed in Section 4.2.1.3.

The use of chloride to estimate percolation fluxes or infiltration rates is directly related to the initial estimate of the effective chloride concentration in precipitation, the spatial variation, and changes over time (Ginn and Murphy 1997, pp. 2065 to 2066). The long-term projection of spatial and temporal patterns of precipitation is uncertain because the patterns have been measured for less than 100 years, which is short compared to the time period over which the chloride concentrations have developed in the unsaturated zone (tens of thousands of years) (Sonnenthal and Bodvarsson 1999, pp. 107 to 111). Given these uncertainties, the chloride mass balance approach is used to estimate ranges in the infiltration rate for comparison to the

flow model. The distribution of chloride in the unsaturated zone is also influenced by lateral flow diversion, as well as diffusion and dispersion processes, and thus may not accurately represent local infiltration conditions. However, the average chloride concentration for pore water in the unsaturated zone is a better indicator of the average infiltration flux.

Bomb-pulse chlorine-36 signatures can be clearly identified in isotopic data. However, the chlorine-36 background analysis is more uncertain because of the possibility for contamination of older chlorine by bomb-pulse chlorine-36. Accordingly, the chlorine-36 method is used to detect clear indications of modern fast pathways and to identify regions of the unsaturated zone with faster transport to the repository horizon (which may also be associated with fast pathways). Bomb-pulse tritium signatures can be attributed to liquid or vapor movement, both of which are prevalent in the unsaturated zone. The presence of bomb-pulse tritium can indicate fast liquid flow from the surface or redistribution of modern infiltration by evaporation and gas-phase movement of water vapor.

Uncertainties Associated with Seepage—Seepage threshold predictions are expected to vary with location. The seepage threshold value of 200 mm/yr (7.8 in./yr) applies to Niche 2 (CRWMS M&O 2000c, Section 3.9.4.7). Further abstraction analysis is used to extend the seepage calibration model to the repository area (CRWMS M&O 2000c, Section 3.9.6.4). Much of the potential repository area is located in the lower lithophysal zone of the Topopah Spring Tuff, which is more permeable than the middle nonlithophysal zone, with shorter fractures and pervasive lithophysal cavities. Some of the frames of Figure 4-18 for Niche 5 in the ECRB Cross-Drift show an example of a large lithophysal cavity and a borehole image of lithophysal cavities.

The greater permeability of the lower lithophysal unit of the Topopah Spring Tuff may enhance the capillary barrier effect (i.e., reduce seepage), either by the presence of more permeable fractures or by higher porosity and permeability in the rock matrix that can absorb more water. Geologic mapping

along the ECRB Cross-Drift indicates that the lower lithophysal zone is very heterogeneous; investigations of the hydrologic properties of this rock unit are ongoing.

4.2.1.3.6 Summary of the Current Understanding of Unsaturated Zone Flow and Seepage into Drifts

Current understanding of unsaturated flow at Yucca Mountain has been gained through collection of site data and modeling of the relevant processes. Table 4-12 summarizes the current understanding of flow parameters and processes. The table identifies features, events, and processes that are important to unsaturated zone flow processes and could affect the waste isolation performance of a repository. The statements listed under the "Current Understanding" column are a mixture of observations, hypotheses, and insights that constitute only abridged, summary information. Additional detail is provided in the *Unsaturated Zone Flow and Transport Model Process Model Report* (CRWMS M&O 2000c). Note that Table 4-12 summarizes current understanding only for flow processes occurring in the unsaturated zone hydrogeologic units and for seepage. A discussion of issues related to flow and transport processes occurring below the potential repository is presented in Section 4.2.8.

4.2.1.4 Total System Performance Assessment Abstraction

4.2.1.4.1 Unsaturated Zone Flow Abstractions for Total System Performance Assessment

A total of nine flow fields are used in the TSPA base case calculations. These consist of three infiltration cases (lower, mean, and upper) within each of the three climate states (present-day, monsoon, and glacial-transition).

Abstraction of Water Table Rise—The two future climate states (monsoon and glacial-transition) are expected to be wetter than the present-day climate, and, as a result, the water table is expected to rise. However, uncertainty exists regarding the amount of water table rise for each climate state.

Therefore, as discussed in Section 4.3.3.1 and in *Abstraction of Flow Fields for RIP (ID: U0125)* (CRWMS M&O 2000ca, Section 6.2), a conservative water table rise of 120 m (390 ft) is used for all flow fields using future climate states. Recent analyses described in Section 4.3.3.1.3 indicate that the maximum rise in the last 2 million years has been about 17 to 30 m (56 to 98 ft).

The impact of the water table rise on transport beneath the potential repository was evaluated in *Analysis of Base-Case Particle Tracking Results of the Base-Case Flow Fields (ID: U0160)* (CRWMS M&O 2000cb, Section 6.2.4). Results showed that the elevated water table reduces transport times beneath the repository (the median breakthrough for a sorbing tracker, neptunium, decreased by nearly a thousand years for the mean infiltration case).

Abstraction of Groundwater Breakthrough—The breakthrough time to the water table of a nonsorbing tracer (technetium) released uniformly in the repository region is simulated for TSPA to gain insight into the range of possible radionuclide transport times that can result based on the different possible infiltration cases for the present-day climate. Breakthrough for future climates is presented in *Analysis of Base-Case Particle Tracking Results of the Base-Case Flow Fields (ID: U0160)* (CRWMS M&O 2000cb, Section 6.2.6).

Breakthrough curves for technetium using the present-day climate and three infiltration cases show that median breakthrough times are approximately 400 years, 2,000 years, and 600,000 years for the upper, mean, and lower infiltration cases, respectively. As expected, the higher infiltration rates yield shorter breakthrough times relative to lower infiltration rates.

More recent modeling of unsaturated zone transport is presented in Volume 1, Section 11 of *FY01 Supplemental Science and Performance Analyses* (BSC 2001a). Influence of model refinements of five issues in the travel of radionuclides between the potential repository horizon and the saturated zone is treated (BSC 2001a, Table 11-1). These issues are the degree of advection–diffusion split-

Table 4-12. Summary of Current Understanding Used to Develop Conceptual and Numerical Models for Unsaturated Zone Flow and Seepage into Drifts

Feature, Event, or Process	Current Understanding	Sections of UZ PMR Where Addressed
Climate/infiltration	Rainfall for the modern mean climate is about 190 mm/yr (7.5 in./yr) resulting in average steady-state net infiltration of 4.6 mm/yr (0.2 in./yr).	3.5.1.8; 3.5.2.10
	After 600 years, the average rainfall is forecast to increase to about 300 mm/yr (11.8 in./yr) for a monsoon climate; in response, the average net infiltration is predicted to increase to 12.2 mm/yr (0.5 in./yr).	3.5.1.8; 3.5.2.10
	After 2,000 years, the average rainfall is predicted to increase to about 320 mm/yr (12.6 in./yr) for a glacial-transition climate; in response the average net infiltration is predicted to increase to 17.8 mm/ year (0.7 in./yr).	3.5.1.8; 3.5.2.10
Infiltration	The net infiltration is episodic, with a significant amount infiltrating only every few years.	3.3.2
	There is large spatial variability of infiltration, with most water infiltrating on ridgetops and in the upper reaches of washes where there is little alluvial cover.	3.3.2; 3.5.2.5; Figures 3.5-4c, 3.5-5a and b
Flow through TCw	Flow through the Tiva Canyon welded hydrogeologic unit (TCw) is episodic as controlled by infiltration.	3.3.3.1; 3.7.3.1
	Fracture flow dominates in the TCw, transmitting water rapidly through the TCw.	3.3.3.1; 3.7.3.1
Flow through PTn	Flow through the Paintbrush tuff nonwelded hydrogeologic unit (PTn) is primarily matrix flow.	3.3.3.2; 3.7.3.1
	The PTn consists of up to nine stratigraphic units with different degrees of welding and alteration and different hydrologic properties.	3.2.2.2
	Lateral flow occurs in the PTn.	3.3.3.2; 3.7.3.1; 3.7.3.2
	Most of the fast flow through the PTn occurs via faults, though this represents only a very small fraction of the total flow.	3.3.7; 3.11.8
Flow through TSw	Episodic flow into the Topopah Spring welded hydrogeologic unit (TSw) is damped by the PTn to the extent that flow can be considered steady-state when it enters the TSw. The exception is that at or near major faults episodic flow may still persist through the PTn.	3.3.3.2; 3.3.3.3; 3.3.5; 3.3.6; 3.7.3.1; 3.7.3.2
	Fracture flow dominates in the TSw because this unit is densely welded and highly fractured; additionally, within some subunits of the TSw, the low-permeability matrix is incapable of transmitting the percolation flux estimated to be moving through the unit.	3.3.3.3; 3.7.4.3
	Fracture flow in the potential repository horizon, which intersects the Topopah Spring middle nonlithophysal, lower lithophysal, and lower nonlithophysal stratigraphic units, is estimated to range from 84 to 94 percent of the total water flow for the three present-day climate scenarios.	3.7.4.2; 3.7.4.3
	Water drainage in the potential repository units, Topopah Spring middle nonlithophysal, lower lithophysal, and lower nonlithophysal stratigraphic units, is expected to be good due to the generally high fracture permeability (~10^{-11} to 10^{-10} m^2 [10^{-10} to 10^{-9} ft^2]).	3.6.5.1, Figure 3.6-6
	Current average percolation flux in the potential repository horizon is estimated to be about 5 mm/yr (0.2 in./yr), with spatial variability between 0 and 60 mm/yr (0 and 2.4 in./yr).	3.7.4.1; 3.7.4.2; 3.7.4.5
	Long-term average percolation flux at the potential repository horizon, averaged over the last 1,000 to 10,000 years, is estimated to be about 6 mm/yr (0.2 in./yr) based on calcite abundances, with a range of 2 to 20 mm/yr (0.1 to 0.8 in./yr).	3.8.4.2
	Evidence for fast/preferential flow is seen at the potential repository horizon, primarily near major faults. It is estimated that the fast component of flow is less than a few percent of the total flow.	2.2.3.3; 3.3.7; 3.8.3; 3.11.8

Table 4-12. Summary of Current Understanding Used to Develop Conceptual and Numerical Models for Unsaturated Zone Flow and Seepage into Drifts (Continued)

Feature, Event, or Process	Current Understanding	Sections of UZ PMR Where Addressed
Seepage	Open emplacement drifts act as capillary barriers, impeding water from seeping into the drifts and diverting some fraction of the prevailing percolation flux around the drifts.	3.3.9; 3.9.1; 3.9.9; 3.9.3.5
	A critical percolation flux (seepage threshold) exists below which no seepage occurs. The distribution of seepage thresholds depends on the hydrologic characteristics and variability of the unit, especially the fracture permeability and the van Genuchten alpha values.	3.9.3.5
	Seepage flux is always smaller than the percolation flux as a result of partial flow diversion around the drift.	3.9.1; 3.9.6.1
	Ventilation reduces seepage of liquid water. Neglecting ventilation effects in seepage models is conservative.	3.9.3.3
	Seepage percentages are expected to be similar for all potential repository units because permeability and capillary strength are inversely related, canceling their respective effects on seepage.	3.9.6.2
Perched water	Several perched water bodies have been found below the potential repository horizon, with the perching layer generally being the basal vitrophyre of the TSw or the zeolitic part of the Calico Hills nonwelded hydrogeologic unit (CHn).	3.3.3.4; 3.3.8; 3.7.3.3
	The largest perched water body is found in the vicinity of Borehole UZ-14, north of the potential repository region; this perched water body may be connected to those found in Boreholes WT-24, SD-9 and SD-12.	3.7.3.3
	A very small perched water body is found in the southern part of the potential repository region at Borehole SD-7. This perched water body is expected to have little impact on the performance of the potential repository.	3.7.3.3
	The perched water bodies contain a mixture of Pleistocene and Holocene water, with average ages ranging from 3,500 to 11,000 years old.	2.2.3.3; 3.3.3.3; 3.8.3; 3.10.3.4
	Infiltration rates needed to form perched water bodies are higher than present-day values.	3.8.2; 3.8.3
	The minute fractions of bomb-pulse ^{36}Cl and tritium in perched water suggest that the fast flow fraction over the past 50 years is very small.	3.8.3
	Perched water is formed because the ambient percolation flux exceeds the capacity of the geologic media to transmit the flux vertically through the underlying low-permeability units. Water may flow either through the units or laterally to major faults or other vertical conduits for flow.	3.7.3.2; 3.7.3.3
Flow through CHn	The CHn consists of unaltered vitric zones, primarily in the south, and altered zeolitic zones, primarily in the north. Water flow through the zeolitic units is primarily in the fractures, while flow through the vitric units is mostly or all in the matrix.	3.7.3.3; 3.3.3.4
	Lateral flow in perched water bodies toward faults and other major permeable features causes partial bypassing of the low permeability zeolitic units of the CHn.	3.7.3.2; 3.7.3.3
	Water entering the CHn vitric unit from the TSw transitions from discrete fracture flow to heterogeneous matrix flow.	3.11.4
Flow through faults	Fault properties are variable and generally controlled by rock type and stratigraphic displacement.	3.2.3; 3.3.5
	Faulting enhances fracturing in the fault zones, contributing to increased permeability. Permeability in the TCw and TSw fault zone is 6 to 9×10^{-11} m^2 (9×10^{-10} ft^2). In the PTn fault zone it is ~2×10^{-11} m^2 (2×10^{-10} ft^2).	3.7.3.2; 3.6.5.1
	Faults are high permeability features through the CHn and Crater Flat undifferentiated hydrogeologic unit (CFu), provide a fast flow path from the TSw to the water table, and allow discharge from perched water bodies.	3.3.5

NOTES: UZ PMR = *Unsaturated Zone Flow and Transport Model Process Model Report* (CRWMS M&O 2000c). Source: Adapted from CRWMS M&O 2000c, Table 1.2-3.

ting in the drift shadow zone; the effects of the drift shadow concentration boundary on engineered barrier system release rates; the effect of matrix diffusion; the significance of three-dimensional transport modeling; and the effects of coupling of thermal-hydrologic, thermal-hydrologic-chemical and thermal-hydrologic-mechanical processes on transport. Results of model refinement of breakthrough time are presented in Volume 1, Section 11 of *FY01 Supplemental Science and Performance Analyses* (BSC 2001a, Figures 11.3.1-7, 11.3.1-8, and 11.3.2-8).

4.2.1.4.2 Seepage Model for Performance Assessment

Abstraction of seepage models for the TSPA, as documented in *Abstraction of Drift Seepage* (CRWMS M&O 2000by), focuses on providing conservative seepage estimates for a wide range of hydrologic conditions.

Selection of Parameter Ranges and Case Studies—Table 4-13 shows four parameters identified for prediction of seepage into the potential repository drifts. Ranges of values are shown for each parameter, which were used as the basis for an extensive sensitivity analysis. The maximum and minimum values for each parameter were selected based on field data and modeling studies. For example, seepage is evaluated for percolation flux as small as 5 mm/yr (0.2 in./yr) and as great as 500 mm/yr (20 in./yr) (CRWMS M&O 2000bx, Section 6.3.6). The higher value accounts for a hypothetical future climate scenario with spatial and temporal focusing effects (CRWMS M&O

2000c, Sections 3.9.3.1, 3.9.3.2, and 3.9.6.4). The rationale for selecting the parameter ranges shown in Table 4-13 is further discussed in supporting documentation (CRWMS M&O 2000bx, Section 6.3). The results of this sensitivity analysis are used in seepage abstraction for the TSPA (CRWMS M&O 2000c, Section 3.9.6) to account for uncertainty in the seepage calibration model.

Results from Modeling of Seepage for Performance Assessment—The seepage percentage is defined as the seepage flux into a drift opening divided by the average percolation flux over the drift footprint (CRWMS M&O 2000c, Section 3.9.1). The seepage model was implemented to evaluate seepage percentage for multiple statistical realizations of the hydrologic property field representing fractured host rock and for many combinations of parameters in Table 4-13 (CRWMS M&O 2000c, Section 3.9.5.3). The results confirm the seepage behavior observed in testing: seepage increases with decreasing permeability, decreasing capillarity, and increasing percolation flux. For most of the realizations examined, the capillary barrier effect resulted in seepage flux that was substantially less than the percolation flux (i.e., seepage percentage much less than 100 percent). Zero seepage was obtained for a significant portion of the realizations calculated.

Abstraction of the Seepage Model for Performance Assessment—The seepage model for performance assessment was used to simulate seepage for a large number of realizations (CRWMS M&O 2000c, Section 3.9.5). Examination of the results revealed that seepage percentage

Table 4-13. Parameter Ranges for Which Seepage is Evaluated Using the Seepage Model for Performance Assessment

Parameter	Minimum	Maximum	Parameter Description
k, m^2 (ft^2)	0.9×10^{-14} (0.9×10^{-13})	0.9×10^{-11} (0.9×10^{-10})	Mean permeability of fracture-continuum
$1/\alpha$, Pa (psi)	30 (4.4×10^{-3})	1,000 (0.15)	van Genuchten's capillary-strength parameter
$\sigma\ln(k)$	1.66	2.50	Standard deviation of log-permeability field
Q_p, mm/yr (in./yr)	5 (0.2)	500 (20)	Percolation flux

Source: CRWMS M&O 2000c, Table 3.9-1.

is most sensitive to a combination of parameters (k/α): the product of fracture permeability, k, and the capillary strength parameter, $1/\alpha$. With this simplification, seepage can be treated as a function of just two variables (i.e., percolation flux and k/α).

The abstraction for TSPA focuses on two quantities: (1) the seepage fraction, which is the fraction of waste package locations (i.e., model realizations) for which seepage is predicted and (2) the seepage flow rate, which is the volumetric flow rate of seepage in a drift segment of specified length. Details of the abstraction procedure are provided in supporting documentation (CRWMS M&O 2000by, Sections 6.2.2 and 6.4). Table 4-14 summarizes the abstracted seepage distributions as they vary with percolation flux for ambient conditions (not the nearly dry conditions expected during repository heating). Seepage threshold values of approximately 200 mm/yr (7.8 in./yr), 15 mm/yr (0.6 in./yr), and 5 mm/yr (0.2 in./yr) are estimated for the minimum, expected (i.e., most likely), and maximum seepage conditions, respectively. Note that these values are different from the previously discussed seepage threshold of 200 mm/yr (7.8 in./yr) (CRWMS M&O 2000c, Section 3.9.4.7) for a single location in Niche 2 in the middle nonlithophysal zone.

Summary and Conclusions for the Drift Seepage Model—Seepage into waste emplacement drifts is important to the performance of a repository at Yucca Mountain. Numerical modeling, field testing, and observations at analogue sites suggest that seepage into repository emplacement drift openings would be substantially less than the local percolation flux. This performance results mainly from capillarity retaining the water in the rock and diverting the flow around the openings. The effectiveness of this capillary barrier principle depends on the percolation flux magnitude, the hydrologic properties of the rock, and the drift opening geometry.

A sequence of models was developed to predict the seepage percentage, seepage threshold, and seepage flow rate for waste emplacement drifts. The seepage model was calibrated against relevant data from liquid injection tests in the Exploratory Studies Facility. Seepage percentages and flow rates were then calculated for a wide range of parameter values representing uncertainty in the model and summarized in a probabilistic abstraction model for TSPA. The results indicate that only 13 percent of waste packages are likely to be

Table 4-14. Uncertainty in Seepage Parameters as a Function of Percolation

q, mm/yr (in./yr)	Minimum Value of k/α			Peak Value of k/α			Maximum Value of k/α		
	f_s	Mean Q_s, m³/yr (ft³/yr)	Std. Dev. Q_s, m³/yr (ft³/yr)	f_s	Mean Q_s, m³/yr (ft³/yr)	Std. Dev. Q_s, m³/yr (ft³/yr)	f_s	Mean Q_s, m³/yr (ft³/yr)	Std. Dev. Q_s, m³/yr (ft³/yr)
5 (0.2)	0	0	0	0	0	0	1.97×10^{-3}	3.21×10^{-3} (0.113)	3.16×10^{-3} (0.112)
14.6 (0.6)	0	0	0	2.45×10^{-3}	7.95×10^{-3} (0.28)	7.09×10^{-3} (0.25)	5.75×10^{-2}	2.26×10^{-2} (0.799)	2.45×10^{-2} (0.865)
73.2 (2.9)	0	0	0	0.250	0.106 (3.74)	0.198 (6.99)	0.744	0.404 (14.3)	0.409 (14.4)
213 (8.4)	4.91×10^{-3}	0.284 (10)	0.188 (6.64)	0.487	1.51 (53.3)	1.15 (40.6)	0.944	3.31 (117)	2.24 (79.1)
500 (20)	6.01×10^{-2}	0.992 (35)	1.05 (37.1)	0.925	5.50 (194)	4.48 (158)	0.999	13.0 (459)	5.74 (203)

NOTES: q = percolation flux; f_s = seepage fraction; Q_s = seep flow rate. Source: Modified from CRWMS M&O 2000by, Table 11.

subject to seepage (CRWMS M&O 2000a, Section 4.1.2). Alternative conceptual models leading to as much as 48 percent of waste packages subject to seepage have been considered (BSC 2001b, Section 4.2.2), although such a high percentage of impacted waste packages is supported only by an inference from an uncalibrated model. The qualitative and quantitative results from seepage testing and modeling, as reflected in the abstraction model, are summarized in Figure 4-37 (CRWMS M&O 2000c, Section 3.9.3).

4.2.2 Effects of Decay Heat on Water Movement

After permanent closure, the heat produced by radioactive decay of the nuclear waste will have an immediate effect on seepage into the repository drifts, water movement through the repository, and the patterns of natural water flow in the unsaturated rock layers. The nature and extent of these effects, however, will depend on thermal loading (or areal heat output), ventilation rates and durations, and attendant thermal operating conditions (i.e., above-
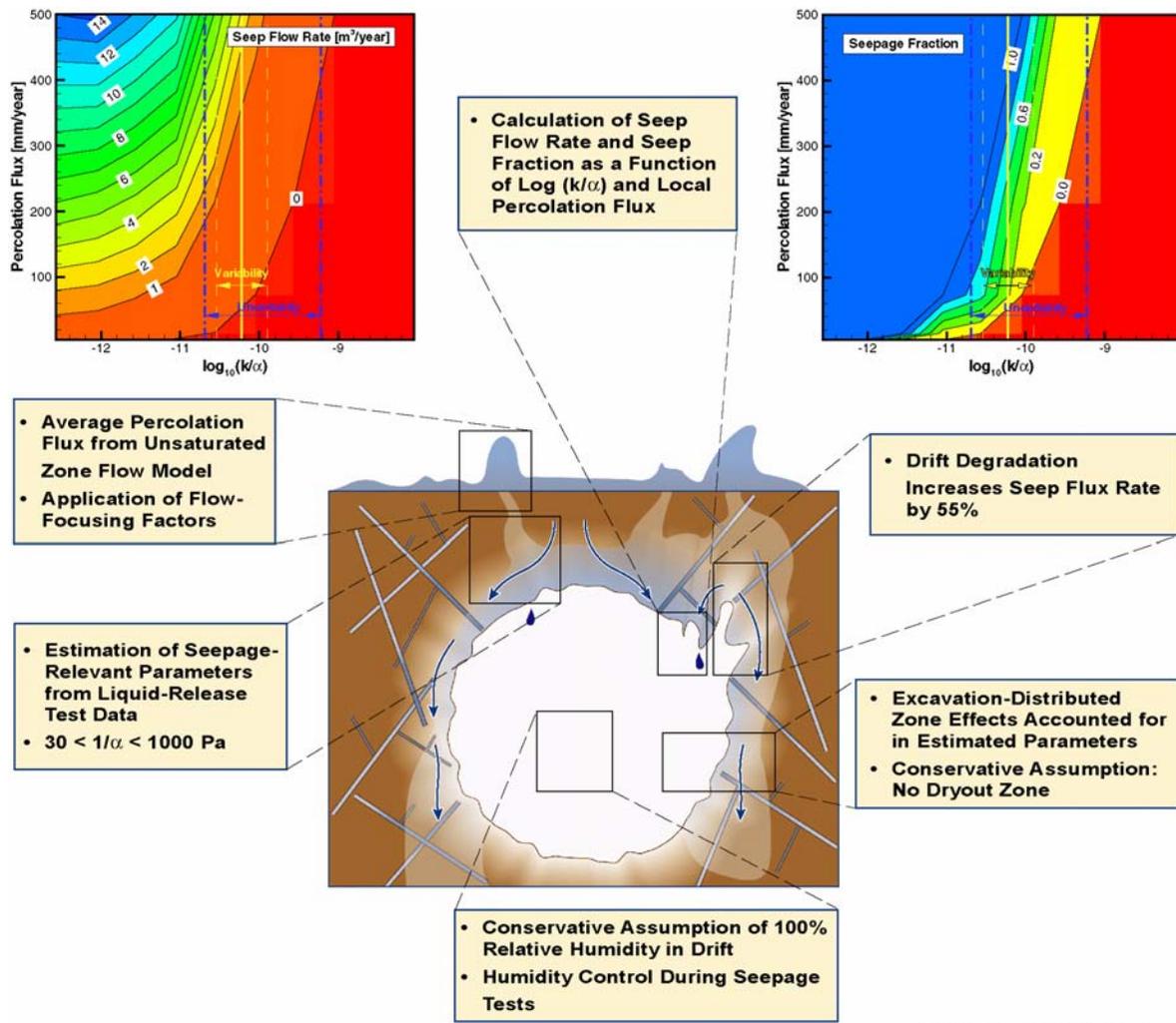
Figure 4-37. Summary of Qualitative and Quantitative Results from Seepage Testing and Modeling
α = van Genuchten "alpha" parameter defining capillary strength; k = fracture permeability. Source: CRWMS M&O 2000c, Figure 3.9-12.

boiling or below-boiling). The analytical and experimental studies conducted to date have examined these heat effects in detail but with emphasis on environmental conditions associated with the higher-temperature operating mode described in Section 2.1.2.3 of this report. The data and analytical results presented in this section mainly describe the effects of higher-temperature conditions on water movement and, specifically, the process models and abstractions employed in the TSPA-SR model, as reported in *Total System Performance Assessment for the Site Recommendation* (CRWMS M&O 2000a).

As noted in Section 4.1.4, the DOE is evaluating operating the repository at lower temperatures, which may reduce the magnitude and duration of the effects of decay heat on water movement described in this section. Alternative thermal operating modes and supplemental uncertainty evaluation results related to thermal hydrology and thermally coupled models are documented or summarized in *FY01 Supplemental Science and Performance Analyses* (BSC 2001a, Sections 4.3.5, 4.3.6., 4.3.7, 5.3, 5.4, and 6.3; BSC 2001b, Sections 3.2, 4.2.2, 4.2.3, and 4.2.4).

This section explains the scientific understanding of how the decay heat from radioactive waste will affect natural water movement into and through the repository and water flow in the surrounding unsaturated rock layers. During the period in which decay heat strongly influences fluid flow, the potential sources of water seeping into emplacement drifts are heat-driven condensate flow (thermal seepage), as opposed to ambient percolation and drift seepage, as discussed in Section 4.2.1. Because of the thermal inertia of the heated rock and the continuing (though declining) heat source, the return to near-ambient temperatures may take many thousands of years (CRWMS M&O 2000al). The goals of the near-field thermal hydrology and thermally coupled process models are to assess the effects of the initial thermal pulse (and longer thermal period) on key environmental conditions, such as temperature and relative humidity in the emplacement drifts. These conditions, in turn, may affect the performance of the engineered barriers and the transport of radionu-

clides (CRWMS M&O 2000al; CRWMS M&O 2000as).

The abstraction of thermal-hydrologic data for use in TSPA represents the potential variability and uncertainty in thermal-hydrologic conditions. It provides a quantitative description of thermal-hydrologic variability (i.e., from variability in the host rock unit, edge proximity, waste package type, infiltration rate, and climate state) and also incorporates uncertainty associated with the infiltration (i.e, lower, mean, and upper). Multiscale model results that are used directly in the TSPA include waste package temperature, relative humidity at the waste package surface, and the percolation flux in the host rock 5 m (16 ft) above the emplacement drift. Temperature and relative humidity are used for the corrosion model, and percolation flux is used for the seepage model. Time-histories of waste package temperature, percolation flux, evaporation rates, and maximum and minimum waste package surface temperatures are also provided (CRWMS M&O 2000cc, Section 6.3).

4.2.2.1 Conceptual Basis

Decay heat generated by radioactive waste may affect the movement of water in the host rock units (CRWMS M&O 2000al, Section 1.1). The conceptual processes described in this section assume thermal loading high enough to result in conditions above the boiling point of water. Under these conditions, decay heat directly affects thermal-hydrologic processes (i.e., movement of water). Heat-driven thermal-chemical processes and thermal-mechanical processes may also affect the movement of water. The conceptual basis for each of these processes is discussed in this section.

4.2.2.1.1 Conceptual Basis of Thermal-Hydrologic Process

Evaporation will occur in the drifts and in the rock immediately surrounding the drift openings. A region of elevated temperature and rock dryout will form around each drift (Pruess, Wang et al. 1990, p. 1241). Heating can change the flow properties of the rock, and the chemical composition of water and minerals in the affected region. These changes can also occur within the drifts in the engineered

barrier system. Figures 4-38 and 4-39 illustrate the conceptual processes of heat-driven water movement.

Calculations indicate that the heat generation rate from radioactive decay decreases rapidly with age relative to the initial output. Heat generation continues at decreased output for thousands of years. Both the initial heat output and its rate of decrease with time depend upon the type of nuclear waste. Calculations indicate that the repository would initially produce approximately 80 MW of thermal power (CRWMS M&O 2000cd, Attachment II). The thermal power output will decrease to approximately 25 percent in 100 years, 12 percent in 300 years, and 2 percent of its initial value in 10,000 years (CRWMS M&O 2000ce, Table I-1).
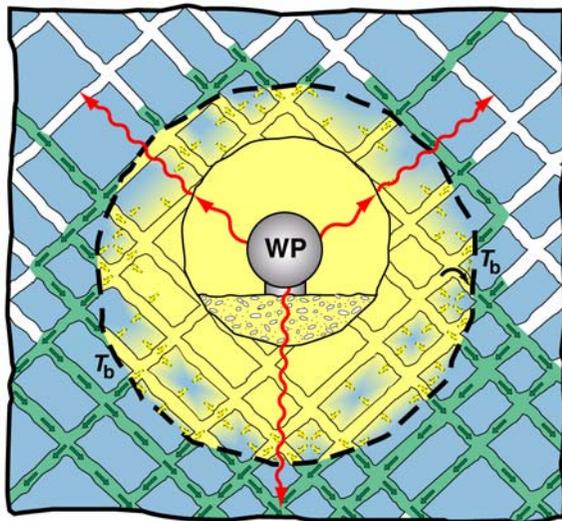
00050DC_ATP_Z1S42_103.ai

Figure 4-38.   Drift-Scale   Schematic   Illustration Showing   Decay-Heat-Driven Thermal-Hydrologic   Flow   and Transport Processes
Fracture flow is shown with solid arrows (green features), water vapor flow is shown with dashed arrows (yellow features), and heat flow is indicated with oscillatory arrows. The ambient (preheating) state of the rock is shown with white fractures and a blue matrix. The boiling isotherm is labeled T_b, and the waste package is labeled WP. The fractures and in-drift features are stylized for the illustration. Source: Modified from CRWMS M&O 2000al, Figure 3-4.

Continuous forced ventilation of emplacement drifts during operations will remove 70 percent of the total decay heat generated during a period of 50 years after the first waste is emplaced. A conservative model, accounting only for heat removed as sensible heat in the ventilation air (and ignoring heat removed by evaporation of moisture), indicates that a ventilation air flow rate of up to 15 m^3/s in each emplacement drift will provide this level of heat removal (CRWMS M&O 2000cd, Section 6.5). The remaining heat output during the preclosure period will be transferred to the host rock by radiation, conduction, and convection, increasing the host rock temperature. Some moisture, and the associated latent heat of evaporation, will be removed by ventilation during this period. At closure, ventilation will cease after drip shields have been placed over the waste packages. This would cause an abrupt increase of heat flux into the host rock.

The major effects of decay heat on water movement would occur after closure (CRWMS M&O 2000cf, Section 6.11.4). Initially, heat will be transported radially away from the drifts by heat conduction through the rock and movement of air through fractures. A portion of the heat will be transported by water that vaporizes near the heat sources and condenses in cooler rock farther away. If the heat flux is high enough, rock near the drifts will be heated to the boiling point of water (nominally 96°C [205°F] at the elevation of the repository) and then to higher temperatures after most of the water in this region has evaporated. The region within which substantially all the water has evaporated is called the dryout zone. Surrounding the dryout zone, a heat pipe zone would form, within which the temperature is essentially constant at the boiling point. The heat pipe zone in turn would be surrounded by a condensation zone of increased water saturation and temperature below the boiling point. After closure, these regions will first expand, then contract as the heat output diminishes over time. The timing of these events will depend on local thermal loading, percolation flux, and location in the potential repository layout (i.e., near the center or the edge). After sufficient time has passed, the temperature will return to preemplacement levels. For purposes of this section, "thermal pulse" is used to describe
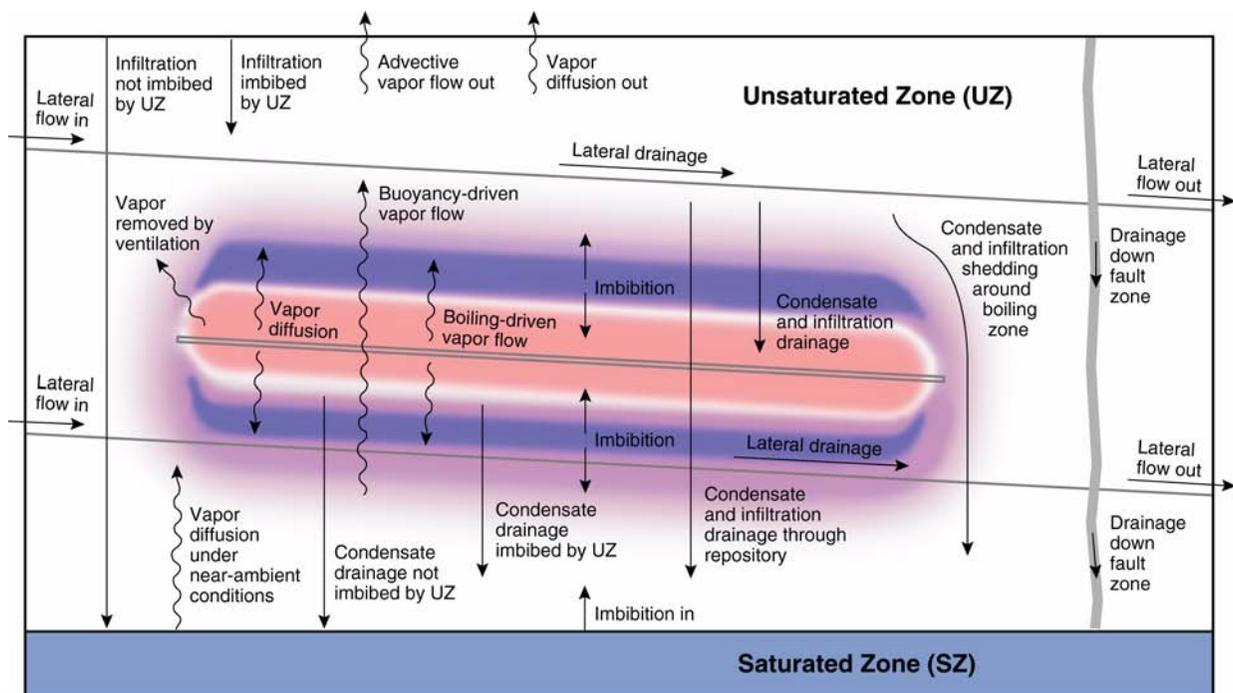
00050DC_ATP_Z1S42_104.ai

Figure 4-39. **Mountain-Scale Schematic Illustration Showing Decay-Heat-Driven Thermal-Hydrologic Flow and Transport Processes that Influence Moisture Redistribution and the Moisture Balance in the Unsaturated Zone**

Source: CRWMS M&O 2000al, Figure 3-5.

the development of above-boiling conditions and the heat pipe zone, a process which may last on the order of a few hundreds of years (CRWMS M&O 2000cf, Figure 6-53). "Thermal period" is generally used to describe the time required for temperatures to return to ambient and may last on the order of tens of thousands of years (CRWMS M&O 2000al). Figures 4-38 and 4-39 provide, respectively, conceptual drift-scale and repository-scale illustrations of thermally driven features and processes during the thermal pulse (CRWMS M&O 2000al, Section 3.2.1).

In the investigation of thermal-hydrologic processes, it has been assumed that heating, cooling, and the resulting movement of water will occur in a system with fixed thermal and hydrologic properties (such as porosity, permeability, and thermal conductivity). Properties of the rock may vary with temperature and water saturation but are assumed to return to preemplacement

values after the temperature returns to ambient levels (CRWMS M&O 2000al, Sections 3.2.2 and 3.3.5). This concept is used to develop process models like those described in Section 4.2.2.3. Thermal-hydrologic processes in the near field will determine the environmental conditions in the drift, including temperature, relative humidity, and seepage at the drift wall.

4.2.2.1.2 Conceptual Basis of Thermal-Hydrologic-Chemical Process

Thermal-hydrologic-chemical processes involve liquid and vapor flow, heat transport, and thermal effects resulting from boiling and condensation; transport of aqueous and gaseous chemical species; mineralogical characteristics and changes; and aqueous and gaseous chemical reactions. Figure 4-40 shows schematically the relationships between thermal-hydrologic and geochemical processes in the zones of boiling, condensation,
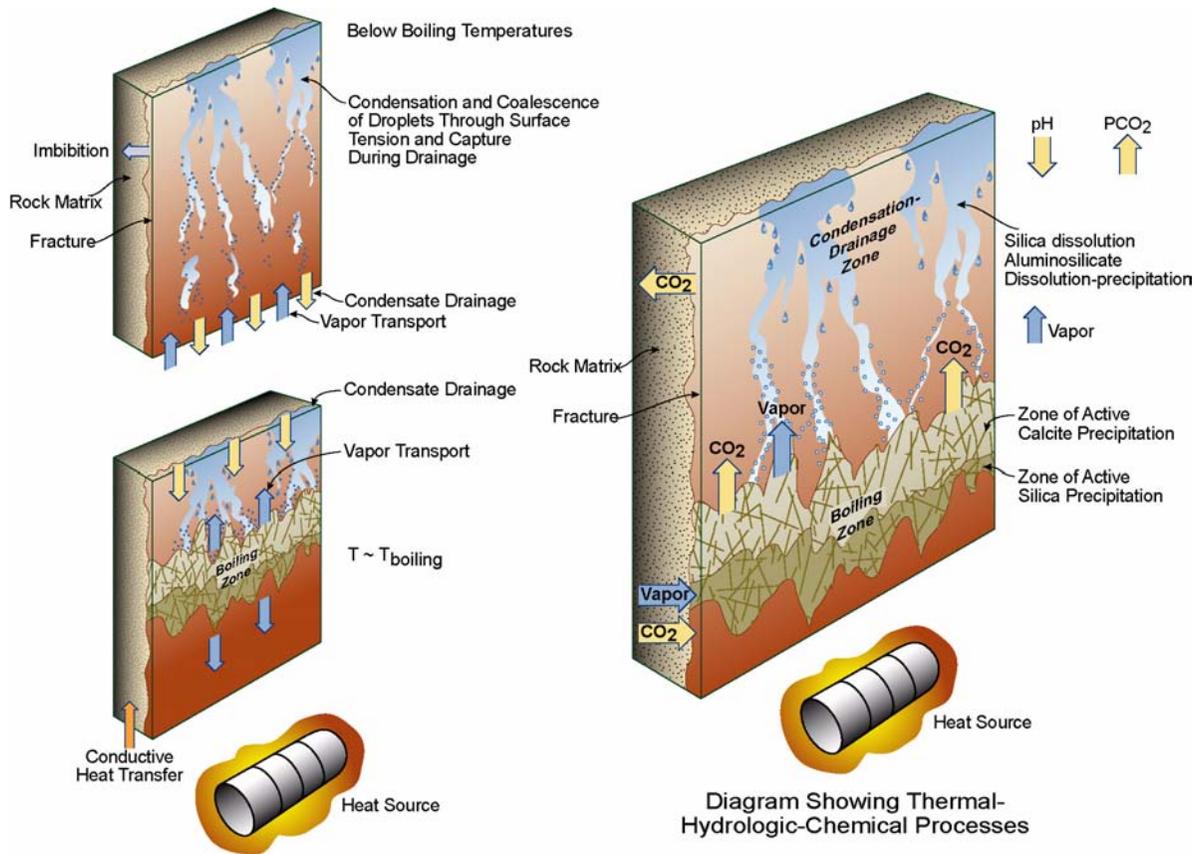
Figure 4-40. Schematic Diagram Showing Relation between Thermal-Hydrologic Processes and Geochemical Processes
Source: CRWMS M&O 2000c, Figure 3.10-2.

and water drainage in the rock surrounding a repository, particularly in the rock above emplacement drifts.

Heat transfer to the drift wall and surrounding rock will evaporate water in fractures first, then the rock matrix. Vapor will migrate out of the matrix blocks and into fractures, where it will move away from the emplacement drifts because of pressure effects and buoyant convection (CRWMS M&O 2000al, Sections 3.1.5 and 3.2.1). In cooler regions further away from the emplacement drifts, vapor will condense on fracture walls. The condensate will then drain through the fracture network; some of this water will drain back toward the heat source.

The resulting localized counter-flow of water vapor and liquid (thermal reflux) is called a heat pipe. A heat pipe zone will develop between the dryout zone and the condensation zone (Pruess, Wang et al. 1990), as discussed previously in Section 4.2.2.1.1.

Chemical evolution of waters, gases, and minerals is coupled to thermal-hydrologic processes. The distribution of condensate in the fracture system will determine where mineral dissolution and precipitation can occur in the fractures and where there can be direct interaction (via diffusion) between matrix pore waters and fracture waters. Investigation of the reactive-transport processes in

the potential repository host rock accounts for different rates of transport in the very permeable fractures, compared to the less permeable rock matrix (Steefel and Lichtner 1998, pp. 186 to 187).

One important aspect of the system is release of carbon dioxide from the liquid phase as temperature increases. The release of carbon dioxide and its transport out of the boiling zone will cause pH to increase in the boiling zone and decrease in the condensation zone. Because gases are more mobile than liquids, the region of gas-phase carbon dioxide transport could be much larger than the region affected by thermally driven water movement (CRWMS M&O 2000al, Section 3.3.1.2).

Conservative species (i.e., those that are unreactive and nonvolatile), such as chloride, will become increasingly concentrated in waters undergoing evaporation or boiling but will be more dilute in the condensate zone. The concentrations of chloride and other constituents in condensate waters will be determined mainly by interaction of fracture waters with matrix pore waters via diffusion. Concentrations of aqueous species, such as calcium, will also be affected by mineral dissolution or precipitation and by reactions involving zeolites, clays, and plagioclase feldspar. Calcite may precipitate in fractures over a broad zone of elevated temperature. Silica precipitation will be confined to a narrower zone where evaporative concentration from boiling causes the silica concentration to exceed solubility limits. Alteration of feldspars to clays and zeolites will be most rapid in the boiling zone. As waters drain away from the emplacement drifts, mineral dissolution and precipitation may occur in fractures or in the adjacent rock matrix (CRWMS M&O 2000al, Section 3.3.1.2).

The composition of the percolating waters above the potential repository (before mixing with condensate) may be similar to matrix pore water, or it may reflect more dilute water that has traveled through fractures (CRWMS M&O 2000al, Section 3.3.1.3). The chemical composition selected for input to the thermal-hydrologic-chemical model is described in Sections 4.2.2.2.1.3, 4.2.2.3.3, and 4.2.3.3.1 of this report.

Changes in the percolation flux can affect the extent of mineral deposition and dissolution because of changes in the fluxes of dissolved species. For example, with more calcium transported toward the emplacement drifts, more calcite would tend to be precipitated. Also, a greater percolation flux will tend to increase the dissolution of minerals that are undersaturated in the fluid (CRWMS M&O 2000al, Section 3.3.1.3).

Mineral dissolution and precipitation in fractures and in the rock matrix can modify the porosity, permeability, and unsaturated hydrologic properties of the potential repository host rock in the vicinity of the emplacement drifts. The extent of mineral–water reactions will be controlled by the surface area of each mineral phase that is exposed to the liquid water. Other factors that may control property changes are the distribution of liquid saturation in fractures, the proportion of fractures with actively flowing water, and the rate of evaporation or boiling, which can control crystal growth and nucleation (CRWMS M&O 2000al, Section 3.3.1.4). Rock–water interactions will affect the chemistry of the water that may seep into the emplacement drifts. The effect of rock–water interactions on hydrologic properties and seepage is evaluated in Section 4.2.2.3.3.

4.2.2.1.3 Conceptual Basis of Thermal-Mechanical Process

The stress field in the rock mass surrounding emplacement drifts would be altered by excavation of drifts and by the heating/cooling cycle associated with emplacement of radioactive waste. The direction and magnitude of principal stresses will change significantly because of thermal loading and then will return to near-ambient values during cooldown—but not completely, since the rock mass will be changed permanently from deformations occurring from stress redistribution; however, the magnitude of changes in hydrologic properties will be limited (CRWMS M&O 2000al, Section 3.5). Compressive stress will build up rapidly in the host rock, especially after the end of the ventilation period. The stress field generally will gradually decay as the temperature in the rock decreases. Potential seismic effects on the repository system are discussed in *Drift Degradation*

Analysis (CRWMS M&O 2000e, Sections 6.3.4 and 7.1); potential effects of fault displacement on the repository system are discussed in *Disruptive Events Process Model Report* (CRWMS M&O 2000f).

The potential repository host rock is a fractured, densely welded, ash-flow tuff. These fractures are expected to deform as stress conditions evolve. Two types of fracture deformations will contribute to thermal-hydrologic-mechanical coupling: normal displacement perpendicular to a fracture plane and shear displacement parallel to a fracture plane.

Rock-mass permeability is an important thermal-hydrologic property for assessment of repository performance. Because the rock has low matrix permeability, the rock mass permeability is mainly associated with fractures, and large changes in rock mass permeability may result from fracture deformation.

The potential effect of fracture deformation on fracture permeability is discussed in Section 4.2.2.3.4. The potential for drift degradation to affect the drip shield (i.e., rockfall on the drip shield) is discussed in Section 4.2.3. The basis for screening these potential processes from the TSPA-SR model is referenced in the process and model and/or the TSPA abstraction sections.

4.2.2.2 Summary State of Knowledge

This section presents a summary of the state of knowledge of properties (rock and fluid) and processes tested in the laboratory and in the field. Much of the information presented in this section is extracted from Hardin and Chesnut (1997).

4.2.2.2.1 State of Knowledge of Laboratory Measured Properties

This section describes the available laboratory data for assessing matrix contributions to thermally coupled processes. Laboratory data for assessing fracture contributions are relatively limited and are described to a lesser extent. Because sample sizes are typically much smaller than the in situ fracture spacing, laboratory measurements generally provide properties of the rock matrix only and do

not directly show the effects of thermally coupled processes on rock-mass behavior. Laboratory data therefore provide only part of the input data required to investigate coupled processes. The properties of fracture networks are also needed and have been inferred from observations and measurements in the field.

4.2.2.2.1.1 Thermal-Mechanical Properties

Variation of matrix thermal and thermal-mechanical properties with temperature is relatively well understood, and data are available. The dependence of matrix and fracture rheology on temperature, including deformation modulus and creep properties, is less well known, but some data at elevated temperature are available. These data do not indicate that rheology is important for prediction of long-term repository performance.

Rock Creep—Laboratory testing of the rock matrix showed that significant creep occurs only when samples are stressed to at least 50 percent, and in some cases more than 90 percent, of their ultimate strength (Martin et al. 1995). Such stress conditions may be uncommon in the host rock, occurring only at fracture asperity contacts. These results also indicate a tendency for fractures in the host rock to close in response to heating and open in response to cooling.

Physical Properties (Porosity and Grain Density)—For the TSw2 welded tuff, these properties change little from ambient temperature up to at least 180°C (356°F). Change in the welded tuff matrix near the emplacement drifts is expected to be minor and will probably be caused mainly by mineral phase transitions (e.g., a→b cristobalite) and dehydration of hydrous phases, such as clinoptilolite and smectites. Of these, dehydration of hydrous fracture-lining minerals has a greater potential to affect host rock performance (Hardin and Chesnut 1997, Section 2.2).

Thermal Conductivity—Laboratory measurements of thermal conductivity have been performed on samples from the Exploratory Studies Facility, in conjunction with field-scale thermal testing (Brodsky et al. 1997). There is a slight increase of thermal conductivity with

temperature for the Topopah Spring welded tuff. Water saturation apparently increases thermal conductivity of the TSw2 welded tuff by approximately 50 percent. A small pressure effect in other rock types, whereby conductivity increases with confining stress, has been observed and is probably caused by closing of microcracks. Pressure effects on thermal conductivity have not been examined for Yucca Mountain tuffs but are likely to be small or highly localized in the host rock.

Heat Capacitance—When measured on dried samples, the heat capacitance of the TSw2 welded tuff increases about 20 percent from ambient temperature to 200°C (392°F) (SNL 1996). Behavior at temperatures greater than 150°C (302°F) is affected by mineral phase transitions, notably that of cristobalite, which occurs at temperatures greater than 200°C (392°F). In polycrystalline rocks, the cristobalite transition apparently occurs over a temperature range of 20 to 50 C° (36 to 90 F°).

Thermal Expansion—The coefficient of thermal expansion for TSw2 welded tuff increases with temperature because of mineral-phase transitions and dilatancy caused by heterogeneous thermal expansion of different minerals. Linear unconfined expansion measurements have been reported for ambient pressure, temperatures to 300°C (572°F), and several saturation states (Brodsky et al. 1997, Table B-5) determined from samples that are somewhat heterogeneous and exhibit some variability between samples. Measured thermal expansion for samples of TSw2 welded tuff varies by a factor of about five. Thermal expansion is relatively insensitive to saturation. Hysteresis becomes apparent at temperatures greater than 200°C (392°F), probably because expansion produces irreversible changes in rock fabric.

Mechanical Properties—For the Topopah Spring welded tuff, long-term (3.5- to 6-month) changes in the mechanical properties of three samples were investigated at temperatures of 80°, 120°, and 180°C (176°, 248°, and 356°F) (Hardin and Chesnut 1997, Section 2.5.1). The results indicate that temperature effects on mechanical properties are smaller than the differences between the samples. More recently, a 0.5-m (1.6-ft) scale block of Topopah Spring welded tuff was subjected to uniaxial loading at temperatures as great as 85°C (185°F) (Hardin and Chesnut 1997, Section 3.8.1). The apparent Young's modulus for the tuff matrix at several locations in the block decreased significantly as temperature increased.

Compressive Strength Versus Saturation—It has been reported that a significant decrease in compressive strength could be associated with increased saturation (Nimick and Schwartz 1987, Section 3.4.2.2.1). This observation was based on early studies that may have been affected by different methods used to control sample saturation (Boyd et al. 1994, Section 4.3).

4.2.2.2.1.2 Hydrologic Properties

Thermal-hydrologic processes in fractured rock have been investigated theoretically and experimentally since the early 1980s (Pruess, Tsang et al. 1984; Pruess, Wang et al. 1990; Buscheck and Nitao 1993; Pruess 1997; Tsang and Birkholzer 1999; Kneafsey and Pruess 1998). The laboratory work and early field studies are reported in *Synthesis Report on Thermally-Driven Coupled Processes* (Hardin and Chesnut 1997) and *Near-Field Environment Process Model Report* (CRWMS M&O 2000al, Sections 2.2 and 3). See also Section 4.2.1.2.5 of this document for hydrologic properties of fractures.

For matrix hydrologic properties, there are fundamental temperature-dependent responses that may be important to understanding the thermal-hydrologic process. These include the temperature effect on hysteresis of wetting and drying characteristic curves, Knudsen diffusion, and enhancement of vapor diffusion (CRWMS M&O 2000al, Section 3.6.3.1).

Matrix Permeability—Variations in matrix permeability of the Topopah Spring welded tuff that are associated with temperature changes have been found to be much less than natural variations between samples (CRWMS M&O 2000al, Section 3.6.3.1).

Unsaturated Hydraulic Conductivity—A limited number of measurements have been made of unsaturated matrix conductivity in Yucca Mountain tuffs. Changes in the properties of water at elevated temperature (viscosity and surface tension) suggest that unsaturated conductivity may increase by as much as an order of magnitude from 20° to 100°C (68° to 212°F). The viscosity effect is taken into account in current thermal-hydrologic simulations, but the surface-tension effect is not. In addition, changes in the water–rock–air contact angle at elevated temperature can also influence unsaturated conductivity (Hardin and Chesnut 1997, Section 2.10).

Enhanced Vapor Diffusion—No enhancement in vapor diffusion was observed in a limited investigation of the Topopah Spring welded tuff matrix (Wildenschild and Roberts 1999).

Knudsen Diffusion—Knudsen diffusion and its variation with temperature are possible mechanisms for transport of moisture in the host rock (Hardin and Chesnut 1997, Section 2.7.4). This is likely to be of little significance and has not been investigated experimentally.

4.2.2.2.1.3 Chemical and Transport Properties

Chemical reactions are strongly temperature-dependent, and laboratory measurements of reaction rates and surface areas under controlled conditions are sparse. However, experimental kinetic data are not generally needed for reactions that can be modeled satisfactorily using qualified thermodynamic equilibrium and reaction-path models, such as EQ3/6 and its associated chemical databases. Determination of which chemical processes in the potential repository can be modeled in this manner rely on results from laboratory and field-scale testing.

Thermodynamic equilibrium data for many aqueous and mineral species have been measured or estimated, and reviewed for accuracy and consistency in preparation for use with qualified analyses. For certain other types of reactions (e.g., surface complexation), equilibrium conditions at elevated temperatures are relatively unknown.

Seepage Water Compositions—Two water compositions have been considered for use in TSPA-SR modeling for various purposes. One is referred to as chloride-sulfate-type water that is based on the chemical analyses of matrix pore waters from near the Drift Scale Test (CRWMS M&O 2000cg, Sections 6.5 and 6.7.4; BSC 2001o, Section 6.1.2). Another is referred to as bicarbonate-type water, based on the composition of J-13 well water (CRWMS M&O 2000cg, Section 6.5; see also Section 4.2.4). The chloride-sulfate-type water is more concentrated in total dissolved minerals and is selected for calculations that evaluate potential changes in fracture properties from precipitation of minerals and salts. The source of water and gas chemistry for use in the thermal-hydrologic-chemical model is based on the chemical composition of matrix pore water collected from Alcove 5 (BSC 2001o, Sections 4.1.3 and 6.1.2).

Behavior of Radionuclides in J-13 Water—Experimental data on the speciation and solubility of important radionuclides at elevated temperature are limited. However, the investigation of spiked J-13 water at temperatures as great as 100°C (212°F) indicates that plutonium solubility decreases, but uranium, neptunium, and americium remain soluble or become increasingly soluble at elevated temperatures (Nitsche 1991). Carbonate complexes appear to be important to the solubility of uranium, neptunium, and americium at elevated temperatures. Knowledge about complexation and solubility of nickel, zirconium, technetium, uranium, neptunium, plutonium, and americium in J-13 water at elevated temperatures was published in a recent review (Wruck and Palmer 1997).

Hydrothermal Tuff Alteration—Batch studies of hydrothermal alteration of wafers of Topopah Spring welded, devitrified tuff have been performed at temperatures from 90° to 250°C

(194° to 482°F) and for durations to 120 days (Knauss 1987; Knauss and Beiriger 1984; Knauss, Beiriger et al. 1987; Knauss, Delany et al. 1985; Knauss and Peifer 1986; Oversby 1984a; Oversby 1984b; Oversby 1985). They show that changes in the composition of water in contact with the tuff are moderate at temperatures as great as 150°C (302°F), with slight alteration of the tuff over a few months. At higher temperatures, similar alteration products are produced, but reaction rates increase significantly. Accelerated experiments on crushed tuff at temperatures greater than 150°C (302°F) have produced more extensive alteration, including metastable phases.

Energetics of Zeolite Dehydration—Zeolites could have a significant effect on the heat and water balance where they are abundant because zeolite dehydration is more energetic than evaporation of water on a molar basis (Bish 1995; Wilder 1996, Section 3.4.3; Hardin and Chesnut 1997, Section 2.6.2.1). Zeolite hydration is apparently reversible at dehydration temperatures as great as 215°C (419°F) for clinoptilolite, so complementary effects will occur during repository cooldown. Altered units above and below the repository horizon contain a large fraction of zeolites; the data produced by these studies indicate that dehydration will cause some amount of shrinkage, increasing porosity and probably also increasing permeability. This could affect the water-perching behavior at altered zones associated with the upper and lower Topopah Spring vitrophyres.

Effect of Hydrothermal Alteration on Flow Paths—Plug-flow reactor studies involving flow-through reaction of J-13 water with crushed tuff at 240°C (464°F) resulted in significant dissolution of alkali feldspar and cristobalite (DeLoach et al. 1997, p. 5). This experiment produced significantly different results from those of batch reactor studies at similar temperatures (i.e., predominantly dissolution instead of alteration). The two approaches span the range of conditions likely to exist in the host rock: stagnant vs. flowing water in the tuff matrix or along fractures. Dissolution and alteration behavior of the major minerals constituting the host rock are temperature-dependent and much slower at temperatures near the boiling point of water.

Limitations of Available Kinetic Data—The available kinetic data for dissolution of mineral phases that may be important to repository performance are limited reflecting the general sparseness of laboratory data on kinetic interactions involving rock. Different investigators have used various investigation and measurement strategies, and test results are sensitive to methodology (e.g., batch methods versus flow-through methods).

Kinetics of Silica Dissolution and Precipitation—Reaction rates for dissolution of quartz and silica polymorphs, and precipitation of amorphous silica, are key parameters in estimating the extent and magnitude of thermal-hydrologic-chemical coupled effects in the host rock. Dissolution will be expressed in heat pipe zones where refluxing water is at approximately 100°C (212°F). Mineral species like silica will then be deposited where the reflux water evaporates or boils. A boiling front will expand outward from each emplacement drift, but eventually reverse because of less heat generation. Depending on how fracture properties and connectivity are affected by precipitated minerals, seepage into the drift openings may become more or less likely during cooldown.

Experimental Data for Silica Kinetics—Dissolution rates are key parameters for estimating the extent and magnitude of thermal-hydrologic-chemical coupled effects in the host rock. In a classic study, the dissolution rate for silica polymorphs increased by 2 orders of magnitude for each 100 C° (180 F°) temperature increase, with a factor of 300 increase in the dissolution rate between 25° and 70°C (77° and 158°F) (Rimstidt and Barnes 1980, Figure 9). In addition, upon cooling a saturated silica solution, decreasing solubility caused supersaturation, while the rate constant for precipitation decreased, producing a maximum precipitation rate at a temperature 25 to 50 C° (45 to 90 F°) less than the saturation temperature. A more recent investigation of quartz dissolution kinetics at 70°C (158°F) (Knauss and Wolery 1988) produced dissolution rate data that were similar, at neutral to mildly alkaline pH, to rates predicted for quartz by the classic model.

Interaction of Radionuclides with Alteration Products of Introduced Materials—Surface

complexation reactions will be important for retardation of actinides, and possibly pertechnetate, in the host rock. Introduced materials, including structural steel, could be a source for potential high-affinity sorbents for radionuclides. If the sorbents are colloidal, the sorbed radionuclides may be transported. Limited test data for radionuclide sorption on these materials (e.g., goethite, clays, or silica polymorphs) are available, mainly for ambient temperature and simplified chemical systems (see, for example, Section 6.6 of *Engineered Barrier System: Physical and Chemical Environment Model* [CRWMS M&O 2000cg]).

Matrix Diffusion Effects—Diffusion of radionuclides into minerals and into the tuff matrix is an important temperature-dependent retardation mechanism. The tuff matrix has been shown to contain ubiquitous nanopores that support slow diffusion, plus a few connected paths through which diffusion is much faster but limited in overall effect. Effective diffusion coefficients have been estimated for uranium migration into polished wafers of Topopah Spring Tuff at ambient temperature (Wilder 1996, Section 7.4.1). Relative diffusivities of actinide and technetium species have been compared at 90°C (194°F) using "tuff cup" experiments (Hardin and Chesnut 1997, Section 2.10). Effective diffusion parameters for migration of strontium and cesium ions in clinoptilolite have been estimated (Hardin and Chesnut 1997, Section 2.6.5.1). These data generally indicate that the rate of diffusion in the tuff matrix and sorbent minerals is enhanced at elevated temperature.

4.2.2.2.1.4 Other Properties

Self-Potential—Naturally occurring electrical potentials were observed in the Single Heater Test and in the Drift Scale Test and were large enough to be considered as a factor in waste package corrosion analyses, but the source of these potentials and the amount of current generated have not been investigated (Hardin and Chesnut 1997, Section 2.10).

Microbial Activity—Investigations have established that the natural microbes present in the unsaturated zone, plus those introduced by excava-tion, include species that can survive exposure to desiccation and elevated temperature. Some species produce metabolic products that could be important in determining rates of corrosion and radionuclide transport in the near-field environment. There are few data that can be used to describe microbial activity at elevated temperatures (Hardin and Chesnut 1997, Section 2.10).

4.2.2.2.2 Laboratory-Scale Process Investigations

Laboratory experiments have included comparison of vapor-phase and liquid-phase rewetting, fracture healing, fracture–matrix coupling with flow into heated tuff, fracture flow visualization, heat pipe formation, and rock–water interaction studies. These physical simulations of thermally coupled processes have advanced conceptual understanding and provided data for testing mathematical models.

Rewetting Behavior—Testing of wafers of welded tuff has indicated (Wilder 1996, Section 2.1.1) that water-retention hysteresis varies at elevated temperatures. Typical wetting/drying hysteresis at ambient temperature was nearly zero at 78°C (172°F) and reversed at 94°C (201°F). Rewetting behavior at elevated temperature is also summarized by Hardin and Chesnut (1997, Section 2.7.5). The effect is probably related to changes in surface tension and the rock–water–air contact angle at elevated temperatures. Hysteresis behavior is generally ignored, for computational expediency, in thermal-hydrologic models, and this appears to be defensible. The possible effects of negative hysteresis have not been considered.

Vapor Resaturation—Tuff matrix rewetting due to the presence of saturated water vapor (100 percent relative humidity) has a different result than rewetting by liquid at the same zero potential. Experimental data (Buscheck et al. 1992) show that rewetting of dry tuff in the presence of water vapor occurs much more slowly than does rewetting by imbibition of liquid water. This effect is incorporated in thermal-hydrologic models by adjusting the matric potential versus saturation relationship so that matrix saturation of 30 to 40 percent or greater corresponds to a relative humidity of nearly 100 percent. The vapor resatu-

ration effect strongly influences the timing of rewetting in the repository (Wilder 1996, Section 10.1) and tends to increase the relative humidity calculated at waste packages during cooldown.

Fracture Healing—An understanding of fracture-permeability reduction has been developed, and observations reported in the literature can be explained by three mechanisms (CRWMS M&O 2000al, Section 3.6.3.3):

1. Dissolution of fracture asperities by flowing water and consequent aperture reduction under the influence of confining stress

2. Dissolution/precipitation reactions that clog porosity by redistributing silica or by creating alteration products with greater molar volume

3. Migration of heated pore water from the rock matrix, toward fractures, where the pressure is lower and evaporation or boiling occurs, clogging fractures or the matrix porosity.

Experiments have shown that flowing water or steam promotes permeability reduction, and the effect is strongest at temperatures greater than 90°C (194°F) (Hardin and Chesnut 1997, Section 3.10) (Figure 4-41). All these mechanisms can lead to changes in fracture porosity and permeability in the host rock where there is sufficient water.

Fracture–Matrix Coupled-Flow Visualization— Fracture flow studies in the laboratory (Hardin and Chesnut 1997, Section 3.3.1) have physically demonstrated fracture–matrix flow coupling in welded tuff, using x-ray imaging to visualize the flow (Figure 4-42). By varying the water injection pressure and the resulting flow velocity, the nonequilibrium nature of flow coupling was demonstrated. When the experiment was repeated with a thermal gradient, a different flow regime resulted, with localized precipitation of the solute tracer (Figure 4-42).

Flow Channelization—Visualization experiments (Hardin and Chesnut 1997, Section 3.4) showed, among other findings, that fracture transport in response to constant boundary conditions can be unsteady and produce intermittent rivulets that "snap off" and reform episodically. The authors related the average repetition rate for episodic flow
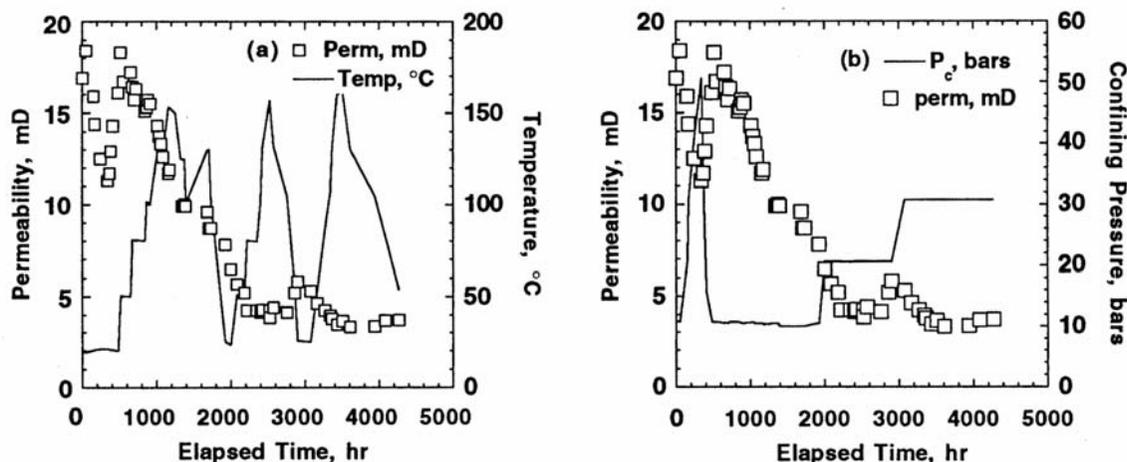
00050DC_ATP_Z1S42_106.ai

Figure 4-41. Permeability of a Single Fracture in a Core Sample of Topopah Spring Welded Tuff as a Function of Time and Exposure to Flowing Water
Temperature (left) and confining pressure (right) during the test series are plotted for comparison. Source: CRWMS M&O 2000al, Figure 3-101.

80°C

85°C

93°C

98°C

103°C

111°C

148°C

00050DC_ATP_Z1S42_107.ai
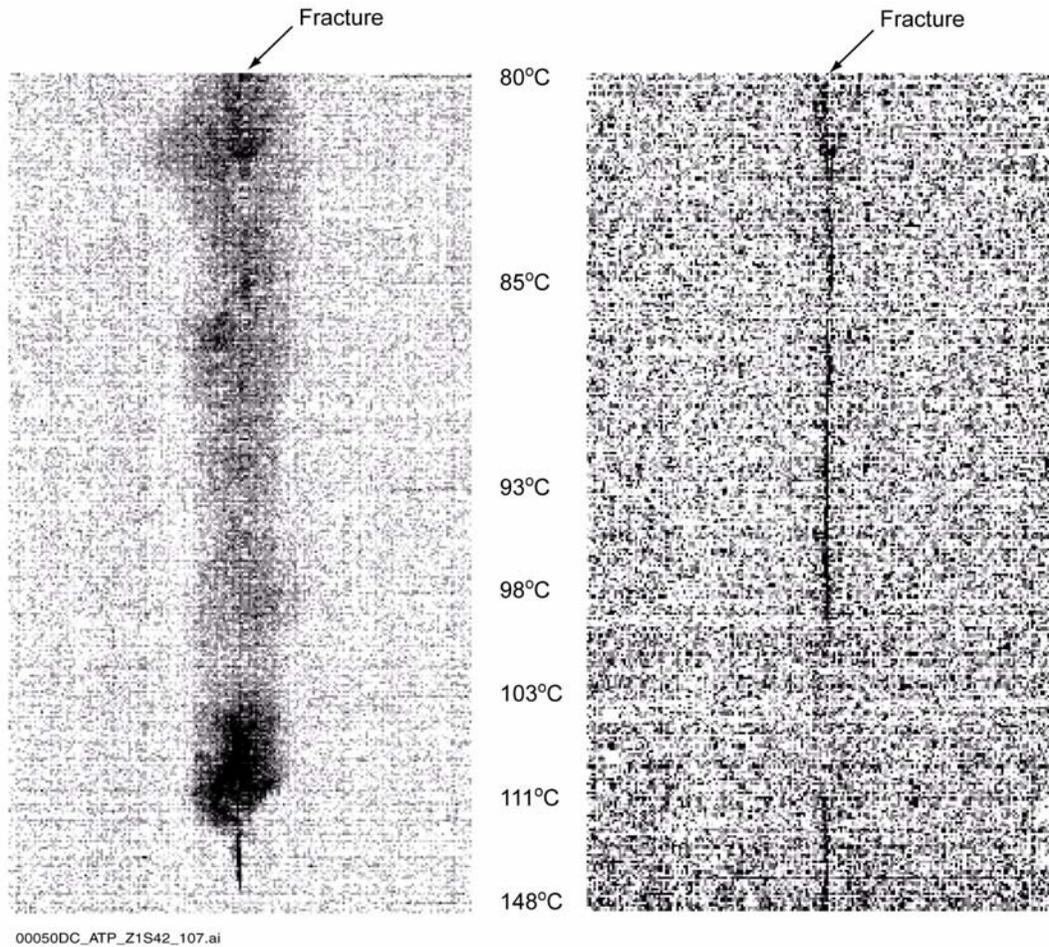
Figure 4-42. Difference X-Ray Radiography Images of 7.2 Hours (left) and 0.67 Hours (right) after Flow was Initiated
Left image 7.2 hours and right image 0.67 hours after flow was initiated. Thermal gradient is indicated between the figures. The difference between these two experiments was the height of the water column: 0.26 m (left) and 0.46 m (right), respectively. The difference in head was large enough to force flow through the boiling region in the right image. Source: CRWMS M&O 2000al, Figure 3-102.

with fracture aperture and wetting properties and the inclination of the models to gravity. These ambient-temperature experiments demonstrated that simple, simulated fractures can produce unsteady fracture flow in response to constant boundary conditions. Similar flow can be expected in the fractures of a heat pipe zone. These data have important implications for fracture–matrix interaction (i.e., there is limited contact time available for fracture–matrix interaction).

Physical Models of Heat Pipes—Fracture thermal-hydrology visualization studies by Kneafsey and Pruess (1997) examined conditions

(e.g., fracture saturation, temperature difference, and fracture dimensions) that support heat pipe development. Heat pipes were observed in parallel plate fractures containing obstacles, heat sources, and vents. Film flow as well as meniscal flow were observed to produce heat pipes (Figure 4-43). Unsteady rivulet-flow behavior, analogous to episodic fracture flow at ambient temperature, was observed (Hardin and Chesnut 1997, Section 3.5.1). Rapid evaporation events occurred when "islands" of fluid became superheated and suddenly boiled, constituting another mechanism for unsteady flow with the potential to rapidly disperse solute. A few of these observations were
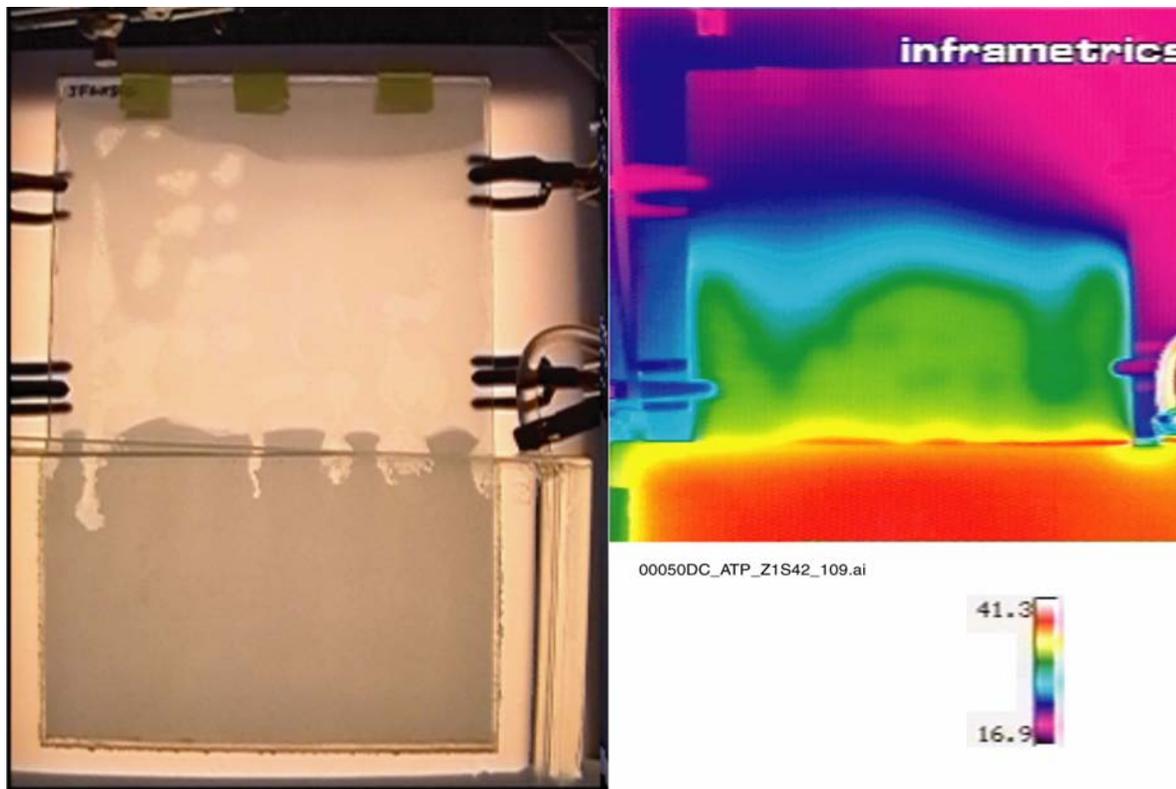
Figure 4-43. Pentane and Temperature Distribution Showing Heat Pipe

Experiment 9: T_{bath} = 42.4°C. Color scale indicates temperatures shown in the right image in °C. The experiment was conducted by injecting a small amount of pentane liquid between panes of glass. The lower half of the apparatus (shown in the left image) was immersed in a temperature bath sufficiently warm to boil pentane. The upper part of the apparatus was warmed by migration and condensation of pentane vapor, as seen in the green region in the right image. This region, in which vapor moved up and liquid moved down, was a heat pipe zone. The temperature in this zone was maintained at nearly the boiling point of pentane by thermal reflux activity. Source: CRWMS M&O 2000al, Figure 3-104.

repeated with a half-cast model incorporating welded tuff as one fracture wall.

Water–Rock Interaction—Chemical analyses of effluent water from matrix flow and fracture flow experiments have indicated water–rock interaction. When J-13 water was flowed through an intact core sample, the concentration of most major anions and cations first increased, then approached influent concentrations (Hardin and Chesnut 1997, Section 3.6.2.2). Anions such as chloride and sulfate were leached in quantities that may be significant to the in-drift chemical environment. Other reported data for similar tests (Hardin and Chesnut 1997, Section 3.6.2.1) included chemical analyses of water that flowed through a healed, natural fracture at elevated temperatures.

Fracture Flow in a Heated and Stressed Block—Laboratory tests were conducted on 0.5-m (1.6-ft) scale blocks to monitor fracture flow and mechanical deformation properties under conditions that approximated the near-field environment expected in a repository at Yucca Mountain (Costantino et al. 1998). In this test, a rectangular block was bisected by an artificial fracture perpendicular to the fabric of the tuff. Water was supplied at a point source at the center of the fracture under various pressures. Both fluid flow and mechanical properties were found to be anisotropic and strongly correlated with the ash-flow fabric of the sample. Fluid flow measurements revealed that only minor imbibition of water occurred through the fracture surfaces, and that flow rates were independent of normal stress up to 14 MPa across the fracture, and at temperatures to 140°C (280°F). Flow through

the fracture occurred largely through uncorrelated porosity that intersected the fracture plane.

4.2.2.2.3   Field-Scale Processes

This section briefly describes selected results from a number of field-scale tests and natural processes having some features in common with processes expected at Yucca Mountain. Emphasis is given to thermally driven coupled processes. The field-scale tests include those presented by Hardin and Chesnut (1997) and those presented in the *Near-Field Environment Process Model Report* (CRWMS M&O 2000al, Section 3.6.1). These tests are grouped into three groups: non-Yucca Mountain tests, Yucca Mountain tests, and natural analogues.

4.2.2.2.3.1 Non-Yucca Mountain Tests

Climax Spent Fuel Test (Hardin and Chesnut 1997, Section 4.1.1; Wilder and Yow 1987)—Acoustic emissions responded to the rate of thermal energy production and may be useful for monitoring the stability of a repository. No significant changes in mineralogy or microfracturing occurred, as a result of heat or irradiation, near the electrical heaters or spent nuclear fuel canisters. Nitric acid formed by radiolysis of atmospheric nitrogen accelerated corrosion of the carbon steel emplacement hole liners. Corrosion was also observed in alloys such as stainless steel, Inconel 600, and super-Invar.

Edgar Mine, Colorado School of Mines (Hardin et al. 1982)—Heating of a fractured gneiss caused significant reductions in the loading and unloading moduli and reductions in the permeability of a test fracture. The largest permeability change occurred during excavation. Compressive loading reduced the permeability, but the permeability did not return to the preexcavation condition. Permeability reduction at elevated temperatures was smaller in magnitude than the effect of excavation.

G-Tunnel Small-Diameter Heater Tests (Zimmerman and Finley 1987)—For the first month of heating in the horizontal heater test in welded tuff, small amounts of water collected in the heater borehole and wetted a sensor located

immediately under the heater. Relative humidity approached saturation within hours after the start. Total pressures remained at ambient. Neutron-probe measurements of moisture content in the heated rock showed that significant changes occurred in the temperature range 70° to 120°C (158° to 248°F). Dewatering apparently began at temperatures less than boiling.

G-Tunnel Heated Block Test (Zimmerman et al. 1986)—A slight dependence of modulus on stress was indicated, but there was no significant temperature effect. Thermal expansion behavior of the heated block was well represented by measurements on intact rock samples. The largest changes in permeability of a test fracture were associated with excavation. Subsequent compressive loading and increased temperature lowered the apparent permeability of a test fracture. Saturation declined, in steps corresponding to successive cycles, from 60 to 80 percent and down to approximately 15 percent as a result of heating. Rehydration upon cooling was not significant on a time scale of weeks.

G-Tunnel Prototype Engineered Barrier System Field Test (Hardin and Chesnut 1997, Section 4.1.3; Ramirez et al. 1991; Lee and Ueng 1991)—The drying front penetrated most rapidly along fractures, and rewetting occurred most rapidly near fractures during the ramping down and cooling phases. Water vapor that condensed below the heater drained away from the boiling zone, and rock below the heater dried out more quickly than it did above the heater. During cooling, rewetting above the heater occurred slightly more quickly than it did below the heater. After heating and cooling back to ambient temperature, measured permeability in the heater borehole increased by 10 to 1,800 percent. The increase was greatest in intervals with the smaller values of preheating permeability. The boiling zone acted as an "umbrella," shielding rock below the heater from drainage of condensate generated above the heater.

Underground Tests at Stripa, Sweden—Fracture closure in response to heating was confirmed by observation of diminished water inflow to heater and instrument boreholes (Nelson et al. 1981).

4.2.2.2.3.2 Yucca Mountain Tests

Large Block Test—The Large Block Test was described by Wilder et al. (1997). Figure 4-44 shows the Large Block Test during its construction, and a schematic of the test showing the instrument boreholes is given in Figure 4-45. One-dimensional heating geometry and moisture movement in the block were achieved as planned. Boiling of the pore water was indicated by temperatures measured near the heaters. Figure 4-46 shows the temperature measured at the TT1-14 and TT2-14 temperature sensors. Note that the boiling temperatures apparent from these two figures are slightly different, indicating heterogeneity in the pore pressure and/or concentration of chemicals in the pore water. Heat pipe activity was observed along the two vertical temperature holes in the block. Figure 4-47 illustrates one aspect of that heat pipe activity, whereby condensate drainage toward the heaters was most evident during the two thermal refluxing episodes of the Large Block Test. Figure 4-48 illustrates one of those refluxing episodes and the

00050DC_ATP_Z1S42_181.ai

Figure 4-44   Photograph of the Large Block Test Site

This photograph shows the Large Block Test during construction, with the block itself exposed as the exterior insulation is being constructed from the bottom to the top.

episodic water movement that followed its onset. Cooler liquid water apparently penetrated the heated interval, causing the temperature in a wider zone extending above and below the heaters to converge to near the boiling point. This was followed by episodic thermal refluxing, which caused the temperature to fluctuate. The redistribution of moisture was monitored by electrical resistivity tomography and neutron logging, as shown in Figure 4-49 and Figure 4-50, respectively. These refluxing events are believed to have been caused by rainstorms, which introduced water into the test.

Drying of the Large Block Test was also nearly one-dimensional. Neutron logging shows that localized dryout reached its maximum after about 334 days of heating. Subsequent heating extended the dryout zone but did not dry out the rock further. Mechanical displacement measurements on the block indicate that during the June 1997 thermal refluxing episode, a major near-horizontal fracture near the top of the block opened approximately 0.0094 to 0.011 cm (0.0037 to 0.0043 in.) at the northern and eastern sides, with a 0.0058 cm (0.0023 in.) shear displacement on the western side. Deformation data also indicate that during heating the block experienced horizontal expansion that increased linearly with height above the base. These deformations may have affected the hydrologic properties of the block. Simulation of the Large Block Test using the thermal-hydrology modeling code NUFT was used to capture the major characteristics of the measured temperatures of the Large Block Test (CRWMS M&O 2000al, Section 3.6.1.1) (see additional discussion below).

Single Heater Test (CRWMS M&O 2000al, Section 3.6.1.2)—The Single Heater Test was described in *Single Heater Test Final Report* (CRWMS M&O 1999m). A schematic of the Single Heater Test is shown in Figure 4-51. Measurement of mechanical displacements in the Single Heater Test showed expansion along the heater hole, with compressive movement at the beginning of the heating, followed by expansion perpendicular to the heater. These results were simulated by calculations using the continuum mechanical modeling code FLAC. Simulation using the thermal-hydrology modeling code
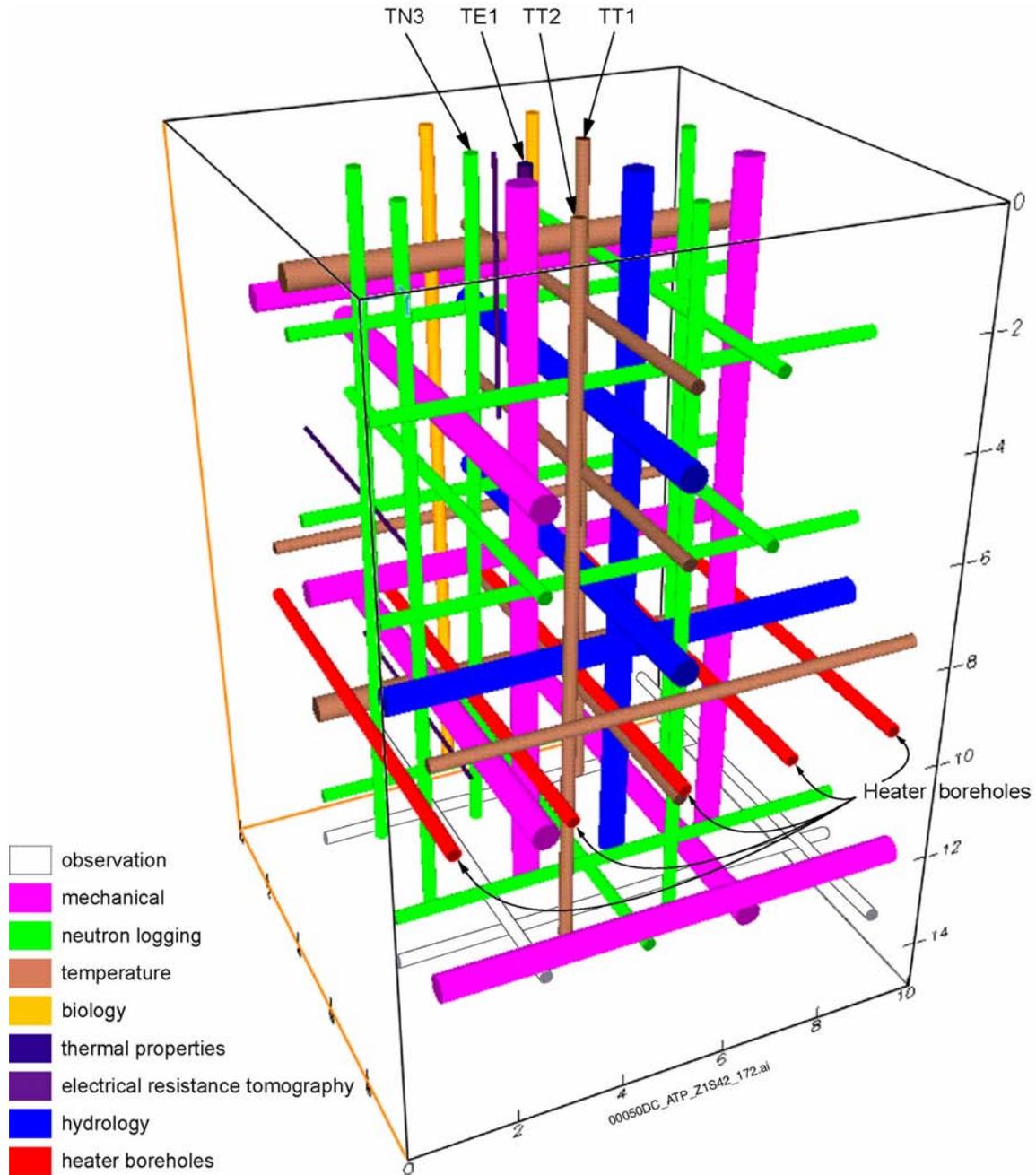
Figure 4-45.   Schematic of the Large Block Test Instrument Boreholes

Borehole diameter is significantly exaggerated in the illustration. Only the heater boreholes and the instrument boreholes discussed in this section (i.e., TE1, TN3, TT1, and TT2) are labeled. Source: Modified from CRWMS M&O 2000al, Figure 3-49.
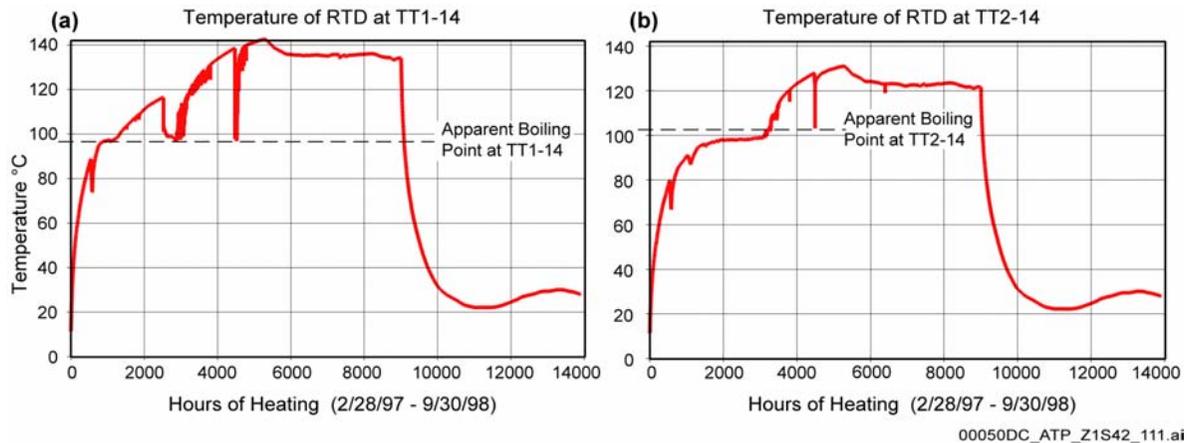
Figure 4-46   Temperatures Measured at (a) TT1-14 and (b) TT2-14 of the Large Block Test as a Function of Elapsed Time

See Figure 4-45 for the locations of Boreholes TT1 and TT2. RTD = resistance temperature detector. Source: CRWMS M&O 2000al, Figures 3-50 and 3-51.
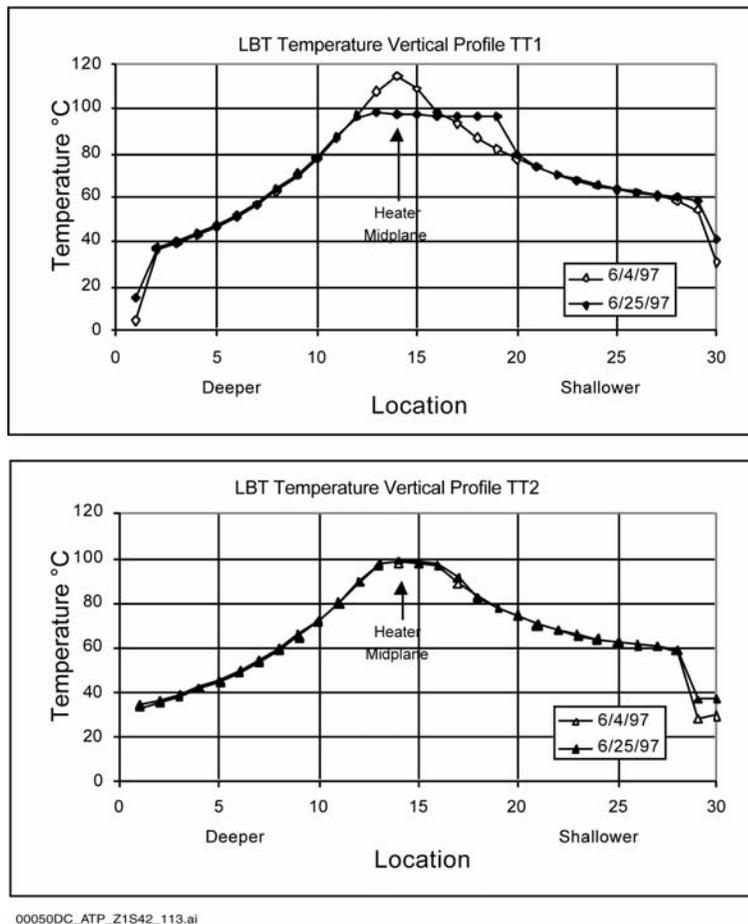
Figure 4-47.   Vertical Temperature Profiles through the Large Block for June 4 and June 25, 1997, Showing Development of a Heat Pipe Zone

The heat pipe zone is indicated by the "flattening" of the temperature curve for TT1 on June 25, 1997, which shows boiling temperatures distributed over a greater length of the borehole. See Figure 4-45 for the locations of Boreholes TT1 and TT2. LBT = Large Block Test. Source: Modified from Hardin and Chesnut 1997, Figure 4-7.
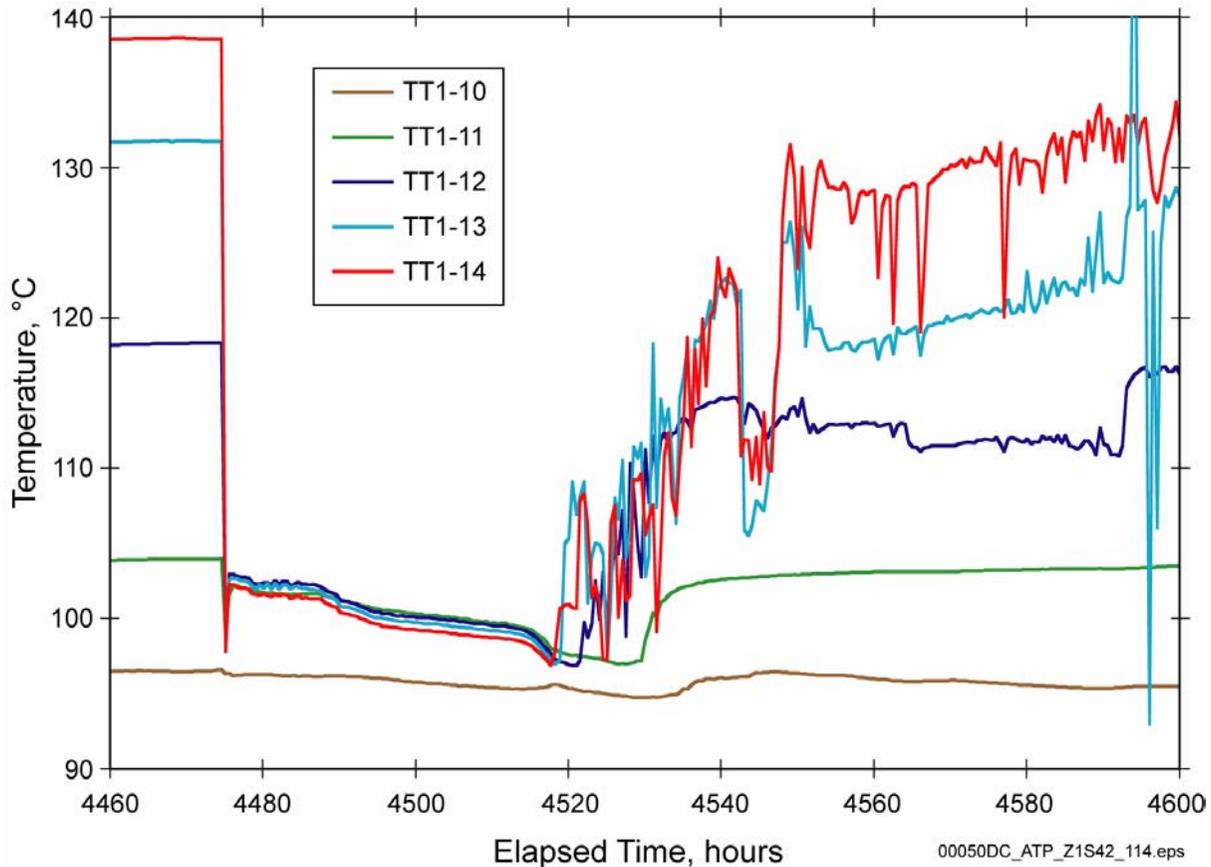
**Figure 4-48.   Temperatures at Several Resistance Temperature Detectors in TT1, Showing the Fluctuations
Due to a Thermal-Hydrologic Event on September 2, 1997**
See Figure 4-45 for the location of Borehole TT1. The beginning of thermal reflux (heat pipe) activity is clearly
indicated by the abrupt change in temperature at about 4,475 hours after the start of heating (i.e., September 2,
1997). Source: CRWMS M&O 2000al, Figure 3-55.

TOUGH2 was used to represent the evolution of measured temperatures. Modeling of this test provided important insights into the hydrologic properties and responses of the fractured tuff. The test confirmed that water moves away from heat sources as vapor, condenses where it is cooler, and tends to drain downward. Condensate was collected in a borehole, where it intersected a fracture drainage pathway. The apparent rapidity of drainage through fractures indicates that rock–water interaction between condensate and fracture surfaces is limited to relatively short residence times. The chemistry of sampled water was similar

to, but more dilute than, J-13 water. Solution equilibrium modeling indicates that the gas-phase carbon dioxide fugacity during the heated portion of the test was about two orders of magnitude greater than atmospheric.

Drift Scale Test—The Drift Scale Test, the largest thermal test conducted by the project to date, involves heating a drift that is approximately 48 m (157 ft) long. The rock mass being heated in this test will experience a thermal environment somewhat hotter than the repository design, with rock surface temperatures reaching a maximum of about
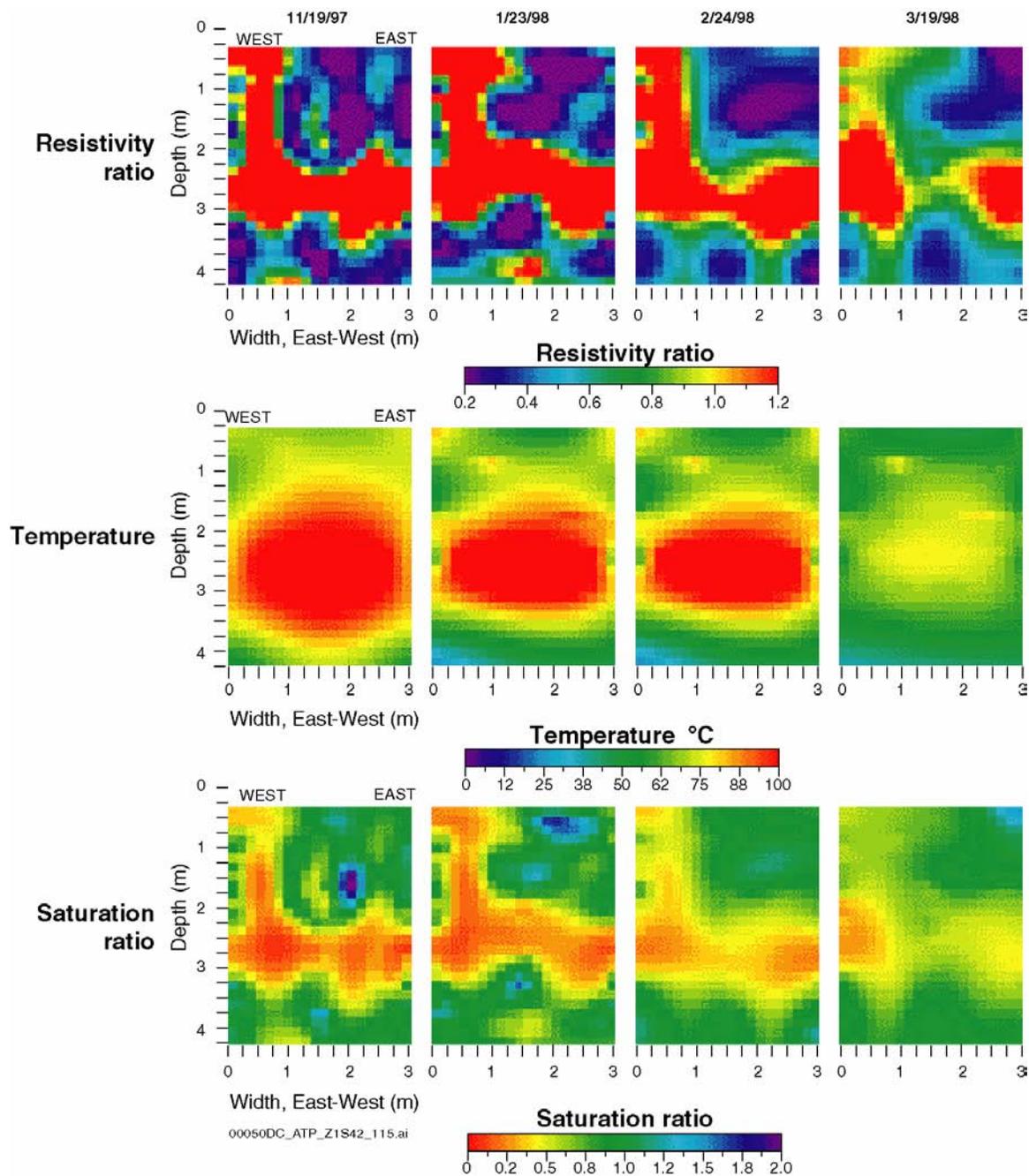
Figure 4-49.   **Electrical Resistance Tomographs of an East–West Vertical Cross Section of the Large Block Test, Showing the Variation of the Moisture Distribution within the Imaging Plane**

The resistivity ratio and saturation ratio results for 2/24/98 and 3/19/98 are of lesser quality than the ratios for the previous dates because fewer measurements met the acceptance criteria for interpretive processing. This probably occurred because dryout of the block surface affected the electrical signal strength. The interpretation of the apparent rewetting in the central region of the block is, therefore, less reliable than the interpretation of dryout from the earlier results. Source: CRWMS M&O 2000al, Figure 3-56.

00050DC_ATP_Z1S42_116.ai
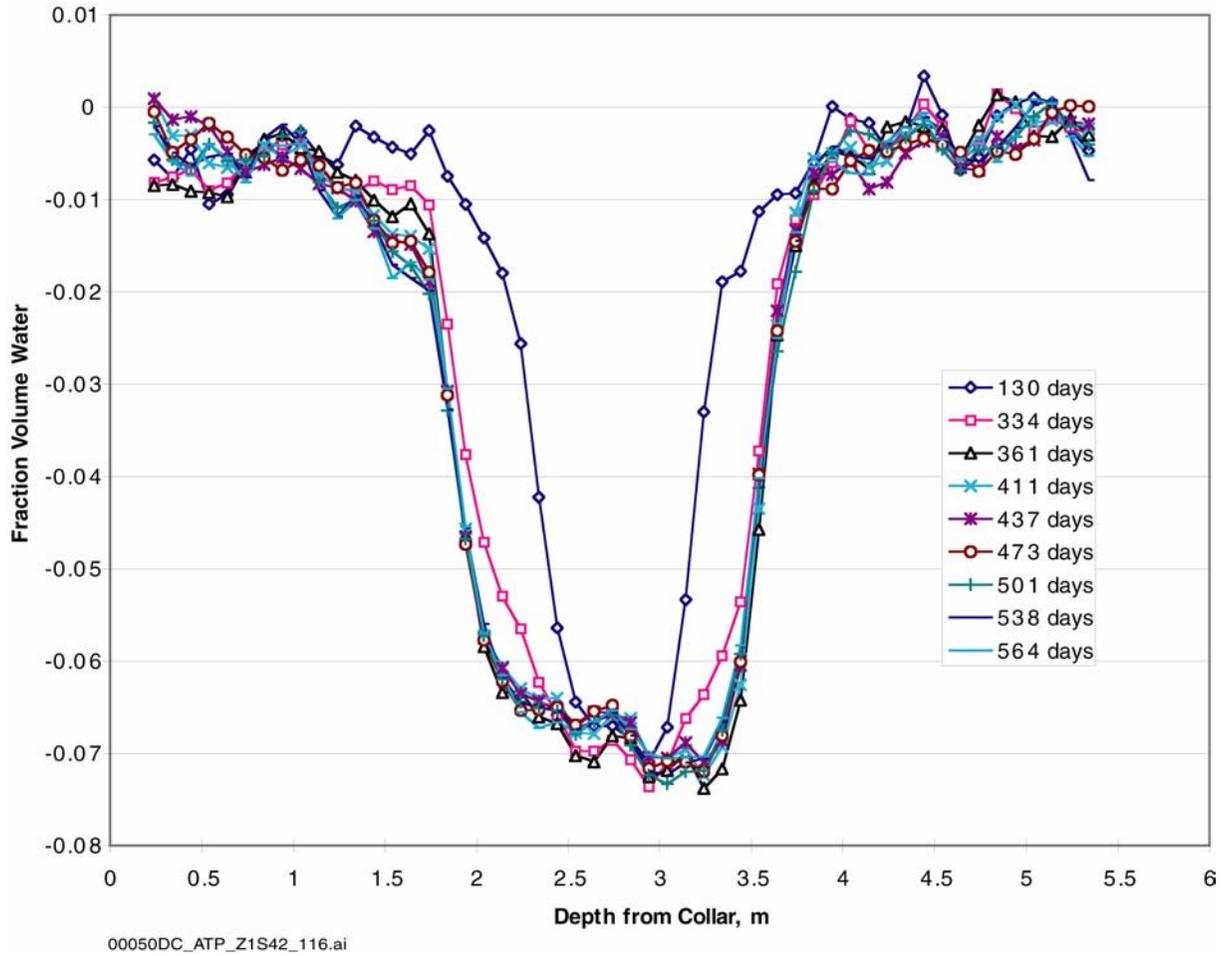
Figure 4-50.   Difference Fraction Volume Water in Large Block Test Borehole TN3 as a Function of Depth, from 103 to 565 Days of Heating

See Figure 4-45 for the location of Borehole TN3. Difference fraction volume water is the change in volumetric water content. As shown by the measurements plotted here, decreased water content resulted from heating. Source: CRWMS M&O 2000al, Figure 3-58.
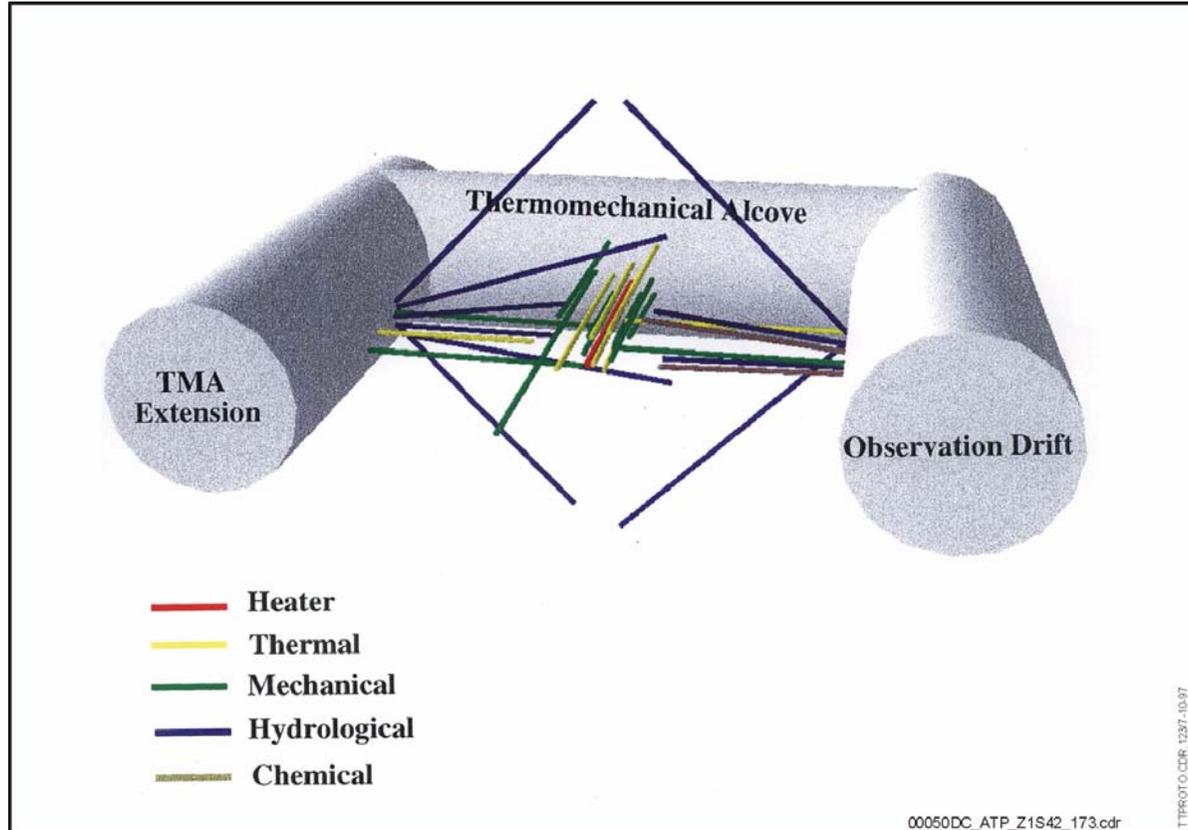
Figure 4-51. Schematic Illustration of the Single Heater Test in the Exploratory Studies Facility
Borehole diameter is significantly exaggerated in the illustration. The Single Heater Test is located near the Drift Scale Test (see Figure 2-78) at the Thermal Test Facility at Alcove 5. TMA = Thermomechanical Alcove. Source: CRWMS M&O 2000c, Figure 2.2-13; modified from CRWMS M&O 1999m, Figure 3-2 and Table 3-1.

200°C (390°F). This test is designed to produce above-boiling temperatures in about 10,000 m^3 of rock. The Drift Scale Test was described in *Near Field Environment Process Model Report* (CRWMS M&O 2000al, Section 3.6.1.3). A schematic of the Drift Scale Test is shown in Figure 4-52. After 4 years of heating, the Drift Scale Test is to begin a 4-year cooling phase beginning in early 2002 (CRWMS M&O 2000ch Section 1; CRWMS M&O 2000al, Section 3.6.1.3). The test results have provided and will continue to provide important insights into analyses of coupled processes, as described in this and following sections. Figure 4-53 shows the effect of boiling, as indicated by the temperature history at a single location. Boiling of pore water is represented by a

relatively flat region at about the boiling point of pore water in the temperature–time curves. Variations in heating rates are due to different distances between the sensors and the heaters. The duration of boiling is apparently affected by the availability of pore water to evaporate and the extent to which condensate flows back toward the heaters at each location.

Drying in regions near the heated drift and the wing heaters has been measured by electrical resistivity tomography, neutron logging, and ground-penetrating radar. Results obtained using these methods are shown in Figures 4-54, 4-55, and 4-56, respectively.
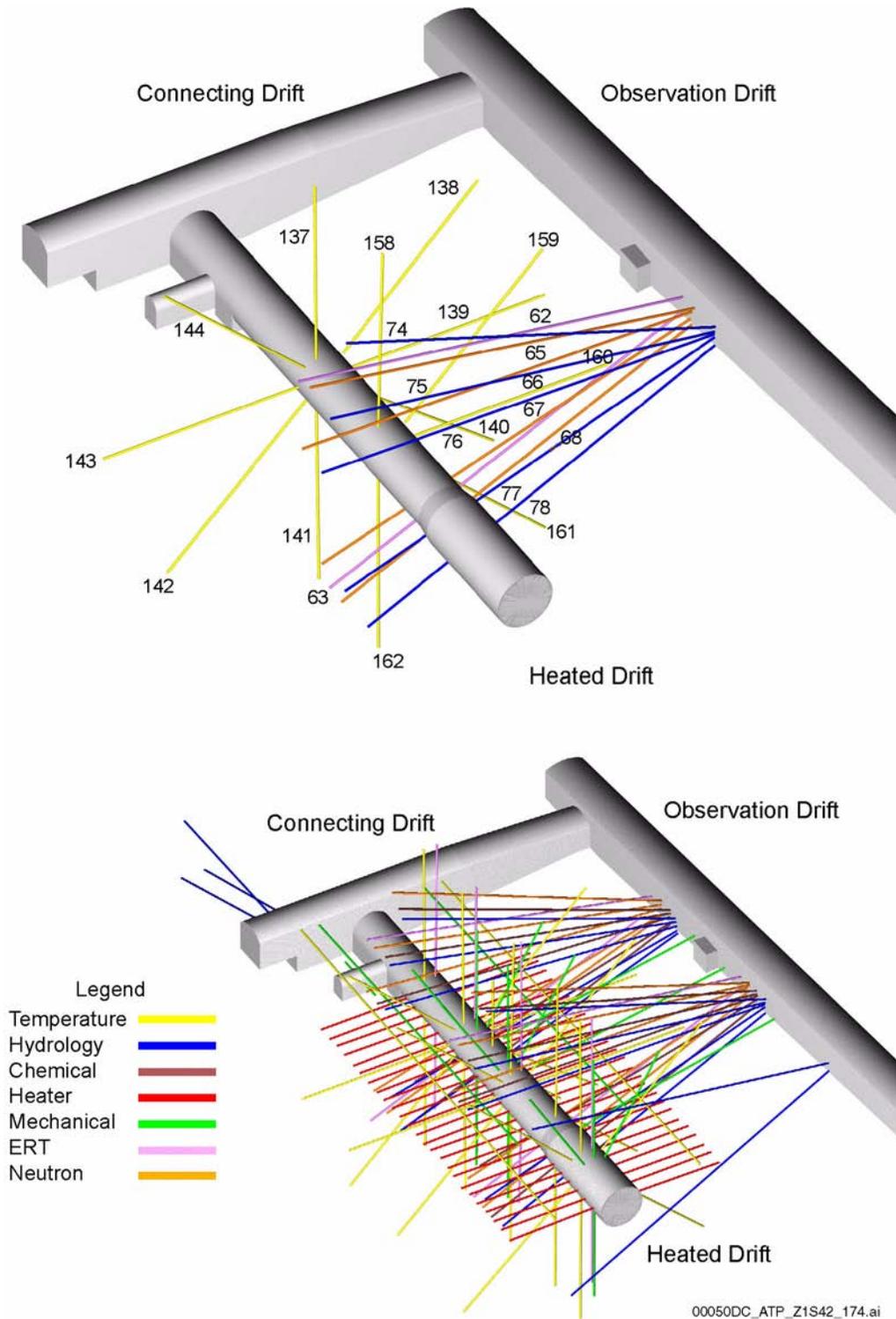
Figure 4-52.   Schematic Illustration of the Drift Scale Test in the Exploratory Studies Facility
Borehole diameter is significantly exaggerated in the illustration. For simplified identification of the boreholes discussed in this section, the top figure shows only those boreholes; the lower figure shows all the Drift Scale Test boreholes. See Figure 2-78 for the location of the Drift Scale Test at the Thermal Test Facility at Alcove 5. ERT = electrical resistance tomograph. Source: modified from CRWMS M&O 2000c, Figure 2.2-14, and CRWMS M&O 1998c, Table 4-1 and Figures 4-2 through 4-4.
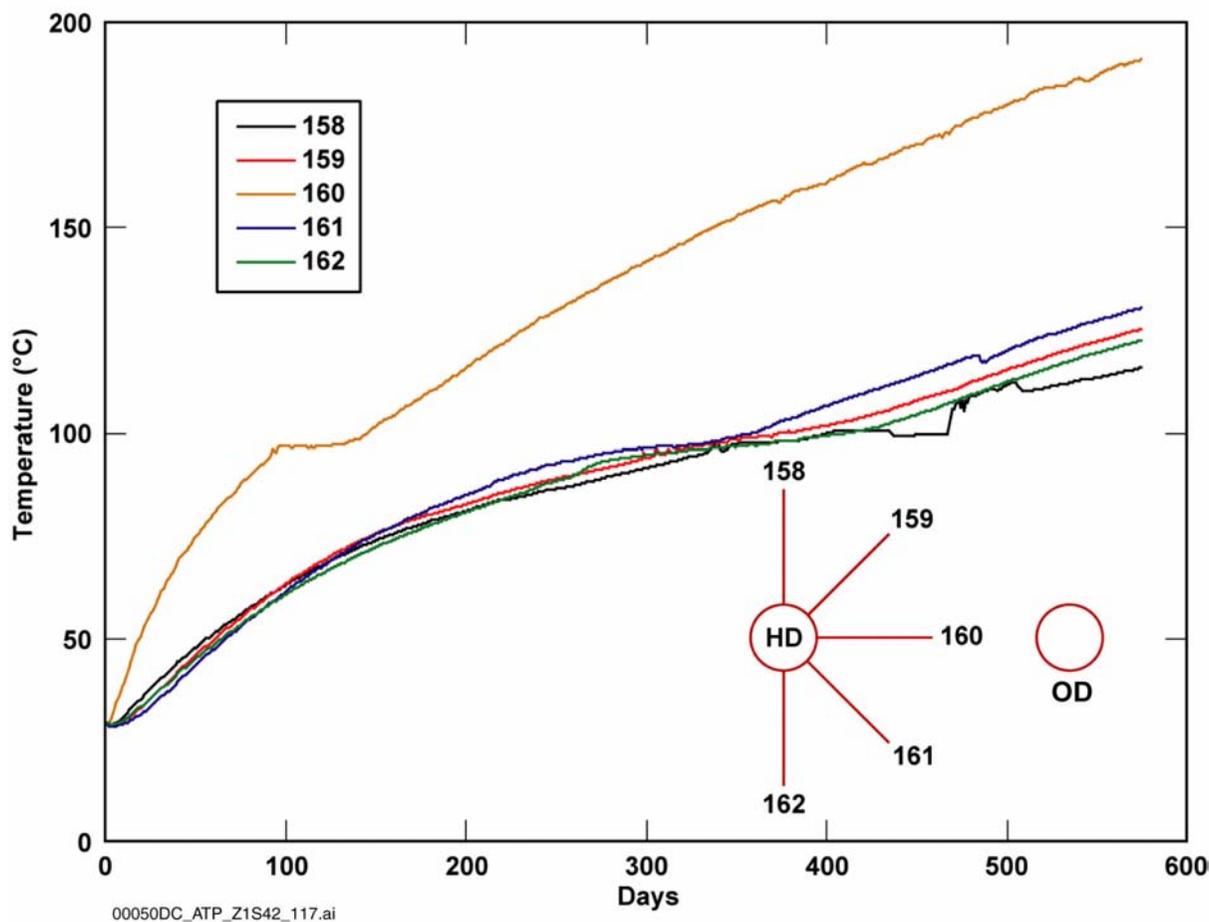
Figure 4-53. Temperature Measured at 2 m (6.6 ft) from the Collar of Boreholes 158 to 162 in the Drift Scale Test as a Function of Time, Showing the Spatial Variation of the Boiling of the Pore Water
Inset shows the location of the heated drift (HD) and Boreholes 158 to 162, where temperature measurements were taken, in relation to the observation drift (OD). See Figure 4-52 for the location of these boreholes. Source: CRWMS M&O 2000al, Figure 3-79.

Heat pipe activity caused by thermal refluxing of condensate water has been observed at some temperature measurement locations, as shown in Figure 4-57.

Thermal Tests Thermal-Hydrological Analyses/ Model Report (CRWMS M&O 2000ch) reports that both the TOUGH2 and NUFT modeling codes have predicted the temperature evolution and the dryout (liquid saturation) for the rock around the heated drift, consistently and with reasonable success. These thermal-hydrologic simulations support high confidence in using the thermal conductivity of rock mass to predict average temperature distributions. In addition, *Drift-Scale Coupled Processes (DST and THC Seepage) Models* (BSC 2001o, Section 6.2.7) shows that the TOUGHREACT modeling code was able to produce reasonable predictions of the evolution of carbon dioxide and composition of collected water samples as affected by heating.

4.2.2.2.3.3 Natural Analogues

Natural analogues related to the effects of heating on water movement and rock mass response were discussed by Hardin and Chesnut (1997) and in *Near Field Environment Process Model Report* (CRWMS M&O 2000al, Section 3.6.2). Additional information on natural analogues is provided in
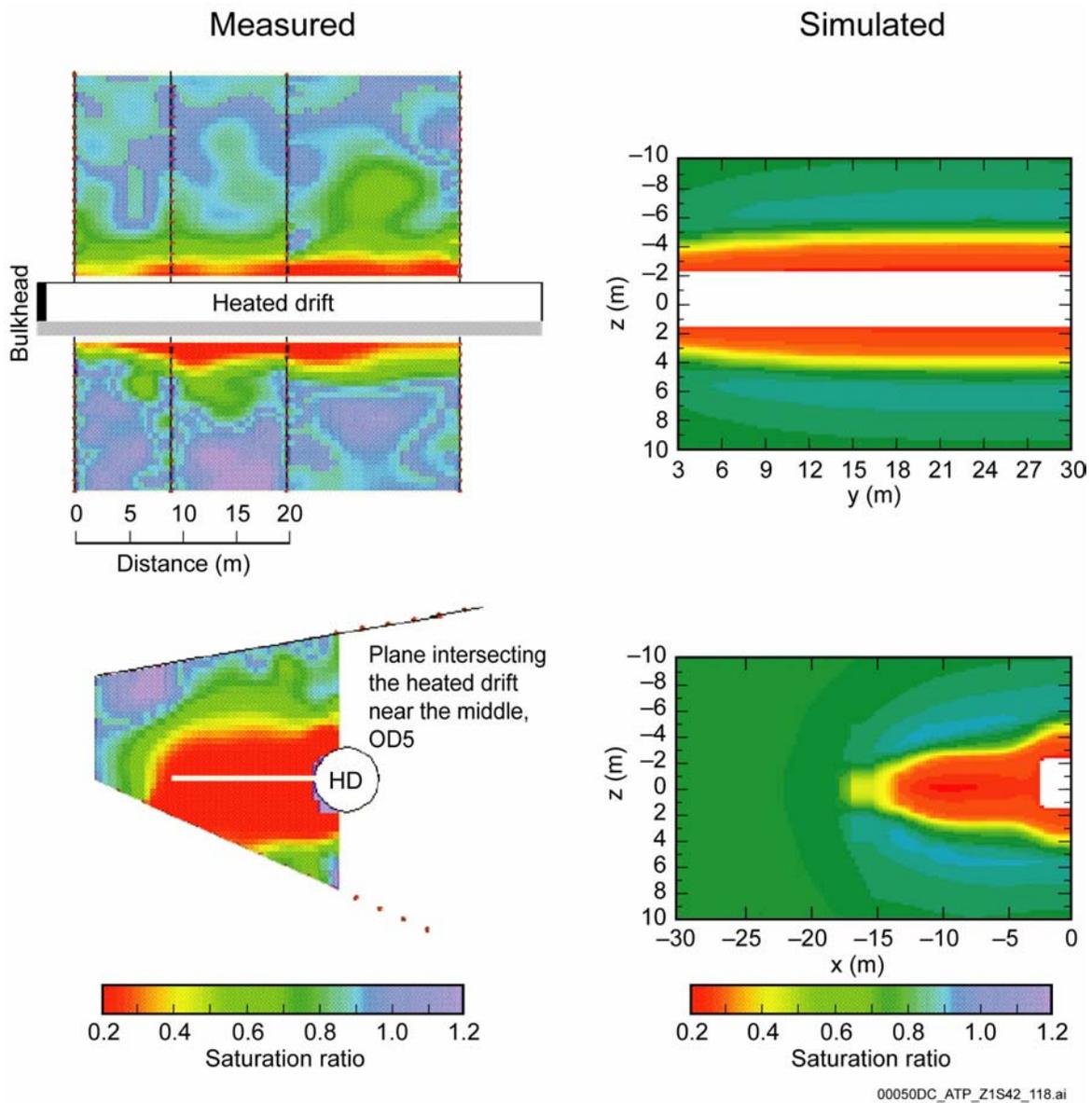
Figure 4-54. **Comparison of Distributions of Drift Scale Test Water Saturation Measured by Electrical Resistivity Tomography and Simulated by NUFT at 547 Days**

Measured saturation ratio was derived from electrical resistivity tomography after 558 days of heating. The top pair show the longitudinal cross section through the heated drift (HD) axis; the bottom pair show the transverse cross section at the plane of Boreholes 62 and 63. See Figure 4-52 for the location of these boreholes. OD = observation drift. Source: CRWMS M&O 2000ch, Figure 56.
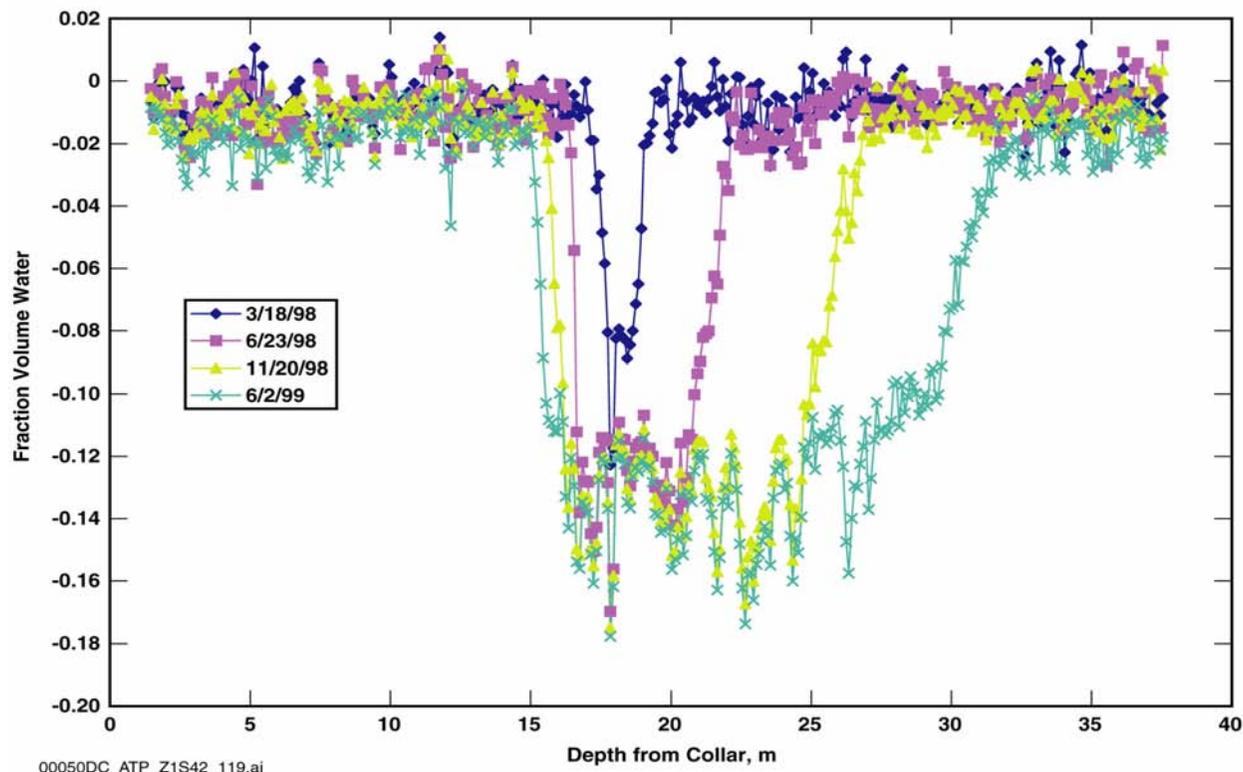
Figure 4-55. **Difference Fraction Volume Water in Borehole 67 of the Drift Scale Test as a Function of Depth from Collar**

These measurements show the change in volumetric water content in the rock in comparison to ambient measurements taken in February 1998. See Figure 4-52 for the location of Borehole 67. Source: CRWMS M&O 2000al, Figure 3-85.

Natural Analogs for the Unsaturated Zone (CRWMS M&O 2000bp) and in *Yucca Mountain Site Description* (CRWMS M&O 2000b, Section 13). Figure 4-58 illustrates selected examples of analogue information for heat induced and coupled processes. The information from geothermal studies can be used to demonstrate that the effects of decay heat on water movement can be evaluated. The available information ranges from core-scale and outcrop evaluations of fossil thermal-hydrologic-chemical coupled processes, understanding of efficient heat transfer mechanism with vapor–liquid counter flow phenomena (heat pipe), induced changes in operating geothermal fields, to dynamic or even disruptive processes with mechanical changes. Some of these phenomena are described in this section.

Geothermal Fields—Heat pipes in the repository will be short-lived, transient features compared to geothermal systems. Thermal-hydrologic characteristics of the repository host rock are similar to vapor-dominated geothermal systems (Hardin and Chesnut 1997; Simmons and Bodvarsson 1997), and similar modeling methods are applicable. Geothermal systems are apparently self-sealing, but conditions for development of a mineral cap above the emplacement drifts in a repository are different and less likely to result in sealing.

Table 4-15 lists selected geothermal systems evaluated in many countries. A photograph of a tuff core with indication of fracture sealing and opening from the Yellowstone geothermal field and a
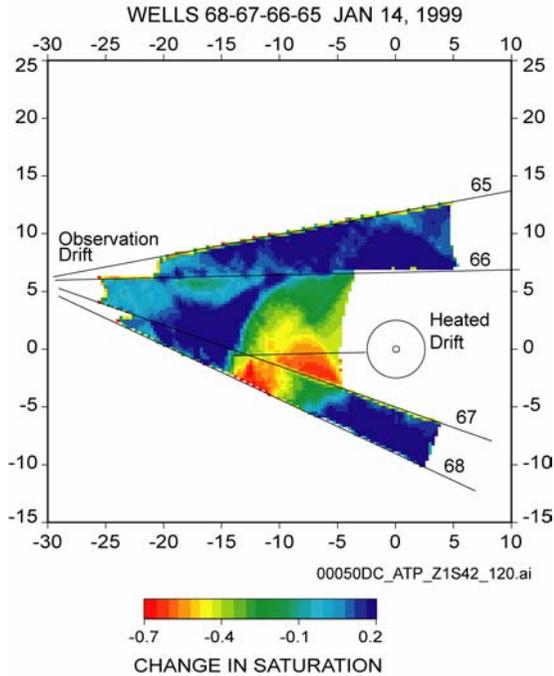
Figure 4-56. Tomogram Showing Saturation Change from Preheat Ambient Values after Approximately 13 Months of Heating

Measurements taken January 14, 1999, from a cross-hole radar survey in the plane of Drift Scale Test Boreholes 64 to 68. See Figure 4-52 for the location of these boreholes. Source: CRWMS M&O 2000ch, Figure 33.

photograph of topographic deformations associated with the high-temperature geothermal field at Krafla, Iceland, are examples illustrated in Figure 4-58. Also included in Figure 4-58 is a photograph of the concrete-lined tunnel, subjected to heating by nuclear reactor processes, at the Kransno-yarsk-26 site in Russia. This is one example of the different kinds of site studies of anthropogenic (human-induced) analogues (CRWMS M&O 2000b, Section 13.3.6.3). Additional information on natural analogues and model calibration and validation for thermal-hydrologic applications is provided below in Section 4.2.2.3.6.

The Geysers—The Geysers is a geothermal field located about 65 km (45 miles) north of Santa Rosa, California. The pressure and temperature of the vapor-dominated geothermal system at The Geysers plot along the liquid-vapor phase boundary for water, whereas the repository host rock will be free-draining, and the pressure of refluxing water will be constrained at about 1 atm (Hardin and Chesnut 1997, Section 4.3.1; Wilder 1996, Chapter 1). The maximum heat flux from the repository will be 50 to 70 times that calculated for The Geysers. Therefore, the calculated reflux magnitude at The Geysers, 4 to 5 mm/yr, does not imply that there will be no dryout zone above the repository. However, heat pipe activity is likely in the repository host rock and may be important for an extended period during cooldown.

Taupo Volcanic Zone and Geothermal Fields, New Zealand—The Taupo volcanic zone analogue was used to compare observed water composition and mineral occurrence in a geothermal well with chemical modeling calculations. In accordance with observations, major phases such as quartz and calcite were calculated to be at near-equilibrium. Other phases were predicted less accurately for several reasons: (1) uncertain kinetics, (2) completeness of thermodynamic data, (3) solid-solution effects (such as heterogeneity), and (4) the influence of boiling on precipitation (Glassley and Christenson 1992; Bruton et al. 1994). Differences were observed between precipitation rates measured in the laboratory and those measured in the field. Earlier studies by Rimstidt and Barnes (1980, p. 1691) argued that precipitation rates for silica polymorphs are the same, but this approach does not explain certain natural analogue observations (Carroll et al. 1995, pp. 7 to 13).

Figure 4-58 includes an example of geothermal fields in New Zealand. At the Wairakei geothermal field illustrated in Figure 4-58, rates of amorphous silica precipitation measured in the field were 400 times faster than those obtained in the laboratory measurements. Similar rates are found at the Broadlands field. Both field data and model results indicate that stable mineral assemblages are sensitive to small differences in fluid chemistry, temperature, and pressure. Silica precipitation under potential repository conditions at Yucca Mountain could exhibit rate behavior somewhere in a range between the laboratory and field experiments (CRWMS M&O 2000b, Section 13.4.1.3).
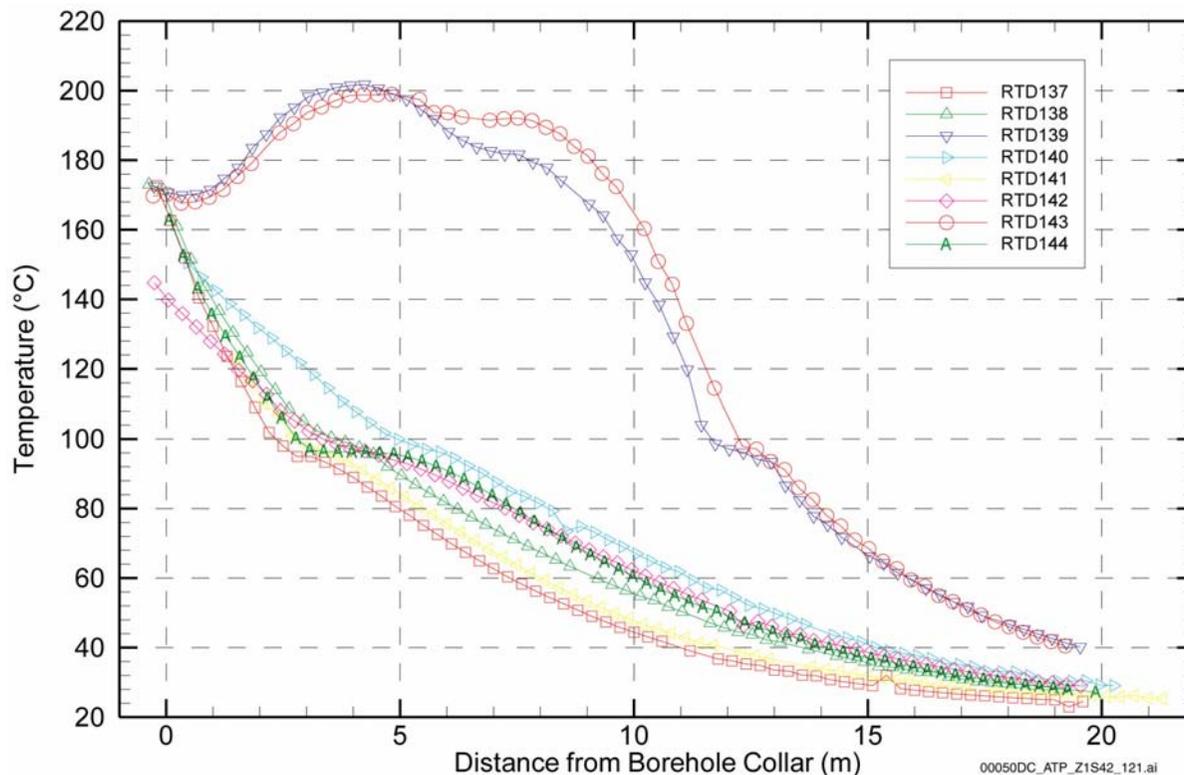
Figure 4-57.   Measured Drift Scale Test Temperatures as a Function of Distance of Sensor Locations from Borehole Collars after 18 Months of Heating

Data shown from resistance temperature detectors (RTDs) in Drift Scale Test Boreholes 137 to 144. See Figure 4-52 for the location of these boreholes. Source: CRWMS M&O 2000ch, Figure 21.

Grants Ridge, New Mexico—Despite the high-temperature basaltic intrusion, there was no evidence of pervasive hydrothermal circulation and alteration in the country rock that could have resulted from thermally driven liquid-phase convection (CRWMS M&O 2000al, Section 3.6.2.1).

Yucca Mountain—Conceptual models for mineral evolution at Yucca Mountain (Carey et al. 1997) suggest that the most likely mineralogical reactions caused by repository heating would include disso-lution of volcanic glass and precipitation of clinoptilolite, clay, and opal-CT; dissolution and precipitation of silica polymorphs (cristobalite, opal-CT, tridymite, and quartz); alteration of feld-spars to clays; and finally, reactions involving calcite and zeolites. Thermodynamic modeling results indicate that the stability of various zeolites

is a function of silica activity, temperature, aqueous sodium concentration, and the mineralogy of silica polymorphs. Increasing temperature or sodium concentration causes the alteration of zeolites to other phases. Kinetic data suggest that water saturation conditions are necessary for significant progress in these reactions. Therefore, under ambient conditions the reactions are likely to proceed more slowly in the Yucca Mountain unsat-urated zone (excluding perched water zones) than below the water table. However, if prolonged boiling occurs in water-saturated tuffs, significant progress in such reactions can occur (CRWMS M&O 2000al, Section 3.6.2.2).

Valles Caldera, New Mexico—The contact between the Banco Bonito obsidian flow and underlying Battleship Rock tuff on the southwest rim of the caldera was studied by Krumhansl and
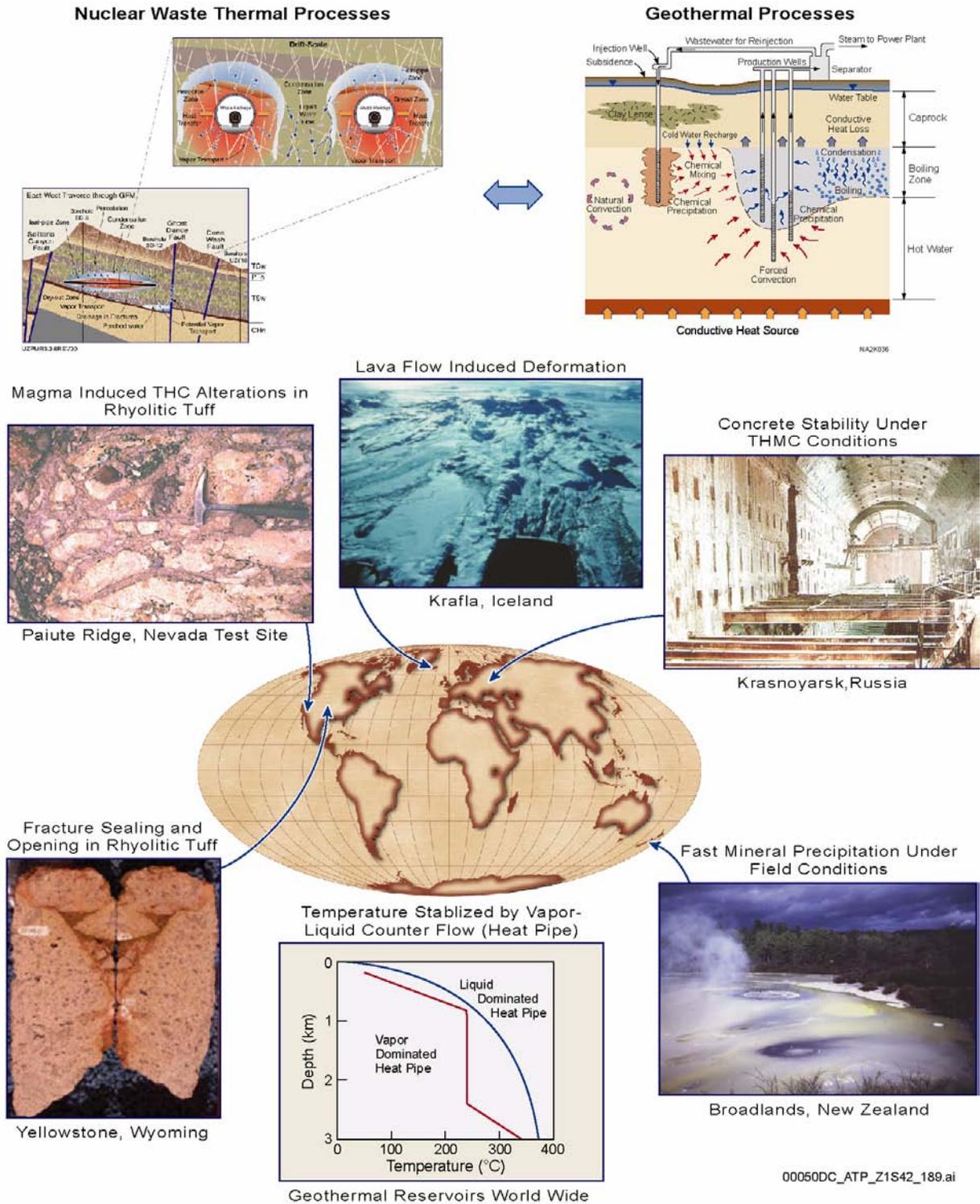
Figure 4-58.   Analogue Studies for the Effects of Decay Heat and Thermal-Hydrologic-Chemical Coupled Processes

THC = thermal-hydrologic-chemical; THMC = thermal-hydrologic-mechanical-chemical.

Table 4-15. Geothermal Analogues for Process Evaluation

Analogue	Data and/or Process
Yucca Mountain as self-analogue	Mineral reaction rates (Bish and Aronson 1993; Carey et al. 1997)
Papoose Lake sill, Paiute Ridge, Nevada Test Site, Nevada	Magma intrusion, coupled thermal-hydrologic-chemical processes (Crowe, Self et al. 1983; Matyskiela 1997; Lichtner et al. 1999)
Dixie Valley, Nevada	Geothermal, coupled thermal-hydrologic-chemical processes, preferential flow, fracture–matrix interaction, mineral precipitation and dissolution, mineral alteration
Cerro Prieto, Mexico	Geothermal, preferential flow, fracture network permeability, mineral reaction rates, self-sealing
East Mesa, California	Geothermal, preferential flow, mineral reaction rates
Heber, California	Geothermal (Lippmann and Bodvarsson 1985)
Long Valley, California	Geothermal, fracture–matrix interaction, mineral precipitation and dissolution
The Geysers, California	Geothermal, preferential flow, fracture network permeability, heat pipes, boiling and condensation, self-sealing
Valles Caldera, New Mexico	Magma intrusion (Stockman et al. 1994, Sections 1.2 and 1.3)
Grants Ridge, New Mexico	Magma intrusion (WoldeGabriel et al. 1999)
Fenton Hill, New Mexico	Geothermal, mineral precipitation and dissolution
Newberry Volcano, Oregon	Geothermal (Sammel et al. 1988)
Yellowstone, Wyoming	Geothermal, fracture–matrix interaction, mineral alteration
Eldora stock and Alamosa River stock, Colorado	Deep hydrothermal intrusions (Brookins 1986; Wollenberg and Flexser 1986)
Wairakei, New Zealand	Geothermal, hydrologic properties, preferential flow, fracture network permeability, mineral precipitation and dissolution, mineral alteration, thermal-hydrologic-mechanical subsidence (Mercer and Faust 1979; Bruton et al. 1993; Glassley and Christenson 1992)
Broadlands, New Zealand	Geothermal, mineral precipitation and dissolution, mineral alteration
Kamojang, Indonesia	Geothermal, hydrologic properties, fracture network permeability, heat pipes, boiling and condensation, self-sealing
Bulalo, Philippines	Geothermal, thermal-hydrologic-mechanical subsidence
Tianjin, China	Geothermal, hydrologic properties
Sumikawa, Japan	Geothermal, hydrologic properties, fracture network permeability
Matsukawa, Japan	Geothermal, fracture network permeability, heat pipes, boiling and condensation, self-sealing
Larderello, Italy	Geothermal, fracture network permeability, heat pipes, boiling and condensation, mineral precipitation and dissolution, self-sealing
Krafla, Iceland	Geothermal, fracture network permeability, thermal-hydrologic-mechanical subsidence (Bodvarsson, Benson et al. 1984)
Reykjanes, Iceland	Geothermal, self-sealing
Olkaria, Kenya	Geothermal, fracture network permeability, fracture–matrix interaction (Bodvarsson, Pruess et al. 1987)

Sources: Adapted from CRWMS M&O 2000c, Table 2.3-1; CRWMS M&O 2000bp, Table 6-13.

Stockman (1988) and Stockman et al. (1994). No evidence of hydrothermal alteration was noted, suggesting that the area was unsaturated at the time of contact. The effects of heating in this unsaturated environment appeared to have been slight and were limited to the tuff nearest the contact. The principal mineralogic change in tuff near the contact was the development of feldspar-silica

linings on voids in the pumiceous tuff matrix; no significant development of zeolites was found.

Paiute Ridge, Nevada Test Site—This characterization has been further developed as a distribution of "key blocks" that are defined by the fractures. An example of a sill observed on the outcrop of Paiute Ridge is illustrated in Figure 4-58.

Matyskiela's (1997) study of alteration surrounding one intrusion, the 50-m-wide (160-ft-wide) Papoose Lake sill, found alteration of glass shards to cristobalite and clinoptilolite within 60 m (200 ft) of the intrusion. He observed complete filling of pore spaces with silica at fracture–matrix interfaces, thus enhancing flow along fractures by inhibiting fracture–matrix interaction. Matyskiela (1997) estimated enhanced fracture flow to be as much as five times ambient conditions. A different kind of response to heating in the repository host rock (i.e., formation of a silica cap) was predicted by Nitao (reported in Hardin 1998, Section 5.6). Those simulations show that both the fractures and the adjacent matrix (at the fracture–matrix interface) could be plugged by dissolved solids transported into the boiling zone by fracture flow. This result depends on the total quantity of dissolved solids (e.g., silica) transported to the boiling zone and on the value of the fracture porosity (a smaller value of the fracture porosity makes plugging more likely). Another set of calculations reported in *Near Field Environment Process Model Report* (CRWMS M&O 2000al, Section 3.2.5) indicates that only minor changes in fracture permeability would result from mineral precipitation during the thermal pulse, based on a larger estimate for fracture porosity and consideration of more complete ranges of minerals and chemical species.

Scoping analyses by Lichtner et al. (1999) provide additional perspective on the potential for plugging of porosity in the fractures and matrix. The approach considers the dissolved silica in the pore water present initially (before heating) in the tuff matrix. During heating, the matrix pore water will evaporate in a region proximal to the drift openings. If the silica contained in the pore water migrates to the fractures as evaporation occurs (ignoring evaporation in the matrix), then the degree of fracture plugging depends on the initial fracture porosity, as well as the particular silica polymorph produced. Based on this analysis, the fracture porosity used in Nitao's models (reported in Hardin 1998, Section 5.6) would be completely filled with amorphous silica for tsw33 and tsw34 units and about 50 percent filled in the tsw35 unit (CRWMS M&O 2000al, Section 3.6.2.2).

4.2.2.3 Process Model Development and Integration

Two models, namely the mountain-scale thermal-hydrologic model and multiscale thermal-hydrologic model, differing primarily in the spatial scales of interest, are used to model the effects of decay heat on water movement (CRWMS M&O 2000al, Section 3.2.2). Both models solve heat and mass balance equations written for a fracture continuum interacting with a matrix continuum. The mountain-scale model evaluates changes in temperature and water movement at greater distance from the potential repository and is used for comparison to analogous geothermal sites. The multiscale thermal-hydrologic model provides detailed output describing temperature and moisture movement in the emplacement drifts and is abstracted directly for use in performance assessment. Both models rely on hydrogeologic properties developed for the unsaturated zone flow model.

Another model is used to calculate the drift-scale thermal-hydrologic-chemical processes and to address the change of chemistry of water entering drifts and the flow properties of the surrounding rock that control the seepage flux (CRWMS M&O 2000al, Section 3.3). A final model is used to calculate the normal and shear displacement of distinct blocks of rock surrounding the heated emplacement drift and to address the consequent change in flow properties of the near-field rock that control the seepage flux (CRWMS M&O 2000al, Section 3.5).

4.2.2.3.1 Mountain-Scale Thermal-Hydrologic Model

The mountain-scale thermal-hydrologic model simulates the effects of repository heating on the unsaturated zone, including a representation of thermally driven processes occurring in regions far away from the potential repository (CRWMS M&O 2000ci, Section 7; CRWMS M&O 2000c, Section 3.12). This model is used to understand the mountain-scale effects of repository heating on water movement and to conclude that the mountain-scale effects of heating on water movement would not degrade the function of the host rock to

divert water from the engineered barriers and the waste form. Thus, the assessment of environmental conditions within the emplacement drifts can be focused on the drift-scale effects of heating on water movement.

The simulations provide predictions for thermally driven flow of liquid water and water vapor, and distributions for temperature and moisture in the unsaturated zone, for a period of 100,000 years. Approaches for simulation of the two-phase heat and mass transport processes in fractured systems are generally based on geothermal and petroleum reservoir simulation methods. Early multiphase modeling studies identified the importance of heat pipe effects in models that include heat sources. The heat pipe phenomenon is associated with boiling conditions and can occur if sufficient liquid is transported back toward the heat source (by gravity or capillarity) to sustain the boiling (Pruess, Wang et al. 1990, p. 1241). In the dryout zone, temperature variation is controlled by heat conduction and the thermal output of the heat source. In previous mountain-scale thermal-hydrology models, planar heat sources were used to represent closely spaced emplacement drifts, with the result that thick heat pipes and condensate zones were predicted (Buscheck and Nitao 1992). In the mountain-scale model, heat sources are more discrete, and drainage can occur through the pillars between emplacement drifts.

The mountain-scale thermal-hydrologic model uses the mathematical formulation employed in previous models (Pruess 1987, pp. 2 to 11; Pruess 1991, pp. 5 to 26). The approach involves volume averaging, the dual-permeability, continuum approach for modeling coupled fluid and heat flow, and fracture–matrix interaction (CRWMS M&O 2000br, Section 6.7; Liu et al. 1998). The model was developed from the unsaturated zone flow model and uses the mathematical formulations employed in the TOUGH2 code to describe flow under thermal-loading conditions (CRWMS M&O 2000c, Section 3.12.1). For the flow model, predictions of the three-dimensional ambient temperature distribution were calibrated against measured temperature profiles in boreholes (CRWMS M&O 2000ci, Section 6.1). The same thermal properties

are used in the mountain-scale thermal-hydrology model, and the ambient temperature distribution is used as the initial condition for modeling thermal effects.

Several numerical models were developed, including a three-dimensional mountain-scale model and two cross-sectional models. Plan views of the three-dimensional grid and the two-dimensional cross-sectional grids are shown in Figures 4-59 and 4-60, respectively. The three-dimensional model represents each emplacement drift and the adjacent pillars as one element, which does not resolve thermal-hydrologic processes in the vicinity of the potential repository. The two-dimensional models are more detailed and therefore allow drainage of condensed water through the pillars between drifts. The two-dimensional cross-sectional models are finer than the three-dimensional model but coarser than the drift-scale models described in Section 4.2.2.3 (see Figure 4-72 in Section 4.2.2.3.6 for a comparison). Accordingly, only the elements outside the drift elements are evaluated in the mountain-scale studies. More detailed discussion of these numerical models is presented in supporting documentation (CRWMS M&O 2000br, Section 6; CRWMS M&O 2000ci, Sections 6.2 and 6.3).

The mountain-scale thermal-hydrologic model uses input parameters that are fully consistent with the unsaturated zone flow model (CRWMS M&O 2000c, Section 3.6; CRWMS M&O 2000cj, Section 6), including hydrologic properties, the mean infiltration distribution, and the evolution of future climate states (CRWMS M&O 2000c, Section 3.5; USGS 2000b, Section 6). The simulations use an average initial thermal loading of 72.7 kW/acre (18.0 W/m^2, equivalent to average areal mass loading of 60 MTHM per acre), based on a potential repository area of 1,050 acres (4,250,000 m^2) (CRWMS M&O 2000c, Section 3.12.2.3; CRWMS M&O 2000ci, Section 5.1). The thermal load is scaled down by the natural decay curve over a total simulation period of 100,000 years. To account for ventilation, only 30 percent of this heat is used during the first 50 years (CRWMS M&O 2000c, Section 3.12; CRWMS M&O 2000ci, Sections 6.10 and 6.11). Figure 4-61
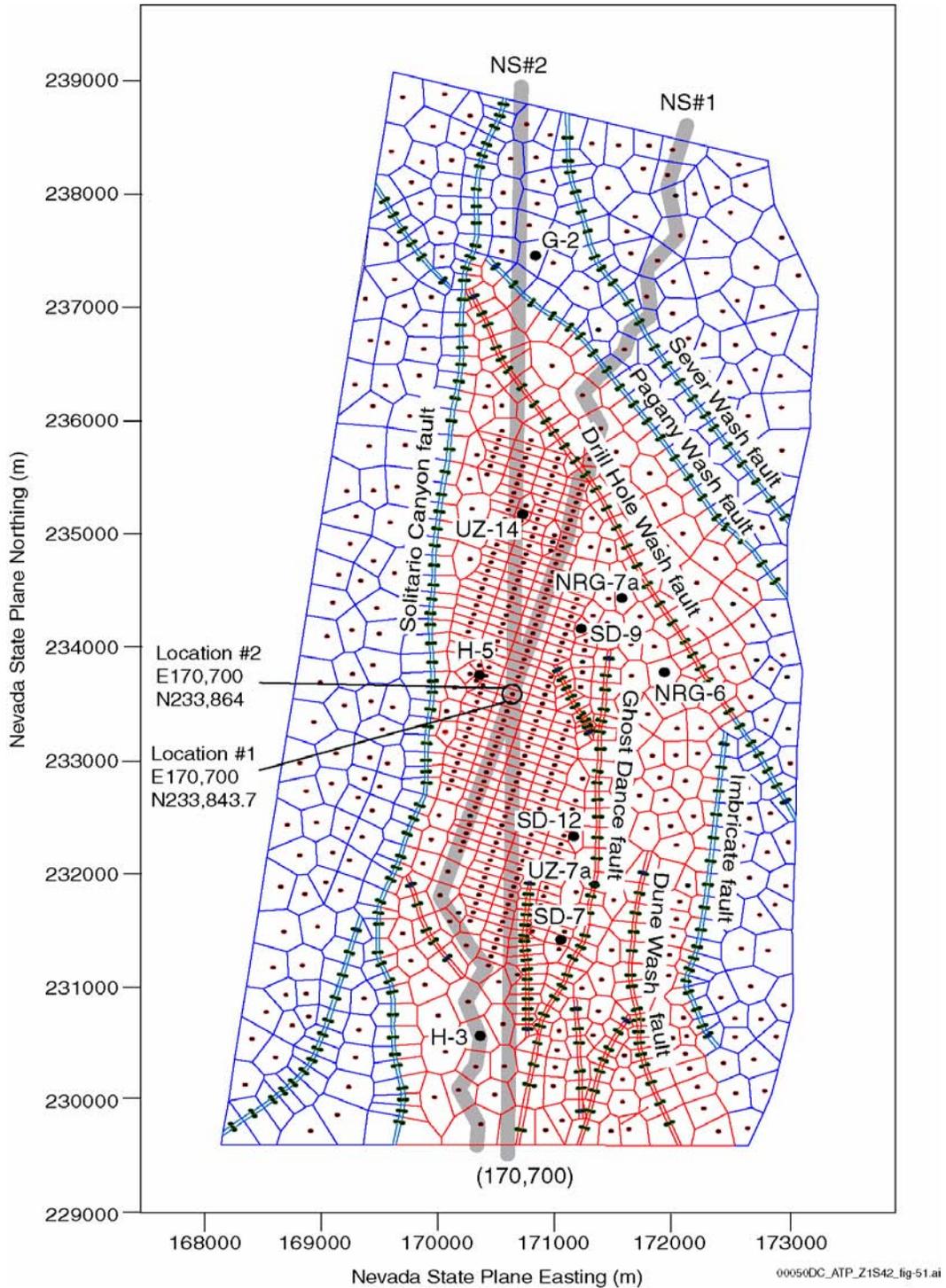
Figure 4-59.   Plan View of the Three-Dimensional Grid Used for the Unsaturated Zone Flow Model and the Mountain-Scale Thermal-Hydrologic Model

Locations #1 and #2 are used for detail plots. Large solid circles represent borehole locations; small circles represent grid column centers. The thick gray lines show the locations of cross sections NS#1 and NS#2. Source: CRWMS M&O 2000c, Figure 3.12-3.
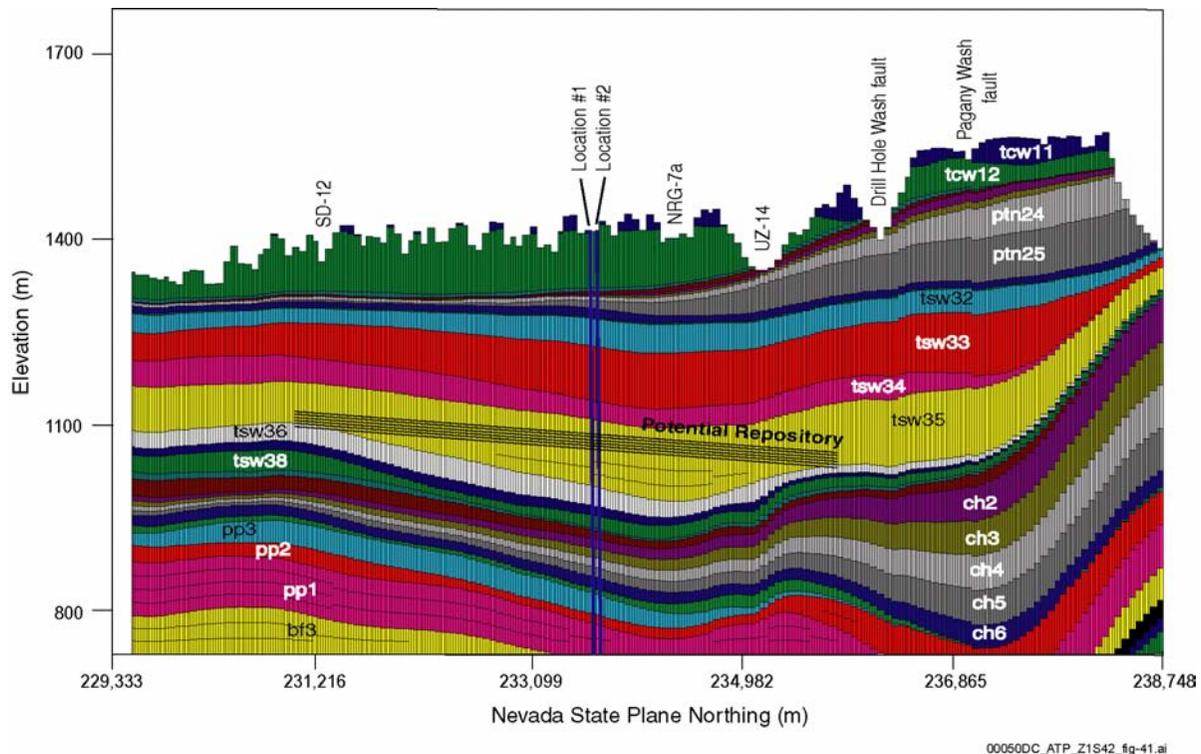
Figure 4-60. **Lateral and Vertical Discretization at the NS#2 Cross Section Based on the Refined Numerical Grid**

Plot shows the location of the potential repository and the unsaturated zone model layering. The figure has approximately 4½:1 vertical exaggeration. The location of this cross section is indicated on the plan view grid in Figure 4-59. Source: CRWMS M&O 2000c, Figure 3.12-4.

depicts the relationship between the thermal-hydrologic model, the input data, and supporting models.

Presented below are some of the results obtained for the two-dimensional cross-sectional models, focusing on the case with ventilation. Discussion of the other two-dimensional and three-dimensional cases is presented in supporting documentation (CRWMS M&O 2000ci, Sections 6.10 and 6.11). The results presented below are based on the higher-temperature operating mode.

Temperature—Figure 4-62 shows the distribution of temperature along cross section NS#2 after 1,000 years of thermal load (a) without ventilation and (b) with ventilation for the first 50 years. The variations in net infiltration across the model influence the evolution of temperature in both cases. Higher temperatures are predicted to occur in areas with less infiltration. The plots show dryout only in

the immediate vicinity of the potential repository. At a lateral distance of 100 m (330 ft) or more from the potential repository, no substantial increases in temperature are predicted, which suggests that buoyant, mountain-scale convection of the gas-phase, driven by production of water vapor and the heating of the gas-phase, will be important within or near the potential repository.

With or without ventilation, the predicted maximum temperatures at the centers of the pillars between emplacement drifts do not exceed boiling. Results also show that the long-term temperature response anywhere in the unsaturated zone is unaffected by 50 years of ventilation. Temperatures at the base of the PTn unit may increase to boiling conditions if the potential repository is not ventilated. Such temperatures could induce property changes in the PTn unit from mineral alteration, particularly in areas with less infiltration. With 50 years of ventilation as planned, temperatures in the
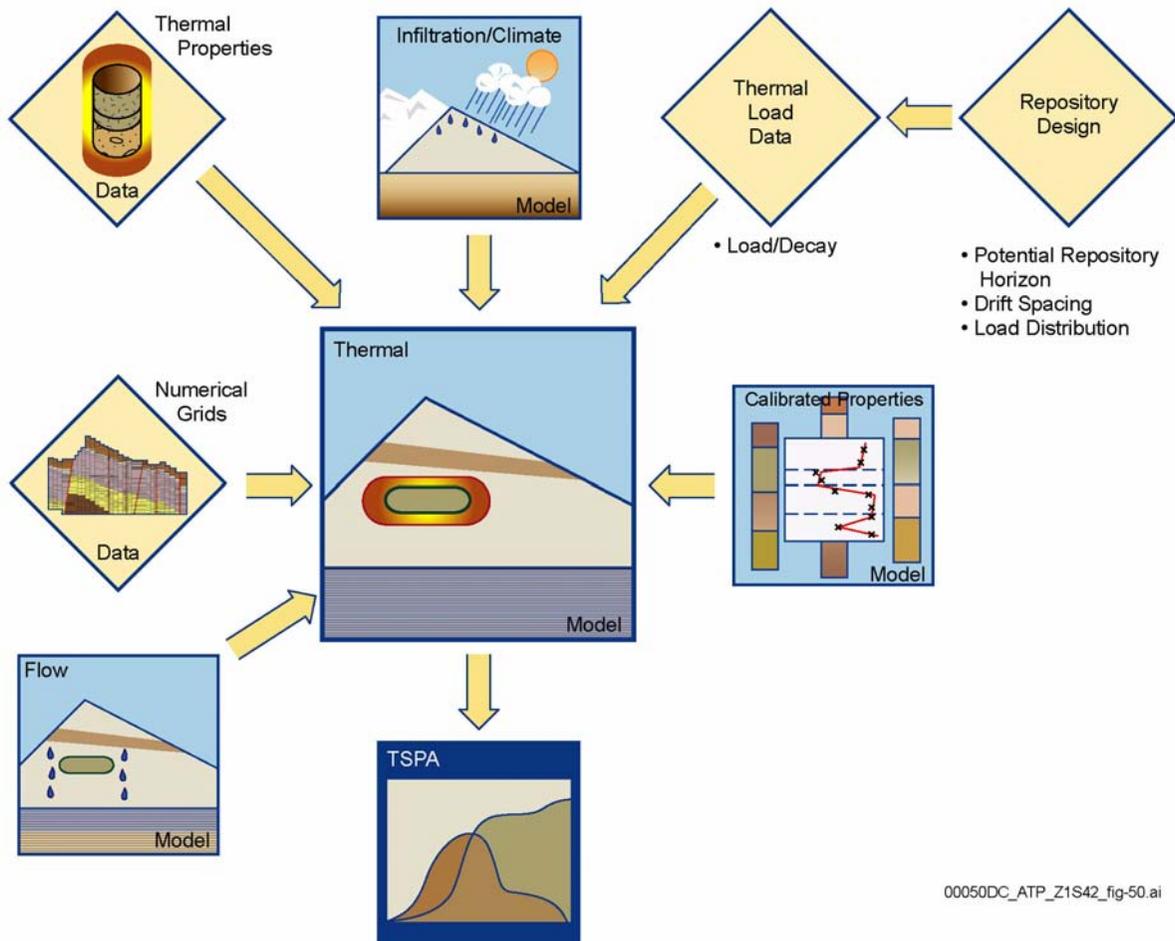
Figure 4-61. Schematic Showing Input Data and the Unsaturated Zone Models that Support the Development of the Thermal-Hydrologic Model
Source: CRWMS M&O 2000c, Figure 3.12-2.

PTn unit are predicted to increase to an average of 40° to 45°C (104° to 113°F). At the top of the CHn unit, below the potential repository, the models predict a maximum temperature of 70° to 75°C (158° to 167°F), which will occur after 2,000 and 7,000 years, depending on location. This temperature range suggests minimal potential for thermally induced mineralogical degradation of zeolites in the CHn unit. At the water table, the models predict a maximum temperature of 65° to 70°C (149° to 158°F), compared to the average ambient temperature of 30°C (86°F).

Saturation—With or without ventilation, all fractures in the drifts at the potential repository horizon are completely dry within the first few years of thermal loading. The dryout zone expands and reaches a maximum thickness between 600 to 1,000 years after thermal loading (CRWMS M&O 2000c, Sections 3.10.5.2 and 3.12.3.2). Thereafter, the dryout zone contracts and persists for several thousand years (i.e., 1,000 to 3,000 years), well after cessation of above-boiling conditions (BSC 2001o, Section 6.3.5.1).

Figure 4-63 shows contour plots of matrix liquid saturation at 1,000 years (a) without ventilation and (b) with ventilation (CRWMS M&O 2000c, Section 3.12.3.2). The plots show large decreases in matrix liquid saturation only near the drifts.
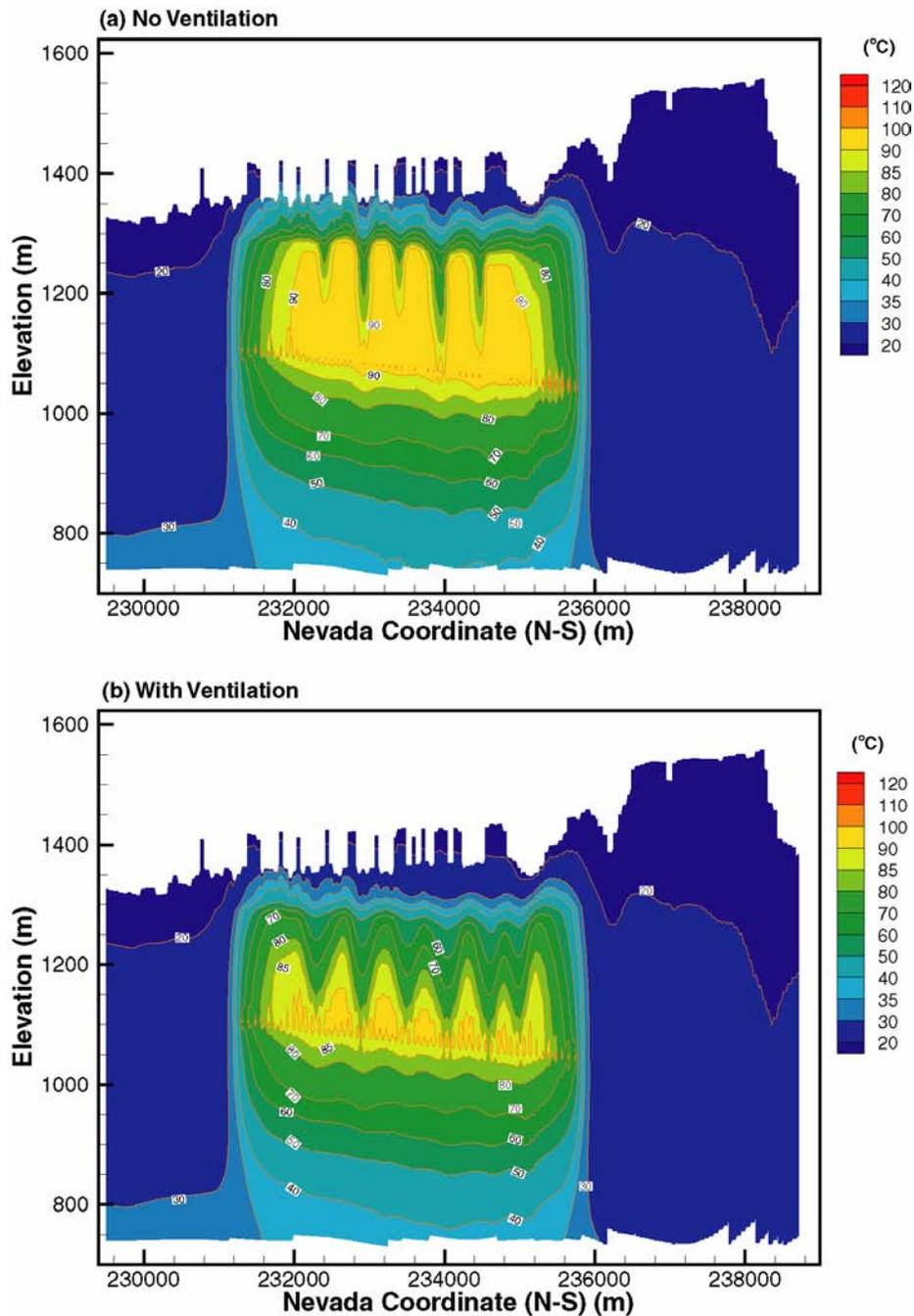
Figure 4-62. Temperature Distribution at 1,000 Years along NS#2 Cross Section from the Mountain-Scale Thermal-Hydrologic Model

(a) No ventilation. (b) With ventilation, removing 70 percent of heat during the 50-year preclosure period. The figure has approximately 8:1 vertical exaggeration. The lateral and vertical cross section used here is shown in Figure 4-60; the location of this cross section is indicated on the plan view grid in Figure 4-59. Source: CRWMS M&O 2000c, Figure 3.12-5.
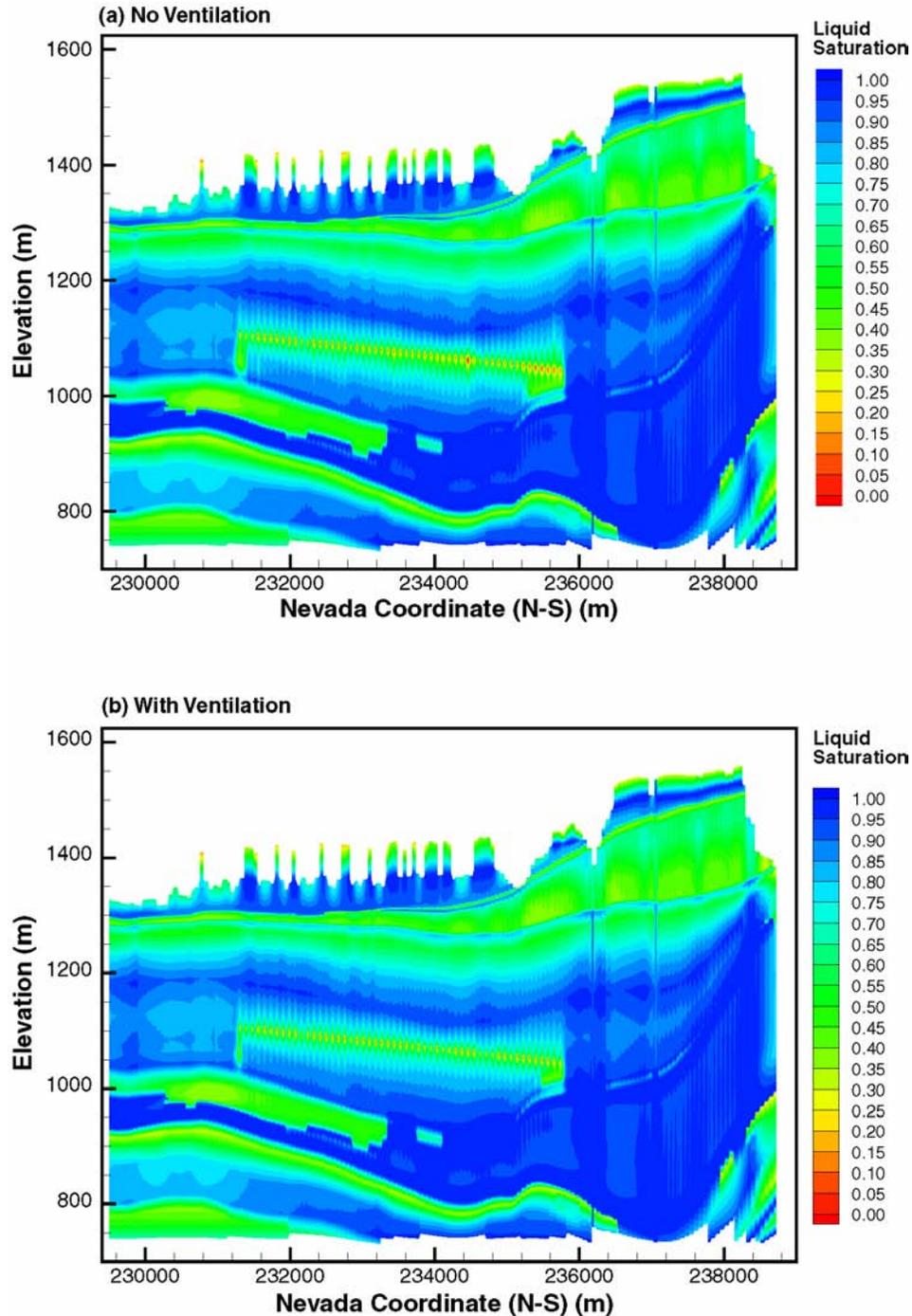
Figure 4-63. **Matrix Liquid Saturation at 1,000 Years along NS#2 Cross Section from the Mountain-Scale Thermal-Hydrologic Model**

(a) No ventilation. (b) With ventilation, removing 70 percent of heat during the 50-year preclosure period. The figure has approximately 8:1 vertical exaggeration. The lateral and vertical cross section used here is shown in Figure 4-60; the location of this cross section is indicated on the plan view grid in Figure 4-59. Source: CRWMS M&O 2000c, Figure 3.12-8.

Liquid saturation at a lateral distance of more than 50 m (160 ft) away from the potential repository is predicted to remain at near-ambient conditions. A zone of decreased saturation extends to about 50 m (160 ft) above and below the emplacement drifts. After 5,000 years, the matrix liquid saturation is almost fully recovered to ambient conditions. The fracture and matrix liquid saturation within the pillars remain at near-ambient levels and are controlled primarily by changes in the climate state.

Thermally Driven Changes in Percolation Flux—Although ventilation lasts only 50 years, it results in changes in flux patterns that persist for hundreds of years. This is because the heat removed by ventilation will delay the onset of boiling conditions. The model results show that ventilation leads to lower thermally driven liquid and gas fluxes because the effective thermal load is only 30 percent of the total heat output during the early period in which the heat output of the emplaced waste is greatest. Figure 4-64 shows the calculated liquid flux through the potential repository horizon with ventilation.

With ventilation, thermal evolution is delayed because the temperature of the rock must rise to boiling conditions to maximize evaporation and heat pipe activity. At 100 years (50 years after closure), the liquid flux is 10 mm/yr (0.4 in./yr). However, flux recovers to more than 150 mm/yr (6 in./yr) at 500 years as a result of higher temperatures. Because of the decay in thermal output, and the increased infiltration imposed by climate change, the liquid flux in the fracture continuum at the potential repository horizon recovers to the ambient percolation flux after approximately 5,000 years. With ventilation, the fracture flux through the pillars between the drifts remains at or above ambient conditions and temperatures remain below boiling throughout the thermal pulse. Beyond approximately 500 years, the fracture liquid flux in the pillars returns to the ambient percolation levels, though these levels change in response to changes in climate state. The liquid saturation within the pillars remains at or above the ambient liquid satu-

ration because of vapor condensation and liquid flux being channeled through the pillars. This flux may be increased by condensate drainage for several hundred years.

Liquid flux through the pillars is the direct result of the counter-current vaporization and condensation (reflux) cycle associated with the development of heat pipe conditions predicted by the mountain-scale thermal-hydrologic model (CRWMS M&O 2000c, Section 3.12.3.3). At early times (less than 100 years), thermally induced liquid fluxes above the drift are up to two orders of magnitude larger than the ambient percolation flux. At around 1,000 years, model results show fracture liquid flux at several locations to be 20 to 50 mm/yr (0.8 to 2.0 in./yr). At around this time, mountain-scale thermal model results suggest liquid flux may occur downward into the drifts (CRWMS M&O 2000c, Section 3.12.3.3).

Mountain-scale thermal-hydrologic modeling shows that temperature increases at the base of the PTn unit and the top of the CHn unit are moderate (much less than boiling) and are not expected to cause mineralogical alteration of these units. Temperatures at a lateral distance of more than 100 m (330 ft) outside the potential repository are expected to remain near ambient conditions. The mountain-scale model predicts little impact on thermal-hydrologic conditions outside the potential repository layout, possibly because large-scale gas-phase buoyant convection promotes upward mass and heat transfer.

4.2.2.3.2 Multiscale Thermal-Hydrologic Model

The multiscale thermal-hydrologic model (CRWMS M&O 2000cf) is used to model the effects of decay heat on water movement at the drift scale and within the emplacement drifts. Simulation results are used either directly or indirectly as input to other process models or abstractions for TSPA. The model uses the nonisothermal unsaturated–saturated flow and transport computer code to solve coupled heat and mass-transfer equations (CRWMS M&O 2000cf, Section 6).
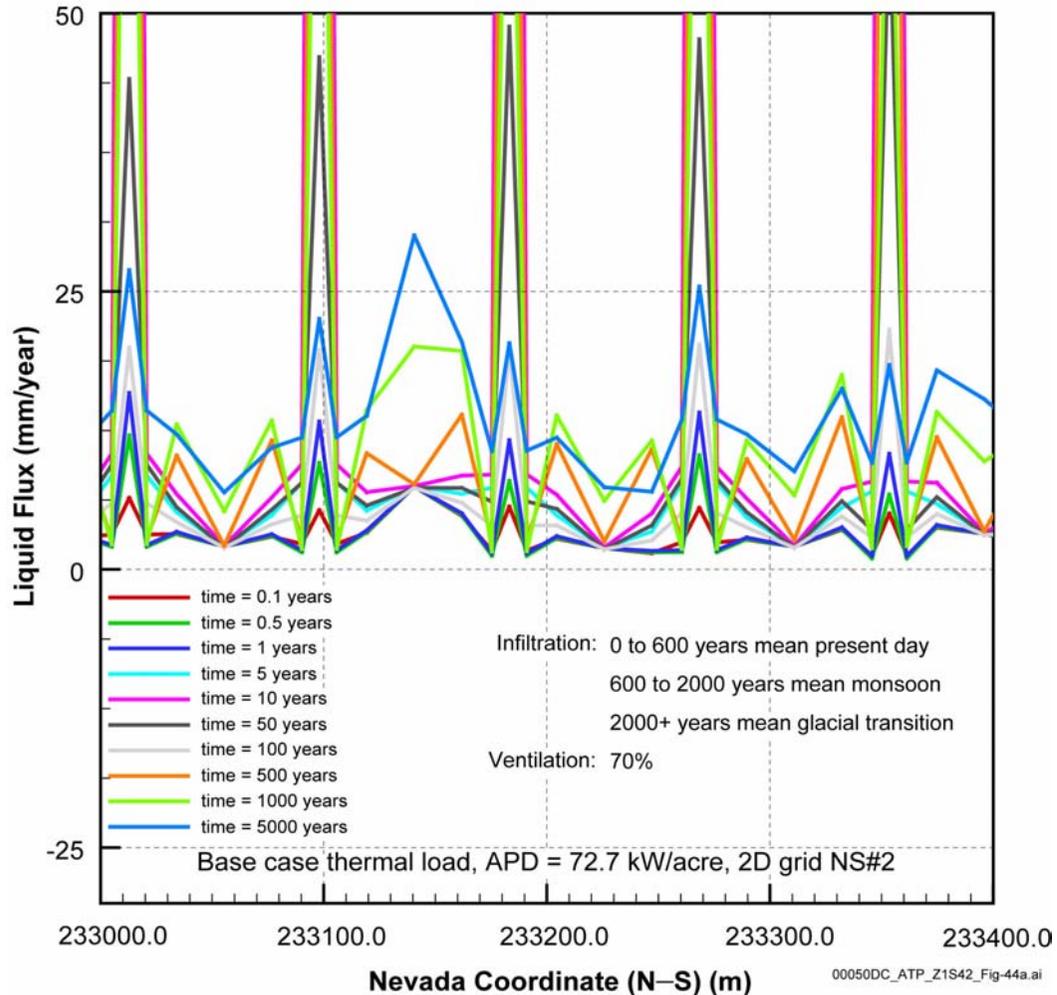
Figure 4-64. Fracture Liquid Flux along NS#2 Cross Section from the Mountain-Scale Thermal-Hydrologic Model

Case with ventilation, removing 70 percent of heat during the 50-year preclosure period. This figure shows the vertical liquid flux along a horizontal profile at the potential repository horizon in a two-dimensional model representing a north–south vertical cross section through the repository. The model is somewhat coarse, but it captures the behavior over multiple drifts at large scale. The maximum fluxes are located at the drifts in early time. This is caused by thermal reflux activity, whereby water evaporates, condenses above the drifts, and flows back down. As the thermal output declines with time, this type of activity diminishes. At later times (e.g., 1,000 years), the flux profile is much more uniform. At 10,000 years, the natural variability of flux conditions at Yucca Mountain, corresponding to predicted future climate conditions, controls the distribution of liquid flux. APD = areal power density. Source: based on CRWMS M&O 2000ci, Figure 69.

This model estimates thermal-hydrologic conditions within the emplacement drifts and the surrounding rock as functions of time, waste package type, and location in the potential repository. The multiscale thermal-hydrologic model is based on drift-scale thermal-hydrologic models of the types used to analyze the field-scale thermal tests, combined with three-dimensional thermal models that incorporate thermal interactions between waste packages and mountain-scale heat transfer. The resulting multiscale model predicts fine-scale behavior within the emplacement drifts while including the effects of repository-scale heat transfer (CRWMS M&O 2000cf, Section 6).

The multiscale thermal-hydrologic model relates the results from different types of smaller models to capture the effects of key factors that can affect

thermal-hydrologic conditions in the emplacement drifts and surrounding rock (CRWMS M&O 2000cf, Section 6):

- Variability of the percolation flux on the scale of the potential repository

- Temporal variability of percolation flux (as influenced by climate change)

- Uncertainty in percolation flux (as represented by the mean, high, and low infiltration flux conditions described in Section 4.2.1.3.3)

- Variability in hydrologic properties (e.g., those properties which control fracture–matrix interaction and capillarity of fractures) on the scale of the potential repository

- Edge-cooling effect (cooling increases with proximity to the edge of the potential repository)

- Dimensions and properties of the engineered barrier system components, such as the drip shield and invert

- Waste-package-to-waste-package variability in heat generation rate

- Variability in overburden thickness on the scale of the potential repository

- Variability in rock thermal conductivity (emphasizing the host rock units) on the scale of the potential repository.

Table 4-16 lists the specific performance measures that are predicted using the multiscale thermal-hydrologic model. This model simulates time-varying thermodynamic conditions such as temperature, relative humidity, and evaporation and condensation. Thermal-hydrologic conditions are also predicted, such as liquid saturation, liquid-flux (percolation flux), gas-phase flux, and capillary pressure. These results are used in coupled models, in engineered barrier system performance analyses, and to describe the overall evolution of the thermo-dynamic and thermal-hydrologic environments in the emplacement drifts and surrounding rock for TSPA (CRWMS M&O 2000al, Sections 2.2.1 and 3.2; CRWMS M&O 2000cf, Sections 6.11 and 6.12).

The need for a multiscale modeling approach stems from the fact that the performance measures depend on thermal-hydrologic behavior within a few meters of the emplacement drifts and also on thermal and thermal-hydrologic behavior at the mountain scale. A single, explicit numerical model would require a large number (many millions) of grid blocks. The multiscale model is used to estimate results that would be obtained if such a single model were feasible. The multiscale thermal-hydrologic model also predicts the effects of different waste package types (e.g., different commercial spent nuclear fuel waste packages, codisposal of DOE high-level radioactive waste) on the various performance measures (CRWMS M&O 2000cf, Section 6.1).

The multiscale thermal-hydrologic model comprises four major models and includes multiple scales (mountain and drift), multiple dimensions (one-dimensional, two-dimensional, and three-dimensional), and different assumptions regarding the coupling of heat transfer to fluid flow (conduction-only and fully coupled thermal-hydrologic). The four types of models are (CRWMS M&O 2000cf, Section 6.1):

- Line-averaged-heat-source, drift-scale, thermal-hydrologic model

- Smeared-heat-source, mountain-scale, thermal-conduction model

- Smeared-heat-source, drift-scale, thermal-conduction model

- Discrete-heat-source, drift-scale thermal-conduction model.

It is useful to think of the line-averaged-heat-source, drift-scale, thermal-hydrologic model as the basis model. These two-dimensional drift-scale thermal-hydrologic models use hydrologic properties and other input data that are fully consistent with the unsaturated zone flow model. The models

Table 4-16.   Thermal-Hydrologic Variables Predicted with the Multiscale Thermal- Hydrologic Model at 610 Locations in the Potential Repository

Thermal-Hydrologic Variable	Drift-Scale Location at Which Predicted
Temperature	Near-field environment host rock (5 m [16 ft] above crown)
	Near-field environment host rock (mid-pillar at potential repository horizon)
	Maximum lateral extent of boiling
	Upper drift wall (crown of the drift)
	Lower drift wall (below invert)
	Drift wall (perimeter average)
	Drip shield (perimeter average)
	Drip shield (upper surface)
	Waste package (surface average)
	Invert (average)
Relative humidity	Drift wall (perimeter average)
	Drip shield (perimeter average)
	Waste package
	Invert (average)
Liquid saturation (matrix)	Drift wall (perimeter average)
	Drip shield (perimeter average)
	Invert
Liquid-phase flux	Near-field environment host rock (5 m [16 ft] above crown)
	Near-field environment host rock (3 m [10 ft] above crown)
	Drift wall (crown)
	Drip shield (crown)
	Drip shield (upper surface average)
	Drip shield (lower side at the base)
	Invert (average)
Gas-phase air-mass fracture	Drip shield (perimeter average)
Gas-phase pressure	Drip shield (perimeter average)
Capillary pressure	Drip shield (perimeter average)
	Invert (average)
	Drift wall (crown; in matrix)
	Drift wall (crown; in fractures)
Gas-phase (water vapor) flux	Drift wall (perimeter average)
Gas-phase (air) flux	Drift wall (perimeter average)
Evaporation rate	Drip shield (crown)
	Drip shield (perimeter total)
	Invert (total)

are run for 31 locations spaced throughout the potential repository area (Figure 4-65) for a range of thermal loading values that represents the influence of edge-cooling. Variability of the hydrologic properties at the scale of the potential repository is represented by the 31 locations (CRWMS M&O 2000cf, Section 5.1.1).

The other three types of models, which are thermal conduction-only models, are required to account for the influence of three-dimensional mountain-scale heat flow and three-dimensional drift-scale heat flow on drift-scale thermal-hydrologic behavior. Further details on these thermal-conduction-only models, the method used to modify the two-dimensional thermal-hydrologic model results to reflect the three-dimensional scale effects, and the representation of air spaces in the drifts are provided in supporting documentation (CRWMS M&O 2000cf, Sections 6 and 7.1).
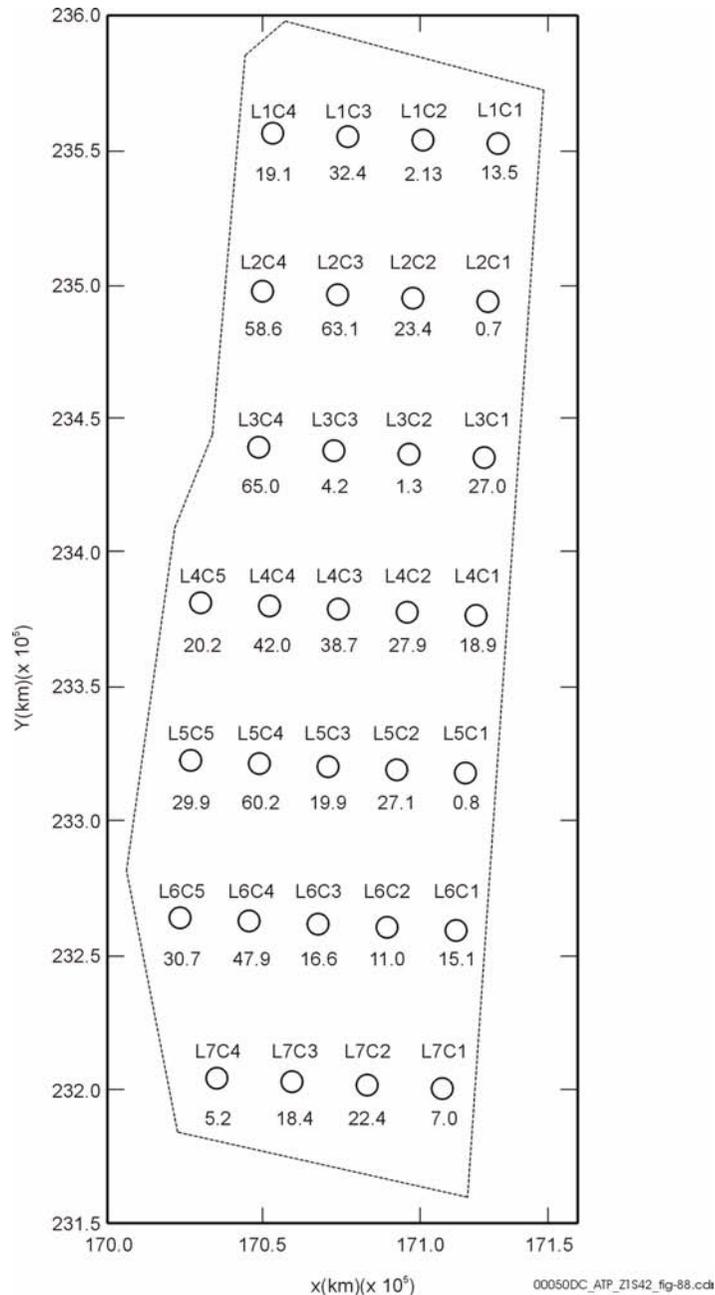
Figure 4-65.   Layout of the Potential Repository Used in the Multiscale Thermal-Hydrologic Model
These 31 locations (labeled L1C1 through L7C4) represent the overall repository in the multiscale thermal-hydrologic model. Detailed modeling is performed for each location to predict temperature and humidity conditions in the emplacement drifts. These models are combined with larger (but coarser) drift-scale and mountain-scale models to incorporate the effects of large-scale features of the site and the repository layout. The values posted at each location are the net infiltration values for the glacial-transition (long-term) climate state. Source: CRWMS M&O 2000as, Figure 3-70.

In the multiscale thermal-hydrologic model, the waste package sequence is explicitly modeled in a drift segment and repeated hundreds of times throughout the footprint of the potential repository. Model geometry is consistent with the design basis described in this report. The emplaced waste packages fall into several categories, representing those that would contain (1) pressurized water reactor spent nuclear fuel, (2) boiling water reactor spent nuclear fuel, (3) DOE high-level radioactive waste, and (4) DOE (naval) spent nuclear fuel. All waste packages are emplaced at the same time and follow the same average thermal decay function (as a percentage of initial heat output). The 70 percent heat-removal efficiency and the 50-year ventilation period are applied uniformly throughout the potential repository footprint. The overall average areal mass loading of the potential repository for multi-scale model applications is 60 MTHM/acre.

Figure 4-65 illustrates the potential repository footprint used in the model; this footprint closely approximates the actual plan view of the perimeter within which waste would be emplaced. Thirty-one locations are shown, which represent the lateral variability in hydrologic properties, stratigraphic thickness, and boundary conditions.

Major results of the multiscale thermal-hydrologic model summarized in this section are based on the higher-temperature thermal operating mode described in Section 2. During the preclosure period, host rock temperatures remain below the boiling point for the mean- and upper-infiltration flux cases, while boiling occurs in the host rock for the lower-flux case.

The expected duration of temperatures above the boiling point of water (96°C [205°F]) on the surfaces of the waste packages varies for three main reasons: (1) location within the repository layout, (2) spatial variation in the infiltration of recharge water at the ground surface, and (3) variability in the heat output of individual waste packages. The repository edges would cool first because they lose heat to the cooler rock outside the layout. The repository center would cool more slowly because heat flow would be limited mainly to the upward and downward directions. Water percolating downward through the

host rock in response to infiltration at the ground surface would hasten cooling of the repository; locations with greater percolation will cool sooner. There will be relatively large variations in the heat output of individual waste packages depending on the type and age of the waste they contain. Each of these effects is represented explicitly in the multi-scale thermal-hydrologic model, and the results of this model are used in TSPA.

During the preclosure period, peak waste package temperatures of 100°C (212°F) for the mean flux case, and 110°C (230°F) for the low flux case, are expected to occur at 10 to 15 years; peak drift-wall temperatures of 86°C (187°F) for the mean flux case, and 96°C (205°F) for the low flux case, are expected to occur at 20 to 25 years. Edge-cooling effects will not strongly affect preclosure temperatures.

During the postclosure period, peak waste package temperatures of 128° to 178°C (262° to 352°F) for the mean flux case, 127° to 189°C (261° to 372°F) for the low flux case, and 124° to 173°C (255° to 343°F) for the high flux case are expected to occur at 60 years. The difference in peak waste package temperature between the hottest and coldest waste packages for the mean flux case would be approximately 50 C° (90 F°). During the very early postclosure period, edge-cooling will have a small effect on temperatures. By 100 years, the influence of edge-cooling will be considerable, with waste package temperatures varying by 65 C° (117 F°) (98° to 163°C [208° to 325°F]) from the edge to the center of the potential repository for the mean flux case.

A typical waste package under nominal conditions would have an average surface temperature above the boiling point of water for about 1,000 years (CRWMS M&O 2000cf, Figure 6-50). For the mean infiltration case, the average temperature on the surfaces of all 21-PWR waste packages would cool to below the boiling point of water after about 1,400 years. Lower infiltration rates could increase the time until the waste packages cool to this temperature. Depending on the infiltration rate and the location in the repository, the time to cool could be less; for example, for the mean infiltration rate a 21-PWR waste package located on the edge of the

repository would cool to below the boiling temperature of water within about 300 years. For brevity, these ranges are described elsewhere in this report as "from hundreds to thousands of years."

Liquid-phase flux in the host rock above the drift would be influenced by dryout and heat pipe activity. Heat pipe behavior can increase the liquid-phase flux in fractures to well above the ambient percolation flux. However, the duration of this effect would be greatly decreased in this design in comparison with the repository design used for the Viability Assessment (CRWMS M&O 1998g, Chapter 3, Section 3.5.4). For the higher-temperature operating mode, the increased liquid-phase flux is calculated to last for less than 600 years (the duration of the present-day climate period).

The maximum lateral extent of boiling temperatures (away from the drift wall) is a good indication of spatial extent of dryout around the emplacement drifts. The lateral extent of boiling would be greater for the low infiltration-flux case than for the mean or upper-flux cases. For the hottest waste package location and the lower flux distribution, the maximum lateral extent of boiling would be 18 m (59 ft); because the drifts would be 81 m (266 ft) apart, a maximum of approximately 44 percent of the potential repository area would exceed the boiling point. If the estimated infiltration increases, this percentage would decrease.

There is a much greater difference in dryout behavior (as evidenced by the maximum lateral extent of boiling and by relative humidity reduction) between the mean and low infiltration-flux cases than between the mean and upper flux cases. Therefore, if one considers a percolation threshold above which rock dryout becomes substantially limited by percolation, the threshold would be near the mean infiltration-flux case. Larger values of the percolation flux greatly limit the calculated extent of boiling temperatures and rock dryout.

4.2.2.3.3 Drift-Scale Thermal-Hydrologic-Chemical Processes and Models

Figure 4-40 shows schematically the relationships between thermal-hydrologic and geochemical processes in the zones of boiling, condensation,

and water drainage in the rock surrounding the potential repository, particularly in the rock above the emplacement drifts. The emphasis in this section is on the changes in flow properties of the host rock due to these processes. Modeling of thermal-hydrologic-chemical effects on the aqueous chemistry of seepage water and gas composition in the potential repository host rock is described in Section 4.2.3.3.

Changes to hydrologic properties were evaluated using the thermal-hydrologic-chemical model. The thermal-hydrologic-chemical models account for two-dimensional heat and mass transfer within the drifts and in the surrounding rock, using separate continua in the rock to represent the connected network of fractures and the rock matrix in which the fractures reside (CRWMS M&O 2000al, Section 3.2.3.4.2). The thermal-chemical model component is implemented using TOUGHREACT, a heat transfer, mass transfer, and reactive-transport code. The model is used to calculate dissolution and precipitation of minerals that could change the porosity and permeability of the fracture system (CRWMS M&O 2000al, Section 3.2.3.4.3).

Thermal-hydrologic aspects of the model, such as the heating rate, ventilation, infiltration flux, and other boundary conditions, are identical to the thermal-hydrologic models discussed previously in this section. Discretization of the model domain is illustrated in Figure 4-66. Several cases were evaluated for different infiltration conditions (i.e., lower, mean, and upper) using the same climate-change scenarios used for the unsaturated zone flow model (BSC 2001o, Section 6.3).

The dual-permeability method was selected for modeling thermal-hydrologic-chemical processes. This is an important selection because a realistic representation of chemical interactions between fractures and the rock matrix depends on realistic representation of hydrologic interactions. The active fracture model is used (Liu et al. 1998; CRWMS M&O 2000bq, Section 6.4.5). Each matrix gridblock and each fracture gridblock has its own pressure, temperature, liquid saturation, water and gas chemistry, and mineralogy. Water–mineral reactions are considered to take place
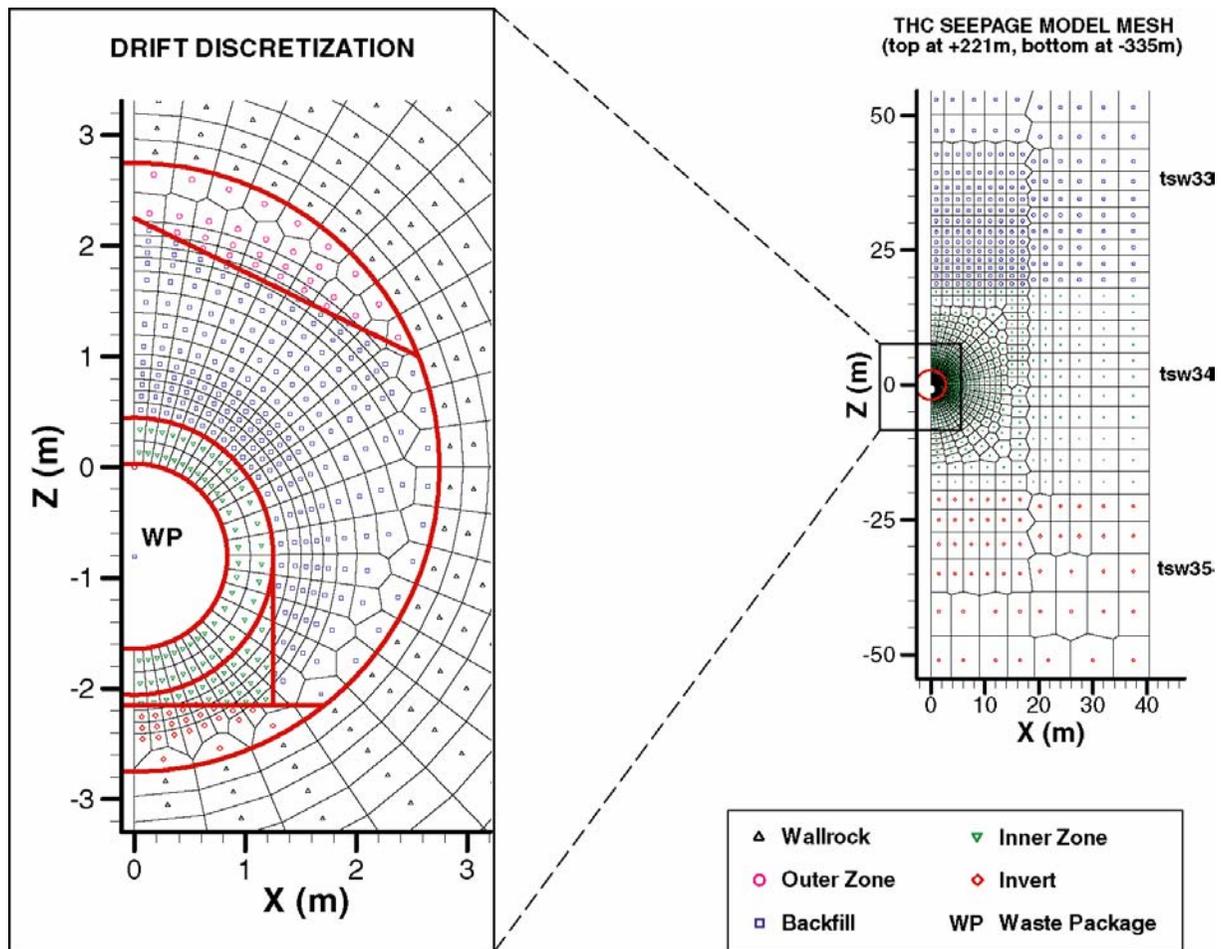
Figure 4-66. **Thermal-Hydrologic-Chemical Seepage Model Mesh Showing Hydrogeologic Units in Proximity of the Drift, and Blowup Showing Discretization of In-Drift Design Components**
The hydrogeologic units shown are the Topopah Spring Tuff upper lithophysal (tsw33), middle nonlithophysal (tsw34), and lower lithophysal (tsw35) units. These model grids are for simulations with backfill. The model results are used to predict thermal, hydrologic, and chemical conditions at the drift wall, rather than inside the drift. The results are therefore considered applicable to the design without backfill. THC = thermal-hydrologic-chemical. Source: CRWMS M&O 2000c, Figure 3.10-6.

under either kinetic or equilibrium conditions, using simulation methods similar to those described by Reed (1982) and Steefel and Lasaga (1994). Because the dissolution rates of many mineral–water reactions are quite slow, most phases are treated using pseudo-order reaction kinetics.

As stated in Section 4.2.2.2.1.3, the initial water and gas chemistry selected for use in the thermal-hydrologic-chemical model is based on the chem-

ical composition of matrix pore water collected from Alcove 5 (BSC 2001o, Sections 4.1.3 and 6.1.2). Although the rock permeability of the matrix is many orders of magnitude smaller in the matrix than in the fractures, the TSPA-SR thermal-hydrologic-chemical model assumes that infiltrating water in the fractures has the same composition as matrix pore water. This is justified in that the chloride-sulfate-type matrix-derived pore water composition is more concentrated in total dissolved minerals. The actual water compo-

sition within fractures tends to be more dilute (i.e., bicarbonate-type water). For all thermal-hydrologic-chemical modeling, the initial water composition is set to be the same in the fractures and matrix throughout the model domain (BSC 2001o, Section 4.1.3). Thermal-hydrologic-chemical model simulations were repeated with two sets of rock minerals to evaluate the sensitivity of calculated results to the mineral assemblage selected (BSC 2001o, Section 6.2). A full-simulation case included the major minerals found in the fractures and matrix of all rock units that are likely to be thermally perturbed based on mineral occurrence in deeper zeolitized units. A limited-simulation case included those minerals needed to represent basic aspects of Drift Scale Test data, such as pH and gas-phase carbon dioxide, while neglecting other species, such as silicates, ferric minerals, and fluorides. Details on derivation of model inputs, the numerical model and supporting sensitivity studies are provided in *Drift-Scale Coupled Processes (DST and THC Seepage) Models* (BSC 2001o, Sections 4.1 and 6.2).

Thermal-hydrologic-chemical model results consist of projections for the composition of water and gas that may enter the emplacement drifts for 100,000 years, including a 50-year preclosure period with ventilation. Figure 4-67 shows liquid saturation and temperature in the rock around the drifts at 600 years for the three infiltration conditions (i.e., lower, mean, and upper). This is the approximate time of the maximum extent of dryout for each infiltration case investigated. Note that these models predict conditions that would be encountered near the center of the potential repository, and that cooler conditions would be found near the edges.

Time histories for gas-phase carbon dioxide concentration, pH, chloride concentration, and total dissolved carbon concentration are predicted for the several locations in the host rock at the drift wall (CRWMS M&O 2000c, Figures 3.10-8 to 3.10-11). These results are summarized in Section 4.2.3.3, where they are used as boundary conditions for the physical and chemical environment in the emplacement drifts.

Comparison with data from the Drift Scale Test shows that the limited simulation (calcite, silica, and gypsum minerals only) matches observed chemical data more closely than the full simulation (including silicates, iron, and fluorides). However, for longer duration of reflux and boiling, as would be encountered in the potential repository, the system may trend toward the chemistry of the more complex full simulation.

Porosity changes in the rock matrix and fractures are directly related to volume changes from mineral precipitation and dissolution. Changes in fracture permeability are approximated using a parallel-plate model approach with fractures of uniform aperture (Steefel and Lasaga 1994, p. 556). Matrix permeability changes are calculated from changes in porosity using the Carmen–Kozeny relation (Bear 1988, p. 134). Capillary pressure in the matrix and fractures is modified using the Leverett scaling relation (Slider 1976, pp. 290 to 297), as previously mentioned in Section 4.2.1.3.2.

The calculated changes in fracture porosity for rock near the emplacement drifts, for the full simulation, at a simulation time of 10,000 years, are shown in Figure 4-68 for the three infiltration conditions (i.e., lower, mean, and upper). The fracture porosity change is expressed as a percentage of the initial porosity. Maximum porosity decrease is predicted for the high-infiltration case, predominantly above the drift. For all cases, the porosity change is relatively small (less than 1 percent of the initial porosity). For the limited simulation, porosity decrease results mainly from calcite precipitation, as was interpreted from the Drift Scale Test simulations. For the full simulation, the fracture porosity change is dominated by zeolite reactions. Because the fracture porosity changes are small compared to total fracture porosity, permeability changes are negligible and thermal-hydrologic processes will not be significantly affected by mineral precipitation or dissolution (CRWMS M&O 2000al, Section 3.2.3.4.3).
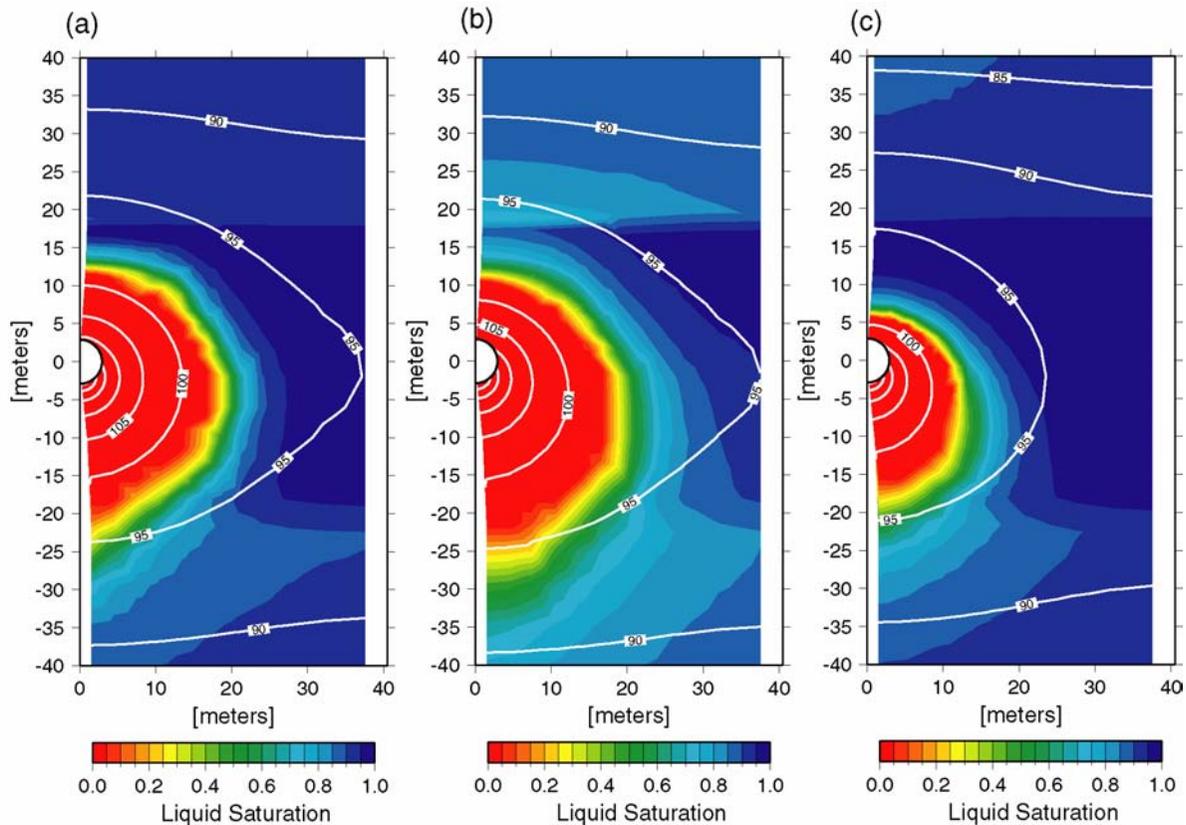
Figure 4-67.   Contour Plot of Modeled Liquid Saturations and Temperatures in the Matrix at 600 Years (Near Maximum Dryout) for Three Infiltration Rate Scenarios

The lower, mean, and upper infiltration rate scenarios are developed for the unsaturated zone flow model to represent the uncertainty of present-day and predicted future infiltration rates. The contour plots shown are (a) lower, (b) mean, and (c) upper scenarios (calcite-silica-gypsum system). The white contour lines show temperature in °C. The white half-circle in each plot is the drift outline, and the models are laterally symmetrical about the drift center. Source: CRWMS M&O 2000c, Figure 3.10-7.

4.2.2.3.4 Drift-Scale Thermal-Hydrologic-Mechanical Processes and Models

The drift-scale thermal-hydrologic-mechanical modeling in support of the TSPA accomplishes two objectives. This section emphasizes the potential effect on hydrologic properties in the surrounding rock resulting from thermal-mechanical changes, specifically potential effects on permeability. The drift degradation analysis presented in Section 4.2.3.3.5 assesses thermally caused movement of blocks on fractures intersecting the drift and the

potential for rockfall to affect the engineered barrier system.

Most prior thermal-mechanical modeling had the objective of determining the evolution of stresses in the near-field rock, in order to estimate the requirements for rock support in the emplacement drifts. These models treated the rock as a continuum and conservatively assumed that the mid-pillar locations were symmetry boundaries. This assumption is conservative (produces higher calculated stresses) because the overall repository footprint can expand due to the heating. The move-
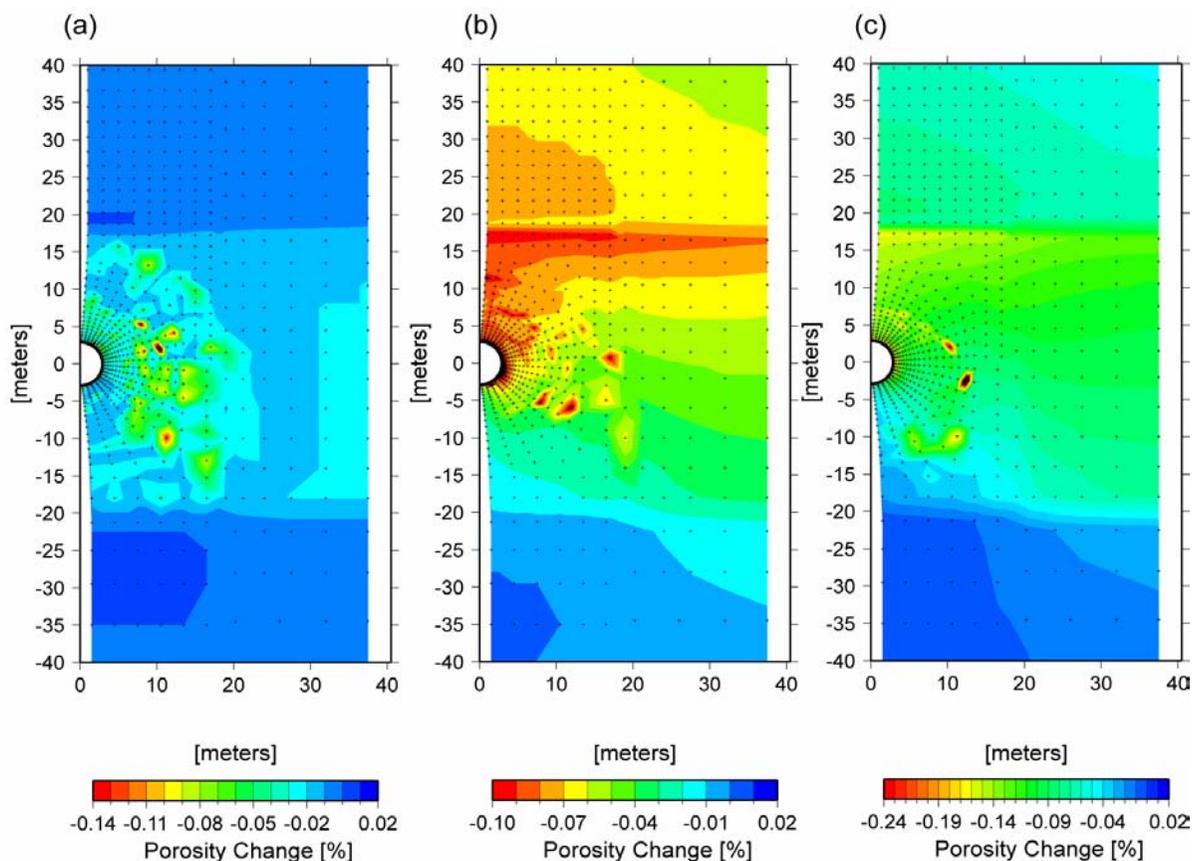
Figure 4-68.   Contour Plot of Calculated Total Fracture Porosity Change at 10,000 Years for Three Infiltration Rate Scenarios

The lower, mean, and upper infiltration rate scenarios are developed for the unsaturated zone flow model to represent the uncertainty of present-day and predicted future infiltration rates. The contour plots shown are (a) lower, (b) mean, and (c) upper scenarios (full simulation). Red areas indicate the maximum decrease in porosity as a result of mineral precipitation. The white half-circle in each plot is the drift outline, and the models are laterally symmetrical about the drift center. Source: CRWMS M&O 2000c, Figure 3.10-12.

ment of rock blocks at fractures was captured in the continuum models by the rock mass properties, such as the coefficient of thermal expansion (the fractional expansion of the rock per degree of temperature rise). Measurements of this coefficient depends on the size of the sample, with the coefficient decreasing as the scale moves from core to small blocks to small field tests and then to large field tests (CRWMS M&O 1999m, Table 9-3). The decrease in expansion coefficient can be attributed to the increased number of fractures which can accommodate expansion of the rock blocks. The results of the modeling indicate that horizontal

compressive stresses increase more than vertical compressive stresses during the thermal pulse, due to the stiff boundary conditions at the mid-pillar locations.

In this analysis supporting the TSPA-SR model, the distinct-element code 3DEC is used to simulate normal and shear displacement and other behavior on discrete fractures in the rock mass surrounding the drift (CRWMS M&O 2000al, Section 3.5.2). Fracture orientations and fracture densities are represented and discretized (gridded) in three dimen-

sions. Fracture orientations are based on field observations (Albin et al. 1997). Joint and rock-mass properties used in the calculation are based on field and laboratory studies of rock and fracture behavior, such as those by Barton et al. (1985) and Olsson and Brown (1994). Fracture densities are based on the assumption that only a few well-connected fractures are mechanically and hydrologically active (CRWMS M&O 2000al, Section 3.5.2).

Calculated joint deformations are used to compute permeability deformation values over a period of 1,000 years to capture the effects of heating and cooling. The mathematical formulation is described in the *Near-Field Environment Process Model Report* (CRWMS M&O 2000al, Section 3.5.2.3). Using this formulation, shear deformation always produces an increase in permeability, while normal deformation will increase permeability if the fracture opens and decrease permeability if the fracture closes. In general, fracture closing is expected during the heating phase in response to thermal expansion, while fracture opening occurs during cooling, the effects of shear displacements notwithstanding.

The results of the calculation (CRWMS M&O 2000al, Section 3.5) are that the major thermal-mechanical effect on fracture permeability occurs during cooldown due to both shear and normal deformation. Shear deformation of fractures during the cooldown causes permeability of the fractures in a region within two drift diameters of a drift wall to increase in permeability as much as an order of magnitude. Specifically, shear deformation on vertical fractures during cooldown produces the maximum amount of permeability change. Farther away from the drift wall, smaller increases in permeability (a factor of five) may occur on vertical fractures (CRWMS M&O 2000al, Section 3.5.3).

Results also indicate that normal deformation of fractures causes permeability to increase but to a lesser degree than shear deformation. Normal deformation during heating causes permeability to decrease significantly within one drift diameter of the drift wall. During cooldown, some vertical fractures above the drift open, thus increasing the permeability by a factor of two from the ambient values (CRWMS M&O 2000al, Section 3.5.3).

Ambient fracture permeability at the repository horizon is high, greater than 10^{-13} m^2 (100 milli-darcy) (CRWMS M&O 2000ch, Table 5). *Near-Field Environment Process Model Report* (CRWMS M&O 2000al, Section 5.5) concludes that the potential order of magnitude increase in permeability due to shear movement is not likely to significantly affect seepage.

4.2.2.3.5 Limitations and Uncertainties

As discussed in Section 4.1.1.2, uncertainties are an inherent component of the TSPA method. Uncertainty is introduced through the conceptual model selected to characterize a process, as well as the mathematical, numerical, and computational approaches used to implement the model. Uncertainty is also introduced from imperfect knowledge of important parameters used for input to the models (e.g., physical properties).

The DOE has performed several supplemental activities to address uncertainties and limitations in the TSPA-SR model. Additionally, as noted in Section 4.1.4, the DOE is evaluating the possibility for mitigating uncertainties in modeling long-term repository performance by operating the design described in this report at lower temperatures. Consequently, some of the models describing the effect of decay heat on water movement have been updated since the TSPA-SR model. Some alternative conceptual models have been implemented, and sensitivity analyses conducted to address parameter and model uncertainties. These supplemental model analyses are summarized in *FY01 Supplemental Science and Performance Analyses* (BSC 2001a, Section 1; BSC 2001b, Section 1).

Mountain-Scale Thermal-Hydrologic Model—The unsaturated zone flow model is the basis for the mountain-scale thermal-hydrologic model. Therefore, uncertainties associated with the unsaturated zone flow model also pertain to the mountain-scale model (see Section 4.2.1.3). The spatial resolution of the numerical mountain-scale thermal-hydrologic model is large enough that it

limits the interpretation of calculated temperature, saturation, and fluxes within the emplacement drifts and in the host rock near the drift openings. Consequently, the multiscale thermal-hydrologic model, with a finer spatial scale than the mountain-scale model, is used for these purposes.

Multiscale Thermal-Hydrologic Model—Two categories of model uncertainties are defined for the multiscale thermal-hydrologic model: (1) uncertainties related to thermal-hydrologic modeling and (2) uncertainties related to the multiscale estimation methodology.

The unsaturated zone flow model provides an important basis for the multiscale thermal-hydrologic model. Consequently, uncertainties associated with the flow model are propagated to the multiscale thermal-hydrologic model. Uncertainties related to the special features of the unsaturated zone seepage process model are not incorporated in the TSPA-SR model. As discussed in this section, the TSPA-SR model uses a conservative approach for calculating seepage during the thermal pulse, based on the percolation flux (5 m [16 ft] above the drift openings) and calculated by the multiscale thermal-hydrologic model. Although this is considered to be a conservative approach (leading to overestimated thermal seepage into drift openings), model improvements have been suggested such as discrete representation of flow focusing along faults and fractures and representation of episodically increased flow in the host rock (BSC 2001a, Section 4.3.5.6).

The percolation flux contains uncertainties related to mean, high, and low infiltration flux conditions, temporal variability (e.g., changes in climate), and spatial variability (e.g., repository cooling at the edges). The principal effects of these uncertainties on TSPA are related to the timing for cooling and return of moisture to the in-drift environment. Differences in timing of hundreds to a few thousands of years (as discussed in Section 4.2.2.3.2) will have a minor impact on the estimated longevity of the drip shield and waste package (with expected lifetimes greater than 10,000 years calculated in the TSPA-SR model). Another uncertainty is the arrangement and heat output of different types of waste packages, either in a lower- or higher-temperature operating mode. An arrangement of waste types with different heat output is used in the multiscale model, but the extent to which this is representative of repository conditions is uncertain, pending final decisions on repository design and operations parameters.

Uncertainties related to the multiscale estimation methodology include the effects of mountain-scale gas-phase convective circulation and the movement of water vapor along the axis of emplacement drifts from warmer to cooler regions. The TSPA-SR modeling approach did not include heat transfer by these mechanisms, probably resulting in overestimation of predicted temperatures and the duration of the thermal pulse.

Supplemental studies have added insight to some uncertainties and limitations identified with the TSPA-SR model. Approaches included alternative thermal property sets representing lithophysal tuff, Monte Carlo simulations of spatially heterogeneous fracture properties, simulation of a through-going vertical fracture zone intersecting the drift opening, and decreased thermal loading representing a lower-temperature operating mode (BSC 2001a, Sections 4.3.5.3, 4.3.5.4, and 4.3.5.5). Specific studies included:

- Alternative thermal seepage models incorporating the effects of flow focusing and episodicity (BSC 2001a, Section 4.3.5). The results support previous TSPA-SR analyses that found thermal seepage to be negligible for the relatively small values of seepage that may occur.

- Representation of fractures by spatially heterogeneous properties (BSC 2001a, Section 5.3.1.4.2).

- Evaluation of the bulk permeability of the host rock, the thermal conductivity of the lithophysal Tptpll unit and the invert, and the effects of lithophysal porosity of the Tptpll unit on vapor storage and heat capacity (BSC 2001a, Sections 5.3.1.4.1, 5.3.1.4.7, 5.3.1.4.8, 5.3.1.4.9, and 5.3.1.4.10).

- Evaluation of mountain-scale gas-phase convective process and the movement of vapor along the axis of the emplacement drifts (BSC 2001a, Sections 5.3.1.4.4 and 5.3.2.4.6).

Supplemental studies substantiate the overall model and analytical results of the TSPA-SR model, providing quantification of uncertainty either quantitatively or qualitatively. Thermal-hydrologic-chemical and thermal-hydrologic-mechanical processes will not significantly affect temperature or relative humidity within the emplacement drifts (BSC 2001a, Sections 5.3.1.4.5 and 5.3.1.4.6). In evaluating a lower-temperature operating mode, supplemental studies show thermal perturbations to be less than in the higher-temperature operating mode (BSC 2001b, Sections 3.2.2.6 and 4.2.2).

Drift-Scale Thermal Hydrologic-Chemical Processes Model—Uncertainties exist in the chemical parameters used to describe mineral precipitation and dissolution. Temperatures and flow rates are better constrained than other parameters of these models. Geochemical reactions are strongly influenced by temperature, the presence of water, and mass transport; so while the spatial distribution of mineral precipitation and dissolution is considered to be representative, the quantities minerals formed or dissolved at a given time and location are more uncertain. Furthermore, the potential for rapid boiling in the rock to cause mineral behavior outside the range of the models is recognized.

The assumed initial water and gas compositions as well as the geochemical conceptual model may also introduce uncertainty. Uncertainty is also recognized in the relationship used to determine fracture permeability based on changes in fracture porosity. These model uncertainties affect predictions of host rock pore water chemistry and changes in permeability in the host rock caused by thermal-hydrologic-chemical processes.

Model parameters, such as the effective reaction rates, are calibrated to results from field thermal tests, including the Drift Scale Test. Comparison of model predictions to geochemical data is important

for confidence building, and such comparisons have shown that the model is reasonable. Results from the full simulations yield higher pH values than measured in water samples from the Drift Scale Test, which results from a greater calculated reaction rate for feldspars. Therefore, porosity changes as a result of feldspar alteration in the potential repository host rock will probably be slower than predicted, suggesting that the TSPA-SR model gives an upper bound on such changes.

Supplemental studies have added insight to some uncertainties and limitations identified with the TSPA-SR thermal-hydrologic-chemical process and abstractions. These activities included a range of different input data and assumptions, such as host rock mineralogy and thermodynamic input data (BSC 2001a, Sections 4.3.6.3.1 and 6.3.1.6). Studies included:

- Supplemental model validation activities of water and gas compositions conducted for Drift Scale Test results (BSC 2001a, Sections 4.3.6.3.1 and 4.3.6.9)

- Supplemental sensitivity studies of different initial water and gas boundary conditions (BSC 2001a, Section 4.3.6.5)

- Simulated evolution of water and gas compositions in the lower lithophysal as well as the middle nonlithophysal tuff unit (BSC 2001a, Section 6.3.1.4.3).

These additional drift-scale thermal-hydrologic-chemical model simulations support the TSPA-SR evaluation, concluding only negligible changes in fracture permeability resulting from thermal-chemical rock and water interactions (BSC 2001a, Sections 4.3.6.7.4 and 4.3.6.9).

Drift-Scale Thermal-Hydrologic-Mechanical Processes and Models—The thermal-hydrologic-mechanical model, used in the TSPA-SR model, used a simplified thermal history to calculate results (CRWMS M&O 2000al, Section 3.5). Coupling the model to the multiscale thermal-hydrologic model has been suggested as a model improvement. Uncertainties in the TSPA-SR

thermal-hydrologic-mechanical model also include mechanical boundary conditions, joint and block properties, block geometry, and the calculation of permeability change due to aperture change.

The model domain for drift-scale near-field thermal-mechanical models is bounded by the mid-pillar locations between the emplacement drifts. For stress calculations, using a zero lateral displacement boundary condition at this location would be conservative (i.e., producing greater horizontal compressive stress) because in reality the entire repository layout can expand, allowing some displacement of the mid-pillar locations during the heating period.

The thermal-hydrologic-mechanical model used in the TSPA-SR model imposed boundary conditions equal to the ambient in situ stress (CRWMS M&O 2000al, Section 3.5). This is nonconservative (producing smaller stresses) because it is equivalent to assuming that more lateral displacement of the repository layout would occur. An alternative method would calculate the overall large-scale repository response in a coarsely gridded model and use the results to develop time-dependent displacement and stress boundary conditions for a drift-scale model. An additional advantage of this method would be the ability to consider the variability of the thermal-hydrologic-mechanical response due to proximity to an edge of the repository.

The joint and rock mass properties are based on field and laboratory studies (CRWMS M&O 2000al, Section 3.5.2). As discussed in Section 4.2.2.3.4, the effective thermal expansion coefficient depends on the size of the sample because of the tendency for fractures to deform in response to thermal stress changes. A similar situation exists for discrete fracture models because the rock between the discretely modeled joint may also include fractures. Also, the input values used for joint friction and cohesion are both variable and uncertain. Possible model improvements include adjusting the model grid for more gradual transitions in block sizes, also using site-specific fracture mapping data to develop the block sizes and shapes.

Supplemental studies have added insight to some uncertainties and limitations identified with the TSPA-SR thermal-hydrologic-mechanical process evaluation. Two models were used to assess selected uncertainties related to thermal-hydrologic-mechanical processes: a revised and extended discrete fracture (distinct element) analysis and a fully coupled thermal-hydrologic-mechanical continuum model (BSC 2001a, Section 4.3.7). These studies evaluated different boundary conceptual models, a simplified cubic-block conceptual model, and alternative empirical nonlinear relationships to calculate permeability change from porosity change (BSC 2001a, Section 4.3.7). Sensitive parameters were identified (e.g., residual permeability and rock stiffness) and conclusions are similar to those reached for the TSPA-SR model: permeability changes are within the range of the ambient seepage model, and thus uncertainty is already captured in the TSPA-SR model (BSC 2001a, Section 4.3.7.5).

4.2.2.3.6   Alternative Conceptual Processes

As with limitations and uncertainties, some of the following alternative conceptual models have been implemented or addressed in supplemental uncertainty analyses. These results are summarized in *FY01 Supplemental Science and Performance Analyses* (BSC 2001a, Section 1; BSC 2001b, Section 1).

Mountain-Scale Thermal-Hydrologic Model and Multiscale Thermal-Hydrologic Model— Alternative conceptual models can be organized in several categories: representation of fractured rock in numerical models, selection of representative property values, the potential for permanent changes in those properties from the effects of heating, and alternative models implemented to quantify uncertainties.

The host rock is represented in the mountain-scale and multiscale models as a continuous porous medium, although the rock contains discontinuities such as fractures and fracture zones. An alternative model represents the fractures discretely, and the resulting discrete fracture model approach has been applied to example problems (Hardin 1998, Section 3.3.3). The approach is very computation-

ally intensive and probably not practical for drift-scale and mountain-scale calculations. In addition, the number of interconnected fractures present in the host rock is so large that features of the network can be represented by a continuous medium (Section 4.2.1.3.1.1). Use of the discrete fracture model approach has been limited to modeling studies that support understanding of thermal-hydrologic processes.

Another category of alternative models involves the manner in which the network of fractures in the host rock is represented by a continuous medium. The thermal-hydrologic models described here represent fracturing using a dual-permeability continuum approach, based on the active fracture concept, which is also used in the unsaturated zone flow model (Section 4.2.1.3.1.1). The dual-permeability approach controls the movement of liquid and gas between fractures and the adjacent intact rock. Other available approaches include dual-porosity models and the equivalent single-continuum model (Hardin 1998, Section 3.3). The need for dual-permeability has been demonstrated by comparison to field thermal test data (Hardin 1998, Section 3.4); other approaches have been determined to provide less realism than the dual-permeability approach.

Alternative models for potential permanent changes in thermal and hydrologic properties of the host rock may be summarized as follows:

- Heating, cooling, and resulting water movement occur in a system with fixed thermal and hydrologic properties (such as porosity, permeability, and thermal conductivity). Properties of the rock may vary with temperature and water saturation but return to pre-repository values after the temperature returns to ambient levels.

- The same processes occur, but thermal effects permanently alter certain properties of the host rock through the action of coupled processes. For example, thermal-hydrologic-chemical coupling may change the hydrologic properties because of dissolution and precipitation of minerals in different regions.

The understanding of thermal-hydrologic-chemical effects on flow is summarized in Section 4.2.2.3.3. The model results indicate that changes in fracture porosity and permeability caused by chemical dissolution and precipitation will be minor compared to total porosity and permeability; hence, the first conceptual model (i.e., stationary properties) is selected as the most credible. This is the conceptual basis for both the mountain-scale thermal-hydrologic model and the multiscale thermal-hydrologic model.

As noted in the previous Section 4.2.2.3.5, supplemental studies have addressed additional alternative models:

- Supplemental studies implemented an alternative seepage method. Instead of using percolation flux as input to the seepage abstraction model, the unsaturated zone seepage model is used, incorporating new models for focusing seepage flow along discontinuities (e.g., faults) and episodic flow (BSC 2001a, Section 4.3.5).

- Supplemental studies implemented effects of mountain-scale gas-phase convective circulation and the movement of water vapor along the axis of emplacement drifts from warmer to cooler regions (BSC 2001a, Sections 5.3.1.4.4 and 5.3.2.4.6).

- Supplemental studies implemented effects of vapor storage and altered heat capacity within lithophysal cavities (porosity) of the Tptpll unit (BSC 2001a, Sections 5.3.1.4.1 and 5.3.1.4.9).

- Sensitivity studies incorporated drift-scale heterogeneity such as the influence of drift-scale heterogeneity of fracture properties, including permeability, porosity, and capillary properties (BSC 2001a, Section 5.3.1.4.2).

Supplemental analyses employing alternative models substantiate the overall model and analytical results of the TSPA-SR model (BSC 2001b, Sections 3.2.2 and 4.2.2).

Drift-Scale Thermal-Hydrologic-Chemical Processes and Models—A model proposed by Matyskiela (1997) suggests that silica precipitation in the rock matrix adjoining fractures will strongly reduce the permeability of the matrix, resulting in significantly decreased imbibition of percolating waters. The time required for strong sealing by silica was estimated for volcanic glasses under saturated conditions. Matyskiela (1997) observed complete filling of pore spaces with silica at fracture–matrix interfaces around a basaltic magma intrusion, the 50-m (160-ft) wide Papoose Lake sill, in the Paiute Ridge area of the Nevada Test Site. He estimated that fracture flow could be enhanced five times in magnitude with the sealing of the matrix pores (Matyskiela 1997, pp. 1117 to 1118). Formation of a silica cap by plugging of fractures with siliceous minerals, as predicted by recent simulations conducted for the potential repository at Yucca Mountain (Hardin 1998, Section 8.5.1), is the opposite behavior. More recent simulation modeling (CRWMS M&O 2000al, Section 3.3.3.5) has shown that fracture plugging will be of limited importance, given estimated fracture porosity of 1 percent.

Lichtner et al. (1999) showed that for a given matrix porosity, fracture plugging depends on the fracture porosity and the particular silica mineral that precipitates. The two-phase numerical simulation results suggest that at distances of tens of meters from the larger Paiute Ridge intrusion in their study, prolonged boiling conditions were established for times on the order of several thousands of years. Amorphous silica, with its higher solubility, is more readily transported by water and therefore produces the largest decrease in porosity, followed by chalcedony and quartz. For substantial sealing of fractures, a very small value of the fracture porosity is necessary. Lichtner et al. (1999) questioned the conclusions of Matyskiela (1997).

Comparison of the geochemical environment around a potential repository at Yucca Mountain with the geochemical environment around a basaltic magma intrusion is provided in supporting documentation (CRWMS M&O 2000c, Section 3.10.9). As discussed in Section 4.2.2.3.3, models of permeability changes due to mineral precipitation indicate that any such changes will be minimal. The sealing effects of silica deposition will probably be less developed at Yucca Mountain because (1) devitrified tuff reacts slowly compared with volcanic glass, (2) unsaturated fractures have less wetted surface area, and (3) the silica concentration in condensate draining through fractures will probably be limited by reaction rate processes.

As noted in Section 4.2.2.3.5, supplemental studies have addressed additional alternative models, including:

- Alternative initial water and gas compositions boundary conditions (BSC 2001a, Section 4.3.6.5)

- Alternative representation of the host rock, including the explicit representation of the Tptpll lithophysal unit mineralogy (BSC 2001a, Section 6.3.1.4.3).

Supplemental analyses employing alternative models substantiate the overall model and analytical results of the TSPA-SR model (BSC 2001b, Section 3.2.4.2).

Drift-Scale Thermal-Hydrologic-Mechanical Processes and Models—Alternative approaches fall into two categories: continuum versus discrete fracture models and method of coupling thermal-mechanical results to hydrologic flow. Both continuum and discrete fracture models have been used on the project. The continuum approach is satisfactory for calculating spatially averaged stress fields but is unable to resolve fracture displacements that affect permeability. The discrete fracture method can calculate movement of a significant number of representative fractures, which can then be related to permeability change.

Fracture displacement through normal or shear movement results in aperture change. The aperture change can be used to calculate both fracture porosity and fracture permeability, based on assumptions about fracture geometry. The approach used in Section 4.2.2.3.4 was to calculate fracture permeability change directly from fracture aperture change, using an empirical relationship based on laboratory studies. An alternative approach, used for thermal-hydrologic-chemical

modeling in Section 4.2.2.3.3, assumes a fracture geometry (parallel plates) and calculates permeability change from theoretical considerations.

As noted in Section 4.2.2.3.5, supplemental studies have addressed additional alternative models, including:

- A revised and extended distinct element analysis and a fully coupled thermal-hydrologic-mechanical continuum model (BSC 2001a, Section 4.3.7)

- A simplified cubic block conceptual model and alternative empirical nonlinear relationships to calculate permeability from porosity (BSC 2001a, Section 4.3.7).

Conclusions from the supplemental studies are similar to those reached for the TSPA-SR model: permeability changes are within the range of the ambient seepage model, and thus uncertainty is already captured in the TSPA-SR model (BSC 2001a, Section 4.3.7.5).

4.2.2.3.7   Model Calibration and Validation

Mountain-Scale Thermal-Hydrologic Model— There are no directly applicable data for validation of the mountain-scale response to thermal loading associated with the potential repository. However, numerical models of geothermal and petroleum systems can be validated from a wealth of field-scale testing and geothermal production data. The validity of mountain-scale model predictions is demonstrated by corroborative results from the modeling of analogue systems, from previously published unsaturated zone modeling studies, and from field-scale thermal tests in the Exploratory Studies Facility.

Table 4-15 in Section 4.2.2.2.3.3 lists selected geothermal systems (and, where available, analyses of those systems) that are comparable to the mountain-scale model. Applications for thermal-hydrologic modeling include detailed studies of the genesis, production history, and future performance of geothermal fields. Justification for the modeling approaches used in the mountain-scale thermal-hydrologic model is found in the

successful modeling of fluid and heat transport in large natural subsurface systems for which extensive field data are available. The magma intrusion analogues for thermal-hydrologic-chemical processes are discussed in Section 4.2.2.3.5. In addition, models for the recently completed Single Heater Test (Tsang and Birkholzer 1999) and the ongoing Drift Scale Test (CRWMS M&O 2000c, Section 2.2.4) use the same approach and input data as the mountain-scale model. In summary, the mountain-scale thermal-hydrologic model is considered valid because of its similarity to the models developed for field tests and the demonstrated validity of the geothermal analogue models.

Multiscale Thermal-Hydrologic Model—The multiscale thermal-hydrologic model uses a method based on industry-standard finite-difference software that includes both mass and energy balances. Model documentation addresses input data, assumptions, initial and boundary conditions, software, uncertainties, and other information required to replicate the model results.

Several validation approaches are used for the multiscale thermal-hydrologic model, including comparison of thermal-hydrologic modeling with results from the Large Block Test and the Drift Scale Test and comparison of multiscale thermal-hydrologic model results with mountain-scale thermal-hydrologic simulation, as described below. These comparisons are discussed in more detail in supporting documentation (CRWMS M&O 2000cf, Section 6.13).

Thermal-Hydrologic Models of the Large Block Test—A similar modeling approach was used to simulate the entire history of the Large Block Test (CRWMS M&O 2000cf, Section 6.13.1). As an example of model comparison with data, Figure 4-69 shows simulated borehole temperature profiles compared to observed temperatures. Evaluation of goodness-of-fit to measured temperatures shows accuracy of a few degrees Celsius.

Figure 4-70 shows the simulated and measured liquid-phase saturation profiles along another borehole in the Large Block Test. The simulated dryout zone develops more slowly than observed, but the
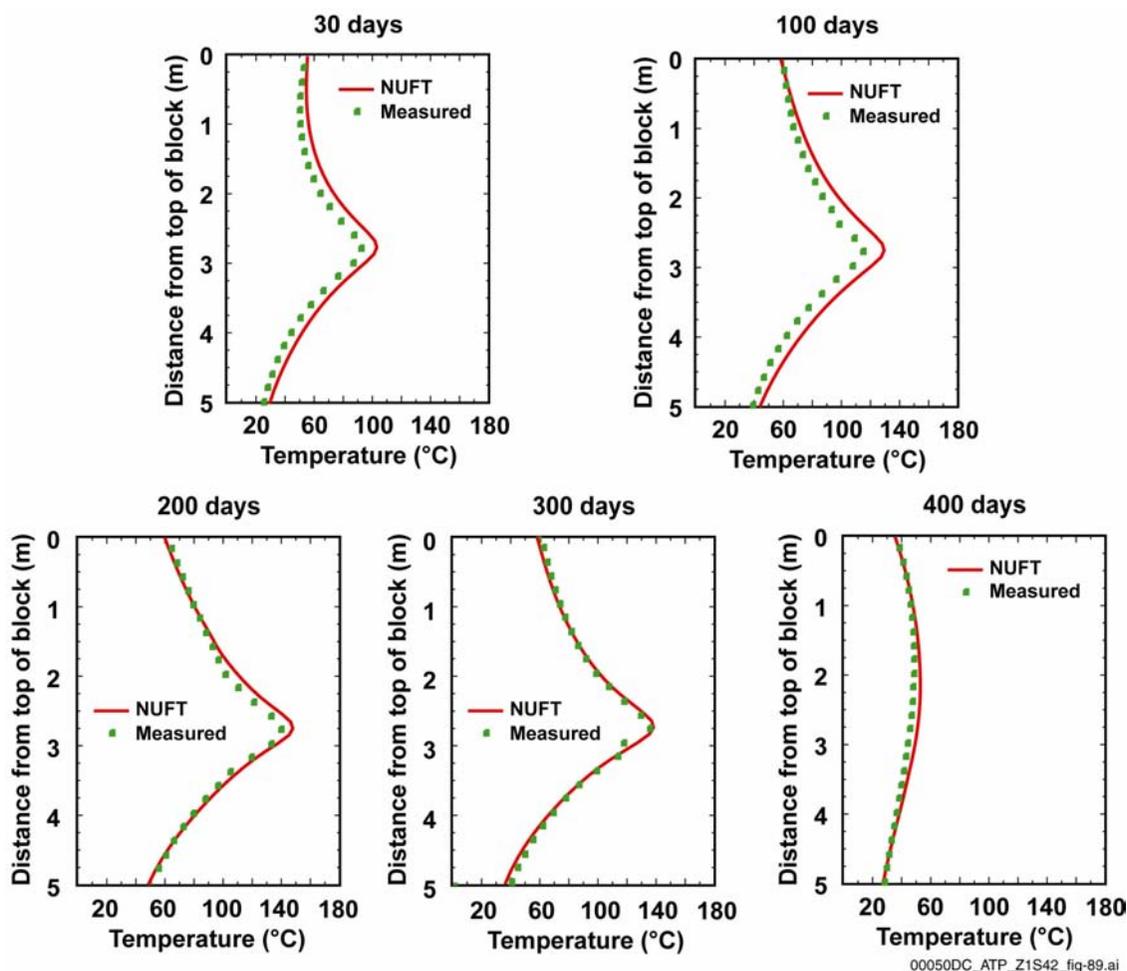
Figure 4-69. Comparison of Simulated and Measured Temperature Profiles along Large Block Test Borehole TT1, at Five Times from 30 to 400 Days
See Figure 4-45 for the location of Borehole TT1. Source: CRWMS M&O 2000cf, Figure 6-65.

difference resolves with time. At later times, the model is in close agreement.

Thermal-Hydrologic Models of the Drift Scale Test—Thermal-hydrologic modeling of the Drift Scale Test heating period, from startup to the present, was compared to observations (CRWMS M&O 2000cf, Section 6.13.2). As an example of model comparison with data, Figure 4-71 compares the simulated and measured temperatures along an observation borehole. The model results are in close agreement with measured temperatures, only slightly overpredicting temperatures in the dryout zone and slightly underpredicting temperatures in the sub-boiling zone.

In general, close agreement with observed temperature in the sub-boiling zone indicates that heat flow there is dominated by conduction and that the value of thermal conductivity is reasonable. Close agreement in the region close to the heated drift indicates that (1) thermal radiation is adequately represented inside the heated drift, (2) heat flow in the boiling and above-boiling zones is dominated by conduction, and (3) the value of thermal conductivity in this region is reasonable.

Comparison of the Multiscale Thermal-Hydrologic Model with the Mountain-Scale Numerical Model—Figure 4-72 compares the drift-wall temperature predicted by the multiscale thermal-hydrologic model with temperatures predicted by east–west cross-sectional mountain-scale thermal-
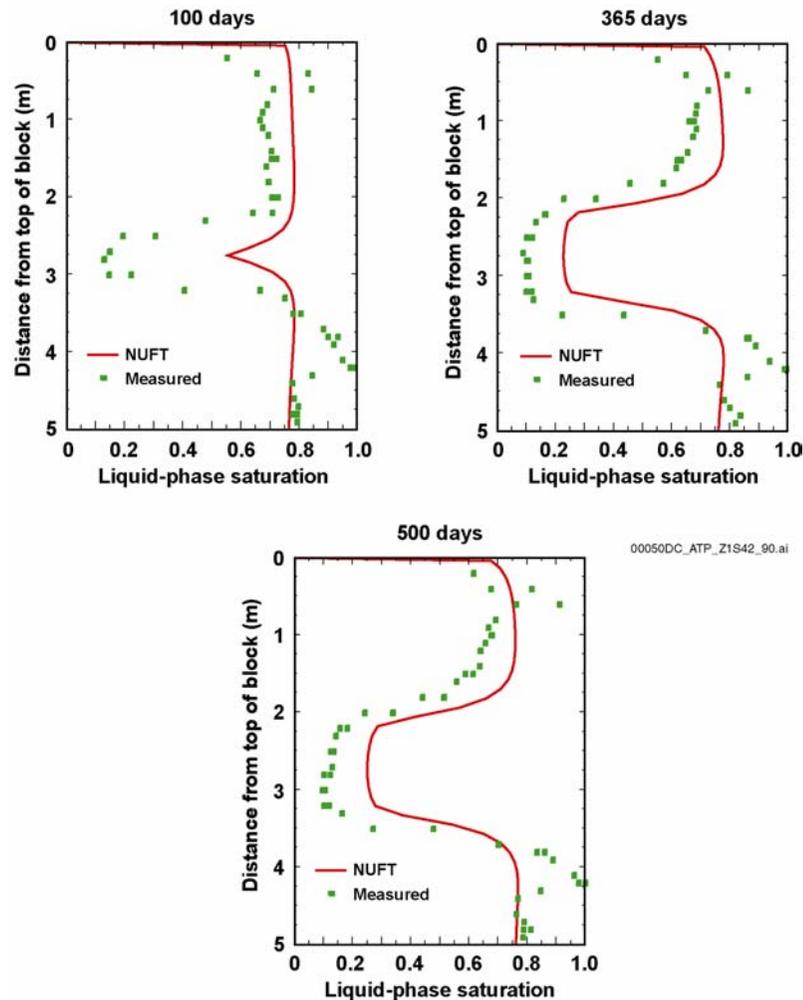
Figure 4-70. **Comparison of Simulated and Measured Liquid-Phase Saturation Profiles along Large Block Test Borehole TN3, at Three Times from 100 to 500 Days**

See Figure 4-45 for the location of Borehole TN3. Source: CRWMS M&O 2000cf, Figure 6-66.

hydrologic models (for details, see CRWMS M&O 2000cf, Section 6.13.3). The mountain-scale thermal-hydrologic model is coarsely gridded, so the comparison is limited to drift-wall temperature from the multiscale thermal-hydrologic model vs. drift temperature from the mountain-scale thermal-hydrologic model.

Before comparing the two approaches (Figure 4-72), it is important to discuss other differences in the models. Differences between the multiscale model and mountain-scale modeling approaches include:

- The temperature predicted by the mountain-scale model is for a grid block that occupies

an entire drift, so it produces a lumped representation of drift temperature, whereas the multiscale model resolves temperature differences within the drift.

- The mountain-scale thermal-hydrologic model uses a line-averaged heat source that axially smooths the differences between hotter and cooler waste package locations.

- The initial areal power density (at emplacement) in the multiscale thermal-hydrologic model is 92.3 kW/acre, compared to 99.4 kW/acre in the mountain-scale thermal-hydrologic model.
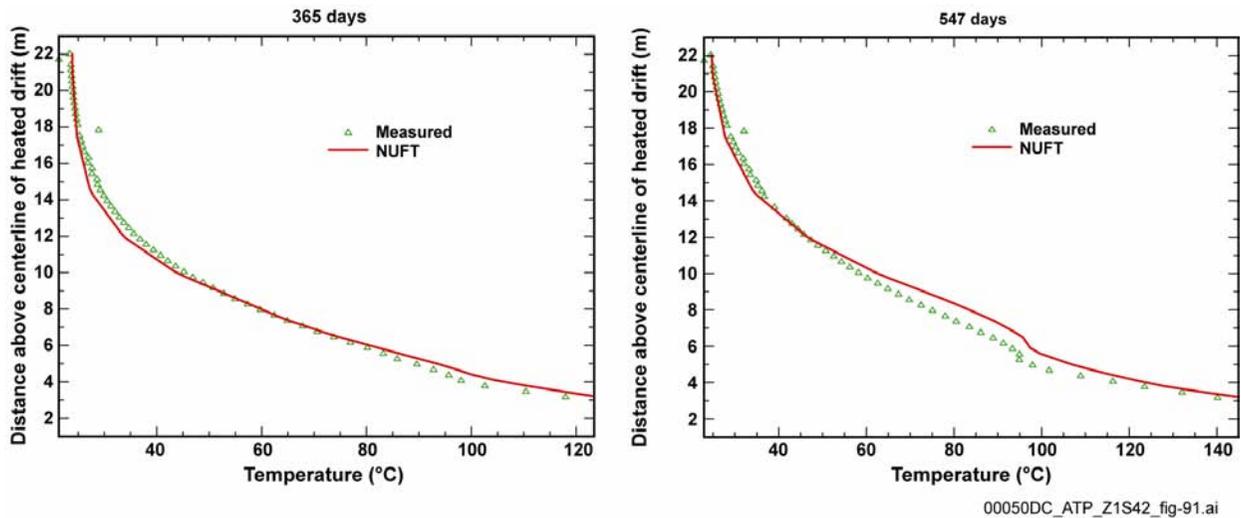
Figure 4-71. **Comparison of Simulated and Measured Temperatures along Single Heater Test Borehole ESF-HD-137 at 365 and 547 Days**

Source: CRWMS M&O 2000cf, Figure 6-67.
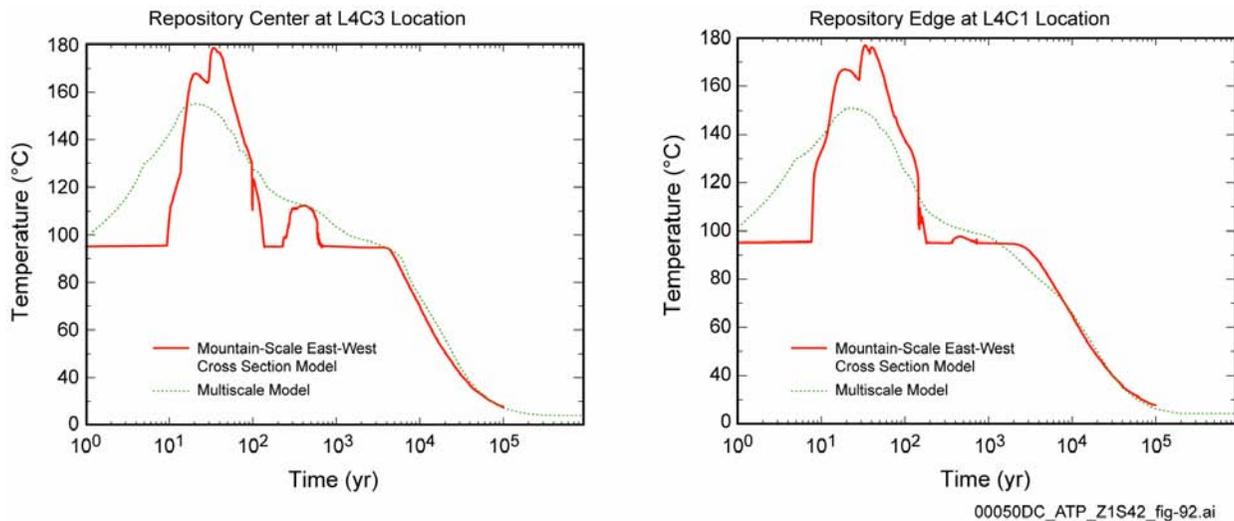
Figure 4-72. **Drift-Wall Temperature Predicted by the Multiscale Thermal-Hydrologic Model Compared to the Temperature Predicted by an East–West Cross-Sectional Mountain-Scale Thermal-Hydrologic Model**

L4C1 and L4C3 locations are shown in Figure 4-65. Source: CRWMS M&O 2000cf, Figure 6-68.

- The mountain-scale thermal-hydrologic model representation of the heated footprint of the potential repository extends slightly further to the west than in the multiscale thermal-hydrologic model.

Near the center of the potential repository, the approaches predict nearly the same duration of boiling (Figure 4-72, left). Near the edge, the mountain-scale model predicts a longer duration of boiling (Figure 4-72, right). During the post-boiling period, the temperatures predicted by the approaches are in close agreement. During the early heating period, the coarse gridding of the mountain-scale model cannot capture the more rapid changes that the multiscale model predicts. Also because of the coarse gridding, the mountain-scale model tends to overpredict heat pipe behavior. Given the differences in technical approach, the models are in reasonable agreement throughout much of the thermal evolution of the potential repository.

Drift-Scale Thermal-Hydrologic-Chemical Processes and Models—Comparison of model predictions with data from the Drift Scale Test involves (1) modeled patterns of fracture drainage compared to locations where water has been collected during the test, (2) comparison of carbon dioxide concentrations from gas samples, and (3) comparison of the evolution of water composition in boreholes sampled over time.

Simulated distributions of temperature and carbon dioxide concentration are shown in Figure 4-73 for the limited simulation approach (Case 2). The comparison shows that the simulations follow general trends in measured carbon dioxide concentration (CRWMS M&O 2000c, Figure 3.10-5). Two exceptions were when heater power loss occurred temporarily and when the gas samples were acquired at boiling temperatures and condensation occurred during the sampling. Detailed comparison of the modeling results and the measured carbon dioxide concentration data is discussed in *Drift-Scale Coupled Processes (DST and THC Seepage) Models* (BSC 2001o, Section 6.2.7.2).

The simulated pH of water in fractures is shifted to pH 6.5 from an initial pH of approximately 8.3, with the lowest pH values predicted where carbon dioxide concentration is greatest. The predicted shift in pH is similar to that observed in water samples collected from the Drift Scale Test. Chloride concentrations in waters collected from hydrology boreholes are considerably more dilute (a factor of 5 to 10) than the matrix pore water predicted by the modeling. Other species, such as calcite and silica, show similar trends in the modeled fracture water compositions compared to measured water compositions.

In the model simulations, calcite is the major phase forming in the zone above the heaters, although the quantity of calcite is small. Amorphous silica also precipitates but is less abundant than calcite. Direct observation of calcite precipitation or dissolution has yet to be observed in the Drift Scale Test, which is ongoing. However, other indications, such as the composition of water samples, provide indirect evidence for calcite precipitation. Fracture porosity changes predicted for the Drift Scale Test after 20 months are very small (on the order of 0.01 percent of the initial fracture porosity). Such small changes would likely have no measurable effect on the hydrologic properties of the rock.

Drift-Scale Thermal-Hydrologic-Mechanical Processes and Models—Model calibration and validation of fracture displacements due to heating and cooling is done using laboratory and field test results. Calibration includes normalizing models to test results and using observations to determine physical phenomena needed in the models. An example of the latter is the observation of sharp movements in multipoint-borehole-extensometer data at specific times; this observation has resulted in the adoption of a discrete fracture conceptual model in Section 4.2.2.3.4. Validation is the comparison of calculated results to test data, with the calculations being done independent of the test data themselves. Both continuum models and discrete fracture models have been compared to test data from the Large Block Test, the Single Heater Test, and the Drift Scale Test; these tests are described in Section 4.2.2.2.3.2.
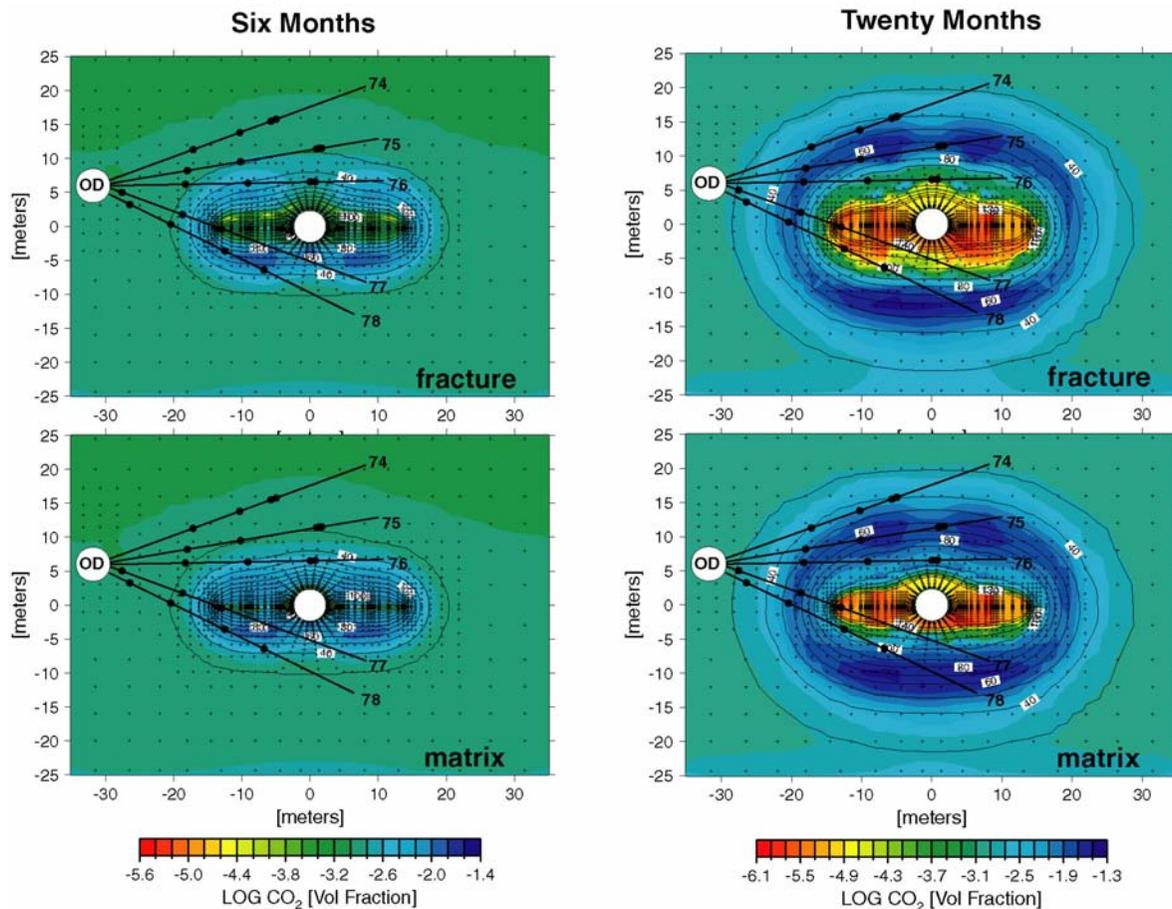
Figure 4-73. **Simulated CO$_2$ Volume Fractions in Fractures and Matrix after 6 Months and 20 Months of Heating During the Drift Scale Test**

The white labels indicate locations of isotherms (in °C). These isotherms correspond approximately to the distribution of volume fraction of CO$_2$, shown by the color contours. The white circle in the center of the plot is the heated drift diameter. "OD" indicates the observation drift from which Boreholes 74 through 78 extend (see Figure 4-52 for the location of these boreholes). Sampling locations in those boreholes are plotted with black dots. Source: Adapted from BSC 2001o, Figures 5 and 6.

4.2.2.4   Total System Performance Assessment Abstraction

Because of the limited thermal effect on water movement at large distances, the mountain-scale thermal-hydrologic model results are not directly included in the TSPA. Abstraction of thermal-hydrologic model results for the TSPA was therefore based on the near-field behavior predicted by the multiscale model.

The mountain-scale thermal-hydrologic model shows that the impacts of repository heating on temperature, saturation, and liquid flux in the unsaturated zone will have limited duration and will be limited to the repository area. Some effects, such as elevated liquid flux associated with heat pipe activity, will be limited to the vicinity of the emplacement drifts. Also, mineralogical alteration of the overlying and underlying hydrogeologic units will be minimal with preclosure ventilation. Accordingly, the thermal-hydrologic effects on far-field flow and transport are not currently considered in the TSPA (CRWMS M&O 2000c, Table 3.13-2).

The purpose of the report *Abstraction of NFE Drift Thermodynamic Environment and Percolation Flux* (CRWMS M&O 2000cc) is to abstract the multiscale, process-level thermal-hydrologic model results (CRWMS M&O 2000cf) so that they can be implemented in the TSPA model. The purpose of the abstraction is to simplify the detailed thermal-hydrologic description of the potential repository that is produced by the multi-scale model. An averaging process ("binning") is used to compute these quantities, based on a subdivision of the repository footprint that preserves a wide range of thermal-hydrologic variability. Multiscale model results used directly in support of the TSPA-SR model include waste package temperature, relative humidity at the waste package surface, and the percolation flux in the host rock 5 m (16 ft) above the emplacement drift. Temperature and relative humidity are used for the corrosion model, and percolation flux is used for the seepage model. Time-histories of waste package temperature, percolation flux, evaporation rates, and maximum and minimum waste package surface temperatures are also provided (CRWMS M&O 2000cc, Section 6.3). The abstraction of thermal-hydrologic data represents the potential variability and uncertainty in thermal-hydrologic conditions. It provides a quantitative description of thermal-hydrologic variability (i.e., from variability in the host rock unit, edge proximity, waste package type, infiltration rate, and climate state) and also incorporates uncertainty associated with the infiltration (i.e., lower, mean, and upper).

Abstraction of predicted water and gas compositions for the mean infiltration rate (with climate change), including both limited and full mineral suite simulations, is summarized in Section 4.2.3.4. Also, since the predicted thermal-hydrologic-chemical coupled effects on flow properties are relatively small, the effects on seepage are not included in the TSPA-SR.

The abstracted seepage model used in TSPA-SR performance assessment calculations did not include changes in permeability due to thermal-mechanical effects. This approach was based on *Near-Field Environment Process Model Report* (CRWMS M&O 2000al, Section 5.5) and was confirmed by supplemental TSPA analyses (BSC 2001a, Section 4.3.7.4.4).

4.2.3 Physical and Chemical Environment

The lifetimes of the drip shield and waste package will depend on the environmental conditions to which they are exposed: the in-drift physical and chemical environment (CRWMS M&O 2000a, Section 3.3). Once a waste package is breached, the transport of radionuclides released from the waste form also depends on the environment in the emplacement drifts.

This section describes estimates of how the physical and chemical conditions in the drifts are expected to evolve with time, based on the thermal operating mode described in Section 2. The description is based on the estimated response of the host rock to heating and on data concerning behavior of the engineered materials used to construct the potential repository. The estimates are based primarily on results from laboratory and field-scale testing, supplemented by observations from natural and man-made analogues.

As noted in Section 4.1.4, the DOE is evaluating operation of the repository at lower temperatures. Operating the repository at lower temperatures may change the evolution of the physical and chemical conditions in the drifts described in this section. The data and analytical results presented in this section reflect the effects of higher-temperature operating mode conditions, specifically the process models and abstractions employed in the TSPA-SR model (CRWMS M&O 2000a). Alternative thermal operating modes and supplemental uncertainty evaluations related to the in-drift physical and chemical environment models are described and summarized in *FY01 Supplemental Science and Performance Analyses,* (BSC 2001a, Sections 6.3.3., 6.3.4, 7.3.1, 7.2.4, and 10.3.4; BSC 2001b, Sections 3.2.4.2 and 4.2.4).

Results of the in-drift models used directly in the TSPA-SR model include time-dependent estimates of the infiltration rate, temperature, and relative humidity at the drift wall, as well as the evolution of the chemical conditions at the drift wall over four discrete time periods: (1) preclosure,

(2) boiling, (3) transitional cooldown, and (4) extended cooldown (CRWMS M&O 2000a, Section 3.3.3.4.2).

Physical Environment—The physical environment is described by the evolution, with time, of thermal-hydrologic conditions in the emplacement drifts. Estimation of the temperature, relative humidity, and rate of evaporation at locations throughout the potential repository is described in Section 4.2.2. The results show that every location in the potential repository could evolve from very dry conditions at temperatures greater than boiling to cooler conditions and increasing humidity. Differences between locations are limited mainly to the timing of these changes—for example, the duration of boiling temperatures on the waste package will depend on its location in the repository layout, local infiltration flux, and the heat output of individual waste packages (see Section 4.2.2.3.2). Cooling, and return of moisture to the emplacement drifts, would occur hundreds to a few thousands of years sooner at the edges of the potential repository, compared with the center. Cooling also would occur sooner at locations where there is greater recharge of water from the ground surface.

The potential for liquid water seepage into the emplacement drifts is described in Section 4.2.1. Seepage is combined with temperature, relative humidity, and evaporation rate to represent the physical environment for the engineered barriers in the TSPA-SR. Diversion of seepage by the drip shield and waste package is described in Section 4.2.5. The potential for condensation under the drip shield during the thermal period is also discussed in that section. A model of the flow of liquid water through breaches in the drip shield and waste package is used to assess advective releases of radionuclides in TSPA-SR. Thermal-hydrology, seepage, and water diversion model results that were developed in Sections 4.2.1, 4.2.2, and 4.2.5 are implicit in the following description of the physical and chemical environment and are not discussed further in this section.

The physical environment also includes the potential for rockfall, which could damage the drip shields or waste packages. The effects of rockfall are estimated based on observations from site char-acterization and use approaches that represent the effects of heating and seismic loading. Estimates of block size and rockfall frequency have been used to design the drip shield, which is designed to withstand rockfall over its design lifetime and thereby protect the waste package. The approach to estimating rockfall events is also described in this section.

Chemical Environment—Important processes affecting the chemical environment include evaporation and condensation of water, the formation of salts, and the effects of gas composition. During the thermal period, relative humidity will likely control the equilibrium solution chemistry and is therefore a principal descriptor of the chemical environment. The approach to analyzing the chemical environment involves several types of predictions:

- Composition of water and gas in the host rock around the drifts that can enter drift openings

- Composition of waters within the drifts that can further evaporate and form precipitates and salts

- The effect of microbial activity on the chemical environment

- The effects of engineered materials such as steel and cement

- The chemical environment at the surfaces of the drip shield and waste package.

These analyses are complementary and together describe the in-drift chemical environment as it is represented for performance assessment. Each is either incorporated explicitly in TSPA-SR or has been considered to have minor consequences to system performance and is excluded from consideration. The approach for each analysis is described in the following sections.

4.2.3.1 Conceptual Basis

This section describes the conceptual models that form the basis for analytical treatment of processes

in TSPA. Although the descriptions may contain statements that appear to be definitive, it is important to recognize that there are uncertainties associated with the selection of appropriate conceptual models. Alternative conceptual models are discussed in Section 4.2.2.3.7. Model results based on the selected conceptual models are generally considered to be best estimates, incorporating uncertainty, such that the models are suitable for use in TSPA.

4.2.3.1.1 Conceptual Basis for the Composition of Liquid and Gas Entering the Drifts

Composition of Liquid Seepage—The chemistry of waters in the host rock will act as a boundary condition on the in-drift chemical environment (CRWMS M&O 2000al, Section 3.4.2). During the thermal pulse, water vapor will move away from the heated drifts while liquid water percolates downward and replaces the water that evaporates in a thermal refluxing process (Section 4.2.2). The percolating waters will contain dissolved chemical species, such as sodium, calcium, sulfate, chloride, carbonate, and silica (CRWMS M&O 2000a, Section 3.3.3.4.2). When evaporation occurs, the chemical species will be left behind in the rock as precipitated minerals and salts.

The areal extent of the dryout zone produced by the higher-temperature operating mode would shrink as the heat output from the waste packages decreased with time. This will cause the region of boiling conditions to slowly converge on the drift openings. Liquid water will tend to sweep through formerly boiling regions, redissolve precipitates and salts, and move them closer to the openings. Soluble salts will tend to be concentrated near the openings. Depending on local hydrologic conditions, this process could cause seepage to be concentrated in soluble salts relative to the ambient (preheating) water composition.

With seepage, salts such as calcium carbonate and sodium chloride can form in the drifts (for example, from dripping and evaporation) directly on the drip shield or waste package. In the TSPA-SR model, only a fraction of the waste package locations in the repository would be affected by seepage (Section 4.2.1), especially during the thermal pulse when the conditions are relatively dry (Section 4.2.2). Without seepage, the effects of chemical processes in the host rock on the in-drift chemical environment will be limited to the gas composition. Seepage will be more likely in the future as the climate changes to the cooler, wetter, glacial-transition conditions discussed in Section 4.2.1. However, by the time the effects of this climate change propagate down to the host rock, cooldown will have progressed so that the drip shield temperature will be below boiling throughout the potential repository (CRWMS M&O 2000cf, Section 6.11.4).

After cooldown, and after soluble salts precipitated during the thermal pulse are redissolved and remobilized, the composition of seepage water will become increasingly similar to the ambient percolation in the host rock units. Some minerals precipitated during the thermal pulse may be stable, or slow to dissolve, but effects from such minerals are incorporated into the thermal-hydrologic-chemical model (BSC 2001o, Section 6.1).

Composition of the Gas Phase—The gas-phase composition in the host rock will also act as a boundary condition on the in-drift chemical environment (CRWMS M&O 2000a, Sections 3.3.3.2.3 and 3.3.3.4.2). The gas composition will initially be similar to atmospheric air, but during the thermal pulse, the gas phase will be strongly modified by evaporation of water and by interaction with carbon dioxide in waters and carbonate minerals (BSC 2001o, Section 6.2.7.2). Change in the in-drift gas flux and composition will affect water pH, including water that may occur on the surface of the drip shield or waste package (CRWMS M&O 2000ck, Section 6.2.4; CRWMS M&O 2000a, Section 3.3). Relationships among thermal, hydrologic, and chemical processes in the host rock around the drift openings, and within the drifts, are depicted schematically in Figure 4-74.

Evaporation of water from heating of the host rock will cause much of the dissolved carbon dioxide to be released as gas (the remainder will be precipitated as carbonate minerals). The gaseous carbon dioxide will form a broad halo around the drift openings that encompasses the cooler region where
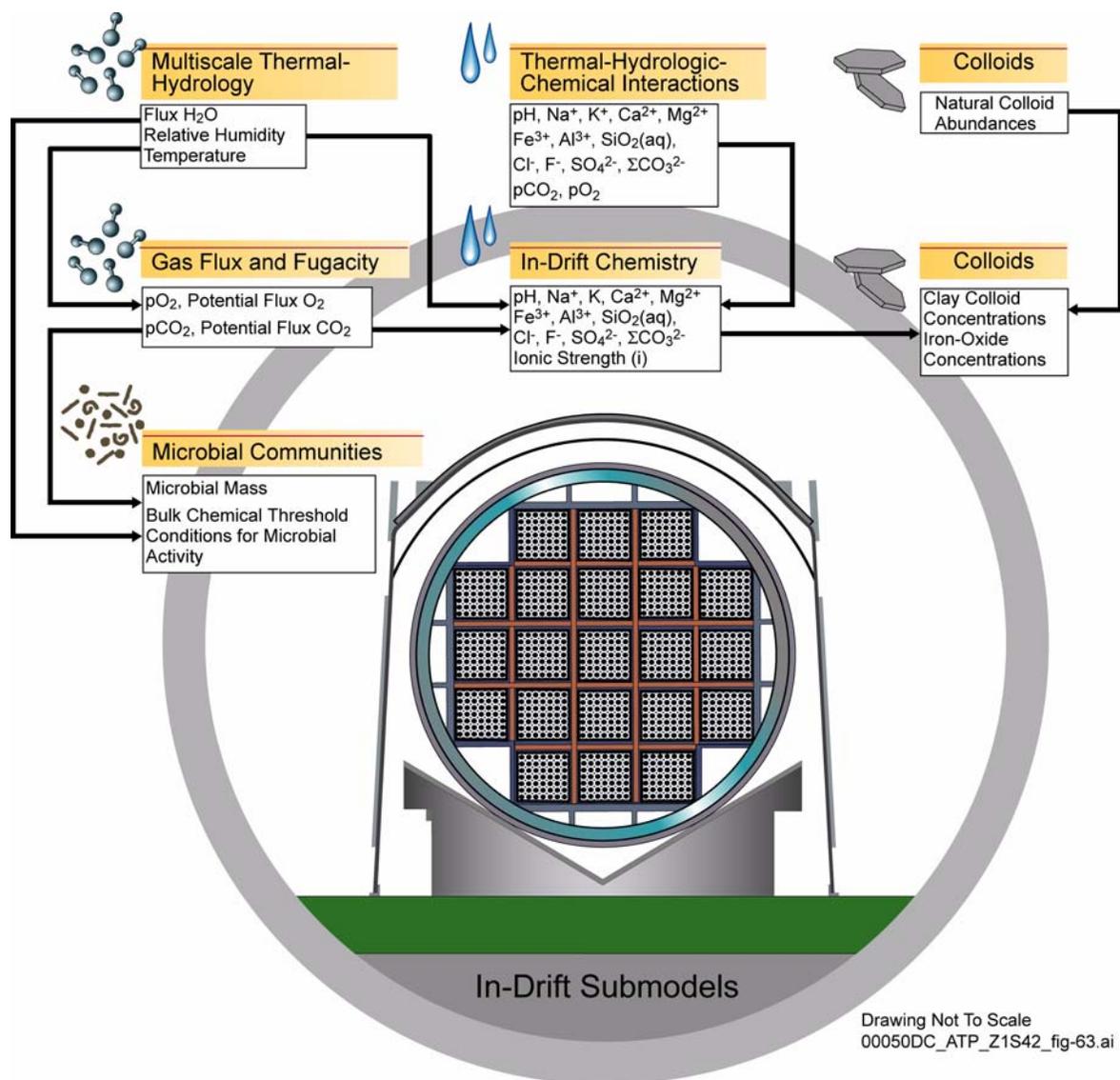
Figure 4-74. Emplacement Drift Cross Section Showing the Processes Considered in the Evolution of the Physical and Chemical Environment, and in the Transport of Radionuclides, within the Emplacement Drifts
Source: Modified from CRWMS M&O 1998g, Chapter 4, Figure 4-1.

water vapor condenses. Condensate will be enriched in carbon dioxide and slightly acidified (CRWMS M&O 2000al, Section 3.6.4.2). In the zone of evaporation closer to the drift openings, calcite and other carbonate minerals will be precipitated but may be redissolved later during cooldown when liquid water returns. Oxygen will exhibit simpler behavior because it is less soluble in water and forms different kinds of minerals. Analyses of uncertainty and the thermal sensitivity of chemical conditions within the drifts are

described in *FY01 Supplemental Science and Performance Analyses* (BSC 2001a, Section 6.3).

4.2.3.1.2   Conceptual Basis for Evolution of the Chemical Environment for the Engineered Barriers

At low relative humidity, any minerals or salts that exist in the emplacement drifts will be dry. These minerals and salts may be introduced as ventilation dust, from evaporation of construction water, or

from the occurrence of seepage when the drifts are hot and dry. As the relative humidity increases during cooldown, salts will condense to trap water vapor from the air (deliquescence) and form brine. Minerals and salts may occur on a small scale, for example, an evaporated droplet on the surface of the drip shield. Eventually, increasing humidity will cause the brines to capture more water vapor and become diluted. Seepage (where it occurs) will flush soluble salts from the drifts and redissolve the less soluble minerals. After the thermal period, the composition of waters and gases in the emplacement drifts will return to ambient (preheating) conditions (CRWMS M&O 2000as, Section 3.1.2.5.1).

Minerals and Salts Formed by Evaporation— Temperatures well above the boiling point of pure water (96°C [205°F] at the potential repository elevation), and associated low relative humidity, will persist hundreds to thousands of years after emplacement, depending on the location within the repository layout, the local infiltration flux, and the heat output from individual waste packages, as discussed in Section 4.2.2.3.2. These conditions are conducive to evaporation. Seepage into the drifts during this period, if it occurs, may be transient, but the nonvolatile dissolved constituents will accumulate in the drifts as salts and minerals. These solids will include soluble salts with the potential to form brines when relative humidity increases to approximately 50 percent and greater (CRWMS M&O 2000as, Section 3.1.2.5.1). Another source of minerals and salts is dust on the drip shield or waste package surfaces, which could be derived from the rock or from aerosols introduced from the atmosphere by ventilation during the preclosure operational period (CRWMS M&O 2000ck, Section 6.2).

Composition of Waters in the Emplacement Drifts—Temperature and humidity would be slowly varying in the repository, so equilibrium relationships will apply between brine concentration and relative humidity. Thus the relative humidity, which is readily predicted from thermal-hydrologic calculations (Section 4.2.2), is a good estimator of brine composition (CRWMS M&O 2000ck, Section 6.4). As noted previously, all waste package locations will evolve to high rela-

tive humidity, but at different rates, so the effect on TSPA is limited mainly to the timing of changes in equilibrium brine composition and seepage.

Where seepage occurs, the rate of seepage entering the drift during cooldown will eventually exceed the rate of evaporation in the drift as the thermal output decays (CRWMS M&O 2000cl, Section 6.2). When this happens, liquid water will begin to flow through the drift. Any brines present will tend to be diluted and flow out of the drifts with the seepage. If seepage is flowing into the drift, then considerable dilution of brines has probably occurred already from the associated humidity. Therefore, the details of seepage mixing with pockets of brine are not critical to predicting the chemical environment.

Microbial Activity in the Emplacement Drifts— Microbial activity is important primarily because of the potential for microbially influenced corrosion of the waste package. Microbes may also increase the rates of degradation for other engineered materials and can contribute to radionuclide transport. Bacteria and fungi, including molds, occur naturally in the host rock and would also be introduced by repository construction and operation. Because of dryness and elevated temperature, heating the rock at the potential repository will arrest microbial activity for time periods on the order of hundreds of years. However, heating will redistribute water so that cooler locations are wetter, which will locally increase the microbial activity. Factors that will limit microbial activity include elevated temperature, low humidity, and availability of nutrients and energy from engineered materials. Engineered materials such as steel may provide metabolic energy sources and limiting nutrients, such as phosphate. Measures to control the use of organic materials during construction and operation will also limit microbial activity (CRWMS M&O 2000as, Section 3.1.2.4).

4.2.3.1.3 Conceptual Basis for the Effects of Engineered Materials on the Chemical Environment

Engineered materials have the potential to affect the chemical environment as they degrade. Drip shield and waste package materials will degrade

slowly, and the effects on oxygen availability will be minor. Structural steel in the emplacement drifts will corrode and consume more oxygen, depending on the relative humidity. Cementitious grout will be used to anchor rock bolts in a portion of the potential repository (CRWMS M&O 2000cg) and may contribute cement leachate to the chemical environment.

Degradation of Steel and Alloys—Measured penetration rates for the titanium drip shield and the Alloy 22 waste package outer barrier are small (see Section 4.2.4). These materials obtain corrosion resistance from a passive layer of oxides on the exposed surfaces. The rate of oxygen consumption from maintaining the oxide layer is directly related to the penetration rate.

Steel will be used in roof supports, rails, and beams in the invert that support the drip shields and waste packages (see Section 2.4). These are preclosure structural applications; the steel will readily degrade during the postclosure period when humidity returns. Steel corrosion will begin when the temperature is near boiling and much of the air is displaced by water vapor. The steel is likely to corrode relatively quickly, within a few hundreds to thousands of years. While it is active, steel corrosion may affect the oxygen budget in the emplacement drifts (CRWMS M&O 2000cm, Section 6.2.2).

Cementitious Materials—Cement that will be used in rock bolt installation (like all Portland-based cements) is an assemblage of minerals and other phases, some of which dissolve to produce highly alkaline leachate. The composition of leachate will be determined by the solubilities of cement mineral phases. The phases present in "fresh" cement are more alkaline than those in aged cement because of carbonation and other processes (CRWMS M&O 2000cg, Section 5.3.1). Therefore, the leachate composition can be bounded using readily available information on cement composition. Several factors will act to limit the quantity and quality of leachate produced, including cement carbonation, low grout permeability, limited exposure to seepage flux, and neutralization of leachate by carbon dioxide in the drift environment (CRWMS M&O 2000cg, Sections 6.3.1 and 6.7.5).

Colloidal Particles Produced by Degradation of Engineered Materials—Colloidal particles are important as carriers for radionuclides, particularly isotopes of relatively insoluble elements, such as americium and plutonium. These radionuclides are transported very slowly (or not at all) in groundwater, except for colloidal modes of transport. Colloid generation and radionuclide transport are discussed at length in Sections 4.2.6, 4.2.7, 4.2.8, and 4.2.9. Colloids derived from the host rock will be present in seepage water. Additional colloids will be generated from degradation of engineered materials in the potential repository, including waste forms and other materials within the waste package (CRWMS M&O 2000cn, Section 6.1; CRWMS M&O 2000cg, Section 6.6).

Engineered materials in the emplacement drifts will consist mainly of corrosion-resistant alloys, cement, crushed rock, and steel. Corrosion products of titanium and Alloy 22 are mechanically stable (hence the corrosion resistance of these materials) and are unlikely to form significant colloids. Degradation of cementitious materials can form colloids (Hardin 1998, Chapter 6), but the usage of cement and its exposure to seepage will be limited. The invert ballast material will be crushed tuff derived from the host rock (see Section 2.4.1); the resulting colloids will be similar to colloids introduced with seepage. By contrast, steel in the emplacement drifts will be an abundant source of ferric-oxide colloids that are potentially important for radionuclide transport.

It is anticipated that quantities of colloids will be mobilized as a result of alteration of both the high-level radioactive waste and spent nuclear fuel waste forms. Colloid abundance within a breached waste package will depend on the extent of waste form alteration and the alteration products formed from in-package steel components. Colloid abundance and stability also depend on many environmental factors, including the ionic strength, pH, cation concentrations, colloid content of groundwater entering the waste package from the drift, presence of fulvic and humic acids, and microbe fragments (CRWMS M&O 2000co,

Section 1). The colloid source term and transport models are described in Sections 4.2.6 and 4.2.7 of this report, respectively.

Contribution of Engineered Materials to Microbial Activity—As stated previously, microbial activity is important primarily because of the potential for microbially influenced corrosion of the waste package; microbial activity may also increase the rates of degradation for other engineered materials and contribute to radionuclide transport. Microbes exploit chemical reactions (oxidation–reduction) that are rate-limited under abiotic conditions by providing faster alternative reaction pathways that also support cell-building and energy production (CRWMS M&O 2000cp, Section 6.3.1.1). Engineered materials include metals, which are important sources of reactants for these chemical reactions.

Engineered materials in the emplacement drifts will consist mainly of corrosion-resistant alloys, steel, cement, and crushed rock. Each of these can interact with microbes in particular ways, but steel will probably be the most important contributor. Steel will oxidize completely in the first few hundred years after sufficient humidity returns to the in-drift environment; after that, it will contribute little to microbial activity.

4.2.3.1.4 Conceptual Basis for the Environment on the Surfaces of the Drip Shield and Waste Package

Behavior of Water on the Barrier Surfaces— The environments on the surfaces of the drip shield and the waste package will determine the potential for corrosion processes and the penetration rates. Surface chemical conditions will be controlled by temperature, humidity, gas-phase composition (especially oxygen and carbon dioxide), the composition of dripping water, and the minerals and salts that may be deposited.

During the thermal pulse, the drip shield will be warmer than the surrounding in-drift environment in some instances, and the local relative humidity at the surface will be lower than the average humidity in the drift. Under these conditions, any water on the drip shield would tend to evaporate,

resulting in concentration of aqueous solutions and precipitation of minerals and salts (CRWMS M&O 2000ck, Section 6.2.3).

The titanium and Alloy 22 surfaces will react with atmospheric oxygen to form thin, resistant layers of metal-oxides (corrosion processes and rates are discussed in Section 4.2.4). These oxide layers will be mechanically stable and chemically unreactive, which confers corrosion resistance to these materials. Because the oxides are chemically inert compared to other species in the environment, they are assumed to not contribute to the chemical evolution of aqueous solutions on the barrier surfaces (CRWMS M&O 2000ck, Section 5).

Waste packages under intact drip shields will be exposed to moisture and chemical species. Humidity will penetrate the air gap between the waste package and drip shield, although the increase of relative humidity at the waste package surface will be delayed because of the warmer temperature there (CRWMS M&O 2000ck, Section 6.2.3). Moisture will form thin films on the surfaces by adsorption or capillary condensation (CRWMS M&O 2000ck, Section 6.3). Minerals and salts will be present in small quantities from dust and aerosols transported in the drift air (CRWMS M&O 2000ck, Section 6.1). If a drip shield is breached, seepage can contact the underlying waste package, which can lead to additional precipitation of minerals or salts on the waste package surface. As the waste package cools, less evaporation will occur on the surface, and accumulation of minerals or salts will be increasingly unlikely.

Potential for Acidic Conditions—There are two mechanisms by which acidic conditions could occur on the surfaces of the drip shield or waste package: radiolysis and localized corrosion. Neither mechanism will be important in the potential repository.

Radiolysis (outside the waste package) will be caused by gamma radiation that penetrates the waste package wall and interacts with air and moisture in the environment to produce small amounts of hydrogen peroxide (CRWMS M&O 2000n, Section 3.1.6.6) and possibly other species, such as

nitric acid. Radiolysis inside the waste package is discussed in Section 4.2.4. Several factors will limit the effect of radiolysis on the environment at the waste package and drip shield surfaces. The rate of gamma radiation from spent fuel and other waste forms will decline steeply within the first 1,000 years from the decay of relatively short-lived fission products. Only a small portion of the gamma radiation from the waste package will interact with the air space between the waste package and drip shield; much of this radiation will penetrate the drip shield or be absorbed within it. Acidic compounds formed in the drift environment during the thermal period will likely condense on cooler surfaces such as the drift wall and not on the drip shield or waste package, which will be warmer than their surroundings. If acidic compounds tend to precipitate on surfaces, then the drip shield will afford some protection to the waste package. Finally, the drip shield and waste package materials are resistant to attack by products of radiolysis (Section 4.2.4).

Localized corrosion can, in principle, cause acidic conditions to develop in cracks, crevices, or interfaces where exposure to the bulk chemical environment in the drifts is limited (CRWMS M&O 2000ck, Sections 6.5 and 6.6). Corrosion modes are discussed at length in Section 4.2.4, and localized corrosion is found to be of minor importance for titanium and Alloy 22.

4.2.3.1.5 Conceptual Basis for Rockfall on the Drip Shield

Fractures intersecting emplacement drifts can form "key blocks" that may become dislodged and fall directly onto the drip shields. Key blocks typically form at the crown of the existing excavations, are of minor size, and fall immediately after excavation, prior to ground support installation (CRWMS M&O 2000a, Section 3.3.1). In the design described in Section 2.4.4, the drip shield segments will be pinned together to prevent movement (with allowance for longitudinal thermal expansion and seismic strain). Structural bracing will provide capacity to resist permanent deformation from rockfall. The drip shield segments will have overlapping and interlocking joints to impede water leakage, even with small displacements between

segments. The connections between segments will tend to stiffen the structure, so that loads will be shared by adjacent segments. Determination of the size distribution for rock blocks that may fall on the drip shield and analysis of the structural response of the drip shield to rockfall are ongoing activities for which preliminary results are presented in Section 4.2.3.3.5.

4.2.3.2 Summary State of Knowledge

4.2.3.2.1 Composition of Liquid and Gas Entering the Drifts

Ambient Water Composition in the Unsaturated Zone—As discussed in Section 4.2.2.1.3, infiltrating water chemistry could be chosen from either the pore water chemistry in the unsaturated zone at or above the repository horizon or from a more dilute composition found in the perched water or saturated zone. These are referred to as a chloride-sulfate-type water composition and a bicarbonate-type water composition, respectively. As discussed in Section 4.2.2.3.3, the thermal-hydrologic-chemical model assumes the chloride-sulfate-type water as the basis for the initial ambient water composition in fractures in the unsaturated zone.

Composition of Evaporatively Concentrated Waters—Laboratory evaporation tests have been performed using both types of waters to investigate the effects of partial evaporation on solution chemistry and to determine which minerals and salts form as the waters are evaporated completely (CRWMS M&O 2000cg, Section 6.5.2). The bicarbonate-type water has been shown to evolve by evaporative concentration to a brine with high pH, whereas the chloride-sulfate-type water evolves to a brine with a nearly neutral pH. The chloride, sulfate, and nitrate concentrations in these waters tend to increase linearly with evaporation, and precipitate only in the later stages, because they are highly soluble. The major differences in behavior are attributed to the relative abundance of bicarbonate and carbonate among the anions present.

Studies of saline lakes in the western United States show that alkaline sodium-carbonate brines of the type that were produced from bicarbonate-type

water in laboratory tests occur in nature (CRWMS M&O 2000cl, Section 6.1.2). Many of these waters occur in volcanic geology similar to Yucca Mountain and have high silica content. These waters also are typically enriched in chloride and sulfate. Similarly, carbonate-poor brines of the type that were produced from matrix pore water in laboratory tests also occur in nature, such as those resulting from evaporation of sea water.

Water samples collected from the rock, in field-scale thermal tests performed at Yucca Mountain, are analogous to waters that would form during the heating of the host rock around the potential repository. The waters were collected where fractures intersected boreholes; therefore, they represent fracture waters that could potentially seep into repository drifts. The composition of such waters has varied with location, temperature, and other conditions but is dominated by condensation and interaction with fracture minerals (CRWMS M&O 2000cg, Section 6.5). The water compositions show that calcite present in the fractures is more readily dissolved than clays, feldspars, quartz, or other forms of silica. The noncalcite constituents of the waters are present in relative amounts that are similar to perched water and water found in well J-13, referred to hereafter as J-13 water (CRWMS M&O 2000cg, Section 6.5). The overall rate of condensation in these tests greatly exceeds the rate of water input from natural percolation, so the waters are dilute. Mixing of condensate with matrix pore waters was limited over the duration of the field tests but may be important over hundreds or thousands of years. From this discussion, it is appropriate to consider a range of water compositions, including bicarbonate-type and chloride-sulfate-type waters, for estimating the effects of evaporatively concentrated water and projecting the evolution of the in-drift chemical environment (CRWMS M&O 2000cg, Section 6.7.4.6).

Ambient Gas Composition—The natural composition of the gas phase in the unsaturated zone at Yucca Mountain is similar to atmospheric air, except that the carbon dioxide concentration is elevated by a factor of three. Elevated carbon dioxide is associated with soil processes near the ground surface and is commonly observed in nature. At other locations where there is more plant

activity, the carbon dioxide activity in the subsurface may be an order of magnitude greater than at Yucca Mountain (CRWMS M&O 2000cg, Section 6.2). The oxygen concentration throughout the unsaturated zone is apparently close to atmospheric, indicating there are no natural processes that consume oxygen at rates nearing the rate of potential supply from the ground surface.

Analysis of radiocarbon data from the site, from sampling of pore gas in surface-based boreholes and analysis of core samples, has been used to investigate the natural processes that deliver carbon dioxide to the unsaturated zone (CRWMS M&O 2000cg, Section 6.2). The influx of carbon dioxide dissolved in infiltrating waters, plus that transported in the gas-phase, has been estimated from isotopic mass balance to be in excess of 500 mg carbon dioxide per square meter per year. The results indicate that carbon dioxide is transported in the unsaturated zone by percolating waters and by gas-phase processes, such as barometric pumping.

Effects of Heating on Gas Composition—With heating of the potential repository, carbon dioxide will be released to the gas phase from evaporating matrix pore water (CRWMS M&O 2000al, Sections 3.3.1.2 and 3.3.3). At the same time, the humidity will increase with temperature, and water vapor will displace the air. This will initially cause increased carbon dioxide activity, as observed in field thermal tests, relative to the ambient level for the unsaturated zone. Years later, the carbon dioxide activity will decrease as the temperature approaches 96°C (205°F) (the boiling point at the potential repository elevation) and air is displaced by water vapor. Eventually, during cooldown, the carbon dioxide concentration in the emplacement drifts will approach the ambient level for the unsaturated zone.

Gas-phase convection during the thermal pulse will have an important impact on the fluxes of carbon dioxide and oxygen to the emplacement drifts and on the resulting gas-phase concentrations available for chemical reactions. As the host rock heats up, and the humidity increases, the density of the gas phase will decrease, and buoyant convection may occur. Buoyant convection can occur in porous

media, and has been interpreted as the cause for thermal effects associated with hot springs and igneous intrusions (Turcotte and Schubert 1982, pp. 367 to 370). Convection could circulate gas in the unsaturated zone, and thereby move air into the emplacement drifts, decreasing the humidity and increasing the availability of carbon dioxide and oxygen during the thermal pulse (CRWMS M&O 2000cg, Section 6.2.2.2). Increased availability of carbon dioxide will have the effect of buffering evaporatively concentrated, alkaline solutions, particularly above pH 10 (CRWMS M&O 2000cg, Section 6.7.5.3). Increased availability of oxygen will lessen the impact of steel corrosion on the in-drift chemical environment (CRWMS M&O 2000cg, Section 6.3.2.2).

The gas-phase concentration of carbon dioxide in the emplacement drifts during the thermal pulse will also be augmented by liquid water percolation in the host rock. As waters percolate downward toward the potential repository, carbon dioxide will exsolve because its solubility decreases with increasing temperature. If the waters are evaporatively concentrated, more carbon dioxide may be produced. The concentration of carbon dioxide species in such waters can be inferred from the composition of perched waters sampled from field thermal tests (CRWMS M&O 2000cg, Section 6.5) and is predicted using the approach described below.

Approach to Modeling the Composition of Liquid and Gas Entering the Drifts—The modeling approach for seepage and gas-phase composition during the thermal period couples thermal-hydrologic processes with both liquid and gas-phase chemistry. Temperature and evaporative concentration are determined from thermal-hydrology, while dissolution and precipitation reactions are modeled simultaneously (CRWMS M&O 2000c, Section 3.10.5). The thermal-hydro-logic-chemical modeling approach is integrated with the unsaturated zone flow model (Section 4.2.1) because the same rock properties and boundary conditions are used. The same coupled model is used in Section 4.2.2 to evaluate the potential for coupled effects on hydrologic properties.

As noted previously, every location in the potential repository will be subject to similar evolution of thermal-hydrologic and chemical processes, but the timing of these processes will depend on local conditions. The principal factors that will control timing are edge versus center locations in the potential repository layout and the local percola-tion flux (CRWMS M&O 2000cg, Section 6.1). Based on similarity of the process evolution at different locations, it is possible to represent thermal-hydrologic-chemical behavior using a limited set of chemical computational models. The major drawback of such an approach is uncertainty of hundreds to thousands of years in the timing of thermally driven changes in chemical conditions. This uncertainty corresponds to the predicted vari-ability in the duration of elevated temperature on individual waste packages, as discussed in Section 4.2.2.3.2.

For developing and validating this model, results from the Drift Scale Test constrain the thermal-hydrologic response, gas composition, and compo-sition of liquid water in fractures for the first few years of repository evolution. Longer-term evolu-tion is predicted by extrapolation. The concentrations of carbon dioxide and oxygen depend on thermally driven gas-phase circulation, and a range of models and properties are consid-ered and compared (CRWMS M&O 2000cg, Section 6.2).

Water and gas compositions are predicted at the drift wall to represent effects of processes in the host rock and used as boundary conditions for processes in the drift (CRWMS M&O 2000c, Section 3.10.5). These predictions are then used as boundary conditions on a different model for in-drift processes, which uses an approach formulated to accommodate evaporatively concentrated waters with high ionic strength (CRWMS M&O 2000cg, Section 6.7.4.6; CRWMS M&O 2001b, Section 1). Evaluation of the carbon dioxide and oxygen budgets for chemical processes occurring in the drifts and the surrounding host rock shows that chemical reactions will probably not strongly perturb conditions in the surrounding rock (CRWMS M&O 2000cg, Section 6.7). The concentrations of carbon dioxide and oxygen will be uniform within the drift air-space (although

relative humidity will vary with temperature) because gas-phase diffusion and convective mixing are rapid compared to the potential rates of consumption of these reactants. Finally, alternative chemical boundary conditions for water composition (i.e., bicarbonate-type and chloride-sulfate-type waters) are used to reflect the present state of knowledge of mobile waters in the host rock (CRWMS M&O 2000cg, Section 6.7.4).

4.2.3.2.2 Evolution of the Chemical Environment

The following discussion describes the summary state of knowledge for processes that will affect the bulk chemical environment in the emplacement drifts. This environment is distinguished from local conditions associated with cracks and crevices, microbial colonies, and within layers of engineered material degradation products.

Minerals and Salts Formed by Evaporation—As Yucca Mountain waters are evaporated to dryness, various minerals and salts are formed in sequence as the solution conditions exceed their solubility constraints. The formation of brines by evaporative concentration of natural waters can be conceptualized as a series of chemical divides, which are caused when salts with limited solubility drop out of solution (CRWMS M&O 2000ck, Section 6.5). The concept of chemical divides is straightforward. When a salt such as calcium sulfate is precipitated from solution during continual evaporation, one or the other of the component species (i.e., calcium or sulfate) will be effectively removed from the water. The remaining one will jointly determine what precipitates next, and so on, in a series of chemical divides. (The situation is more complex for solutions with multiple soluble species, as discussed below.) The complete precipitation of all limited-solubility species is observed in natural waters that have been concentrated by evaporation, such as Owens Lake in southeastern California (CRWMS M&O 2000ck, Section 6.5).

As discussed previously, for particular conditions of temperature and relative humidity, there is a specific extent of evaporative concentration for Yucca Mountain waters, such that the solution is in

moisture equilibrium with the gas phase. In other words, the solution will either evaporate or absorb moisture from the air until equilibrium is reached. This equilibrium behavior is well known and has been observed in laboratory tests (CRWMS M&O 2000ck, Section 6.6). Below a critical value of the relative humidity, or deliquescence point, the solution evaporates completely and the resulting salts remain dry. Coligative behavior is observed when solutions are concentrated by boiling; the boiling temperature increases with solution concentration until a limit is reached and the salt precipitates. The deliquescence point and the boiling point have been measured for a number of solutions of pure salts, as shown in Figure 4-75. Various salts exhibit different behavior, but solutions of salts with lower deliquescence points have consistently higher boiling points.

During cooldown of the potential repository, dissolution of salts will occur rapidly when the relative humidity exceeds the critical value for each salt present. Rapid dissolution is consistent with the observation that puddles of dissolved salt (primarily sodium chloride) occur overnight on salt flats when the relative humidity exceeds the deliquescence point for sodium chloride, but the temperature remains above the dew point (CRWMS M&O 2000cl, Section 6.1.4.2). These puddles can then dry up during the day when the relative humidity decreases.

Laboratory evaporation tests have been used to identify the minerals and salts that could form in the emplacement drifts. Tests were conducted using two different water compositions: a bicarbonate-type water and a chloride-sulfate-type water (CRWMS M&O 2000cg, Section 6.5). Evaporation was performed at below-boiling conditions (85°C [185°F]) to represent the behavior of slowly migrating waters in the engineered barrier system. At this temperature, the assemblage of mineral phases resulting from evaporation is controlled by precipitation kinetics. It is thought that the assemblages are representative of potential repository conditions.

The first set of tests using bicarbonate-type water (similar to water from well J-13) showed that the salts formed during complete evaporation included
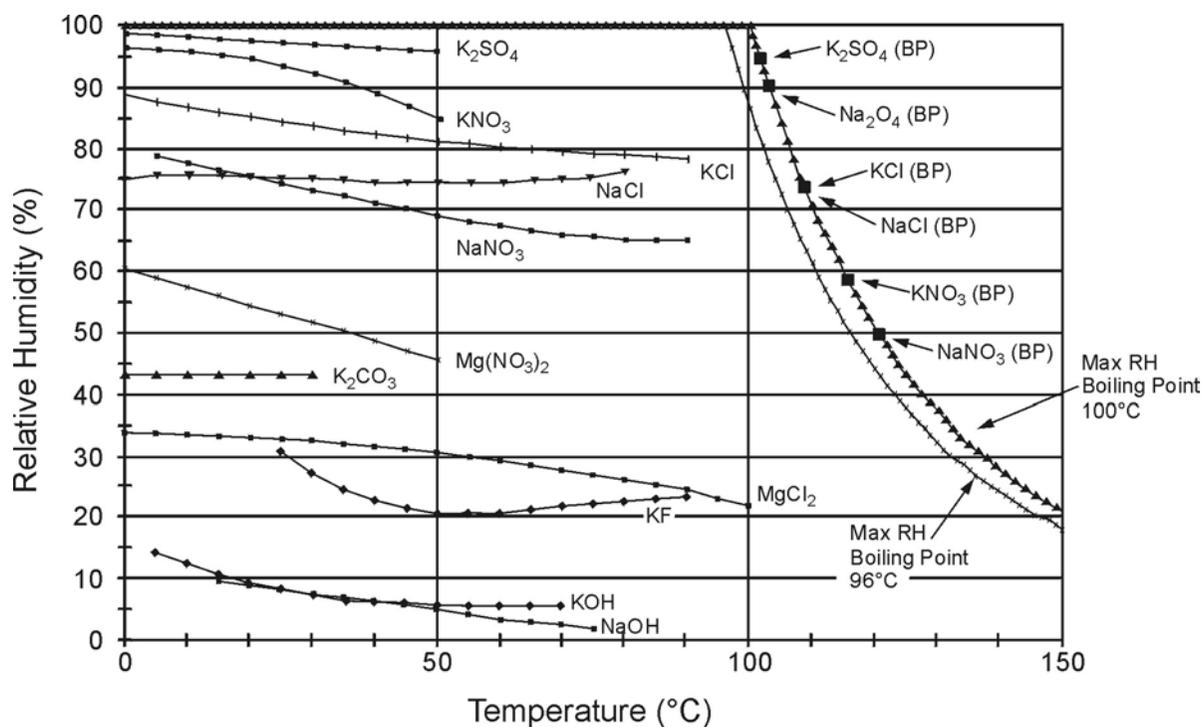
00050DC_ATP_Z1S42_87b.cdr

Figure 4-75.   Deliquescence Points (Expressed as Relative Humidity) and Boiling Points for Several Pure Salts

This figure plots handbook data for the equilibrium relative humidity, as a function of temperature, for saturated aqueous solutions of some pure salts. Some of these may be present in the emplacement drifts, and these data represent minimum relative humidity conditions when aqueous conditions can occur. Each data curve probably terminates at the boiling curves to the right, but these are gaps in the available handbook data at intermediate temperatures. BP = boiling point; RH = relative humidity. Source: CRWMS M&O 2000ck, Figure 8.

niter, halite, thermonatrite, calcite, and silica (CRWMS M&O 2000cg, Section 6.5). Calcium and magnesium precipitated as carbonates early in the evaporation process, while halite and niter, being more soluble, precipitated when evaporation was nearly complete. The precipitates formed are sensitive to the concentration of carbon dioxide in the environment, which affects the pH environment. The tests provided no evidence of hydroxide precipitates, which would indicate very high pH. When the tests were repeated with tuff particles mixed with the water, similar results were obtained.

Test results for the chloride-sulfate-type water (similar to matrix pore water or sea water)

concluded that chloride and sulfate are the major anionic brine constituents, and that carbonate species are substantially less important (CRWMS M&O 2000cg, Section 6.5). As the water was evaporatively concentrated, the pH decreased to approximately 6 or lower. On complete evaporation, chloride and sulfate salts (such as halite and gypsum) predominated. In summary, test results show that calcium and magnesium carbonates, if present, will precipitate early in the evaporation process, while halite and niter are among the last salts to form. Other, additional chloride and sulfate salts will precipitate from chloride-sulfate-type waters.

Composition of Waters in the Emplacement Drifts—Throughout most of the repository performance period, composition of water in the drifts will be similar to that of ambient percolation in the host rock. During the thermal pulse, development of brine compositions that could potentially accelerate corrosion of the drip shield and waste package will depend on the chemical composition in late stages of evaporation.

In the laboratory tests described previously, evaporation of the bicarbonate-type water (similar to J-13 well water) produced a carbonate-rich brine that was highly concentrated in sodium, chloride, sulfate, carbonate, and silica. The pH increased to at least 10 and possibly higher as evaporation progressed. Evaporation of chloride-sulfate-type water (similar to matrix pore water or sea water) produced a carbonate-poor brine that was concentrated in sodium, chloride, sulfate, calcium, and magnesium (CRWMS M&O 2000cg, Section 6.5). Other dissolved components that can be enriched in natural brines include fluoride, bromide, strontium, phosphate, and boron (CRWMS M&O 2000ck, Section 6.1). Laboratory test results have shown that fluoride is not concentrated in brines representing Yucca Mountain waters, probably because these waters contain sufficient calcium and sodium to precipitate fluoride minerals (CRWMS M&O 2000cg, Section 6.5). Other components of natural brines (bromide, strontium, phosphate, and boron) are trace constituents in Yucca Mountain waters and are unlikely to achieve significant concentrations. Thus, the major chemical constituents of concentrated brines in the potential repository drifts will be sodium, calcium, magnesium, chloride, sulfate, and nitrate. For high-pH carbonate-rich brines, silica species and carbonate will also be present.

Brine compositions are outside the range that can be calculated exactly with widely used chemical activity models (i.e., much greater than 1 molal ionic strength). Accordingly, descriptions of brine behavior are more empirical, particularly with multiple dissolved species (not a single salt). The Pitzer approach (CRWMS M&O 2000cl, Section 6.4.2; CRWMS M&O 2000cg, Section 6.7.3) is based on observations of analogous ion interactions and for simulating brine behavior at ionic strengths as high as 10 molal.

Microbial Activity in the Emplacement Drifts—Laboratory testing, combined with microbial test results in the scientific literature, show that threshold conditions for microbial activity and growth are relative humidity above 90 percent, and temperature below 120°C (248°F) (CRWMS M&O 2000cg, Section 6.4.5.1). Field investigations have been performed at Yucca Mountain and at nearby Rainier Mesa to characterize microbial populations in situ (CRWMS M&O 2000cg, Section 6.4). Additional microbial observations from the exploratory tunnels at Yucca Mountain are underway.

Site characterization investigations have shown that in situ microbial growth and activity are limited by availability of water and nutrients, particularly phosphate and organic carbon. In the potential repository environment, microbial activity will also be limited by temperature and radiation (CRWMS M&O 2000cg, Section 6.4). Water will be locally available during the repository thermal evolution, as discussed previously. Phosphate is a trace constituent of J-13 water, probably because the Topopah Spring Tuff contains apatite, a phosphate mineral. Organic carbon may be limiting for some classes of organisms, such as molds, but microorganisms that fix carbon from carbon dioxide are common in rock samples obtained underground at Yucca Mountain; therefore, a source of organic carbon is not required for bacterial growth and activity. Temperature will decrease over time, so microbial activity will be possible within a few hundred years after permanent closure. Radiation from the waste package may sterilize the surrounding environment, but the shielding effect of the host rock will ensure that nearby microbes can recolonize the emplacement drifts. From this discussion, it is evident that microbial activity will occur in the emplacement drifts. The effects of microbial activity on the degradation of the waste package outer barrier material are discussed in Section 4.2.4.3.3. The potential effects on radionuclide transport are discussed in Section 4.2.7.

Approach to Modeling the Evolution of the In-Drift Chemical Environment—In this approach,

relative humidity is used as a "master variable" to control the evolution of brines. Initially, the formation of minerals and salts, as seepage waters are evaporated to dryness, is modeled using a normative approach based on the laboratory tests described previously (CRWMS M&O 2000cg, Section 6.5). As relative humidity increases in the emplacement drifts, the salts formed by evaporation gradually become brines and are diluted. For the salts formed from evaporation of bicarbonate-type water (similar to J-13 well water), and considering the behavior of the salts separately and without interaction, deliquescence begins at relative humidity of 50 percent (CRWMS M&O 2000ck, p. 75 and Figure 8). At a greater value of relative humidity, all the salts are considered to be dissolved, and further changes in solution composition are calculated using the Pitzer modeling approach (or other more widely used modeling approaches) as the environment approaches ambient (preheating) conditions. If seepage occurs, it either evaporates completely, forming minerals and salts, or it is partially evaporated and the evaporative concentration effect is accommodated in the chemical modeling approach (CRWMS M&O 2000cg, Section 6.5).

To evaluate the effects of microbial activity on the bulk chemical environment while taking into account the importance of engineered material degradation, an approach is used that incorporates energy balance and mass balance. Threshold conditions determine when microbial growth and activity can resume, then degradation rates for the materials present in the in-drift environment determine the biomass that can be supported. The result of this calculation can be compared with other descriptors of the in-drift environment to assess whether microbial effects are significant (CRWMS M&O 2000cg, Section 6.4).

The same threshold conditions apply to the onset of microbially influenced corrosion of the waste package. While the drip shield and waste package materials are included in the energy- and mass-balance approach, the corrosion rates are developed directly from laboratory tests (see Section 4.2.4).

4.2.3.2.3 Effects of Engineered Materials on the Chemical Environment

Degradation of Steel and Alloys—The product of drip shield corrosion is predominantly titanium dioxide. Alloy 22 corrosion produces oxides of major components nickel, chromium, iron, and molybdenum. These oxides tend to be chemically inert and do not react with other chemical species in the drift environment. They will accumulate slowly, corresponding to general corrosion rates on the order of 10 to 1,000 nm/yr (0.0000004 to 0.00004 in./yr) (see Section 4.2.4). This will consume oxygen at a rate that is negligible compared with the rate of gas flux through the drift openings (CRWMS M&O 2000cg, Section 6.3).

Steel corrosion products are insoluble ferric-oxides or oxyhydroxides. The concentration of ferric iron for aqueous solutions in equilibrium with hematite, goethite, and other iron oxides is very small, comparable to the concentration associated with iron-bearing nontronite clays (CRWMS M&O 2000cg, Section 6.7).

The rate of degradation for structural carbon steel, for vapor-phase conditions representative of the drift environment, has been measured for many samples, at different temperatures, in close proximity to different solutions conditions, such as pH and chloride concentration (CRWMS M&O 2000cg, Section 6.3). The measured penetration rates are on the order of tens to hundreds of microns per year. The corresponding consumption rates for oxygen are comparable to the convective flux of oxygen through the drift openings during the time period when this corrosion will occur.

Corrosion products can increase in volume, and particles can move in the drifts, potentially changing flow characteristics. These effects are neglected because the liquid flux in the drifts will be orders of magnitude smaller than the flow capacity, and redistribution of particulate matter can therefore have only a minor impact on the flow.

Effects of Cementitious Materials—A modified Type-K (Portland-based) expansive cement would be used for rock bolt anchorage in the potential

repository. The mix will contain silica fume, plasticizer, and a low water-cement ratio to promote strength, durability, and low permeability (10^{-19} m^2).

The alkaline composition of leachate from rock bolt cement grout will be bounded by equilibrium with portlandite. This approximation is conservative because portlandite will be carbonated over tens or hundreds of years from exposure to carbon dioxide in the gas phase. This behavior is known to occur with long-term exposure of concrete to air (CRWMS M&O 2000cg, Section 6.3).

Colloidal Particles Produced by Degradation of Engineered Materials—The following paragraphs describe laboratory data and field analogue data that are used to estimate the importance of ferric colloids for radionuclide transport.

Naturally percolating, mobile fracture waters have not been intercepted or sampled in the host rock, so groundwater analogues have been used to estimate colloid concentrations in seepage water. Colloids have been sampled by pumping of groundwater from 18 well intervals, from the saturated zone, at or near Yucca Mountain. The concentrations of particles in different size ranges were determined by instrumental analysis (CRWMS M&O 2000cg, Section 6.6). It is assumed that these results are analogous to unsaturated zone fracture waters in the potential repository host rock because the waters are derived from broadly similar rock types and likely have similar compositions. Accordingly, colloids are probably of similar types, consisting mainly of clays and silica.

It is noted that for more concentrated waters with greater ionic strength, such as will be produced by evaporative concentration during the thermal pulse, colloid concentrations are suppressed (Section 4.2.6). As the solution concentration increases, colloid stability decreases (i.e., the maximum possible concentration of colloids, which may vary for different sizes).

Production of colloids from engineered materials will be dominated by steel corrosion products, as discussed previously. The maximum concentration of ferric colloids in seepage waters can be estimated using the groundwater analogue. The affinity of these colloids for radionuclides has been measured in the laboratory (CRWMS M&O 2000cg, Section 6.6). Ferric-oxide colloids were shown to have high affinity for plutonium and americium.

Application to Modeling the Effects of Engineered Materials—The effects of steel on oxygen consumption in the drifts, and radionuclide transport, are modeled using the available information. Consumption of oxygen by steel is modeled by applying the average of measured corrosion rates, subject to a condition that the onset of steel corrosion occurs when the relative humidity is 70 percent. Consumption of oxygen by titanium and Alloy 22 corrosion, and the effects of cementitious materials on the bulk chemical environment, are not included in performance analyses, based on the previous discussion.

Use of groundwater colloids as an analogue for the concentration of ferric-oxide colloids in the drifts is conservative because pumping wells are highly dynamic, and not all colloids in the drift will be ferric-oxide or derived from steel. Also, different types of colloids become unstable in certain pH ranges (point of zero charge), and ferric-oxide colloids are unstable near pH 8, which is very close to the predicted pH of seepage. Use of laboratory test data for radionuclide affinity is also a conservative approach because smaller distribution coefficients would probably be observed in chemical systems with more components, containing anions and cations that could compete with radionuclides for sorption sites.

It is noted that the majority of ferric-oxide corrosion products in the drifts will be immobile in the drift environment and yet exposed to seepage water so that released radionuclides can be immobilized by sorption. The potential for retardation by corrosion products in the drifts was not incorporated into the TSPA-SR model but has been considered in supplemental studies. This supplemental evaluation is described further in Section 4.2.7.

4.2.3.2.4 Environment on the Surfaces of the Drip Shield and Waste Package

Behavior of Water on the Barrier Surfaces—As discussed previously, the deliquescence point defines the minimum relative humidity at which a salt will absorb water from the atmosphere and form a concentrated brine. Figure 4-75 shows deliquescence points for a number of pure salts as functions of temperature. Among the salts which have been identified from evaporation of representative waters, sodium nitrate has the lowest deliquescence point (50 percent). Humidity corrosion of the drip shield and waste package can therefore begin at a relative humidity of 50 percent. This is conservative because deliquescence apparently occurs at greater humidity for mixtures of salts. For example, the deliquescence point for a mixture of salts evaporated from J-13 well water can be inferred from the observed boiling point of a concentrated brine representing the result of evaporating a bicarbonate/carbonate solution. The boiling point for such a brine is approximately 112°C (234°F) (CRWMS M&O 2000ck, Section 6.12.5), which is less than the boiling point of a saturated sodium nitrate solution (Figure 4-75). This means that humidity corrosion of the drip shield or waste package is not actually likely to occur until relative humidity reaches a value greater than 50 percent.

Potential for Acidic Conditions—Inorganic acids could form in small quantities from chemical evolution of brines, or they could be produced in conjunction with localized corrosion processes. These acids, such as hydrochloric acid, have known vapor pressures and will tend to evaporate over time, especially at elevated temperature (CRWMS M&O 2000ck, Section 6.10).

Application to Modeling the Environment on Barrier Surfaces—Consideration of the environment on the drip shield and waste package surfaces is limited mainly to identifying the value of relative humidity at which corrosion will begin. Humidity corrosion begins at 50 percent relative humidity, which is conservative, as discussed previously. The relative humidity is determined from thermal-hydrologic predictions that represent the metallic barriers explicitly.

Once corrosion begins, the water composition is estimated using the approach described previously for the in-drift chemical environment. Possible water compositions range from a concentrated sodium nitrate brine to dilute bicarbonate-type or chloride-sulfate-type waters. The corrosion rates used with these water compositions in the TSPA-SR model are based on laboratory-measured corrosion data for several different water compositions ranging from dilute bicarbonate-type water to concentrated brine, including elevated temperature conditions and both acidified and basified compositions (CRWMS M&O 2000ck, Section 6.12). The selection of these water compositions for corrosion test conditions is central to the approach for representing environmental conditions on the surface of the drip shield and waste package.

Considering the factors limiting production and deposition of inorganic acids and hydrogen peroxide, radiolysis outside the waste package is considered to be of minor importance to corrosion and is not considered in the performance analyses.

4.2.3.2.5 Rockfall on the Drip Shield

The geotechnical parameters required to predict rockfall include data and information collected either by field mapping or by laboratory testing. Joint mapping data for the subunits that constitute the emplacement horizon of the potential repository have been collected from the Exploratory Studies Facility, including the ECRB Cross-Drift (CRWMS M&O 2000e, Section 4.1). Joint strength parameters, including cohesion and friction angle, have been developed from laboratory shear strength test data from core samples and are used to predict both the size and number of fallen rock blocks (CRWMS M&O 2000e, Section 4.1). Rock density data and intact rock elastic properties are used to assess seismic effects and to determine the load applied to the drip shield; these data have also been obtained from laboratory tests performed on core samples (CRWMS M&O 2000e, Section 4.1).

Key block analysis in underground excavations located in jointed rock masses has been considered for a number of design situations. Deterministic methods of block theory in rock engineering were advanced by Warburton (1981) and Goodman and

Shi (1985). The literature provides examples for deterministic analysis of the maximum block size, given the spacing and orientation of three joint sets, and the excavation size and orientation. Subsequent work by other authors has been oriented toward probabilistic risk assessment of key block failure (CRWMS M&O 2000e, Section 6.3). These more recent methods are considered suitable for the analysis of densely jointed and faulted rock masses (i.e., greater than three joint sets) where planar joint surfaces can reasonably be assumed. Such conditions typically exist in the potential host rock units at Yucca Mountain. The probabilistic approach used in the TSPA-SR model is distinguished from traditional key block analysis because it not only assesses the maximum size of key blocks, but it also predicts the number of potential key blocks that will be formed in a certain length of tunnel for any tunnel orientation.

4.2.3.3   Process Model Development and Integration

The discussion of the physical and chemical environment is divided into five parts: (1) the chemical composition of seepage water and gas flux into the emplacement drifts (these are near-field conditions and are bounding conditions to the chemical and physical environment for the engineered barriers); (2) the chemical environment in emplacement drifts; (3) the effects of engineered materials on the chemical environment; (4) the chemical environment on the surfaces of the drip shield and waste package; and (5) the model for the rockfall on the drip shield.

4.2.3.3.1   Modeling the Composition of Liquid and Gas Entering the Drifts

Thermal-Hydrologic-Chemical Seepage Model Approach—This section discusses implementation of the thermal-hydrologic-chemical seepage model. The unsaturated zone flow model and the drift seepage model, which are the bases for thermal-hydrologic modeling, are discussed in Section 4.2.1. This model predicts, at the drift scale, the composition of seepage and the associated gas-phase chemistry for 100,000 years, including the effects of heating.

The effects of heating on gas composition are important for predicting the composition of incoming seepage. The concentration of carbon dioxide in the immediate vicinity of the drift openings will decrease because of displacement and dilution by water vapor. This will be accompanied by decreased carbon dioxide activity in any associated seepage, which will cause pH to increase. In the zone of condensation further from the drift openings, carbon dioxide enrichment will occur, causing pH to decrease. Diffusivity for gaseous species is much greater than for aqueous species, and transport is more rapid. The result is that the region affected by changes in gas composition will be larger than that affected by changes in liquid-phase transport.

Flow of information from various models and data sources to the thermal-hydrologic-chemical seepage model is shown in Figure 4-76. The model uses input from modeling of the Drift Scale Test, the unsaturated zone flow model (CRWMS M&O 2000c), and other sources of geochemical data (CRWMS M&O 2000al, Section 3.3). These inputs ensure consistency between the thermal-hydrologic-chemical seepage model and the other models and data used to calculate drift seepage and the movement of water in response to heating. Other model inputs, including reactive surface areas of minerals, fracture–matrix interaction area, and the mineral volume fractions, are estimated from observed data (CRWMS M&O 2000al, Section 3.2.2).

Comparison with observations from the Drift Scale Test (CRWMS M&O 2000ch) and sensitivity studies on mineral assemblages and water compositions were used to guide development of the model. An example of the comparison of model results and observed data is shown in Figure 4-77. Evolution of the concentration of carbon dioxide in the gas-phase, over time, is compared with model results at four sampling intervals in the Drift Scale Test. For some data, calculated results are shown for nearby points in the model grid. For example, locations labeled "above" or "below" are calculated somewhat above or below the sampled location in the test. Similarly, locations labeled "center" or "end" were calculated near the center or the far end, respectively, of the sampled loca-
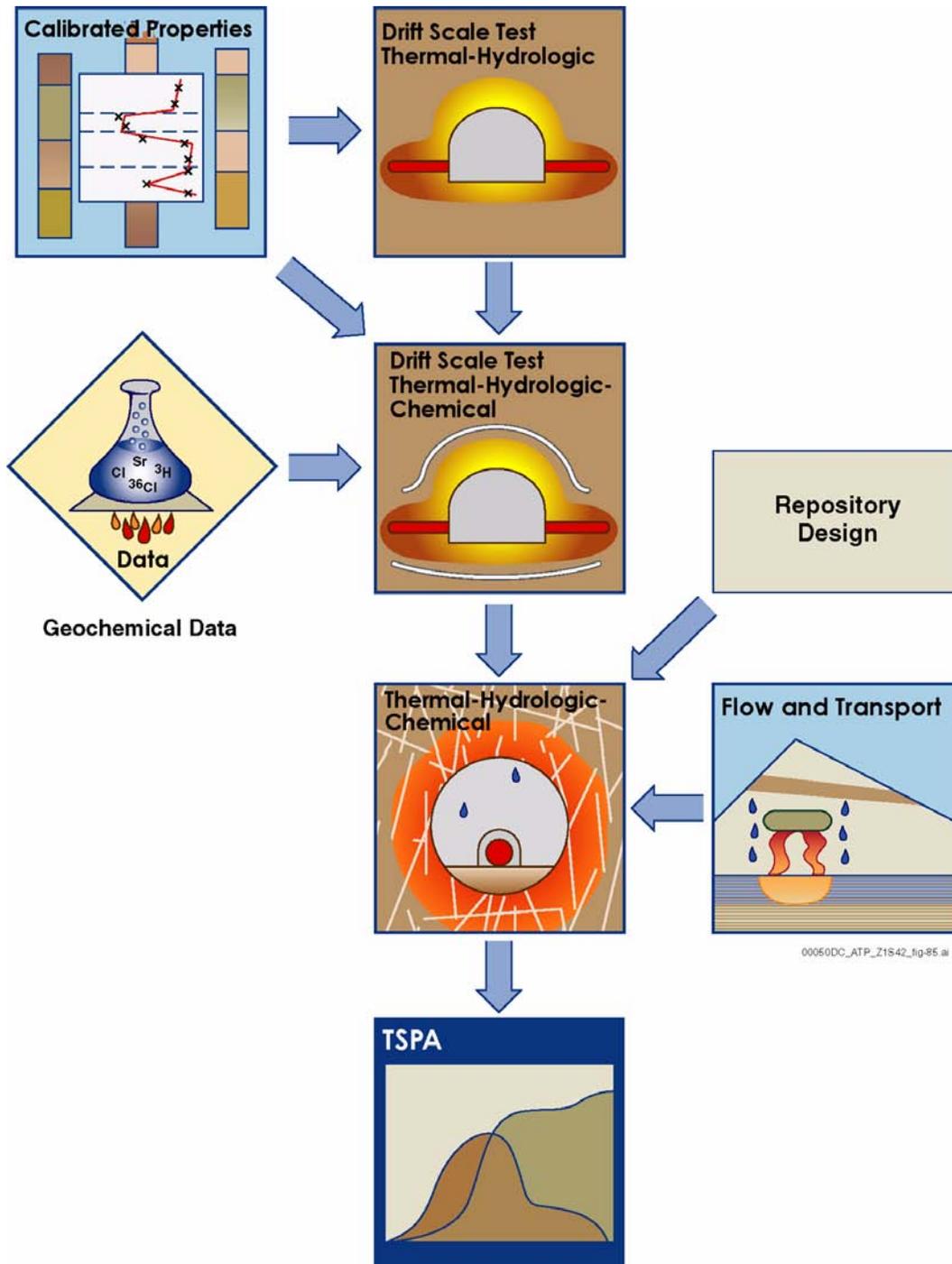
Figure 4-76. **Model Diagram Relating Inputs and Outputs for the Thermal-Hydrologic-Chemical Seepage Model, with the Thermal-Hydrologic Drift Scale Test Model, Thermal-Hydrologic-Chemical Drift Scale Test Model, Calibrated Properties Model, Unsaturated Flow and Transport Model, Other Data Input, and Design Information**
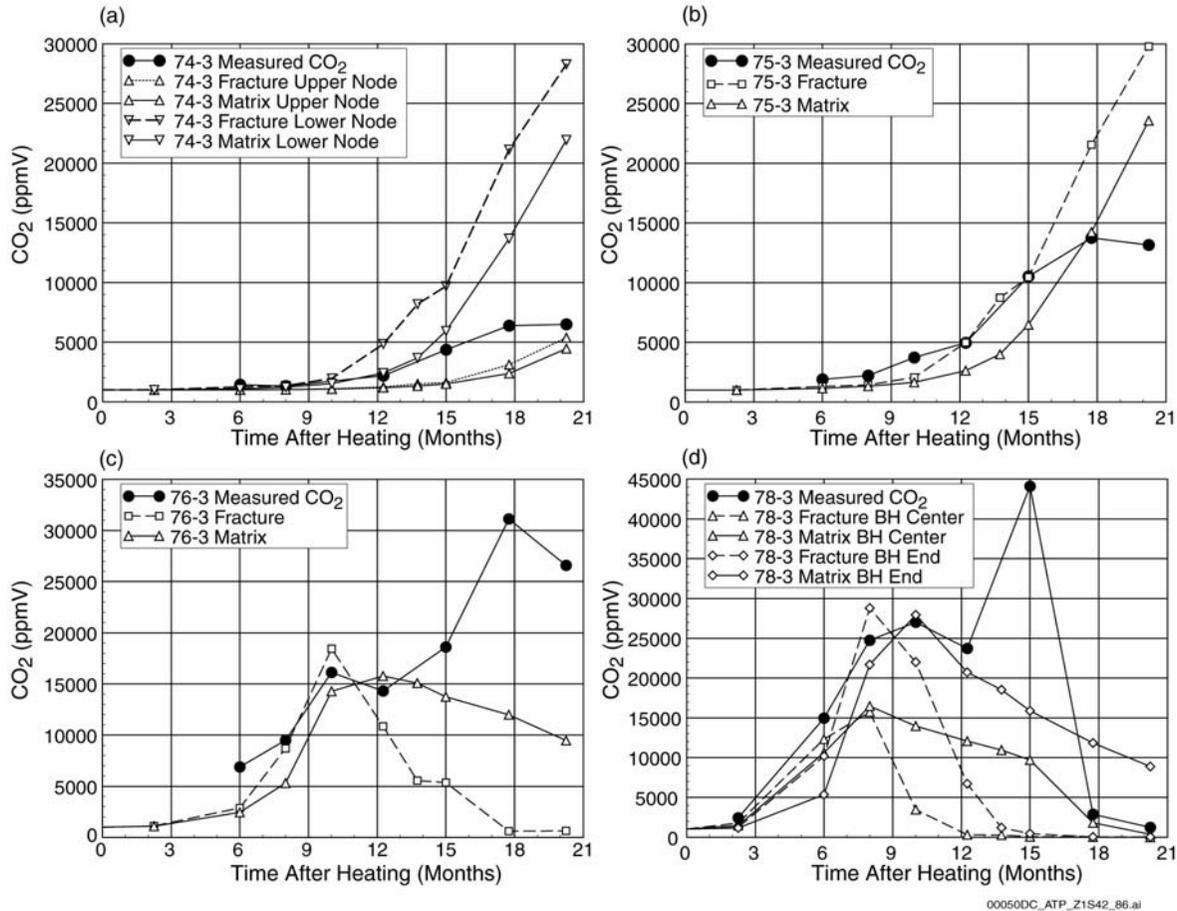
Figure 4-77. Comparison of Modeled Carbon Dioxide Concentrations in Fractures and Matrix to Measured Concentrations in Boreholes for the First 21 Months of the Drift Scale Test
(a) Borehole interval 74-3. (b) Borehole interval 75-3. (c) Borehole interval 76-3. (d) Borehole interval 78-3. Measured data are plotted with black dots; calculated results are shown using other symbols. The model results are from the grid points in the model domain closest to the sampling intervals. The predictive model is based on a limited mineral assemblage that includes calcite, gypsum, and silica phases. See Figure 4-52 for the location of Boreholes 74, 75, 76, and 78. Source: BSC 2001o, Figure 10.

tion. There are comparable trends between the test data and the calculations, and agreement is obtained in an average sense throughout much of the time period modeled.

Thermal-Hydrologic-Chemical Seepage Model Results—The model incorporates elements of the repository thermal operating mode nominally described in Section 2 to represent waste package heating over time, changes in heating from ventilation, heat transfer within the drift, and thermal-hydrologic-chemical processes (CRWMS M&O 2000al). As an example of model results, time profiles for gas-phase carbon dioxide concentra-

tions at three locations around the drift, for one simulation using chloride-sulfate-type water, are shown in Figure 4-78. Carbon dioxide concentrations in fractures decrease significantly during dryout and increase again during rewetting. The increase during rewetting is caused by the dissolution of calcite deposited during dryout and by heating of ambient percolation and condensate waters as they approach the drift opening (the solubility of carbon dioxide in water decreases as temperature increases).

Using the chloride-sulfate-type water as the initial condition, the chloride concentration in fracture
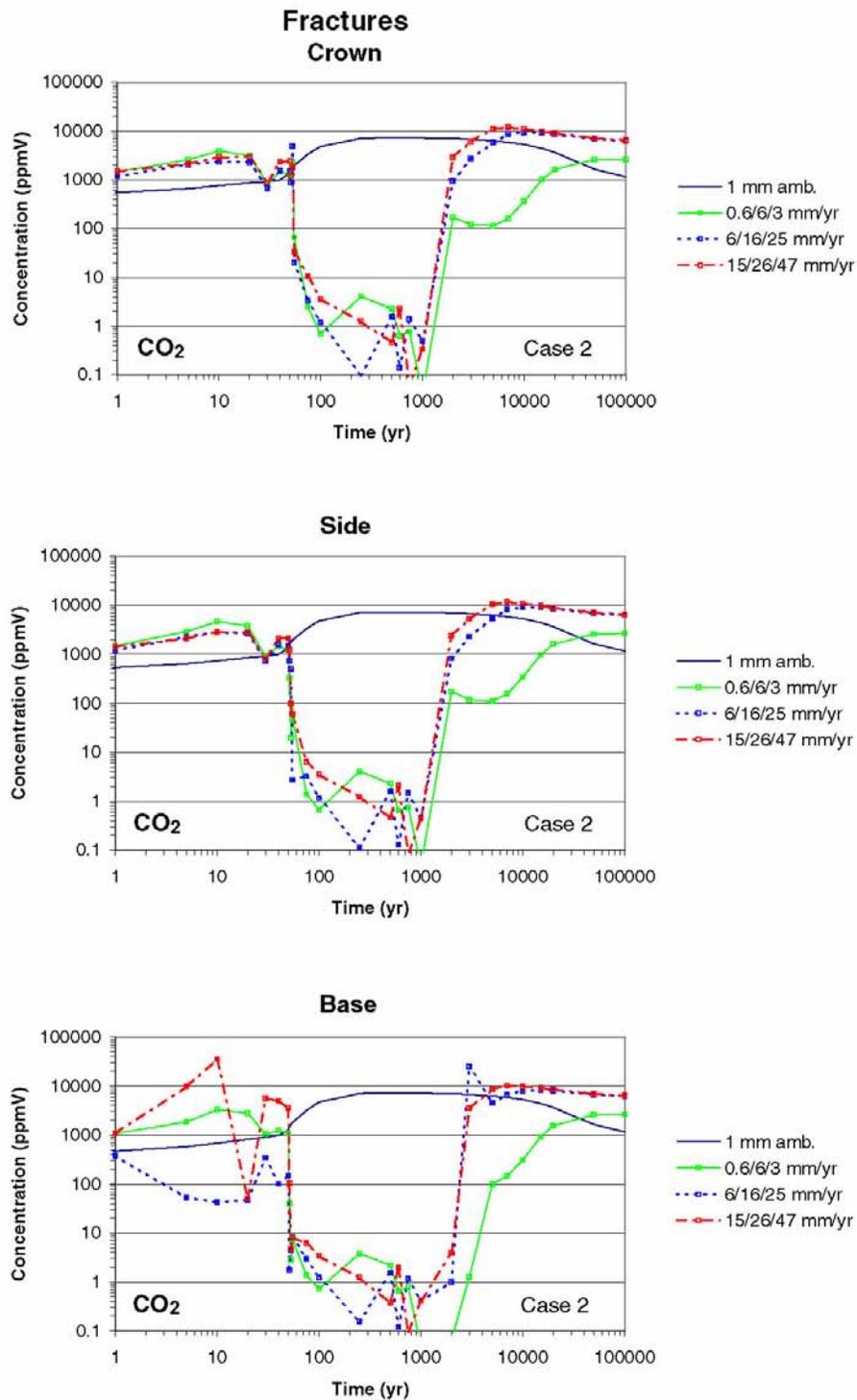
Figure 4-78.   Time Profiles of Modeled Carbon Dioxide Concentrations in the Gas Phase in Fractures at Three Drift Wall Locations for Different Climate Change Scenarios

The climate change scenarios are indicated as net infiltration flux values (in mm/yr) for the present-day, monsoonal, and glacial-transition climate states (calcite–silica–gypsum system). For all scenarios, the transitions between these sites occur at 600 and 2,000 years. Source: BSC 2001o, Figure 40.

water immediately above the drifts is estimated to increase approximately fourfold from evaporative concentration. Higher concentrations could occur below the drifts. Upon rewetting, chloride concentrations are estimated to decrease to near-ambient values. The results indicate that seepage water should not be concentrated more than approximately one order of magnitude in chloride, compared to the ambient pore water. For the same simulation, the estimated pH for waters reaching the drift wall ranges from near-neutral (pH 7.2 to 8.3) to sub-alkaline (pH 8.6 to 9.0), depending on the chemical system properties used in the calculation, such as mineral assemblage and gas-phase carbon dioxide (CRWMS M&O 2000al, Section 3.3; CRWMS M&O 2000cl).

4.2.3.3.2 Modeling the Evolution of the In-Drift Chemical Environment

Three complementary modeling approaches are used to describe the formation and behavior of salts under different relative humidity conditions:

- **Normative Precipitates and Salts Model**—Based on empirical data, this model is used to estimate which minerals and salts will form when waters are completely evaporated.

- **Low-Relative-Humidity Salts Model**—The low-relative-humidity salts model describes the behavior of salts when relative humidity is less than 85 percent.

- **High-Relative-Humidity Salts Model**—The high-relative-humidity salts model calculates water composition and dissolution/precipitation reactions for solutions that can occur when relative humidity is greater than 85 percent.

These models are used to determine the timing of in-drift environmental conditions that permit aqueous corrosion and to estimate the composition of waters that can transport released radionuclides.

Normative Precipitates and Salts Model—For waters having compositions similar to either bicarbonate-type water or chloride-sulfate-type water, a set of precipitates is identified that is consistent

with the laboratory test data discussed previously. This model describes an assemblage of precipitates formed by complete evaporation. It is approximate in that the laboratory tests may not exactly duplicate evaporation conditions in the potential repository. It is supported by arguments based on thermodynamic data, which indicate that:

- Thermonatrite and calcite are favored over hydroxides such as portlandite because of the presence of sufficient carbon dioxide in the environment.

- Anhydrite is favored to form over gypsum (both forms of calcium sulfate) for the humidity conditions that will be present in the drifts.

- Thenardite (sodium sulfate) and calcite are a more stable assemblage than thermonatrite and anhydrite.

The final species considered in the assemblage is amorphous silica (silicon dioxide), which was detected in all the laboratory samples derived from the bicarbonate-type water. The presence of the tuff would allow for more geochemical processes, such as formation of clays, cation exchange, and silicate buffering associated with tuff dissolution (CRWMS M&O 2000cg, Section 6.5).

Low-Relative-Humidity Salts Model—This model begins at a point in time during the thermal period when the emplacement drifts are dry and at low humidity. Incoming seepage (if it occurs) is completely evaporated, and the salts and minerals that form are determined from the normative approach. As relative humidity continues to increase over time, the salts are allowed to dissolve according to their deliquescent behavior. The amount and composition of brine produced are controlled by the solubilities of the salts and the fraction of each salt that is allowed to dissolve. For the nitrate salts, the entire amount is allowed to dissolve when the relative humidity reaches 50 percent. For the remaining salts, the fraction dissolved is abstracted from the individual salt properties. For simplicity in performance assessment analyses, all of the remaining salts are modeled to dissolve exponentially from zero to

unity as relative humidity increases from 50 percent to 85 percent. The timing of relative humidity evolution at different locations in the potential repository is obtained from thermal-hydrologic calculations (Section 4.2.2). At 85 percent relative humidity, all the accumulated soluble salts are considered to be completely dissolved.

High-Relative-Humidity Salts Model—The high-relative-humidity salts model is used for relative humidity greater than 85 percent, conditions for which soluble salts are fully dissolved and the relative rates of evaporation and seepage control the aqueous chemistry. Modeling the behavior of concentrated aqueous solutions (greater than 1 molal ionic strength) is performed using a Pitzer approach, implemented using the EQ3/6 chemical modeling code (CRWMS M&O 2000cl, Section 6.4.2). A modified Pitzer database was developed from existing published data, adding chemical species such as nitrate and silica, and extending the temperature range of applicability to 95°C (203°F). Details are provided in supporting documentation (CRWMS M&O 2000cl, Section 5.3). It is a conservative, approximate model that is used for predicting the composition of water in the emplacement drifts for a time interval during the thermal period when seepage is strongly concentrated by evaporation.

Three sources of experimental data were used for validation of the model (but not for model development or calibration; CRWMS M&O 2000cl, Section 4.1.2). All three studies involved evaporation of synthetic J-13 well water in a beaker open to the atmosphere and maintained at constant elevated temperature. In one study, 30 L (7.9 gal) of synthetic average J-13 water were evaporated to 30 mL and the precipitated solids analyzed. In a second study, the pH of the water was monitored during evaporation, and, in a third, 100-times concentrated average J-13 well water was dripped through a column of heated tuff and final solution composition compared to the initial composition (CRWMS M&O 2000cl, Section 4.1.2).

Results from the high-relative-humidity salts model show that sodium, potassium, chloride, sulfate, and carbonate species simply concentrate without much precipitation. As J-13 water is concentrated to a total ionic content of 10 molal, the pH approaches 10. Species containing silicon, aluminum, calcium, magnesium, iron, and fluoride tend to precipitate in significant amounts relative to their aqueous concentrations. Among the precipitates included in the model, calcite and chalcedony are produced in greatest quantity; magnesium-bearing clay (represented in the model by sepiolite) and fluorite are the next most abundant.

Model for Microbial Activity in the Emplacement Drifts—The approach to assessing the potential effects from microbial activity has two parts: (1) a threshold model for environmental conditions that permit microbial growth and activity and (2) a quantitative model to bound the quantity of biomass, including microbes, that could develop in the emplacement drifts.

Relative humidity, temperature, and radiation dose conditions are combined to formulate threshold environmental conditions for microbial activity. Published results based on extreme behaviors of known organisms are used as a guide where site-specific data are sparse. More precise estimates based on characterization of organisms at Yucca Mountain are unwarranted because of the uncertainty about which types of organisms will be present and the potential for biological adaptation.

Microbial growth and activity does not occur until the local temperature decreases to less than 120°C (248°F) and relative humidity increases to 90 percent. Microbially influenced corrosion of the waste package is conservatively assumed to begin when the relative humidity reaches 90 percent.

The microbial communities model quantifies the abundance and metabolic activity of microorganisms in the engineered barrier system environment. It is based on models used in the Swiss and Canadian nuclear waste programs (CRWMS M&O 2000cp, Section 6). An idealized elemental composition for microbial biomass is used, consisting of carbon, nitrogen, sulfur, and phosphorous in fixed proportions, plus water. The rates of supply for these constituents are input as constant release rates for each natural and engineered material present in the drifts. The other major constraint is

the chemical energy available for microbes to grow, which is maximized from possible oxidation/reduction reactions.

The presence of water, nutrients, and energy sources is required for microbial growth and activity. There are three main categories of introduced materials that could furnish nutrients and energy: steels/alloys, cementitious materials, and organic substances (CRWMS M&O 2000as, Section 3.1.2.4.2.1).

Three basic approaches to modeling microbial nutrient and energy balances are possible, based on nutrient balance, thermodynamic energy balance, and chemical kinetics. The microbial communities model (CRWMS M&O 2000cp, Section 6) combines the nutrient and thermodynamic approaches. The available materials are decomposed into their basic elements and combined with the constituents available from groundwater and gas fluxes through the repository. Release of chemical constituents is controlled by estimating the degradation lifetime of each material. The model assumes that all available nutrients and redox energy sources are used for microbial processes and is therefore bounding.

Application of the microbial communities model to the potential repository design shows that approximately 10 grams of biomass would be produced per lineal meter of emplacement drift per year, during the first 10,000 years. Based on this small generation rate, effects on the bulk chemical environment are considered negligible for the TSPA-SR analyses (CRWMS M&O 2000as, Section 5.3.2.4). Localized effects of microbial activity could nevertheless alter the longevity of materials and the transport of radionuclides. For that reason, microbially influenced corrosion of the waste packages was included in TSPA-SR calculations (CRWMS M&O 2000a, Section 3.4.1.6).

4.2.3.3.3 Modeling the Effects of Engineered Materials on the Chemical Environment

Modeling the Effects from Corrosion of Steel and Alloys—Steels and alloys introduced to the potential repository as ground support and other

structural materials will degrade with time. The important effects of metal corrosion on the bulk chemical environment, and the approaches used to represent those effects, are summarized as follows.

Oxygen in the drift environment will be consumed, decreasing the partial pressure of oxygen while corrosion is active. This effect is modeled by converting rates of metal corrosion to rates of oxygen consumption and comparing the results with estimates of the available oxygen flux (CRWMS M&O 2000as, Section 3.1.2.3.4).

A corrosion-rate model for structural steel was used to develop estimates of oxygen availability. The potential consumption of oxygen from corrosion of other alloys is also discussed briefly. Corrosion rates for A516 carbon steel have been measured for representative vapor-phase conditions (not immersion), elevated temperature, and proximity to synthetic groundwater with a composition similar to evaporatively concentrated J-13 water. These data are used to represent corrosion of structural steel in the drifts, as there is a paucity of equivalent data for other steels. The rate can vary with temperature, pH, and water composition. In addition, laboratory data for a similar carbon steel composition (CRWMS M&O 2000cg, Section 6.4) suggest an approximate sixfold increase in the corrosion rate once moisture returns to the drifts because of microbial activity. Steel corrosion will be insignificant until the relative humidity exceeds 70 percent (CRWMS M&O 2000cg, Section 6.3.2.2).

Applying measured corrosion rates for structural steel and using environmental conditions representing the potential repository environment yields the following results (CRWMS M&O 2000cg, Section 6.3):

- Steel present in the drifts will completely corrode within a few hundred years, starting at times from approximately 300 to 2,000 years after waste emplacement. (Timing will depend on the duration of preclosure operations and location in the repository layout; steel corrosion can begin at 300 years after emplacement if the preclosure period is

50 years, and corrosion first occurs near the repository edge, which cools fastest.)

- The calculated rate of steady-state oxygen consumption will be replenished by the flux of oxygen that is transported to the drifts by buoyant gas-phase convection.

Results indicate that oxygen partial pressure in the drifts would be decreased but that the flux of oxygen would probably be sufficient to maintain oxic (i.e., corrosive) conditions. In the potential repository, the corrosion rate for structural steel will tend to decrease as the oxygen partial pressure decreases, prolonging the degradation process but moderating the impact on oxygen partial pressure. This model is therefore conservative because the laboratory corrosion data on which the rate model is based were acquired for oxic conditions (CRWMS M&O 2000as, Section 3.1.2.3.4).

The drip shield, waste package, and waste package supports in the design described in this report would be made from titanium, Alloy 22, and stainless steel. Corrosion of these materials will be much slower than for carbon steel and therefore slower to consume oxygen. Consumption of oxygen by corrosion of Grade 7 titanium or Alloy 22 could contribute slightly to depletion of oxygen in the engineered barrier system. However, the potential rate of consumption is a small fraction of the oxygen availability (CRWMS M&O 2000cg, Section 6.3).

Modeling the Effects from Cementitious Materials—The model for the effects of cement grout used in rock bolts is based on dissolution of cement mineral phases and subsequent interaction of cement leachate with carbon dioxide in the drift environment. The results indicate that the potential contribution of cement leachate to the bulk chemical environment will be minor (CRWMS M&O 2000cg, Sections 6.3 and 6.7).

Chemical equilibrium calculations for cement are performed using a mineral assemblage that includes constituents of young cement as a bound on the potential to produce alkaline leachate (CRWMS M&O 2000cg, Section 6.3). Mineral assemblages representing alteration of Portland

cement by aging and carbonation are available but tend to produce less alkaline leachate.

The initial composition of water that interacts with cement is assumed to be that of J-13 water, but the potential contribution of influent water chemistry to the leachate is minor because leachate composition (before reaction with carbon dioxide) will be dominated by the cement. Reaction of groundwater with the grout is assumed to be closed (i.e., it does not include reactions with gas-phase carbon dioxide), which maximizes the leachate pH. Biotic processes are also assumed to have a negligible effect on leachate composition because the organic content of the plasticizer admixture probably has very low biological reaction rates (CRWMS M&O 2000cg, Section 6.3).

Once the leachate flows into the drift opening or the surrounding rock, it will be exposed to carbon dioxide in the emplacement drifts, which will moderate the pH. Because of the small amount of leachate compared to the total percolation through the host rock, open-system conditions are used for evaluating this interaction. In addition, contact with silica, such as the cristobalite present in the host rock, will also moderate leachate pH.

The grout permeability is small, which limits chemical interaction with the drift environment while increasing the longevity of the grout to dissolution. Very small flow rates (a few milliliters per year per rock bolt) are obtained using the saturated hydraulic conductivity of the grout. A more conservative bounding approach is used to account for the possibility of grout cracks, allowing higher water contact rates. This approach is based on the ratio of the rock bolt grout cross-sectional area to the drift diameter. This method produces flow rates on the order of a few percent of the total seepage inflow to the drifts.

Results from this model show that prior to contact with carbon dioxide or siliceous minerals, the leachate will be highly alkaline, with a pH value of 11 or greater. This is caused primarily by dissolution of portlandite, which has retrograde solubility (higher solubility at lower temperatures). Buffering on contact with carbon dioxide and near-field rock in the drift environment will result in substantial

decrease in leachate pH. Accordingly, elevated pH values from the leachate are unlikely to be present at the drip shield or waste package.

The model does not consider the possibility that grout could break up into fragments, some of which may fall and come to rest on the drip shield. A transient pulse of alkaline leachate could result from such failure, and the current model does not explicitly address rapid leaching. However, the analysis shows that if such leaching occurs during the thermal pulse, the chemical composition of the leachate will be similar to evaporatively concentrated waters that will form in the drift. During and after cooldown, the concentration of carbon dioxide will increase in the drift environment, and cement fragments will be exposed to increased carbon dioxide levels. The potential for strongly alkaline conditions will then be moderated by reaction of leachate with the drift environment. Also, carbon dioxide gas will diffuse into the grout and react directly with the cement. This process is not considered in the current model but will be more important for fragmented grout. Finally, the current model indicates that the quantities of leachate produced are likely to be small, whether or not the grout is fragmented.

Modeling the Effects of Colloids Produced from Engineered Materials—Ferric-oxide colloids with strong affinity for plutonium and americium will be produced from corrosion of steel in the emplacement drifts. The size and concentration distributions of natural colloids observed in local groundwaters are used to represent the behavior of ferric-oxide colloids. This is justified because these waters are similar in composition to seepage waters that are likely in the potential repository (CRWMS M&O 2000al, Section 3.3.2.4). It is conservative because the effect of ionic strength in evaporatively concentrated waters, and the behavior of ferric-oxide at near-neutral pH, will decrease the stability of ferric-oxide colloids. Colloids are discussed further in Section 4.2.7 in the context of the radionuclide transport model.

4.2.3.3.4 Modeling the Environment on the Surfaces of the Drip Shield and Waste Package

Conditions for Aqueous Corrosion and Humidity Corrosion—At permanent closure, the surfaces of the drip shield and waste package will be dry, with relative humidity less than 50 percent, and no humidity corrosion or aqueous corrosion processes active. This condition will continue through the period of peak temperatures. During cooldown, the relative humidity on the barrier surfaces will gradually increase (CRWMS M&O 2000n, Section 3.1.3).

Figure 4-75 shows that aqueous salt solutions on the drip shield and waste package can exist for relative humidity less than 100 percent but greater than the deliquescence point. Analysis of salts formed from laboratory evaporation tests shows that the salt with the lowest deliquescence point is sodium nitrate (CRWMS M&O 2000n, Section 3.1.3.1).

For modeling purposes, it is assumed that sodium nitrate—the salt with the lowest deliquescence point among all the salts likely to be present—will determine the minimum relative humidity at which aqueous conditions can occur (50 percent). Another value of relative humidity is selected to represent the condition at which all salts, including chlorides, sulfates, and carbonates, are dissolved as brine (85 percent). This value is greater than the deliquescence points for all salts that are likely to be present. The low-relative-humidity salts model is used to predict the composition of brines present on the drip shield and waste package surfaces as the relative humidity increases from 50 to 85 percent. This is a conservative approach because waste packages under intact drip shields will be affected only by dust and aerosols, which may be more benign than the brine conditions considered in the model.

The high-relative-humidity salts model is used to calculate the composition of brines as they undergo further dilution at relative humidity greater than 85 percent. If seepage occurs during the thermal pulse, the waters that contact the drip shield and waste package surfaces will be evaporatively

concentrated because the relative humidity on the surfaces will be less than in the surroundings. The high-relative-humidity salts model is used to calculate the composition of evaporatively concentrated seepage waters. The degree of evaporative concentration will decrease with time as the relative humidity increases.

The high-relative-humidity submodel of the in-drift precipitates and salts analysis was implemented for relative humidity greater than 85 percent. In this regime, the steady-state water composition is controlled by the ratio of the evaporation rate to the seepage rate; this ratio is always less than one. The submodel calculates water composition, pH, chloride molality, and ionic strength in the repository for several temperatures, relative humidities, relative evaporation rates, and carbon dioxide gas fugacity values (CRWMS M&O 2000cl, Section 6.4.2).

Composition of Aqueous Solutions Used for Corrosion Testing—The exact chemistry of the water that contacts the drip shield and waste package surfaces cannot be known precisely. However, several test solutions have been developed for laboratory corrosion testing of titanium, Alloy 22, and other materials. These solutions were selected to represent a range of dilute and concentrated conditions, pH, and temperatures that could result from evaporative concentration in the repository. The test solutions are described in Section 4.2.4.2.

The chemistry of the waters that contact drip shield and waste package surfaces would vary in a repository, and the test solutions described previously represent a range of possible conditions. Results from corrosion testing with these solutions are discussed in Section 4.2.4.

4.2.3.3.5 Model for Rockfall onto the Drip Shield

The effect of rockfall on the emplaced drip shield was screened from the TSPA-SR model based on the following analysis. *Drift Degradation Analysis* summarizes the analysis of key blocks, including block failure due to seismic and thermal effects (CRWMS M&O 2000e, Section 6), using the prob-abilistic Discrete Region Key Block Analysis method (CRWMS M&O 2000a, Section 3.3.1; CRWMS M&O 2000e, Attachments VIII through XI).

Based on mapping data and results from key block analysis, the orientation of the emplacement drifts, as discussed in Section 2.1.2, was selected to maximize drift stability (CRWMS M&O 2000e, Sections 1.4 and 6.4). Considering static plus seismic loads, rockfalls were estimated using the probabilistic key-block analysis. The results include probability distributions for the size of fallen key blocks and the number of such blocks per length of emplacement drifts.

Heating and subsequent cooling of the repository host rock would impose stresses, deposit minerals, and shift rock joints. This was represented in the analysis as reduction in joint cohesion from the time of closure until about 2,000 years after closure and thereafter. The resulting changes in estimated rockfall are provided in supporting documentation (CRWMS M&O 2000e, Section 6). Results for combined thermal and static loads are similar to those for combined seismic and static loads.

Given the distribution of key block size, a structural calculation was performed to determine the stresses in the titanium drip shield (BSC 2001l). The analysis considered a range of rock sizes falling onto a 3-m (10-ft) length of drip shield. This length is half that of a drip shield segment and was chosen to take advantage of symmetry and thereby reduce computational effort. A range of rock sizes up to 10 metric tons (approximately 4.15 m^3 [147 ft^3]) is the design basis for the drip shield. For rock sizes up to 4 metric tons, the entire volume of a rock can be located above a 3-m (10-ft) partial-length drip shield. An analysis of the joint geometry suggests that an increase in rock size must occur by an increase in length of the rock block along the drift, rather than an increase in block height (CRWMS M&O 2000e, Attachment IX). The probabilistic key-block analysis showed that the maximum block size could be greater than 10 metric tons, but such large blocks would be relatively unlikely. Probabilistic key-block analysis was performed for the middle nonlithophysal, lower lithophysal, and lower nonlithophysal host

rock units. For these units, the proportion of rock blocks simulated that exceeded 10 metric tons ranged from 0 to 5.8 percent (CRWMS M&O 2000e, Figures 27 to 29 and Attachment II). Also, because of their large dimensions, each block would be distributed over more than one 6-m (20-ft) drip shield segment, so the loads would be shared. Using the concept of effective rock mass over a 3-m (10-ft) partial-length drip shield, the maximum rock mass is determined to be 10 metric tons per 3-m (10-ft) partial-length drip shield. In other words, any rock mass greater than 10 metric tons will load a 3-m (10-ft) partial-length drip shield the same as a 10-metric-ton rock. Calculations for the effective rock mass for different size blocks were calculated using finite element techniques and are documented in *Rock Fall on Drip Shield* (BSC 2001l, Section 5.2 and Table 7-1). Preliminary results from the analysis indicated that the impact would not dent the drip shield in such a way that it would contact the waste package. (Design criteria are presented in *Emplacement Drift System Description Document* [CRWMS M&O 2000ab].) The impact from a 10-metric-ton block was estimated to produce one 13-cm (5-in.) long crack in a 3-m (10-ft) long portion of a drip shield segment because of stress corrosion cracking that could occur after the rockfall (BSC 2001l, Table 6-1). Smaller rocks, such as a 2-metric-ton rock, were estimated not to produce enough residual stress to initiate stress corrosion cracking. It is expected that such stress corrosion cracks would be narrow and would not conduct much water flow (see Section 4.2.4). The calculation is conservative because it does not take credit for energy expended by fracturing of the rock or dislocation of the drip shield.

Effects from rockfall events involving multiple rock blocks have not been analyzed explicitly. However, because the dimensions of the maximum expected block size are of the order of the dimensions of the waste packages, it is reasonable to assume that multiple falls of blocks of the maximum size would have to act independently. The effects from multiple, smaller-size block falls would be bounded by the analyses of the effects of the maximum block size.

4.2.3.3.6 Limitations and Uncertainties

As discussed in Section 4.4.1.2 of this report, uncertainties are an inherent component of the TSPA method. Uncertainty is introduced through the conceptual model selected to characterize a process, as well as the mathematical, numerical, and computational approaches used to implement the model. Uncertainty is also introduced from imperfect knowledge of important parameters used for input to the models (e.g., physical properties). This section emphasizes limitations and uncertainties relative to the in-drift physical and chemical environment: (1) the thermal-hydrologic-chemical model used to characterize seepage water chemistry that enters the drift, (2) the in-drift chemical environment model and supporting analyses, and (3) the rockfall model and supporting analyses.

Since the TSPA-SR model, the DOE has performed several supplemental activities to address uncertainties and limitations in the TSPA-SR model. Additionally, as noted in Section 4.1.4, the DOE is evaluating the possibility for mitigating uncertainties in modeling long-term repository performance by operating the design described in this report at lower temperatures. Consequently, some of the models describing the thermal-hydrologic-chemical model, precipitates salts model, and the drift degradation model have undergone further evaluation since the TSPA-SR model. Some alternative models have been implemented and sensitivity analyses conducted to address parameter and model uncertainties. These supplemental analyses are summarized in *FY01 Supplemental Science and Performance Analyses* (BSC 2001a, Sections 4, 5 and 6). The sensitivity of TSPA model results to alternative process models is discussed in Volume 2, Sections 3.2 and 4.2 of *FY01 Supplemental Science and Performance Analyses* (BSC 2001b) and is summarized in Section 4.4.5.5 of this report.

Thermal-Hydrologic-Chemical Seepage Model Limitations and Uncertainties—Uncertainties exist in the thermodynamic and kinetic input data used in the model. For example, as the concentrations of dissolved solutes increase during evaporation, the theoretical limitations of the chemical activity model may be exceeded. Rapid boiling can lead to mineral precipitation that is

controlled by nucleation kinetics and other surface-related phenomena. The specific conditions for which the model becomes invalid, however, may not be important for the overall dynamics of the system. Geochemical reactions are a strong function of temperature and the presence of water, both of which are better constrained than the rates of reaction and may control the spatial distribution even if the exact quantities of the phases at a given time are uncertain (CRWMS M&O 2000al, Section 3.3.4).

The model is based on information obtained from thermal testing in the middle nonlithophysal unit of the Topopah Spring Tuff, which may exhibit somewhat different thermal-hydrologic behavior or mineralogy than lower lithophysal units, in which most of the repository emplacement drifts would be located. Although this could change the system response, it is noted that the bulk chemistry is similar for all the welded host rock units (CRWMS M&O 2000al, Section 3.3.4). Thermal testing that is planned for the lower lithophysal unit will evaluate the applicability of the current model over the repository footprint.

Another aspect of thermal-hydrologic response that will affect aqueous and gas-phase chemistry in the host rock is buoyant gas-phase convection (CRWMS M&O 2000cm), controlled by the large-scale permeability. As discussed previously, gas-phase convection will be an important source of carbon dioxide and oxygen as chemical reactants to the in-drift chemical environment. Buoyant gas-phase convection is not evident from the Drift Scale Test, probably because the rock bulk permeability at this location does not support it. However, results from the unsaturated zone flow model (Section 4.2.1) indicate that permeability of the host rock increases with scale, and current thermal-hydrologic models do not incorporate mass transfer along the axes of the drift openings. Therefore, it is likely that further investigation will show that gas-phase convection in the potential repository will exceed that observed in the Drift Scale Test. It is anticipated that the magnitude of gas phase convection will be great enough to supply sufficient amounts of gas through drift openings to preclude depletion of gas components

through chemical reactions with drift components (CRWMS M&O 2000cg, Sections 6.3.2 and 6.3.3).

Section 4.2.2.3.5 summarized supplemental studies to the TSPA-SR model related to physical changes in permeability and seepage resulting from thermal-hydrologic-chemical processes. These studies also addressed thermal-hydrologic-chemical model uncertainties related to the chemistry of potential seepage water. Specific studies included:

- Supplemental sensitivity studies of different initial water and gas boundary conditions (BSC 2001a, Section 4.3.6.5)

- Simulated evolution of water and gas compositions in the Tptpmn and Tptpll units (BSC 2001a, Section 6.3.1.4.3)

- Modified base-case and extended case geochemical systems (BSC 2001a, Sections 4.3.5.3.2, 4.3.6.4, and 6.3.1.5).

These activities included a range of different input data and assumptions, including thermodynamic and kinetic data input data (BSC 2001a, Sections 4.3.6.4 and 6.3.1.4).

Precipitates and Salts Model Limitations and Uncertainties—This modeling approach is based on literature data that describe the minerals and salts produced by evaporative concentration and the relations between solution composition and relative humidity. In certain aspects, the thermal-chemical data support is incomplete. Therefore, the accuracy of this model was tested using independent collected laboratory data for the evolution of solids and water composition during evaporation. As described in *In-Drift Precipitates/Salts Analysis* (CRWMS M&O 2000cl, Section 7.3), the precipitates and salts model is expected to provide results that are within an order of magnitude for chloride concentrations and ionic strength and within a pH unit for pH predictions. This degree of accuracy is acceptable because it greatly reduces the potential ranges of these variables, thereby considerably reducing uncertainty.

Data were not available to directly evaluate the accuracy of the low-relative-humidity salts model.

The model did, however, produce reasonable trends and results in chloride and ionic strength outputs in its applied relative humidity range and produces consistent results at 85 percent relative humidity, where the high-relative-humidity salts model takes over (CRWMS M&O 2000cl, Section 7.3).

Simplifying assumptions were required to reduce the complexity of the precipitates and salts analysis and to avoid sophisticated approaches where data were lacking, although these assumptions tended to be conservative. The greatest uncertainties in the analysis are likely the thermal-hydrologic and thermal-hydrologic-chemical predictions and other predicted inputs to the analysis (CRWMS M&O 2000cl, Section 7.3). Therefore, the models were applied for a variety of these conditions.

The precipitates/salts model has been modified in several ways since the TSPA-SR model analyses. Each modification involved the high relative humidity submodel. The Pitzer database was improved by the addition of several minerals and thermodynamic data, and the amount of output data reported in lookup tables was increased (BSC 2001a, Section 6.3.3.4).

Additional discussion of uncertainties related to the precipitate and salts model is described in supplemental studies (BSC 2001a, Sections 6.3.3.3, 6.3.3.4, and 6.3.3.5). Supplemental studies emphasized selected uncertainties, including the sensitivity of starting water composition on evaporative chemical evolution and effects of mineral suppression (BSC 2001a, Section 6.3.3.5.1). Sensitivity studies show in-drift chemistry to be sensitive to starting water composition and that thermodynamic and kinetic data are secondary in importance or negligible (BSC 2001a, Section 6.3.3.5). These studies also show that using the water composition obtained from the thermal-hydrologic-chemical model is reasonable, as implemented in the TSPA-SR model and supplemental TSPA model analyses.

Microbial Communities Model Limitations and Uncertainties—This model is not intended to quantify localized microbial activity or its consequences but bounds overall microbial growth and activity in the engineered barrier system. It has been validated by testing against laboratory data, natural system observations, and other modeling efforts, as described in Section 6.6 of *In-Drift Microbial Communities* (CRWMS M&O 2000cp). Comparison with these independent data sets indicates that the estimates are within an order of magnitude of the actual values.

The approach uses a well-mixed reaction system to represent the emplacement drift and provides estimates of total biomass production that can be used to bound the extent of microbially influenced corrosion of the waste package. In this approach, one of the primary uncertainties is in the degradation rates that supply nutrients and energy for microbial growth. This is evaluated by varying the rates over large ranges and using bounding results (CRWMS M&O 2000cp, Section 6).

Engineered Materials Effects Modeling Limitations and Uncertainties—The rate of steel corrosion for sub-oxic conditions, including the effects of microbial activity, is an important factor in predicting the oxygen budget in the emplacement drifts. Current estimates for steel corrosion are based on (1) abiotic test results obtained for similar steel under oxic conditions and (2) preliminary data for microbially influenced corrosion of similar steel at water-saturated and nutrient-augmented culture conditions. The results for oxic conditions overestimate the rate of oxygen consumption for conditions of decreased oxygen availability, which could occur for a few hundred years in the repository during peak thermal conditions. Applicability of the available microbial testing data to environmental conditions in the repository is more uncertain (CRWMS M&O 2000cg, Section 6.3).

Boiling of water during the thermal event will produce water vapor that will displace much of the air from the drift, with the result that oxygen will be depleted. This may lead to decreased corrosion rates, but the extent of such decreases is uncertain for steel and corrosion-resistant materials such as titanium and Alloy 22. In any case, the effect of decreased oxygen availability will be of limited duration.

Supporting analyses to the TSPA model has previously demonstrated that including these uncertainties would increase the potential for reduced corrosion and solubility, which would have a beneficial impact on performance (BSC 2001a, Section 6.3.2.3.1).

Conceptualization of leachate that could be contributed from degradation of cement grout is adapted from simplifying assumptions and studies of concrete reported in the literature (CRWMS M&O 2000cg, Section 6.3.1; CRWMS M&O 2000as, Section 3.1.2.3.5). Confirmatory testing of rock bolt longevity, carbonation of the grout, microbial attack of organic superplasticizers, and other aspects of grouted rock bolt performance has not been undertaken. The final design of ground support in the emplacement drifts is under development, and analysis of ground support function is preliminary. Accordingly, the longevity of grouted rock bolts in response to thermal loading and environmental conditions remains somewhat uncertain. Rock-mass deformation could lead to failure of the rock bolts (not necessarily associated with failure of the drift openings).

Supporting the TSPA-SR model analyses, supplemental analyses have provided additional confirmation indicating cement leachate-influenced seepage water would have a negligible affect on in-drift chemistry (BSC 2001a, Section 6.3.2.3.2).

Limitations and Uncertainties on Conditions Used to Model Barrier Corrosion—Microbial activity on the waste package surface under an intact drip shield may be negligible, even above 90 percent relative humidity, as long as water has not leaked through the drip shield onto the waste package and the waste package has not directly contacted the invert. Thus, significant corrosion would not commence until the drip shield fails and water contacts the waste package. Similarly, if salt-tolerant organisms are present, the relative humidity threshold for microbially influenced corrosion may decrease to 75 percent, which would mean that the onset of microbially influenced corrosion could shift to an earlier time. Such a shift represents only a small fraction of the time that microbial processes are modeled to be present.

Furthermore, uncertainty as to the timing for the onset of general corrosion or microbially influenced corrosion is of low importance for performance assessment because the expected corrosion rate for the waste package, even with microbes present, is low enough that a shift in the timing of the onset of corrosion is insignificant to the overall performance of the potential repository. Further discussion of corrosion rates for the drip shield and waste package is provided in Section 4.2.4.

Common scale minerals that are produced from natural waters include calcite, gypsum, and silica (CRWMS M&O 2000ck, Section 6.1.1). If seepage occurs, the chemical components of these minerals will be present in waters that contact the drip shield and waste package. The tendency for scale formation is enhanced by evaporative concentration and changes in pH. Scale can protect the underlying material if it forms a dense adherent layer, but it may have a deleterious effect if it forms a porous layer or a crevice with the underlying material. Interfaces between scale-covered and bare regions of the surfaces might be subject to corrosion. Few data on the effects of scale are presently available, but related laboratory tests have been performed to evaluate the potential for crevice corrosion. The results show that crevice corrosion is insignificant for titanium and Alloy 22 at the expected repository temperature and humidity. By inference, the effects of scale are also thought to be insignificant.

Another potentially important aspect of scale formation is the production of decomposition products, such as lime, from scale minerals at elevated temperatures. Subsequent dissolution of such products by seepage water or deliquescence could produce highly alkaline solutions. Decomposition temperatures for potential scale minerals are known, and some are within the operating temperature limits for the waste package (CRWMS M&O 2000ck, Sections 4.1.11 and 6.11). However, as discussed previously, the presence of gaseous carbon dioxide in the drift environment implies that the formation of highly alkaline hydroxide species is unlikely.

Rockfall Model Limitations and Uncertainties—The usefulness of the rockfall model is

affected by how well the data inputs describe the actual fracture conditions. The natural variability of fractures within a rock mass always represents uncertainty in the design of structures in rock. The extensive fracture data collected at Yucca Mountain provide a good representation of fracturing at the emplacement drift horizon. The range of fracture variability from tunnel mapping has been captured in the rockfall model through multiple Monte Carlo simulations of the rock mass. To account for uncertainties associated with seismic, thermal, and time-dependent effects on rockfall, a conservative reduction of joint strength parameters has been included in the approach (CRWMS M&O 2000e, Section 5).

Sensitivity analyses supplemental to the TSPA-SR model did not change the results of the rockfall model analyses (BSC 2001a, Section 6.3.4.9). Consequently, the process remains insignificant to performance and remains screened from TSPA analyses (BSC 2001a, Section 6.3.4.6).

4.2.3.3.7   Alternative Conceptual Processes

As with limitations and uncertainties, some of the following alternative conceptual models have been addressed in supplemental analyses and summarized in *FY01 Supplemental Science and Performance Analyses* (BSC 2001a, Section 1; BSC 2001b, Section 1).

Alternative Concepts for Thermal-Hydrologic-Chemical Seepage Model—Alternative approaches for modeling the compositions of the gas-phase and liquid seepage have been evaluated in *Engineered Barrier System: Physical and Chemical Environment Model* (CRWMS M&O 2000cg, Sections 6.2 and 6.7). Both the bicarbonate-type and chloride-sulfate-type waters were evaluated for a range of carbon dioxide conditions. The results were used to evaluate the carbon dioxide budget, taking into account processes in the host rock and within the drifts, as discussed previously. The liquid and gas compositions obtained are comparable to results from the thermal-hydrologic-chemical seepage model, which were abstracted for the TSPA-SR model.

As noted in Section 4.2.2.3.5, supplemental studies have evaluated a number of additional alternative starting water compositions in sensitivity analyses. Additional water compositions included water perched on top of the Calico Hills formation, water collected from the Drift Scale and Single Heater Tests, and water predicted by the thermal-hydrologic-chemical model, as well as other seepage water compositions discussed in this section (BSC 2001a, Section 6.3.3.5). Alternative conceptual models described in Sections 4.2.2.3.5 and 4.2.3.3.6 include alternative initial water and gas compositions, alternative host rock assumptions, and modified base-case and extended case geochemical systems (BSC 2001a, Sections 4.3.5.3.2, 4.3.6.4, 4.3.6.5, 6.3.1.4.3, and 6.3.1.5). In general, the sensitivity studies suggest that the models incorporated in the TSPA-SR are reasonable or conservative.

Alternative Concepts for Precipitates and Salts Model—An alternative approach for representing the composition of waters contacting the drip shield and waste package would be a bounding concept. Considering that some dripping of water onto the drip shields may occur throughout the repository in small quantities because of condensation, small accumulations of minerals and salts, on the scale of individual droplets, could occur in locations where seepage will never occur. Microscopic quantities of salts would interact with changes in the relative humidity but would not be mobilized by flow or diluted by seepage. In this alternative bounding approach, the environment on the drip shield surface would be represented by the permanent presence of minerals and soluble salts or the solutions obtained when they equilibrate with water vapor in the air (CRWMS M&O 2000cg). Although simpler than the current precipitates and salts model used for TSPA-SR, this approach would not yield very different corrosion conditions. Current estimates of corrosion rates are small, with limited sensitivity to the presence of soluble salts (see Section 4.2.4).

An alternative model for seepage/invert interactions has been developed but has not yet been implemented in its entirety (BSC 2001a, Section 6.3.3.4.2.1). This alternative model abstracts in-drift mixed solutions using ionic strength, pH, and

an acid neutralizing capacity parameter (which is an indication of the resistance of a solution to pH changes). The abstracted solutions are mixtures of seepage fluxes from the crown above the drift, the water wicked through the rock and corroded metals in the invert, and the diffusion film or flux from a waste package after failure.

Alternative Concepts for Microbial Communities Model—As stated previously, the implemented model bounds the overall production of biomass in the emplacement drifts. Two approaches, while not precisely alternatives to the microbial communities model, could be used to extend the model from estimation of biomass to estimation of bounding rates for microbially influenced corrosion. The first approach is an empirical approach based directly on microbial corrosion laboratory test data. The second approach, which is the principal alternative concept for predicting microbial effects on the bulk chemical environment, is the chemical kinetics approach mentioned previously. In this concept, biotic and abiotic chemical reactions are treated similarly, as quantitatively explicit reactions distinguished by different reaction rates. Reaction pathways would include organic species and compounds produced by microbial activity. This approach has long been recognized as an alternative but has not been used because reasonable data support is not available. The advantages of the approach would include quantitative predictions involving specified chemical systems. Pathways for microbially mediated reactions can be complex, and extensive laboratory testing could be required to represent conditions in the repository. Process models for these approaches have not been developed.

Alternative Concepts for Engineered Materials Effects Modeling—An alternative concept for the possible effect of steel on the performance of the titanium drip shield was analyzed. Specifically, the potential for hydrogen embrittlement and cracking of the titanium was evaluated. It is likely that steel ground support members will eventually fail from corrosion, possibly augmented by rock support loads, and fall onto the drip shields so that steel would come to rest on the titanium. This concept is neglected in the TSPA-SR model because (1) at the time of failure the steel will probably be coated

with oxides that have no deleterious effect on titanium and (2) fine cracks in the drip shields will not transmit significant amounts of water (CRWMS M&O 2001c, Section 6.1), similar to stress corrosion cracks in the waste package (see Section 4.2.4).

Alternative Approaches for Modeling Rockfall—An alternative approach that was considered for modeling rockfall involved the use of multidimensional distinct-element analysis (CRWMS M&O 2000e). The approach has the benefit of directly applying dynamic loading to the rock mass. However, the approach is deterministic and cannot readily accommodate the available data on variability of fracturing in the potential host rock units. Accordingly, distinct element modeling was used only to confirm results obtained with the probabilistic key-block analysis and to assess thermal effects on host rock permeability (see Section 4.2.2.3.4).

4.2.3.3.8 Model Calibration and Validation

Thermal-Hydrologic-Chemical Seepage Model Calibration and Validation—The goal of model validation is to determine reasonable bounds on the system behavior over 10,000 years or longer, based on relatively short-term tests. The thermal-hydrologic-chemical Drift Scale Test model is an implementation of the repository-scale thermal-hydrologic-chemical seepage model for the situation of the Drift Scale Test. The results were compared to gas and water samples, representing potential seepage collected during the Drift Scale Test (CRWMS M&O 2000al, Section 3.6.3.2) as a means to validate the repository scale model. These comparisons include gas-phase carbon dioxide concentrations as a function of time and space, the pH of waters collected in boreholes, and general observations on changes in concentrations of chloride and other aqueous species.

Gas-phase carbon dioxide concentrations in the model results and in the measured values showed a similar halo of strongly elevated values (approximately 2 orders magnitude greater than the air in the observation drift) around the Drift Scale Test heaters that grew outward over time. Modeled pH values of fracture waters in the drainage zones of

around 6.5 to 7.5 (calcite–silica–gypsum system) are within one pH unit of waters collected from boreholes during the Drift Scale Test. Increases in the modeled pH of the waters as the rock around the boreholes heated further and began to dry out were also similar to the measured values where multiple samples were collected over time. This indicates that the model also captured the time-dependence of thermal-hydrologic-chemical processes. Simulations employing a more complex set of minerals and aqueous species estimate pH values about 0.5 to 1 pH unit higher than for the calcite–silica system. Such behavior may be more characteristic of longer time-scale water–rock interaction, which can be validated as the Drift Scale Test produces data that reflect conditions of more stable isotherms, as opposed to the data that were collected during the more transient first two years of the heating phase.

Concomitant increases (with pH and temperature) in measured silica concentrations and depletions in calcium suggest silicate mineral dissolution and calcite precipitation, trends that were also predicted by the model. Ongoing studies (by side-wall sampling and overcoring) of the actual minerals precipitated in fractures and their effect on hydrologic properties will allow for further comparisons to model results.

Measured chloride concentrations (a conservative species that shows the effects of dilution, boiling, and fracture–matrix interaction) are 5 to 10 times lower than in the pore water, a characteristic that was also captured by the model in the drainage zones. This validates that the model approximates fairly well the overall effects of dilution through condensate formation and fracture–matrix interaction (diffusive equilibration).

Precipitates and Salts Model Calibration and Validation—The normative precipitates and salts model approach (CRWMS M&O 2000cg, Section 6.5) was applied to the laboratory test results on a qualitative basis, and the results were in reasonable agreement for the bicarbonate-type water. There evidently is some sensitivity to the relative availability of calcium and sodium to form sulfate salts, which is not accounted for in the model. Minor species such as sylvite were identified by the

normative model but were not detected in the laboratory tests because they were scarce and because of interference from ambient humidity. Additional testing with the chloride-sulfate-type water produced similar agreement between the normative assemblage and the minerals observed on complete evaporation. From these results, the normative model is determined to provide a valid approximation to the major minerals and salts formed on complete evaporation of waters with composition similar to either J-13 water or matrix pore water.

The low- and high-relative-humidity salts models were independently developed and validated with laboratory data (CRWMS M&O 2000cl, Section 4.1.2). The low-relative-humidity salts model approach is conservative because it tends to shorten the dry period by not allowing dry conditions for relative humidity greater than 50 percent in the presence of nitrate salts. Also, it predicts elevated chloride concentrations at low relative humidity (CRWMS M&O 2000cl, Section 7.1). The model is valid because it reproduces trends in the known behavior of salts and provides results that are within an order of magnitude of independently developed data. Such accuracy reduces uncertainty associated with the processes that control water composition at low relative humidity. The low-relative-humidity salts model results that are important for TSPA modeling are a decrease in ionic strength (due to the thicker water film) and an increase in chloride concentration as the relative humidity rises from 50 to 85 percent.

Validation of the high-relative-humidity salts model is approached using results from laboratory tests, including those described previously in which bicarbonate-type and chloride-sulfate-type waters were evaporated, and handbook solubility values for pure salts. Reasonable agreement is obtained between measured and modeled values for pH and the concentrations of sodium, carbonate species, fluoride, chloride, and sulfate (CRWMS M&O 2000cl, Section 6.5.1). Agreement to within an order of magnitude is obtained for other constituents, which is acceptable for use in abstracted models for the TSPA. As an additional check, the model is also used to calculate the solubilities of several sodium and potassium salts that are potentially important products of evaporating J-13 water.

Calculated values are within a factor of 2 of the handbook values, up to 10 molal (the limit of the Pitzer model).

Microbial Communities Model Calibration and Validation—This is a bounding model that has been validated by comparison to laboratory and field data. Both model validation and code verification are described in Section 6.6 of *In-Drift Microbial Communities* (CRWMS M&O 2000cp). In these applications, agreement was obtained with observed microbial abundances within the order-of-magnitude tolerance level identified for the use of this model. Three comparisons were used:

- Replication of model results originally calculated for the Swiss repository program demonstrates that the code used for the microbial model (MING) functions correctly where natural materials are combined with engineered materials.

- Modeling of microbial conditions investigated underground at Yucca Mountain and at an analogue site at Rainier Mesa replicated the ambient microbial abundance to within an order of magnitude and confirmed that water and phosphorous availability are limiting factors to microbial growth.

- Modeling of the laboratory tests shows that the numbers of organisms calculated by MING can agree to within an order of magnitude with independently measured data from both energy-limited and nutrient-limited tests.

Engineered Materials Effects Model Calibration and Validation—Models for oxygen consumption by steel corrosion, the effects of cementitious materials, and the impact of ferric-oxide colloids on radionuclide transport are based on bounding approaches, and the best available supporting data are used. Key uncertainties and approaches to confirmation of these bounding arguments have been identified (CRWMS M&O 2000cg, Sections 6.3 and 6.6).

Rockfall Model Calibration and Validation—The rockfall model involved the use of probabi-

listic key block theory, which is an accepted approach for analyzing this type of geotechnical problem. The static key block results are in agreement with observed key block occurrence in the Exploratory Studies Facility main drift and cross-drift (CRWMS M&O 2000e, Section 7.2). The results from the rockfall model have shown that key blocks are most predominant in the Tptpmn unit, which agrees with field observations. The size of key blocks observed in the field is generally less than one cubic meter, which agrees with the simulated distribution of block sizes.

The seismic component of the rockfall model involves a quasi-static method of reducing the joint strength parameters. This method was verified based on the test runs using the dynamic functions of the distinct element code UDEC. Comparison between results from the dynamic and quasi-static analyses shows a consistent prediction of block failure at the opening roof (CRWMS M&O 2000e, Attachment V).

4.2.3.4 Total System Performance Assessment Abstraction

This section describes abstraction of only those models selected for inclusion in the TSPA. The microbial communities model and the models used to bound the effects of engineered materials are determined to have minor impacts on calculated waste isolation performance (although it is acknowledged that microbially influenced corrosion may affect the longevity of Alloy 22 locally) and are excluded from the base case. Also, design analysis has shown that rockfall will not degrade the functionality of the drip shield or waste packages, so the rockfall model is also not included in TSPA-SR.

Abstraction of the Thermal-Hydrologic-Chemical Seepage Model for the Total System Performance Assessment—The thermal-hydrologic-chemical abstraction using the mean distribution of infiltration rate (CRWMS M&O 2000a, Section 3.3.3.4.2), including climate change, is calculated for both geochemical systems discussed above. The abstracted results for both the less complex and more complex chemical systems are shown in Table 4-17 (CRWMS M&O 2000al,

Table 4-17. Thermal-Hydrologic-Chemical Abstraction for the Mean Infiltration Rate Case with Climate Change

Parameter	Preclosure (Period 1) 0 to 50 years Abstracted Values 80°C	Boiling (Period 2) 50 to 1,000 years Abstracted Values 96°C	Transitional Cooldown (Period 3) 1,000 to 2,000 years Abstracted Values 90°C	Extended Cooldown (Period 4)[a] 2,000 to 100,000 years Abstracted Values 50°C
Constituents from the Limited Chemical System (calcite–silica–gypsum)				
log CO_2, vfrac	-2.8	-6.5	-3.0	-2.0
pH	8.2	8.1	7.8	7.3
Ca^{2+}, molal	1.7×10^{-3}	6.4×10^{-4}	1.0×10^{-3}	1.8×10^{-3}
Na^+, molal	3.0×10^{-3}	1.4×10^{-3}	2.6×10^{-3}	2.6×10^{-3}
SiO_2, molal	1.5×10^{-3}	1.5×10^{-3}	2.1×10^{-3}	1.2×10^{-3}
Cl^-, molal	3.7×10^{-3}	1.8×10^{-3}	3.2×10^{-3}	3.3×10^{-3}
HCO_3^-, molal	1.3×10^{-3}	1.9×10^{-4}	3.0×10^{-4}	2.1×10^{-3}
SO_4^{2-}, molal	1.3×10^{-3}	6.6×10^{-4}	1.2×10^{-3}	1.2×10^{-3}
Constituents from the More Complete Chemical System (including aluminosilicates)				
Mg^{2+}, molal	4.0×10^{-6}	3.2×10^{-7}	1.6×10^{-6}	7.8×10^{-6}
K^+, molal	5.5×10^{-5}	8.5×10^{-5}	3.1×10^{-4}	1.0×10^{-4}
AlO_2^-, molal	1.0×10^{-10}	2.7×10^{-7}	6.8×10^{-8}	2.0×10^{-9}
$HFeO_2^-$, molal	1.1×10^{-10}	7.9×10^{-10}	4.1×10^{-10}	2.4×10^{-11}
F^-, molal	5.0×10^{-5}	2.5×10^{-5}	4.5×10^{-5}	4.5×10^{-5}

NOTES: [a]Thermal-hydrologic-chemical calculations have been carried out to 100,000 years, while TSPA calculations have been carried out to 1 million years. Source: CRWMS M&O 2000c, Table 3.10-3.

Section 3.3.1). The evolution of chemical conditions at the drift wall is presented as a series of four discrete time periods for the TSPA-SR calculations: (1) preclosure, (2) boiling, (3) transitional cooldown, and (4) extended cooldown. The log carbon dioxide value represents the composition of gas at the drift wall. These time periods are selected so that relatively constant concentrations can be defined for constituents of interest. After the extended cooling period, the system is considered to have returned to the ambient conditions before thermal perturbation. For both chemical systems considered, major differences in concentrations for key constituents (factor of 10) are limited to calcium, sodium, and bicarbonate ions.

Abstraction of the Precipitates and Salts Model for the Total System Performance Assessment—For the TSPA-SR model, the evolution of water in the repository drifts as temperature decreases and relative humidity increases over time is generalized as an evolution from brine to increasingly dilute water. This evolution is modeled as a succession of time intervals. In each interval, the incoming seepage flow and its composition, as well as temperature, are assigned constant values; the

evaporation rate varies, and the in-drift chemical environment is determined from the evolution of thermal-hydrologic conditions at the particular location evaluated (CRWMS M&O 2000a, Section 3.3.4).

Below 50 percent relative humidity, any salts present in the drift environment will exist in crystalline form and will not form brines. At relative humidities between 50 and 85 percent, salts in the environment will deliquesce and form brines; compositions are provided by the low-relative-humidity salts model. Above 85 percent relative humidity, all of the salts are considered dissolved, and the composition is estimated by the high-relative-humidity salts model using a quasi-steady-state approximation of the degree of evaporative concentration (CRWMS M&O 2000a, Section 3.3.4.5.1).

For each time interval, values of the temperature, carbon dioxide partial pressure, seepage, and evaporation rate are obtained from other models. Lookup tables are then developed for the in-drift water composition to be used in the TSPA, based on a set of calculations using the low-relative-

humidity salts model and the high-relative-humidity salts model. The lookup tables are developed for the following conditions: temperature at 95°, 75°, 45°, and 25°C (203°, 167°, 113°, and 77°F); carbon dioxide partial pressure at 10^{-1}, 10^{-3}, and 10^{-6} atmospheres; and evaporative concentration ranges up to a thousandfold (CRWMS M&O 2000a, Section 3.3.4.5.1).

Inputs to and outputs from the precipitates and salts model were abstracted for use in the TSPA-SR model (CRWMS M&O 2001b, Section 1; CRWMS M&O 2000cg, Section 6.7.4). The abstracted results used in the TSPA-SR model were based on the thermal-hydrologic-chemical model as follows:

- Incoming seepage composition represented by the thermal-hydrologic-chemical abstraction

- Carbon dioxide fugacity and temperature fixed at thermal-hydrologic-chemical abstracted values.

The supplemental TSPA model used a modified abstraction of the thermal-hydrologic-chemical model. Modifications included the effects of operating temperature, the effects of different carbon dioxide partial pressures, and the effects of different initial pore water (and infiltration) compositions (BSC 2001a, Sections 6.3.1.6.3 and 6.3.1.9).

Likewise, the precipitates and salts model abstraction has been updated in supplemental TSPA modeling to include the effect of the concentrations of a revised suite of elements and a select number of aqueous species used to estimate alkalinity (BSC 2001a, Section 6.3.3.6). Another improvement to the precipitates and salts model is consideration of condensation. The combined effect of improvements to the near-field geochemical model shows differences at the subsystem level composition (BSC 2001a). However, supplemental analyses do not show a significant impact at the TSPA level for either higher- or lower-temperature operating modes (BSC 2001b, Sections 3.2.4.2 and 4.2.4).

4.2.4 Waste Package and Drip Shield Degradation

The roles of the waste package and drip shield are discussed in detail in Section 3. This section addresses the expected performance of these components in the potential repository and, along with Sections 4.2.1 through 4.2.6, provides an explanation of the relationship of the waste package and the geologic environment at Yucca Mountain.

The degradation process models and the abstracted models discussed in this section serve as feeds to the WAPDEG code, which integrates the various models to address the overall performance (degradation rates) of the waste package and the drip shield. WAPDEG results, in turn, are used as feeds to the overall TSPA-SR. Specifically, the integrated model included in the WAPDEG performance assessment code used repository environmental conditions as a function of time from other process models to estimate the performance of the waste package and drip shield in terms of time to failure.

As noted in Section 4.1.4, the DOE is evaluating operation of the repository at lower temperatures. The conceptual basis and model abstractions presented in this section reflect the effects of higher-temperature operating modes, specifically those implemented in *Total System Performance Assessment for the Site Recommendation* (CRWMS M&O 2000a, Section 3.4). Alternative thermal operating modes and/or conservatisms and conceptual uncertainties have been reevaluated since the TSPA-SR model and are reported or summarized in *FY01 Supplemental Science and Performance Analyses* (BSC 2001a, Section 9; BSC 2001b, Sections 3 and 4).

4.2.4.1 Conceptual Basis

Lifetimes of the drip shield and waste package depend on the environmental conditions to which they are exposed and the degradation processes that occur in that environment. Section 4.2.3 describes the conceptual understanding of the evolution of physical and chemical conditions in the repository emplacement drifts, the models used to represent those conditions, and the experimental

data that support and contribute to the validation of the models. Environmental conditions within the drifts that influence the degradation of the waste package and drip shield are tightly coupled to the thermal-hydrologic and geochemical processes occurring in the rock surrounding the drifts. These processes involve the vaporization and condensation of water under changing thermal conditions, redistribution and precipitation of dissolved salts, and the effects of gaseous species on solution chemistry. Included in the conceptualization are the contributions of construction material degradation processes (i.e., rock structural support materials and cementitious grout) and the effects of microbial action.

Once the exposure environments have been established, the most important and relevant degradation processes can be identified, which in turn can be used for selecting engineered materials for the drip shield and the waste package. This section discusses the degradation modes of the waste package and drip shield materials under the changing environmental conditions. Corrosion is the degradation process most relevant and important to the selection of the materials for the waste package and drip shield. Mechanical deformation of the waste package and drip shield are estimated to be less significant to the waste package containment time than corrosion (CRWMS M&O 2000n, Section 1.5). A number of corrosion processes have been investigated in detail and the results used to support the selection of materials and the design of these components.

Waste Package and Drip Shield Materials—Degradation modes for the drip shield and waste package are dependent on the materials used in these components and as mentioned earlier, on the environment in which they function. Performance of these materials are reviewed in *General Corrosion and Localized Corrosion of Waste Package Outer Barrier* (CRWMS M&O 2000cq) and *General Corrosion and Localized Corrosion of the Drip Shield* (CRWMS M&O 2000cr). Titanium alloys were selected for construction of the drip shield because of their high resistance to corrosion. This corrosion resistance is due to the formation of a passive oxide film, which is stable over a relatively wide range of environments. The rates of general corrosion and dry oxidation (or dry-air oxidation) of this material have been shown to be very low (CRWMS M&O 2000n, Sections 3.1.1.1, 3.1.5.1, and 3.1.5.4).

Alloy 22 (UNS N06022) was selected for construction of the waste package outer barrier. The main alloying elements of this material are nickel, chromium, molybdenum, iron, tungsten, and cobalt. Alloy 22 is less susceptible to localized corrosion in environments that contain chloride ions than Alloys 825 and 625, materials of choice in earlier waste package designs (CRWMS M&O 2000n, Section 3.1.1.2). This material is one of the most corrosion-resistant nickel alloys for the expected range of repository environments (Gdowski 1991, Section 1.2.5). Alloy 22 and its predecessor alloys have been in use for the past 50 years in a variety of environments and have performed extremely well. Figure 4-79 shows the appearance of a test coupon made from Alloy C, which is a predecessor of Alloy 22, after almost 60 years of exposure to a marine environment. Its shiny, mirror-like appearance was restored by rinsing the dirt and sand from the surface. In comparison to Alloy C and C-4, Alloy 22 has greater corrosion resistance. This is based on the fact that Alloy C-4 and Alloy C-276 have a comparable corrosion resistance (Gdowski 1991, Section 1.2.4), and resistance of Alloy 22 to crevice corrosion is greater than Alloy C-276 (Gdowski 1991, Tables 22 and 25).

Stainless Steel Type 316NG will be used for construction of the structural support container inside the waste package outer barrier to increase the overall strength of the waste package. This material is less susceptible to localized corrosion in environments that contain chloride ions than stainless steel 304, but it is more susceptible than other corrosion-resistant materials such as Alloys 22, 625 and 825, which were considered in various waste package designs (CRWMS M&O 2000n, Section 3.1.1.3). However, the stainless steel layer is used primarily for structural support for the outer barrier and not as a corrosion barrier to the ingress of water into the waste package. The key factor in placing the structural material on the inside is that its strength does not begin to degrade until the outer shell is breached by corrosion or other degradation modes. This is in contrast to the VA design
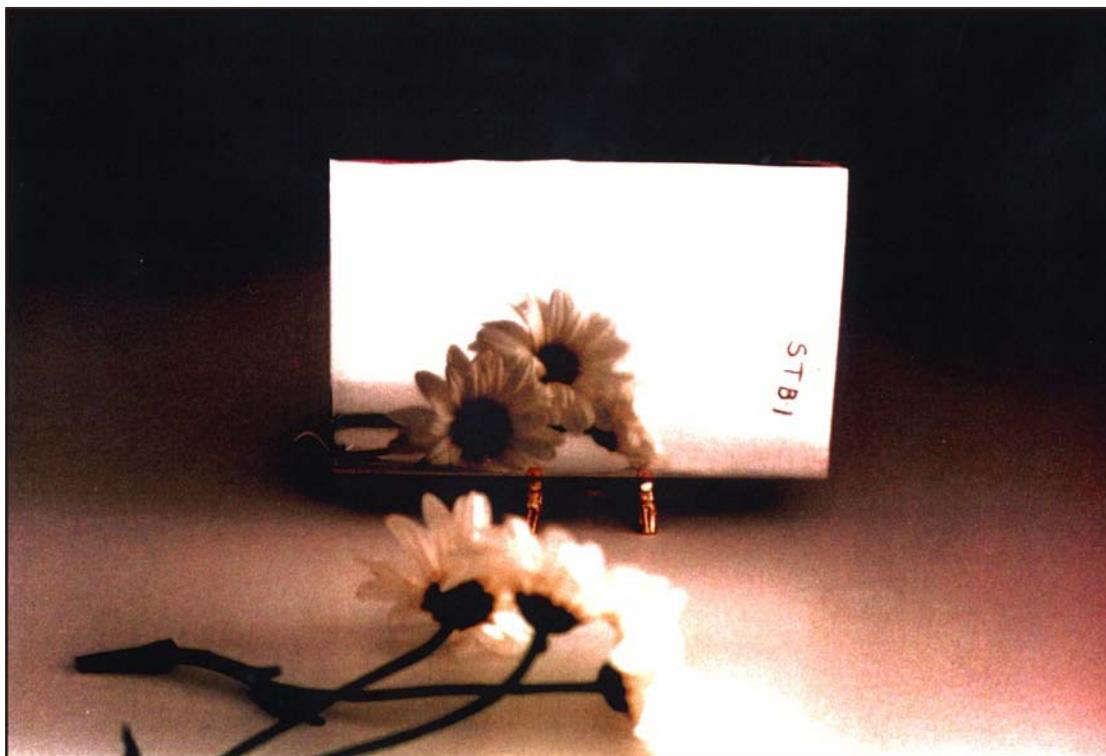
Figure 4-79.   Alloy C Test Coupon after Almost 60 Years of Exposure to a Marine Environment
This test coupon has maintained its mirror finish even after 56 years of exposure to a saltwater atmosphere at the Kure Beach (North Carolina) Marine Atmosphere Test Lot. The coupon was cleaned by simply rinsing it with water.

in which the structural carbon steel was the outer shell, with degradation of strength beginning soon after repository closure.

Figures 4-80 and 4-81 provide a visual perspective to illustrate the physical arrangement of the waste packages and the drip shield within the drift. Figure 4-80 shows schematically the arrangement of different types of waste packages and drip shield. Figure 4-81 shows a schematic sketch of a typical waste package designed for 21 pressurized water reactor fuel assemblies, along with the materials used for the various components.

The dual-barrier design of the waste package and the number of options for the thermal design of the potential repository required a comprehensive testing program to evaluate how materials would perform under the wide range of possible conditions in the potential repository.

Degradation processes evaluated for the drip shield and the waste package include general and localized corrosion under humid air and aqueous conditions, stress corrosion cracking, and hydrogen-induced cracking. The effects of microbially influenced corrosion and aging of the waste package outer barrier were also included in the modeling. An integrated model was developed to evaluate the combined effects of the various degradation modes and was used to estimate the range of lifetimes of the drip shields and the waste packages, including an evaluation of uncertainties.

4.2.4.2   Summary State of Knowledge

Surface Environment—The starting waters present at Yucca Mountain are classified into two types: (1) bicarbonate-type water (e.g., J-13 water) and (2) unsaturated zone pore water (chloride-sulfate water). Chemical modeling and laboratory testing of these water compositions have shown that the bicarbonate-type water evolves by evapo-
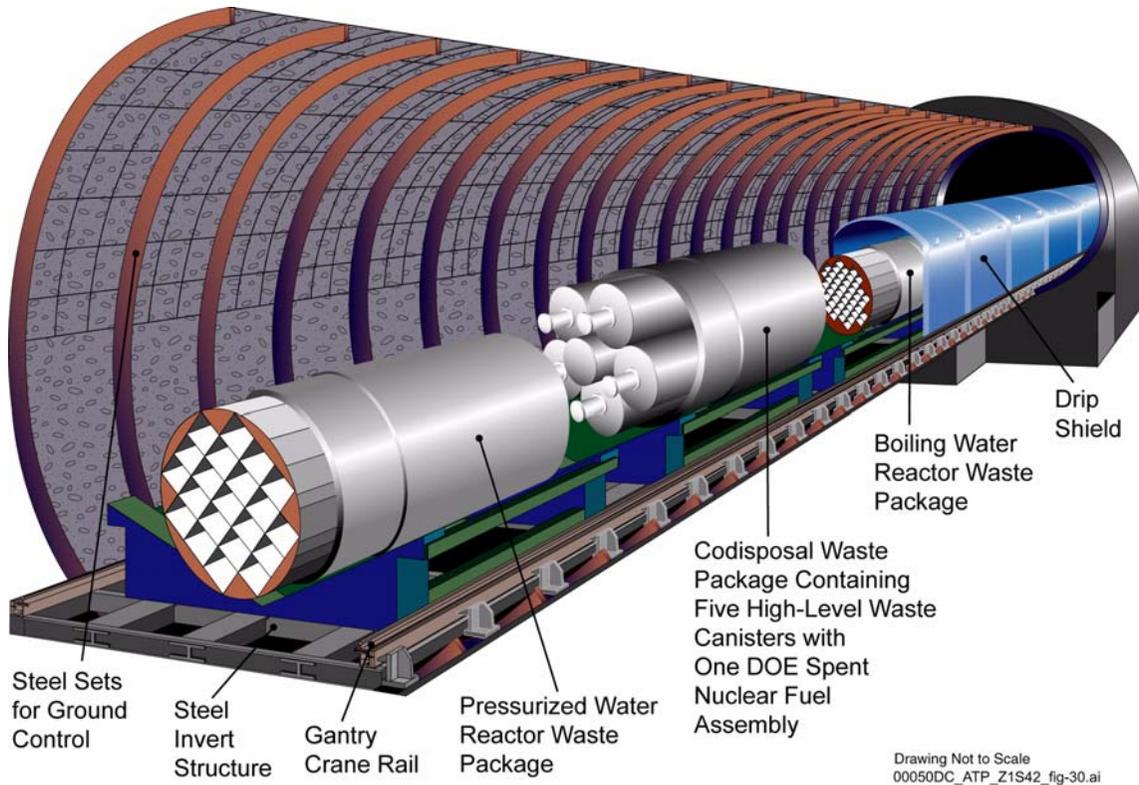
Figure 4-80.   Schematic Illustration of the Arrangement of Waste Packages and Drip Shield
Waste packages are shown in cutaway view to illustrate different waste streams, such as commercial spent nuclear
fuel and high-level radioactive waste. Source: CRWMS M&O 2000n, Figure 1-2.

rative concentration to a high-pH brine, whereas the chloride-sulfate-type water evolves to a brine with nearly neutral pH (CRWMS M&O 2000ck, Section 6.1).

In the model used, hygroscopic salts on the drip shield or waste package formed due to evaporation of the dripping water will be limited to sodium or potassium salts. As a bounding condition, it is assumed that sodium nitrate—the salt with the lowest deliquescence point at elevated temperature—will determine the minimum relative humidity at which aqueous conditions can occur (CRWMS M&O 2000ck, Section 6.4.2).

The exact chemistry of the water that contacts the drip shield and waste package surfaces cannot be known precisely. However, the range of potential types of aqueous solutions has been estimated from the range of potential starting water compositions, from knowledge of near-field and in-drift

processes that can alter these compositions, and from laboratory experiments and natural analogue observations. From these results, a range of water compositions was developed and is being used for corrosion testing; the range also includes the potentially important effects of processes at the engineered component surfaces.

Composition of Aqueous Solutions Used for Corrosion Testing—Test solutions developed for laboratory corrosion testing of titanium, Alloy 22, and other materials were selected to represent a range of dilute and concentrated conditions, pH, and temperatures that could result from evaporative concentration in the potential repository (CRWMS M&O 2000ck, Section 6.12). The test solutions include the following:

• **Simulated Concentrated Water**—Formulated to simulate evaporative concentration of J-13 water by a factor of 1,000. The resulting
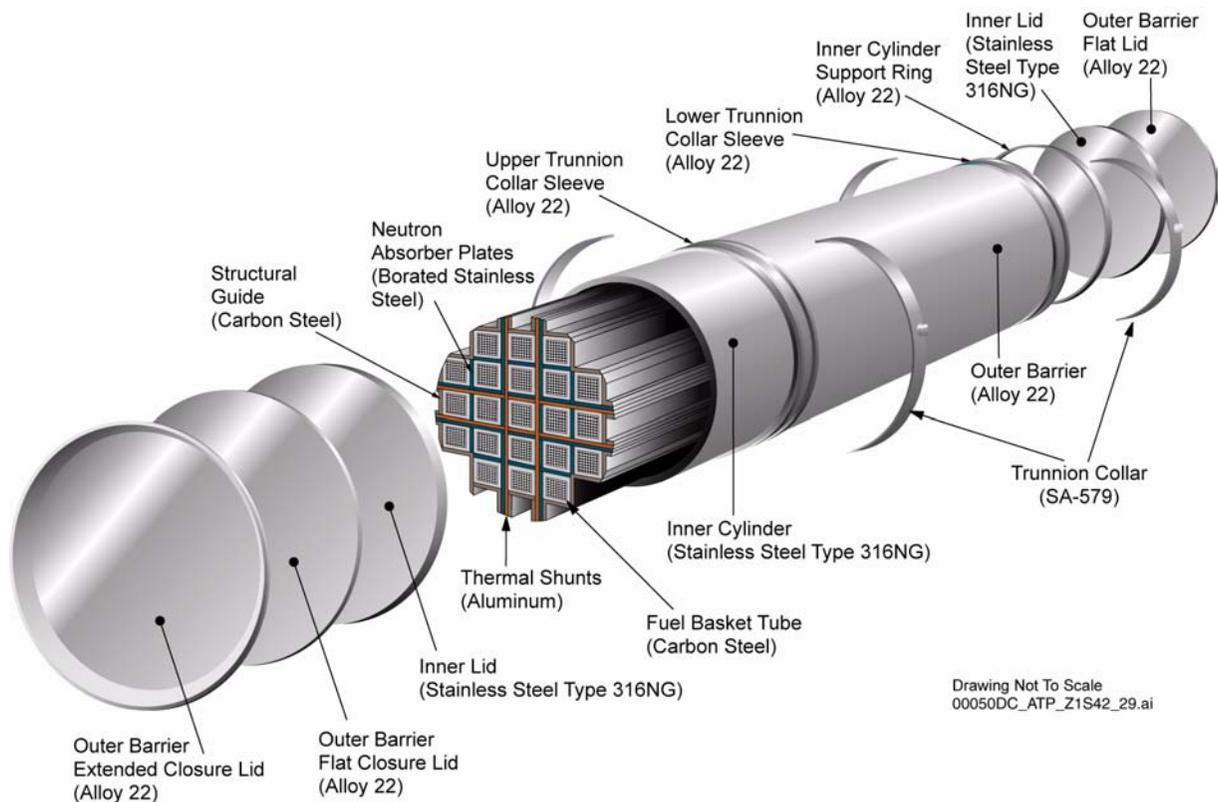
Figure 4-81. Schematic Illustration of a Typical Waste Package Designed for 21 Pressurized Water Reactor Fuel Assemblies, and the Materials Used for the Various Components
This figure shows the arrangement of the two cylinders and the location of trunnions used for lifting and handling of the waste packages. The internal parts of the waste package include basket tubes, a structural guide, and neutron absorber plates. Source: CRWMS M&O 2000n, Figure 1-1.

solution has a moderately high pH (9 to 10) (CRWMS M&O 2000ck, Section 6.12.1).

- **Simulated Dilute Water**—Formulated to simulate evaporative concentration of J-13 water by a factor of 10. This type of water might exist on the drip shield or waste package when the temperature difference between these components and the surrounding drift environment is small and evaporation is slow (CRWMS M&O 2000ck, Section 6.12.2).

- **Simulated Acidic Water**—Similar to the simulated concentrated water solutions but acidified to pH 2.7. This solution is intended to simulate acidification of J-13 water, or pore water from the tuff matrix, by surface

processes on the engineered components (CRWMS M&O 2000ck, Section 6.12.3).

- **Simulated Saturated Water**—Simulates solutions that can become concentrated in the most soluble constituents, namely nitrate and chloride salts. In the host rock around the emplacement drifts, soluble salts can become separated from other constituents of the starting water and concentrated. This test solution is therefore a concentrated solution of sodium nitrate with some additional potassium chloride and with the concentrations adjusted to promote oxygen solubility (CRWMS M&O 2000ck, Section 6.12.4).

- **Basic Saturated Water**—Formulated to simulate extreme evaporative concentration of a bicarbonate-type water such as J-13

water. In addition, three values of pH are used (controlled by addition of sodium hydroxide) to simulate different values of carbon dioxide partial pressure (CRWMS M&O 2000ck, Section 6.12.5).

Corrosion tests were conducted at Lawrence Livermore National Laboratory on specimens of waste package and drip shield materials, including titanium and Alloy 22, exposed to the above environments. The tests were comprehensive and examined many forms of corrosion: pitting, stress corrosion cracking, galvanic corrosion, corrosion in crevices, and general corrosion. In addition, some long-term tests had counterpart shorter-term tests for stress corrosion cracking and galvanic corrosion. The results of the tests were used for developing various corrosion models to predict the long-term behavior of the materials in the repository.

Long-Term Corrosion Testing—Test environments for long-term corrosion testing were structured to simulate concentrated solution conditions. The samples were exposed in the aqueous phase, in the vapor phase above the solutions, and at the waterline (DOE 1998, Volume 2, Section 5.1.4.1). To date, some 13,000 specimens, including welded samples, have been tested in water for periods from 6 months to 2 years in duration. The first materials tested were arranged in three categories: corrosion-allowance materials, intermediate corrosion-resistance alloys, and corrosion-resistant alloys (DOE 1998, Volume 2, pp. 5-44 to 5-45). The specimen designs and test procedures were based on specifications developed by the American Society for Testing and Materials, including specifications ASTM G 1-90, *Standard Practice for Preparing, Cleaning, and Evaluating Corrosion Test Specimens*, ASTM G 30-94, *Standard Practice for Making and Using U-Bend Stress-Corrosion Test Specimens*, and ASTM G 46-94, *Standard Guide for Examination and Evaluation of Pitting Corrosion*. Figure 4-82 shows the arrangement of the test specimens in the racks, and Figure 4-83 shows the typical appearance of the specimens after 12 months of exposure in the corrosion test facility.

Complementary Short-Term Tests—The long-term corrosion tests were a key component for evaluating waste package materials. They were complemented by short-term tests designed to develop mechanistic understanding. For example, short-term tests measured the relative susceptibilities of the candidate materials to general, localized, and microbially influenced corrosion. The short-term tests were important for developing models of corrosion behavior.

Field Test Assessment—Field tests provide an independent confirmation of the performance of materials in the Yucca Mountain environment. Specimens included in the accelerated thermal field tests were characterized to determine how candidate materials degrade with exposure to actual field environments at Yucca Mountain under repository temperature conditions. The specimens are subjected to changing environmental conditions, including temperature, relative humidity, and possible intermittent water contact. In comparison, laboratory experiments are being run at fixed and constant environmental conditions (DOE 1998, Volume 2, Section 5.1.4.1), and the laboratory experiments also include bounding or conservative aggressive environments.

In each field study, test specimens were placed in drifts and boreholes that were well characterized with respect to temperature and relative humidity (DOE 1998, Volume 2, Section 5.1.4.1). The data on corrosion generated from the field tests were used in activities related to performance assessment, materials selection, model development, and potential repository design.

The materials selected for the drip shield (titanium) and the waste package outer barrier (Alloy 22) are highly corrosion-resistant. Based on literature and prior industrial experience, these materials are not expected under repository exposure conditions to be subject to degradation processes that could lead to failure in a short time period (Gdowski 1991, pp. 1 to 3; Gdowski 1997, pp. 38 to 39). Those degradation modes are localized corrosion (pitting and crevice corrosion), stress corrosion cracking, and hydrogen-induced cracking (applicable only to the drip shield). Both the drip shield and waste package degrade by general corrosion at very low
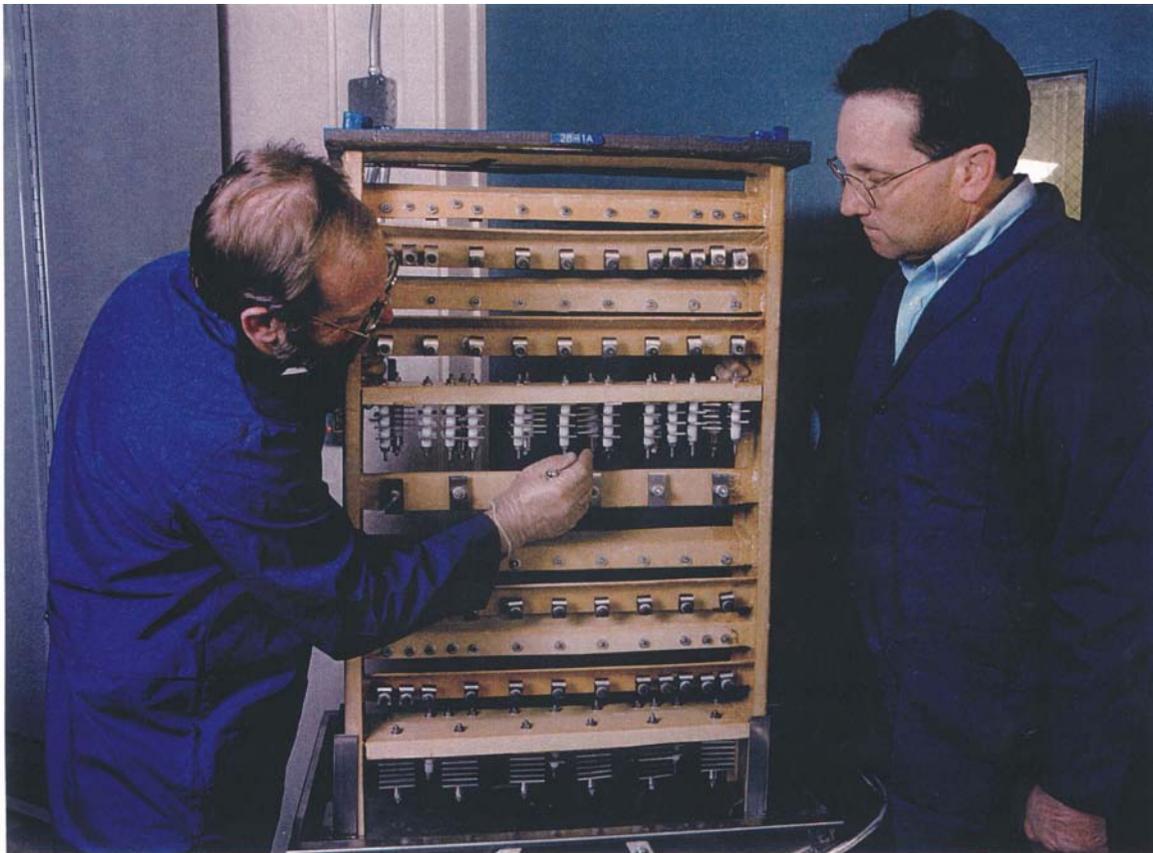
00050DC_ATP_Z1S42_fig.28.cdr

Figure 4-82.   Arrangement of the Test Specimens in the Racks

rates. The current experimental data and detailed process-level analyses also indicate that the candidate materials would not be subject to rapidly penetrating corrosion modes under the expected repository conditions. The exception to this is the closure-lid welds of the waste package, where unmitigated residual stresses could potentially lead to stress corrosion cracking. To preclude this occurrence, weld residual stress mitigation processes will be implemented on each of the dual-lid Alloy 22 waste package closure welds. As a result, the estimated long lifetime of the waste packages in the current analyses is attributed mostly to two factors: (1) stress mitigation in the dual closure lid weld area and (2) the low general-corrosion rate, which will very slowly remove the beneficial compressive stress zones at each weld surface, thereby providing a long delay before stress corrosion cracking can potentially initiate and grow to penetrate the weld thickness.

Models were created to predict the performance of the various materials in the expected repository environment. The modeling effort served the following two major purposes:

1. It supported the selection of materials for which a key selection criterion was the predictability of the component material performance.

2. It furnished information about how the selected materials would perform in the repository environment. Consistent with ASTM C 1174-97, *Standard Practice for Prediction of the Long-Term Behavior of Materials, Including Waste Forms, Used in Engineered Barrier Systems (EBS) for Geological Disposal of High-Level Radioactive Waste*, relevant data from testing activities were interpreted with a mechanistic understanding of how materials behave.
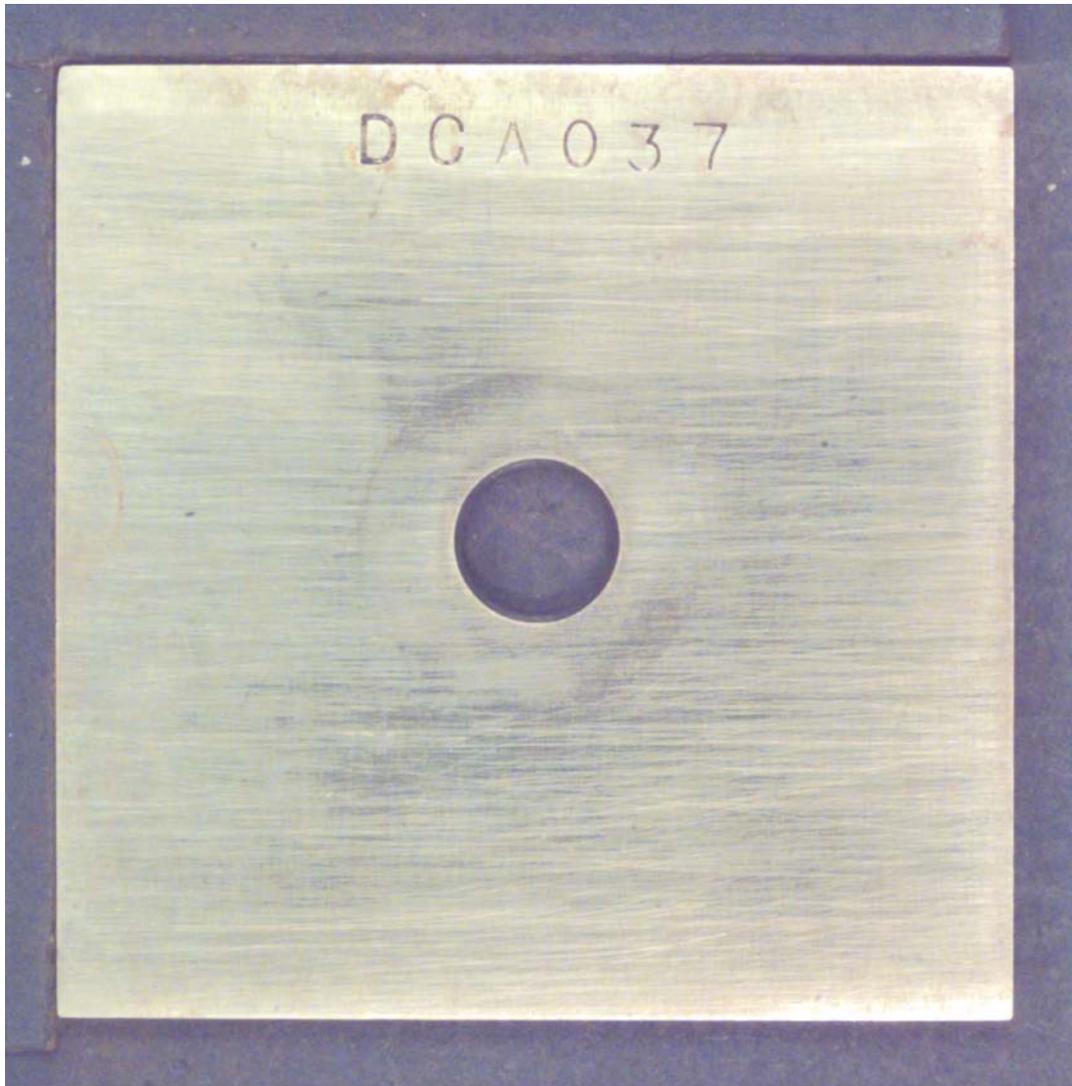
00050DC_ATP_Z1S42_fig 23.cdr

Figure 4-83.   Typical Appearance of an Alloy 22 Specimen after 12 Months of Exposure to an Aqueous Environment in the Long-Term Corrosion Test Facility

The "scratched" appearance of the surface finish is the same as that observed before the start of testing. The small, faint circular area of discoloration in the center is caused by a Teflon washer used to create a creviced area.

4.2.4.3   Process Model Development and Integration

This section addresses waste package and drip shield material degradation models and their abstractions and alternative models considered for the waste package and drip shield lifetimes. Degradation modes for the components are discussed and the dominant modes determined. Available test data are summarized. The section concludes that the modes of waste package and drip shield degra-dation (i.e., corrosion) and their dependence on expected thermal-hydrologic and geochemical conditions are sufficiently understood and conser-vatively captured in the model abstractions to support evaluation of postclosure performance.

Waste Package Material Degradation Modes—The degradation processes were selected for modeling on the basis of an extensive review of available information on the candidate materials for the waste package and drip shield. These

processes have been documented in a number of degradation mode surveys (Gdowski 1991; Gdowski 1997). In addition, a review and analysis of features, events, and processes relevant to the degradation of the waste package and drip shield was recently completed and is described in Section 4.3. The degradation models provided a quantitative analysis of early failure of waste packages. The degradation models also calculated the range of expected degradation histories of both waste packages and drip shields. These models consisted of several individual process models or analyses and associated abstraction models. Figure 4-84 shows the elements of each process model, associated abstraction models, and the interrelationships among the various process and abstraction models (CRWMS M&O 2000n, Figure 1-4). The process models for general and localized corrosion of the waste package outer barrier include dry oxidation, humid-air corrosion, and the expected environment

on the surface. In addition, the figure also shows how the process models feed the integrated model for waste package and drip shield degradation (WAPDEG), which is used to predict the lifetimes of these two components. Details of the process models and abstraction models are presented in the following analysis model reports and calculations (which also document evaluation of the applicable modes of degradation of the waste package and the drip shield and their models):

- *Environment on the Surfaces of the Drip Shield and Waste Package Outer Barrier* (CRWMS M&O 2000ck)

- *Analysis of Mechanisms for Early Waste Package Failure* (CRWMS M&O 2000cs)

- *Aging and Phase Stability of Waste Package Outer Barrier* (CRWMS M&O 2000ct)
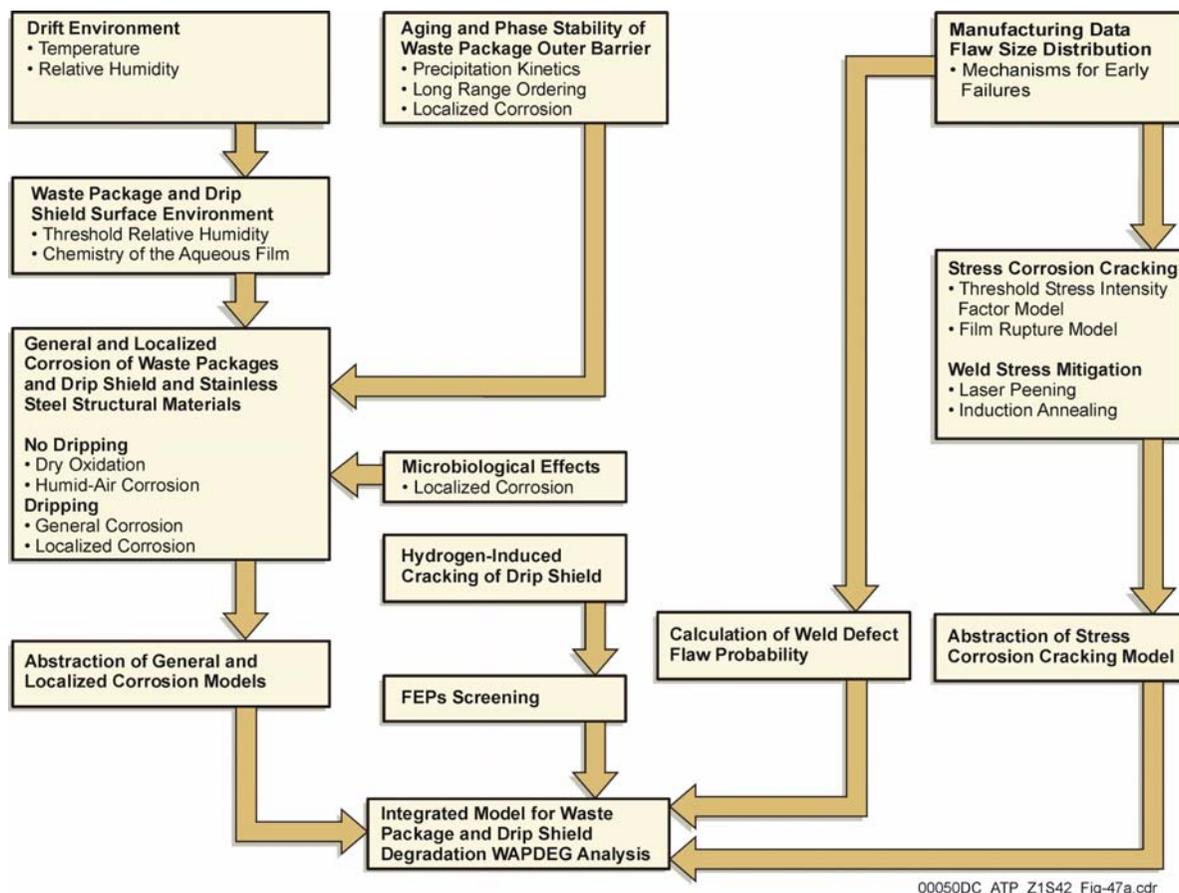
Figure 4-84. Schematic Representation of the Elements of Process Models and the Interrelationships among the Process Models

- *General Corrosion and Localized Corrosion of Waste Package Outer Barrier* (CRWMS M&O 2000cq)

- *General Corrosion and Localized Corrosion of the Drip Shield* (CRWMS M&O 2000cr)

- *Stress Corrosion Cracking of the Drip Shield, the Waste Package Outer Barrier and the Stainless Steel Structural Material* (CRWMS M&O 2000cu)

- *Hydrogen Induced Cracking of Drip Shield* (CRWMS M&O 2000cv)

- *Degradation of Stainless Steel Structural Material* (CRWMS M&O 2000cw)

- *FEPs Screening of Processes and Issues in Drip Shield and Waste Package Degradation* (CRWMS M&O 2000cx)

- *Calculation of Probability and Size of Defect Flaws in Waste Package Closure Welds to Support WAPDEG Analysis* (CRWMS M&O 2000cy)

- *Calculation of General Corrosion Rate of Drip Shield and Waste Package Outer Barrier to Support WAPDEG Analysis* (CRWMS M&O 2000cz)

- *Abstraction of Models for Pitting and Crevice Corrosion of Drip Shield and Waste Package Outer Barrier* (CRWMS M&O 2000da)

- *Abstraction of Models of Stress Corrosion Cracking of Drip Shield and Waste Package Outer Barrier and Hydrogen Induced Corrosion of Drip Shield* (CRWMS M&O 2000db)

- *WAPDEG Analysis of Waste Package and Drip Shield Degradation* (CRWMS M&O 2000dc).

Figure 4-85 shows the model confidence foundation, along with the inputs and outputs for the various degradation process models. This figure shows the critical input parameters for the degradation mechanisms and data inputs and sources, which provide lifetimes for the components. Confidence in the overall model is based on the comprehensive nature of the input parameters, data, and degradation mechanisms considered in the overall performance assessment. Highlights of the waste package degradation process models are addressed in the following subsections.

4.2.4.3.1   Mechanisms for Early Failures

There is a potential for early failures of the waste package due to material defects and waste package fabrication processes, including welding. The probability of waste package fabrication defects, the uncertainty and variability of those defects, and the consequences of the defects on waste package failure times (e.g., number of potential failure sites and flaw-size distribution) were assessed.

A literature review was performed to determine the rate of failure from manufacturing defects for various types of welded metallic containers. Types of components examined included boilers and pressure vessels, nuclear fuel rods, underground storage tanks, radioactive cesium capsules, dry-storage casks for spent nuclear fuel, and tin-plate cans. In addition to providing examples of the rate at which defective containers occur, this information provided insight into the various types of defects that can occur, and the mechanisms that cause defects to propagate to failure (CRWMS M&O 2000cs, Section 6.1).

The fraction of the total population that failed due to defect-related causes during the intended lifetime of the component was generally in the range of 10^{-3} to 10^{-6} per waste package (equivalent to 1 component in 1,000 to 1,000,000 components). In most cases, defects that led to failure of the component required an additional stimulus to cause failure (i.e., the component did not fail immediately when it was placed into service). In fact, there were several examples that indicated that even commercial standards of quality control could reduce the rate of initially failed components well below 10^{-4} per package (or 1 out of 10,000 components) (CRWMS M&O 2000cs, Section 7).
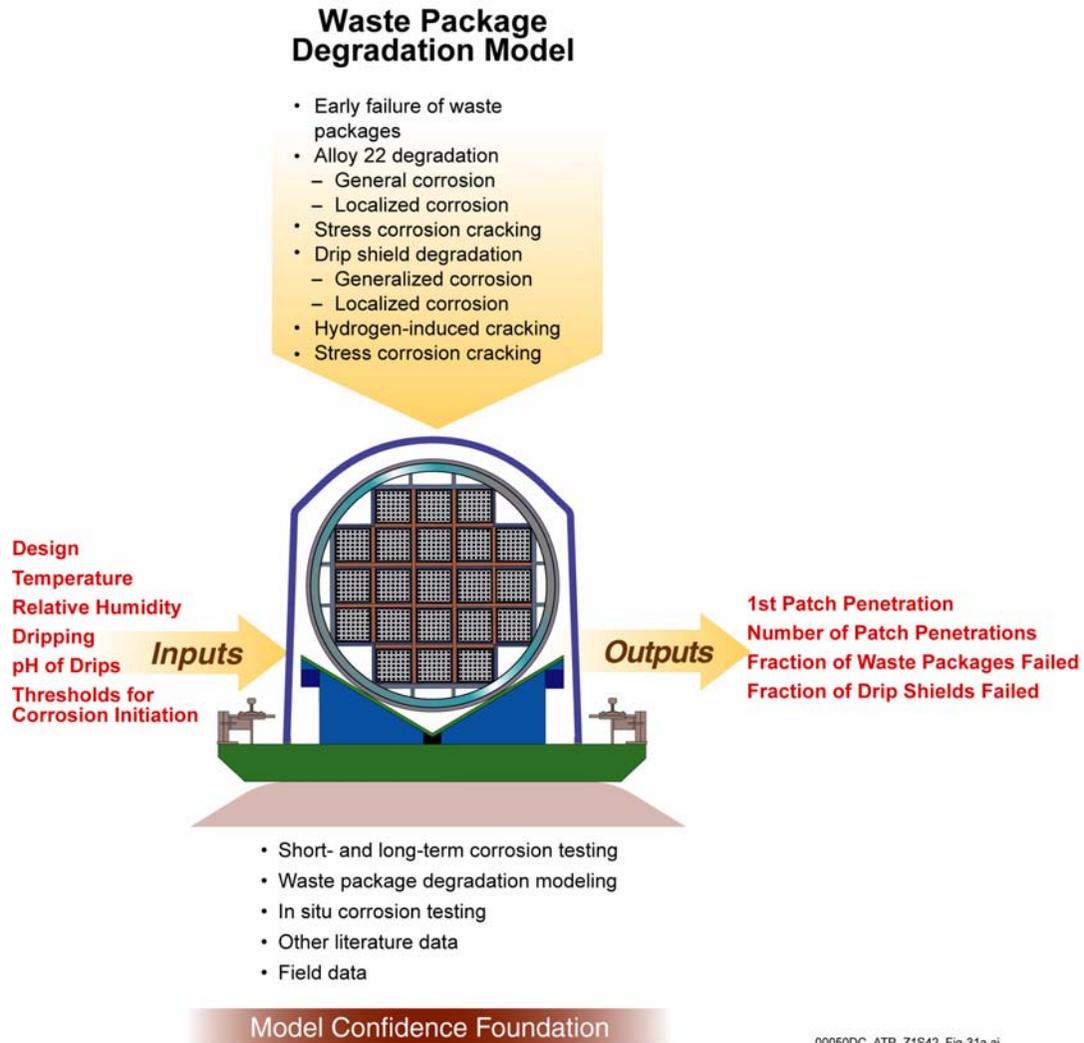
Figure 4-85. Foundation for Model Confidence, including Inputs and Outputs for the Various Degradation Process Models

Confidence in the outputs of the degradation model is influenced by the accuracy of the inputs, such as design parameters and repository environments. These inputs are used in combination with testing data and descriptions of predictive models. It is therefore important to have reliable data and models that address all credible degradation mechanisms. Source: CRWMS M&O 2000n, Figure 1-3.

The literature review identified 11 generic types of defects that could cause early failures in the components examined (CRWMS M&O 2000cs, Section 6.1.7). These were:

1. Weld flaws
2. Base metal flaws
3. Improper weld material
4. Improper heat treatment
5. Improper weld flux material
6. Poor weld joint design
7. Contaminants
8. Mislocated welds
9. Missing welds
10. Handling and installation damage
11. Administrative error resulting in an unanticipated environment.

Four of these defect types were not considered applicable to the waste package: improper weld flux material, poor joint design, missing welds, and mislocated welds. This conclusion was based on

the processes to be used for welding and the process qualification and weld inspection programs that will be implemented (CRWMS M&O 2000cs, Section 7).

The analysis also estimated the probability that specific defect types would occur on a given waste package, considering the expected preventive quality controls. The analysis applies to those defects for which probabilities are estimated using event sequence trees, namely: drip shield emplacement error, waste package handling error, waste package surface contamination, thermal misload, and improper heat treatment. The method used to establish an upper bound value for event sequences combines the human error rates probabilistically. Uncertainties are considered only for human error probabilities related to failures. Probability components for success are treated at their nominal level (i.e., without uncertainty), which produces conservative results. No upper bounds were estimated for other failure probabilities related to mechanical failure or based on historical data. Accordingly, the upper bound for an event sequence probability is adjusted for only human error probability uncertainties. This analysis is much more rigorous and mathematically defensible in comparison to the prior analyses conducted for the Viability Assessment.

Results of the analysis for the remaining seven types of defects showed that, with the exception of the administrative error category, all the defect probabilities were less than 10^{-4} per waste package. This is equivalent to less than one waste package failure out of 10,000 in the entire repository. The administrative error defect rate will be reduced through implementation of stringent administrative controls (CRWMS M&O 2000cs, Section 7).

Subsequently, in reevaluating the potential of early failure mechanisms and their potential consequences, a more conservative approach resulted in the inclusion of improper heat treatment and subsequent failure of a few waste packages in the supplemental TSPA analysis. To ensure that the potential consequence of early waste package failures is treated conservatively, it is included in the nominal scenario, not as a sensitivity analysis (BSC 2001a, Section 7.3.6).

4.2.4.3.2   Aging and Phase Stability of the Waste Package Outer Barrier

Alloy 22, a nickel-based alloy, has excellent corrosion resistance and good strength and ductility. Under certain conditions, changes in the internal structure of the material can degrade its corrosion resistance and/or ductility. Three general areas were addressed in the models: complex phases, ordering, and welds.

Complex phases are known to form in Alloy 22 at temperatures above approximately 600°C (1,100°F). They can presumably form at lower temperatures, but it would take much longer than is typically observed in the laboratory because these types of changes require thermal energy and occur more slowly at lower temperatures. The rate at which these phases form in Alloy 22 was measured at temperatures above 600°C (1,100°F) as a function of temperature. Extrapolation of this rate relation to 300°C (570°F), the expected peak temperature in the emplacement drift, indicates that the rate of complex phase formation would be very slow under potential repository conditions and would have an insignificant contribution to corrosion. To bound this effect, however, a worst case was defined for the fully aged material with complete coverage of the grain boundaries with precipitates (CRWMS M&O 2000n, Section 3.1.4.2). Figure 4-86 shows the effects of aging on precipitation in the grain boundaries.

Samples with this worst-case structure were created and provided for corrosion testing. Samples of Alloy 22 were aged at 700°C (1,292°F) for either 10 or 173 hours. The corrosion resistance of these aged samples is compared to that of base metal in several standardized test media using cyclic polarization technique. The results of this testing showed that the fully aged material exhibited a slightly higher corrosion rate than the unaged material. The maximum increase in corrosion rate was by a factor of 2.5 over the unaged sample. The results are described in greater detail in *General Corrosion and Localized Corrosion of Waste Package Outer Barrier* (CRWMS M&O 2000cq, Section 6).
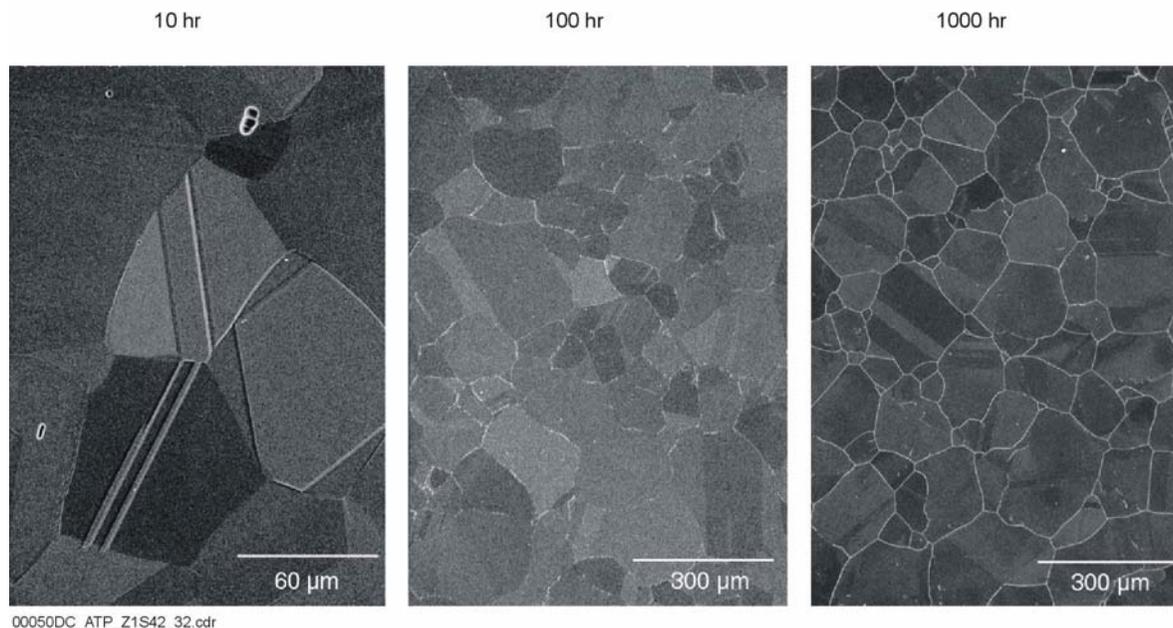
Figure 4-86.   Effects of Aging on Precipitation at Alloy 22 Grain Boundaries
The figure shows the amount of precipitation of complex phases in the boundaries of grains due to aging at high temperatures. After 10 hours of aging at 649°C (1,200°F), few or no precipitates are seen in the left photomicrograph. After 100 hours, as shown in the center, parts of the grain boundaries are decorated (covered) with white precipitates. After 1,000 hours, the grain boundaries are completely covered with precipitates, as seen in the photo on the right. Source: CRWMS M&O 2000n, Figure 3-5.

The second general area is ordering. Commercially available Alloy 22 is a single-phase alloy. At temperatures below approximately 600°C (1,100°F), the atoms slowly transform from a somewhat random arrangement into an ordered pattern, with the highest rates of transformation at higher temperatures below the 600°C (1,100°F) temperature limit. This process results in the rearrangement and segregation of alloying elements into specific locations in the crystal structure. This is a slow process, occurring over a long period of time. Ordering may affect the mechanical properties of alloy systems. For example, ordering can increase the strength of the alloy and reduce its ductility, which also decreases its resistance to stress corrosion cracking and hydrogen embrittlement. Because ordering occurs only at lower temperatures and because these reactions are slow, the data for the rate of ordering in Alloy 22 are limited. However, based on the available data, ordering will not become a problem, provided the temperature does not go above about 260°C (500°F) for significant periods of time (CRWMS

M&O 2000n, Section 3.1.4.4). Testing will continue into the performance confirmation period to more accurately predict the performance of this alloy in the potential repository environment.

The third general area is welds. Complex phases form during welding of Alloy 22 and are present in the as-welded condition. These phases and segregation in the weld cause the welds to have lower corrosion resistance than the base metal. Work to determine the effects that long-term exposures to repository-relevant temperatures have on the properties of Alloy 22 welds is ongoing (CRWMS M&O 2000n, Section 3.1.4.3).

The aging times for the various stages of intermetallic precipitation in Alloy 22 base metal as a function of temperature were obtained from the examination of aged samples after approximately 1, 10, 100, 1,000, and in some cases 16,000 hours (CRWMS M&O 2000n, Section 3.1.4.2). These measurements are only intended as an initial estimate of the precipitation kinetics. These obser-

vations were used to generate the isothermal time–temperature transformation diagram for Alloy 22 base metal shown in Figure 4-87.

The long-term aging of Alloy 22 at elevated temperatures can cause the precipitation of undesirable intermetallic phases if the temperature is sufficiently high. The data shown in Figure 4-87 do not indicate that the phase stability of Alloy 22 base metal will be a problem at less than about 300°C (572°F). It is expected that the waste package surface temperature will stay below 300°C (572°F) in the emplacement drift (CRWMS M&O 2000n, Section 3.1.4). While this estimate is bounding, it is based on limited data. The analysis will be further refined and improved as additional data and analysis become available.

For comparison, estimated temperature of the waste package surface as a function of time in the repository is shown in Figure 4-88 for repository designs with and without backfill. This figure shows that even for the hottest waste package containing design basis spent fuel waste the peak temperature does not exceed 250°C (482°F) for the design with no backfill. The sharp increase in surface temperature seen in both curves is due to the assumed (for this analysis only) termination of ventilation at 25 years after emplacement. Based on this comparison, the impact of aging and phase instability on the corrosion of Alloy 22 is not expected to be a problem for the repository design without backfill (CRWMS M&O 2000n, Section 3.1.4.2). The significance of the uncertainties in this data is discussed in Section 3.
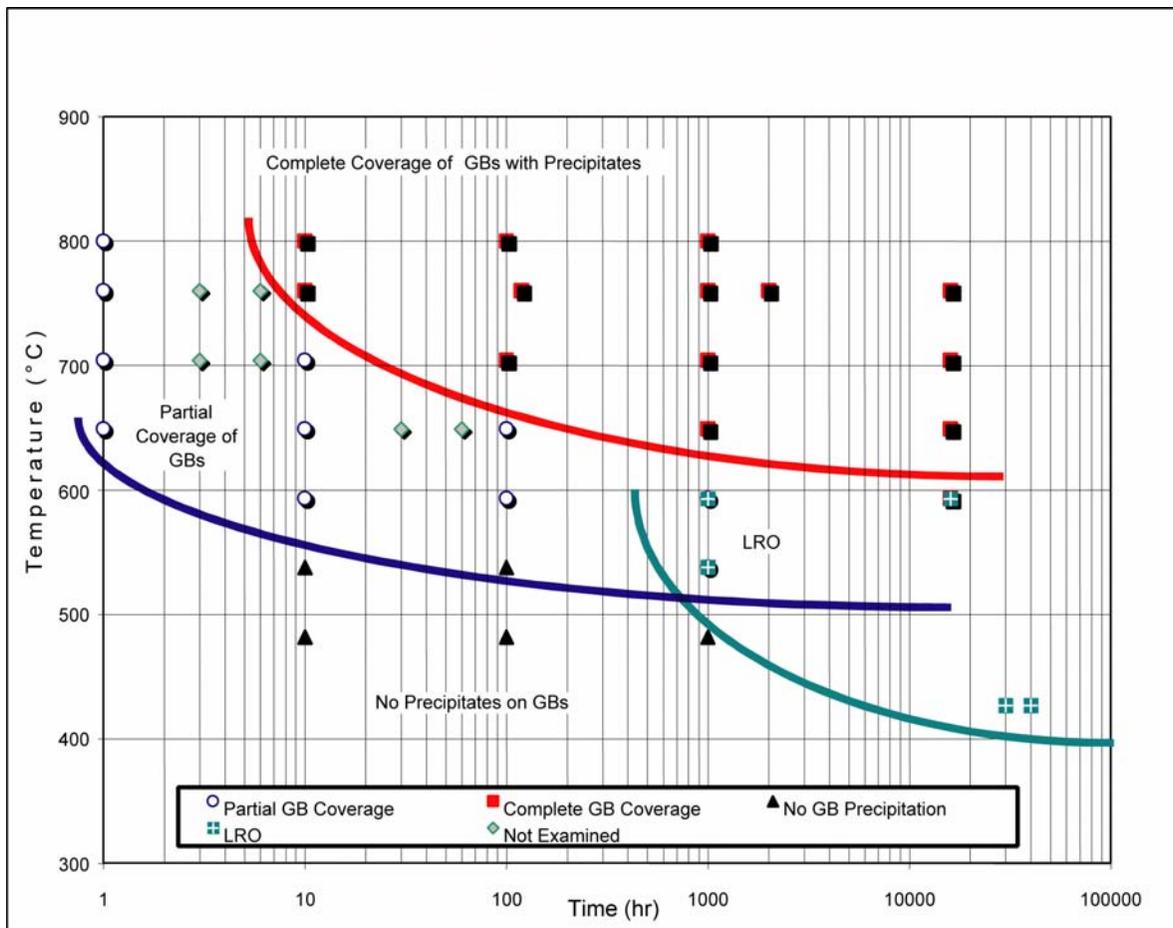
00050DC_ATP_Z1S42_102.ai

Figure 4-87. Isothermal Time–Temperature Transformation Diagram for Alloy 22 Base Metal
GB = grain boundary; LRO = long-range ordering. Source: CRWMS M&O 2000n, Figure 3-4.
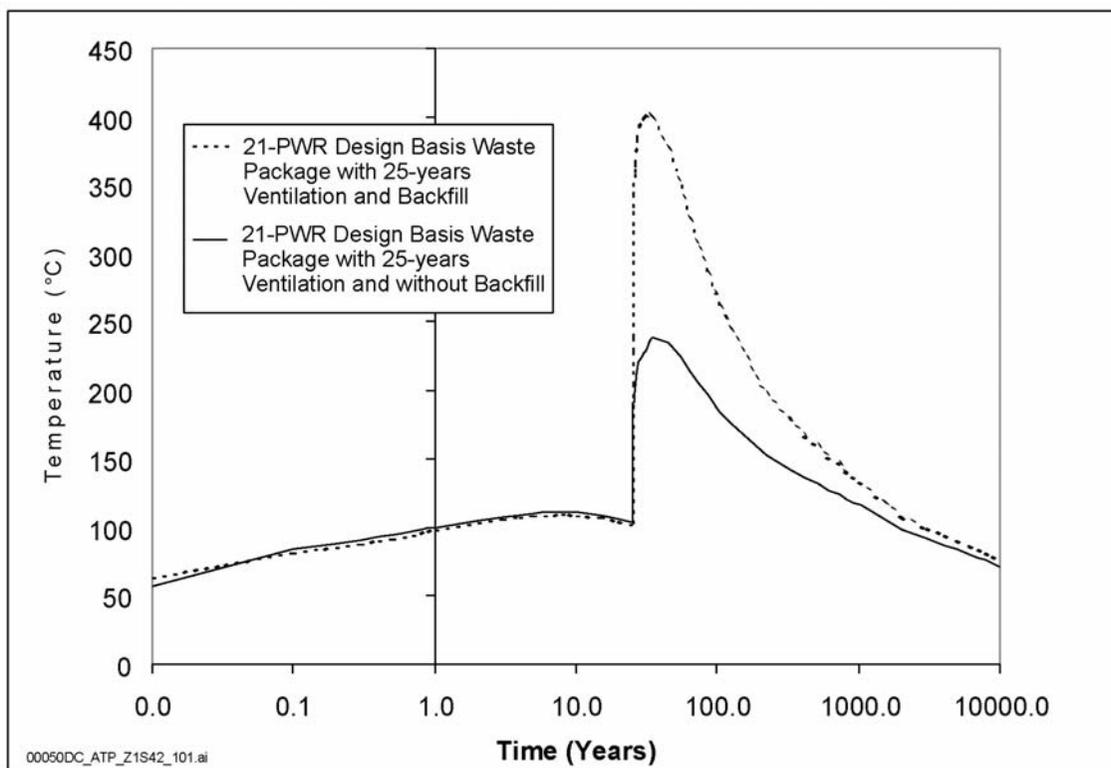
Figure 4-88. **Temperature of the Waste Package Outer Barrier Surface as a Function of Time for the Hottest Waste Package**

The sharp rise in temperature for both cases is due to the termination of ventilation which in this analysis is assumed to occur after 25 years. The use of backfill results in much higher waste package surface temperature because the backfill acts as an insulator against heat dissipation. Source: CRWMS M&O 2000n, Figure 3-7a.

Since the completion of the TSPA-SR model, aging and phase stability of Alloy 22 was reevaluated using new data and analyses. These analyses confirm the conclusion of the TSPA-SR model that aging of the Alloy 22 barrier is not a concern (BSC 2001a, Section 7.2.1).

4.2.4.3.3   General and Localized Corrosion

Three separate process models were developed to address general and localized (including microbial) corrosion of the drip shield, waste package outer barrier, and stainless steel structural material. The design described in this report uses Grade 7 titanium for the drip shield, Alloy 22 for the waste package outer barrier, and Stainless Steel Type 316NG as stainless steel structural material. While the stainless steel structural material is not specifically intended to be a corrosion barrier, it may affect the chemistry and the rate of water entering

the waste package and retard the rate of radionuclide release from the breached waste package. Given the limited availability of corrosion data for Stainless Steel Type 316NG, data for Stainless Steel Type 316L were used as representative class of materials. This is appropriate since the compositions of the two materials are similar, and aqueous corrosion characteristics are expected to be similar (CRWMS M&O 2000n, Section 1.5.4).

The process model for general and localized corrosion includes submodels for dry oxidation, humid-air and vapor-phase corrosion, and aqueous phase corrosion.

Dry Oxidation—The dry oxidation submodel assumes that dry oxidation could be treated as a single mode of attack, that is, as general corrosion. Corrosion rates were estimated as a function of

temperature (CRWMS M&O 2000n, Section 1.5.4.1).

Humid-Air and Vapor-Phase Corrosion—Humid-air and vapor-phase corrosion are treated as a single mode of attack, that is, as general corrosion. Corrosion rates were estimated as a function of temperature (CRWMS M&O 2000n, Section 1.5.4.2).

Aqueous-Phase Corrosion—The process model for aqueous-phase corrosion of the drip shield and waste package accounts for both general and localized corrosion. Two different modeling methods were used to model this process. The first method determined the threshold corrosion potential for localized attack of the material from short term experiments that used relevant test media. Test environments covered the range from the least aggressive environment of J-13 water to the most aggressive environment of concentrated J-13 water, and the temperature range was between 30° and 90°C (86° and 194°F). Using data from published literature and tests at elevated temperature and pressure, the second method determined the threshold temperature for localized attack. The aqueous-phase corrosion model was applied independently to a large number of small regions (patches) on each waste package (CRWMS M&O 2000n, Section 1.5.4.3).

Abstracted models were developed to account for general and localized corrosion of the drip shield and waste package materials. The abstracted models were input to the TSPA analysis using the WAPDEG code. The abstracted models included thresholds for initiation of various modes of corrosion, as well as the corresponding penetration rates. The relative humidity and temperature thresholds for initiation of humid-air and aqueous-phase corrosion were included, as well as the electrochemical potential for initiation of localized corrosion during aqueous-phase corrosion.

In the case of the drip shield and waste package outer barrier, distributions of general corrosion rates were based upon data from the Long-Term Corrosion Test Facility, while project and published data were used as the basis of estimating localized corrosion rates. For the Stainless Steel Type 316NG inner barrier, both general and localized corrosion rates were based upon data presented in *Degradation of Stainless Steel Structural Material* (CRWMS M&O 2000cw, Section 6). These general and localized corrosion rates included estimates of the uncertainty and variability. Sufficient information was also provided to determine expected failure mode characteristics (e.g., number of failure sites and opening size).

General and Localized Corrosion of Alloy 22—Based on a detailed analysis of the test data, the mean value of the general corrosion rate of Alloy 22 after 24 months of exposure was 10 nm/yr (0.0000004 in./yr). The mean is the average over the number of duplicate samples in the range of test temperatures and the chemical environments summarized earlier. The general corrosion rates determined thus far are so low that the depth of penetration is not deep enough to accurately determine the sensitivity to the temperature and chemical composition of the water. The low general corrosion rates at all test temperatures and chemical environments indicate that the sensitivity is not large. Extrapolation of the mean corrosion rate to 10,000 years implies an average penetration of the Alloy 22 of only 0.1 mm (0.004 in.) of the waste package outer barrier. Even at the highest corrosion rate measured in this data set, the maximum penetration would be less than 1 mm (0.04 in.) over a 10,000-year time period, far less than the package thickness. The TSPA-SR uses the entire range of measured values from the long-term tests using a stochastic approach.

At planned times, some of the samples were withdrawn from the tests for examination. No evidence of localized corrosion was observed on the surfaces of the exposed Alloy 22 specimens for the three exposure times—6, 12, and 24 months (CRWMS M&O 2000n, Section 3.1.5.4). The tests are continuing with the remaining samples. Because of the low general-corrosion rate and the absence of localized corrosion and stress corrosion crack initiation, Alloy 22 is expected to be extremely long-lived as a waste package shell.

General and Localized Corrosion of Titanium—General corrosion rates for the titanium drip shield material were based on Long-Term Corrosion Test

Facility weight-loss samples. These rates appeared to be independent of temperatures between 60° and 90°C (140° and 194°F) and the chemistry of the test medium. The median rate was approximately zero, with most measurements for uncreviced samples lying between -200 and +200 nm/yr.

Crevice corrosion rates also appeared to be independent of temperature and test medium. As with the uncreviced samples, the median rate was approximately zero, with most of the corrosion rates between -350 and +350 nm/yr. The largest measured rate was less than +0.35 µm/yr and would not lead to failure of the drip shield during the first 10,000 years of its lifetime. Based upon these data, the life of the drip shield does not appear to be limited by crevice corrosion of titanium at temperatures less than those involved in the test (90°C [194°F]). Testing and model results indicate that the highest probable corrosion rate for titanium is approximately 25 nm/yr and the maximum rate is less than 350 nm/yr.

Microbially Influenced Corrosion of Alloy 22 and Stainless Steel—It has been observed that nickel-based materials such as Alloy 22 are relatively resistant to microbially influenced corrosion (CRWMS M&O 2000cq, Section 6.8). Corrosion rates of Alloy 22 are enhanced by microbially influenced corrosion by only a factor of approximately two (CRWMS M&O 2000cq, Table 25). The augmentation of corrosion rates due to microbially influenced corrosion is accounted for in the model documented in *General Corrosion and Localized Corrosion of Waste Package Outer Barrier* (CRWMS M&O 2000cq, Section 6.8). Corrosion studies have shown that microbes can enhance corrosion rates of 304 stainless steel by a factor of approximately ten (CRWMS M&O 2000cq, Table 25). It is assumed that microbially influenced corrosion will have the same effect on Stainless Steel Type 316NG.

The principal nutrient-limiting factor to microbial growth in situ at Yucca Mountain has been determined to be low levels of phosphate. Yucca Mountain bacteria grown in the presence of Yucca Mountain tuff are apparently able to dissolve phosphate contained in the tuff to support growth to levels of 10^6 cells per milliliter of groundwater.

When exogenous phosphate is added (10 mM), then levels of bacterial growth increase to 10^7 to 10^8 cells per milliliter. It may be noted, however, that the two-fold enhancement of corrosion included in the model was in the presence of sufficient phosphate to sustain higher levels of bacterial growth (in an effort to achieve accelerated Alloy 22 attack).

Other environmental factors that could affect levels of bacterial growth include temperature and radiation. However, these factors are closely coupled to relative humidity. As temperature and radiation decrease in the repository, relative humidity is predicted to increase. There are some types of microorganisms that can survive elevated temperatures (up to 120°C [248°F]) and high radiation doses; if there is no available water, then bacterial activity is completely prevented. Thus, because water availability is the primary limiting factor, and this factor is coupled to other less critical limiting factors, water availability (as expressed by relative humidity) was used as the primary gauge of microbial activity.

It has been assumed that a critical mass of bacteria exists for microbially influenced corrosion. Bacterial densities in Yucca Mountain rock have been determined to be on the order of 10^4 to 10^5 cells per gram of rock. In absolute terms, this is almost certainly above the threshold required to cause microbially influenced corrosion. Further, bacterial densities were shown above to increase 1 to 2 orders of magnitude when water was available. More germane concerns are the types of bacteria present, their abundance, and how their relative numbers are affected when water is available for growth. Corrosion rates will be affected (at least on some waste package materials), for example, if organic acid producers outcompete sulfate reducers or inorganic acid producers for available nutrients when water is sufficient to support growth. No data are currently available regarding the composition of the bacterial community over the changing environmental conditions anticipated during repository evolution. As described previously, this issue has been addressed for Alloy 22 in the current model with a corrosion enhancement factor that was determined from the ratio of measured corrosion current densities for inoculated and abiotic

samples. The enhancement factor has an upper bound of 2 (for the inoculated condition) and a lower bound of 1 (for the sterile condition). The enhancement factor is applied to the entire surface of the waste package outer barrier when the relative humidity at the surface is greater than a threshold value (i.e., 90 percent relative humidity).

Effect of Gamma Radiolysis on Corrosion Potential—Anodic shifts in the open circuit corrosion potential of stainless steel in irradiated aqueous environments have been experimentally observed (CRWMS M&O 2000cq, Section 6.4.4). Experiments performed at ambient-temperature cyclic polarization of Stainless Steel Type 316L samples in 0.018 M NaCl solution during exposure to 3.5 Mrad/hr gamma radiation showed that the corrosion potential shifted in the anodic direction by approximately 200 mV. This shift in corrosion potential was shown to be due to the formation of hydrogen peroxide. This finding was subsequently confirmed by another cyclic polarization experiment at ambient-temperature with 316 stainless steel in acidic (pH~2) 1.5 M NaCl during exposure to 0.15 Mrad/hr gamma radiation which showed a 100 mV anodic shift in the corrosion potential, with very little effect on the corrosion current. Note that these experiments were performed on stainless steels, not Alloy 22.

To determine the maximum impact that gamma radiolysis could have on the corrosion potential, hydrogen peroxide was added to the test media used for testing Alloy 22. As the concentration of hydrogen peroxide in simulated acidic concentrated water approaches 72 ppm (calculated from number of added drops of hydrogen peroxide), the corrosion potential asymptotically approaches 150 mV, well below the potentials where localized attack would be expected. Similarly, as the concentration of hydrogen peroxide in simulated concentrated water approaches 72 ppm, the corrosion potential asymptotically approaches -25 mV, well below any threshold where localized corrosion would be expected. Therefore, gamma radiolysis is not expected to result in the localized corrosion of Alloy 22 since the maximum shift in corrosion potential (induced by hydrogen peroxide additions) is less than that required for initiation of localized corrosion.

Pitting and Crevice Corrosion of Alloy 22 and Titanium—Short-term tests evaluating the susceptibility of Alloy 22 and titanium to pitting and crevice corrosion were conducted in accordance with ASTM G 61-86, *Standard Test Method for Conducting Cyclic Potentiodynamic Polarization Measurements for Localized Corrosion Susceptibility of Iron-, Nickel-, or Cobalt-Based Alloys*, to determine relative susceptibility to these types of localized corrosion. The results of these tests do not indicate a susceptibility to localized corrosion in plausible repository environments.

Since the completion of *Total System Performance Assessment for the Site Recommendation* (CRWMS M&O 2000a), the DOE has performed further research and analysis utilizing available project data to develop a temperature-dependent general corrosion rate and calculated the change in performance of the waste package over a range of operating modes. The inclusion of a temperature-dependent corrosion rate was included as a supplemental sensitivity analysis (BSC 2001b, Section 3.2.5.3). In the revised supplemental TSPA model discussed in *Total System Performance Assessment—Analyses for Disposal of Commercial and DOE Waste Inventories at Yucca Mountain—Input to Final Environmental Impact Statement and Site Suitability Evaluation* (Williams 2001a, Section 5.2.4.1), the general corrosion model was independent of temperature. Results of both supplemental analyses are consistent with the conclusions drawn from the results of the TSPA-SR model analyses and also provide additional insights into the behavior of the disposal system.

4.2.4.3.4 Stress Corrosion Cracking Models

Stress corrosion cracking is a mechanism of cracking in some materials caused by tensile stresses in an aggressive environment (CRWMS M&O 2000cu). This mechanism requires a combination of three elements: material susceptibility, tensile stresses, and an appropriate environment. Unique aspects of the stress corrosion cracking mechanism include brittle-type cracking in ductile materials, crack initiation and propagation under constant load without a need for cyclic load, and occurrence of cracking at lower stresses than would be expected without the presence of an

aggressive environment. This process model accounted for the possibility of stress corrosion cracking of the drip shield, the waste package outer barrier, and the stainless steel structural material. The model for stress corrosion cracking evaluated two alternative methods. The first method was based on the stress-intensity threshold criterion; the second method was based on a mechanistic film-rupture model yielding a finite rate of stress corrosion crack propagation. The modeled rate of stress corrosion crack propagation was dependent upon both the local environment and the stress intensity factor at the crack tip. The stresses for initiation and propagation of stress corrosion cracking in the models were due to unannealed closure welds, deformation caused by rockfall, and the weight of the waste package.

Stress Corrosion Cracking of the Stainless Steel Waste Package Inner Shell—The stainless steel structural material may or may not be susceptible to stress corrosion cracking. However, because the corrosion rate of stainless steel is expected to be much higher than that of Alloy 22, the TSPA is using a simplified model in which the stainless steel is assumed to fail immediately after the Alloy 22 outer barrier. Potential performance contribution of the stainless steel structural material will be evaluated as additional data and analyses become available.

Stress Corrosion Cracking of the Titanium Drip Shield—Stress corrosion cracking of the titanium drip shield is not expected in a design that uses backfill, because drip shield stresses that are relevant to stress corrosion cracking are insignificant in this case. The major source of drip shield stress is loading due to earthquakes.

For designs without backfill, rockfall directly on the titanium drip shields could result in localized areas of high residual stresses which could lead to stress corrosion cracking and through-wall penetration of the drip shields. While this is possible, it is expected that, because of their size, these penetrations will not prevent the drip shields from performing their intended function of diverting seepage water away from the waste package surface.

Stress corrosion cracks in passive alloys, such as Titanium Grade 7 and Alloy 22, tend to be very tight (small crack opening displacement) by nature (CRWMS M&O 2000cu). Stress analyses that consider rockfall have estimated the local residual titanium stresses following a large (i.e., greater than 4 metric tons) rock impact. The subsequent stress corrosion crack is expected to be approximately 100 µm (0.1 mm, or 0.004 in.) wide. The crack faces are expected to corrode slowly and eventually fill the crack space with corrosion products. While the crack faces are corroding slowly, there may be a small amount of water transported by surface diffusion into the crack and through the drip shield. However, the small temperature gradient present across the drip shield wall will result in evaporation of the slowly flowing water, and a resultant scale deposit will form over and within the crack on the upper drip shield surface. This formation of scale deposits is well documented in seawater environments and in heat exchangers. Such deposits form rapidly under flowing conditions and must be regularly removed to avoid loss of heat exchanger efficiency. In the case of J-13 water concentrated by evaporation, calcium carbonate precipitation is the first stage of the concentration process. Consequently, evaporation of J-13 water slowly flowing through an approximately 100-µm crack opening would lead to rapid scale deposition. The rate of plugging would be inversely proportional to the volume flow rate through the crack. For a 100-µm wide crack through a 15-mm (15,000-µm) thick drip shield, scale deposition would be an efficient process involving the need for only a small volume flow through the crack. In addition, because of the expected high density of the deposits and lack of a pressure gradient to drive water through the crack, the probability of solution flow through the plugged crack would approach zero. It is therefore concluded that the function of the drip shield will not be compromised even in the event of stress corrosion cracking (CRWMS M&O 2000cu).

Stress Corrosion Cracking of the Alloy 22 Waste Package Outer Shell—For Alloy 22, the stress corrosion cracking film rupture model (the second model) assumes crack growth could begin at any surface defect that could generate a stress intensity, regardless of size and surface tensile

stress level. However, examination of the relevant literature indicated that there is a threshold stress below which stress corrosion cracking would not initiate on a "smooth" surface. In the case of the waste package closure weld, the range of threshold stress was conservatively estimated at 10 to 40 percent of the material yield stress (CRWMS M&O 2000cu, Section 6.5.2). This threshold stress range was based on literature reporting stress corrosion cracking-initiation test results for stainless steels and nickel alloys (with known susceptibility to stress corrosion cracking) with comparable surfaces exposed to very aggressive environments.

Mitigation of the Alloy 22 Closure Weld Residual Stress—Examination of the weld residual stress profiles for the initial waste package outer barrier closure design revealed that tensile stresses exceeding 20 percent of Alloy 22 yield stress existed in the vicinity of the closure weld surface in both the radial and circumferential directions. This indicated stress corrosion cracking initiation in unacceptably short times could not be precluded for that design. Further, the stress intensity plot indicated that, at least for radially oriented stress corrosion cracks, through-wall crack propagation was possible once a crack initiated.

To reduce weld residual tensile stresses below the stress corrosion cracking-initiation threshold, improved waste package closure designs were evaluated. These included low residual-stress welding techniques and postweld residual tensile-stress-reduction techniques such as induction annealing (heating of the weld) and laser peening (subjecting the weld to laser-generated compressive stresses). Based on these evaluations and a review of the relevant literature (CRWMS M&O 2000cu, Section 6), the Alloy 22 closure design was improved to add a second flat closure lid on the top end of the waste package. This lid will be placed between the extended Alloy 22 closure lid and the stainless steel inner lid (see Figure 3-2 in Section 3). In the improved design, the inner lid closure weld is relieved of its tensile stress using laser peening. Then the outer lid closure weld is completed and its residual tensile stresses are relieved using postweld induction annealing.

To optimize the new Alloy 22 closure design, experimental measurements were made to quantify the expected stress reduction benefit resulting from laser peening. In addition, extensive ANSYS finite element model calculations were performed to determine the expected stress and stress intensity reduction benefits resulting from the application of both processes. The results of these calculations show that both processes reduced the surface residual tensile stresses below 20 percent of the yield stress (the threshold value for initiation of stress corrosion cracking). These stress reductions persist to depths of about 2 to 3 mm (0.08 to 0.12 in.) for laser peening and at least 6.5 mm (0.25 in.) for postweld induction annealing.

As the waste package outer surface corrodes away, the beneficial low-tensile-stress surface layers resulting from either process are removed. Use of the dual Alloy 22 closure lids in the design improved the longevity of the overall closure, since the flat closure lid does not begin to corrode until the extended closure lid is breached. Figure 4-89 shows the schematic of the dual closure lid design, and Figure 4-90 shows conceptual details of remote welding, annealing, and laser peening for the closure weld area of the waste package.

The closure lid design, as mentioned earlier, helps extend the life of the waste package. The closure weld area of the extended lid is subjected to localized induction annealing to mitigate the weld residual stresses. Stress corrosion cracking of this lid is delayed until the stress-mitigated layer is removed by corrosion. The closure weld area of the flat closure lid is subjected to residual stress mitigation by laser peening. This lid is exposed to the repository environment only after the extended lid is breached, and the stress corrosion cracking of this lid is delayed until after the mitigation layer corrodes away.

Figure 4-90 shows how welding, inspection, laser peening, and induction annealing can be performed at a single work station in the transfer cell facility. This conceptual arrangement will continue to evolve during the next few years.

Additional analyses and quantification of uncertainties performed since the completion of the
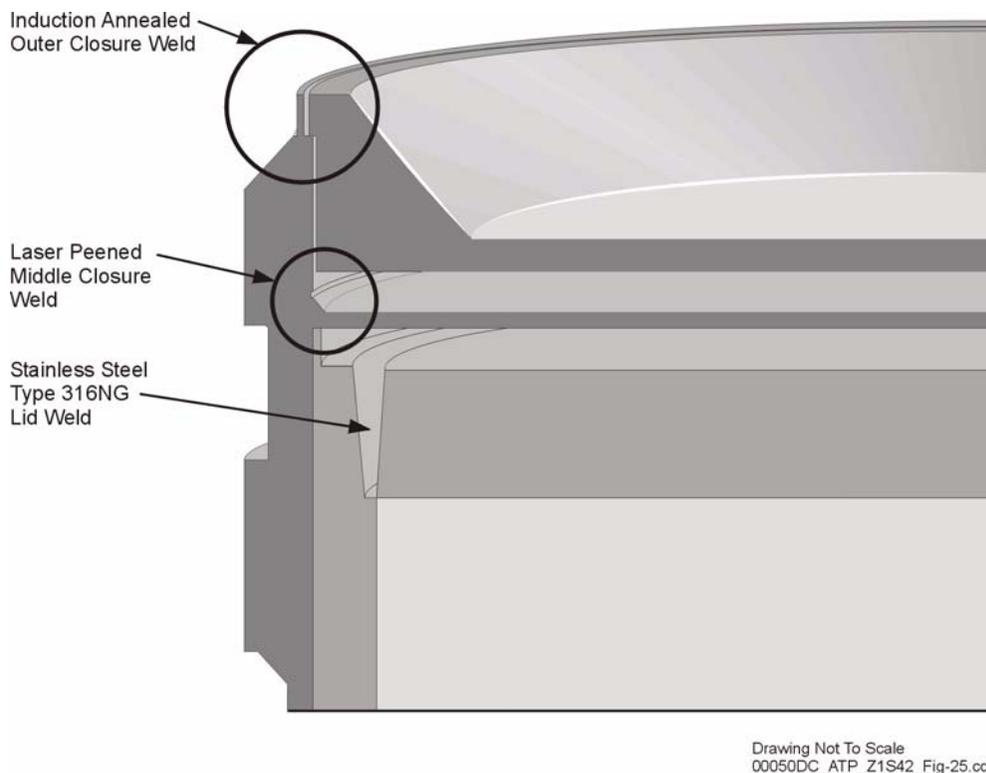
Figure 4-89.   Schematic Illustration of the Dual Alloy 22 Lid Waste Package Design
The use of two lids for the outer barrier extends the waste package lifetime.

TSPA-SR model provide additional confidence that the stress corrosion cracking model used in the TSPA-SR model is conservative and that the likelihood of stress corrosion cracking of the waste package in the repository environment will be less than predicted by the TSPA-SR model (BSC 2001a, Sections 7.2.5 and 7.3.3).

4.2.4.3.5   Hydrogen-Induced Cracking of the Titanium Drip Shield

Another potential failure mechanism for titanium and its alloys under waste disposal conditions is hydrogen absorption leading to hydrogen-induced cracking. Hydrogen-induced cracking is also called "hydrogen embrittlement," which is a process resulting in a decrease of fracture toughness or ductility of a metal due to the presence of atomic hydrogen. The usual failure mode for a ductile material is the ductile tearing observed during slow crack growth. In this case, the material will fail as the stress intensity factor reaches a threshold value.

The decrease of fracture toughness can also cause fast crack growth (brittle fracture) of a normally ductile material under a sustained load. During fast crack growth, the same material will fail as the stress intensity factor reaches another threshold value, which is less than threshold value for slow crack growth. The process model developed for this degradation mode established the conditions under which the drip shield would experience hydrogen uptake, potentially leading to hydrogen embrittlement and hydrogen-induced cracking.

Generally, the passive oxide film on titanium acts as an excellent barrier to the transport of hydrogen, and hydrogen absorption under natural corrosion conditions would not be expected and is generally not observed over normal operating periods (up to tens of years). In a repository situation, even very slow hydrogen absorption may be significant over thousands of years, leading to a significant accumulation of hydrogen and the danger of hydrogen-
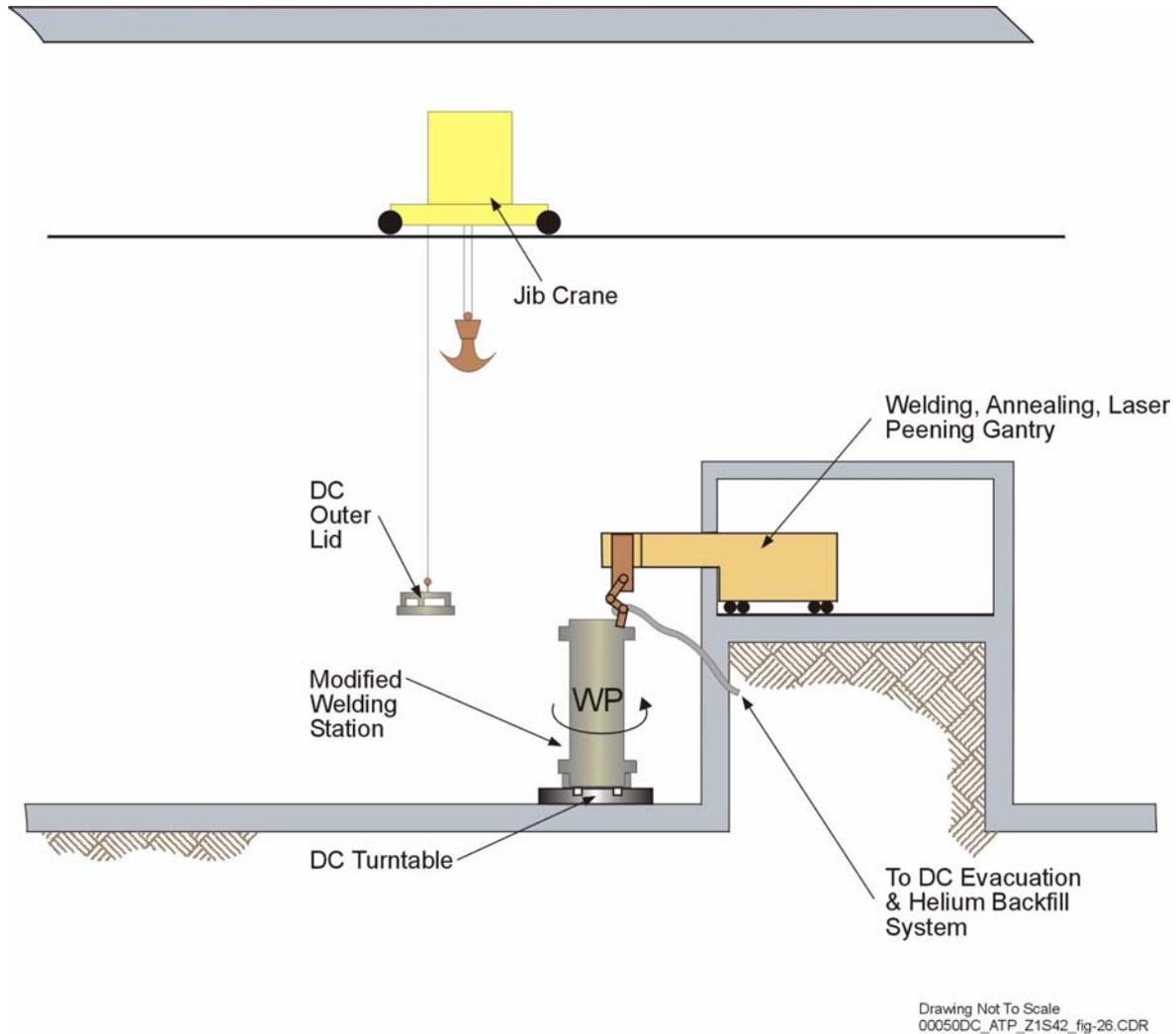
Figure 4-90.   Conceptual Design of Remote Welding, Annealing, and Laser Peening for the Closure Welding of the Waste Package
This design allows remote welding, induction annealing, and laser peening to be conducted at a single station. DC = disposal container; WP = waste package.

induced cracking. The model addressed these considerations, which are summarized below:

1. The passive oxide is assumed to be permeable to atomic hydrogen.

2. Atomic hydrogen is generated at the surface of the titanium alloy. This is described by a hydrogen generation rate, which is taken to be proportional to the general passive corrosion rate.

3. A fraction of the hydrogen is absorbed into the oxide and assumed to directly enter the alloy. The remainder combines to yield hydrogen gas, which is lost to the surroundings. The rate of absorption is taken to be directly proportional to the hydrogen generation rate multiplied by an absorption efficiency coefficient.

4. Once in the alloy, the hydrogen is distributed uniformly throughout the entire thickness of the material. That is,

transport processes within the alloy are rapid compared to the rate of absorption.

5. The hydrogen content of the alloy is allowed to increase until a critical level is reached. The material then is assumed to fail immediately. The model allows for the calculation of hydrogen content and for comparison with the critical concentration.

The hydrogen-induced cracking model was presented in *Hydrogen Induced Cracking of Drip Shield* (CRWMS M&O 2000cv, Section 6). In that report, extensive evidence supported a qualitative assessment of titanium alloys as an excellent choice of material for the drip shield with regard to degradation caused by hydrogen-induced cracking, where the hydrogen source is from general corrosion of the titanium. Quantitative evaluation based on this model indicated that the drip shield material was able to sustain the effects of hydrogen-induced cracking. Using available general corrosion test data, the model calculated a hydrogen concentration below 120 µg per gram, which is less than the critical hydrogen concentration of 400 µg per gram for the titanium grade that was tested.

The source of the hydrogen for embrittlement can also be through galvanic coupling of the titanium drip shield with less corrosion-resistant materials, such as carbon steel. At the bottom of the drip shield, this galvanic coupling is precluded by the use of a small Alloy 22 "foot" separating the drip shield and the carbon steel invert structure (CRWMS M&O 2000cv).

In a design without backfill, steel components such as rock bolts, wire mesh, and steel liners used in the drift may fall on the drip shield and undergo active corrosion. This could potentially lead to generation of hydrogen on the surface of the drip shield, leading in turn to hydrogen pickup levels higher than the critical levels needed for cracking. Preliminary evaluation shows that these embrittled titanium regions are likely to be self-limiting "hotspots" from the point of view of hydrogen absorption and embrittlement of the drip shield. The buildup of carbon steel corrosion products at

the contact site would be expected to eventually break the contact. The drip shield is expected to be unaffected by contact with iron corrosion products, since the galvanic connection would be poor (CRWMS M&O 2000cv).

4.2.4.3.6 Limitations and Uncertainties

Uncertainties in each of the process models were identified in the discussion of the models in the previous sections and in the individual analysis model reports. The approach generally used in dealing with these uncertainties is to be conservative and bound the uncertainties. In several cases combinations of approaches were used. For example, in the case of Alloy 22 thermal aging, accelerated testing (i.e., higher-temperature aging) was used to predict long-term behavior based on short-term data, in accordance with ASTM C 1174-97. The data were then used with conservative bounding estimates. In the case of general corrosion, aggressive test media were used to represent potential concentrating effects in the repository. Features, events, and processes were evaluated to screen out degradation processes that have very low probability of occurrence (less than 10^{-4}/yr) or that have very low consequences. Examples of screened-out processes include radiolysis-enhanced corrosion and inside-out corrosion of waste package barrier materials.

As noted in Section 4.1.1.2, the DOE has performed several activities to improve the treatment of uncertainty in current models. Additionally, as noted in Section 4.1.4, the DOE has evaluated the effect that operating the repository at lower temperatures would have on repository performance models. Uncertainty about the waste package corrosion rate may be reduced by avoiding the conservatively defined window of corrosion susceptibility for Alloy 22, which can be accomplished by keeping waste package temperatures at or below 85°C (185°F) or maintaining the relative humidity in emplacement drifts below 50 percent. The results of the analyses of lower-temperature operating modes are described in *FY01 Supplemental Science and Performance Analyses* (BSC 2001a; BSC 2001b).

A review of the uncertainties in the various models is presented below.

Thermal Aging—A graphical approach to bounding the uncertainty in the aging model is used. In Figure 4-91, the line representing a "best fit" to the data for "complete grain boundary coverage" predicts that more than 10,000 years at 300°C (572°F) will be required to completely cover the grain boundaries of Alloy 22 with inter-metallic precipitates. However, the line with the "minimum slope possible within the error bars" shows that complete grain boundary coverage might occur in as few as 100 years (very unlikely bounding case). The "best fit" line is the most likely scenario. In the case of bulk precipitation, none is predicted with the line representing the minimum possible slope. Thus, it can be concluded with reasonable certainty that no bulk precipitation will occur before 10,000 years at 300°C (572°F).

From the corrosion tests conducted, it appears that a fully aged sample of Alloy 22 could change the observed corrosion potential. For example, corrosion potential was shifted in a less noble (negative) direction by a small value (less than 100 mV) in simulated acidic concentrated water and simulated concentrated water at 90°C (194°F). The shift was not considered significant, and it was concluded that full aging of Alloy 22 (complete coverage of the grain boundaries) does not significantly alter passive film stability and result in significantly enhanced corrosion.

Thermal aging of Titanium Grade 7 at 300°C (572°F) is expected to have little impact on the corrosion resistance of this material. Since no credit is claimed for the corrosion resistance of Stainless Steel Type 316NG, all TSPA calculations are insensitive to the uncertainty associated with the corrosion of Stainless Steel Type 316NG.

Dry Oxidation—In the case of Alloy 22 and Stainless Steel Type 316NG, the rates of dry oxidation are negligible even over hundreds of years and the expected repository temperature. Therefore, uncertainty in the dry oxidation rate is not expected to have any significant impact on the performance of these materials. The current model is based upon

published data and does not include estimates of uncertainty.

Humid-Air and Aqueous-Phase Corrosion—Uncertainty in the threshold relative humidity for these corrosion modes is primarily due to the composition of the salt film. The waste package and drip shield would always experience some combination of humid-air and aqueous-phase corrosion. The uncertainty in this parameter is discussed in more detail in *Degradation of Stainless Steel Structural Material* (CRWMS M&O 2000cw, Section 6), *General Corrosion and Localized Corrosion of the Drip Shield* (CRWMS M&O 2000cr, Section 6), and *General Corrosion and Localized Corrosion of Waste Package Outer Barrier* (CRWMS M&O 2000cq, Section 6).

The distribution of general corrosion rates for either humid air corrosion or aqueous phase corrosion is represented by the curves given in Section 3.1.5.4 of the *Waste Package Degradation Process Model Report* (CRWMS M&O 2000n, Figures 3-14 through 3-26). Distributions for Stainless Steel Type 316NG are represented by distributions formed from published data. The distribution of rates for Alloy 22 and the distribution for Titanium Grade 7 rates are based upon data from the Long-Term Corrosion Test Facility. The dispersion in these curves is assumed to be entirely due to uncertainty. A detailed analysis of the error in general corrosion rate was given in each supporting report (CRWMS M&O 2000cw, Section 6; CRWMS M&O 2000cr, Section 6; CRWMS M&O 2000cq, Section 6).

Determinations of corrosion and threshold potential are based upon three replicate cyclic polarization measurements at each combination of environment and temperature. The results are tabulated in *General Corrosion and Localized Corrosion of Waste Package Outer Barrier* (CRWMS M&O 2000cq, Section 6). The uncertainty in the corrosion potential due to gamma radiolysis (i.e., a maximum positive shift in error of about 250 mV) is also addressed in *General Corrosion and Localized Corrosion of Waste Package Outer Barrier* (CRWMS M&O 2000cq, Section 6.4.4) and *Waste Package Degradation Process Model Report* (CRWMS M&O 2000n,
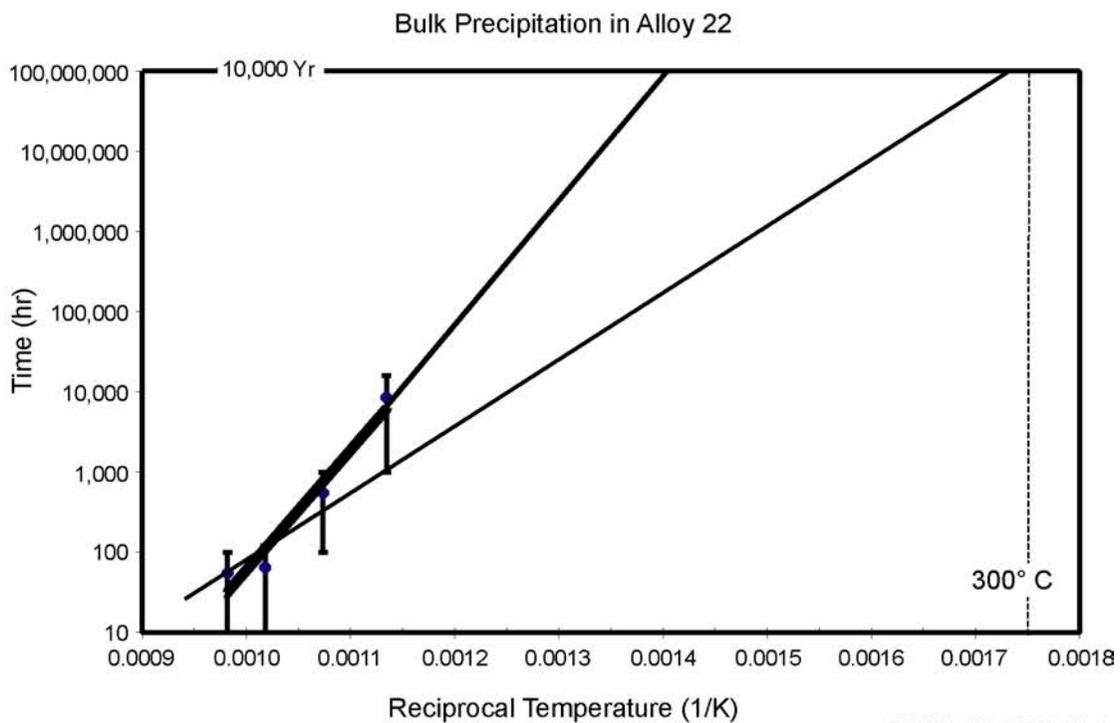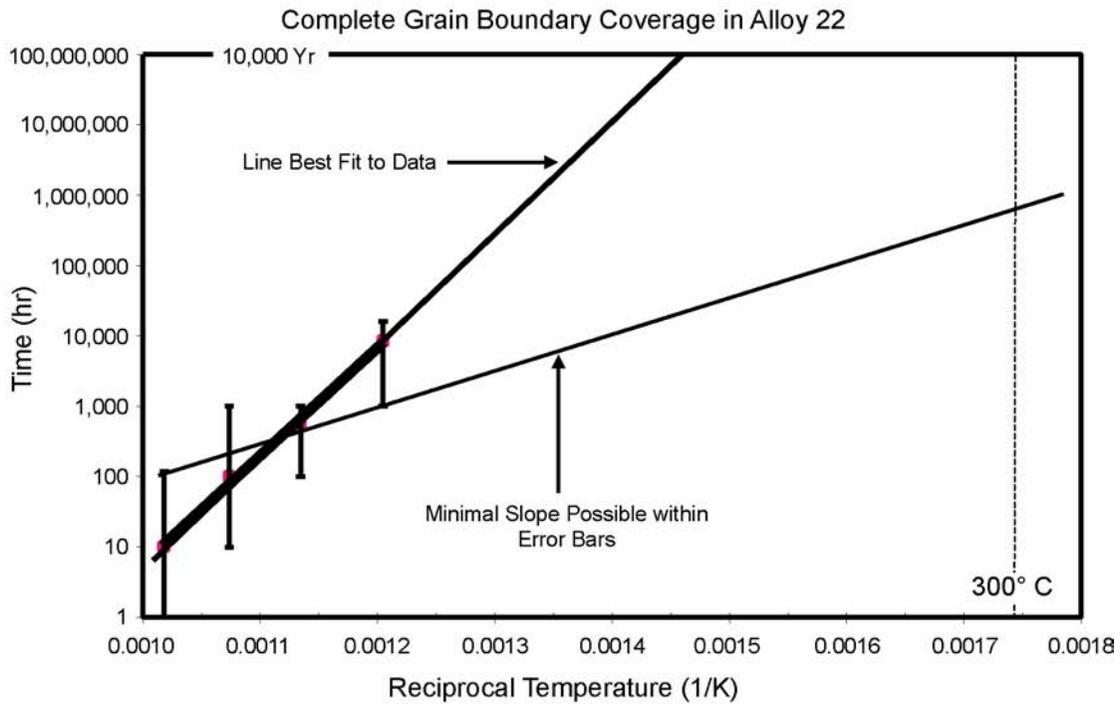
Figure 4-91. Graphical Extrapolation of the Curves to Repository-Relevant Temperatures
Source: CRWMS M&O 2000ct, Figure 98.

Section 3.1.6). Estimates of uncertainty in the selection of corrosion and threshold potential have been made and are embedded in WAPDEG analyses.

The rates of localized corrosion have been bounded with the range of values found in the published literature.

Stress Corrosion Cracking—Two alternative stress corrosion cracking models have been considered, one based upon a threshold stress intensity factor (Method A) and another based upon a threshold stress for a smooth surface (Method B) (CRWMS M&O 2000cu). In the second approach, cracks are assumed to propagate by the slip-dissolution mechanism after initiation. Method B is used as the basis of the performance assessment. The slip-dissolution model, Method B, predicts that crack propagation is a function of the local stress intensity at the crack tip. Thus, the uncertainty in this driving force must be estimated.

Local stress intensity is calculated from the local stress and the crack penetration. The uncertainties in the stress distribution (stress versus depth) are based upon analyses of measured residual stresses in welds, before and after mitigation, as well as finite element modeling with the ANSYS code. These uncertainties are abstracted for WAPDEG. Aside from the stress intensity, the parameters in the slip-dissolution model for stress corrosion cracking propagation are based upon measurements for stainless steel from the boiling water reactor industry. Since stainless steels are much more prone to stress corrosion cracking than Alloy 22, these parameter estimates are conservative for Alloy 22.

The threshold stress for initiation of stress corrosion cracking on a smooth surface is conservatively estimated to be approximately 10 to 40 percent of the yield stress, based upon the determination of such thresholds for related but more susceptible alloy systems exposed to very aggressive environments, such as boiling magnesium chloride.

Since completion of the TSPA-SR model, the DOE has continued to explore uncertainties associated with the model. Volume 1, Section 7 of *FY01*

Supplemental Science and Performance Analyses (BSC 2001a) describes in detail the additional work performed to further defend, model, and understand uncertainties associated with the waste package degradation models. It further discusses uncertainties related to mechanisms for early failures, aging and phase stability of the waste package outer barrier, general and localized corrosion, and stress corrosion cracking. In order to assess the performance consequences of early waste package failures, the supplemental TSPA model described in Volume 2 of *FY01 Supplemental Science and Performance Analyses* (BSC 2001b) included a model that assumed that improper heat treatment of welds could lead to cracks forming in a small fraction of waste packages. The formation of cracks in a few waste packages (up to three) resulted in the calculation of small doses (approximately 2×10^{-4} mrem/yr) in the supplemental TSPA model (compared to zero dose in the TSPA-SR model). The inclusion of a thermally-dependent corrosion rate in the waste package performance model resulted in significantly improved long-term performance of the waste packages. In summary, the results of the additional analysis provide added confidence that the TSPA-SR model is conservative and that the behavior of the waste package in the repository environment is likely to be better than predicted by the TSPA-SR model.

4.2.4.3.7   Alternative Approaches or Models

Alternative models have been considered for oxidation, localized corrosion thresholds, stress corrosion thresholds, stress corrosion cracking, stress mitigation, and hydrogen-induced cracking. These alternatives are summarized below.

As with limitations and uncertainties, alternative conceptual models for corrosion, early waste package failure, and stress corrosion cracking have been updated in supplemental analyses as summarized in *FY01 Supplemental Science and Performance Analyses* (BSC 2001a, Section 7; BSC 2001b, Sections 3.2.5 and 4.2.5). These analyses generally tend to confirm the results of the TSPA-SR. These analyses are also summarized in Section 4.4.5.5 of this report.

Dry Oxidation—This process can be represented by two different methods: the parabolic growth law and the logarithmic growth law. In the parabolic growth law, the oxide film is assumed to grow continuously with the rate of film growth controlled by the diffusion of oxygen through the film. The thickness of the oxide is proportional to the square root of the exposure time. In the case of the logarithmic growth law, the oxide film asymptotically approaches a small maximum thickness. In the case of dry oxidation, parabolic growth law is used for Alloy 22 and Stainless Steel Type 316NG, while logarithmic growth law is used for Titanium Grade 7. These model selections were based upon the published literature for these types of corrosion-resistant materials (CRWMS M&O 2000n, Section 3.1.5.1).

Localized Corrosion Threshold—Localized corrosion process can be expressed in terms of the threshold electrochemical potential or threshold temperature for the initiation of the localized corrosion. For the highly corrosion resistant materials under consideration, the threshold potential model is used because it is more solidly rooted in the theoretical concepts underlying passive film stability. Furthermore, it is expected that a good correlation of threshold and corrosion potential can be used to deduce a threshold temperature. The threshold temperature would be the temperature at which the corrosion and threshold potentials are equivalent.

Stress Corrosion Cracking—The stress corrosion cracking model includes two separate models, one based on the threshold stress intensity factor at the tip of a preexisting flaw and the second based on the threshold stress for propagation by slip-dissolution mechanism. The second method is used in the abstraction for TSPA because it is the more conservative model and because it has been used for predicting the performance of boiling water reactors. The method is considered to be conservative because it is based upon data for stainless steel, a material more prone to stress corrosion cracking than Alloy 22 (CRWMS M&O 2000cu). Predictions based upon a correlation for stainless steel would yield a conservative prediction for Alloy 22.

Weld Stress Mitigation—Two methods will be used for mitigation of the weld residual stresses: localized induction annealing and laser peening. Induction annealing will be used for the outer lid, and laser peening will be used for the inner lid on the Alloy 22 outer barrier of the waste package. This selection is based upon the ability of the induction annealing process to place compressive stress deeper into the weld. Laser peening is more compatible with the design of the inner lid weld, due to the occluded nature of such a weld.

Hydrogen-Induced Cracking of Titanium—Two methods are available to address hydrogen induced cracking: threshold electrochemical potential and threshold hydrogen concentration. The first method is applicable primarily for conditions that would lead to galvanic coupling of titanium. As this will be avoided by design, this method has not been used in the model. Therefore, hydrogen-induced cracking evaluation is based upon a threshold hydrogen concentration. Also, since such concentrations are possible to be measured with secondary iron mass spectrometry, this method is preferred.

The threshold concentration model is a simple and conservative model. The basic premise of the model is that failure will occur once the hydrogen content exceeds a certain limit or critical value. This model is conservative because it assumes that, once the environmental and material conditions can support that particular corrosion process, failure will be effectively instantaneous. Quantitative evaluation based on the hydrogen-induced cracking model described in *Hydrogen Induced Cracking of Drip Shield* (CRWMS M&O 2000cv, Section 6) indicates that the drip shield material (Titanium Grade 7) is able to sustain the effects of hydrogen-induced cracking. Available test data show that the hydrogen concentration is below 180 μg per gram, which is less than the critical hydrogen concentration of 400 μg per gram for Titanium Grade 7.

With the removal of backfill from the repository design, the potential for that galvanic interaction between carbon steel ground support and the drip shield is increased. The impact of this on the potential hydrogen pickup has been evaluated using the

threshold concentration model. Preliminary results show that hydrogen-induced cracking is not a problem (CRWMS M&O 2000cv).

4.2.4.3.8   Model Calibration and Validation

According to ASTM C 1174-97, *Standard Practice for Prediction of the Long-Term Behavior of Materials, Including Waste Forms, Used in Engineered Barrier Systems (EBS) for Geological Disposal of High-Level Radioactive Waste*, model validation is the process through which independent measurements are used to ensure that a model accurately predicts an alteration behavior of waste package materials under a given set of environmental conditions (e.g., in the repository environment over 10,000 years). Obviously, models cannot be tested for 10,000 years. Therefore, validation relies on accelerated testing. According to the same standard, an accelerated test is a test that results in an increase in the rate of an alteration mode, when compared with the rates for service condition. Changes in alteration mechanism, if any, must be accounted for in the use of the accelerated test data.

The thermal aging model assumes Arrhenius-type kinetics (CRWMS M&O 2000ct, Sections 6.2 and 6.5). Precipitation and long-range ordering can be accelerated by increasing the temperature above those levels expected in the repository. If the model can accurately predict the kinetics of these phenomena at combinations of time and elevated temperature, it will be considered valid for making predictions at lower temperature and longer time.

Since all available data has been used to establish these correlations, the correlations are considered valid for their intended use. Additional data that are being collected will help to reduce uncertainties and improve the level of confidence in the model.

The effects of precipitation and long-range ordering on corrosion are determined with electrochemical techniques. Through application of electrochemical potentials more anodic than the open circuit corrosion potential, corrosion phenomena can be accelerated (CRWMS M&O 2000cq, Section 6.7). Variations in corrosion and threshold potential can be correlated with the extent of thermal aging. Similarly, variations in

rates of dissolution through the stable passive film can also be correlated with the extent of thermal aging. These rates of dissolution are accelerated by application of a potential between the corrosion and threshold potentials and are proportional to the passive current density (CRWMS M&O 2000cq, Section 6.7.1). The corrosion rate enhancement factor is determined by calculating the ratio of measured passive current densities for aged and unaged samples (CRWMS M&O 2000cq, Section 6.7.3). Since all available electrochemical data has been used to establish the corrosion model for thermally aged samples, this model is considered valid for its intended use.

The models for dry oxidation of Alloy 22 (CRWMS M&O 2000cq, Section 6.1), Titanium Grade 7 (CRWMS M&O 2000cr, Section 6.1), and Stainless Steel Type 316NG (CRWMS M&O 2000cw, Section 6.1) are based upon published data found in the scientific literature. More specifically, the model for dry oxidation of Alloy 22 is based upon the parabolic growth of the oxide film at elevated temperature (CRWMS M&O 2000cq, Section 6.1). However, in the absence of any such low-temperature data, the parabolic rate constant for high temperature is applied at low temperature. Given the extremely small magnitudes of these rates, dry oxidation is expected to have no significant impact on waste package performance (CRWMS M&O 2000cq, Section 6.1).

The threshold relative humidity for humid-air corrosion is based on the deliquescence point of sodium nitrate (CRWMS M&O 2000ck, Section 7; CRWMS M&O 2000cq, Section 4.1.2). The threshold for salt films deposited in the repository may be slightly different. However, salt deposits produced by evaporating simulated J-13 water to dryness support this basis.

Rates of humid air corrosion are expected to follow general distributions based upon weight-loss data from the Long-Term Corrosion Test Facility (CRWMS M&O 2000cq, Section 6.5.2; CRWMS M&O 2000cr, Section 6.5.2). The distributions are for Alloy 22 data for 6, 12, and 24 months of exposure to a variety of test media. Corroborative measurements made with the atomic force microscope and other surface analytical techniques have

also been used as further means of model validation (CRWMS M&O 2000cq, Section 6.5.5). The test program will continue, ultimately providing data for 60 months of exposure. Future data will be considered independent and corroborative, and will be used to reduce uncertainties and conservatism in the model.

The threshold relative humidity for aqueous phase corrosion is the same as that used for humid air corrosion (CRWMS M&O 2000ck, Section 6.3; CRWMS M&O 2000cq, Section 6.3). The same approach has been used for validation. Rates of general corrosion in the aqueous phase also obey the general distributions based upon weight-loss data from the Long-Term Corrosion Test Facility. The same approach described for validation of the rate model for humid air corrosion has been employed for validation of the rate model for general corrosion in the aqueous phase.

Comparisons of corrosion and threshold potentials are used to determine whether rates for general or localized corrosion are applicable. The initial correlations given in the *Waste Package Degradation Process Model Report* (CRWMS M&O 2000n, Sections 3.1.5 and 3.1.6) are based upon standard cyclic polarization measurements in simulated dilute water, simulated concentrated water, simulated acidic concentrated water, and simulated saturated water, covering a broad range of temperature.

The stress corrosion model is primarily based on published data. Limited data have been obtained under repository-relevant conditions. The data obtained under the Yucca Mountain project include precracked specimens tested under very aggressive environments (CRWMS M&O 2000cu, Sections 4.1.3 and 6.3.2). Thus, the model uses a conservative approach. Future data will serve to reduce the level of conservatism and improve the confidence in the model.

4.2.4.4 Total System Performance Assessment Abstraction

An integrated model was developed from the process and abstraction models for the various degradation modes. The integrated model included in the WAPDEG performance assessment code used repository environmental conditions as a function of time from other process models to estimate the performance of the waste package and drip shield. The WAPDEG model uses a stochastic approach to sample model parameters over the ranges including uncertainties. The following sections discuss model abstractions for the TSPA-SR. Details of the abstraction of individual process models and the development of the integrated model parameters are provided in Section 3.2 of the *Waste Package Degradation Process Model Report* (CRWMS M&O 2000n).

Abstraction of General Corrosion Models—The model abstractions are to develop two cumulative distribution functions to represent the general corrosion rate distribution for Alloy 22 outer barrier and the titanium drip shield. For each material, the weight loss and crevice sample penetration rate data were combined to yield one general corrosion rate data set. For Alloy 22, the general corrosion rate data with 6-month, 1-year, and 2-year exposure were considered. Since the variance in the corrosion rate data is reduced with the exposure time, and the median rate also decreases with the exposure time, it was concluded that the 2-year data are sufficiently conservative to represent the long-term general corrosion rate. Therefore, only the 2-year data were used in the model abstraction. For the drip shield, only the 12-month data were used in the model abstraction. The cleaning method employed with the 6-month titanium samples caused significant metal loss, thereby yielding inaccurate corrosion rates. Assumptions shown below were employed in the model abstraction.

- For both alloys considered (Alloy 22 and Titanium Grade 7), corrosion penetration rate data from the weight loss of both plain and creviced geometry test coupons were considered to represent general corrosion penetration rate.

- The maximum general corrosion rate for Alloy 22 was set to 7.30×10^{-5} mm/yr (0.073 µm/yr). This assumed upper bound is greater than the maximum penetration rate of 7.25×10^{-5} mm/yr (0.0725 µm/yr) observed.

- The maximum general corrosion rate of Titanium Grade 7 was set to 3.25×10^{-4} mm/yr (0.325 µm/yr). This assumed upper bound is greater than the maximum penetration rate of 3.19×10^{-4} mm/yr (0.319 µm/yr) observed.

As discussed in Section 6.5.5 of *General Corrosion and Localized Corrosion of Waste Package Outer Barrier* (CRWMS M&O 2000cq), the formation of silica scale deposit on the surface of the Alloy 22 sample coupons could bias the estimated general corrosion rate. The potential measurement bias for the weight loss sample coupons was estimated to be 0.063 µm/yr, and the Alloy 22 general corrosion rate was corrected for the maximum bias by adding a constant value of 0.063 µm/yr to the estimated value of the general corrosion rate. The same data treatment was used for the Titanium Grade 7 drip shield general corrosion rate data. As a result, the corrosion rate correction increased the median rate (50th percentile value) by about 50 percent.

Abstraction of Localized Corrosion Models—This section discusses the approaches and assumptions used in the abstraction of localized corrosion models for the waste package outer barrier and drip shield, as well as the abstraction results.

The model abstractions are to develop two localized corrosion initiation criteria: one representing the localized corrosion initiation criterion for the waste package outer barrier (Alloy 22) and the other for the localized corrosion initiation criterion for the drip shield (Titanium Grade 7). Cyclic polarization measurements were made in several synthetic concentrated J-13 waters. For each curve obtained, the critical potential for localized corrosion initiation and the corrosion potential were determined. The potential difference between these two was then fit to a function of relevant exposure parameters. According to the model, localized corrosion should initiate if the corrosion potential exceeds the critical potential. The abstraction results showed that localized corrosion of Alloy 22 and titanium do not initiate under repository conditions, based on extrapolation of the repository-relevant experimental data used in the analysis.

Abstraction of Stress Corrosion Cracking Model—In the current waste package degradation analysis, two alternative stress corrosion cracking models, the slip dissolution (or film rupture) model and the threshold stress intensity factor model, are considered (CRWMS M&O 2000cu, Section 6). In the threshold stress intensity factor model, this factor is used to determine when stress corrosion cracking will occur. Provided that an initial flaw and corrosive environment are present, a stress corrosion cracking failure will occur when the applied stress intensity factor is greater than or equal to the threshold stress intensity factor. The slip dissolution model also assumes that incipient cracks or defects grow continuously when the oxidation reaction that occurs at the crack tip ruptures the protective film via an applied strain in the underlying matrix. The rate at which the crack grows is a function of the crack tip strain rate and environmental and material chemistries.

In the waste package degradation analysis (WAPDEG), the slip dissolution model is employed to calculate the growth rate of cracks initiated by stress corrosion cracking. The waste package degradation analysis employs a stochastic approach to model the initiation and propagation of cracks from stress corrosion. The major efforts in the abstraction are to develop an approach to represent the uncertainty and variability associated with the stress corrosion cracking initiation and crack propagation processes. The associated parameters in the model include two model parameters (*A* and *n*), stress intensity factor, threshold stress, and incipient crack density and size. The analysis also includes preexisting manufacturing defects in the closure lid welds. The manufacturing defect sizes are sampled for the closure lid weld patches, and the sampled flaws are included in the analysis. Because manufacturing defects are much larger than the incipient cracks, the closure lid weld patches with manufacturing defects are likely to fail initially because of stress corrosion cracking.

Abstraction of Stress and Stress Intensity Factor Profile—The Alloy 22 barrier has dual closure lids, referred to as outer and inner lids. The process model analyses calculated the stress and stress intensity factor profiles along the circumference of the welds for each of the closure lids

(CRWMS M&O 2000cu, Section 6), and the results were analyzed to develop abstracted models to represent the uncertainty and variability of the profiles in the closure lid welds.

Assumptions employed in the abstraction are:

- The hoop stress (and the corresponding stress intensity factor for radial cracks) is the prevailing stress in the closure lid welds that could lead to stress corrosion cracking through wall cracks in the closure lid weld of waste packages.

- The hoop stress and corresponding stress intensity factor profiles as a function of depth in the closure lid welds from the process model analyses represent the mean profiles.

- The hoop stress and stress intensity factor profiles vary along the circumference of the closure lid welds, and those represent the variability in the profiles on a given waste package.

- As a crack propagates in the closure lid welds or the weld is thinned by general corrosion, the residual stresses in the welds may redistribute in such a way that the stress corrosion cracking initiation and crack growth are mitigated. Such stress redistribution or relaxation is not considered in the current abstraction. This is a conservative approach.

Three cases have been evaluated: "optimum," "realistic," and "most conservative." The uncertainty range in the hoop stress (and corresponding stress intensity factor profiles based on the hoop stress) is bounded between ±5, ±10, and ±30 percent, respectively, of the yield strength and centered around the mean hoop stress profile. The technical basis for the three uncertainty ranges is discussed in Section 6.2.2.5 of *Stress Corrosion Cracking of the Drip Shield, the Waste Package Outer Barrier and the Stainless Steel Structural Material* (CRWMS M&O 2000cu).

Abstraction for Manufacturing Defects in Waste Package Closure Welds—Abstracted models were developed for the probability and size of manufacturing defects in the waste package closure lid welds. The flaw density is used as the parameter to represent the frequency of occurrence of flaws in a given length of closure weld. The flaw sizes are given as a probability density function on each closure lid weld.

Further details of the assumptions used in the abstraction analyses are discussed in Section 3.2 of *Waste Package Degradation Process Model Report* (CRWMS M&O 2000n). Major assumptions employed in the abstraction are:

- For the cases analyzed, both surface-breaking flaws and embedded flaws are considered.

- Flaws occur randomly.

- The fraction of surface breaking flaws is uniformly distributed. The use of the uniform distribution is a reasonable representation of the uncertainty in expressing this value.

The number of flaws that appear on a waste package patch is sampled stochastically as a Poisson random variable. For each flaw that occurs, a flaw size is randomly assigned to it by sampling from the calculated flaw size cumulative distribution function. This flaw's location and size are then used in the stress corrosion cracking analysis.

Because embedded defects can become surface breaking defects as general corrosion proceeds, the consideration only of preexisting surface breaking defects may not be appropriate. As an alternative conservative abstraction, both surface breaking defects and embedded defects within the outer quarter region of the weld surface are considered. Three observations for the sum of the fraction of surface breaking flaws and the fraction of flaws embedded within the outer quarter region of the surface are used in the alternative conservative abstraction. This, however, may be overly conservative because most embedded defects would be oriented in the radial direction that would not lead to stress corrosion cracking. The stress corrosion cracking analysis considers that hoop stress is the dominant stress in the closure lid welds and drives radial crack propagation.

Integrated Analyses for Drip Shield and Waste Package Degradation—This section reports WAPDEG analysis results for drip shield and waste package degradation. The section includes the discussion of results for the three cases (optimum, realistic, and most conservative) that are likely to represent the potential range of major corrosion model parameter values that could affect the long-term performance of the waste package and the drip shield in the repository. The optimum case represents the parameters achievable through stringent control of such processes as stress mitigation, material variability, welding, and other fabrication steps. The realistic case represents what is achievable through appropriate levels of process controls. The most conservative case represents the combination of the worst case parameters that might result from inadequate control of the processes. In the WAPDEG analyses for the three cases, the potential performance credit of the stainless steel structural material is not considered.

The WAPDEG model, an integrated model used for waste package and drip shield degradation analysis, is based on a stochastic simulation approach. It describes waste package degradation, which occurs as a function of time and repository location for specific design and thermal hydrologic modeling assumptions. The corrosion modes that were included in the analyses are:

- Humid-air phase general corrosion of the drip shield

- Aqueous phase general corrosion of the drip shield

- Localized (pitting and crevice) corrosion of the drip shield

- Humid-air phase general corrosion of the waste package outer barrier

- Aqueous phase general corrosion of the waste package outer barrier

- Localized (pitting and crevice) corrosion of the waste package outer barrier

- Stress corrosion cracking of closure lid welds of the waste package outer barrier.

The following corrosion parameters were abstracted and included in the analyses:

- Relative humidity threshold for corrosion initiation of the drip shield and waste package outer barrier

- Corrosion potential-based threshold for localized corrosion initiation of the drip shield and waste package outer barrier

- Probability of the occurrence and size of manufacturing defects in closure lid welds of the waste package outer barrier

- Stress and stress intensity factor profiles in the closure lid welds of the waste package outer barrier (incorporating stress mitigation techniques)

- Threshold stress intensity factor for the waste package outer barrier (used with the threshold stress intensity factor model)

- Threshold stress for the initiation of stress corrosion cracking crack growth for the waste package outer barrier (used with the slip dissolution model)

- Corrosion enhancement factor for aging and phase instability of the waste package outer barrier

- Corrosion enhancement factor for microbiologically influenced corrosion of the waste package outer barrier.

For the stress corrosion cracking analysis of the waste package closure lid welds in the WAPDEG analysis, the slip dissolution model has been adopted over the threshold stress intensity factor model. For the analysis with the slip dissolution model, the following should be met before initiating a stress corrosion cracking crack propagation in a patch: (1) the stress intensity factor (K_I) should be positive, and (2) the stress state must be greater than or equal to the threshold stress. In the

WAPDEG analysis, for those patches with a compressive stress zone (or layer) in the outer surface, the compressive stress zone is removed by general corrosion, and this delays the application of the slip dissolution model for the crack propagation rate. The delay time depends on the compressive zone thickness and the general corrosion rate sampled for the patch.

In addition, preexisting manufacturing defects in a patch are all assumed to be surface breaking for the optimum case. For the most conservative and the realistic cases, all flaws within the outer quarter thickness were included. All of the surface breaking flaws grow at the same general corrosion rate as each sampled patch. Growth of the defects at the general corrosion rate of the patch is a conservative assumption. Therefore, patches with preexisting defects would be subject to stress corrosion cracking earlier than patches without defects.

Corrosion enhancement factors for microbially influenced corrosion and aging and for phase instability are applied to the general corrosion rate of the waste package outer barrier. No microbially influenced corrosion and aging or phase instability factor is applied to the localized corrosion rate because no localized corrosion occurs.

Because temperature and relative humidity do not significantly affect waste package and drip shield degradation, except in the case of relative humidity threshold for corrosion initiation, a representative set of histories for these parameters were used in the current analysis. In addition, the threshold for localized corrosion initiation for the drip shield and waste package outer barrier, which requires the presence of drips, is much higher than the conditions expected in the repository. The stainless steel inner layer of the waste package was not considered in the analysis.

Additional waste package degradation model improvements were implemented after completion of the TSPA-SR analyses. After incorporation of new analyses, models, and data, the predicted performance against general and localized corrosion of the waste package was shown to improve. The TSPA-SR model shows no waste package failures before 10,000 years (CRWMS M&O 2000a, Section 5.3). The supplemental TSPA model conservatively included a small number of waste package failures (up to three) due to improper heat treatment of welds. These failures lead to small calculated doses before 10,000 years. Excluding those early failures, the supplemental TSPA models show significant improvement in waste package lifetime (BSC 2001a, Section 7.5; Williams 2001a, Figure 6-1). The results of the additional analyses provide added confidence that the TSPA-SR model is conservative and that the behavior of the waste package in the repository environment is likely to be better than that predicted by the TSPA-SR model.

The various cases analyzed for waste package and drip shield degradation constitute 100 realizations of WAPDEG simulation (or 100 WAPDEG runs) that used 100 inputs for uncertain corrosion model parameters sampled from their respective range. The parameters used in the analysis are:

- Temperature, relative humidity, and contacting solution pH histories in the presence of backfill

- 400 waste package and drip shield pairs

- Thickness of the waste package outer barrier (Alloy 22)

- 15-mm (0.6-in.) thick drip shield (titanium)

- 1,000 patches per waste package

- 500 patches per drip shield.

The DOE codisposal waste package and the naval spent nuclear fuel waste package have a thicker outer barrier than commercial spent nuclear fuel packages. Therefore, the calculation of patch penetration times by general corrosion of those waste packages is conservative (i.e., the model calculates faster corrosion than is expected). However, radionuclides that contribute most to the peak dose (technetium-99, iodine-129, neptunium-237, and plutonium-239; see Section 4.4.2.2) from DOE spent nuclear fuel and high-level radioactive waste in the codisposal waste packages represent only

about 10 percent of the total inventory of radionu-clides in the repository (CRWMS M&O 2000bm, Table 3.1-4). Therefore, the delayed patch penetrations of the codisposal waste packages by general corrosion would not affect the peak dose significantly. In addition, because stress corrosion cracks, once initiated, propagate very rapidly, the crack penetration times by stress corrosion cracking in the closure lid welds would not be affected significantly for the codisposal and naval spent nuclear fuel waste packages with the thicker outer barrier. The WAPDEG analysis results (i.e., waste package and drip shield failure time and number of crack, pit, and patch penetrations) are reported as a group of degradation profile curves that represent the potential range of the output parameters.

The optimum case (the upper bound profile, which is the upper extreme of the probable range of the failure time) indicates that the earliest possible waste package failure time is about 51,000 years. An extremely low probability is associated with the estimated earliest possible failure time. The failure time of the median profile is about 80,000 years. The time to fail 10 percent of waste packages for the two profiles is about 80,000 and 97,000 years, respectively.

Because conditions for localized corrosion do not develop, degradation of the drip shield occurs primarily because of general corrosion. Stress corrosion cracking of the drip shield due to rockfall is not expected to affect drip shield functions (CRWMS M&O 2000cu, Section 6.5.5). Both the top and under sides of the drip shield are exposed to emplacement drift conditions and subject to corrosion. In addition, both sides are assumed to experience the same exposure conditions, regardless of whether the drip shields are dripped on or not. Results of the WAPDEG analysis show that for the optimum case (i.e., the upper bound profile), the drip shield failure starts at about 24,000 years, and 50 percent of the drip shields fail within several thousand years after the initial failure.

The most conservative case analysis was to evaluate the effects of the alternative conservative model abstractions of several key corrosion model parameters. Those parameters are stress corrosion cracking-related parameters and general corrosion parameters, along with corrosion rate bias to account for silicate deposits. This case represents the worst case combination of those parameters from the perspective of first waste package failure time. As shown in Figure 4-92, the results of this case indicate that in the TSPA-SR model the earliest possible failure time of a waste package for the upper bound profile is about 12,000 years, much earlier than the realistic case (about 50,000 years) (see Section 4.4.2.2 for the analysis result summary). This estimated earliest possible failure time has a very low probability. The results also show that the initial failure comes from a stress corrosion crack penetration. The failure time of the median profile is about 50,000 years. The time to fail 10 percent of waste packages for the upper bound profile is about 22,000 years. These results do not include the possibility of small releases resulting from early failures described in *FY01 Supplemental Science and Performance Analysis* (BSC 2001a).

For the most conservative case, the failure profiles of drip shields are not significantly affected because the failures occur only by general corrosion. The difference between the conservative and optimum cases consists only of bias correction for the silicate deposits. As with the optimum case analysis, both the outer and inner sides of the drip shield are exposed to the same conditions in the emplacement drift and subject to general corrosion. The results show that for the upper bound profile, drip shield failure starts at about 20,000 years, and 50 percent of the drip shields fail within a thousand years after the initial failure.

The realistic case represents what is achievable for fabrication and material parameters under present-day processes. The results for this case fall between those of the optimum and most conservative cases.

Analysis Summary—The candidate materials for the drip shield (Titanium Grade 7) and the waste package outer barrier (Alloy 22) are highly corrosion resistant. Under the expected repository exposure conditions, these materials are not expected to be subject to degradation modes that, if initiated, could lead to failure in a short time.
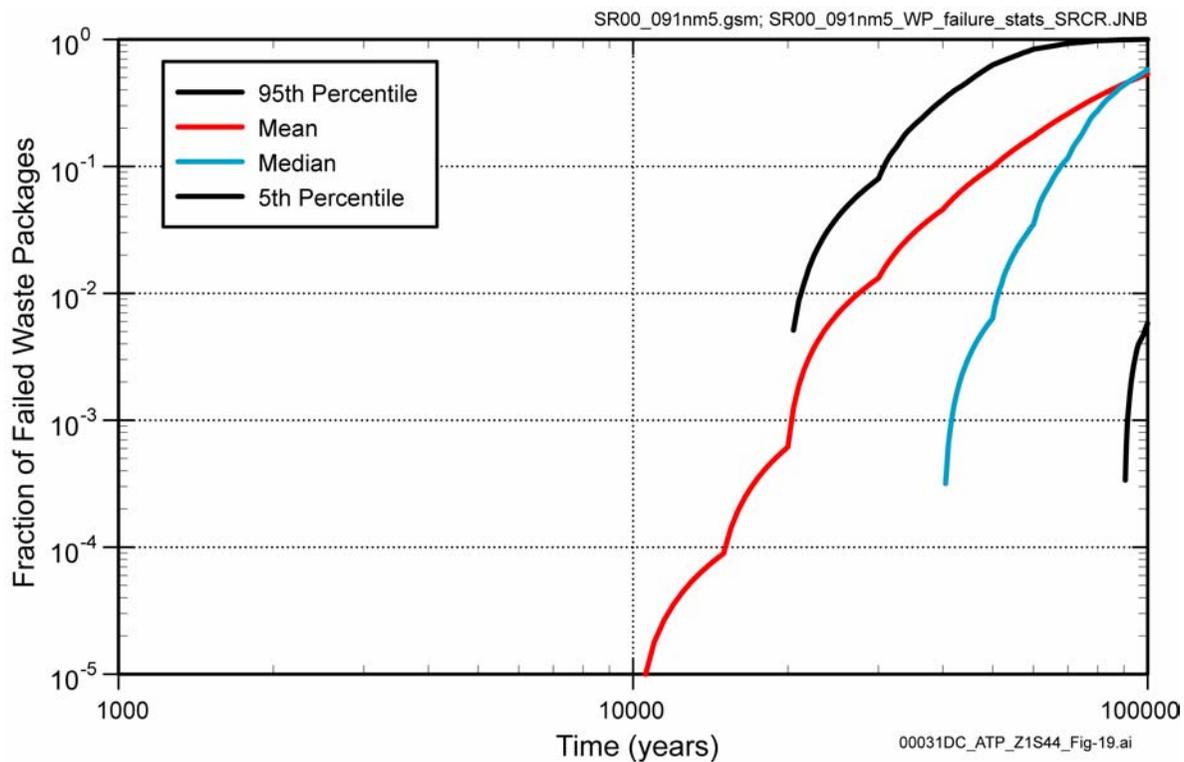
Figure 4-92.   TSPA-SR Performance Assessment Results for Waste Package Degradation (Nominal Scenario)
Source: Modified from CRWMS M&O 2000a, Figure 4.1-9.

Those degradation modes are localized corrosion (pitting and crevice corrosion), stress corrosion cracking, and hydrogen-induced cracking (applicable to drip shield only). Both drip shield and waste package degrade by general corrosion at a very low passive dissolution rate. The current experimental data and detailed process-level analyses, upon which the model abstractions that have been incorporated in the WAPDEG analysis are based, indicate that, except for the closure lid welds of the waste package, the candidate materials would not be subject to those rapidly penetrating corrosion modes under the expected repository conditions. The waste package and drip shield degradation analyses for the two "end-member" cases (i.e., the optimum case and the most conservative case) have shown that, based on the TSPA-SR corrosion model abstractions and assumptions, both the drip shields and waste packages do not fail within 10,000 years. From the perspective of first waste package failure, the analysis results are encouraging because the most

conservative case represents the worst case combination of key corrosion model parameters that significantly affect the long-term performance of waste packages in the repository. The most conservative case accounts for potential uncertainties in the fabrication and process control steps, such as stress mitigation. However, the estimated long lifetime of the waste packages in the TSPA-SR model analysis is attributed primarily to two factors: (1) stress mitigation to substantial depths in the dual closure lid welds and (2) the very low general corrosion rate applied to the closure lid welds to corrode the compressive stress zones. Complete stress mitigation as proposed may not be possible for the closure lid welds, and because of the potential residual stresses, the closure lid welds may be subject to stress corrosion cracking. Once a stress corrosion crack begins, it penetrates the closure lid thickness in a very short time. Thus, stress mitigation in the closure lid welds is a key design element to avoid premature waste package failures from stress corrosion cracking.

Movement of Water into Breached Waste Packages to Contact Waste—The temperature conditions in the waste package over time (before and after waste package breach) are used to calculate the number of spent nuclear fuel rods that develop pinholes due to creep rupture, in addition to those that have pinholes prior to being delivered to the repository. If waste package breaches occur while temperatures are high, oxygen can enter the waste package, and thermally-driven oxidation of the spent fuel pellets exposed through the pinholes can cause large length cracks (unzipping) in a significant number of fuel rods. The amount of cracking is very small if the waste package breaches occur after temperatures fall, which is the more likely situation. In the TSPA-SR, the amount of water that is calculated to have access to the waste package interior is based on the degraded areas of both the drip shield and the waste package. The distribution of water within the waste package is modeled using a conservative mixing cell approach. Resident water within the cell is based on the water fraction in saturated corrosion products of the spent nuclear fuel of the high-level radioactive waste glass. No credit is taken in this model for the potential for water to not fully wet the large surface area available in the waste package interior or the possibility that residual heat in the waste package could evaporate the water before it contacts the waste. The mobilization of radionuclides by the water from the exposed waste (through the cladding pinholes and cracks) is described in Section 4.2.6.

Once radionuclides are mobilized, they are transported to the exterior of the waste package by a simple one-dimensional diffusion model. No credit is taken in this model for the time it could take for the radionuclides to reach the inner surface of the waste package breach location or for sorption by corrosion products within the waste package. The diffusion model uses the crack width to determine the cross-sectional area, the thickness of the closure weld for the diffusion distance, the mixing-cell concentration as the source concentration, and a zero sink concentration (by assuming advection of the contaminated effluent from the outer surface of the crack). The output of this diffusion model is the source term for the sequential engineered barrier system, unsaturated zone, and saturated zone transport calculations described in Sections 4.2.7, 4.2.8, and 4.2.9.

4.2.5 Water Diversion Performance of the Engineered Barriers

The water diversion functions of the engineered barrier system are to limit or delay the amount of water contacting waste packages for at least 10,000 years (CRWMS M&O 2000ab, Section 1.2.1.8) and to increase the predictability of environmental conditions at the waste package surface. The engineered barrier system components that will perform these functions include the drip shield, the invert (consisting of a steel support structure with crushed rock ballast), the waste package pallet, and the steel ground support. Engineered barriers are described in Section 2.4.

This section describes how the engineered barriers in the potential repository will function together with the natural barriers to minimize water contact with waste packages. Over time, the drip shields and waste packages will become susceptible to corrosion, as discussed in Section 4.2.4. Once these processes result in breaches in the drip shield and the waste package, water can contact the waste form and mobilize radionuclides. The water diversion model described in *Total System Performance Assessment for the Site Recommendation* (CRWMS M&O 2000a, Sections 3.6.1 and 3.6.2) identifies flow pathways and calculates, among other things, leakage through a breached drip shield as well as leakage from a breached waste package. Another aspect of engineered barrier system performance is to moderate the transport of released radionuclides from breached waste packages to the host rock at the drift wall. This will be accomplished for the case of a breached waste package under an intact drip shield using a diffusion barrier concept (see Section 4.2.7). For the case of a breached drip shield, transport will be moderated through partial performance of the drip shield by reducing the amount of water that contacts the waste package.

Finally, free drainage from the drifts is important for engineered barrier system performance. Sufficient drainage capacity will prevent partial

inundation of waste packages or their supports, promote diffusion-barrier performance of the invert, and prevent saturated flow conditions that could lead to faster transport for released radionuclides through the engineered barrier system and the host rock. Complete saturation of the invert is possible if seepage inflow exceeds the drainage capacity of the floor.

As noted in Section 4.1.4, the DOE has conducted sensitivity studies of the operation of the repository at lower temperatures. The conceptual basis and model abstractions presented in this section reflect the effects of higher-temperature operating conditions, specifically those implemented in *Total System Performance Assessment for the Site Recommendation* (CRWMS M&O 2000a, Section 3.6). Alternative thermal operating modes and/or conservatisms and conceptual uncertainties in the model have been reevaluated since the TSPA-SR model and are reported or summarized in *FY01 Supplemental Science and Performance Analyses* (BSC 2001a, Sections 8 and 15; BSC 2001b, Sections 3.2.6 and 4.2.6).

The issues reevaluated since the TSPA-SR model include evaporative reduction of seepage, condensation under the drip shield, geometric constraints on advective flux into the waste package, and the effect of allowing accumulation of water within the waste package (i.e., the "bathtub effect").

4.2.5.1 Conceptual Basis

Initially, preclosure ventilation will remove heat and moisture from the emplacement drifts. Ventilation at ambient temperature in the Exploratory Studies Facility has been observed to dry the surrounding rock (Section 4.2.2), and even more drying of the rock will occur during preclosure operations because of the duration and the elevated temperature. After permanent closure, the emplacement drifts and the surrounding rock will heat up, and depending on the thermal loading, the dryout zone will extend around the drifts. Eventually, within approximately 1,000 years (for the mean and upper infiltration distributions, see Section 4.2.2), moisture will return to the

surrounding rock. At a few locations in the potential repository, seepage of liquid water into the drifts may occur. The drip shield will prevent such seepage from contacting waste packages.

Seepage in the future may increase because of altered climate conditions or episodic fluctuations in infiltration at the ground surface. In addition, at a limited number of locations in the potential repository, faults or fractures may focus percolation into an emplacement drift. Drainage capacity will ensure water diversion performance for extreme seepage conditions.

Conceptual Basis for Types of Flow on the Drip Shield and Waste Package—Water that enters the emplacement drifts as seepage can flow along three types of pathways: (1) water flow directly to the invert; (2) water flow that contacts the drip shield, but is diverted to the invert; and (3) water flow through breaches in the drip shield or waste package. Breaches in the drip shield or waste package can take different forms, ranging from fine cracks caused by stress corrosion cracking of the waste package to patches where general corrosion has penetrated a larger area of the drip shield or waste package (Section 4.2.4). Conceptual features related to film flow and droplet formation are discussed in this section, some aspects of which are not directly modeled (CRWMS M&O 2001c, Section 6.1). As outlined in the process model and abstraction sections 4.2.5.3 and 4.2.5.4, the TSPA-SR conceptual model for fluid flux through the drip shield and waste package bounds many of the discussed conceptual processes using simplified and conservative approaches (CRWMS M&O 2000a, Sections 3.6.1 and 3.6.2).

Thin films can be predicted to form on any wetting or partially wetting surface that is exposed to humidity (Middleman 1995, Chapter 9). Films may then flow because of gravity or possibly because of other differences in water potential on the surface. Film flow capacity is limited by viscosity, the extent of the flow area, surface roughness, and other factors. Film flow on the engineered barriers can deliver liquid water at significant flow rates and could be significant to waste isolation performance. However, film flow through breaches in the drip shield is likely to continue as film flow on the

underside of the drip shield and thus will tend to be diverted from the waste package. Also, film flow through fine cracks into the waste package will be limited by heat generation within the waste package, which will cause water to be rejected as vapor (CRWMS M&O 2000as, Section 3.1.1).

Depending on the aperture of a breach, capillary flow and droplet flow modes can occur. For fine cracks, flow will be dominated by capillarity. In capillary flow, water will be either strongly imbibed or excluded in a crack, depending on whether the surfaces are wetting or nonwetting, respectively. If the local environment has low relative humidity, which would occur mainly during the thermal pulse, a fine crack may dry out. Molecular films of water could then form on the crack surfaces, but the flow capacity would be negligible because the films would be very thin. As the relative humidity increases during cooldown, water films will thicken, and fine cracks will become increasingly water-saturated (CRWMS M&O 2001c, Section 6.1).

As saturation increases and water bridges a fine crack or pore, it will be held there at a negative potential by capillarity. It will not flow unless the adjacent downstream flow pathway is at a more negative potential, or unless sufficient water pressure is applied upstream to overcome the negative potential. For the case of water flowing through the drip shield or through the waste package under the impetus of gravity, neither of these conditions is likely unless the water evaporates at the downstream end (CRWMS M&O 2001c, Section 6.1). Thus, the movement of water through fine cracks is limited to very thin water films that can form in the crack and, when humidity conditions permit, to evaporation of water from the downstream end.

Wetting behavior of the crack surfaces is required for capillary effects to occur, and the assumption of wetting behavior is conservative because it increases the liquid pathways available for radionuclide transport (CRWMS M&O 2000as, Section 3.1.1). If the crack surface is nonwetting, water cannot enter and bridge the crack except if pushed by greater water pressure, which is unlikely in the emplacement drifts.

As breaches in the drip shield or waste package increase in size, capillary flow will be more important. As the relative humidity increases during cooldown, and especially when seepage water is present, wider aperture cracks and other types of flow channels will become partially or fully water-saturated. As the relative humidity approaches 100 percent, the saturation and flow capacity of cracks and pores in the drip shield or waste package will increase. Water droplets can form at the downstream end of such channels, and depending on the relative humidity and the channel aperture, they may be released. Once released, droplets can flow on the surface (e.g., the underside of the drip shield) or fall (e.g., onto the waste package). If the crack or channel aperture is fine enough, droplet release will not occur. There is a limit to the aperture above which drops can form and fall from the lower end of the channel. This limit will depend in a complex manner on the geometry of breaches, the wetting properties of the surfaces, and relative humidity (CRWMS M&O 2001c, Section 6.1).

The foregoing discussion applies to an equilibrium situation in which drop size and relative humidity are related (CRWMS M&O 2001c, Section 6.1), so that for a given relative humidity there is an associated equilibrium drop size. If the equilibrium drop size is greater than or equal to the aperture of a potential flow channel, then the channel can be considered fully saturated and flow will depend on the conditions described previously. This is the basis for the capillary flow concept, which can be used to establish a lower threshold of aperture below which flow does not occur for given relative humidity conditions.

A different mode of flow may result when drops fall from the roof of the emplacement drift at locations where seepage contacts the drip shield or waste package. The kinetic energy at impact can produce smaller droplets that are not at equilibrium with the relative humidity and can travel through smaller channels without forming films or causing the channels to become saturated. For breaches due to general corrosion, even equilibrium droplets could do this. Thus, there is another mode of flow that is dynamic and not limited by capillary retention.

The dynamic droplet mode of flow will be limited by several factors (CRWMS M&O 2001c, Section 6.1). Firstly, production of smaller drops will increase the surface energy, and the increase must be less than the kinetic energy of impact, which constrains the distribution of drop sizes produced by the impact. Secondly, as debris accumulates in the drifts, falling drops may dissipate their kinetic energy before contacting the drip shield or waste package. Thirdly, the breaches may fill with corrosion products or debris, so that the resulting flow channels are smaller than the droplets produced. The interlocking drip shield joint design will obstruct and prevent dynamic penetration by water droplets. Finally, multiple breaches will tend to interfere, whereby an upper breach intercepts the flow to a lower breach.

In summary, for fine cracks and pores the flow of water because of gravity will be negligible, especially at low relative humidity, compared with the potential diffusion of radionuclides through such channels. There is an aperture threshold above which flow through cracks or other channels can occur, depending on the relative humidity conditions. Dripping behavior is complex and depends on the channel geometry, material surface characteristics, and relative humidity. This aperture threshold concept does not apply to droplets that are smaller than the channel aperture, which can penetrate dynamically. The dynamic droplet mode is limited by several factors but is taken into account in the interlocking joint of the drip shield design described in this report.

Conceptual Basis for the Environment Under the Drip Shield—During the thermal pulse, the relative humidity at the waste package surface will be less than in the drift environment, primarily because the temperature will be greater. Several studies supporting the TSPA-SR model evaluated the potential for water vapor emanating from the invert to condense on the underside of the drip shield (CRWMS M&O 2001c, Section 6.4; CRWMS M&O 2000dd, Section 6.3.3). As a minimum, this would require very wet conditions in the invert, corresponding to high rates of seepage inflow to the drifts during the thermal pulse. Without such seepage, moisture conditions in the invert material will be too dry to produce

water vapor partial pressures that can condense on the underside of the drip shield. An important reason for this is that the vapor pressure in unsaturated porous media, such as the invert, is lowered by capillarity (CRWMS M&O 2001c, Section 6.4).

The drip shield must also be cooler than the invert for condensation to occur. As the thermal output of the waste decays, the driving force for condensation under the drip shield will be greatly diminished, so the potential condensation rate will be diminished even if condensation is still possible. Differences in temperature and relative humidity between the waste package and the drift environment will gradually decay and become insignificant after a few thousand years. The timing will depend on location within the potential repository and hydrologic factors, as discussed in Section 4.2.2.

The chemical environment under the drip shields will be protected from liquid or solid-phase mass transport, and thermally driven coupled chemical processes taking place outside the drip shields, for as long as the drip shields are intact and functional. Gas-phase composition, including humidity and the partial pressures of oxygen and carbon dioxide, will be similar to the drift environment and is readily predicted (see Section 4.2.3). There will be dust present on the waste package, derived mainly from the host rock and construction materials and also including particles that may be contributed by the preclosure ventilation air.

Finally, condensate under the drip shield would be pure water that interacts with carbon dioxide in the gas phase, dust on the surfaces, and the metal oxide corrosion products. The resulting bulk composition of condensate would be dilute and well within the range of corrosion resistance for the waste package and drip shield materials (discussed in Section 4.2.4). Condensate would tend to moderate chemical conditions by dilution and flushing of dust and salts. The thickness of water films that form on the surfaces of the waste package or drip shield will increase with time as the relative humidity increases. However, the potential rate of condensation will decrease with time, as the thermal output of the waste package decays.

In summary, the physical and chemical environment under the drip shields will be protected from potential seepage and thermally driven chemical coupled processes taking place outside the drip shields.

Conceptual Basis for Drainage—Free drainage is an important attribute of the potential repository host rock at the Yucca Mountain site. Drainage from the emplacement drifts will be facilitated by the permeability of the rock immediately below the drift floor. If drainage capacity is exceeded locally, water will flow from less permeable to more permeable regions. Thus, the spatial distribution of seepage and drainage capacity could be used to develop greater estimates of drainage capacity.

Excess drainage capacity is desirable because the permeability of the rock below the emplacement drifts may be decreased by thermal-hydrologic-chemical-mechanical coupled processes occurring early in the thermal period. The possibility for fracture plugging increases from migration of fines from the drift into fractures and from thermally driven reaction of those fines to form clays or other products, particularly on contact with water. Fracture plugging may also be associated with thermal-mechanical loading of the host rock (Hardin and Chesnut 1997, Section 3.2.2).

4.2.5.2 Summary State of Knowledge

Results from Laboratory Testing of Drip Shield Concepts—A series of drip shield tests was conducted in a mockup of an emplacement drift to investigate drip shield performance. Results from the tests demonstrated the capillary flow mode and showed, for a set of thermal conditions similar to those of the design and operating mode described in this report, that condensation does not form on the underside of the drip shield. The following description, summarized from *Water Distribution and Removal Model* (CRWMS M&O 2001c), pertains to one of the tests in the series, which involved water injection onto a simulated drip shield, without backfill, at elevated temperature.

The drip shield test configuration shown in Figure 4-93 consists of an outer steel canister, simulated drip shield, invert structure, and simulated waste package. At one-fourth scale, the outer canister represented a 5.5-m (18-ft) diameter emplacement drift. The canister was thermally insulated on the outside, and the total weight was monitored to measure bulk water content. The scale-model drip shield was fabricated from stainless steel and was similar to the design concept described in this report (see Section 2.4), except that simple overlap joints were used between sections rather than the interlocking design. Drift seepage was simulated using an array of drippers at the top of the canister, which injected water at a rate of 1 L/hr (0.26 gal/hr). The water contained a blue dye to facilitate tracing of water movement. Temperature and humidity measurements were made in the canister and under the drip shield. Moisture content and temperature were measured in the invert material. The dripper locations, measurement locations, and other details are shown in Figure 4-94.

The temperature of the simulated waste package was maintained at 80°C (176°F) and that of the outer canister wall at 60°C (140°F). The volume of water recovered from the test as a function of time is shown in Figure 4-95. Of the 760 L (200 gal) introduced, approximately 650 L (170 gal) were recovered; the difference was retained in the granular invert material. The water injection rate represented localized seepage conditions extreme, that might be encountered in the potential repository. Relative humidity above the drip shield typically remained around 85 percent, while under the drip shield the relative humidity was typically 65 percent (Figure 4-96). Condensation under the drip shield can occur only if the relative humidity approaches 100 percent. Observation with remote television cameras indicated no condensation under the drip shield or on the waste package.

Observations of Drainage from Exploratory Tunnels—Water use is limited in exploratory excavation and scientific testing in tunnels at Yucca Mountain. The amount of water used during excavation was monitored and was typically in the range of 1,900 to 2,700 L (500 to 700 gal) per meter of drift. Ponded water on the tunnel floor evaporated and drained into the rock and did not persist. Drainage was difficult to quantify because construction water was removed along with the waste rock and because ventilation also removed
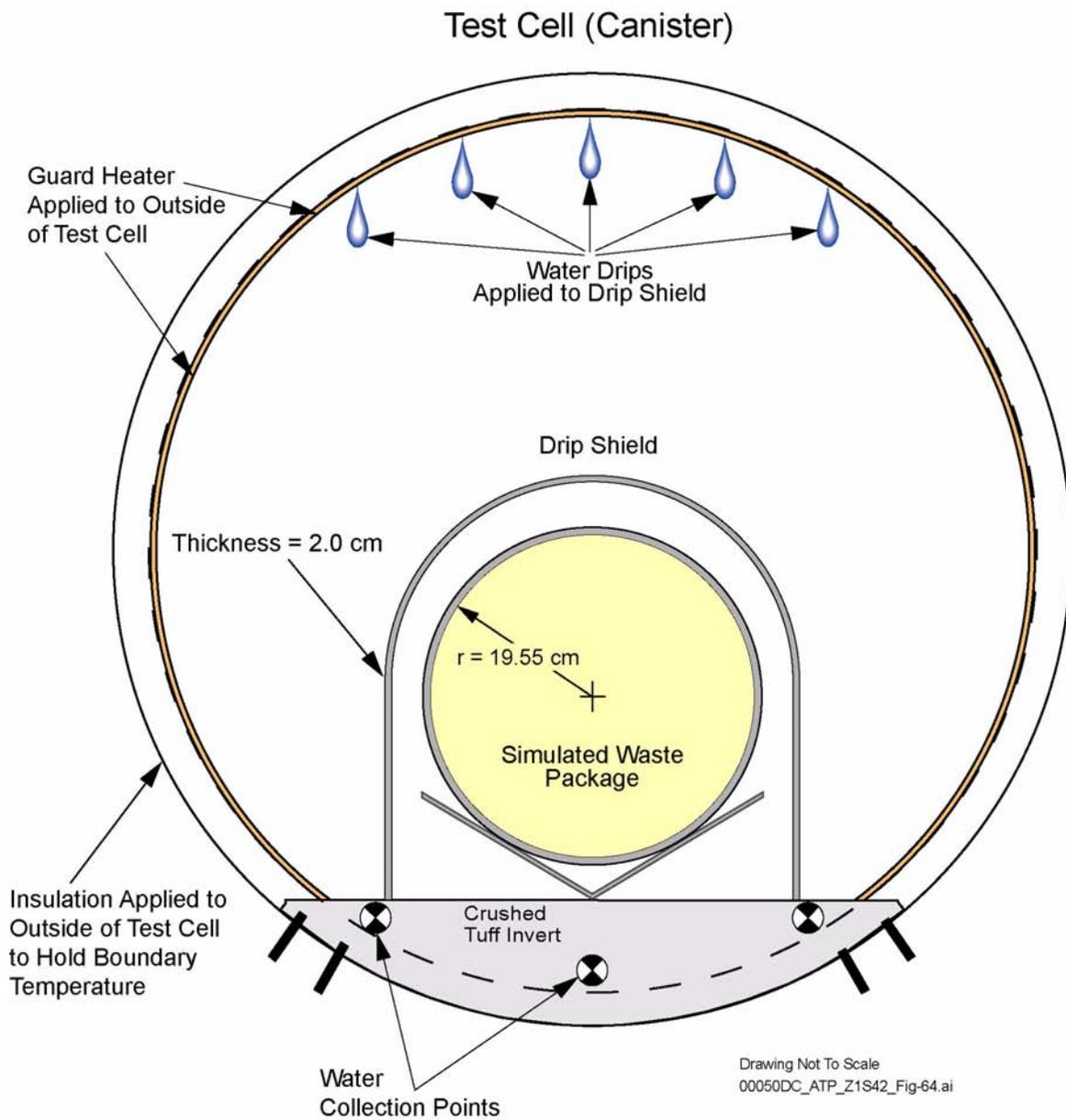
Figure 4-93.   Schematic of Drip Shield Test
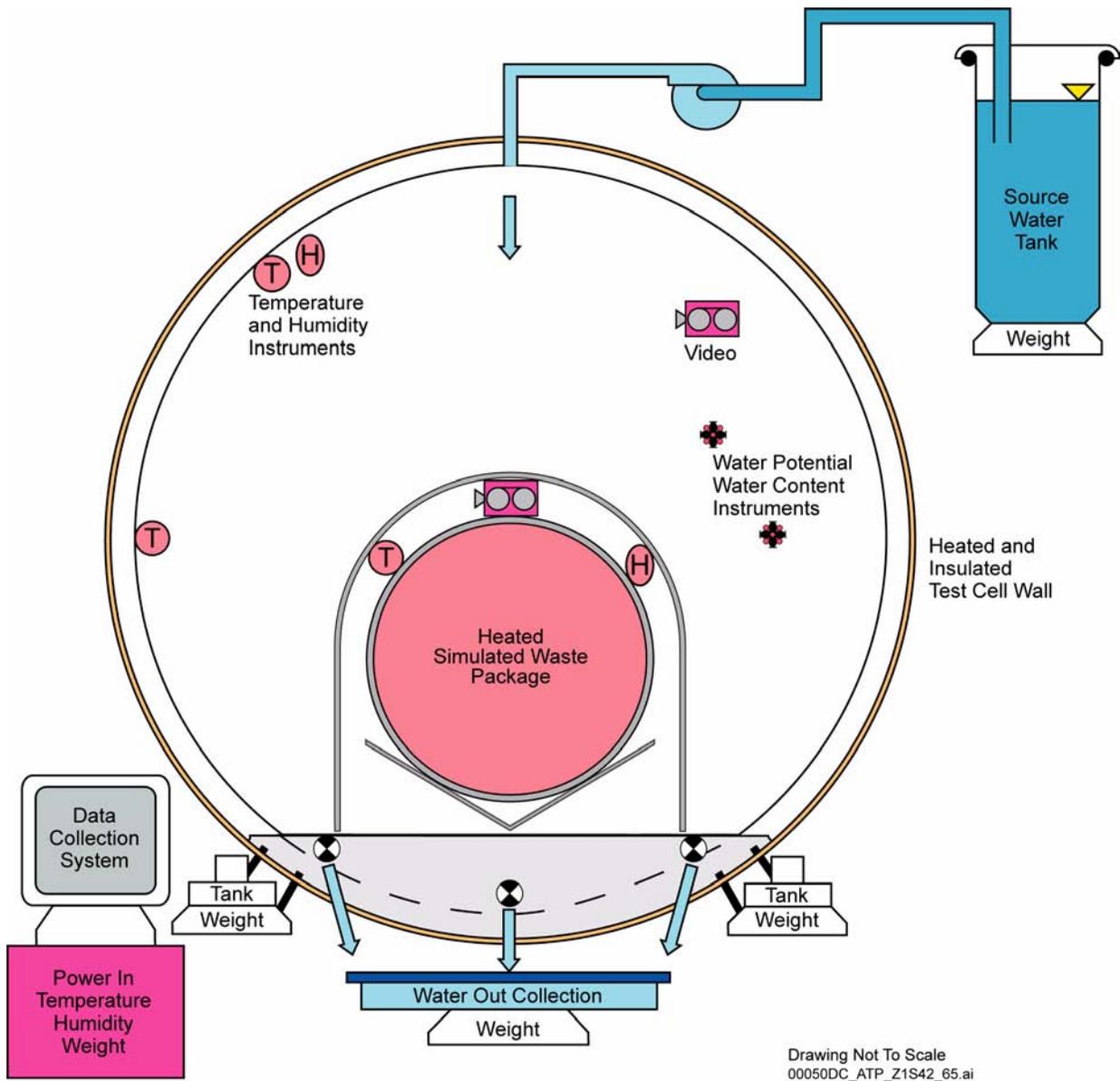
Figure 4-94.   Schematic of Drip Shield Test Measurements
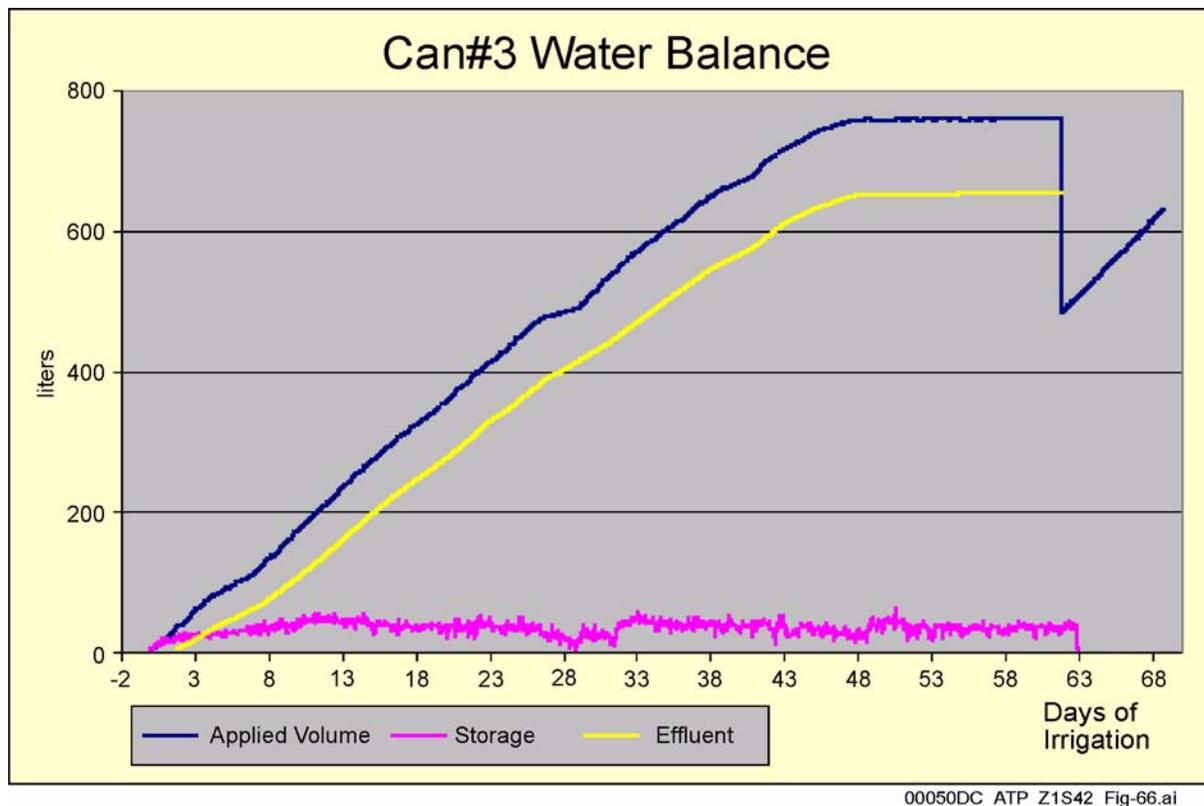
Figure 4-95.   Water Balance for the Pilot-Scale Drip Shield Test without Backfill
This figure shows the total water injected into Canister Test #3 (blue curve), the total collected (yellow curve), and the difference, representing water stored in the test (magenta curve). The test was terminated at approximately 62 days. Source: Modified from Howard et al. 2001, Figure 58.

water. Temporary ponding of construction water on the floor did not occur uniformly, so drainage capacity was apparently heterogeneous.

Measurements from the Yucca Mountain site have shown that the ambient, in situ bulk permeability of the rock exceeds the necessary drainage capacity by orders of magnitude, on average. Hydrologic properties developed for the welded tuff host rock units, constrained by air injection testing in boreholes, indicate that bulk permeability is 1 darcy or more (CRWMS M&O 2000cj, Tables 13, 14, and 15). This permeability corresponds to water drainage capacity of more than 300 m/yr (1,000 ft/yr), which exceeds the drainage capacity requirement for the most extreme seepage criterion (CRWMS M&O 2000ab, System Performance Criterion 1.2.1.8) by at least an order of magnitude.

4.2.5.3   Process Model Development and Integration

Drip Shield Design Features for Water Diversion, Rockfall, and Seismic Stability—The interlocking drip shield joint will maintain a functional configuration capable of diverting water, mitigating impact loads from rockfall, and resisting the effects of seismic motion. A description of the drip shield concept is provided in Section 2.4.4. Design requirements are presented in *Emplacement Drift System Description Document* (CRWMS M&O 2000ab). Drip shield design requirements include corrosion resistance and structural strength. Corrosion resistance is required so that drip shields can function with high reliability as water diversion barriers for at least 10,000 years. Structural strength is needed so they can withstand rockfall (see Section 4.2.3). Drip shield degrada-
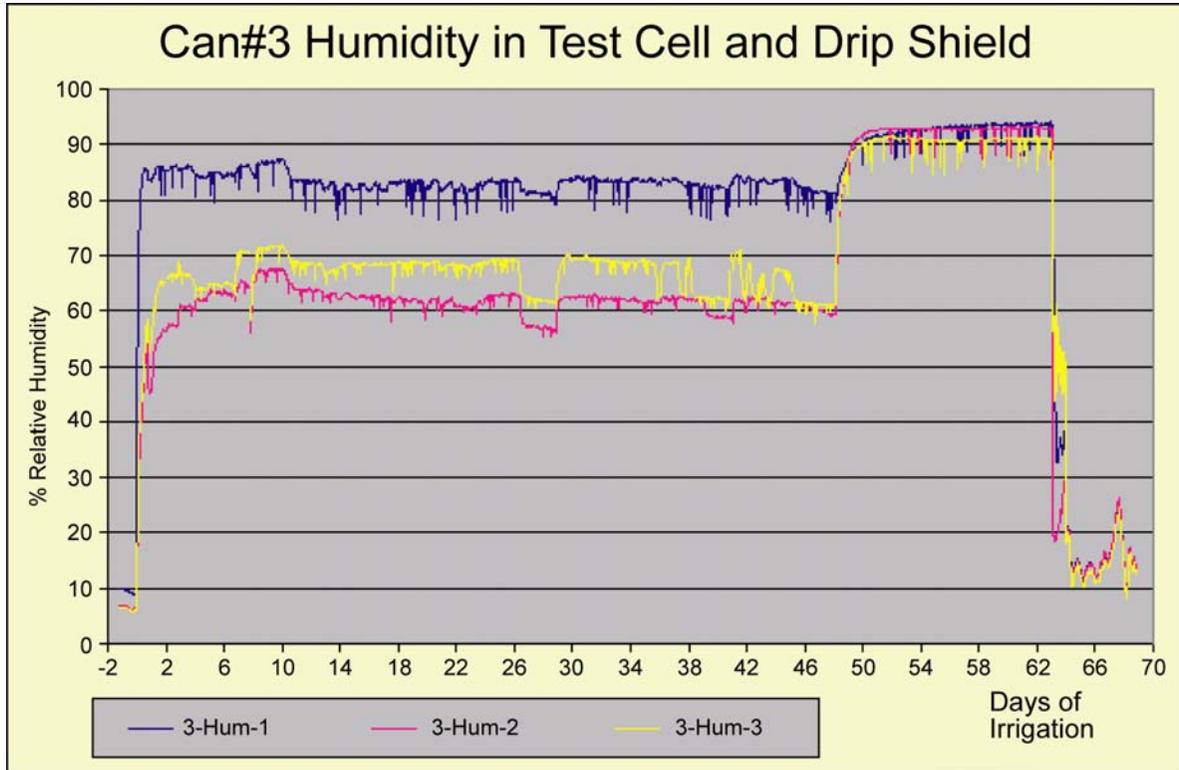
Figure 4-96.   Relative Humidity in the Pilot-Scale Drip Shield Test without Backfill
This figure shows relative humidity measured at three locations in Canister Test #3. The blue curve shows relative humidity in the test cell outside the drip shield. The yellow and magenta curves show relative humidity at two locations in the air space between the drip shield and the simulated waste package. The relative humidity under the drip shield was substantially lower, and condensation was not observed there. The period of heating was terminated at approximately 48 days, and temperature returned to ambient values. Source: Modified from Howard et al. 2001, Figures 48 and 49.

tion from dislocation, deformation, and corrosion processes is the focus of ongoing analyses.

In the design described in this report, the drip shield sections will interlock to prevent separation between adjacent segments (see Figure 2-74 in Section 2.4.4.1). Interlocking will be accomplished by overlapping the specially designed ends of adjacent segments. Each segment will be lowered into place over the end of its predecessor. This will engage interlocking channels located on the top and sides of each segment. To separate the segments will require relative movement of approximately 1 m (3.3 ft) in the vertical direction, which is more than seismic ground motion or rockfall are likely to produce.

The interlocking design of the joint will include water diversion channels to capture and divert dripping water that may penetrate the joints between drip shield segments, so that the water runs downward to the invert rather than to the underside of the drip shield. The water diversion channels will also provide capillary breaks between adjacent diversion rings (Figure 2-74) so that water cannot wick into the joint as observed in the pilot-scale test. The interlocking joint design will prevent droplet flow and capillary flow for as long as the joints remain intact. The joints are designed to accommodate thermal expansion and seismic displacement (Figure 2-74). Joint stability under rockfall is currently being analyzed.

Significant structural strength is required so the drip shield can protect the waste package from

damage by rockfall. The drip shield will be designed to withstand damage from rocks up to several tons in size (CRWMS M&O 2000ap, Section 4.2.1.1, Table 3). The drip shield must also withstand static loads from rock debris due to collapse of the emplacement drift. Titanium Grade 7 will provide superior corrosion resistance for the drip skin, while Titanium Grade 24 will be used for internal bracing because of its greater strength (see Section 2.4.4).

The drip shield legs will rest on transverse steel support beams in the drift invert and will be set alongside longitudinal steel guide beams (see Section 2.4.4, Figures 2-71 and 2-72). These longitudinal guide beams will maintain the geometry of the pallet that supports the waste package and the drip shield, even when they are exposed to seismic shaking. The pallet will also be designed to restrain the waste package and prevent dislocation relative to the drip shield, when exposed to seismic shaking. The invert ballast will support and constrain the drip shield and waste package after the steel beams have failed from corrosion.

Water Diversion by the Drip Shield and Waste Package—Film flow will not provide a significant advective pathway for release of radionuclides, particularly through fine cracks or when the waste packages are warm. However, transport of radionuclides may occur by molecular diffusion in water films. Capillary flow and droplet flow will be negligible in fine cracks. The most likely cause of fine cracks is stress corrosion cracking, particularly around the waste package closure welds, but these cracks will probably be protected from dripping water by a skirt on the waste package. Capillary flow and droplet flow in the joint between drip shield segments has been considered in the drip shield joint design.

The drip shields are not expected to be penetrated by rockfall and will remain in place for 10,000 years. When drip shields or waste packages are eventually penetrated by general corrosion, capillary or droplet flow (where there is seepage) could transport water through breaches.

Conceptually, if seepage water leaks through the drip shield, only a portion of the water would actu-

ally contact the waste package, and it would be distributed over only a portion of the waste package area. Realistically, breaches in the waste package would capture water emanating from a co-located breach in the drip shield above. In other words the capture area should depend on the relative location of the breaches. Where multiple breaches occur in the drip shield or waste package, there would also be interference between them, limiting the total leakage.

Flux Through the Drip Shield and Waste Package—In the process model for water diversion by the drip shield, all seepage into the drift falls onto the crown of the drip shield (CRWMS M&O 2000a, Sections 3.6.1 and 3.6.2). Breaches in the drip shield intercept this flow and permit a fraction of the incoming seepage to flow through the drip shield (CRWMS M&O 2000a, Section 3.6.2.1). Fluid flux only occurs through drip shield patches, as pitting of the titanium drip shield does not occur in the modeled near-field geochemical environment. The remainder of the water flows directly down to the invert and then drains into the host rock.

The process model for water diversion by the waste package in the TSPA-SR model specifies that all water transmitted through the drip shield contacts the waste package (CRWMS M&O 2000a, Sections 3.6.1 and 3.6.2). Breaches in the waste package intercept this flow and permit a fraction of the incident water to flow into the waste package. Conceptually, continuous flow paths are assumed through breaches penetrating the waste package (i.e., patches and stress corrosion cracks). The fraction of water flowing into a waste package is the ratio of the summed axial length of the patch breaches in the waste package to the total length of the waste package. The remainder flows off the waste package, down to the invert, and then into the host rock.

The TSPA-SR model conservatively assumes no resistance to flow in the waste package. The model conservatively ignores a fundamental physical requirement for leakage to occur: breaches in the upper and lower areas of the waste package. This means through-flow is assumed possible through the waste package even with only penetration(s) on

the upper surface (CRWMS M&O 2000dd, Section 6.3.3).

Advection is modeled as the dominant transport process through any patches that form in the drip shield or waste package whenever there is an appreciable amount of water dripping (CRWMS M&O 2000a, Section 3.6.1.2). Diffusion will be the dominant transport process through fine cracks in the waste package so long as the drip shield remains functional. In both cases:

- WAPDEG output (i.e., timing and location of breaches) is used by the engineered barrier system flow abstraction to define the time-dependent fluxes that flow through (or are diverted around) the drip shield and the waste package (CRWMS M&O 2000a, Section 3.6.1.1)

- All of the seepage entering the drift falls on the crown of the drip shield. Conservatively, a patch at any axial location on the drip shield or waste package will collect fluid, even if the axial location of the drip and breach area do not coincide (CRWMS M&O 2000a, Section 3.6.2.1).

Environment Under the Drip Shield—Heat transfer between the waste package and drip shield and humidity under the drip shield are simulated using the multiscale thermal-hydrologic model (Section 4.2.2). Predicted relative humidity is less than 100 percent for most conditions that control the thermal-hydrologic response (rock properties, infiltration flux, thermal loading, and location). For certain conditions, some studies suggest that condensation under the drip shield may be possible (CRWMS M&O 2001c, Sections 6.3.3 and 6.4). Such conditions are limited to many thousands of years after closure, when cooldown has progressed and the temperature differences between engineered barrier system components (e.g., invert and drip shield) approach only a few degrees. At such late time, the thermal output of the waste and the potential for thermally driven condensation would be greatly reduced. In summary, the potential for condensate to drip from the underside of the drip shield is not included in the TSPA-SR model. This is based on TSPA-SR supporting calculations indi-

cating that either condensation would not occur or the effect would be inconsequential (CRWMS M&O 2000dd, Section 6.3.3; CRWMS M&O 2001c, Section 6.4; CRWMS M&O 2000cc, Section 6.4.6).

The chemical environment at the waste package surface will be slowly varying and predictable while the drip shields are intact. Dust derived from repository operations will be present on the waste package surface. Humidity conditions in the presence of dust may support microbially influenced corrosion activity, so for TSPA-SR the corrosion rate is conservatively increased to account for possible microbial activity (see Section 4.2.3). Once drip shield breach occurs, the chemical environment at the waste package surface will be similar to the environment on the drip shield surface.

Water Drainage from the Emplacement Drifts—Numerical modeling of drainage from the emplacement drifts, using extreme seepage, was performed to confirm the conditions that could lead to complete saturation of the invert. The hydrologic simulations were similar to the thermal-hydrologic models described in Section 4.2.2, except that heating was not applied for many of the calculations, and a sand backfill was included in the drift (CRWMS M&O 2001c, Section 6.2). These calculations are applicable to the design without backfill described in this report because drainage through the invert must occur in either case. The same hydrologic properties used in the unsaturated zone flow model for the host rock (as described in Section 4.2.1) were used, along with the same boundary conditions, except that the infiltration boundary condition was manipulated to simulate different values of extreme seepage (CRWMS M&O 2001c, Section 6.2).

The approach to drainage is to establish that there is sufficient drainage capacity throughout the potential repository to handle extreme seepage. The value of seepage flow used for this purpose is approximately 2,000 L (528 gal) per meter of drift, recurring once per year (CRWMS M&O 2000ab, System Performance Criterion 1.2.1.8). Such seepage can occur in only a small portion of the potential repository because the estimated future

infiltration flux will be less, even for the wettest conditions anticipated (see Section 4.2.1). This seepage value is several times greater than the maximum average percolation flux that is estimated to occur anywhere in the host rock for the glacial-transition climate state (CRWMS M&O 2000cf, Figure 6-48). In addition, the numerical simulations were two-dimensional, without provision for diversion of seepage inflow axially along the emplacement drifts to more permeable locations. Accordingly, the approach for evaluating drainage is conservative. The results nevertheless lead to a conclusion that sufficient drainage capacity exists or can be accommodated in design and construction of the emplacement drifts.

The effects of fracture plugging were investigated in the numerical models by setting fracture permeability to zero below the drift for a distance of 3 m (10 ft) from the opening. The most important result was further increase in liquid saturation in the invert and complete saturation given sufficient seepage flux. Drainage was still possible even with fractures plugged, such that the invert remained unsaturated up to a limiting value of the seepage flux.

In summary, model calculations show that the invert could become completely saturated only if the fracture permeability in the host rock is plugged, and seepage exceeds a threshold value. Complete saturation of the invert did not occur in the simulations, even with very high seepage rates, if the fracture permeability was unmodified.

4.2.5.3.1 Limitations and Uncertainties

As noted in Section 4.1.1.2, the DOE performed several activities to improve the treatment of uncertainty in certain TSPA-SR models. The following limitations and uncertainties have been assessed in supplemental TSPA model results as summarized in *FY01 Supplemental Science and Performance Analyses* (BSC 2001a, Section 15; BSC 2001b, Section 3.2.6). These include the following:

- **Evaporative Reduction of Seepage on the Drip Shield and Waste Package**—Evaporative reduction of the amount of water

contacting the drip shield and waste package is ignored in the TSPA-SR model. When accounted for in the model, supplemental TSPA model studies suggest a negligible effect (BSC 2001b, Section 3.2.6.1).

- **Geometrical Constraint in Flux into Waste Package**—In the TSPA-SR model, geometrical constraints on flux through the waste package (such as the coincidence of the axial locations of the breaches and the assumption that any breach is located so that it collects dripping fluid) are ignored. Supporting the conservatism of the TSPA-SR model, supplemental TSPA model studies implemented alternative assumptions and the representation of the fraction of water flowing through the waste package (BSC 2001b, Section 3.2.6.3).

- **Condensation under the Drip Shield**—Condensation under the drip shield as a source for additional water on the waste package is reevaluated in supplemental TSPA model studies. The results corroborate the approach used in the TSPA-SR model (BSC 2001b, Section 3.2.6.2).

- **Bathtub Model for the Waste Package**—Inundation of the waste package, caused by considering the timing of breaches on the top and bottom of the container, result in short-term releases and a negligible, short-term effect on performance (BSC 2001b, Section 3.2.6.4).

Water Diversion Performance of the Drip Shield—Water diversion performance of the drip shield design, and resistance to dislocation by rockfall and seismic motion, are based on design criteria (CRWMS M&O 2000ab, Section 1.2). Consistency with many of these criteria has been evaluated, and some confirmatory testing has been performed (Section 4.2.5.2).

Environment Under the Drip Shield—As stated above, supplemental studies have addressed uncertainties pertaining to the potential for condensation under the drip shield. The reevaluation supports the TSPA-SR approach. Fundamentally, the effect

remains negligible in the nominal scenario because the waste packages do not fail in the period when evaporation might be important (BSC 2001b, Section 3.2.6.2).

Water Drainage from the Emplacement Drifts—The uncertainties in the calculation of seepage entering drifts is addressed in Section 4.2.1.4.2 and Table 4-14. However, 2,000 liters per meter of drift assumed in this analysis exceeds the maximum value in Table 4-14. Site characterization data, such as permeability testing in boreholes, does indicate that the drainage capacity of the drift floor is sufficient to ensure free drainage from the drifts.

4.2.5.3.2   Alternative Conceptual Processes

Water Diversion Performance of the Drip Shield—The rate of seepage inflow may vary with time and location, driven by episodic hydrologic conditions or changes in properties of the host rock (CRWMS M&O 2000by, Section 6.3). At locations where seepage occurs, dripping could occur at a point, then move around to other points as time passes. If there is a breach in the drip shield at such a location, seepage may flow through directly or may be diverted to another part of the drip shield. Such behavior will be random and is accommodated by associating the model results with the average response of multiple breached drip shields to seepage. The maximum and minimum rates of flow through a single breach are not represented, but the average behavior overall is represented. A similar argument applies to modeling of flow through breaches in the waste package. Such an approach has been implemented in supplemental TSPA model studies to quantify conservatism (BSC 2001b, Section 3.2.6.3).

Environment Under the Drip Shield—The chemical environment on the surface of the waste package under an intact drip shield may not support microbially influenced corrosion, as conservatively assumed. The overall rate of microbial activity is known to be limited by the availability of water, nutrients, and energy sources (CRWMS M&O 2000cg, Section 6.4). Water could be provided by humidity on the waste package surface, and energy could be provided by the waste

package outer barrier material, but nutrients will be very scarce under intact drip shields. The available phosphorus and other nutrients will be limited to what may accumulate in the form of dust on the waste package surface during preclosure operations.

Water Drainage from the Emplacement Drifts—Modeling described in Section 4.2.3 has shown that fracture plugging in the host rock from thermal-hydrologic-chemical processes (i.e., chemical precipitation) is unlikely to significantly affect host rock hydrologic properties. However, those results did not include the potential effects of fines migration within the engineered barrier system and thermal-mechanical loading of the host rock. Also, if there is seepage during the thermal pulse and the invert is the last part of the engineered barrier system to cool (as indicated by models described in Section 4.2.2), then precipitates and salts could accumulate near the drift floor. As stated previously (Section 4.2.5.3), the combination of excess drainage capacity in the host rock, plus the possibility of axial flow in the drifts in response to localized extreme seepage, support a conclusion that complete saturation of the invert in the emplacement drifts will not be important to waste isolation performance.

4.2.5.3.3   Model Calibration and Validation

Modeling has been conducted to evaluate water diversion by the drip shield and the potential for condensation under the drip shield (CRWMS M&O 2001c, Section 6.3.3; CRWMS M&O 2000dd, Section 6.4; CRWMS M&O 2000cc, Section 6.4.6). Bounding models are useful where complex phenomena limit modeling approaches, for example, in assuming that all seepage falls as drops and that all water which flows through breached drip shields contacts the underlying waste packages. Model validation for water diversion models is addressed using a combination of bounding approaches and preliminary results from pilot-scale testing. When engineered barrier system pilot-scale testing results become available, this quantitative test data can be compared to predicted model results using NUFT to provide full validation of the model (CRWMS M&O 2001c, Section 6.2.7).

4.2.5.4 Total System Performance Assessment Abstraction

The water diversion model described in the TSPA-SR model identifies eight key flow pathways used in the TSPA-SR abstraction for water diversion for use in engineered barrier system transport models (CRWMS M&O 2000a, Section 3.6.2.1):

- **Seepage Flux Entering the Drift**—This water may be flowing or dripping slowly through the engineered barrier system. Alternatively, this water may form a continuous film of stationary liquid.

- **Flow through the Drip Shield**—Fluid flux through the drip shield begins once patches form due to general corrosion.

- **Flow Diversion around the Drip Shield**—The portion of the flux that does not flow through the drip shield is assumed to bypass the invert and flow directly into the unsaturated zone.

- **Flow through the Waste Package**—Fluid flow through the waste package does not occur until the drip shield failures begin and patch breaches occur in the waste package. Leakage of liquid water through stress corrosion cracks in the waste package is considered negligible because these cracks will be so fine that leakage will not occur by capillary flow or droplet flow. Diffusion of radionuclides through such cracks is included in transport models. There is no assumed locational correspondence between breaches in the drip shield and waste package because corrosion of the different barriers is initiated under different environmental conditions. Microbially influenced corrosion of waste packages is initiated when humidity conditions permit, even under intact drip shields (CRWMS M&O 2000cg, Section 6.4).

- **Flow Diversion around the Waste Package**—The portion of the flux that does not flow into the waste package is assumed to

bypass the waste form and flow directly to the invert.

- **Evaporation from the Invert**—The magnitude of the evaporative flux from the invert is based on the thermal-hydraulic abstraction (CRWMS M&O 2000cc). Condensation as a source for dripping on the waste package is neglected based on supporting studies (see Section 4.2.5.3).

- **Flow from the Waste Package to the Invert**—All flux from the waste package flows to the invert, independent of the breach location on the waste package. The presence of the emplacement pallet is ignored, and the waste package is assumed to be lying on the invert so that a continuous liquid pathway for diffusive transport exists at all times.

- **Flow through the Invert into the Unsaturated Zone**—All fluid and mass flux into the invert is immediately released into the unsaturated zone.

Uncertainties in abstraction inputs were accommodated in general by using bounding values and building conservatism into the models. In this way, it is believed that significant uncertainties have been adequately accounted for in the TSPA calculations in *Total System Performance Assessment for the Site Recommendation* (CRWMS M&O 2000a). This has been confirmed in supplemental work (see Section 4.2.5).

Exclusion of Drainage Effects from the Total System Performance Assessment—From the foregoing discussion, the invert will not be completely saturated unless there is extreme seepage and fracture plugging. Extreme seepage on the order of 1,000 mm/yr (39 in./yr) is extremely unlikely, and although useful for design criteria, such seepage is not included in the performance assessment. The calculations described above have shown that complete saturation of the invert will not occur unless both extreme seepage and fracture plugging occur. Therefore, complete saturation of the invert is screened out as a process that requires explicit representation in the TSPA-SR due to its low probability. In conjunction with this approach,

a bounding approach is taken for representing the diffusion-barrier performance of the invert (see Section 4.2.7).

4.2.6   Waste Form Degradation and Radionuclide Release

The waste form degradation process models provide technically defensible methods for predicting the long-term ability of the waste forms to control radionuclide release from the immediate vicinity of the waste. These models were provided as eight key feeds to TSPA: radionuclide inventory, in-package chemistry model, cladding degradation model, commercial spent fuel degradation model, high-level waste glass degradation model, other waste form degradation models, solubility model, and colloid model.

Section 4.2.6.1 is an introductory summary of the general concepts used to represent the phenomena applicable to waste form degradation and radionuclide release. Section 4.2.6.2 summarizes the current information available, including the ongoing work that forms the basis for understanding the degradation and mobilization processes. These processes and their data inputs and outputs are shown schematically in Figure 4-97. Process model development is provided in Section 4.2.6.3. It describes the approach taken for modeling the degradation of each of the major waste forms. These are commercial, naval, and DOE spent nuclear fuel and high-level radioactive waste glass, which are described in Sections 3.2 and 3.3. This section also discusses the feedback between the degradation processes and in-package chemistry. In-package chemistry in turn controls the radionuclide solubility and colloid stability. For
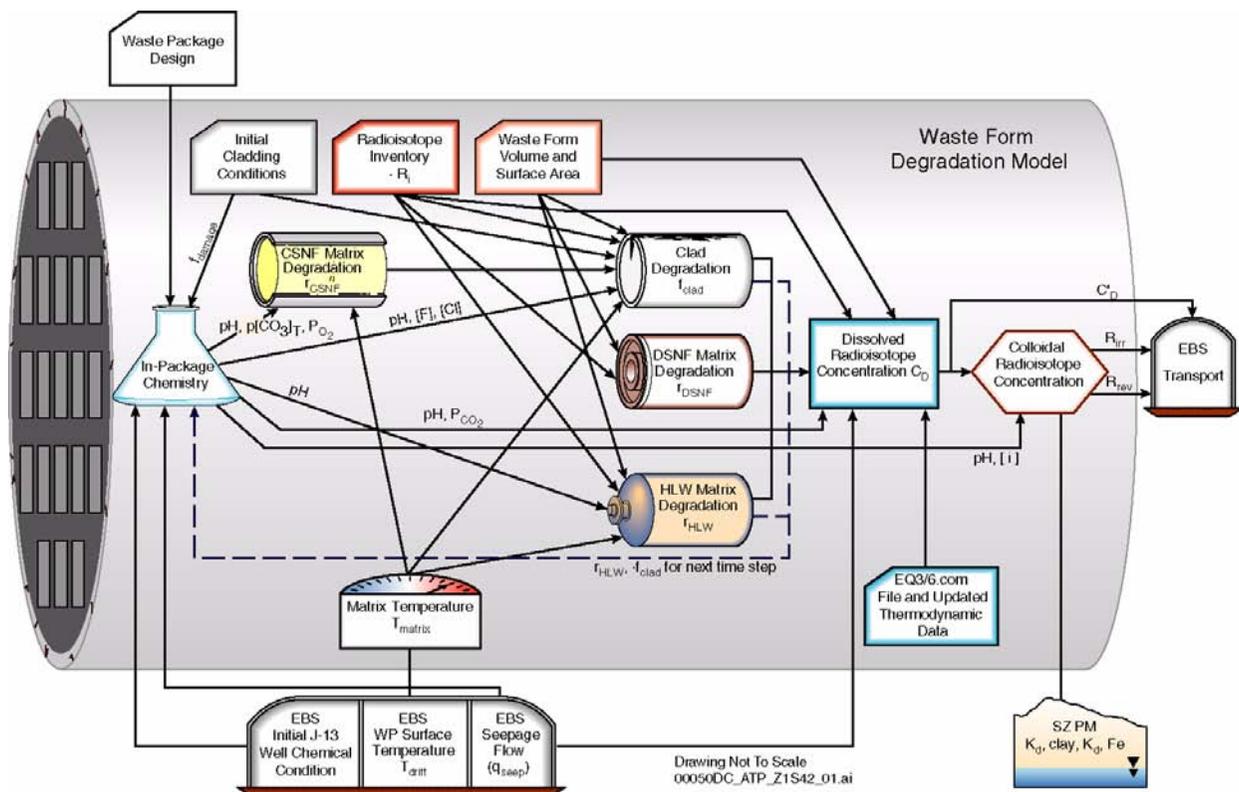
Figure 4-97.   Components of the Waste Form Degradation Model
For detailed discussion of the model and its components, see the *Waste Form Degradation Process Model Report* (CRWMS M&O 2000bm), Section 3. EBS = engineered barrier system; CSNF = commercial spent nuclear fuel; DSNF = DOE spent nuclear fuel; HLW = high-level radioactive waste; SZ PM = saturated zone process model; WP = waste package. Source: CRWMS M&O 2000bm, Figure 1.5-3.

each of the modeled processes, limitations and uncertainties of using the developed models, alternative conceptual processes, and model calibration and validation are discussed. The TSPA abstractions are presented in Section 4.2.6.4.

As noted in Section 4.1.4, the DOE has evaluated operation of the repository at lower temperatures. The conceptual basis and model abstractions presented in this section primarily reflect the effects of higher-temperature operating modes, specifically those implemented in *Total System Performance Assessment for the Site Recommendation* (CRWMS M&O 2000a, Section 3.5). Alternative thermal operating modes and/or conservatisms and conceptual uncertainties have been reevaluated since the TSPA-SR model and are reported or summarized in *FY01 Supplemental Science and Performance Analyses* (BSC 2001a, Section 9; BSC 2001b, Sections 3 and 4).

4.2.6.1   Conceptual Basis

Radionuclide release from the waste forms is a three-step process requiring (1) degradation of the waste forms, (2) mobilization of the radionuclides from the degraded waste forms, and (3) transport of the radionuclides away from the waste forms. Water strongly influences all three processes. The release of specific isotopes may be limited in any step. The release of insoluble elements such as plutonium is usually limited by the mobilization step. The solubility and colloid stability of plutonium is so low that it remains with the waste form degradation products unless large flow rates flush it away. The opposite is true for technetium, which is quite soluble in an oxidizing environment. Technetium release is usually limited only when the waste form degradation rate or technetium inventory is very low, or when there is not enough water for effective diffusive transport. Water flow and radionuclide transport are discussed in Sections 4.2.5 and 4.2.7. This section focuses on the degradation and mobilization processes, their interactions, and the controls they exert on radionuclide release.

Waste form degradation and radionuclide mobilization are part of a highly coupled thermal-hydrologic-chemical system that may follow many scenarios. An overall description of the processes that may occur is provided here, followed by a summary of the testing that has led to this conceptualization in Section 4.2.6.2.

Water Contact and Chemistry—Radionuclide release begins after breach of the waste package and the ingress of air. If the breach is early, the waste may still be highly radioactive and physically hot. The thermal output of hot waste packages, particularly from commercial spent nuclear fuel, will limit groundwater access at early times. When water enters the package, the rate of water inflow and evaporation will determine when and if water accumulates. During this period, gamma radiolysis of the humid air within the package may cause production of nitric acid, which could condense into any accumulated water. If the breach is late, radiation levels and heat will be much lower, and evaporation and radiolytic acid production will be less important. During either period, water may enter the package either as water vapor or as flowing groundwater. The groundwater species entering the package may have a significant effect on in-package chemistry only if evaporation has concentrated them by orders of magnitude. This is unlikely to occur unless the waste package is breached only at the top, and large amounts of water enter and evaporate within the package (Figure 4-98). During this period, there is no water transport of groundwater species or radionuclides out of the package. If the package overflows, or if holes in the bottom allow flow-through, fresh groundwater will dilute the groundwater components, and water-based radionuclide releases may begin. Chemistry within the package is important because it influences the rate of degradation of the package and waste forms (including cladding), and it determines the mobility of radionuclides as dissolved or colloidal species. Films of stagnant, concentrated, acidified groundwater are considered the worst possible scenario for degradation because they do not inhibit oxygen and carbon dioxide transport and may support localized corrosion of the cladding and waste. Such films, however, do not support significant mobilization and transport of radionuclides, and are only possible at times when there is an exact balance of water inflow and evaporation.
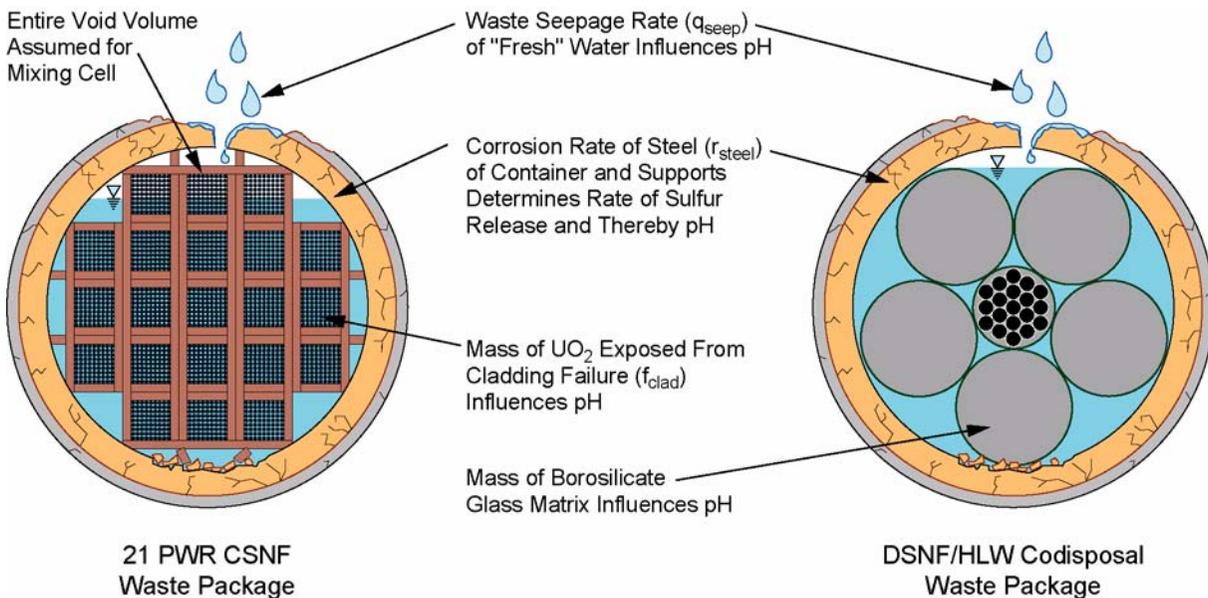
Figure 4-98. Conceptual Model of In-Package Chemistry
DSNF = DOE spent nuclear fuel; HLW = high-level radioactive waste; CSNF = commercial spent nuclear fuel.
Source: CRWMS M&O 2000bm, Figure 3.2-1.

Cladding Degradation—The release of radionuclides does not begin until after the breach of the cladding (for spent fuel). Stainless steel cladding is expected to be susceptible to stress corrosion cracking and therefore cannot be relied upon for long term protection. Some spent fuels, such as N Reactor, have high fractions of damaged cladding, so little protection is expected. Most commercial spent fuel, however, will have intact Zircaloy cladding at the time of emplacement. Zircaloy is a highly corrosion resistant material that is expected to provide significant protection of the waste. The mechanisms that may initially fail Zircaloy produce small flaws such as pinholes or cracks. These mechanisms include ones that are expected only in-reactor (fretting, baffle-jetting) and those that may occur after reactor operation (creep, hydride reorientation, earthquake damage). Under some circumstances, the initial flaw may propagate, splitting open the cladding. This has been rarely observed in reactors, due to hydride effects, and during exposure to hot air due to oxidation and swelling of the fuel.

Waste Form Degradation—There are many waste form types that may be emplaced within a repository, but most of them are thermodynamically unstable under moist, oxidizing conditions. Uranium dioxide fuels will oxidize and hydrate; glass waste forms will react with water and form clays, zeolites, and oxides; and all but a few of the over 250 DOE spent fuel types will undergo similar reactions. The rate of these reactions, however, will in most cases be quite slow and may be limited by the rate that reactants such as oxygen and water can be transported to the waste form surface. Although a few radionuclides such as cesium and iodine may concentrate between the fuel and cladding during reactor operation, most of the radionuclides will be tied up within the various waste forms and cannot be released from the waste package until the waste forms degrade.

Radionuclide Mobilization—Once the waste form degrades, radionuclides may be mobilized in flowing or diffusing water. Water-mobilized radionuclides include dissolved species and suspended particles (Figure 4-99). Larger suspended particles
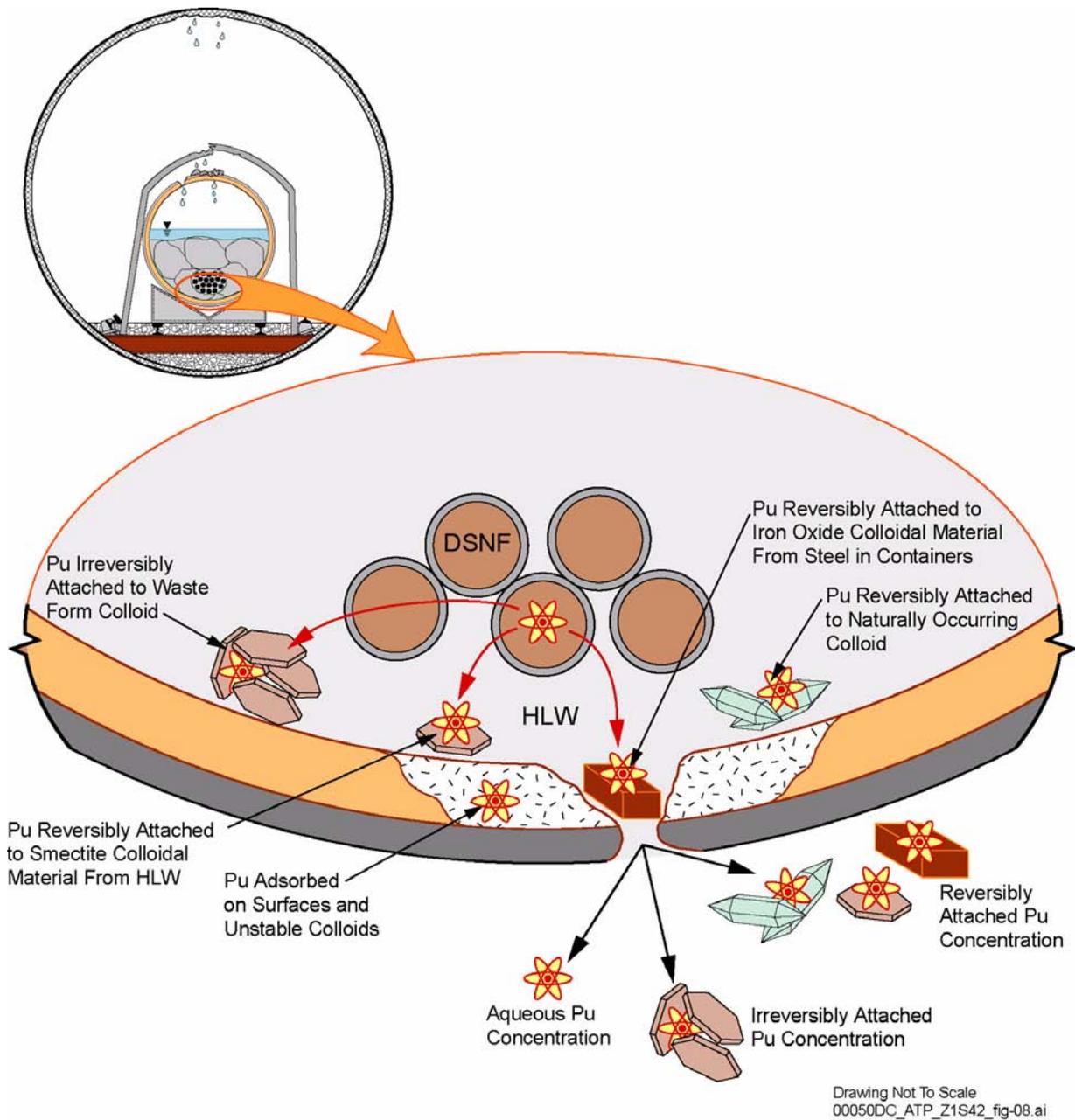
Figure 4-99. Conceptual Model of the Formation of Reversibly and Irreversibly Attached Radionuclides on Colloids

DSNF = DOE spent nuclear fuel; HLW = high-level radioactive waste. Source: CRWMS M&O 2000bm, Figure 3.8-1.

quickly settle out of solution or are trapped in small openings. Only after gross failure of the package would these larger particles fall or wash out of the package. Particles in the colloid size range, however, can remain suspended by Brownian forces and may travel significant distances. The concentration of radionuclides associated with colloids is limited by the colloid concentration and radionuclide carrying capacity of the colloids. The concentration of dissolved species is limited by the elemental solubility of the radionuclide within the local environment.

4.2.6.2 Summary State of Knowledge

This section discusses the testing done to elucidate the degradation and mobilization processes for commercial light water reactor spent nuclear fuel, DOE spent nuclear fuel, and other high-level radioactive waste encased in borosilicate glass or ceramics. The work briefly summarized below is presented in more detail in *Waste Form Degradation Process Model Report* (CRWMS M&O 2000bm) and fully discussed in the analyses and models reports referenced therein. The tests identify degradation and mobilization mechanisms, as well as inputs for predictive models as described in Section 4.2.6.3.

4.2.6.2.1 Inventory Characterization Tests

The radionuclide inventory of commercial spent nuclear fuel depends upon the initial enrichment of uranium-235 and burnup. Burnup is determined by the total neutron fluence to which the fuel was subjected and thus depends on both the total time the fuel is in the reactor and the location of the fuel within the core during its irradiation history. The burnup of a given rod varies both axially and radially, with the highest burnup at the central height and at the fuel pellet periphery. Modern core management techniques allow for a fairly uniform axial burnup profile, the exception being at the ends of the rods.

The fuels used in waste form tests have been extensively characterized prior to testing (Guenther, Blahnik, Jenquin et al. 1991; Guenther, Blahnik, Campbell, Jenquin, Mendel, and Thornhill 1988; Guenther, Blahnik, Campbell, Jenquin, Mendel,

Thomas, and Thornhill 1988, 1991). This characterization includes electron and optical microscopy (scanning electron microscopy, transmission electron microscopy, ceramography), X-ray diffraction, and, most importantly, radionuclide inventory determination. The burnup and inventory determination procedures follow the approved radiochemical and analytical methods in appropriate American Society for Testing and Materials standards. These procedures are well developed and have validated the codes used to predict burnup and inventory.

4.2.6.2.2 In-Package Chemistry Tests

Most testing relevant to in-package chemistry has considered the role of heat and the interaction of water chemistry and waste form degradation, although recent testing has also included interaction of water with drift gases, waste package materials, and engineered barrier system materials (see Sections 4.2.2 through 4.2.4). The tests with waste forms and radionuclides are summarized in Sections 4.2.6.2.3 through 4.2.6.2.7.

4.2.6.2.3 Cladding Degradation Tests

Zirconium was initially used in the chemical industry to handle extremely corrosive liquids and gasses. The experimental bases for this are discussed by Yau and Webster (1987). Zirconium alloy (Zircaloy) was introduced as a nuclear fuel cladding material in the late 1950s because of its corrosion resistance and neutron absorption characteristics. Extensive research has been continuous since that time as the nuclear industry has been driven to limit fuel defects and increase fuel longevity. Cladding degradation tests are published at regular intervals in publications such as *Zirconium in the Nuclear Industry* (published by the American Society for Testing and Materials every two and a half years), *Proceedings of the International Topical Meeting on Light Water Reactor Fuel Performance* (published by the American Nuclear Society every 3 years), and *Journal of Nuclear Materials* (published monthly by Elsevier Science), as well as in many other publications. As an example of the extent of data available, an International Atomic Energy Agency document summarizing waterside corrosion cites 538 sources

on corrosion (IAEA 1998, pp. 281 to 309). The TSPA-SR cladding degradation model is based on cladding tests reported in the open literature, as well as data collected specifically for the Yucca Mountain Project. These include tests used to generate the cladding characteristics as it is received at Yucca Mountain (CRWMS M&O 2000de), corrosion tests (CRWMS M&O 2000df), experiments on hydride effects in cladding (CRWMS M&O 2000dg), tests on wet and dry splitting of cladding (CRWMS M&O 2000dh; CRWMS M&O 2000di), and experiments on creep failures (CRWMS M&O 2000dj). In addition, there is an active dry storage testing program in Europe that is generating additional data on cladding behavior under conditions very similar to the early phases of repository placement.

4.2.6.2.4   Commercial Spent Nuclear Fuel Degradation Tests

Many tests have been performed to evaluate the mechanism and rate of degradation of commercial spent nuclear fuel under various conditions. These tests are summarized in *CSNF Waste Form Degradation: Summary Abstraction* (CRWMS M&O 2000dk). These include: oxidation tests, batch tests, unsaturated drip tests, vapor phase tests, electrochemical tests, and flow-through tests.

Oxidation Tests—Hot oxidation testing of spent fuel and uranium dioxide fragments has been done for over 40 years and is summarized in *Clad Degradation—Dry Unzipping* (CRWMS M&O 2000di). Tests have been conducted from about 200° to 360°C (390° to 680°F) using either dry baths or thermogravimetric apparatus. These tests demonstrate the influence of fuel characteristics (e.g., fission gas release, burnup, fuel type) and atmospheric variables (e.g., moisture content or radiation field) on oxidation rates and mechanisms. Results obtained by the project and those from outside laboratories are very similar, which has permitted the development of oxidation models for spent fuel and uranium dioxide. Results indicate that the oxidation rate is very temperature-dependent and too slow to be significant at temperatures expected when waste packages breach.

Batch Tests—Immersion tests were performed on segments of spent fuel rods, as well as unclad fuel particles, in both deionized water and J-13 well water. The fuel rod segments were fitted with watertight end fittings. Small holes were laser-drilled through the cladding of one, a slit was machined in one, and another was tested intact. In a fourth experiment, unclad fuel particles removed from the cladding plus the cladding hull sections were immersed. The tests were semi-static in that they were run for several months, solutions removed and analyzed, and the vessel walls were acid stripped to recover any deposited radionuclides. Tests were performed at both 25° and 85°C (77° and 185°F). These tests showed that secondary phases form on the surface of the reacting fuel, colloidal sized particles form in solution, the concentration of most dissolved actinides remained quite low, and the release rate of actinides is much higher from unclad fuel than from defected clad fuel.

Unsaturated Drip Tests—To simulate dripping under repository conditions, small samples of spent nuclear fuel fragments were held within Zircaloy or stainless steel cups with screens on both ends. The cups were held within the top of a sealed stainless steel autoclave-like vessel, and water was dripped over the samples at controlled rates and collected in a catch basin below. The tests were performed at 90°C (194°F) to maximize the reaction rates, and J-13 water was equilibrated with tuff rock at 90°C (194°F) prior to use. Both low and high drip rate tests were conducted to cover a range of possible repository dripping rates. Solutions from the bottom of the test vessels were collected and analyzed about every six months for both dissolved and colloidal materials. In addition, small samples of the reacted fuel were removed for detailed analysis. Tests on several different fuels, as well as uranium dioxide fragments, have been ongoing since 1992. These tests have provided information on the forward dissolution rates, chemistry of water interacting with fuel, the sequence of alteration products, and concentrations of dissolved and colloidal species under dripping conditions. The alteration phases are similar to those observed in the corrosion of natural uraninite deposits, indicating that the experimental results are indeed relevant to long-term behavior.

Vapor Phase Tests—The configuration for the vapor phase tests was similar to the unsaturated drip tests and was designed to study the degradation of fuel that is not directly contacted by flowing water but exposed to 100 percent relative humidity. Small amounts of water were introduced into the collection basin of the vessels, which were placed in ovens and heated to the test temperatures, usually around 200°C (390°F) to accelerate the reactions. The water evaporated from the collection basin and condensed on the waste forms. Alteration of the test samples and transport of radionuclides to the collection basin was observed, although much less than in the drip tests. It is believed that thin-film flow and waste form and secondary product spallation were the mechanisms of transport.

Electrochemical Tests—Electrochemical tests with spent nuclear fuel are similar in concept to tests performed with metallic materials. An electrochemical cell is established between a corroding electrode (a spent fuel or uranium dioxide pellet) and a noncorroding (e.g., platinum) electrode in an electrolyte, under an impressed voltage. The current passed between the electrodes is measured over time. This information can then be utilized to establish the oxidation state of the spent fuel or uranium dioxide surface and the dissolution rate as a function of the voltage and water chemistry in relatively short-term experiments. These tests shed light on the dissolution process and provide the basis for understanding aqueous attack of these materials.

Flow-Through Tests—Flow-through tests were designed to measure the fundamental spent fuel dissolution/oxidation rates. Under the stagnant or slow flowing conditions of the other tests, secondary phases precipitate on the surface of the reacting fuel, which complicates the interpretation of results. In flow-through tests, the water is flowed over the reacting surfaces fast enough to prevent saturation and precipitation of secondary minerals. These tests provide the fundamental forward dissolution rate at the given tests conditions. These tests were performed on many fuel types (burnup 0 through 70 GWd/MTHM), at many laboratories, under many conditions (21° to 75°C [70° to 167°F], pH of 3 to 10, various carbon

dioxide and oxygen pressures). These tests have provided the mechanistic and empirical basis for the fuel dissolution rate model.

From the many experiments performed (CRWMS M&O 2000dk), an understanding of the mechanisms of spent nuclear fuel dissolution has emerged. Commercial nuclear fuel is composed primarily of uranium dioxide which, when exposed to mildly oxidizing solutions, is oxidatively dissolved to uranyl ion, UO_2^{2+}. The rate of uranium dioxide oxidation depends on the interaction of specific surface species that control the rate-determining dissolution step. The increase in commercial spent nuclear fuel degradation rates with decreasing pH (at low pH), and with increasing carbonate levels (at high pH), suggests that adsorbed protons and/or carbonate ions control the dissolution reaction under flow-through conditions. Important aqueous species that might also affect dissolution rates are calcium and silicon ions, which can form stable corrosion products possessing low solubilities.

4.2.6.2.5   Tests on Vitrified High-Level Radioactive Waste

High-level waste glass currently being tested includes mock and real radioactive glasses from the Savannah River (South Carolina) Technology Center and the West Valley (New York) Demonstration Program. Glass compositions corresponding to those expected from the Hanford Site high-level waste glass program will be tested when they become available. Because glass degradation is quite slow, various methods have been used to elucidate mechanisms and rates under fully saturated conditions:

- Testing at elevated temperatures, which accelerates reaction rates

- Testing at high surface-area-to-volume ratios, which accelerate rates proportionally to the exposed surface area of the glass

- Flow-through tests and closed-system tests.

Like the flow-through tests of spent nuclear fuel, the glass flow-through tests were designed to

prevent secondary phase formation and measure the forward dissolution rate over a range of conditions that bounded anticipated repository conditions (CRWMS M&O 2000dl).

Parallel efforts have also been undertaken to better calibrate glass dissolution mechanisms. The results of standard static leaching tests based on ASTM C 1220-98, *Standard Test Method for Static Leaching of Monolithic Waste Forms for Disposal of Radioactive Waste*, have been compared to the measurements of glass surface chemistry to link glass surface chemistry and dissolution mechanisms. Measured dissolution rates have been compared against long-term glass degradation rates measured on geologic samples. Lastly, two types of nonsaturated glass degradation experiments were done to examine degradation under conditions that might exist upon waste package breach: drip tests and vapor hydration degradation.

4.2.6.2.6 Tests on U.S. Department of Energy Spent Nuclear Fuel and Other Waste Forms

The National Spent Nuclear Fuel Program has been conducting degradation testing on several of the DOE spent fuel types. To date partial test results are available only on N Reactor and uranium–aluminum spent nuclear fuel, but testing on mixed-oxide spent nuclear fuel is also underway. The preliminary N Reactor spent nuclear fuel results indicated that dissolution rates were significantly faster than that of commercial spent nuclear fuel and high-level waste glass, whereas the uranium–aluminum spent nuclear fuel showed dissolution rates lower than for the commercial spent nuclear fuel and high-level radioactive waste glass. Differences could also exist in neptunium solubility, colloid formation, and radionuclide transport through and out of the engineered barrier system. However, for the TSPA-SR, bounding values have been used. Details of this analysis are provided in Section 4.2.6.3.

4.2.6.2.7 Solubility Tests

The solubilities of a number of radionuclide-bearing solids were measured as a function of fluid composition and temperature. These measurements were used to update thermodynamic databases describing radionuclide stabilities. This in turn involved performing critical reviews of the thermo-chemical literature and reliance on international efforts (e.g., the Nuclear Energy Agency of the Organization for Economic Cooperation and Development) to develop internally consistent thermodynamic databases.

Uranium—Uranyl (UO_2^{2+}) minerals are expected to precipitate under the oxidizing conditions likely to prevail when breached waste packages are initially altered by incoming fluids. Laboratory experiments and field observations suggest that the most common secondary uranyl minerals to form at low temperatures are schoepite, soddyite, uranophane, and/or sodium boltwoodite.

Neptunium—Neptunium solubilities in Yucca Mountain waters as a function of pH and temperature have been described by Nitsche et al. (1993). Efurd et al. (1998) measured neptunium solubilities up to approximately pH 8 in carbonate-containing media and up to approximately pH 12 in carbonate-free systems. Results of the neptunium solubility experiments from both over- and under-saturation were found to converge to approximately the same steady-state concentrations. With increasing temperature, a slight decrease in solubility is observed at pH 7 and 8.5, while at pH 6 the neptunium solubility remains approximately constant. The soluble neptunium concentrations are similar at pH 7 and 8.5, while at pH 6 the solubility is about one to two orders higher depending on the temperature. Note that although neptunium dioxide is expected to be the most stable neptunium-bearing phase, it has only rarely been observed to precipitate in laboratory experiments, presumably because kinetic obstacles prevent its nucleation and growth over short periods of time.

Plutonium—Plutonium solubility was studied by Efurd et al. (1998) only from oversaturation. In general, plutonium is about three orders of magnitude less soluble than neptunium, and pH does not affect the soluble concentration as much as seen in the neptunium solubility studies. Increasing temperature decreases the plutonium solubility below 10^{-8} mol/L. The plutonium concentrations at 60°C (140°F) and 90°C (194°F) are pH indepen-

dent, while at 25°C (77°F) they show higher variability. The plutonium precipitates were dark green in color, which is characteristic of plutonium (IV) solid phases, and plutonium hydroxides and/or plutonium colloids, aging toward $PuO_2 \cdot xH_2O$, are interpreted to be the solubility-controlling solids. Since the crystalline phase forms within the laboratory time scale, it is reasonable to assume that over geological time, plutonium hydroxides will convert to plutonium dioxide. However, α-decay of plutonium isotopes has been observed to decrease the crystallinity of plutonium dioxide, while at the same time plutonium hydroxide can gradually convert to anhydrous, though poorly crystalline, material.

Americium, Actinium, Curium, Samarium— Nitsche et al. (1993) showed that $AmOHCO_3$ precipitates from J-13 water at a pH range from 5.9 to 8.4, and temperatures from 25° to 90°C (77° to 194°F), and is therefore the most likely phase to control americium solubility. Additional americium thermodynamic data has been developed by the Nuclear Energy Agency.

Technetium, Carbon, Chlorine, Iodine, Cesium, and Strontium—Under the conservative assumption of oxidizing repository conditions, laboratory measurements and thermodynamic analysis indicate that no insoluble salts of technetium, chlorine, iodine, or cesium form. Each forms relatively large monovalent ions in solution that are exceedingly soluble. Therefore, the solubility of each is set to 1.0 mol/L, which will let the waste inventory control their respective release. Carbon and strontium both form less soluble metal carbonate minerals—either pure-phase or solid solution. An involved prediction of carbon and strontium solubility was not done. Instead, the solubility for each was set to 1.0 mol/L, which will let the waste inventory control release.

4.2.6.2.8   Colloid Tests

Colloid testing has focused on spallation (i.e., flaking) of colloids from glass, the stability and abundance of smectite colloids, and sorptive uptake and release of actinides from colloidal material. Long-term tests done with high-level waste glass (CRWMS M&O 2000dl) indicate that

colloids are produced through spallation of altered glass at the glass–water interface. The colloids are primarily smectite clay that contain discrete radionuclide-bearing phases incorporated ("entrained") into the clay. Some iron silicate colloids are also observed. Several entrained actinide and rare earth-containing phases were identified, including brockite (thorium calcium orthophosphate) and an amorphous thorium-titanium-iron silicate similar to thorutite. Uranium was detected within the clays and iron silicates in some samples.

The entrained phases are often engulfed in a smectite clay substrate, and the properties of the latter are such that the entrained phases are expected to destabilize only at pH of about 2. Since a pH this low is not anticipated in the repository, smectite colloids are expected to remain stable under repository conditions. Smectite colloids become increasingly sensitive to ionic strength as pH drops below about 8 (Tombacz et al. 1990).

During static glass dissolution tests, colloids developed and increased in concentration with time up to a point where the colloid concentration reached a maximum and then became unstable. This was attributed to the ionic strength increasing to a threshold above which the colloids precipitated and agglomerated. These data provide an experimental basis for evaluating the ionic strength regimes in which the waste form colloids are stable or unstable.

Sorption of plutonium (IV) and plutonium (V) onto colloidal dispersions of hematite, goethite, montmorillonite, and silica was measured over time periods of 4 to 10 days. Information on americium (III) was also collected for the same minerals—except goethite. The observed ranges of the adsorption coefficients (K_d) are generally consistent with those found in the literature. Experimental evidence from plutonium sorption experiments (CRWMS M&O 2000cn, Section 6.1.3) with colloidal hematite and goethite show that the rate of desorption (backward rate) of plutonium is significantly slower than the rate of sorption (forward rate). More importantly, over a significant time period (up to 150 days in some experiments), the extents of desorption is somewhat less than the extent of sorption.

Groundwater colloids may include those already present in the geosphere, such as microbes, organic macromolecules (humic substances, including humic and fulvic acids), and mineral colloids (primarily clay minerals, silica, and iron-oxide or iron-hydroxide minerals). Microbe-facilitated radionuclide transport is disregarded because the relatively large size of microbes makes them susceptible to filtration. Experimental studies indicate that Yucca Mountain humics possess a very low complexation capability. Mineral colloids present at the site are assumed to consist of smectite clays, which are fairly strong sorbers.

4.2.6.3   Process Models

This section provides a description of the individual process models and the interfaces between them. It builds upon the overall concepts described in Section 4.2.6.1 and the summary state of knowledge given in Section 4.2.6.2. The components of the waste form degradation model are shown in Figure 4-97. The inputs to the waste form degradation models include the waste package design and the drift environment as a function of time.

4.2.6.3.1   Inventory Modeling

In TSPA modeling of repository performance, it is important to have good estimates of the initial inventory for all radioisotopes important to human dose. These estimates are provided by the fuel and waste generators using records of reactor and reprocessing operations, burnup calculations and experimental validation of calculations.

Fuel burnup at any location along a fuel rod can be accurately calculated using complex, multidimensional neutronics codes. Simpler and more general calculations of burnup and inventory are performed using the ORIGEN (ORIGEN, ORIGEN-2, and ORIGEN-S) code, which uses experimental data to develop burnup-dependent neutron cross sections. ORIGEN is used to compute time-dependent concentrations of numerous radionuclides that are both generated and depleted through neutronic transmutation, fission, and radioactive decay. ORIGEN is a point depletion (i.e., no spatial dependence) model where the neutron cross section data and spectral parameters are averaged over the spatial region of interest, making these codes valuable for rod- or assembly-average inventory calculations.

Validation of the ORIGEN codes within the limiting conditions (burnup, enrichment, etc.) of each neutron cross section library has been performed by comparing the code output with both project-generated and literature data. Results are usually well within 10 percent for measured fuel actinide and fission product data; some of the higher-order actinides have predicted results that differ by 15 to 25 percent with measured results (Parks 1992). Larger discrepancies for the radionuclides of importance to the repository are most often explained by large analytic uncertainties or sample preparation. ORIGEN has been shown to predict radionuclide inventories with reasonable accuracy. Continuing verification of additional approved test materials with predictions is performed whenever a new fuel is subjected to testing.

4.2.6.3.2   In-Package Chemistry Model

Outputs of the in-package chemistry model, such as pH and ionic strength, are used as inputs by several other models (see Figure 4-97) that describe processes that depend on the chemistry of in-package fluids. The latter include the degradation of cladding, the degradation of the matrix of the waste forms, the dissolved concentration of radioisotopes, and the stability of colloids. The in-package chemistry model is summarized in *Waste Form Degradation Process Model Report* (CRWMS M&O 2000bm) and described in detail in *Summary of In-Package Chemistry for Waste Forms* (CRWMS M&O 2000dm).

The in-package chemistry model component estimates over time the fluid chemistry inside the waste package after the initial breach of the waste package. In-drift solutions seeping into breached waste packages would contact several materials whose reaction rates and effective reaction surface areas are imprecisely known (see Figure 4-98). These materials include waste forms and waste package internal structures, such as canisters, baskets, and heat conductors. Waste forms include uranium dioxide fuel within Zircaloy cladding;

DOE spent nuclear fuels, such as graphite, mixed plutonium–uranium oxides, uranium metal, and thorium oxides; and high-level radioactive waste glass or ceramic. Waste package internals include aluminum alloy, Type 316L and 304L stainless steels (with and without neutron absorbers, such as boron or gadolinium phosphate), A516 low-carbon steel, and Alloy 22. Other uncertainties affecting the in-package chemistry modeling include flow rates and chemical composition of water and drift gases entering the package. To encompass the accumulated uncertainties, many of the input parameters used in the model were sampled from broad ranges or conservatively bounded. In particular, clad coverage and water flow rates were varied orders of magnitude. Partial pressures of carbon dioxide and oxygen were conservatively set to 10^{-3} and $10^{-0.7}$ bar respectively.

As described in *Summary of In-Package Chemistry for Waste Forms* (CRWMS M&O 2000dm), simulations of waste package and waste form alteration by ambient groundwater were done using the qualified reaction path code EQ3/6 (CRWMS M&O 1998h; CRWMS M&O 1999n), which titrates masses of waste package and waste form components at a rate determined by input reaction rates and fluid influxes into the breached waste package. EQ3/6 estimates the elemental composition of the reacting fluid for the duration of the reaction path calculation while at the same time providing estimates of the nature and masses of secondary phases that are predicted to form. The code cannot predict kinetic inhibitions, which must instead be done on the basis of expert judgment. Moreover, the code cannot account for local nonequilibrium effects such as galvanic coupling or radiolysis.

Table 4-18 summarizes the range of in-package fluid compositions predicted to occur for both the waste package types.

Table 4-18. Range of In-Package Fluid Compositions

Variable	Commercial Package	Codisposal Package
pH	3.6 to 8.1	4.8 to 10.0
Ionic Strength	0.003 to 1.7	0.003 to 5.8
Carbon	2.8×10^{-5} to 0.002	3.5×10^{-5} to 0.5

NOTES: Measurements given in mol/L for all except pH.
Source: CRWMS M&O 2000dm, Table 3.

For the waste packages containing spent nuclear fuel, the in-package chemistry model predicts a decrease in pH, caused by dissolution of low-carbon steel, followed by a subsequent rise in pH due to the dissolution of commercial spent nuclear fuel, the oxidation of aluminum alloy, and the inflow of additional water. The lowest predicted pH levels are those calculated for the least amount of clad failure, as shown in Figure 4-100. Yet the bulk pH is not expected to go low enough to cause significant increases in clad failure rates. Under the bounded fixed carbon dioxide conditions assumed for the simulations, carbonate levels are relatively high at high pH and low at low pH. Because both uranium and plutonium form soluble complexes with carbonate, the dissolved levels of each tend to increase at high pH and decrease at neutral pH. However, the lowest pH levels occur in the early stages of the reaction paths, before appreciable amounts of uranium or plutonium have been dissolved from the commercial spent nuclear fuel matrix.

In the codisposal simulations (Figure 4-101), the moderately alkaline pH of the input solution prevails initially, then progresses towards a minimum, primarily due to the oxidation of the A516 carbon steel (degradation of fast flux test facility waste packages was modeled to bound degradation of codisposal waste packages). The high specific rate and relatively high surface area of the latter mean that its dissolution tends to dominate the whole reaction path, at least as long as it remains (oxidation of sulfur in the steel to sulfate is the primary proton-producing reaction). After the steel is exhausted, dissolution of base cation-containing high-level radioactive waste glass leads to increased pHs. pHs as high as 10 and ionic strengths as high as about 5.8 mol/L were predicted for codisposal waste packages under conditions of high glass dissolution and low flow rates. At ionic strengths greater than about 0.7 mol/L, the calculations are less accurate than for dilute systems. Because the solubilities of many minerals do not appear to depend strongly on ionic strength at and above this range, the lack of exactness does not prevent the results from providing useful bounding ranges of fluid chemistry (CRWMS M&O 2000dm).
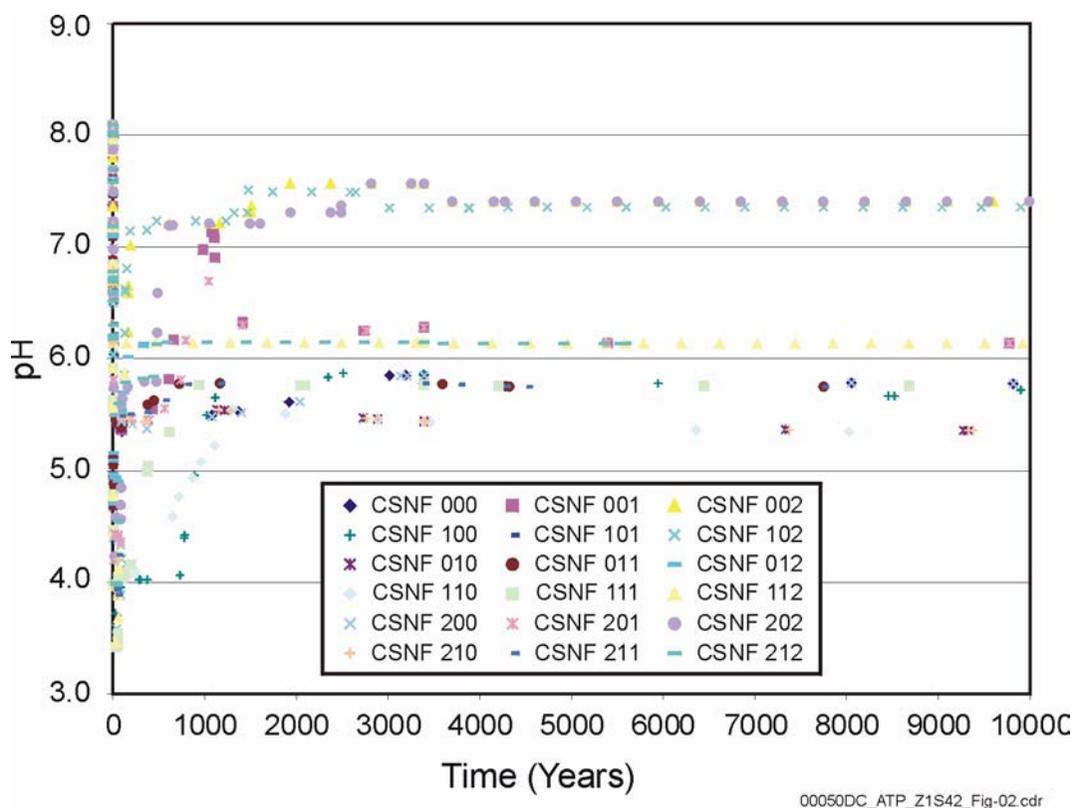
Figure 4-100. pH History for Commercial Spent Nuclear Fuel Process Model Calculations
The numbers in the legend indicate individual calculation runs. For details, see *In-Package Chemistry Abstraction* (CRWMS M&O 2000dn). Source: CRWMS M&O 2000bm, Figure 3.2-3.

Since the completion of the TSPA-SR models, the DOE has developed additional information to further understand and quantify uncertainties associated with the in-package chemistry models. Uncertainties in the in-package chemistry models include those associated with steel and glass degradation rates, oxygen fugacity, in-package sorption, and choice of solubility limiting phase. In the TSPA-SR models, the DOE utilized bounding approximations or conservative inputs for these processes. Since completion of the TSPA-SR analyses, a series of sensitivity studies were performed to assess the impact of uncertainty with these processes on repository performance. Volume 1, Section 9.3.1 of *FY01 Supplemental Science and Performance Analyses* (BSC 2001a) provides detailed discussions of the additional studies, specifically the investigation of the impact on pH–time trajectories from lower degradation rates of

glass and steel. The lower-temperature operating mode is reflected in the model because the degradation rates and themodynamic data were developed for ambient temperature conditions (25°C [77°F]).

Since the completion of the TSPA-SR models, an updated in-package chemistry model was developed to provide a sensitivity study on the effect of input fluid chemistry on calculated reaction paths (i.e., the likely variation in major-element composition of in-package fluids), to provide a sensitivity study on the effect of different partial pressures of oxygen and carbon dioxide on reaction paths, and to provide a formal examination of the potential for radiolysis-induced corrosion on spent fuel rod cladding. Results of these sensitivity studies are discussed in detail in *In-Package Chemistry for Waste Forms* (BSC 2001p) and are included in
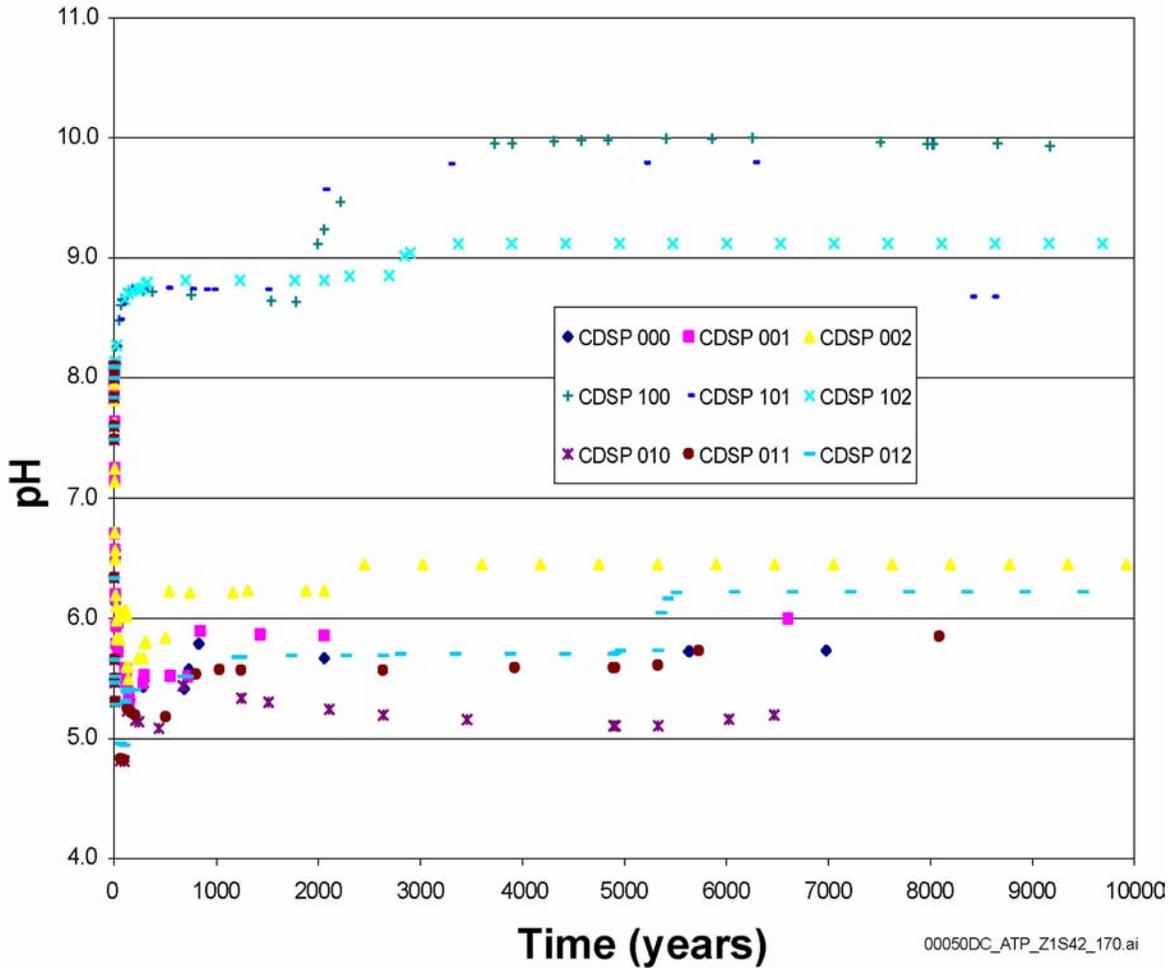
Figure 4-101. pH History for Codisposal Process Model Calculations
The numbers in the legend indicate individual calculation runs. For details, see *In-Package Chemistry Abstraction*
(CRWMS M&O 2000dn). Source: CRWMS M&O 2000bm, Figure 3.2-4.

Volume 1, Section 9 of *FY01 Supplemental Science and Performance Analyses* (BSC 2001a). This additional work has provided additional confidence that the models used in the TSPA-SR analyses are reasonable.

4.2.6.3.3   Cladding Degradation Model

Since the 1950s, most commercial spent nuclear fuel has been clad with less than 1 mm (0.04 in.) — usually between 600 through 900 μm (0.024 through 0.035 in.)—of Zircaloy, an alloy that is about 98 percent zirconium with small amounts of tin, iron, nickel, and chromium. The Zircaloy cladding is not a designed engineered barrier of the

Yucca Mountain disposal system; rather it is an existing characteristic of the commercial spent nuclear fuel important to determining the rate of release of radionuclides once engineered barriers such as the waste package have breached. Zircaloy is very resistant to corrosion, and cladding failure is expected to be minimal in the first 10,000 years. However, while Zircaloy provides excellent protective properties, characterization of the uncertainty in its performance is important. This characterization is possible because data has been collected on its performance over the past 40 years by the nuclear industry and by others in several different harsh environments.

The cladding degradation model predicts the rate at which the commercial spent nuclear fuel matrix is exposed and altered based on the number of rods with perforated cladding at any one time. The technical basis for the model is summarized in *Waste Form Degradation Process Model Report* (CRWMS M&O 2000bm) and described in more detail in the following analysis and modeling reports:

- *Clad Degradation—Summary and Abstraction* (CRWMS M&O 2000dj)

- *Initial Cladding Condition* (CRWMS M&O 2000de)

- *Clad Degradation—Dry Unzipping* (CRWMS M&O 2000di)

- *Hydride-Related Degradation of SNF Cladding Under Repository Conditions* (CRWMS M&O 2000dg)

- *Clad Degradation—FEPs Screening Arguments* (CRWMS M&O 2000do)

- *Clad Degradation—Wet Unzipping* (CRWMS M&O 2000dh)

- *Clad Degradation—Local Corrosion of Zirconium and Its Alloys Under Repository Conditions* (CRWMS M&O 2000df).

The conceptual model for the degradation of commercial spent nuclear fuel cladding is shown in Figure 4-102. Cladding degradation is assumed to proceed through two distinct steps: (1) rod failure (perforation of the cladding) and (2) progressive exposure of uranium dioxide spent fuel matrix from tearing of the cladding.

In the TSPA-SR model, perforation of the cladding may occur because (1) the cladding initially fails within the reactor or during storage, (2) the cladding fails from creep or stress-corrosion cracking, (3) an earthquake severely shakes and severs the rods, or (4) the cladding fails from localized corrosion. Other mechanisms of initiating cladding perforations, such as diffusion controlled cavity growth or delayed hydride cracking, were specifi-cally evaluated using features, events, and processes screening analyses and were screened out based on either low consequence or low proba-bility (CRWMS M&O 2000do).

Local corrosion was included because corrosion of zirconium has been observed in concentrated fluo-ride or chloride solutions at very low pHs or very high oxidation potential (CRWMS M&O 2000df, Section 4.1). These conditions are not predicted to occur in the bulk solution (see Section 4.2.6.3.2) but have not yet been ruled out for localized or nonequilibrium effects such as microbially influ-enced corrosion, galvanic coupling, radiolysis in a humid environment, and extreme concentration by evaporation. Each of these mechanisms may locally depress the pH or increase the concentra-tion of corrosive species such as fluoride or chloride, at least temporarily. None of these condi-tions is expected to impact cladding performance under repository conditions. However, until they can be ruled out or shown to be too transitory to have negative consequences on cladding, a conser-vative model that includes local corrosion mechanisms will be used to bound the uncertainty associated with cladding corrosion.

The localized corrosion model is just one example of the conservative models included in TSPA to bound the uncertainty of cladding performance (CRWMS M&O 2000dj). For each of the cladding perforation mechanisms assumed in the TSPA-SR, conservative bounding estimates were generated for the number of cladding failures, their timing, and their character. These estimates were based upon one or more of the following: analyses of data from decades of reactor operations for fuel handling and wet and dry storage; fuel perfor-mance reports; analytical methods and assumptions previously used in licensing of storage or transpor-tation designs; interim guidance from the NRC; corrosion studies; and experiments reported in the literature.

The release of radionuclides does not occur until after the waste package fails and air and water can enter the waste package. The release occurs in two stages, fast release of immediately accessible radi-onuclides followed by slower release as the matrix degrades.
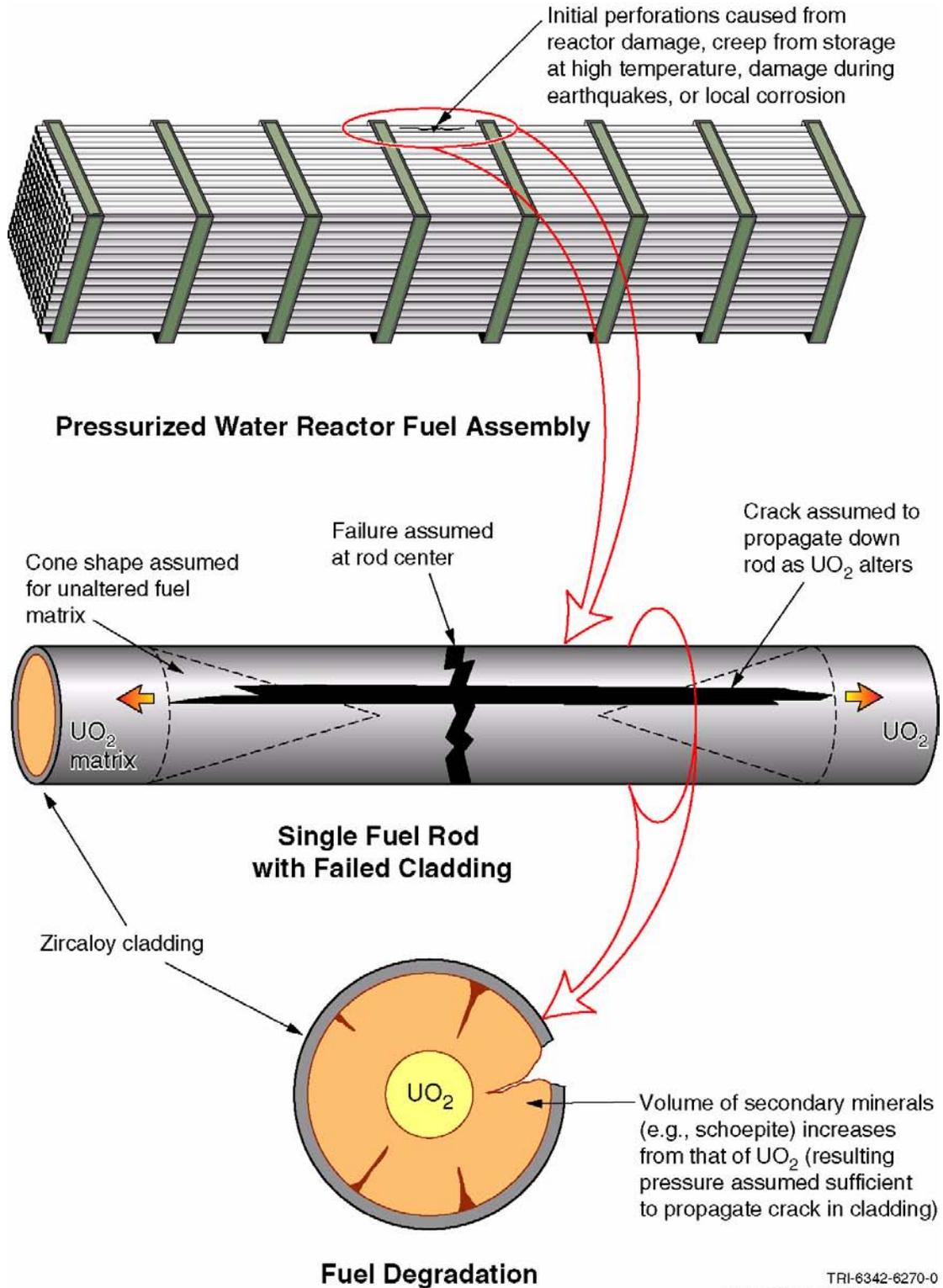
Figure 4-102. Conceptual Model of Commercial Spent Nuclear Fuel Cladding Degradation
Source: CRWMS M&O 2000bm, Figure 3.8-2.

Fast release refers to the inventory of radionuclides that are in the gap between the fuel pellets and the cladding (gap inventory) and the radionuclides at the grain boundaries of the spent nuclear fuel matrix. A small percentage of the inventory of iodine, cesium, and a few other radionuclides resides in the gap between the cladding and waste matrix. For the TSPA-SR, the release of the gap inventory is conservatively assumed to be instantaneous when the cladding is perforated and, thus, independent of the cladding tearing. Cladding that was initially perforated releases the gap inventory when the waste package is breached. The inventory of the radionuclides in the grain boundaries is also released quickly.

As water and air enter the fuel rods, they slowly react with any available exposed spent fuel surfaces. This may include a gap between the fuel and cladding and cracks through the fuel pellets. Under slow flow or unsaturated conditions, secondary phases precipitate at the reaction front. The phases that precipitate depend on the water chemistry, but metaschoepite has been used as representative phase. As these phases precipitate, they will fill the void spaces within the fuel and may exert force outward force on the fuel cladding. If there is sufficient force, the cladding may tear open in a process called "unzipping." Unzipping has been observed under dry, high-temperature, oxidizing conditions but has not been observed in failed fuel rods under wet conditions outside of the reactor. A wet unzipping model has been developed based on analogy to dry unzipping (CRWMS M&O 2000dh). This model predicts that hundreds of years are required for the void spaces to be filled and for unzipping to start. During this time, a small faction of the matrix is predicted to react, and the radionuclides contained within this matrix are assumed to be released instantly along with the other fast releases.

Wet unzipping is modeled to start at waste package failure for rods perforated prior to waste package failure or to start when rod perforation occurs if after waste package failure. The fuel matrix is modeled to dissolve at the intrinsic dissolution rate for the predicted temperature and in-package chemistry and precipitate as metaschoepite. The volume increase is modeled to split the cladding,

exposing more of the spent nuclear fuel matrix as the cladding unzips along its length. The reaction region is conservatively assumed to be cone-shaped based on experimental observations of dry unzipping, and it is assumed that the perforation is in the center of the rod. The unzipping is modeled to propagate along the rod at a rate approximately 40 times (range 1 to 240 times) as fast as the intrinsic dissolution rate discussed in Section 4.2.6.3.4. This results in most sampled unzipping times greater than 10,000 years. The long time periods associated with unzipping mean that cladding contributes to a significant delay in radionuclide release from the commercial spent nuclear fuel waste form.

The anticipated temperature of the fuel matrix is not high enough, nor do the high temperatures occur for a long enough period, to cause unzipping in a dry environment, so dry unzipping is not included in the TSPA-SR. Based on observed behavior within storage pools at reactors, unzipping in a wet environment does not occur in observed time periods of 40 years once the Zircaloy cladding has been perforated. However, these observations are not sufficient to entirely rule out the possibility of a wet environment unzipping process. By including in the TSPA-SR the possibility of the clad unzipping in a wet environment, the assumed complete exposure of the fuel matrix conservatively bounds diffusive releases of radionuclides through the perforations. Exposure of the spent nuclear fuel is evaluated through a hypothetical but bounding rate of unzipping of the cladding such that the entire inventory of radionuclides can eventually be exposed over sufficient time.

Since the completion of the TSPA-SR analysis, the DOE has developed additional information to further understand and quantify uncertainties associated with the cladding model. Uncertainties exist related to the fraction of cladding perforated because of creep rupture and stress corrosion cracking, the localized corrosion rate, the potential for mechanical damage (seismic and rock overburden), and the unzipping velocity of the cladding. In the TSPA-SR models, the DOE utilized bounding approximations or conservative inputs for these processes. Volume 1, Section 9.3.3 of *FY01 Supplemental Science and Performance*

Analyses (BSC 2001a) provides detailed discussions on how the sensitivity model reduced uncertainties by utilizing the more realistic approach for many aspects of the cladding model. The behavior of cladding within the repository is not expected to differ significantly between a lower- and higher-temperature operating mode as long as the cladding temperature limit of 350°C (660°F) is not exceeded (BSC 2001a, Section 9.3.3).

4.2.6.3.4 Commercial Spent Nuclear Fuel Degradation Model

The commercial spent nuclear fuel degradation model is important to TSPA because it predicts the rate at which soluble isotopes important to humans dose (e.g., technetium-99) become available for transport and release. *CSNF Waste Form Degradation: Summary Abstraction* (CRWMS M&O 2000dk) documents the development of this semi-empirical model from flow through test data, and the validation of the model by comparison to other test data and natural analogues. Because it directly relies upon only the flow through tests, which give upper limits to the actual dissolution rates, this model is a bounding one, and has been validated as such.

Figure 4-103 shows the predicted rate of degradation of the fuel rate in mg/(m^2·day) as a function of temperature and pH for the oxygen and carbon
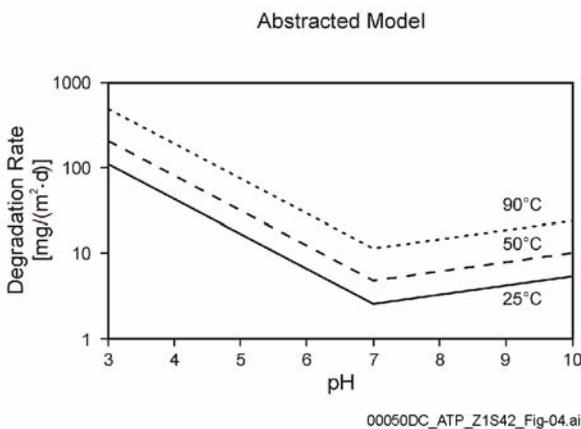
Figure 4-103. Abstracted Degradation Rates for Commercial Spent Nuclear Fuel
Source: CRWMS M&O 2000dk, Figure 2.

dioxide partial pressures used in the TSPA calculations. This model uses two linear regression equations based on pH, the partial pressures of oxygen and carbon dioxide, and temperature. One equation is applicable for pH less than or equal to 7 and another for pH greater than 7. Considering the uncertainty of the applicability of data from young spent nuclear fuel (less than 30 years out of reactor) and unburned uranium dioxide toward the prediction of long-term (greater than 1,000 years) performance of spent fuel, the dissolution model was estimated to be valid to within 1.5 orders of magnitude. Comparisons of the abstracted dissolution model for commercial spent nuclear fuel with long-term unsaturated drip tests, batch tests, and literature results provide confidence that the model adequately accounts for all dissolution rates and provides conservative overestimates of dissolution rates for use in the TSPA-SR. In addition, a comparison of the phases produced in the unsaturated drip tests compare well with that of the natural analogue at Nopal I, a uranium mining site at Peña Blanca, Mexico (CRWMS M&O 2000dk, Section 6.6). This site is one of the best natural analogues for spent fuel degradation in Yucca Mountain because it contains substantial quantities of uraninite in a geologic, geochemical, and hydrogeologic setting similar to Yucca Mountain. Overall, the phase assemblage observed at Nopal I is similar to that derived experimentally in the commercial spent nuclear fuel alteration drip tests. The general agreement between the observed alteration products in the various tests, the natural analogues, and the geochemical modeling provide confidence that the mechanisms of spent nuclear fuel corrosion are well understood and that the forward dissolution model is bounding for long-term prediction of commercial spent nuclear fuel degradation rates.

4.2.6.3.5 High-Level Radioactive Waste Glass Degradation Model

The high-level radioactive waste degradation model is used to predict conservative borosilicate glass degradation rates over the range of conditions (i.e., immersion, humid air, and dripping water) expected after waste package failure. The rate of radionuclide release from high-level radioactive waste is calculated by multiplying the glass degra-

dation rate by the mass fraction of the radionuclide in the glass. Although much of the glass will be exposed only to humid air or dripping water conditions, a conservative bounding scenario of complete saturation is used in modeling dissolution.

The area of the glass surface available for corrosion in the disposal environment is difficult to estimate precisely. The logs of waste glass will crack within the pour canister due to thermal and mechanical stresses generated as the glass cools and as the waste form is handled, ultimately increasing the total surface area available for contact with water. The key differences between the dissolution rates of the glass within cracks and at the outer surface are the transport rates of reactant and products, respectively, into and out of the crack. Surface-area-normalized dissolution of fractured glass is therefore sometimes found to be slower than that of nonfractured glass. The conservative, bounding approach that has been followed assumes they are equal (CRWMS M&O 2000dl, Section 6.1.2).

The rate expression for high-level waste glass degradation contains two main parts: a forward reaction rate term, which represents the dissolution rate in the absence of feedback effects of dissolved silica (and other aqueous species), and a reaction affinity term $(1-Q/K)$, which quantifies the feedback effects. Q represents the concentration of dissolved silica in the solution, in units of mass/volume, while K represents the quasi-thermodynamic fitting parameter equal to the apparent silica saturation concentration for the glass, in units of mass/volume. The dissolution rate will decrease as the value of the affinity term decreases (i.e., as the value of Q approaches K) until a minimum rate is reached (CRWMS M&O 2000dl, Section 6.1.1).

Corrosion proceeds in three stages:

- **Stage I**—The value of the affinity term is one, and glass dissolves at the forward rate for the specific temperature and pH conditions involved. Stage I will not occur when glass is contacted by groundwater containing high levels of dissolved silica (from the dis-

solution of minerals present in the tuff rock and from the dissolution of the glass itself).

- **Stage II**—The value of the affinity term approaches zero due to the accumulation of glass components in solution. The value of the affinity term cannot become zero because glass is thermodynamically unstable; therefore, it cannot equilibrate with the solution.

- **Stage III**—The dissolution rate increases concurrently with the formation of alteration phases. The formation of alteration phases is believed to cause a decrease in the value of Q due to the consumption of dissolved silica as silica-bearing phases form.

Dissolution rates were independent of the glass composition within the limits prescribed by the high-level radioactive waste glass waste acceptance product specification (CRWMS M&O 2000dl, Section 6.2), but high-level waste glass degradation rates do depend on pH and temperature. Abstracted degradation rates are shown in Figure 4-104.

Since the completion of the TSPA-SR models, the DOE has performed additional sensitivity studies on high-level waste glass degradation rates. In the TSPA-SR models, conservative estimates of important model parameters were used to calculate degradation rates. In Volume 1 of *FY01 Supplement Science and Performance Analyses* (BSC 2001a, Section 9), the DOE utilized a more realistic treatment of glass degradation rates that resulted in slower calculated degradation. These analyses indicated that dose calculations are not highly sensitive to glass degradation rates.

4.2.6.3.6   U.S. Department of Energy Spent Nuclear Fuel and Other Waste Form Degradation Modeling

The degradation rates of all waste forms other than commercial spent nuclear fuel and high-level radioactive waste are summarized in *Waste Form Degradation Process Model Report* (CRWMS M&O 2000bm, Section 3.5). Over 250 distinct types of DOE spent nuclear fuel may be disposed in the potential repository at Yucca Mountain. The
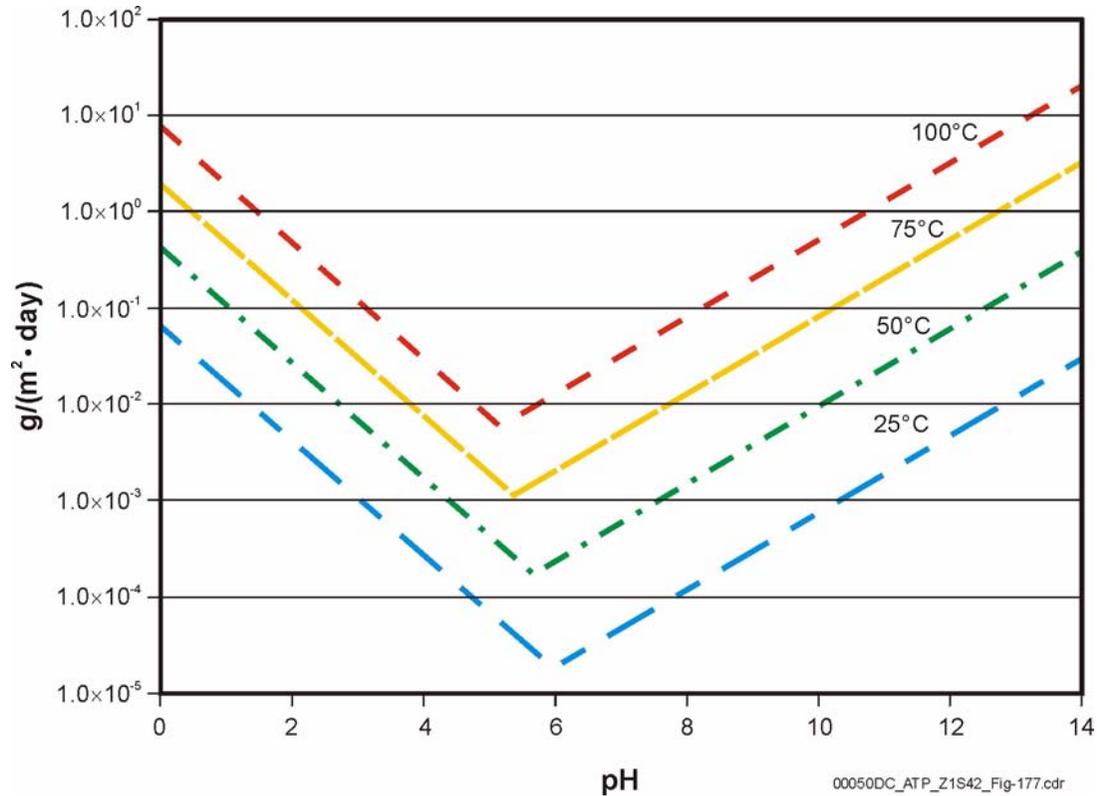
Figure 4-104. Abstracted Degradation Rates for High-Level Radioactive Waste Glass
Source: Modified from CRWMS M&O 2000bm, Figure 3.6-2.

Office of Civilian Radioactive Waste Management and the National Spent Nuclear Fuel Program have collaborated in the identification of spent nuclear fuel "groups" (CRWMS M&O 2000bm, Section 3.5) to simplify the analysis of their effects on repository preclosure safety analyses or for postclosure TSPA.

The DOE spent nuclear fuel groups are:

- Group 1—Naval spent nuclear fuel
- Group 2—Plutonium/uranium alloy
- Group 3—Plutonium/uranium carbide
- Group 4—Mixed oxide and plutonium oxide fuels
- Group 5—Thorium/uranium carbide
- Group 6—Thorium/uranium oxide
- Group 7—Uranium metal
- Group 8—Uranium oxide
- Group 9—Aluminum-based spent nuclear fuel
- Group 10—Unknown
- Group 11—Uranium-zirconium-hydride.

In addition, the immobilized ceramic plutonium waste form was also evaluated. This waste form will consist of disks of a plutonium-containing, titanium-dioxide-based ceramic that will be enclosed in stainless steel cans, which in turn will be encased in a borosilicate glass matrix within the high-level radioactive waste canisters.

Waste Form Degradation Process Model Report (CRWMS M&O 2000bm, Section 3.5) summarized three types of degradation models for the DOE spent nuclear fuel and plutonium-ceramic waste forms: upper-limit, conservative, and best-estimate, to provide the user of the models appropriate flexibility in their application to any particular postclosure performance scenario. An upper-limit model predicts release rates always well in excess of actual dissolution rate data. The conservative degradation model provides an estimate of dissolution rate that reflects the higher rate end of available dissolution data on the spent nuclear fuel groups or similar materials. A best-estimate model is appropriate only when sufficient

dissolution data exist and the characteristics of the waste form can be shown to correspond to the characteristics of the materials that provided the dissolution database. For the conservative and best-estimate models, various surrogate spent nuclear fuels were evaluated for degradation behavior. In general, the degradation rates of the oxide fuels are much lower than the metallic uranium or carbide fuels. Because the metallic uranium and carbide fuels degrade very rapidly compared to repository time scales, the TSPA results have been very insensitive to these rates. In addition, TSPA analyses have shown that the overall performance of the potential repository is driven primarily by the commercial spent nuclear fuel and high-level radioactive waste inventories. For these reasons, the conservative Hanford N Reactor fuel model (1.75 kg/m^2·day) was recommended as the surrogate to bound all the DOE spent nuclear fuel groups 2 through 11.

The best-estimate for the degradation of the immobilized ceramic plutonium is given by a titanate ceramic model, with an exposed surface area corresponding to the geometric surface area of the plutonium-containing ceramic disks. For the TSPA-SR, however, the immobilized plutonium inventory was averaged into the high-level radioactive waste inventory, and the higher rates for high-level radioactive waste degradation were used.

The application of the DOE spent nuclear fuel and other waste degradation models involves the extrapolation of the models over long periods of time, which are orders of magnitude greater than the experimental test periods used to generate the data used to derive the models. The general lack of qualified experimental dissolution and degradation data for many of the DOE spent nuclear fuel waste forms was addressed by the use of conservative degradation models for the TSPA.

One of the types of DOE-owned spent nuclear fuel to be disposed in the potential repository is naval spent nuclear fuel. There are 65 MTHM of naval spent nuclear fuel included in the base case repository design. The Naval Nuclear Propulsion Program modeled the performance of naval spent nuclear fuel with the same environmental condi-

tions used in the commercial spent nuclear fuel degradation model (Mowbray 2000).

4.2.6.3.7   Solubility Model

Doses calculated for groundwater pathways from the repository to the environment depend significantly on the concentrations of radionuclides in fluids issuing from breached waste packages. While dissolution of the waste forms is the primary source of radionuclides, formation of secondary phases often limits available levels of radionuclides for subsequent groundwater transport. The primary report supporting the radioisotope concentration model component is *Summary of Dissolved Concentration Limits* (CRWMS M&O 2000dp).

The dissolved concentration calculation builds upon three primary feeds: (1) estimates of in-package fluid major element composition (i.e., pH, Eh, ionic strength, carbonate levels); (2) measured (and estimated) thermodynamic parameters describing the stabilities of aqueous species and solid radioisotope phases; and (3) determination/estimation of solubility-controlling phases. The thermodynamic databases that were used are described in *Summary of Dissolved Concentration Limits* (CRWMS M&O 2000dp) and *Pure Phase Solubility Limits—LANL* (CRWMS M&O 2000dq).

Modeling was based on EQ3NR (a component of EQ3/6) analyses and a recently revised thermodynamic database incorporating experimental solubility data and critical reviews of parameterizations used internationally. Important components of this effort included the measurement and critical analysis of neptunium and plutonium solubility in J-13 groundwater and an analysis of technetium and uranium silicate thermodynamic data. The chosen solubility-controlling phase can affect the calculated radionuclide concentrations by orders of magnitude and is one of the sources for uncertainty in the predicted concentration. For the TSPA-SR analysis, the pure phases were chosen because in general they yield higher dissolved concentrations. See *Secondary Uranium-Phase Paragenesis and Incorporation of Radionuclides into Secondary Phases* (CRWMS M&O 2000dr) for discussion of the effects of secondary phases on radionuclide

concentration. The phases were chosen based upon geologic and/or experimental observations or crystallochemical arguments. These issues are discussed in *Summary of Dissolved Concentration Limits* (CRWMS M&O 2000dp) for each radionuclide. Schoepite was assumed to be the solubility-controlling mineral for uranium because (1) schoepite is the first mineral to be formed during spent fuel corrosion; (2) field observations and modeling study indicate that schoepite can persist for more than 10,000 years; (3) schoepite is the most soluble of the common secondary phases; and (4) the temperature dependence of schoepite solubility is known. Relatively soluble Np_2O_5 (or $Np(OH)_4$(am) under reducing conditions) are assumed to be the solubility-controlling minerals for neptunium. $Pu(OH)_4$(am) was chosen as the solubility-controlling phase for plutonium, though less soluble plutonium dioxide might form instead. $AmOHCO_3$ was chosen as the conservative solubility-controlling phase for americium. Because of chemical similarities, the solubility functions for actinium, curium, and samarium were set identical to that of americium.

Three radioisotope solubilities were abstracted as a direct function of in-package chemistry (neptunium, uranium, americium); three solubilities were set equal to that used for americium (actinium, curium, samarium); four were defined by probability distributions (plutonium, lead, protactinium, nickel); and bounding values were used for the remainder. Figure 4-105 shows the neptunium solubility as a function of pH abstraction and the neptunium solubility data (CRWMS M&O 2000bm).

Since the completion of the TSPA-SR models, the DOE has performed additional uncertainty analyses on the solubility model. The radionuclides considered most important to dose and which are conservatively modeled in the TSPA-SR models are thorium, neptunium, plutonium, and technetium. Volume 1, Section 9 of *FY01 Supplemental Science and Performance Analyses* (BSC 2001a) describes the uncertainties associated with these radionuclides and how these uncertainties were modeled in supplemental analysis. Utilizing more realistic solubility models for key radionuclides has a significant effect on peak dose calculations (reducing calculated doses) although doses during the first 10,000 years are not affected.

4.2.6.3.8   Colloid Model

Critical to repository performance are the availability and the stability of three types of colloids: (1) existing colloids in the groundwater, (2) colloids generated by degradation of the waste, and (3) colloids generated during degradation of the disposal container (ferric iron-oxide and iron-hydroxide minerals). Figure 4-99 illustrates this conceptually, and Figure 4-106 shows how these concepts are reflected in colloid modeling.

Colloid transport is potentially most important for low solubility, highly sorbing radionuclides. Plutonium and americium are the most likely such radionuclides to affect dose in the regulatory time period (CRWMS M&O 2000ds, Table 11).

The colloid abstraction (CRWMS M&O 2000cn) builds on waste form corrosion testing and measurements of plutonium and americium adsorption and desorption from clay and iron-(hydr)oxide colloids. A model was developed to calculate the colloid radioisotope concentration for each of the three colloid types. The model for the waste form colloids includes the contributions of the engulfed (irreversibly attached) plutonium observed in waste glass tests. The models for all three colloid types include reversibly attached radionuclides. These models are based on the population of each colloid type (expressed in terms of mass of colloids per volume of fluid) and experimental data for the sorption of radionuclides onto the colloid substrate materials involved. The effects of pH and ionic strength on the stability of dispersions of each colloid type are considered. Specifically, the location of the boundaries between pH and ionic strength regimes in which each type of colloid substrate is stable or unstable are defined, together with the colloid mass concentration in each regime.

The mobile colloidal radionuclide source term is the sum of the radionuclide contribution from waste form colloids (reversibly and irreversibly attached), corrosion product colloids, and groundwater colloids. The total colloid mass
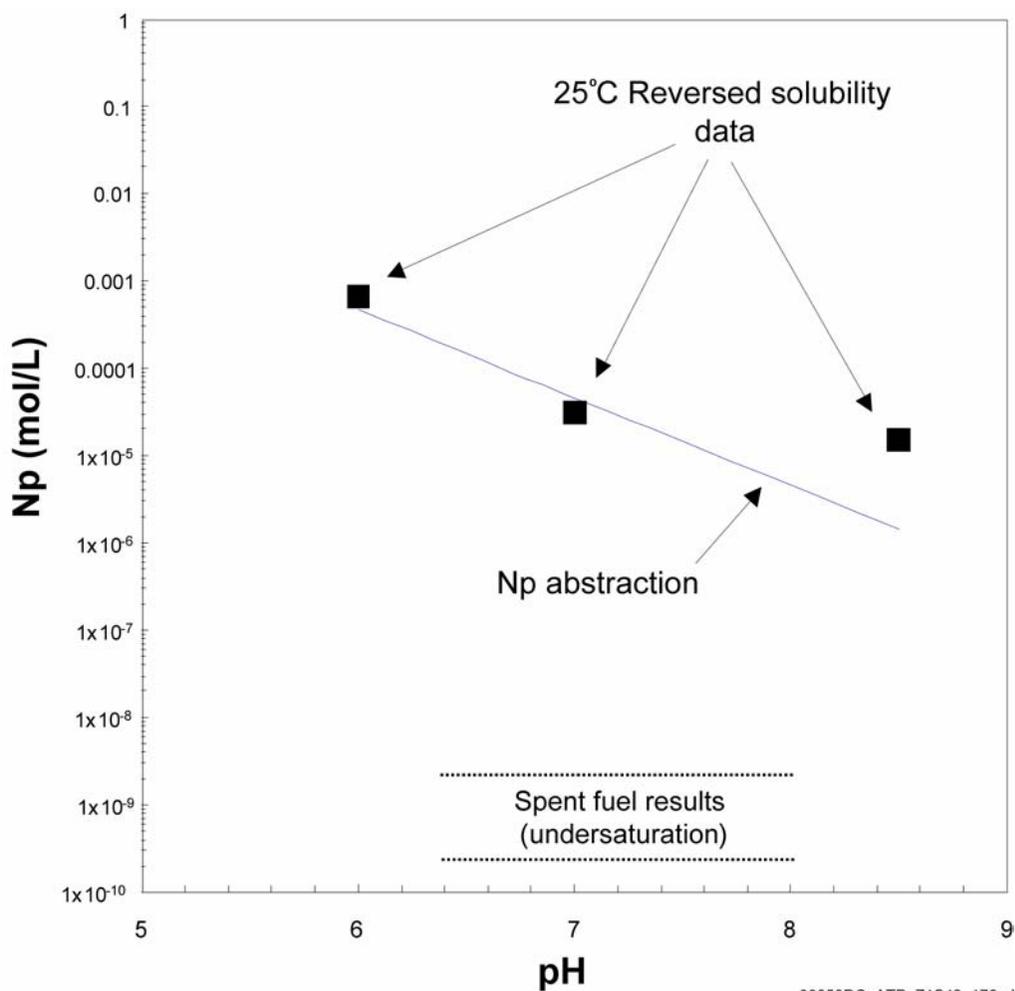
Figure 4-105. Neptunium Solubility Abstraction and Neptunium Solubility Data
Source: CRWMS M&O 2000bm, Figure 3.7-3.

concentration is also used to estimate reversibly attached radionuclide concentrations as dissolved concentrations change during transport. Reversibly attached actinides can subsequently re-equilibrate with adjacent fluids, whereas engulfed radionuclide-bearing phases cannot.

The sorption processes controlling the attachment and detachment of soluble materials to colloidal substrates are complex but are similar to sorption of dissolved materials to rock surfaces. The most common approach used in assessing such interactions is the linear isotherm, as described in *Waste Form Colloid-Associated Concentrations Limits:*

Abstraction and Summary (CRWMS M&O 2000cn).

Waste Form Colloid Concentration Model and Abstraction—The waste form concentration model includes contributions from colloids with reversibly and irreversibly attached radionuclides. The concentration of irreversibly attached colloidal plutonium is calculated in part from the ionic strength conditions adjacent to the waste form. The details of these calculations are described more fully in *Colloid-Associated Radionuclide Concentration Limits: ANL* (CRWMS M&O 2000dt). The concentration of reversibly sorbed radionuclides is
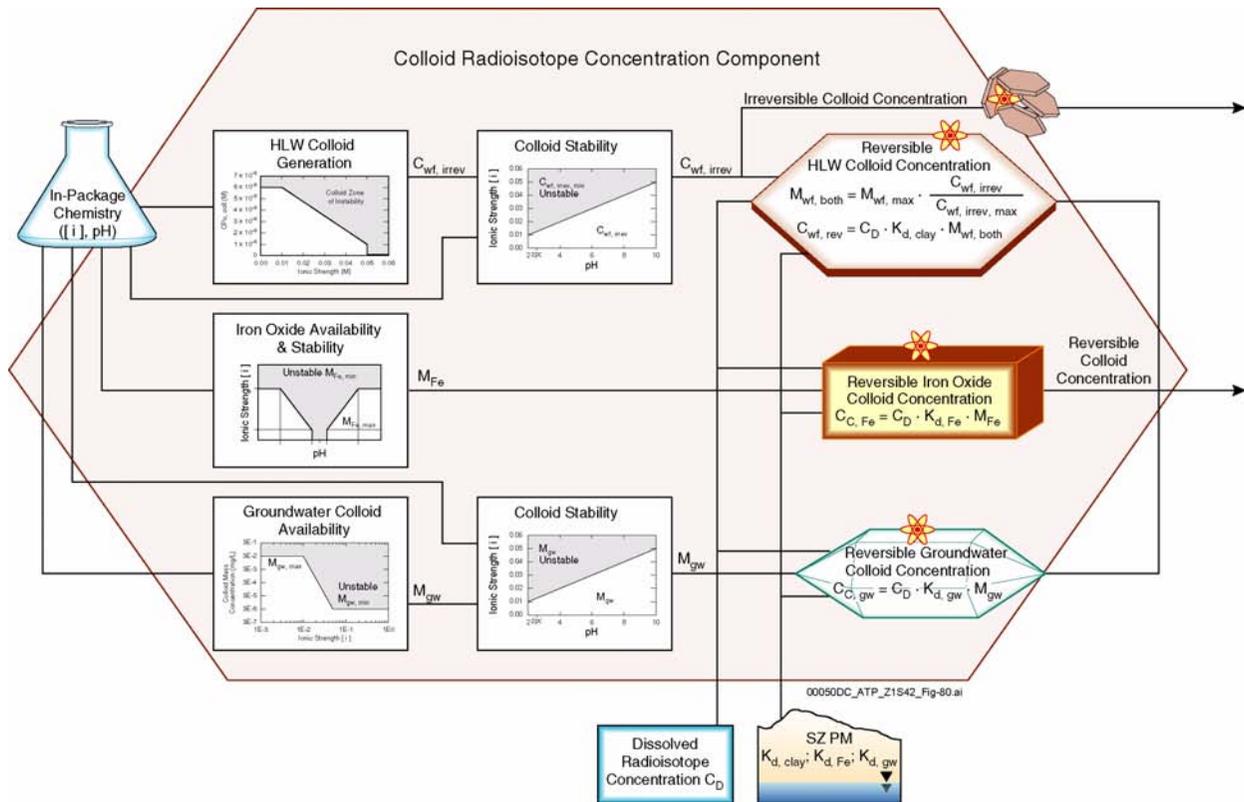
Figure 4-106. Linkage of Subcomponents of the Waste Form Degradation Process Model Colloidal Radionuclide Component

HLW = high-level radioactive waste; SZ PM = saturated zone process model. Source: CRWMS M&O 2000bm, Figure 3.8-2.

determined using technically applicable sorption coefficients and a mobile mass determined by scaling from the predicted mass of irreversibly attached colloidal plutonium.

Groundwater Colloid Model and Abstraction— McCarthy and Zachara (1989) and McCarthy and Degueldre (1993) studied and compiled the characteristics of colloids in groundwaters from crystalline and sedimentary rocks in saturated and unsaturated hydrologic regimes. The data show a general inverse correlation above an ionic strength of about 0.01 M and provide a predictive tool for estimating groundwater colloid mass concentration. For TSPA-SR analysis calculations, these data were converted to mass or surface area per unit volume. It is assumed that sorption for groundwater colloids is similar to clay minerals (CRWMS

M&O 2000cn, Section 6.2.3), and the same sorption coefficients that were used for waste form colloids were used for groundwater colloids. The concentration of reversibly sorbed radionuclides is determined using technically applicable sorption coefficients.

Corrosion Product Colloid Concentration Model and Abstraction—It is assumed that corrosion product colloid concentrations will be similar to the concentration of iron-hydroxide colloids found adjacent to the iron-rich rock at the Morro de Ferro natural analogue site (CRWMS M&O 2000bm, Section 3.8.2.3.1). The stability behavior of iron-oxide and iron-hydroxide colloids was abstracted as a function of ionic strength and pH. Given the mass concentration of the corrosion product colloids, the concentration of reversibly

sorbed radionuclides is determined using appropriate sorption coefficients.

Since the completion of the TSPA-SR models, the DOE has performed additional uncertainty analyses on the colloid model. Uncertainties can be roughly grouped as pertaining to amounts of colloids available, nature and extent of sorption to colloids, and colloid retardation. Generally, in the TSPA-SR models, uncertainties were addressed by following bounding approaches and choosing conservative inputs and/or conceptual models. In Volume 1, Section 9 of *FY01 Supplemental Science and Performance Analyses* (BSC 2001a), the DOE further defines these uncertainties and describes how these uncertainties were modeled in supplemental analyses. These analyses indicate that colloidal transport can have a significant impact on dose calculations in some cases. The supplemental analyses also suggest that the assumptions used in the TSPA-SR model were reasonable or conservative (BSC 2001a, Section 10.3.5).

4.2.6.3.9 Limitations and Uncertainties

Because models are imperfect representations of complex processes, it is important to identify their limitations and associated uncertainties, to outline alternative models that might describe the respective process, and, where possible, to fully validate the chosen process model. For most waste form models, process uncertainties are addressed by using bounding approximations or by using conservative inputs.

As noted in Section 4.1.1.2, the DOE has initiated several activities to improve the treatment of uncertainty in current models. Additionally, as noted in Section 4.1.4, the DOE has evaluated the possibility of mitigating uncertainties in modeling long-term repository performance by operating the design described in this report at lower temperatures. Some of the models that evaluate the performance of the waste form, particularly those that have used bounding approximations or conservative inputs, may be updated as a result of those activities. The model updates and evaluation results will be documented in future reports. The limitations of each waste form model described in this report are discussed below.

Radionuclide Inventory—The representative TSPA inventories (see Section 4.2.6.4.1) were derived from projections of future waste streams. The actual waste streams will be known only at the time of actual repository loading. The projected waste streams could differ from the actual waste streams in their fuel burnups, fuel ages, fuel enrichments, and utility efficiencies. As discussed in *Waste Form Degradation Process Model Report* (CRWMS M&O 2000bm, Section 3.1.1.4), the numbers of waste packages were specified for this analysis. As described in Section 1.2.1, these numbers are subject to change if a second repository is available or if the Nuclear Waste Policy Act is amended. However, changes that might be expected in the waste stream would produce only minimal changes in the average per-package radionuclide activities for commercial spent nuclear fuel used in TSPA modeling. The total curies of isotopes important to TSPA were between 1×10^4 and 1×10^5 for over 99 percent of the commercial fuel assemblies modeled in the TSPA-SR, with totals between 1×10^3 and 1×10^4 for the rest, as summarized from *Waste Packages and Source Terms for the Commercial 1999 Design Basis Waste Streams* (CRWMS M&O 2000bb). The inventory within the codisposal packages is more variable than the commercial spent fuel packages but on average is much lower. The range of total curies of isotopes important to TSPA for high-level glass waste canisters is 1×10^3 to 1×10^5, as summarized in *Source Terms for HLW Glass Canisters* (CRWMS M&O 1999o), and the range for DOE spent nuclear fuel canisters is 1×10^1 to 1×10^6, as summarized from *Per Canister Inventories of DOE SNF for TSPA-SR* (CRWMS M&O 2000du). Changes in waste stream are more likely to change the average per-package inventory of codisposal packages, but because these packages have significantly lower total activity, these changes are less likely to affect the TSPA results. The calculated average initial inventories in commercial spent nuclear fuel and codisposal waste packages are valid for the waste stream, as described in *Inventory Abstraction* (CRWMS M&O 2000ds).

In-Package Chemistry—The in-package chemistry model is limited by its reliance on reaction paths calculated at 25°C (77°F), by uncertainties in

the kinetic and thermodynamic database, and by uncertainties in the mode of water contact with the breached waste package (CRWMS M&O 2000dm). The difference between 25°C (77°F) reaction paths and those expected in reality should not be great after the thermal pulse has passed and temperatures approach ambient. At ionic strengths greater than about 0.7 mol/L, the calculations are less accurate than for dilute systems. Because the solubilities of many minerals do not appear to depend strongly on ionic strength at and above this range, the lack of exactness does not prevent the results from providing useful bounding ranges of fluid chemistry. To address thermokinetic uncertainties, where possible, conservative reaction parameters have been assumed. Specifically, rates tend to be overestimated, and solubility-limiting phases that tend be the most soluble are chosen. Other parameter uncertainties, such as estimated extents of clad failure and fluid influxes, have been addressed by considering a range of values as inputs.

Cladding Degradation—There are limitations to the cladding model. The model is strictly applicable only to commercial pressurized water reactor fuel with Zircaloy cladding, but it is used for boiling water reactor fuel and fuel with advanced zirconium-base cladding as well. Such application is conservative because boiling water reactor fuel is less heavily stressed and advanced cladding alloys have better performance than Zircaloy. The model is also limited to fuel exposed to normal operation and anticipated operational events; it is not applicable to fuel that has been exposed to severe accidents. Fuel burnup projections have been limited to the current licensing environment with restrictions on fuel enrichment, oxide coating thickness, and rod plenum pressures. Cladding degradation from surface facility handling and operation was not considered. Ranges of uncertainties have been established and conservatism was used in developing this analysis.

Commercial Spent Nuclear Fuel—The dissolution model is appropriate for repository conditions, as discussed in Section 4.2.6.3.11. From an analysis of the fit of the model to the data, and from further consideration of the uncertainty of application of data from young spent fuel (less than 30

years out of reactor) and unburned uranium dioxide toward the prediction of long-term (greater than 1,000-year) performance of spent fuel, the model was estimated to be valid to about one order of magnitude (a factor of ten). The model and uncertainty range adequately accounted for, or overestimated, all dissolution rate data.

High-Level Radioactive Waste Glass Degradation—The primary uncertainties in the long-term corrosion rate of high-level radioactive waste glass are associated with the value of the k_{eff} (i.e., $k_{eff} = k_0 \cdot [1 - Q/K]$, where k_0 is the intrinsic dissolution rate and Q and K are as defined in Section 4.2.6.3.5) term in the model. The value of k_{eff} is mathematically constrained to the range $k_0 > k_{eff} > 0$, but the appropriate value to use for k_{eff} is uncertain. The available data show that the dissolution rate decreases monotonically over time in static or nearly static systems. However, for some compositions, after initially decreasing, the dissolution rate has been observed to increase to an apparently constant value. Because the factors that trigger this increase in the glass corrosion rate are not well understood, the abstracted model conservatively assumes that an increase in the rate will occur for all waste glass compositions.

DOE Spent Nuclear Fuel—Because of their robust design (see Section 3.3.1), releases from naval spent nuclear fuel waste packages are very small (Mowbray 2000). Releases from naval spent nuclear fuel are significantly less than releases from commercial spent nuclear fuel (CRWMS M&O 1998g, Chapter 6, Appendix A-2.1.14). This comparison shows that it is very conservative to represent releases from naval spent nuclear fuel waste packages with releases from commercial spent fuel waste packages.

The application of models for the remaining DOE spent nuclear fuel and immobilized ceramic plutonium involves the extrapolation of the models over long periods of time. The sparseness of directly relevant experimental dissolution/degradation data precludes the development of a mechanistic model. In addition, uncertainties in the data—such as in the surface area measurements used to calculate normalized dissolution rates—produce significant uncertainties even in the short-term application of

the models. For this reason and because preliminary TSPA analyses have shown that the overall performance of the repository is very insensitive to the degradation rate of DOE spent nuclear fuel, upper-limit or bounding degradation models were used.

Solubility—The limitations of the in-package chemistry model also apply to the solubility model. Inherent limitations within the databases can lead to an uncertainty, up to a factor of 2, when the ionic strength exceeds about 0.7 M. Uncertainties in the kinetic and thermodynamic databases are bounded by suppressing many of the more insoluble actinide solids and using experimentally confirmed solids as the solubility limiting phases. For example, a recent study on the reaction of PuO_2 with water has found that in the presence of water and oxygen, PuO_2 may be metastable and can be converted into PuO_{2+x} (Haschke et al. 2000). This new finding has raised the concern that plutonium may be more soluble than previously believed. This concern, however, is mitigated by the use of the much more soluble $Pu(OH)_2$(am) instead of PuO_2(c) as the solubility controlling solid. While PuO_{2+x} may be more soluble than PuO_2(c), it is not clear that PuO_{2+x} is more soluble than $Pu(OH)_2$(am). Because $Pu(OH)_2$(am) solubility is quite high relative to dissolved plutonium concentrations observed in spent fuel tests, this model is believed to be conservative.

Colloids—Uncertainty was captured directly in distribution functions for the adsorption coefficients, and bounding values or bounding estimates from experimental results were used for mass concentrations of groundwater and waste-form colloids. Another large uncertainty comes from the limited available information describing formation of colloids from degradation of N Reactor fuel and its potential contribution to repository performance. In the absence of useful data, it is assumed that, due to the small quantity of N Reactor fuel, any colloids generated from degradation of the fuel will have little or no effect on repository performance.

A less significant uncertainty is the mass of colloids produced by commercial spent nuclear fuel degradation. Little colloidal material was observed experimentally. Colloids formed were smectites, some apparently possessing adsorbed plutonium, and uranium silicates. However, no embedded radionuclide phases were observed in the few clay colloids produced during degradation testing. If any contain embedded (irreversibly attached) radionuclides, the consequences for waste package releases would be minimal, since it is assumed that all colloid-associated radionuclides leave a breached waste package.

Since completion of the TSPA-SR models, the DOE has continued to explore uncertainties associated with these models. Volume 1, Section 9 of *FY01 Supplemental Science and Performance Analyses* (BSC 2001a) describes in detail the additional work performed to further define, model, and understand uncertainties associated with the waste form degradation models. In general, Volume 1 of *FY01 Supplemental Science and Performance Analyses* (BSC 2001a) further discusses uncertainties related to the in-package chemistry model, the dissolved concentration abstraction (solubilities), the high-level waste glass degradation model, the cladding model, and the colloid model. Detailed descriptions and analyses performed since the TSPA-SR model are available in Volume 2 of *FY01 Supplemental Science and Performance Analyses* (BSC 2001b).

In general, these analyses indicate that uncertainty in the relevant processes did not significantly affect performance (e.g., high-level radioactive waste glass dissolution rates, cladding degradation) or that the assumptions used in the TSPA-SR models were conservative (e.g., radionuclide solubilities). In addition, several improved process model representations (e.g., neptunium solubility) were developed and implemented in the supplemental TSPA model. Results of the supplemental analyses support the conclusions drawn from the TSPA-SR analyses in the evaluation of the site's long-term performance.

4.2.6.3.10 Alternative Conceptual Models

Alternate conceptual models were considered in the development of all waste form models. The model chosen for the TSPA-SR was either the one with the most mechanistic and experimental basis

or one that is most easily demonstrated to be bounding. Some model alternatives are discussed below.

As with limitations and uncertainties, alternative conceptual models for engineered barrier system transport processes have also been updated in supplemental analyses, summarized in *FY01 Supplemental Science and Performance Analyses* (BSC 2001a, Section 1; BSC 2001b, Section 1).

Radionuclide Inventory—Although the radionuclide inventory is not a model, the use of alternative approaches is nevertheless of interest. In previous TSPAs (e.g., TSPA for viability assessment), radionuclide activities for commercial spent nuclear fuel were developed by assuming an average set of fuel characteristics (enrichment, burnup, and age of the waste) and calculating the radionuclide inventory for that type of fuel having the specified characteristics (CRWMS M&O 2000bm, Section 3.1.3). Radionuclide inventories for high-level radioactive waste were similarly based on an average waste glass. Radionuclide activities for DOE spent nuclear fuel were developed by combining these fuels into a few representative groups and calculating the inventory for a representative fuel from each group.

The current inventory analysis is more detailed and flexible than previous analyses and is tied to the waste stream. Changes in waste package configuration or waste stream are more easily reflected in the per-package inventory of representative waste packages.

In-Package Chemistry—The in-package chemistry model provides an average composition for the water in a waste package. Local variations in composition (e.g., crevice chemistries) are possible, but it would be difficult to validate and defend such models.

The in-package chemistry will have some dependence on the composition of the incoming groundwater. Ongoing sensitivity studies are addressing this subject.

Cladding Degradation—In the TSPA-VA model, the fuel in rods that were failed before emplace-

ment was assumed to be completely exposed for dissolution. The fuel in an area below an impacting rock or a failed corrosion patch was available for dissolution, but the remaining ends of the rods were not. This model was not necessarily conservative.

Creep rupture of cladding by diffusion-controlled cavity growth has been accepted by the NRC as the predominant mechanism for failure of cladding during dry storage (NRC 2000a, p. 8-5). Dry storage conditions are similar to repository conditions for the period before the waste packages are breached. However, more recent guidance from the NRC (NRC 2000b) allows the use of other models for creep rupture and admits a lack of experimental evidence for diffusion-controlled cavity growth in Zircaloy (NRC 1999a, p. 56).

Other performance assessments have assumed no credit for cladding protection of the fuel. No cladding credit is easily defended as the worst case for repository performance during the regulatory period. However, this alternative is extremely conservative and gives unrealistically high releases at early times.

Commercial Spent Nuclear Fuel—This semi-empirical model was based on an understanding of the chemistry of uranium dioxide dissolution. This understanding was used to choose the functional form of the equation for dissolution rate. More complex empirical functions were also considered, but the current form was chosen for its simplicity.

The spent fuel dissolution model was based on results from flow-through experiments in which dissolved material is washed away rapidly. As a result, the model does not reflect the effects of saturation or formation of secondary phases. More realistic models might be constructed to include these effects, but they would necessarily be much more complex, require more data, and be more difficult to validate.

High-Level Radioactive Waste Glass Degradation—An alternative model of waste glass degradation envisions corrosion under humid air and dripping water conditions. Water vapor will continually condense in the film of saline water on

the exposed waste glass as the glass corrodes. Continuous exposure to water-saturated air will result in a process of vapor condensation, flow across the sample, and dripping, wherein dissolved species can be transported away from the glass as solution drips from the glass, and fresh water vapor condenses. The corrosion rate of the glass under these conditions will be affected by the rates at which water vapor condenses in the film and solution drips from the sample. These processes will affect the glass dissolution rate through their effects on the solution chemistry of the film. The fully saturated model described elsewhere results in a more rapid dissolution rate and was therefore used instead.

DOE Spent Nuclear Fuel—As discussed in Section 4.2.6.3.6, upper-limit, conservative, and best-estimate models have been proposed for each of the groups of DOE spent nuclear fuel, other than naval spent nuclear fuel. The Naval Nuclear Propulsion Program modeled the performance of naval spent nuclear fuel with the same environmental conditions used in the commercial spent nuclear fuel degradation model (Mowbray 2000).

Solubility—An alternative approach to estimating dissolved levels of radionuclides is to use dissolved levels measured in contact with experimentally altered fuels. Figure 4-105 shows neptunium concentrations measured in contact with spent fuels in long-term degradation experiments. In general, reliance on values derived from long-term degradation measurements would result in estimated radionuclide concentrations several orders of magnitude below those estimated from solubility measurements.

Colloids—An alternative model for waste-form colloid generation was proposed in *Waste Form Colloid-Associated Concentrations Limits: Abstraction and Summary* (CRWMS M&O 2000cn) and *Colloid-Associated Radionuclide Concentration Limits: ANL* (CRWMS M&O 2000dt), in which the rate of colloid formation was based on the rate of release of a tracer ion (boron and technetium), high-level radioactive waste glass and spent nuclear fuel corrosion, and plutonium concentrations. This model was not recommended

for implementation because it is based on limited laboratory data, but it may be useful in the future.

The use of a mass-based adsorption coefficient (K_d) or a surface-area-based adsorption coefficient (K_a) may be significant in some colloid systems because the effectiveness of colloids at facilitating contaminant transport is largely due to their very large mobile surface area available for sorption. The greatest variability exists in situations in which an inordinately large number of very small colloids exist, which have a high surface-area-to-mass ratio. Based on experimental measurements and observations of colloid characteristics in Yucca Mountain groundwater, this situation does not exist at Yucca Mountain, and the use of a mass-based K_d is believed to be satisfactory.

In the approach used in the TSPA for the viability assessment, a constant steady-state mass concentration of colloids in groundwater was assumed. The steady-state mass concentration was embedded in a sorption term referred to as K_c. The approach used in the TSPA-SR is more comprehensive, in that by not assuming a uniform colloid mass concentration, the effect of ionic strength and pH on mass concentration is included, and mass concentration is used in conjunction with K_d values. This approach provides more realism by accounting for the destabilizing effect of high ionic strength conditions and some pH conditions. The K_c approach, however, is well suited for far-field transport, where transients in aqueous chemical conditions are not expected.

4.2.6.3.11 Model Validation

In all waste form models, some model validation has been performed. In most cases this has been done by comparing model outputs against experimental observations or geologic occurrences. A number of these comparisons are summarized below.

Radionuclide Inventory—Since the radionuclide inventory is simply an accounting analysis, rather than a model, it is not subject to model validation. However, see Section 4.2.6.3.10 for a discussion of other approaches and their effects on inventory.

In-Package Chemistry—EQ3/EQ6, the reaction-path code used to model waste package degradation, has been used over the past 20 years to successfully model such complex natural processes/features as seawater speciation and evaporation, hydrothermal ore formation, granite weathering, and high temperature alteration of mid-ocean ridge basalts by seawater. A degree of confidence in the model is also implied by the successful validation of model inputs—thermodynamic data and rate constants.

Cladding Degradation—The cladding degradation model is based on over 40 years of experiments and observations of cladding behavior. The analysis of initial cladding conditions is based on reactor fuel performance reports that have been published since the start of the industry. Creep, stress corrosion cracking, and delayed hydride cracking analyses are supported by extensive experimental data. Zirconium alloys were originally developed for use in the chemical industry to handle very corrosive fluids such as hydrochloric acid. In water environments, continuous corrosion experiments have been performed for 27.5 years. Fuel has been exposed in spent fuel pools for over 25 years and in dry storage research programs. The models, including ranges and uncertainties, developed for TSPA are based primarily on experimental observations.

Commercial Spent Nuclear Fuel—The dissolution model was based on a large set of qualified flow-through experiments under a wide range of environmental conditions. It is valid from pH 3 to 10, oxygen pressure from 0.002 to 0.2 atmospheres, and total carbon concentrations from 2×10^{-4} to 2×10^{-2} molar. At pHs less than or equal to 7, this model is valid at carbon dioxide pressures of 10^{-3} atmospheres. To provide additional confidence, the model was compared to unsaturated drip tests, batch tests, and a range of literature results.

High-Level Radioactive Waste Glass Degradation—To show that the model provides a conservative upper bound to the long-term rate under basic conditions, calculated rates were compared with the Stage III rates measured with long-term product consistency tests (CRWMS

M&O 2000dl, Section 6.2.3). This was done by first estimating the pH at the reaction temperature of 90°C (194°F) and then using the mean values for the model parameters. The calculated rates are plotted against the experimentally measured rates in Figure 4-107. A diagonal line is drawn to indicate where the calculated and measured rates are equal. All of the points lie above the diagonal line, which indicates that the model provides an upper bound estimate of the long-term rates for these glasses. Note also that model rates have been compared against long-term alteration of submarine basalt glass and been shown to be conservative.

DOE Spent Nuclear Fuel—The initial results of TSPA sensitivity analyses for DOE spent nuclear fuel (CRWMS M&O 2000dv, Section 7) indicate that the performance of the repository is very insensitive to its degradation kinetics. Even if all radionuclides are released instantaneously, the calculated boundary dose is well within requirements. Use of a less conservative model would not significantly lower the calculated boundary dose, because even with the upper-limit model, releases due to DOE spent nuclear fuel are significantly lower than those due to high-level waste and commercial spent nuclear fuel.

00050DC_ATP_Z1S42_178a
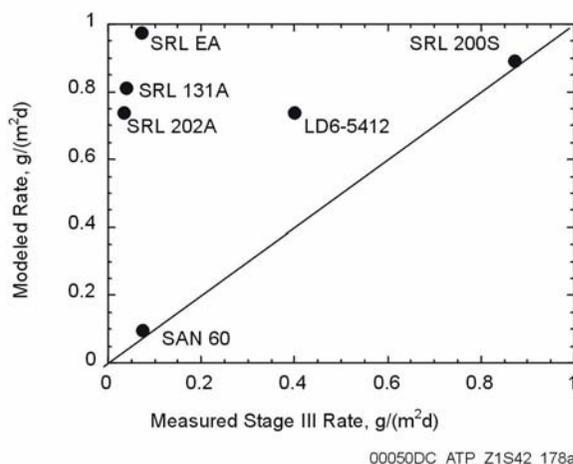
Figure 4-107. Plot of Long-Term Estimated Glass Dissolution Rates vs. Stage III Measured Product Consistency Test Rates
Source: Derived from data in CRWMS M&O 2000dl, Table 3.

The conservative and best estimate models for DOE spent nuclear fuel waste forms are primarily impacted by the validity of the uranium metal-based DOE spent nuclear fuel dissolution models.

Solubility—The solubility model is based on well-established chemical principles, so model validation is primarily validation of the thermodynamic data used in the model. A systematic review of thermodynamic data and controlling phases has been performed for a large range of chemical conditions. When uncertainties were encountered, choices were made that would result in higher predicted solubilities. Inherent limitations within the databases can lead to an uncertainty up to a factor of 2 when the ionic strength exceeds about 0.7 mol/L. However, this uncertainty is small relative to other uncertainties within the system. Figure 4-105 shows neptunium concentrations measured in contact with spent fuels in long-term degradation experiments. In general, reliance on values derived from long-term degradation measurements would result in estimated radionuclide concentrations several orders of magnitude below those estimated from solubility measurements. These observations provide validation that the solubility model will bound the radionuclide concentrations.

Colloids—The colloid model abstraction is based on laboratory results from waste-form corrosion testing and testing of adsorption and desorption properties of plutonium and americium on clay and iron-(hydr)oxide colloids. The development of the conceptual model and implementation requires consideration of colloid generation, colloid-radionuclide interaction, colloid stability behavior, and to some extent, colloid transport/retardation behavior. Information used for groundwater colloids, waste-form colloids, and corrosion-product colloids was obtained primarily from Yucca Mountain-specific studies. Consequently, the colloid-concentration model is expected to be representative of Yucca Mountain behavior.

Field evidence of small concentrations of radionuclides associated with colloids migrating considerable distances has provided insight into possible colloid behavior at Yucca Mountain. At the Benham nuclear test site at the Nevada Test Site, colloid-associated plutonium appears to have been rapidly transported (Kersting et al. 1999). At a point about 1.3 km (0.8 mi) from the blast site, 1×10^{-14} mol/L colloid-associated plutonium was detected 30 years after the detonation. It is plausible that the plutonium was transported as plutonium irreversibly attached to colloids, a possibility which underscores the potential significance of the irreversibility of radionuclide attachment to smectite colloids observed in Argonne National Laboratory waste form corrosion experiments (CRWMS M&O 2000dt, Figures 11 and 13). Irreversibly attached colloids are included in the abstracted model as a contribution to the colloid-associated radionuclide concentration.

4.2.6.4 Total System Performance Assessment Abstraction

The process models described in Section 4.2.6.3 are not fully implemented until they are combined within the TSPA model, as shown in Figure 4-97. While the fundamental features specific to each process model are retained where possible in the TSPA, a number of further simplifications have been made. These are outlined in greater detail below.

4.2.6.4.1 Inventory Abstraction

The radioisotope inventory abstraction provided the radioisotope inventory for TSPA. This abstraction is described in *Inventory Abstraction* (CRWMS M&O 2000ds) and nine supporting calculations. Three important aspects of the radionuclide inventory abstraction are (1) obtaining the radioisotope inventories of various fuels and wastes, (2) selecting the most important radionuclides for human dose out of the few hundred found within the fuel and waste, and (3) grouping the fuels and wastes into the waste packages selected for modeling in the TSPA-SR analysis.

Data Sources—Four main sources were used for inventory data: (1) commercial utilities, for commercial spent nuclear fuel (CRWMS M&O 1999a); (2) DOE National Spent Nuclear Fuel Program, for DOE spent nuclear fuel (DOE 1999d); (3) Yucca Mountain Environmental Impact Statement (EIS) program, for DOE high-level radioactive waste, mixed oxide, and plutonium

ceramic wastes (DOE 1999a); and (4) *Monitored Geologic Repository Project Description Document* (Curry 2001, Table 5-5).

Isotope Selection—The relative importance of individual radionuclides to offsite doses was evaluated for several waste types, time frames, and release scenarios (CRWMS M&O 2000bm, Section 3.1.1.1). This evaluation considered the effects of inventory abundance, radionuclide longevity, element solubility, and element transport affinity. Inventory abundance was addressed by examining eight waste types (average and bounding types for boiling water reactor, pressurized water reactor, high-level radioactive waste, and DOE spent nuclear fuel waste forms). To address radionuclide longevity, these fuels were evaluated between 100 years and 1 million years after repository closure. The elements were separated into two solubility groups—the relatively soluble and the relatively insoluble (americium, curium, zirconium, thorium, niobium, protactinium, and tin)—and three transport affinity groups: (1) highly sorbing, (2) moderately sorbing, and (3) slightly sorbing to nonsorbing. The isotopes within each group were ranked against one another in relative importance (CRWMS M&O 2000ds, Section 4.1.1.4). Three release scenarios were considered: nominal case, human intrusion, and direct volcanic release. Two time frames were considered: 100 years to 10,000 years and 100 years to 1 million years. The set of important isotopes was different for each scenario and time frame. The resulting 23 screened-in isotopes are shown in Table 4-19, along with isotope selection from previous performance assessments. The differences between the isotope selection in these performance assessments are primarily due to (1) modification made to remain consistent with licensing-related regulations concerning, for example, dose, groundwater protection, the time period—10,000 years or 1 million years, and human intrusion, (2) inventory data relied upon, and (3) screening techniques.

Grouping of Fuels and Wastes—The waste types, allocations, and waste packages for commercial spent nuclear fuel, high-level radioactive waste (including immobilized plutonium), and DOE spent nuclear fuel are shown in Figure 4-108.

For the base case, over 220,000 commercial spent nuclear fuel assemblies will need to be disposed, and each assembly will have a unique isotopic composition. In 1995, the utilities supplied historical information about reactor assembly discharges up through December 1995 and five-cycle forecasts for assembly discharges. With this information, the forecasts for assembly discharges over the lifetime of each commercial power reactor were developed for use in defining the commercial spent nuclear fuel inventory for the TSPA (CRWMS M&O 1999a). For the base case repository design of 70,000 MTHM, three alternative schedules were developed for shipping the assemblies to Yucca Mountain. Radionuclide activities for each assembly in the waste stream were estimated, and the waste package configuration that could accommodate the assembly based on its potential criticality level was determined.

The proposed technology for immobilization of the high-level radioactive waste is vitrification in a borosilicate glass. Because the reprocessed fuel at each of the vitrification sites differs, the radionuclide inventory of the waste and resultant glass product will vary slightly among the sites.

Up to approximately 33 metric tons of surplus plutonium will be fabricated into uranium-plutonium fuel (mixed-oxide fuel) and irradiated in commercial reactors. The spent fuel will be treated as part of the commercial waste stream. About 17 metric tons of surplus plutonium will be immobilized with neutron absorber material in small canistered ceramic disks. These disks will be placed within standard high-level radioactive waste canisters and the remaining void filled with high-level radioactive waste glass.

DOE spent nuclear fuel consists of more than 250 distinct types, and much like commercial spent nuclear fuel, radionuclide inventories for these fuels will vary widely depending on the history of the fuel. The National Spent Nuclear Fuel Program divided the fuels into 11 groups.

Arrival scenarios were developed for all fuels and wastes. The immobilized plutonium, DOE spent nuclear fuels, and high-level radioactive wastes will be packaged in the 10 canister designs listed in

Table 4-19. Isotope Selection

Isotope	TSPA-SR[a] & Final EIS 2000	TSPA 1993[b]	TSPA 1995[c]	TSPA-VA 1998[d]	NRC Iterative Performance Assessment 1995[e]
^{227}Ac	X	X	X		
^{108m}Ag		X			
^{241}Am	X	X	X		X
^{242m}Am		X	X		
^{243}Am	X	X	X		X
^{14}C	X	X	X	X	X
^{36}Cl		X	X		
^{243}Cm		X			
^{244}Cm		X	X		
^{245}Cm		X	X		X
^{246}Cm		X	X		X
^{135}Cs		X	X		X
^{137}Cs	X	X			X
^{129}I	X	X	X	X	X
^{93}Mo		X			
^{93m}Nb			X		
^{94}Nb		X	X		X
^{59}Ni		X	X		X
^{63}Ni		X	X		
^{237}Np	X	X	X	X	X
^{231}Pa	X	X	X	X	X
^{210}Pb	X	X	X		
^{107}Pd		X	X		
^{238}Pu	X	X	X		
^{239}Pu	X	X	X	X	X
^{240}Pu	X	X	X		X
^{241}Pu		X	X		
^{242}Pu	X	X	X	X	
^{226}Ra	X	X	X		X
^{228}Ra			X		
^{79}Se		X	X	X	X
^{151}Sm		X	X		
^{121m}Sn		X			
^{126}Sn		X	X		
^{90}Sr	X	X			
^{99}Tc	X	X	X	X	X

Table 4-19. Isotope Selection (Continued)

Isotope	TSPA-SR[a] & Final EIS 2000	TSPA 1993[b]	TSPA 1995[c]	TSPA-VA 1998[d]	NRC Iterative Performance Assessment 1995[e]
^{229}Th	X	X	X		
^{230}Th	X	X	X		X
^{232}Th			X		
^{232}U	X	X	X		X
^{233}U	X	X	X		X
^{234}U	X	X	X	X	X
^{235}U		X	X		
^{236}U	X	X	X		
^{238}U	X	X	X		X
^{93}Zr		X	X		

NOTES: [a]CRWMS M&O 2000ds, Sections 7.1 and 7.2.
[b]Wilson, M.L. et al. 1994.
[c]CRWMS M&O 1995.
[d]DOE 1998, Volume 3.
[e]Wescott et al. 1995.
Source: CRWMS M&O 2000bm, Table 3.1-1.

Section 3.3 and Table 4-20. These canisters and the commercial spent nuclear fuel assemblies will be emplaced in the 10 waste package designs listed in Tables 3-2 and 4-21. The waste packages and canisters combine to give a total of 13 waste package configurations, as shown in Table 4-22.

Average and bounding inventories were developed for each package configuration recommended for the potential repository (CRWMS M&O 2000dw). Then, the package-specific radionuclide activities were combined, using the number of waste packages in each group as a weighting factor, to estimate the per-package radionuclide activities for TSPA modeling purposes (see Table 4-23). For each commercial spent nuclear fuel configuration, the average radionuclide activity is the number of assemblies multiplied by the average per-assembly radionuclide activity. For the TSPA representative commercial spent nuclear fuel waste package, a weighted average of these five configurations was used. For the TSPA representative codisposal waste package, the average radionuclide activity from DOE spent nuclear fuel is the number of DOE spent nuclear fuel canisters multiplied by the

average per canister radionuclide activity calculated. Similarly, the average radionuclide activity from high-level radioactive waste for one of these configurations is the number of waste canisters multiplied by the average per canister radionuclide activity calculated. This average was performed for all waste and fuel that was represented in the TSPA by the codisposal packages.

Because of its robust design (see Section 3.3.1), releases from naval spent nuclear fuel waste packages are very small (Mowbray 2000). Releases from naval spent nuclear fuel are significantly less than releases from commercial spent nuclear fuel (BSC 2001q). This comparison shows that it is very conservative to represent releases from naval spent nuclear fuel waste packages with releases from commercial spent fuel waste packages.

Three radionuclides appear in Table 4-23 that were not listed in Table 4-19: radium-228, thorium-232, and uranium-235. These isotopes were not identified as important contributors to dose. However, radium-228 and thorium-232 are required for the proposed groundwater protection scenario, and
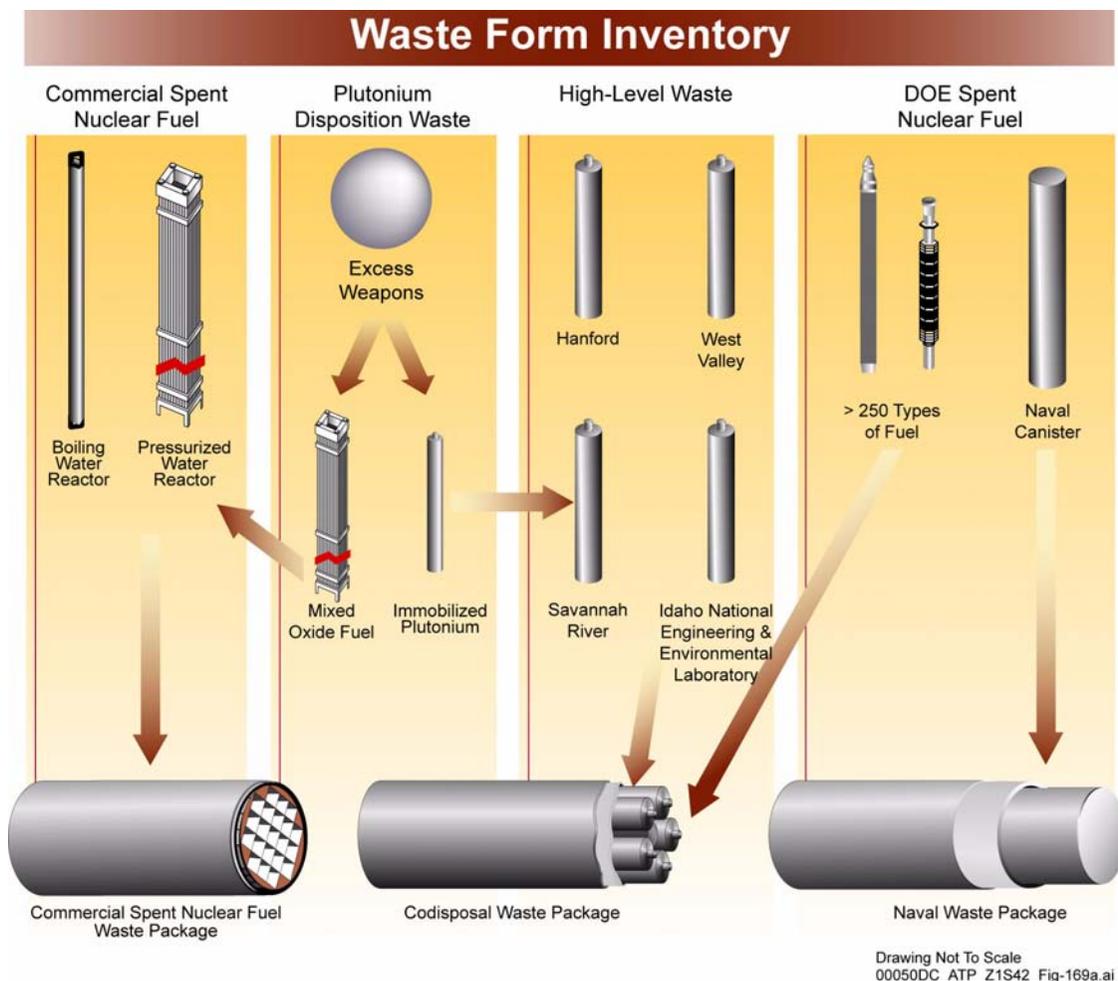
Figure 4-108. The Waste Form Inventory, Detailing Waste Types, Allocation, and Waste Packages
Source: Adapted from CRWMS M&O 2000bm, Figure 3.1-1.

uranium-235 is required for calculations of the dose from protactinium-231.

Projected waste streams could differ from the actual waste streams in their fuel burnups, fuel ages, fuel enrichments, and utility efficiencies, which introduces some uncertainty in the model. However, the analysis performed for TSPA-SR is more detailed and flexible than previous analyses and is tied to the waste stream. Changes in waste package configurations or waste streams are more easily reflected in the per-package inventory of representative waste packages.

4.2.6.4.2   In-Package Chemistry Abstraction

Summary of In-Package Chemistry for Waste Forms (CRWMS M&O 2000dm, Section 6) uses

reaction-path modeling to predict the broad range of effluent compositions emanating from a breached waste package and provides a basis from which to estimate radioisotope solubilities.

The analysis of calculated in-package fluid compositions reveals four common characteristics. Carbonate alkalinity increases with pH due to the assumed fixed partial pressure of carbon dioxide. System Eh decreases with pH due to the assumed constant partial pressure of oxygen. Low early pHs are only seen with low cladding failures, and alkalinities typically correlate with high ionic strengths associated with high glass dissolution and low flow rates. Typically, reaction times of less than 1,000 years result in relatively minor degradation of waste package components; hence, the concentrations of many radionuclides are often well below

their respective solubility limits. In effect, their concentrations depend directly on the dissolution rates of waste package components. At much greater time spans (over 1,000 years), many, but not all, radionuclides have reached saturation with at least one mineral phase. Once this has occurred, dissolved levels of the particular radionuclides will depend on the thermodynamics of secondary phase stability and much less directly upon the dissolution rates of the waste package components.

Table 4-20. Canister Designs

Canister Design	Canister Design Code
Naval short	C1
Naval long	C2
DSNF short	C3
DSNF long	C4
DSNF short, wide	C5
DSNF long, wide	C6
HLW short	C7
HLW long	C8
HLW short with Pu-ceramic	C9
Multicanister overpack	C10

NOTES: DSNF = DOE spent nuclear fuel; HLW = high-level radioactive waste.

Table 4-21. Waste Package Designs

Waste Package Design	Waste Package Design Code
21-PWR Absorber Plate	W1
21-PWR Control Rod	W2
12-PWR Long	W3
44-BWR	W4
24-BWR	W5
5-DHLW/DOE SNF Short	W6
5-DHLW/DOE SNF Long	W7
2-MCO/2-DHLW Long	W8
Naval SNF Short	W9
Naval SNF Long	W10

The abstraction of in-package processes consists of multiple linear regression analyses of the output from the EQ3/6 simulations described in the *In-Package Chemistry Abstraction* (CRWMS

M&O 2000dn). The multiple linear regression analyses take explicit account of the change in process control with time and treat results for times less than 1,000 years after waste package breach separately from those for later times.

The pH abstraction follows two lines of reasoning based on the waste package type (commercial spent nuclear fuel waste package or codisposal waste package) and the difference in kinetic rate laws between the two. The rate law for commercial spent nuclear fuel is proportional to the hydrogen ion activity, i.e., proportional to pH, such that at low pH the dissolution rate increases (CRWMS M&O 2000dm, Section 6.1.1). For high-level radioactive waste glass, the rate law is "U" shaped, with the minimum at pH 7 and the rate increasing above and below pH 7 (CRWMS M&O 2000dm, Section 6.1.1). For the commercial spent nuclear fuel, at times less than 1,000 years after waste package breach, minimum pH values for each flux/cladding/corrosion scenario were regressed to produce two abstractions of pH; one for low waste package corrosion rates and the other for high waste package corrosion rates. This process was repeated for times greater than 1,000 years after breach, where the average pH for the entire modeled duration (0 to 10,000 years after breach) was used to calculate the average pH.

The results are four response surfaces for each waste type, two surfaces for less than 1,000 years, and two for more than 1,000 years. The parameter space between two surfaces may be sampled by the TSPA code where pH can be calculated as a function of time, water flux Q (m³/yr), waste package corrosion rates, and cladding coverage, or glass dissolution rate for the case of codisposal waste packages. In the case of the commercial spent nuclear fuel, assuming the lowest observed pH for the less than 1,000-year period, and the averaged pH for greater than 1,000-year period is the most conservative, while still honoring the pH–time history. However, for the codisposal package using the lowest observed pH is conservative for the less than 1,000-year period but not for the greater than 1,000-year period when use of the maximum pH is conservative. The difference in the rate laws between glass and commercial spent nuclear fuel and the difference in the pH–time profiles for the

Table 4-22. Waste Configurations Used in the Inventory Abstraction

Configuration	Waste Package Design Code	Number[a]	DSNF Canisters per Waste Package	HLW Canisters per Waste Package
21-PWR Absorber Plate	W1	4500	—	—
21-PWR Control Rod	W2	100	—	—
12-PWR Long	W3	170	—	—
44-BWR	W4	3000	—	—
24-BWR	W5	90	—	—
Total Commercial Spent Nuclear Fuel		**7860**		
Pu-ceramic in HLW	W6	100	—	Five C7 (short)
Codisposal short	W6	1100	One C3 (short)	Five C7 (short)
Codisposal long	W7	1500	One C4 (long)	Five C8 (long)
Codisposal mixed	W7	130	One C3 (short)	Five C8 (long)
HLW-only	W7	600	—	Five C8 (long)
2-MCO/2-DHLW Long	W8	160	Two C10	Two C8 (long)
Total Codisposal		**3590**		
Naval SNF Short	W9	200	One C1 (short)	—
Naval SNF Long	W10	100	One C2 (long)	—
Total Naval		**300**		

NOTE: [a]Curry 2001, Table 5-5.

two waste forms predicate the use of different assumptions in the abstractions.

The balance of acid production from A516 carbon steel and base production from the glass determine the pH in codisposal waste packages. At early times (less than 1,000 years after breach), acid production dominates, but as the steel is consumed, base production overcomes the acid production. In most cases, this is not calculated to occur until considerably after 10,000 years after breach.

Total dissolved carbonate affects the solubilities of a number of actinide phases as well as the degradation rate of commercial spent nuclear fuel. The total dissolved carbonate is abstracted as a function of pH by assuming a partial pressure of 10^{-3} atm for carbon dioxide and equilibrium between the carbonate, bicarbonate, and carbonic acid in solution. The system Eh is important in particular for determining the solubilities of many of the actinides. Calculating Eh directly from the pH and an assumed partial pressure of oxygen (0.20 atm) tends to be conservative, as it maximizes the solubilities of a number of radionuclides.

For the period before 1,000 years after breach, the minimum ionic strength was calculated for each flux/cladding and glass-rate/corrosion-rate scenario. At times greater than 1,000 years after breach, the average value of ionic strength was used from each scenario to calculate the ionic strength range used in the colloid abstraction.

4.2.6.4.3   Commercial Spent Nuclear Fuel Cladding Degradation Abstraction

The cladding degradation process models are abstracted to a family of distributions, lookup tables, or simple calculations for inclusion in the TSPA. The following summarizes this abstraction.

Cladding Condition as Received—The groups (bins) of waste packages have an average initial cladding failure distribution of 0.095 percent (range 0.0155 to 1.29 percent, triangular distribution).

Creep Failures—Table 5 of *Clad Degradation— Summary and Abstraction* (CRWMS M&O 2000dj) gives the percentage of rods failed as a function of peak waste package surface temperature. Because of the comparatively low temperatures of the design, the creep failures are due only to creep failures in dry storage and transportation to Yucca Mountain. This produces an initial cladding failure distribution of 2.44 percent (range 1.05 to 19.4 percent, triangular distributed).

Table 4-23.   Average Radionuclide Inventory in Grams in Commercial Spent Nuclear Fuel and Codisposal Waste Packages for TSPA-SR

Isotope	Specific Activity (Ci/g)	Grams in TSPA-SR CSNF Packages	Grams in TSPA-SR Codisposal Packages	
			From Spent Fuel	From HLW glass
Actinium-227	7.24×10^1	3.09×10^{-6}	1.13×10^{-4}	4.67×10^{-4}
Americium-241[a]	3.44×10^0	1.09×10^4	1.17×10^2	6.57×10^1
Americium-243	2.00×10^{-1}	1.29×10^3	1.49×10^0	3.99×10^{-1}
Carbon-14	4.46×10^0	1.37×10^0	4.96×10^{-2}	6.43×10^{-3}
Cesium-137	8.65×10^1	5.34×10^3	1.12×10^2	4.51×10^2
Iodine-129	1.73×10^{-4}	1.80×10^3	2.51×10^1	4.80×10^1
Neptunium-237	7.05×10^{-4}	4.74×10^3	4.79×10^1	7.23×10^1
Protactinium-231	4.72×10^{-2}	9.87×10^{-3}	3.25×10^{-1}	7.96×10^{-1}
Lead-210	7.64×10^1	0.00×10^0	1.40×10^{-8}	1.14×10^{-7}
Plutonium-238	1.71×10^1	1.51×10^3	6.33×10^0	9.33×10^1
Plutonium-239	6.21×10^{-2}	4.38×10^4	2.30×10^3	3.89×10^3
Plutonium-240	2.27×10^{-1}	2.09×10^4	4.89×10^2	3.81×10^2
Plutonium-242	3.93×10^{-3}	5.41×10^3	1.11×10^1	7.77×10^0
Radium-226	9.89×10^{-1}	0.00×10^0	1.87×10^{-6}	1.67×10^{-5}
Radium-228	2.72×10^2	0.00×10^0	6.98×10^{-6}	3.19×10^{-6}
Strontium-90	1.37×10^2	2.24×10^3	5.54×10^1	2.88×10^2
Technetium-99	1.70×10^{-2}	7.68×10^3	1.15×10^2	7.29×10^2
Thorium-229	2.14×10^{-1}	0.00×10^0	2.66×10^{-2}	4.08×10^{-3}
Thorium-230	2.06×10^{-2}	1.84×10^{-1}	1.06×10^{-2}	7.82×10^{-3}
Thorium-232	1.10×10^{-7}	0.00×10^0	1.49×10^4	7.31×10^3
Uranium-232	2.20×10^1	1.01×10^{-2}	1.47×10^{-1}	8.23×10^{-4}
Uranium-233	9.66×10^{-3}	7.00×10^{-2}	2.14×10^2	1.11×10^1
Uranium-234	6.24×10^{-3}	1.83×10^3	5.72×10^1	4.72×10^1
Uranium-235	2.16×10^{-6}	6.28×10^4	8.31×10^3	1.70×10^3
Uranium-236	6.47×10^{-5}	3.92×10^4	8.53×10^2	3.98×10^1
Uranium-238	3.36×10^{-7}	7.92×10^6	5.09×10^5	2.61×10^5

NOTES: [a]Part of the americium-241 inventory is due to decay of plutonium-241 and curium-245.
Source: *Inventory Abstraction* (CRWMS M&O 2000ds, Section 7 and Attachment I). These numbers have been updated from the numbers used in TSPA-SR, which were provided in the initial version of *Inventory Abstraction* (CRWMS M&O 2000dx). CSNF = commercial spent nuclear fuel; HLW = high-level radioactive waste.

This failure rate is added to the cladding condition as received failures.

Localized Corrosion—This conservative model uses two severe assumptions. The first assumption is that there is no filling or flushing of the waste package by water. This is the worst case for concentration of aggressive species and breach of cladding. It is assumed that groundwater entry occurs while there is still significant heat and/or radiation. The water flow rate must nearly match the evaporation rate within the package. If the flow is too high, the package will fill and overflow. The scenario of a filled, well-mixed, overflowing package is covered by the in-package chemistry model, which shows only moderate pH reduction. The scenario with flushing is the worst for transport of species out of the package but is not the worst for cladding performance. Filling the package with water displaces the nitrogen that otherwise might be radiolytically converted to nitric acid. Overflow will flush out aggressive species and prevent groundwater from concentrating to the point of promoting galvanic corrosion of the carbon steel basket materials. Oxygen influx is also greatly reduced in a flooded waste package, so the corrosion potential and corrosion rates are reduced, as are many radionuclide solubilities.

The second assumption is that aggressive species concentrate in the worst possible way. Because fluoride and chloride are consumed by reaction with Zircaloy (CRWMS M&O 2000df, Section 6.2.2.3.2) and carbon steel (McCright 1998, Section 2.1.8), respectively, it is assumed that aggressive species from incoming water will concentrate where they can do the most damage. For fluoride, this would be nearly total evaporation of incoming drops on a drop-width section of a single fuel rod. For chloride, this would be in a crevice between Zircaloy and carbon steel basket materials. It is assumed that the incoming water species are directed to a single rod, until they have breached that rod. Then it is assumed that new aggressive species are directed to another single rod until it is breached, and so on. In this approach, the fraction of cladding perforated is linearly dependent on the water inflow, which generally increases with time as the waste package degrades. Inflow, however, is also a function of other factors such as climate and location within the repository. The likelihood of significant concentration of aggressive species decreases with time; as decay heat and radioactivity decrease, likelihood of good galvanic connection to the Zircaloy decreases, and amount of reduced iron as an energy source for microbes decreases. The trend toward less aggressive conditions is ignored, however, as it is assumed that the aggressive species concentrate in the worst possible way for all time.

This conservative model estimates that the fraction of rods failed from localized corrosion is equal to the amount of water (in m^3) that has entered the average waste package in a group (bin) divided by 2,424 m^3 (85,648 ft^3). Thus, all rods will fail by the time 2,424 m^3 (85,648 ft^3) of water has entered the package. This is evaluated at each time-step, and as the waste package corrodes, more water enters the waste package and more rods fail.

Fast Release of Radionuclides—When the waste package fails, the inventory of isotopes that have migrated to the gap between the fuel and cladding is modeled as instantly released. This was 1.4 percent of the cesium inventory and 4.2 percent of the iodine inventory. In addition, 0.2 percent (range of 0 to 0.4 percent uniformly distributed) of

the inventory of all radionuclides in failed commercial spent fuel rods was modeled as instantly released to account for spent fuel dissolution that occurs before wet unzipping starts.

Wet Unzipping—The fuel rods that have failed at time of waste package breach, or later fail from localized corrosion, are modeled as unzipping as the uranium dioxide fuel matrix reacts. The fraction of fuel that is reacted within the waste package is calculated each time step (after waste package failure) based on the intrinsic commercial spent nuclear fuel dissolution rate. The wet unzipping velocity is modeled as 40 times (range 1 to 240, triangular distributed) the intrinsic dissolution velocity. Unzipping starts at the rod center and progresses in both direction. The intrinsic dissolution velocity is evaluated using the in-package chemistry at each time step.

Seismic Failures—Seismic failures that are severe enough to fail the cladding are estimated to occur with a frequency of 1.1×10^{-6} per year. When such an event is predicted within a TSPA time-step, all the cladding is assumed to fail and start unzipping.

Stainless Steel Cladding—The waste packages that contain the stainless steel clad commercial spent nuclear fuel are treated as a special type of commercial spent nuclear fuel waste package in TSPA. These waste packages are modeled as 3.5 percent of the total number of commercial spent nuclear fuel waste packages and are assumed to contain 33 percent stainless steel clad fuel and 67 percent Zircaloy clad fuel. The stainless steel clad fuel within these packages is assumed to fail and start unzipping at waste package breach.

4.2.6.4.4 Commercial Spent Nuclear Fuel Degradation Abstraction

The degradation rate function is combined with the in-package chemistry and waste package temperature to determine a rate, which is then directly used by the cladding degradation model (see Section 4.2.6.3.3) to determine the rate at which the fuel cladding splits open and exposes more of the fuel matrix. The abstracted dissolution model is shown in Figure 4-102.

4.2.6.4.5 Glass Degradation Abstraction

Dissolution rates are independent of the glass composition within the limits prescribed by the high-level radioactive waste glass waste acceptance product specification, but high-level waste glass degradation rates do depend on pH and temperature. Abstracted degradation rates are shown in Figure 4-104. Uncertainty is included in all three terms of the abstracted model: the effective forward dissolution rate, the pH term, and the activation energy term. These are combined with the pH from abstracted codisposal package chemistry model and the waste package temperature to determine the rate of glass dissolution with time. The resulting uncertainty in the degradation rate included in the model is about four orders of magnitude with a log-uniform distribution.

4.2.6.4.6 DOE Spent Nuclear Fuel and Other Waste Form Degradation Abstraction

The conservative Hanford N Reactor fuel model (1.75 kg/m^2·day) was recommended as the surrogate to bound DOE spent nuclear fuel groups 2 through 11. Naval spent fuel can be bounded by commercial spent fuel, and immobilized plutonium degradation was bounded by high-level radioactive waste glass degradation.

4.2.6.4.7 Solubility Abstraction

A systematic review of thermodynamic data and controlling phases was performed for a large range of chemical conditions. The amount of thermodynamic data available for the radionuclides, the sensitivity of solubilities to in-package chemistry, and the importance of radionuclides to total system performance is quite uneven. For these reasons, the implementation of solubility within the TSPA-SR analysis ranged from (1) multitermed functions of chemistry for uranium, neptunium, and americium; (2) distributions for plutonium, protactinium, lead, and nickel; and (3) constant bounding values for technetium, iodine, thorium, cesium, strontium, chlorine, carbon, niobium, zirconium, radium, and selenium. For the multitermed functions, the radionuclide solubility was calculated as a function of time for each simulation. For the distribution type,

a value for the simulation was sampled from the distribution and used for the entire simulation. For the last type, the same bounding value was used for all times in all simulations. Detailed discussions for each radionuclide are provided in *Summary of Dissolved Concentration Limits* (CRWMS M&O 2000dp). The concentration limits are given in Table 4-24.

In TSPA, solubilities were calculated for each computational cell, using the abstracted chemistry of that cell. Thus for isotopes whose solubilities were functions of chemistry, the solubilities varied spatially and with time.

Table 4-24. Dissolved Concentration Limits for TSPA-SR

Element	Distribution Type	Min (mol/L)	Max (mol/L)
Americium	Function	$\sim 10^{-7.7}$	~0.19
Actinium	Function	$\sim 10^{-7.7}$	~0.19
Samarium	Function	$\sim 10^{-7.7}$	~0.19
Curium	Function	$\sim 10^{-7.7}$	~0.19
Carbon	Constant	1	1
Chlorine	Constant	1	1
Cesium	Constant	1	1
Iodine	Constant	1	1
Niobium	Constant	10^{-7}	10^{-7}
Nickel	Log Uniform	$10^{-5.9}$	$10^{0.5}$
Neptunium	Function	$\sim 10^{-5.7}$	$\sim 10^{-1.8}$
Protactinium	Log Uniform	10^{-10}	10^{-5}
Lead	Log Uniform	10^{-10}	10^{-5}
Plutonium	Log Uniform	10^{-10}	$10^{-3.7}$
Radium	Constant	10^{-6}	10^{-6}
Tin	Constant	$10^{-7.3}$	$10^{-7.3}$
Strontium	Constant	1	1
Technetium	Constant	1	1
Thorium	Constant	10^{-5}	10^{-5}
Uranium	Function	$\sim 10^{-6.3}$	$\sim 10^{-3.4}$
Zirconium	Constant	$10^{-9.2}$	$10^{-9.2}$

Source: Excerpted from *Summary of Dissolved Concentration Limits* (CRWMS M&O 2000dp).

4.2.6.4.8 Colloids Abstraction

The mobile colloidal radionuclide source term consists of three colloid types: waste-form colloids, corrosion-product colloids, and groundwater colloids. As illustrated in Figure 4-106, the mobile colloidal radionuclide source term is the sum of the radionuclide contribution from those colloid types. The total colloid mass concentration

is also provided for recalculating reversibly attached radionuclide concentrations as dissolved concentrations change during transport.

For codisposal packages, the colloidal source term includes (1) waste-form smectites produced from high-level radioactive waste glass, (2) iron-(hydr)oxide colloids produced from steel packaging material, and (3) naturally occurring groundwater colloids found in the infiltrating water. Plutonium and americium are bound irreversibly in waste form colloids, and along with their daughter products are permanently entrained within the colloid. Waste-form colloids can also serve as substrates for reversibly sorbed plutonium and americium. For commercial spent nuclear fuel packages, only iron-(hydr)oxide and naturally occurring groundwater colloids are available for uptake of radionuclides. Following the conceptual model, the TSPA calculations use in-package and in-drift pH and ionic strength conditions to calculate the generation and stability of waste-form colloids and the stability of corrosion-product and groundwater colloids.

4.2.7 Engineered Barrier System Transport

The purpose of the engineered barrier system transport process model is to provide a description of radionuclide transport within the emplacement drift as a result of releases from one or more breached waste packages (CRWMS M&O 2000as). Radionuclide transport out of the waste form and waste package through the invert and into the unsaturated zone is dependent on a complex series of processes, including development of potential flow pathways through the engineered barrier system discussed in Section 4.2.5. This section emphasizes the mobilization and transport of dissolved or colloidal radionuclide species through the engineered barrier system by flowing or slowly dripping water or alternatively through continuous water films formed by adsorptive condensation of humidity on engineered barrier system materials (CRWMS M&O 2000a, Sections 3.6.1 and 3.6.2). In the TSPA-SR model, the principal processes included in the abstraction are diffusion (i.e., the diffusion barrier effect when advection is negligible) and advection without

sorptive retardation (when there is greater water content).

As noted in Section 4.1.4, the DOE has evaluated operation of the repository at lower temperatures. The conceptual basis and model abstractions presented in this section primarily reflect the effects of higher-temperature operating conditions described in Sections 4.2.2 through 4.2.6, specifically those implemented in the TSPA-SR model (CRWMS M&O 2000a, Section 3.6). Conservatisms and conceptual uncertainties in the model have been reevaluated since the TSPA-SR model and are reported or summarized in *FY01 Supplemental Science and Performance Analyses* (BSC 2001a, Sections 10 and 15; BSC 2001b, Sections 3.2.8 and 4.2.8).

New or reevaluated processes modeled in the supplemental TSPA model and found to have a potential affect on radionuclide releases from the engineered barrier system include:

- Waste package diffusion, specifically in-package diffusion (BSC 2001a, Sections 10.3.1 and 10.4.1)

- Sorption of radionuclides to corrosion products derived from mild steel and stainless steel used in the waste package and in the structural support for the invert (BSC 2001a, Sections 10.3.4 and 10.4.4).

Uncertainties in the TSPA-SR colloidal transport model and invert diffusion model were also reevaluated in the supplemental TSPA model (BSC 2001a, Sections 10.3.3, 10.3.5, 10.4.3 and 10.4.5; BSC 2001b, Sections 3.2.8 and 4.2.8). In general, the supplemental TSPA model results suggest that the TSPA-SR model results are reasonable to conservative.

4.2.7.1 Conceptual Basis

The waste form is the source of radionuclides considered for the engineered barrier system. Radionuclides can be transported downward from breached waste packages, through the invert, and into the unsaturated zone. Transport can occur through advection, by which dissolved chemical

species or colloidal particles are carried along by the fluid when there is a fluid flux through the waste package and invert. Transport can also occur by diffusion, whereby dissolved chemical species or colloidal particles migrate from zones of high to low concentration. Diffusion can occur in the absence of an advective liquid flux, if there is a continuous liquid pathway via thin films on the waste form, the waste package, and in the invert (CRWMS M&O 2000a, Section 3.6.2.2).

A one-dimensional transport model is used to represent advection and diffusion in the engineered barrier system. Further, because the duration of radionuclide releases from the waste package will generally be much greater than the travel time through the invert (when advective flow and release conditions pertain), transport dispersivity is neglected in the model. Also, the invert materials have little sorptive affinity for several important radionuclides, so in the TSPA-SR model no performance credit is taken for sorptive retardation (CRWMS M&O 2000a, Section 3.6.1.2).

The engineered barrier system elements through which radionuclides can migrate are conceptually similar to a laboratory column test. That is, radionuclides are introduced at the top of the "column" and migrate downward through materials representing the invert.

Transport Modes Considered—Transport of radionuclides through the waste package and into the invert can occur in several possible modes. Dissolved and colloidal radionuclides will diffuse through thin films of water and stress corrosion cracks in the waste package wall. They may also migrate by advection through larger patches formed by general corrosion. Migration through the invert may be by diffusion, advection, or both (CRWMS M&O 2000a, Sections 3.6.1 and 3.6.2; CRWMS M&O 2000dd, Section 6.1.2).

Colloid-facilitated transport of radionuclides is important for certain radionuclides that have limited solubility (as dissolved species) but strong affinity for colloidal-size particles that are mobile in water. Three types of colloids are expected in the engineered barrier system: (1) waste form colloids, (2) colloids produced from corrosion of repository materials, and (3) groundwater colloids. Radionuclides may become irreversibly embedded in waste form colloids, reversibly attached by sorption, or both modes may exist. Radionuclide sorption to corrosion-product and groundwater colloids is likely to be reversible, although sorption of metal ions to iron-oxide colloids can be quite strong (CRWMS M&O 2000dd, Section 6.1.2).

4.2.7.2 Summary State of Knowledge

4.2.7.2.1 Hydrologic Properties of the Invert

The drip shield is designed to divert water flow to the invert (CRWMS M&O 2001c, Section 6.3). The invert ballast material will be crushed tuff derived from the excavated host rock and will exhibit the hydraulic characteristics of a porous medium. Permeability, porosity, thermal properties, and unsaturated hydrologic properties of candidate invert ballast materials have been measured (CRWMS M&O 2001c).

4.2.7.2.2 Analogue Studies

Advection—Laboratory testing of radionuclide migration downward through a crushed-tuff column was performed with several radionuclides (neptunium-237, plutonium-239, tritium, and pertechnetate) in two groundwaters with different chemical compositions (Triay, Meijer et al. 1997, Section V.A). The purpose of the tests was mainly to compare column transport characteristics with radionuclide sorption parameters from batch-sorption tests. The tests, therefore, provided analogous information on advective transport modified by sorption. The engineered barrier system transport model is analogous to these laboratory tests.

Diffusion—A different series of tests was performed to gather information on the diffusive uptake of radionuclides by intact samples of tuff (Triay, Meijer et al. 1997, Section VI). It was observed that certain radionuclides could diffuse through minute water-filled pores, depending on the porosity, heterogeneity of the pore structure, and sorptive retardation. The tests show that diffusion through the intact tuff is a slow process, particularly for radionuclides with sorptive affinity

such as actinides. For unsaturated conditions, diffusive transport is very slow.

In another set of tests (Conca and Wright 1992), transport parameters including diffusion coefficients were measured in unsaturated gravels over a range of water content. It was observed that in granular materials, diffusive behavior depends on the presence of small amounts of water on grain surfaces, which presumably facilitate grain-to-grain contact. This was apparent even in materials consisting of grains with significant intra-granular porosity. The electrical conductivity of partially saturated materials was measured, from which the analogous solute diffusivity behavior (diffusion coefficient) was estimated using the Nernst–Einstein relation.

4.2.7.2.3 Colloid-Facilitated Radionuclide Transport

Colloid Stability at Engineered Barrier System Conditions—For radionuclide-bearing colloids to affect repository performance, the colloidal dispersion must be stable for the duration of transport and must carry significant amounts of radionuclides. Transport times can range from days to years for advective transport out of a breached waste package and up to hundreds of thousands of years for retarded transport to the receptor location. Thus, some relatively unstable colloids generated at the waste form may persist long enough to be transported out of the waste package and through the invert, but not long enough to be transported a significant distance away from the potential repository. More stable colloids, however, may remain suspended for years and travel a much greater distance (CRWMS M&O 2000cn, Section 6.1.2).

Iron-(hydr)oxide colloids from corrosion of steel and naturally occurring in groundwater are least stable around pH 8.5, and at this pH they will tend to agglomerate (i.e., form larger, immobile particles) (CRWMS M&O 2000cn, Section 6.1.2). At higher or lower pH, however, iron-(hydr)oxide colloids may be more mobile, depending on other factors, such as ionic strength. It is anticipated that ionic strength of water in the drifts will be relatively low during the post-thermal period when waste package breach is most likely, which will facilitate colloid mobility.

Analogues—There is field evidence that suggests colloid-facilitated transport of radionuclides. Buddemeier and Hunt (1988, p. 536) found plutonium and americium more than 30 m (100 ft) below a low-level waste site in unsaturated tuff after approximately 30 years of operation. At the Nevada Test Site, the isotope ratio of plutonium-240 to plutonium-239 in groundwater suggested that plutonium may have been colloidally transported more than 1.3 km (0.8 mi) over a 30-year period, although plutonium is strongly sorbing at the Nevada Test Site and assumed to be immobile (Kersting et al. 1999). In water samples from the Nevada Test Site, plutonium was found to be attached to colloids. In the Pahute Mesa drainage, Buddemeier and Hunt (1988, p. 537) found colloid concentrations of 0.8 to 6.9 mg/L for particles greater than 30 nm (0.000001 in.) in size.

Treated liquid wastes containing traces of plutonium and americium have been released into Mortandad Canyon at Los Alamos National Laboratory (Triay, Meijer et al. 1997, Section V.D). The shallow alluvium at that location is composed of sandy to silty clays formed from weathering of volcanic rocks. Detectable amounts of plutonium and americium have been observed in monitoring wells up to about 3.4 km (2.1 mi) downgradient from the discharge point. Sorption studies had predicted that movement of plutonium and americium would be restricted to a few meters. This suggests that plutonium and americium are strongly associated with colloid materials and that they can be mobile for large distances (Triay, Meijer et al. 1997, Section V.D).

4.2.7.3 Engineered Barrier System Process Model Development

In this section, an overview of radionuclide transport in the engineered barrier system is presented. The engineered barrier system model is described more fully in *EBS Radionuclide Transport Model* (CRWMS M&O 2000dy), *EBS Radionuclide Transport Abstraction* (CRWMS M&O 2000dd), and *Total System Performance Assessment for the*

Site Recommendation (CRWMS M&O 2000a, Section 3.6).

The approach uses the analytical solution to the one dimensional advection–dispersion equation for a continuous source to determine radionuclide breakthrough curves for various postclosure scenarios. Breakthrough curves are plots of relative concentration (i.e., the downstream concentration relative to the concentration at the source) at the point of interest (the floor of the drift) versus the amount of time that has passed since the radionuclide was first released from the source (the waste form). Because of the effects of diffusion and dispersion, relative concentrations gradually increase from 0 to 1 as a contaminant front arrives. Breakthrough times for relative concentrations of 0.01 and 0.5 are used to facilitate comparison of the results (CRWMS M&O 2000dd, Section 6.3.3).

The primary hydrologic input to the engineered barrier system analysis is the pore water velocity, which in turn depends on the Darcy flux (volumetric flow rate per unit area) and the moisture content (fractional volume of the invert material that is occupied by water). This input was derived by inspecting output from *Multiscale Thermohydrologic Model* (CRWMS M&O 2000cf, Section 7).

In addition, a correlation based on laboratory-determined diffusion coefficients is used for calculating diffusive transport when the advective pore water velocity is negligible. This correlation is a power law similar to Archie's Law for electrical conductivity (CRWMS M&O 2000dz) that accounts for the effect of moisture content. In the TSPA calculations, the multiscale thermal-hydrologic model provides the invert water content from which the invert diffusion properties are calculated.

Transport calculations are made using the one-dimensional analytical solution and the average pore water velocity immediately beneath the waste package (i.e., at the drift centerline) (CRWMS M&O 2000dy, Section 6). Sensitivity calculations were performed to evaluate breakthrough times (defined by relative concentration of 50 percent) for various combinations of model input parameters. For advective transport, breakthrough is most

sensitive to the sorptive retardation coefficient. For diffusive transport, transport is most sensitive to the diffusion coefficient.

Model assumptions include one-dimensional vertical migration of radionuclides, negligible transport of radionuclides in the vapor phase, and negligible radioactive decay along the transport pathway (CRWMS M&O 2000dd, Sections 5.5 and 5.7). The invert material is assumed to be homogeneous. These assumptions are justified because the most direct pathway is used, and the pathway is short relative to downstream pathways through the host rock. Radionuclides which can contribute to potentially significant doses at the biosphere, do not form gaseous species at conditions present in the engineered barrier system when releases are most likely to occur.

4.2.7.3.1 Limitations and Uncertainties

As noted in Sections 4.1.1.2 and 4.2.7, the DOE performed several activities to improve the treatment of uncertainty in TSPA-SR models. As stated in Section 4.2.7, uncertainties in the TSPA-SR colloidal transport model and invert diffusion model were reevaluated in the supplemental TSPA model (BSC 2001a, Sections 10.3.3, 10.3.5, 10.4.3, and 10.4.5; BSC 2001b, Sections 3.2.8 and 4.2.8).

Although sorptive distribution coefficients for invert materials are uncertain, this does not affect the modeling approach described here because the distribution coefficient for the TSPA-SR model is assumed to be zero: that is, no credit is taken for any retardation that may occur in the engineered barrier system. This assumption produces a conservative estimate of the transport of dissolved species out of the engineered barrier system (CRWMS M&O 2000dd, Section 5.2.7).

If advection is the dominant mode of transport, then differences in travel time at the center of the invert, compared to near the edges, could be important. However, advective travel times are relatively fast, on the order of a few tens of years or less. Therefore, the model is insensitive to the location of the fastest advective pathway through the invert. If advection is negligible (i.e., at low water content), then the invert can behave as a diffusion

barrier. However, by relying on a conservative diffusion coefficient model, the TSPA-SR model and supplemental model studies show limited diffusion resistance to radionuclide transport in the invert (BSC 2001b, Section 3.2.8).

4.2.7.3.2   Alternative Conceptual Processes

Several concepts that could be examined as relevant alternatives were considered but, because they are improbable or not supported by available data, are not incorporated in the engineered barrier system analyses. Transport was represented using a one-dimensional model. Expanding the model to multiple dimensions would provide insights into the spreading of a radionuclide contaminant from a point source, but the resulting differences in the estimated rate of transport would probably be small.

It is possible that complete saturation could occur in the emplacement drift invert due to clogging in the invert or in the host rock that drains the invert. Drainage pathways could become clogged with fine materials by geochemical alteration of engineered barrier system materials or by precipitation of uranium compounds derived from the waste form. Possible consequences include an increased rate of radionuclide release and transport by saturated flow in a direction parallel to the drift axis. Radionuclides might then be transported laterally through the invert to a major fault or fracture zone where relatively rapid drainage through the host rock could occur. Transport of radionuclides through the unsaturated zone would potentially occur at higher velocity, and with fewer water–rock interactions, than if the drainage was more uniform. However, the fracture permeability and drainage capacity of the host rock are considered sufficient that complete saturation of the invert is unlikely, and this condition is excluded from the TSPA-SR model (CRWMS M&O 2001c, Section 6.2.5).

It is also possible that radionuclides could be sorbed by solids (e.g., steel corrosion products) in the engineered barrier system, and that episodes of increased fluid flux could cause temporarily increased rates of radionuclide release. As for episodes of increased flux, this process would

cause dilution downstream, which would tend to mitigate the effects on dose rates at the biosphere. Alternative conceptual processes were conservatively unaccounted for in the TSPA-SR model but were implemented in supplemental models to quantify conservatism. These processes included sorption of radionuclides to corrosion products in the emplacement drifts and in-package diffusion of radionuclides, which were found to have a beneficial affect on total performance. These conclusions have provided additional confidence in the TSPA-SR model (BSC 2001a, Sections 10.3.1, 10.3.3, and 10.3.4).

It is possible that precipitates and salts could accumulate in the invert early in the thermal period. The change in porosity could produce changes in the transport properties. However, the salts would be readily dissolved when water returned during cooldown, leaving the less soluble precipitates (consisting mainly of silica and calcite) at later times when waste package breach is most likely to occur. These precipitates constitute only a fraction of the maximum accumulation (CRWMS M&O 2000cg, Section 6.5) and would occupy only a portion of the available porosity (CRWMS M&O 2001c, Section 6.1). Consequently, the effect on transport properties of the invert ballast material would be limited.

Another possibility is that constituents of the waste form (e.g., uranyl compounds) could precipitate in the invert and change the transport properties. This is unlikely because the waters that contact the waste form will have already reacted with the host rock and because conditions that lead to advective flow through the waste package would be associated with additional water flow that is diverted to the invert and is available for dilution. This possibility is the subject of ongoing analysis.

Microbially facilitated radionuclide transport was considered but was screened out for the TSPA-SR model (CRWMS M&O 2001d, Section 6.4.61). Microbial action tends to increase colloid size, which would make them susceptible to gravitational settling and filtration. Consequently, exclusion of microbially facilitated transport may be considered conservative.

4.2.7.3.3 Engineered Barrier System Radionuclide Transport Model Validation

The one-dimensional advection–dispersion equation is widely accepted for evaluating solute transport, and the analytical solution to this equation provides a robust and reliable method for evaluating transport through a homogeneous material like the invert ballast. Applicability of the model depends on understanding possible changes that could occur in the invert ballast material with time. The model relies on results from *Water Distribution and Removal Model* (CRWMS M&O 2001c, Section 6) for scoping of such changes.

4.2.7.4 Engineered Barrier System Flow and Transport Abstraction

The following sections provide a summary of how the results of the engineered barrier system radionuclide transport process modeling were abstracted for use in the TSPA-SR model. The principal processes included are diffusion (i.e., the diffusion barrier effect when advection is negligible) and advection without sorptive retardation (when there is greater water content) (CRWMS M&O 2000a, Section 3.6).

Over tens of thousands of years the drip shields and waste packages will gradually degrade, leading to the release and transport of radionuclides through the engineered barrier system (Section 4.2.4.3). Water is expected to be the primary transport medium. Flowing water, or a continuous film of stationary water, is necessary for radionuclide transport out of the waste package, through the invert, and into the unsaturated zone (CRWMS M&O 2000a, Section 3.6).

After a waste package is breached, moisture may enter the waste package as vapor and form water films on the internal surfaces (Section 4.2.5.1). If the cladding is breached, radionuclides may dissolve in the water and be transported out of the waste package by diffusion (Figures 4-109 and 4-110). Breaches formed by general corrosion ("patches") can provide a path for advective liquid flux to enter the waste package and mobilize radionuclides. Advective transport is anticipated to be the main transport mechanism through corrosion patches. Diffusive transport will be the dominant mechanism through stress corrosion cracks because their small size and associated capillary forces resist advective flux.

The dissolved concentration of each mobilized radionuclide cannot exceed the radionuclide solubility limit, unless suspended colloids are present. Colloids are important because they can increase the concentration of radionuclides in the liquid. Colloids can also increase the transport velocity of radionuclides, although this will be a minor effect over the short distances in the engineered barrier system (CRWMS M&O 2000a, Section 3.6; see also Section 4.2.6.3).

Once outside the package, the radionuclides will be transported through the invert by diffusion if advection in the invert is sufficiently slow, or by advection if an appreciable amount of water is flowing through the invert. For TSPA-SR, the one-dimensional advection–diffusion transport model described previously combines these mechanisms. The conceptual model for the engineered barrier system flow and transport abstraction is summarized in Figure 4-111. The important elements for transport are the flow abstraction and the transport abstraction.

4.2.7.4.1 Flow Abstraction

The source of advective inflow to the engineered barrier system is seepage flux, flowing from discrete fractures in the roof of the drift, falling vertically onto the drip shield and any other exposed components (Figure 4-109). The most important part of the engineered barrier system flow abstraction is the algorithm for splitting the seepage flux into the portion that flows through breaches in the drip shield or waste package and the remainder that flows around the drip shield or waste package (Sections 4.2.5.3 and 4.2.5.4). As discussed in Section 4.2.5.4, the result of the flow abstraction is that fluid flux occurs along eight pathways through the engineered barrier system. Only the flux through the waste package and the flux to the unsaturated zone are used directly in the transport calculations for the TSPA-SR model (CRWMS M&O 2000dd, Section 6.4).
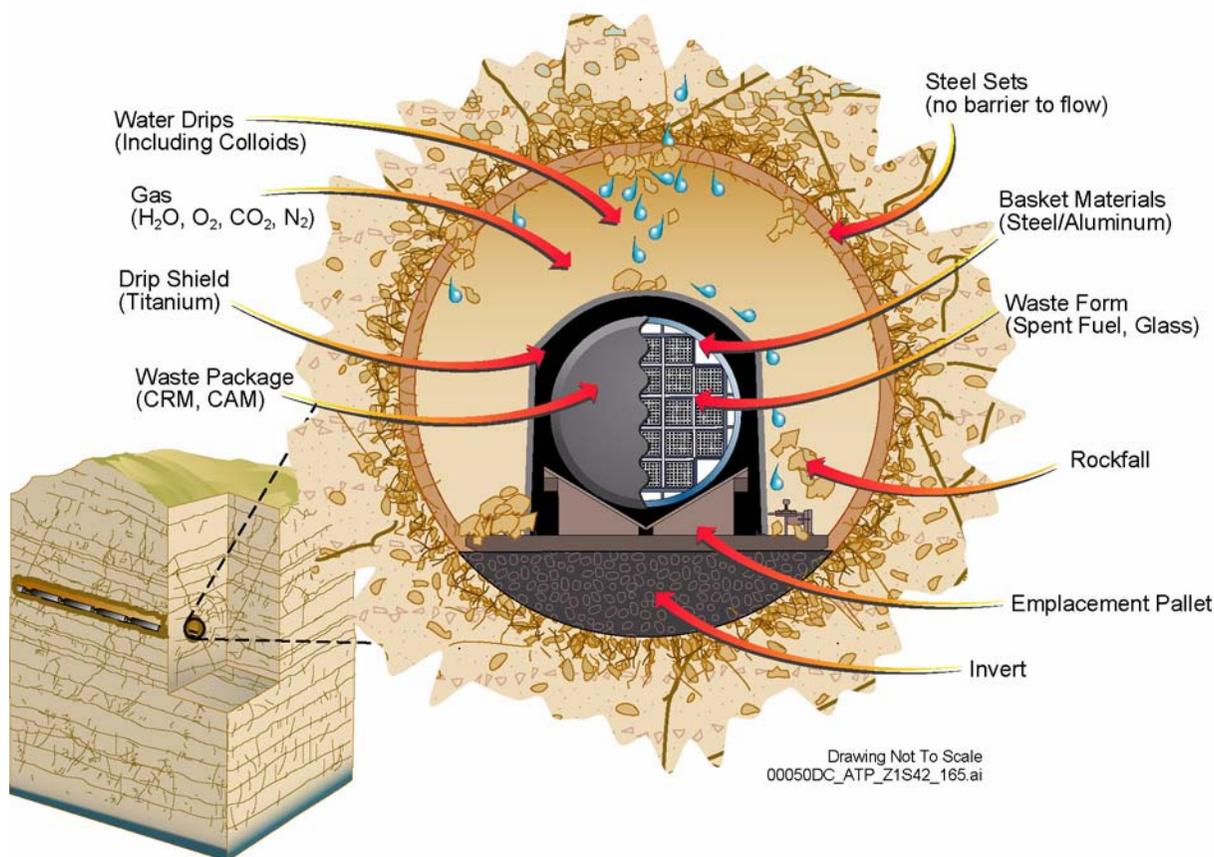
Figure 4-109. Conceptualization of an Emplacement Drift with the Major Components of the Engineered Barrier System, and Seepage Diverted by the Drip Shield
CRM = corrosion-resistant material; CAM = corrosion-allowance material.

The flow abstraction is conservative in several aspects, as discussed in Sections 4.2.5.3 and 4.2.5.4. First, leakage of liquid water through the drip shield always falls on a waste package, although is it also possible that such leakage could be diverted as film flow on the underside of the drip shield. In addition, where seepage occurs, it is assumed to uniformly wet the surface of the drip shield or waste package. Thus, every breach is exposed to seepage; however, no breach is exposed to the full flow of dripping at a point. This approach is justified because it represents the average response of the many waste package locations where seepage can occur. It also accommodates the average response when seep locations move around with time. Finally, evaporation within and on the waste package is ignored. Either diffusive or advective transport will cease if the liquid films on the waste form or the waste package evaporate. The potential for evaporation to eliminate radionuclide transport is conservatively ignored in the TSPA-SR model (CRWMS M&O 2000dd, Section 5.1.17).

Modifications to the flow abstraction are discussed in Section 4.2.5 of this report. These changes include a revised method for splitting the seepage flux through the engineered barriers. See Sections 4.2.5.3 and 4.2.5.4 of this report for further discussion.

4.2.7.4.2   Engineered Barrier System Transport Abstraction

The waste form is the source of all radionuclides considered for the engineered barrier system. After
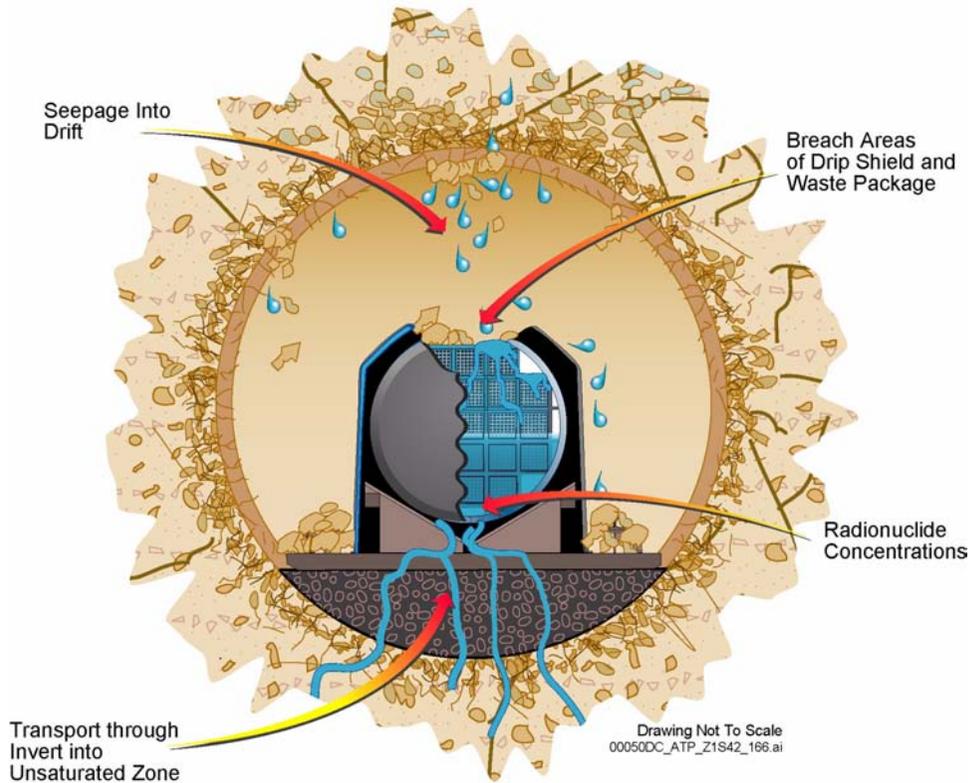
Figure 4-110. Conceptualization of an Emplacement Drift after the Drip Shield and Waste Package are Breached
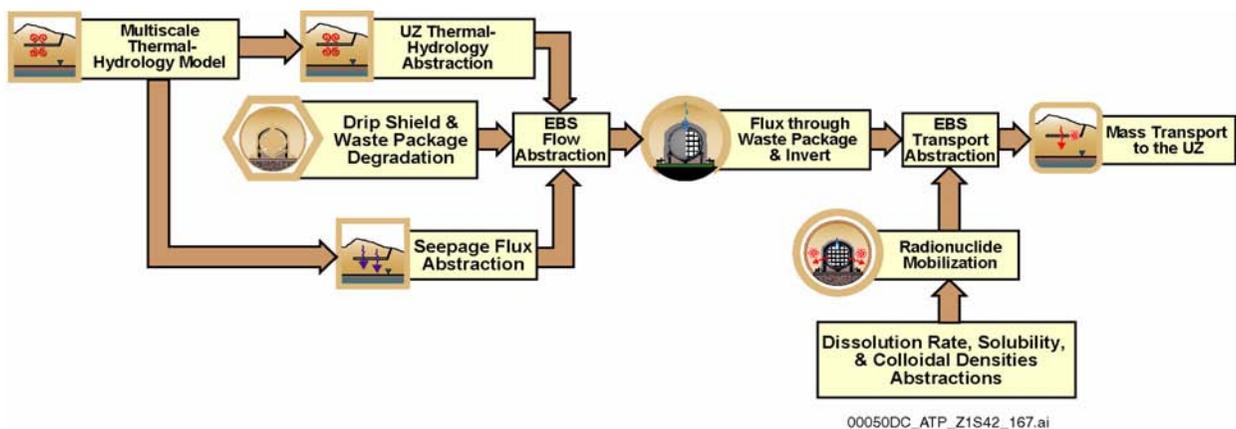
Figure 4-111. Schematic Representation of Inputs and Outputs of Engineered Barrier System Flow and Transport Model for Total System Performance Assessment

UZ = unsaturated zone; EBS = engineered barrier system.

a breach of the drip shield and waste package, radionuclides could be transported downward, through the invert, and into the unsaturated zone (Figure 4-110). After stress corrosion cracks appear in the waste package, diffusive transport is allowed to commence regardless of whether conditions may be consistent with existence of a continuous liquid pathway. Radionuclides are then mobilized to the unsaturated zone when a significant advective liquid flux is present in the invert (CRWMS M&O 2000dd, Section 7.1).

Colloid-facilitated transport of radionuclides is included as an additional source term. Radionuclide transport from the waste package occurs in a fluid containing colloids and dissolved radionuclides. The total concentration for certain radionuclides, particularly plutonium and americium, can be increased well above the solubility limit by colloidal transport. Plutonium and americium are included on the basis of their transport behavior and observations from laboratory and field studies. Protactinium and thorium are highly sorptive and are included for conservatism. Selected daughters of these parent radionuclides are also included in the TSPA-SR model (CRWMS M&O 2000a, Section 3.5.6.2). Colloid-associated radionuclide concentrations, colloid masses, and water chemistry parameters (ionic strength and pH) from the waste package serve as inputs to the in-drift colloids model, where colloid stability and advective transport through the invert are modeled (CRWMS 2000co, Section 6.3.4).

Mixing cells are used in TSPA-SR to represent the waste package and the invert. A mixing cell is a fluid volume with well-mixed, homogeneous conditions throughout. Representation of radionuclide solubility, waste form dissolution rate, cladding performance, and inventory by waste package type are defined by other abstractions for the TSPA-SR (CRWMS M&O 2000a, Section 3.5).

The transport abstraction in the TSPA-SR model is also conservative in several aspects. Firstly, as mentioned in Section 4.2.7.3.1, there is no retardation of dissolved species in the waste package or invert (CRWMS M&O 2000dd, Section 5.2.7). Corrosion products from the waste package, structural steel in the drifts, and spent nuclear fuel have

the potential to be strong sorbents for actinides but are conservatively ignored. Secondly, diffusive transport cannot occur if liquids are not present, and the waste form may actually remain dry for hundreds or thousands of years after the waste package is breached. This effect is conservatively ignored, and diffusion is allowed to occur immediately when a breach occurs. In addition, the waste package is assumed to be in contact with the invert, providing a continuous liquid pathway for diffusion (CRWMS M&O 2000a, Section 3.6.2). Finally, release of radionuclides by advective transport is modeled to be independent of the location of breaches in the waste package. Thus, in the TSPA-SR abstraction, a waste package with only one penetration, or a waste package with one or more penetrations on its upper surface and none on its lower surface, would still have advective transport into the invert (CRWMS M&O 2000dd, Section 7.2).

The supplemental TSPA model has incorporated selected changes to the engineered barrier system transport model resulting from supplemental uncertainty analyses. These modifications include waste package diffusion (BSC 2001a, Sections 10.3.1 and 10.4.1) and sorption of radionuclides to corrosion products (BSC 2001a, Sections 10.3.4 and 10.4.4). The affects of these changes at the TSPA level are discussed in Volume 2, Section 4.2.8 of *FY01 Supplemental Science and Performance Analyses* (BSC 2001b). In general, inclusion of the supplemental models results in slight reductions in dose calculations by the supplemental TSPA model, indicating that the TSPA-SR model may be somewhat conservative.

4.2.8   Unsaturated Zone Transport

In the event of radionuclide mobilization and migration away from the potential emplacement drifts at Yucca Mountain, the rate of radionuclide transport through the unsaturated zone is determined by the percolation flux and by the hydrologic properties and sorptive characteristics of tuff units. Water carrying radionuclides would percolate vertically through fractured tuff units, or it may be laterally diverted around low-permeability horizons (particularly where perched water occurs) to fault zones. Diffusion, sorption, and

dispersion would retard the radionuclide movement. Each of these processes potentially affects the distribution and concentration of radioactive particles at the water table.

Unsaturated zone transport depends on inputs from the unsaturated zone flow and seepage into drifts (described in Section 4.2.1) and on rates of radionuclide releases from the waste emplacement drifts (described in Sections 4.2.2 to 4.2.7). The unsaturated zone transport model supplies to the TSPA temporal evolutions and spatial distributions of radionuclide concentrations at the water table. The current understanding of transport in the unsaturated zone is documented in *Unsaturated Zone Flow and Transport Model Process Model Report* (CRWMS M&O 2000c, Sections 2.2 and 3.11), *Radionuclide Transport Models Under Ambient Conditions* (CRWMS M&O 2000ea, Section 6), *Unsaturated Zone and Saturated Zone Transport Properties (U0100)* (CRWMS M&O 2000eb, Sections 6.4 to 6.8), and *In Situ Field Testing of Processes* (CRWMS M&O 2000bu, Section 6.9; BSC 2001a, Section 11).

4.2.8.1 Conceptual Basis of Unsaturated Zone Transport

This section summarizes basic concepts about transport through the unsaturated zone at Yucca Mountain. The transport of aqueous/colloidal radionuclide species can occur in both the fractures and the porous matrix. The flow pathways are determined by the characteristics of hydrogeologic units, faults, and perched water. These characteristics control the extent of downward versus lateral flow, fracture–matrix interaction, and the partitioning of flow between fractures and rock matrix. Fractures and faults can be fast flow paths, with diffusion into the matrix and sorption to the rock being the important processes for radionuclide retardation. Radionuclide retardation may be important to the safety of a potential repository at Yucca Mountain (CRWMS M&O 2000c, Section 3.11.1.1).

The concentration of radionuclides and their daughter products are diminished according to their radioactive decay rates, the extent of sorption onto the solid phase, and dilution as a result of

mixing (i.e., dispersion). The effects of advective flow processes, sorption (solutes) or filtration (colloids), matrix diffusion, hydrodynamic dispersion, and radioactive decay on unsaturated zone transport are summarized below.

Advection (CRWMS M&O 2000c, Section 3.11.2.2)—Advection is the movement of dissolved or colloidal species resulting from the bulk flow of fluid (Fetter 1993, p. 47). Flow and advective transport within Yucca Mountain are predominantly downward because of gravity. The presence of perched water may result in lateral flow and subsequent transport of the radionuclides. Advection through fractures is expected to dominate transport behavior in welded units and in the zeolitic portions of the Calico Hills nonwelded hydrogeologic unit and other lower tuff units. In some welded and zeolitic layers, the matrix permeability is insufficient to carry the net infiltration, which implies that a portion of the percolation is likely to be carried by fractures (CRWMS M&O 2000c, Section 3.6.3.1). Matrix flow dominates in the vitric Calico Hills nonwelded hydrogeologic unit.

Matrix Diffusion (CRWMS M&O 2000c, Section 3.11.2.5)—Matrix porosity, saturation, and mineralogy affect the extent of diffusion and sorption of species. Matrix diffusion can play an important role in radionuclide exchange between the fractures and the rock matrix. It depends on the effective contact area between fracture and matrix (CRWMS M&O 2000bq, Section 6.2). The presence of inactive and relatively dry fractures, accounted for with the active fracture model, would affect matrix diffusion. Radionuclide diffusion into the rock matrix and away from the fracture surface is driven by a concentration gradient, and it will slow the advance of radionuclides by removing them from the faster flowing fractures. The effective matrix diffusion coefficient can be expressed as the product of molecular diffusion coefficient (for diffusion process in aqueous solution), tortuosity (for measure of deviation from straight flow path through porous medium), porosity, and water saturation to account for the rock characteristics and saturation effects on matrix diffusion.

Sorption (CRWMS M&O 2000c, Section 3.11.2.4)—Sorption is a general term to describe the binding of a solute (radionuclide) onto the sorbent (either the immobile rock matrix or colloids). As a result of sorption onto the rock matrix, the advancing rate of sorbing radionuclides is retarded. In Yucca Mountain studies, the effective sorption distribution coefficient (K_d) approach is employed to quantify the extent of radionuclide–sorbent interactions. This approach does not require identifying the specific underlying processes of sorption, such as surface adsorption, precipitation, and ion exchange.

Hydrodynamic Dispersion (CRWMS M&O 2000c, Section 3.11.2.3)—Hydrodynamic dispersion includes both mechanical dispersion arising from local velocity variations and molecular diffusion driven by concentration gradients. Hydrodynamic dispersion dilutes and smears sharp concentration gradients and reduces the breakthrough time of radionuclides to the water table. Dispersion of radionuclides occurs both along (longitudinally) and transverse to the average flow direction.

Radioactive Decay and Daughter Products (CRWMS M&O 2000c, Section 3.11.2.6)—The decay of the radioactive species of interest and their half-lives are well documented. The transport simulations must compute the total radioactivity distribution (i.e., the sum of the concentrations of all the members of the radioactive decay chain). This is especially significant if the daughters from the decay chains have long half-lives. The daughter products may have significantly different transport behavior than the parent radionuclide.

Colloidal Transport (CRWMS M&O 2000c, Section 3.11.2.7)—Colloids are very fine particles (e.g., clay minerals, metal oxides, viruses, bacteria, and organic macromolecules) that range in size from 1 to 10,000 nm (0.00000004 to 0.0004 in.) (McCarthy and Zachara 1989, pp. 496 to 502). Radionuclides can be transported as intrinsic colloids. Intrinsic colloids are also referred to as waste-form colloids or true colloids of elemental particles (e.g., plutonium colloidal forms plutonium (IV) and colloidal plutonium (V), with Roman numerals representing the valence or

oxidation states). Radionuclides can also be adsorbed to naturally occurring fine particles and be transported as radionuclide-bearing pseudo-colloids (e.g., for plutonium-239 and americium-243). The transport of colloidal species is further affected by their size, which determines the nature of pore exclusion and filtration processes. Colloidal transport differs from solute transport because of colloidal particle interactions (e.g., flocculation or formation of aggregated mass of suspended particles), pore exclusion, and surface reactions (e.g., deposition or attachment).

4.2.8.2 Summary State of Knowledge

This section presents data that support the conceptual basis and modeling of radionuclide transport through the unsaturated zone. The in situ field tests in the Exploratory Studies Facility at Yucca Mountain and at the unsaturated transport test site at Busted Butte are first described in Section 4.2.8.2.1. The laboratory measurements of transport properties conducted on tuff samples from deep boreholes and from field sites are summarized in Section 4.2.8.2.2. In addition, natural analogues for unsaturated zone transport processes are discussed in Section 4.2.8.2.3.

4.2.8.2.1 Field Tracer Tests

All liquids released in the alcove and niche test sites in the Exploratory Studies Facility contain tracers. The tracer analyses provide data and information on flow and transport processes. Some flow tests are summarized in Section 4.2.1.2 and in *Unsaturated Zone Flow and Transport Model Process Model Report* (CRWMS M&O 2000c, Section 2.2). The tracer transport data from seepage tests and fracture–matrix interaction tests are presented in *In Situ Field Testing of Processes* (CRWMS M&O 2000bu, Sections 6.3, 6.4, 6.6, and 6.7).

Construction Water Migration (CRWMS M&O 1998i)—Construction water used in the excavation of the Exploratory Studies Facility drifts contained lithium bromide as a tracer. The presence of the tracer (measured as bromide to chloride ratio, leached out of crushed borehole samples) is illustrated in Figure 4-112 along three construction
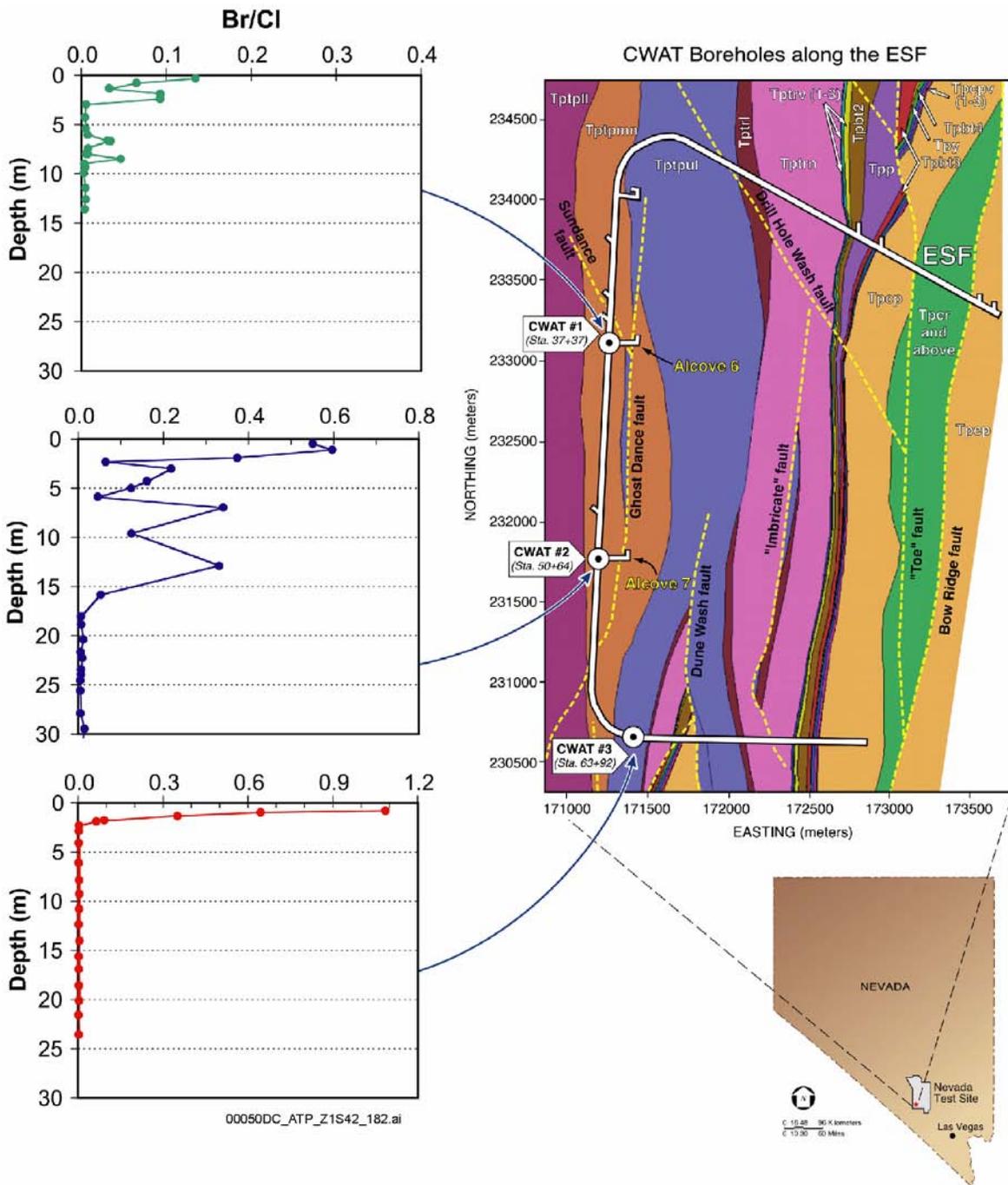
Figure 4-112. Construction Water Distribution below the Exploratory Facilities Drift
Sources: Bromide to chloride ratios taken from Figure 3.1-1 of *Model Prediction of Local Plume Migration from the Cross Drift* (CRWMS M&O 1998i); geologic framework map based upon the geologic framework model (CRWMS M&O 2000bs). ESF = Exploratory Studies Facility.

water boreholes (designated "CWAT") drilled in the Exploratory Studies Facility. The deepest tracer penetration was at borehole CWAT#2, in which construction water had reached the bottom of the hole (30 m, or 98 ft). CWAT#2 is located in an intensely fractured zone (illustrated in Figure 4-10) of the middle nonlithophysal zone of the Topopah Spring welded hydrogeologic unit. In CWAT#1, the construction water was detected in all samples to a depth of 2.4 m (8 ft) with two isolated peaks at greater depths. In CWAT#3, located in the upper lithophysal zone, the construction water was detected only in the top 2 m (7 ft).

Figure 4-112 also illustrates that the Exploratory Studies Facility main drift is primarily through the middle nonlithophysal zone, with the main potential repository block in the lower lithophysal zone located to the west of the main drift horizon. Both the variations in hydrologic properties of different tuff units and in the construction usage rates could have effects on the construction water penetrations. Another test was conducted in the upper lithophysal zone at the starter tunnel of the ECRB Cross-Drift. Wetting front signals were detected up to depths close to 10 m (33 ft) by electrical resistivity probes and psychrometers after the excavation by the tunnel boring machine (CRWMS M&O 2000bu, Section 6.9).

Alcove 1 El Niño Infiltration and Seepage Tests (CRWMS M&O 2000bw, Section 6.8.1)—A large-scale infiltration and seepage test in the Exploratory Studies Facility is located in Alcove 1 near the North Portal (Figure 4-113). In this test, a drip irrigation system on the outcrop above Alcove 1 is used to simulate large infiltration events associated with high precipitation during El Niño conditions. The crown of Alcove 1 is approximately 30 m (100 ft) below the ground surface. The infiltration test at Alcove 1 involved applying water at the ground surface. At a late stage of the test, lithium bromide at high concentration was introduced into the infiltrating water. Seepage into the alcove and the tracer arrival time were recorded. The tracer was first detected after 28 days.

Hydrologic properties calibrated to earlier Alcove 1 seepage data were used in the tracer simulation. The simulated breakthrough curve closely matches

the tracer concentration data for a tortuosity value of 0.75, which is close to the value of 0.7 given by Francis (1997, p. 5). This relatively high tortuosity value is possibly related to the nearly saturated conditions in the test. Comparison with early test results indicate that the continuum approach is valid for modeling flow and transport in unsaturated fractured rock. An active fracture model can capture the major features of fingering flow and transport in fractures. Matrix diffusion has a large effect on the overall transport behavior in unsaturated fractured rock, while dispersion in fractures does not (CRWMS M&O 2000bw, Section 6.8.1.2).

Test results show that matrix diffusion is important in diluting the tracer concentration and increasing the tracer breakthrough times in the Tiva Canyon welded hydrogeologic unit (CRWMS M&O 2000bw, Section 6.8.1). Both the Tiva Canyon and Topopah Spring hydrogeologic units contain fractured and welded tuff rock. While the Alcove 1 test site in the Tiva Canyon welded hydrogeologic unit is above the potential repository horizon, the test results on the importance of matrix diffusion may be applied to the similarly fractured Topopah Spring welded hydrogeologic unit below the potential repository horizon.

Alcove 8–Niche 3 Cross-Drift Tests (CRWMS M&O 2000bu, Section 6.9)—Alcove 8 has been excavated in the ECRB Cross-Drift, approximately 20 m (66 ft) directly above Niche 3 in the main drift. Alcove 8 is for controlled liquid-release tests with Niche 3 instrumented for seepage detection, as illustrated in Figure 4-114. The Cross-Drift test block includes the interface between the upper lithophysal zone and the middle nonlithophysal zone of the Topopah Spring welded hydrogeologic unit. A localized release test has been initiated and a 3 m × 4 m (10 ft × 13 ft) areal liquid release plot will be used for the Cross-Drift tests. The test results, when available, would be used to understand large-scale flow and seepage processes across a tuff layer interface at the potential repository horizon.

Where the Cross-Drift crosses over the main drift, the migration of construction water from the excavation of the Cross-Drift was monitored, as
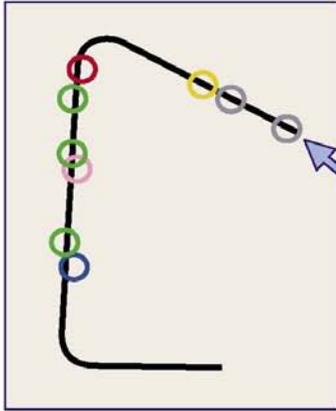
(a) Photograph of Exploratory Studies Facility North Portal and Infiltration Plot (Blue Cover)

Objectives:
- Quantify large-scale infiltration and seepage processes in the bedrock.
- Evaluate matrix diffusion mechanism in long-term flow and transport tests.

Approaches:
- Water applied on the surface 30 m directly above the alcove.
- Tests conducted in two phases: March – August 1998 and May 1999 – present, with Phase 1 focusing on flow and Phase 2 focusing on tracer transport.

Results:
- Over 100,000 liters infiltrated in Phase 1, with observed seepage rates of up to 300 liters/day.
- First seepage was observed 58 days after Phase 1 test initiation. Pressure/flow response of the system was observed to be ~2 days once a nearly steady-state system had developed.
- High concentrations of LiBr were used in Phase 2 tracer test.
- First tracer breakthrough in Phase 2 observed in 28 days with a nearly steady-state flow system using a conservative tracer.
- Tracer recovery data were used to compare with model predictions and to evaluate the importance of matrix diffusion.

00050DC_ATP_Z1S42_158a.ai

(b) Schematic of Alcove 1 Infiltration Test
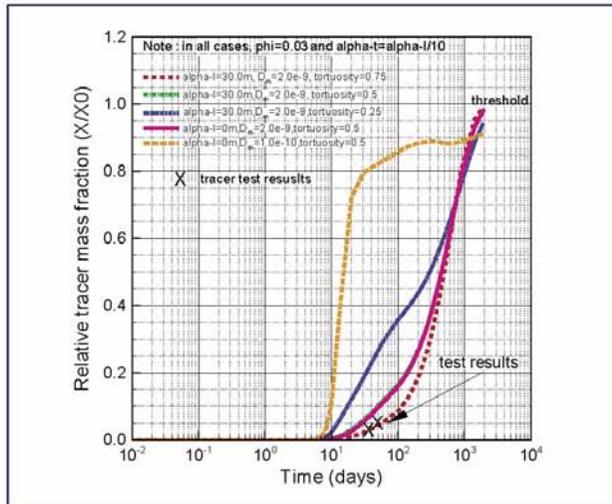
(c) Tracer Breakthoughs Test Results and Model Predictions with Matrix Diffusion

Figure 4-113. El Niño Infiltration and Seepage Test at Alcove 1
Source: CRWMS M&O 2000c, Figure 2.2-8.

(a) Schematic of the Cross-Drift Test Bed

Objectives:
- Quantify large-scale infiltration and seepage processes in the potential repository horizon.
- Evaluate matrix diffusion mechanism in long-term flow and transport tests across a lithophysal—nonlithophysal interface.

Approaches:
- Water releases are in Alcove 8 and seepage collections are in Niche 3.
- Niche 3 is instrumented with seepage collectors and wetting front sensors.
- Geophysical tomographs are conducted in vertically slanted boreholes.

Status:
- Drill-and-blast phase of Alcove 8 excavation was completed in 1999.
- Tests are prepared to be conducted after alcove excavation.

Supporting Results:
- Seepage tests at Niche 3 behind bulkhead demonstrate the existence of seepage threshold under high-humidity conditions.
- During ECRB Cross-Drift construction, no water was observed to seep into the ESF Main Drift 20 m below.

(b) Photograph of Partial Excavated Alcove 8 in ECRB Cross-Drift

(c) Photograph of Water Collection Trays on the Ceiling of the ESF Main Drift

00050DC_ATP_Z1S42_183c.ai

Figure 4-114. Alcove 8–Niche 3 Cross-Drift Tests
ESF = Exploratory Studies Facility. Source: CRWMS M&O 2000c, Figure 2.2-9.

illustrated in Figure 4-114. No seepage was observed when the tunnel boring machine passed over the main drift.

Busted Butte Transport Tests (CRWMS M&O 2000c, Section 3.11.11.2)—Transport processes in the vitric Calico Hills nonwelded hydrogeologic unit have been and are currently under investigation at the Busted Butte underground facility (Figure 4-115). The principal basis for the Busted Butte tests is that the test results can be extended to characterize the transport properties of the Calico Hills nonwelded geologic unit in the unsaturated zone beneath the potential repository. Busted Butte is located approximately 8 km (5 mi) southeast of the potential Yucca Mountain repository area. This facility consists of a drift complex excavated 70 m (230 ft) below the ground surface to reach a distal extension of the vitric Calico Hills nonwelded hydrogeologic unit below Yucca Mountain. Tracer-injection tests, partial mine-out, and geophysical measurements (ground-penetrating radar, electrical resistivity tomography, and neutron logging) were performed to map solute migration patterns. Results of the ongoing tests are presented in *Unsaturated Zone and Saturated Zone Transport Properties (U0100)* (CRWMS M&O 2000eb, Section 6.8).

Phase 1A results indicate that transport through the vitric Calico Hills nonwelded hydrogeologic unit is dominated by capillary-driven flow, with a well-defined plume developing after tracer injection. Plumes from the ongoing larger-scale Phase 2 test are tracked by sorbing pads in monitoring boreholes and by geophysical imaging techniques. Examples of a fluorescent plume photograph from the Phase 1A test and a ground-penetrating radar tomograph from Phase 2 are presented in Figure 4-115.

The radar data were acquired in two-dimensional planes defined by two boreholes. Regions with elevated moisture content correspond to regions of low transmission velocity of the radar signals. The radar tomographs, together with neutron logging and electrical resistivity tomography results, are compared with tracer breakthrough logs in boreholes. Injected fluid may displace the pore fluid

based on preliminary results of Phase 2 tests. Some fluid breakthrough occurred in the boreholes, but it did not contain injected tracers (CRWMS M&O 2000eb, Section 6.8.4.1.4).

Microspheres are used as a colloidal tracer at the Busted Butte transport test as well as in the saturated zone C-Wells tests (CRWMS M&O 2000eb, Section 6.9). Results of transport tests using sorbing tracers that represent sorbing radionuclides provide evidence of whether or not laboratory-measured retardation factors can be used to predict field-scale transport processes. The Busted Butte transport tests are discussed in more detail in *Unsaturated Zone Flow and Transport Model Process Model Report* (CRWMS M&O 2000c, Section 3.11.11.2), *Radionuclide Transport Models Under Ambient Conditions* (CRWMS M&O 2000ea, Section 6.10), and *Unsaturated Zone and Saturated Zone Transport Properties (U0100)* (CRWMS M&O 2000eb, Section 6.8).

4.2.8.2.2 Transport Properties

As described in Section 4.2.8.1, the unsaturated zone transport processes include advection, matrix diffusion, sorption, hydrodynamic dispersion, radioactive decay, and colloidal transport. The unsaturated zone flow properties affecting advective transport are discussed in Section 4.2.1 and will not be repeated in this section. This section describes unsaturated zone transport properties based primarily on laboratory measurements of tuff samples.

Matrix Diffusion Coefficients—The effective diffusion coefficient, which is the product of the molecular diffusion coefficient, tortuosity, porosity, and water saturation, is used to account for rock geometry and saturation effects on matrix diffusion. Some experimental data exist on the tortuosity distribution in the various hydrogeologic units at Yucca Mountain. *Radionuclide Transport Models Under Ambient Conditions* (CRWMS M&O 2000ea, Section 6.1.2.4) employed the approach of using the porosity value to approximate tortuosity. Tortuosity measurements on devitrified tuffs showed good agreement with this approximation.

Objectives:
- Quantify unsaturated zone transport processes in Calico Hills nonwelded unit.
- Measure retardation coefficients in the field to compare with laboratory measured values.

Approaches:
- A test bed was excavated 70 m below the surface in mainly vitric CHn underlying the vitrophyre.
- A mixture of conservative and sorbing tracers is used in tracer injection tests.
- Absorbent pads are used to sample periodically the tracer distributions below injections.
- Ground-penetrating radar tomography, together with electrical resistivity tomography and neutron logging, is used to track plume migrations.

Results:
- Phase 1A was conducted with single point injections from April 1998 to mineback in 1999. Capillary-driven flow mechanism is confirmed.
- Phase 2 tests with aerial injections are ongoing with breakthroughs and plume migrations monitored.

00050DC_ATP_Z1S42_157b.ai

(a) Ground Penetrating Radar Tomograph of Injected Plume (Phase 2)

(b) Schematic of Busted Butte Test Area

(c) Tracer Plume from Injection in the Side Wall of the Main Adit, Opposite to the Test Alcove (Phase 1A)

Figure 4-115. Unsaturated Zone Transport Test at Busted Butte
ERT = electrical resistance tomography; GPR = ground penetrating radar. Source: CRWMS M&O 2000c, Figure 2.2-12.

A probabilistic description of matrix diffusion was developed using a beta distribution and the distribution parameters listed in Table 4-25 (CRWMS M&O 2000eb, Section 6.6.3). The assigned parameter values were developed based on analyses of data from literature reviews and limited laboratory data (CRWMS M&O 2000eb, Section 6.6.1.3, Table 16, and Figures 29 and 30). The cationic (positively charged and sorbing) radionuclides are assigned values representative of the coefficient for tritium. Based on measured diffusion behavior of cationic radionuclides, this is conservative (CRWMS M&O 2000eb, Section 6.6.1.3). The coefficient for technetium (as pertechnetate, the predominant aqueous species of technetium) is approximately 10 times lower than that for tritium. The anionic (negatively charged) radionuclides are more likely to be excluded from the matrix pores, which are also negatively charged.

Table 4-25. Distribution Parameters for Matrix Diffusion Coefficients

Radionuclide Type	Mean (m²/s)	Standard Deviation (m²/s)	Maximum (m²/s)	Minimum (m²/s)
Anionic	3.2×10^{-11}	1.0×10^{-11}	1×10^{-9}	0
Cationic	1.6×10^{-10}	0.5×10^{-10}	1×10^{-9}	0

Source: CRWMS M&O 2000eb, Section 6.6.3.

Sorption Coefficients—Most experimentally determined sorption values at Yucca Mountain have been derived from batch experiments using crushed tuff (crushed to 75 to 500 µm [0.003 to 0.02 in.]) under water-saturated conditions (CRWMS M&O 2000eb, Section 6) for a variety of rock types and elements. Probabilistic descriptions and distribution parameters of sorption coefficients for selected radionuclides are given in Table 4-26 for three rock types: devitrified tuff (including welded tuff), vitric tuff, and zeolitic tuff (CRWMS M&O 2000eb, Table 2a). These distributions and parameter values were derived from an expert elicitation conducted in 1993 as modified by additional new data (CRWMS M&O 2000eb, Section 6.4.2). The water compositions from Wells J-13 and UE-25 p#1 were used to provide an adequate range of compositions to capture the influence of water compositional variability on sorption in the unsaturated zone. The effects of temperature were bounded by measurements at ambient tempera-

tures. The batch experimental approach with crushed tuff may overestimate the sorption values for unsaturated zone transport, as discussed in Section 4.2.8.3.5.2.

The assumptions used to develop values of sorption are discussed in *Unsaturated Zone and Saturated Zone Transport Properties (U0100)* (CRWMS M&O 2000eb, Section 5). The complete table (CRWMS M&O 2000c, Table 3.11-1; CRWMS M&O 2000eb, Table 2a) contains data for additional elements, and, in addition to tuff rocks, sorption coefficients for iron oxide are also presented for some elements. Sorption onto fracture surfaces can retard radionuclide migration. Laboratory sorption experiments showed that trace minerals might be effective at retarding the transport of neptunium-237 when they are concentrated on fracture surfaces (CRWMS M&O 2000eb, Section 6.5.3). Numerical simulations showed that the limited sorption on the fracture walls was sufficiently important to retard transport of strongly sorbing radionuclides (e.g., plutonium-239) (CRWMS M&O 2000ea, Section 6.17.1). However, sorption in fractures is not included in the TSPA transport evaluations because of limited data and the conservative nature of this approximation regarding radionuclide transport to the water table.

Experimental sorption coefficients (K_d values) were obtained using rock samples collected from the Topopah Spring welded and Calico Hills nonwelded hydrogeologic units at Busted Butte (Table 4-27). Sorption coefficients for neptunium and americium from Busted Butte (Table 4-27) are similar to values from batch experiments (Table 4-26); however, sorption values for plutonium are significantly larger.

Dispersivities—The dispersion coefficient is a function of dispersivity and flow velocity. Dispersivity has been shown to increase as a function of observation scale, attributed mainly to mixing as more heterogeneities are sampled at larger scales (Gelhar et al. 1992). Field measurements show that the transverse dispersivity is significantly less than longitudinal dispersivity (Fetter 1993, pp. 65 to 66).

Table 4-26. Sorption Coefficient Distributions for Unsaturated Zone Hydrogeologic Units from Batch Experiments

| Element | Rock Type | K_d (mL/g) | | | Coefficient of Variation | Distribution Type |
		Minimum	Maximum	Mean		
Neptunium	Devitrified	0	1.0	0.3	0.3	Beta
	Vitric	0	1.0	0.3	1.0	Beta (exp)
	Zeolitic	0	3.0	0.5	0.25	Beta
Plutonium	Devitrified	5	70	—	—	Uniform
	Vitric	30	200	100	0.25	Beta
	Zeolitic	30	200	100	0.25	Beta
Uranium	Devitrified	0	2.0	0.5	0.3	Beta
	Vitric	0	1.0	0.5	0.3	Beta
	Zeolitic	0	10.0	4.0	1.0	Beta (exp)
Americium	Devitrified	100	2000	—	—	Uniform
	Vitric	100	1000	400	0.20	Beta
	Zeolitic	100	1000	—	—	Uniform
Chlorine, Technetium, Iodine	—	0	0	0	0	N/A

NOTE: N/A = not applicable. Source: Adapted from CRWMS M&O 2000eb, Table 2a.

Table 4-27. Summary of Radionuclide Sorption Results from Busted Butte Tests

Element	Geologic Unit	Model Layer	Sample Source	Approximate Average K_d (mL/g)
Neptunium	Tptpv2	tsw39	Phase 1B, BH 7	1.1
	Tptpv1	ch1v	Phase 1A, BH 3	0.3
	Tac	ch2v	Phase 1A, BH 4	1.4
Plutonium	Tptpv2	tsw39	Phase 1B, BH 7	1100
	Tptpv1	ch1v	Phase 1A, BH 3	19
	Tac	ch2v	Phase 1A, BH 4	2500
Americium	Tptpv2	tsw39	Phase 1B, BH 7	460
	Tptpv1	ch1v	Phase 1A, BH 3	380
	Tac	ch2v	Phase 1A, BH 4	470

Source: Adapted from CRWMS M&O 2000c, Table 3.11-4.

No data are available to determine dispersivity in the unsaturated zone over the transport distance between the potential repository horizon and the water table. In transport simulations, longitudinal dispersion results in earlier arrival but generally lower concentration. Given this behavior, no simple conservative bound exists for the longitudinal dispersion. A distribution consistent with the dispersivity versus scale correlation of Neuman (1990) is used in TSPA calculations. Transverse dispersion acts only to reduce concentration, with generally little effect on breakthrough time. Therefore, a conservative value of zero for transverse dispersivity is used in TSPA.

The potential repository emplacement area is broad relative to the distance to the water table. For this reason, hydrodynamic dispersion is not expected to play an important role in unsaturated zone transport at Yucca Mountain (CRWMS M&O 2000bq, Section 6.2.5).

Decay Chains—The plutonium-239 decay chain (plutonium-239 → uranium-235 → protactinium-231) is particularly important because the daughter uranium-235 has significantly smaller K_d values compared to its parent plutonium-239, as shown in Table 4-26. The listed decay chain includes only the most important radioactive chain members and omits daughters with short half-lives. The neptunium-237 decay chain (neptunium-237

→ uranium-233 → thorium-229) has also been evaluated. The daughter contribution is less than 2 percent at 1 million years (CRWMS M&O 2000ea, Section 6.13.1.2). As such, daughter contributions to the neptunium-237 transport are relatively insignificant.

Colloid-Facilitated Transport Parameters— Anthropogenic colloids may be produced from the waste or from potential repository construction and sealing materials. This was demonstrated in an experiment on simulated weathering of a high-level radioactive waste glass, where the amounts of plutonium and americium released from waste forms were orders of magnitude greater than their respective concentrations in the dissolved phase (Bates et al. 1992). Constraints on these types of colloids are described in Section 4.2.7 and are treated in *Waste Form Degradation Process Model Report* (CRWMS M&O 2000bm, Section 3.8). Relative to waste form colloids, natural colloid-facilitated transport is much lower and plays a minor role in releases from the repository (CRWMS M&O 2000ec, Section 6.6).

The association of radionuclides with colloids is modeled using two end-member representations: (1) reversible equilibrium exchange with the aqueous phase and (2) irreversible attachment. Radionuclides associated with colloids in either condition (reversible or irreversible) may be subject to size exclusion for fracture–matrix exchange. Colloids are excluded from moving from a fracture into matrix pores smaller than the colloid diameter. This tends to keep colloids (and the associated radionuclides) in the fractures, which leads to more rapid transport of the radionuclides. The chance of exclusion of a colloid from the matrix during fracture–matrix exchange is computed using a probabilistic method that considers different colloid-size and pore-size distributions (CRWMS M&O 2000ec, Section 6.2.1).

The description of reversible, colloid-facilitated radionuclide transport for the particle-tracking transport model used in performance assessment is quantified through two parameters (CRWMS M&O 2000ed, Section 6.1.4). One parameter defines the equilibrium partitioning of radionu-clides between the aqueous phase and colloids. The other parameter is a retardation factor that captures the details of an equilibrium balance between colloid deposition and resuspension. The retardation factor in the colloid model abstraction applies to the transport through fractures. The distribution of retardation factors used is derived from C-Wells data for saturated-zone colloid transport (CRWMS M&O 2000ed, Section 6.2.5). The accessibility factors of colloids of different sizes were evaluated for different geological units (CRWMS M&O 2000ec, Table 3). The linear kinetic model of colloid filtration was used, with the forward kinetic coefficient directly computed (CRWMS M&O 2000ea, Section 6.16).

Colloid concentrations have been measured in several groundwater samples from Yucca Mountain and from other areas at the Nevada Test Site. The measured particle concentrations vary between 1.05×10^6 and 2.72×10^{10} particles per mL, with the lowest being for water from Well J-13 and the highest for water from Well U19q on Pahute Mesa (CRWMS M&O 2000ec, Section 6.2.2.2). These values are consistent with what has been reported in the literature for various groundwaters around the world.

4.2.8.2.3 Analogues for Unsaturated Zone Radionuclide Transport

Natural and anthropogenic sites around the world potentially provide sources of long-term data on the behavior of radionuclides and various metals that may serve as analogues to radionuclide transport at Yucca Mountain (CRWMS M&O 2000c, Section 3.11.12). In this section, some of the more important analogue sites for transport in the unsaturated zone are discussed; additional discussion is presented by *Natural Analogs for the Unsaturated Zone* (CRWMS M&O 2000bp).

Colloid Transport at the Nevada Test Site— There is some field evidence for the occurrence of colloid-facilitated transport of radionuclides at or near the Nevada Test Site. In one case, migration of plutonium and americium, attributed to colloidal transport, was found more than 30 m (100 ft) downward through unsaturated tuff over the period of approximately 30 years below a low-level waste

site (Buddemeier and Hunt 1988, p. 536). In a saturated zone study at the Nevada Test Site, the isotopic ratio of plutonium-240 to plutonium-239 in groundwater showed that plutonium had been transported more than 1.3 km (0.8 mi) from an underground explosion cavity to a test well over a 30-year period, although plutonium is strongly sorbing at the Nevada Test Site and assumed to be immobile (Kersting et al. 1999). Filtration of groundwater samples from the test well indicated that the plutonium was on colloidal material. It is difficult to interpret the plutonium observed at the Nevada Test Site because it originated from an underground nuclear bomb test. The effects of the underground blast on the movement of plutonium are not fully understood.

Uranium Migration at Peña Blanca, Mexico—Since the 1980s, the Nopal I uranium deposit at Peña Blanca (see Figure 4-19b in Section 4.2.1) has been recognized as a natural analogue for the potential repository at Yucca Mountain. From the uranium–thorium age data, it appears that the primary transport of uranium occurred more than 300,000 years ago. Subsequently, there has been little redistribution of uranium-238 and uranium-235. The 300,000-year stability of uranium-235, uranium-238, thorium, and protactinium in fracture-fill minerals has survived recent hydrologic disturbances from surface water infiltration of the fractures. Recent data indicate that the geochemical system at Nopal I restricts actinide mobility in the unsaturated environment. By analogy, the tuffs at Yucca Mountain should have similar retentive properties and impede the mobility of oxidized uranium.

The McDermitt Caldera uranium deposits and other uranium deposits in northwestern Nevada and southeastern Oregon, together with many other uranium sites and contaminated sites worldwide, are discussed in *Natural Analogs for the Unsaturated Zone* (CRWMS M&O 2000bp). These natural analogue studies build confidence in the flow and transport process models.

Artifact Preservation at Akrotiri, Greece—Akrotiri, Greece has silicic volcanic rocks, a dry climate, and oxidizing, hydrologically unsaturated subsurface conditions that are similar to those at Yucca Mountain. The Minoan eruption, an eruption of volcanic ash 3,600 years ago, buried bronze and lead artifacts under 1.5 to 2.0 m (5 to 6 ft) of ash. Researchers looked for plumes of copper, tin, and lead beneath the artifacts by selectively leaching packed earth and bedrock samples that were collected beneath the artifacts. Little of the bronze material had been transported away from the artifacts. Copper and lead plumes were found beneath the artifacts, but neither was detected below a depth of about 45 cm (18 in.). The Akrotiri study shows preservation of artifacts for a long period of time in an oxidizing environment, indicating that unsaturated systems in arid environments may provide favorable sites for geologic disposal of radioactive waste (Murphy et al. 1998).

4.2.8.3 Unsaturated Zone Flow and Transport Process Models

Section 4.2.1 described seepage into the drifts. In this section, additional understanding of flow diverted around drifts and of condensate shed away from the drifts is discussed in Section 4.2.8.3.1. After the radionuclides are transported to the tuff units below the potential repository horizon, the current understanding of the impact of perched water is summarized in Section 4.2.8.3.2. The modeling results on the temporal and spatial distributions of particle released from the potential waste emplacement drifts to the water table are described in Section 4.2.8.3.3. Alternative conceptual processes and limitations and uncertainties are discussed in Sections 4.2.8.3.4 and 4.2.8.3.5, respectively.

4.2.8.3.1 Seepage Diversion and Condensate Shedding

Both the advective and diffusive transport processes determine the rates of radionuclide releases in the drift and transport below the drift. With percolation flux below the seepage threshold and limited amount of seepage flux available (as described in Section 4.2.1.4.2) for advective transport, the release rate is sensitive to enhanced diffusive transport (CRWMS M&O 2000a, Sections 3.6.3.1 and 5.2.5.1). Figure 4-116 is a conceptual sketch that illustrates the concepts of the possible diffusion-dominated flow field or the

advection-dominated flow field in the zone below the drift, discussed in the following paragraphs. The results of analyses of drift seepage for performance assessment (CRWMS M&O 2000bx, Section 6.6.6) indicate that the drift acts as a barrier to downward percolation and that the region below the drift is a drier shadow zone, as illustrated in Figure 4-117. More recent modeling and analysis of the drift shadow zone are presented in Volume 1, Sections 11.2.1 and 11.3.1 of *FY01 Supplemental Science and Performance Analyses* (BSC 2001a).

As long as waste packages are warm enough to heat the air in emplacement drifts, the heat will tend to desaturate the rock around the drifts and redistribute the water. If liquid water is boiled away near the drift during the thermal period, little or no seepage into the drifts is expected. The functioning of the hot and dry barrier is illustrated in Figure 4-118, based on the thermal-hydrologic model and the thermal seepage model (CRWMS M&O 2000ci, Section 6.11.2; BSC 2001o, Section 6.3.5). The drift shadow zone remains relatively dry during the thermal period. The percolation and

seepage after the waste heat decays will be essentially equal to the preemplacement rates if the hydrologic properties and conditions are not significantly altered.

4.2.8.3.2 Lateral Flow Associated with Perched Water Bodies

This section summarizes the effects of perched water bodies on the unsaturated flow field below the potential repository (CRWMS M&O 2000c, Section 3.7.3.3). The geological setting of perched water bodies was presented in Section 4.2.1.1.2 (and illustrated there in Figure 4-7). The occurrence of perched water indicates that the base of the Topopah Spring welded hydrogeologic unit and the zeolitic layers within the Calico Hills nonwelded hydrogeologic unit may serve as barriers to vertical flow and cause lateral diversion of flow. The spatial distribution of low-permeability zeolites has been modeled using mineralogic and petrologic data from several boreholes and is presented in *Integrated Site Model Process Model Report* (CRWMS M&O 2000i).
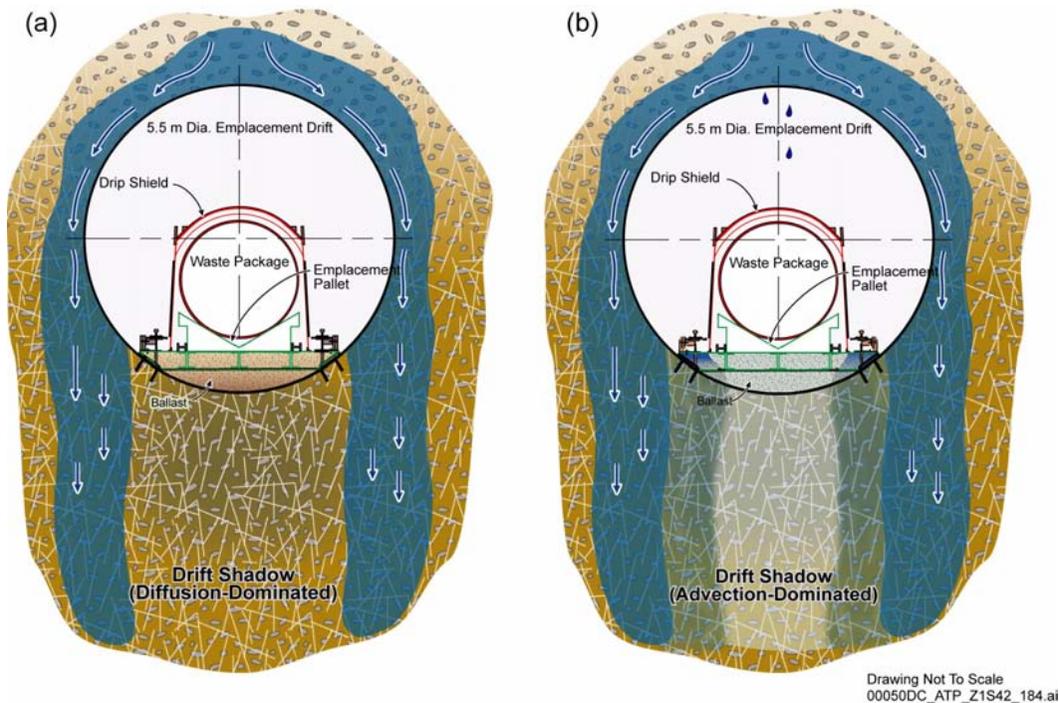
Figure 4-116. Schematic Diagram of Diffusion Barriers in Invert and Drift Shadow Zone
(a) Schematic with diffusion barriers enhanced by seepage diversion and drip shield. (b) Schematic with diffusion barriers influenced by surface diffusion and advective transport. See also Section 2.4.1, Figures 2-71 and 2-72 for the invert structure selected for the potential emplacement drift.
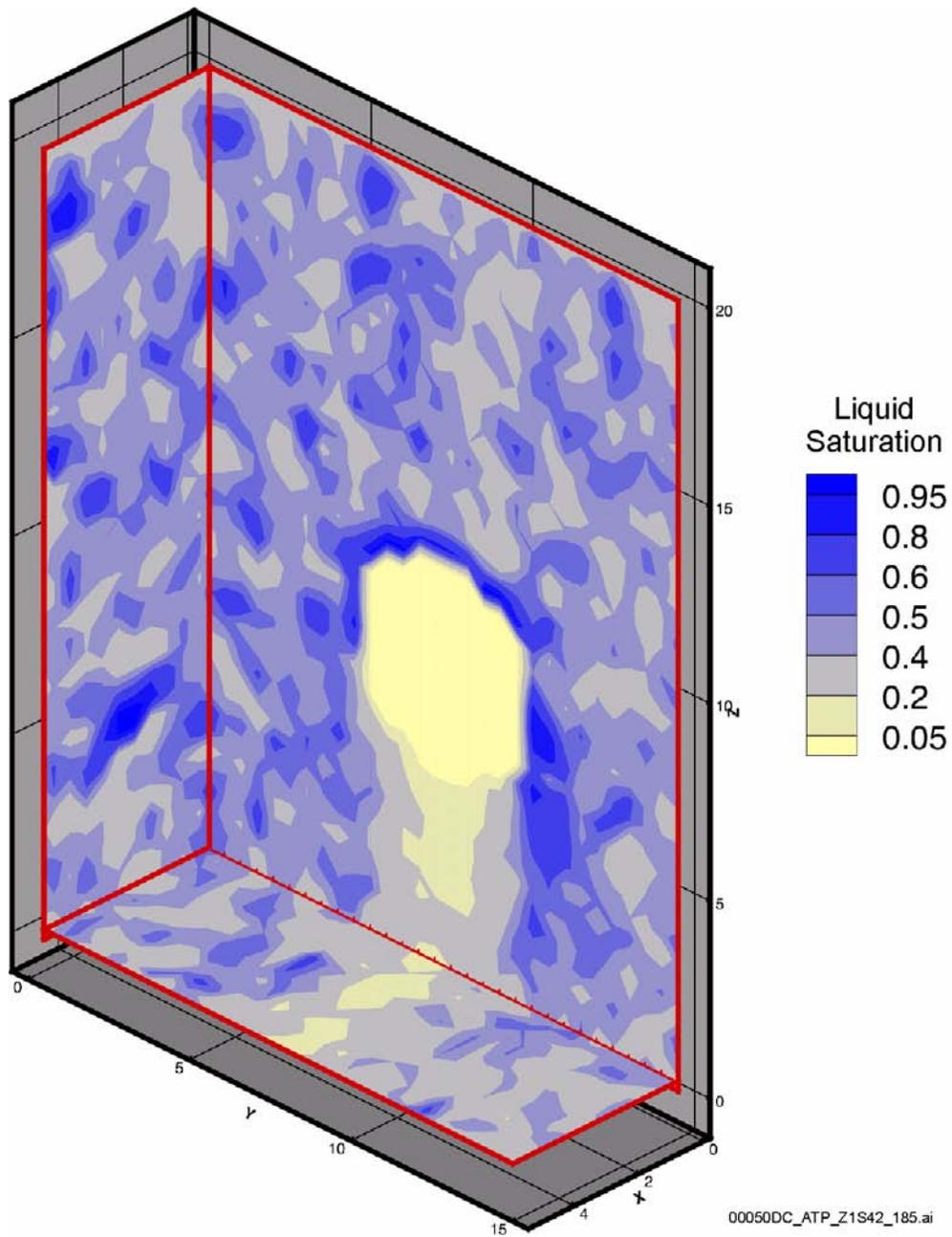
Figure 4-117. Saturation Profiles around a Drift from a Seepage Model for Performance Assessment
Source: CRWMS M&O 2000bx, Figure 5.
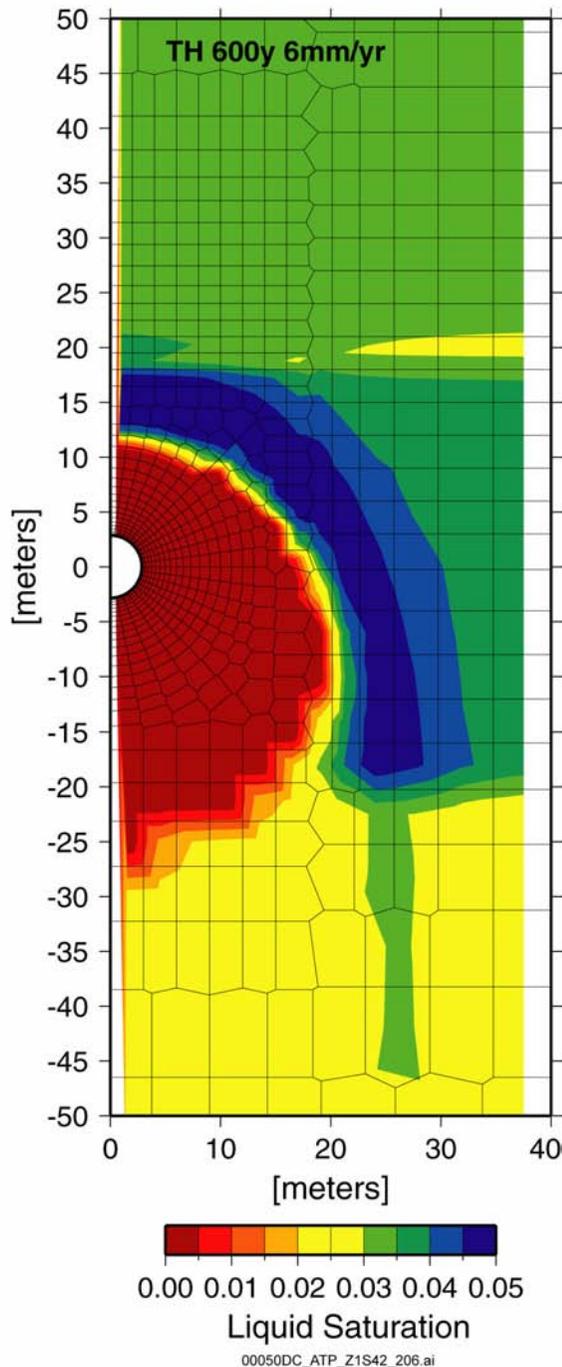
Figure 4-13 (see Section 4.2.1.2.10) shows the modeled distribution of zeolites for layers within the lower Topopah Spring welded and the upper Calico Hills nonwelded hydrogeologic units. Areas with 3 percent or less zeolite by weight are considered vitric, or unaltered.

Zeolites within the Calico Hills nonwelded hydrogeologic unit are prevalent in the northern and eastern portion of the model domain (Figure 4-13). The areal extent of the vitric region diminishes with depth and is considered to be largely confined to the fault block bounded on the north and east by the Sundance and Ghost Dance faults, respectively, and in the west by the Solitario Canyon fault. The northern half of the potential repository area is underlain by the predominantly zeolitic Calico Hills nonwelded hydrogeologic unit, while the southern half is underlain by the predominantly vitric upper portion of the Calico Hills nonwelded unit. However, below the vitric Calico Hills nonwelded hydrogeologic unit (yet above the water table) are nonwelded portions of the Prow Pass, Bullfrog, and Tram tuffs that are pervasively altered to zeolites. Thus, there appears to be no direct vertical pathway from the potential repository horizon to the water table that does not intersect zeolitic units, except perhaps within fault zones.

The spatial distributions of vitric and zeolitic material within the Calico Hills nonwelded hydrogeologic unit, along with the characterization of the basal vitrophyre of the Topopah Spring welded hydrogeologic unit, are important for understanding the distribution of perched water and for determining potential flow paths for radionuclides. Figure 4-119 shows a perspective view of the extent of perched water in the lower Topopah Spring welded hydrogeologic unit based on three-dimensional simulations with mean, present-day infiltration rates.

Performance assessment analyses, described in *Analysis of Base-Case Particle Tracking Results of the Base-Case Flow Fields (ID: U0160)* (CRWMS M&O 2000cb, Sections 6.2.1 and 6.2.2), considered the particle breakthrough locations and times resulting from two perched water conceptual models. Figure 4-120 shows the particle-break-

Figure 4-118. Condensate Shedding during the Thermal Period
Source: BSC 2001o, Figure 32b.
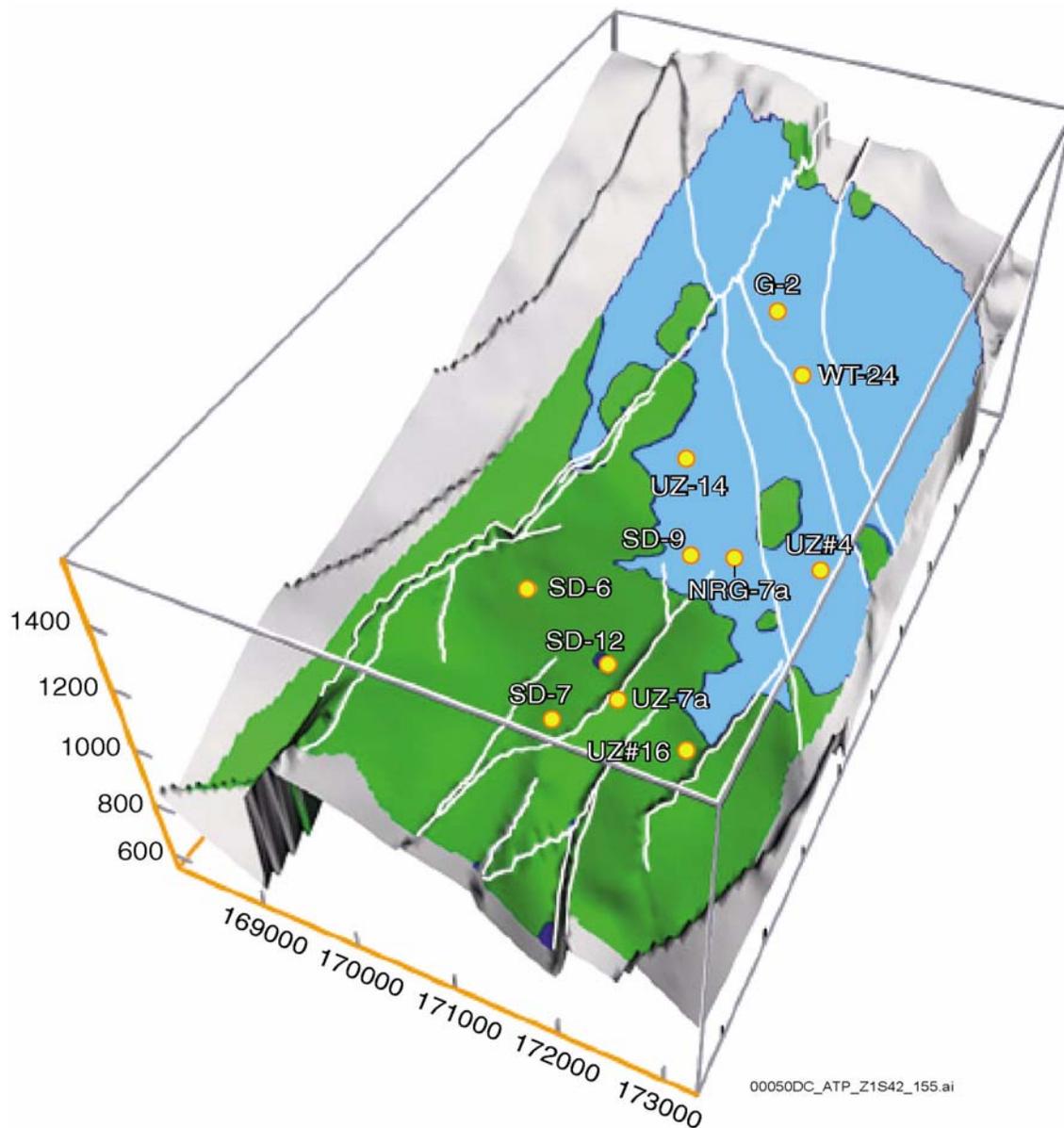
Figure 4-119. Perched Water at the Base of the Topopah Spring Welded Hydrogeologic Unit
Figure based on a simulation with present-day mean infiltration rates. Blue indicates 100 percent liquid saturation (perched water) within fractures; green indicates less than 100 percent fracture liquid saturation. Elevation is given in meters; horizontal coordinates are Nevada State Plane, Easting. Source: CRWMS M&O 2000bw, Figure 6-9.

through locations at the water table for an advective tracer (no diffusion, sorption, or dispersion) released uniformly as a pulse in the outlined potential repository region using the mean infiltration case for the glacial-transition climate. Both perched-water models show a large amount of lateral diversion of particles beneath the northern portion of the potential repository. Many of the diverted particles are concentrated in faults, which, based on the simulated fault properties, channel water to the water table. Perched-water model #2 (permeability barrier, unfractured zeolite model) shows more lateral diversion in the southern portion of the potential repository area because of the absence of enhanced fracture permeability in zeolitic units of the Calico Hills nonwelded hydro-

geologic unit. Perched-water model #1 (permeability barrier, fractured zeolite model) shows breakthrough over a large area in the southern half of the potential repository footprint because of enhanced fracture permeability in zeolitic portions of the Calico Hills nonwelded hydrogeologic unit in areas where perched water is absent.

Additional results from modeling studies that investigate flow distribution within the Calico Hills nonwelded hydrogeologic unit, perched water occurrence, and the effects on flow and transport of major faults below the potential repository horizon are summarized in Section 4.2.1.3.
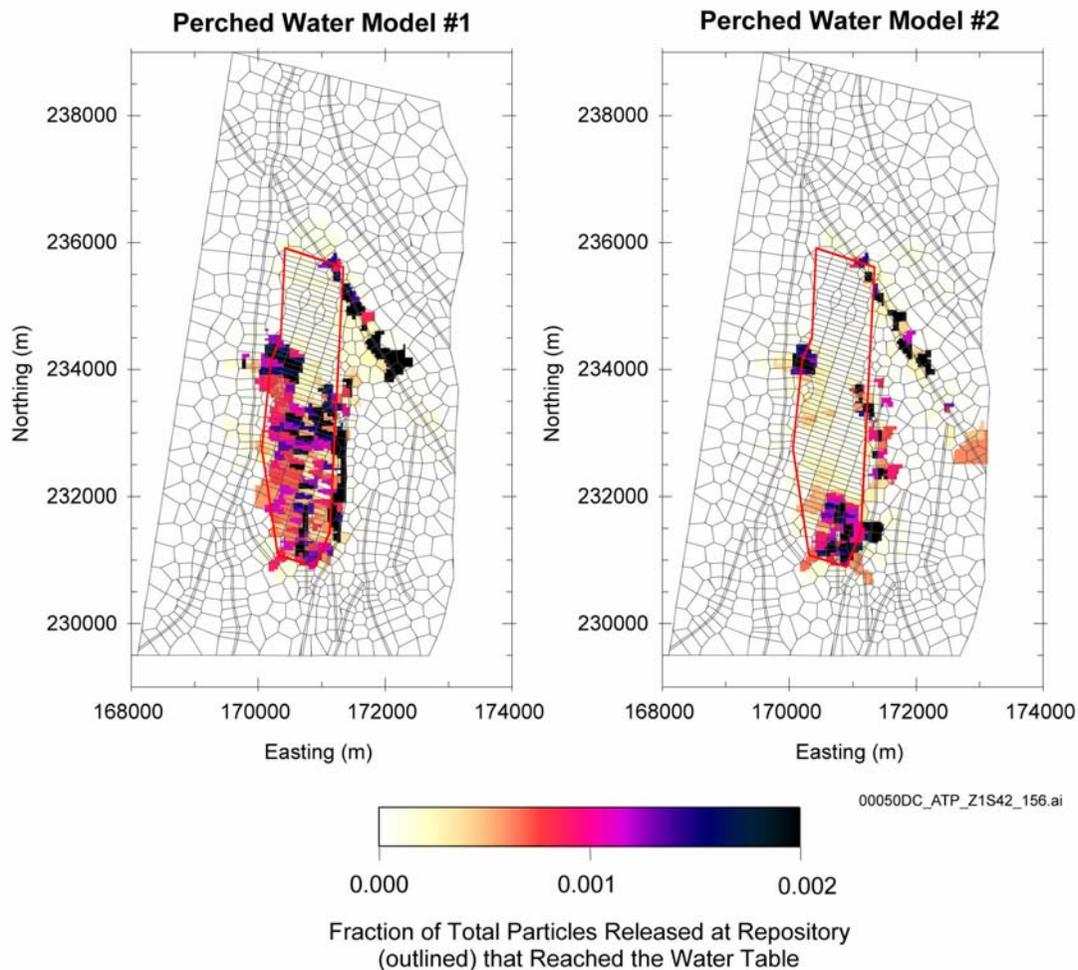
Figure 4-120. Locations of Particle Breakthrough at the Water Table for the Mean Infiltration, Glacial-Transition Climate Using Two Perched Water Models
Source: CRWMS M&O 2000c, Figure 3.7-16.

4.2.8.3.3 Flow and Transport in Geological Layers below the Potential Repository

In addition to unsaturated zone flow processes, radionuclide migration depends on transport properties, colloid transport mechanisms, and the geochemical environment. The relationship of other models and data feeds to the unsaturated zone transport model are schematically illustrated in Figure 4-121. Most of the model assumptions and approaches are similar to the corresponding unsaturated zone flow model components. The integrated flow and transport model is presented more fully in *Unsaturated Zone Flow and Trans-port Model Process Model Report* (CRWMS M&O 2000c, Section 3.11).

4.2.8.3.3.1 Transport of Nonsorbing and Sorbing Radionuclides through the Hydrogeologic Units

For transport assessment, nonsorbing and weakly sorbing radionuclides with long half-lives are the primary concern. In sensitivity analyses, processes, properties, and model results are presented for the representative radionuclides: technetium-99 (nonsorbing), neptunium-237 (moderately sorbing), plutonium-239 (strongly sorbing), and its long-lived daughter uranium-235 (moderately
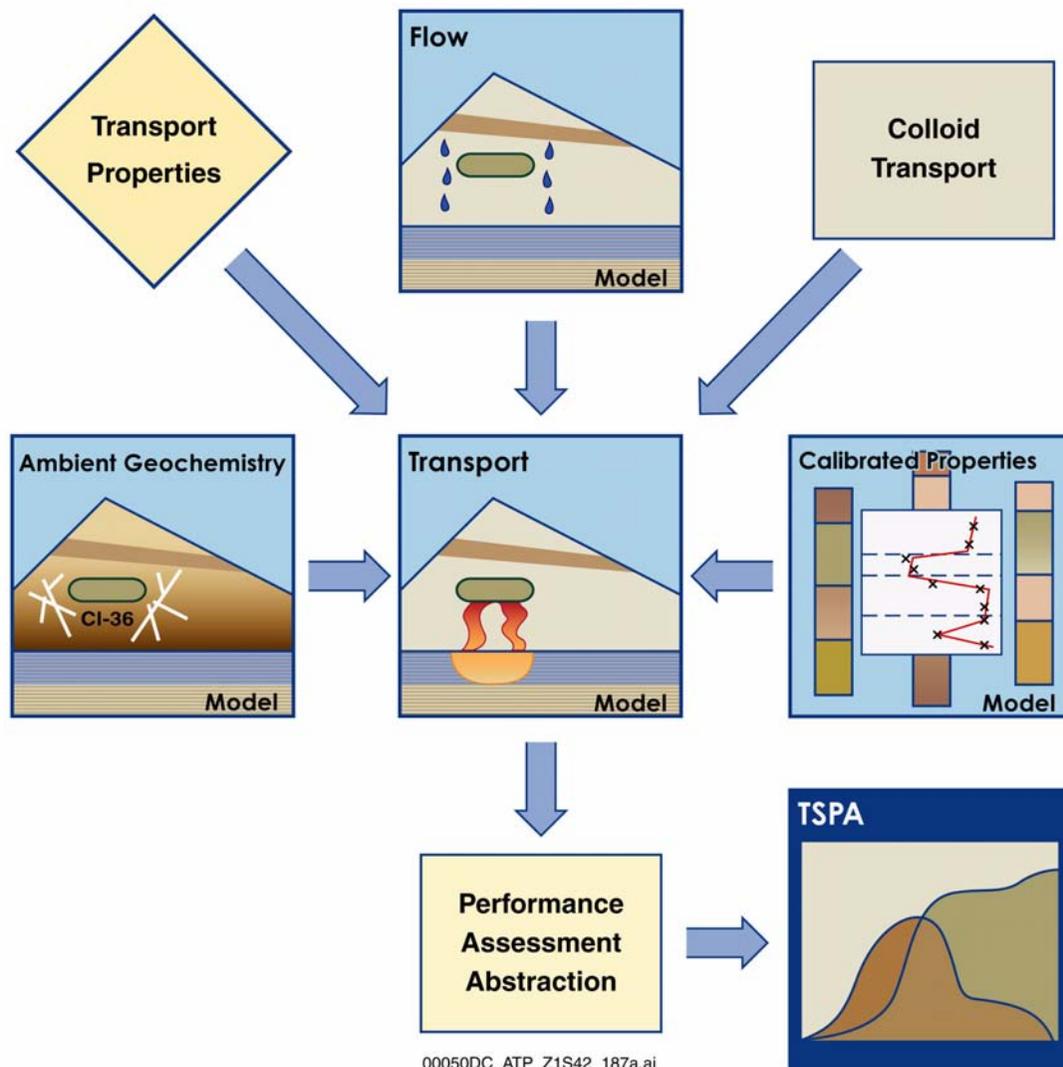
00050DC_ATP_Z1S42_187a.ai

Figure 4-121. Relationships of Other Models and Data Inputs to the Unsaturated Zone Transport Model
Source: CRWMS M&O 2000c, Figure 3.11-2.

sorbing). In these analyses, the radionuclides are released continuously at the top of the model domain (which coincides with the location of the potential repository), and the contaminant distribution is monitored over time for different percolation rates. In TSPA, the full inventory of radionuclides and their daughters are included to assess the total radioactivity distribution.

Flow in the zeolitic portions of the Calico Hills nonwelded hydrogeologic unit is judged to be dominated by fracture flow. In some welded and zeolitic layers, the matrix permeability is insufficient to carry the net infiltration, which implies that a portion of the percolation is likely to be carried by fractures (CRWMS M&O 2000c, Section 3.6.3.1). In vitric portions of the Calico Hills nonwelded hydrogeologic unit, matrix and fracture permeabilities are on the same order of magnitude; therefore, these layers behave as porous (rather than fractured) media, and flow is matrix-dominated. Fracture flow in the Topopah Spring welded hydrogeologic unit will be strongly attenuated,

transport velocities greatly reduced, and contact of dissolved radionuclides with the rock matrix enhanced by the slower velocities, longer contact time, and stronger fracture–matrix interaction, which leads to more retardation for sorbing radionuclides. Based on current understanding, the Prow Pass and Bullfrog tuffs are heterogeneous, with some zeolitic layers and some devitrified and unaltered layers (CRWMS M&O 2000c, Section 3.11.4).

4.2.8.3.3.2 Two-Dimensional Radionuclide Transport at Representative Borehole Locations

The effect of geologic layers on radionuclide migration below the potential repository is illustrated in Figure 4-122, which illustrates, conceptually, flow and transport processes in two representative hydrogeologic profiles. Borehole USW UZ-14 is located in the northern part of the potential repository site, while borehole USW SD-6 is located in the southern part. Narrow-width
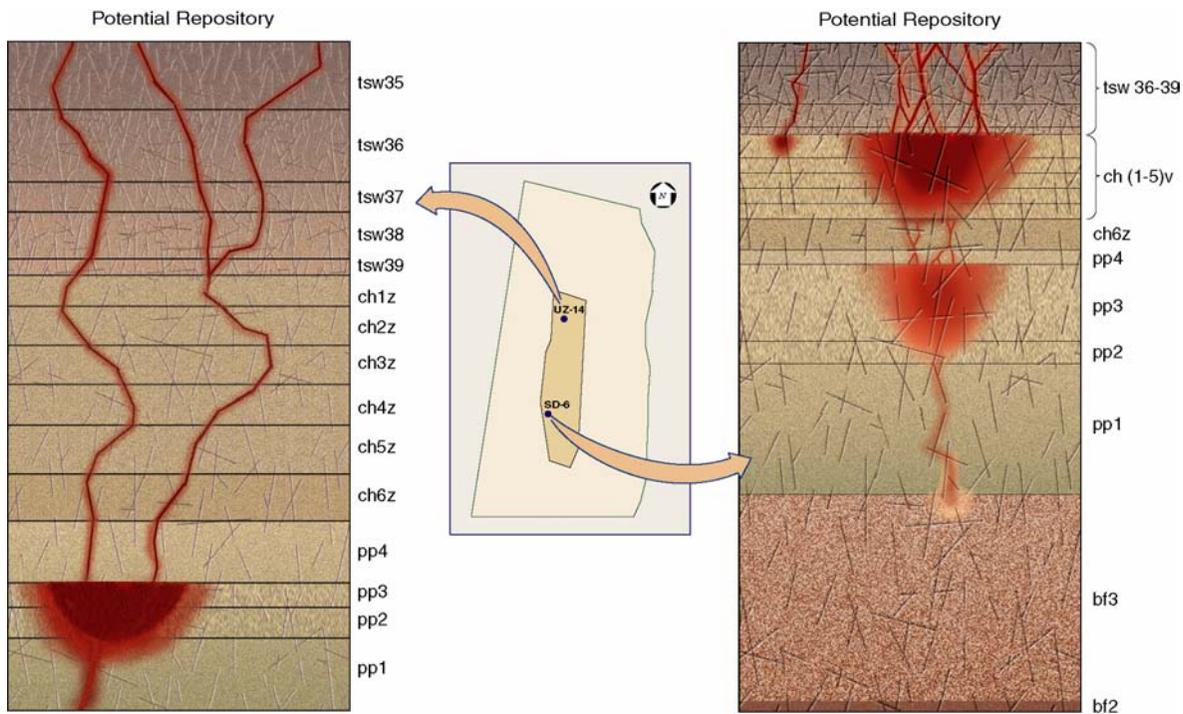
Figure 4-122. Flow and Transport in Two Representative Unsaturated Zone Hydrogeologic Profiles
Source: CRWMS M&O 2000c, Figure 3.11-3.

cross-sectional (two-dimensional) models were developed at each of these locations. As radionuclides leave the potential repository, they could quickly migrate through the Topopah Spring welded hydrogeologic layers with limited matrix diffusion and sorption. Vitric layers could retard migration because of the matrix-dominated flow in these layers, while radionuclides could quickly pass through zeolitic layers due to the fracture-dominated flow (CRWMS M&O 2000c, Section 3.11.4).

The difference in the capacity to retard radionuclides between vitric and zeolitic tuffs is illustrated in Figure 4-123 for two-dimensional simulations with a percolation rate of 6 mm/yr (0.24 in./yr) (close to the mean present-day rate). At 10,000 years, the breakthrough to the water table for the moderately sorbing neptunium-237 occurs through zeolitic layers (in a cross section including borehole USW UZ-14) and does not occur through mainly vitric layers (in a cross section including borehole USW SD-6). Transport of other radionuclides through individual layers is summarized in *Unsaturated Zone Flow and Transport Model Process Model Report* (CRWMS M&O 2000c, Section 3.11.5). The two-dimensional simulations do not allow lateral diversion in the third dimension.

4.2.8.3.3.3 Three-Dimensional Mountain-Scale Radionuclide Transport

In the three-dimensional model (CRWMS M&O 2000c, Section 3.11.6), the spatial distribution of percolation is heterogeneous with perched water and faults affecting the percolation distribution below the potential repository. Modeling of radionuclide transport using the mountain-scale three-dimensional grids (CRWMS M&O 2000ea, Sections 6.11 to 6.16) were performed, and breakthrough is described by a normalized release rate, R, (i.e., the ratio of radionuclide mass release rates at the water table versus that at the potential repository).

The normalized release rate for nonsorbing technetium-99 depends strongly on the infiltration rate (Figure 4-124). As the infiltration rate increases from lower-bound to mean present-day level, the

t_{10} time, defined as the time at which $R = 0.1$, decreases from about 10,000 years to about 300 years. The t_{50}, the time at which $R = 0.5$, decreases from about 45,000 years to about 4,000 years. The upper-bound infiltration rate further reduces t_{10} and t_{50}. The maximum attainable normalized release rate decreases with the infiltration rate because lower infiltration results in lower velocities and slower transport, thus higher radioactive decay.

From t_{10} and t_{50} values, the moderate sorption and resulting retardation of neptunium-237 is sufficient to increase the time to reach the water table by a factor of about 40. The $R = 1.0$ limit is not achieved within the simulation period. At 1 million years, R is 0.98, 0.86, and 0.42 for the upper-bound, mean, and lower-bound infiltration rates, respectively.

The normalized release rate for strongly sorbing plutonium-239 never reaches the 0.1 level, even after 1 million years of continuous release. The picture changes dramatically, however, if the daughter contributions to the release rate at the water table are accounted for in the computations. Given the half-life of plutonium-239 and the much longer half-life of uranium-235, the daughter contributions can become important. The relative flux fractions, M_R, are also shown in Figure 4-124. The plutonium contribution to the release rate starts declining rapidly after 1,000 years, and uranium-235 is by far the dominant species after 10,000 years (CRWMS M&O 2000ea, Section 6.14.1.2). After 1,000 years, the release at the water table consists mostly (over 95 percent) of uranium-235 under the lower-bound, present-day infiltration rate. The protactinium-231 contribution is negligible because of the very long half-life of uranium-235.

Direct comparison of perched-water hydrogeochronology and modeled radionuclide breakthrough times is hindered by the differences in the flowpaths of the water in both cases and the role and magnitude of retardation of the different radionuclides in the transport models. There are, nonetheless, some inferences that can be drawn about the percolation flux rates in the deep unsaturated zone and the style of flow in that region that
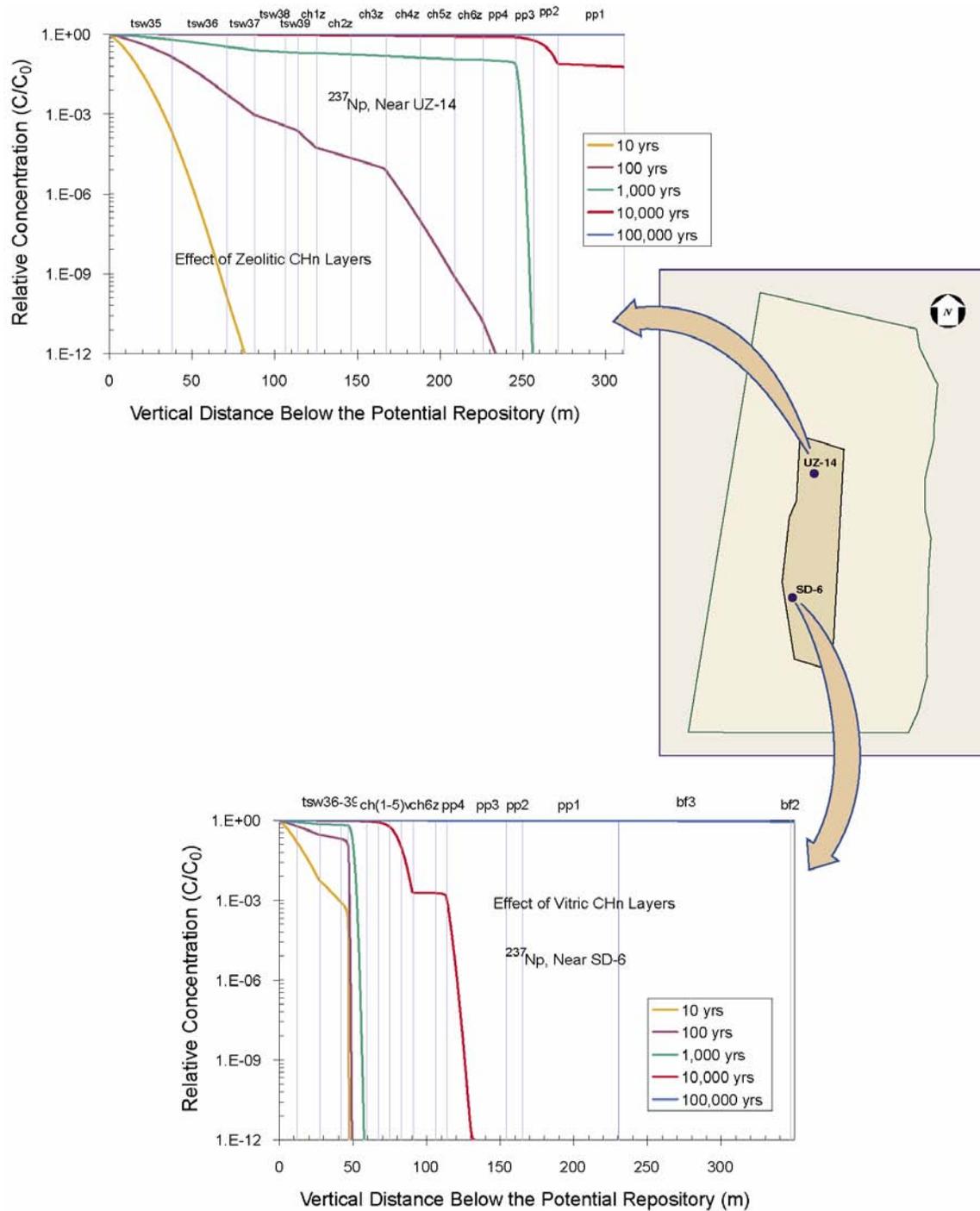
Figure 4-123. Comparison of Transport Characteristics in USW UZ-14 and USW SD-6
The data shown in this figure are based on a model that is appropriately conservative for TSPA analysis and not intended to represent expected breakthrough of radionuclides of the water table. Source: CRWMS M&O 2000c, Figure 3.11-4.
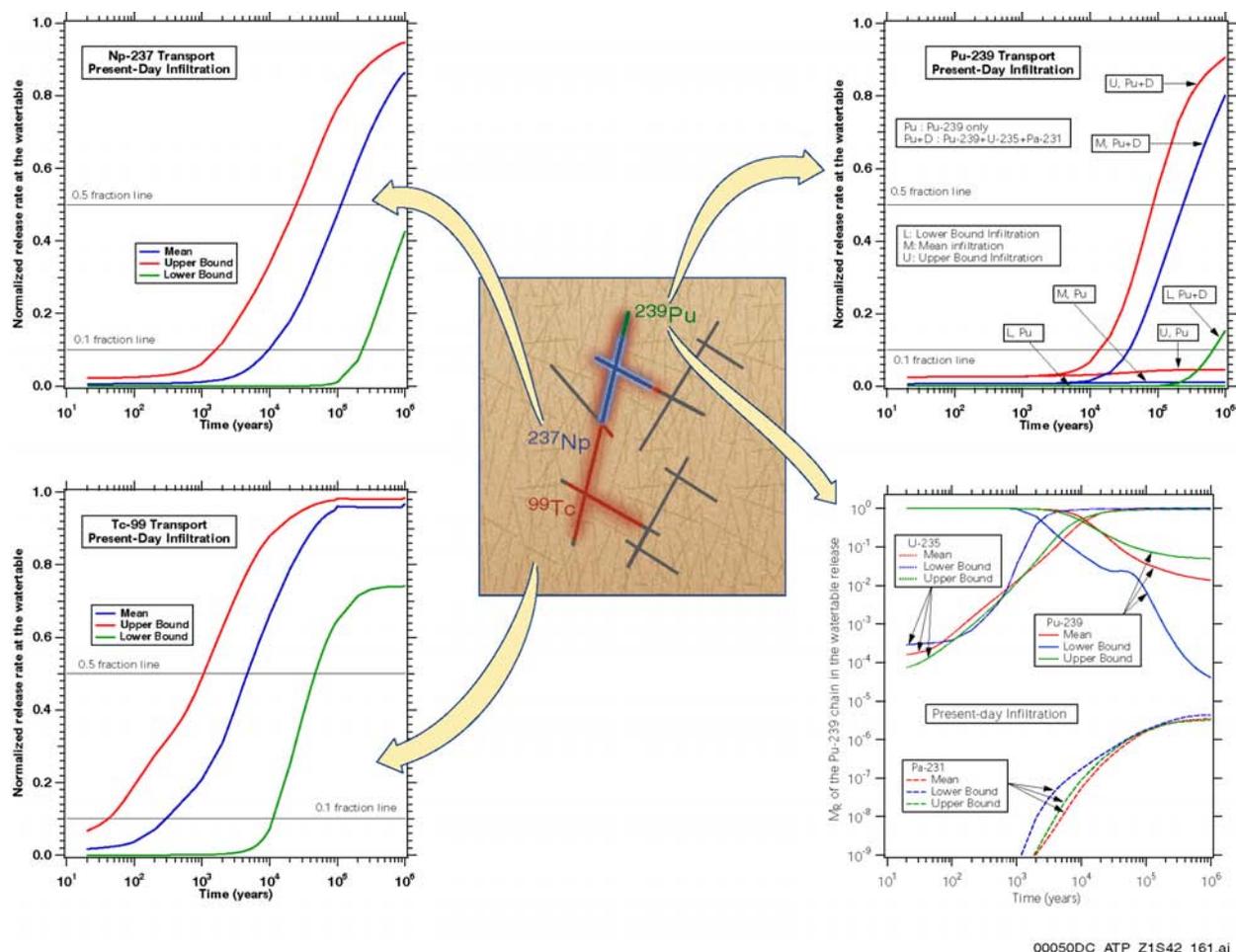
Figure 4-124. Normalized Release Rate and Dependence of Technetium-99 Transport on Infiltration Rates
The data shown in this figure are based on a model that is appropriately conservative for TSPA analysis and not intended to represent expected breakthough of radionuclides at the water table. Source: CRWMS M&O 2000c, Figure 3.11-5.

are useful in supporting the understanding of unsaturated zone transport.

Perched water is a mixture of old and young water, with the oldest water perhaps being the product of flow during past wetter climates and the youngest water being the result of fast fracture flow. The chlorine-36 analyses of perched water indicate ages ranging from 2,000 to 12,000 years, in general agreement with the carbon-14-based ages (BSC 2001r, Section 6.6.3.6; Yang, Rattray et al. 1996). Variation in ages from place to place in the perched water bodies indicates incomplete mixing of old and young water. Pore water near fault zones (borehole UZ#16) is sometimes apparently some-

what younger than the water in nearby perched-water bodies (Yang, Rattray et al. 1996).

Major ion concentrations and uranium isotope data indicate that the perched-water bodies formed from water different from water in the matrix of the host rock and that little equilibration has taken place between these waters (BSC 2001r, Section 7.5). This suggests that perched water arrived at its present location by fracture flow in a flow system in which there was little liquid exchange between the fractures and the matrix. This observation supports the dual permeability model used in evaluating unsaturated zone transport.

The apparent radionuclide transport times from the repository horizon to the water table average about 5,000 years (CRWMS M&O 2000c, Section 3.11.8), falling at about the median age of perched water (BSC 2001s, Section 6.2.1.2). Although the flowpaths and details of radionuclide retardation are different, the fracture-dominated dual-permeability flow mechanism is comparable, and the youngest perched water is not much younger than the predicted breakthrough times. The hydrogeo-chronology of the perched water therefore permissively supports the modeled breakthrough times by demonstrating slow percolation in the deep unsaturated zone and the geochemistry of the fracture and matrix water supports the dual perme-ability model used in the breakthrough modeling.

Where transported radionuclides intersect perched water, the role of the perched-water bodies in trans-port includes the dilution of radionuclides and delay associated with residence time in the perched-water bodies. The residence times and subsequent transport flowpaths are represented by two conceptual models, one representing vertically downward flow and another representing lateral diversion to faults and subsequent rapid downward flow to the water table (BSC 2001s, Section 6.5.3.2). These are known as the flow-through and flow-by models. The flow-through model is used in performance assessment because it is slightly faster and therefore more conservative.

Results of the three-dimensional simulation indi-cate that flow is diverted above the zeolitic Calico Hills nonwelded hydrogeologic unit and that radio-nuclides move slowly through the perched water to faults and to the vitric Calico Hills nonwelded hydrogeologic unit. In the three-dimensional model, transport is controlled by faults, especially at the early times (approximately 100 years). The Ghost Dance (southern splay), Sundance, and Drill Hole Wash faults are the main transport-facilitating features, providing fast pathways to the water table (CRWMS M&O 2000ea, Section 6.12.2.2). The main Ghost Dance fault does not play an important role in transport at the bottom of the Topopah Spring welded hydrogeologic unit, as the techne-tium-99 does not reach the fault at this level even after 100,000 years (CRWMS M&O 2000ea, Section 6.12.2.2). This fault is more important at

the water table, where it acts as a barrier to lateral transport while facilitating downward migration into the water table.

The transport pattern illustrated in Figure 4-125 indicates that radionuclide transport to the ground-water is expected to be faster in the southern part of the potential repository block, where it is also areally concentrated. There are several reasons for this. First, the rates and direction of water flow dictate the advective transport pattern, and the maximum water flow within the footprint of the potential repository is in its southern part in perched water model #1. Second, the presence of the highly conductive faults (e.g., Splay G of the Solitario Canyon fault and the Ghost Dance fault splay) act as the venue for fast transport, despite the fact that the vitric Calico Hills nonwelded hydrogeologic unit behaves as a porous medium (with relatively lower water velocities). These faster transport pathways may be facilitated by flow focusing in the vitric Calico Hills nonwelded hydrogeologic unit, which has a funnel-shaped distribution in the south. Third, the low-perme-ability zones at the Topopah Spring welded–Calico Hills nonwelded hydrogeologic unit interface in the northern part of the potential repository, act as barriers to water drainage, and lead to low water velocities and the presence of perched water bodies. Radionuclides move slowly through the perched water before reaching the underlying conductive zeolitic Calico Hills nonwelded hydro-geologic unit, hence the delay in transport. Radionuclide breakthrough at the water table occurs before 1,000 years and over a large area by 10,000 years in the southern part of the potential repository block.

4.2.8.3.3.4 Three-Dimensional Mountain-Scale Transport of Plutonium True Colloids

Plutonium, a major nuclear fuel element, can be present as a waste-form colloid (i.e., true or intrinsic colloid as elemental particle). The waste-form colloids will play a more significant role than natural colloids as pseudocolloids with radionu-clides adsorbed to the naturally occurring fine particles (CRWMS M&O 2000ec, Section 7). Colloid size has an important effect on transport,
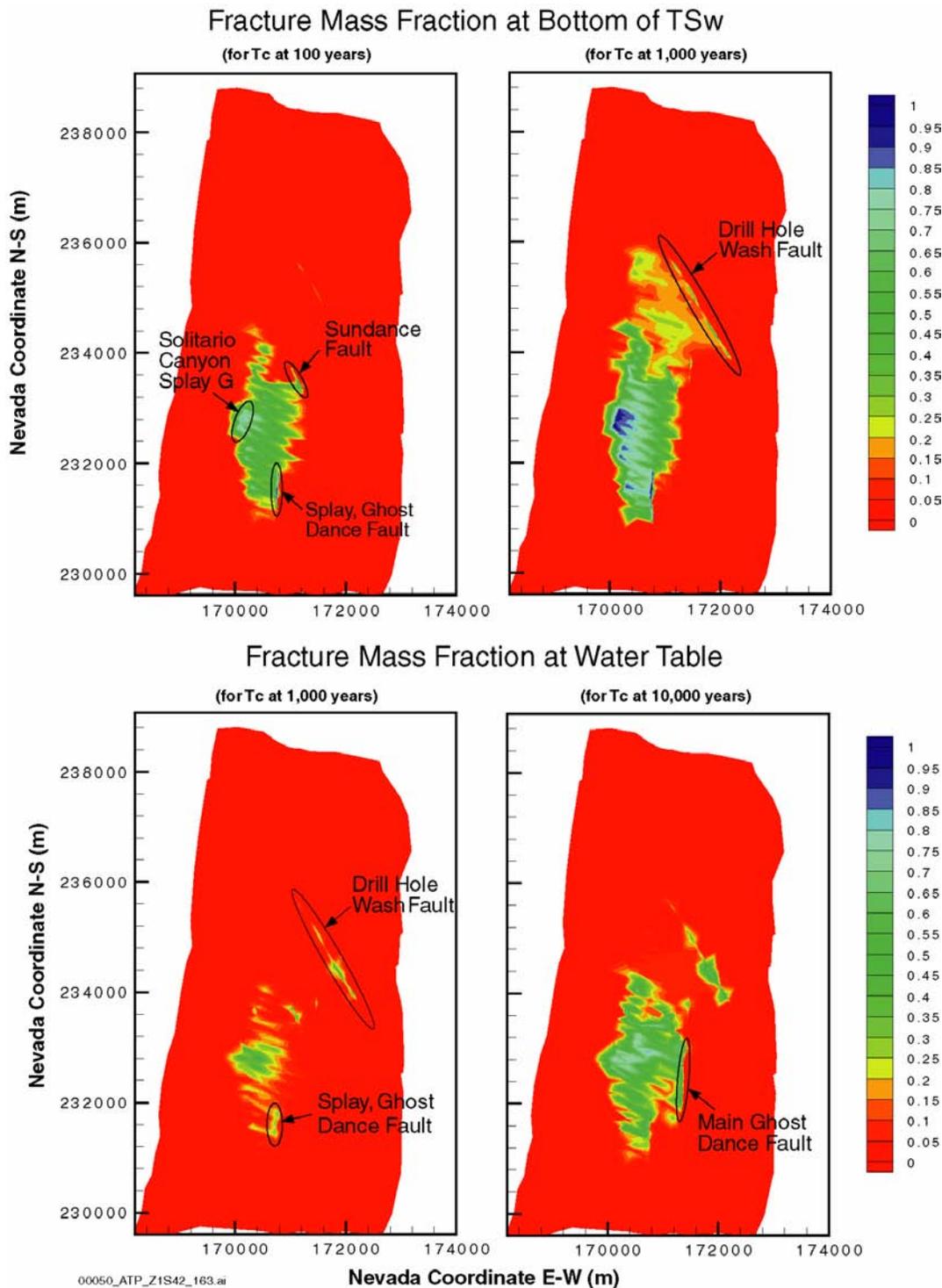
Figure 4-125. Normalized Mass Fraction Distribution of Technetium-99 in Fractures at the Bottom of the Topopah Spring Welded Hydrogeologic Unit and at the Water Table

The data shown in this figure are based on a model that is appropriately conservative for TSPA analysis and not intended to represent expected breakthough of radionuclides at the water table. Source: CRWMS M&O 2000c, Figure 3.11-6.

and the size exclusion (inability of larger colloids to move into the matrix) results in enhanced transport to the groundwater. Smaller colloidal particles can diffuse more easily into the matrix, and their transport is thus more retarded. Size exclusion at the interfaces of different geologic units leads to colloid concentrations that can be significantly higher than that in the water released from the potential repository (CRWMS M&O 2000ea, Section 6.16). These high concentrations are observed behind (i.e., they do not penetrate) the interfaces because the large-size colloids cannot move across the interface.

4.2.8.3.4   Alternative Conceptual Approaches

The alternative conceptual processes for unsaturated flow below the potential repository horizon, as described in Section 4.2.1.3.4, have the same large impacts on the unsaturated zone transport. These alternative processes include episodic flow within the Topopah Spring welded hydrogeologic unit, flow through the perched water into the Calico Hills nonwelded unit without significant lateral diversion, and faults in the Calico Hills unit and below having low permeabilities. The conservatism and optimism associated with the advective transport are similar to the discussions in Section 4.2.1.3.4 and are not reiterated in this section.

Drift Shadow—If the shadow zone of drier conditions exists below the drift, the advective and diffusive transport will be greatly reduced in the vicinity of the radionuclide release points, as illustrated in Figures 4-116 to 4-118. Omitting the shadow process from the unsaturated zone transport model results in a conservative evaluation. A realistic representation, with drift-scale processes below the drift taken into account, would likely result in performance analyses that indicate more retardation of radionuclide transport in the unsaturated zone. More recent modeling and analyses, which show that the drift shadow may increase the radionuclide transport time from the repository horizon to the water table by several orders of magnitude, are presented in Volume 1, Sections 11.2.1 and 11.3.1 of *FY01 Supplemental Science and Performance Analyses* (BSC 2001a).

Matrix Diffusion—Some previous hydrologic models of Yucca Mountain have ignored the effects of matrix diffusion, an assumption that is very conservative because it ignores the interaction between water in fractures and the rock matrix, particularly in unwelded tuffs. This results in unrealistically fast predictions of transport. The available analyses of Alcove 1 infiltration tests indicate that the inclusion of matrix diffusion is important in interpreting the data and in validating the models. Ongoing testing and modeling of the Alcove 8 to Niche 3 Cross-Drift test can further validate the importance of matrix diffusion. While neglecting matrix diffusion is conservative, the alternative process model with no matrix diffusion is not realistic. In the TSPA-SR abstraction, matrix diffusion is explicitly incorporated and modeled (CRWMS M&O 2000c, Section 3.11.13.1).

4.2.8.3.5   Uncertainties and Limitations

The uncertainties and limitations for unsaturated flow, as described in Section 4.2.1.3.5—in climate, hydrologic properties in lower tuff units, geochemical analyses, and numerical approaches—are also applicable to unsaturated zone transport. In this section, uncertainties and limitations associated with field testing are first discussed, followed by evaluations of transport properties.

4.2.8.3.5.1   Uncertainties and Limitations for Field Testing in Lower Hydrogeologic Units

The field tests in construction water monitoring and liquid release testing are mainly limited to the tuff units accessible from the Exploratory Studies Facility, in and above the middle nonlithophysal zone of the Topopah Spring welded hydrogeologic unit. Ongoing tests along the Cross-Drift are generating additional data for the lower lithophysal unit, with additional tests in the lower nonlithophysal and the western part of the potential repository block planned. Uncertainties about transport below the drift can be reduced with relevant data collected.

The unsaturated zone transport test site at Busted Butte is in a distal extension of the vitric Calico Hills nonwelded hydrogeologic unit. The site-

specific information about the zeolitic Calico Hills nonwelded hydrogeologic unit is based on borehole cores. The uncertainties and limitations are being assessed by comparing tests in fractured units and in vitric units to demonstrate that core-scale data are adequate for site-scale assessment.

4.2.8.3.5.2 Uncertainties and Limitations in Transport Properties

Many conservative approximations are used in the performance assessments, leading to overestimation of radionuclide transport. Conservative assignments of transport parameters, potentially overconservative alternative models, and potentially optimistic (nonconservative) approaches all contribute to uncertainties in the assessment of transport processes in the unsaturated zone. In addition to the diffusion processes discussed in Section 4.2.8.3.4, some of the uncertainties and limitations of other flow and transport processes are further discussed below.

Matrix Sorption—The experimentally determined K_d values are mostly from batch experiments using crushed tuff under saturated conditions. These saturated conditions are not representative for ambient conditions in the unsaturated zone. The crushed rock tests can overestimate sorption, and fine particles generated in grinding can lead to irreproducible or high K_d values (CRWMS M&O 2000ea, Section 6.1.3.1). Measurements of tracer penetration into unsaturated core-size solid tuff samples can generate K_d values that are more directly related to processes of transport through fractured blocks observed in the field (CRWMS M&O 2000bu, Section 6.4).

Rate-Limited Sorption—Rate-limited sorption could be important, especially for fluid–radionuclide–rock systems with large sorption potential. Breakthrough curves for neptunium-237 transport in tuffs from the column experiments can only be analyzed by considering rate-limited sorption (Viswanathan et al. 1998, p. 267). This result indicates the existence of rate-limited sorption under flowing conditions. Nonlinear and irreversible sorption are also evident from the diffusion and transport studies in *Unsaturated Zone and Saturated Zone Transport Properties (U0100)*

(CRWMS M&O 2000eb, Sections 6.5 and 6.6). Overall, rate-limited sorption and nonlinear sorption are uncertainties in evaluating the validity of the linear equilibrium sorption adopted in unsaturated zone transport studies. Rate-limited sorption reduces sorption in the matrix and increases the concentration and duration of migration through the fractures. In the TSPA-SR, the sorption coefficients (K_ds) of linear sorption for different radionuclides are represented by distribution functions to quantify the uncertainties (CRWMS M&O 2000a, Section 3.7.3).

Colloid Declogging—The kinetic declogging (reverse) coefficient, κ^-, is treated as a fraction of κ^+ to examine the sensitivity of this parameter on colloidal transport (CRWMS M&O 2000c, Figure 3.11-7). When no declogging is allowed, no colloids reach the water table (CRWMS M&O 2000ea, Section 6.16). Small values of κ^- (i.e., slow declogging) lead to retardation of colloids and slow transport to the water table. Large values of κ^- (i.e., fast declogging) lead to fast transport to the water table for radioactive colloids. For the TSPA-SR, the colloid retardation factor is conservatively set to 1 for all colloids in the unsaturated zone.

Surface Diffusion—It is possible that surface diffusion can be supported in zeolites. Surface diffusion can be important for radionuclides that exhibit strong sorption (e.g., plutonium). A larger K_d clearly indicates stronger sorption, but this does not mean immobilization of the dissolved species when the fractured porous medium supports surface diffusion (Moridis 1999, Section 6.1.2). For the TSPA-SR, the uncertainties of molecular diffusion coefficients (as described in Section 4.2.8.2.2, based on sorbing tritium and nonsorbing technetium measurements) and the retardation factors are independently sampled. The uncertainties associated with surface diffusion may be large for media supporting surface diffusion.

Desorption from Radioactive Decay—Daughters of sorbed parents may be ejected from grain surfaces because of recoil from radioactive decay. The alpha decay is evaluated and the potential implications for kinetically controlled sorption are discussed in *Radionuclide Transport Models under Ambient Conditions* (CRWMS M&O 2000ea,

Section 6.2.8). For equilibrium sorption, this is not an issue.

Particle Tracking—Different approaches to represent matrix diffusion could yield different transport behavior. Comparisons between the FEHM V2.10 particle tracker and DCPT code were performed by *Analysis Comparing Advective–Dispersive Transport Solution to Particle Tracking* (CRWMS M&O 2000ee, Section 6.4). The two particle-tracking routines agree only if diffusion and dispersion are neglected. For the cases that include diffusion and dispersion, the median breakthrough for FEHM V2.10 occurs at times more than one or two orders of magnitude earlier. The difference is more pronounced for radionuclides undergoing sorption in the matrix. These differences stem from different implementations of the diffusive mass flow between fractures and the matrix in the two codes (CRWMS M&O 2000ee, Section 7). The conservative FEHM V2.10 particle tracker is used for the TSPA-SR abstraction. The flow fields derived from the three-dimensional site-scale model are inputs to the particle tracker and are used to calculate transport velocities.

4.2.8.4 Total System Performance Assessment Abstraction

Unsaturated zone transport is important as the first natural barrier to radionuclides that escape from the potential repository. The unsaturated zone acts as a barrier by delaying radionuclide movement. If the transport time is long compared to the radionuclide half-life, then the unsaturated zone may have an important effect on decreasing the dose from that radionuclide at the biosphere. In this section, the abstraction of unsaturated zone process modeling results into the TSPA-SR is presented (CRWMS M&O 2000a, Section 3.7).

Within the unsaturated zone, radionuclides can migrate in groundwater as dissolved molecular species or associated with colloids (CRWMS M&O 2000a, Section 3.7.1). Five basic processes affect the movement of dissolved or colloidal radionuclides: advection, diffusion, sorption, hydrodynamic dispersion, and radioactive decay. Sorption is potentially important because it slows, or retards, the transport of radionuclides. Diffusion

of radionuclides out of fractures into matrix pores is also a potential retardation mechanism because matrix transport is generally slower than fracture transport. However, sorption and matrix diffusion have less effect on colloids, so radionuclides can be more mobile if they are attached to colloids than if they are dissolved in the water. Radioactive decay is potentially important because daughter products may have sorption behavior different than that of the parent radionuclide, thus affecting transport. The key processes and issues for unsaturated zone transport are summarized in Figure 4-126. The unsaturated zone flow and transport model is used to represent the key processes, assess the uncertainties, and provide direct inputs to the TSPA-SR.

4.2.8.4.1 Abstraction and Direct Use of the Unsaturated Zone Flow and Transport Fields

A dual-permeability model is used to represent mountain-scale unsaturated zone flow. The same concept is used to model radionuclide transport: a dual-continuum model in which fractures and matrix are distinct interacting continua that coexist at every point in the modeling domain. Each continuum is assigned transport properties in addition to its hydrologic properties. The properties can vary spatially.

The unsaturated zone transport model is directly coupled, that is, dynamically linked, with the TSPA-SR model (CRWMS M&O 2000a, Section 3.7.2). The unsaturated zone flow calculations are done ahead of time, and the flow fields are saved for use by the TSPA-SR model. During a TSPA simulation, radionuclide mobilization and transport through the engineered barrier system are calculated and the radionuclide mass flux at the engineered barrier system boundary at each time step is provided as the boundary condition for unsaturated zone transport.

The use of pregenerated flow fields implies the assumption of quasi-steady flow. That is, flow is modeled as a sequence of steady states (as an approximation). Mountain-scale unsaturated zone flow is represented as a sequence of steady states as determined by climate change and infiltration models. The transport calculation (particle
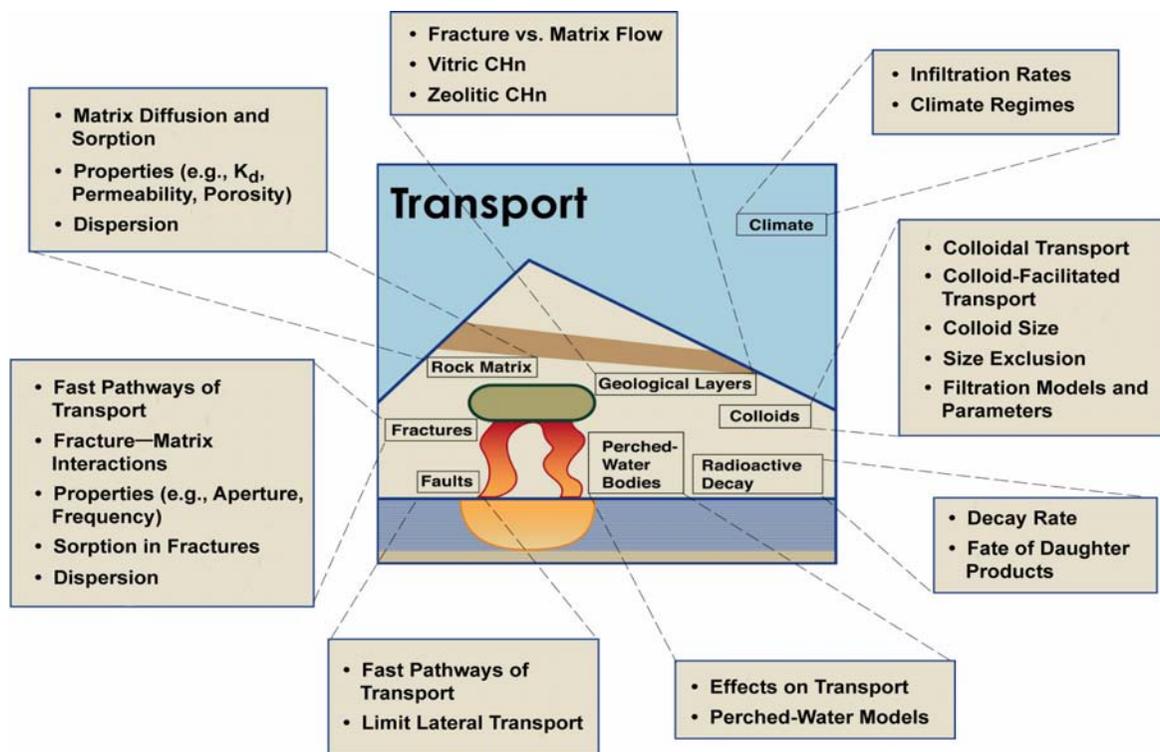
00050DC_ATP_Z1S42_188a.ai

Figure 4-126. Key Issues of Unsaturated Zone Transport
Source: CRWMS M&O 2000c, Figure 3.11-1.

tracking) itself is fully transient, with radionuclides moving downward from the potential repository as they are released. Each TSPA realization uses one set of flow fields: low infiltration, mean infiltration, or high infiltration; each set has three flow fields, for present-day, monsoon, and glacial-transition climates.

The flow field is changed from one to another at the time of a climate change. The transport calculation then continues with the new flow field. In addition to the step change in the flow field, the location of the water table is also changed at the time of climate change. The water table for the future climates (monsoon and glacial-transition) is taken conservatively to be 120 m (390 ft) higher than the present-day water table (CRWMS M&O 2000ca, Section 6.2). When the water table rises with a climate change, radionuclides in the unsaturated zone between the previous and new water table elevations are moved to the saturated zone.

4.2.8.4.2 Abstraction of Matrix Diffusion, Sorption, and Dispersion

The incorporation of matrix diffusion in the unsaturated zone transport model is simplified by conservatively neglecting flow in the matrix continuum in the diffusion calculation. This allows use of an analytical solution for matrix diffusion (CRWMS M&O 2000ed, Section 6.1.3). Fracture properties (aperture, spacing) are modified to take into account that only some fractures actively flow and transport radionuclides (CRWMS M&O 2000ed, Section 6.2.1). Colloids are larger than solute molecules, so they have much smaller diffusion coefficients. Because of this and possible size-exclusion effects, matrix diffusion is conservatively neglected for colloids. Anionic species such as pertechnetate (the predominant aqueous species of technetium) have lower diffusion coefficients than cationic species (CRWMS M&O 2000c, Section 3.11.3.2) and are assigned different diffusion coefficients.

In TSPA simulations, the sorption characteristics of the tuff units are taken to be constant in time. Changes in sorption (or other transport properties) brought about by thermal effects of the potential repository or from climate change have been considered and found to be insignificant (CRWMS M&O 2000ef, Sections 6.3.8 and 6.8).

In unsaturated zone TSPA transport calculations, dispersion in fractures is represented independently of that in the matrix (CRWMS M&O 2000a, Section 3.7.1.4). Dispersion is a way of including small-scale velocity variations in the transport model, but these small-scale variations are not very important to unsaturated zone transport because they have less effect over long distances than the large-scale velocity variations that are explicitly included in the model. Also, the explicitly modeled differences in transport velocity between fractures and matrix, and the transfer of radionuclides between them, introduce considerable dispersion into the transport simulations. Transverse dispersivities are normally small compared to longitudinal dispersivities (CRWMS M&O 2000a, Section 3.7.1.4). Any transverse dispersion (spreading) that occurs in the unsaturated zone is eliminated at the water table by starting the saturated zone transport model at a small number of discrete points.

4.2.8.4.3   Abstraction of Colloidal Transport

Colloids diffuse more slowly than dissolved radionuclides because of their larger size, and as a result, matrix diffusion of colloids is neglected in TSPA. Colloids can, however, move between fractures and rock matrix advectively (i.e., moving with the water) as long as they are smaller than the matrix pores. Most of the pores in the welded and zeolitic tuffs are small, so most colloids remain in the fractures in those hydrogeologic units (CRWMS M&O 2000c, Section 3.11.3.4). Because transport in fractures is faster than transport in the matrix, this size-exclusion effect results in faster colloidal transport in those units. Most flow and transport in those units is through fractures, so the result of this effect is not large. In addition, a size-exclusion effect is possible at hydrogeologic unit interfaces. This exclusion is not applied to colloids transporting through fractures because fractures are relatively large compared to matrix pores, but it is applied to colloids transported in the matrix from one hydrogeologic unit to another. In this situation a portion of the colloids, corresponding to the fraction of them that are smaller than the pores in the downstream unit, is stopped at the unit interface. This exclusion is taken to be a permanent filtration for irreversible colloids; it is not applied to reversible colloids because the radionuclides can desorb from the colloids and continue to move (CRWMS M&O 2000c, Section 3.11.13.3).

Colloids may be temporarily "detained" at the interface of fractures and matrix or sorbed to fracture walls (reversible filtration), and this interaction can be included in the colloid transport model as a retardation factor for colloid transport in the fracture system (CRWMS M&O 2000c, Section 3.11.13.3; CRWMS M&O 2000ed, Section 5.3). The effective transport velocity is reduced by this retardation factor. However, the data available on this effect are for the saturated zone, so the retardation factor is conservatively set to 1 in the unsaturated zone (i.e., no retardation due to this factor).

For reversible colloids, radionuclides sorbed to colloids are assumed to be in equilibrium with radionuclides in solution. The ratio of the concentration of a radionuclide sorbed to colloids to the concentration in solution is represented by a colloid partitioning factor in the models (CRWMS M&O 2000ed, Section 5.3). The ratio is a function of the concentration of colloids and the sorption coefficient for the given radionuclide onto the given type of colloid. Diffusion of dissolved radionuclides into the matrix can reduce the concentration in the fractures, which reduces the amount of radionuclides sorbed to the colloids in equilibrium with radionuclides in solution. Thus, matrix diffusion can effectively slow the transport. The colloid partitioning factor is one of the key transport parameters sampled in the TSPA-SR (CRWMS M&O 2000a, Section 3.7.3).

4.2.8.4.4   Abstraction with Particle Tracking

Radionuclide transport modeling for the unsaturated zone uses the residence time transfer function particle-tracking technique (CRWMS M&O

2000c, Section 3.11.13.3). This technique is a cell-based approach in which particles move from cell to cell in a numerical grid. Particle locations within cells are not tracked as they are in some particle-tracking techniques, but rather movement from cell to cell is computed probabilistically based on transfer functions. The transfer functions are defined using analytical or semi-analytical solutions of the transport equations and represent probability distributions of the residence time (the amount of time that a particle resides in a cell). The probability that a particle will move to a neighboring cell is proportional to the water flow rate to that cell. Only outflows are included in this calculation; particles are not moved to a cell if water flows from that cell to the current cell. A dual-continuum conceptual model is used for transport, so there is a network of fracture cells and a network of matrix cells, with each fracture cell connected to a corresponding matrix cell.

4.2.8.4.5 Abstraction of Spatial and Temporal Variabilities

Releases from the engineered barrier system are computed for 30 environmental groups that are based on infiltration, waste type, and seepage condition (CRWMS M&O 2000a, Section 3.7.2). Because infiltration is important for unsaturated zone transport, radionuclides are released into the unsaturated zone at locations consistent with the environmental group from which they are released. Each environmental group is associated with one of five infiltration categories that are based on the percolation at each spatial location during the glacial-transition climate. The ranges for the categories are 0 to 3 mm/yr (0 to 0.1 in./yr), 3 to 10 mm/yr (0.1 to 0.4 in./yr), 10 to 20 mm/yr (0.4 to 0.8 in./yr), 20 to 60 mm/yr (0.8 to 2.4 in./yr), and greater than 60 mm/yr (2.4 in./yr).

To avoid artificial dispersion, the model of radio-nuclide release into the unsaturated zone takes into account the number of failed waste packages within each of the five infiltration categories (CRWMS M&O 2000a, Section 3.7.2). If only one waste package has failed in a category, then releases for that category are put into a single unsaturated zone cell, sampled randomly from the cells in that category. If two waste packages fail,

then releases are put into two randomly selected cells. This process continues for additional waste packages until the number of failed waste packages is equal to the number of cells in the category; at that point the releases are spread over all cells in the category, and additional waste package failures cause no change in the release locations. For any number of failed waste packages in a particular category, releases are always divided evenly among the cells that have been selected. Artificial dispersion in the unsaturated zone is further reduced by gathering releases from the unsaturated zone into a few discrete locations at the water table for input to the saturated zone transport model.

In the unsaturated zone transport model, spatial variability is included by use of a three-dimensional model that incorporates the appropriate geometry and geology (CRWMS M&O 2000a, Section 3.7.3). Temporal variability is included by using different unsaturated zone flow fields for different climate states, but none of the other transport properties change with time.

4.2.8.4.6 Uncertainty and Conservatism

Uncertainty is included in the unsaturated zone transport model by defining uncertainty distributions for a number of input parameters. Values of these parameters for each TSPA realization are sampled from the distributions. Thus, each realization of the total system has a unique set of input parameters, each of which is within the range that is considered to be defensible (CRWMS M&O 2000a, Section 3.7.3). Normally each realization is considered to be equally likely, but importance sampling may be used to emphasize some realizations (usually to increase the probability of sampling an unlikely parameter value).

Current performance assessment models of unsaturated zone transport consider and account for uncertainties and conservatisms. These are detailed in *Unsaturated Zone Flow and Transport Model Process Model Report* (CRWMS M&O 2000c); they include:

- The significance of fracture flow in the vitric Calico Hills nonwelded hydrogeologic unit

- The effectiveness of perched water to divert water away from the zeolitic Calico Hills nonwelded hydrogeologic unit

- The reduction of fracture–matrix interaction along fractured flow paths within the Topopah Spring welded hydrogeologic unit

- The extrapolation of properties for the fault intervals in the Calico Hills nonwelded hydrogeologic unit and the Crater Flat undifferentiated hydrologic unit from fault data collected in the Topopah Spring welded hydrogeologic unit

- The use of a conservative particle tracker for performance assessment.

This conservatism may be partially offset by the use of batch-derived retardation factors (obtained from crushed-rock samples) for radionuclide migration, which may overestimate sorption (CRWMS M&O 2000c, Section 3.11.10.2). In general, the abstraction represents a balance of conservative assumptions and nominal parameters and processes to yield a reasonably realistic representation and assessment.

As noted in Section 4.1.1.2, the DOE has completed several activities to improve the treatment of uncertainty in current models, and the results are reported in *FY01 Supplemental Science and Performance Analyses* (BSC 2001a; BSC 2001b). Modeling based on new information and one-off sensitivity studies were focused on model aspects that were identified as unevaluated or that were perceived as having overly conservative estimates of uncertainty associated with them (BSC 2001b, Table 1.3-1). Descriptions of each analysis are contained in Volume 1 of *FY01 Supplemental Science and Performance Analyses* (BSC 2001a) and an assessment of the impact of the analyses on performance is presented in Volume 2 (BSC 2001b). In addition, analyses and assessments were carried out that provide a basis for evaluation of the role of repository thermal operating mode on performance and uncertainty. Analyses of performance of thermal modes are presented in Volume 2, Section 4 of *FY01 Supplemental Science and*

Performance Analyses (BSC 2001b). The supplemental analyses indicate that the TSPA-SR model is generally conservative to reasonable. The sensitivity studies are also briefly described in Section 4.4.5.5.

4.2.9   Saturated Zone Flow and Transport

Yucca Mountain is part of the Alkali Flat–Furnace Creek subbasin of the Death Valley flow system. Recharge within the Death Valley flow system occurs at high altitudes, where relatively large amounts of snow and rainfall occur. Water inputs to the Alkali Flat–Furnace Creek subbasin include groundwater inflow along the northern boundary of the subbasin, recharge from precipitation in high-elevation areas of the subbasin, and recharge from surface runoff in Fortymile Canyon and Fortymile Wash. North and northeast of Yucca Mountain, recharge from precipitation is believed to occur also at Timber Mountain, Pahute Mesa, Rainier Mesa, and Shoshone Mountain (CRWMS M&O 2000bn, Section 3.2).

The geologic strata at Yucca Mountain form a series of alternating volcanic aquifers and confining units above the regional carbonate aquifer. The volcanic rocks generally thin toward the south, away from their eruptive sources in the vicinity of Timber Mountain. The volcanic aquifers and confining units are intercalated with undifferentiated valley-fill and the valley-fill aquifer to the south and southeast of Yucca Mountain (USGS 2000d, Section 6.1).

The general conceptual model of saturated zone flow in the site-scale saturated zone flow and transport model area is that groundwater flows to the south from recharge areas of higher precipitation at higher elevations north of Yucca Mountain, through the Tertiary volcanic rocks into the valley-fill aquifer, and toward the Amargosa Desert. Within the site-scale model area, recharge occurs from infiltration of precipitation and infiltration of flood flows from Fortymile Wash and its tributaries. Outflow from the model area mostly occurs across the southern boundary of the model, and to pumpage by irrigation wells in the Amargosa Farms area (CRWMS M&O 2000bn, Section 3.2).

In the event of waste mobilization and migration away from the potential emplacement drifts at Yucca Mountain, the rate of radionuclide transport through the saturated zone is determined by the groundwater flux, the hydrologic properties, and sorptive properties of tuff and alluvium units.

The objective of the saturated zone flow and transport process model and the corresponding components of the TSPA-SR is to evaluate the migration of radionuclides from their introduction at the water table below the potential repository to

the release point to the biosphere, as illustrated in Figures 4-127 and 4-128. The release point is at the accessible environment downgradient (i.e., the direction of groundwater flow) from the site. The main output of the saturated zone flow and transport process models used directly by the TSPA is an assessment of the concentration of radionuclides in groundwater and the time it takes for various radionuclides to be transported from areas beneath the potential repository to the accessible environment. The current understanding of saturated zone transport is documented in *Saturated Zone Flow*
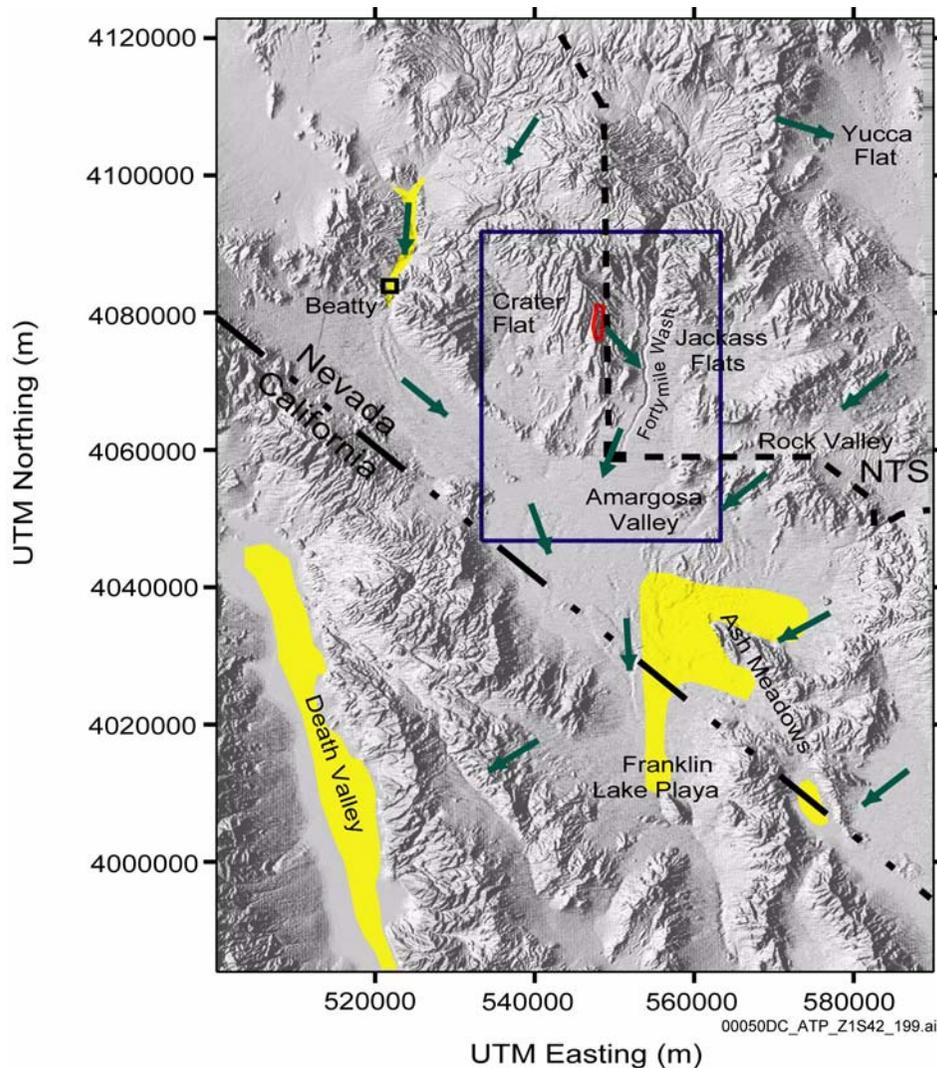
Figure 4-127. Regional Map of the Saturated Zone Flow System Showing Direction of Flow and Outline of the Three Dimensional Saturated Zone Flow Model Domain

Arrows give direction of flow from regional flow models. The solid rectangle shows the boundary of the site-scale three-dimensional saturated zone flow model. Flow from Yucca Mountain is southeast to Fortymile Wash and then south to the site-scale model boundary. NTS = Nevada Test Site. Source: (CRWMS M&O 2000a, Figure 3.8-4).
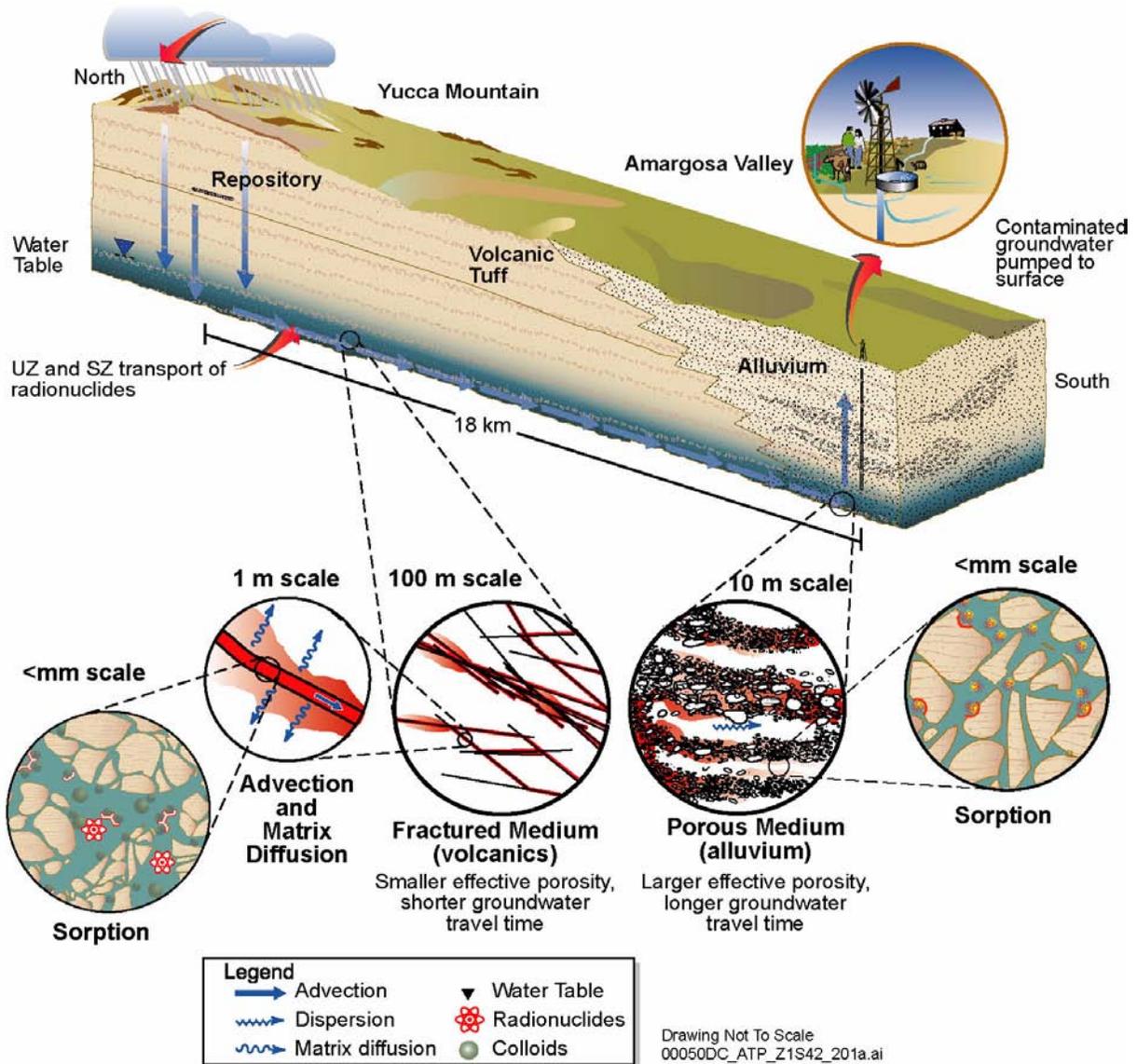
Figure 4-128. Conceptualization of Features and Processes Important to Saturated Zone Transport
This schematic illustration presents transport processes in fractured and porous media flow at Yucca Mountain, providing a conceptualization of transport through the saturated zone to the location of the reasonably maximally exposed individual in the Amargosa Valley. Moving groundwater carries (advects) dissolved or suspended radionuclides in fractures in the volcanic rocks and in pores between individual rock grains in the alluvium. The processes of diffusion and sorption slow the transport of radionuclides to the accessible environment. Radionuclides diffuse into and out of the unfractured portion (matrix) of the volcanic rocks. In the alluvium, radionuclides diffuse into and out of regions where water is stagnant or flows very slowly. UZ = unsaturated zone; SZ = saturated zone.

and Transport Process Model Report (CRWMS M&O 2000bn).

4.2.9.1 Conceptual Basis of Flow and Transport

The following discussion of the conceptual basis for the site-scale saturated zone flow and transport model is a summary of information presented in Section 3.2 of *Saturated Zone Flow and Transport Process Model Report* (CRWMS M&O 2000bn).

Flowing groundwater transports radionuclides either in solution (dissolved) or in suspension, bound to very small particles known as colloids. Colloid particles are small enough to travel with flowing water through fractures in volcanic rocks, pores in the unfractured portion (matrix) of volcanic rocks, and pores in alluvium. Radionuclide releases from water contacting breached waste packages in the potential repository would have to migrate a distance ranging from approximately 210 m (690 ft) to 390 m (1,300 ft) downward to the water table, then migrate downgradient in the saturated zone to reach the accessible environment. The average distance of the potential repository above the elevation of the water table is about 300 m (1,000 ft). Groundwater in the saturated zone generally moves southeast from beneath the potential repository before flowing south out of the volcanic rocks and into the thick valley fill deposits of the Amargosa Desert.

The water table under most of the potential repository is in the Tertiary age Crater Flat Group. This stratigraphic unit is also referred to by a hydrostratigraphic name, the lower volcanic aquifer. It is composed of three tuffs: the Tram, Bullfrog, and Prow Pass. After reaching the water table, flow continues away from the immediate vicinity of the potential repository site in the Crater Flat Group. Permeability of tuffs in the Crater Flat Group is small where the rocks are not fractured. Consequently, most flow of groundwater in these rocks occurs in fractures.

The volcanic rocks are about 2,000 m (6,500 ft) thick at the site, but they gradually thin to 0 m (0 ft) with increasing distance from the site. At a distance of 10 to 20 km (6 to 12 mi) along the travel path from the potential repository, groundwater flow enters alluvium and remains in alluvium to the accessible environment. Flow in alluvium is modeled as movement through pores between rock grains rather than in fractures.

The quantity of groundwater that flows through a unit area of rock per unit period of time is known as the specific discharge. To maintain the same specific discharge in volcanic rocks and alluvium, the velocity of flow must be slower in the alluvium because the effective porosity of the alluvium is larger than the fracture porosity of the volcanic rocks. Results of the saturated zone site-scale flow model show that specific discharge does not change greatly along flow paths from the repository to the receptor location. Consequently, flow velocities are faster in volcanic rocks than in alluvium. Figure 4-129 shows possible flow paths from the potential repository, as well as the portions of the flow paths in tuff and alluvium. The portion of the flow paths in tuff is shown in red, and the portion in alluvium is blue. The location of the contact of tuff and alluvium is uncertain and is treated stochastically in TSPA-SR calculations. This figure shows the contact to be at the expected-value location.

The flow paths described previously are inferred from a site-scale flow model. This model results in a flow field that is consistent with available information concerning geology, rock hydraulic properties, groundwater chemistry, and measured water levels. One feature of the simulated three-dimensional flow field is higher hydraulic head in carbonate rocks at depth than in the rocks containing the simulated flow paths from below the potential repository. The carbonate rocks are relatively permeable and laterally continuous. They are sometimes referred to by the hydrostratigraphic name, the regional carbonate aquifer. The upward gradient of hydraulic head from the carbonate rocks to the overlying tuffs is observed in boreholes located within the more extensive Death Valley Regional Flow System and is supported by regional-scale flow modeling (D'Agnese, Faunt et al. 1997). In addition, the upward gradient is observed in the only borehole in the vicinity of Yucca Mountain to penetrate the regional carbonate aquifer. This potential for upward flow is
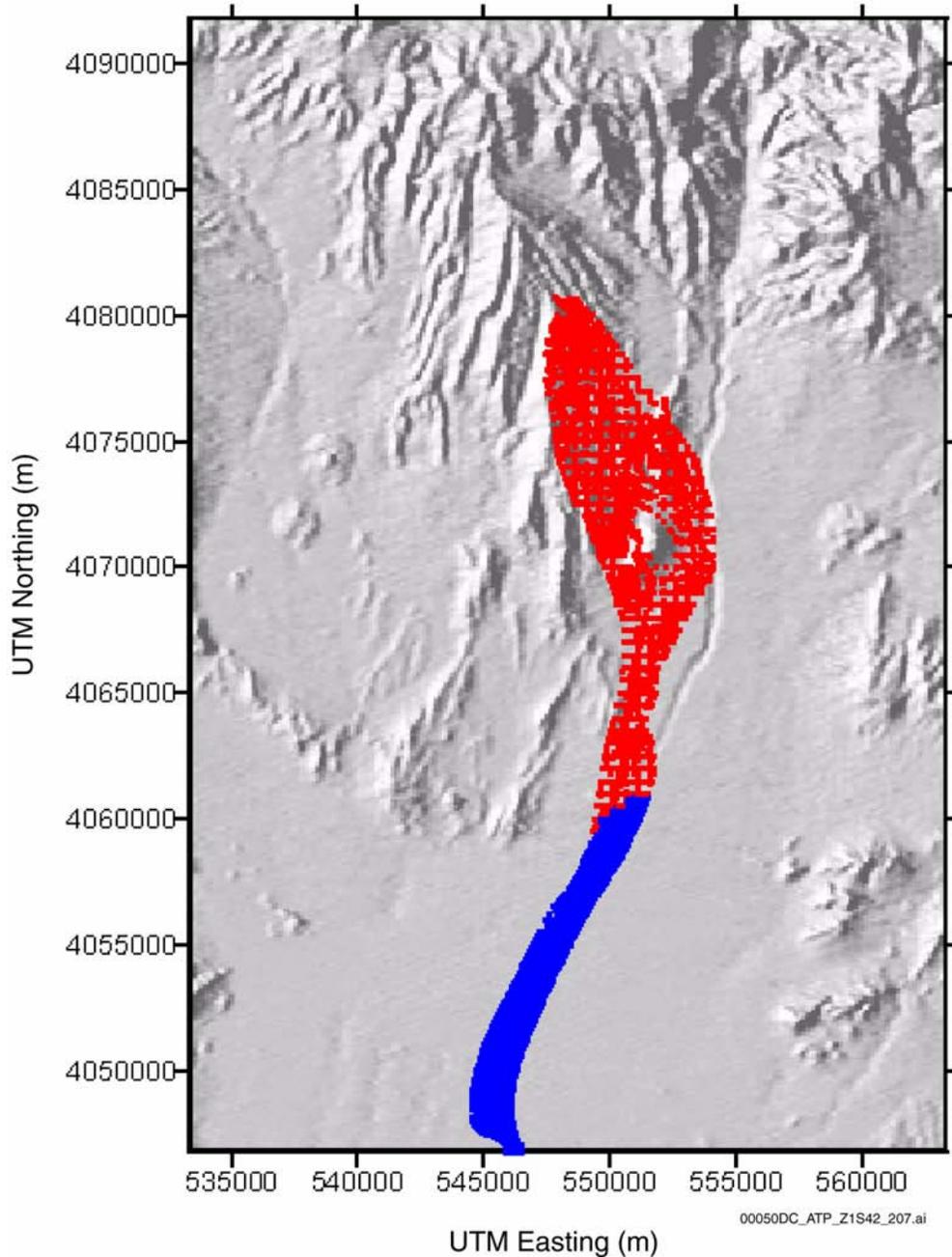
Figure 4-129. Flow Paths Predicted by the Site-Scale Saturated Zone Flow and Transport Model for the TSPA-SR

The repository is located in the upper central part of the figure. The released particles move from the upper central area in the figure to the bottom. The red portion of the illustrated particle positions corresponds to an area of flow through fractured volcanic tuff while the blue part of the flow path is through alluvium, modeled as a porous medium. The spatial pattern in the volcanic tuff reflects the numerical algorithm that illustrates particle positions at grid boundaries or at the end of a time step. The location of the contact of tuff and alluvium is uncertain and is treated stochastically in TSPA-SR calculations. This figure shows the contact to be at the expected-value location. Source: Adapted from CRWMS M&O 2000a, Figure 3.8-21.

significant for the performance of the potential repository because it prevents downward flow of contaminants from Yucca Mountain into the regional carbonate aquifer.

Several processes act to slow the movement of radionuclides or to dilute their concentration (Figure 4-128). The processes that slow, or retard, the movement of radionuclides are important in that longer travel times allow more time for radioactive decay to occur. One important retardation process is sorption onto mineral surfaces. The sorption process is reversible. Consequently, a portion of the radionuclides at a particular location will be sorbed to rock surfaces, and a portion will be in solution in the groundwater. Multiple cycles of sorption and desorption slow the movement of radionuclides relative to the groundwater flow rate.

Diffusion of dissolved or colloidal radionuclides into regions of very slowly moving groundwater is a second important retardation process. Diffusion will occur from water flowing in the fractures of the volcanic rocks into the matrix, or nonfractured, portion of these rocks, as well as from water in pores between rock grains in the alluvium into porosity within the rock grains. In either case, the radionuclides will eventually diffuse back out into the moving groundwater. However, multiple cycles of diffusion into and out of the rock matrix and grains slows the rate of transport.

Finally, hydrodynamic dispersion, or spreading of solutes, along the flow path can decrease the concentration of radionuclides in groundwater (Figure 4-130). Dispersion is mainly due to differences in flow velocity at a microscopic scale or by larger-scale heterogeneity of permeability.

4.2.9.2   Summary State of Knowledge

In this section, data are presented that support selected aspects of the conceptual basis and modeling of radionuclide transport through the saturated zone. In addition, natural analogues for these processes are discussed.

The transport of radionuclides potentially released from a repository is closely tied to the behavior of water flowing through the host subsurface material

because liquid water is the principal medium in which radionuclides are transported to the potential downgradient receptor (CRWMS M&O 2000bn, Section 3). If released, radionuclides would primarily move in groundwater as solute or attached to colloids. The transport of radionuclides as solute is affected by the three processes discussed in the previous section—advection, diffusion, and dispersion—and, for reactive constituents, by sorption. In addition, transport of radionuclides attached to colloids is affected by filtering, in which colloids with diameters greater than the pore openings are "sieved" by the medium. Transport of filtered particles is thereby retarded with respect to advective flow. Chemical precipitation, retardation (slowing the movement of radionuclides to less than the velocity of groundwater), and dilution (reducing the concentration) of radionuclides in the groundwater all affect the concentration of radionuclides released to the environment.

4.2.9.2.1   Advection

C-Wells Testing—Results from the hydraulic and tracer testing completed at the C-Wells Complex (Figure 4-131) were used to identify and confirm the conceptualization of flow and transport in the fractured tuff and to derive flow and transport parameters used in the modeling. Data from the testing are discussed in the next sections on advection, dispersion, matrix diffusion, and sorption. Ongoing testing at the Alluvial Testing Complex located at Nye County Well 19D, shown in Figure 4-131, will provide additional information on flow and transport in the alluvium.

Advection in the Fractured Porous Media—Hydrologic evidence supports the model of fluid flow within fractures in the moderately to densely welded tuffs of the saturated zone (CRWMS M&O 2000bn, Section 3.2.2). Bulk hydraulic conductivities measured in the field tend to be several orders of magnitude higher than hydraulic conductivities of intact tuff core samples measured in the laboratory. Also, there is a positive correlation between fractures identified using acoustic televiewer or borehole television tools and the zones of high transmissivity and flow (Erickson and Waddell 1985, Figure 3).
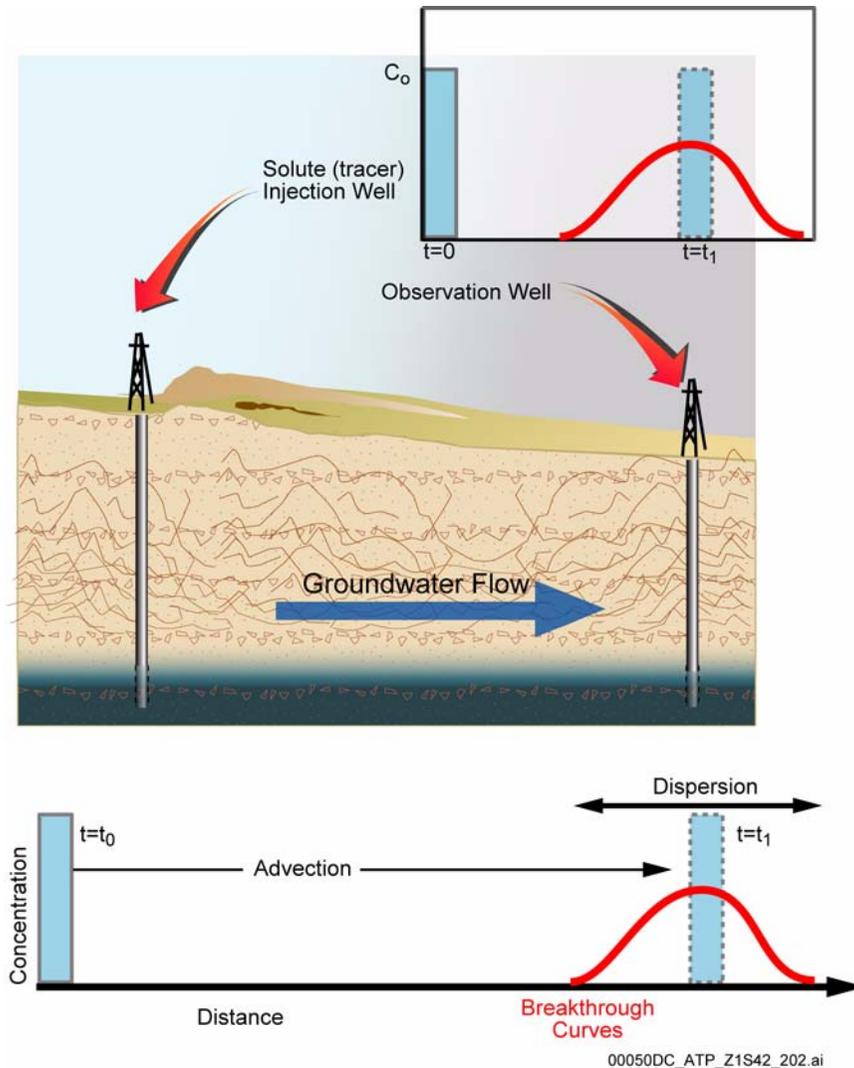
Figure 4-130. Concepts of Advection and Dispersion in Porous Medium and the Resulting Breakthrough Curves Defined by the Time History of Solute Concentration Measured in a Well
The initial volume at the well on the left illustrates the introduction of a solute plume at time t=0. As the solute moves downstream (by advection) to an observation well, it spreads by dispersion. The dotted volume illustrates the effect of advection only. The breakthrough curve gives the time-dependent concentration history at the observation well.

Fractures have important effects on the hydrology at Yucca Mountain, and the permeability distribution and principal flow directions depend strongly on the spatial distribution and orientations of fractures.

The laboratory work of Peters et al. (1984, Appendix E), in which fracture hydraulic apertures were found to be relatively insensitive to confining pressures, suggests that the spatial distribution of fractures (densities and interconnectivities) is more important in determining hydraulic conductivity as a function of direction than the effect of the stress field on the apertures of individual joints.

Numerical simulations (Brown 1987) suggest that there is a propensity of fluid and solutes to travel preferentially along channels in fractures where apertures are largest. Thus, for flow within fractures in the saturated zone, a fracture-flow model recognizing and accounting for flow channels may be necessary.
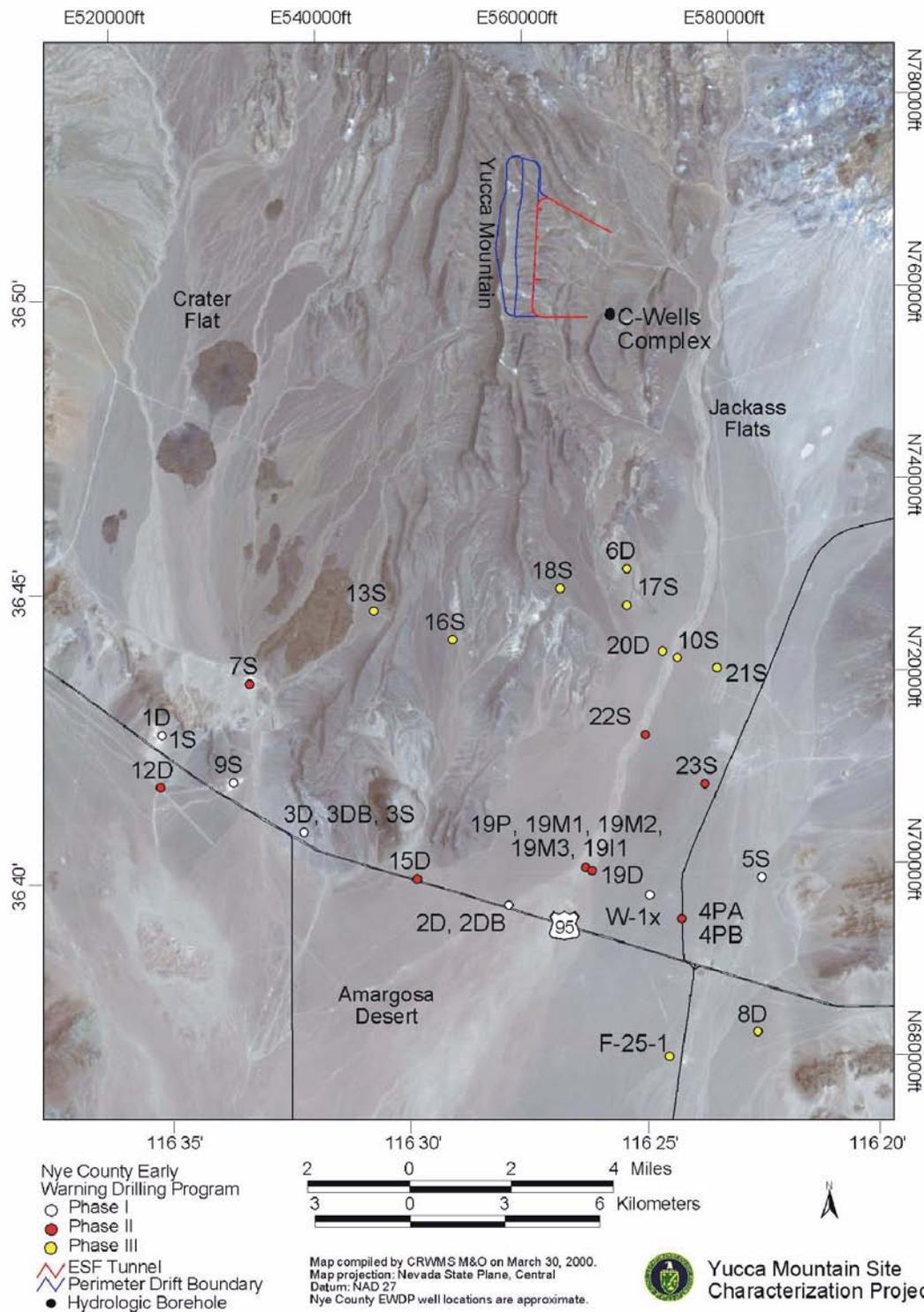
Figure 4-131. Nye County Early Warning Drilling Program Boreholes, the C-Wells Complex, and 19D (the Location of the Alluvial Testing Complex)

Source: CRWMS M&O 2000bn, Figure 2-3.

Fractures generally are found within the moderately to densely welded tuffs, so the range of matrix porosities of these tuffs (0.06 to 0.09 for densely welded and 0.11 to 0.28 for moderately welded) probably best reflects the matrix fluid storage capacity of interest for saturated zone transport calculations (CRWMS M&O 2000bn, Section 3.2.4.1.1).

Advection in the Alluvium—Due to the more porous and less fractured nature of the porous alluvial material, fluid flow in the alluvium is well represented using a porous continuum conceptual model. However, this assumption does not mean that the medium is homogeneous. On the contrary, flow is likely to occur through the more permeable regions within the medium, with the low-permeability regions acting as flow barriers that groundwater flows around rather than through. Ongoing Nye County Early Warning Drilling Program drilling and the Alluvial Testing Complex

testing will provide more data to quantify the alluvium portion of the flow. Hydrologic parameters used in numerical models were selected to be conservatively bounding. Fluid flow is represented using a porous continuum with a constant and conservative permeability value. Transport parameters are assigned based on uncertainty distribution of the parameters.

Fracture Properties—Fracture properties (such as aperture, frequency, mineralogy, and saturation, as shown in Figure 4-132) affect fracture–matrix interactions, dispersion, sorption, and the transport of aqueous and colloidal species. The fracture apertures are derived from the fracture porosity and fracture–matrix connection area (CRWMS M&O 2000ed, Section 6.2.1). A log-normal distribution of apertures for all the model layers beneath the potential repository is sampled stochastically in the transport calculations for TSPA.
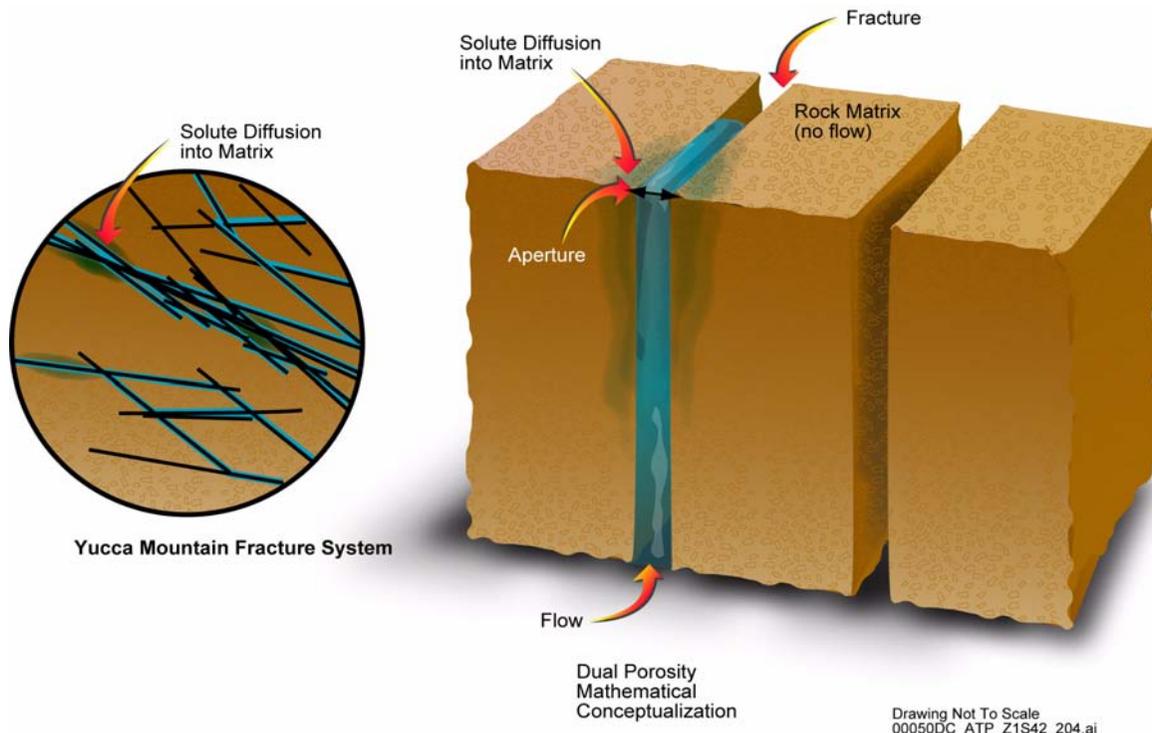
Figure 4-132. Fracture Properties of Aperture (Width), Length, and Frequency (Number of Fractures per Volume)

These parameters vary spatially in real geological media. The dual-porosity mathematical conceptualization assumes stagnant water in a porous rock matrix of high porosity and low permeability and relatively rapid flow in the fracture network of low porosity and high permeability. Solute enters and leaves the matrix rock through matrix diffusion.

In the saturated zone, the main distinction between the volcanic aquifers and the confining units is that the aquifers tend to be more welded and contain more permeable fractures. However, alteration of the tuffs to zeolites and clays, which reduces permeability, is more pronounced at depth, and the greater pressure at depth tends to reduce fracture permeability. Consequently, a combination of factors, including fracture properties, mineralogy, and depth, rather than just rock type, determines the hydrologic character of the volcanic rocks below the water table at Yucca Mountain.

Hydraulic tests have been performed to determine the properties of the saturated zone volcanic units. The analyses are limited by uncertainties about the extent to which fractures affect the unit conductivity (a measure of the ability of the subsurface material to transmit flow) (Luckey et al. 1996, pp. 32 to 36). However, the confining units had a low range of conductivities (0.000005 m to 0.26 m [0.00002 to 0.85 ft] per day), whereas the aquifers had a range of moderate to high conductivities (0.00004 m to 18 m [0.0001 to 59 ft] per day). Intervals without open fractures in all units tend to have low hydraulic conductivity, reflecting the conductivity of the rock matrix or of small fractures (Luckey et al. 1996, p. 32). Conversely, larger values of apparent hydraulic conductivity for both aquifers and confining units can generally be attributed to fractures.

Hydraulic tests at Yucca Mountain were performed in single-borehole and multiple-borehole tests (C-Wells Complex). Transmissivities, which are a measure of the ability of the entire thickness of the rock unit to transmit water, were measured in the multiwell tests and tend to be approximately 100 times greater than those determined from single-borehole tests in the same borehole. This observation suggests that the multiwell tests, which sample larger subsurface volumes, are also encountering a larger number of permeable fractures (Luckey et al. 1996, p. 36). The test results also support the hypothesis that fractures are more important than matrix in controlling hydraulic conductivity of the volcanic rocks in the saturated zone.

Groundwater Flow Paths—The concentrations of chemical constituents in groundwater that do not react with the subsurface material (i.e., conservative constituents) can be used to help delineate groundwater flow paths both on a regional and a local basis (CRWMS M&O 2000eg, Figure 5). Maps of areal variations in the concentrations of such constituents as chloride in the Yucca Mountain region delineate flow paths with generally north–south orientations (Figure 4-133). Flow paths from the potential repository first trend to the southeast towards Fortymile Wash and then, after reaching Fortymile Wash, trend more southerly. Whether water from the potential repository horizon mixes with water moving southward along Fortymile Wash is unclear. If such mixing does take place, it could substantially dilute the concentrations of any radionuclides that might be released from the potential repository. If not, radionuclides that might be released from the potential repository could be confined to the somewhat slower flow paths generating from below Yucca Mountain.

The time at which a given body of water is recharged can generally be bounded through an analysis of isotopic data for hydrogen, oxygen, carbon, and chlorine. Data on isotopic compositions of hydrogen and oxygen in saturated zone waters in the Yucca Mountain region suggest that the waters of southern Yucca Mountain and eastern Crater Flat infiltrated under cooler conditions than the waters of northern and eastern Yucca Mountain, which in turn were infiltrated under cooler conditions than waters along Fortymile Wash (CRWMS M&O 2000eg, Section 6.5.4.1). Through comparisons of the isotopic data for waters in modern climatic regimes, it is likely that the cooler conditions reflected in the waters of southern Yucca Mountain and eastern Crater Flat were associated with the end of the last ice age approximately 10,000 years ago. Carbon isotopic data (including carbon-14 measurements) for these waters are consistent with such a conclusion (CRWMS M&O 2000eg, Section 6.5.4.2.1). Unfortunately, the carbon isotopic data do not allow the derivation of more accurate groundwater ages because of uncertainty in the degree to which the original atmospheric carbon-14 signal in infiltrated waters may have been modified by dissolution of preexisting carbonate minerals. As a
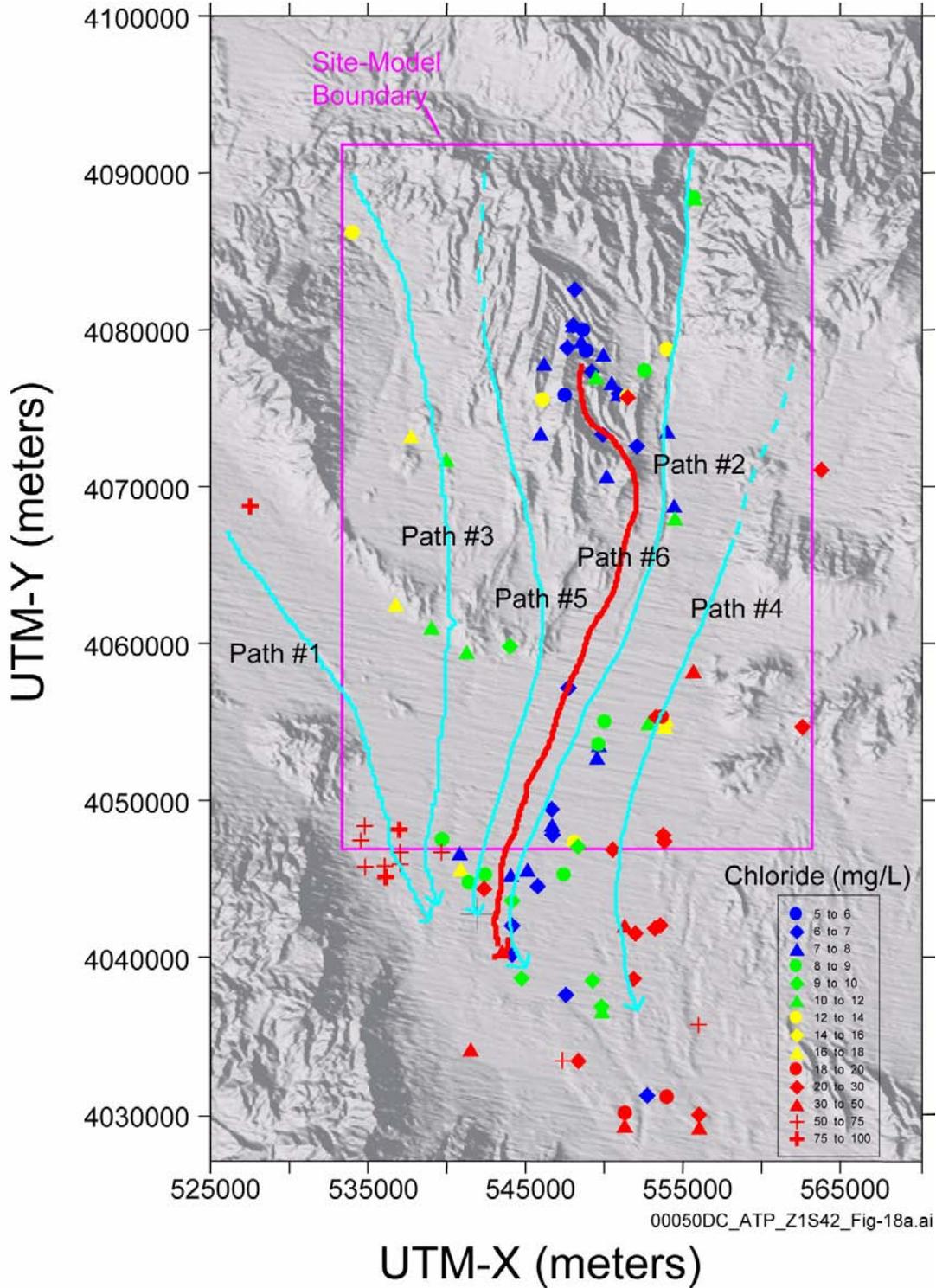
Figure 4-133. Groundwater Flow Paths near Yucca Mountain as Inferred from Chloride Concentrations at Sites near Yucca Mountain

The red arrow shows the groundwater flow path from Yucca Mountain. The blue arrows show other regional groundwater flow paths that constrain the Yucca Mountain flow path. UTM = Universal Transverse Mercator. Source: Modified from CRWMS M&O 2000bn, Figure 3-3.

consequence, groundwater ages calculated on the basis of observed carbon-14 values are maximum ages (CRWMS M&O 2000eg, Section 6.5.4.2.1).

The apparent age of groundwater in Fortymile Wash is younger than the age of groundwater beneath the potential repository (CRWMS M&O 2000eg, Section 6.5.4.2.1). This result implies that, if there is groundwater mixing, groundwater below the potential repository makes up at most a small fraction of the groundwater beneath Fortymile Wash. It also suggests the possibility that flow paths from the area of the potential repository may have a more southerly orientation than suggested by the chlorine data (Figure 4-133).

The expected flow path of groundwater moving away from the potential repository in the saturated zone passes into the valley-fill deposits approximately 15 km (9.3 mi) or more south of Yucca Mountain. Beginning in 1999, numerous boreholes have been drilled in the valley fill as part of the Nye County Early Warning Drilling Program (Figure 4-131). Additional holes are scheduled to be drilled in later phases. In addition to providing a monitoring system for Amargosa and Pahrump valleys, these holes are designed to provide information about the lithology, water levels, hydraulic properties, and transport properties of the valley fill. This information should enable the DOE to limit the uncertainties and conservatism in the current site-scale saturated zone flow and transport model.

4.2.9.2.2 Matrix Diffusion

Instead of simply traveling at the flow rate of the fluid in the saturated zone, radionuclides will potentially undergo physical and chemical interactions that must be characterized to predict large-scale transport behavior. In the laboratory, the effect of matrix diffusion has been clearly demonstrated by rock-beaker, diffusion-cell, and fractured-rock-column experiments (CRWMS M&O 2000eb, Section 6.6). Transport models incorporating matrix-diffusion concepts have been proposed to explain the inconsistencies between groundwater ages obtained from carbon-14 data and those predicted from flow data. In the field, interwell tracer tests that demonstrate the effect of

matrix diffusion have been conducted (CRWMS M&O 2000eb, Section 6). These laboratory experiments and field tests have demonstrated the validity of matrix diffusion and provided a basis for quantifying the effect of matrix diffusion on radionuclide migration through the moderately and densely welded tuffs of the saturated zone at Yucca Mountain. Because the effect of matrix diffusion on transport through the saturated zone could be important, it is incorporated into the TSPA model of radionuclide migration.

When a dissolved species travels with the groundwater within a fracture, it may migrate by molecular diffusion into the relatively stagnant fluid in the rock matrix. When a molecule enters the matrix, its velocity effectively goes to zero until Brownian motion carries it back into a fracture. The result of moving into the stagnant matrix is a delay in the arrival of the solute at a downgradient location from that predicted if the solute had remained in the fracture.

As described in *Saturated Zone Transport Methodology and Transport Component Integration* (CRWMS M&O 2000eh), mathematical models were first used to demonstrate the likely effect of matrix diffusion and flow in fractured media. In these studies, transport was idealized as plug flow in the fracture with diffusion into the surrounding rock matrix. Experiments were performed on transport in natural fissures in granite, and it was concluded that matrix diffusion was necessary to model conservative tracer data. The concept of matrix diffusion was extended to examine the coupling between matrix diffusion and channel flow usually thought to occur within natural fractures.

Often, groundwater ages obtained from carbon-14 data are greater than those predicted from flow data. Sudicky and Frind (1981) developed a model of flow in an aquifer with diffusion into a surrounding aquitard and showed that the movement of carbon-14 can be much slower than that predicted assuming only movement with the flowing water. Maloszewski and Zuber (1985) reached a similar conclusion with a model for carbon-14 transport that consists of uniform flow through a network of equally spaced fractures with

diffusion into the surrounding rock matrix. Their model also includes the effect of chemical-exchange reactions in the matrix, which further slows the migration velocity. They also present analyses of several interwell tracer experiments showing that the matrix-diffusion model can be used to provide simulations of these tests that are consistent with the values of matrix porosity obtained in the laboratory and aperture values estimated from hydraulic tests. In all cases, the results are superior to previous analyses that did not include the effects of matrix diffusion. Finally, of greatest relevance to the saturated zone beneath Yucca Mountain is the C-Wells reactive tracer test (CRWMS M&O 2000bn, Section 3.1.3.2), which demonstrated that models incorporating matrix

diffusion provide more reasonable fits to the tracer-experiment data than those that assume a single continuum. Maloszewski and Zuber (1985) demonstrated that a suite of tracers with different transport characteristics (diffusion coefficient, sorption coefficient) produced breakthrough curves that can be explained with a model that assumes diffusion of tracers into stagnant or near-stagnant water in the matrix pores (Figure 4-134).

Data from naturally occurring isotopes such as carbon-14 provide valuable clues into the processes controlling transport in the saturated zone. The apparent ages of saturated zone fluids are several thousand years or more (CRWMS M&O 2000bn, Section 3.1.2.3). These ages imply
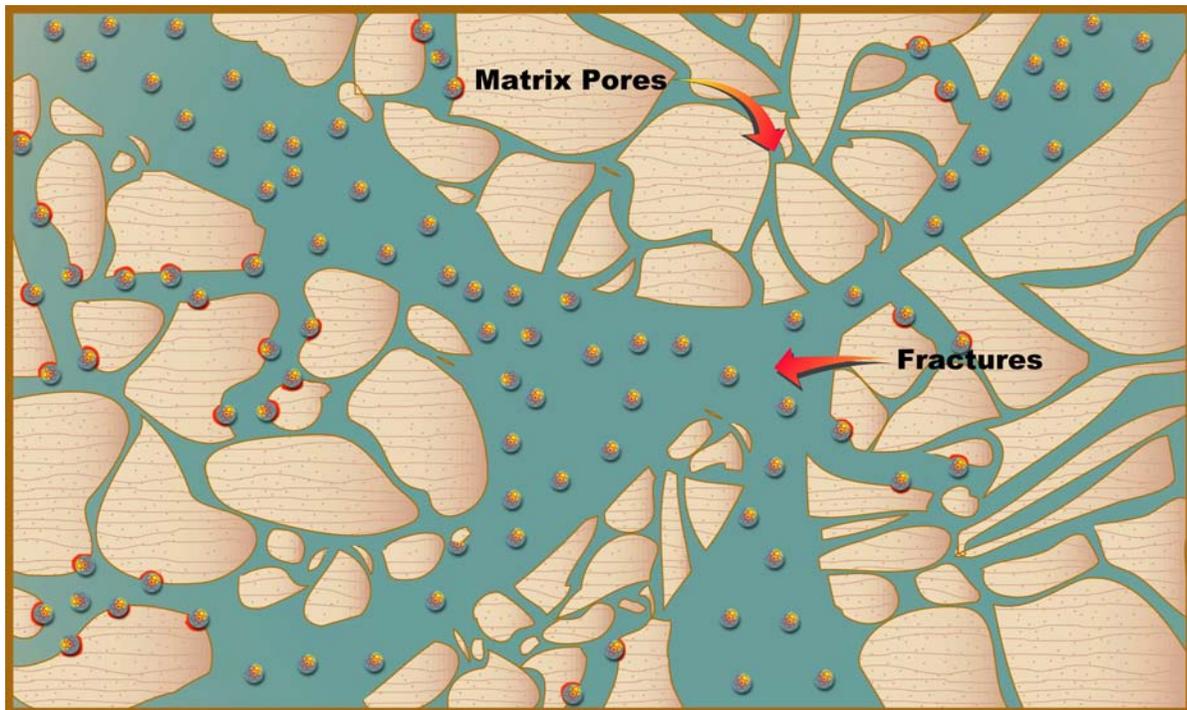
00050DC_ATP_Z1S42_198.ai

🔵 Radionuclide

🔴 Sorbed Radionuclide

Figure 4-134. Conceptualization of Solute and Colloid Transport in a Fracture with Sorption in the Rock Matrix
Sorption in the fracture rock is conservatively ignored in TSPA-SR calculations. After diffusing into the matrix, solutes are sorbed into the rock matrix. Source: CRWMS M&O 2000a, Figure 3.7-4.

that either transport of carbon is slowed by matrix diffusion or advective porosity is much larger than expected for a fractured media. This argument is consistent with the conceptual model of inter-change of solutes between the fractures and matrix found in the matrix-diffusion model (CRWMS M&O 2000bn, Section 3.2.4.2).

4.2.9.2.3 Hydrodynamic Dispersion

Dispersion is caused by heterogeneities from the scale of individual pore spaces to the thickness of individual strata and the length of structural features such as faults. The spreading and dilution of radionuclides that results for these heterogene-ities could be important to performance of the potential repository. The largest heterogeneities are represented explicitly in the site-scale saturated zone flow and transport model (CRWMS M&O 2000bn, Section 3.2.4.4) in that these features are embodied in the hydrogeologic structure on which the model is built. For dispersion at smaller scales, dispersion is characterized using an anisotropic dispersion coefficient tensor consisting of a three-dimensional set of values: longitudinal, horizontal-transverse, and vertical-transverse dispersivities.

Transport field studies have been conducted at a variety of length scales from meters to kilometers to address the issue of dispersion, as discussed in *Saturated Zone Flow and Transport Process Model Report* (CRWMS M&O 2000bn, Section 3.2.4.4). Figure 4-135 shows estimated dispersivity as a function of length scale. The dispersivity values determined for the C-Wells reactive tracer experi-ment (CRWMS M&O 2000bn, Section 3.1.3.2), shown as a black diamond, illustrate a trend toward larger dispersion coefficients for transport over longer distances. Solutes encounter larger-scale heterogeneities at greater distances, and thus spreading is more pronounced. There is uncertainty in this estimate due to uncertainty in the exact flow paths taken by a tracer during the test. Neverthe-less, the estimate falls within the range of values from other sites, suggesting that transport in the fractured tuffs exhibits similar dispersive charac-teristics. The values used in the simulations of radionuclide transport are somewhat higher than those estimated from the C-Wells because of the
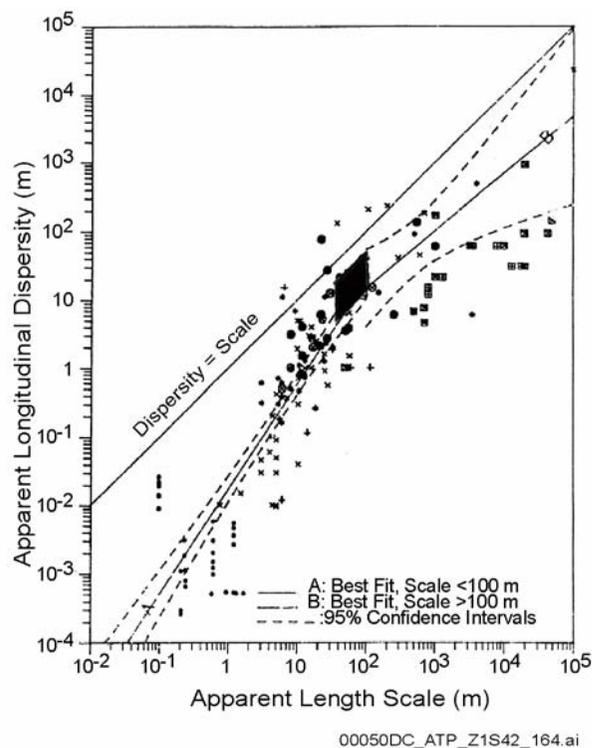
Figure 4-135. Estimated Dispersivity as a Function of Length Scale
The black diamond represents the dispersivity determined for the C-Wells reactive tracer experiment. Source: CRWMS M&O 2000eb, Figure 100.

larger scale that is relevant for radionuclide migra-tion to the receptor location. A discussion of the numerical and field studies used to set transverse dispersivities is presented in *Saturated Zone Flow and Transport Process Model Report* (CRWMS M&O 2000bn, Section 3.7.2).

Dispersivities—The dispersion coefficient is a function of dispersivity and flow velocity and determines the rate that the contaminant plume spreads within a medium. Dispersivity has been shown to increase as a function of observation scale, attributed mainly to mixing as more hetero-geneities are sampled at larger scales (Gelhar et al. 1992). Field measurements show that the trans-verse dispersivity is significantly less than longitudinal dispersivity (Fetter 1993, pp. 65 to 66).

In transport simulations, longitudinal dispersion results in earlier arrival but generally lower concentration. Given this behavior, no simple conservative bound exists for the longitudinal dispersion. A distribution consistent with the dispersivity-versus-scale correlation of Neuman (1990) is used in TSPA calculations. Transverse dispersion acts only to reduce concentration, with generally little effect on contaminant breakthrough time.

For comparison with regulations, concentrations are computed by dividing all the mass crossing into the accessible environment by a specified volume of water. For this reason, hydrodynamic dispersion is not expected to play an important role in saturated zone transport simulations at Yucca Mountain.

Decay Chains—The plutonium-239 decay chain (plutonium-239 → uranium-235 → protactinium-231) is particularly important because the uranium-235 daughter has significantly smaller K_d values compared to its plutonium-239 parent (CRWMS M&O 2000c, Section 3.11.2.6). This decay chain includes only the most important radioactive chain members and omits daughters with short half lives. The neptunium-237 decay chain (neptunium-237 → uranium-233 → thorium-229) has also been evaluated. The daughter contribution is less than 2 percent at 1 million years (CRWMS M&O 2000ea, Section 6.13.1.2). As such, daughter contributions to neptunium-237 transport are relatively insignificant.

Matrix-Diffusion Coefficients—The effective matrix-diffusion coefficient, which is the product of the molecular diffusion coefficient, tortuosity, and porosity, is used to account for rock geometry effects on matrix diffusion. The matrix diffusion coefficient determines the rate of contaminant flux between the matrix and the fracture. Tortuosity, a measure of deviation from straight flow path through porous medium, is a parameter that reflects the effect of the geometry of the pore structure on the flow within the matrix (it varies between zero and one). The concepts of porosity and molecular diffusion in the matrix are discussed in Section 4.2.9.1.

Experimental data on the tortuosity distribution in the various hydrogeologic units at Yucca Mountain were supplemented by an approach using porosity values to approximate tortuosity (CRWMS M&O 2000ea, Section 6.1.2.4). Tortuosity measurements on devitrified tuffs showed good agreement with this approximation.

Distribution parameters for matrix diffusion coefficients (see Table 4-25 in Section 4.2.8.2.2) are based on the measured diffusion coefficients of tritium and technetium (CRWMS M&O 2000eb, Section 6.6.1.3). The cationic (positively charged and sorbing) radionuclides are assigned values representative of the coefficient for tritium. Based on measured diffusion behavior of cationic radionuclides, this is conservative (CRWMS M&O 2000eb, Section 6.6.1.3). The anionic radionuclides (negatively charged) are assigned values representative of the coefficient for technetium, which (as pertechnetate, the predominant aqueous species of technetium) is approximately 10 times lower than that for tritium. Anionic radionuclides are more likely to be excluded from the matrix pores, which are also negatively charged.

4.2.9.2.4 Sorption

Sorption reactions are chemical reactions that involve the attachment of dissolved chemical constituents to solid surfaces. Although these reactions can be complex in detail, they are typically represented in transport calculations by a constant called the sorption coefficient (CRWMS M&O 2000bn, Section 3.2.4.3).

In the case of the Yucca Mountain flow system, an important performance assessment goal is the prediction of radionuclide transport rates to the receptor location. Radionuclide sorption onto either fracture or matrix surfaces will decrease radionuclide transport rates.

Sorption in Fractured Tuff—Sorption reaction interactions can potentially occur on the surfaces of fractures and within the rock matrix. However, because of a lack of data and to be conservative, sorption on fracture surfaces is neglected, and only sorption within the matrix is included in the saturated zone process models and the TSPA

simulations. For the C-Wells field experiments, analogue tracers were used in place of radionuclides because of environmental considerations. The experiment's reactive tracer, lithium (an analogue for a sorbing radionuclide), was modeled using a matrix-diffusion model with the sorption coefficient of the matrix as an adjustable parameter (CRWMS M&O 2000bn, Section 3.1.3.2). The matrix sorption coefficient that fit the data agreed quite well with the value determined in laboratory sorption tests, thus providing an additional degree of confidence in the matrix-diffusion model. The fact that the early breakthrough of lithium had the same timing as that of the nonsorbing tracers, but with a lower normalized peak concentration, is consistent with matrix diffusion followed by sorption in the matrix.

Transport parameters obtained from the model fits for the saturated zone, with the exception of lithium sorption parameters, are listed in Table 4-28 for the Bullfrog and Prow Pass tuff tests. Further discussion of how these parameters were obtained and how they compare with other studies is provided in *Unsaturated Zone and Saturated Zone Transport Properties (U0100)* (CRWMS M&O 2000eb, Section 6.9).

Lithium sorption parameters were deduced from the field tracer tests. In these tests, lithium sorption always was approximately equal to or greater than the sorption measured in the laboratory (CRWMS M&O 2000bn, Table 3-5). Details of the methods used to obtain the field lithium sorption parameters and discussions of possible alternative interpretations of the lithium responses are provided in Reimus et al. (1999). Microsphere filtration and detachment rate constants deduced from these tracer tests are provided in *Saturated Zone Colloid-Facilitated Transport* (CRWMS M&O 2000ei, Section 6.1.2).

Experimental sorption coefficients (K_d values) were obtained using rock samples collected from the Topopah Spring welded and Calico Hills nonwelded hydrogeologic units at Busted Butte. The fine particles produced during sample crushing were not removed during the Busted Butte sorption study (CRWMS M&O 2000eb, Section 6.8.5.1.2.2) to duplicate in situ conditions, whereas fine materials were removed in the standard batch-sorption tests. Values for K_d could be influenced by small crushed-rock sizes used for sorption measurement, with the fine materials generating large K_d values. The Busted Butte transport tests are discussed in more detail in *Unsaturated Zone Flow and Transport Model Process Model Report* (CRWMS M&O 2000c, Section 3.11.11.2), *Radionuclide Transport Models Under Ambient Conditions* (CRWMS M&O 2000ea, Section 6.10), and *Unsaturated Zone and Saturated Zone Transport Properties (U0100)* (CRWMS M&O 2000eb, Section 6.8).

Table 4-28. Transport Parameters Deduced from Bullfrog Tuff and the Prow Pass Tuff Tracer Tests

Parameter (units)	Bullfrog Tuff		Prow Pass Tuff
	Pathway 1[a]	Pathway 2[b]	
Mass Fraction in Pathway (unitless)	0.12	0.59	0.75
Residence Time, Linear Flow (hr)	37	995	1230
Longitudinal Dispersivity, Linear Flow (m)	5.3	18.8	23.1
Residence Time, Radial Flow (hr)	31	640	620
Longitudinal Dispersivity, Radial Flow (m)	3.6	10.7	6.3
Effective Flow Porosity, Linear[c] (unitless)	0.0029	0.026	0.0068
Effective Flow Porosity, Radial[c] (unitless)	0.0025	0.017	0.0034
Effective Matrix-Diffusion Mass Transfer Coefficient[d] (sec$^{-1/2}$)	0.00158	0.000458	0.000968

NOTES: [a] Pathway 1 refers to pathways that resulted in the first tracer peak.
[b] Pathway 2 refers to pathways that resulted in the second peak.
[c] Based on flow log information, it was assumed that 75 percent of the production flow contributed to the Pathway 1 responses and 25 percent of the flow contributed to the Pathway 2 responses.
[d] The value of the parameter for pentafluorobenzoate (PFBA) was assumed to be 0.577 times that for bromide.
Source: Adapted from CRWMS M&O 2000eb, Tables 51 and 52.

Sorption data for the saturated zone were also determined during batch experiments, and selected results of those tests are presented in Table 4-29.

Sorption in the Alluvium—In contrast to the fractured tuffs, there are no field-scale tracer transport tests as of yet in the alluvium south of Yucca Mountain to confirm the validity of the sorption coefficient data. Tracer testing activities are underway in the Alluvium Testing Complex. However, transport of sorbing solutes in porous media not controlled by fractures has been well studied (CRWMS M&O 2000bn, Section 3.2.4.3), and it is reasonable to assume that the transport velocities of sorbing radionuclides in the alluvium can be conservatively represented using an equilibrium sorption coefficient. Sorption onto alluvium from the Nye County Early Warning Drilling Program wells has been measured for a few key radionuclides (CRWMS M&O 2000eb, Section

6.4.5). For the remaining radionuclides, sorption coefficients are estimated based on values measured for crushed tuff (CRWMS M&O 2000eb, Section 6.9.3.3).

4.2.9.2.5   Colloid-Facilitated Transport

Colloid-Facilitated Transport Experiments—Figure 4-136 provides a conceptual illustration of colloid-facilitated transport processes. Colloids in the saturated zone are capable of facilitating the transport of radionuclides over long distances if (1) a large percentage of the colloids do not irreversibly filter or attach to surfaces of subsurface materials and (2) radionuclide desorption rates from the colloids are slow (i.e., radionuclides are strongly sorbed to colloids), or if (3) colloid concentrations are so high that colloid surfaces can effectively compete with immobile surfaces for radionuclides. However, analyses of colloid

Table 4-29. Sorption-Coefficient Distributions for Saturated Zone Units From Laboratory Batch Tests

Element	Rock Type	K_d (mL/g)			
		Minimum	Maximum	Mean	Coefficient of Variation
Americium	Devitrified	100	2000	N/A	N/A
	Vitric	100	1000	400	0.20
	Zeolitic	100	1000	N/A	N/A
	Iron oxide	1000	5000	N/A	N/A
Neptunium	Devitrified	0	2.0	0.5	0.3
	Vitric	0	2.0	0.5	1.0
	Zeolitic	0	5.0	1.0	0.25
	Iron oxide	500	1000	N/A	N/A
	Alluvium	0	100	18	1.0
Plutonium	Devitrified	5	100	50	0.15
	Vitric	50	300	100	0.15
	Zeolitic	50	400	100	0.15
	Iron oxide	1000	5000	N/A	N/A
Uranium	Devitrified	0	5.0	N/A	N/A
	Vitric	0	4.0	N/A	N/A
	Zeolitic	5	20.0	7.0	0.3
	Iron oxide	100	1000	N/A	N/A
	Alluvium	0	8.0	N/A	N/A
Chlorine, Technetium, Iodine	All tuffs	0	0	N/A	N/A
Technetium	Alluvium	0.27	0.62	N/A	N/A

NOTES: N/A = not applicable. Source: CRWMS M&O 2000eb, Table 2b.
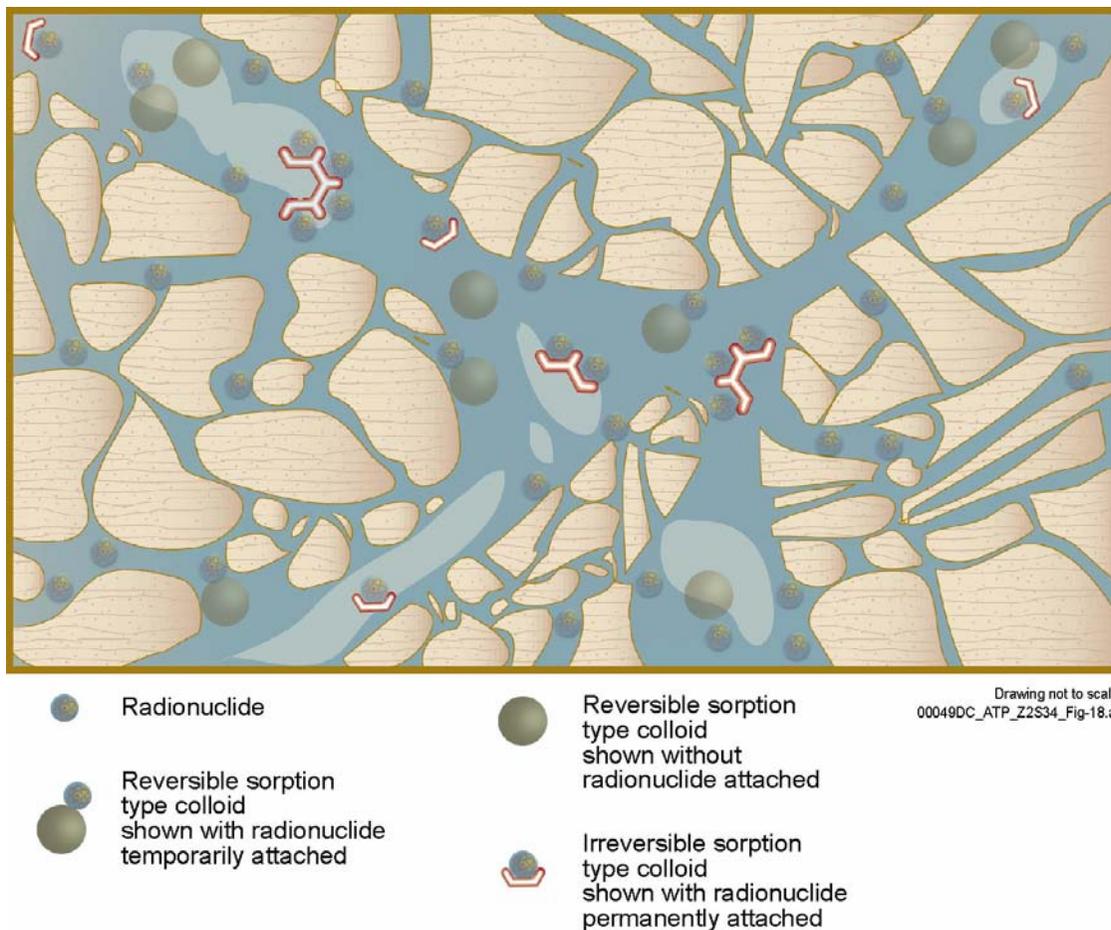
Figure 4-136. Colloid-Facilitated Transport
Colloids are small particles ranging from 0.1 to 5 μm (0.000004 to 0.0002 in.) in diameter. Some radionuclides are sorbed to colloids and thereby transported in groundwater. Source: CRWMS M&O 2000a, Figure 3.7-6.

concentrations and size distributions in Yucca Mountain groundwater have not found high concentrations of colloids. Published correlations of colloid concentrations as a function of water chemistry, which draw upon a global database of measurements, also suggest that colloid concentrations are unlikely to be high enough for the third condition to be met even under perturbed conditions (Triay, Degueldre et al. 1996).

The DOE has addressed the filtering or attachment of colloids to surfaces of subsurface materials using polystyrene microsphere data from the C-Wells field tests to obtain conservative estimates of colloid attachment and detachment rates in frac-

tured tuffs. The DOE also has used published data to obtain bounding estimates of attachment and detachment rates in alluvium (CRWMS M&O 2000bn, Section 3.2.4.5.3). The published correlations of colloid concentrations as a function of water chemistry also support indirect estimates of attachment rates, as it is widely accepted that lower concentrations occur under conditions in which colloids are less stable and, hence, more likely to attach to surfaces. Details of stability-based arguments for bounding colloid concentrations and attachment rates in Yucca Mountain waters are provided in *Colloid-Associated Radionuclide Concentration Limits: ANL* (CRWMS M&O 2000dt, Section 6).

Recent laboratory experiments focused on addressing the magnitude and reversibility of radionuclide sorption onto colloids. Some of the earliest laboratory experiments involved the transport of cesium-137 and silica colloids in columns packed with glass beads. Cesium sorption to the silica was fast and reversible, and it was shown that under these conditions, the ability of the colloids to facilitate cesium-137 transport was limited because of the large amount of competing sorptive surface area presented by the glass beads. Nevertheless, these experiments helped establish equilibrium- and kinetic-based modeling approaches for describing colloid-facilitated transport in the saturated zone. These experiments also made it clear that considerable colloid-facilitated transport would only be an issue for radionuclides that sorbed to colloids more strongly than did cesium-137.

Further laboratory experiments focused on measurements of the magnitude and rates of sorption and desorption for strongly sorbing, long-lived radionuclides onto several different types of colloids that may be present in the near-field (iron oxides such as goethite and hematite that might result from degradation of waste package materials) or in the far-field (silica, montmorillonite clay) environment at Yucca Mountain (CRWMS M&O 2000bm, Section 3.8). These studies used the radionuclides plutonium-239 and americium-243, with the plutonium being prepared in two different forms: colloidal plutonium (IV) and soluble plutonium (V). Also, water from Well J-13 and a synthetic sodium-bicarbonate solution have been used in the experiments. Colloid concentrations were varied in some of the experiments to determine the effect of colloid concentration. Details of the experiment and summaries of the plutonium-239 sorption and desorption rates onto the different colloids are provided in *Colloid-Associated Radionuclide Concentration Limits* (CRWMS M&O 2000dt). The results can be summarized as follows:

- The sorption of plutonium-239 onto hematite, goethite, and montmorillonite colloids was strong and rapid, but the sorption of plutonium-239 onto silica colloids was slower and not as strong.

- The desorption rates of plutonium-239 from hematite colloids were so slow that they are essentially impossible to measure after 150 days. Desorption from goethite and montmorillonite colloids was also slow, but not as slow as for hematite. The desorption rates of plutonium-239 from silica colloids was rapid relative to the other colloids studied.

- For a given form of plutonium-239, sorption was generally stronger, faster, and less reversible in the synthetic sodium-bicarbonate water than in the natural Well J-13 water. Apparently, the presence of other ions, probably most notably calcium, in the natural water tended to suppress slightly the sorption of plutonium-239.

- There was no clear trend of colloidal plutonium (IV) or soluble plutonium (V) being more strongly sorbed to the colloids. In general, it appeared that plutonium (V) was sorbed slightly more to hematite and silica, while plutonium (IV) was sorbed slightly more to goethite and montmorillonite.

- The sorption of plutonium-239 was greatest per unit mass of colloid at the lowest colloid concentrations, which implies that the most conservative K_d values for performance assessment will come from sorption data generated at low colloid concentrations.

The sorption of americium-243 onto hematite, montmorillonite, and silica colloids showed the same trends as plutonium-239 sorption (i.e., for both americium-243 and plutonium-239, sorption onto hematite was stronger than sorption onto montmorillonite, and sorption onto montmorillonite was stronger than it was for silica), and the magnitudes of sorption for the two radionuclides were similar for the different colloids.

This ongoing work indicates:

- Waste form colloids such as hematite pose the greatest risk for colloid-facilitated transport, although these colloids would have to

travel through the unsaturated zone before reaching the saturated zone.

- Natural clay colloids will facilitate plutonium or americium transport more than silica colloids in the saturated zone.

4.2.9.2.6 Analogues to Saturated Zone Radionuclide Transport

In this section, natural analogue studies conducted in saturated environments are reviewed. These sites occur around the world in uranium ore deposits and rare-earth deposits in different types of host rocks (Figure 4-137). Characteristic of these sites is the presence of redox fronts (e.g., Poços de Caldas and Oklo) or weathering and periodic influx of oxidizing water (e.g., Alligator Rivers and Poços de Caldas). Although Cigar Lake applies to reducing groundwater that is not relevant to conditions at Yucca Mountain, localized oxidation may have resulted from radiolysis and could be useful. Additional details of these and other sites are presented in *Saturated Zone Flow and Transport Process Model Report* (CRWMS M&O 2000bn, Section 3.4.5).

Nevada Test Site (CRWMS M&O 2000bn, Section 3.4.5.3.3)—There is some field evidence of colloid-facilitated transport of radionuclides at the Nevada Test Site. Plutonium was detected in groundwater from a well on the Test Site. The isotope ratio of plutonium-240 to plutonium-239 showed that the plutonium had originated from an underground test detonated in the saturated zone. The results indicated that plutonium had transported more than 1.3 km (0.8 mi) over a 30-year period, although plutonium is strongly sorbing at the Nevada Test Site and assumed to be immobile (Kersting et al. 1999). Filtration of the groundwater samples showed that the plutonium was attached to colloidal material in the water. However, it should be noted that the plutonium observed in this study originated from an underground nuclear bomb test and the effects of the blast itself on plutonium transport are not fully understood. Other evidence suggests that transport rates in the saturated zone are significantly lower than would be inferred from the distance travelled by the plutonium.

Colloid concentrations have been measured in several groundwater samples from Yucca Mountain and from other areas at the Nevada Test Site. The measured particle concentrations vary between 1.05×10^6 and 2.72×10^{10} particles per milliliter, with the lowest being for water from Well J-13 and the highest for water from Well U19q on Pahute Mesa (CRWMS M&O 2000ec, Section 6.2.2.2). These values are consistent with what has been reported in the literature for various groundwaters
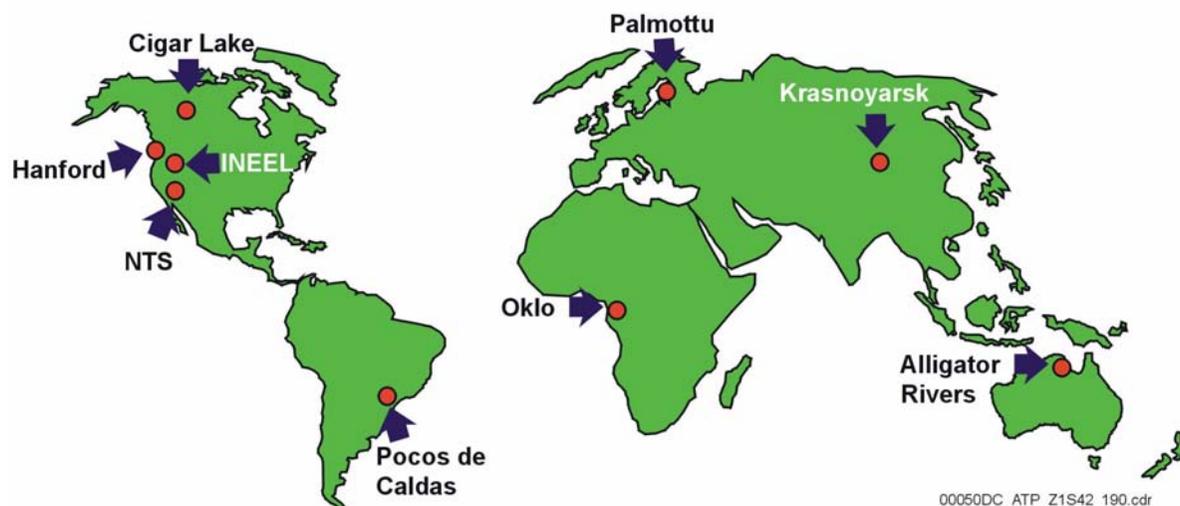
Figure 4-137. Natural Analogue Sites Used for Comparison with Yucca Mountain
INEEL = Idaho National Engineering and Environmental Laboratory; NTS = Nevada Test Site. Source: CRWMS M&O 2000bn, Figure 3-26.

around the world. In the Pahute Mesa drainage, Buddemeier and Hunt (1988, p. 537) found colloid concentrations of 0.8 to 6.9 mg/L for particles greater than 30 nm (0.000001 in.) in size.

Poços de Caldas, Brazil (CRWMS M&O 2000bn, Section 3.4.5.2.2)—The Poços de Caldas caldera in Brazil was the focus of a study involving the Osamu Utsumi mine (a uranium ore body with subsidiary thorium, zirconium, and rare-earth element enrichment) and Morro do Ferro (a thorium and rare-earth element ore body with subsidiary uranium). This site is important as a saturated zone analogue for sorption in alluvium and onto fracture coatings, for matrix diffusion, and for colloidal transport. The Osamu Utsumi uranium mine is known for a well-developed redox front in the uranium ore, and the primary mineralization is mostly low-grade and dispersed throughout the rock. The redox front generally is sharp but irregular in profile as it follows the dips of faults and fractures along which oxidizing waters have penetrated. Uranium mineralization occurs at the redox front itself. At Morro do Ferro, the ore occurs in elongated mineralized lenses. The groundwater at Osamu Utsumi has high concentrations of uranium (up to 10 mg/L), but those at Morro do Ferro are lower. Thorium-232 concentrations generally are low in groundwater from both sites (less than 0.1 µg/L). Most colloids are composed of iron and organic species. Only minor amounts of uranium are associated with colloids, but thorium and rare-earth elements are transported in the colloidal fraction.

Oklo, Gabon (CRWMS M&O 2000bn, Section 3.4.5.2.3)—The Oklo uranium mine in Gabon contains the only known examples of natural fission reactors, and 14 reactor zones have been identified among 3 uranium deposits (see Section 4.3.2.1). This site is important as a saturated zone analogue for sorption in alluvium and onto fracture coatings and for matrix diffusion. At this site, low-grade ore contains 0.1 to 1.0 percent uranium oxide, whereas high-grade ore contains up to 10 percent uranium oxide. High-grade ore occurs within fractures in sandstone rocks. The formation of high-grade ore is attributed to the remobilization of low-grade ore by oxidizing hydrothermal fluids, which transported the uranium along faults,

followed by precipitation in fractures when conditions became more reducing.

Alligator Rivers, Australia (CRWMS M&O 2000bn, Section 3.4.5.2.1)—The Alligator Rivers Analogue Project in Australia was conducted to investigate the migration of radionuclides from an enriched uranium deposit. Leaching of primary ore resulted in the formation of four distinct zones: unaltered primary ore; a uranium silicate zone formed by in situ alteration of the primary ore; a zone of secondary uranyl phosphate minerals that are currently being leached by groundwater; and a zone with uranium in association with clays and iron oxyhydroxides. Dissolved uranium is transported from the uranium oxide zone at depth to the silicate zone, also at depth, then upward to the phosphate zone. The uranyl phosphate zone exists near the surface in the most oxidized weathered zone. A dispersion fan occurs in the weathering zone where uranium has been mobilized, and secondary minerals are found as far as 50 m (160 ft) downstream from the ore body, with detectable concentrations of uranium-series nuclides for about 300 m (1,000 ft) downstream in the dispersion fan. Groundwater samples taken from boreholes were studied with respect to their colloidal contents. Boreholes closest to faults had the greatest variety of colloids. The colloids identified included particles of iron, kaolinite, chlorite, silica, lead, uranium, and titanium. All colloid samples were dominated by iron-rich particles, and uranium was only found in iron-rich species. Low colloid concentrations (about 10^6 particles per liter or less) and the absence of radionuclides in colloids outside the center of the ore body indicated little colloidal transport of radionuclides at this site.

4.2.9.3 Saturated Zone Flow and Transport Process Model Development and Integration

To provide the basis for the analysis of radionuclide transport from the water table beneath the potential repository to the point of regulatory compliance, a numerical site-scale saturated zone flow model was developed to simulate groundwater flow in the area of the potential repository. The flow model is a steady-state model that is calibrated to represent current groundwater flow

conditions in the Yucca Mountain area. A continuum approach for simulating groundwater flow through the fractured rock and alluvial materials is adopted in this model. This approach allows the use of widely accepted mathematical equations describing groundwater flow through porous medium as the mathematical basis for the model. A numerical solution to these equations is obtained using the FEHM code (Zyvoloski et al. 1997a). FEHM uses a method that has been used extensively in petroleum reservoir engineering, the control-volume finite element method, to obtain the numerical solution (Forsyth 1989).

Flow Model Development—The area selected as the domain of site-scale saturated zone flow model is shown in Figure 4-138. The model domain covers an area of approximately 1,350 km^2 (521 mi^2) and is 45 km (28.0 mi) long by 30 km (18.6 mi) wide. The model domain extends to a depth of approximately 2,750 m (9,020 ft) below the interpreted water table. A number of criteria were used to establish the model domain. The model area was made sufficiently large to minimize the effects of the boundary conditions on the estimated permeability values and simulated flow paths at Yucca Mountain, to assess groundwater flow and contaminant transport at the regulatory compliance points downgradient from the potential repository area, and to include wells in the Amargosa Desert at the southern end of the modeled area. However, the area was selected to be small enough to minimize the number of nodes required in the computational grid. The thickness of the model was established to include part of the regional Paleozoic carbonate aquifer (CRWMS M&O 2000bn, Section 3.2.1).

A structured computational grid using orthogonal hexahedral elements was developed for the site-scale saturated zone flow and transport model (Figure 4-139). A horizontal grid spacing of 500 m (1,640 ft) was selected based on previous modeling studies, which demonstrated that this grid spacing provided sufficient horizontal resolution for the model. Although a uniform horizontal spacing was adopted, a nonuniform vertical spacing was established to provide the resolution necessary for accurately representing flow and transport along critical flow and transport pathways in the satu-

rated zone. A finer grid spacing was adopted for shallower portions of the model (10 m [33 ft]) near the water table, and a progressively coarser grid was adopted for deeper portions of the aquifer (550 m [1,800 ft]) at the bottom of the model domain (CRWMS M&O 2000bn, Section 3.3.5.1).

The physical hydrogeologic unit present at each node in the site-scale saturated zone flow model grid was identified using the three-dimensional hydrogeologic framework model (USGS 2000d). The hydrogeologic framework model was constructed using available data from the Death Valley regional flow model (D'Agnese, Faunt et al. 1997), geologic maps and cross sections, borehole data, geophysical data, digital elevation data, and the previously developed geologic framework model for the immediate 40-km^2 (15-mi^2) potential repository area. Geologic units were classified into hydrogeologic units based on their hydraulic properties and lateral extent. A basic principle followed is that the hydrogeologic units at Yucca Mountain form a series of alternating volcanic aquifers and confining units overlying the regional carbonate aquifer. To represent the stratigraphy at a level of detail that would allow a computationally efficient flow model at reasonable computation times, the geologic units are simplified based on their general hydrologic properties. In all, a complex three-dimensional spatial pattern of hydrogeologic units was delineated in the site-scale saturated zone flow and transport model area (Figure 4-140) (CRWMS M&O 2000bn, Section 3.2.1).

Development of a numerical flow model requires specification of boundary conditions for the model domain (CRWMS M&O 2000bn, Section 3.3.5.3). Fixed-head boundary conditions were established around the periphery of the computational grid based on the water levels identified on the potentiometric map previously developed for the site-scale model area (Figure 4-141). The constant head identified for each node was applied uniformly through each layer of the model. In spite of such "constant-head" boundary conditions, vertical gradients develop internally in the model domain in response to geohydrologic conditions, and the calibrated model is capable of representing the upward vertical gradients observed between the carbonate aquifer and overlying volcanic aquifers
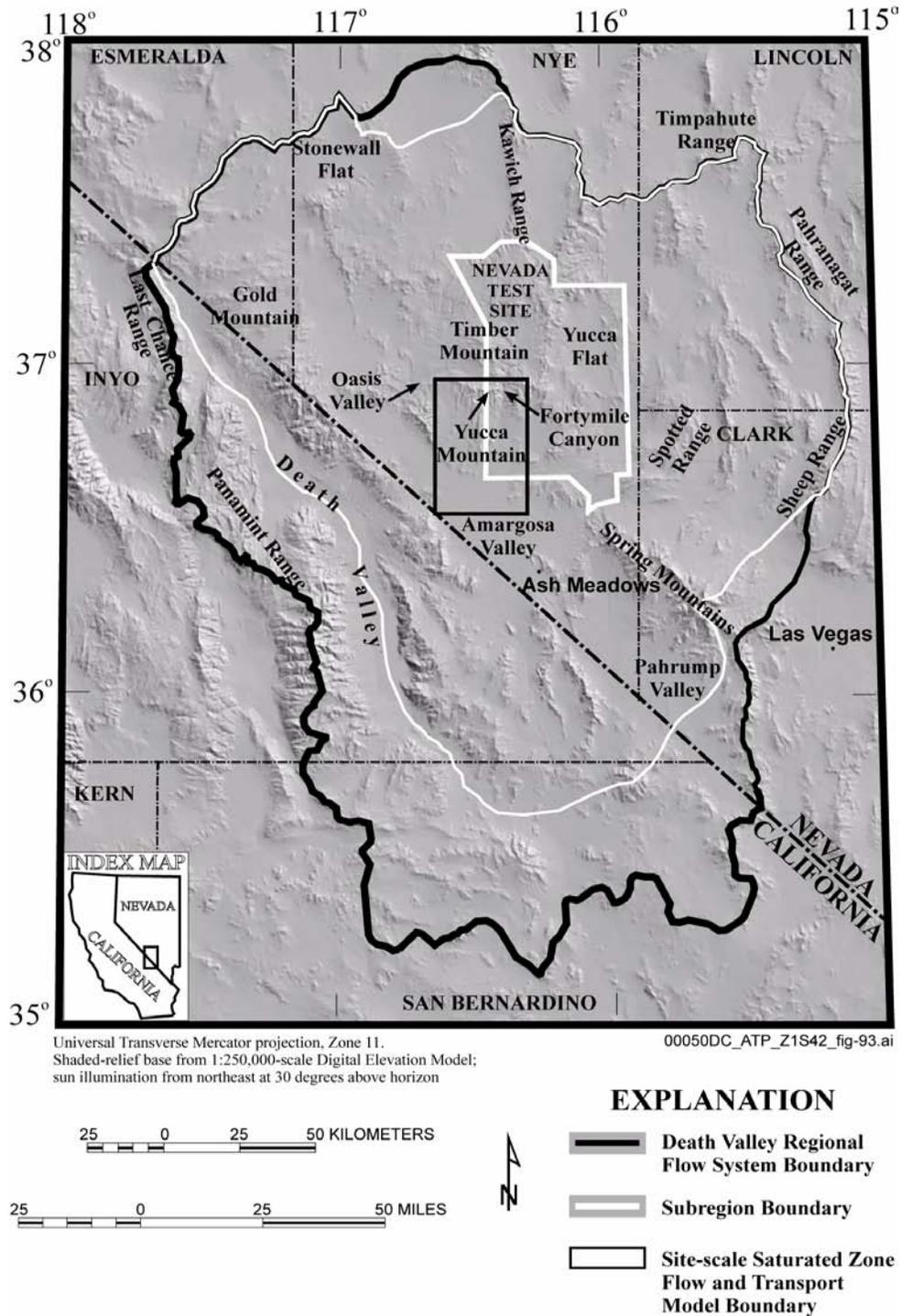
Figure 4-138. Domain of Site-Scale Saturated Zone Flow and Transport Model for the TSPA-SR
The Death Valley regional flow system is the model domain of the regional model used to provide the site-scale flow and transport model with the boundary conditions and to simulate future climate changes. Source: CRWMS M&O 2000bn, Figure 2-1.

00050DC_ATP_Z1S42_fig-14.ai
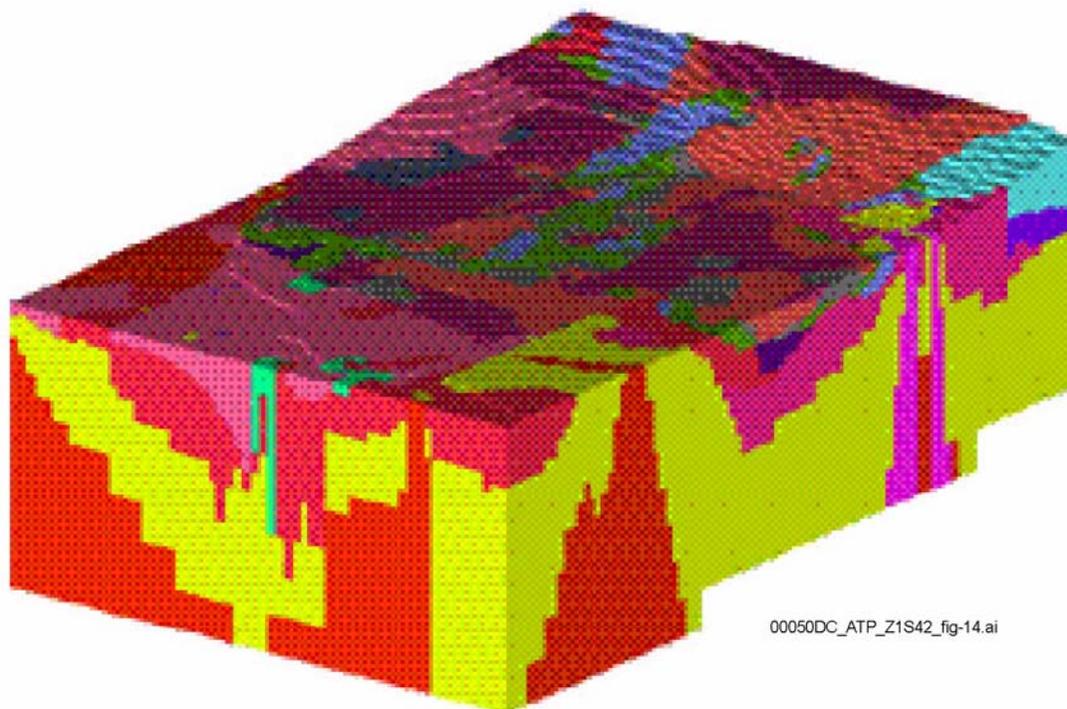
Figure 4-139. Computational Grid Developed for the Site-Scale Saturated Zone Flow and Transport Model
This representation of the computational grid illustrates the complex three-dimensional spatial relation among the units within the site-scale model area. Colors represent different hydrogeologic units. Grid cells are 500 m on each side in the north–south and east–west directions, and the cells vary in depth from about 10 m to about 550 m. Source: CRWMS M&O 2000bn, Figure 3-18.

(CRWMS M&O 2000ej, Section 6.1.2). A no-flow boundary was established at each node located along the bottom of the computational grid. Although flow conditions in the deeper portions of the model domain are not well established, the depth of the bottom boundary is such that this boundary condition is not likely to exert an important influence on flow at shallower levels where groundwater flow and transport is of greater interest to the performance assessment. At the top of the model, a flux boundary condition was established to represent recharge to the system (Figure 4-142).

Representative hydrologic properties were assigned for each node in the computational grid. For flow modeling, these properties include permeability, porosity, and viscosity. Permeability values were assigned to each node during model calibration (Figure 4-143). Because steady-state flow is simulated in site-scale saturated zone flow, the specific storage values assigned at each node does

not influence the water levels predicted by the model (CRWMS M&O 2000bn, Section 3.3.5.5). However, to facilitate the calculation of the specific discharge, which is the volume of water flowing through a unit area of rock at unit time, a porosity value of 1.0 was assigned to all nodes. Because the viscosity of groundwater depends on temperature, the nodal values for viscosity were assigned based on the expected temperature distribution in the subsurface.

4.2.9.3.1 Limitations and Uncertainties

In any numerical simulation of a physical process using a mathematical model, assumptions are made and limitations apply (CRWMS M&O 2000bn, Section 3.5). The following sections discuss the critical assumptions and limitations of the site-scale saturated zone flow and transport model and the parameters that are used as input in this model. Many of the parameter values used in the model are estimated using simple mathematical models.
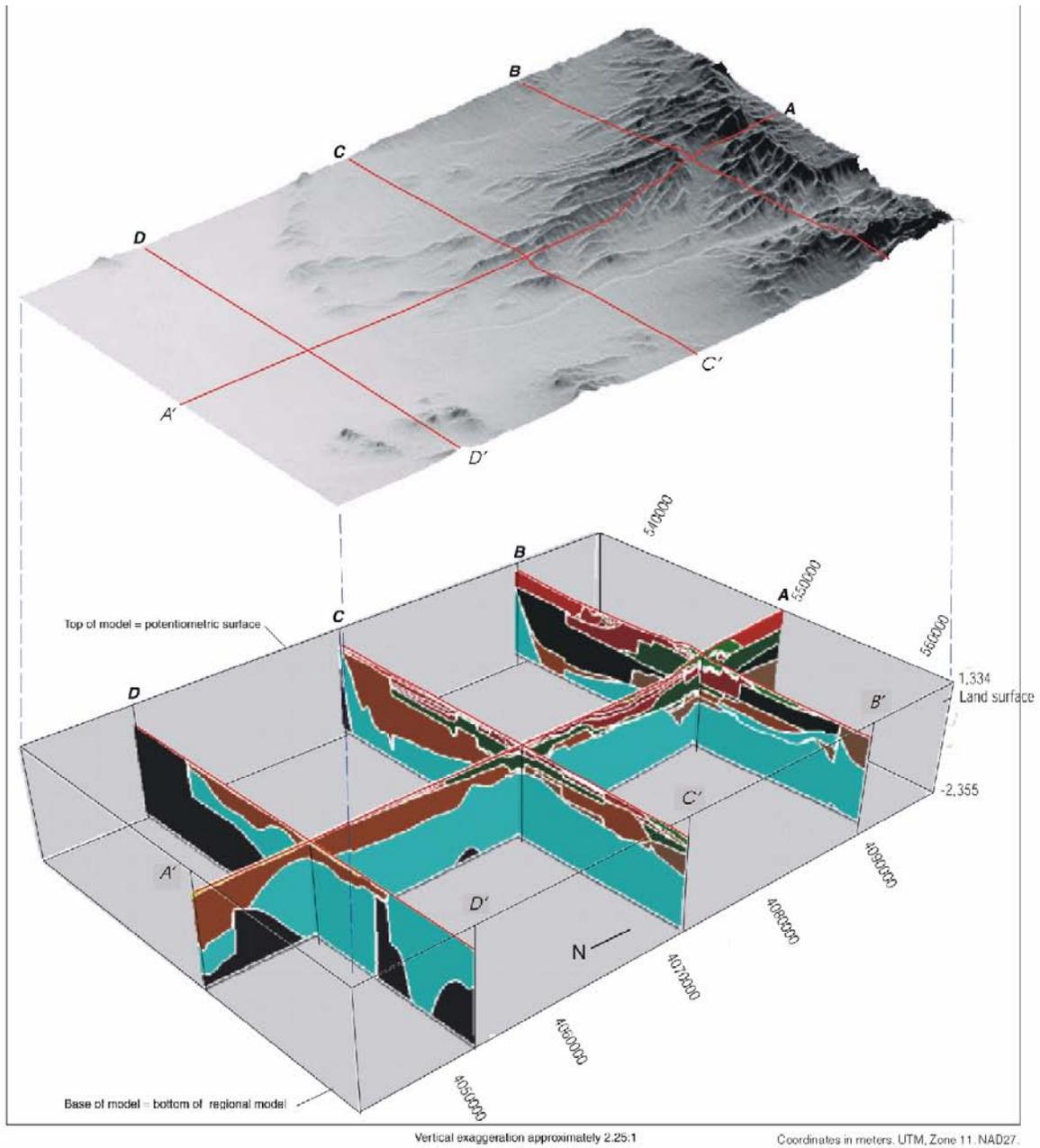
EXPLANATION

Color and model unit number

20 Valley-fill aquifer	15 Upper volcanic confining unit	10 Older volcanic aquifer	5 Upper clastic confining unit
19 Valley-fill confining unit	14 Middle volcanic aquifer -Prow Pass	9 Older volcanic confining unit	4 Lower carbonate aquifer
18 Limestone aquifer	13 Middle volcanic aquifer -Bullfrog	8 Undifferentiated valley-fill	3 Lower clastic confining unit
17 Lava-flow aquifer	12 Middle volcanic aquifer -Tram	7 Upper carbonate aquifer	2 Granitic confining unit
16 Upper volcanic aquifer	11 Middle volcanic confining unit	6 Lower carbonate aquifer (thrust)	1 Base

00050DC_ATP_Z1S42_fig-10.ai

Figure 4-140. Complex Spatial Pattern of Hydrogeologic Units Depicted as a Fence Diagram
Source: CRWMS M&O 2000bn, Figure 3-13.
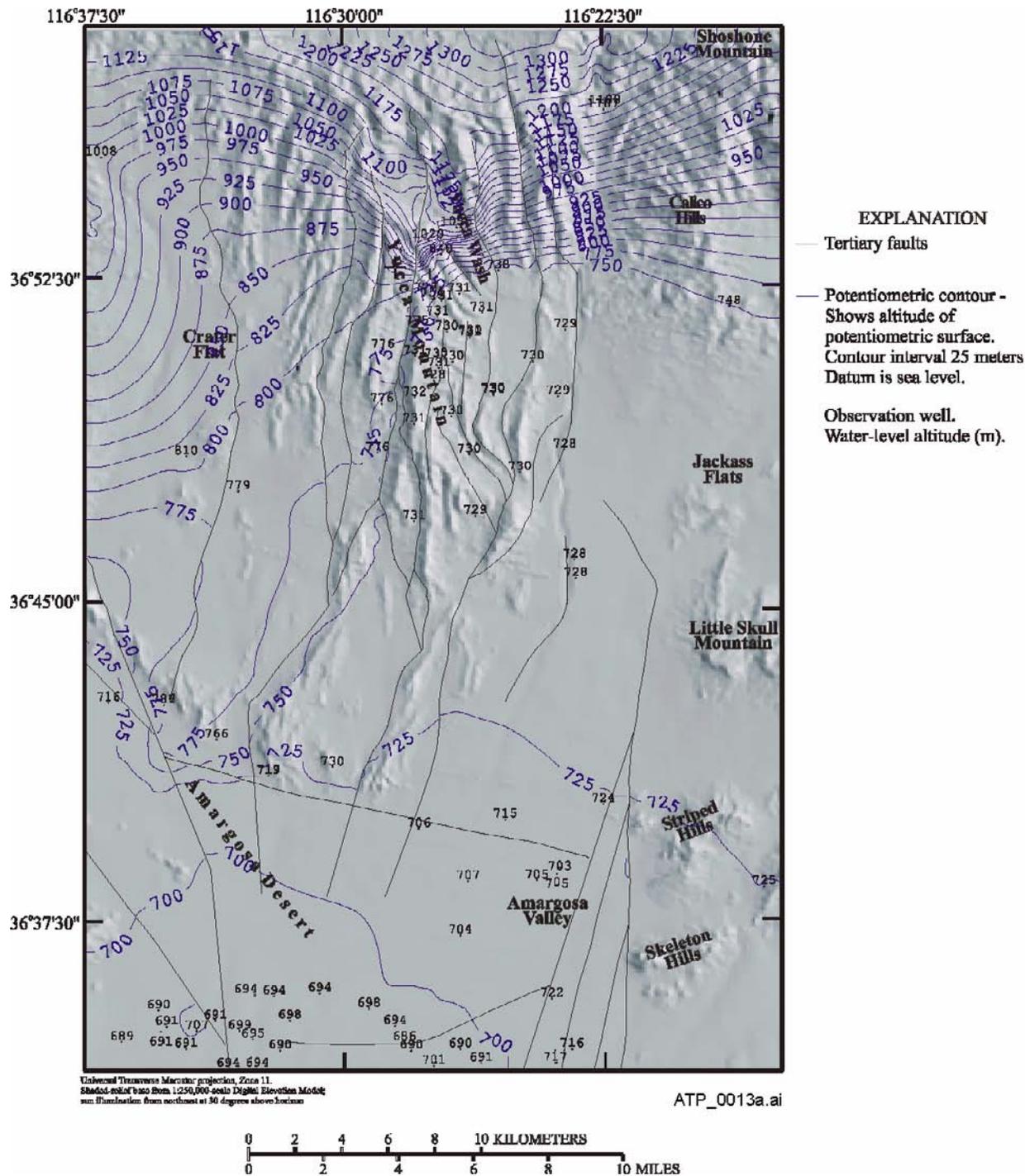
Figure 4-141. Site-Scale Saturated Zone Model Area, Showing Potentiometric Surface Contours, Water Level Altitudes, and Tertiary Faults

Source: USGS 2000d, Figure 6-2.
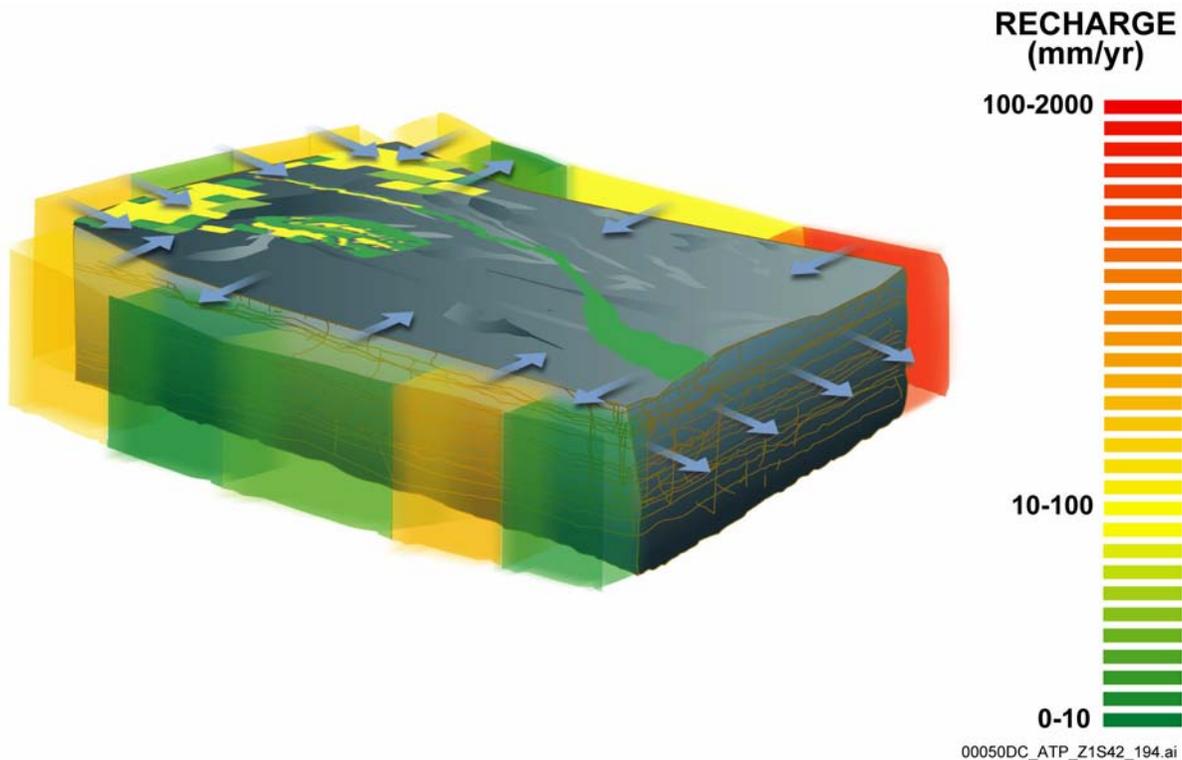
Figure 4-142. Lateral and Top Boundary Conditions for the Three-Dimensional Saturated Zone Flow Model for the Present-Day Climate
Source: CRWMS M&O 2000a, Figure 3.8-6.

Other parameter values may be estimated from data. However, extracting model parameter values from data is often not straightforward, and statistical methods that require extrapolation or corrections are used. Assumptions embedded in these methods influence the estimated individual parameter values and are described in the analysis and model reports. For example, stochastic parameters and their associated uncertainty distribution are presented in *Uncertainty Distribution for Stochastic Parameters* (CRWMS M&O 2000ek).

Taken in total, these data provide an appropriate and adequate basis for the conceptual model and numerical model of the site-scale saturated zone flow and transport system (CRWMS M&O 2000bn, Section 3.5). The site characterization information, along with inferences based on that information, support a conceptual model in which groundwater flow is controlled by the spatial distri-

bution of geologic units and structural features. Site-specific data, together with regional-scale studies, suggest that a large fraction of groundwater flowing in the saturated zone enters the Yucca Mountain site area as lateral flow from the north with a small fraction contributed by recharge near Yucca Mountain. The conceptual model of radionuclide transport in fractured rocks includes the processes of advection, dispersion, matrix diffusion, sorption, and colloid-facilitated transport, as supported by site data. These components of the conceptual model are implemented numerically in the site-scale saturated zone flow and transport model, which represents the processes relevant to radionuclide migration from Yucca Mountain to the biosphere.

Groundwater Flow Processes—Assumptions used in modeling the groundwater flow process include those of the regional-scale models and the
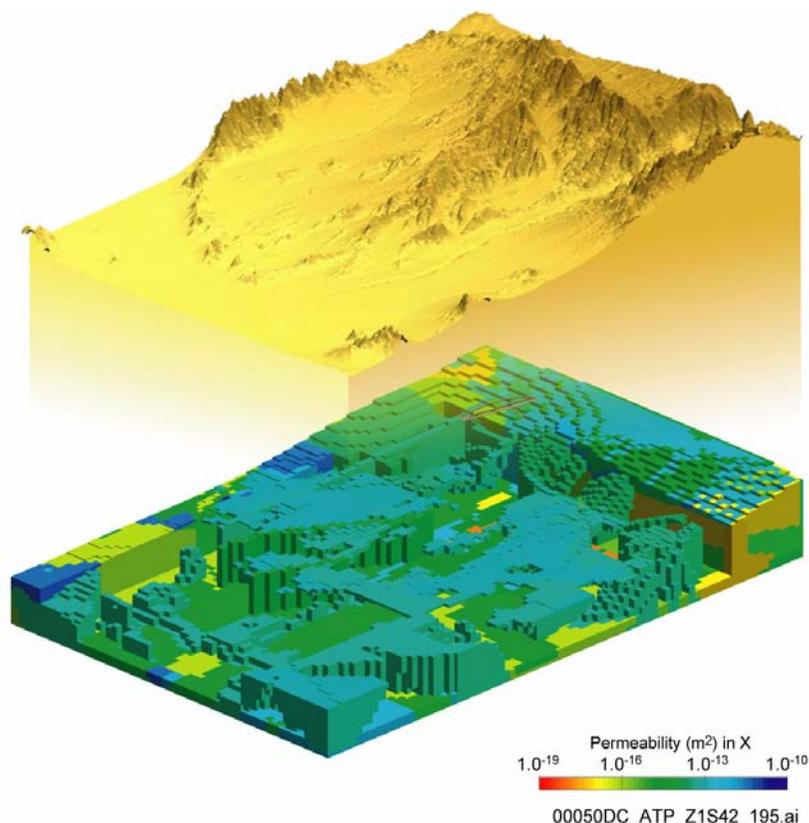
Figure 4-143. Three-Dimensional Saturated Zone Model Domain Showing the Different Permeability Fields
Permeabilities are assigned on a zone basis. Each zone represents hydrogeologic characteristics. Source: CRWMS M&O 2000a, Figure 3.8-7.

site-scale saturated zone flow and transport model and those made in estimating parameters that are used as input to these models. The following assumptions apply to the TSPA-SR continuum modeling approach (CRWMS M&O 2000el, Section 5):

- On the scale represented by the site-scale saturated zone flow and transport model, the site is well represented by a continuum flow model. The reasons for this choice rather than a discrete fracture model are discussed in detail in the section on alternative conceptual models.

- Estimates of specific discharge from the volcanic aquifer, elicited from the saturated zone expert elicitation panel, are assumed to be applicable to the entire flow path from the potential repository to the receptor location. The estimates were based primarily on data

from hydraulic testing in wells in volcanic units and the hydraulic gradient inferred from water level measurements (CRWMS M&O 1998j, p. 3-8).

- Horizontal anisotropy in permeability is adequately represented by a permeability tensor that is oriented in the north–south and east–west directions. For the purposes of the TSPA nominal case, both horizontal isotropy and anisotropy are considered for radionuclide transport. Analysis of the probable direction of horizontal anisotropy shows that the direction of maximum transmissivity is N 33° E (Winterle and La Femina 1999, p. iii), indicating that the anisotropy applied on the site-scale saturated zone model grid is within approximately 30° of the inferred anisotropy.

- Horizontal anisotropy in permeability applies to the fractured and faulted volcanic units of

the saturated zone system along the groundwater flow paths that run from the potential repository to points south and east of Yucca Mountain. Given the conceptual basis for the anisotropy model, it is appropriate to apply anisotropy only to those hydrogeologic units that are dominated by groundwater flow in fractures.

- Current groundwater flow conditions in the saturated zone system are at steady state. A steady-state model of the flow conditions is used to reflect the assumption that a steady-state representation of the saturated zone system is accurate. Studies by Luckey et al. (1996, pp. 29 to 32) indicate that there are no long-term consistent trends in the data from wells at Yucca Mountain.

- Changes in the water table elevation (due to future climate changes) will have negligible effect on the direction of the groundwater flow near Yucca Mountain. This assumption has been studied in regional-scale (D'Agnese, O'Brien et al. 1999) and subregional-scale (Czarnecki 1984) flow models. These studies found that the flow direction did not change significantly under increased recharge scenarios.

- Future water supply wells that might be drilled near Yucca Mountain (including outside the controlled area) will have a negligible effect on the hydraulic gradient.

- Possible effects due to temperature gradients and heat transport are assumed to be negligible. Heat transport can affect flow modeling through the temperature dependence of fluid viscosity and density.

Radionuclide Transport Properties—Radionuclide transport is modeled using a particle-tracking methodology (CRWMS M&O 2000eh). This three-dimensional particle-tracking model assumes transport along streamlines and takes into account advection, dispersion, sorption, and matrix diffusion. This particle-tracking model is semi-analytical in nature and has been developed to include anisotropic structures. Using particle

tracking to model radionuclide transport using particle tracking has some advantages over numerical solutions to an advection–dispersion equation. Two of these advantages include less numerical dispersion and the ability to model plumes on a subgrid block scale. Disadvantages include the facts that computations of concentration may require the use of a large number of particles and that particles may move into zones of low advection, requiring a long time to exit. The method allows for matrix diffusion, but does not account for advective flow in the matrix, where advection is slower than in the fractures. Particles are allowed to exit the matrix through Brownian motion into the fractures, where they are transported by advection. The transport model carries the following assumptions:

- On the scale represented by the site-scale saturated zone flow and transport model, the site is well-represented by a continuous flow and transport model. In particular, the specific discharge field computed by the FEHM flow model (Zyvoloski et al. 1997b) represents the specific discharge averaged over grid cells that are 500 m (1,640 ft) long, which means that possible long (more than 500 m [1,640 ft]) high-permeability conduits would not be represented accurately by the present transport model. The possible existence of relatively long, high-permeability structural features with a north–south orientation is explicitly incorporated in the model through the inclusion of horizontal anisotropy.

- An appropriate method for scaling transport to account for increasing mass flux in response to changes in the future climate is the convolution integral method. An assumption inherent in this method is that the system being simulated exhibits a linear response to the input function. In the case of solute transport in the saturated zone system, this assumption implies, for example, that a doubling of the input mass flux results in a doubling of the output mass flux. This assumption is valid for the site-scale saturated zone flow and transport model because the underlying transport processes (e.g.,

advection and sorption) are linear with respect to solute mass.

- Fractures are equally spaced, smooth, and have constant aperture. The numerical representation of matrix diffusion assumes equally spaced, smooth, constant aperture fractures. The assumption that the fracture aperture width is equal to that of a flowing interval tends to underestimate fluid velocity, whereas the assumption that no flow occurs in the matrix tends to overestimate the fluid velocity in the fracture.

- Fluid in the matrix of volcanic rocks is stagnant. This assumption is conservative from the perspective of the performance of the potential repository because if mass flows in the matrix, then the mass available for faster transport and flow velocities in the flowing intervals (fractures) is reduced.

- The mathematical representation assumes linear sorption at equilibrium due to the large temporal and spatial scales involved in radionuclide transport. Furthermore, the low relative concentrations of radionuclides support this assumption (CRWMS M&O 2000eb, Section 6.4).

Modeling Limitations—The site-scale saturated zone flow and transport model is adequate for its intended purpose, which is to model groundwater flow and radionuclide transport from the potential Yucca Mountain repository to the site-scale model boundary under present day and potential future climate conditions (CRWMS M&O 2000bn, Section 3.5.4). Here, adequate means that the transport model is an internally consistent representation of the saturated zone, which is subject to considerable uncertainty due to assumptions and simplification inherent in groundwater flow and transport modeling. Both the important processes and the subprocess models that address them have been identified. Many processes are inherently uncertain, and this uncertainty is handled through the use of stochastic realizations. The site-scale saturated zone flow and transport model is not appropriate (and was not used) for the following

types of simulations (CRWMS M&O 2000bn, Section 3.5.4):

- Computing transport over short distances. Over short distances (less than 1 km [0.6 mi]), transport likely is dominated by discrete fractures or fracture zones.

- Computing scenarios involving heavy well pumpage near Yucca Mountain. These scenarios would violate the conditions of a steady-state groundwater system, since they might involve large changes to the water table.

- Computing short-term transient hydrologic conditions. The site-scale saturated zone flow and transport model is not appropriate for computing short-term transient hydrologic conditions because it has not been calibrated using transient pumping tests.

- Performing analyses of the effects of certain disruptive events. Disruptive events, such as intrusive volcanic events, could affect the hydrogeologic environment at Yucca Mountain, for example, by altering the permeability field or causing transient changes to the water table. Such an analysis would require modifying the hydrogeologic framework model, regridding, or modifying other subprocess models and parameters to account for transient changes to the water table.

Process Model Uncertainty—The site-scale saturated zone flow and transport model and its components are comprehensive and complex. The model was used by TSPA-SR to characterize flow and transport processes that operate in the saturated zone below Yucca Mountain. The accuracy and reliability of predictions from the site-scale saturated zone flow and transport model are critically dependent on the accuracy of estimated model properties to which the model is sensitive, other types of input data, and conceptual models of the hydrology and geology. These models are limited mainly by the current characterization of the saturated zone system (including the geological and conceptual models), the continuum modeling

approach, steady-state flow, and the available field and laboratory data.

Investigations have indicated that a large amount of variability exists in the flow and transport parameters over the spatial scale of the saturated zone flow and transport model domain. Even though considerable progress has been made in this area, the major remaining uncertainties in model parameters are: (CRWMS M&O 2000bn, Section 3.5.5):

- Transport properties, including effective porosity in the alluvium

- Sorption coefficients for different elements in the alluvial and volcanic units

- Matrix molecular diffusion in different hydrogeological units for different radionuclides

- Dispersivities in volcanic and alluvial units

- Location of the transition zone where the flow path from the potential repository to the transitions from volcanic to alluvial hydrogeological units.

Uncertainty is addressed in the analysis of the performance of the potential repository system by considering selected parameters as stochastic variables and sampling from parameter uncertainty distributions in realizations of the saturated zone. The stochastic parameter uncertainty distributions are developed from limited field and laboratory data, expert elicitation, and literature surveys. These uncertainties are addressed in Sections 3.7.1 and 3.7.2 of the *Saturated Zone Flow and Transport Process Model Report* (CRWMS M&O 2000bn), and in Section 6 of *Uncertainty Distribution for Stochastic Parameters* (CRWMS M&O 2000ek). The matrix porosity in the volcanic units, bulk density in the volcanic units and the alluvium, and temperature were not treated as probability distributions. Rather, a deterministic value was used to represent these parameters in the simulations. The deterministic values vary from node to node in the model, as taken from the Integrated Site Model. Descriptions of how each parameter is

represented and associated justifications are included in Section 6 of *Uncertainty Distribution for Stochastic Parameters* (CRWMS M&O 2000ek).

Several supplemental analyses related to the saturated zone have been conducted since the TSPA-SR model was completed. The first supplemental analysis is part of the effort made by the DOE to improve the treatment of uncertainty in current models (Section 4.1.1.2) and concerns several changes made to refine the uncertainty in the saturated zone flow and transport model. The remaining analyses are sensitivity studies that examine specific parameter values. The second and third new analyses look at the question of how the results of the TSPA-SR model would change if there was no matrix diffusion and if there was more matrix diffusion in the volcanic rocks in the saturated zone. The fourth analysis looks at how the TSPA-SR results would change if the flow paths in the saturated zone encountered minimum alluvium in the southern half of the model domain. The fifth analysis looks at how the results would change if greater uncertainty is included in the parameters for the two models describing colloid-facilitated transport.

Unquantified Uncertainty in the Saturated Zone—The saturated zone flow and transport model was modified to include new information and in response to the effort to evaluate unquantified uncertainty in the TSPA-SR model. These modifications have been based on insights from the uncertainty analyses (BSC 2001a, Section 12.3; BSC 2001b, Section 3.2.10.2) and to include new data (BSC 2001a, Section 12.3.2.2) developed since the completion of the TSPA-SR model. A more realistic representation of the bulk density of the alluvium is included based on new borehole gravimeter data (BSC 2001a, Section 12.3.2.4). Continuing data collection from batch and column sorption experiments for iodine-129 and technetium-99 with alluvium samples indicates that the sorption coefficients for these radionuclides are zero under oxidizing conditions (BSC 2001a, Section 12.3.2.2). A more detailed discussion is contained in Volume 1, Section 12.5.1 of *FY01 Supplemental Science and Performance Analyses* (BSC 2001a). Changes that are most significant to

TSPA dose calculations include the following (BSC 2001b, Section 3.2.10.2.1):

- Bulk density of the alluvium, a factor in determining the amount of sorption that a radionuclide undergoes, was changed from a constant (1.27 g/cm^3) to a variable (normal distribution with a mean of 1.91 g/cm^3 and standard deviation of 0.08 g/cm^3).

- The sorption coefficients in the alluvium for technetium and iodine were set to zero; they were previously represented with uncertainty distributions with very low values.

- The sorption-coefficient distribution for neptunium was assigned to somewhat lower values: the sorption-coefficient distribution of uranium is made equal to that of neptunium, and the two distributions were correlated in the alluvium.

- The diffusion coefficient was changed from a log-uniform distribution to a log-triangular distribution with the same range but with a mode of 3.2×10^{-11} m^2/s.

- The amount of uncertainty in the saturated zone flux was reduced. For the TSPA-SR model, three saturated zone fluxes were considered: high, medium, and low. Each differed by a factor of 10: 6, 0.6, and 0.06 m/yr (20, 2, and 0.2 ft/yr), respectively, in the vicinity of the repository. For the analysis of unquantified uncertainties, the high, medium, and low fluxes differed by a factor of 3: 1.8, 0.6, and 0.2 m/yr (6, 2, and 0.7 ft/yr).

There is virtually no difference between the mean annual doses calculated by the TSPA-SR model and by the supplemental saturated zone model incorporating these changes (BSC 2001b, Section 3.2.10.2, Figure 3.2.10-1(a)). From a total-system perspective, the overall effect of changes made for the analysis of unquantified uncertainties tend to counteract each other.

No Matrix Diffusion in the Saturated Zone—For the purposes of this sensitivity study, the diffusion coefficient is reduced by 10 orders of magnitude. A

more detailed discussion of the changes made to the saturated zone modeling is contained in Volume 1, Section 12.5.2.1 of *FY01 Supplemental Science and Performance Analyses* (BSC 2001a).

The differences between results of the TSPA-SR model with matrix diffusion and the model without are slight (BSC 2001b, Section 3.2.10.2.2). The most likely reason for this is that approximately half of the TSPA-SR realizations have little or no matrix diffusion because of a low diffusion coefficient, large flowing interval spacing, or a high groundwater flux. The mean annual dose is primarily influenced by the realizations that produce the high annual dose values, particularly for neptunium-237. On average, approximately a fourth of the high-dose realizations include a saturated zone that has little or no matrix diffusion. Reducing matrix diffusion in the other half of the realizations that have matrix diffusion does little to increase the mean annual dose (BSC 2001b, Section 3.2.10.2.2).

Enhanced Matrix Diffusion in the Saturated Zone—To create an enhanced matrix diffusion model, the flowing interval spacing in the saturated zone site-scale flow and transport model is reduced; in particular the mean of the distribution was reduced by a factor of 100. A more detailed discussion of the changes made to the saturated zone modeling is contained in Volume 1, Section 12.5.2.2 of *FY01 Supplemental Science and Performance Analyses* (BSC 2001a).

The differences between the results of the TSPA-SR model and the model with enhanced matrix diffusion are generally less than 20 percent, and the simulated doses are somewhat lower for the model with enhanced matrix diffusion, as expected (BSC 2001b, Section 3.2.10.2.3, Figure 3.2.10-3(a)). The mean annual dose in the TSPA-SR model is primarily influenced by the realizations that produce the high annual dose values, particularly for neptunium-237. The sorption coefficient for neptunium in the volcanic matrix averages 0.5 ml/g; thus, even if neptunium does diffuse into the matrix, there is little retardation. The modeled combination of high groundwater fluxes, low diffusion coefficient, and low neptunium sorption coefficient tends mostly to

override the effect of a reduced flowing interval spacing, at least in the mean annual dose (BSC 2001b, Section 3.2.10.2.3).

Minimum Flow Path Length in the Alluvium— The alluvial uncertainty zone is a region in the TSPA-SR saturated zone site-scale model (CRWMS M&O 2000a, Section 3.8.2.4; CRWMS M&O 2000bn, Section 3.7.2) that encompasses the area where flow paths from a repository at Yucca Mountain might enter alluvial deposits in southern Jackass Flats. The alluvial uncertainty zone is approximately 5 km (3 mi) wide by 8 km (5 mi) long (in the north–south direction). In this sensitivity study, the length of the alluvial uncertainty zone is set to zero in the saturated zone model. There is still approximately 1 km (0.6 mi) of alluvium at the 20-km (12-mi) boundary used in the model. As discussed in Volume 2, Section 3.2.10.2.4 of *FY01 Supplemental Science and Performance Analyses* (BSC 2001b), the results from the sensitivity analysis differ only slightly (generally less than 10 percent) from TSPA-SR model results.

Increased Uncertainty in the Colloid-Facilitated Transport Models—For TSPA-SR, the colloid concentrations for both irreversible colloids and reversible colloids were calculated from functions of ionic strength that included no uncertainty. The sensitivity study defined here is for a new colloid-facilitated transport model as discussed in Volume 1, Sections 9.3.4 and 10.3.5 of *FY01 Supplemental Science and Performance Analyses* (BSC 2001a), which includes probability distributions for colloid concentrations and an expanded probability distribution for the sorption coefficient for radionuclides onto colloids.

For irreversible colloids, a mass flux of plutonium and americium associated with these colloids is introduced to the saturated zone at the unsaturated zone-saturated zone interface and their transport is tracked. In the volcanic units, these colloids are restricted to the fractures where they undergo transport and retardation as in the TSPA-SR model. In the alluvium, a new distribution of the retardation factor for radionuclides irreversibly sorbed onto colloids is used in this sensitivity study. The distribution results in lower retardation factors than

the retardation distribution used in the TSPA-SR model (BSC 2001a, Section 12.3.2.4.5.2). For reversible colloids, a mass flux of radionuclides associated with these colloids is also tracked from the unsaturated zone–saturated zone interface (BSC 2001a, Section 12.5.2.4; BSC 2001b, Section 3.2.10.2.5).

There is virtually no difference in the mean annual dose using the supplemental colloid model compared with the colloid model used in the TSPA-SR analyses (BSC 2001b, Section 3.2.10.2.5, Figure 3.2.10-5). The two radionuclides that comprise greater than 70 percent of the annual dose in the TSPA-SR model are technetium at earlier times and neptunium at later times. Both of these radionuclides are transported as solute and thus are unaffected by the new colloid model. Also, in the new colloid model the means of the distributions (for colloid concentrations, sorption coefficients for radionuclides onto colloids, and sorption coefficients for radionuclides onto the rock matrix and alluvium) are similar to values used in TSPA-SR, and thus the mean behavior was not expected to be significantly different.

4.2.9.3.2   Alternative Conceptual Processes

Luckey et al. (1996, p. 52) reviewed the major conceptual uncertainties relating to the saturated zone flow system at Yucca Mountain. They identified the following major areas of uncertainty:

- Whether the flow system can be simulated as a porous medium or if discrete features need to be simulated

- Behavior of the flow system in the areas of the large hydraulic gradient and the moderate hydraulic gradient

- Recharge and the time-scale at which it comes into equilibrium with climate

- How best to translate data from field sampling and borehole testing to the scale of the flow models.

Numerical modeling of fracture properties is done in one of two ways: discrete fracture models or

effective continuum models. Discrete fracture models represent each fracture as a distinct object within the modeling domain. The effective continuum representation of fracture permeability is used for the site-scale saturated zone flow and transport model for the following reasons (CRWMS M&O 2000bn, Section 3.5.1):

- The exact characterization of hydraulic and geometric properties of fractures necessary to construct an accurate discrete fracture model does not exist for Yucca Mountain.

- At Yucca Mountain, studies of the density and spacing of flowing intervals generally indicate that flow occurs through fracture zones (CRWMS M&O 2000em, Figure 15).

- Part of the flow system is an alluvium unit for which flow and transport is appropriately modeled using a continuum model.

- The drawdown response (drop in water level) to pumping at wells surrounding the C-Wells Complex in multiwell pump tests indicates a well-connected fracture network in the Miocene tuffaceous rocks in this area (Geldon, Umari, Earle et al. 1998, p. 31).

- Although the discrete fracture approach retains the discrete nature of the observed fractures within the model, the computational burden of calculating a flow solution using a discrete fracture model becomes extremely large even for relatively simple fracture models.

Whether the flow system can be simulated as an effective continuum model is addressed in *Calibration of the Site-Scale Saturated Zone Flow Model* (CRWMS M&O 2000ej, Section 6.1.1), which notes that the site-scale saturated zone flow and transport model uses the effective continuum representation of fracture permeability.

Although the site-scale saturated zone flow and transport model is a continuum model, special hydrologic features, including selected major faults, fault zones, and zones of chemical alteration, are treated in the model as zones of enhanced or reduced permeability (CRWMS M&O 2000ej, Table 6). Because the major faults and fault zones are represented directly in the model and because of the scale of use of the model, no impact results from using a continuum model over a discrete fractures model.

Luckey et al. (1996) present detailed descriptions of the gradient features and discuss interpretations of their causes (CRWMS M&O 2000bn, Section 3.2.2.3). The large hydraulic gradient, particularly, has been the subject of numerous theories. Current models assume that the hydraulic gradient is caused by semi-perched water. This assumption is based on the formal expert elicitation and recent test results discussed next.

An expert elicitation panel on saturated zone flow and transport, which was convened by the DOE, addressed the cause of the large hydraulic gradient (CRWMS M&O 1998j, pp. 3-5 to 3-6). The panel narrowed the theories to the two most credible hypotheses: the large hydraulic gradient is caused by flow through the upper volcanic confining unit or it is a result of semi-perched water. The consensus of the panel slightly favored semi-perched water. The experts were in agreement that the issue was mainly one of technical credibility, that the probability of any large transient change in the configuration of the large gradient is low, and that long-term transient readjustment of gradients was of low probability (CRWMS M&O 1998j, p. 4-3).

The only important new results pertaining to the cause of the large gradient include the drilling of borehole WT-24 in the area of the large gradient and the analysis of hydrochemical data in *Geochemical and Isotopic Constraints on Ground-Water Flow Directions, Mixing, and Recharge at Yucca Mountain, Nevada* (CRWMS M&O 2000eg, Section 6.4.2). The drilling of borehole WT-24 supported the previous portrayal that the large gradient (Tucci and Burkhardt 1995, Figure 4) probably included perched water; however, the question of whether perching of water is the cause of the large gradient was not fully resolved.

Hydrochemical information on the ratio of uranium-234 to uranium-238 presented in

Geochemical and Isotopic Constraints on Ground-Water Flow Directions, Mixing, and Recharge at Yucca Mountain, Nevada (CRWMS M&O 2000eg, Section 6.5.3) suggests that local recharge, as represented by perched water, is a major component in the groundwater at Yucca Mountain.

Perched water was encountered in seven boreholes near the potential repository (CRWMS M&O 2000b, Section 8.5.2). The contact zone between the Topopah Spring welded and the Calico Hills nonwelded hydrogeologic units is characterized by a basal vitrophyre stratum in the Topopah Spring welded hydrogeologic unit above a zone of zeolitic altered tuffs in the Calico Hills nonwelded hydrogeologic unit. For a perched zone to exist, the vertical permeability of the perching units would have to be low (less than 1 microdarcy) and fracture permeability would have to be negligible.

Horizontal Anisotropy—Anisotropic conditions exist if the permeability of media varies as a function of direction. Because groundwater primarily flows in fractures within the volcanic units downgradient of Yucca Mountain and because fractures and faults occur in preferred orientations, it is possible that anisotropic conditions of horizontal permeability exist along the pathway of potential radionuclide migration in the saturated zone (CRWMS M&O 2000bn, Section 3.2.5.3). Performance of the potential repository could be affected by horizontal anisotropy because the flow could be diverted to the south, causing transported solutes to remain in the fractured volcanic tuff for longer distances before moving into the valley fill alluvial aquifer. A reduction in the length of the flow path in the alluvium would decrease the amount of radionuclide retardation that could occur for those radionuclides with greater sorption coefficients in alluvium than in fractured volcanic rock matrix. In addition, potentially limited matrix diffusion in the fractured volcanic units could lead to shorter transport in the volcanic units relative to the alluvium.

A conceptual model of horizontal anisotropy in the tuff aquifer is reasonable, given that flow in the tuff aquifer is believed to occur in a fracture network that exhibits a preferential north–south strike azimuth (CRWMS M&O 2000en, Section 5.5). Major faults near Yucca Mountain that have been mapped at the surface also have a similar preferential orientation (Figure 4-144). In addition, north to north-northeast striking structural features are optimally oriented perpendicular to the direction of least principal horizontal compressive stress thus promoting flow in that direction, suggesting a tendency toward dilation and potentially higher permeability (Ferrill et al. 1999, pp. 5 to 6).

Evaluation of the long-term pumping tests at the C-Wells Complex supports the conclusion that large-scale horizontal anisotropy of aquifer permeability may occur in the saturated zone (Ferrill et al. 1999, p. 7). Results of this hydrologic evaluation generally are consistent with the structural analysis of potential anisotropy. However, there are important uncertainties, including differences in pumping test analysis methods; the fact that only a minimum number of observation wells were used; and the additional uncertainty regarding the validity of assuming a homogenous effective continuum over the scale of the test (Winterle and La Femina 1999, p. 4-29).

Taken together, these observations and inferences support an alternative conceptual model (Figure 4-145) in which large-scale horizontal anisotropy of permeability, with higher permeability in a north-northeasterly direction, occurs in the volcanic units of the saturated zone to the southeast of the potential repository. Because of existing uncertainty in the interpretation of the large-scale horizontal anisotropy in permeability, the simpler, horizontal isotropic model of permeability was retained as the nominal conceptual model. The large-scale horizontal anisotropy in permeability is considered an alternative plausible model. To evaluate the uncertainty in anisotropy (isotropy/anisotropy), two discrete cases were examined. These consist of two alternative models: the isotropic case and the anisotropic case with a 5 to 1 anisotropy ratio. To evaluate the uncertainty in groundwater flux, three discrete cases were examined. These consist of the mean case (corresponding to the mean flux of the calibrated site-scale saturated zone flow model), the low case (mean flux time 0.1), and the high case (mean flux time 10). The flux multiplier and the corresponding probabilities for these cases are quantified based on the uncertainty distribution for discharge in the
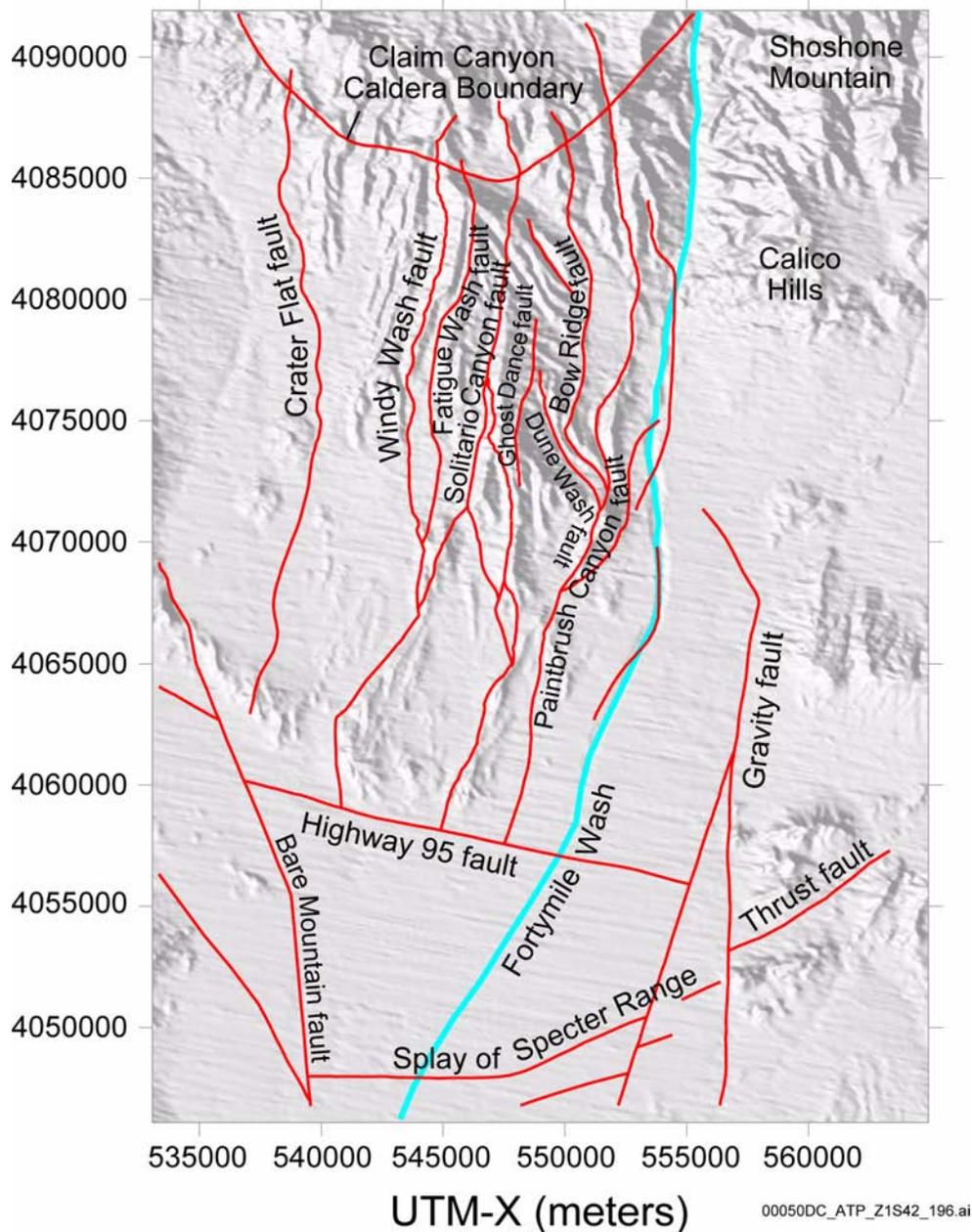
Figure 4-144. Structural and Tectonic Features within the Site-Scale Saturated Zone Model
Large known features are implicitly represented in the site-scale flow and transport model. UTM = Universal Transverse Mercator. Source: CRWMS M&O 2000bn, Figure 3-4.
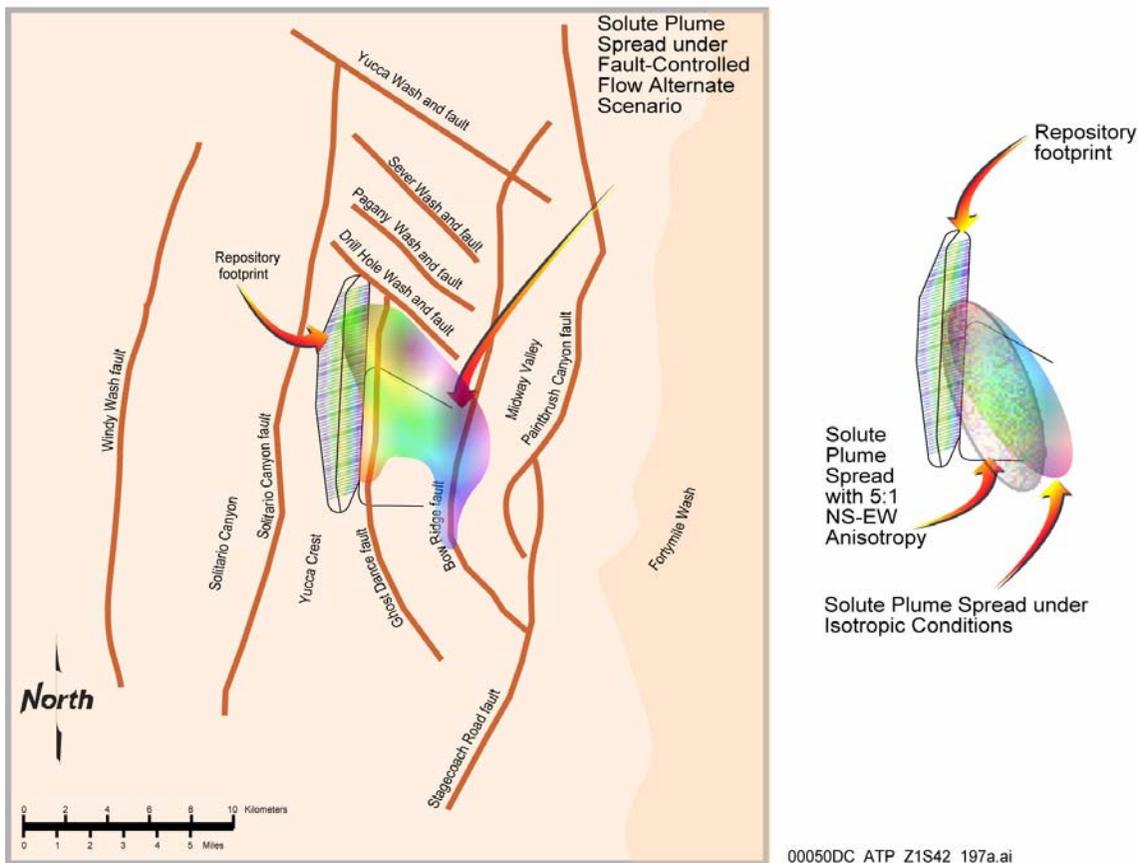
Figure 4-145. The Use of Anisotropy to Simulate an Alternate Conceptual Flow and Transport Model
In this case it is assumed that observed faults to the south and east of Yucca Mountain tend to divert flow to the south. The north–south hydraulic conductivity in the upper layers of the porous medium flow model were increased by a factor of five to increase the southerly flow and simulate the effect of the faults. The solute plumes in the right panel conceptually illustrate the effect of faults on transport and the effect of the introduction of anisotropy in the porous media flow model on transport in the mathematical model.

volcanic aquifer from the saturated zone expert elicitation (CRWMS M&O 1998j, Section 3.2.3). The analysis is provided in *Input and Results of the Base Case Saturated Zone Flow and Transport Model for TSPA* (CRWMS M&O 2000el, Section 6.2.5). The results of considering both types of uncertainty are six alternative groundwater flow fields (three flux cases times two anisotropy cases).

Implementation of the alternative groundwater flow fields is accomplished by establishing a steady-state solution of groundwater flow in the site-scale saturated zone model for each of the six cases. Small variations in the simulated heads (i.e., hydraulic pressure) exist among the six steady-state flow solutions (generally variations of less than 1 m [3.3 ft]). All six flow fields represent acceptable matches to measured water levels. The steady-state conditions for each of these cases are imposed as the initial conditions for TSPA simulations of radionuclide transport. In addition, a separate set of input files for the site-scale saturated zone flow and transport model that incorporate modifications to the boundary conditions and value of permeability for each case are constructed. Each simulation is assigned to the appropriate flow field based on the values of the stochastic parameters that represent uncertainty in flux and horizontal anisotropy.

4.2.9.3.3 Saturated Zone Flow and Transport Model Calibration and Validation

4.2.9.3.3.1 Flow Model Calibration

Calibration, also known as inverse modeling, is the process by which values of important model parameters are estimated and optimized to produce the best fit of the model output to the observed data. Calibration is generally accomplished by varying model parameters to minimize the difference between observed and simulated conditions. The site-scale saturated zone flow and transport model was calibrated largely by automated procedures, but manual adjustments to the calibration were also performed to ensure an accurate and conservative model. During the calibration process, nodal values of permeability were adjusted to minimize the differences between observed and simulated values of water levels and groundwater fluxes along the northern and eastern boundaries of the model domain. One hundred fifteen water level and head measurements were used as calibration targets (CRWMS M&O 2000bn, Section 3.3.6).

During the calibration process, special emphasis or weighting was given to minimizing the difference between observed and simulated water levels at selected locations. Preferential weighting was applied to approximately thirty calibration targets in the low-gradient region to the south and east of Yucca Mountain. These calibration targets were given high weighting because they are in the likely pathway of fluid leaving the potential repository site and because small changes in head in this area could produce a large effect on the flow direction. The single head measurement in the carbonate aquifer was also given preferential weighting because of the importance of this calibration target for reproducing an upward gradient in the calibrated model. The inclusion of an upward gradient within the calibrated site-scale saturated zone flow and transport model is considered important for generating a realistic model. Calibration targets north of Yucca Mountain were given low weighting, primarily because of the possibility of perching and the attendant uncertainty in water-level measurements in this region.

During calibration, sets of nodes were grouped into specific permeability zones based on similar permeability characteristics, and a single permeability variable was assigned to each zone. These values of zonal permeability variables served as the parameters that were optimized during model calibration. Permeability zones were created for each of the hydrogeologic units identified in the hydrogeologic framework model and for specific hydrogeologic features. All of the nodes within a specific hydrogeologic unit were assigned to that permeability zone unless they were included in one of the permeability zones established for specific hydrogeologic features. The hydrogeologic features for which special permeability zones were established were primarily faults, fault zones, and areas of chemical alteration. Twenty-seven permeability zones were established for model calibration, and permeability values or multipliers were assigned to each zone. Upper and lower bounds were placed on each permeability variable during calibration. The upper and lower bounds for the permeabilities and permeability multipliers were chosen to reflect maximum and minimum field values (permeability) or a realistic range of values (permeability multipliers). Horizontal isotropy in permeability was assumed at all nodes.

4.2.9.3.3.2 Calibration Results

A potentiometric surface was generated using the calibrated site-scale saturated zone flow and transport model, and residual heads remaining after calibration were computed by subtracting the observed head from the predicted head (Figure 4-146). The largest head residuals (about 100 m [330 ft]) are in the northern part of the model (in the high-head gradient area). These head residuals are largely the result of the low weighting assigned to these calibration targets and of the uncertainty in these measurements due to the perched conditions that may exist in this area. The next highest group of head residuals border the east–west barrier and Solitario Canyon fault. These residuals likely result from a grid resolution insufficient to resolve the 780- to 730-m (2,560- to 2,400-ft) drop in head that occurs over a short distance in this area. Head residuals in the low-gradient area along the expected migration pathway away from the poten-
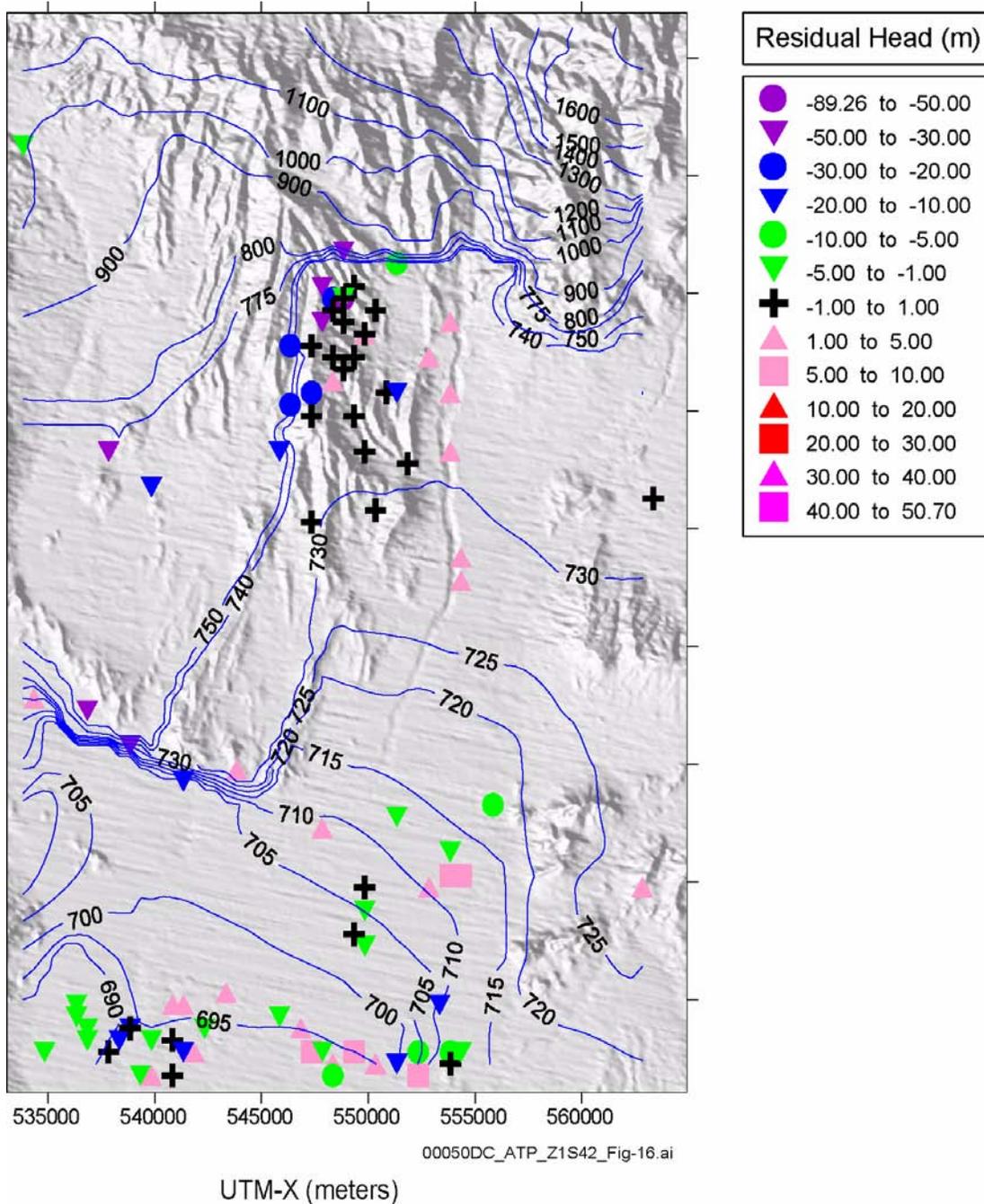
Figure 4-146. Simulated Potentiometric Surface with Three-Dimensional Flow Model Calibration Residuals
The calibration residual is computed by taking the difference between the observed hydraulic head and the predicted hydraulic head. This calibration supported the TSPA-SR. UTM = Universal Transverse Mercator. Source: CRWMS M&O 2000bn, Figure 3-20.

tial repository are generally low (CRWMS M&O 2000bn, Section 3.3.7).

The particle-tracking capability of FEHM was used to demonstrate the predicted flow paths from the potential repository (Figure 4-147). The predicted pathways generally leave the potential repository and lead in a south-southeasterly direction to the accessible environment. From the accessible environment to the end of the model domain (approximately the 30-km [19-mi] boundary), the flow paths trend to the south-southwest and generally follow Fortymile Wash.

The calibrated flow model was used to estimate the specific discharge for a nominal fluid path leaving the potential repository area and traveling to 5, 20, and 30 km (approximately 3.1, 12, and 19 mi). For these three points, values for specific discharge of 0.6 m/yr, 2.3 m/yr, and 2.7 m/yr (2.0, 7.5, and 8.9 ft/yr), respectively, were obtained. An expert elicitation panel estimated a specific discharge of 0.71 m/yr (2.3 ft/yr) for the volcanic aquifer at 5 km (3.1 mi) (CRWMS M&O 1998j, Figure 3-2e). Thus, agreement between the specific discharge predicted by the calibrated model and that estimated by the expert elicitation panel for 5 km (3.1 mi) is good, and the value predicted by the calibrated model is conservative. The expert elicitation committee did not consider other boundaries.

4.2.9.3.3.3 Flow Model Validation

Model validation is the process of testing the validity of the conceptualization of the processes represented in the model and testing the validity of the mathematical representation and numerical implementation. The results of the calibrated site-scale saturated zone flow and transport model have undergone analyses to validate the model (CRWMS M&O 2000bn, Section 3.4). These analyses include a comparison of the calibrated permeability values with observed permeability data, a comparison between boundary fluxes predicted by the regional-scale flow model and the calibrated site-scale saturated zone flow and transport model, a comparison between the observed and predicted gradients between the carbonate aquifer and overlying volcanic aquifers, and a

comparison between hydrochemical data and particle pathways predicted by the model.

Permeability—For model validation, the permeabilities estimated during calibration of the site-scale saturated zone flow and transport model were compared to permeabilities determined from aquifer test data from the Yucca Mountain area and elsewhere at the Nevada Test Site (CRWMS M&O 2000bn, Section 3.4.1). Data from reports pertaining to the Nevada Test Site were included in the comparison to help constrain permeability estimates for hydrogeologic units that were not tested or that underwent minimal testing at Yucca Mountain. The logarithms of permeability estimated during calibration of the model were compared to the mean logarithms of permeability determined from aquifer test data from Yucca Mountain (Figure 4-148) and to data from elsewhere at the Nevada Test Site (Figure 4-149). For most of the geologic units, the calibrated permeabilities were within the 95 percent confidence limits of the mean permeabilities estimated from the data (Figure 4-148). The model-calibrated permeability value for the carbonate aquifer is well within the 95 percent confidence interval for the mean permeability of the carbonate aquifer beneath Yucca Mountain, which has been estimated from field testing (Figure 4-148). However, both of these permeability values are about an order of magnitude less than the estimated mean permeability of the carbonate aquifer derived from aquifer tests performed elsewhere on the Nevada Test Site (Figure 4-149). Given these available data, the agreement between the model-calibrated value and the estimated site permeability value for the carbonate aquifer is considered to provide an adequate basis for confidence in the validity and representativeness of the site-scale flow model. Figure 4-149 also suggests a discrepancy between the model-calibrated permeability value for the upper volcanic aquifer and the estimated mean value obtained from field testing elsewhere on the Nevada Test Site. The field test permeability data, however, have been inferred from only two transmissivity values estimated from drawdown curves in two boreholes and are insufficient to either yield reliable permeability values or estimate confidence intervals for these data (CRWMS M&O 2000ej,
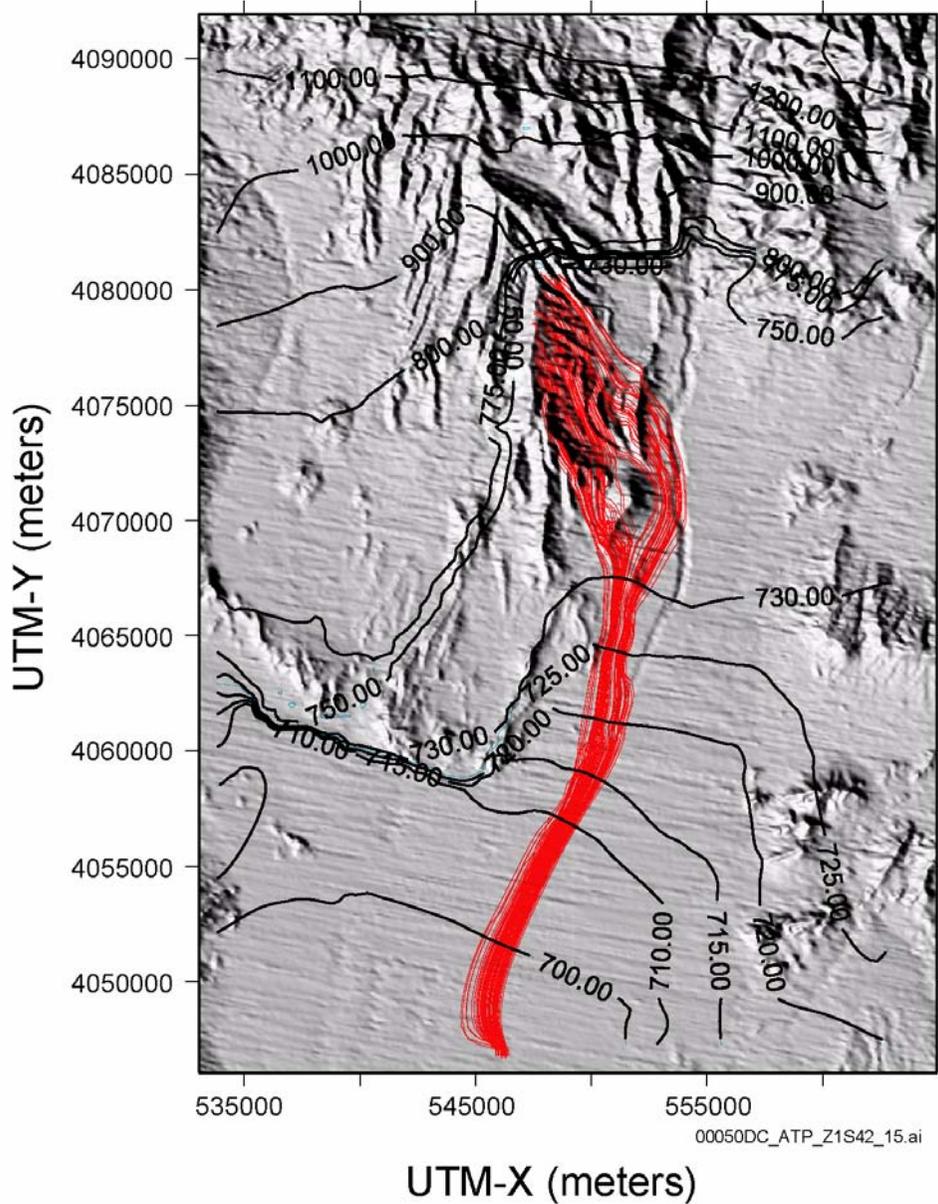
Figure 4-147. Simulated Particle Paths after a Hypothetical Radionuclide Release from the Potential Repository

The particle paths were superimposed on a shaded relief map of the surface topography. The particles were distributed in the repository footprint in the saturated zone. This analysis supported the TSPA-SR. UTM = Universal Transverse Mercator. Source: CRWMS M&O 2000bn, Figure 3-21.
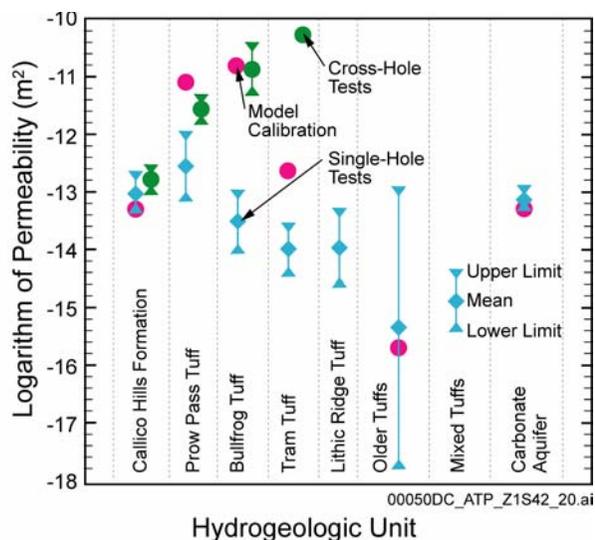
Figure 4-148. Estimated and Observed Permeabilities for Nine Stratigraphic Units at Yucca Mountain

Estimated permeabilities calculated from the site-scale saturated zone flow and transport model. Observed permeabilities calculated from pump-test data. Bars indicate 95 percent confidence intervals; diamonds indicate the mean value. Source: CRWMS M&O 2000bn, Figure 3-22.
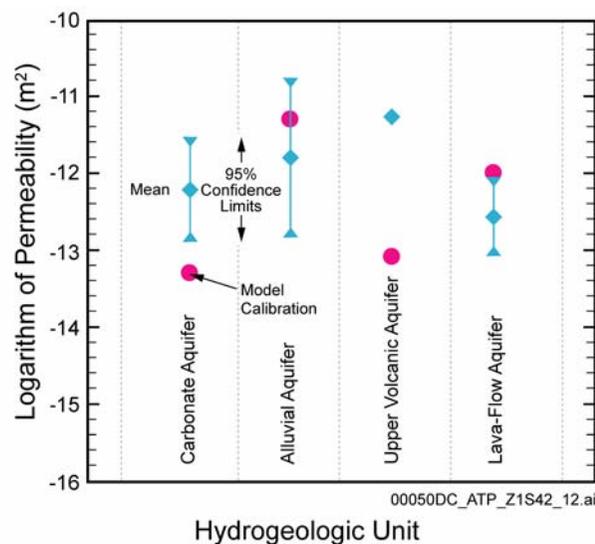
Figure 4-149. Estimated and Observed Permeabilities for Four Aquifers at Yucca Mountain

Estimated permeabilities calculated from the site-scale saturated zone flow and transport model. Observed permeabilities calculated from pump-test data. Bars indicate 95 percent confidence intervals; diamonds indicate the mean value. Source: CRWMS M&O 2000bn, Figure 3-23.

Section 6.7.7.6). Because the upper volcanic aquifer is expected to contribute little to potential radionuclide transport through the saturated zone (CRWMS M&O 2000ej, Figure 17), the model-calibrated permeability value for this unit is considered to be adequate for the intended application of the model.

With the exception of the calibrated values for the upper volcanic aquifer, the calibrated permeabilities generally are consistent with most of the permeability data from Yucca Mountain and elsewhere at the Nevada Test Site. A discrepancy exists between the calibrated permeability for the Tram Tuff of the Crater Flat Group and the mean permeability derived from the cross-hole tests. However, the permeabilities measured for the Tram Tuff of the Crater Flat Group may have been enhanced by the presence of a breccia zone in the unit at boreholes UE-25 c#2 and UE-25 c#3 (Geldon, Umari, Fahy et al. 1997, Figure 3).

Boundary Fluxes—A comparison of the fluxes predicted at the boundary of the site-scale model domain by the calibrated site-scale saturated zone flow and transport model and by the regional-scale model was used to further validate the model (CRWMS M&O 2000bn, Section 3.4.2). The mass fluxes computed along the boundaries by the two models match reasonably well. The total fluxes across the northern boundary computed by the regional-scale model and the site-scale saturated zone flow and transport model were 189 kg/s and 169 kg/s (416 lbs/s and 372 lbs/s), respectively, a difference of 11 percent. The fluxes computed for individual segments along the northern boundary by the two models are distributed somewhat differently. However, this difference in distribution can be expected because the regional-scale and site-scale models are based on different hydrogeologic framework models. The comparison of the boundary fluxes computed along the east side of the site-scale saturated zone flow model domain also indicates a good match. The total fluxes across the eastern boundary computed by the regional-scale model and the site-scale model were 561 kg/s (1,236 lb/s) and 517 kg/s (1,139 lbs/s), respectively. The match is particularly good along the lower thrust area, where both models predict large fluxes across the model boundary. Both models

also predicted small fluxes across the remainder of the eastern boundary.

The fluxes across the western boundary computed by the regional-scale model and the site-scale model do not match as well as along the northern and eastern boundaries. The regional-scale model predicts greater inflow along the western boundary than does the site-scale model. The discrepancy in fluxes computed along the western boundary by the two models is largely the result of the different hydrogeologic framework models upon which the two models are based. For example, the newer hydrogeologic framework model used as the basis for the site-scale model includes a large amount of low permeability clastic rock along the southernmost portion of the western boundary that was not included in the regional-scale model. This zone of low-permeability rock would not support the large flux predicted by the regional-scale model across this portion of the western boundary. For these reasons, it is concluded that the site-scale model estimated flux is appropriate.

The southern boundary flux is simply a sum of the other boundary fluxes plus the recharge. A comparison of the fluxes across the southern boundary computed by the regional-scale model and the site-scale saturated zone flow and transport model indicates a relatively good match. The difference in the fluxes computed by the two models across the southern boundary is approximately 21 percent.

Upward Hydraulic Gradient—An upward hydraulic gradient between the lower carbonate aquifer and the overlying volcanic rocks has been observed in the vicinity of Yucca Mountain. Principal evidence for this upward gradient is provided by data from the only borehole at Yucca Mountain that has been drilled into the upper part of the carbonate aquifer. Hydraulic head measurements in this borehole indicate that the head in the carbonate aquifer is about 752 m (2,470 ft), about 22 m (72 ft) higher than the head measured in this borehole in the overlying volcanic rocks. Although the head in the carbonate aquifer at this borehole location was not held fixed, but was estimated as part of the model calibration process, increasing head with depth at this location (but not the precise magnitude of the observed hydraulic gradient) was

preserved during model calibration. As indicated by geochemical data, preserving the sense of the upward gradient is important to ensure that the modeled flow paths in the carbonate aquifer remain shallow and confined within the upper part of the aquifer. The difference in predicted and observed values of the upward hydraulic gradient at this location results, in part, because the constant vertical head boundary conditions imposed on the lateral boundaries of the model domain restricted the accurate representation of vertical groundwater flow and gradients within the model interior (CRWMS M&O 2000ej, Sections 6.7.11 and 6.1.2).

The failure to fully represent the entire magnitude of this upward vertical gradient can be attributed, in part, to the constant-head conditions established at the boundaries of the model (the same value of the constant-head boundary was specified for all layers (i.e., the same with depth)). The constant-head conditions applied to each layer of the model at each boundary did not allow vertical flow at the boundaries. However, vertical gradients developed within the model domain in response to geohydrologic conditions. Although the upward gradient produced by the model is not as large as that indicated by field measurements, it nevertheless is sufficient to keep the simulated fluid path lines downgradient from the potential repository in the shallow volcanic aquifers.

Hydrochemical Data Trends—To provide further validation of the site-scale saturated zone flow and transport model, the flow paths (Figure 4-147) predicted by the calibrated model were compared with those estimated using groundwater chemical and isotopic data (Figure 4-133) (CRWMS M&O 2000bn, Section 3.4.4). Flow paths predicted by the calibrated site-scale saturated zone flow model were generated using the particle-tracking capability of the FEHM code by placing particles at various depths along the western, northern, and eastern boundaries and running the model to trace the paths of these particles for 1 million years.

Comparison of the flow paths predicted by the calibrated model with those estimated using groundwater chemical and isotopic data indicate that some differences exist between the flow direc-

tions determined by the two approaches. The most prominent difference is the stronger eastward component of flow in the Crater Flat area predicted by the numerical model as compared to flow directions determined with the hydrochemical data. The differences in flow directions estimated for Crater Flat could be due to the inability of the simple hydrochemical analysis to account for vertical mixing due to recharge or mixing between aquifers, the assumption in the numerical model that the permeability of subsurface material in Crater Flat is isotropic, or a combination of these factors. However, the important flow paths leading away from the potential repository area are similar for both methods.

Saturated Zone Transport Model—To test conceptual models of saturated zone transport in fractured tuffs, the DOE conducted several cross-hole tracer and hydraulic tests at the C-Wells Complex between 1995 and 1999 (CRWMS M&O 2000eb, Section 6.9). The discussion here focuses on two tracer tests involving the injection of multiple tracers, as these tests provided the most

rigorous and convincing testing of conceptual transport model for saturated, fractured tuffs (Figure 4-150). One of these tests was conducted in the lower Bullfrog Tuff, the most transmissive interval at the C-Wells, and the other was conducted in the lower Prow Pass Tuff, which had relatively low transmissivity. Additional information on the field testing and the parallel laboratory studies is presented in *Saturated Zone Flow and Transport Process Model Report* (CRWMS M&O 2000bn, Section 3.1.3.2.1).

The principal conclusions from the C-Wells field and laboratory tests relevant to performance assessment of the potential Yucca Mountain repository are (CRWMS M&O 2000bn, Section 3.1.3.2.1.2):

- The relative response of nonsorbing tracers in fractured tuffs are consistent with matrix diffusion. This result supports the use of a dual-porosity conceptual model to describe radionuclide transport through the saturated, fractured rocks near Yucca Mountain.
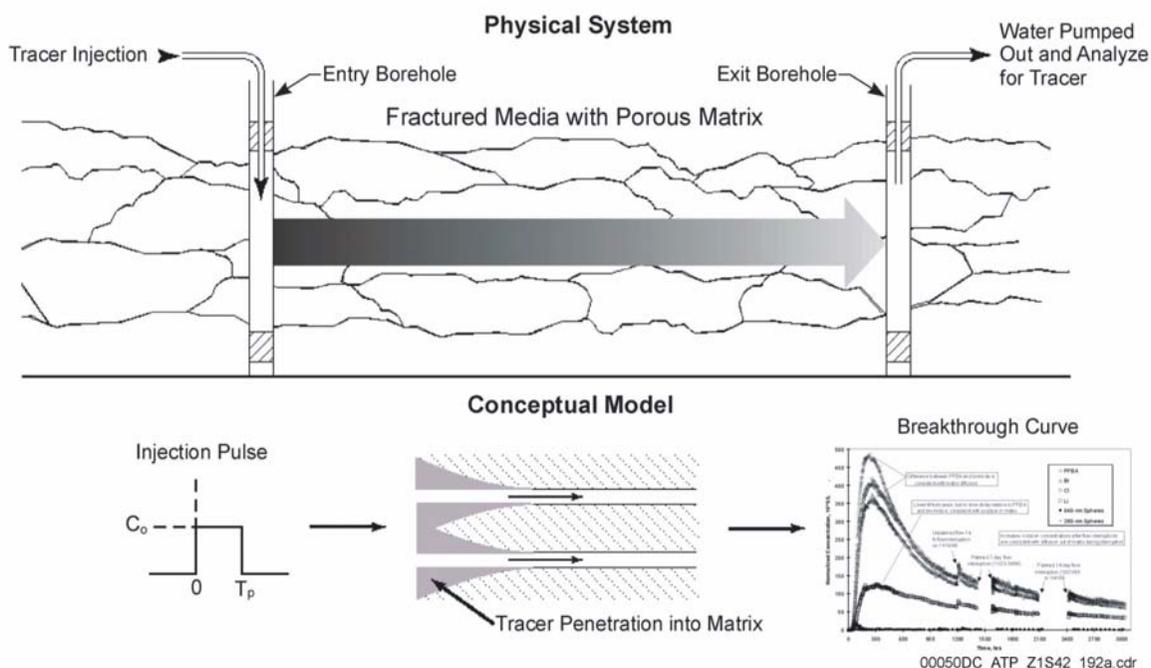
Figure 4-150. Physical System, Conceptual Model, and Normalized Tracer Responses from the Prow Pass Multiple Tracer Test
Source: CRWMS M&O 2000bn, Figure 3-8.

- Sorption of lithium ions (the sorbing radionuclide analogue) in the field was greater than or equal to measured sorption in the laboratory. Although lithium does not behave identically to any radionuclide, this result suggests that the use of laboratory-derived radionuclide sorption parameters in field-scale transport predictions is defensible and may even be conservative.

Other transport parameters derived from the C-Wells tracer tests include effective porosity, longitudinal dispersivities, matrix-diffusion mass transfer coefficients, colloid filtration and detachment rate constants, and horizontal anisotropy ratios. Conclusions related to these parameters are provided in *Unsaturated Zone and Saturated Zone Transport Properties (U0100)* (CRWMS M&O 2000eb, Section 6.9).

To simulate radionuclide transport through the site-scale model domain, a numerical approach for solving the mathematical equations describing solute transport is incorporated into the FEHM code. This numerical approach relies on the same computational grid developed for the site-scale saturated zone flow and transport model. The groundwater velocity field generated by that calibrated transport model provides the basis for predicting radionuclide migration through the site-scale model domain. Those factors that govern radionuclide mobility, including advection, dispersion, sorption, matrix diffusion, and colloid-facilitated transport, have been included in the transport model. The transport parameters used to model radionuclide transport were established during model abstraction for the TSPA analysis.

Mathematical Formulation of the Transport Model—Widely accepted mathematical equations describing the advective and dispersive transport provide the mathematical basis for the transport model. Matrix diffusion is incorporated into the mathematical formulation of the transport through the use of an analytical solution developed by Sudicky and Frind (1981) that describes transient contaminant transport in equally spaced parallel fractures. The model is a dual-porosity model for contaminant concentration that takes into account advective transport in the fractures, molecular diffusion from the fracture to the porous matrix, adsorption on the fracture face, and adsorption within the matrix. The model uses a no-flux condition at the midpoint of the matrix between fractures. The analytical solution requires the definition of a number of specific parameters, including the fracture aperture, the mean fracture spacing, the linear groundwater velocity within the fracture, the porosity of the matrix, the retardation factors in the matrix, and the effective matrix diffusion coefficient. Based on the values specified for these parameters, this analytical solution can be used to identify the distribution of a contaminant along the fracture at any point in time.

Sorption in the matrix is incorporated into the mathematical formulation of the transport model using a linear isotherm model (CRWMS M&O 2000bn, Section 3.3.2.3). Based on this linear isotherm model, distribution coefficients (K_d) are defined. These distribution coefficients identify the relative partitioning that will occur between the solid and liquid phases as radionuclides migrate through subsurface materials. The distribution coefficients may then be used to define retardation coefficients that identify the ratio of linear groundwater velocity to the retarded migration rate of radionuclides, based on the partitioning of radionuclides to subsurface materials.

Colloid-facilitated transport is incorporated into the mathematical formulation of the transport model in a manner similar to sorption (CRWMS M&O 2000bn, Section 3.3.2.4). The mathematical treatment for colloid-facilitated transport is focused on colloid attachment and detachment processes. The model conservatively assumes that in saturated fractured tuffs, colloids will move exclusively through fractures with negligible matrix diffusion and that colloid attachment and detachment to fracture surfaces can be described by first-order rate expressions. A local equilibrium assumption also has been adopted to describe these processes. Using these assumptions, an effective retardation factor for colloid transport through fracture tuffs can be defined based on a filtration rate constant, a detachment rate constant, and the fracture aperture. The mathematical model for colloid-facilitated transport in alluvium is identical to that for fractured tuffs, with the exception that

the effective retardation factor for colloid transport is defined using alluvial attachment and detachment rates and the density and porosity of the alluvium.

Numerical Solution of Transport Equation— The numerical approach implemented in FEHM to obtain a solution for the transport equation was selected based on a number of important requirements (CRWMS M&O 2000bn, Section 3.3.4). The transport model needs to be able to handle extremes of the advective–dispersive transport that include a wide range of dispersivity values. It may be necessary for the transport model to simulate the transport of plumes that have smaller dimensions than the gridblock size of the flow model. The numerical approach used to solve the transport equation also must include a method for introducing the radionuclide source term into the model that is flexible enough to handle both small and large source regions at the water table. Finally, the numerical approach must be able to capture the important physicochemical processes known or suspected to occur as radionuclides migrate from the potential repository.

To meet these requirements, a particle-tracking method has been implemented in FEHM to provide a solution to the advection–dispersion transport equation (CRWMS M&O 2000bn, Section 3.3.4). In this approach, transport is decomposed into three interrelated components: advective, dispersive, and physiochemical. For the advective component, a particle-tracking method is used. A random-walk algorithm has been combined with the particle-tracking approach to account for the dispersive component of the advection–dispersion transport equation. To incorporate the dual-porosity transport and sorption components of transport equation, special modules have been incorporated into the FEHM code.

The particle-tracking method incorporated into FEHM is based on placing particles at specific points in the flow field to represent a specified mass of solute. These particles can be placed throughout the model domain to represent existing solute concentrations and can be introduced as necessary over time at specific source locations to represent radionuclide migration from the unsatur-

ated zone. The particle-tracking method assumes a Lagrangian point of view, in which these particles move with the prevailing flow velocity. Based on a velocity field derived from the flow model, the trajectories for each particle are computed one at a time. Through a series of time steps, the particles are moved according to these computed trajectories.

The dispersive component of the transport is calculated using the random-walk method (Tompson and Gelhar 1990). This approach is based on the analogy between the mass transport equation and the Fokker–Plank equation of statistical physics (Van Kampen 1984). The dispersive displacement of each particle is computed using uniform random numbers, based on the dispersivity tensor and the porous flow velocity field at the particle location. In this model, the proper terms in the random-walk algorithm are derived from an anisotropic version of the dispersion coefficient tensor. During each time step, the trajectory of each particle is computed using the advective component of transport, which is modified through a series of displacements due to the dispersion calculated for each particle.

To incorporate the influence of matrix diffusion and sorption, the residence time transfer function particle-tracking method has been adapted to the particle-tracking algorithm (Zyvoloski et al. 1997a, pp. 41 to 42). In this method, adjustments to the transport time of a particle are made to account for the influence of physicochemical processes, such as sorption and matrix diffusion. During its path along a streamline, the particle transport time is governed by a transfer function describing the probability of the particle spending a given length of time on that portion of its path. The form of the transfer function is derived from an analytical or numerical solution to capture the appropriate processes being considered. The analytical solution identified above, matrix diffusion in fractured rock, and the retardation coefficients developed to account for sorption and colloid-facilitated transport are used by the model in developing the transfer function and determining the value of the delayed travel time along a path line for each particle resulting from the effects of matrix diffusion, sorption, and colloid-facilitated transport.

4.2.9.4 Total System Performance Assessment Abstraction

The saturated zone flow and transport component of the TSPA-SR evaluates the migration of radionuclides from their introduction at the water table below the potential repository to the accessible environment to the biosphere (Figure 4-128). This component of the analysis is coupled with the transport calculations for the unsaturated zone that describe the movement of contaminants in downward percolating groundwater from the potential repository to the water table. The input to the saturated zone flow-and-transport calculations is the spatial and temporal distribution of simulated mass flux at the water table that has been transported through the unsaturated zone. The transport of radionuclides in the saturated zone is linked to the biosphere analysis by the simulated time history of radionuclide concentration in groundwater at the accessible environment (Figure 4-151). Additional analyses have been done to evaluate the concentrations at the accessible environment. Radionuclide concentrations in the water are used in the biosphere component to calculate radiation dose rates received by the reasonably maximally exposed individual.

The site-scale saturated zone flow and transport model (CRWMS M&O 2000bn, Section 3) represents a synthesis of data on the groundwater flow system at the Yucca Mountain site, as well as information from regional-scale studies of the saturated zone. Key information used in the construction of the site-scale saturated zone flow model includes a three-dimensional representation of the geology of the system, water level measurements from wells, pumping tests of the volcanic units, hydrochemical data, and simulations of groundwater flux from the saturated zone regional-scale flow model. The calibration process for the site-scale saturated zone flow model provides an internally consistent representation of the saturated zone flow system that reproduces the key field observations of the system.

Information on radionuclide migration in the saturated zone is also incorporated in the site-scale saturated zone flow and transport model (CRWMS M&O 2000bn, Section 3). Key information incorporated into the model includes sorption coefficients for sorbing radionuclides, flowing interval spacing and porosity, matrix porosity in fractured volcanic units, effective porosity in alluvial units, dispersivity, and the effective diffusion coefficient. Additional data and inferences regarding colloid-facilitated transport of radionuclides are used in the site-scale saturated zone flow and transport model to simulate this process.

In the nominal case, migration of radionuclides from the unsaturated zone to the saturated zone is assumed to occur by undisturbed, natural movement of groundwater as recharge at the water table. Radionuclides migrating from the repository must be transported approximately 300 m (1,000 ft) downward by groundwater in the unsaturated zone to the water table, where they enter the saturated zone. Radionuclides are then carried downstream in the groundwater system. Radionuclides reach the accessible environment, where they could become a source of contamination in the biosphere (Figure 4-128).

Radionuclides may be dissolved in water or attached to colloids, as appropriate for the given radionuclide. Transport of parent radionuclides is simulated using the three-dimensional site-scale saturated zone flow and transport model (CRWMS M&O 2000bn, Section 3). Because the model is not currently formulated to simulate daughter products, the simultaneous transport of daughter products is carried out using a separate one-dimensional transport model (CRWMS M&O 2000el, Section 6.5). Reversible colloid transport, assuming equilibrium with the surrounding fluid, is simulated in the three-dimensional and one-dimensional transport calculations. A portion of the waste is vitrified, which produces colloids with irreversibly attached isotopes of plutonium and americium. The migration rate of these irreversibly sorbed colloids is retarded based on their expected rates of attachment and detachment in the fractured bedrock and alluvial materials. The total dose of any radionuclide computed in the assessment is the dose due to the sum of the above transported radionuclide mass through all forms of transport.

A number of processes contribute to the retardation of transported radionuclides and the dilution of the
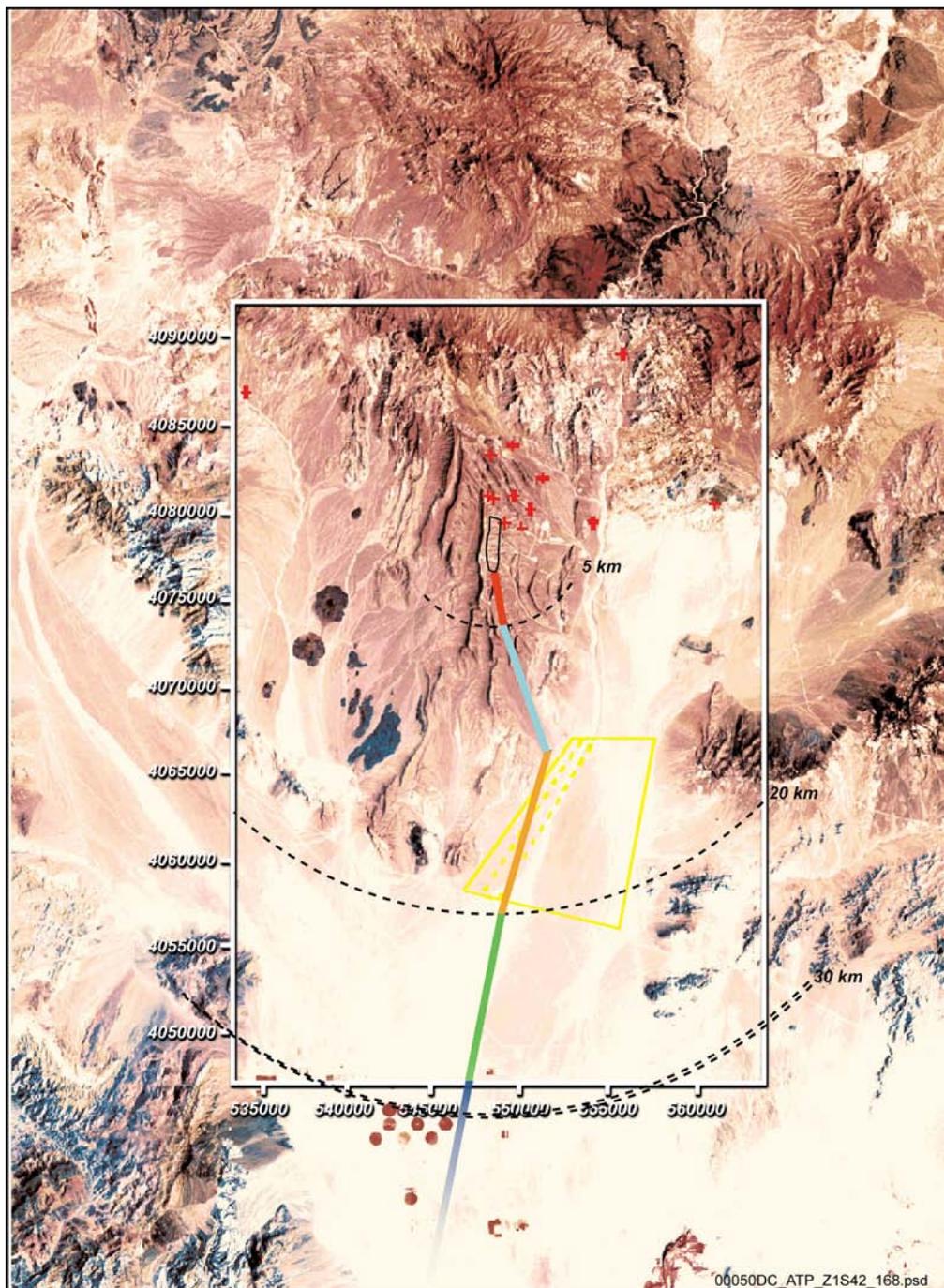
Figure 4-151. Map of Yucca Mountain Area with the Site-Scale Model Boundary
The multicolored line shows the generalized groundwater flow path from the one-dimensional saturated zone transport model, which provides the output of radionuclide mass at the exit of each pipe segment. See Figure 4-147 for a more detailed illustration of flow paths from Yucca Mountain. This analysis was performed to support the TSPA-SR. Source: Modified from CRWMS M&O 2000a, Figure 3.8-16.

radionuclide concentrations at the accessible environment downstream from Yucca Mountain. Important processes relevant to radionuclide transport in the saturated zone that are explicitly included in the TSPA-SR analyses are advection in groundwater, dispersion, matrix diffusion in fractured media, sorption of radionuclides, colloid-facilitated transport, radioactive decay, and radioactive ingrowth (production of radionuclides as decay products of other radionuclides during transport). Sorption of radionuclides is simulated to occur in the rock matrix of volcanic units but is conservatively disregarded in fractures of the saturated zone. Sorption of radionuclides is also simulated to occur in the porous media of the alluvium. Colloid-facilitated transport is included in the transport simulations as occurring in two modes: as irreversible attachment of radionuclides to colloids originating from the waste and as equilibrium attachment of radionuclides to colloids. Radioactive decay is simulated to occur for all radionuclides, and the effect of radionuclide ingrowth is simulated for the daughter radionuclides in four key decay chains in a separate one-dimensional saturated zone transport model (CRWMS M&O 2000el, Section 6.5).

The primary result of this synthesis is the site-scale saturated zone flow and transport model used for simulations of radionuclide transport in TSPA-SR analyses. This model includes modification of the final calibrated flow model (CRWMS M&O 2000ej) to accommodate variable parameter values for stochastic radionuclide transport parameters and consists of six alternative groundwater flow fields that incorporate uncertainty in groundwater flux and horizontal anisotropy. The site-scale saturated zone flow and transport model for TSPA-SR also produces simulation results in the appropriate format for coupling the radionuclide transport results with other components of the TSPA-SR analyses (CRWMS M&O 2000a).

Results of the site-scale saturated zone flow and transport model (CRWMS M&O 2000bn, Section 3.6.3) are abstracted by repeatedly performing simulations using a constant, unitary radionuclide mass flux corresponding to each radionuclide source considered for transport at the upstream end of the saturated zone. This process is done for each time step in the simulation. The calculations underlying this analysis were developed to provide insights about the sensitivities of saturated zone flow processes to individual flow parameters. The calculations were designed to accentuate and emphasize important saturated zone transport processes, and they are based on highly conservative representations of model components. In particular, the results illustrated in Figure 4-152 are based on a model that is appropriately conservative for TSPA analyses and not intended to represent expected breakthrough of radionuclides or groundwater travel time for the saturated zone portion of the Yucca Mountain flow system (CRWMS M&O 2000bn, Section 3.7.4). Accordingly, the breakthrough times are not a correct representation of the travel time of the water.

Groundwater carbon-14 data from well NC-EWDP-2D about 20 km (12 mi) downgradient from the repository along the groundwater flow path from the repository (Figures 4-131 and 4-133) offers a method of providing a rough travel-time estimate to the area of the accessible environment. Carbon-14 analyses (CRWMS M&O 2000eg, Section 6.5.7.2.2) indicate a minimum groundwater age of about 7,900 years.

In order to estimate the time required for water to move from the potential repository to the environment, the time required for flow from the point of recharge at the ground surface to the repository must be subtracted from the total age. Assuming that rapid fracture flow through the welded units results in negligibly small travel times through these units and that most of the travel time from between the ground surface and repository horizon is the result of slow matrix flow through the nonwelded tuffs of the Paintbrush nonwelded hydrogeologic unit (PTn), the travel time through the PTn can be calculated from the average moisture content of rocks in the PTn (20 percent) and the PTn thickness. The PTn ranges in thickness from about 100 m (330 ft) to 25 m (80 ft). Complete piston displacement of the in situ water is assumed in order to maximize the estimated travel time through the PTn. The water column heights of 20 m (66 ft) (for a 100-m [330-ft] thick PTn) and 5 m (16 ft) (for a 25-m [80-ft] thick PTn) are divided by the average flux over the repository
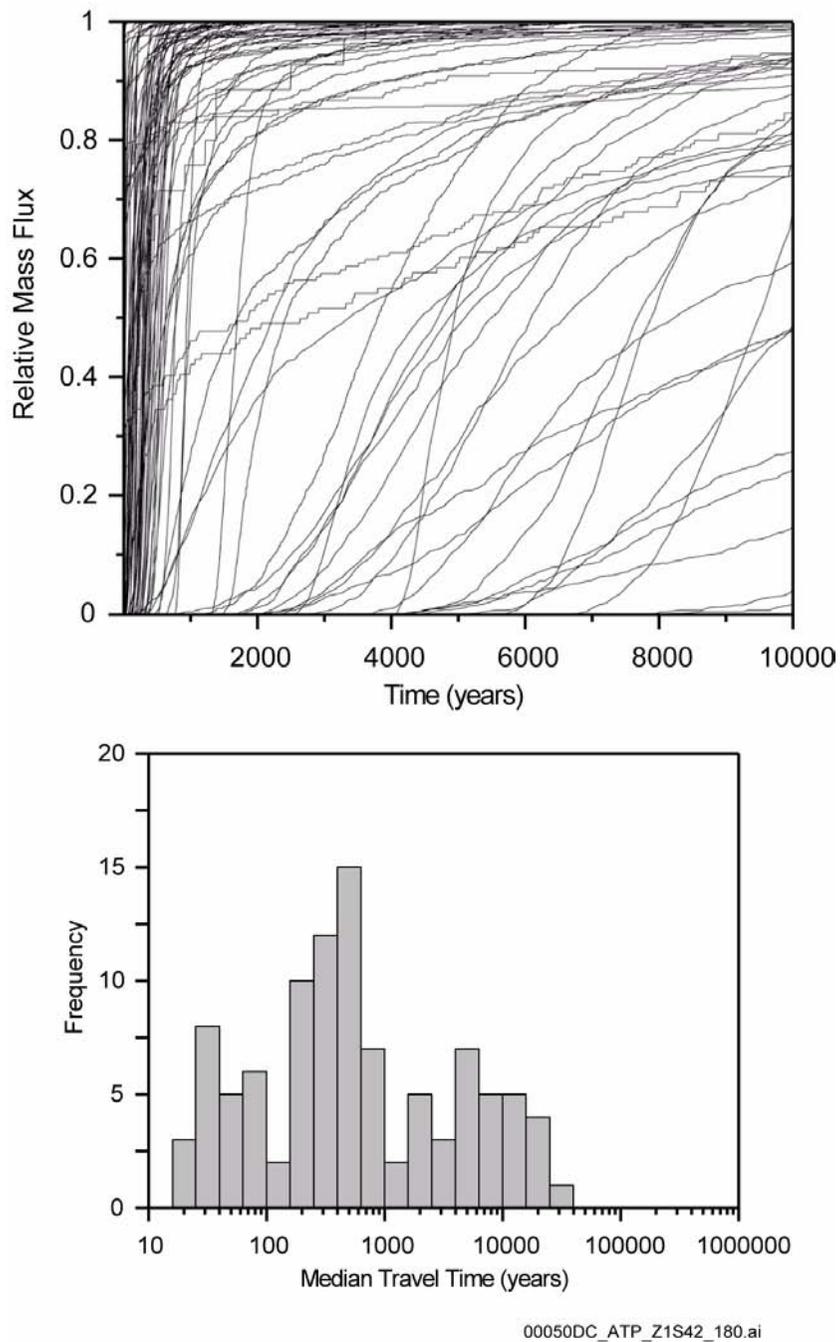
Figure 4-152. Representative Breakthrough Curve and Histogram
In this case, the simulated unit breakthrough curves and histogram of median transport times of mass flux were generated for carbon. Additional curves are presented in *Input and Results of the Base Case Saturated Zone Flow and Transport Model for TSPA* (CRWMS M&O 2000el, Section 6.3.2). The data shown in this figure are based on a model that is appropriately conservative for TSPA analyses and not intended to represent expected breakthrough of radionuclides or groundwater travel time for the saturated zone portion of the Yucca Mountain flow system. Source: CRWMS M&O 2000bn, Figure 3-31.

(5 mm/yr or 0.005 m/yr [0.2 in./yr]) resulting in estimates of travel time from the ground surface to the potential repository that range from approximately 1,000 to 4,000 years.

Subtracting these values from the groundwater carbon-14 ages provides a rough estimate of 3,900 to 6,900 years for travel time from the potential repository to the environment. This range represents an averaged duration that is generally consistent with the results of groundwater flow models. Although the carbon-14 data do not preclude the existence of some faster flow paths, it suggests that on average, the time required for water to move from the potential repository to the environment is on the order of thousands of years.

The radionuclide mass breakthrough curves at the downstream end of the saturated zone contain information about the model behavior for those source and receptor locations, assuming steady groundwater flow (Figure 4-152). The radionuclide mass breakthrough curves are saved for later computation of radionuclide mass transport by the TSPA-SR simulator. These computations are performed by scaling the mass breakthrough for a source by the mass input at each time step. In this way it is unnecessary to perform flow simulations when only the mass input for a radionuclide changes (i.e., for changes in the source or transport through the unsaturated zone).

The source of radionuclide contamination entering the site-scale saturated zone flow and transport model is specified as a point within each of four source regions beneath the potential repository (CRWMS M&O 2000bn, Section 3.6.3.4.1). The point source is located at an elevation of 725 m (2,380 ft) above mean sea level in the nominal case, which is approximately 5 m (16 ft) below the water table over most of the area beneath the potential repository. The horizontal location of the point source in each of the four source regions varies stochastically from simulation to simulation, reflecting uncertainty in the location of leaking waste packages and transport pathways in the unsaturated zone. Radionuclide transport simulations with the site-scale saturated zone flow and transport model are performed using 4,000 particles, 1,000 of which are released at each

of the four point source locations at the beginning of the simulation. The mass of radionuclide for each particle was not varied during the simulations.

Radionuclide transport is directly simulated for radionuclides (except the products of radioactive decay and ingrowth) using the site-scale saturated zone flow and transport model (CRWMS M&O 2000bn, Section 3.6.3). The convolution integral method is used in the TSPA-SR calculations to determine the time-varying radionuclide mass flux at the interface of the saturated zone and the biosphere, downgradient from the potential repository (Figure 4-153). This method combines information about the response of the system, as simulated by the site-scale saturated zone flow and transport model, with the radionuclide source history from the unsaturated zone to calculate transient system behavior. The most important assumptions of the convolution integral method are linear system behavior and steady-state flow conditions in the saturated zone. The two inputs to the convolution integral method are a radionuclide mass breakthrough curve in response to a unit step-function mass flux source as simulated by the site-scale saturated zone flow and transport model and the radionuclide mass flux history as simulated by the unsaturated zone flow and transport model (CRWMS M&O 2000c, Section 3.11). The output is the radionuclide mass flux history at the biosphere.

The presence of faults and fracture zones that are not explicitly represented in the site-scale saturated zone flow and transport model (CRWMS M&O 2000bn, Sections 3.3.6.3 and 4.2.1.2) and their potential impact on groundwater flow is implicitly included in the nominal case through consideration of horizontal anisotropy of the permeability in the fractured volcanic units downgradient of the potential repository. There is uncertainty in the potential anisotropy of permeability in the horizontal direction over the scale of the transport path length. Given the uncertainty in anisotropy, and to simplify the model, the potential effects of anisotropy are bounded by setting the anisotropy ratio to 1 (isotropic) or 5 (anisotropic), values that are based on the results of tests at the C-Wells Complex at Yucca Mountain (Winterle and La Femina 1999, Section 4.5).
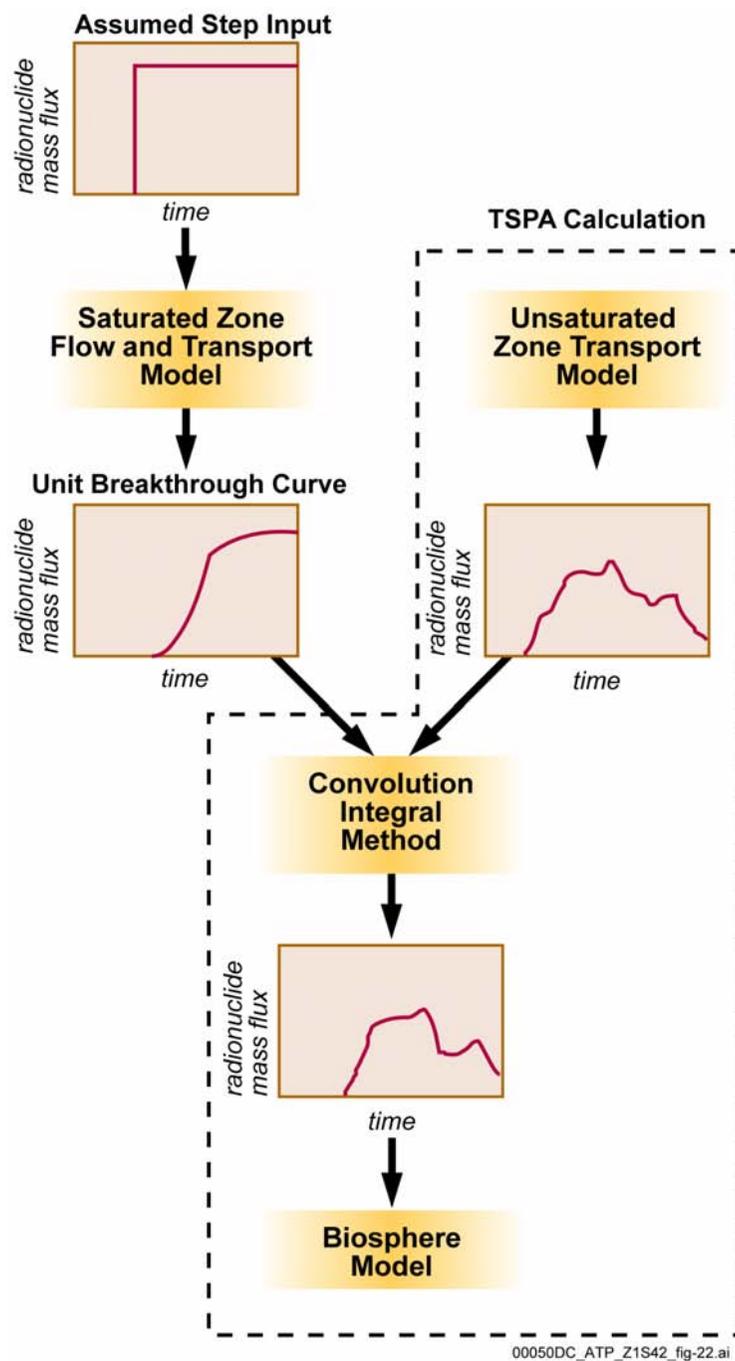
Figure 4-153. Convolution Integral Method Used in Saturated Zone Flow and Transport Calculations for Total System Performance Assessment–Site Recommendation

The dashed line is to distinguish between the saturated zone flow and transport model calculation and the TSPA-SR calculation. The TSPA-SR calculation is explained in Section 4.4.1. This figure only reflects a portion of the complete TSPA-SR calculation. Source: CRWMS M&O 2000bn, Figure 3-28.

Features, events, and processes, or FEPs (Freeze et al. 2001), include expected behavior and scenarios outside of the expected behavior of the repository, which could result in significant changes in radionuclide release to the biosphere. An example of a FEP is the possible eruption of a volcano in the Yucca Mountain area. Saturated zone flow and transport for the TSPA-SR explicitly incorporates many FEPs of the saturated zone system and implicitly includes others (CRWMS M&O 2000bn, Section 1.3). Those FEPs that are implicitly incorporated are primarily captured in the range of uncertainty assigned to parameters varied in the stochastic analyses. The most important features of the saturated zone system that are explicitly represented in the simulations are the geometry and variability in properties among hydrogeologic units in the subsurface. Of particular importance is the distinction between units consisting of fractured volcanic rock media and those that consist of porous media (alluvium). In addition, numerous hydrologic features corresponding to faults and geologic zones are explicitly incorporated into the site-scale saturated zone flow and transport model as part of the calibration process.

For the nominal TSPA-SR case (CRWMS M&O 2000bn, Section 3.7), analyses of saturated zone flow and transport incorporate uncertainty in the saturated zone groundwater flow system and in horizontal anisotropy. Uncertainty in groundwater flow is incorporated through the use of six discrete flow fields. The six fields correspond to low, average, and high flux crossed with either isotropic or horizontal anisotropic (5:1 north–south) permeability to consider uncertainty in the magnitude of groundwater flux and horizontal anisotropy. The effect of the assumption of anisotropy (5:1 north–south) does not result in a large change in the transport paths.

Climate-change forecasts for Yucca Mountain based on the analysis of past climate changes and on the assumption that climate is cyclical (USGS 2000a) are used to predict future infiltration at Yucca Mountain. Climate change is explicitly included in the nominal case of saturated zone flow and transport for TSPA-SR. Increases in the

groundwater flux of the saturated zone for a monsoonal climate state (forecast to occur in about 400 to 600 years and to have a duration of 900 to 1,400 years) and the glacial-transition climate state (forecast to occur after the monsoonal climate and to persist beyond 10,000 years) are included in the analyses. For conservatism, the impact of a rising water table on groundwater flow paths in the saturated zone is not explicitly included in the saturated zone flow and transport model for the nominal case. This is conservative because radionuclides are transported in shallow flow paths at the water table, and a rising water table would result in those flow paths rising up and radionuclides being transported in less permeable material and with a slower travel time. Thus, the current model, which ignores the impact of a rising water table on groundwater flow paths and transit time, produces transport times that are conservative with respect to dose.

Multiple simulations of the saturated zone transport model are performed using continuous distributions for the parameters that define the transport characteristics of the saturated zone system. The probabilistic analysis of uncertainty is implemented through Monte Carlo simulations of the saturated zone flow and transport system in a manner consistent with the TSPA-SR simulations implemented with the GoldSim software code. Alternative models of groundwater flux and horizontal anisotropy are included as the six saturated zone groundwater flow fields. Uncertainty in the location of the contact between volcanic units and the alluvium is incorporated as geometric variability in the alluvium zone in the site-scale saturated zone flow and transport model. Colloid-facilitated transport is considered in the uncertainty analysis through the use of two coexisting modes of colloid-facilitated transport.

In general, parameters to which the model results are sensitive, due to the combination of the numerical importance of the parameter in the model or the uncertainty in the parameter value, are represented stochastically. Parameters to which the model results are not sensitive are represented by constant values. This approach is a reasonable simplifying assumption because the results are not significantly altered by those parameters.

The following parameters are considered either wholly or partially stochastic:

- Groundwater specific discharge
- Alluvium boundary
- Effective porosity in the alluvium
- Flowing interval spacing, flowing interval porosity
- Effective diffusion coefficients
- Bulk density
- Sorption coefficients
- Longitudinal dispersivity
- Horizontal anisotropy
- Source region definitions
- Retardation of radionuclides irreversibly sorbed on colloids (volcanics and alluvium)
- Retardation of radionuclides reversibly sorbed on colloids.

The stochastic distributions and constant values used in the site-scale saturated zone flow and transport model for TSPA-SR are presented in *Uncertainty Distribution for Stochastic Parameters* (CRWMS M&O 2000ek, Section 6). Matrix porosity, a parameter used in matrix diffusion, is recognized as an uncertain parameter. Matrix diffusion is very sensitive to flowing interval spacing and matrix-diffusion coefficient but not sensitive to matrix porosity. As a result, matrix porosity was treated as a constant value in all TSPA simulations.

For the purposes of the TSPA-SR model, the breakthrough curves of radionuclide mass arrival at the accessible environment are simulated with the site-scale saturated zone flow and transport model by obtaining output of particle travel time from the FEHM code when a particle crosses a fence of nodes in the model grid. Three fences, corresponding to travel distances of 5, 20, and 30 km (approximately 3, 12, and 19 mi), are specified for output of breakthrough curves. These fences of grid nodes are located at the prescribed distance from the southern corner of the outline of the potential repository and extend from the upper surface to the lower surface of the site-scale saturated zone flow and transport model domain. The saturated zone groundwater flow pathway from beneath the potential repository extends in a generally southerly direction and all particles are counted as they cross the intervening fences of grid

nodes. The model setup of the one-dimensional saturated zone transport model provides output of radionuclide mass at the exit of each pipe segment, and these segments are constructed to end at distances of 5, 20, and 30 km (approximately 3, 12, and 19 mi) (Figure 4-151).

The contributions of radionuclide mass flux at the 20-km (12-mi) fence from the four source regions in the site-scale saturated zone flow and transport model are summed to obtain the total radionuclide mass flux for a time step in the TSPA-SR simulator. Summing these values of radionuclide mass flux occurs following the convolution integral calculation. The mass flux of the daughter radionuclides from the one-dimensional saturated zone transport model is also included in the calculation at this point.

Radionuclide concentrations in groundwater are used in the biosphere component of the TSPA-SR analysis to calculate radiological dose to the receptor of interest using biosphere dose conversion factors. The concentrations of radionuclides are calculated by dividing the radionuclide mass delivered to the biosphere per year for that time step by the total groundwater use per year of the receptor of interest.

Additional breakthrough curves were calculated for a location consistent with NRC licensing-related regulations at 10 CFR Part 63 (66 FR 55732), which provide a new definition of the boundary between the controlled area and the accessible environment. This location was evaluated where the hypothetical reasonably maximally exposed individual is assumed to live at the point above the highest concentration of radionuclides in the simulated plume of contamination where the plume crosses the southernmost boundary of the controlled area (at a latitude of 36° 40' 13.6661" North) and reaches the accessible environment. This distance is approximately 18 km (11 mi) from the repository footprint, compared to the original distance of approximately 20 km (12 mi) used in the saturated zone transport modeling calculated for the TSPA-SR model. To provide a preliminary assessment consistent with the final NRC regulation at 10 CFR Part 63, a conservative sensitivity analysis was performed for a nonsorbing radionu-

clide and a sorbing radionuclide (carbon-14 and neptunium-237, respectively) to evaluate how long radionuclides are projected to take in being transported from the saturated zone directly beneath the potential repository to a downgradient location where they could enter the accessible environment (BSC 2001a, Section 12.5.3). These radionuclides were chosen because they are representative of the solutes that would be most rapidly transported (i.e., nonsorbing carbon-14) or are among the larger contributors to the potential dose (i.e., neptunium-237), and together they bound the range of solute transport.

The sensitivity analysis was conducted using the saturated zone flow and transport model with conservative values for process model parameters. The results of comparisons between the different transport distances for a nonsorbing radionuclide (carbon-14, which is representative of other nonsorbing radionuclides such as technetium-99 and iodine-129) and a slightly sorbing radionuclide (neptunium-237) are illustrated in Volume 1, Section 12.5.3 of *FY01 Supplemental Science and Performance Analyses* (BSC 2001a). The simulated radionuclide breakthrough curves at 18 km (11 mi) have shorter radionuclide transport times than those at 20 km (12 mi) (BSC 2001a, Section 12.5.3) under the same set of conservative assumptions.

The effect of the reduced advective transport times (due to the shorter distance) is to shift the breakthrough curves to correspondingly earlier times (BSC 2001b, Section 5.4). During the time period of regulatory concern (10,000 years), when the doses are dominated by low-probability early waste package failures (due to improper heat treatment of the closure welds), the releases and resulting doses are primarily related to nonsorbing radionuclides (BSC 2001b, Section 3.2.5). Therefore, reducing the advective transport time would reduce the breakthrough of the radionuclides by roughly the same amount of time. This reduction would have no effect on the magnitude of the peak mean annual dose because this is controlled by the temporally dispersed release from the engineered barrier system (BSC 2001b, Section 5.4).

Additional saturated zone breakthrough curves, which describe the time-related arrivals of radionuclides at the reasonably maximally exposed individual location, were calculated in *Total System Performance Assessment—Analyses for Disposal of Commercial and DOE Waste Inventories at Yucca Mountain—Input to Final Environmental Impact Statement and Site Suitability Evaluation* (Williams 2001a) to evaluate long-term performance with respect to the criteria established in 10 CFR Part 63 (66 FR 55732). The saturated zone breakthrough curves were used in analyses to simulate radionuclide transport from the water table beneath the potential repository to the reasonably maximally exposed individual location at the accessible environment. The simulated radionuclide breakthrough curves at the reasonably maximally exposed individual location exhibited shorter transport times than those used in *Supplemental Science and Performance Analyses* (BSC 2001a, Section 12.3.2.3) on a realization-by-realization basis. In particular, those radionuclides that may have significantly greater sorption in the alluvium than in the volcanic units (e.g., neptunium-237) exhibit shorter transport times to the reasonably maximally exposed individual location in this analysis relative to the location used in analyses for *Total System Performance Assessment for the Site Recommendation* (CRWMS M&O 2000a). This result is related to the fact that the reasonably maximally exposed individual location in *Total System Performance Assessment—Analyses for Disposal of Commercial and DOE Waste Inventories at Yucca Mountain—Input to Final Environmental Impact Statement and Site Suitability Evaluation* (Williams 2001a) results in a decrease in the length of transport through the alluvium relative to the previously computed transport path.

4.2.10 Biosphere

The biosphere is the ecosystem of the earth and the organisms inhabiting it and includes the soil, surface waters, air, and all living organisms. The purpose of the TSPA-SR biosphere analyses is to develop dose conversion factors reflecting the transport and retention of radionuclides within the biosphere. These dose conversion factors, called biosphere dose conversion factors, are subse-

quently used directly in the TSPA abstraction to calculate dose. The biosphere analyses are designed to provide the capability to predict radiation exposures to persons living in the general vicinity of the potential repository if there is release of radioactive material to the biosphere after closure of the repository (CRWMS M&O 2000a, Section 3.9). Analysis of the biosphere transport and uptake processes requires conceptually interpreting the important contaminant transport pathways (ways in which potential releases from a geologic repository could reach a human being and result in a radiation dose) (CRWMS M&O 2000bo, Section 3.1.4).

4.2.10.1   Conceptual Basis

The biosphere is the last component in the chain of TSPA component models considered in the overall performance assessment of the potential repository site (Section 4.2). Upstream from the biosphere, there are two connections: (1) the biosphere is coupled to the saturated zone flow and transport model for the contaminated groundwater use scenario (nominal case); and (2) the biosphere is coupled to the volcanic dispersal model for the direct volcanic release scenario.

The biosphere component of TSPA analyses addresses processes and pathways that could either disperse or concentrate radionuclides released from the repository. The biosphere analyses focus on the behaviors (i.e., lifestyles, including dietary and activity habits) that would be significant to radiation exposure and the environment around these potentially exposed people that would be important to their radiation exposure (Figure 4-154) (CRWMS M&O 2000bo, Section 3.1.2). For the TSPA-SR model and the supplemental TSPA model, the conceptual basis for the biosphere component is consistent with the proposed rules promulgated by the NRC and EPA (BSC 2001a, Section 13.1; BSC 2001b, Section 3.2.11). With the promulgation of the final rules by each agency, additional biosphere model sensitivity and supplemental performance analyses evaluate the potential impacts consistent with the final licensing-related rules (Williams 2001a, Section 5.2.5; Williams 2001b, Section 6.3).

The biosphere analyses for the TSPA-SR model considered a hypothetical human receptor to evaluate the effects of the potential contaminant pathways and processes, consistent with proposed regulations. Subsequent biosphere analyses are based on the receptor concept of the reasonably maximally exposed individual consistent with 40 CFR 197.21 and 10 CFR 63.312 (66 FR 55732).

There have been four prior TSPA iterations conducted for the disposal of spent nuclear fuel and high-level radioactive waste at Yucca Mountain (Eslinger et al. 1993; CRWMS M&O 1994; 1995; 1998g, Chapter 9). The TSPA-VA was the first effort by the DOE to incorporate an all-pathway biosphere model for radiation dose assessment (CRWMS M&O 1998g, Chapter 9). With a few changes, the approach developed for *Viability Assessment of a Repository at Yucca Mountain* (DOE 1998) is used in the TSPA-SR.

Changes incorporated into the TSPA-SR analyses include the following:

- A comprehensive list of FEPs is used to identify the attributes of the conceptual biosphere pathway analyses (CRWMS M&O 2000bo, Section 3.1.3).

- The receptor and the reference biosphere concepts specified by the regulatory agencies are used in calculations.

- Radionuclide buildup in soils resulting from continued irrigation with contaminated groundwater is considered in the analyses, and estimates of soil and radionuclide removal by erosion are incorporated into overall dose calculations.

- An assessment of the annual water usage by a hypothetical farming community was conducted.

In TSPA-SR, the two basic scenarios for radionuclide transport to the biosphere are analyzed as the following:

- Use of contaminated groundwater for domestic and agricultural purposes
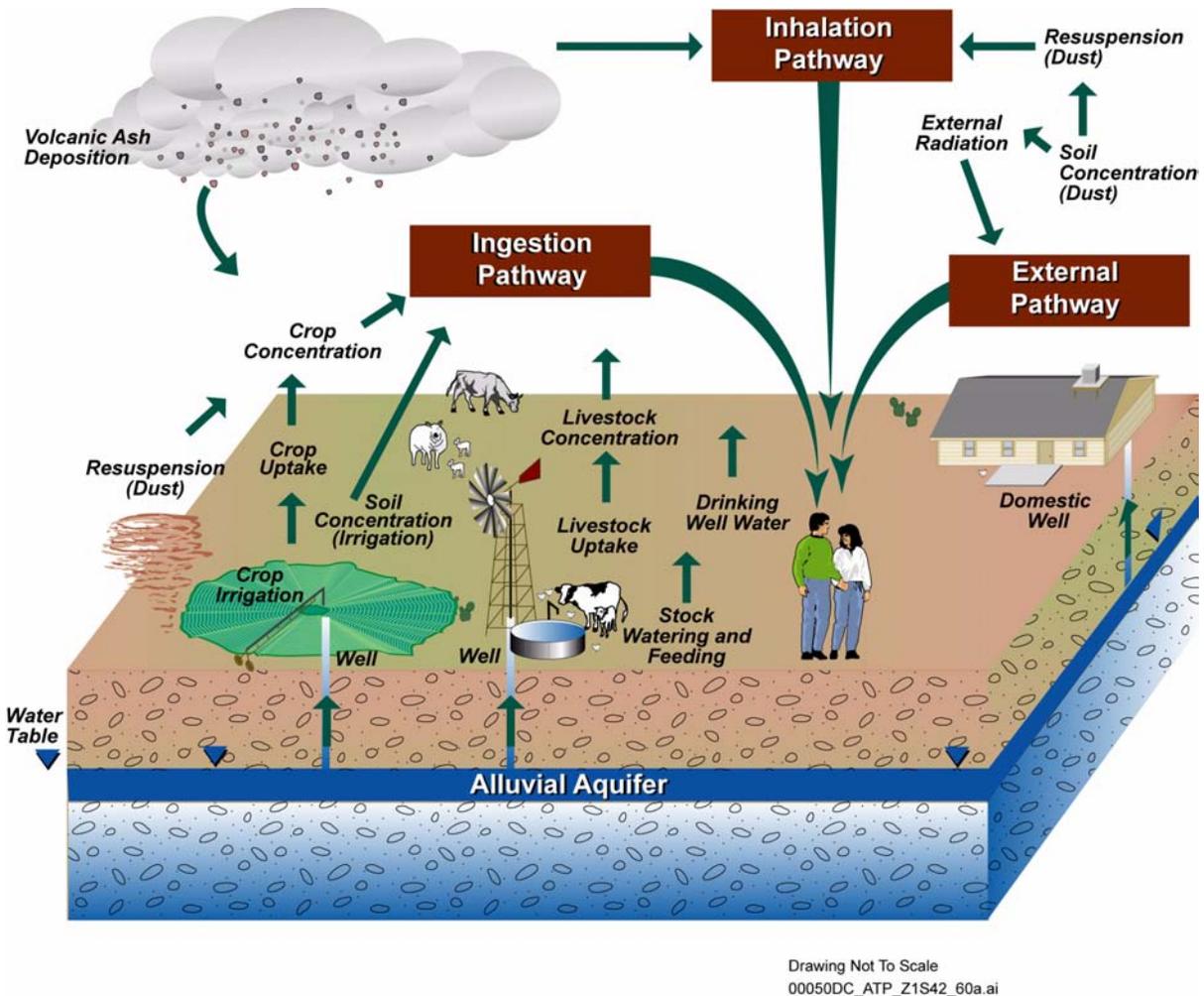
Figure 4-154. Illustration of the Biosphere Transport Pathways and Processes Contributing Dose to the Biosphere Receptor(s)

- Dispersal of radionuclide contaminants onto the earth's surface by a direct volcanic release (ash deposition).

The TSPA-SR biosphere analyses include a conceptual representation of the local population, as receptors, and contaminant transport pathways, represented as a mathematical expression. GENII-S (Leigh et al. 1993), a computer code for predicting radiation dose, is used to calculate radionuclide-specific biosphere dose conversion factors. The biosphere dose conversion factors consider the pathways of radionuclides (Figure 4-154) through the environment (such as irrigation and uptake of a contaminant by food crop plants and the subsequent ingestion of the plant by the person in question). GENII-S calculates a

biosphere dose conversion factor for each of the radionuclides considered in the analysis by assuming a unit concentration of that radionuclide in water and then evaluating radionuclide transfer through pathways to the human receptor (CRWMS M&O 2000bo, Section 3.2.1). In other words, this computer program calculates a factor by which scientists can estimate a receptor's annual committed dose from the release of a particular radionuclide into the biosphere. The multiplication factor calculated by GENII-S is determined using input parameters that characterize radionuclide transport in the biosphere and human exposure. Human exposure parameters include the amount of groundwater the person drinks and the amount of locally grown foodstuffs (both animal and vegetable) the person consumes. The conversion factors

also include such lifestyle elements as the amount of time spent outdoors (CRWMS M&O 2000bo, Sections 3.1 and 3.3). Once a conversion factor for a particular radionuclide is determined, it can be multiplied by the actual radionuclide concentrations in groundwater (determined by the saturated zone flow and transport modeling component of the TSPA-SR) to calculate the dose the person(s) would receive.

Many of the input parameters used in the biosphere analyses (e.g., quantity of groundwater and locally produced foodstuffs ingested annually) were obtained through a survey of inhabitants residing within an 80-km (50-mi) grid centered on Yucca Mountain (CRWMS M&O 2000bo, Section 3.2.4). The survey was designed to permit an accurate representation of dietary patterns. Over one thousand interviews were completed for the survey. A detailed discussion of the survey method and the confidence levels of the resulting data is found in *The 1997 "Biosphere" Food Consumption Survey Summary Findings and Technical Documentation* (DOE 1997d). Lifestyle characteristics, including employment attributes, of the inhabitants in the area were determined based on 1990 Census Data (Bureau of the Census 1999). Based on existing employment classifications, the highest exposure due to outdoor employment activity would be for agricultural or construction workers. A major portion of the data related to the surface soil layer considered in the analyses was obtained from a U.S. Department of Agriculture Natural Resource Conservation Service database that provides chemical and physical properties for the soils for southern Nye County, including the Amargosa Valley (CRWMS M&O 2000eo, Section 4.1, Table 1). Other data used in biosphere pathway analyses were obtained from credible literature sources, including refereed journal articles (CRWMS M&O 2000bo, Section 3.2.4).

It is important to note that the biosphere pathway analysis component of the TSPA-SR does not, in itself, perform dose assessment calculations (CRWMS M&O 2000bo, Section 3.1.2.1). Rather, the biosphere analyses provide the capability to the integrated TSPA model to calculate dose to the human being considered most at risk once radionuclide concentrations in the groundwater and volcanic ash have been determined through the calculations of the other performance assessment subsystem component models (e.g., unsaturated zone flow and transport, saturated zone flow and transport).

Receptor Concepts—For the TSPA-SR model, project scientists determined a critical group representing those individuals in the general population who, based upon conservative assumptions, are expected to receive the highest potential doses in the event of radionuclide release from the repository. As discussed previously, the biosphere pathway analyses for TSPA-SR were conducted for the hypothetical receptor called the average member of the critical group (consistent with proposed 10 CFR Part 63 [64 FR 8640]). Supplemental TSPA analyses were conducted consistent with the receptor in the EPA standard and NRC regulations, which is identified as a "reasonably maximally exposed individual." Consistent with the final rules, the reasonably maximally exposed individual is the hypothetical person who would:

- Live in the accessible environment above the highest concentration of radionuclides in the plume of contamination

- Have a diet and living style representative of the people who now reside in the Town of Amargosa Valley, Nevada. The DOE must use projections based upon surveys of the people residing in the Town of Amargosa Valley, Nevada, to determine their current diets and living styles and use the mean values of these factors in the assessments

- Use well water with average concentrations of radionuclides based on an annual water demand of 3,000 acre-ft

- Drink 2 L (0.53 gal) of water per day from the wells drilled into the groundwater at the reasonably maximally exposed individual location in the accessible environment

- Is an adult with metabolic and physiological considerations consistent with present knowledge of adults.

Comparison of the biosphere model results for the receptor indicates that the dose conversion factors calculated for the average member of the critical group adequately represent the potential exposure for the reasonably maximally exposed individual (Williams 2001a, Section 5.2.5).

4.2.10.2   Summary State of Knowledge

Reference Biosphere—The climate in the vicinity of Yucca Mountain is arid, and the site is located within the sparsely populated region between the Great Basin and the Mojave deserts in southern Nevada. The natural vegetation is predominantly desert scrub and grasses (CRWMS M&O 2000bo, Section 3.1.1.1).

The nearest community in the direction of groundwater flow from the potential repository site is the Town of Amargosa Valley (Figure 4-155). The Town of Amargosa Valley is an area of approximately 1295 km^2 (500 mi^2) that was defined as a tax district by the Nye County commissioners in the early 1980s. The closest inhabitants to Yucca Mountain are within Amargosa Valley, approximately 20 km (12 mi) south at the intersection of U.S. 95 and Nevada State Route 373, a location known as Lathrop Wells (there are approximately eight inhabitants at this location) (CRWMS M&O 2000bo, Section 3.1.1.3). This area is near the location of the reasonably maximally exposed individual in the accessible environment at the southernmost boundary of the potential repository controlled area (Williams 2001a, Section 5.2.3). The Amargosa Farms area (a triangle of land bounded by the Amargosa Farm Road to the north, Nevada State Route 373 to the east, and the California border running from the northwest to the southeast) is the closest agricultural area.

The Amargosa Valley area is sparsely populated and primarily rural agrarian in nature. The area supports a population of approximately 900 in about 450 households (DOE 1997d, Section 2.4). Agricultural activity is directed primarily towards livestock feed production (e.g., alfalfa; see Figure 4-155b), but gardening and animal husbandry are common. Water for both domestic and agricultural use is taken from local wells, mostly privately owned. Commercial agriculture in the Amargosa Valley farming triangle includes a dairy operation (approximately 4,500 milk cows) employing about 50 people, a catfish farm that sustains approximately 15,000 catfish, and a garlic farm that annually produces about one ton of garlic per year. Approximately 728 hectares (1,800 acres) are dedicated to alfalfa production, 12 hectares (30 acres) to oats production, 32 hectares (80 acres) are in pistachios, and 4 hectares (10 acres) in grape vineyards. The area has a general store (Figure 4-155c), community center, senior center, elementary school, public library, medical clinic, restaurant, hotel-casino, and motel (CRWMS M&O 2000bo, Section 3.1.1.3).

Previous TPSA analyses have shown that, given the lifestyle habits in the Amargosa Valley, the greatest potential contributors to dose are the drinking of contaminated groundwater and the consumption of locally produced leafy vegetables (DOE 1998, Volume 3, Section 3.8.3.1).

Groundwater Demand—TSPA-SR and *Total System Performance Assessment—Analyses for Disposal of Commercial and DOE Waste Inventories at Yucca Mountain—Input to Final Environmental Impact Statement and Site Suitability Evaluation* (Williams 2001a) used an average water demand of about 2,000 acre-ft (a mean of 1,938 acre-ft with a range from 887 to 3,367 acre-ft) (CRWMS M&O 2000bo, Section 3.4.6) based on a survey of current usage. Consistent with the final 10 CFR 63.312(c) (66 FR 55732), revised supplemental TSPA analyses assumed the use of 3,000 acre-ft/yr. This higher water demand results in a subsequent decrease in expected mean annual dose via the groundwater pathway (Williams 2001b, Section 6.3).

In the TSPA-SR analyses, the input parameter defining the quantity of drinking water consumed by the receptor was based upon human consumption data obtained by the survey of the Amargosa Valley area; this value is 753 L/yr (199 gal/yr), or 2.1 L/day (0.55 gal/day) (CRWMS M&O 2000ep, Table 4; CRWMS M&O 2000a, Section 3.9.1). Consistent with final licensing-related NRC regulations, the daily drinking water consumption value for the receptor is 2 L/day (0.53 gal/day) (730 L/yr [193 gal/yr]) (10 CFR 63.312(c) [66 FR 55732]).
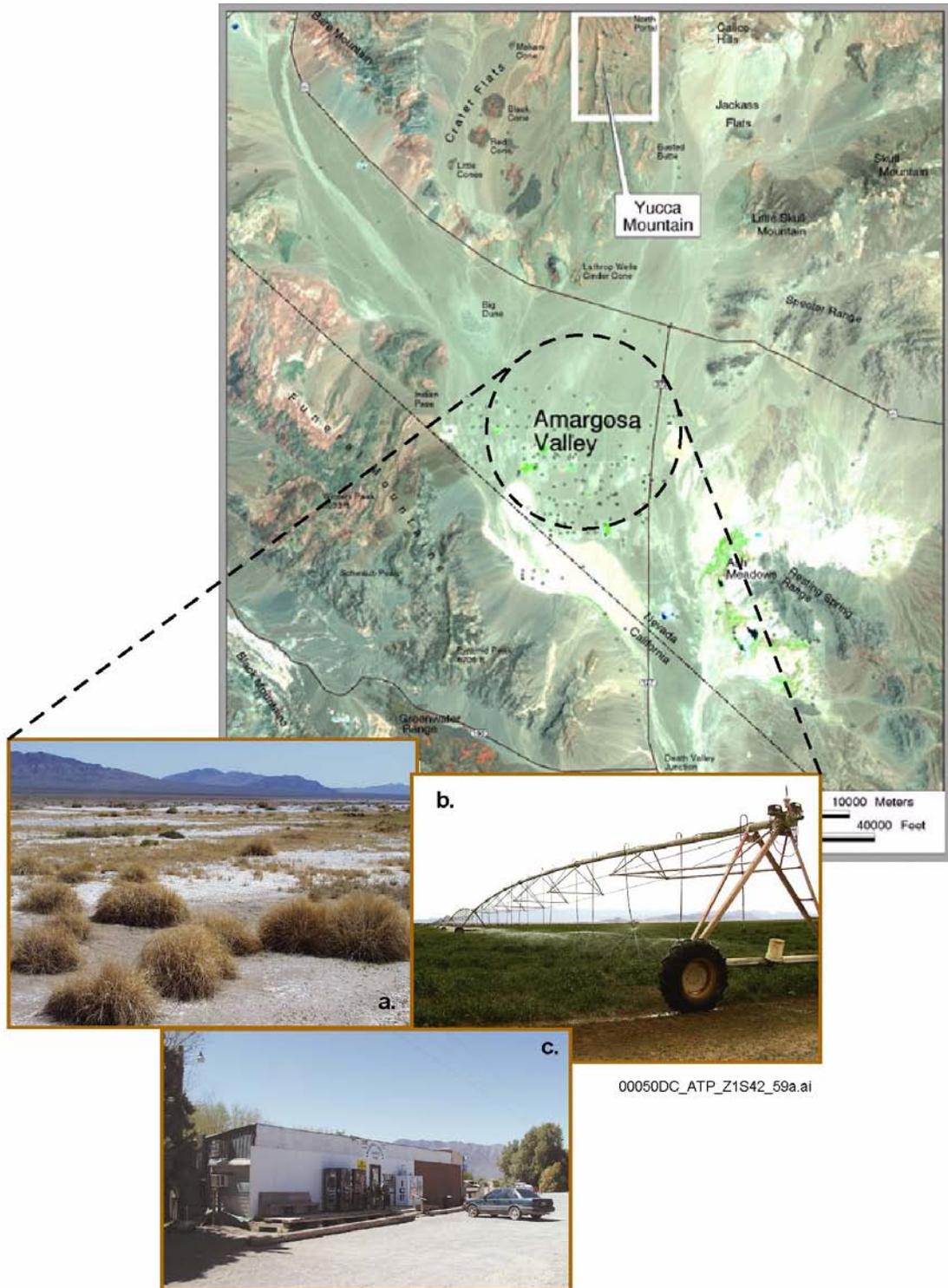
Figure 4-155. Satellite Image Showing the Yucca Mountain Area, Including the Amargosa Valley, with Details of the Area

(a) Characteristic sparsely vegetated desert grassland/shrubland in undeveloped areas. (b) Alfalfa produced with groundwater distributed through sprinkler irrigation is the dominant agricultural practice. (c) General store in Amargosa Valley. Source: Modified from CRWMS M&O 2000a, Figures 3.9-3 and 3.9-4.

The 2 L/day (0.53 gal/day) drinking water consumption value used in the supplemental biosphere analyses is slightly less than the 2.1 L/day (0.55 gal/day) used in TSPA-SR model and has minimal impact on the biosphere dose conversion values used for supplemental TSPA model analyses (Williams 2001a, Section 5.2.5).

4.2.10.3 Process Model Development and Integration

4.2.10.3.1 Biosphere Process Model

As described earlier, the biosphere conceptual model is a set of hypotheses consisting of assumptions, simplifications, and idealizations that describe the essential aspects of the biosphere in the vicinity of Yucca Mountain. This conceptual model is used to evaluate the transport of radionuclides potentially released from the source (repository) throughout the environment to the receptor of interest, as well as internal and external exposure of the receptor to the radionuclides present in the environment.

Two repository release scenarios are evaluated: (1) pumping of contaminated groundwater to be used for both domestic and agricultural purposes by the receptor under nominal repository performance; and (2) deposition of contaminated ash resulting from a volcanic (igneous activity) release from the repository (CRWMS M&O 2000bo, Section 3.1.5).

The biosphere conceptual model includes the following components: the surface soil above the lower bounds of the plant root zone (including volcanic ash, in the case of a volcanic eruption), the surface water (e.g., large, man-made containers filled from groundwater sources), the atmosphere, and flora and fauna. Thus, the biosphere includes biological components that may be a part of the various potential pathways for radionuclide transport to humans. The upper boundary of the biosphere includes that portion of the atmosphere that controls the transport and dispersal of airborne radionuclides. For the TSPA-SR, the effects of surface soil removal by erosion or other processes (e.g., mechanical removal as in harvesting of soil along with crop) was estimated based upon land

use and conservation practices. The objective for considering the effects of surface soil removal was to allow for the evaluation of radionuclide buildup in soil following continuous irrigation with contaminated groundwater (CRWMS M&O 2000eq, Section 7.3).

After the permanent closure of the potential repository, radionuclides may eventually be leached to the underlying groundwater, or saturated zone, and then migrate hydrologically downgradient to the location beneath the receptor. This water could then eventually reach the earth's surface through the pumping of well water (CRWMS M&O 2000bo, Section 3.1.4.2).

Potential cooler, wetter future climate (glacial-transition) could effect biosphere pathways and performance assessment. A climate evolution pathway analysis to evaluate the potential effects on the biosphere model resulted in a reduction in expected biosphere dose conversion factor values for the future climate (BSC 2001a, Section 13.3.7). The TSPA-SR and supplemental TSPA models use the modern climate condition biosphere model (CRWMS M&O 2000bo, Section 3.1.1) because it is more conservative than the evolved climate model.

In the contaminated groundwater use scenario, a groundwater well is considered the source of drinking and irrigation water (CRWMS M&O 2000bo, Section 3.1.5.1). The affected farming community is presumed to be located approximately directly south of the potential repository in the Amargosa Valley. In the TSPA-SR, based on proposed regulations, the community (and the average member of the critical group) was assumed to be 20 km (12 mi) south of the repository. In the revised supplemental TSPA analyses, based on final regulations, the reasonably maximally exposed individual was assumed to be 18 km (11 mi) south. The receptor (average member of the critical group or reasonably maximally exposed individual) is an adult who lives at this location year round and uses a well as the primary source of water and otherwise has habits (e.g., consumption of locally produced foods) that are similar to those of the population of the Amargosa Valley. The contaminant transport pathways, routes taken by

radionuclides through the biosphere from the source to a receptor, are typical for a farming community in this desert environment. Inhalation and direct exposure from surface contamination are intensified by the significant outdoor activity of a farming lifestyle. The exposure pathways (Figure 4-154) considered for the contaminated groundwater use scenario include consumption of tap water, locally produced leafy/root vegetables, fruits, grain, meat (beef and pork), poultry, milk and eggs, fish, inadvertent soil ingestion, inhalation of resuspended particulate matter, and external exposure to contaminated soil. Supplemental biosphere exposure pathway analyses for the groundwater use scenario consider a groundwater well at the location of the reasonably maximally exposed individual in the accessible environment (southernmost boundary of the controlled area) as the source of contamination. The reasonably maximally exposed individual is a hypothetical rural-resident receptor exposed to contamination through the same general exposure (transport) pathways as a farmer (as stated in the preamble of 40 CFR Part 197 [66 FR 32074, p. 32092]).

Since the biosphere modeling for the TSPA-SR model, some supporting documentation for the biosphere groundwater release exposure scenario has been revised, including updates of a limited number of parameter values. Discussion of the changes made to the biosphere model is contained in Volume 1, Section 13.4 of *FY01 Supplemental Science and Performance Analyses* (BSC 2001a). The most significant changes in the groundwater release exposure scenario are related to:

- Parameters defining employment and recreational behavior (duration of inhalation and external exposure times) (BSC 2001a, Section 13.2.1.4)

- Particulate concentrations in the air based on measurement of total suspended particles at Yucca Mountain and PM10 measurements from arid farming communities in the southwestern United States and the Yucca Mountain area (BSC 2001a, Section 13.2.1.4)

- Consumption rates of locally grown food for the critical group represented by distributions (BSC 2001a, Section 13.3.1)

- Parameters associated with the ingestion pathway for the current climate updated and new values developed for the cooler and wetter climate (glacial transition) (BSC 2001a, Section 13.2.1.5).

For the nominal scenario, the most significant contributing pathway to exposure is ingestion (CRWMS M&O 2001e, Section 6.7). The changes made based on the updated data had little impact on the nominal exposure ingestion pathway (BSC 2001b, Section 3.2.11.2).

The direct volcanic release scenario provides the framework for evaluating the radiological consequences of a volcanic eruption, wherein it is assumed that such an event would result in the deposition of radionuclide-contaminated ash on the soil surface. For the biosphere dose conversion factor calculations, the initial surface deposition of ash is assumed to remain on the soil surface rather than to become distributed (and thus diluted) throughout the surface soil layer. This approach maximizes the contribution to the inhalation pathway, considered the most important for direct volcanic releases. In addition, it accounts for the process of volcanic ash transfer from uncultivated areas (CRWMS M&O 2000bo, Section 3.1.5.2). Biosphere model supplemental analyses for volcanic release scenario confirm the importance of the inhalation pathway for this exposure scenario (BSC 2001a, Section 13.4.3).

The conditions for human exposure from volcanic ash deposition are the same as those considered for undisrupted performance. That is, the receptor is assumed to live year round in the farming community. The person is also assumed to be similarly involved in the activities typical of the current inhabitants of the region (e.g., has the same patterns of consumption of locally produced foods and similar periods of time spent in outdoor activities) (CRWMS M&O 2000bo, Section 3.1.5.2). Supplemental biosphere analyses indicate that the biosphere dose conversion factors for the average member of the critical group conservatively repre-

sent the reasonably maximally exposed individual (Williams 2001a, Section 5.2.5).

Updates in the biosphere model volcanic-eruption exposure scenario (radionuclides introduced to the biosphere by volcanic ash) since the TSPA-SR include revision of parameter values. A more detailed discussion of the changes made to the biosphere model is contained in Volume 1, Section 13.4 of *FY01 Supplemental Science and Performance Analyses* (BSC 2001a). The most significant changes include:

- Revision of parameters defining employment and recreational behavior (duration of inhalation and external exposure times) (BSC 2001a, Section 13.2.1.4)

- Revision to distribution of particulate concentrations in air for the volcanic scenario based on measurement from Mount St. Helens and Cerro Negro (BSC 2001a, Section 13.2.1.4)

- Development of new set of particle-resuspension factors for use after a volcanic event (BSC 2001a, Section 13.2.1.6)

- Development of distributions to represent consumption rates of locally grown food for the critical group (BSC 2001a, Section 13.3.1)

- Revision of parameters associated with the ingestion pathway for the current climate and develop values for the cooler and wetter climate (glacial transition) (BSC 2001a, Section 13.2.1.5).

Reevaluation of factors in the biosphere model volcanic-eruption exposure scenario (BSC 2001a, Section 13.4.3) results in changes to the expected annual doses. The particulate concentration in air was increased by a factor of 2.5. For the direct releases by volcanic eruption (ash fall), inhalation is the dominant pathway when integrated over time. (BSC 2001a, Section 13.3.6).

4.2.10.3.2 Mathematical Model

GENII-S, a computer program for statistical and deterministic simulations of radiation doses to humans from radionuclides in the environment (Leigh et al. 1993), was chosen to support the biosphere analyses for TSPA-SR. The program was found to be the most comprehensive code available for the analyses. GENII-S is flexible enough to address the FEPs applicable to Yucca Mountain, and it has been accepted by regulatory agencies for the purpose of environmental dose assessment. Furthermore, the program has the capability to sample over a range of environmental transport and human exposure parameter values for uncertainty and sensitivity analyses. Other criteria used in selecting GENII-S for use in the biosphere analyses are outlined in the *Biosphere Process Model Report* (CRWMS M&O 2000bo, Section 3.2.1.1).

Using a comprehensive set of environmental pathway models, GENII-S calculates the environmental transport of radionuclides following contamination of groundwater or contamination of soil resulting from the deposition of volcanic ash containing radionuclides. Based on the defined source term and exposure scenario, radionuclide transport through the biosphere as well as human internal and external exposure to key radionuclides are assessed. The entire process is an effort to describe the complex behavior of radionuclides in the environment and in humans using a mathematical abstraction, with the results of the modeling process being influenced by all uncertainties associated with the model itself, as well as with the model parameters (CRWMS M&O 2000bo, Sections 3.3.1 and 3.3.2). Uncertainty analyses summarized in Volume 1, Sections 13.2 and 13.3 of *FY01 Supplemental Science and Performance Analyses* (BSC 2001a) discuss the potential impact of fixed or single input values instead of distributions for parameters limited by the GENII-S calculation process, as well as the sensitivity of biosphere modeling to alternative receptor concepts. The many individual model components, including fixed parameter values or constraints on receptor parameters, contribute to the overall uncertainty. The analyses and multiple lines of evidence indicate that mathematical uncertainties

contribute little additional uncertainty to the biosphere model (BSC 2001a, Section 13.2.2.2).

The principal results of the biosphere pathway analyses, biosphere dose conversion factors, are expressed as the radiation dose received from annual exposure to radionuclides in the environment for each unit of radioactivity concentration at the source of contamination. The dose conversion factors are then used in the TSPA-SR model and supplemental TSPA model analyses to estimate potential radiation dose based on the concentrations of a particular radionuclide at the source of that radionuclide (i.e., radioactivity per unit volume of well water for the contaminated groundwater use scenario, and activity per unit area of surface soil for the direct volcanic release scenario) (CRWMS M&O 2000a, Section 3.9; BSC 2001b, Section 2.2.2; Williams 2001a, Section 2; Williams 2001b, Section 2).

4.2.10.3.3 Biosphere Dose Conversion Factors for Contaminated Groundwater Use Scenario

For the contaminated groundwater use scenario, calculations of biosphere dose conversion factors were performed for radionuclides selected through an analysis designed to determine which radionuclides should be included in the TSPA-SR based on their expected contribution to the total potential dose (CRWMS M&O 2000dx). The groundwater contamination scenario is used to evaluate the radiological consequences of both undisturbed potential repository system performance and selected disruptive processes and events. The latter include the potential consequences of earthquakes and igneous intrusions, as well as consequences following a stylized human intrusion event (CRWMS M&O 2000bo, Section 3.1.5.1).

Radionuclide inventory was specified in terms of radionuclide concentrations in groundwater at the well head in units of pCi/L. The conversion factors, expressed as total effective dose equivalent from annual exposure (here also called annual dose) per unit activity concentration in groundwater, were calculated in units of mrem/yr per pCi/L. To incorporate the results of the calculations into the TSPA-SR predictive code in a computationally

efficient manner, statistical distributions were fitted to the biosphere dose conversion factor data and distribution parameters were determined (CRWMS M&O 2000bo, Section 3.3.1.1). As noted before, a distribution of biosphere dose conversion factors represents the uncertainty due to the possible variabilities and uncertainties in the input parameters used (BSC 2001a, Section 13.4.1.2).

When contaminated groundwater is used to irrigate agricultural soil, the concentration of each contaminant in the soil will build up at a rate determined by the chemical properties and radioactive half-life of the material. Long-lived isotopes of elements that bind readily to soil particles may not reach an equilibrium concentration in soil for many hundreds of years, whereas relatively short-lived or mobile radioisotopes may approach their maximum concentrations in soil after only a few years of irrigation (CRWMS M&O 2000bo, Section 3.3.1.1).

To account for the radionuclide buildup in soil, biosphere dose conversion factors were calculated for each of six periods of cumulative years of irrigation with contaminated groundwater (CRWMS M&O 2000bo, Section 3.2.4.1.2, Table 3-6). With these calculations, it was possible to evaluate whether potential buildup of radioactivity in soil would change the estimated radiation doses received by the receptor. The irrigation time periods are the number of years that the land has been irrigated with contaminated groundwater before the point in time for which the biosphere dose conversion factors are calculated. The periods of previous irrigation are correlated with the period of time it takes until the equilibrium radionuclide concentration in soil is reached under the continuous irrigation conditions. The first of the six sets of biosphere dose conversion factors were always calculated under the assumption of no prior irrigation (i.e., radionuclide contamination in soils is absent). The remaining five irrigation periods were selected so that the biosphere dose conversion factors at each period would be approximately equally spaced between their no-prior-irrigation values and their long-term asymptotic (leveling off) contamination levels.

Table 4-30 outlines the biosphere dose conversion factors and soil buildup factors calculated for the contaminated groundwater use scenario and the distributions recommended by project scientists for use in the TSPA-SR analyses. Most of the conversion factors presented in Table 4-30 increased with the duration of previous irrigation (increasing time steps) (CRWMS M&O 2000bo, Section 3.3.1.1.1, Table 3-17), reflecting radionuclide buildup in soil. Supplemental biosphere dose conversion factor for supplemental TSPA model analyses are described in Volume 1, Section 13.4.1 of *FY01 Supplemental Science and Performance Analyses* (BSC 2001a) and *Total System Performance Assessment—Analyses for Disposal of Commercial and DOE Waste Inventories at Yucca Mountain—Input to Final Environmental Impact Statement and Site Suitability Evaluation* (Williams 2001a, Section 5.2.5). The radionuclide-specific conversion factors represent combined contributions from all pathways under consideration for a particular exposure scenario. Not every pathway component is influenced by the changing radionuclide concentration

in soil. For example, the contributions to biosphere dose conversion factors due to ingestion of drinking water and the intake of the radionuclides that enter the food chain by deposition on plant surfaces during irrigation with contaminated water are insensitive to radionuclide buildup in soil. Examples of pathways that are sensitive to soil buildup include external exposure to radiation from contaminated soil, inhalation of resuspended soil particles, and radionuclide uptake by edible plants through their roots (CRWMS M&O 2000eq).

For most radionuclides, radionuclide buildup represented by the buildup factor was less than 15 percent (i.e., the soil buildup factor in Table 4-30 is less than 1.15). Because the estimated degree of buildup is not significant to the recommendation decision, for simplicity it was recommended that the biosphere dose conversion factor distributions appropriate to the longest periods of irrigation be used for these radionuclides (CRWMS M&O 2000bo, Section 3.3.1.1; CRWMS M&O 2000er, Section 7.1). These distributions

Table 4-30.   Biosphere Dose Conversion Factor and Soil Buildup Factors for Radionuclides Introduced into the Biosphere through Irrigation with Contaminated Groundwater

| Radionuclide | Biosphere Dose Conversion Factor | | Soil Buildup Factor | Leveling Off Period (years)[a] |
| | Geometric Mean | Geometric Standard Deviation | | |
	mrem/yr per pCi/L			
Thorium-229	5.392	1.167	2.85	8,448
Cesium-137	0.1841	1.163	2.21	78
Strontium-90	0.1121	2.736	1.93	53
Americium-243	5.030	1.163	1.62	5,031
Uranium-232	2.064	1.150	1.13	93
Plutonium-239	4.976	1.151	1.10	1,456
Plutonium-240	4.953	1.151	1.10	1,456
Americium-241	5.012	1.156	1.08	1,117
Uranium-238	0.3512	1.159	1.04	93
Uranium-233	0.384	1.161	1.03	93
Uranium-234	0.3769	1.162	1.03	93
Uranium-236	0.3564	1.164	1.03	93
Technetium-99	0.001495	1.8423	1.01	5
Plutonium-238	4.109	1.161	1.01	227
Actinium-227	18.01	1.162	1.01	56
Neptunium-237	6.738	1.163	1.01	14
Iodine-129	0.3562	1.1874	1.00	5
Carbon-14	0.00055	1.5177	1.00	7,401

NOTES: [a]Approximate times required for biosphere dose conversion factor buildup to reach asymptotic value.
Sources: CRWMS M&O 2000a, Table 3.9-2; CRWMS M&O 2000bo, Table 3-19.

(one for each radionuclide) can be efficiently sampled by the TSPA computer code to generate the dose to the defined receptor from radionuclide contamination in the groundwater.

Of the four radionuclides that displayed greater than 15 percent increase due to soil buildup, thorium-229 showed the greatest degree of buildup, increasing by a factor of 2.85 relative to prior conditions (CRWMS M&O 2000bo, Table 3-19). For thorium-229 and americium-243, in the absence of soil loss, the time to approach the buildup limit was a few thousand years. As reported in a previous analysis (CRWMS M&O 2000eq, Section 7.2), soil loss has a significant effect on biosphere dose conversion factor buildup for these three radionuclides. The effect of soil erosion on cesium-137, strontium-90, and uranium-232 (with much shorter GENII-S buildup time) was much less pronounced due to their relatively short half-life.

The GENII-S program does not consider the mechanism of radionuclide removal by soil erosion. However, this issue was addressed in an analysis (CRWMS M&O 2000eo, Section 6.1) focusing on the major soils present in the Amargosa Valley area near the proposed location of the receptor. These annual soil loss estimates were incorporated into the overall modeling calculations to account for radionuclide removal from the 15-cm (6-in.) surface soil layer. The rate of soil removal by erosion under natural conditions is generally in approximate equilibrium with the rate of soil formation from the transformation of underlying bedrock, alluvium, colluvium, or other geologic material comprising the parent material. Under these conditions, the soil depth (or thickness) is maintained at a near constant depth through time (Troeh et al. 1980, p. 4). Human activities, including tilling of cropland, removal of vegetation, and grazing of pasture or rangeland, typically tend to accelerate the natural rate of soil removal. Disturbed soil is generally left with less protection against the action of water and wind. Thus, the formation of new soil cannot keep pace with the accelerated erosion rate, and the soil material may progressively become thinner (Troeh et al. 1980, pp. 5 and 6). The annual rate of soil loss for the major soil series in the vicinity of the proposed

receptor generally was estimated to be between 0.06 and 0.08 cm/yr (0.024 to 0.031 in./yr) (CRWMS M&O 2000eo, Section 6.1.1).

The degree of buildup for thorium-229 and americium-243, once soil loss was considered, was sufficiently small (less than 20 percent) that there was little benefit of incorporating a probabilistic sampling for the time of previous irrigation. Thus, for simplicity, the asymptotic (i.e., long time irrigation buildup period) biosphere dose conversion factor mean was used. Although americium-243, thorium-229, and uranium-232 are predicted to have more significant buildup in soil, these radionuclides have not been significant contributors to dose in previous TSPA evaluations. For thorium-229 and americium-243, the periods needed for maximum buildup are 8,448 and 5,031 years, respectively, and continuous farming activity on a single plot of irrigated land over such extended periods of time is unlikely (CRWMS M&O 2000bo, Section 3.3.1.1). Comparing the mean values of biosphere dose conversion factors for the nominal scenario used in the TSPA-SR model (given in CRWMS M&O 2000er, Table 3) with the new data (CRWMS M&O 2001f, Section 7.2) indicates the small net effect of the change in biosphere dose conversion factors. The TSPA-SR model identified the radionuclides contributing most to annual dose as technetium-99, iodine-129, neptunium-237, and plutonium-239 (CRWMS M&O 2000a, Figure 4.1-6). As an indication of the relative differences for technetium-99, iodine-129, and neptunium-237, the revised biosphere dose conversion factor values are lower by no more than 20 percent than those used in TSPA-SR. The change for plutonium-239 in the biosphere dose conversion factor is less than 20 percent (BSC 2001b, Section 3.2.11.2).

The relatively small effect of updates to the biosphere model on the expected annual dose for the nominal scenario is reflected in the supplemental TSPA model results (BSC 2001b, Figure 3.2.11-1a). The mean annual dose using the updated uncertainty distributions for the biosphere dose conversion factors (BSC 2001a, Section 13.4.) is compared to the results calculated in the TSPA-SR model in Volume 2, Figure 3.2.11-1a of *FY01 Supplemental Science and Performance*

Analyses (BSC 2001b). The differences between the previously calculated annual dose (TSPA-SR base-case results) and the supplemental TSPA model results (of less than 10 percent in simulated annual dose for most times) do not constitute a large change (BSC 2001b, Section 3.2.11.2). Supplemental biosphere dose conversion factors for supplemental TSPA model and revised supplemental model analyses are described in Volume 1, Section 13.4.1 of *FY01 Supplemental Science and Performance Analyses* (BSC 2001a) and *Total System Performance Assessment—Analyses for Disposal of Commercial and DOE Waste Inventories at Yucca Mountain—Input to Final Environmental Impact Statement and Site Suitability Evaluation* (Williams 2001a, Section 5.2.5).

4.2.10.3.4 Biosphere Dose Conversion Factors for Direct Volcanic Release Scenario

The biosphere model for a direct volcanic release (volcanic eruption) considers both inhalation of contaminated ash during the eruption and radionuclide transport and uptake following the deposition of contaminated volcanic ash (CRWMS M&O 2000bo, Section 3.1.5.2). Human exposure may occur as a result of inhalation of fine particles of contaminated ash during the eruptive event, inhalation of resuspended ash after deposition, ingestion of larger particulates after inhalation both during and after the event, and ingestion of contaminated crops and animal products. Consumption of contaminated water, which is an important pathway for the nominal scenario, is not included as a pathway for the direct volcanic release scenario because there is no significant quantity of surface water in the Yucca Mountain region that might be contaminated by volcanic ash.

Ash concentrations in the air may be extremely high during the eruptive event, and humans who do not leave the region may be exposed to radiation by both inhalation and ingestion of particulates. Dose factors that account for inhalation of fine and coarse particulates were developed for an eruptive event duration spanning between 33 minutes and 73 days. Analysis of potential doses as a result of inhalation during the eruption shows that it is a minor contributor to total probability-weighted dose from volcanic eruption because of the relatively brief duration of the event compared to the long-term exposure that could occur from ash after it is deposited (CRWMS M&O 2000a, Section 5.2.9.9). The TSPA analyses of doses from direct volcanic releases were therefore focused on consideration of exposures incurred after contaminated ash is deposited. Detailed description of the processes and assumptions considered for the modeling of the scenario are in Section 3.10.3.1 of *Total System Performance Assessment for the Site Recommendation* (CRWMS M&O 2000a).

Biosphere dose conversion factors developed for the direct volcanic release scenario are outlined in Table 4-31. Seventeen radionuclides were identified as relevant for calculation of biosphere dose conversion factors under a volcanic (igneous activity) event contamination scenario (CRWMS M&O 2000a, Section 3.10.3.5, Table 3.10-8; CRWMS M&O 2000bo):

- Strontium-90
- Cesium-137
- Lead-210
- Radium-226
- Actinium-227
- Thorium-229
- Thorium-230
- Protactinium-231
- Uranium-232
- Uranium-233
- Uranium-234
- Plutonium-238
- Plutonium-239
- Plutonium-240
- Plutonium-242
- Americium-241
- Americium-243.

The list of radionuclides of interest is somewhat different than that considered for the contaminated groundwater use scenario because it reflects the radionuclide inventory directly released from the repository during a volcanic eruption, as opposed to radionuclides transported to the biosphere by groundwater in the saturated zone, where substantial retardation and sequestering of many radionuclides may occur within the geologic strata.

Table 4-31. Statistical Output for Direct Volcanic Release Scenario Biosphere Dose Conversion Factors for the TSPA-SR

Radionuclide	Biosphere Dose Conversion Factors (rem/yr per pCi/m²)	
	Arithmetic Mean	Arithmetic Standard Deviation
Strontium-90	1.22×10^{-8}	1.91×10^{-8}
Cesium-137	1.28×10^{-9}	1.52×10^{-9}
Lead-210	6.05×10^{-8}	6.68×10^{-8}
Radium-226	5.66×10^{-9}	3.42×10^{-9}
Actinium-227	7.34×10^{-7}	6.46×10^{-7}
Thorium-229	2.31×10^{-7}	2.06×10^{-7}
Thorium-230	3.47×10^{-8}	3.09×10^{-8}
Protactinium-231	1.63×10^{-7}	1.24×10^{-7}
Uranium-232	7.39×10^{-8}	6.45×10^{-8}
Uranium-233	1.50×10^{-8}	1.30×10^{-8}
Uranium-234	1.48×10^{-8}	1.28×10^{-8}
Plutonium-238	4.94×10^{-8}	3.78×10^{-8}
Plutonium-239	5.48×10^{-8}	4.19×10^{-8}
Plutonium-240	5.47×10^{-8}	4.19×10^{-8}
Plutonium-242	5.11×10^{-8}	3.91×10^{-8}
Americium-241	5.60×10^{-8}	4.27×10^{-8}
Americium-243	5.59×10^{-8}	4.26×10^{-8}

Source: CRWMS M&O 2000a, Table 3.10-8.

Revised volcanic eruption scenario biosphere dose conversion factors are developed for evaluation of transition and steady-state phases of a potential eruption. Mass loading is the most important biosphere model parameter distinguishing the different phases of the scenario. The impact of mass loading and the development of updated biosphere dose conversion factors is described in Volume 1, Section 13.4.3 of *FY01 Supplemental Science and Performance Analyses* (BSC 2001a). Table 13.4-10 in Volume 1 of *FY01 Supplemental Science and Performance Analyses* (BSC 2001a) summarizes the updated biosphere dose conversion factors for the volcanic eruption scenario.

The receptor of interest for the direct volcanic release scenario was the same as used in the nominal groundwater release scenario. Radionuclide inventory was specified in terms of basic concentrations that exist after transport of volcanic ash has occurred. The inventory activity concentration units selected (pCi for activity and m² for soil inventory) resulted in basic concentrations in surface soil in the units of pCi/m². Biosphere dose conversion factors expressed as annual total effective dose equivalent per unit activity deposition, per unit area, were calculated in units of rem/yr per pCi/m².

As with the case of biosphere dose conversion factors for the contaminated groundwater use scenario, calculations of conversion factors for the direct volcanic release scenario were performed in a series of probabilistic runs to propagate the uncertainties of input parameters into the output. A Latin Hypercube sampling method (a form of stratified Monte Carlo sampling) was used in the stochastic (probabilistic) analysis with the number of realizations set to 160, which was the maximum that the software could perform due to its computing limitation. However, it was determined that this number of realizations was sufficient to obtain statistically valid results (CRWMS M&O 2000bo, Section 3.3.2).

Input values were reflective of the air quality conditions (increased dustiness) following volcanic eruption (CRWMS M&O 2000bo, Section 3.3.2.2). Specifically, probability distribution functions of total suspended particulates in air and of the respirable fraction of suspended particulates were developed based on the documented air quality data from volcanic eruptions, such as Mount St. Helens and Montserrat. These data were also used to develop other GENII-S parameters whose values were affected by the conditions of increased particulate concentration in air, such as the crop resuspension factor and the inadvertent soil ingestion.

Similar to the case of groundwater contamination, the effects of surface soil removal by erosion were included in the evaluation of the expected annual dose to the receptor from volcanic eruption (CRWMS M&O 2000a, Section 3.10.3.2).

Reevaluation of factors influencing the biosphere dose conversion factors for the volcanic eruption scenario (BSC 2001a, Section 13.4.3) results in updated uncertainty distributions of biosphere dose conversion factors. The particulate concentration in air increased by a factor of 2.5 (BSC 2001a, Section 13.3.6), resulting in an increase in

biosphere dose conversion factors that propagates through to potentially significant changes to the predicted dose. Biosphere dose conversion factors are developed for three phases (eruption, transition, and steady-state) during and following the assumed volcanic eruption. The biosphere dose conversion factor distributions for the transition phase (BSC 2001a, Section 13.4.3) are the more conservative values used in supplemental TSPA model calculations. The biosphere dose conversion factors that are applicable for the eruption phase are not used in TSPA analyses because of the short duration of the eruptive phase. The transition phase biosphere dose conversion factors are conservative relative to the biosphere dose conversion factors for the steady-state phase following eruption because the volcanic ash is more available for resuspension in air during the transition phase. The case with the highest biosphere dose conversion factors (i.e., the 1-cm [0.4-in.] thick ash layer with annual average airborne particulate concentration) is used for supplemental TSPA model analyses (BSC 2001b, Section 3.2.11.2). The expected mean annual dose using the updated uncertainty distributions for the volcanic eruption biosphere dose conversion factors compared to the results calculated in TSPA-SR is approximately 2.5 times greater. This represents a significant increase relative to previous results and is primarily due to the increase in the respirable fraction of particulate concentration in air within the biosphere model (BSC 2001a, Section 13.3.6.2). However, the higher expected annual dose from direct exposure to contaminated volcanic ash using the updated volcanic eruption biosphere dose conversion factors is still lower than the expected annual dose from the igneous groundwater pathway at later times (compare to Figure 4.2-1 of *Total System Performance Assessment for the Site Recommendation* [CRWMS M&O 2000a]).

4.2.10.3.5 Limitations and Uncertainties

A review of the list of FEPs applicable to the Yucca Mountain Project identified primary FEPs that were potentially applicable to the biosphere (CRWMS M&O 2000bo, Section 3.1.3). Each of these primary FEPs was screened to determine if it was applicable to Yucca Mountain considering the proposed NRC regulations (10 CFR Part 63 [64 FR

8640]) and the local environment. The results of this screening process are outlined in Appendix B of the *Biosphere Process Model Report* (CRWMS M&O 2000bo). Additional screening of biosphere FEPs, consistent with EPA and NRC rules, is discussed in *Evaluation of the Applicability of Biosphere-Related Features, Events, and Processes (FEPs)* (BSC 2001t, Section 6.1). Those FEPs which were screened out as not applicable to Yucca Mountain included either (1) issues precluded from consideration by the proposed NRC regulations (e.g., social and institutional development, technical development, species evolution) or (2) FEPs that were deemed unlikely to occur in the Yucca Mountain biosphere (e.g., capillary rise of water from the saturated zone to the repository, marine features).

As with any modeling effort, uncertainty is inherent in the biosphere model (CRWMS M&O 2000bo, Sections 3.3.1.2 and 3.3.2.2). This means that modeling results carry uncertainty resulting from both uncertainties in the model itself and uncertainties in model parameters. Uncertainty and sensitivity analyses were used to assist in interpreting the results of analysis. The probabilistic approach was used for both sensitivity and uncertainty analyses. The objective of sensitivity analysis was to determine which parameters affect the model results the most, whereas the objective of uncertainty analysis was to determine how the uncertainty in model parameters affects the model results.

Uncertainty analysis shows quantitatively the effect of propagation of input parameter uncertainties on the resulting biosphere dose conversion factors. Uncertainty in the modeling results includes contribution from both the model and the parameter uncertainty. Uncertainty analysis for the conversion factors was focused on the parameter uncertainty, which represents uncertainty in the data, parameters, and coefficients used in mathematical models and the supporting computer program, GENII-S. Parameter uncertainty originates from a number of sources including uncertainty in determining parameter and coefficient values used in the biosphere model, and uncertainty associated with the temporal and spatial heterogeneity of the biosphere system.

Contribution of parameter uncertainty to the overall uncertainty of the modeling outcome can be more readily quantified than model uncertainty. In the case of the biosphere modeling, the probabilistic approach was taken which allows statistical sampling of parameter values described by their probability distribution functions.

Because the biosphere environment is complex in nature, any representation of the contaminant transport pathways is a simplified version of the reality on which it is based. For the TSPA-SR, some input parameters were obtained through field measurements and the regional survey, while others were derived from existing literature. The parameters used in the biosphere analyses can be classified into two main categories: (1) parameters that influence, or are related to, the transport and accumulation of radionuclides in the biosphere; and (2) parameters related to characteristics of the receptor (i.e., consumption patterns, lifestyle characteristics, and land use). Each parameter value or range of values used represented either a reasonable or conservative estimate regarding potential contribution to the total dose to the receptor. The GENII-S computer code allows the representation of certain input parameters as variable in nature (probability distributions), while others may only be represented as fixed values. The parameters selected for use in the biosphere analyses are described in detail in the *Biosphere Process Model Report* (CRWMS M&O 2000bo, Section 3.2.4).

In the TSPA-SR biosphere analyses, the assessment philosophy is to use generally conservative assumptions to ensure that the results are unlikely to underestimate the corresponding values of dose conversion factors for the radionuclide transport and uptake conditions and mechanisms considered. For example, it is conservatively assumed that all (100 percent) of the water used or consumed in the biosphere is contaminated. This assumption applies to several aspects of the total biosphere model, including parameters that describe:

- Drinking water for human consumption

- Water for beef cattle and dairy cow consumption

- Water for poultry and laying hen consumption

- Irrigation water for terrestrial food production (leafy and root vegetables, fruit, and grain for human consumption)

- Irrigation water for production of fresh and stored feed for animals used directly or indirectly as food sources.

A thorough discussion on the various GENII-S input parameters and the degree of conservatism assumed for these parameters are in Section 3.2.4 of the *Biosphere Process Model Report* (CRWMS M&O 2000bo).

Limitations to the biosphere pathway analyses are generally associated with the uncertainty within the mathematical representation of the conceptual model and the input parameters used in the analyses. Input parameters were quantified using site specific data and other accepted information (e.g., government publications, and journal articles and reports). Validation of the biosphere process concluded that the combination of the conceptual model, appropriately selected input parameters, and the mathematical expressions of the processes involved are valid for use in evaluating the Yucca Mountain biosphere (CRWMS M&O 2000bo, Section 5.2).

Sensitivity and pathway analyses were conducted for the biosphere dose conversion factors calculated for both the contaminated groundwater irrigation scenario and the disruptive event scenario. The purpose of these analyses was to determine which pathways and input parameters have the greatest influence on the biosphere dose conversion factors. Uncertainty analysis shows quantitatively the effect of propagation of input parameter uncertainties on the calculated conversion factors. Information on pathway sensitivity, input parameter sensitivity, and biosphere dose conversion factor uncertainty provides a context for the estimates of biosphere dose conversion factors while focusing attention and resources on parameters and modeling decisions that could have the greatest influence on the calculations for the various scenarios (CRWMS M&O 2000es). Details

on the methodology used to conduct the sensitivity and uncertainty analyses are provided in Sections 3.3.1.2 and 3.3.2.2 of the *Biosphere Process Model Report* (CRWMS M&O 2000bo).

Additional analyses discussed in Volume 1, Section 13.3 of *FY01 Supplemental Science and Performance Analyses* (BSC 2001a) provides a better understanding of various uncertainties and sensitivities inherent in the biosphere model. Of special interest to the biosphere model is the sensitivity of the mathematical code to alternative receptor concepts (details of dietary and lifestyle definition). The receptor in the biosphere model is evaluated as a source of uncertainty by varying the dietary characteristics. Uncertainty due to the receptor is likely to be bounded by the biosphere dose conversion factors used in the TSPA-SR model (BSC 2001a Section 13.3.1.8). Other uncertainties evaluated included the effect of the partition coefficients on biosphere dose conversion factors, the impact of fixed ingestion pathway parameters inputs within GENII-S, and water-usage in future cooler, wetter climates. GENII-S treats radionuclide accumulation in and depletion from the surface soil. The depletion (leaching and removal by decay or plant uptake) is subject to uncertainty of a fixed input parameter (partition coefficient of the element). For certain radionuclides, a large change in the assumed coefficient causes an insignificant change (few tens of percent) while changes for other radionuclides are more significant (increase by a factor of five). The net effect can be approximated resulting in an increased spread in the distribution in the biosphere dose conversion factors representing increased total uncertainty in the biosphere model if applied (BSC 2001a, Section 13.3.3). Additional uncertainty due to fixed ingestion pathway parameters can be approximated with large estimated uncertainties noted for important radionuclides (BSC 2001a, Section 13.3.4). The water-usage uncertainty analysis predicted a decrease for the cooler, wetter (future glacial-transition) climate (BSC 2001a, Section 13.3.5). The overall uncertainty associated with the mathematical model is not quantified; however, the multiple lines of evidence indicate that the mathematical uncertainties contribute little additional model uncertainty (BSC 2001a, Section 13.2.2).

For the contaminated groundwater use scenario, the inhalation and external exposure pathways are not significant, and the ingestion pathway accounts for essentially all of the biosphere dose conversion factor. The most important parameters for all radionuclides of interest, except carbon-14 and cesium-137, are ingestion of drinking water, followed by ingestion of leafy vegetables. Consumption of fish, assumed to be raised in large, man-made containers filled from groundwater sources, is the greatest contributor (more than 90 percent) of carbon-14. Fish consumption is the leading contributor to the conversion factor for cesium-137, followed by drinking water, leafy vegetables, and meat. Additional pathway exposure analysis confirms the importance of the ingestion pathway within the biosphere dose conversion factors (BSC 2001a, Section 13.4.1.4).

4.2.10.3.6   Alternative Conceptual Processes

As stated previously, no alternative conceptual models were developed for the overall biosphere modeling process consistent with the licensing-related regulatory framework (CRWMS M&O 2000bo, Section 3.5). In addition, review of publicly available documents produced by the DOE and external agencies and organizations indicates that there are no alternative conceptual processes or major opposing views to the overall biosphere analysis process consistent with the regulatory framework. The main reason for the absence of opposing views regarding alternative conceptual models is that the strategy for conceptualizing the biosphere pathway analyses is consistent with similar activities being pursued by the international scientific community (BIOMOVS II Steering Committee 1994; BIOMOVS II 1996; National Research Council 1995). Furthermore, the biosphere analyses have been based on the reference biosphere consistent with the licensing-related regulations (10 CFR Part 63 [66 FR 55732]). This limits the biosphere system being studied/modeled as well as alternative locations for the reasonably maximally exposed individual or future population and socioeconomic considerations.

4.2.10.3.7   Model Calibration and Validation

Model validation is a process used to establish confidence that a conceptual model represented in a mathematical model, by software, or by other analytical means, adequately represents the phenomenon, process, or system under consideration. In the case of the biosphere pathway analyses for the potential repository at Yucca Mountain, complete validation of the model is not feasible because direct observation of the actual outcome will not be possible for many years to come, if ever. However, an independent technical review of the model was commissioned to enhance confidence in the biosphere conceptual model (CRWMS M&O 2000bo, Section 3.2.3). A variety of reports with a similar scope were evaluated, and it was determined that the biosphere model developed does reasonably reflect the environmental conditions in the Amargosa Valley. The review also concluded that the methods, references, and data sources used by the analysts were sound and that the GENII-S input values were reasonable for the environment conditions of the biosphere pathway analyses (CRWMS M&O 2000bo, Section 3.2.3).

The GENII-S code was also subjected to the DOE software qualification process (CRWMS M&O 1998k). The qualification process makes use of test cases supplied by the software developer to verify that the software, as installed on project computers, produces outputs that are consistent with values expected for a prescribed set of inputs. Additionally, a special test case tailored to exercise all the GENII-S pathways and features relevant to Yucca Mountain analyses was developed. The expected results of the analysis were calculated by hand using the equations from the GENII-S mathematical model. Agreement of the GENII-S results and hand calculations were found to be within ±5 percent, and the code was subsequently designated as qualified software. Finally, an analysis was conducted to evaluate the reconciliation of the biosphere dose conversion factors for the Yucca Mountain case with other dose calculations obtained by the GENII-S and GENII (the predecessor code to the GENII-S code). Project scientists identified several recent applications of the codes that provided a basis for comparison of the predicted dose to a receptor as a consequence of exposure to radioactive contaminants in surface soil and groundwater. The annual total effective dose equivalent from unit concentrations of various radionuclides in groundwater and soil was then inferred from the different calculations and compared to the dose conversion factors for the Yucca Mountain case. This comparative analysis showed that the calculated Yucca Mountain biosphere dose conversion factors were largely consistent with the estimated dose per unit activity concentrations in groundwater and soil, once the effects of the different input parameter values and settings associated with the various applications were taken into account.

4.2.10.4   Total System Performance Assessment Abstraction

4.2.10.4.1   Contaminated Groundwater Use Scenario

To obtain annual radiation dose (mrem/yr) to the receptor (the reasonably maximally exposed individual in supplemental and revised supplemental TSPA analyses), the biosphere dose conversion factor (mrem/yr per pCi/L) for each radionuclide calculated in the biosphere pathway analyses was multiplied by its corresponding concentration (pCi/L) in the groundwater at the accessible environment.

The steps that occur within the TSPA model to calculate annual dose are as follows. Radionuclide amounts in groundwater are specified in terms of mass flux (specified in units of grams per year [g/yr]) which, when multiplied by the activity for the particular radionuclide (in units of curies per gram [Ci/g]), is converted to an activity flux. When divided by the water-usage volume of the hypothetical farming community (specified in units of liters per year [L/yr]), the activity flux is converted to an activity concentration, specified in units of picocuries per liter (pCi/L). The biosphere dose conversion factors, expressed as annual dose per unit activity concentration in groundwater, are calculated in units of mrem/yr per pCi/L. Thus, the radionuclide concentration in the water-usage volume is multiplied by the appropriate biosphere dose conversion factor to determine the annual dose (in units of rem/yr). The annual dose is there-

fore the sum of the products of the biosphere dose conversion factors for each radionuclide and the radioactivity available for each radionuclide from agricultural and domestic processes, based upon the groundwater concentrations.

4.2.10.4.2 Direct Volcanic Release Scenario

In the case of the direct volcanic release scenario, volcanic ash contaminated with radionuclides is assumed to be dispersed in the air and eventually settles to the ground, thereby contaminating the agricultural soils in the reference farming community. The biosphere exposure scenario involves individuals exposed to contaminated ash during and following volcanic eruption. Biosphere dose conversion factors for the volcanic eruption are expressed in units of rem/yr per pCi/m^2.

Within the TSPA model, the areal mass of a radionuclide in the ash deposited on the ground surface is calculated, considering radioactive decay and soil removal. The areal mass is then converted to areal activity, and the areal activity is multiplied by the appropriate biosphere dose conversion factor to realize the annual total effective dose equivalent for that radionuclide. Within the model, at every time step, the annual doses for all the radionuclides are summed to determine the total annual dose. Doses are calculated separately for the volcanic eruptive release mechanism, igneous intrusion groundwater release mechanism, and the nominal scenario. These doses are subsequently combined to obtain the expected annual dose to the receptor.

The probability-weighted dose attributed to the direct volcanic release scenario is combined with the dose attributed to contaminated groundwater use (nominal scenario) to calculate the total system dose to the receptor of interest.

For the overall TSPA-SR analyses and supplemental TSPA model, uncertainties in the biosphere modeling input parameters were carried forward in the TSPA calculations by sampling from the full distribution for the biosphere dose conversion factors developed by the biosphere process model.

4.3 SCENARIOS OF FUTURE CONDITIONS THAT COULD AFFECT REPOSITORY PERFORMANCE

The TSPA examines a range of possible future conditions (i.e., features, events, and/or processes) that could affect the repository's long-term performance. The TSPA considers a range of possible future conditions because it is not possible to forecast future conditions precisely. The uncertainty in future conditions is due to a combination of limited information about the FEPs that could affect repository performance and the inherent variability or randomness in natural processes. In principle, more information can be gained through further testing and analysis. However, complete knowledge is unattainable because investigations of site features must sample limited parts of the site, and monitoring of events and investigations of long-term processes must be conducted over limited periods of time.

The condition identification and screening process that is described below ensure that potentially relevant FEPs are considered in the TSPA. The amount of uncertainty associated with each feature, event, or process will vary. However, one of the key advantages of TSPA as an analytical and decision-aiding tool is that it provides a structured framework for expressing and evaluating the significance of uncertainties in future conditions. The structured screening process and the TSPA ensure that the range of possible future conditions are factored explicitly into the projections of repository performance. The uncertainty in inputs to the TSPA results in a range of possible future outcomes (i.e., a range of possible future doses to the receptor group). Probabilities assigned to the various TSPA inputs are carried through the analysis so that the range of potential doses is defined by a probability distribution. The mean dose can then be calculated from the probability distribution.

The TSPA approach followed here uses scenarios to evaluate the significance of uncertainty in the future system conditions and to assess its impact on projected exposures. Scenarios are combinations of possible future conditions and are grouped into two general categories: (1) a nominal scenario and

(2) disruptive scenarios. The nominal scenario includes the most likely conditions that could occur in the future (e.g., climate change, seismic activity, or repository heating). The disruptive scenario category includes conditions that are very unlikely (e.g., nuclear criticality, or water table rise) but that could, if they were to happen, adversely impact the capability of the repository system to isolate radioactive waste.

As noted in Section 4.1.1.2, the DOE has initiated several activities to improve the treatment of uncertainty in current models. Additionally, as noted in Section 4.1.4, the DOE has evaluated the possibility of mitigating uncertainties in modeling long-term repository performance by operating the design described in this report at lower temperatures. The nominal scenario (particularly with respect to repository heating) and the disruptive scenarios described above have been reevaluated and documented in *Yucca Mountain Preliminary Site Suitability Evaluation* (DOE 2001b).

The following sections provide additional information and background on how the DOE arrived at the scenarios that were analyzed for this report. Specifically, the subsequent sections focus on:

- Outlining the systematic methodology used to select the scenarios analyzed to evaluate repository system performance

- Describing the characteristics of the nominal, disruptive, and human intrusion scenarios considered in the TSPA

- Explaining the basis for the exclusion of certain scenarios historically debated by scientists.

More detailed technical information on future system conditions and scenarios can be found in the *Total System Performance Assessment for the Site Recommendation* (CRWMS M&O 2000a), *FY01 Supplemental Science and Performance Analyses* (BSC 2001a; BSC 2001b), *Total System Performance Assessment—Analyses for Disposal of Commercial and DOE Waste Inventories at Yucca Mountain—Input to Final Environmental Impact Statement and Site Suitability Evaluation*

(Williams 2001a), *The Development of Information Catalogued in REV00 of the YMP FEP Database* (Freeze et al. 2001), and a series of analysis model reports on FEPs (e.g., BSC 2001t; CRWMS M&O 2000cx, 2000ef, 2000et, 2000eu, 2000ev, 2000ew, 2000ex).

4.3.1 Methodology for Developing Scenarios

The method used to develop the nominal and disruptive scenarios is summarized on Figure 4-156 and in the following five sections. A more detailed explanation of the scenario development methodology can be found in *Total System Performance Assessment—Site Recommendation Methods and Assumptions* (CRWMS M&O 2000ey).

As used in this report, a scenario is defined as a combination of FEPs. In the specific context of scenarios, features are physical, chemical, thermal, or temporal characteristics of the site or repository system. Examples of features are fracture systems or faults. Processes are typically phenomena and activities that have gradual, continuous interactions with the repository system or subsystem. Percolation of meteoric water into the unsaturated rock layers above the potential repository is an example of a process. Events and processes can be interrelated, but in general, events are discrete occurrences for which probability and consequence can be assessed. Volcanism, for example is an event that is relevant to disruptive scenarios.

Step 1: **Identify and Classify Potentially Relevant Conditions**—The DOE assembled an initial list of possible future conditions (i.e., FEPs) that could affect the repository system using a draft list in the Nuclear Energy Agency's working group database (NEA 1999b). Scientists working on nuclear waste programs in several countries compiled this comprehensive database as a collaborative effort. They identified generic future conditions using a variety of methods, which included informal expert elicitation, judgments of subject matter experts, logic tree analyses, stakeholder reviews, and regulatory criteria. The Nuclear Energy Agency database, which currently contains more than 1,200 entries for future conditions, was constructed using input from scientists

Identify and Classify Future Conditions
Potentially Important to Postclosure
Performance

Screen List of Future Conditions Using
Probability and Consequence to Determine
Inclusion and Exclusion of Specific Conditions

Construct Nominal and Disruptive
Scenarios from Retained Future Conditions

Screen Disruptive Scenarios Using
Probability and Consequence Criteria

Specify the Characteristics of Nominal
and Disruptive Scenarios and Implement
in TSPA

PSWIFT1NRC.125NRC.9/28/98 11

00050DC_ATP_Z1S43_fig-12.cdr

Figure 4-156. Major Steps in Scenario Selection Methodology

affiliated with the U.S. Waste Isolation Pilot Plant program; Canadian, Swiss, and Swedish spent nuclear fuel programs; and the intermediate- and low-level waste programs of the United Kingdom.

The DOE expanded the initial list of potential future conditions by adding site-specific FEPs identified in previous Yucca Mountain performance assessment studies (Ross 1987; Wilson, M.L. et al. 1994, Section 3.2; CRWMS M&O 1995, Section 2.7). These additional future conditions represent the specific and unique geologic and hydrologic characteristics of the Yucca Moun-

tain region. They also reflect future conditions that could affect the repository facility, waste package, and other engineered barriers.

The DOE developed an electronic database with over 1,700 entries from the Nuclear Energy Agency and DOE lists of potential future conditions. The entries in the DOE database were classified using the Nuclear Energy Agency's classification method. The DOE streamlined the database by combining similar entries and organizing them into primary and secondary categories. The primary entries, which collectively form a site-

specific list of future conditions, then went into the scenario methodology. The entries that were redundant or that otherwise could be appropriately combined into a single representation of a future condition were placed in a secondary category. The rationale for primary and secondary categorizations is described in the DOE's database (Freeze et al. 2001). Eleven additional FEPs were added to the list in 2001 (Freeze et al. 2001).

Step 2: **Screen the List of Future Conditions**—The next step in the scenario methodology, shown in detail in Figure 4-157, involved refining the list by excluding future conditions due to low probability or consequence consistent with NRC licensing-related regulations (see 10 CFR 63.114(c) and (d) [66 FR 55732]). These criteria establish the technical basis for excluding FEPs from further analysis.

The first reason involves the probability of the event occurring (10 CFR 63.114(d) [66 FR 55732]). The TSPA considers events that have at least 1 chance in 10,000 of occurring in 10,000 years. Therefore, any event with an estimated probability of occurrence less than 10^{-4} in 10^4 years was excluded from further consideration in the TSPA. For example, an impact by a meteorite is a low-probability event not considered in the TSPA because the estimated probability for this event is about 10^{-12} per year (Ross 1987, p. 42).

The second reason addresses the significance of the radiological consequences of potential future conditions. The DOE did not consider, in detail, potential future FEPs with low consequences. For example, surface processes that are certain to occur, such as erosion and sedimentation, have no significant impact on a repository's capability to meet the radiation protection standard and were, therefore, excluded from consideration in the TSPA.
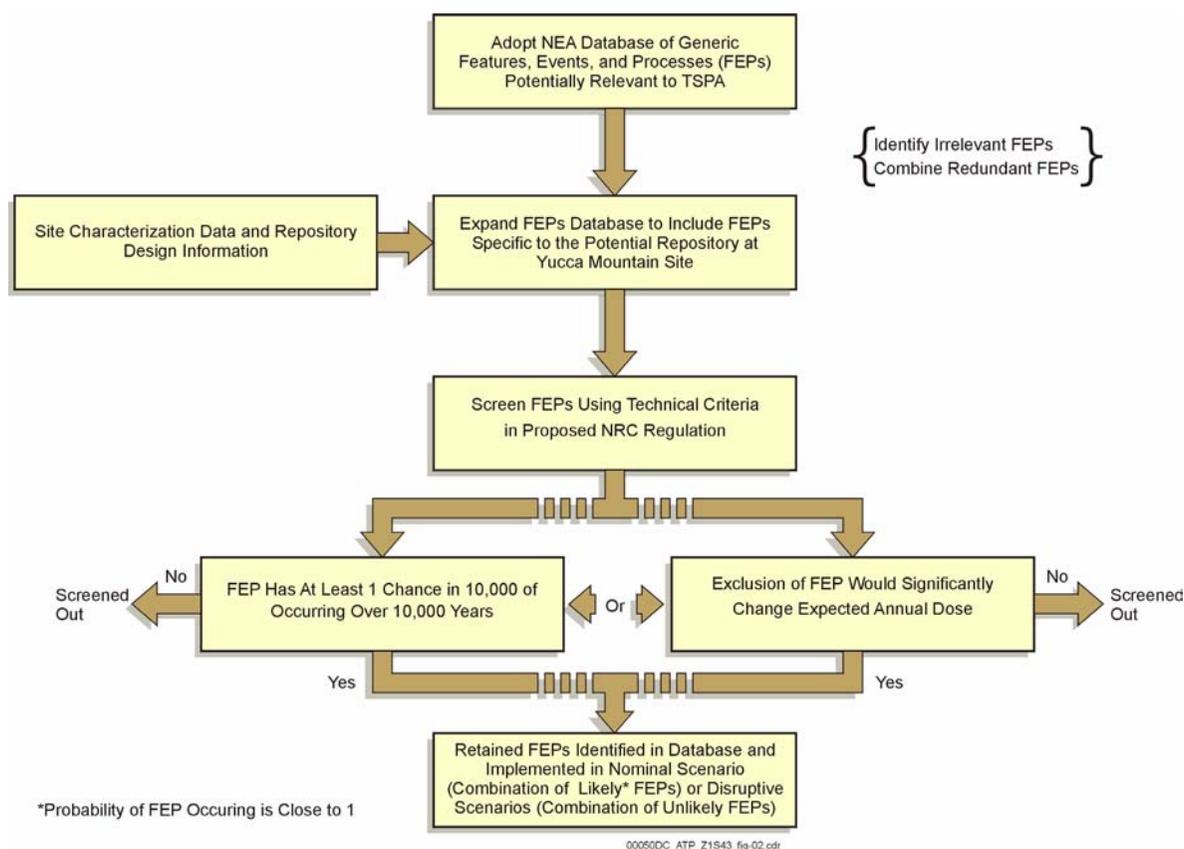
Figure 4-157. Schematic Illustration of the Screening Process
NEA = Nuclear Energy Agency.

Step 3: **Construct Nominal and Disruptive Scenarios**—The nominal scenario was constructed using all expected conditions (i.e., future conditions that are very likely to operate after closure) that were retained after screening. Stated simply, the nominal scenario represents the most plausible evolution of the geologic repository system and includes both favorable and adverse (e.g., seismicity) future conditions. Similarly, disruptive scenarios were developed using combinations of the adverse future conditions. These disruptive scenarios represent low-probability (but greater than the screening probability) perturbations to the expected evolution of the geologic repository system. To a limited extent, logic diagrams (Cranwell et al. 1990), which are mathematically equivalent to the NRC "Latin square" approach (NRC 2000c, Section 4.4.2), have also been used. Both approaches provided a systematic and transparent method for establishing all possible combinations of disruptive conditions and for calculating the probabilities of those combinations (Wescott et al. 1995, Chapter 3). In addition, the logic diagrams were used to establish the empirical probability for the nominal scenario (i.e., computed by taking one minus the sum of the disruptive scenario probabilities).

Step 4: **Screen Scenarios**—Analysts further refined the specification of the nominal scenario and screened the initial set of disruptive scenarios. The screening of the disruptive scenarios was performed using probability and consequence discussed in the previous screening step. As a result of this screening, a number of scenarios associated with faulting, nuclear criticality (within 10,000 years following emplacement), and water table rise were eliminated from consideration. In addition, the scenarios were reviewed by groups of subject matter experts to ensure that the uncertainties in future conditions were properly represented.

Step 5: **Implement Scenarios for Total System Performance Assessment**—Collectively, the nominal scenario and selected disruptive scenario (i.e., igneous activity) effectively specify the range of possible future events and processes that could affect the repository's capability to provide long-term isolation of the radioactive waste. The TSPA evaluates each scenario separately to account for

the uncertainties in models and parameters. TSPA calculations for the individual scenarios and the overall evaluation are summarized in Section 4.4 and documented in more detail in *Total System Performance Assessment for the Site Recommendation* (CRWMS M&O 2000a). Additional calculations are documented in *FY01 Supplemental Science and Performance Analyses* (BSC 2001a; BSC 2001b). Further supplemental calculations are documented in *Total System Performance Assessment—Analyses for Disposal of Commercial and DOE Waste Inventories at Yucca Mountain—Input to Final Environmental Impact Statement and Site Suitability Evaluation* (Williams 2001a).

4.3.2 Scenarios Considered in Total System Performance Assessment

The potential repository's capability to isolate radioactive waste is evaluated by modeling scenarios of the evolution of the geologic system and the occurrence of unlikely adverse conditions. Using the systematic procedure described in Section 4.3.1, earth scientists and engineers have developed scenarios of future system evolution and unlikely adverse conditions. These scenarios, which were developed by combining FEPs relevant to the site, are grouped into two basic categories: a nominal scenario and disruptive scenarios.

The nominal scenario includes the most likely FEPs expected to occur in the future (e.g., climate change, repository heating). The disruptive scenario category includes adverse conditions that are extremely unlikely (e.g., volcanism) but that could, if they were to happen, significantly reduce the capability of the repository to isolate waste. In addition to analyses of scenarios in these two categories, the TSPA analyzes a separate scenario for human intrusion, which assumes a drill hole penetrating the repository during a hypothetical groundwater exploration operation.

The following are examples of specific disruptive conditions that were considered in the TSPA evaluation:

- **Igneous activity**—Magmatic processes causing releases of radioactive wastes directly (i.e., to the atmosphere) and/or indi-

rectly (i.e., in the subsurface) into the environment (disruptive scenario)

- **Seismic activity**—Vibratory ground motion and fault displacement potentially causing damage to the engineered barriers and/or alteration of the performance attributes of the natural barriers (nominal scenario)

- **Human intrusion**—Inadvertent drilling through the repository and penetrating a single waste package, causing radionuclide releases to the groundwater aquifer (human intrusion scenario).

Igneous activity (or, alternatively, volcanism) was the principal disruptive scenario retained after the comprehensive screening/selection process described in Section 4.3.1. Potential seismic effects on the underground facilities and waste packages were screened out (i.e., excluded from consideration) because the waste packages would not be adversely damaged by design basis rockfalls or vibratory ground motion (CRWMS M&O 2000ex, Section 6.2). However, because vibratory ground motion from seismic events might damage the commercial spent nuclear fuel cladding, the effect of this potential damage to cladding by a discrete seismic event is included in the TSPA model in the nominal scenario. The frequency assumed for this event is 1.1×10^{-6} per year. For this analysis, when the vibratory ground motion event occurs, all commercial spent nuclear fuel cladding in the repository is assumed to fail by perforation, and further cladding degradation is calculated according to the cladding degradation. A drilling scenario of inadvertent human intrusion is considered in a separate TSPA calculation.

The following sections provide background information relevant to the disruptive scenarios that have been considered in the TSPA.

4.3.2.1 Volcanic/Igneous Activity

For more than two decades, scientists have performed extensive volcanism studies at Yucca Mountain. Their studies identified the location, age, volume, geochemistry, and geologic setting of past volcanic activity in the area. The results from

these studies are described in *Yucca Mountain Site Description* (CRWMS M&O 2000b, Section 12.2). Although scientists cannot predict future volcanic activity with total certainty, the resulting data provide a comprehensive basis for estimating the probability of future volcanic activity and for determining the effects on people and the environment if volcanic activity were to disrupt the potential repository (CRWMS M&O 2000f, Section 3.1).

4.3.2.1.1 Past Volcanic Activity in the Yucca Mountain Region

Volcanoes have played an important role in the development of the Yucca Mountain region. From 15 million to about 7.5 million years ago, a series of large, silicic, explosive volcanic eruptions occurred in the region. These eruptions produced dense clouds of incandescent volcanic glass (silica), ash, and rock fragments, which melted or compressed together to create layers of rock called tuff. Some of the explosive volcanoes in the Yucca Mountain region formed large calderas as much as 20 km (12 mi) in diameter. Calderas are circular depressions that form when large volumes of magma erupt rapidly, causing the volcano's surface to collapse.

The large-volume, silicic type of volcanic activity no longer occurs in the Yucca Mountain region and has not occurred for more than 7.5 million years. The layers of ash-fall and ash-flow tuff formed by these eruptions have since been disrupted by faulting and erosion. The subsurface bedrock units of Yucca Mountain are made up of ash-fall and ash-flow tuffs that were deposited approximately 13 million years ago, during the episode of silicic volcanism.

Basaltic volcanism began during the latter part of the caldera-forming phase, as rates of extension of the earth's crust waned; small-volume basaltic volcanism continued in the Quaternary Period (the past approximately 2 million years). Collectively, the calderas and basaltic eruptions in the Yucca Mountain region are called the southwestern Nevada volcanic field (Sawyer et al. 1994). Approximately 99.9 percent of the volume of the southwestern Nevada volcanic field erupted

between 15 and 7.5 million years ago. The last 0.1 percent of eruptive volume of the volcanic field, consisting entirely of basalt, erupted since 7.5 million years ago. Considered in terms of total eruption volume, frequency of eruptions, and duration of volcanism, basaltic volcanic activity in the Yucca Mountain region defines one of the least active basaltic volcanic fields in the western United States (CRWMS M&O 2000ez, Section 6.2).

In the Yucca Mountain region, there are more than 30 basaltic volcanoes that were formed between 9 million and 80,000 years ago. These volcanoes can be separated into two distinct periods of volcanism that are separated both temporally and spatially. The older basaltic volcanoes formed between about 9 and 7.3 million years ago (during the Miocene epoch). The younger (post-Miocene) basaltic volcanoes erupted between approximately 5 million and 80,000 years ago. As shown in Figure 4-158, the general location of the younger, post-Miocene volcanoes shifted substantially to the southwest (CRWMS M&O 2000ez, Section 6.2).

The post-Miocene volcanoes were formed during at least six different episodes that occurred within 50 km (31 mi) of the proposed Yucca Mountain repository (Figure 4-158). Three of these episodes produced six cinder cones that are in or near the Crater Flat basin, within 20 km (12 mi) of Yucca Mountain (Figure 4-159). The latest volcanic episode, about 80,000 years ago, created the Lathrop Wells Cone, about 18 km (11 mi) south of the potential repository site.
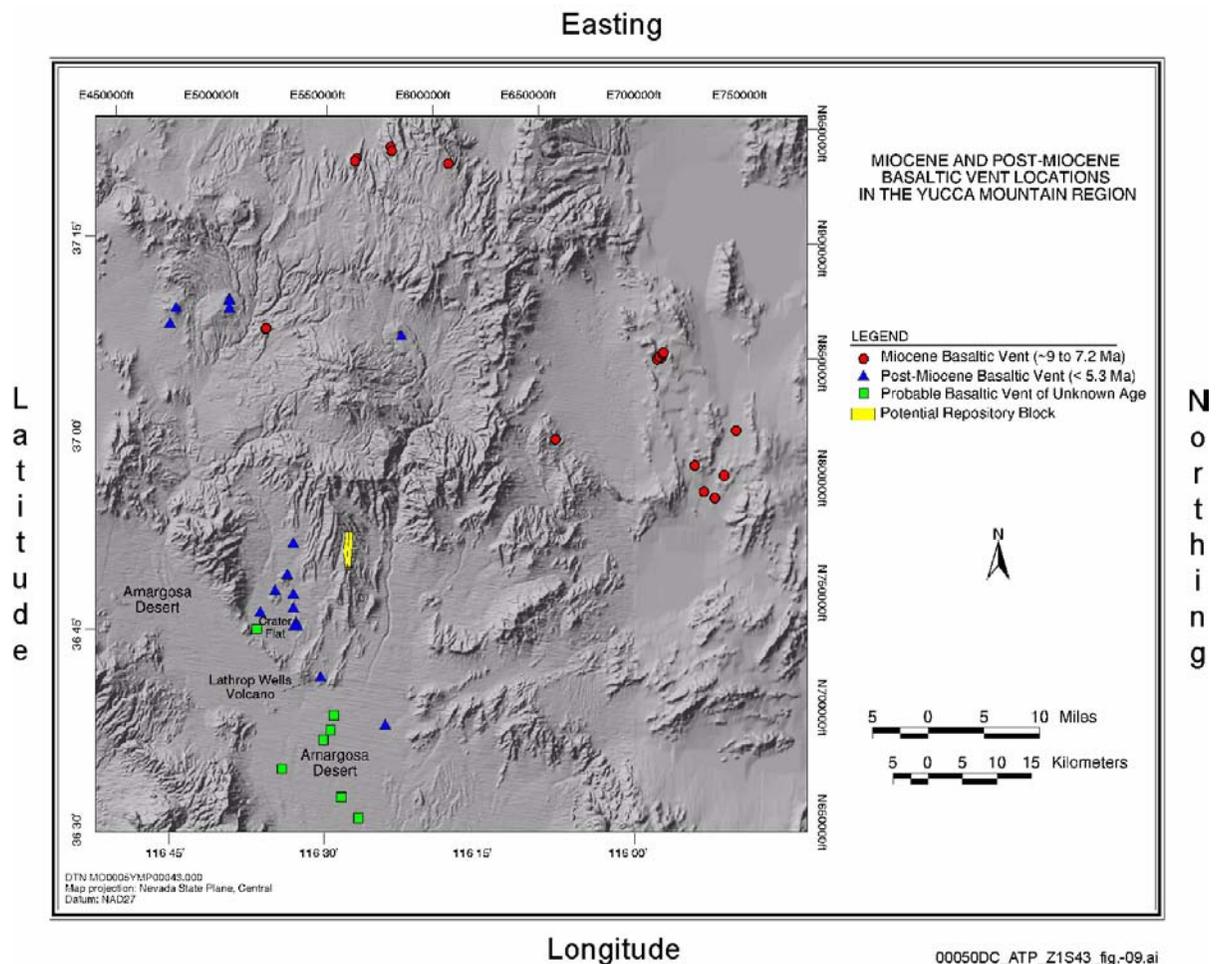
Figure 4-158. Location of Miocene (Circles) and Post-Miocene (Triangles) Basaltic Vents of the Yucca Mountain Region
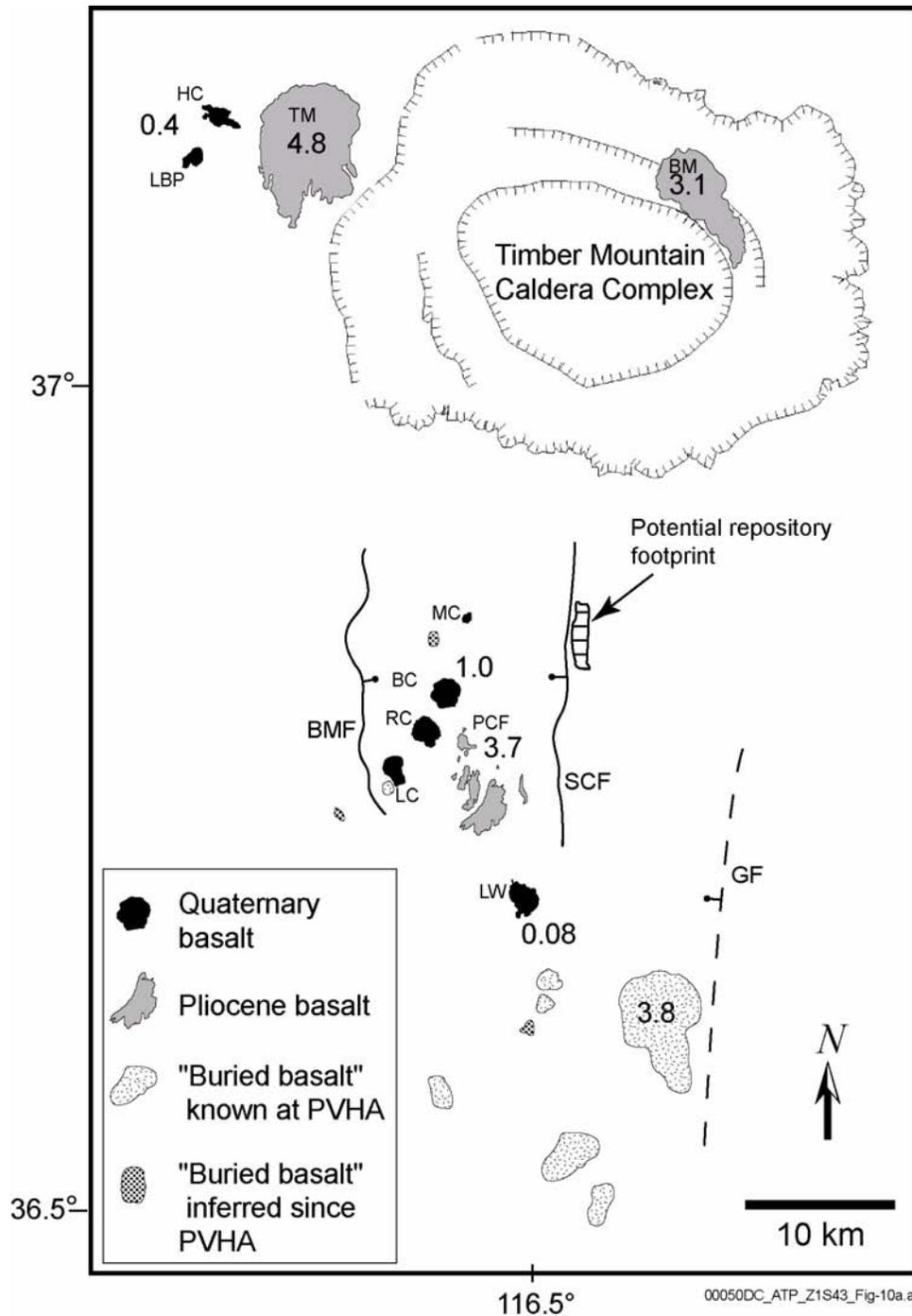
Figure 4-159. Location and Age of Quaternary (<2 Million Years) and Pliocene (2 to 5 Million Years) Volcanoes (or Clusters where Multiple Volcanoes have Indistinguishable Ages) and Probable Buried Basalt in the Yucca Mountain Region

Numbers by each volcano indicate approximate age in millions of years. BM = Buckboard Mesa; TM = Thirsty Mesa; HC = Hidden Cone; LBP = Little Black Peak; MC = Makani Cone; BC = Black Cone; RC = Red Cone; LC = Little Cones; PCF = Pliocene Crater Flat; LW = Lathrop Wells; BMF = Bare Mountain fault; SCF = Solitario Canyon fault; GF = Gravity fault. PVHA = *Probabilistic Volcanic Hazard Analysis for Yucca Mountain, Nevada* (CRWMS M&O 1996b). Buried basalt is assumed to be post-Miocene based on the age of one buried basalt sampled by drilling. Source: CRWMS M&O 2000ez, Figure 3.

Basaltic volcanoes form from magma that has a low silica and water content. In the southern Great Basin, basaltic volcanoes generally do not erupt as violently as magmas with higher silica and water content. Basaltic volcanoes in the Yucca Mountain region typically form cinder cones associated with small-volume lava flows. However, if the water content is high enough or the magma encounters groundwater during its ascent, explosive phases can also occur, resulting in eruption of an ash plume and deposition of an ash blanket. The youngest basaltic volcanoes in the Yucca Mountain region contain deposits that record moderately violent eruptions that may have produced ash plumes 5 to 10 km (3 to 6 mi) high, along with evidence for less violent and even nonexplosive eruptions.

Most observed basaltic eruptions begin as fissure eruptions, discharging magma where a dike (a vertical, tabular sheet of intrusive magma) intersects the earth's surface. They rapidly become focused at one or more vents into semicircular conduit eruptions. Volcanoes in the Yucca Mountain region are each fed by one main dike, along which a central cone and other vents may form, although subsidiary dikes are also present (CRWMS M&O 2000fa, Section 6.1). Typical basaltic dikes in the Yucca Mountain region are approximately 1.5 m (5 ft) wide (CRWMS M&O 2000fa, Section 6.1) and about 1,000 to 5,000 m (3,000 to 16,000 ft) long (CRWMS M&O 2000ez, Figure 13).

4.3.2.1.2 Probabilistic Volcanic Hazard Analysis

To assess the probability of volcanic activity disrupting a repository, the DOE has performed numerous analyses and conducted extensive volcanic hazard assessments. A panel of ten experts representing a wide range of expertise in the fields of physical volcanology, volcanic hazards, geophysics, and geochemistry were assembled to evaluate the volcanic hazard. The scientists reviewed extensive information presented by representatives of the DOE, U.S. Geological Survey (USGS), State of Nevada, NRC, and others regarding the timing and location of possible future volcanic activity near Yucca Moun-

tain. This study included a careful evaluation of the uncertainties in all the analyses. The expert panel devoted considerable effort to evaluating the existing data, testing alternative models and hypotheses, and ultimately, incorporating a wide variety of alternative models and parameters in their evaluations. Their evaluations (elicitations) were then combined to produce an integrated assessment of the volcanic hazard that reflects a range of alternative interpretations.

To estimate the probability of future volcanic activity at Yucca Mountain, the panel of experts used sophisticated modeling techniques documented in *Probabilistic Volcanic Hazard Analysis for Yucca Mountain, Nevada* (CRWMS M&O 1996b). As defined in *Probabilistic Volcanic Hazard Analysis for Yucca Mountain, Nevada*, a volcanic event is the formation of a volcano (with one or more vents) from the ascent of basaltic magma through the crust as a dike or system of dikes (CRWMS M&O 1996b, Appendix E). For the hazard analysis, the panel of experts considered a volcanic event as a point in space representing a volcano and an associated dike having length, azimuth, and location relative to the point event (CRWMS M&O 2000ez, Figures 10 and 12). This hazard analysis evaluated the annual probability of a future basaltic dike intersecting the subsurface area of the potential repository, based on considerations of the locations and recurrence rates of past volcanic activity in the region.

The hazard analysis models are based on data from Yucca Mountain volcanic studies, along with other data and observations from analogue studies of both modern and ancient volcanic eruptions. From these studies, scientists infer how and where magmas form and the processes that control the timing and location of magma ascent through the earth's crust. The panel of experts agreed that future volcanism is more likely to occur within or near existing clusters of geologically recent volcanism than elsewhere in the Yucca Mountain region. While the experts considered the entire 15-million-year history of volcanism in the Yucca Mountain region, they assigned the highest weights for assessing the volcanic hazard in the probabilistic analysis to the past 5 million years. They also emphasized the Crater Flat basin because of the

frequency of past volcanic activity there and its proximity to the potential repository (Figure 4-159). One difficulty, however, in evaluating past basaltic volcanic activity in the area is that evidence of basaltic volcanoes, particularly those that are older than 2 million years, may have been eroded or buried by younger sediments. The panel of experts recognized the possibility that there may be additional undetected basaltic volcanoes in the Yucca Mountain region and factored this into their uncertainty estimates for the number of volcanic events that have occurred.

The results of the probabilistic volcanic hazard analysis (CRWMS M&O 1996b) form the basis for probabilistic volcanic risk estimates that account for the repository layout described in this report and the probability of eruption through the repository, conditional on dike intrusion within the repository footprint. These latter results are included in *Total System Performance Assessment for the Site Recommendation* (CRWMS M&O 2000a).

The results of the hazard analysis estimate that 1.6×10^{-8} igneous events per year could be expected to disrupt the potential repository (CRWMS M&O 2000ez, Section 6.5.3). This translates to approximately one chance in 6,250 of an igneous event disrupting the repository during the first 10,000 years after repository closure. This is the probability of a future basaltic dike intersecting the subsurface area of the potential repository (intrusive scenario). If a dike does intersect the repository, analysts estimate about a 77 percent chance that a volcano would form at the surface with magma flowing through the repository (eruptive scenario) (CRWMS M&O 2000ez, Table 13a). This translates to approximately 1 chance in 7,700 of a volcano forming above the repository during the first 10,000 years. The annualized probabilities for both disruptive events are just slightly greater than the probability cutoff of 10^{-8}/yr; therefore, both intrusive and eruptive igneous scenarios have been included in the TSPA. Earlier versions of the TSPA analyses used lower estimates of the likelihood that magma contacting the repository would erupt at the surface (a probability of 0.36). Nevertheless, both intrusive and eruptive scenarios were also included in those analyses.

Analysis of new data collected in the Yucca Mountain region since the completion of the hazard assessment demonstrates the thoroughness of the results. Post-elicitation studies by the NRC (Connor et al. 1997) provided evidence to support the possibility of a greater volume for one of the volcanic centers in the Crater Flat basin and an additional volcanic center in the Amargosa Valley. Sensitivity studies showed that these new data did not significantly affect the results of DOE's hazard assessment (Brocoum 1997). The DOE will continue to monitor data and will incorporate significant new information into future technical and licensing documents.

4.3.2.1.3   Consequence Analyses for Volcanic/Igneous Disruptive Events

The DOE evaluated the possible consequences of volcanic activity disrupting the potential repository and estimated the risk to people and the environment that would result from such a disruption. Models of the consequences of an igneous intrusion into, or a volcanic eruption through, a repository at Yucca Mountain require specific information about the nature of the igneous event and the response of the repository to intrusion. This analysis considered the full range of basaltic eruptive processes that have occurred in the Yucca Mountain area during the Quaternary Period, from explosive to nonviolent basaltic eruptions. Information used in the TSPA-SR model to characterize these intrusive and eruptive processes comes from three sources: (1) examination of the geologic record of past intrusive and eruptive events in the Yucca Mountain region, (2) observations of eruptive processes during analogous modern volcanic events elsewhere in the world, and (3) consideration of the range of physical processes that might occur during the interaction between the repository and an igneous dike. The first two sources of information are described in the analysis model reports *Characterize Framework for Igneous Activity at Yucca Mountain, Nevada* (CRWMS M&O 2000ez) and *Characterize Eruptive Processes at Yucca Mountain, Nevada* (CRWMS M&O 2000fa). The analysis model report *Dike Propagation Near Drifts* (CRWMS M&O 2000fb) and the calculation *Waste Package Behavior in Magma* (CRWMS

M&O 1999p) provide additional information regarding dike and repository interactions.

Figure 4-160 is a schematic illustration of the hypothetical igneous activity modeled in the analysis. Two possible scenarios for igneous disruption are included in the consequence analysis: a model for volcanic eruptions that intersect drifts and bring waste to the surface; and a model for igneous intrusions that damage waste packages and expose radionuclides to groundwater transport processes. These models are described in detail in *Igneous Consequence Modeling for the TSPA-SR* (CRWMS M&O 2000fc) and represented schematically in Figure 4-161.

The scenario for a volcanic eruption assumes that magma erupts through a section of the repository, forming a volcano at the surface (Figure 4-161a). This scenario assumes that an igneous dike rises through the earth's crust and intersects one or more drifts in the repository. An eruptive conduit (the vertical cylindrical passageway through which

magma and pyroclasts move upward) forms somewhere along the dike as it nears the land surface, feeding a volcano at the surface. Waste packages in the path of the conduit are destroyed, and the waste is available to be entrained in the eruption. Volcanic ash is contaminated, erupted, and then transported by wind. Ash settles out of the plume as it is transported downwind, resulting in an ash layer on the land surface. The receptor receives a radiation dose from various pathways associated with the contaminated ash layer.

The scenario begins with an eruptive event, which is characterized in the TSPA by both its probability (CRWMS M&O 2000ez, Section 6.5.3) and its physical properties, such as energy and volume of the eruption, composition of the magma, and properties of the pyroclastic ash. Interactions of the eruption with the repository are described in terms of the damage to the engineered barrier system and the waste package. Characteristics of the waste form in the eruptive environment are described in terms of waste particle size. Atmospheric transport
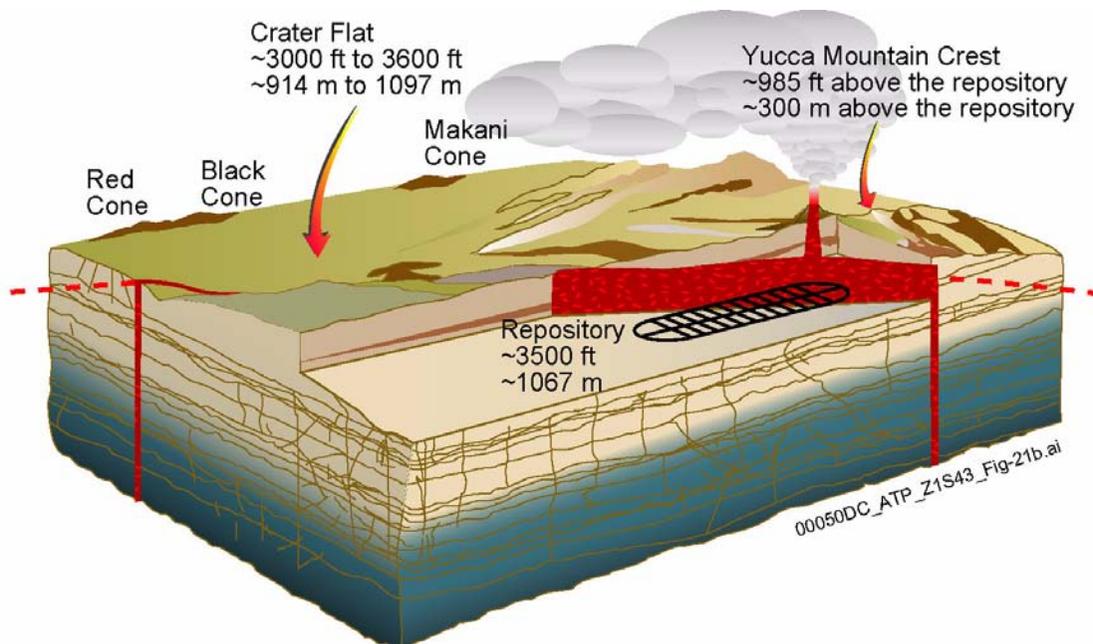
Figure 4-160. Schematic Illustration of Hypothetical Igneous Activity at Yucca Mountain
In the hypothetical case shown here, an intrusive dike rises through the earth's crust and intersects the repository. An eruptive conduit forms above the dike and feeds a volcano at the earth's surface. TSPA scenarios include cases both with and without eruptions that intersect the repository. Elevations of Crater Flat and the potential repository horizon are distances above sea level.
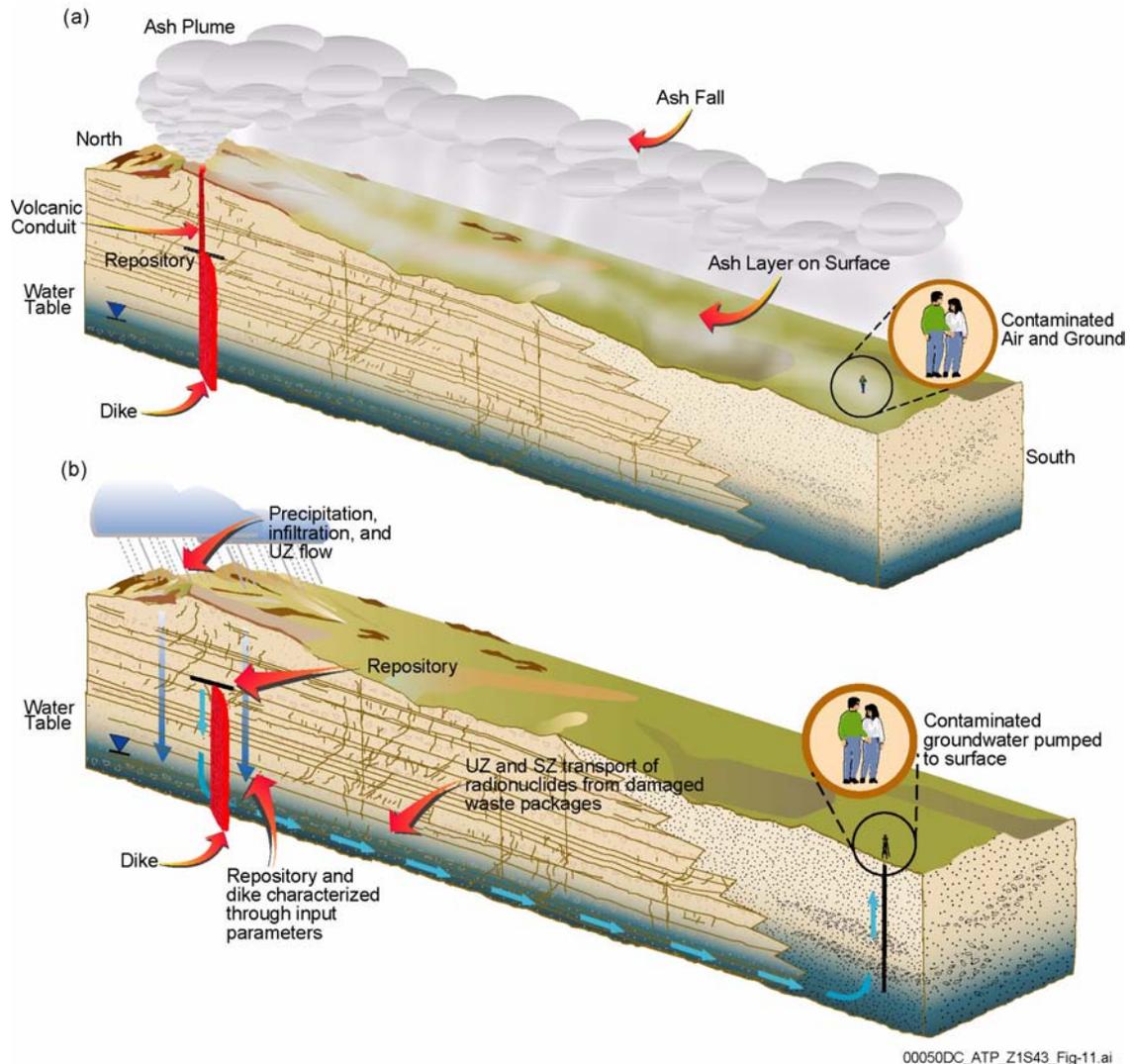
Figure 4-161. Schematic Representation of the Two Volcanism Scenarios Analyzed for TSPA-SR
(a) Volcanic eruption at Yucca Mountain, showing development of an eruptive conduit through a part of the repository, entrainment of waste particles in an ash cloud, and deposition of contaminated ash downwind of the potential repository. (b) Igneous intrusion at Yucca Mountain, showing the intersection of one or more emplacement drifts by an ascending dike followed by flow of magma in drifts, engulfing and damaging waste packages, and subsequent transport of radionuclides by groundwater moving through the solidified intrusion. UZ = unsaturated zone; SZ = saturated zone.

of waste in the volcanic ash plume begins with entrainment of waste particles in the pyroclastic eruption and is affected by wind speed and direction. Biosphere dose conversion factors are developed specifically for exposure pathways relevant to atmospheric deposition of contaminated ash, rather than the groundwater pathways considered for nominal performance. As a final step, the volcanic eruption biosphere dose conversion factors are used to determine radiation doses

resulting from exposure to contaminated volcanic ash in the accessible environment, approximately 18 km (11 mi) from the repository.

The other scenario in the analysis models the possible effects of a basaltic dike that intersects a section of the repository and partially or completely engulfs waste packages in magma (Figure 4-161b). This may or may not be accompanied by an eruption from the surface of the

mountain. Radionuclide releases from waste packages damaged by the intrusion are then available for transport in groundwater. The rate of transport depends on the solubility limits of the waste and the availability of water. The movements of radionuclides released by this type of an event are modeled directly in the TSPA using existing flow-and-transport models.

This scenario begins with an intrusive event (dike intersection), which is characterized in the TSPA by its probability and physical properties. Although the intrusion damages waste packages and other components of the engineered barrier system, it does not significantly alter the long-term flow of water through the mountain. Possible effects of a dike intrusion on the mountain hydrology in the unsaturated and saturated zones are discussed in *Features, Events, and Processes: Disruptive Events* (CRWMS M&O 2000ex, Section 6.2.8). Based on natural analogue sites, there is no indication of extensive hydrothermal circulation and alteration related to magmatic intrusion. In particular, natural analogue studies at sites on the Nevada Test Site show that alteration is limited to less than 10 m (30 ft) into the country rock adjacent to a dike intrusion (CRWMS M&O 2000ex, Section 6.2.9). Therefore, the disruptive event scenario uses nominal models to describe groundwater flow and radionuclide transport through the mountain.

For calculation of the annual dose resulting from radionuclides that are transported in groundwater following a disruptive igneous event, conditions in the biosphere at the location of the receptor are assumed to be the same as the conditions for nominal performance. Biosphere dose conversion factors for this pathway are therefore the same as those used in the nominal scenario. Because the total expected annual dose in the TSPA models is the sum of probability-weighted doses from both the nominal and disruptive scenarios, any additional increment of dose due to nominal processes that might occur following an igneous disruption is appropriately included in the overall analysis.

The TSPA-SR conceptual models take a conservative approach to modeling uncertainty in several respects. For the purposes of the analysis, the contents of all packages that are fully or partially damaged by an eruption (i.e., that lie in part or entirely within the circumference of the conduit, as described in Section 4.4.1) are assumed to be fully available for entrainment in the eruption. Likewise, it is conservatively assumed that any waste package that is partially or completely intersected by an intrusive dike is fully destroyed. The model does not take credit for the possibility of the magma encapsulating the waste and waste package, which could slow or even prevent water from reaching the waste. In the eruptive scenario, the entire volume of erupted material is conservatively assumed to have been involved in a violent phase of eruption. Observations of both modern and past analogue volcanoes indicate that the violent phases account for only a portion of the total eruption. This assumption overestimates, perhaps significantly, the amount of energy in the eruption and, therefore, the amount of ash transported away from the site. The TSPA evaluates the risk to people and the environment from both disruptive igneous event scenarios. These include (1) doses from the direct release of contaminated ash from an explosive volcanic eruption and (2) doses resulting from the release of radionuclides into the groundwater from waste packages damaged by magma intrusion. The results of these analyses are discussed in Section 4.4.3. Indirect effects that result from volcanic activity outside the repository (e.g., changes to the hydrologic and mineralogical properties of the rock or alteration of water flow and transport) have such low consequences that they are not evaluated further (CRWMS M&O 2000ex).

4.3.2.2 Seismic Activity

The geologic setting of a region influences potential earthquake effects by controlling:

- Location and size of earthquakes

- Potential for the ground's surface to rupture by faulting

- Amount of ground shaking at a specific site from earthquakes at various distances.

During site characterization, the DOE performed extensive studies at Yucca Mountain to estimate the potential sizes and frequencies of future earthquakes and to determine the level of ground motion and fault displacement that might affect potential repository facilities, both on the surface and underground. The DOE has used the results from these studies to design repository facilities that will withstand future earthquakes and to assess the long-term performance of the total repository system.

Scientists cannot predict the exact location and timing of future earthquakes. However, through intensive study of an area's surface and underground geology, with particular attention to past faulting, scientists can estimate the frequency and size of future earthquakes, the potential intensity of ground movement, and the possible effects from earthquakes on the area's geologic features and man-made structures.

The Yucca Mountain region is one of the most intensively studied areas in the world. Since 1978, scientists have collected and analyzed data on the geologic features of the surface and underground environments. These features provide information on the area's past seismic activity, which is important in estimating the characteristics of future earthquakes. Using these studies, scientists rate the Yucca Mountain region as having low to moderate seismicity (Figure 4-162) (CRWMS M&O 2000fd, Section 6.3.1).

Most of the movement in the earth's crust that formed the mountains and valleys of the southern Nevada landscape ended about 10 million years ago, but slow movement has continued into the present. Some of this movement occurs along faults, which are zones of weakness in the earth's crust. Future movement on some faults will produce future earthquakes. Therefore, intensive study has focused on the faults in the Yucca Mountain region to determine which faults are likely to move in the future and to estimate the potential magnitude and frequency of those earthquakes.

Scientists have used the data from site characterization studies to assess the seismic hazard at the site by defining the potential for ground shaking and fault rupture related to earthquakes. The type

of analysis used is called a probabilistic seismic hazard analysis. This type of analysis provides estimates on where and how often earthquakes might occur and on how much fault displacement and ground motion could result. To assess the seismic hazard for Yucca Mountain, scientists factored in different interpretations to account for uncertainties in evaluation of the data for each geologic feature.

Recent earthquakes near Yucca Mountain have been consistent with the seismic hazard analysis for the Yucca Mountain site. For example, in 1999 a magnitude 4.7 M_w (moment magnitude) earthquake occurred at Frenchman Flat about 45 km (28 mi) east of Yucca Mountain (for an earthquake of this size, moment magnitude is approximately equal to magnitude on the Richter scale). This was a moderate-magnitude event in a zone that scientists had identified as a seismic source. This earthquake did not exceed the ground motion estimates from the seismic hazard analysis. (See Sections 6.3 and 6.5 in *Characterize Framework for Seismicity and Structural Deformation at Yucca Mountain, Nevada* [CRWMS M&O 2000fd] for a discussion of seismic source characterization.) The results from the seismic hazard analysis are a sound basis for designing repository facilities to withstand potential earthquakes and for assessing future repository performance.

Engineers use proven techniques to design structures to withstand the potential earthquakes within that area. The repository surface facilities, where waste would be received, prepared for emplacement, then moved into the repository, would be subject to stronger earthquake ground shaking than subsurface facilities. (See Section 4.3.2.2.1 for more on the effects of seismic activity underground.) Extensive experience in designing and operating critical facilities, such as nuclear power plants, will be relied on in the design of the structures used during repository operations, so they will perform their safety functions during and after an earthquake. After all the waste is emplaced underground, the risks related to seismic activity would decrease. However, a strong earthquake could cause rock falls in the emplacement drifts or alter the pathways followed by groundwater. Scientists have studied these potential conse-
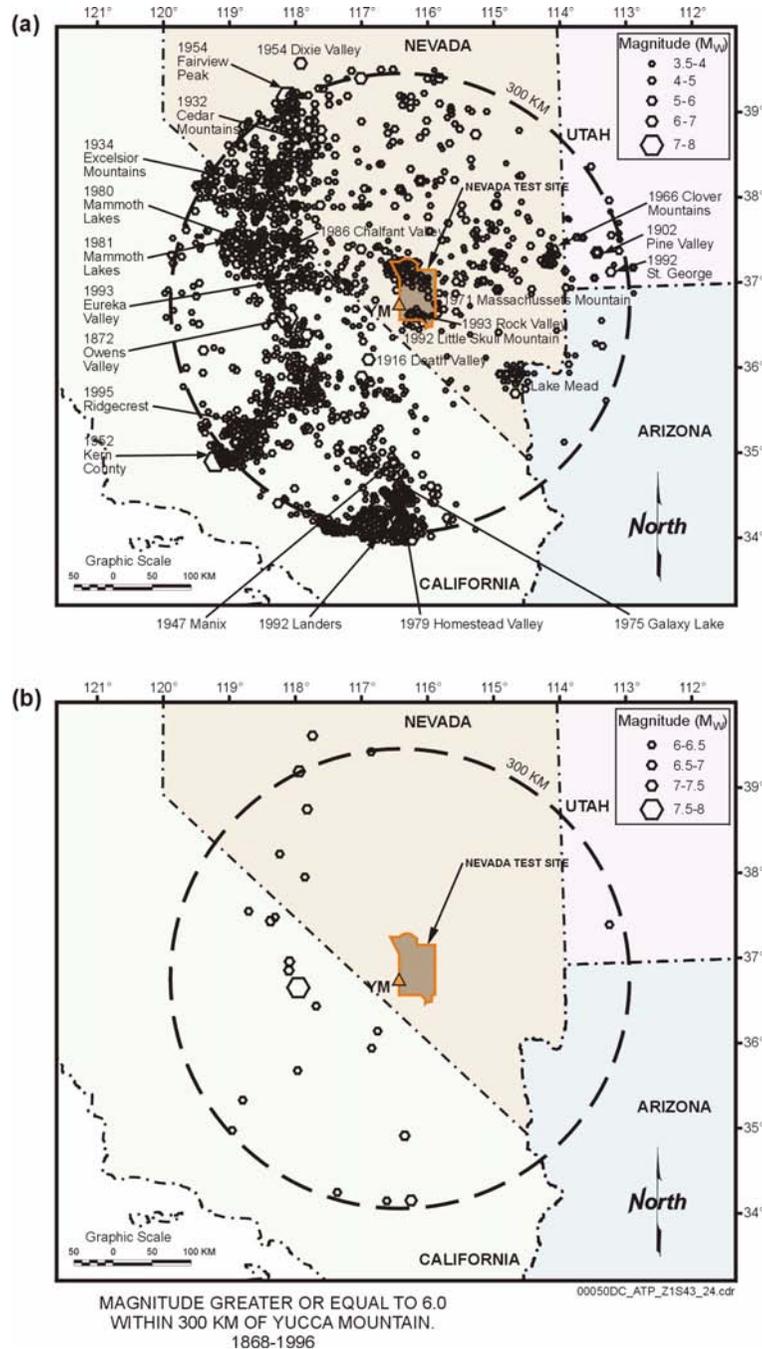
Figure 4-162. Historical Seismicity (1868 to 1996) Showing Events of M_w 3.5 or Modified Mercalli Intensity III and Larger within 300 km (186 mi) of Yucca Mountain

This seismicity catalog was compiled from a variety of sources. Coverage of older seismicity is sparse because of the absence or limited availability of seismographic coverage in the late 1800s and early 1900s. The cluster of earthquakes near the southern border of the Nevada Test Site represents the 1992 Little Skull Mountain earthquake and its numerous aftershocks; many of the events in the northern half occurred in response to underground nuclear weapons tests. Part b shows events of M_w 6 and larger within this time period. Earthquakes designated by name and year of occurrence are discussed in Section 12.3 of the *Yucca Mountain Site Description* (CRWMS M&O 2000b). For a more detailed discussion of these issues and how an earthquake catalog is used to assess seismic hazard, see Section 12.3.3 of the *Yucca Mountain Site Description* (CRWMS M&O 2000b) and Appendix G of *Probabilistic Seismic Hazard Analyses for Fault Displacement and Vibratory Ground Motion at Yucca Mountain, Nevada* (Wong and Stepp 1998).

quences and concluded that it is extremely unlikely that the consequences would be significant to repository performance. (See Section 4.3.2.2.3 for a discussion of fault displacement effects.)

4.3.2.2.1 Effects of Seismic Activity Underground

Underground openings are less likely to sustain damage from earthquakes than structures on the surface. This is because ground shaking is stronger on the surface than underground. When an earthquake occurs deep underground, locations at the surface receive ground motion energy simultaneously from the upward-traveling waves and from waves reflected back at the earth's surface. In addi-

tion, subsurface rock generally is stronger than weathered near-surface rock, which results in a smaller ground motion at depth.

A seismometer (an instrument that records earthquake waves) at the ground level and another in the Exploratory Studies Facility recently measured seismic waves from a 3.5 M_w earthquake at Frenchman Flat (this event was an aftershock of the 4.7 M_w earthquake described previously). Recordings from this earthquake, as shown in Figure 4-163, clearly indicate the decrease in amplitude of ground motion deep within the mountain (Savino et al. 1999). Scientists have observed this effect around the world for underground structures. For example, tunnels near the 1995 Kobe,
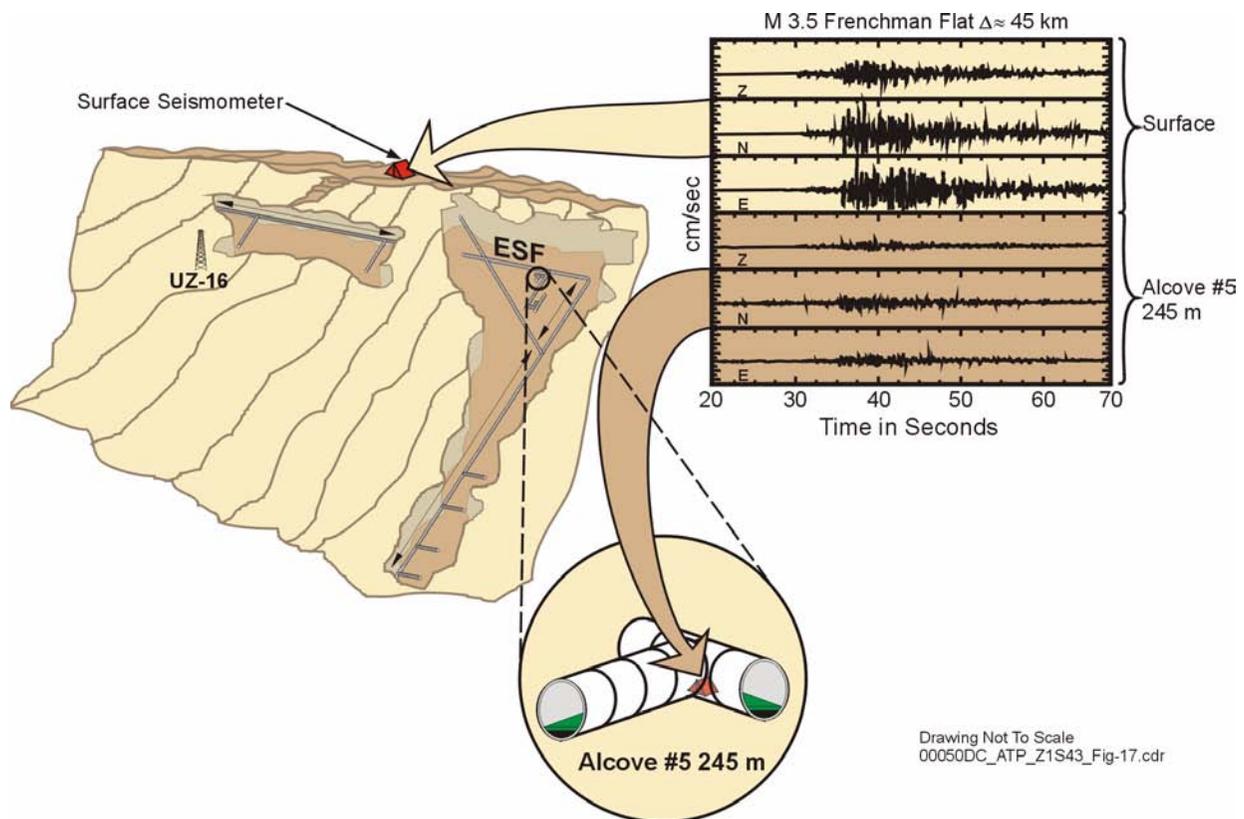
Figure 4-163. Recordings of Frenchman Flat Earthquake at the Ground Surface and the Thermal Test Alcove 245 m (804 ft) Underground

The seismograms for the surface and underground at the Thermal Test Alcove of the Exploratory Studies Facility (i.e., Alcove #5, at 245 m depth) are to the same vertical scale. M = magnitude; Δ = distance; Z = up–down; N = north–south; E = east–west; ESF = Exploratory Studies Facility. Source: Savino et al. 1999.

Japan earthquake (6.9 M$_w$) experienced no major damage despite high surface ground motion and extensive damage to surface facilities (Savino et al. 1999).

4.3.2.2.2 Probabilistic Seismic Hazard Analysis

The probabilistic seismic hazard analysis identifies the potential earthquake ground motion and fault displacement that could occur at the Yucca Mountain site. The results from this analysis were incorporated into estimates of seismic consequences and used in designing the repository's facilities. The following paragraphs describe the DOE's methods for performing the seismic hazard analysis (CRWMS M&O 2000fd).

The probabilistic seismic hazard analysis involved a multistep process. First, scientists identified the location of potential earthquake sources and defined their characteristics. Next, they estimated how frequently earthquakes of various magnitudes might occur at each source location. In the third step, experts calculated potential earthquake effects at Yucca Mountain, including the level of vibratory ground motion and amount of fault displacement, given earthquakes of a particular magnitude. Finally, they combined all of the information from the previous steps into "hazard curves" that show the probability of exceeding different levels of ground motion or fault displacement at a particular location during a specific period in time.

The method for performing the seismic hazard analysis of Yucca Mountain is state-of-the-practice and consistent with recent guidance developed by government agencies (e.g., the U.S. Army Corps of Engineers, the USGS). The NRC uses this method to evaluate the safety of existing nuclear power plants, and it would be the basis for licensing new plants (CRWMS M&O 2000fd, Section 6.1.4; CRWMS M&O 2000f). Specific information provided by the probabilistic seismic hazard analysis includes:

- The location of seismic sources that could contribute to fault displacement and vibratory ground motion at Yucca Mountain

- Estimates of the maximum magnitude of potential earthquakes from each seismic source (i.e., the largest earthquake the source can generate)

- Estimates of the frequency or recurrence rate of earthquakes having various magnitudes, up to the probable maximum magnitude

- Characterization of ground motion attenuation (decrease in amplitude of ground motion with distance from the source)

- Estimated probabilities for both fault displacement and vibratory ground motion

- Incorporated uncertainties into the analyses to reflect the range of views of experts.

Many scientists and engineers contributed to these activities. These individuals were associated with universities (including the University of Nevada, Reno and the University of Utah), government agencies (including the DOE, USGS, and U.S. Bureau of Reclamation), and private companies.

Seismic Source Location and Geometry—A seismic source is a region of the earth's crust that has certain characteristics indicating that earthquakes could originate there. In the probabilistic seismic hazard analysis, seismic sources can be of two basic types: fault sources and areal sources.

Fault sources are known fractures in the earth's crust containing characteristics that indicate past movement along the fault's surfaces. A fault is considered to have the potential to move in the future if it has moved in the past 2 million years (the Quaternary Period). Evidence from historically active faults around the world indicates that, in general, faults that show characteristics of having moved in the recent past, or "active faults," are those most likely to sustain future movement. Studies of faults in the Yucca Mountain region have focused on active and potentially active faults.

To represent the full range of possible fault rupture patterns and interactions near Yucca Mountain, experts used various combinations of possible fault

orientations and behaviors in their analyses of each potentially active fault. They also used alternate lengths for each fault to compensate for uncertainties in geologic mapping and different rupture patterns. Figure 4-164 shows the faults that were considered in the seismic analysis. Table 4-32 shows selected fault parameters for potentially significant faults within 10 km (6.2 mi.) of the repository that potentially could rupture independently (that is, rupture of a single fault and not simultaneous rupture of multiple faults). The slip rates are relatively low in comparison with rates for significant regional faults (such as the Furnace

Creek and Death Valley faults, which have slip rates of 2.5 to 8 mm/yr [0.1 to 0.3 in./yr]).

Areal sources represent areas where experts believe that potential earthquakes could occur on faults not singularly recognized as significant earthquake sources, such as buried faults. These areas are treated as having relatively uniform earthquake frequency and maximum earthquake magnitudes.

Maximum Earthquake Magnitudes—Experts used two basic approaches to estimate the
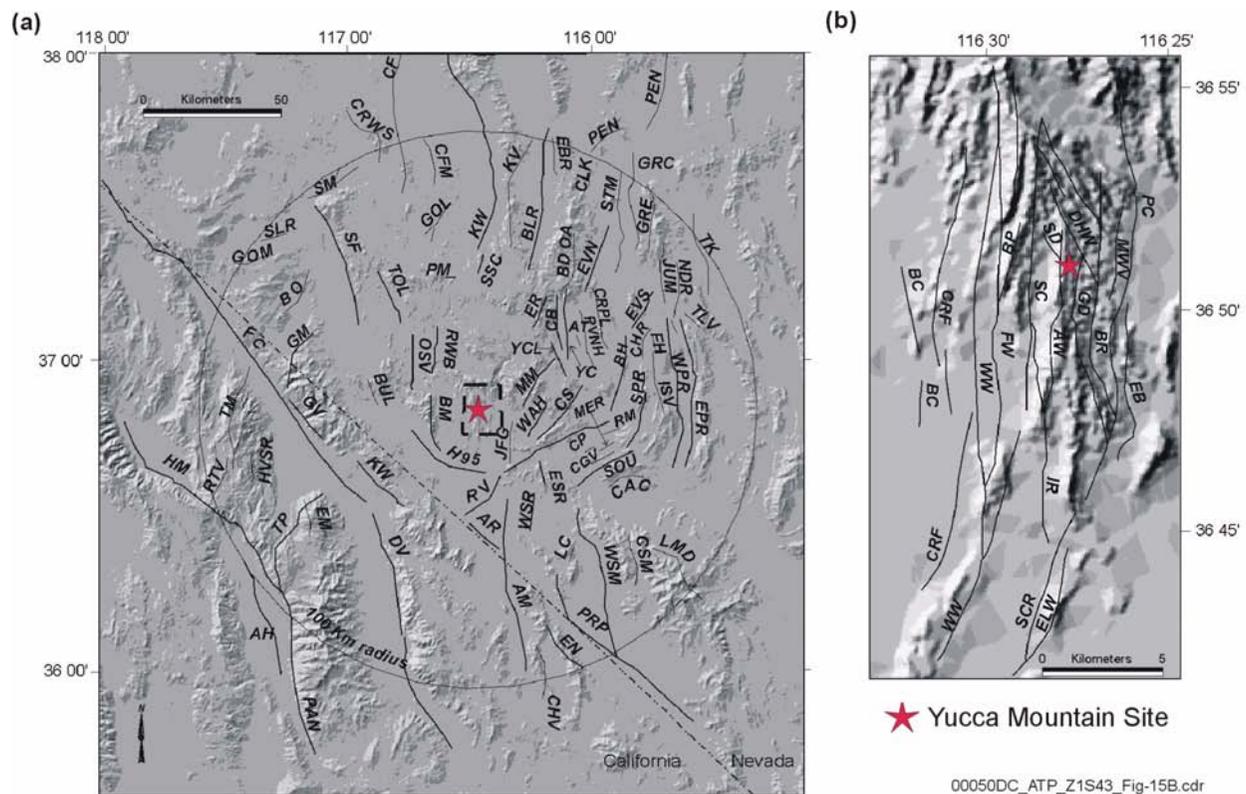
Figure 4-164. Known or Suspected Quaternary Faults and Potentially Significant Local Faults within 100 km of Yucca Mountain

(a) Known or suspected Quaternary faults within 100 km (62 mi) of Yucca Mountain; the two faults of interest are the Furnace Creek (FC) and Death Valley (DV) faults.

(b) Detail of (a), showing known or suspected faults near Yucca Mountain; these faults are the Abandoned Wash (AW), Black Cone (BC), Boomerang Point (BP), Crater Flat (CRF), Drill Hole Wash (DHW), Dune Wash (DW), East Busted Butte (EB), East Lathrop Wells (ELW) Fatigue Wash (FW), Ghost Dance (GD), Iron Ridge (IR), Midway Valley (MDV), Paintbrush Canyon (PC), Solitario Canyon (SC), Stagecoach Road (SCR), Sundance (SD), and Windy Wash (WW) faults.

Also see Figure 1-14 for the locations of the block-bounding and intrablock faults relative to the Exploratory Studies Facility and the potential repository block. For detailed identification of each fault labeled with initials in (a) but not identified in these notes, see the *Yucca Mountain Site Description* (CRWMS M&O 2000b, Figure 12.3-12). Source: CRWMS M&O 2000f, Figures 2-8 and 2-9.

Table 4-32. Potentially Significant Faults and Fault Parameters within 10 km (6.2 mi) of the Potential Repository

Fault Name	Rupture Length[a] (km)	Distance[b] (km)	Slip Rate[a] (mm/yr)
Solitario Canyon	16 to 18.7	1	0.01 to 0.03
Iron Ridge	6.5 to 8.5	2.5	0.002 to 0.004
Bow Ridge	6.7 to 8	2.5	0.002 to 0.003
Fatigue Wash	9.5 to 17	3.5	0.002 to 0.009
Paintbrush Canyon	12 to 19.4	4	0.002 to 0.017
Windy Wash	5 to 27	4.5	0.003 to 0.03
North Crater Flat	6.5 to 13.3	6	0.001 to 0.003
South Crater Flat	6.1 to 8.1	8	0.001 to 0.008
Stagecoach Road	4.5 to 10	10	0.016 to 0.05

NOTES: [a]Range of preferred values interpreted by the experts.
[b]Approximate shortest distance to repository.

Only significant and potentially independent fault sources are included here; see Appendix E of *Probabilistic Seismic Hazard Analyses for Fault Displacement and Vibratory Ground Motion at Yucca Mountain, Nevada* (Wong and Stepp 1998) for a complete discussion of all local fault sources, including multiple fault rupture scenarios. Source: Modified from CRWMS M&O 2000fd, Table 6.

maximum magnitudes of potential earthquakes in the Yucca Mountain region. The primary approach was based on estimates of the maximum dimensions of fault rupture. Multiple sources of uncertainties were considered in estimating physical dimensions of maximum rupture on faults (e.g., uncertainties in rupture length, rupture area, and displacement per event). Experts then compared these estimated dimensions with the estimated dimensions of ruptured faults and known magnitudes of earthquakes observed throughout the world. The second approach considered historical data on the seismicity of the region and the potential size of unrecognized faults in that region.

Earthquake Recurrence—Earthquake recurrence relationships express the rate or annual frequency of earthquakes occurring on a seismic source. Seismic sources generate a range of earthquake magnitudes, up to some maximum magnitude. A magnitude-distribution model defines the relative number of earthquakes having particular magnitudes. Methods for developing these relationships are usually different for fault sources than for areal sources. Experts estimated recurrence rates for fault sources from geologic data and rates for areal sources from historical seismicity data.

Vibratory Ground Motion Hazard—The level, or amplitude, of ground shaking is influenced by three main elements. The first element is how the size and nature of an earthquake controls the generation of earthquake waves. The second element is the travel path of seismic waves from the source of the earthquake to a particular site. The length of this path is important because the amplitude of ground motion will decrease (attenuate) with distance. The third element is the local site condition, or the effect of the uppermost several hundred feet of rock and soil, and the surface topography. Experts explicitly addressed all three of these elements in the Yucca Mountain seismic hazard analysis. Combining the ground motion analysis with seismic source characteristics produces a probabilistic representation of vibratory ground motion hazard that gives annual exceedance probabilities associated with different levels of earthquake ground motion.

Fault Displacement Hazard—Fault displacement hazard is the hazard related to rupture along a fault triggered by an earthquake. Based on the careful study of fault ruptures associated with earthquakes around the world, the potential for fault displacement is categorized as either principal or distributed faulting. Principal faulting occurs along the main plane of a fault. Distributed faulting

is rupture that occurs on other faults in the vicinity of an earthquake in response to the principal displacement.

The DOE's method for assessing probabilistic fault displacement hazard is very similar to that for vibratory ground motion hazard and relies heavily on the detailed geologic studies of individual faults in the Yucca Mountain vicinity. Experts evaluated the fault displacement hazard at nine locations within the Yucca Mountain site. These locations span the range of known faulting conditions in the area, which include recognized faults to small fractures and unfaulted rock. For the period of repository operations (i.e., before closure of the repository surface facilities), results of the hazard assessment show that, in the areas where waste would be emplaced, fault displacements of 0.1 cm (0.04 in.) have less than one chance in 100,000 of being exceeded each year (CRWMS M&O 2000fd, Section 6.6.3). DOE studies have also shown that the consequences of fault displacement in the repository after the repository is closed will not significantly affect performance (see Section 4.3.2.2.3 for a discussion of fault displacement effects).

4.3.2.2.3 Application of Seismic Hazard Analyses

Based on the results of the probabilistic seismic hazard analyses, a team of scientists computed the vibratory ground motion inputs to be used for preclosure design analyses. These inputs were developed for the following areas:

- At the repository elevation, about 300 m (1,000 ft) below the ground surface (Point B)

- On a rock outcrop at the ground surface directly above the repository (Point C)

- Near the North Portal of the Exploratory Studies Facility, where the Waste Handling Building would be located during the preclosure period (Point D).

Analysts selected these three areas, shown in Figure 4-165, because they represent the range of locations and conditions where the potential repos-

itory's facilities would be located. The ground motion for the three areas was derived from the ground motion developed for a "reference rock outcrop" (Point A) during the probabilistic seismic hazard analysis. The ground motion at each of the three areas is different because of local site conditions. The estimated ground motion at these areas will be used in designing repository facilities and in performance assessments of the potential repository during the postclosure period. Figure 4-166 shows calculated preliminary design ground motion for the Point B and C areas only. These are defined for a probability of 1 chance in 10,000 of being exceeded each year. The design ground motion is represented by response spectra (curves) that indicate the strength of ground shaking at different frequencies of motion (frequency, in Hertz [Hz], is the number of cycles per second of a seismic wave or the vibration of a structure). The shape and stiffness of engineered structures determine which frequencies of seismic waves are important. In addition, the frequencies of strong seismic waves at a site are determined by the size of the earthquake, its distance from the site, and the physical properties of the earth between the site and the earthquake. Two design earthquake spectra are shown on each panel of Figure 4-166 because two kinds of earthquakes control the ground shaking hazard at Yucca Mountain (CRWMS M&O 1998l). The shaking hazard at moderate frequencies (5 to 10 Hz) is due predominately to earthquakes of magnitude M_w 5.5 to 6.5 within 15 km (9 mi) of the site. The shaking hazard at low frequencies (1 to 2 Hz) is due predominately to earthquakes of approximately magnitude M_w 7 and larger at a distance of about 50 km (31 mi). The sources for these larger, more distant earthquakes are the Death Valley and Furnace Creek faults. The DOE has collected additional geotechnical data to refine analyses of ground motion at the Point B, C, and D sites.

The DOE has also studied the potential effects and consequences of fault displacements associated with both known and unknown faults. Experts conducted analyses to evaluate potential effects of fault displacement on emplacement drifts and the engineered barriers in the drifts (i.e., drip shields and waste packages) (CRWMS M&O 2000fe). They also examined how fault displacement could
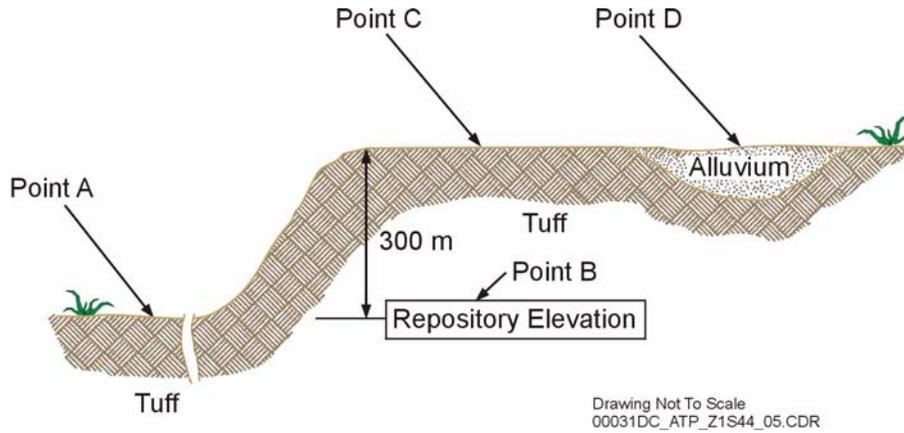
Figure 4-165. Locations of Specified Design Basis Earthquake Ground Motion Input
Point A: Reference rock outcrop at potential repository elevation (Point A is a hypothethetical site and does not correspond to an actual location at Yucca Mountain); Point B: Potential repository elevation with tuff overburden; Point C: Rock surface; Point D: Soil surface. Source: Modified from CRWMS M&O 1998l, Figure 2.3-1.
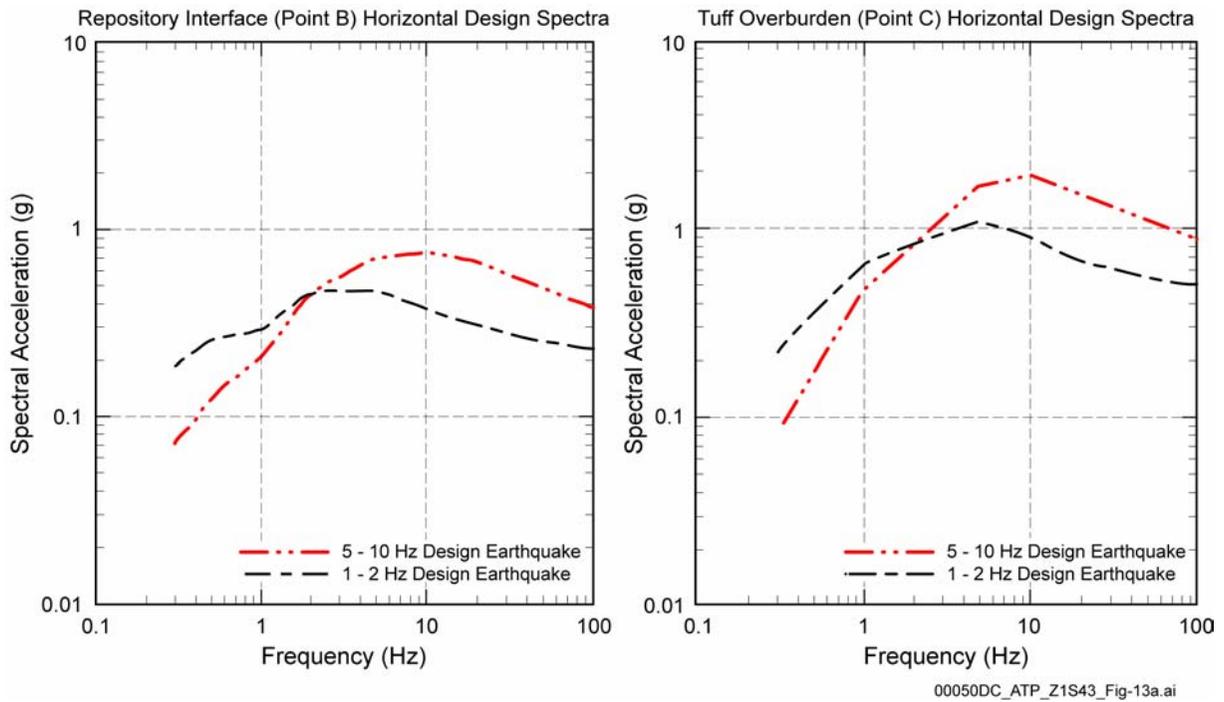
Figure 4-166. Preliminary Ground Motion Calculated by the TSPA-SR Model at Points B and C with 1 Chance in 10,000 of being Exceeded Each Year
Locations of the two points are shown in Figure 4-165. The DOE is currently collecting additional data to refine analyses of ground motion at these sites. Source: Modified from CRWMS M&O 1998l, Figures 6.2-1 and 6.2-3.

affect water movement within Yucca Mountain, which could affect the movement of radionuclides into the groundwater (CRWMS M&O 2000ff). These detailed studies show that hydrologic changes resulting from fault displacement are highly unlikely, and that faulting events will not affect the safety of the potential repository.

4.3.2.3 Human Intrusion Scenario

The DOE conducted a separate TSPA (see Section 4.4.4) to evaluate how well the repository system would limit radiological exposures under the hypothetical condition of a human intrusion. This scenario assumes a drill penetrating the repository during a possible exploration for groundwater resources. To determine the impacts from this type of disruptive event, the scenario involves site-specific data that represent the repository's natural and engineered barriers. Specifications for this scenario also include such information as the type of drilling, the size of the borehole, and the location of the borehole. By mathematically modeling this scenario, experts evaluated the repository's performance under this disrupted condition and projected the effects. This section describes the basis and assumptions for the TSPA evaluation of the human intrusion scenario.

4.3.2.3.1 Scenario Basis and Assumptions

Human intrusion analyses were performed in *Total System Performance Assessment for the Site Recommendation* (CRWMS M&O 2000a), *Total System Performance Assessment—Analyses for Disposal of Commercial and DOE Waste Inventories at Yucca Mountain—Input to Final Environmental Impact Statement and Site Suitability Evaluation* (Williams 2001a, Section 5.2.7), and *Total System Performance Assessment Sensitivity Analyses for Final Nuclear Regulatory Commission Regulations* (Williams 2001b).

The purpose of the TSPA for human intrusion scenario is to provide a basis for judging the resilience of the geologic repository to inadvertent human intrusion (National Research Council 1995, Chapter 4). Unlike analyses of other potential disruptive scenarios, the human intrusion scenario does not evaluate the probability of such an event

occurring but instead assumes the event probability of 1. The TSPA analysis uses a "stylized" human intrusion scenario, which refers to specific characteristics that define the scenario.

The human intrusion scenario assumes:

- A single human intrusion occurs as a result of exploratory drilling for groundwater.

- The intrusion occurs some time after the repository is permanently closed.

- A drill bit penetrates a waste package and continues to the water table.

- The drillers use common techniques and practices currently used for drilling operations in the Yucca Mountain region.

- The drillers do not seal the borehole, and natural degradation processes gradually modify the borehole.

- No particulate waste material falls into the borehole.

- The analysis only considers the amount of radionuclide release that results from the intrusion.

- The analysis does not include any radionuclide releases caused by unlikely natural processes and events.

The DOE has estimated that this event could happen no sooner than about 30,000 years after closure without recognition by the driller that he had penetrated a waste package. Therefore, human intrusion is assumed to occur at 30,000 years in *Total System Performance Assessment—Analyses for Disposal of Commercial and DOE Waste Inventories at Yucca Mountain—Input to Final Environmental Impact Statement and Site Suitability Evaluation* (Williams 2001a, Section 5.2.7). For conservatism and consistent with NRC proposed regulations, the DOE also analyzed a human intrusion scenario that assumed (TSPA-SR) that the intrusion occurs at 100 years.

For the purposes of analysis, it was necessary for the DOE to provide supplemental information and data to completely specify the human intrusion scenario. This information and data includes:

- Surface water collection and flow rate in the hypothetical borehole
- Borehole size and condition
- Type of waste exposed (e.g., spent nuclear fuel, high-level waste glass)
- Water flow conditions in the waste package
- Waste form dissolution rates
- Location of the borehole within the repository.

Therefore, all of the DOE's human intrusion scenarios assume that someone unknowingly drills for groundwater at Yucca Mountain and the drill penetrates a waste package containing commercial spent nuclear fuel or DOE high-level radioactive waste glass. The drill continues down approximately several hundred meters to the water table.

The exposed radioactive waste is mobilized by degradation of the waste form and mixing with the infiltrating water, which then travels down the uncased drill hole and into the water table. After entering the water table, the radionuclides, in dissolved and colloidal forms, are transported by the groundwater to the receptor location. This scenario is illustrated in Figure 4-167.

For an intrusion at 100 years after repository closure, a waste package containing commercial spent nuclear fuel would still be thermally hot, so that any water entering the waste package would convert to vapor (CRWMS M&O 2000fg, Table 10). Thus, the absence of liquid water would prevent waste form degradation and transport of radionuclides down the drill hole. At that time, any water entering the package would convert to vapor, and the absence of liquid water would prevent the transport of radionuclides down the drill hole. However, to add a conservative bias to the analysis, the scenario does not reflect this fact and instead
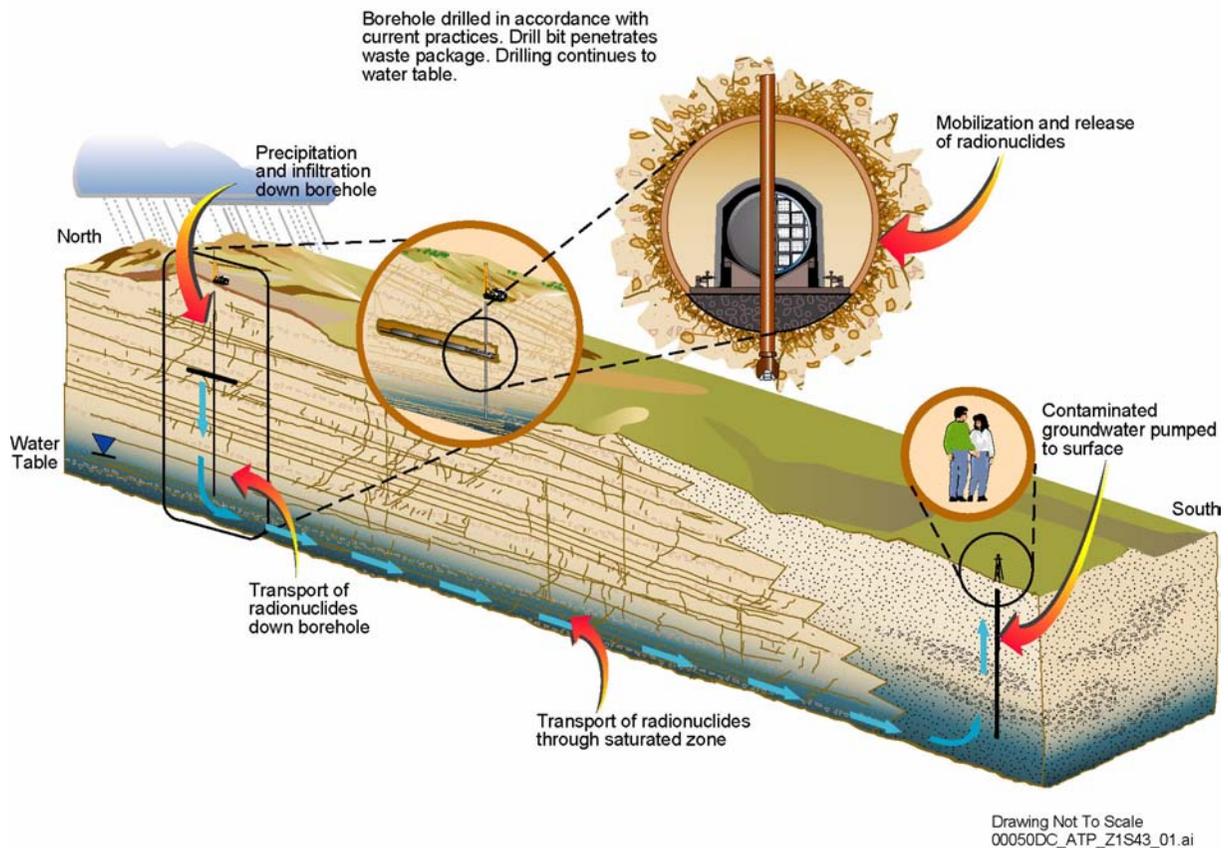
Figure 4-167. Human Intrusion Scenario

assumes liquid water flows continuously through the penetrated waste package and mobilizes radionuclides. A lower-temperature repository might not be hot enough to vaporize liquid water which then would flow continuously through the penetrated waste package. In either case, the TSPA for a 100-year intrusion would be similar. Additional specifications and assumptions for this human intrusion scenario are presented in Section 4.4.4.1.

4.3.2.3.2 Total System Performance Assessment Evaluation and Sensitivity Analyses

The TSPA-SR and supplemental TSPA evaluations and sensitivity analyses of the human intrusion scenario focused on such aspects as:

- Infiltration of water down the borehole and into the penetrated waste package

- Mobilization and release of radionuclides from a penetrated waste package

- Transport of radionuclides down the borehole to the water table

- Type and amount of radionuclides that could be transported through groundwater (i.e., water table) to the human environment

- Projected annual doses.

To compensate for uncertainty, the TSPA-SR and supplemental TSPA evaluation of the human intrusion scenario does not account for factors within the unsaturated zone (the rock between the repository and the water table) that would limit the transport of some radionuclides. The TSPA-SR evaluated the consequences of the scenario (with human intrusion at 100 years) during the remaining part of the 10,000-year compliance period following the hypothetical intrusion. The analysis assumed the same climatic and hydrogeologic conditions as the nominal scenario (i.e., the representation of the most plausible evolution of the repository system).

The TSPA-SR analysis (intrusion at 100 years after closure) focused on:

- Radionuclides with long half-lives relative to the compliance period, which will not decay away before reaching the point of compliance

- Radionuclides that are highly to moderately soluble in water (i.e., quickly mobilized after waste package failure) and nonsorbing or low sorbing (i.e., transport is minimally delayed)

- Radionuclides with the potential to produce significant radiation exposures if contacted or consumed by the group receptor

- Radionuclides in the form of tiny (i.e., approximately 0.1 to 5 µm (0.000004 to 0.0002 in.) colloidal particles that are carried at the speed of the groundwater.

The DOE performed a sensitivity analysis (see Section 4.4.5) of this evaluation to identify the factors that have the greatest influence on the release, transport, and radiation exposure to the hypothetical receptor group.

Section 4.4.4 summarizes the results of the TSPA-SR model evaluation of the 100-year human intrusion scenario. In addition, Section 4.4 of *Total System Performance Assessment for the Site Recommendation* (CRWMS M&O 2000a) documents the results in detail. *Total System Performance Assessment—Analyses for Disposal of Commercial and DOE Waste Inventories at Yucca Mountain—Input to Final Environmental Impact Statement and Site Suitability Evaluation* (Williams 2001a, Section 5.2.7) summarizes the results of the human intrusion scenario occurring at 30,000 years.

4.3.3 Scenarios Addressed and Screened Out of Total System Performance Assessment

Over the past decade, scientists have hypothesized and considered many possible scenarios of conditions that could occur in the distant future and have the potential to affect the repository's capability to isolate radioactive waste. They selected the most

probable of these conditions and developed scenarios for further analysis in the TSPA. Many conditions and scenarios were screened out according to probability or consequence. The technical basis for excluding these scenarios from consideration in analyses of the performance of the design described in this report is presented in the various process model and analysis model reports and in the DOE FEPs database (Freeze et al. 2001).

Two particular scenarios that the DOE considered but ultimately excluded from further TSPA analysis have been the focus of past scientific interest. They are:

1. **Rise of the water table**—a hypothesis that speculates that tectonic and hydrothermal events could cause the water table to rise to the repository level

2. **Nuclear criticality**—the possibility of the spent nuclear fuel in the repository causing a self-sustaining chain reaction (as a result of chemical or physical processes affecting the waste) either in or after release from breached waste packages.

As explained in the following sections, the DOE and others have determined that the water table rise scenario is not scientifically credible and that the nuclear criticality scenario is highly improbable. A model detailed analysis has shown that the probability of a nuclear criticality event falls below the screening threshold of less than 1 chance in 10,000 in the first 10,000 years following emplacement (see Section 4.3.3.2.3). This is primarily because there are few failures of waste packages, which are designed to prevent breach before 10,000 years. Therefore, it was screened out. However, because these scenarios have been the subject of much discussion, Sections 4.3.3.1 and 4.3.3.2 present the scientific investigations that led to the DOE's conclusions.

4.3.3.1 Long-Term Stability of the Water Table

The current elevation of the water table beneath Yucca Mountain is about 730 m (2,400 ft) above sea level, and the potential repository horizon would be an average of about 300 m (1,000 ft) above this elevation. The minimum height of an emplacement drift above the water table is about 210 m (690 ft) in the northernmost section of the repository. Geologic, geochemical, and hydrologic investigations of the site indicate that the elevation of the water table has fluctuated in the past and that the maximum elevation in the Yucca Mountain region was about 120 m (390 ft) above the current level, primarily as a result of variation in climate. Paces and Whelan (2001) have recently re-estimated the maximum climate-caused water table rise during the Pleistocene, including glacial climates, to be 17 to 30 m (56 to 98 ft). Based on this evidence and on numerical modeling, and to conservatively account for uncertainties related to future climate states, the DOE's analyses of repository performance include future variations in water table elevation of up to 120 m (390 ft). In 1987, a DOE scientist hypothesized that much larger variation in the water table could occur as a result of tectonic processes (Szymanski 1989). Szymanski (1989) postulated that tectonic stress could cause fracture apertures to be opened wider than they would be under normal stress and that during an earthquake the extensional stress could be released, causing the fracture apertures to decrease. He further postulated that, in a process called "seismic pumping," the water in the fractures would be compressed, forcing the water upward to the level proposed for storage of nuclear waste (Szymanski 1987, 1989). A group of 23 project scientists (DOE 1989) reviewed this hypothesis and concluded it was not supported by available information.

Since that initial internal review, Szymanski and colleagues have written several additional papers in support of the hypothesis that the repository could be inundated by a rising water table (Davies and Archambeau 1997a, 1997b; Dublyansky and Reutsky 1995; Hill et al. 1995). This new information has been systematically evaluated by the DOE and in a series of external peer reviews, which are discussed in this section. These external peer reviews included:

- A five-member peer review panel composed of outside reviewers convened by the Yucca Mountain Site Characterization Project, with

conclusions published separately as a majority report (Powers et al. 1991) and a minority report (Archambeau and Price 1991).

- A single reviewer from the USGS, at the request of one of the members of the five-member panel (Evernden 1992).

- A 17-member panel established by the National Academy of Science/National Research Council at the request of the DOE (National Research Council 1992).

- NRC contractors at the Center for Nuclear Waste Regulatory Analyses (Leslie 1994).

- The saturated zone flow and transport expert elicitation panel (CRWMS M&O 1998j, Section 3.2.9.3).

- The Nuclear Waste Technical Review Board (NWTRB), which, through a panel of outside experts, reviewed documents in support of the upwelling groundwater model submitted in 1997 (Cohon 1998).

Except for the minority report of Archambeau and Price (1991), these reviews all concluded that the available evidence does not support the proposed upwelling groundwater hypothesis.

This section will discuss:

- Data and analyses related to the origin of mineral deposits that led to Szymanski's conclusions

- Data and analyses related to the past elevation of the water table

- Analyses of the future potential for variation in the elevation of the water table.

4.3.3.1.1 Evidence for the Origin of Surficial Deposits of Calcite and Opaline Silica

A trench, designated Trench 14, was excavated to a depth of 1.8 m (6 ft) in 1982 to study the Bow Ridge fault along the west side of Exile Hill. The trench exposed a vein-like deposit of calcium carbonate and subordinate opaline silica, as well as a breccia deposit (angular fragments of older rock cemented within a fine-grained matrix) in the bedrock on the footwall. The origin of these deposits was the subject of considerable debate, so in 1984 the trench was deepened to 3.6 m (12 ft) to help elucidate the origin of the deposits. Taylor and Huckins (1986) proposed that the deposits were formed by evaporation of precipitation, leaving behind dissolved minerals (a pedogenic, or soil forming, origin). After examination of deposits in Trench 14, Szymanski (1987) hypothesized that the potential repository was at risk because of upwelling water. Varying hypotheses on the origin of the deposits and peer reviews of the hypotheses are discussed in this section.

Field Observations—Stuckless, Peterman et al. (1992) examined several lines of evidence and concluded that a pedogenic origin provided the best explanation for the deposits observed at Trench 14. This evidence includes field relationships, such as the slope-parallel orientation and great lateral extent of the calcic or caliche deposits below the surface of soils in the desert Southwest. Additionally, some carbonate layers continue upslope beyond their supposed feeder-vein source. A second deepening of Trench 14 in 1989 showed (Taylor and Huckins 1995) that the veins pinch out with depth (Figure 4-168). In addition, the veins are not visible in the Exploratory Studies Facility where the tunnel intersects the Bow Ridge fault, although minor calcite may occur on the footwall. These observations contrast sharply with the morphology observed at Travertine Point (Figure 4-169), a site of known groundwater discharge along Furnace Creek on the east side of Death Valley.

Textural and Mineralogical Evidence—Vaniman, Bish et al. (1988) have shown that the deposit at Trench 14 is similar mineralogically and texturally to soil deposits and distinct from spring deposits. For example, the vein material in Trench 14 is poorly indurated (soft and not well cemented together), porous, and fine grained. In contrast, feeder veins, like those at Travertine Point, are coarse grained and well indurated (having a solid, hard structure). The deposit at

00050DC_ATP_Z1S43_Fig-08.cdr

Figure 4-168. Veins in Trench 14 Pinching Out with Depth

ATP_0012.cdr

Figure 4-169. Photograph of Travertine Deposit and Feeder Vein at Travertine Point, along Furnace Creek, Death Valley, California
The leftmost vein is about 0.5 m (1.6 ft) wide.

Trench 14 exhibits intimate intergrowths of calcite and opal, as well as abundant ooids (egg-shaped particles) and pellets. Both features are atypical of any type of spring deposits, but they are common in soils. Springs and seeps have abundant biogenic evidence of their past higher water content, including fossils of aquatic animals, such as ostracodes and mollusks, and algal or diatomaceous deposits of opal-A. These biogenic features are not found at Trench 14. Biogenic evidence found at springs and seeps also includes poorly preserved root casts of phreatophytic plants (i.e., plants that obtain moisture from below the water table). In contrast, Trench 14 has well-preserved, very delicate filaments that are common in pedogenic calcretes and are associated with roots of xerophytic plants (i.e., plants adapted to low moisture conditions, typically with deep roots).

Monger and Adams (1996) examined the microscopic structure of the deposits at Trench 14 and elsewhere and compared the textures with known pedogenic and phreatic (from groundwater) deposits. They used a combination of thin sections, scanning electron microscopy, x-ray diffraction, and cathodoluminescence, and concluded that the vein deposits appear to be of pedogenic origin.

Geochemical Evidence—Vaniman, Chipera et al. (1994) note that the major- and trace-element chemistry of the deposit at Trench 14 is distinct from the chemistry of spring deposits and similar to the chemistry of soils. The iron and scandium abundance data are most distinctive. The weathering process that forms soils elevates the concentrations of these elements. The elevated iron and scandium content in the veins has the same ratio as the local soils. Lanthanum/ytterbium ratio

values in the Trench 14 deposit also match those of the soils. This correspondence can be accounted for only if the material in the veins is derived from soil.

Isotopic data—Isotopes are atoms of a chemical element with the same atomic number (i.e., the same number of protons) but a different atomic mass (containing a different number of neutrons). Several types of isotopic data can be used to demonstrate that local groundwater was not involved in the formation of the Trench 14 veins. The isotopic evidence and references to isotopic work are summarized by Stuckless, Marshall et al. (1998). Oxygen isotopes in the calcite found in veins at Trench 14 indicate that their origin would have been at unreasonably low temperatures if they had been precipitated from either of the aquifers beneath Yucca Mountain. Carbon isotopes preclude involvement of the deepest groundwater aquifer at Yucca Mountain. Strontium in the vein deposit has a greater proportion of the isotope strontium-87 than strontium found in either aquifer beneath Yucca Mountain, which precludes the involvement of either aquifer in the formation of the veins. In contrast, the isotopic composition of strontium in the Trench 14 deposits is within the range measured for soil deposits, which is permissive evidence for formation of the deposits by soil-forming processes. The uranium-234/uranium-238 activity ratio in groundwater beneath Yucca Mountain is anomalously large relative to most groundwaters (greater than 5 in the volcanic aquifer). In comparison, the uranium-234/uranium-238 activity ratio values for both soils and the calcite from Trench 14 are less than 1.5. This isotopic system again shows that the local groundwater could not have formed the deposits, but that they may be closely related to soil-forming processes. Finally, lead isotope data also support a pedogenic origin for the calcite and identify a detrital origin as the probable source of the lead.

Radioactive elements decay at known rates, so the relative abundance of radioactive elements and their decay products can sometimes be used to determine the age of a sample. Alternatively, if one knows the amount of a radioactive element initially present, one can measure the amount currently remaining to calculate an age. Carbon-14 dating is

an example of the latter. Samples of modern groundwater from volcanic tuffs sampled within 1 km (0.6 mi) of the potential repository block have apparent carbon-14 ages of 12,000 to 18,500 years (Benson and McKinley 1985). In contrast, apparent thorium-230/uranium-234 ratio ages of calcite found at Trench 14 range from about 80,000 to more than 400,000 years. Data from a drill hole into calcite at Devils Hole (a fault-controlled cavern in limestone in Ash Meadows) show little variation in the isotopic composition of strontium, uranium, oxygen, and carbon for the last 500,000 years (Stuckless, Peterman et al. 1992; Ludwig, Simmons et al. 1992; Winograd et al. 1992). Because the isotopic composition of groundwater beneath Yucca Mountain has not likely varied significantly during the last 500,000 years, the comparison of modern groundwater with that of the deposits provides a valid means of assessing the origin of the deposits.

4.3.3.1.2 Peer Reviews and Evaluations of New Evidence

In 1990, the DOE requested that the National Academy of Sciences/National Research Council consider whether the water table had risen in the geologically recent past to the level of the potential repository and whether a water table rise was likely to occur over the life of the repository in the manner proposed by Szymanski (1989). The National Research Council established a panel that reviewed the pertinent literature and data available up to 1992. This panel consulted with scientists involved in related field and laboratory studies. The panel's conclusion (National Research Council 1992, p. 3) was that none of the evidence offered as proof of groundwater upwelling in and around Yucca Mountain could reasonably be attributed to that process. Furthermore, the panel stated (p. 130): "The preponderance of features [ascribed to ascending water] (1) were clearly related to the much older (13-10 Ma) volcanic eruptive processes that produced the tuffs in which the features appear, (2) contained contradictions or inconsistencies that made an upwelling groundwater origin geologically impossible or unreasonable, or (3) were classic pedogenic features recognized worldwide." The panel concluded that the physical and textural evidence from the veins in the trenches

indicated a sedimentary, low-temperature origin from descending meteoric water (infiltration) rather than an origin involving upwelling of thermal water from deep within the crust. The panel also concluded (p. 56): "…to date the preponderance of evidence supports the view that the calcretes and other secondary carbonates in veins of the area formed from meteoric water and surface processes."

Other independent reviewers reached similar conclusions, which were considered by the National Research Council. In the majority report of the independent peer review panel convened in 1991, Powers et al. (1991, p. s-2) concluded: "Surficial deposits cited by Szymanski as evidence of upwelling fluids are consistent in isotopic and physical character with surficial, pedogenic processes; these deposits are not consistent isotopically with known groundwater in the area of Yucca Mountain." Although Archambeau and Price (1991), in their minority report, supported Szymanski's hypothesis, a colleague they selected to review their report concluded the model was "a set of unsupported and unsupportable assertions" (Evernden 1992, p. 65).

After the National Academy of Sciences/National Research Council reached its conclusions, Szymanski and others, as documented by Hill et al. (1995), asserted in 1995 that much of the data available for the calcite/opal deposits could be explained by the upwelling of warm, carbon dioxide-rich water along faults. Hill et al. postulate that once this upwelling water reaches the surface, it flows downhill back into the ground. Therefore, they argued, the resulting deposits are slope-parallel and acquire a pedogenic character. In a critique of this hypothesis, Stuckless, Marshall et al. (1998, p. 70) concluded the hypothesis was based on misstatements, omissions of available information, and misleading generalizations that lead to an erroneous conclusion. In addition, Vaniman, Carey et al. (1999) have examined the chemistry of zeolitic strata beneath the potential repository horizon and concluded that flow in the unsaturated zone has been downwards and predominately gravity-driven for the last 12 million years.

The NWTRB (Cohon 1998) reviewed a group of reports submitted by the Nevada Nuclear Waste Project Office. One of the reports cited evidence from fluid inclusion studies that the authors asserted were an indication of a purported high-temperature origin for secondary calcite collected in the Exploratory Studies Facility (Dublyansky and Reutsky 1995). However, the age of the secondary calcite was unknown, and there was a well-documented thermal period that affected the volcanic rock for a long time after its formation. Because of this and other evidence from the Exploratory Studies Facility excavation, discussed below, the NWTRB concluded that the fluid inclusion data does not significantly affect the conclusions of the National Academy of Sciences/ National Research Council report (National Research Council 1992). The NWTRB did, however, recommend further studies of this type in conjunction with age determinations.

In response to this recommendation, the DOE sponsored research at the University of Nevada, Las Vegas and the USGS on age and thermal history indicated by fluid inclusions. Representatives of the state of Nevada participated in the sampling program and were given splits of all materials collected. In addition, the representatives participated in biannual meetings to review and interpret the data. The general conclusion reached by USGS and University of Nevada, Las Vegas researchers was that the fluid inclusions formed in the vadose environment by downward percolating meteoric water and that the environment was warmer than ambient until at least 5 million years ago; however, there is no evidence for above-ambient temperature precipitation during the last 1.9 million years (Paces, Whelan et al. 2000; Paces, Neymark, Persing et al. 2000; Whelan, Roedder, Paces, Neymark et al. 2000; Wilson, N.S.F., Cline, Rotert, and Amelin 2000; and Wilson, N.S.F., Cline, and Amelin 2001).

Evidence for precipitation in a vadose environment includes (1) only 1 to 40 percent of the cavities are mineralized in a given area, whereas precipitation in a saturated environment would predict that most, if not all sites would be mineralized (Marshall, Neymark et al. 2000); (2) mineralization is restricted to floors of cavities and footwalls of frac-

tures (Marshall and Whelan 2000); and (3) the fluid inclusion assemblage of all liquid, all vapor, liquid and vapor in variable proportions is most consistent with a vadose environment (Whelan, Roedder, Paces, Neymark et al. 2000).

Fluid inclusion temperatures for all but the earliest calcites range from 35° to 75°C (95° to 167°F) (Whelan, Roedder, Paces, Neymark et al. 2000; Wilson, N.S.F., Cline, Rotert, and Amelin 2000). Most of these temperatures were determined for calcite that is clearly older than 4 to 5.3 million years (Wilson, N.S.F., Cline, and Amelin 2001). The chemical composition of calcite changed between 2.8 and 1.9 million years ago to include a few percent magnesium, and this calcite lacks two-phase inclusions, thereby indicating precipitation at ambient temperatures (Wilson, N.S.F., Cline, and Amelin 2001).

The isotopic composition of strontium in secondary calcite collected in the Exploratory Studies Facility is more radiogenic (containing more of the isotope strontium-87) in successively younger layers, which is consistent with an origin of meteoric water reacting with rocks that are getting older and accumulating radiogenic strontium (Marshall and Whelan 2000). Carbon isotopes also show an evolution in time that can be related to a change in plant community at the earth's surface, which in turn reflects changing climate (Whelan and Moscati 1998). In contrast to evidence for downward percolating water, groundwater beneath Yucca Mountain is undersaturated with respect to calcite and could not precipitate that mineral without significant degassing or evaporation.

Considerable geochronology has been done on the secondary minerals. Uranium–lead dating shows a long-term slow average growth rate, which is consistent both for an entire secondary mineral coating or for parts of a coating where layers of opal are separated by calcite (Neymark et al. 1998). Uranium series dating yields similar growth rates for the outer layers of secondary minerals (Paces, Whelan et al. 2000; Paces, Neymark, Persing et al. 2000). Disagreement in apparent ages between techniques with different half-lives and the correlation between initial uranium-234/uranium-238 and

apparent age is best explained by a continuous growth model and slow growth rates (Neymark et al. 1998; Neymark and Paces 2000).

4.3.3.1.3 Evidence Related to Past Water Table Elevation

Field Observation—Although the calcite and opaline silica deposits provide no direct information on past water table elevations, estimates can be made from other evidence for former high levels of the water table in the region surrounding Yucca Mountain during the past 2 million years. The evidence includes:

- Tufas and travertines

- Calcitic veins and calcite-lined tubes that mark the routes of former groundwater flow to springs

- Former water levels marked by calcite cave deposits on the walls of Brown's Room within Devils Hole

- Widespread marsh deposits (composed of silty marls, diatomaceous earth, and clays) formed from past groundwater discharge.

Most of these features are attributable to the carbonate aquifer, which is the deep and probably confined aquifer beneath Yucca Mountain. Nonetheless, this aquifer and the one hosted by the volcanic rocks and valley fill likely have responded similarly to past conditions. Available evidence indicates (1) an apparent lowering of the water table of 50 to 70 m (160 to 230 ft) for the carbonate aquifer in the east-central Amargosa Desert since the middle Pleistocene and (2) an apparent lowering of perhaps as much as 130 m (430 ft) since the end of the Pliocene. This estimated general lowering does not preclude small water table fluctuations in response to climate changes superimposed on the general trend.

There are also several discharge deposits from the volcanic and valley-fill aquifer, including three small deposits near the south end of Crater Flat. Root casts from these deposits have yielded uranium-series ages of approximately 10,000 to

20,000 years (Paces, Mahan et al. 1995). Four carbon-14 ages for root casts range from approximately 6,000 to 16,000 years and confirm the young (and possibly Holocene) age for groundwater discharge in Crater Flat. The initial uranium-234/uranium-238 ratio values and the initial strontium-87/strontium-86 values (Marshall, Stuckless et al. 1993) agree with the values obtained for samples from the volcanic and valley-fill aquifer in Crater Flat (Ludwig, Peterman et al. 1993; Peterman and Stuckless 1993). This correspondence confirms the origin of the Crater Flat deposits as groundwater discharge from a regional aquifer.

The largest and most extensive past discharge site for the volcanic and valley-fill aquifer is near Stateline, Nevada. This site is particularly significant in that it occurs where the regional groundwater flow model predicts that—under conditions of nearly a 15-fold increase in recharge and a water table rise of about 100 m (330 ft) beneath Yucca Mountain—discharge would occur (Czarnecki 1984); note that the amount of water table rise predicted to initiate spring discharge is less than the conservative, maximum water table rise calculated by Czarnecki and discussed in Section 4.3.3.1.4. Eight uranium-series ages on five different samples from this site range from approximately 11,000 to 110,000 years, but the ages cluster around the times of the last two pluvial periods (times with higher rainfall) (Paces, Neymark, Marshall et al. 1996). This suggests that maximum water table rises correspond to the wettest past climates. Recent work by Paces and Whelan (2001) on spring discharge deposits from Nye County Early Warning Drilling Program wells is interpreted to indicate that the maximum Pleistocene groundwater table rise was only 17 to 30 m (56 to 98 ft).

Devitrification and Other Mineralogical Evidence—The maximum water table rise suggested by past discharge deposits south of Yucca Mountain is supported by data from drill holes at Yucca Mountain. Bish and Vaniman (1985) noted that the volcanic tuffs were devitrified (i.e., glass was altered to minerals) below the current water table and for as much as 80 to 100 m (260 to 330 ft) above that surface. Devitrification is attributed to prolonged contact with water; therefore, the top of the devitrified zone marks the high stand of the water table. Dibble and Tiller (1981) have concluded that the time required to form zeolites from glass is on the order of 10,000 years, so larger short-term fluctuations are not precluded by the elevation of devitrified tuff. This suggests that the water table must have remained about 100 m (330 ft) higher than at present over the thousands of years required for zeolitization of the glassy tuffs (NRC 1999b, pp. 27 and 28).

Levy (1991) reevaluated the base of the vitric tuff as an indicator of the hydrologic past, considering structures and uplift occurring after devitrification. She noted that the uppermost boundary of the devitrified tuff, which occurred farthest above the current water table, was not parallel to the water table, suggesting that it formed before tilting of the tuffs. Therefore, at least some of the devitrification must have occurred more than 12 million years ago. The most recent water level fluctuations would postdate major tectonic events, but would be difficult to date. The base of the vitric tuff shown on Bish and Vaniman's (1985) cross sections is 10 m (33 ft) to more than 100 m (330 ft) below the base of the potential repository horizon. Thus, it appears likely that the maximum water table elevation is well below the potential repository. If the structural interpretations proposed by Levy (1991) are taken into account, the maximum past rise in the water table, for enough time to cause devitrification, was about 60 m (200 ft).

Because the shallow groundwater beneath Yucca Mountain is undersaturated with calcite, calcite can dissolve in the groundwater. Consequently, secondary calcite is rare below the current water table, occurring only where it is armored, such as in a tightly sealed fracture. Secondary calcite is also rare in a zone as much as 85 m (280 ft) above the water table (Marshall, Stuckless et al. 1993), suggesting that the water table could have risen as much as 85 m (280 ft) in the past.

Carbon isotopes in unsaturated zone calcite are consistent with the carbon isotopic signature acquired in the soil zone by downward percolating water (Marshall, Whelan et al. 1992). This consistency is also corroborated by strontium isotopic

compositions for calcite and pore water that are closely similar to values in the soil zone at shallow depth and become more similar to values for the volcanic rock as water reacts with the rock during downward percolation (Marshall, Futa et al. 1998).

Evidence from the Exploratory Studies Facility Excavation—Studies of secondary minerals from the Exploratory Studies Facility show that these minerals formed in the unsaturated zone (Paces, Neymark, Marshall et al. 1996). For example, mineralization in the Exploratory Studies Facility is found only on the floors of cavities and footwalls of open fractures, which contrasts with the locus of mineralization for geodes or veins that formed in the saturated zone. Most cavities are devoid of the mineralization that would be expected in a saturated environment. Uranium–lead and uranium-series dating have shown that the environment of deposition for the secondary minerals has stayed the same for millions of years (Neymark et al. 1998; Neymark and Paces 2000).

4.3.3.1.4 Future Water Table Elevations

Although nothing in the geologic record suggests that the water table might rise sufficiently to flood the potential repository horizon, there are two general mechanisms proposed as capable of doing so in the future: climate change and tectonic activity. A careful examination of both of these mechanisms shows that neither is likely to be able to cause flooding of the repository level.

The long-term climate history has been examined and correlated with variations in the Earth's orbit over the past 400,000 years (USGS 2000a). This climate study concluded that most of the next 10,000 years will be wetter, cooler, and more like the glacial periods in the past and that the climate will be much like the current climate in northern Nevada. Czarnecki (1984) modeled the regional groundwater flow system to examine water table rises due to increased precipitation (i.e., pluvial periods). He calculated a maximum increase in water table altitude of about 130 m (430 ft) beneath the emplacement horizon. This analysis is considered conservative because a 100-percent increase in precipitation during pluvial periods was assumed. This in turn results in a 15-fold increase

in recharge from the assumed modern rate of 0.5 mm (0.02 in.) per year to about 8 mm (0.3 in.) per year at Yucca Mountain. Half of the calculated recharge flux in the model was applied directly east of the potential repository site, along a segment of Fortymile Wash, which is consistent with the proposal of Claassen (1985) that Fortymile Wash is an area of recharge under wetter climatic conditions. The flux at Fortymile Wash causes about three-quarters of the computed water table rise of 130 m (430 ft). Czarnecki (1984) notes, however, that under a 100-percent increase in precipitation, large quantities of runoff might flow away from the area down Fortymile Wash and other drainage ways. This would have the effect of decreasing the effective groundwater recharge to less than the calculated values.

Based on past discharge deposits, Quade et al. (1995) calculated a maximum past water table elevation. They concluded that the maximum increase in water table elevation under Yucca Mountain in response to climate change was less than or equal to 115 m (380 ft) during the last full glacial period. They estimated the paleo-water table rise at the Lathrop Wells diatomite spring deposits based on water table information from Winograd and Thordarson (1975). The rise of 115 m (380 ft) was needed to establish spring flow in the past. Nye County drilling at these spring deposit sites established that the water table is currently about 16 to 30 m (52 to 98 ft) below the land surface (NRC 1999b, pp. 25, 26, and 31). This 115 m (380 ft) value is now recognized as a significant overestimate. Recent work by Paces and Whelan (2001) on results from the most recent Nye County drilling indicates that the maximum water table rise during the Pleistocene was between 17 to 30 m (56 to 98 ft). Thus, multiple lines of evidence suggest that a 120-m (390-ft) rise in water table elevation is a reliable estimate of the potential maximum increase due to climate change, based on a projected wetter future climate (CRWMS M&O 2000c, Section 3.7.5.2). Future climate changes are not expected to cause the emplacement drifts to flood because they would be located at a distance ranging between approximately 210 m (690 ft) and 390 m (1,300 ft) above the water table. The average distance of the repository above the water table would be about 300 m (1,000 ft).

Possible tectonic-induced changes in water table elevation include volcanic and seismic effects. If basaltic intrusion formed barriers downstream from Yucca Mountain, those barriers could raise the elevation of the water table, much like a dam impounds water. Similarly, a dike that is formed upgradient from the repository could lower the water table at Yucca Mountain. The heat associated with a volcanic intrusion could also cause the water table to rise. However, the only potential volcanism near Yucca Mountain would be basaltic dikes that tend to form along faults in extensional tectonic areas and are typically less than two, but potentially up to four, meters in width (Carrigan, King, and Barr 1990). Thus, future intrusion would be expected to be small and to trend in a northerly direction, which coincides with the principal strike of faulting. Movement of groundwater at Yucca Mountain is parallel to the direction of possible dike formation, so an intrusive dike would be unlikely to form a barrier to flow. As described previously, Szymanski (1989) and Archambeau and Price (1991) have postulated seismic activity as a driving mechanism to raise the water table to the level of the potential repository. Carrigan, King, Barr, and Bixler (1991) and the National Research Council (1992) examined this mechanism and concluded that it would not raise the water table more than a few meters. In fact, the opposite effect is more common. Increased stream flow and decreased wellheads have been observed after moderate earthquakes (Rojstaczer and Wolf 1992; National Research Council 1992).

Davies and Archambeau (1997a, 1997b) developed a variation of the seismic pumping model. Their model posits that variations in the state of stress cause changes in water table elevation and that these changes may be as great as several hundred meters. The NWTRB asked an independent expert to review this hypothesis and other material. The reviewer concluded, "The interpretations depend significantly upon theoretical models that have never been tested or previously used and run counter to observations in nature and in the laboratory" (Rojstaczer 1998; see also Rojstaczer 1999). Based on this review, the Board concluded that the material reviewed: "…does not make a credible case for the assertion that there has been ongoing, intermittent hydrothermal activity at Yucca Moun-

tain or that large earthquake-induced changes in the water table are likely at Yucca Mountain. This material does not significantly affect the conclusions of the 1992 NAS report" (NWTRB 1999a, p. 20).

4.3.3.1.5   Conclusion

Despite the suggestion that the water table could rise to the level of the potential repository, the preponderance of evidence shows that the water table has not risen to this level in the past and is not likely to do so in the future. Earthquakes are known to have an impact on the water table, but water table excursions are likely to be small and short-lived. For these reasons, tectonically induced fluctuations of the water table have not been included in the TSPA-SR. Future, wetter climates have the potential to cause the water table to rise to levels that were experienced during past, wetter climate periods. Multiple lines of evidence suggest that 120 m (390 ft) is a reliable estimate of the potential increase in water table elevation for a future, wetter climate (CRWMS M&O 2000c, Section 3.7.5.2). Paces and Whelan (2001) estimate that the maximum water table rise during the Pleistocene was only 17 to 30 m (56 to 98 ft). Future climate changes are not likely to result in flooding of the waste emplacement drifts due to a water table rise because the emplacement drifts would be located a distance above the water table ranging between approximately 210 m (690 ft) and 390 m (1,300 ft) (see Figure 1-13 in Section 1). At the northernmost end of the repository block, the design described in this report has portions of the layout outside the emplacement area that would be less than 120 m (390 ft) above the water table. The repository layout shown in Figure 1-13 includes a ramp at the northernmost areas that serves as an access to an observation drift located below the emplacement area (see Figure 2-38 in Section 2.3.1 for labeled repository components). Sections of that ramp and the east repository main north extension that it connects to are located such that portions of the excavations could be flooded if the water table rose as much as 120 m (390 ft). Water would not be expected to flow to the emplacement drifts. Future assessment of performance and design work will consider this situation, together with more specific details of the water table and its

potential rise, and ensure that the design is developed to take advantage of opportunities to contribute positively to performance. Variation in the water table caused by climate is included within the nominal dose for the TSPA-SR.

4.3.3.2 Nuclear Criticality

This section describes the FEPs that could lead to a nuclear criticality event, together with the possible consequences. It begins with a discussion of the physics of nuclear criticality, followed by a brief summary of the methods used to evaluate the post-closure criticality potential of the waste forms that may be emplaced in the potential repository. These methods ensure that all the critical configurations that could result from the degradation of the waste forms are identified and the results quantified. Criticality control is an important objective of waste package design because a criticality event can result in an increased radionuclide inventory, potentially increasing the radiation dose to the receptor. For the 10,000-year period after disposal, nuclear criticality is screened out from the TSPA nominal case analysis based on its low probability. Nevertheless, because of significant interest in this topic, the DOE investigated the potential consequences of a criticality event. The results of the investigation indicate that a nuclear criticality would not have a significant impact on repository performance.

4.3.3.2.1 Physics of Nuclear Criticality

Nuclear fission is the splitting of an atomic nucleus by an impacting neutron. Only certain isotopes of very heavy elements can be split; the most commonly known of these are the uranium-235 and plutonium-239 isotopes. The nucleus of each element has a constant number of protons but may have a varying number of neutrons; these variations identify isotopes of an element.

The key factors associated with the potential fissioning of a nucleus are the energy or speed of the impacting neutron and the characteristics of the nucleus, which affect the manner in which it reacts to the neutron. The nuclear reaction most important for criticality occurs when a nucleus absorbs a free neutron, creating an unstable compound nucleus.

The compound nucleus splits into fission fragments (lighter elements), releases energy in the form of gamma rays, and emits two or three additional neutrons in the process. The released neutrons are free to collide with other nuclei, which may absorb one of them and fission as well (Duderstadt and Hamilton 1976, Chapter 2).

There are other possible outcomes from a neutron interacting with a nucleus besides fissioning. The neutron may simply collide and be scattered, transferring kinetic energy to the nucleus in the process, or it may be absorbed by the nucleus without fissioning. The likelihood of any of these interactions depends heavily on the energy of the neutron. Neutrons emitted from fission have high energy. However, the likelihood of an interaction resulting in fission increases as the energy of the neutron decreases. As a result, fission is more likely if the energy or speed of a neutron is reduced.

Each time a neutron collides with a nucleus but is not absorbed, it loses energy, its speed decreases, and its potential for fissioning a nucleus increases. This slowing down of energetic neutrons is referred to as moderation; the material that provides the nuclei that cause this slowing down is called a "moderator." In general, the lighter the element, the better it works as a moderator because it scatters neutrons much better than it absorbs them. Hydrogen, the lightest element, is a very efficient moderator. Since water contains hydrogen nuclei, it also is a very effective moderator. The silicon in sand and rocks, such as those at the potential repository site, can also serve as a moderator, but silicon is a much less efficient moderator than water.

A nuclear chain reaction can be initiated once a neutron interacts with a fissile isotope, inducing it to fission. This releases additional neutrons that are, in turn, available to cause more fissions. Of the neutrons resulting from each fission, some will be absorbed in a nucleus without a resulting fission, some will escape from the system before colliding with a potentially absorbing nucleus, and some will be absorbed and cause fission. When each fission releases just enough neutrons to cause one additional fission, the effective neutron multiplication factor (k_{eff}) equals one, the chain reaction becomes

self-sustaining, and the system is considered critical.

For a nuclear criticality to occur, there must be the proper combination of material and geometric configuration, known as the critical mass and critical geometry. Fissile material is essential for criticality. The only naturally occurring fissile isotope is uranium-235. However, it is not the only isotope that can support a critical reaction. Uranium-233 and plutonium-239 can also support criticality; these isotopes are produced in a reactor by fast neutrons that are absorbed by thorium-232 and uranium-238, respectively. In general, the greater the amount of fissile material, the more likely it is to have a criticality. The presence of neutron absorbers—materials that absorb neutrons without causing fission—is also important. The greater the amount of neutron absorber material, the less likely it is to have a criticality. Isotopes of boron and gadolinium are good neutron absorbers.

The geometrical arrangements of the fissile material and any neutron-absorbing material are of equal importance in determining whether an accumulation of a fissile material can achieve criticality. Because neutrons can leak out of a system without causing fission, the most efficient geometry for the occurrence of criticality is a sphere, which has the least surface area per unit volume of any shape.

With the presence of moderating materials like water, the likelihood of fission can be greatly increased, and a reduced amount of fissile material is necessary to form a critical mass. However, criticality is possible without the presence of a moderator. These situations are known as fast criticalities because they can occur in the presence of predominantly high-energy neutrons.

In addition to the release of energy and additional neutrons, the fission process effectively removes fissile nuclei from the system by splitting them into other, lighter elements. This is referred to as fuel depletion, or burnup. Also, many of the fission products—the lighter elements resulting from the fragmenting of nuclei—are strong neutron absorbers. Their existence in the area where the critical reaction is ongoing dampens the reaction. Thus, as commercial spent nuclear fuel is depleted, its ability to support a criticality is reduced from the combination of the removal of fissile material and the creation of materials that absorb neutrons through the fission process. This is the primary reason fuel is discharged from operating reactors after several years: it can no longer effectively support a critical reaction. Incorporating fuel depletion in the criticality evaluation of systems is called "burnup credit."

A repository would contain fissile material, mostly from commercial spent nuclear fuel in the form of a reduced amount of uranium-235 (compared to what was initially loaded into the reactor) and plutonium-239. Moderating materials, primarily consisting of silicon dioxide, would be present; some water may be present as well. As a result, a criticality event is possible: (1) inside one or more degraded waste packages; (2) in the rock surrounding the emplacement drifts, as a result of water transporting fissile materials from degraded waste packages; or (3) in the rock at some distance from the emplacement drifts as a result of an accumulation of fissile materials under favorable conditions in the nearby rock. An example of the last situation would be a deposit of organic material, which could accumulate dissolved fissile material from a flow of water that had originated in or previously passed through the repository area. The probability of a criticality depends on the probability of occurrence of three conditions: (1) a waste package breach, (2) the separation of the neutron absorber from the fissile material, and (3) the presence of sufficient amounts of a moderator. The spacing between fuel rods will affect the probability of criticality for certain waste forms.

If a critical event were to occur in a repository, the characteristics and consequences of the event may be considered as falling into two categories: steady-state and transient.

In a steady-state criticality, the reaction remains constant, with the k_{eff} equal to one. The magnitude of this type of criticality is limited by the fact that the energy released as a result of the criticality serves, in part, to evaporate surrounding water. Since the water is necessary for moderation of the neutrons, removing the water through boiling restrains the reaction and would, over time, make the system no longer critical.

One of the principal consequences of a steady-state criticality would be an increase in radionuclide inventory, particularly in fission products and actinides (i.e., elements heavier than uranium, formed primarily from the initial absorption of neutrons by uranium-238 for those waste forms which contain a significant fraction of this isotope). Another result would be the production of heat from the fissioning of nuclei, which would incrementally increase the heat generated from the ongoing decay of fission products already present in the waste. The additional heat could create localized hot spots in the repository, potentially affecting nearby geochemical and other conditions. These changes could marginally affect the amount and rate of release of radioactive materials from the repository. However, evaluations have shown that neither the inventory increase nor the thermal effects are significant enough to adversely impact repository performance (CRWMS M&O 1998m, Sections 9 and 10).

A natural analogue for steady-state criticality is the family of natural reactors that occurred in a sedimentary formation approximately 2 billion years ago at Oklo, a site in what is now Gabon, Africa. These natural reactors occurred in several closely linked, very rich uranium ore bodies that were saturated with water, which served as a moderator. Criticality at Oklo continued periodically for approximately one million years, pausing when the heat from the reaction evaporated the water and resuming when the site reflooded. Such a natural reactor was possible because, two billion years ago, the natural enrichment of uranium was greater than 3 percent (by weight) (enrichment is the percentage of uranium-235 by weight contained in the total uranium content). The radioactive decay process of uranium-235 has since dropped the worldwide natural uranium enrichment from

greater than 3 percent at that time to its current value of 0.72 percent. The natural reactors at Oklo at that time period are unique; no other place in the world has been found where natural reactors existed (Smellie 1995). A reactor like the one that occurred at Oklo is not probable in a repository at Yucca Mountain because (1) the prevailing geochemical conditions for the Oklo deposit allow a higher concentration of uranium than any known deposit in the world, while the geochemistry and lithology characteristics of the Yucca Mountain site are not conducive to such concentrated accumulations of fissile materials, and (2) the effective enrichment (uranium-235 plus plutonium-239) of most commercial spent nuclear fuel that would be emplaced in the potential repository is less than the enrichment of the Oklo reactors during the time they were critical (Smellie 1995).

Transient criticalities could occur if there were a sudden change in the geometry or material composition of a disposed waste. A transient criticality would increase the rate of fission rapidly so that a very large burst of neutrons would be produced for a brief period; the accompanying increased rate of energy release could lead to a large increase in pressure and temperature. A transient criticality ends when the neutron multiplication factor decreases below unity, usually because of the loss of the moderating effects of water, which boils off during heightened temperatures. If some water were to return (recharge) after the criticality ended, it could increase neutron moderation, and the critical reaction could start again. However, the recharge of water would require a relatively long time compared with the duration of the criticality, so the total radionuclide increment from a transient criticality would be much smaller than the total for a steady-state criticality enduring over the same total elapsed period. The potential for damage to waste packages in the repository because of the peak temperature pulse from a transient criticality has been investigated, and evaluations (as presented in Section 4.3.3.2.3) indicate that such effects are not sufficient to significantly alter repository performance (CRWMS M&O 1999q).

A special subset of transient criticality is autocatalytic criticality, which is a transient criticality where the usual mechanisms that tend to shut down

a criticality, such as the loss of moderator or loss of confinement, are delayed until a high fission rate is achieved. Although the probability of occurrence of an autocatalytic criticality at the potential repository is so low as to be considered not credible (Paperiello 1995), it is addressed for completeness and for evaluation of any hypothetical consequences. Scientists have pointed out that an autocatalytic criticality could occur when silica is the primary moderator (Bowman and Venneri 1996), but this would require extraordinarily unusual conditions that cannot occur in the waste package or at all outside the waste package unless (1) the entire fissile content of the waste package is spread uniformly in a nearly spherical shape or (2) fissile material from multiple waste packages accumulates in a small region of rock. Either configuration is essentially impossible to achieve. If such an event were to occur, it could create a much higher peak temperature and pressure than would result from transient criticality. If such an event were to result in a large and rapid release of kinetic energy, it could be considered an explosion. The possibility of an explosion as a result of an autocatalytic criticality in the potential repository has been examined by the scientific community and found not to be credible (Canavan et al. 1995; Kastenberg et al. 1996).

4.3.3.2.2 Methodology for Criticality Evaluation

The complete evaluation process for postclosure criticality has been documented in *Disposal Criticality Analysis Methodology Topical Report* (YMP 1998), which has been reviewed by the NRC. Some aspects of the methodology have already been accepted by the NRC (Reamer 2000), which is providing additional information and refinement to allow for the acceptance of remaining aspects of the methodology (YMP 2000c).

The postclosure criticality methodology is based primarily on a risk-informed approach. The objective of the risk-informed methodology is to provide assurance that all known waste forms and associated degradation products that can result in configurations that can support criticality are considered and evaluated based on probability of occurrence and potential consequences. The bases

of this risk-informed methodology are the estimated probabilities of the potential configurations that could lead to a criticality and the evaluation of the consequences of those criticalities. This methodology was designed to, and can, encompass time frames much greater than 10,000 years. This methodology requires a redesign of any proposed design concept that may result in a critical event that has a frequency of occurrence of greater than 1 in 10,000 per year for the entire repository in any of the first 10,000 years. The methodology also identifies potentially critical configurations that have such a low probability of occurrence that they are deemed not credible.

Figure 4-170 provides a visual representation of the postclosure criticality methodology. The starting point is the establishment of the range of:

1. Potential waste forms
2. Waste package and engineered barrier system designs
3. Characteristics of the site
4. Degradation characteristics of the waste package materials.

Some of these parameters can be specified deterministically, but some are most readily characterized probabilistically. Based on the established parameters, scenarios are developed encompassing how the emplaced material may degrade, which results in various degraded configurations. These configurations are grouped into classes reflecting a range of related parameters. Detailed degradation analyses are then performed on these configuration classes to identify the parameters that affect criticality potential: when the calculated k_{eff} of the configuration exceeds an established analytical value called the critical limit, the configuration is considered potentially critical (Section 3.5.2). These parameters include the respective quantities of fissile material, neutron absorber material, corrosion products, and moderator present in the configuration. Evaluations are then performed to determine the potential for criticality in the various proposed configuration classes (Section 3.5.2). Initially, the worst combination of parameters that define the range is used to determine whether that configuration class is potentially critical. If no combination of parameters can be
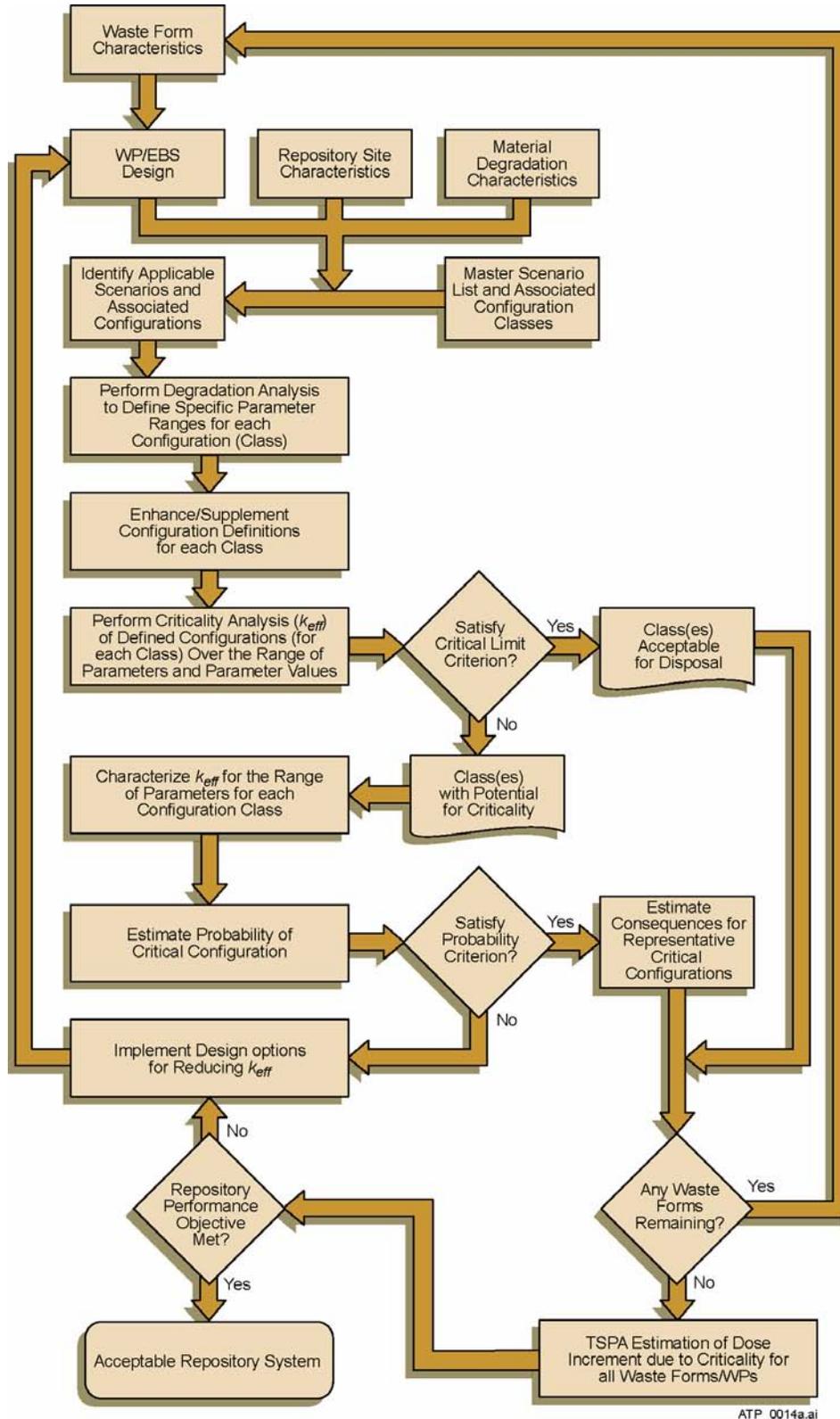
Figure 4-170. Representation of the Postclosure Criticality Methodology
WP = waste package; EBS = engineered barrier system. Source: YMP 2000c, Figure 3-1.

constructed such that probability of exceeding the critical limit is below the screening value, then that configuration class is considered acceptable for inclusion in the repository. Configuration classes that show a potential for criticality are evaluated further to more precisely define which parametric combinations result in a k_{eff} that exceeds the critical limit criterion.

The results of these k_{eff} calculations are tabulated to cover the range of parameter values. These tables are then used to determine whether a specific combination of parameters within a configuration class can be considered potentially critical.

The probability of exceeding the critical limit is estimated for each configuration class by comparing the characteristics of the waste stream to the established parameter ranges. A probability criterion is established to identify when the probability of criticality is considered so high that a redesign of the waste package or engineered barrier system is needed to reduce the probability of criticality. The probability criterion requires that the overall frequency of criticality be less than 1 in 10,000 per year for the entire repository in any of the first 10,000 years. The criticality limit and probability criterion form design criteria for limiting the potential for criticality in the repository during postclosure (CRWMS M&O 2000au; CRWMS M&O 2000bg).

If any configurations are determined to be capable of supporting criticality events and have an estimated probability of occurrence below the probability criterion, but contribute to a total probability of criticality for the entire repository inventory above the 10 CFR 63.114(d) (66 FR 55732) screening probability threshold of 10^{-4} in 10,000 years, consequence analyses are performed. The probability tested against this screening threshold is the sum of the probabilities for all the scenarios that can lead to criticality for all waste forms in the repository.

The consequence analyses are primarily concerned with the increase in the radionuclide inventory resulting from a criticality, but they include other potential consequences, such as increased waste

package degradation due to the increased heat generated from the criticality.

In addition to the establishment of probability criteria, the overall risk of potential critical events is determined. The probabilities and associated consequences of all configurations that would contribute to the probability of exceeding the screening probability threshold (1 chance in 10,000 in 10,000 years) are collected into an input set to perform an additional TSPA. This TSPA, which includes the total criticality risk, is performed to determine if the health and safety of the public would be maintained within the proposed regulatory limit. If necessary, additional design features for reducing the potential level of criticality would be implemented.

As Figure 4-170 shows and the preceding paragraphs describe, the postclosure disposal analysis criticality methodology includes both deterministic and probabilistic aspects. The evaluation of the various long-term processes, the combination of events, any potential criticality, and the consequences resulting from a potential criticality are all deterministic analyses. However, probabilistic analyses are performed to establish the likelihood of a criticality occurrence.

The methodology as described in this section pertains to commercial and DOE spent nuclear fuel, DOE high-level radioactive waste, and immobilized plutonium. Criticality analyses for naval spent nuclear fuel employ a separate methodology that is primarily deterministic (YMP 1998, Section 1.2) and show that intact naval spent nuclear fuel cannot go critical for any credible configuration within the repository.

4.3.3.2.3 Criticality Results: Probability and Consequences

The methodology described in the previous section has been applied to postulated configurations that could result from the degradation of commercial spent nuclear fuel waste packages and their contents (CRWMS M&O 2000fh), as well as from several of the possible DOE spent nuclear fuel types (CRWMS M&O 1999j, 2000bh, 2000bi). The results, which demonstrate a very low proba-

bility of criticality and minimal consequences, are summarized below. These results apply to commercial spent nuclear fuel, except as otherwise noted. The 21-PWR waste package was chosen for these calculations because it is the design for fuel with the highest reactivity (CRWMS M&O 2000bg). Other waste forms with lower reactivity planned for repository disposal are expected to have a lower probability of criticality.

Probability of Criticality within 10,000 Years Following Repository Closure—The postulated earliest time to breaches in the waste package barrier that could allow criticality exceeds 10,000 years because of the limited water available in the natural system to contact the waste packages, the use of an extremely corrosion-resistant material for the waste package outer barrier, and a titanium drip shield that covers the tops of the waste packages and is designed to divert water away from the waste packages. Even with postulated early breaches, the initial conditions required for criticality would have a very low probability. The probability of a critical event, internal or external to the waste package, is expected to be less than 1 chance in 10,000 within 10,000 years (CRWMS M&O 2000fh, Section 6). The main possible exception to this pre-10,000-year conclusion is in the event of igneous intrusion. In that case, the combination of low probability for breach by igneous intrusion and the other conditions required for criticality (filling with water moderator and separating fissile material from neutron absorber) have been shown, for commercial spent nuclear fuel, to be well below the screening probability threshold (CRWMS M&O 2000fh, Section 6). Because of the combination of low probability for breach by igneous intrusion and other conditions required for criticality, other waste forms are expected to show similar results.

Probability of Internal Criticality—As mentioned previously, the probability of a waste package breach and subsequent loss of neutron absorber will increase with time after 10,000 years. Figure 4-171 depicts the different stages of internal degradation for a typical 21-PWR Absorber Plate waste package (YMP 1998, Appendix C). The final stages of degradation, shown in this figure, illustrate the collapse of the assemblies, which reduces

the probability of criticality because of the reduced volume between fuel rods available for the moderator to fill. Another factor tending to reduce the probability of criticality with time is the eventual breach of the bottom of the waste package, which can drain most of the moderating water. Evaluations have shown that the potential for criticality of commercial spent nuclear fuel is maximized when the internal basket is fully degraded, but the assemblies remain intact (CRWMS M&O 1997d) and there is no breach of the bottom of the waste package. Using the TSPA-SR waste package degradation models, the probability of a critical event within the total inventory of the 21-PWR Absorber Plate waste packages is calculated to be 2×10^{-7} in 10,000 years (CRWMS M&O 2000fh, Section 6).

Probability of Internal Criticality for Codisposed U.S. Department of Energy Spent Nuclear Fuel and High-Level Radioactive Waste—Evaluations have been performed of the criticality potential of waste packages that would contain high-level radioactive waste glass and certain types of codisposed DOE spent nuclear fuel (CRWMS M&O 1996c, 1999j, 2000bh, 2000bi). These evaluations have generally shown the probability of criticality to be less than that for commercial spent nuclear fuel, which is very small to begin with. The primary reasons are the lower fissile loading per waste package for many of the DOE fuel types and the greater flexibility to install insoluble neutron absorber. This flexibility arises because of the smaller fuel mass per waste package.

Probability of Criticality for the Immobilized Plutonium Waste Form—The range of possible degradation scenarios for this waste form has been examined to identify potentially critical configurations. It was found that the design of the immobilized plutonium waste form itself provides several layers of defense in depth, so that criticality is virtually impossible (CRWMS M&O 2000ba). The degradation rate of the ceramic waste form is so slow that in the unlikely event that the waste package is breached and filled by a continuous dripping of water, it will be nearly 50,000 years after emplacement before enough of this waste form has degraded to permit any significant separa-
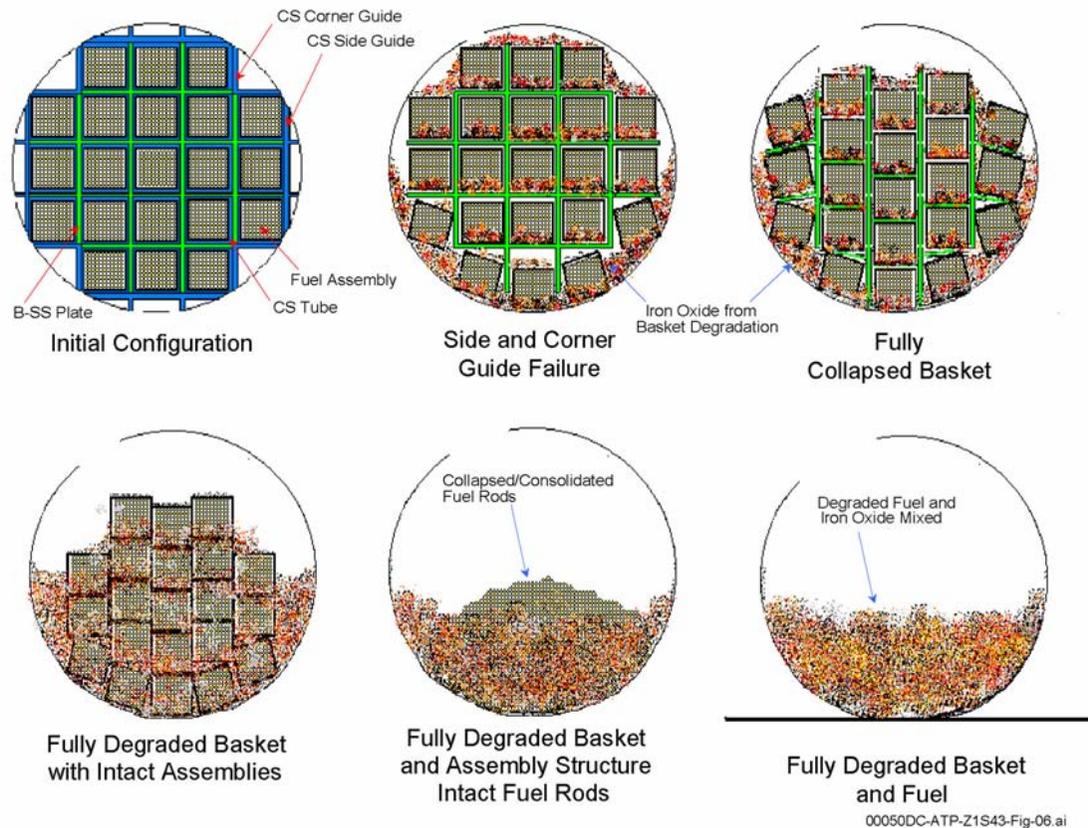
Figure 4-171. Different Stages of Internal Degradation for a Typical 21-PWR Absorber Plate Waste Package After 10,000 Years

CS = carbon steel; B-SS = borated stainless steel. Source: YMP 1998, Figure C-15.

tion of the uranium and plutonium from the gadolinium and hafnium neutron absorbers. Even after degradation of the waste form, the gadolinium and hafnium are generally less soluble than the fissile material, so they cannot be transported out of the waste package while the fissile material remains. Even with the additional conservative assumption of extremely unlikely chemistry conditions that would make the gadolinium sufficiently soluble to be removed before the fissile material, enough of the completely insoluble hafnium would remain to prevent criticality (CRWMS M&O 2000ba).

Probability of External Criticality—The probability for an external criticality to occur before 10,000 years is based on the igneous intrusion scenario. The probability for igneous intrusion is 1.6×10^{-4} in 10,000 years, which is just above the criticality-screening threshold of 1×10^{-4} in 10,000 years. However, subsequent processes to transport and accumulate the fissile material have a very small probability, so the combined probability of criticality before 10,000 years from igneous intrusion is less than the screening threshold (CRWMS M&O 2000fh, Section 6.2). Evaluations have shown that the probability, not considering igneous intrusion, of an external criticality even in the rock beneath the waste packages containing immobilized plutonium waste forms is less than 4×10^{-12} (McClure and Alsaed 2001, Section 8.4) and occurs beyond 10,000 years. This is primarily a result of (1) limited dripping water available to transport enough fissile mass out of the waste package and into a geometry favorable for criticality; (2) limited fracture intensity and lithophysae frequency to allow for fissile material accumulation in a geometry favorable for criticality; (3) low

concentration of fissile material in the water trickling out of a breached waste package due to low waste form solubility; and (4) limited fresh water needed to dilute the effluent water and neutralize and precipitate the fissile minerals (McClure and Alsaed 2001, Section 8.4).

Steady-State Criticality Consequences—If a steady-state criticality were to occur, it would be very unlikely to have a power level greater than 5 kW because the power is limited by the evaporation of the water moderator, which increases with power level or temperature. The duration is likely to be limited to 10,000 years, which is the average period of a climate cycle that might have a high enough rainfall or drip rate to sustain the required level of water moderation against evaporation (YMP 1998, Appendix C, Section 5.1). For a typical commercial spent nuclear fuel waste package, a continuous steady-state criticality would result in an increase of the radionuclide inventory in that waste package by less than 30 percent at approximately 10,000 years (YMP 1998, Appendix C, Section 5.1). The return of a moist climate cycle, upwards of 10,000 years after the shutdown, would be very unlikely because continued degradation of the waste package would have removed some conditions necessary for criticality (e.g., intact waste package bottom that supports water ponding, or optimum spacing between fuel rods). When this moderate increase is spread over all the waste packages likely to be degraded and not critical, the increment in radionuclide inventory is likely to be much less than the 10 percent stated in the criticality consequence criterion in Section 4.3.3.2.2. The temperature increase during steady-state criticality will be too small to measurably enhance waste form or waste package degradation. Steady-state criticalities would not operate above boiling temperatures because such temperatures would boil away the water moderator and shut down the criticality (YMP 1998, Appendix C, Section 5.1), and no increased degradation rates have been observed in iron-based materials at 150°C (302°F) (CRWMS M&O 1996d, Volume III, p. 8-4). As a result, the incremental impact of steady-state criticality events on the total inventory for the repository is expected to be insignificant.

Transient Criticality Consequences—In the unlikely event that a transient criticality were to occur, a worst-case rapid initiating event would provide a uniform ramp of positive reactivity insertion lasting 90 seconds and producing a peak power level of 10 MW for less than 60 seconds (CRWMS M&O 1999q). This reactivity insertion profile reflects the most rapid redistribution of moderator from the initial configuration to one most favorable to criticality, most likely caused by a seismic disturbance. After this brief period, rapid boiling of the water moderator would shut down the criticality. Although 10 MW is 2,000 times larger than the power level of the steady state criticality, the short duration would limit the increase in radionuclide inventory. The inventory increment would be a factor of 100,000 smaller than that generated by the 10,000-year steady state criticality and a factor of 1 million smaller than that generated by the fuel during its use in a commercial reactor. Other consequences of a transient criticality would be a peak average fuel temperature of 233°C (451°F) and a peak overpressure of about 20 atmospheres (CRWMS M&O 1999q, Section 6.1). Both conditions would last 10 seconds or less and would not be expected to cause enough damage to the waste package or its environment to have a significant impact on repository performance.

Autocatalytic Criticality—This type of criticality has been found to be not credible for the potential repository (Paperiello 1995). Autocatalytic criticality is not possible at all for low-enriched waste forms, nor is it possible for the waste form inside the waste package. Even for highly enriched waste forms or those containing nearly pure plutonium-239, achieving a critical mass outside a waste package would require the entire fissile content of the waste package to be spread uniformly in a nearly spherical shape, or it would require the extremely unlikely commingling of large amounts of transported fissile material from at least two waste packages containing highly enriched waste forms (Canavan et al. 1995; CRWMS M&O 1996e). Because the igneous rock at Yucca Mountain is not likely to contain deposits that can efficiently accumulate fissile material, the probability of creating such a critical mass from a single or multiple waste packages containing highly

enriched waste forms is so low as to be not credible (Kastenberg et al. 1996).

Disruptive Natural Events—The potential impact of disruptive natural events (e.g., seismic or igneous intrusion) on the risk of criticality in the repository has also been studied. Seismic events can produce a rapid change in the configurations of waste forms and waste packages. If the resulting configuration has a k_{eff} above the critical limit, the seismic event has provided a rapid reactivity insertion mechanism that could lead to a transient criticality. The identification of the initial, preinsertion configurations has been incorporated into the repository criticality analysis methodology.

Igneous intrusion was considered because its expected probability, 1.6×10^{-4} in 10,000 years, is above the screening threshold. The potential adverse criticality impacts of igneous intrusion into the repository include (1) the possibility of immediate waste package breach; (2) the separation of a significant fraction of the fissile material from the neutron absorber by magma transport; and (3) the accumulation of a critical mass of fissile material from, or within, the transporting magma. The potential for criticality following igneous intrusion has been evaluated for commercial spent nuclear fuel, under extremely conservative assumptions, and no mechanism for accumulating a critical mass has been identified (CRWMS M&O 2000fh). It is expected that a similar analysis for higher enriched spent nuclear fuel would give similar results. In particular, it is expected that although the probability of igneous intrusion is slightly greater than the screening probability threshold, when the low probability of the other conditions required for criticality is included, the combined probability of criticality will be below the screening probability threshold (CRWMS M&O 2000fh).

4.3.3.2.4 Conclusions

To ensure thorough consideration of all possibilities for criticality, a risk-informed methodology for postclosure criticality has been developed, as described in *Disposal Criticality Analysis Methodology Topical Report* (YMP 1998; YMP 2000c). The methodology encompasses time frames well beyond 10,000 years. It identifies configurations

that can become critical and estimates the probability of occurrence and the consequences of those criticalities. The methodology also includes threshold criteria that identify potentially critical configurations having too high a probability of occurrence. The purpose of these criteria is to identify any need for criticality design enhancement. These criteria are applied before any inclusion of potential criticalities into TSPA analyses. Additional TSPA analyses will be performed, including criticality results, if the combined probability of all the criticality events is above the screening probability threshold (1 chance in 10,000 in 10,000 years) or if a particular criticality event would significantly affect repository performance.

Evaluations have thus far shown that the probability of postulated criticality events before 10,000 years is below the threshold for inclusion in the nominal case for *Total System Performance Assessment for the Site Recommendation* (CRWMS M&O 2000a, Section 4.5.6). Accordingly, criticality is not included in the TSPA-SR nominal case. While the criticality methodology has not been fully applied to evaluation of all the waste forms expected to be placed in the potential repository, many have been evaluated, and the rest are expected to yield similar results. Therefore, the calculations performed to date indicate that the expected total probability of criticality will remain below the threshold for inclusion in the TSPA nominal case before 10,000 years.

In the unlikely event that a criticality occurs, it would most likely be steady-state, and the primary consequence would be an increase in the radionuclide inventory. The principal consequences of a transient criticality would be increased temperature and pressure. These have been evaluated and found to be of such short duration that they would be insignificant to repository performance. Potential autocatalytic criticalities have been evaluated and are not credible events.

4.4 ASSESSMENT OF PERFORMANCE

A major component of the postclosure repository safety case is the quantitative analysis of repository performance presented in this section. The DOE has conducted a TSPA to evaluate the performance

of a potential geologic repository at Yucca Mountain.

The TSPA was divided into separate evaluations: (1) a nominal (or reference) scenario and (2) a disruptive scenario. For groundwater protection, "undisturbed performance" was analyzed, consistent with 10 CFR 63.331 (66 FR 55732), and considered in this report equivalent to the nominal scenario. For individual protection, overall system performance was analyzed, consistent with 10 CFR Part 63. Therefore, the individual protection analyses combined the TSPA results for both the nominal and disruptive scenarios but excluded the human intrusion scenario, consistent with 10 CFR 63.113(d).

Presentations of TSPA-SR model results and supporting analyses for the evaluation of individual protection and groundwater protection are found in Section 4.4.2 and in *Total System Performance Assessment for the Site Recommendation* (CRWMS M&O 2000a, Sections 4.1 and 4.2). These analyses were consistent with proposed EPA (64 FR 46976) and NRC (64 FR 8640) rules.

Additional information on the supplemental TSPA model results is found in Volume 2 of *FY01 Supplemental Science and Performance Analyses* (BSC 2001b), Sections 3.2, 4, 4.1, and 4.2 (for the nominal scenario) and Section 3.3 (for the disruptive scenario). These results were also based on proposed EPA and NRC rules, but the report did provide a qualitative assessment of results consistent with the final EPA standard at 40 CFR Part 197.

Revised supplemental TSPA model results consistent with the final EPA rule can be found in *Total System Performance Assessment—Analyses for Disposal of Commercial and DOE Waste Inventories at Yucca Mountain—Input to Final Environmental Impact Statement and Site Suitability Evaluation* (Williams 2001a, Section 6). Results of TSPA sensitivity analyses consistent with the final NRC rule at 10 CFR Part 63 (66 FR 55732), using the revised supplemental TSPA model, are presented in *Total System Performance Assessment Sensitivity Analyses for Final Nuclear*

Regulatory Commission Regulations (Williams 2001b).

The DOE evaluated the performance of the system where there is a human intrusion, consistent with NRC regulations. The evaluation method in both cases is the same, except that the TSPA method for human intrusion used assumptions about the human intrusion scenario consistent with 10 CFR Part 63 (66 FR 55732). The DOE determined that, after about 30,000 years, the waste packages could degrade sufficiently that a human intrusion could occur without recognition by the driller. A human intrusion at that time was analyzed, and the results of the analysis are presented in the Yucca Mountain EIS and Section 4.4 of this report. Summary results of the earlier TSPA-SR model evaluation of inadvertent human intrusion at 100 years, consistent with proposed NRC (64 FR 8640) and EPA (64 FR 46976) rules, were discussed in *Yucca Mountain Preliminary Site Suitability Evaluation* (DOE 2001b) and are presented in Section 4.4.4 of this report. Results of the supplemental and revised supplemental TSPA models are discussed in Volume 2, Section 4.1.3 of *FY01 Supplemental Science and Performance Analyses* (BSC 2001b), in *Total System Performance Assessment—Analyses for Disposal of Commercial and DOE Waste Inventories at Yucca Mountain—Input to Final Environmental Impact Statement and Site Suitability Evaluation* (Williams 2001a), and in Section 4.4.4 of this report.

A human intrusion preceded by an unlikely igneous intrusion is analyzed in *Total System Performance Assessment Sensitivity Analyses for Final Nuclear Regulatory Commission Regulations* (Williams 2001b, Section 6.2).

This section focuses on explaining the primary results and technical findings of the TSPA calculations. For the purposes of this discussion, the analyses are presented in three scenarios: nominal (i.e., reference), disruptive (i.e., igneous activity), and human intrusion (i.e., penetration of the repository as a result of exploratory drilling for groundwater).

The analysis of FEPs conducted to determine their importance to the performance of the repository

system led to the exclusion of some FEPs because of low probability or low consequence. For example, the criticality and large seismic event FEPs were excluded from the nominal and disruptive analyses based on these criteria.

The TSPA results quantify the performance of the potential repository for 10,000 years. To complement the results of the 10,000-year performance assessment, the peak dose to the reasonably maximally exposed individual beyond the 10,000-year time period has been calculated. TSPA results for 100,000 and 1 million years were calculated for the nominal case to gain insight into possible peak dose levels at times significantly beyond 10,000 years.

Section 4.4.1 describes the TSPA model in general, together with a discussion of how uncertainty is identified and incorporated in the model. It also describes the disruptive scenarios analyzed and summarizes the radionuclides considered in the dose assessment. The sections that follow present the primary TSPA results for:

1. Evaluation of system and barrier component performance for the nominal scenario (Section 4.4.2)

2. Evaluation of the effect on repository performance of direct and indirect releases for the disruptive scenario associated with igneous activity (Section 4.4.3)

3. Evaluation of the impact on repository performance associated with inadvertent human intrusion by drilling through the repository (Section 4.4.4)

4. Sensitivity and uncertainty analyses for the nominal, disruptive, and human intrusion scenarios (Section 4.4.5).

Summary of Results—Table 4-33 presents a summary of recent TSPA results for: (1) individual protection, (2) human intrusion, and (3) groundwater protection. The combined dose calculated from the nominal and disruptive events scenarios for individual protection is 0.1 mrem/yr. The TSPA-SR model calculated a combined dose of

0.08 mrem/yr, whereas the revised supplemental TSPA analyses yielded a calculated dose of 0.1 mrem/yr. TSPA results for each scenario (nominal, disruptive, and human intrusion) are presented below.

Nominal Scenario—The DOE has assessed the repository's performance for the nominal case. The TSPA-SR model projected no dose over a 10,000-year period. The supplemental TSPA model projected a dose to the reasonably maximally exposed individual of 2×10^{-4} mrem/yr, while the revised supplemental TSPA model projected a dose of 1.7×10^{-5} mrem/yr over a 10,000-year period. The doses calculated by the supplemental and revised supplemental TSPA models would be reduced by approximately one-third if an annual water demand of 3,000 acre-ft consistent with NRC regulations was used (see 10 CFR 63.312) (Williams 2001b, Section 6.3).

Disruptive Scenario—The primary disruptive event considered in these analyses is igneous activity. The TSPA models evaluated two igneous disruptions: a volcanic eruption that intersects drifts and brings waste to the surface; and an igneous disruption that damages waste packages and exposes radionuclides for groundwater transport. The probability of igneous disruption is extremely low (the mean annual probability is about one chance in 70 million per year of occurring). The TSPA-SR model projected a dose from igneous activity of 0.08 mrem/yr over a 10,000-year period, and both the supplemental TSPA model and the revised supplemental TSPA model projected a dose to the receptor of 0.1 mrem/yr over 10,000 years.

Human Intrusion Scenario—The DOE has assessed the consequences of a stylized human intrusion into the repository at 100 years after closure, pursuant to the proposed NRC regulation. The results of this analysis show that the peak mean dose is approximately 0.01 mrem/yr over a 10,000-year period. Consistent with final NRC regulations at 10 CFR 63.321, the DOE analyzed the period of time that would be necessary for waste packages to degrade sufficiently that a human intrusion could occur without recognition by a driller. The DOE subsequently found that

Table 4-33. Summary Postclosure Dose and Activity Concentration Limits and Evaluation Results

		Results from TSPA-SR Model[a]	Results from Supplemental TSPA Model[b]	Results from Revised Supplemental TSPA Model[c]	Summary of Results
Individual protection		0.8 mrem/yr[d]	0.1 mrem/yr[d] (HTOM) 0.1 mrem/yr[d] (LTOM)	0.1 mrem/yr[d] (HTOM) 0.1 mrem/yr[d] (LTOM)	0.1 mrem/yr[d] (HTOM) 0.1 mrem/yr[d] (LTOM)
Human intrusion		≤0.01 mrem/yr[e]	0.0 mrem/yr[f]	0.0048 mrem/yr[e] 0.0 mrem/yr[f]	0.0 mrem/yr[f]
Groundwater protection	Combined radium-226 and radium 228, including natural background	≤1.04 pCi/L[g]	≤1.04 pCi/L[g] (HTOM) ≤1.04 pCi/L[g] (LTOM)	≤1.04 pCi/L[g] (HTOM) ≤1.04 pCi/L[g] (LTOM)	≤1.04 pCi/L[g] (HTOM) ≤1.04 pCi/L[g] (LTOM)
	Gross alpha activity (including radium-226 but excluding radon and uranium), including natural background	≤1.1 pCi/L[g,h]	≤1.1 pCi/L[g,h] (HTOM) ≤1.1 pCi/L[g,h] (LTOM)	≤1.1 pCi/L[g,h] (HTOM) ≤1.1 pCi/L[g,h] (LTOM)	≤1.1 pCi/L[g,h] (HTOM) ≤1.1 pCi/L[g,h] (LTOM)
	Dose to the whole body or any organ from combined beta- and photon-emitting radionuclides	0.0 mrem/yr[i]	5×10^{-5} mrem/yr (HTOM) 2×10^{-5} mrem/yr (LTOM)	2.2×10^{-5} mrem/yr (HTOM) 1.5×10^{-5} mrem/yr (LTOM)	2.2×10^{-5} mrem/yr (HTOM) 1.5×10^{-5} mrem/yr (LTOM)

NOTES: [a]Source: CRWMS M&O 2000a, Sections 4.1.5, 4.2.2, and 4.4.2.
[b]Source: BSC 2001a, Appendix A; BSC 2001b, Sections 5.1, 5.2, and 5.5.
[c]Source: Williams 2001a, Sections 6.2, 6.4, and 6.6.
[d]Probability-weighted peak mean dose equivalent for the nominal and disruptive scenarios, which include igneous activity; results are based on an average annual water demand of approximately 2,000 acre-ft; the mean dose for groundwater-pathway-dominated scenarios would be reduced by approximately one-third by using 3,000 acre-ft.
[e]Peak mean annual dose for a human intrusion at 100 years.
[f] Human-intrusion-related releases are not expected during the period of 10,000 years after disposal; the DOE has determined that the earliest time after disposal that the waste package would degrade sufficiently that a human intrusion could occur without recognition by the driller is at least 30,000 years.
[g]These values represent measured natural background radiation concentrations; calculated activity concentrations from repository releases are well below minimum detection level and background radiation concentrations.
[h]Gross alpha background concentrations are 0.4 pCi/L ±0.7 (for maximum of 1.1 pCi/L).
[i]Nominal scenario showed no releases from waste packages before 10,000 years.
HTOM = higher-temperature operating mode; LTOM = lower-temperature operating mode.

human intrusion would not occur for more than about 30,000 years. Therefore, no doses related to human intrusion would occur within 10,000 years. The dose from a human intrusion at 30,000 years is analyzed and presented in the final EIS.

4.4.1   Total System Model

The Yucca Mountain repository system is a combination of integrated processes. The system can be conceptualized and modeled as a collection of component models that are coupled. The basic objective of the waste disposal system is to contain and isolate the radioactive wastes so that the dose impact to humans does not exceed levels considered potentially harmful to human health and the environment, as specified by applicable radiation protection standards. Analysis of the system requires development of conceptual and numerical models for each of the major components.

Figure 4-172 illustrates the process for constructing a TSPA model using the performance assessment pyramid. It shows how more detailed underlying information builds the technical basis for the total system models. The breadth of the pyramid's lowest level represents the complete suite of process and design data and information, along with the field and laboratory studies that are the first step in understanding the system. The next higher level indicates how the data feed into

00050DC_ATP_Z1S42_55.ai
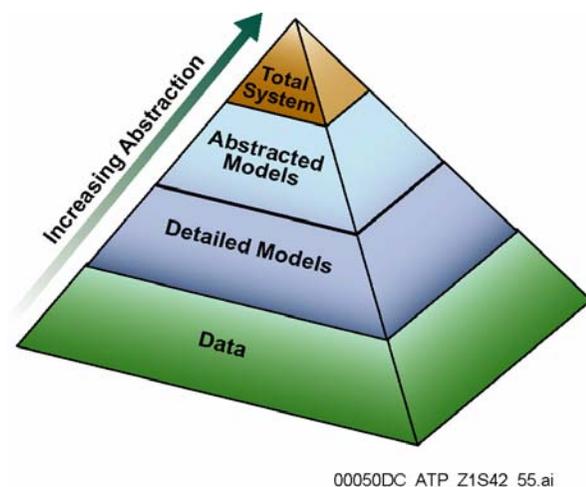
Figure 4-172. Relationship of Data, Models, and Information Flow in the Total System Performance Assessment Model

conceptual models that visualize the operation of the individual system components.

The next higher level represents the synthesis of information from lower levels of the pyramid into computer models. At this point, the subsystem behavior may be described by linking models together into representations; this is where performance assessment modeling is usually thought to begin. The term "abstraction" is used to indicate the extraction of essential information. TSPA models are usually referred to as abstracted models.

The upper level shows the final level of distillation of information into only the most critical aspects to represent the total system. At this point, all the models are linked together. These are the models used to forecast system behavior and estimate the likelihood that the behavior will comply with proposed regulations and ensure long-term safety.

As information is transferred up the pyramid, it generally is distilled into progressively more simplified forms, or becomes more abstracted, as Figure 4-172 indicates. However, abstraction is not necessarily synonymous with simplification. If a particular component model cannot be simplified without losing essential aspects, it ceases to move

up the pyramid and becomes part of the TSPA calculation tool. Therefore, an abstracted model in a TSPA may take the form of something as simple as a table of values calculated using a complex computer model or as complex as a fully three-dimensional computer simulation. However, even the most complex models of specific processes are still abstractions of reality.

Several considerations dictate the level of complexity used to represent a process. One is the sensitivity of the results of the TSPA to that particular process. The more sensitive the process or parameter, the more detailed the model representation tends to be. However, the degree of complexity is also limited by the state of knowledge concerning the model.

Figure 4-173 shows, and Table 4-34 lists, the major components in the TSPA model. Starting in the upper left part of the wheel for the nominal scenario, the components are unsaturated zone flow, engineered barrier system environment, waste package and drip shield degradation, waste form degradation, engineered barrier system transport, unsaturated zone transport, saturated zone flow and transport, and biosphere. The volcanic scenario affects these components but does not increase their number. The human intrusion scenario is a stylized calculation (consistent with EPA and NRC regulations); it requires alteration of the engineered barrier system components, but does not require additional components.

TSPAs are based on a number of building blocks. Principal among these are models that describe what happens to Yucca Mountain in the presence of a repository and how the engineered system behaves within the environmental setting of the mountain. Each model is designed to describe the behavior of individual and coupled physical and chemical processes. A significant portion of the DOE site characterization program has been aimed at developing the scientific basis for the most reasonable representation of the Yucca Mountain site and its associated engineered barriers. This scientific basis serves as the foundation for the process models used in the development of the TSPA. Section 4.2 describes the basis for these models in more detail.
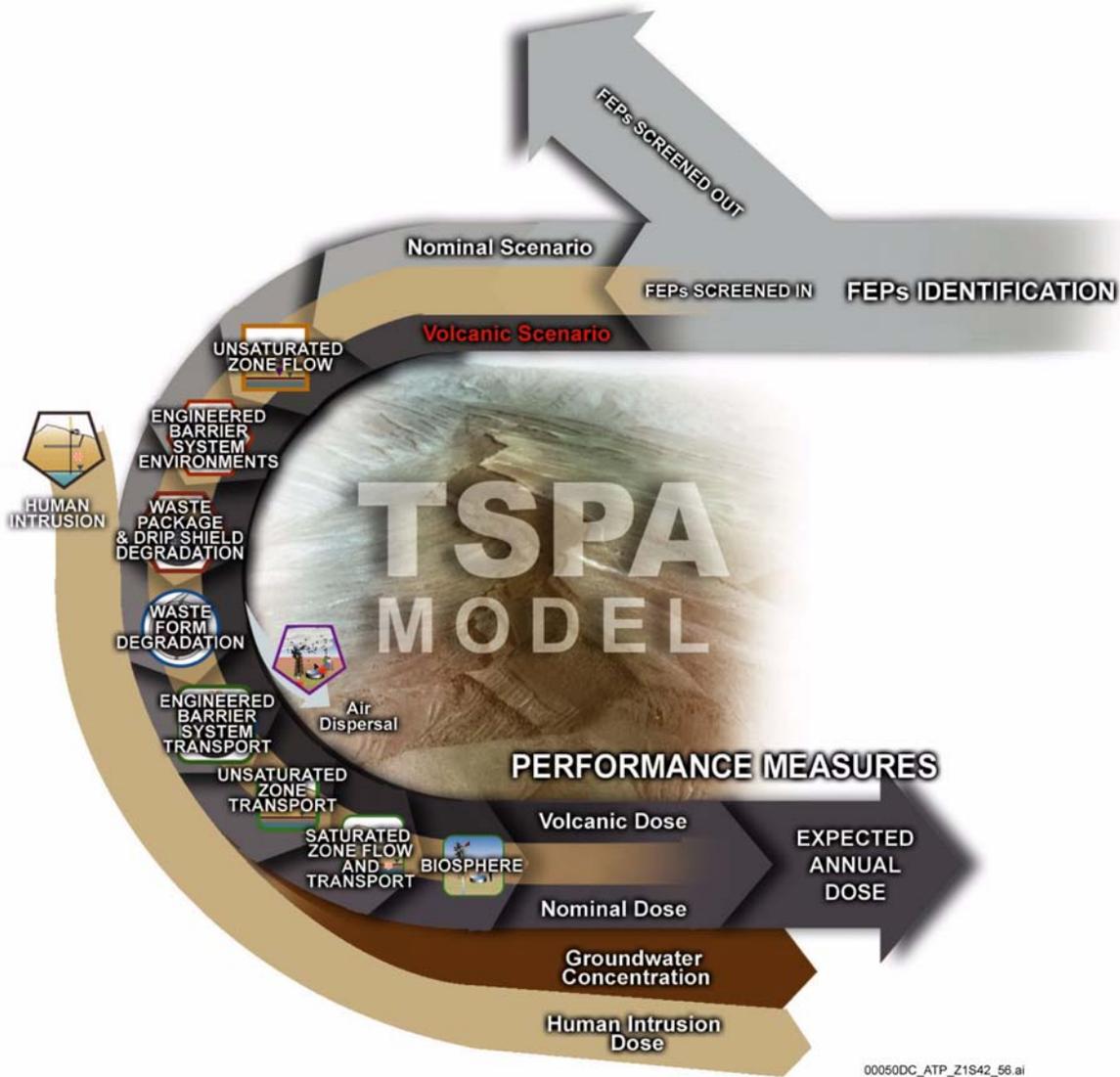
Figure 4-173. Schematic of the Principal Process Models Included in the Nominal and Disruptive Event Scenarios

Table 4-34. Total System Performance Assessment Model Components

TSPA Model Components	Subsystem Model
Unsaturated zone flow	Climate, infiltration, unsaturated zone flow above repository, seepage, coupled processes effects on unsaturated zone flow
Engineered barrier system environment	Mountain scale thermal-hydrologic model, drift scale thermal-hydrologic model, in-drift geochemical model
Waste package and drip shield degradation	Waste package and drip shield degradation model
Waste form degradation	Solubilities, inventory, in-package chemistry, colloid model, cladding degradation model, waste form dissolution model, seismic cladding model
Engineered barrier system transport	Radionuclide transport model, colloid model
Unsaturated zone transport	Unsaturated zone transport model, colloid model
Saturated zone flow and transport	Saturated zone flow and transport model
Biosphere	Soil removal, biosphere dose conversion factor, well head dilution
Volcanism	Direct release model, indirect release model

4.4.1.1 Components and Integration of the Total System Performance Assessment Model

The Yucca Mountain repository system consists of the geologic setting and engineered barriers, which together are aimed at reducing the exposure of humans to radioactive materials to acceptable levels. This section briefly describes the key aspects of the individual component models identified in Table 4-34 and Figure 4-173. Section 4.2 presented more detailed discussion of the processes that may affect repository performance.

Several components—climate, infiltration, and unsaturated zone flow—define the temporal and spatial distribution of water flow through the unsaturated tuffs above the water table at Yucca Mountain and the temporal and spatial distribution of water seeps into the repository drifts. As described in Section 4.2.1, long-term climate variations are expected to occur. In addition, the thermal conditions generated by the decay of the radioactive wastes can mobilize water until the heat of the waste has decreased. The movement of water around drifts varies as a function of temperature (BSC 2001a, Section 11.2.5; BSC 2001b, Section 3.2.2.1). For these reasons, the amount of water flowing in the rock and seeping into drifts is expected to vary with time.

Additional components (drift-scale thermal hydrology, in-drift geochemical environment, and drip shield and waste package degradation) define the spatial and temporal distribution of the calculated breach of the waste packages. The most important environmental factors affecting waste package containment time are the thermal, hydrologic, and geochemical processes acting on the surface of a waste package. The degradation characteristics of the waste package materials (e.g., susceptibility to corrosion) also impact the timing of waste package breaches. Mechanical degradation processes (e.g., from rockfall) are insignificant in affecting containment time.

The environmental processes acting on the surface of a waste package, as well as the timing and extent of waste package degradation, relate directly to the selected design. It is appropriate to review the key aspects of the design described in Section 2 as they relate to the expected behavior of the repository system. Most relevant to performance is the waste package reference design, which consists of a dual barrier of metal: an outer metal barrier of Alloy 22 and an inner metal barrier of Stainless Steel Type 316NG. The principal waste forms to be disposed of within these waste packages are:

- Commercial spent nuclear fuel from pressurized water reactors or boiling water reactors

- DOE spent nuclear fuel, including N Reactor fuel from Hanford, research reactor fuel, and naval spent nuclear fuel

- High-level radioactive waste, in the form of glass logs in stainless steel canisters from Savannah River, South Carolina; Hanford, Washington; and Idaho National Engineering and Environmental Laboratory, Idaho

- DOE stabilized excess weapons-grade plutonium in a ceramic matrix placed in canisters of vitrified DOE high-level radioactive waste.

The waste packages are designed to contain up to 21 pressurized water reactor assemblies, 44 boiling water reactor assemblies, 5 glass logs codisposed with DOE spent nuclear fuel assemblies, or other canistered DOE spent nuclear fuel, including naval spent nuclear fuel.

The engineered barrier system contains a drip shield system over the waste packages, intended to shield the waste packages from dripping water and rockfall. The drip shield consists of a 15-mm (0.6-in.) thick titanium alloy.

Key aspects of the design that influence the long-term performance of the disposal system include:

- Areal thermal loading, which is a function of the contents of waste packages and the spacing between waste packages and between emplacement drifts

- Size of the drifts

- Characteristics of the engineered materials placed in the drifts to support the waste package (the waste package supports and inverts).

These aspects of the design affect (1) the thermal load of the repository, which affects the distribution of water in and around the waste packages; (2) the degradation of the waste packages; and (3) the release pathways and characteristics from the waste packages through the invert.

The analysis of the performance of the disposal system involves an evaluation of the release of radionuclides from breached waste packages. The design is used as a basis for the analysis, then other key processes are imposed on the design, including seepage into the waste package, cladding degradation, colloid formation and stability, waste form degradation, and transport within the waste package. The degradation of the waste form components leads to a determination of the spatial and temporal distribution of the mass of radioactive wastes released from the waste packages. Waste package degradation and radionuclide release depends on the thermal, hydrologic, and geochemical conditions inside the waste package, which change with time.

Evaluation of the concentration of radionuclides in groundwater includes an evaluation of the evolution of the designed system, as well as radionuclide transport through the engineered barrier system, the unsaturated zone, and the saturated zone and radionuclide transport in the biosphere. These components of the total system cause the spatial and temporal variation of radionuclide concentrations in groundwater. The groundwater concentration ultimately yields the mass of radionuclides that may be ingested or inhaled by individuals exposed to that groundwater, which in turn causes a level of radiological dose or risk associated with that potential exposure. Radionuclides may be transported either by advection (radionuclide movement that occurs with the bulk movement of the groundwater), diffusion (radionuclide movement that occurs because of a concentration gradient), or colloid-facilitated transport. The concentration depends on both the mass release rate of the radionuclides and the volumetric

flow of water along the different pathways in the different components.

Each of these aspects of the TSPA model is used in describing the behavior of the Yucca Mountain repository system. They describe the FEPs that are expected to occur in the potential repository throughout the period of interest. Igneous activity, with its low probability of occurrence, is considered separately in the disruptive events scenario in TSPA analyses. In addition, a human intrusion scenario is considered by a separate TSPA.

4.4.1.2 Treatment of Uncertainty in Total System Performance Assessment Analyses

Because uncertainty is unavoidable in long-term assessments of repository performance, both EPA and NRC regulations describe a TSPA methodology that is designed to explicitly incorporate uncertainty in the analyses. Therefore, the DOE has developed a TSPA method that applies a probabilistic framework in which uncertainties associated with scenarios, models, and parameters are explicitly incorporated into the performance assessments.

The result of a TSPA is a quantitative estimate of the expected annual dose, weighted by probability of occurrence, to an individual whose characteristics are consistent with definitions in the regulations. The performance assessment analyzes what can happen at the repository after permanent closure, how likely it is to happen, and what can result, in terms of dose. Taking into account, as appropriate, the uncertainties associated with data, methods, and assumptions used to quantify repository performance, the performance assessment is expected to provide a quantitative evaluation of the overall system's ability to achieve the performance objective.

Consistent with EPA and NRC regulations, the expected annual dose calculated by the TSPA is the expected value of the annual dose considering the probability of the occurrence of the events and the uncertainty, or variability, in parameter values used to describe the behavior of the geologic repository. The expected annual dose is calculated by accumu-

lating the dose estimates for each year, where the dose estimates are weighted by the probability of the events and the parameters leading to the dose estimate. All of the TSPA models described in this report have been developed consistent with EPA and NRC regulations.

Assessment of the long-term performance of a potential repository at Yucca Mountain involves complex modeling of various coupled hydrologic, geochemical, thermal, and mechanical processes taking place within the engineered and natural barriers over an extended period of time. The future evolution of the geologic and environmental conditions surrounding the repository is also considered.

This section discusses the nature and sources of the uncertainties involved in assessing performance, describes the probabilistic framework to be used in the TSPA calculations, and presents the steps required for the propagation of uncertainty in the TSPA model.

Nature and Sources of Uncertainty—Uncertainty will exist in any projection of the geologic and environmental conditions surrounding the potential repository 10,000 years into the future.

Scenario uncertainty refers to uncertainty about future states of the repository system. Plausible future states of the repository system, as well as their likelihood of occurrence, must be inferred from direct and indirect field evidence and incorporated into performance assessment analyses. Examples of uncertain scenarios include volcanic activity, resulting in upward magma flow to the repository horizon and damage to the waste containers, or a change in climate from present-day conditions to a wetter climate.

Model uncertainty can be separated into mathematical model uncertainty and conceptual model uncertainty. Mathematical model uncertainty arises from the simplifying assumptions and approximations made in formulating the mathematical equations used in the TSPA component models. Consequently, component models of the individual natural or engineered barriers are limited in their capability to simulate accurately the behavior of real processes (see Section 4.2). Conceptual model uncertainty refers to an incomplete understanding of what processes dominate system behavior or how different processes might affect one another; therefore, conceptual model uncertainty reflects a state of imperfect or incomplete knowledge. Mathematical model uncertainty can be characterized by comparing computer model calculations with field and laboratory experiments which constitutes a form of model validation. In contrast, conceptual model uncertainty is addressed by evaluating plausible alternative conceptual models of process relationships. The parameters of the model used to predict the performance of the repository system are subject to uncertainty and variability. Uncertainty in model parameters arises from incomplete field-scale knowledge or limited data. Uncertainty can be reduced with additional measurements; an example is the additional data being gathered on the solubility of neptunium in groundwater, which is not known with certainty.

Variability arises from the randomness or heterogeneity of physical or behavioral characteristics. Since variability is an intrinsic property of a system, it can be quantified, but it cannot be reduced with additional information; an example is the infiltration flux into the unsaturated zone at the surface of Yucca Mountain.

Variability and uncertainty are often combined in a single parameter because the information that scientists can obtain is imprecise; an example would be the seepage flux contacting waste packages. This flux varies from location to location within the repository horizon because of underlying heterogeneities in hydrogeologic properties. In addition, the value of flux at any given location is uncertain because of limited characterization of the natural system.

Since many of the TSPA model inputs (i.e., scenarios, mathematical/conceptual models, and parameters) are uncertain or variable, the output of the model will also reflect that uncertainty. A probabilistic framework has been adopted in the TSPA-SR model and supplemental TSPA models for addressing variability and uncertainty in a manner that is consistent with the regulatory standards promulgated by the EPA and NRC.

Probabilistic Framework for Implementing Performance Assessment—The DOE has performed a quantitative evaluation of the potential performance of a repository at Yucca Mountain using probabilistic methods so as to explicitly incorporate the various possible states and their relative likelihoods. The probabilistic framework used in TSPA calculations is a relatively well-established methodology for incorporating the effects of uncertainties in scenarios, conceptual models, and parameters. It has been used extensively in probabilistic risk analyses for evaluating the safety of nuclear reactors and power plants (Rechard 1999). Several probabilistic performance assessments have also been carried out in the national radioactive waste disposal program. These include a series of studies for the disposal of transuranic waste at the Waste Isolation Pilot Plant in New Mexico (Helton, Bean et al. 1998), as well as a series of calculations performed for the disposal of high-level radioactive waste at Yucca Mountain

by the DOE (Barnard et al. 1992; Wilson, M.L. et al. 1994; CRWMS M&O 1994, 1996f, 1998g) and the NRC (Codell et al. 1992; Wescott et al. 1995).

Monte Carlo simulation, the most commonly employed technique for implementing the probabilistic framework in engineering and scientific analyses, is a numerical method for solving problems by random sampling (Cullen and Frey 1999). As shown in Figure 4-174, this method allows a full mapping of the uncertainty in model parameters (inputs) and future system states (scenarios), expressed as probability distributions, into the corresponding uncertainty in model predictions (output). Output is also expressed in terms of a probability distribution. Uncertainty in the model outcome is quantified through multiple model calculations, using parameter values and future states drawn randomly from prescribed probability distributions. The Monte Carlo simulation technique is also called the method of statistical trials
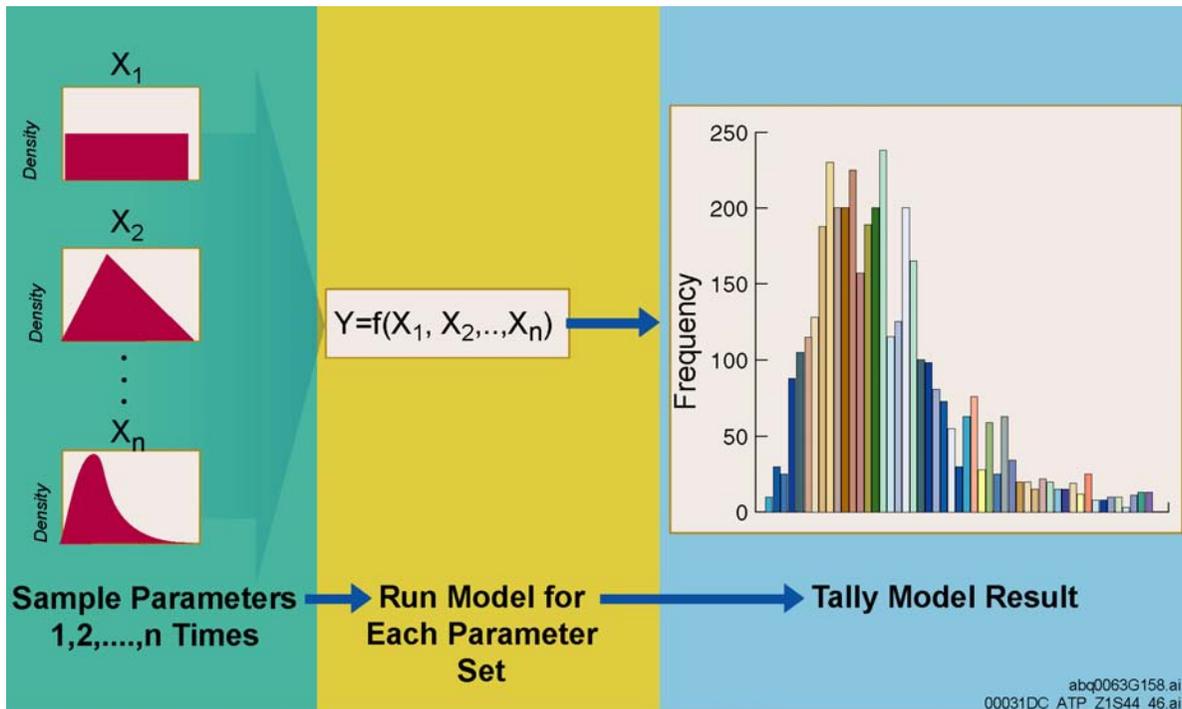
Figure 4-174. Monte Carlo Simulation
The most commonly employed technique for implementing the probabilistic framework in engineering and scientific analyses is a numerical method for solving problems by random sampling (Morgan et al. 1990). This method allows a full mapping of the uncertainty in model parameters (inputs) and future system states (scenarios), expressed as probability distributions, into the corresponding uncertainty in model predictions (output).

because it uses multiple realizations of the inputs to compute a probabilistic outcome.

The probabilistic modeling approach is computationally demanding. It requires several hundred model calculations for each scenario of interest. However, it provides important information not available from a deterministic "best-guess" or "worst-case" calculation. The benefits of probabilistic modeling include (1) obtaining a reasonable approximation of the full range of possible outcomes (and the likelihood of each outcome) to quantify predictive uncertainty and (2) analyzing the relationship between the uncertain inputs and the uncertain outputs to provide insight into the most important parameters.

Quantified Uncertainties in the TSPA Model—To describe system properties realistically, input parameters used in the TSPA component models must reflect the associated degree of uncertainty and variability in the numerical values. Uncertainty in input values can arise because of (1) limited data, (2) measurement resolution, (3) estimation error, and (4) scaling approximations. In contrast, variability in model parameters can be the direct result of the heterogeneous nature of the process, as in the case of geologic materials. Laboratory data for physical properties of geologic media, such as porosity and permeability, exhibit a scattering of values, which is the effect of spatial variability. In a number of cases, input parameters exhibiting spatial variability follow well-known statistical distributions. In addition, input parameters can exhibit variability in time, as in the cases of precipitation, wind speed, wind direction, and other meteorologic parameters.

Input uncertainty and variability are explicitly represented in the TSPA by assigning empirical probability distributions, derived in one of the following ways:

1. Fitting of laboratory or field data with standard statistical distributions

2. Abstracting (i.e., distilling and simplifying) the quantitative results from process model simulations

3. Selecting bounding distributions (i.e., covering the range of variability of data) based on scientific inferences from theoretical calculations or indirect evidence

4. Translating expert judgment into statistical distributions through a formal elicitation procedure.

These probability distributions are then sampled in the Monte Carlo simulation (Cullen and Frey 1999, Chapter 7) to propagate their effects on the TSPA projections for annual dose.

The DOE quantified many uncertainties in Volume 2, Section 3 of *FY01 Supplemental Science and Performance Analyses* (BSC 2001b). These analyses were based on reevaluating uncertainty in several component models:

1. Seepage into drift(s)

2. Coupled effects on seepage

3. Water diversion performance of engineered barrier systems

4. In-drift moisture distribution

5. Drip shield degradation and performance

6. In-package environments

7. Cladding degradation and performance

8. DOE high-level radioactive waste degradation and performance

9. Dissolved radionuclide concentrations

10. Colloid-associated radionuclide concentrations

11. Invert degradation and transport.

These component models are also discussed in Sections 4.2 and 4.4.5.5 of this report.

Propagation of Parameter Uncertainty—The propagation of parameter uncertainty involves performing a Monte Carlo analysis with the TSPA model, a four-step process that is described below.

In the TSPA methodology, the Monte Carlo approach is applied to each scenario separately, and then the results are combined based on the probability of each scenario. All the TSPA models use the same basic methodology.

1. **Identifying imprecisely known model input parameters to be sampled**—The TSPA-SR model and supplemental and revised supplemental TSPA models consist of approximately 1,000 parameters, many of which are uncertain or variable. Scientists determine which of these have a significant range of uncertainty or variability and, therefore, should be statistically sampled during model calculations and during the development of individual process models or abstractions. Section 3 of *Total System Performance Assessment for the Site Recommendation* (CRWMS M&O 2000a) provides more explanation on the selection of these parameters for the TSPA-SR model. The *FY01 Supplemental Science and Performance Analyses* (BSC 2001a; BSC 2001b) and *Total System Performance Assessment—Analyses for Disposal of Commercial and DOE Waste Inventories at Yucca Mountain—Input to Final Environmental Impact Statement and Site Suitability Evaluation* (Williams 2001a) present more information on the parameters used in the supplemental and revised supplemental TSPA models.

2. **Constructing probability distribution functions for each of these parameters**—The probabilistic framework employed in the Monte Carlo simulations requires that the uncertainty in model inputs be quantified using probability distributions. The construction of probability distributions has focused on the full range of defensible and reasonable parameter distributions that can be justified on the basis of available information or expert elicitation. These distributions are specified either as empirical distribution functions (i.e., individual values and their likelihood) or as the coefficients of para-

metric distributions fit to data (e.g., the mean and standard deviations of a normal distribution fit to porosity data).

3. **Generating a sample set by selecting a parameter value from each distribution**—The next step in the Monte Carlo process requires generating a number of equally likely input data sets. These consist of parameter values randomly sampled from the prescribed range and distributions. An improved form of random sampling is the Latin Hypercube sampling procedure, where the range of each parameter is divided into several intervals of equal probability and a value is selected at random from each interval (Helton, Bean et al. 1998). This method, which was employed in the TSPA-SR, the supplemental and revised supplemental TSPA models, helps achieve a statistically more uniform coverage of the uncertain parameter range than random sampling. The issue of interdependence or statistical correlation between parameters is also important. The sampling algorithm used in the TSPA-SR and supplemental TSPA models, ensures that any desired correlation between input parameters is retained, while any spurious correlation that might arise because of the finite size of the sample is eliminated.

4. **Calculating the model outcome for each sample set and tallying the results for all samples**—In this step, scientists evaluate the model that describes the behavior of the system in the scenario of interest for each of the equally likely, randomly generated parameter sets. This is a simple operation consisting of multiple model calls, where the outcome (i.e., annual dose as a function of time) is computed for each sampled parameter set. Once all the required model runs have been completed, the overall uncertainty in the predicted outcome can be characterized by summary statistics, such as the mean and median, and/or by the cumulative probability distribution.

Incorporating Conceptual Model Uncertainty—Conceptual model uncertainty refers to an incomplete understanding of what processes dominate system behavior and how different processes might affect one another; in other words, conceptual model uncertainty reflects a state of imperfect or incomplete knowledge. Multiple conceptual models can be hypothesized that fit the empirical data equally well. Conceptual model uncertainty is addressed by evaluating plausible alternative conceptual models of process relationships. The conceptual model that best fits empirical data, when such a model exists, is used in the integrated TSPA model. When multiple conceptual models are plausible, either a conservative model is chosen or the models are weighted and combined, and the resulting combination is used in the integrated TSPA model. An alternative approach for incorporating conceptual model uncertainty is via a bounding model, such that the consequence can be "bounded." Note that conservative/bounding models are used as additional tools for representing uncertainty in the TSPA model, in addition to the detailed representation of parametric uncertainty via probability distributions.

Incorporating Scenario Uncertainty—Uncertainty related to future states arises because the geologic and environmental conditions occurring over thousands of years cannot be predicted with certainty. As a result, scenarios of plausible future system states (e.g., system changes arising from the evolution of the geologic setting) have been derived from scientific inferences drawn from direct and indirect field evidence from the Yucca Mountain site. Through the FEPs screening procedure, scenarios of system perturbations are conceptualized and characterized in terms of both likelihood of occurrence and potential impact on natural and engineered barriers. As discussed below, the scenarios have been organized into two groups: (1) nominal and disruptive conditions (e.g., repository heating, climate change, seismicity effects, igneous activity) and (2) human intrusion. These scenarios have been evaluated as part of the probabilistic TSPA and the associated consequences included in the projected annual doses.

As discussed, the TSPA done without human intrusion analyzes two scenarios—the nominal and disruptive events scenarios. The mean dose for each of these scenarios was probability-weighted and summed to calculate the dose to the receptor (i.e., the average member of the critical group for the TSPA-SR model analyses and the reasonably maximally exposed individual for the revised supplemental TSPA model).

Presentation of Results—The data from the multiple realizations are graphically summarized by showing time versus annual dose (i.e., annual dose histories) for all realizations (i.e., 300 realizations for the nominal case and 5,000 realizations for the igneous-activity scenario). Graphical representations that display all the realizations of the output from the multiple-realization simulations are termed "horsetail plots." These results of the multiple-realization simulations can be displayed along with statistical measures of the output. Typically, the graphical representations show the mean and the median of the output along with 5th and 95th percentile of the output. In the same manner as described for *Total System Performance Assessment for the Site Recommendation* (CRWMS M&O 2000a, Section 2.2.4.6, pp. 2-39 to 2-40), these statistical measures are calculated using the data from all realizations of the probabilistic simulations at each time step of the dose histories. The plot of the mean represents the arithmetic average of data points from each realization at each time step. For each point on the plot of the median dose, 50 percent of the data have a value greater than the plotted point and 50 percent have a value less than the plotted point. Likewise, for the 95th and 5th percentiles, the plotted data points are such that 5 percent of data are greater (or less) than the plotted point and 95 percent of the data points are less (or greater) than the plotted points, for each point, or time step, plotted. The statistical measures can be superimposed in contrasting colors on the horsetail plots (Williams 2001a).

4.4.1.3   Treatment of Potentially Disruptive Scenarios

Evaluation of the postclosure performance of a potential geologic repository at the Yucca Mountain site considers disruptive processes and events important to the total system performance of the geologic repository. These disruptive processes and

events include (1) volcanism; (2) seismic events; (3) nuclear criticality; and (4) inadvertent human intrusion. These processes have been examined through the FEPs screening process. The results include the following observations:

- Volcanism (including an igneous intrusion that does not erupt at the surface) has occurred in the Yucca Mountain region in the past. Current evaluations indicate a probability of recurrence slightly more than 1 chance in 10,000 during the next 10,000 years. Therefore, the TSPA models explicitly consider the impact of volcanism in a subsystem model. The TSPA treatments for the two volcanic disruption scenarios are described in Sections 4.4.1.3.1 and 4.4.1.3.2. The TSPA results for these scenarios are described in Section 4.4.3.

- Most impacts of seismic events have been excluded from the TSPA on the basis of insignificant consequence or low probability. More specifically, seismic changes in hydrology (including seismic pumping) are not great enough to have a significant effect on overall performance; seismically induced rockfall will not be large enough to degrade the drip shield and waste package significantly; and the probability of fault displacement within the repository is below 1 chance in 10,000 of occurring over 10,000 years. Because vibratory ground motion from seismic events of uncertain magnitude is likely to occur at Yucca Mountain in the future and might damage the spent nuclear fuel cladding, the effect of this potential damage to cladding by a discrete seismic event is included in the TSPA model in the nominal scenario (rather than the disruptive scenario). The frequency assumed for this event is 1.1×10^{-6} per year. For the analysis, when the vibratory ground motion event occurs, all commercial spent nuclear fuel cladding in the repository is assumed to fail by perforation, and further cladding degradation is calculated according to the cladding degradation model.

- The DOE has considered postclosure criticality using the risk-informed methodology described in *Disposal Criticality Analysis Methodology Topical Report* (YMP 2000c). The NRC had issued a Safety Evaluation Report (Reamer 2000) for the initial postclosure criticality methodology (YMP 1998) with a few open items. The postclosure criticality methodology has been updated in *Disposal Criticality Analysis Methodology Topical Report* (YMP 2000c) to address the open items. This assessment included consideration of site characteristics relevant to criticality as determined by a comprehensive assessment of site data and information obtained during site characterization. Three potential criticality scenarios were considered for the TSPA: (1) inside one or more degraded waste packages; (2) in rock surrounding emplacement drifts, as a result of the transport of fissile materials from degraded waste packages; and (3) in rock at some distance from the emplacement drifts, as a result of the accumulation of fissile materials under favorable conditions.

The results from these analyses indicate that the probability of a criticality in the 10,000 years is less than 1×10^{-4} for all commercial pressurized water reactor spent nuclear fuel waste packages (Section 4.3.3.2.3). This low probability is expected to apply to all waste forms placed in a potential repository. Additional scenarios, including criticality without the presence of water and autocatalytic criticality, were considered and eliminated from further consideration because the probabilities of such events are so low that they are not credible. Criticality external to the waste package would require sufficient water flux to carry substantial amounts of fissile materials from breached waste packages to a location in the rock with favorable conditions for accumulating large amounts of fissile material. Lower water flux would mean a lower probability of this phenomenon occurring. Potential early waste package failures from improper heat treatment are modeled to fail by cracking in the closure weld areas. This failure mode, along with the existence of an

intact drip shield, would not allow significant water flux through the waste package, thereby reducing the probability of a criticality event. Section 4.3.3.2 provides a brief description of the methodology and results from this analysis.

- Human intrusion has been analyzed in a stylized scenario. Section 4.4.4 presents the results of the TSPA-SR model and supplemental TSPA model analysis. Human intrusion is not included in either the nominal or disruptive scenarios, and the consequences of human intrusion are not included in the estimates of performance presented in Sections 4.4.2 and 4.4.3.

Analyses of these disruptive processes have been performed by the TSPA-SR model and the supplemental and revised supplemental TSPA models. Detailed results of these analyses are presented in *Total System Performance Assessment for the Site Recommendation* (CRWMS M&O 2000a), *FY01 Supplemental Science and Performance Analyses* (BSC 2001a; BSC 2001b), and *Total System Performance Assessment—Analyses for Disposal of Commercial and DOE Waste Inventories at Yucca Mountain—Input to Final Environmental Impact Statement and Site Suitability Evaluation* (Williams 2001a).

The treatment of potentially disruptive scenarios associated with volcanism addresses models for two types of disruption of the repository: volcanic eruptions that intersect drifts and bring waste to the surface and igneous intrusions that damage waste packages and expose radionuclides for groundwater to transport. These two types of disruption were described in the *Viability Assessment of a Repository at Yucca Mountain* (DOE 1998, Volume 3, Section 4.4) as the direct release scenario and the enhanced source term scenario, respectively. Descriptive terms used for these scenarios are volcanic eruption and igneous intrusion groundwater transport, respectively. These terms, as well as combined igneous activity, are used in the reports documenting the results of TSPA analyses of disruptive events (BSC 2001a; BSC 2001b; Williams 2001a; Williams 2001b). This treatment of volcanism does not address the indirect effects of igneous activity that does not intersect the repository. As described in *Features, Events, and Processes: Disruptive Events* (CRWMS M&O 2000ex), the indirect effects of igneous activity are shown to have such small consequences that they are not included in TSPA-SR estimates of overall system performance.

The treatment of potentially disruptive scenarios draws extensively on activities performed specifically to define the disruptive events to be modeled in the TSPA and to provide the distributions assigned to parameters. In addition, full implementation of the igneous consequence models in the TSPA-SR model and supplemental TSPA models also requires information from other sources. Figure 4-175 shows the relationship among the major products developed specifically to support the igneous consequence modeling and shows how these products support each other and the TSPA analyses. The reports associated with analyses, models, and calculations performed explicitly to address the disruptive scenarios are shown in this figure in boxes with solid lines. Reports from activities that provide other inputs into the TSPA necessary to evaluate the consequences associated with the disruptive scenarios are shown in dashed boxes.

Characterize Framework for Igneous Activity at Yucca Mountain, Nevada (CRWMS M&O 2000ez) provides basic information about volcanic activity in the Yucca Mountain region and derives the probability of future volcanic activity from information provided in *Probabilistic Volcanic Hazard Analysis of Yucca Mountain, Nevada* (CRWMS M&O 1996b). Information from this analysis about the general nature of volcanic activity in the Yucca Mountain region is also used in *Characterize Eruptive Processes at Yucca Mountain, Nevada* (CRWMS M&O 2000fa) to support detailed characterization of the events and processes associated with a volcanic eruption. *Dike Propagation Near Drifts* (CRWMS M&O 2000fb) provides an estimate of the extent of damage to waste packages near an intrusive dike. Information from these three reports is used in *Number of Waste Packages Hit by Igneous Intrusion* (CRWMS M&O 2000fi) to support the calculation of cumulative distribution functions that characterize the number of
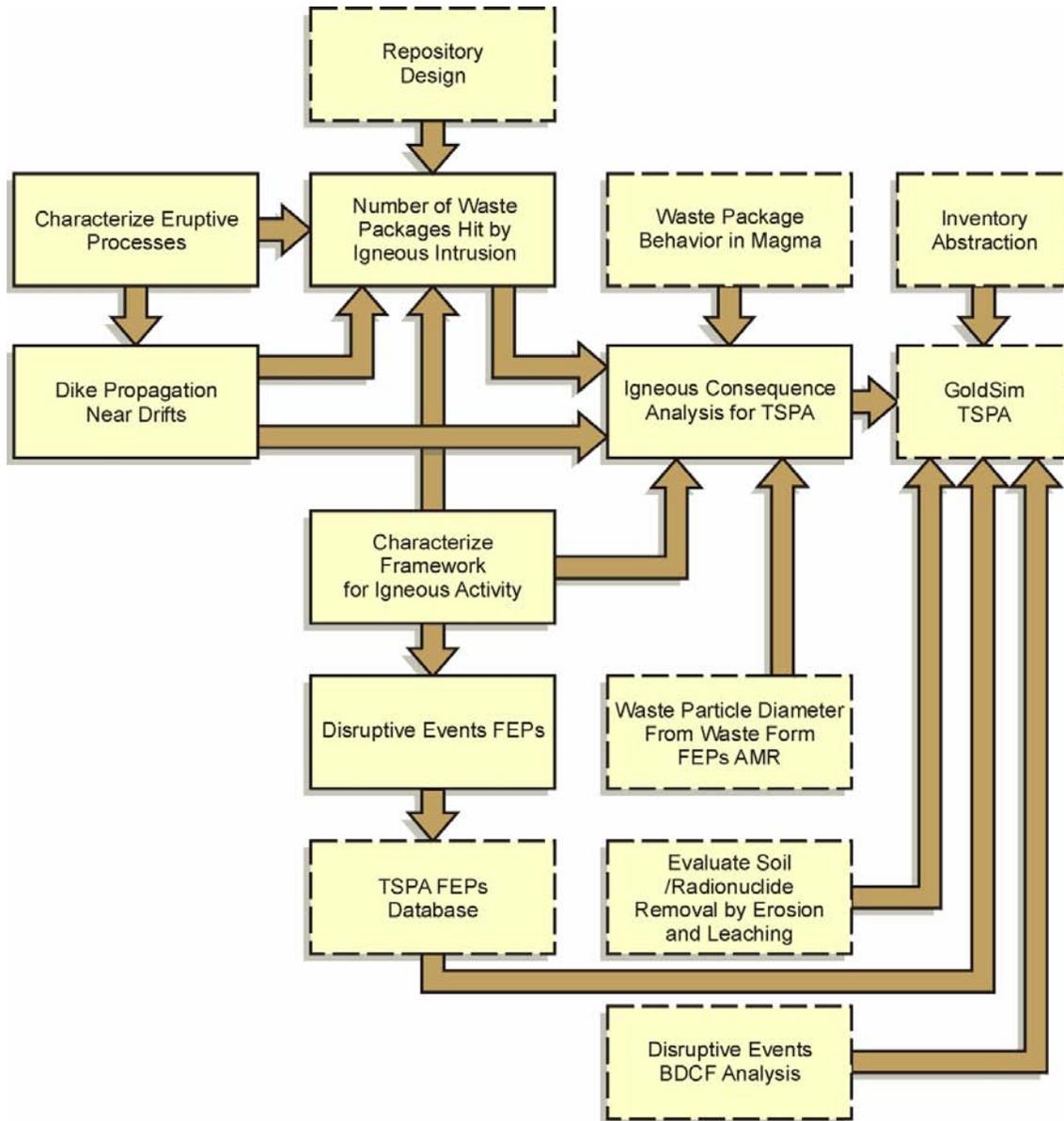
00050DC_ATP_Z1S42_Fig-54.cdr

Figure 4-175. Information Feeds to Igneous Consequence Modeling in the Total System Performance Assessment

Reports from activities that provide other inputs into the TSPA necessary to evaluate the consequences associated with the disruptive scenarios are shown in dashed boxes. AMR = analysis model report; BDCF = biosphere dose conversion factor.

waste packages affected by intrusions and eruptions. As shown in Figure 4-175, *Igneous Consequence Modeling for the TSPA-SR* (CRWMS M&O 2000fc) draws information from *Characterize Framework for Igneous Activity at Yucca Mountain, Nevada* (CRWMS M&O 2000ez), *Characterize Eruptive Processes at Yucca Mountain, Nevada* (CRWMS M&O 2000fa), *Number of Waste Packages Hit by Igneous Intrusion* (CRWMS M&O 2000fi), *Miscellaneous Waste-Form FEPs* (CRWMS M&O 2000eu), and *Waste Package Behavior in Magma* (CRWMS M&O 1999p).

4.4.1.3.1   Volcanic Eruption Scenario

Igneous Consequence Modeling for the TSPA-SR (CRWMS M&O 2000fc) evaluated three models for evaluating volcanic eruptions and concluded that the volcanic eruption scenario should be modeled in the TSPA-SR model using the code ASHPLUME (CRWMS M&O 2000fc, Section 6.1). ASHPLUME has also been used by the supplemental TSPA models (BSC 2001a; BSC 2001b). This recommendation is based on the relative maturity of the model and code and the wide acceptance of the underlying Suzuki model. The ASHPLUME code was developed at the Center for Nuclear Waste Regulatory Analyses sponsored by the Southwest Research Institute. The Center is assisting the NRC in assessing site characterization and long-term safety at the proposed Yucca Mountain site. The ASHPLUME code implements the Suzuki igneous model (Suzuki 1983), a mathematical implementation of an atmospheric dispersal model. The Suzuki model does not attempt to model the subsurface physics of the igneous event but relies on expert inputs for the physical characteristics of the volcano and models the atmospheric dispersal of the ash particles downwind until the ash settles on the ground. The modified ASHPLUME code used for TSPA models added the coupling of waste particles to the ash particles to model a volcanic igneous event through the potential repository. The resulting model maintained all the physical characteristics of the Suzuki model (Suzuki 1983).

The TSPA-SR implementation of the ASHPLUME model is the same as the TSPA model in the VA,

with improvements in the input parameter values. Engineers obtained the current input parameter values from the reports and calculations referenced earlier in this section, as well as Jarzemba et al. (1997); Lide (1994); Suzuki (1983); Reamer (1999); Wilson, L. and Head (1981); and Quiring (1968). One key additional improvement is the model for the intersection of a conduit with the repository drifts in *Number of Waste Packages Hit by Igneous Intrusion* (CRWMS M&O 2000fi) and *Waste Package Behavior in Magma* (CRWMS M&O 1999p). This allows a more complex, detailed analysis of the number of drifts and waste packages that would be intersected by one or more conduits, which provides a means of tracing the justifications behind the input values and allows for an improved accountability for their use.

4.4.1.3.2   Igneous Intrusion Groundwater Transport Scenario

The igneous intrusion groundwater transport scenario evaluates the effect of an igneous intrusion on waste packages in the drifts. For this scenario, the affected waste packages are modeled as compromised to the extent that the waste form inside is completely exposed (i.e., the waste package and cladding have been severely degraded or destroyed). After the magma cools, groundwater begins to flow through the zone with the flow characteristics and transport properties described in the unsaturated zone flow model; on reaching the water table, the transport continues under the conditions described by the saturated zone flow and transport model.

Table 4-35 summarizes the igneous intrusion groundwater event input parameters recommended in *Igneous Consequence Modeling for the TSPA-SR* (CRWMS M&O 2000fc). The table lists the input parameter, the format of the input parameter, and the input data source.

Additional assessments evaluated the effect on dose of the volcanic eruption scenario and the igneous intrusion groundwater transport scenario. Results are documented in Volume 2, Section 4.3.1 of *FY01 Supplemental Science and Performance Analyses* (BSC 2001b). Revised supplemental analyses are reported in *Total System Performance*

Table 4-35. Igneous Intrusion Groundwater Event Scenario Input Parameters

Input Parameter	Input Parameter Format	Addressed In
Event Probability	Cumulative Distribution Function	CRWMS M&O 2000ez, Section 6.5.1.3
Percentage of Hit Packages that Fail	Assume 100%	CRWMS M&O 1999p
Number of Packages Hit	Cumulative Distribution Function	CRWMS M&O 2000fi, Figure 1-8

NOTES: CRWMS M&O 1999p: *Waste Package Behavior in Magma.*
CRWMS M&O 2000ez: *Characterize Framework for Igneous Activity at Yucca Mountain, Nevada.*
CRWMS M&O 2000fi: *Number of Waste Packages Hit by Igneous Intrusion.*

Assessment—Analyses for Disposal of Commercial and DOE Waste Inventories at Yucca Mountain— Input to Final Environmental Impact Statement and Site Suitability Evaluation (Williams 2001a, Section 6.3). These results are presented in Section 4.4.3 of this report.

4.4.1.4   Summary of Radionuclides of Concern Considered in Dose Assessment

The purpose of the TSPA models is to investigate the potential for and impact of radionuclides escaping a potential repository at Yucca Mountain. Many radionuclides only exist for microseconds, and some do not contribute significantly to potential dose. There are hundreds of radionuclides in the waste inventory, and some will be created and destroyed in the cascading process of radioactive decay and ingrowth. It is not practical to numerically portray the behavior of all these radionuclides, their daughter products, and their progeny. Instead, a screening approach was used to identify those radionuclides that would contribute significantly to the potential dose to a receptor living in the vicinity of Yucca Mountain. The most significant contributors to potential dose are included in the TSPA models; these account for at least 95 percent of the potential dose. This section summarizes the screening process. The result of this process—a list of radionuclides—is an impor-

tant part of the TSPA analyses discussed in the rest of this report.

Radionuclide Screening Based on Contribution to Dose—The metric for screening radionuclides for the TSPA models is the radiation dose that a radionuclide could impose on a human living in the vicinity of Yucca Mountain. A methodology has been developed that identifies the important dose contributors, based on an estimate of the amounts of radionuclides that could reach a human receptor (CRWMS M&O 2000ds). Identification of the important dose contributors involves three steps:

1. For the waste form under consideration, the relative dose contribution from an individual radionuclide is calculated by multiplying its inventory abundance (in terms of its radioactivity) by its dose conversion factor (a number that converts an amount of a radionuclide into the dose that a human would incur if the radionuclide were exposed to, ingested, or inhaled). This multiplication gives a result that is not significant by itself; however, when it is compared to values derived in the same manner for other radionuclides in the waste form, the radionuclide that is the more important contributor to the dose can be determined.

2. The individual radionuclides are ranked, with the highest contributor to the dose given the highest ranking, and the percent contribution of each radionuclide in the list to the total dose (the sum of the doses from the radionuclides in the list) is calculated.

3. Radionuclides that are included in the TSPA models are the highest-ranked radionuclides that, when their dose contributions are combined, produce at least 95 percent of the potential dose.

These steps identify which radionuclides would be included in the dose estimate, should all radionuclides in a waste form be released to the environment in proportion to their inventory abundance. However, radionuclides are not always

released in proportion to their inventory abundance. Factors that can affect releases of radionuclides, depending on the scenario being considered, include radionuclide longevity, solubility, and transport affinity.

Radionuclide longevity is the lifetime of a radionuclide before it decays. Solubility is the amount of a radionuclide that will dissolve in a given amount of water. Transport affinity is a radionuclide's potential for movement through the environment. This movement can involve a number of mechanisms, for example: fracture flow (the advective movement of radionuclides with water flowing in fractures), matrix diffusion (the diffusion of radionuclides from water in the fractures into water in the matrix), or colloid-facilitated transport (the movement of radionuclides associated with small particles of rock or waste form degradation products). Transport affinity is not a measurable property but a qualitative description of the likelihood of transport. If a group of radionuclides is transported via a particular mechanism, and that mechanism dominates release, the group of radionuclides will be preferentially released (relative to radionuclides not in the group) to the environment. If a radionuclide has a short half-life, it will have a higher activity in the waste form at early times (close to repository closure); however, at later times, the radionuclide will have all but disappeared from the waste form. If a radionuclide is not soluble in the near-field environment around the waste package, it may not be released to the environment through groundwater transport, even if it is abundant and available.

Because radionuclide longevity, solubility, and transport affinity can affect releases of radionuclides, the identification of important dose contributors includes examination of possible "what-if" scenarios that could result in releases of radionuclides to the environment. For example, "What if radionuclide releases are the result of a colloidal transport mechanism?" If the steps described previously are applied to the subset of radionuclides that could be released through a colloidal transport mechanism (radionuclides that readily bind to rock and colloidal particles), which of those radionuclides would be identified as the important contributors to dose?" Or, "What if a volcanic direct release to the environment occurs?" If the steps described previously are applied to the radionuclides present in the waste form involved in a direct release, which of those radionuclides would be identified as the important contributors to dose?" The radionuclide screening examined over 1,200 potential what-if scenarios and identified the important dose contributors for each one. The cases examined consider times from 100 years to 1 million years after repository closure (100, 200, 300, 400, 500, 1,000, 2,000, 5,000, 10,000, 100,000, 300,000, and 1 million years); eight waste forms (average and bounding pressurized water reactor fuel, average and bounding boiling water reactor fuel, average and bounding DOE spent nuclear fuel, and average and bounding DOE high-level radioactive waste) three transport affinity groups (highly sorbing, moderately sorbing, and slightly to nonsorbing); and two exposure pathways (inhalation and ingestion).

As noted previously, the radionuclides considered in calculating potential dose to the reasonably maximally exposed individual living in the vicinity of Yucca Mountain were selected based on their contribution to dose. The importance of a particular radionuclide is also related to pathway and time of release. Table 4-36 lists the radionuclides considered for three release scenarios, summarizing the differences in importance of particular radionuclides relative to the pathway and time of release for these scenarios. The supplemental TSPA models used the same radionuclides in their analyses (BSC 2001a; BSC 2001b; Williams 2001a). A direct volcanic release scenario involves pathways (e.g., inhalation) that can be different from those modeled in the nominal scenario. If a radionuclide is important for estimating the dose from DOE spent nuclear fuel, it is included in the TSPA models, even though these waste forms would occupy a small fraction of the repository. Similarly, if a radionuclide is important for estimating the dose from the highly sorbing transport group, it is included in the TSPA models, even if analyses show that colloid transport is a minimal contributor to release.

Consideration of Decay Chains and Transport Characteristics—In addition to the radionuclides selected based on contribution to dose, other

Table 4-36. Radionuclides Selected for Consideration in Total System Performance Assessment–Site Recommendation Based on Contribution to Dose

Isotope	Direct Volcanic Release Scenario	Nominal Scenario			Human Intrusion		
		Strongly Sorbing	Moderately Sorbing	Slightly to Nonsorbing	Strongly Sorbing	Moderately Sorbing	Slightly to Nonsorbing
Actinium-227	X	X			X		
Americium-241	X	X			X		
Americium-243	X	X			X		
Carbon-14				X			X
Cesium-137[b]	X				X		
Iodine-129				X			X
Neptunium-237			X			X	
Protactinium-231	X	X[a]			X[a]		
Lead-210	X[a]	X[a]			X[a]		
Plutonium-238	X	X			X		
Plutonium-239	X	X			X		
Plutonium-240	X	X			X		
Plutonium-242	X[a]	X[a]			X[a]		
Radium-226	X[a]	X[a]			X[a]		
Strontium-90[b]	X				X		
Technetium-99				X			X
Thorium-229	X	X			X		
Thorium-230	X[a]	X[a]			X[a]		
Uranium-232	X		X			X	
Uranium-233	X		X			X	
Uranium-234	X		X			X	
Uranium-236			X			X	
Uranium-238			X			X	

NOTES: [a]Important for calculations after 10,000 years, specifically peak-dose calculations (DOE 1999a).
[b]Not included in nominal scenario.
Source: CRWMS M&O 2000ds.

radionuclides (in particular radium-226 and radium-228) are considered for groundwater protection consistent with 40 CFR 197.30 and 10 CFR 63.331 (66 FR 55732). Other radionuclides are also considered in the TSPA models because they belong to decay chains; they were included to accurately track other members of the decay chains. (A decay chain is a sequence of radionuclides that, because of radioactive decay, change from one to the other; thus, the amount of one is dependent on the amounts of the others.)

The radionuclides selected for consideration in the TSPA models fall into two basic categories: fission products (plus carbon-14 and uranium-232) and actinides (plus lead-210 and radium isotopes). Fission products are the lighter elements that result when the heavier, fissionable elements that consti-

tute nuclear fuel, primarily uranium-235, are split to release energy. The fission products of concern here do not decay into other radionuclides of concern; that is, they do not form decay chains. Therefore, the fission products can be considered as single species, with no interdependence on other species. Carbon-14 and uranium-232 are technically not fission products—they are activation products formed by neutron capture— but they are included in the fission-product group because they are not members of decay chains.

The actinide group includes the heavy elements that comprise nuclear fuel and the heavy-element by-products formed by neutron capture or decay of these elements (including lead and radium). The actinides typically decay by losing an alpha particle. Therefore, they tend to form decay chains

in which the isotopes are spaced by an atomic weight of four. For example, uranium-238 loses an alpha particle and decays to uranium-234, which similarly decays to thorium-230, etc. (The actual radionuclide decay chains are much more complicated than this explanation suggests, involving not only alpha radiation, but also beta, gamma, and neutrino radiation and, typically, many intermediate products. However, the significant chain members—those that exist for relatively long times—are separated primarily by release of an alpha particle.) For the actinides that are important

to dose, the decay of parent radionuclides (those higher in the decay chain) and the ingrowth of daughter radionuclides (those lower in the chain) must be tracked during transport.

Figure 4-176 shows the complete list of the radionuclides considered in the TSPA-SR, including how the radionuclides considered in the TSPA-SR are related by membership in decay chains. What follows is a brief discussion of each radionuclide modeled in the TSPA-SR, and—because how radionuclides are modeled in the TSPA-SR depends, to
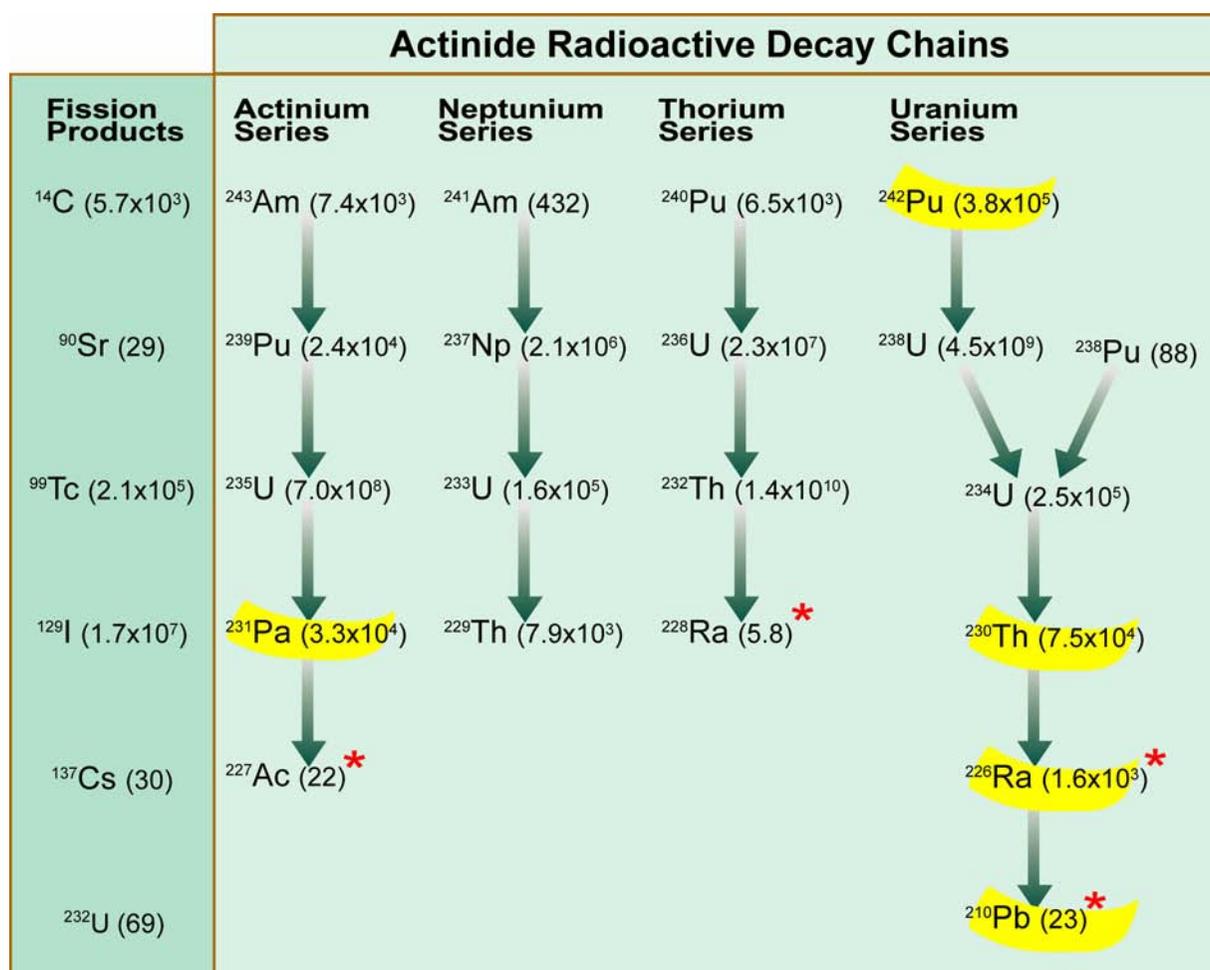
Figure 4-176 All Radionuclides Considered in the TSPA model, Showing Decay-Chain Relationships (with Half-Lives in Years)
Source: Modified from CRWMS M&O 2000a, Figure 3.8-13.

a certain extent, on radionuclide-specific character-istics—the radionuclide-specific characteristics that are important to modeling the radionuclide in the TSPA-SR. These include the half-life and the transport mechanism. This discussion is summarized from Section 3.5 of *Total System Performance Assessment for the Site Recommendation* (CRWMS M&O 2000a). The same radionuclides were considered in the supplemental TSPA model and the revised supplemental TSPA model. Detailed information can be found in *FY01 Supplemental Science and Performance Analyses* (BSC 2001a; BSC 2001b) and *Total System Performance Assessment—Analyses for Disposal of Commercial and DOE Waste Inventories at Yucca Mountain—Input to Final Environmental Impact Statement and Site Suitability Evaluation* (Williams 2001a).

Fission Products—Carbon-14 is a relatively nonsorbing radionuclide with a short half-life that moves easily in groundwater; as such, it is tracked in the human intrusion analysis and the nominal scenario. Carbon-14 does not contribute substantially to dose at periods after 10,000 years and is not considered in the post-10,000-year analyses. Carbon-14 transports as solute. Strontium-90 and cesium-137 are both strongly sorbing radionuclides with short half-lives. Although the initial inventory of the repository would contain substantial amounts of these radionuclides, they are only important to dose if they are released at very early times and transported rapidly. Because early release and rapid transport are not expected, these radionuclides are only considered for direct volcanic and human intrusion releases. Strontium-90 and cesium-137 are relatively immobile in groundwater, except perhaps when associated with colloids; to respect this possibility, colloid-facilitated transport of these radionuclides is considered in the TSPA models. Technetium-99 and iodine-129 are radionuclides with relatively long half-lives that are fairly mobile in groundwater; they are considered for all analyses except direct volcanic releases, in which case they are not important because they do not constitute a large part of the initial inventory. Technetium-99 and iodine-129 transport as solute. Uranium-232 is a radionuclide with a short half-life that is sufficiently present in the initial inventory to be important to inhalation

dose if released early enough; therefore, it is considered in the direct volcanic release scenario.

Actinium Series—Americium-243, plutonium-239, and actinium-227 are important to dose in all analyses. Uranium-235 and protactinium-231 are not important to dose, but both are followed to track actinium-227. Americium-243 and plutonium-239 are both strongly sorbing and only transport when associated with colloids. Uranium-235 is only moderately sorbing and thus transports as solute. Protactinium-231 is a strongly sorbing radionuclide and is relatively immobile, except perhaps when associated with colloids; as with strontium-90 and cesium-137, to respect this possibility, colloid-facilitated transport of protactinium-231 is considered in the TSPA-SR. Actinium-227, because of its brief lifetime, is assumed to be in secular equilibrium with protactinium-231. (Secular equilibrium is when a daughter radionuclide has reached a steady-state amount, in terms of radioactive activity, with respect to the amount of its parent radionuclide. The secular-equilibrium assumption tends to overestimate the amount of a daughter product when there is no significant daughter source; in this regard, it is typically a conservative assumption.)

Neptunium Series—Americium-241, neptunium-237, uranium-233, and thorium-229 are important to dose in all the analyses, except that americium-241 is not important to the long-term performance because of its relatively short half-life. Americium and thorium are only transported when associated with colloids. Neptunium and uranium are transported as solute. The amount of americium-241 is increased to account for ingrowth from the very short-lived plutonium-241.

Thorium Series—Plutonium-240 and uranium-236 are important to dose in all analyses, except that uranium-236 is not important in direct volcanic releases and plutonium-240 is not important past 10,000 years because of its relatively short half-life. Thorium-232 is considered only because it is part of the decay chain that generates radium-228. Radium-228 is specified by the proposed and final EPA regulation for groundwater protection. Plutonium and thorium are transported only when associated with colloids; uranium is

transported as solute. Because of its short half-life, radium-228 is considered to be in secular equilibrium with thorium-232 in the TSPA models.

Uranium Series—The radionuclides selected for consideration in the TSPA-SR are shown in Table 4-36. Plutonium-242 is only important to long-term repository performance analysis. Plutonium-238 is important to all analyses except the longer time-period peak-dose analysis (because of its short half-life). The plutonium isotopes are only transported when associated with colloids. Uranium-238 is important to nominal-scenario dose, primarily because of its tremendous inventory in the repository. Uranium-234 is important to all analyses. The uranium isotopes are mobile as solute. Thorium-230 is only important to dose in long-term repository performance analysis, but must be tracked in the groundwater protection analysis to complete the uranium series decay chain. Thorium is only transported when associated with colloids. Radium-226 is important to long-term repository performance analysis, direct volcanic release analysis, and the groundwater protection analysis. Radium-226 has a short half-life and, for simplicity, is assumed to be in secular equilibrium with thorium-230 (Parrington et al. 1996).

4.4.2   Total System Performance for the Nominal Scenario

This section summarizes the TSPA-SR model and supplemental TSPA models' postclosure performance assessment results for the nominal scenario. The nominal scenario is used for calculations of the groundwater radionuclide activity concentrations and dose to the whole body (or any critical organ) for groundwater protection. The dose projected for the nominal scenario is also combined with the probability-weighted dose from the disruptive scenario for individual protection consistent with 40 CFR Part 197 and 10 CFR Part 63 (66 FR 55732).

Following a discussion of the elements of the nominal scenario in Section 4.4.2.1, the nominal performance results for dose to the hypothetical receptor are presented in Section 4.4.2.2. The nominal performance results for the groundwater

concentrations are presented in Section 4.4.2.3. In addition, Section 4.4.2.4 presents the projected results of postclosure performance during the time period of geologic stability, also presented in *Final Environmental Impact Statement for a Geologic Repository for the Disposal of Spent Nuclear Fuel and High-Level Radioactive Waste at Yucca Mountain, Nye County, Nevada* (DOE 2002) (see 40 CFR 197.35 and 10 CFR 63.341 [66 FR 55732]).

The postclosure performance measures applicable to the Yucca Mountain repository system extend to a time period of 10,000 years after repository closure. An important element of the DOE repository safety strategy (CRWMS M&O 2001a, Volume 2) is the use of a safety margin to offset uncertainties associated with the analyses used to demonstrate compliance with the postclosure performance objective. The safety margin considered by the DOE has two components: (1) the margin in the dose rate during the first 10,000 years and (2) the margin over time periods greater than 10,000 years. To address the second element of the safety margin, analyses have been conducted to 100,000 years after repository closure. These analyses are performed to provide insights into the robustness of the repository system performance (CRWMS M&O 2001a, Volume 2, Section 5.2.1). In addition to these 100,000-year analyses, analyses out to the peak dose during the time period of geologic stability (1 million years) have been conducted. These analyses are described in Section 4.4.2.4.

4.4.2.1   Definition of the Nominal Scenario

The nominal scenario includes all relevant FEPs that are expected to occur over 10,000 years following the closure of the repository after emplacement of the waste packages. The nominal scenario is distinguished from the potentially disruptive scenario described in Section 4.4.3. In the nominal scenario, the expectation is that the processes included in the analyses are anticipated to occur with a probability of close to one within the 10,000-year time period, while the probability of events for the disruptive scenario is on the order of 0.0001 over the 10,000-year period.

TSPAs are projections of the behavior of individual processes described by distinct component models. These projections describe the relevant processes affecting the containment and isolation of radioactive wastes from the biosphere. Uncertainty is explicitly included in the models and the resulting analyses in the form of discrete probability distributions that encompass the range of possible outcomes. In the results presented in this section, uncertainty in the possible performance is evaluated through the use of these probabilistic analyses. Although the expected or mean performance of the repository system can be determined from the range of probabilistic outcomes, this section focuses on examining the full range of possible outcomes and the probability of each projected performance occurring.

The nominal scenario consists of models and parameters of the processes described in Section 4.2. The principal process models for the nominal scenario may be grouped into four key attributes of postclosure safety for the Yucca Mountain repository system. A fifth attribute reflects the likelihood that disruptive events would not affect repository performance over 10,000 years. The attributes and the principal process models within each attribute are:

- **Limited water entering emplacement drifts**—includes models describing climate, infiltration, unsaturated zone groundwater flow, water seepage into drifts, and the effects of thermal hydrology on groundwater flow and seepage.

- **Long-lived waste package and drip shield**—includes models describing the effects of the in-drift geochemical, thermal, hydrologic, and mechanical environments on the drip shields and waste packages, as well as the degradation characteristics of the titanium drip shield and the Alloy 22 waste package.

- **Limited release of radionuclides from the engineered barriers**—includes models describing the alteration of the different radioactive waste forms, as well as the mobil-

ity of the wastes in either dissolved or colloidal form.

- **Delay and dilution of radionuclide concentration by the natural barriers**—includes models describing (1) the retention and transport of different radionuclide species in the unsaturated zone beneath the repository, (2) radionuclide transport through the saturated zone, and (3) the biosphere pathways that may bring dissolved radionuclides into contact with humans.

- **Low mean annual dose considering potentially disruptive events**—includes models describing the probability and consequences of igneous or volcanic intrusions into or near the repository, with potential radionuclide releases through enhanced groundwater transport pathways or through airborne volcanic eruption pathways.

Models of all the above processes are integrated into the TSPA, as illustrated in Figures 4-177 and 4-178. These figures illustrate how information flows within the context of the TSPA model. The model is used to predict how the integrated and interdependent processes evolve over time and space, following the emplacement of the waste packages and drip shields and the ultimate closure of the repository. *Total System Performance Assessment for the Site Recommendation* (CRWMS M&O 2000a) contains a detailed description of the TSPA-SR model.

FY01 Supplemental Science and Performance Analyses (BSC 2001a; BSC 2001b) describes the supplemental TSPA model, and *Total System Performance Assessment—Analyses for Disposal of Commercial and DOE Waste Inventories at Yucca Mountain—Input to Final Environmental Impact Statement and Site Suitability Evaluation* (Williams 2001a) describes the revised supplemental TSPA model.

Each of the component models included in the TSPA models directly quantifies the uncertainty in the underlying process or bounds that uncertainty appropriately by selecting parameters that bound potential consequences of the model from an
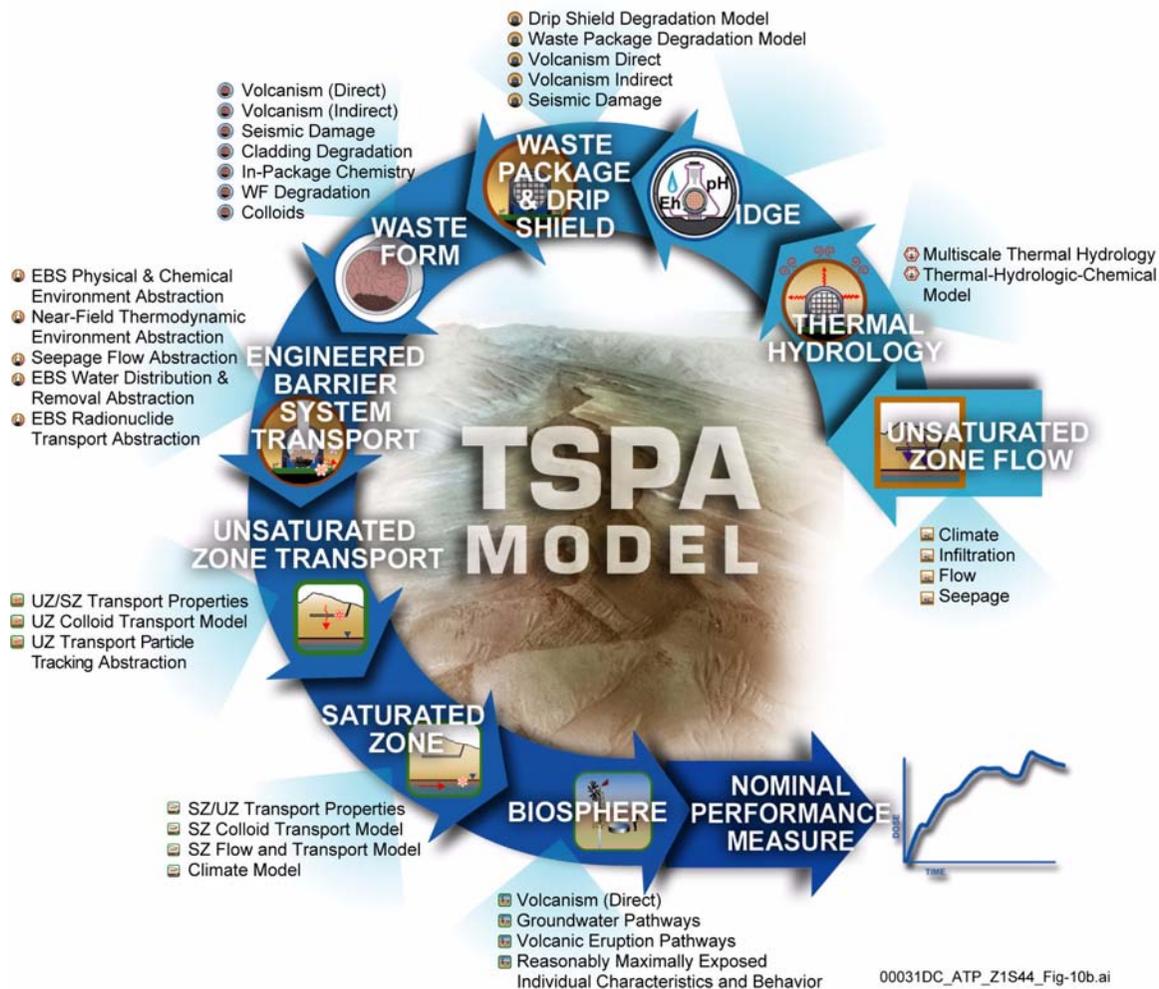
Figure 4-177. Component Models and Information Flow in the Total System Performance Assessment Model
IDGE = in-drift geochemical environment; WF = waste form; EBS = engineered barrier system; UZ = unsaturated zone; SZ = saturated zone.

overall performance perspective (i.e., that bound the expected dose to the receptor). The choice of whether a model or parameter directly incorporates the quantified uncertainty in the TSPA or uses reasonably conservative bounds was based on the availability of data. In cases where the uncertainty could be reasonably quantified with a sound scientific basis, the preferred option was to include this uncertainty directly in the TSPA model. In cases where the uncertainty could not be reasonably quantified as a probability distribution or alternative model, the analyst or modeler chose bounding conditions. The technical descriptions in Section 4.2, the nine process model reports, and Section 3 of the *Total System Performance Assessment for the Site Recommendation* (CRWMS M&O 2000a) present detailed discussions of the basis for the uncertainty that is contained in the models and analyses.

Volume 1, in its entirety, and Volume 2, Section 3 of *FY01 Supplemental Science and Performance Analyses* (BSC 2001a; BSC 2001b) further discuss uncertainty and the quantification of previously unquantified uncertainty.
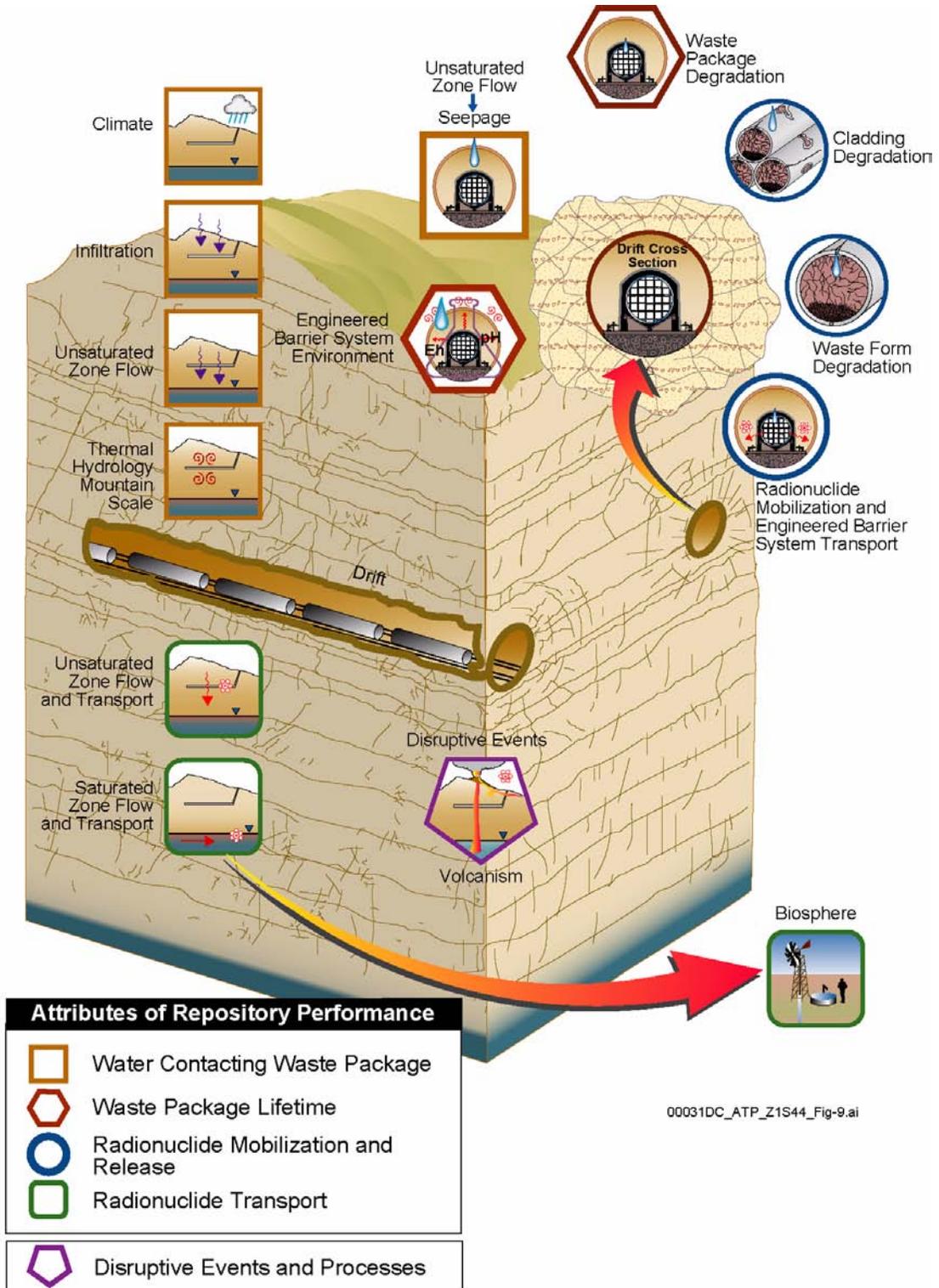
Figure 4-178. Component Models in the Total System Performance Assessment Nominal Scenario Model

In addition to grouping the process models into the different key attributes of postclosure safety, it is also worthwhile to briefly describe the component models in the sequence that represents the evolution of the repository system following the emplacement of the waste packages. This sequence essentially describes the processes that occur that ultimately lead to a release of radionuclides from the engineered barriers (e.g., after the containment provided by the waste packages has been breached) and the transport of these radionuclides to locations that they may come into contact with humans. The nominal scenario TSPA model evaluates the following sequence of processes:

- The temporal and spatial evolution of the physical and chemical environments on the engineered barriers (notably the drip shields and waste packages)

- The degradation of the engineered barriers within this range of possible physical and chemical environments

- The physical and chemical environments within the waste packages once the primary containment has been degraded to the point that throughgoing cracks penetrate the waste package

- The alteration rate of the waste form within the waste package, whether it is commercial spent nuclear fuel, DOE spent nuclear fuel (including naval spent nuclear fuel), or high-level radioactive waste, including immobilized plutonium waste forms

- The release of dissolved or colloidal radionuclides through the degraded engineered barriers to the host rock

- The transport of dissolved or colloidal radionuclides through the unsaturated zone to the water table

- The transport of dissolved or colloidal radionuclides through the saturated zone to the accessible environment

- The transport of radionuclides in the biosphere through a range of possible biological pathways to the point where they are either ingested or inhaled by humans.

Section 4.2 presents the models of each of these processes used as a basis for the TSPA model. *Total System Performance Assessment—Analyses for Disposal of Commercial and DOE Waste Inventories at Yucca Mountain—Input to Final Environmental Impact Statement and Site Suitability Evaluation* (Williams 2001a) assesses transport of radionuclides to the accessible environment consistent with 10 CFR Part 197.

4.4.2.2 Nominal Performance Results for Individual Protection Performance Measure

Information in this section is taken from *Total System Performance Assessment for the Site Recommendation* (CRWMS M&O 2000a), *FY01 Supplemental Science and Performance Analyses* (BSC 2001a; BSC 2001b), *Total System Performance Assessment—Analyses for Disposal of Commercial and DOE Waste Inventories at Yucca Mountain—Input to Final Environmental Impact Statement and Site Suitability Evaluation* (Williams 2001a), and *Total System Performance Assessment Sensitivity Analyses for Final Nuclear Regulatory Commission Regulations* (Williams 2001b). Figure 4-179 illustrates the TSPA results for the nominal scenario. The time period of interest consistent with relevant NRC and EPA regulations is 10,000 years after the closure of the repository.[1] Nevertheless, this figure illustrates the dose that is projected to occur out to 100,000 years to gain insight. Because of the large uncertainty in applying the models to 100,000-year time frames, these projections should not be interpreted as predictions of probable future performance. They

---

[1] To complement the results of the 10,000-year performance assessment and consistent with EPA and NRC regulations at 40 CFR 197.35 and 10 CFR 63.341 (66 FR 55732) respectively, the peak dose to the reasonably maximally exposed individual beyond the 10,000-year time period has been calculated and included in the EIS as an indicator of long-term performance.
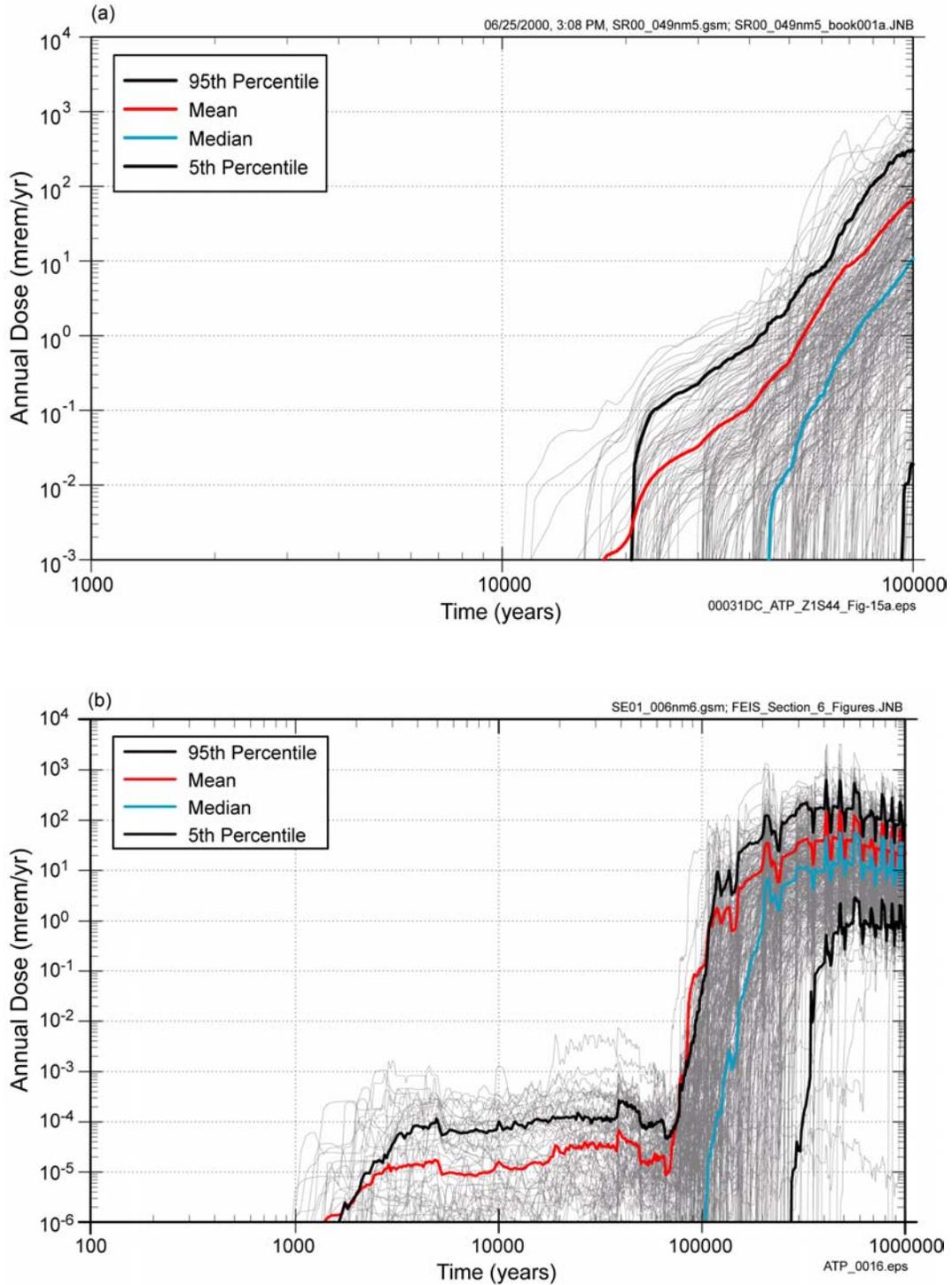
Figure 4-179. TSPA-SR Model and Revised Supplemental TSPA Model Results of Annual Dose to a Receptor for the Nominal Scenario

(a) Annual dose projected by the TSPA-SR model. (b) Annual dose projected by the revised supplemental TSPA model. The figures display the results for each simulation plotted, as well as the 5th and 95th percentiles, and the mean and median of these simulations to better examine the effects of uncertainty on the projected dose. Source: Modified from CRWMS M&O 2000a, Figure 4.1-5; Williams 2001a, Figure 6-5.

are simply indicators of the possible range of performance.

Figure 4-179 illustrates several statistical measures of how the repository system is likely to evolve and the projected dose rates associated with that probable evolution. The uncertainty in the overall projected performance is indicated by the wide range of possible outcomes. Each of the thin lines (also known as "horsetails") represents a single realization of the possible future performance of the repository system. The wide spread in the predicted outcomes is a direct result of the uncertainty in the component models summarized in Section 4.4.2.1 and described in detail in the subparts of Section 4.2. In addition to the complete distribution of results (represented by 300 distinct realizations), summary statistics indicating the 95th, 50th (or median), and 5th percentiles of the dose rate and the mean (or "expected") dose rate are also illustrated. These later statistical representations allow for an examination of the central tendency of the results.

As projected by the TSPA-SR model, no dose occurs for any of the 300 realizations for the nominal scenario of processes until more than 10,000 years after closure (Figure 4-179a). At 40,000 years, there is about a 5 percent probability of the dose rate being on the order of 1 mrem/yr or higher. At 60,000 years, there is about a 50 percent probability of the predicted dose being less than 1 mrem/yr. At 100,000 years, there is about a 50 percent probability of the predicted dose being on the order of 10 mrem/yr.

Based on updated information developed after completion of the TSPA-SR model, supplemental analyses were conducted to provide the basis for a modification of the TSPA-SR model. The results of these analyses are described in Volume 2, Section 3.2 of *FY01 Supplemental Science and Performance Analyses* (BSC 2001b) and in Section 4.4.5 of this report. Based on these sensitivity analyses, 20 component models were updated for the nominal scenario and one component model (igneous activity) was updated for the disruptive scenario to form the supplemental TSPA model (BSC 2001b, Sections 2.3 and 4.1). The peak mean dose projected by the supplemental TSPA model

during the first 10,000 years is 2.0×10^{-4} mrem/yr for the higher-temperature operating mode and 6.0×10^{-5} mrem/yr for the lower-temperature operating mode, as presented in Volume 2, Section 4.1.1 of *FY01 Supplemental Science and Performance Analyses* (BSC 2001b). The supplemental TSPA analyses (Figure 4-180) and revised supplemental TSPA analyses (Figure 4-179b) include nonmechanistic early waste package failures that result in doses to the reasonably maximally exposed individual during the first 10,000 years. Doses after 10,000 years projected by the supplemental and revised supplemental TSPA models are lower than the results of the TSPA-SR model for the same time period (see Figure 4-180). The doses calculated for the nominal scenario by the supplemental TSPA model would be reduced by approximately one-third using an annual water demand of 3,000 acre-ft, consistent with NRC licensing regulations (see 10 CFR 63.312) (Williams 2001b, Section 6.3).

The waste package degradation model was further evaluated in *FY01 Supplemental Science and Performance Analyses* (BSC 2001a; BSC 2001b), and these changes were incorporated into the revised supplemental TSPA model used to project peak mean annual dose to the reasonably maximally exposed individual consistent with the EPA rule at 40 CFR Part 197. The peak mean dose projected by the revised supplemental TSPA model over a 10,000-year period is 1.7×10^{-5} mrem/yr for the higher-temperature operating mode and 1.1×10^{-5} mrem/yr for the lower-temperature operating mode. These evaluations are presented in *Total System Performance Assessment—Analyses for Disposal of Commercial and DOE Waste Inventories at Yucca Mountain—Input to Final Environmental Impact Statement and Site Suitability Evaluation* (Williams 2001a, Section 6 and Table 6-1). These calculated doses would be reduced by approximately one-third using an annual water demand of 3,000 acre-ft, consistent with NRC regulations at 10 CFR 63.312 (66 FR 55732) (Williams 2001b, Section 6.3).

The supplemental and revised supplemental TSPA models forecast doses before 10,000 years, whereas the TSPA-SR model forecasts no dose in the first 10,000 years. The primary reason for this
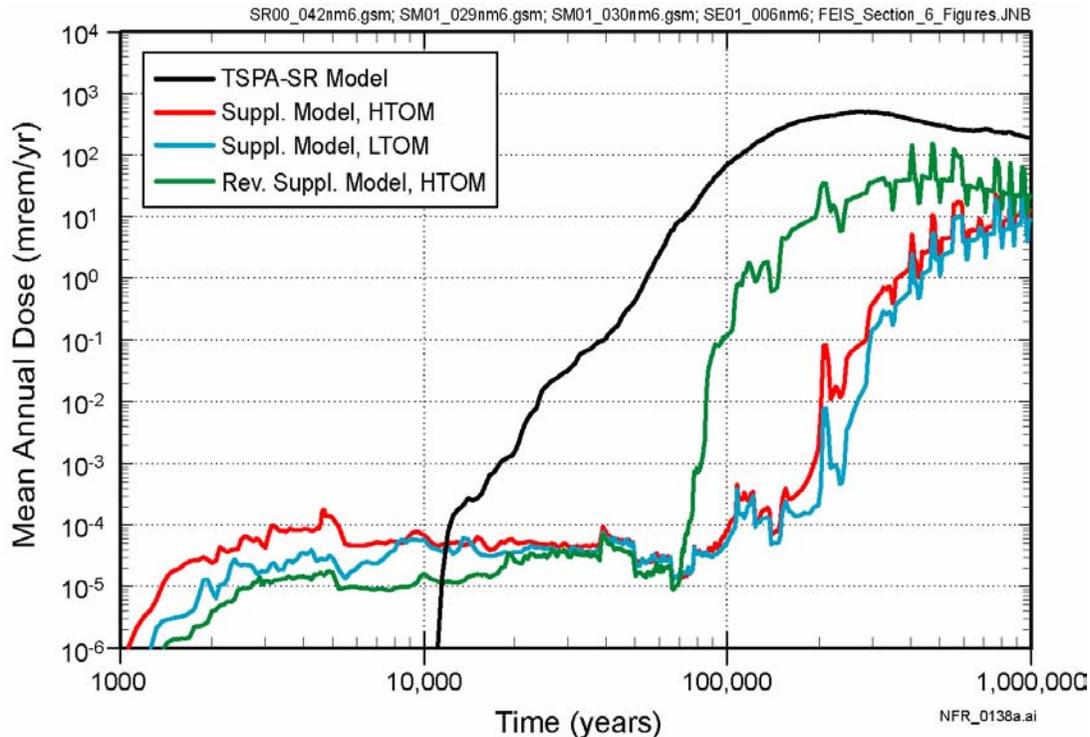
Figure 4-180. TSPA Model Results: Million-Year Annual Dose Histories for Nominal Performance
Mean annual dose histories are shown for the supplemental TSPA model for both higher-temperature and lower-temperature operating modes (HTOM and LTOM, respectively). These results are documented in Volume 2 of *FY01 Supplemental Science and Performance Analyses* (BSC 2001b). The nominal scenario results from the revised supplemental TSPA model for the higher-temperature operating mode, as documented in *Total System Performance Assessment—Analyses for Disposal of Commercial and DOE Waste Inventories at Yucca Mountain—Input to Final Environmental Impact Statement and Site Suitability Evaluation* (Williams 2001a), are also shown. These calculated doses would be reduced by approximately one-third using an annual water demand of 3,000 acre-ft, consistent with NRC regulations. The effect of the 3,000 acre-ft annual water demand is discussed further in *Total System Performance Assessment Sensitivity Analyses for Final Nuclear Regulatory Commission Regulations* (Williams 2001b, Section 6.3). These revised supplemental TSPA model results are presented along with the nominal scenario TSPA-SR model results documented in *Total System Performance Assessment for the Site Recommendation* (CRWMS M&O 2000a). Source: Williams 2001a, Figure 6-14.

is the incorporation of nonmechanistic early waste package failures as described in the supplemental TSPA models (BSC 2001b, Section 4.1; Williams 2001a, Section 5.2.4.2). No mechanisms that could lead to early failure of waste packages were included in the TSPA-SR model. This was based on the low probability and the use of administrative controls to further reduce the probability of mechanisms that could lead to early failure. In reevaluating the potential of early failure mechanisms and their potential consequences, a more conservative approach resulted in the inclusion of improper heat treatment and subsequent possible failure of up to three waste packages in the

supplemental TSPA analyses. The early waste package failure assumes failure of both the inner and outer Alloy 22 lids and the stainless steel inner lid. To ensure that the potential consequence of early waste package failures is treated conservatively, it was included in the nominal scenario, not as a sensitivity analysis, for the supplemental and revised supplemental TSPA model analyses. In the revised supplemental model, assuming nonmechanistic early failure of all waste packages would result in an annual dose during the first 10,000 years of less than 1 mrem/yr, or less than one-third of one percent of the average dose from natural background radiation.

The use of administrative (procedural) controls, engineering controls, and multiple checks included as part of the development of the induction annealing process, will reduce the probability of failures due to improper heat treatment. The inclusion of early failures has built conservatism into the nominal scenario simulated by both supplemental TSPA models. For the nominal scenario, these early failures are the only contributor to the early dose that begins at approximately 2,000 years and extends out to approximately 80,000 years in the supplemental and revised supplemental TSPA model evaluations of nominal performance (BSC 2001b, Section 5.1; Williams 2001a, Section 5.2.4.2).

The difference in projected dose between the TSPA-SR model and both supplemental TSPA models for the nominal case after 10,000 years resulted from an effort to quantify uncertainties and address conservatism found in the TSPA-SR model (Figure 4-180). The drop in peak annual dose for the supplemental and revised supplemental TSPA models after 10,000 years as compared to the TSPA-SR model is largely due to the more realistic treatment of radionuclide solubilities, particularly neptunium, thorium, and plutonium (BSC 2001b, Section 4.1). The increase in peak annual dose after 10,000 years from the supplemental TSPA model compared to the revised supplemental TSPA model is primarily due to the exclusion of the consideration of temperature dependence in Alloy-22 corrosion rates. The revised supplemental TSPA model used biosphere dose conversion factors based on the reasonably maximally exposed individual, whereas the TSPA-SR and supplemental TSPA model used biosphere dose conversion factors based on the average member of the critical group. Reasonably maximally exposed individual biosphere dose conversion factors are lower than those for the average member of the critical group. As a result, doses projected by the revised supplemental TSPA model were lower (Williams 2001a, Section 5.2.5) for the first 10,000 years. Calculated values of dose for the nominal scenario would be reduced by approximately one-third using an annual water demand of 3,000 acre-ft consistent with NRC regulations at 10 CFR 63.312. The effects of the change in annual water demand in the final NRC rule are

discussed further in *Total System Performance Assessment Sensitivity Analyses for Final Nuclear Regulatory Commission Regulations* (Williams 2001b, Section 6.3).

Figures 4-181 and 4-182 illustrate the distribution of key radionuclides projected by the TSPA-SR model that contribute to the mean dose response depicted on Figure 4-179a. These figures indicate that for the first 50,000 years, the doses are dominated by the mobile, high solubility and poorly sorbing radionuclides, such as iodine-129 and technetium-99. After about 50,000 years, the doses are dominated by less mobile, lower solubility, and more sorbing radionuclides, such as neptunium-237 and both colloidal and dissolved plutonium-239.

The preceding figures describe the total system results in terms of the total annual dose to the receptor and the uncertainty in these results. However, it is also important to understand the causal relationships that determine these results. The following discussion describes the evolution of the potential repository as it relates to the performance of the overall system.

Before liquid water can contact the waste packages, the titanium drip shield must be breached. The drip shields are projected by the TSPA-SR model to remain intact for about 20,000 years; however, about half of the drip shields are projected to be breached after about 30,000 years.

The range of initial drip shield breach generally occurs between about 20,000 and 40,000 years, although there is a low probability that some drip shields remain intact for the entire 100,000-year simulation period. While the drip shields are intact, there is no liquid water which contacts the waste package; therefore, there is no possibility for advective releases from the waste package during this time period, even if a waste package were to degrade. The supplemental TSPA model projects drip shield lifetimes of 30,000 to 120,000 years (BSC 2001a, Section 7.4; BSC 2001b, Section 3.2.6.3).

The doses in the nominal scenario are delayed until after the waste packages are breached. In the
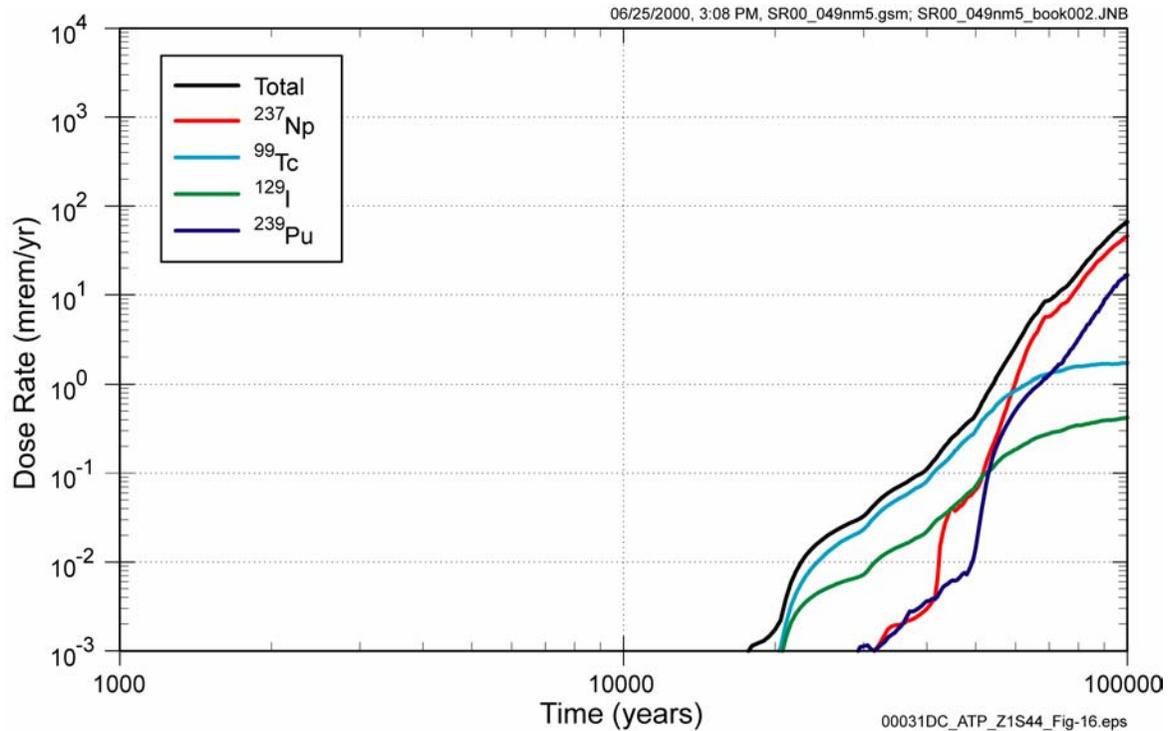
Figure 4-181. Mean Annual Dose Rate for Key Radionuclides for the Nominal Scenario Projected by the TSPA-SR Model
Source: Modified from CRWMS M&O 2000a, Figure 4.1-5.

TSPA-SR model, there is a 95 percent probability that the waste packages will remain intact until about 20,000 years, and there is a 50 percent probability that the waste packages will remain intact until about 40,000 years. However, there is a very small probability that the waste packages will begin to breach at about 11,000 years. The fact that the mean waste package failures occur prior to the 95th percentile failure distribution is indicative that there is a small probability (but less than five percent) that some waste packages will be degraded prior to 20,000 years. The supplemental TSPA model projects up to three waste package failures before 10,000 years due to nonmechanistic improper heat treatment of welds (BSC 2001a, Section 7.3.6).

Additional analyses of corrosion and waste package performance are described in *FY01 Supplemental Science and Performance Analyses* (BSC 2001a; BSC 2001b) and *Total System Performance Assessment—Analyses for Disposal of Commercial and DOE Waste Inventories at Yucca Mountain—Input to Final Environmental Impact*

Statement and Site Suitability Evaluation (Williams 2001a).

The analyses assume that once the outer corrosion-resistant barrier (Alloy 22) of the waste package has degraded, moisture can enter the package. These analyses conservatively assumed that no time delay is attributed to the containment and isolation potentially afforded to the inner, less corrosion-resistant barrier of the waste package (stainless steel). In addition, no credit is taken for the pour canisters that encapsulate the high-level waste glass. Therefore, with the exception of the corrosion-resistant Zircaloy cladding that surrounds about 99 percent of the commercial spent nuclear fuel, once the waste package is breached by a crack penetrating the waste package, the waste form is exposed to moisture.

Once the waste form is exposed, it will begin to degrade and radionuclides will be released to the aqueous phase (whether liquid water or a thin film of moisture) in contact with the waste form. The rate of release to this aqueous phase is a function of
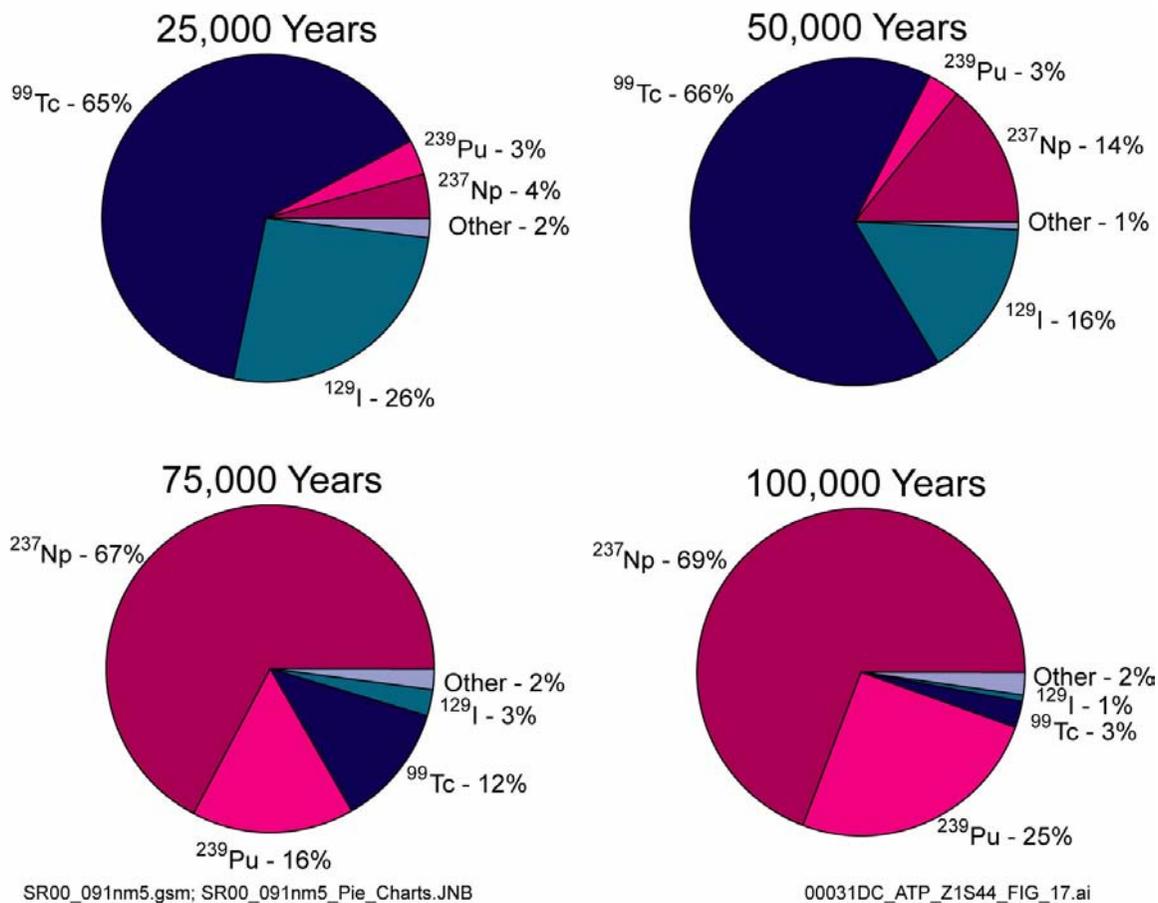
Figure 4-182. Fraction of Mean Total Annual Dose Attributed to Different Radionuclides for the Nominal Scenario Projected by the TSPA-SR Model

Times depicted are (a) 25,000 years, (b) 50,000 years, (c) 75,000 years, and (d) 100,000 years after closure. More mobile radionuclides, such as iodine-129 and technetium-99, dominate the dose at times less than 40,000 years, while neptunium-237 dominates the dose at longer times. Source: Modified from CRWMS M&O 2000a, Figure 4.1-6.

the rate of exposure of the waste, which includes the rate of waste package degradation and the rate of cladding degradation, as well as the rate of waste form degradation. In addition, the release rate is dependent on the solubility of the radionuclide in the moisture film that surrounds the exposed waste form. Once radionuclides are released from the waste form into the aqueous phase, they may be transported by advection (i.e., within flowing water) or diffusion (i.e., by concentration gradients through a continuous water film) through the waste package. Mobile radionuclides—those that are highly soluble or attached to mobile colloids—are transported through the degraded waste package and the invert material beneath the waste package to the host rock. The rate of release to the host rock depends on the

mobility of the radionuclide and the amount of water available for transport.

Plutonium-239 is a low solubility, highly sorbed radionuclide that is generally immobile in aqueous environments. However, in the presence of colloidal material, plutonium-239 can sorb onto the colloid particles and be transported in the aqueous phase with the colloids. Two different types of colloids have been considered in TSPA: reversible colloids (where the radionuclide can sorb and desorb from the colloid) and irreversible colloids (where the radionuclide can not desorb from the colloid).

Mean radionuclide release rates from five locations for key radionuclides were assessed in the

TSPA-SR for the nominal scenario. These correspond to the following boundaries: (1) the edge of the waste form; (2) the edge of the waste package; (3) the edge of the engineered barrier system, which corresponds to the base of the drift invert; (4) the base of the unsaturated zone, which corresponds to the top of the water table; and (5) 20 km (12 mi) from the repository footprint. *Total System Performance Assessment—Analyses for Disposal of Commercial and DOE Waste Inventories at Yucca Mountain—Input to Final Environmental Impact Statement and Site Suitability Evaluation* (Williams 2001a) describes a nominal scenario TSPA with the controlled area extended approximately 18 km (11 mi) south from the repository footprint, consistent with 40 CFR 197.12 and 10 CFR 63.302 (66 FR 55732).

The analyses reveal several important insights into repository system behavior:

1. The initial mean rate of release of these radionuclides from the waste form is dependent on the mean time for initial degradation of the waste package. As soon as the packages are degraded, some mobile radionuclides may be released to the aqueous phase. The mean rate of release can precede the mean time to failure because the mean release rate is dependent on some very low probability early waste package failures. For example, there is a 1 percent chance of having at least one waste package failure at about 11,000 years, projected by the TSPA-SR model.

    The supplemental TSPA model results found in Volume 2, Section 3.2.5.4 of *FY01 Supplemental Science and Performance Analyses* (BSC 2001b, Figure 3.2.5.4-1) and the revised supplemental TSPA model results found in *Total System Performance Assessment—Analyses for Disposal of Commercial and DOE Waste Inventories at Yucca Mountain—Input to Final Environmental Impact Statement and Site Suitability Evaluation* (Williams 2001a, Section 6.2.1, Figures 6-4 and 6-6) describe a nominal scenario in which

doses from nonmechanistic early waste package failures occur as early as 1,000 years after closure.

2. The release rate from the waste form to the aqueous phase is significantly greater than the mean release rate from the waste package. This is a result of the fact that even though the waste package has failed (in that it no longer provides complete containment of the inventory), the initial failure is by very small stress corrosion cracks at the closure welds. These small cracks are sufficiently small to significantly reduce any diffusive (prior to drip shield degradation) or advective (after drip shield degradation) transport through them. Once a significant fraction of the waste package has been degraded, the release rate from the waste form and from the waste package become more equivalent.

3. In most instances, the release rate from the engineered barrier system is similar to the release rate from the waste package. This is a function of the diffusive release rate through the invert materials, for the assumed diffusivity in the partially saturated invert materials, being greater than that through the small cracks in the waste package.

4. The residence time of radionuclides through the unsaturated zone is dependent on the radionuclide. For nonsorbing radionuclides such as technetium-99, the residence time is on the order of hundreds of years for the glacial transition climate state present at the time radionuclides are released from the engineered barrier system. For more sorbing radionuclides such as neptunium-237, the residence time is on the order of thousands of years for the glacial transition climate state.

5. The delay in radionuclides that are released at the base of the unsaturated zone from reaching the accessible environment is also dependent on the degree

of sorption of the radionuclides. Less sorbing radionuclides have a short residence time, while more highly sorbed radionuclides have a longer residence time.

4.4.2.3 Nominal Performance Results for Groundwater Protection

The results of the TSPA-SR groundwater protection performance analyses are illustrated in Figures 4-183 and 4-184 for the concentration and dose performance measures, respectively. Figure 4-183 illustrates the combined radium-226 and radium-228 concentrations in the representative volume of groundwater, as well as the gross alpha-activity concentration (including radium-226 but excluding radon and uranium). Figure 4-184 shows the dose associated with the beta and photon emitting radionuclides (iodine-129, technetium-99, and carbon-14). The critical organs for these three radionuclides are the thyroid (for iodine-129), the gastrointestinal tract (for technetium-99), and fat (for carbon-14).

The natural background concentrations are not shown in these figures. The measured natural gross alpha background is 0.4 pCi/L ± 0.7 pCi/L. The measured natural total radium background is 1.04 pCi/L. The calculated activity concentration of radium-226 and radium-228, with background included, is still less than 5 pCi/L. If the background gross alpha activity is included, the sum of TSPA-SR projected gross alpha activity concentration plus natural background approaches 15 pCi/L at 100,000 years (CRWMS M&O 2000a, Section 4.1.5).

Consistent with proposed 40 CFR 197.35 (64 FR 46976), the TSPA-SR and supplemental TSPA models considered the radionuclide activity concentration in the groundwater, where the water volume considered is that equivalent to a representative volume of 1,285 acre-ft/yr. Groundwater protection was analyzed at the receptor location above the highest concentration of radionuclide in the plume. The plume volume was equivalent to a volume that would yield 1,285 acre-ft of annual groundwater withdrawal. The radionuclide concentrations were calculated by dividing the annual release of radionuclides that pass the receptor location by the representative volume. The water has been measured to have 385 mg/L of total dissolved solids (CRWMS M&O 2000a, Section 4.1.5). For the purposes of the maximally exposed organ dose, these analyses also assumed that the water was consumed at a rate of 2 L (0.5 gal) per day and that the ICRP-2 dose conversion factors were used.

Total System Performance Assessment—Analyses for Disposal of Commercial and DOE Waste Inventories at Yucca Mountain—Input to Final Environmental Impact Statement and Site Suitability Evaluation (Williams 2001a) assumes a representative volume of 3,000 acre-ft/yr. and an accessible environment location consistent with 40 CFR 197.31. These assumptions are included in the revised supplemental TSPA model.

Over 10,000 years, the peak mean annual activity concentration calculated by the supplemental TSPA model for combined radium-226 and radium-228 is 7×10^{-11} pCi/L (not including background radiation) for the higher-temperature operating mode (BSC 2001b, Section 4.1.4). The combined radium concentration for the lower-temperature operating mode is less than 10^{-10} (BSC 2001b, Section 4.1) (not including background radiation). The calculated peak mean activity concentration for gross alpha-emitting radionuclides is 7×10^{-8} pCi/L (not including background radiation) for the higher-temperature operating mode (BSC 2001b, Section 4.1.4). Plots of the gross alpha concentration for the lower-temperature operating mode indicate the activity concentration is approximately 3×10^{-8} pCi/L (BSC 2001b, Section 4.1) (not including background radiation). The calculated maximum dose to any critical organ projected by the supplemental TSPA model is 5×10^{-5} mrem/yr for the higher-temperature operating mode and 2×10^{-5} mrem/yr for the lower-temperature operating mode (BSC 2001b, Section 4.1.4). Further discussion of radionuclide concentrations and critical organ doses calculated by the supplemental TSPA model are given in Volume 2, Sections 4.1.4 and 5.5 of *FY01 Supplemental Science and Performance Analyses* (BSC 2001b).
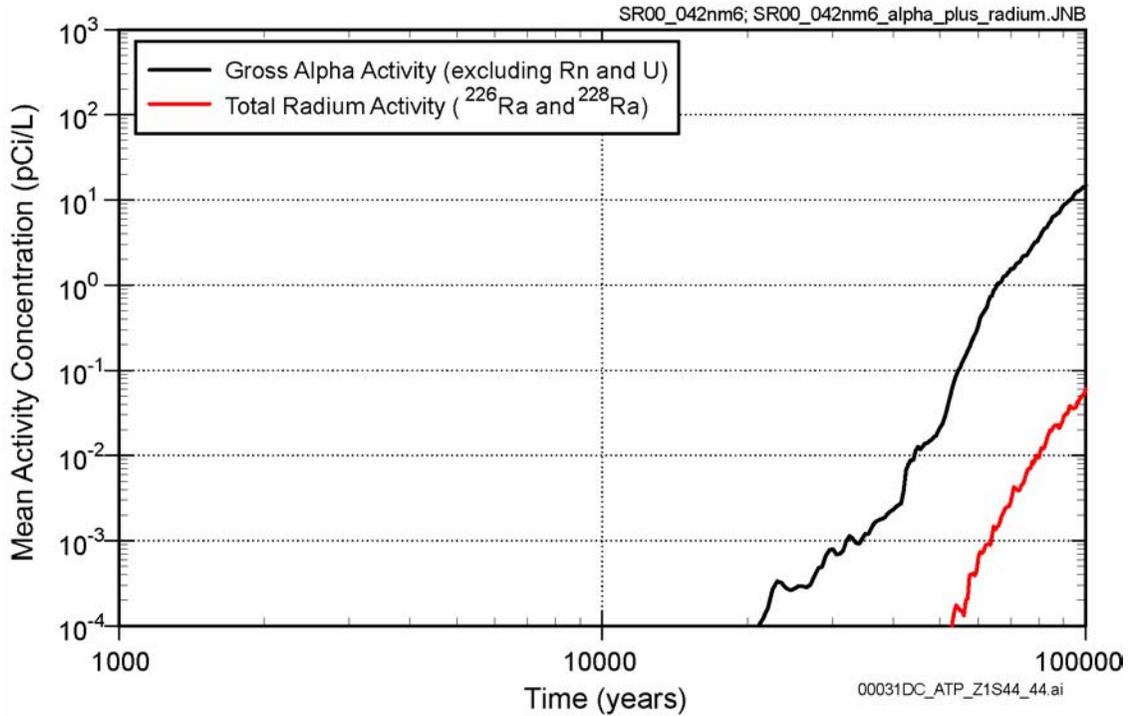
Figure 4-183. Mean Groundwater Concentrations for Gross Alpha and Total Radium Activity Projected by the TSPA-SR Model
Source: CRWMS M&O 2000a, Figure 4.1-24.
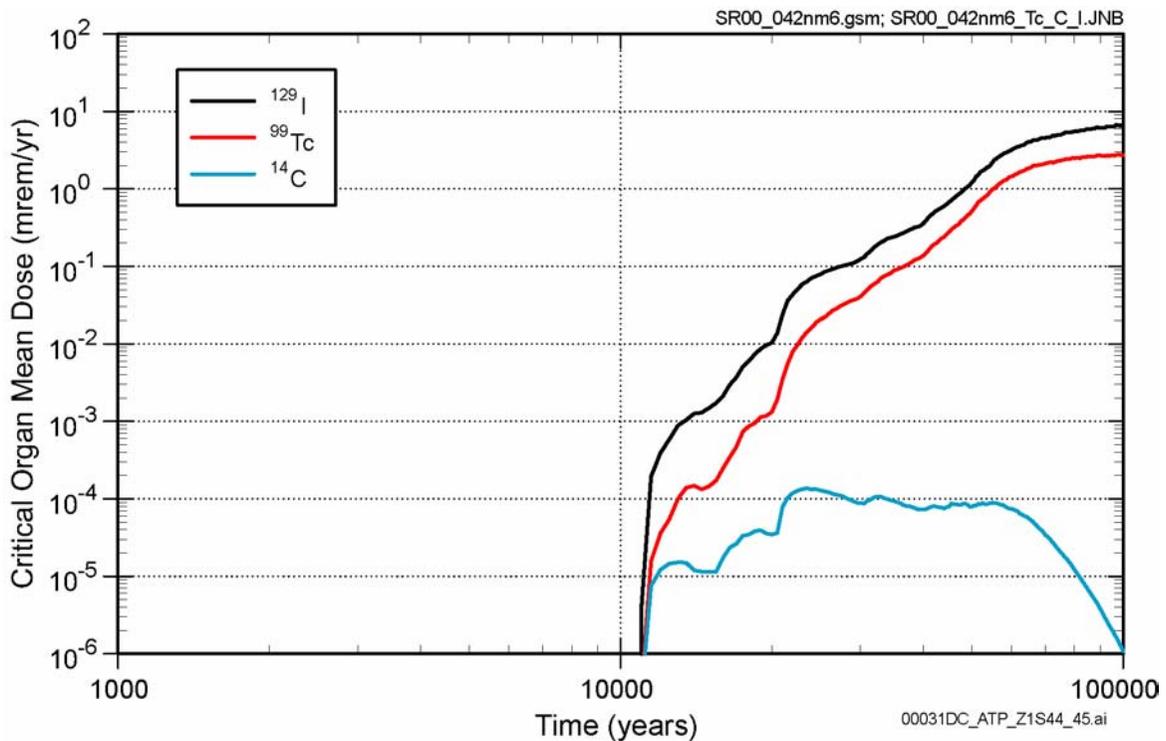
Figure 4-184. Mean Critical Organ Dose Rates Combined Beta- and Photon-Emitting Radionuclides Projected by the TSPA-SR model
Source: CRWMS M&O 2000a, Figure 4.1-27.

As shown in Figures 4-185 and 4-186, the peak mean annual activity concentration calculated by the revised supplemental TSPA model for combined radium-226 and radium-228 for the first 10,000 years is less than 10^{-10} pCi/L for both the higher-temperature and lower-temperature operating modes (not including background radiation) (Williams 2001a, Table 6-3). Figures 4-185 and 4-186 also show that the calculated peak mean activity concentration for gross alpha-emitting radionuclides for the first 10,000 years is 1.8×10^{-8} pCi/L (not including background radiation) for the higher-temperature operating mode and 3.3×10^{-8} pCi/L (not including background radiation) for the lower-temperature operating mode (Williams 2001a, Table 6-2).

As indicated, data taken from a Nevada Department of Transportation well approximately 20 km (12 mi) from the potential repository indicate that gross alpha background concentrations are 0.4 pCi/L $\pm$ 0.7 pCi/L; total radium background concentrations are no greater than 1.04 pCi/L (CRWMS M&O 2000a, Section 4.1.5). Because the calculated gross alpha and total radium concentrations are orders of magnitude lower than their natural background concentration, the combined background and calculated concentrations, when rounded, are the same as the natural background. The maximum mean dose to any critical organ projected by the revised supplemental TSPA model from combined beta- and photon-emitting radionuclides is 2.3×10^{-5} mrem/yr for the higher-temperature operating mode and 1.3×10^{-5} mrem/yr for the lower-temperature operating mode (Williams 2001b, Table 6-3). Radionuclide concentrations and critical organ doses calculated by the revised supplemental TSPA model are discussed in
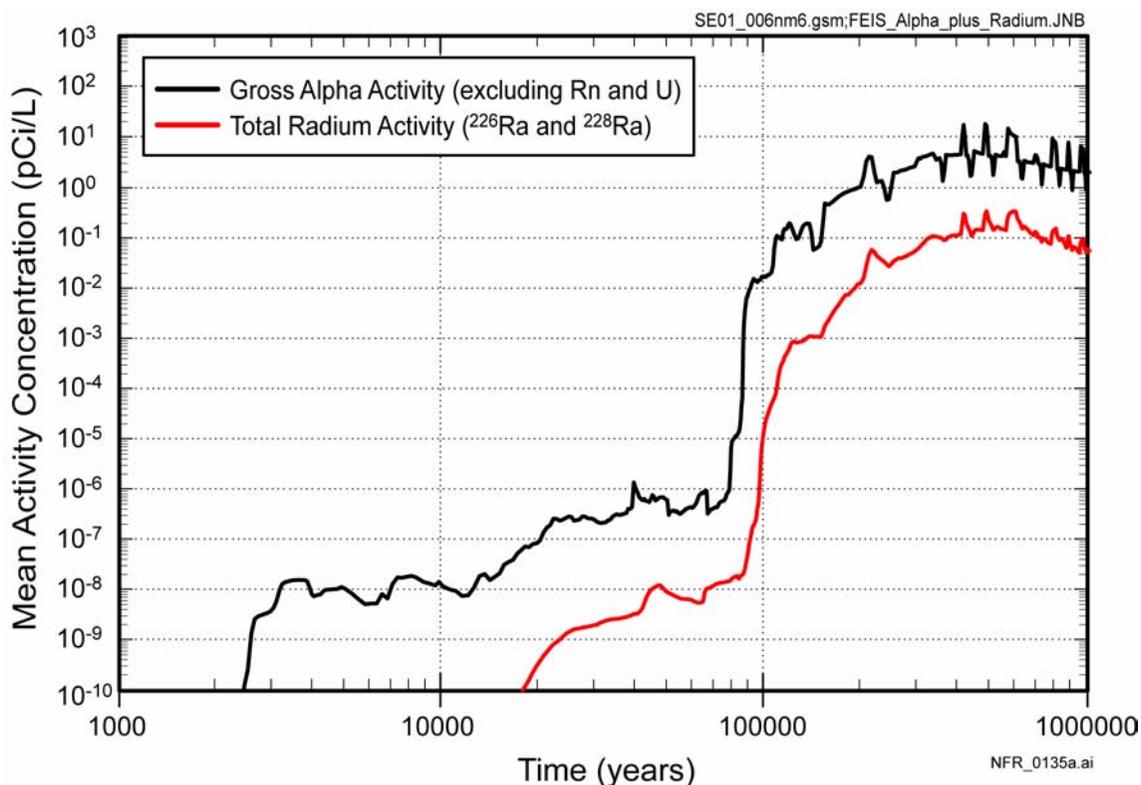
Figure 4-185. Mean Activity Concentrations of Gross Alpha Activity and Total Radium in the Groundwater, Higher-Temperature Operating Mode

Nominal scenario revised supplemental TSPA model results for 1 million years. Concentrations calculated for an annual representative volume of water of 3,000 acre-ft, approximately 18 km (11 mi) from within the potential repository footprint. Naturally occurring background radionuclide concentrations are not included. Source: Williams 2001a, Figure 6-17.
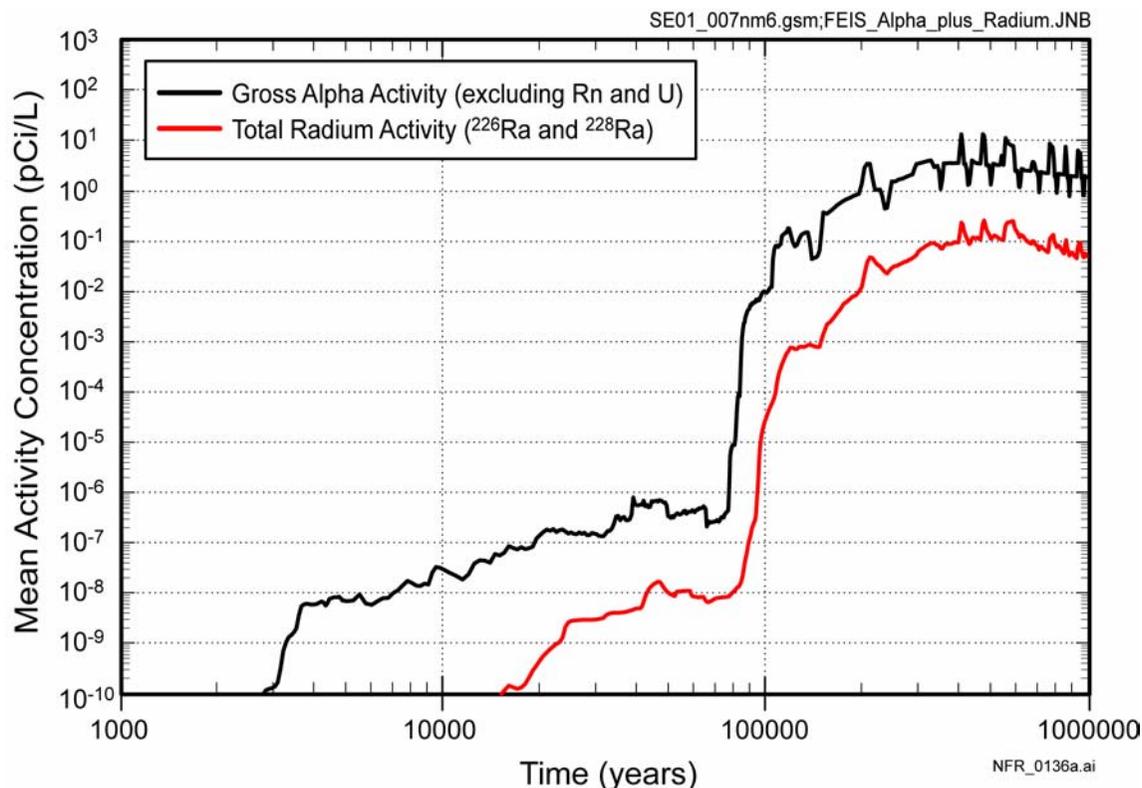
Figure 4-186. Mean Activity Concentrations of Gross Alpha Activity and Total Radium in the Groundwater, Lower-Temperature Operating Mode

Nominal scenario revised supplemental TSPA model results for 1 million years. Concentrations calculated for an annual representative volume of water of 3,000 acre-ft, approximately 18 km (11 mi) from within the potential repository footprint. Naturally occurring background radionuclide concentrations are not included. Source: Williams 2001a, Figure 6-18.

more detail in Section 6.6 of *Total System Performance Assessment—Analyses for Disposal of Commercial and DOE Waste Inventories at Yucca Mountain—Input to Environmental Impact Statement and Site Suitability Evaluation* (Williams 2001a).

The DOE conducted additional sensitivity analyses and documented these in *Total System Performance Assessment Sensitivity Analyses for Final Nuclear Regulatory Commission Regulations* (Williams 2001b). The report includes estimates of activity concentrations and dose estimates from combining releases from the nominal scenario with those from an unlikely event (igneous intrusion scenario) for the evaluation of groundwater protection. Because the nominal scenario results are negligible compared to the results calculated for an unlikely igneous intrusion, the activity concentrations and dose estimates for groundwater

protection considering igneous intrusion are approximated as those calculated for an igneous intrusion. Gross alpha concentration for the igneous intrusion scenario was calculated as 2.9×10^{-2} pCi/L for the higher-temperature operating mode and 5.5×10^{-2} pCi/L for the lower-temperature operating mode. These concentrations are about 10 percent of natural background radiation. Total radium concentration was 5×10^{-6} pCi/L for the higher-temperature operating mode and 5.2×10^{-6} pCi/L for the lower-temperature operating mode. These concentrations are orders of magnitude lower than natural radiation. The calculated maximum dose to any critical organ for the igneous intrusion scenario was 2.5×10^{-1} mrem/yr for the higher-temperature operating mode and 2.4×10^{-1} mrem/yr for the lower-temperature operating mode (Williams 2001b, Tables 6-1, 6-2, and 6-3).

4.4.2.4 Nominal Performance Results for Peak Dose

Consistent with both EPA and NRC rules (40 CFR 197.35 and 10 CFR 63.341 [66 FR 55732] respectively), the DOE has evaluated the peak dose to the reasonably maximally exposed individual during the period of geologic stability and has included these results in the EIS. The National Academy of Science has estimated the period of geologic stability at Yucca Mountain to be on the order of 1 million years (National Research Council 1995, pp. 71 and 72). There are several important limitations that should be emphasized in interpreting the results of the million-year calculations.

The models developed for use in the nominal performance assessment have focused on the first 10,000 years, consistent with EPA and NRC regulations. As a result, these models have not considered longer term processes such as long-term climate change in their development. For example, the climate change considered in the nominal performance analyses for the TSPA-SR model is limited to changes over the next 10,000 years and has neglected the possible changes during full glacial time periods. As a result, the climate model had to be modified to include glacial time periods to perform peak dose analyses.

The post-10,000-year analyses are designed to provide additional confidence that public health and safety will be protected. Extending nominal performance results beyond 10,000 years provides a reasonably conservative representation of the peak dose.

The main reason for estimating peak doses is to provide the DOE, regulators, and the public with additional information about long-term repository performance. It is important to note that the component models in the TSPA-SR model are believed to be relatively conservative for the 10,000-year time period and may be highly conservative when applied to time periods on the order of 100,000 or 1 million years. One of these conservative models is the retention of moderate and low-solubility radionuclides, such as neptunium-237 and plutonium-239, in the secondary phases of uranium that are formed as the spent fuel waste forms are altered. Models of secondary phase (CRWMS M&O 2000dr) on radionuclide solubility have been developed based on data from long-term drip tests conducted at Argonne National Laboratory (CRWMS M&O 2000dk).

Analyses in Volume 2 of *FY01 Supplemental Science and Performance Analyses* (BSC 2001b) had as one of their primary goals to quantify previously unquantified uncertainties. This was done primarily to aid in understanding the degree of conservatism in the calculation.

A second goal of this evaluation was to assess the impact of the conservatisms on the peak dose calculation. For example, not taking secondary phase effects into account simplifies the modeling process, but it makes the peak dose estimate highly pessimistic. In contrast, assuming the climate state at 10,000 years stays the same for the next 990,000 years probably makes the peak dose calculation optimistic. Both processes must be accounted for to make the peak dose calculation. These two processes in particular may represent the most significant potential sources of optimism and pessimism in the TSPA-SR model peak dose. As other optimistic or pessimistic simplifications were identified, however, sensitivity studies have been done to evaluate their importance to the peak dose determination.

The results of the TSPA-SR model mean peak dose performance assessments assuming the models developed for the 10,000-year time period and extrapolated to 1 million years (CRWMS M&O 2000a, Section 4.1.3) are illustrated in Figure 4-187. This plot essentially continues the trends illustrated on the 100,000-year nominal performance analyses illustrated in Figure 4-179. The mean peak dose to the receptor for this plot is about 460 mrem/yr and occurs at about 270,000 years.

The results of the TSPA-SR model mean peak dose performance assessments using a preliminary secondary-phase solubility model (CRWMS M&O 2000a, Section 4.1.3) are illustrated in Figure 4-188. The mean peak dose to the receptor for this plot is about 30 mrem/yr and occurs much later (i.e., 500,000 to 600,000 years).
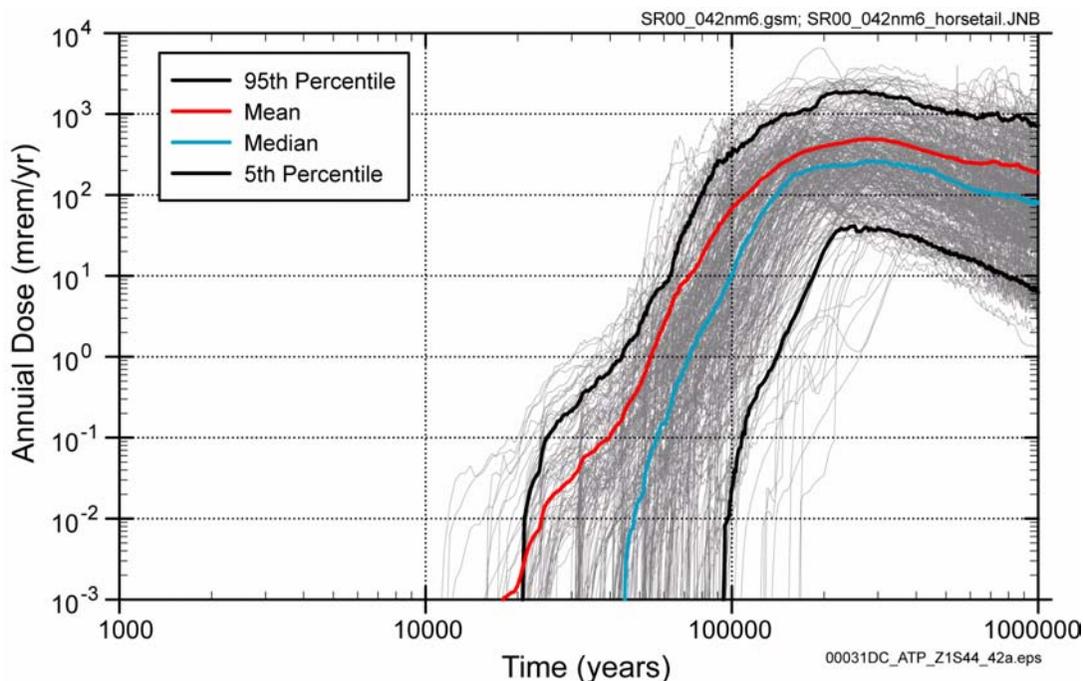
Figure 4-187. TSPA-SR Model Results for the Million-Year Annual Dose to a Receptor for the Nominal Scenario Using Nominal TSPA Models

The figure displays the results for each simulation as well as the 5th and 95th percentiles, and the mean and median of these simulations to better examine the effects of uncertainty on the projected dose. Source: CRWMS M&O 2000a, Figure 4.1-19a.
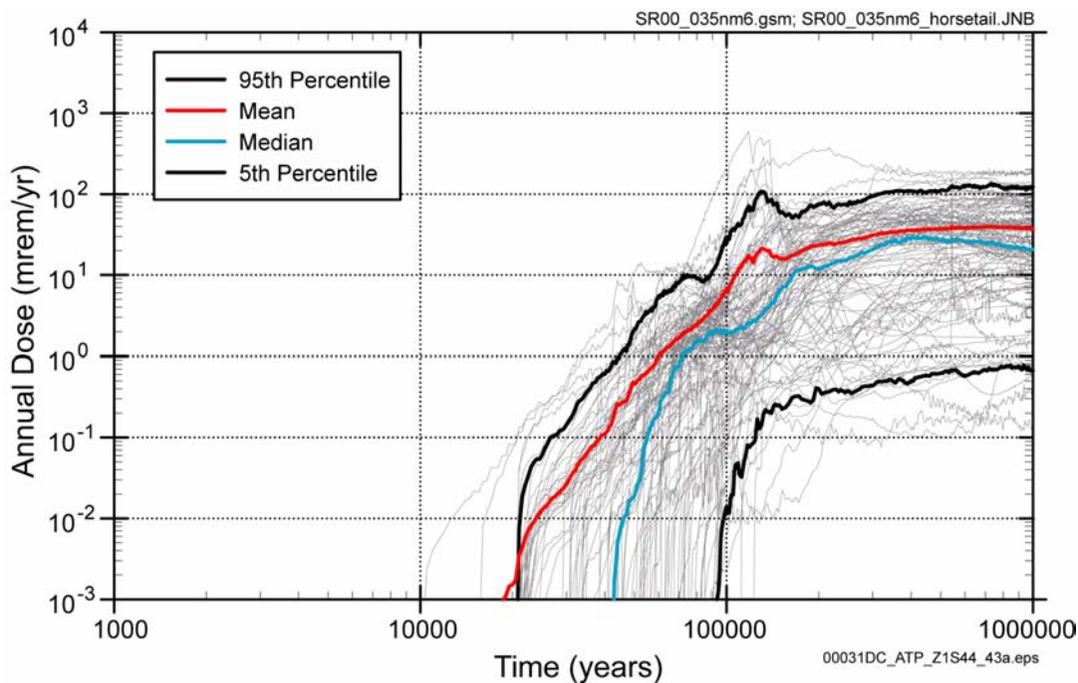
Figure 4-188. TSPA-SR Model Results for the Million-Year Annual Dose to a Receptor for the Nominal Scenario Using Nominal TSPA-SR Models and Revised Solubility Model

The figure displays the results for each simulation, as well as the 5th and 95th percentile, and the mean and median of these simulations to better determine the effects of uncertainty on the projected doses. Source: Modified from CRWMS M&O 2000a, Figure 4.1-21 (all realizations included).

The results of the TSPA-SR model mean peak dose performance assessments using a more representative long-term climate model and the revised secondary-phase solubility model (CRWMS M&O 2000a, Section 4.1.3) are illustrated in Figure 4-189. The peak dose to the receptor for this plot is about 100 mrem/yr. This current estimate for the peak dose value is about a third of the average annual background dose currently experienced in Amargosa Valley (DOE 1999a, Table 3-28).

The revised supplemental TSPA model calculations of peak mean annual dose to the reasonably maximally exposed individual after 10,000 years can be found in Section 6 of *Total System Performance Assessment—Analyses for Disposal of Commercial and DOE Waste Inventories at Yucca Mountain—Input to Environmental Impact Statement and Site Suitability Evaluation* (Williams 2001a). As shown in Figure 4-190, the peak mean annual dose over the first 100,000 years after closure for the nominal scenario is 1.2×10^{-1} mrem/yr for the higher-temperature operating

mode and 8.5×10^{-2} mrem/yr for the lower-temperature operating mode (Williams 2001a, Table 6-1). The peak mean annual dose over the first million years after closure for the nominal scenario is 152 mrem/yr for the higher-temperature operating mode and 122 mrem/yr for the lower-temperature operating mode (Williams 2001a, Figure 6-3 and Table 6-1). Note that calculated doses for the nominal scenario would be reduced by approximately one-third using an annual water demand of 3,000 acre-ft, consistent with NRC regulations (Williams 2001b, Section 6.3). The DOE also included the results of this analysis (peak dose after 10,000 years) in the final EIS.

4.4.2.5 Summary of Nominal Scenario Performance Assessment Results

This section has described three measures (individual protection, groundwater protection, and peak dose) for evaluating the performance of the Yucca Mountain repository system. These analyses have been conducted to 100,000 years to evaluate
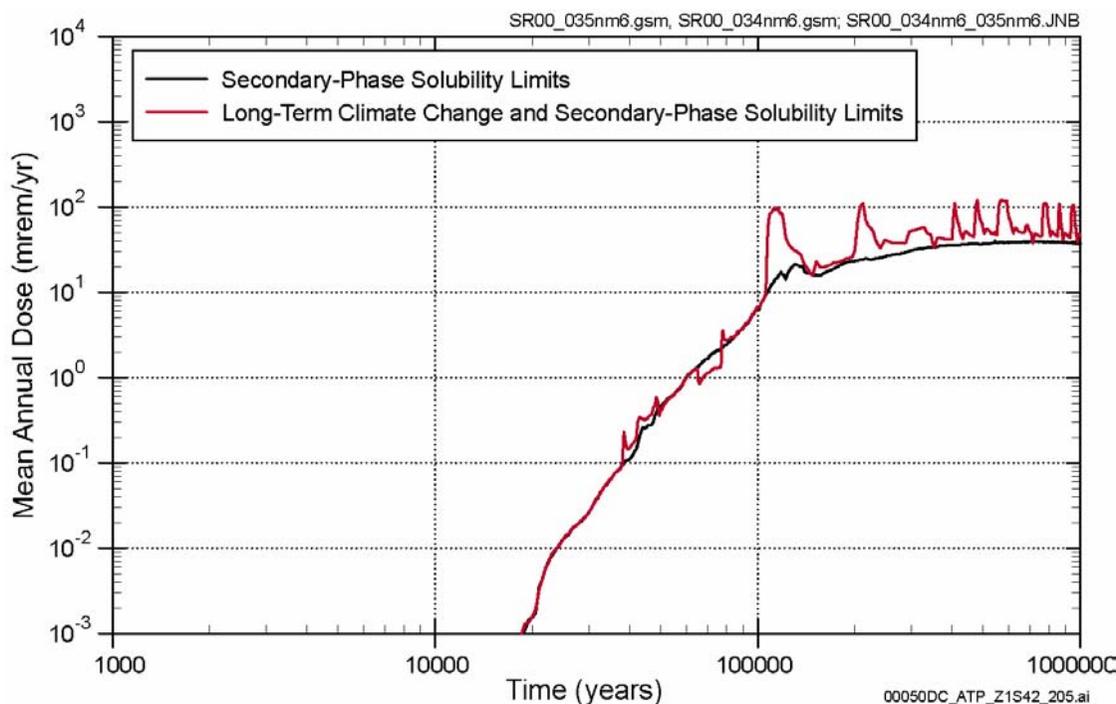
Figure 4-189. TSPA-SR Model Results for Million-Year Annual Dose to a Receptor for the Nominal Scenario Using Nominal TSPA-SR Models and Revised Solubility and Climate Models
Source: Modified from CRWMS M&O 2000a, Figure 4.1-21.

SR00_042nm6.gsm; SE01_006nm6.gsm; SE01_007nm6.gsm; SE01_001im5.gsm;
SE01_002im5.gsm; SR_EIS_Igneous_Mean_Dose.JNB
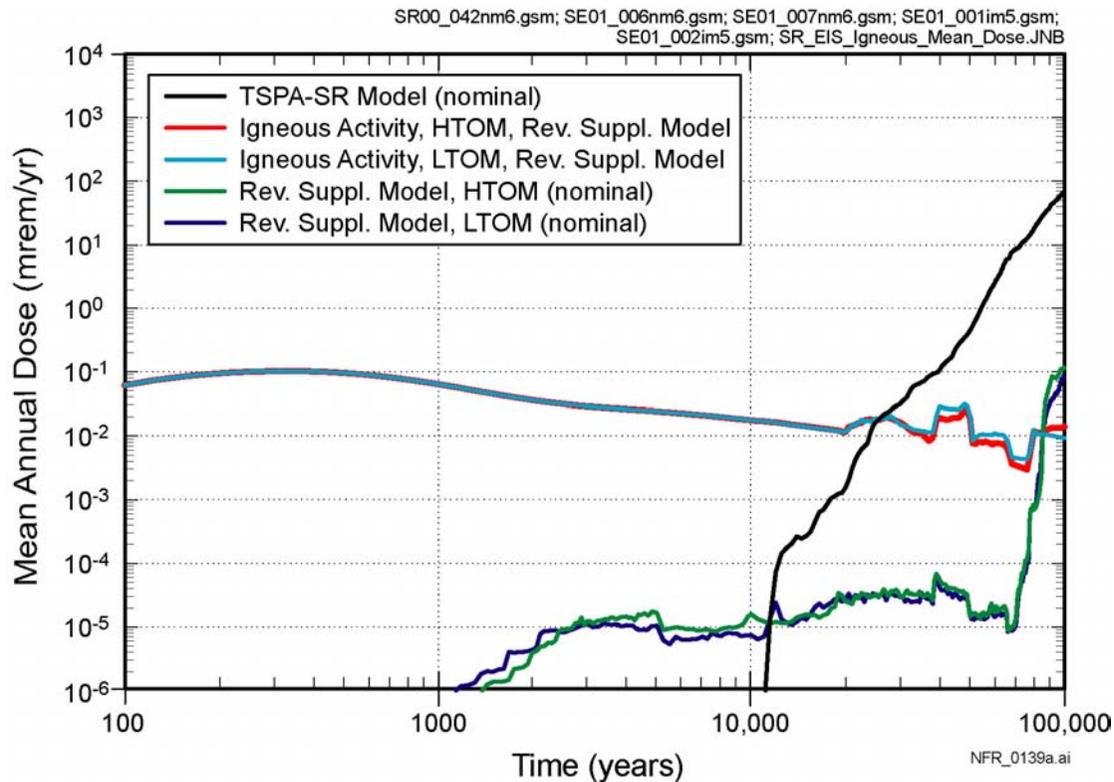
Figure 4-190. 100,000-Year Annual Dose Histories: TSPA-SR Model and Revised Supplemental TSPA Model (Nominal Scenarios) and Revised Supplemental TSPA Model (Igneous Activity)

Mean annual dose histories are shown for the TSPA-SR model and the revised supplemental TSPA model for the nominal scenarios, along with the probability-weighted mean annual dose history for the igneous activity disruptive scenario for the revised supplemental TSPA model for both the higher-temperature operating mode (HTOM) and the lower-temperature operating mode (LTOM). The results from the TSPA-SR model are documented in *Total System Performance Assessment for the Site Recommendation* (CRWMS M&O 2000b). The results from the revised supplemental TSPA model are documented in the *Total System Performance Assessment—Analyses for Disposal of Commercial and DOE Waste Inventories at Yucca Mountain—Input to Final Environmental Impact Statement and Site Suitability Evaluation* (Williams 2001a). Source: Williams 2001a, Figure 6-16.

the robustness of the repository performance beyond 10,000 years. In addition, peak dose analyses required in the EIS have also been presented in *Total System Performance Assessment—Analyses for Disposal of Commercial and DOE Waste Inventories at Yucca Mountain—Input to Final Environmental Impact Statement and Site Suitability Evaluation* (Williams 2001a). The peak mean annual dose calculated by the revised supplemental TSPA model for 100,000 years after closure is 1.2×10^{-1} mrem/yr for the higher-temperature operating mode and 8.5×10^{-2} mrem/yr for the lower-temperature operating mode (Williams 2001a, Table 6-1). The peak mean annual dose over 1 million years calculated by the revised supplemental TSPA model is 152 mrem/yr for the

higher-temperature operating mode and occurs at 476,000 years. The peak mean annual dose for 1 million years for the lower-temperature operating mode is 122 mrem/yr and also occurs at 476,000 years. Calculated values of dose for the groundwater-pathway-dominated scenarios, such as the nominal scenario, would be reduced by approximately one-third using an annual water demand of 3,000 acre-ft, consistent with NRC regulations (Williams 2001b).

The next two sections, Sections 4.4.3 and 4.4.4, describe other analyses for assessing the performance of the repository system, namely, disruptive events scenario performance and human intrusion scenario performance. Section 4.4.5 provides a

discussion of the sensitivity of the projected repository performance to the uncertainties in the component models described in Section 4.2.

4.4.3   Total System Performance for the Disruptive Scenario

As described in Section 4.4.1.3, volcanic activity has been identified as the only disruptive event that has the potential to affect disposal system performance during the first 10,000 years. Other disruptive FEPs, such as seismic perturbations of the water table and nuclear criticality, were analyzed and found either to be unsupported by scientific evidence or to have probabilities less than 1 in 10,000 in 10,000 years. As a result, these disruptive FEPs were not incorporated into the TSPA models through the formal FEPs screening procedure (BSC 2001t; CRWMS M&O 2000f, Table 2-2; see also Section 4.3 of this report). Potential seismic effects on the underground facilities and waste packages were screened out (i.e., excluded from consideration) because the waste packages would not be adversely damaged by design basis rockfalls or vibratory ground motion (CRWMS M&O 2000ex, Section 6.2). However, because vibratory ground motion from seismic events might damage the commercial spent nuclear fuel cladding, the effect of this potential damage to cladding by a discrete seismic event is included in the TSPA model in the nominal scenario. The frequency assumed for this event is 1.1×10^{-6} per year. For this analysis, when the vibratory ground motion event occurs, all commercial spent nuclear fuel cladding in the repository is assumed to fail by perforation, and further cladding degradation is calculated according to the cladding degradation.

The disruptive scenario considers two distinct types of volcanic activity: (1) eruptive volcanism at the repository location and (2) igneous intrusion (or magmatic flooding) of some of the emplacement drifts in the repository. *Disruptive Events Process Model Report* (CRWMS M&O 2000f) documents the geological basis and data for these scenario conceptualizations. The disruptive scenario assumed that the eruptive event consisted of a magmatic penetration of the repository facility after permanent closure. The conceptualization of the eruptive event assumes that the magma flow intersects and destroys waste packages, bringing waste to the surface through one or more eruptive conduits. The igneous intrusion event assumes that a hypothetical igneous dike intersects drifts of the repository and that the associated waste packages are damaged, exposing the waste within to percolating water. In the eruptive event, the TSPA models analyzed the atmospheric transport of radionuclides bound in the particles of volcanic ash that were then dispersed downwind and ultimately deposited on the ground at the receptor location. In the igneous intrusion event, the TSPA models accounted for the additional waste package failures and analyzed the transport of radionuclides through the groundwater pathway to the location of the receptor (average member of the critical group for the TSPA-SR and supplemental TSPA models and the reasonably maximally exposed individual for the revised supplemental TSPA model).

A probabilistic volcanic hazards assessment study (CRWMS M&O 1996b) focused on the task of examining available geologic data for the Yucca Mountain region and estimated the annual probability for the scenario of the repository footprint being intersected by a basaltic dike. A group of about 30 earth scientists from such organizations as the U.S. Geological Survey; the University of Nevada, Las Vegas; the Center for Nuclear Waste Regulatory Analyses; and Los Alamos National Laboratory contributed to this study. After this study, a formal elicitation of expert judgment was conducted in accordance with NRC guidance on elicitation procedures (Kotra et al. 1996). The expert panel used in the formal elicitation was composed of ten internationally recognized volcanism experts. The probability estimate obtained from the expert panel was 1.5×10^{-8} per year (or a probability of 1.5×10^{-4} of occurring over 10,000 years) (CRWMS M&O 1996b, Section 4.3). The probability estimate for the igneous intrusion event was subsequently recalculated based on a change in the configuration of the repository layout. The more recent probability estimate for the igneous intrusion event is 1.6×10^{-8} per year (CRWMS M&O 2000ez, Section 6.5.3.1). If a dike does intersect the repository, there is about a 77 percent chance that a volcano will form at the surface with magma flowing through a portion of the repository (the eruptive event) (CRWMS M&O 2000ez,

Section 7.1.3 and Table 13a). This translates to approximately 1 chance in 7,700 of a volcano forming above the repository during the first 10,000 years. The annualized probabilities for each of the disruptive events are just slightly greater than the probability cutoff of 10^{-8} per year. Therefore, both intrusive and eruptive events have been included in the TSPA model analyses of the disruptive scenario.

The following sections briefly summarize the two models. More details on the results of the TSPA-SR model can be found in the *Total System Performance Assessment for the Site Recommendation* (CRWMS M&O 2000a, Section 3.10.2). The results of the supplemental and revised supplemental TSPA models for the volcanic eruption and igneous intrusion models are summarized in Volume 2, Section 4.3 of *FY01 Supplemental Science and Performance Analyses* (BSC 2001b), *Total System Performance Assessment—Analyses for Disposal of Commercial and DOE Waste Inventories at Yucca Mountain—Input to Final Environmental Impact Statement and Site Suitability Evaluation* (Williams 2001a), and *Total*

System Performance Assessment Sensitivity Analyses for Final Nuclear Regulatory Commission Regulations (Williams 2001b).

4.4.3.1 Total System Performance Assessment Model for Volcanic Eruption

The TSPA model for the consequences of a volcanic eruption at Yucca Mountain is a simplification of the complex processes that could occur during an eruption. At a conceptual level, the overall model is straightforward (Figure 4-191): an igneous dike rises through the earth's crust and intersects one or more drifts in the repository. An eruptive conduit forms somewhere along the dike as it nears the land surface, feeding a volcano at the surface. Waste packages in the direct path of the conduit are sufficiently damaged that they provide no further protection, and the waste is available to be entrained in the eruption. Volcanic ash is contaminated, erupted, and transported by wind toward the receptor. Ash settles out of the plume as it is transported downwind, resulting in an ash layer on the land surface. Receptors (the average
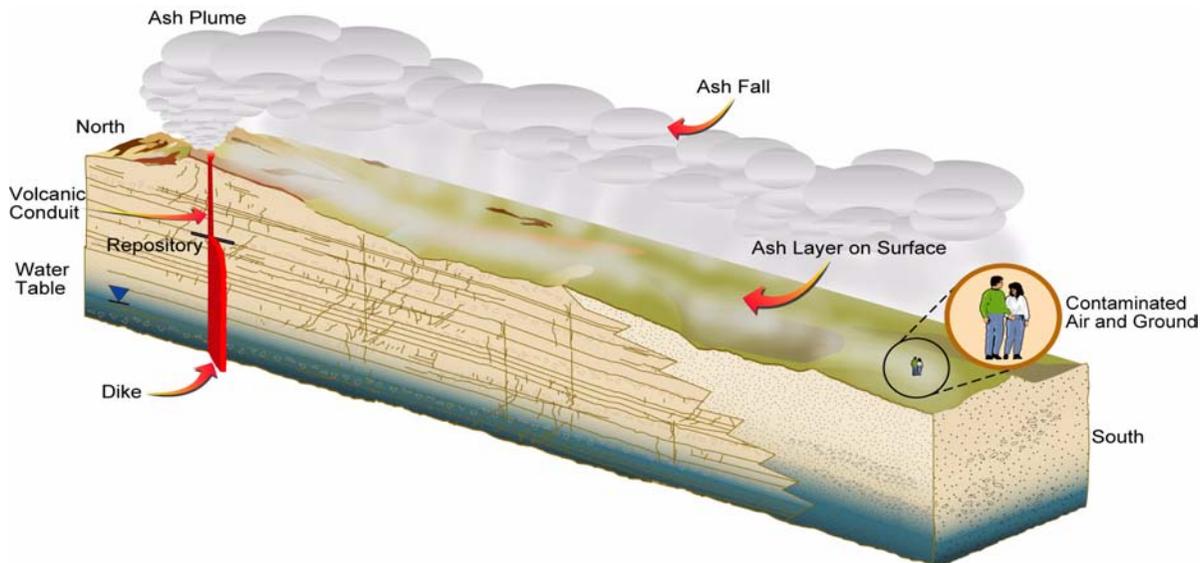
Figure 4-191. Schematic Representation of a Volcanic Eruption at Yucca Mountain, Showing Transport of Radioactive Waste in an Ash Plume

member of the critical group was the receptor used in the TSPA-SR model and supplemental TSPA models, while the reasonably maximally exposed individual was the receptor used in the revised supplemental TSPA model) could receive a radiation dose from various pathways associated with the contaminated ash layer.

This component model is implemented in the TSPA models through the selection of reasonable assumptions about many aspects of the event, the development of input parameter distributions characterizing important physical properties of the system, and the use of a computational model to calculate entrainment of the waste in the erupting ash and concentration of waste reaching the receptor.

Each intrusive event (i.e., a swarm of one or more dikes) is assumed to generate one or more volcanoes somewhere along its length, but eruptions need not occur within the repository footprint. In the TSPA-SR model (CRWMS M&O 2000a), approximately 36 percent of intrusive events that intersect the repository are associated with one or more (up to a maximum of five) eruptions within the footprint. Characteristics of the eruption, such as eruptive power, style (violent versus normal), velocity, duration, column height, and total volume of erupted material, are included in the analysis.

The number of waste packages damaged by an eruptive event is determined by the diameter of the eruptive conduit. Conduit diameter is a sampled parameter in the TSPA-SR calculation. Analogue sites were evaluated in *Characterize Eruptive Processes at Yucca Mountain, Nevada* (CRWMS M&O 2000fa, Section 6.1), and the distribution for conduit diameter was identified as log normal, with a minimum value equal to dike width, with a median value of 50 m (164 ft) and a maximum value of 150 m (490 ft). As a conservative assumption, *Number of Waste Packages Hit by Igneous Intrusion* (CRWMS M&O 2000fi) defined the minimum conduit diameter for the TSPA-SR calculation as 15 m (49 ft). For the purposes of the TSPA-SR model, the contents of all packages that are fully or partially damaged by an eruption (i.e., that lie partly or entirely within the circumference of the conduit) are assumed to be fully available for

entrainment in the eruption. Waste packages, drip shields, cladding, and all other components of the engineered barrier system are assumed to be so damaged that they provide no further protection for the waste. This assumption provides a conservative bound to the possible behavior of the engineered barriers in the eruptive environment.

The physical properties of the waste in the eruptive environment are estimated based on the assumption that the waste form is directly exposed to the eruption, which is consistent with the assumption that the waste packages provide no protection.

The volcanic eruption and subsequent transport of radioactive material in the ash plume are modeled using a parametric characterization of the properties of the eruption to calculate a source term of ash for atmospheric transport. The quantity of ash deposited at any specified point is a function of the wind speed and direction, the volume of ash erupted (which determines the duration and height of the eruption), and the ash particle diameter. The ash particle diameter distribution used in the TSPA-SR model is based on observations from violent eruptions at modern analogue volcanoes and is defined as a log triangular distribution with a minimum value of 0.01 mm (0.00039 in.), a mode value of 0.1 mm (0.0039 in.), and a maximum value of 1 mm (0.039 in.) (CRWMS M&O 2000fa, Section 6.5.1). Waste particles are entrained in the eruption based on the ratio between their diameter and the diameter of the ash particles. In the TSPA-SR, it is assumed that waste particles one half the diameter of the ash or smaller are incorporated into the ash particles and transported downwind.

Projections of future wind conditions at Yucca Mountain are based on the speed and direction data sampled from distributions developed from past observations in the region. As with most weather data, short-term variability is relatively high, covering a broad range of uncertainty appropriate for the analysis of relatively brief volcanic events. Although speed and direction are reported as paired data for each observation at each elevation, the two parameters are sampled independently in the TSPA-SR model, allowing for a full coverage of wind speeds in each direction. Speeds range

from 0 to approximately 2,000 cm/s (0 to 65.6 ft/s), with a median speed of approximately 650 cm/s (21.3 ft/s). Direction is variable, consistent with the observed data, but the decision to treat direction and speed as uncorrelated parameters allows flexibility in the TSPA to consider cases in which the wind direction is fixed toward a specific location in all realizations, rather than allowed to vary. For the TSPA-SR model, results are calculated assuming wind blows to the south in all realizations. This assumption is unrealistic but provides a conservative bound to uncertainty regarding wind direction and compensates for uncertainty regarding the possibility that contaminated ash deposited by winds blowing in directions other than south might later be redistributed to the location of the receptor.

More recent analyses of igneous activity can be found in Volume 2, Sections 4.3 and 5.2 of *FY01 Supplemental Science and Performance Analyses* (BSC 2001b), *Total System Performance Assessment—Analyses for Disposal of Commercial and DOE Waste Inventories at Yucca Mountain—Input to Final Environmental Impact Statement and Site Suitability Evaluation* (Williams 2001a), and *Total System Performance Assessment Sensitivity Analyses for Final Nuclear Regulatory Commission Regulations* (Williams 2001b). These analyses assessed the impact of higher wind speeds and larger waste particles. Using a median wind speed of 1,000 cm/sec (393.7 in./sec), the probability-weighted annual doses for the supplemental TSPA model were increased by a factor of 2. Performance is relatively insensitive to uncertainty in waste package diameter within the range considered in the supplemental TSPA model analysis (BSC 2001b, Section 3.3.1.2).

4.4.3.2 Total System Performance Assessment Model for Groundwater Transport of Radionuclides Following Igneous Intrusion

The TSPA models for radionuclide release and transport away from packages damaged by an igneous intrusion that intersects the repository is similar to the nominal model for radionuclide release and transport but modified to include the intrusion (Figure 4-192). Because flow and transport occur in the same units modeled for nominal

performance, there is no separate set of computational models used in the TSPA to simulate the consequences of intrusion (CRWMS M&O 2000a, Section 3.10.2.3). Instead, the igneous intrusion groundwater transport model consists of a set of input parameters used to define a modified source term for calculations using the flow and transport models developed for the nominal case. There are three main components to the model: the behavior of waste packages and other elements of the engineered barrier system that have been damaged because of their nearness to an igneous intrusion; groundwater flow and radionuclide transport away from the waste packages; and calculation of the number of waste packages that are damaged.

The behavior of a waste package in the intrusive environment is bounded by the conservative assumption that packages close to the point of intrusion are so damaged that they provide no further protection for the waste. As in the case for the eruptive environment, actual conditions are uncertain, and damage is likely to range from moderate to extensive. Abstracted models for seepage, radionuclide mobilization, and transport are used in place of a separate set of detailed source term, flow, and transport models for the conditions in the drift following intrusion. Possible effects of uncertainty regarding conditions in the drift following intrusion are incorporated in the TSPA models through the assumption that all waste in the most severely damaged packages is immediately available for transport in the unsaturated zone, depending on solubility limits and the availability of water. The thermal, chemical, and mechanical effects of the intrusion that might tend to limit water seepage into the drift, at least temporarily, are neglected. No credit is taken for water diversion by pyroclastic debris, chilled lava, or the remnants of the drip shield or waste package, and cladding is assumed to be fully degraded.

For repository design alternatives that include backfill, damage within a drift is limited to the three packages on either side of the intrusion. Backfill pushed up by displaced waste packages and debris from damaged drip shields will stop magmatic material as it moves away from the dike, and the drift is assumed to be plugged relatively close to the intrusion. Pressure will increase in the
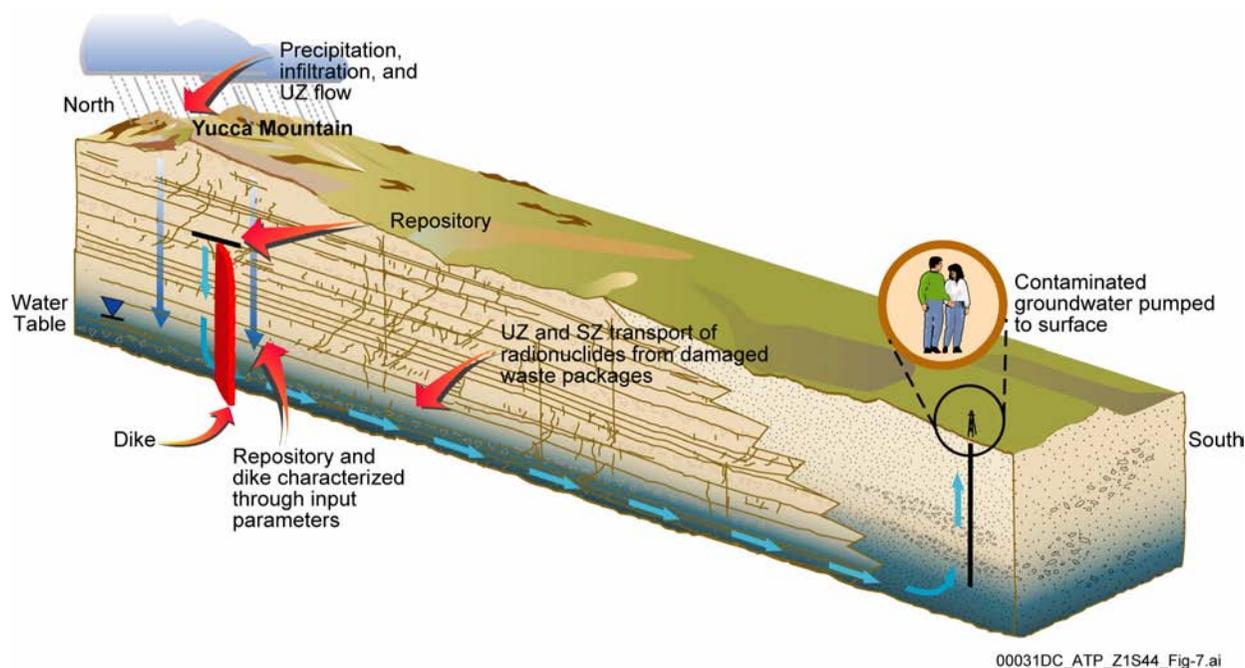
Figure 4-192. Schematic Diagram Showing an Igneous Intrusion at Yucca Mountain and Subsequent Transport of Radionuclides in Groundwater
UZ = unsaturated zone; SZ = saturated zone.

isolated section of the drift to the lithostatic pressure of the magma, further damaging the waste packages, and the dike will continue to propagate upward. Damage in the affected region will be severe, but it will be relatively minor further down the drift, behind the plug of backfill and debris.

For repository design alternatives that do not include backfill, damage within the drift will be much more extensive. Actual conditions are uncertain, but the pressure wave following decompression of the magma appears likely to propagate the full length of the affected drift. Immediate mechanical damage from the displacement of waste packages will be limited to the region around the point of intrusion, as in the backfill case, but damage to the drip shield and ground support will occur throughout the drift. More importantly, debris from the remains of the engineered barrier system may not be sufficient to create a plug within the emplacement drifts. Pyroclastic material (or liquid lava, in the case of extremely dry magma) could fill up to the entire length of the drift, and pressure could rise from atmospheric toward litho-

static before the dike can continue to propagate upward. The combination of high temperature (approximately 1,040° to 1,170°C [1,904° to 2,138°F]) and high pressure (approaching the magmatic lithostatic pressure of 7.5 MPa at the repository depth) could cause partial failure of the lid welds on affected packages. Therefore, for the no-backfill design, the TSPA-SR assumes that three packages on either side of the point of intrusion fail completely and that all other packages in drifts intersected by intrusive dikes are breached by cracks sufficient to allow pressure to equalize within the packages. Drip shields and cladding are assumed to fail completely in all drifts intersected by the intrusion. The number of drifts intersected is calculated probabilistically, based on the drift spacing and distributions for the azimuth and length of intrusive events.

4.4.3.3 Results and Interpretation

The approach taken in the TSPA models to calculating doses resulting from igneous disruption of the repository is consistent with the probabilistic

methodology described in Section 4.4.1.[2] Scenario consequences are multiplied ("weighted") by the probability of the occurrence of the scenario to yield an appropriate estimate of the overall risk posed by low probability events.

Figure 4-193 shows a range of probability-weighted dose histories representing possible doses to a reasonably maximally exposed individual following disruption of the potential Yucca Mountain repository by igneous activity. Results do not include doses that might result from the nominal performance of the repository in the absence of igneous activity. These doses are discussed in Section 4.4.1. Results shown in Figures 4-193a and 4-193b are based on an analysis of 5,000 individual calculations, or realizations, using different sets of sampled values for uncertain input parameters in the model. Rather than showing the full set of 5,000 realizations included in the analysis, which would result in a display too dense to interpret, the figure shows 500 individual curves (in gray) that represent every tenth realization. The range of results shown by these individual curves displays the uncertainty in the calculated dose history that results from uncertainty in model parameter values.

Four additional curves, shown in color, provide summary information about the distribution of results from the full set of 5,000 realizations. The mean curve, shown in red, is the average probability-weighted annual dose rate. The percentile curves, shown for the 95th, 50th (i.e., median), and 5th percentile, show the annual dose rate that is greater than 95 percent (or 50 percent or 5 percent) of the calculated values at that time. The mean curve on Figure 4-193a lies above the 95th percentile curve throughout the interval between approximately 3,000 and 8,000 years because the mean is dominated by the relatively small fraction of the total number of realizations that contribute to a high groundwater dose rate at early times. The number of realizations contributing to this pathway increases through time as the cumulative proba-

bility of an intrusion having occurred increases, causing the 95th percentile curve to climb above the mean at later times.

Figure 4-194 shows the mean probability-weighted dose histories for the individual radionuclides that contributed to the total igneous dose rates shown in Figure 4-193a. These individual radionuclide doses are discussed in more detail in the following paragraphs in the context of the discussion of the mean total igneous dose history.

For approximately the first 2,000 years, the dose history is a smooth curve that is dominated by the effects of a volcanic eruption. As shown in Figure 4-193a, the probability-weighted mean total effective dose equivalent during this period reaches a peak of approximately 0.004 mrem/yr roughly 300 years after repository closure and then drops off due to radioactive decay of the relatively shorter-lived radionuclides that contribute to doses from the ash fall exposure pathway. As shown in Figure 4-194, the major contributors to the eruptive dose are americium-241 and plutonium-240, -239, and -238. Strontium-90 is a significant contributor at extremely early times, but drops off rapidly because of radioactive decay. Inhalation of resuspended particulates in the ash layer is the primary exposure pathway during this period and the smooth decline of the mean dose curve from approximately 300 to 2,000 years results from decay of americium-241, which has a half-life of 432 years.

From approximately 2,000 years after closure onward, the mean igneous dose is dominated by groundwater releases from packages damaged by igneous intrusion. The irregular shape of the curve from this point forward reflects the occurrence of intrusive events at random times, rather than the prescribed intervals used for the extrusive simulations. Close examination of Figures 4-193a and 4-193b shows that individual realizations display distinct peaks occurring at times that are controlled by the sampled time of intrusion and the time

---

[2]   See Section 4.4.1 of *Issue Resolution Status Report Key Technical Issue: Total System Performance Assessment and Integration* (NRC 2000c), where the NRC describes the method for weighting consequences of individual scenarios by their probability before summing the scenario consequences to determine the overall expected annual dose. See also Reamer (1999, Section 3.4) for a discussion of the NRC's implementation of this approach for igneous activity.
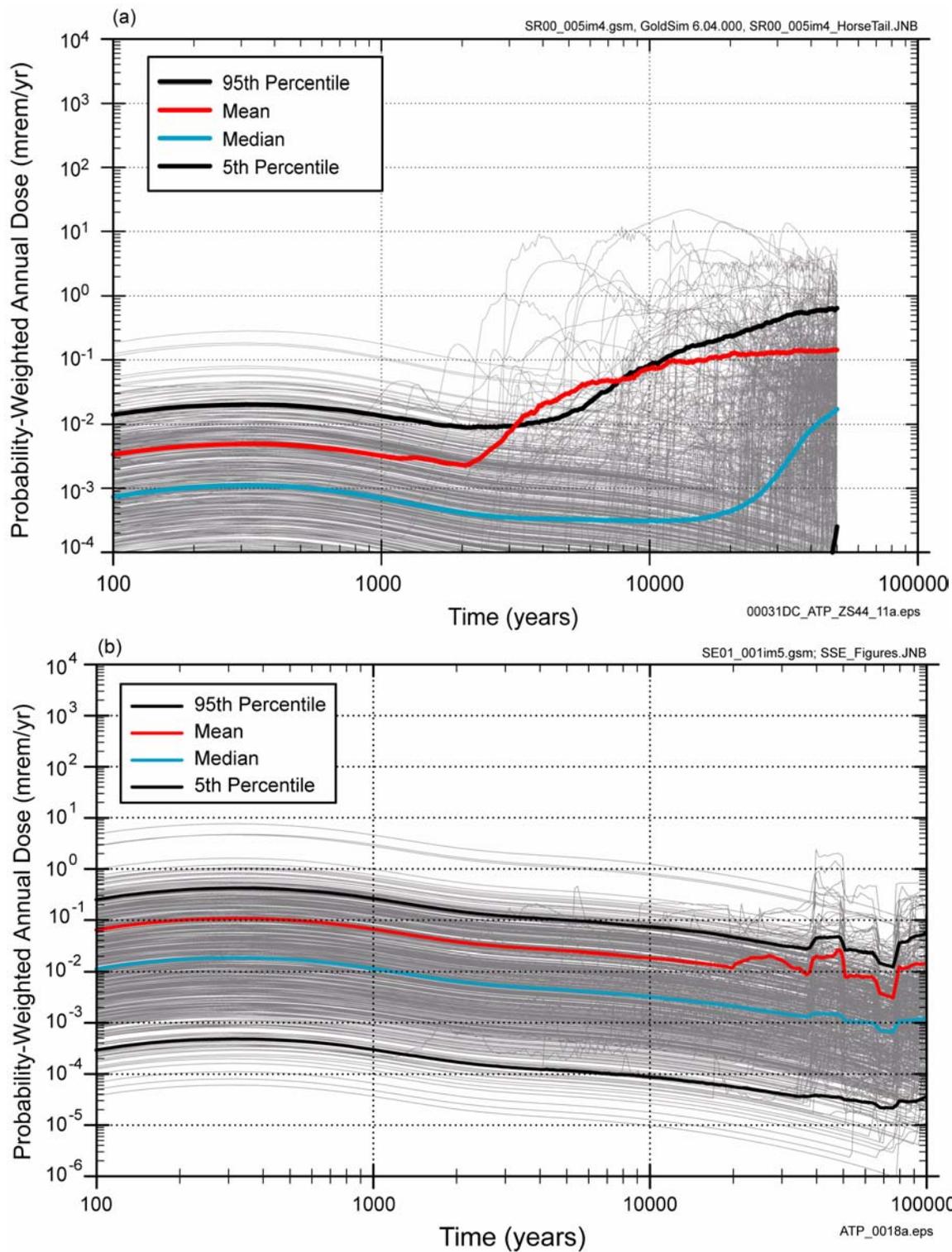
Figure 4-193. TSPA-SR Model and Revised Supplemental TSPA Models Results of Annual Dose to a Receptor for Igneous Activity Scenario

(a) Doses projected by the TSPA-SR model. (b) Doses projected by the revised supplemental TSPA model. Source: CRWMS M&O 2000a, Figure 4.2-1; Williams 2001a, Figure 6-10a.
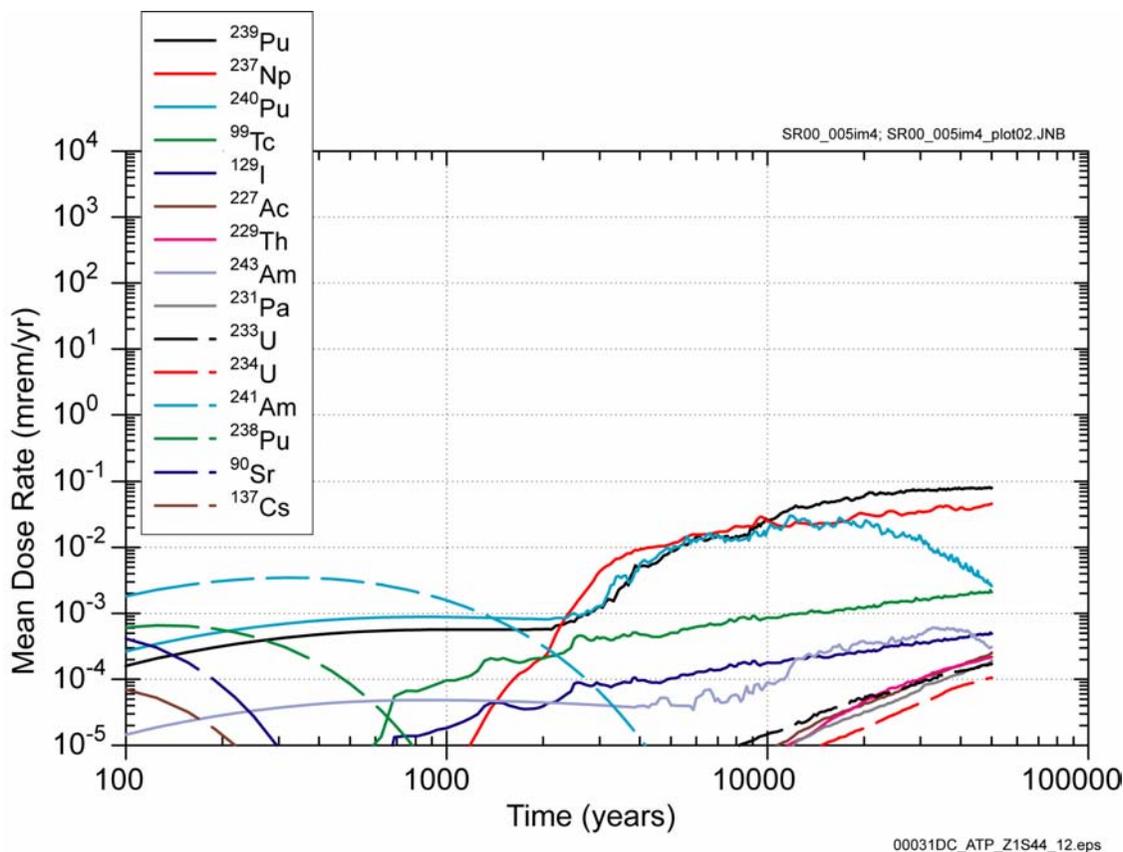
Figure 4-194. Igneous Dose Histories for Major Contributing Radionuclides Projected by the TSPA-SR Model
Source: CRWMS M&O 2000a, Figure 4.2-2.

required for radionuclide transport through the geologic system. The intrusive event may occur at any time, and the first appearance of groundwater doses in the mean curve at approximately 2,000 years reflects retardation during transport rather than the absence of intrusions at earlier times. The observation that some of the 500 individual curves continue to be dominated by the smooth, eruptive doses for essentially all of the 50,000-year period indicates either that, for those realizations, the sampled time of intrusion was relatively late or that, in some cases, retardation in the geologic system was effective for a relatively long period of time.

The overall probability-weighted mean igneous dose rate projected by the TSPA-SR model reaches a peak during the first 10,000 years of approximately 0.08 mrem/yr, occurring at 10,000 years. At later times, the calculated mean igneous dose rate is higher, increasing slowly to approach 0.2

mrem/yr at the end of the 50,000-year period. This peak mean igneous dose is dominated entirely by the groundwater releases following igneous intrusion. As shown in Figure 4-194, plutonium-239 and neptunium-237 are the primary contributors to the peak mean dose.

The probability-weighted dose histories projected for the disruptive scenario by the TSPA-SR model and the revised supplemental TSPA model are shown in Figure 4-195. The time histories are associated with a random occurrence of the disruptive events in the compliance period.

TSPA results for the volcanic disruptive scenario based on the TSPA-SR model, the supplemental TSPA model, and the revised supplemental TSPA model are summarized as follows:

- The TSPA-SR model projected a probability-weighted peak mean annual dose for the first
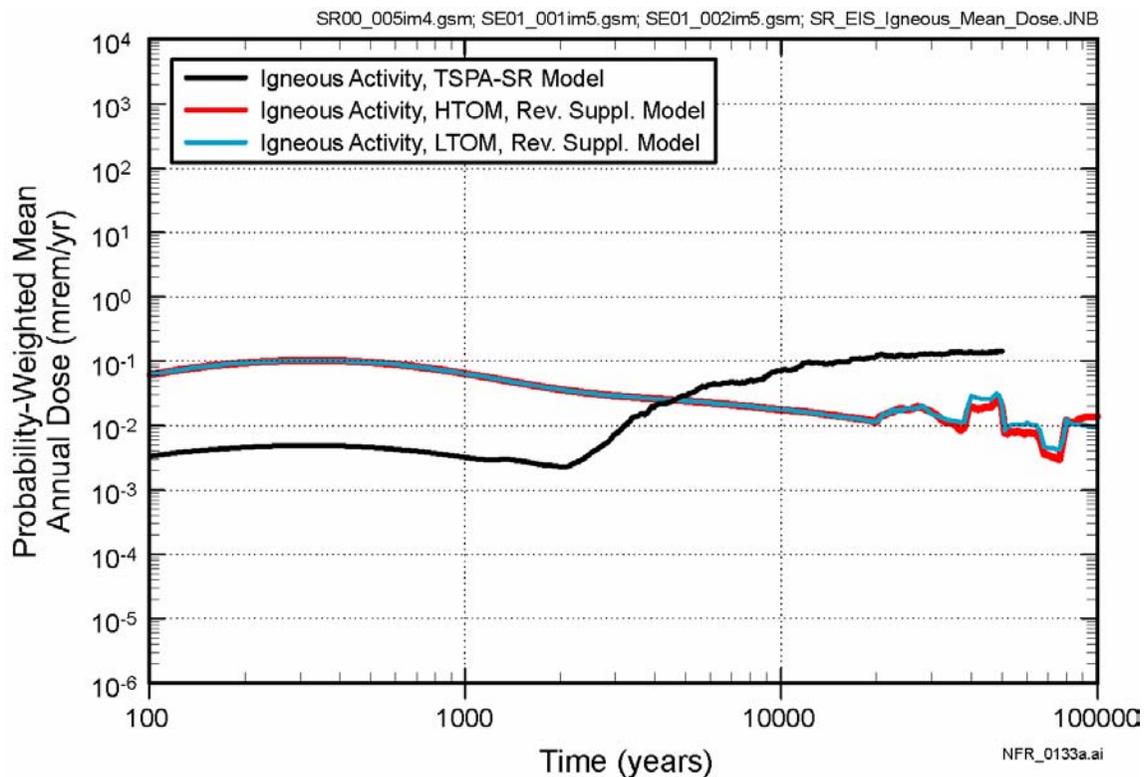
Figure 4-195. Projected Annual Doses for the Igneous Activity Disruptive Scenario
Probability-weighted mean annual dose histories are shown for the TSPA-SR model for the igneous activity scenario documented in *Total System Performance Assessment for the Site Recommendation* (CRWMS M&O 2000a). These results are presented along with revised supplemental TSPA model results for both higher-temperature operating mode (HTOM) and lower-temperature operating mode (LTOM), as documented in *Total System Performance Assessment—Analyses for Disposal of Commercial and DOE Waste Inventories at Yucca Mountain—Input to Final Environmental Impact Statement and Site Suitability Evaluation* (Williams 2001a). Source: Williams 2001a, Figure 6-10c.

10,000 years of approximately 0.08 mrem/yr (occurring at 10,000 years) for the combined volcanic disruptive scenario (CRWMS M&O 2000a, Section 4.2.2). The dose history is dominated by the effects of volcanic eruption for about the first 2,000 years. After about 2,000 years, doses from volcanism are dominated by releases to the groundwater from waste packages damaged by igneous intrusion events. At that time, the projected doses from eruptive events gradually diminish due to the decay of the radioactive waste inventory in the repository (CRWMS M&O 2000a, Section 4.2.2).

- Model and parameter changes for the supplemental TSPA model for the volcanic

disruption scenario class are described in Volume 1, Sections 13 and 14 of *FY01 Supplemental Science and Performance Analyses* (BSC 2001a). Updated scientific information considered in the supplemental TSPA model increases the probability-weighted peak mean annual dose during the first 10,000 years to approximately 0.1 mrem/yr, which occurs about 300 years after closure (BSC 2001b, Section 4.3.1).

- The revised supplemental TSPA model was used to project probability-weighted peak mean annual dose to the reasonably maximally exposed individual. The probability-weighted peak mean annual dose projected for the combined volcanic disruption

scenario (igneous intrusion and volcanic eruption) during the first 10,000 years using this model showed no change from the results projected using the supplemental TSPA model. Results were 0.1 mrem/yr for both the higher- and lower-temperature operating modes (Williams 2001a, Table 6-1).

Both the supplemental and revised TSPA models show the probability-weighted peak mean annual dose occurring approximately 300 years after closure and being dominated by doses from eruptive events for more than 10,000 years (BSC 2001b, Section 4.3.1; Williams 2001a, Figures 6-10b and 6-11b). The largest single contributor to the increase in the projected dose (compared to dose projected by the TSPA-SR model) comes from changes in biosphere dose conversion factors. Other factors include a change in wind speed, an increase in the conditional probability of an eruption at the repository location (from 0.36 to 0.77), and an increase in the total number of eruptive conduits possible within the repository (BSC 2001b, Section 4.3.1).

In the supplemental and revised supplemental TSPA models, after 10,000 years doses to the receptor (i.e., average member of the critical group for the supplemental TSPA models and reasonably maximally exposed individual for the revised supplemental TSPA model) following igneous intrusion are lower than the TSPA-SR model results, generally by a factor of five or more, with the TSPA-SR model peak mean dose from igneous intrusion occurring between 40,000 and 50,000 years after closure (BSC 2001b, Section 4.3.1; Williams 2001a, Figure 6-10c). Decreases in the probability-weighted annual dose from igneous intrusion are due to changes in the nominal scenario models for radionuclide mobilization and transport (BSC 2001b, Section 4.3.1). The distributions used to characterize uncertainty in the number of waste packages affected by igneous intrusion were modified, resulting in a larger number of packages damaged for the supplemental TSPA analyses conducted (BSC 2001a, Section 14.3.3.7; Williams 2001a, Section 6.1). This increase, however, is more than offset by decreases in radionuclide mobilization and transport (see Figure 4-195) (BSC 2001b, Section 4.3.1).

Results from revised supplemental TSPA model analyses also show that thermal operating conditions have no effect on the doses from the eruptive case. Higher- and lower-temperature operating mode curves overlay each other until releases (resulting from igneous intrusion) begin to cause noticeable divergence after about 20,000 years, when mean annual dose for the lower-temperature operating mode becomes greater than the dose from the higher-temperature operating mode by up to a factor of 3 (BSC 2001b, Section 4.3.1; Williams 2001a, Figure 6-10c).

These interpretations of the performance results for the disruptive scenario are valid for the wide range of quantifiable uncertainties that were considered in TSPA models. The TSPA results for the disruptive scenario are presented in more detail and fully documented in *Total System Performance Assessment for the Site Recommendation* (CRWMS M&O 2000a, Section 4.2), Volume 2, Section 3.3.1 of *FY01 Supplemental Science and Performance Analyses* (BSC 2001b), and *Total System Performance Assessment—Analyses for Disposal of Commercial and DOE Waste Inventories at Yucca Mountain—Input to Final Environmental Impact Statement and Site Suitability Evaluation* (Williams 2001a, Section 6.3).

4.4.3.4 Combined Releases from the Nominal and Disruptive Scenarios

To combine the expected annual doses from the nominal and disruptive scenarios, the dose for each scenario was weighted by the scenario probability, so the summed expected annual dose includes both consequence and probability and, therefore, represents the expected risk for the repository. The DOE calculated the annual dose to the reasonably maximally exposed individual as a result of releases from the Yucca Mountain disposal system (considering nominal and disruptive scenarios) that are projected to occur during the first 10,000 years, consistent with EPA and NRC regulations for individual protection (see 40 CFR Part 197 and 10 CFR Part 63 [66 FR 55732]).

The revised supplemental TSPA model calculations supporting the evaluation of individual protection were performed within a probabilistic

framework combining the most likely ranges of behavior for the various component models, processes, and corresponding parameters in the process models describing repository performance. The TSPA analyses evaluated both the nominal scenario (70,000 MTHM) and the disruptive scenario (igneous activity) under both the higher- and lower-temperature operating modes (Williams 2001a). The nominal scenario was analyzed by operating the revised supplemental TSPA model for 300 realizations, and the disruptive scenario was analyzed using 5,000 realizations (Williams 2001a, Sections 6.2.1 and 6.3).

The mean annual dose from the results of the model simulations using the revised supplemental TSPA model is presented in *Total System Performance Assessment—Analyses for Disposal of Commercial and DOE Waste Inventories at Yucca Mountain—Input to Final Environmental Impact Statement and Site Suitability Evaluation* (Williams 2001a, Figure 6-14). Table 4-37 summarizes the results of these simulations and shows the peak mean annual dose for the nominal and disruptive scenarios for both higher- and lower-temperature operating modes. Table 4-37 presents the peak 95th percentile dose for the multiple realizations for the same cases. These data provide confidence in the expected repository performance because 95 percent of the realizations yielded a peak dose that are less than the values shown on the table. For example, the 10,000-year peak 95th percentile value for the disruptive scenario (igneous-activity case), higher-temperature operating mode, is 4.1×10^{-1} mrem/yr, indicating that 4,750 of the 5,000 realizations for that case had a peak value less than 4.1×10^{-1} mrem/yr, and only 250 realizations resulted in a peak value higher than 4.1×10^{-1} mrem/yr. Further, examination of the plots presented in *Total System Performance Assessment—Analyses for Disposal of Commercial and DOE Waste Inventories at Yucca Mountain—Input to Final Environmental Impact Statement and Site Suitability Evaluation* (Williams 2001a, Figures 6-10a and 6-11a) shows that the peak annual dose for all realizations is less than 10 mrem/yr.

For purposes of individual protection (combined nominal and disruptive scenario), the revised

Table 4-37. Tabulated Peak Mean Annual Dose and Peak 95th Percentile Dose for the Nominal Case and the Disruptive (Igneous Activity) Case

Peak Mean Annual Dose		
	10,000-Year Peak	
Case	**Value (mrem/yr)**	**Year**
70,000 MTHM, HTOM	1.7×10^{-5}	4875
70,000 MTHM, LTOM	1.1×10^{-5}	3438
Igneous Activity, HTOM	1.0×10^{-1}	313
Igneous Activity, LTOM	1.0×10^{-1}	313
Peak 95th Percentile Annual Dose		
	10,000-Year Peak	
Case	**Value (mrem/yr)**	**Year**
70,000 MTHM, HTOM	1.2×10^{-4}	4938
70,000 MTHM, LTOM	8.6×10^{-5}	5000
Igneous Activity, HTOM	4.1×10^{-1}	313
Igneous Activity, LTOM	4.1×10^{-1}	313

NOTES: These data are based on the same probabilistic annual water usage model used in the TSPA-SR, and would be approximately 1/3 lower if 3,000 acre-feet/yr was used, consistent with NRC regulations model (not 3,000 acre-ft/yr).
HTOM = higher-temperature operating mode;
LTOM = lower-temperature operating mode.
Source: Williams 2001a, Table 6-1.

supplemental TSPA model calculated doses consistent with the final EPA rule at 40 CFR 197.21 as discussed in *Total System Performance Assessment—Analyses for Disposal of Commercial and DOE Waste Inventories at Yucca Mountain—Input to Final Environmental Impact Statement and Site Suitability Evaluation* (Williams 2001a). Dose is calculated to the reasonably maximally exposed individual, a hypothetical person, located at the point above the highest concentration of radionuclides in the simulated plume of contamination where the plume crosses the southernmost boundary of the controlled area (at a latitude of 36° 40' 13.6661" North) and reaches the accessible environment. This distance is approximately 18 km (11 mi) from the repository footprint, compared to the original distance of approximately 20 km (12 mi) used in the saturated zone transport modeling calculations supporting the TSPA-SR model and supplemental TSPA model analyses.

The revised supplemental TSPA model utilized a slice-of-the-plume method to calculate the dose to the reasonably maximally exposed individual based on an average annual water demand of 2,000 acre-ft of groundwater. Using this method, 100 percent of the released radionuclides reaching the accessible environment are contained in that groundwater volume which represents the amount of water that would be withdrawn and used annually by the reasonably maximally exposed individual. This method minimizes the effects of natural dilution processes that would occur along the flow path and bounds potential consequences. This volume of water was an average volume necessary to operate 15 to 25 farms, representing a range of groundwater volumes from 887 to 3,367 acre-ft, consistent with proposed 10 CFR 63.115 (64 FR 8640). In addition, the revised supplemental TSPA model, consistent with 40 CFR 197.21, used a daily average groundwater consumption of 2.0 L (0.53 gal), compared to the daily average groundwater consumption volume of 2.1 L (0.55 gal) in the earlier TSPA models.

The calculated peak mean annual doses over the first 10,000 years for the nominal scenario using the revised supplemental TSPA model are thousands of times smaller than the probability-weighted mean annual dose for the disruptive scenario. Therefore, the combined mean annual dose for comparison with individual protection standards as calculated by the revised supplemental TSPA model is approximated as the probability-weighted mean annual dose from the disruptive scenario, or 0.1 mrem/yr, during a 10,000-year period (Williams 2001a, Section 6.2 and Table 6-1). This is the calculated dose for both the higher- and lower-temperature operating modes, as shown in Figure 4-190.

It is noted that the final NRC individual protection standard specifies an annual water demand of 3,000 acre-ft (10 CFR 63.312(c) [66 FR 55732]). An average annual water demand of approximately 2,000 acre-ft was used in the TSPA-SR and supplemental and revised supplemental TSPA analyses. The TSPA analyses assumed that 100 percent of the released radionuclides reaching the accessible environment is contained in that groundwater volume for use and consumption. The TSPA mean

doses calculated for the evaluation of individual protection, therefore, represent conservative (higher) estimates. Doses from the groundwater-pathway-dominated scenarios would be reduced by about one-third using an annual water demand of 3,000 acre-ft. The effects on dose calculations of an annual water demand of 3,000 acre-ft are discussed further in *Total System Performance Assessment Sensitivity Analyses for Final Nuclear Regulatory Commission Regulations* (Williams 2001b, Section 6.3).

The TSPA results can be summarized as follows:

- Initial calculations for individual protection used the TSPA-SR model. The probability-weighted mean peak dose occurring within the first 10,000 years, as calculated by the TSPA-SR model was approximately 0.08 mrem/yr, resulting from the disruptive scenario (Figure 4-195). The nominal scenario showed no projected dose to a receptor in the 10,000-year period (CRWMS M&O 2000b, Section 4.2.2). Therefore, the combined nominal plus igneous activity dose over the 10,000-year period is 0.08 mrem/yr.

- The supplemental TSPA model results show the peak mean annual doses for both the higher- and lower-temperature operating modes over the 10,000-year period are approximately 0.1 mrem/yr, resulting from the disruptive scenario (BSC 2001b, Section 4.3).

- Results using the subsequent revised supplemental TSPA model were the same (Williams 2001a, Table 6-1). Because the calculated mean annual doses over the 10,000-year period for the nominal scenario (2×10^{-4} mrem/yr for the higher-temperature operating mode and 6×10^{-5} mrem/yr for the lower-temperature operating mode) are thousands of times smaller than the probability-weighted mean annual doses for the disruptive scenario, the combined mean annual doses, when rounded, are the same as the probability-weighted peak mean annual dose from the disruptive scenario (0.1 mrem/yr

during the first 10,000 years) (see Figure 4-190).

4.4.4 Assessment of Human Intrusion Scenario

4.4.4.1 Background

The stylized human intrusion scenario performed by the TSPA-SR model can be summarized as follows:

- The human intrusion occurs at 100 years after permanent repository closure, consistent with proposed NRC regulations.

- The intrusion results in a single, nearly vertical borehole that penetrates a waste package and extends down to the saturated zone.

- Current practices for resource exploration are used to establish properties (e.g., diameter of the borehole, composition of drilling fluids).

- The borehole is not adequately sealed to prevent infiltrating water, and natural degradation processes gradually modify the borehole.

- Only releases through the borehole to the saturated zone are considered; hazards to the drillers or to the public from material brought to the surface by the assumed intrusion are not included.

These features of the human intrusion scenario are illustrated conceptually in Figure 4-196, and key aspects and technical assumptions are given in Table 4-38.
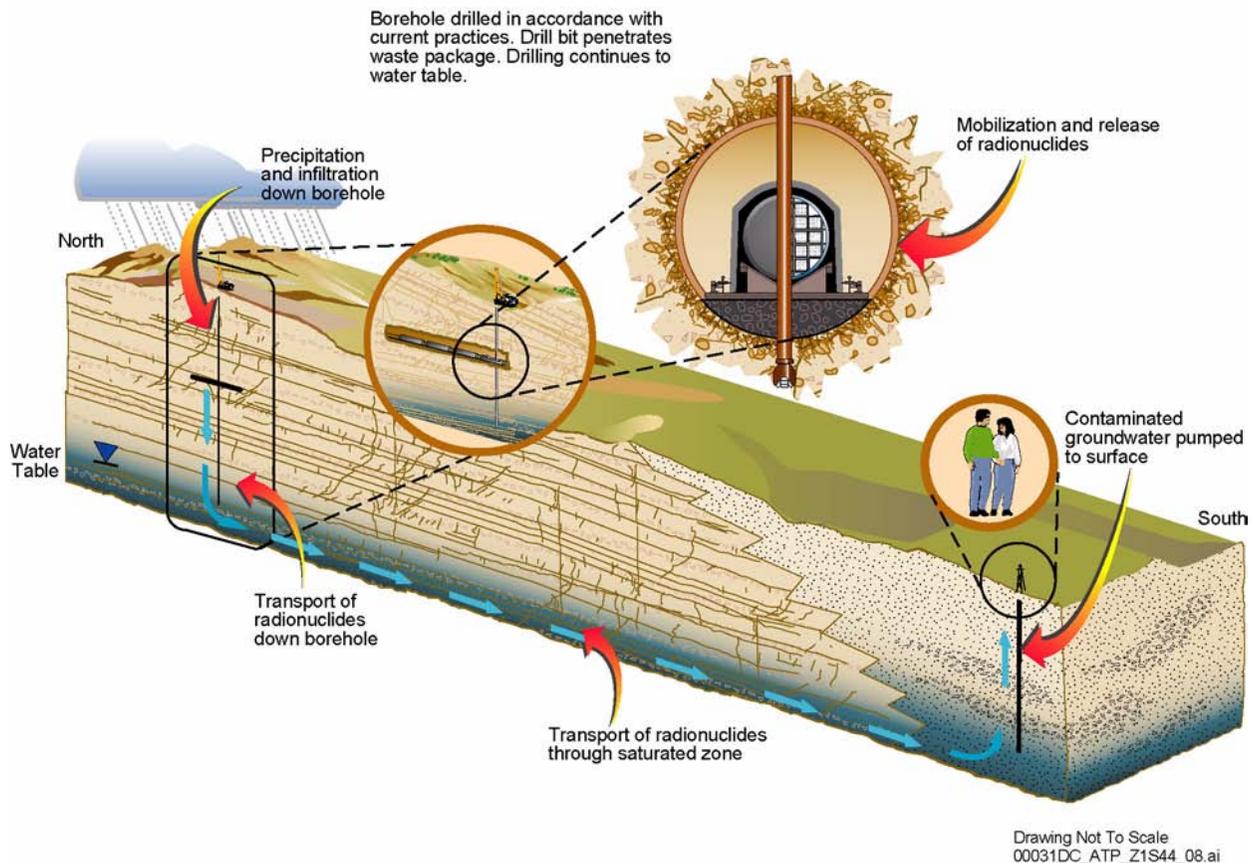
Figure 4-196. Conceptualization of Human Intrusion Scenario in the TSPA-SR Model

Table 4-38. Key Aspects and Technical Assumptions in the Human Intrusion Scenario in the TSPA-SR Model

Key Aspect	Associated Technical Assumptions
Infiltration of water down the borehole and into the penetrated waste package	Borehole diameter Flux into borehole based on infiltration, climate, catchment basin focusing Seepage through borehole into penetrated waste package
Mobilization and release of radionuclides from the penetrated waste package	Type of waste package penetrated Potential dissolved and colloidally transported radionuclide inventory Surface area and volume of waste exposed Waste form and cladding degradation Thermal and geochemical conditions in waste package Dissolution rates
Transport of radionuclides down the borehole to the water table	Borehole flow and transport properties including porosity and sorption Borehole length
Transport of radionuclides through the saturated zone	Borehole location Nominal case saturated zone flow and transport properties
Exposure pathways and dose calculation at the receptor location	Nominal case biosphere pathways and properties

For human intrusion in the supplemental and revised supplemental TSPA models, the DOE first determined the earliest time at which the waste packages would degrade sufficiently that a human intrusion could occur without recognition by the driller. Consistent with final NRC licensing-related regulations (10 CFR 63.321 [66 FR 55732]), the DOE estimated that this could not occur until about 30,000 years after closure. The DOE has also analyzed this human intrusion scenario and included the analysis in the final EIS. The results of a human intrusion at 30,000 years are also summarized below in Section 4.4.4.2.2.

4.4.4.2 Results

4.4.4.2.1 TSPA-SR Model Results

The 100-year human intrusion results were calculated probabilistically by the TSPA-SR model. Figure 4-197a shows the mean annual dose rate for 100,000 years resulting from a human intrusion 100 years after repository closure, together with the 95th, 50th (i.e., median), and 5th percentile curves from a set of 300 simulations. The peak mean total expected dose equivalent from human intrusion during the first 10,000 years is approximately 0.008 mrem/yr, and the peak mean total expected dose equivalent for the 100,000 year period of analysis is also approximately 0.008 mrem/yr. TSPA-SR human intrusion scenario performance assessment results are documented in

more detail in Section 4.4 of the *Total System Performance Assessment for the Site Recommendation* (CRWMS M&O 2000a).

Even though the human intrusion scenario was not evaluated to a million years, the doses would not be expected to be significantly greater than the doses out to 100,000 years because the sorbing, long half-life radionuclides that would start to contribute beyond 100,000 years are not significant contributors to dose. In addition, the million-year human intrusion doses would be less than the nominal case doses.

4.4.4.2.2 Revised Supplemental TSPA-SR Model Results

The first failure of the Alloy 22 waste package material due to general corrosion is projected to occur after approximately 30,000 years. The DOE has, therefore, determined that the earliest time a human intrusion could occur without recognition by a driller (intruder) is at least 30,000 years. This determination was based on analyses presented in Volume 1, Appendix A of *FY01 Supplemental Science and Performance Analyses* (BSC 2001a). Additional information supporting the timing of the human intrusion (at 30,000 years) is presented in *Total System Performance Assessment Sensitivity Analyses for Final Nuclear Regulatory Commission Regulations* (Williams 2001b). The compressive strength and ductility of the metals

from which the drip shields and waste packages are fabricated differ significantly from the rock that would surround them. Drillers (intruders) would notice these differences. For example, the drilling assembly would buckle and bend when the bit attempted to penetrate the titanium drip shield and waste package (drill bits that are designed for rock do not easily penetrate metal, particularly titanium). The drillers (intruders) should, therefore, recognize that they have attempted to drill into some material other than rock for at least as long as the drip shield or waste packages are intact. Analyses calculate a 95 percent probability that the waste packages will remain intact for about 30,000 years. Thus, the human intrusion is not expected to occur within the first 10,000 years.

The analysis of the human intrusion scenario at 30,000 years is presented in *Final Environmental Impact Statement for a Geologic Repository for the Disposal of Spent Nuclear Fuel and High-Level Radioactive Waste at Yucca Mountain, Nye County, Nevada* (DOE 2002) and *Total System Performance Assessment—Analyses for Disposal of Commercial and DOE Waste Inventories at Yucca Mountain—Input to Final Environmental Impact Statement and Site Suitability Evaluation* (Williams 2001a, Section 6.4). The human intrusion scenario at 30,000 years considers an "intruder" to be someone drilling a land-surface borehole using a drilling apparatus and the common techniques and practices that are currently employed in exploratory drilling for groundwater in the region around Yucca Mountain. In the scenario, the intruder drills directly through a degraded waste package and subsequently into the uppermost aquifer underlying the Yucca Mountain repository. The intrusion then causes the subsequent compromise and release to groundwater of the contaminated waste in the penetrated waste package.

Two human intrusion scenarios were simulated and discussed in *Total System Performance Assessment—Analyses for Disposal of Commercial and DOE Waste Inventories at Yucca Mountain—Input to Final Environmental Impact Statement and Site Suitability Evaluation* (Williams 2001a, Section 6.4). One intrusion occurs at 100 years after repository closure, and the other occurs at 30,000 years,

the earliest time after disposal that the waste package would degrade sufficiently that a human intrusion could occur without recognition by the drillers. The results of the revised supplemental TSPA model simulations for a human intrusion at 100 years after closure showed a peak mean dose of 0.0048 mrem/yr (at 875 years) over the 10,000-year period. This is similar to the dose projected by the TSPA-SR model (approximately 0.008 mrem/yr) for a 100-year human intrusion (Figure 4-197a). The revised supplemental TSPA model projected a peak mean annual dose over a million-year period of 2.3×10^{-3} mrem/yr for the 30,000-year human intrusion, as shown in Figure 4-197b. The peak mean dose occurs at 108,000 years (Williams 2001a).

The DOE conducted a sensitivity analysis to consider an unlikely event (igneous intrusion) in the evaluation of the human intrusion scenario and documented it in *Total System Performance Assessment Sensitivity Analyses for Final Nuclear Regulatory Commission Regulations* (Williams 2001b, Section 6.2). The report discusses the scenario of a human intrusion preceded by an unlikely igneous intrusion event with a mean annual probability of an igneous intrusion at the location of the repository of 1.6×10^{-8} (CRWMS M&O 2000a, Table 3.10-5). In the analysis, it was determined that the mean annual dose due to a human intrusion following an unlikely igneous intrusion can be approximated by multiplying the conditional dose of a human-intrusion event by the probability of the initiating igneous-intrusion event by the probability of the drillers not detecting the waste package (assumed to be equal to one if the drilling is preceded by an igneous intrusion event).

The conditional human intrusion dose would be a function of when the initiating igneous intrusion occurs. The worst case would be if the intrusion occurs immediately following the loss of institutional controls. This calculation was presented in *Total System Performance Assessment—Analyses for Disposal of Commercial and DOE Waste Inventories at Yucca Mountain—Input to Final Environmental Impact Statement and Site Suitability Evaluation* (Williams 2001a) for a human intrusion at 100 years, and the resultant maximum mean dose was 4.8×10^{-3} mrem/yr (Williams
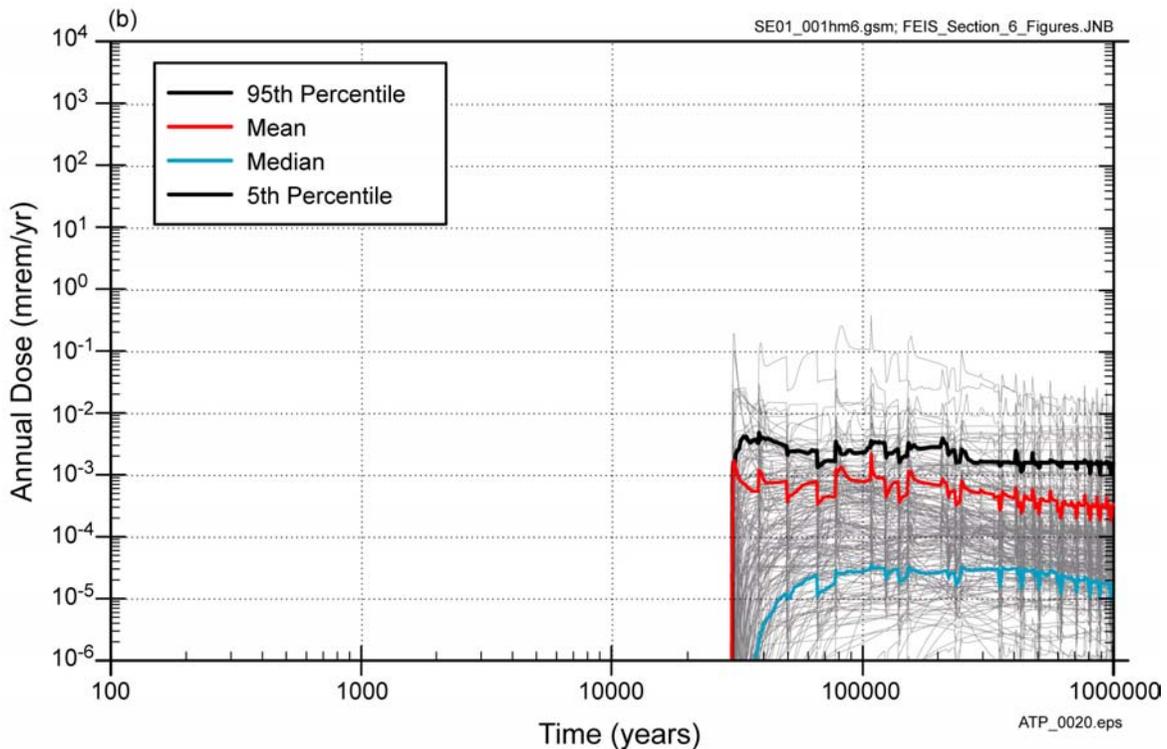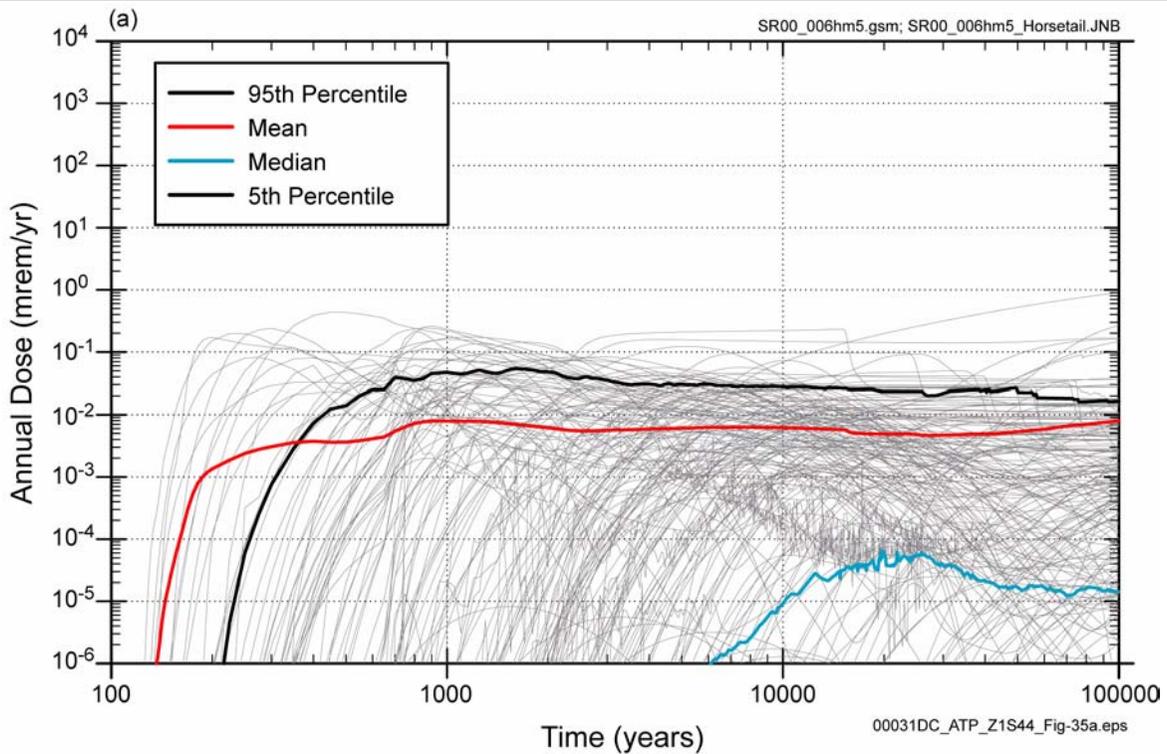
Figure 4-197. TSPA-SR Model and Revised Supplemental TSPA Results of Annual Dose to a Receptor for the Human Intrusion Scenario

(a) Human intrusion at 100 years projected by the TSPA-SR model. (b) Human intrusion at 30,000 years projected by the revised supplemental TSPA model. Source: CRWMS M&O 2000a, Figure 4.4-11; Williams 2001a, Figure 6-12.

2001a, Table 6-1). Considering the probability of the igneous initiating event occurring sometime in 30,000 years (4.8×10^{-4}), the earliest time after disposal that drillers would not recognize they had been penetrated a waste package, it was determined that the approximate maximum mean dose due to a human intrusion following an igneous intrusion would be the probability (4.8×10^{-4}) times the maximum mean dose (4.8×10^{-3} mrem/yr) or 2.3×10^{-6} mrem/yr. The maximum mean dose is much lower than the maximum mean dose due to the igneous intrusion alone of 4.3×10^{-4} mrem/yr (Williams 2001b, Section 6.2).

4.4.5 Sensitivity Analysis and Evaluation of Robustness of Repository Performance

The TSPA-SR model and supplemental TSPA model results for the nominal scenario are presented in Section 4.4.2, those for the disruptive events scenario are presented in Section 4.4.3, and those for the human intrusion scenario are presented in Section 4.4.4. These results illustrate a range of possible performance that is affected by the uncertainty in the individual component models and parameters used to describe the behavior of the system. An important goal of performance assessment is the clarification of the significance of these uncertainties on the overall performance of the potential repository. This section describes the sensitivity analyses conducted on these three scenarios. More details of these results and conclusions are included in *Total System Performance Assessment for the Site Recommendation* (CRWMS M&O 2000a, Sections 5.1 and 5.2) and Volume 2, Section 3 of *FY01 Supplemental Science and Performance Analyses* (BSC 2001b).

Two different approaches have been used to evaluate the contribution of the uncertainty of different component models and parameters to the uncertainty in the dose rate projected by the TSPA-SR model. The first method, called either "stochastic sensitivity analysis" or "uncertainty importance analysis," uses the full suite of results available from the Monte Carlo-type analyses presented for each of the three scenarios. In this method, various statistical techniques are used to determine which models and parameters most significantly affect the mean and the variance (or spread) of the dose

distribution. Other statistical techniques have been used to examine the models and parameters that most significantly affect the extremes (e.g., the top 10 percent) of the resulting dose distribution. These later analyses are informative because it is frequently the extremes (or tails) of the dose distributions that most affect the mean of the projected dose.

The second method, generally called "one-off sensitivity analysis," examines the effects of each component model or parameter on overall system performance. These analyses are conducted by fixing a particular model or parameter at either its expected value (generally the median or 50th percentile value) or a specified extreme value (e.g., either the 5th or 95th percentile value). In these analyses, all other models and parameters other than the fixed value are still sampled from the uncertainty distribution used in the base case analysis. These sensitivity analyses are used to display the effect of the change on the mean predicted dose (or other measures of the system or subsystem performance) as well as on the variance (or spread) of the predicted dose. By fixing a particular parameter that significantly affects the spread of the overall system performance results, especially if the effect is on the upper 5 to 10 percent of the projected dose consequences, it is possible to directly examine the significance that particular parameter has on the resulting performance of the system.

Both of the above sensitivity analysis methods have been used in evaluating the sensitivity of the projected dose of the Yucca Mountain repository system. Detailed discussion of a wide range of TSPA-SR sensitivity analyses are presented in the *Total System Performance Assessment for the Site Recommendation* (CRWMS M&O 2000a, Section 5). All analyses described in Volume 2, Section 3 of *FY01 Supplemental Science and Performance Analyses* (BSC 2001b) were conducted as one-off comparisons in which all models and input parameters are the same as those used in the TSPA-SR model except for the model or parameters being examined. Therefore, differences in performance measures between these results and those of the TSPA-SR base case provide insights into the importance of uncertainty in individual model

components. Details may be found in Volume 2, Section 3.2 of *FY01 Supplemental Science and Performance Analyses* (BSC 2001b). Sections 4.5.1, 4.5.2, 4.5.3, and 4.5.4 in this document report on TSPA-SR sensitivity analyses. Section 4.5.5 reports on supplemental sensitivity analyses reported in Volume 2 of *FY01 Supplemental Science and Performance Analyses* (BSC 2001b).

4.4.5.1   TSPA-SR Model Nominal Scenario Sensitivity Analysis

The nominal performance scenario includes the models and parameters (and their corresponding uncertainty) for all relevant FEPs as they are expected to evolve over time for the Yucca Mountain repository system. The nominal performance results indicate a broad uncertainty in the predicted dose for several tens of thousands of years. As time proceeds, there is a broad range of possible dose rates. The causes for the broad range in projected dose rates are described in this section, and addi-

tional discussion of intermediate results is presented in the *Total System Performance Assessment for the Site Recommendation* (CRWMS M&O 2000a, Sections 4.1, 5.1, 5.2, and 5.3).

Stochastic sensitivity analyses of the nominal performance scenario indicate that the dominant factors in the uncertainty of the projected dose rate (i.e., the variance of the predicted dose rates) vary with time from 40,000 to 100,000 years. Prior to about 40,000 years, there is an insufficient number of realizations with nonzero doses to perform representative stochastic sensitivity analyses. The temporal evolution of the importance is illustrated in Figure 4-198. The uncertainty importance factor is a measure of the importance of the uncertainty in the parameter as this uncertainty affects the uncertainty in the predicted dose; the higher the uncertainty importance factor, the more that parameter affects the distribution or spread in the projected doses.
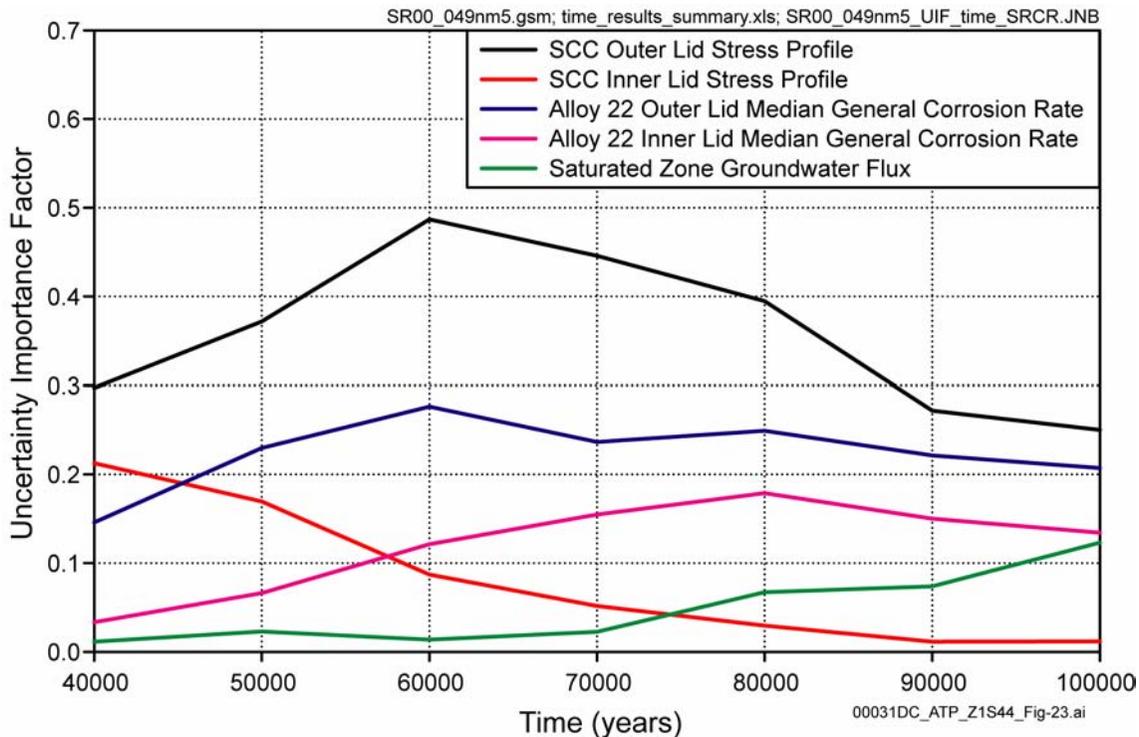
Figure 4-198. Summary of TSPA-SR Model Stochastic Sensitivity Analyses for Nominal Scenario—Parameters Affecting Dose Rate Uncertainty at Various Times

SCC = stress corrosion cracking. Source: CRWMS M&O 2000a, Figure 5.1-4.

The principal uncertainty importance factors determined from the regression analysis (ranked in their order of significance at 40,000 years) are:

- Uncertainty in the stress profile at the welds of the stress-mitigated outer Alloy 22 closure lids of the waste package that are subject to stress corrosion cracking

- Uncertainty in the stress profile at the welds of the stress-relieved inner Alloy 22 closure lids of the waste package that are subject to stress corrosion cracking

- Uncertainty in the median value of the general corrosion rate of Alloy 22 in the region of the outer Alloy 22 closure lid

- Uncertainty in the median value of the general corrosion rate of Alloy 22 in the region of the inner Alloy 22 closure lid

- Uncertainty in the groundwater flux in the saturated zone.

These five factors explain about two-thirds of the total variance of the dose results at 40,000 years.

In addition to examining the uncertainty importance factors as a function of the time at which a particular dose is projected to be received by the individual receptor (as is done in Figure 4-198), additional stochastic sensitivity analyses have been performed at four discrete dose levels (10, 1, 0.1, and 0.01 mrem/yr). The results of these uncertainty importance analyses are illustrated in Figure 4-199. These results confirm the results illustrated in Figure 4-198 in that it is the stress profile and corrosion rate of Alloy 22 that most significantly affects the degradation of the engineered barriers and determines the timing and magnitude of the distribution of doses projected to be received by the receptor.

The previous list illustrates the significant effect that uncertainty in the waste package corrosion rates and stress states at the closure welds could have on the time it takes for waste packages to breach and on the total amount of degradation of
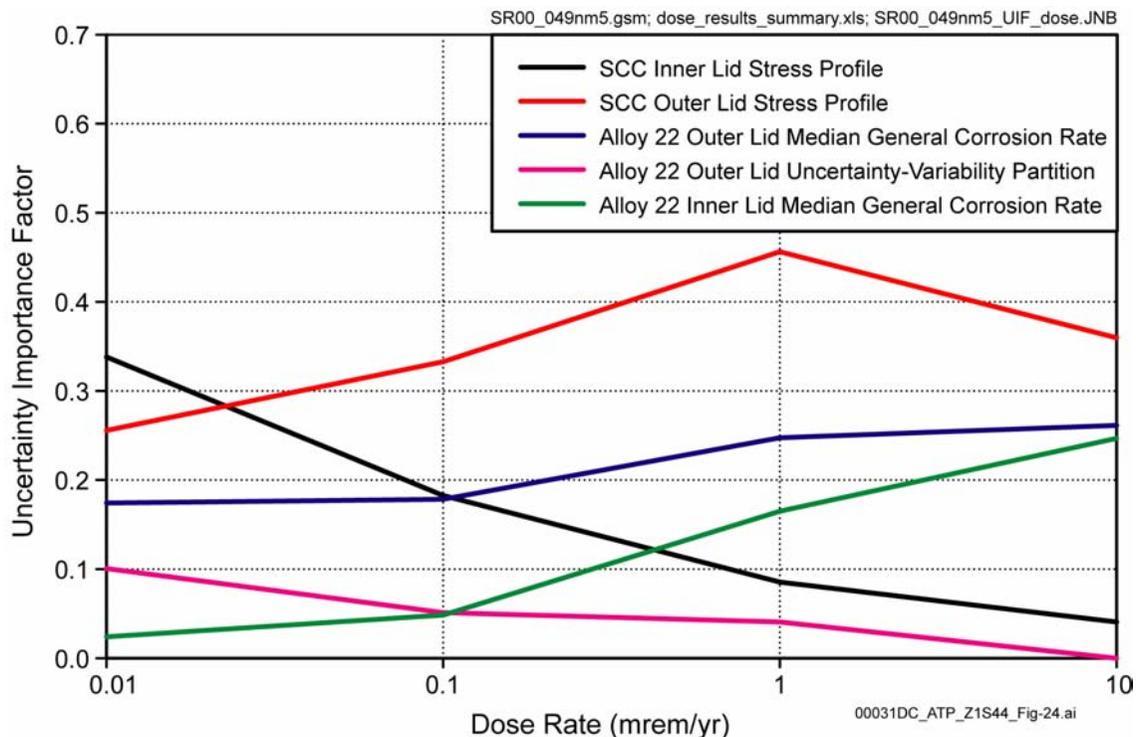
Figure 4-199. Summary of Stochastic TSPA-SR Model Sensitivity Analyses for Nominal Scenario— Parameters Affecting Uncertainty in Time of Dose Rate for Various Dose Rates
SCC = stress corrosion cracking. Source: CRWMS M&O 2000a, Figure 5.1-10.

the waste packages. Until the principal containment barrier of the waste packages is breached, there can be no release from the waste packages and therefore no doses. Therefore, the key parameters that affect the waste package degradation are also the key parameters that affect the total system dose.

The two natural system parameters determined to be most significant are the infiltration rate and the saturated zone advective flux (the former appears more prominent in the 1-million-year analyses described in Section 5.1 of the *Total System Performance Assessment for the Site Recommendation* [CRWMS M&O 2000a]). The infiltration scenario affects the advective transport time through the unsaturated zone (due to the effect on the percolation flux and the height of the water table) and the fraction of waste packages likely to encounter seeping conditions in the repository. The saturated zone groundwater advective flux affects the transport time of key radionuclides through the saturated zone (in particular, moderately sorbing radionuclides like neptunium-237) and the fraction of the total travel path that is in the alluvial aquifers.

In addition to the regression analysis that determines the most significant parameters affecting the variance of the projected dose rate versus time, classification and regression tree analyses have been performed to identify the key variables controlling the extreme realizations (e.g., the top 10 percent). These analyses confirm that the causes of early waste package failures and, therefore, the causes of doses are determined by a few waste package-specific parameters that affect the degradation rates (due both to corrosion and stress corrosion cracking) at the middle lid and outer lid closure welds (CRWMS M&O 2000a, Section 5.1).

4.4.5.1.1 TSPA-SR Model Sensitivity Studies for the Higher-Temperature Operating Mode

Using the factors identified as the most significant contributors to performance based on the stochastic sensitivity analyses described previously, one-off sensitivity analyses have been performed to illus-

trate the significance of these factors on the mean dose rate. These analyses are performed by fixing one or more models or parameters at their extreme values (5th and 95th percentiles) and then rerunning the calculations with all other models and parameters sampled from their "base case" distributions. In the following figures, comparisons of the one-off sensitivity analyses are made using the mean of the overall performance distribution. Additional analyses described in *Total System Performance Assessment for the Site Recommendation* (CRWMS M&O 2000a, Section 5.2) evaluate the variance reduction of the projected dose response from these one-off sensitivity analyses. As in the previous sections, these analyses have been conducted out to 100,000 years to gain insights into the system behavior.

Figure 4-200 illustrates the mean in the predicted dose rate when the stress state at both the inner and outer Alloy 22 closure welds is fixed at the 95th and 5th percentile values from the total uncertainty distribution described in Section 4.2.4. The results are compared to the base case results presented in Section 4.4.2. As expected, the timing of a particular mean dose is significantly affected by changes in the stress state. When the stress profile is fixed at the 95th percentile of the considered distribution, the fraction of the lid thickness that must be corroded before stress corrosion processes are initiated is significantly reduced, which significantly reduces the time required for a breach of the waste package at the lid closure welds. Conversely, when the stress profile is fixed at the 5th percentile, the fraction of the lid thickness that must be corroded before stress corrosion processes are initiated is increased significantly, which significantly delays the breach time of the waste package at the lid closure weld.

Figure 4-201 illustrates the mean in the predicted dose rate when the median value of the general corrosion rate for Alloy 22 for the region of both the outer and middle closure lids is fixed at the 95th and 5th percentile values. Again, as the corrosion rate is fixed at a high (e.g., the 95th percentile) value within the range of possible corrosion rates, the time for the mean waste package breach is reduced. Conversely, when the corrosion rate is fixed at a low (e.g., the 5th percentile) value within
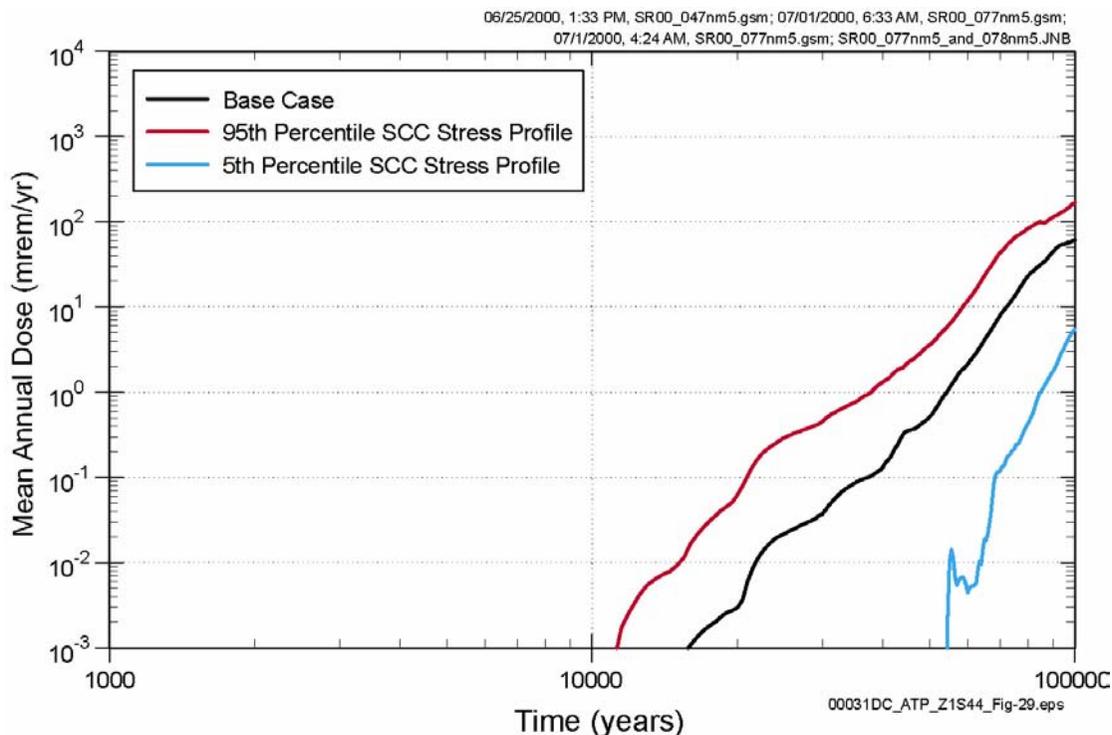
Figure 4-200. Sensitivity of the Mean Annual Dose Calculated by the TSPA-SR Model to Uncertainty in the Stress State at Closure Welds

SCC = stress corrosion cracking. Source: CRWMS M&O 2000a, Figure 5.2-3.

the range of possible corrosion rates, the time for the mean waste package breach is increased. This parameter significantly affects the rate of degradation of the waste packages and the variability in the waste package failures.

In separate barrier importance analyses discussed in Section 4.5.4, all of the important waste package degradation parameters described previously were fixed at their 5th and 95th percentiles. The barrier importance analysis results presented in Section 4.5.4 confirm the individual sensitivity analysis presented above.

Figure 4-202 illustrates the significance of fixing the infiltration rate at the low or high values of the distribution presented in Section 4.2.1. Again, the results are compared to the "base case" results described in Section 4.4.2. The significance of the parameter illustrated in this figure is less than that observed in the waste package degradation sensitivity analysis. The slight difference between the mean dose when the infiltration is fixed at its

maximum value and the mean dose when the infiltration is sampled illustrate that the mean dose response of the base case is already significantly affected by the maximum values of the infiltration rates. However, the 5th percentile infiltration rate has a significant effect on the predicted dose response. This result is primarily due to the effect of reduced seepage flux as the infiltration rate is reduced (CRWMS M&O 2000a, Section 5.2).

Figure 4-203 illustrates the significance of seepage to system performance. In this particular sensitivity analysis, the seepage flow focusing factor is fixed at the 95th or 5th percentile. At high ends of the flow focusing factor, more water is allowed to focus on the drifts and may potentially seep if the capillarity of the fractures is insufficient to keep the water in the rock. As expected, seepage has a minimal significance until such times that the dose is dominated by solubility-limited releases (i.e., greater than about 50,000 years) because the more soluble radionuclides, such as technetium-99, can more readily diffuse through the engineered
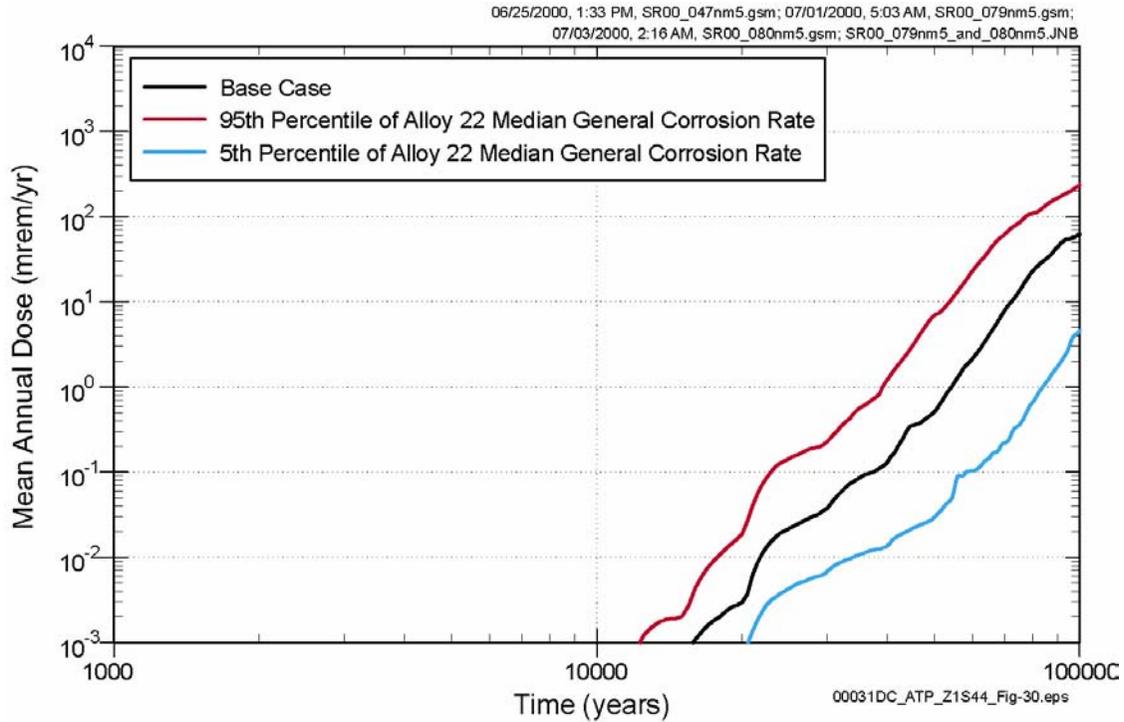
Figure 4-201. Sensitivity of the Mean Annual Dose Calculated by the TSPA-SR Model to Uncertainty in the Median General Corrosion Rate of Alloy 22

Source: CRWMS M&O 2000a, Figure 5.2-9.
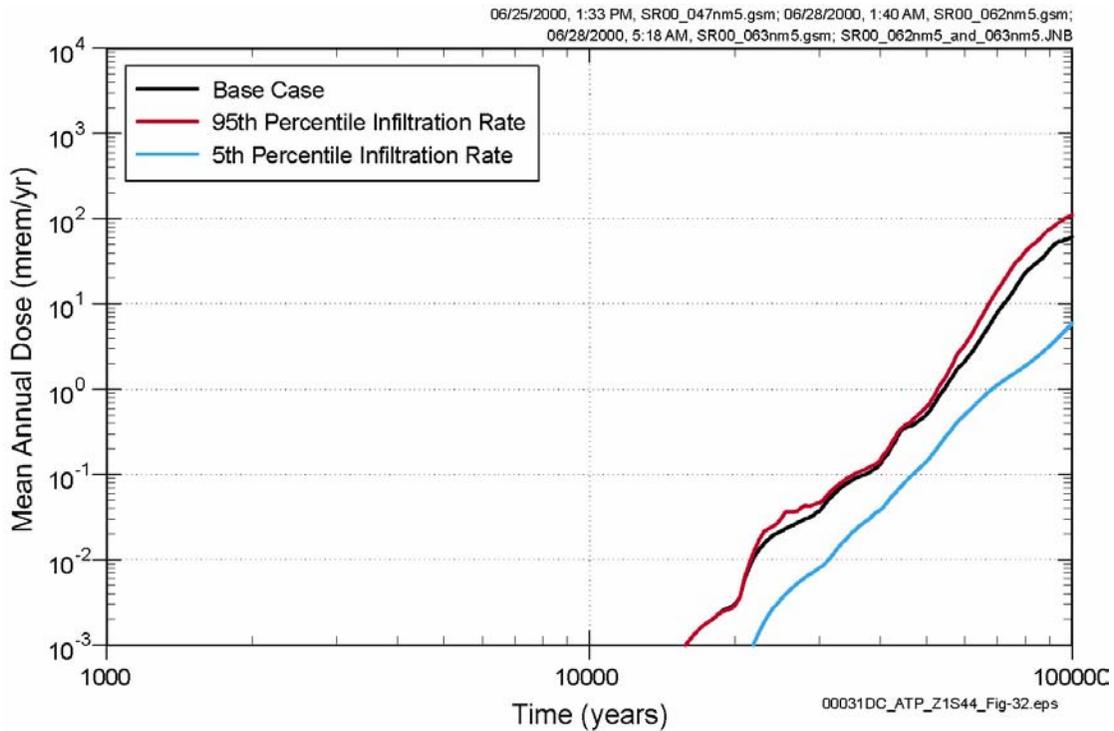
Figure 4-202. Sensitivity of the Mean Annual Dose Calculated by the TSPA-SR Model to Uncertainty in Infiltration Rate

Source: Modified from CRWMS M&O 2000a, Figure 5.2-1.
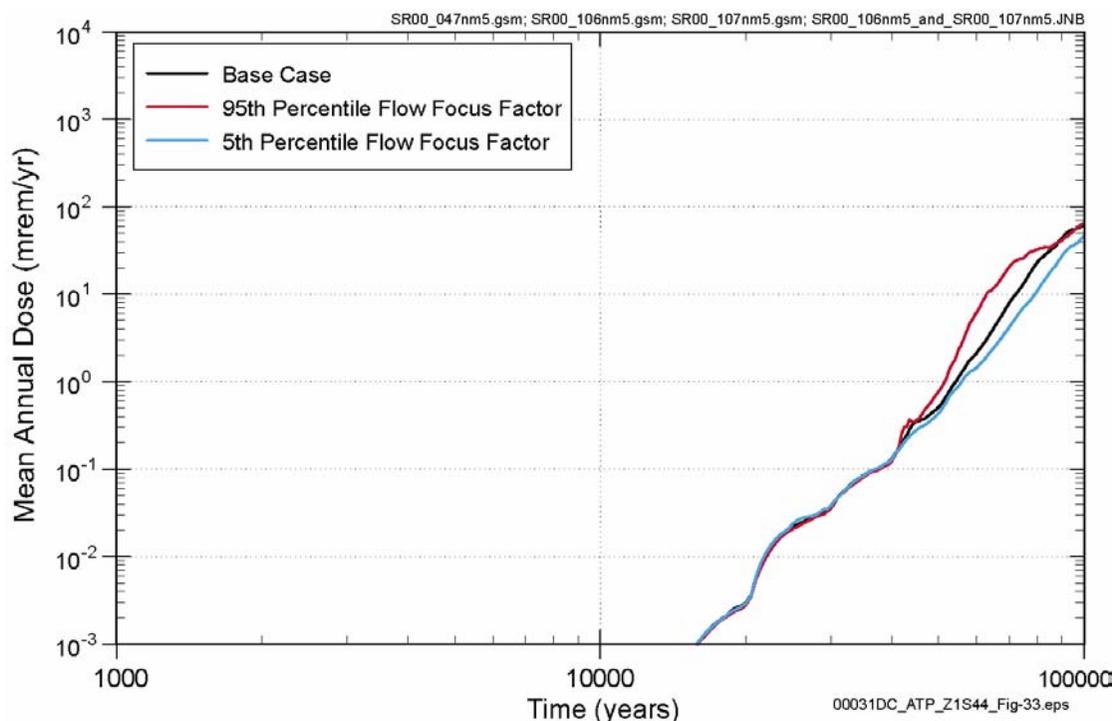
Figure 4-203. Sensitivity of the Mean Annual Dose Calculated by the TSPA-SR Model to Uncertainty in the Seepage Rate
Source: CRWMS M&O 2000a, Figure 5.2-2a.

barriers once they have been breached. In addition, seepage will only be significant when an advective pathway through the drip shields and waste packages is created, which requires a significant fraction of both the drip shields and waste packages to have been degraded.

The above discussion illustrates the significance of some of the most important parameters affecting the projected dose rate for the nominal performance scenario. Other parameters and models that are uncertain and for which sensitivity analyses have been performed are presented in Section 5.2 of the *Total System Performance Assessment for the Site Recommendation* (CRWMS M&O 2000a). The barrier importance analyses presented in Sections 4.5.3 and 4.5.4, in which the variables affecting several process model factors are varied simultaneously, identify additional parameters of potential significance to overall system performance.

4.4.5.1.2 TSPA-SR Model Sensitivity Studies for Alternative Design Features and Lower-Temperature Operating Modes

This section describes analyses that have been performed to address alternative operating modes that could result in lower temperatures. Specifically, these modes would not allow temperatures above the boiling point of water to occur in the host rock.

The sensitivity studies for the lower-temperature operating mode described in this section were undertaken using the process and TSPA models described in this section. Section 2.1 contains descriptions of other lower-temperature operating modes. Design studies were used to develop an understanding of the environmental conditions associated with these operating modes. Enhancements were made to the performance assessment models to conduct the performance assessment and sensitivity evaluations of the additional lower-

temperature operating modes. These enhancements incorporate the results of efforts to quantify uncertainties and extend the applicable range of the process models (BSC 2001a; BSC 2001b). Of particular interest are enhancements that address the performance-related responses of the design and operating mode, considering temperature-sensitive parameters and coupled thermal-mechanical-chemical-hydrologic processes. This approach is intended to ensure that the performance evaluations appropriately consider the potentially detrimental and potentially beneficial aspects of the repository's performance over a range of operating modes encompassing above- and below-boiling conditions.

Sensitivity analyses were also performed to assess the performance-related impacts of the potential addition of backfill. In theory, backfill could have several desirable attributes, such as limiting the potential effect of rockfall and providing a well-

controlled thermal-hydrologic-chemical environment in which the rest of the engineered barriers reside. Backfill also has a potential benefit of reducing the humidity on the waste package surface for several thousand years after closure, delaying the onset of the aqueous corrosion processes that can take place in humid environments. However, backfill could also have negative effects, such as increasing the cladding peak temperature and accelerating the amount and rate of cladding degradation. The effect of adding backfill to the repository design was evaluated, and the results are shown in Figure 4-204. This analysis indicates little net effect of the potential positive and negative performance aspects of backfill.

For the higher-temperature operating mode, the design described in Section 2 includes a 50-year ventilated preclosure period, a linear thermal loading of 1.45 kW/m, and a constant drift to drift spacing of 81 m (266 ft). For the higher-tempera-
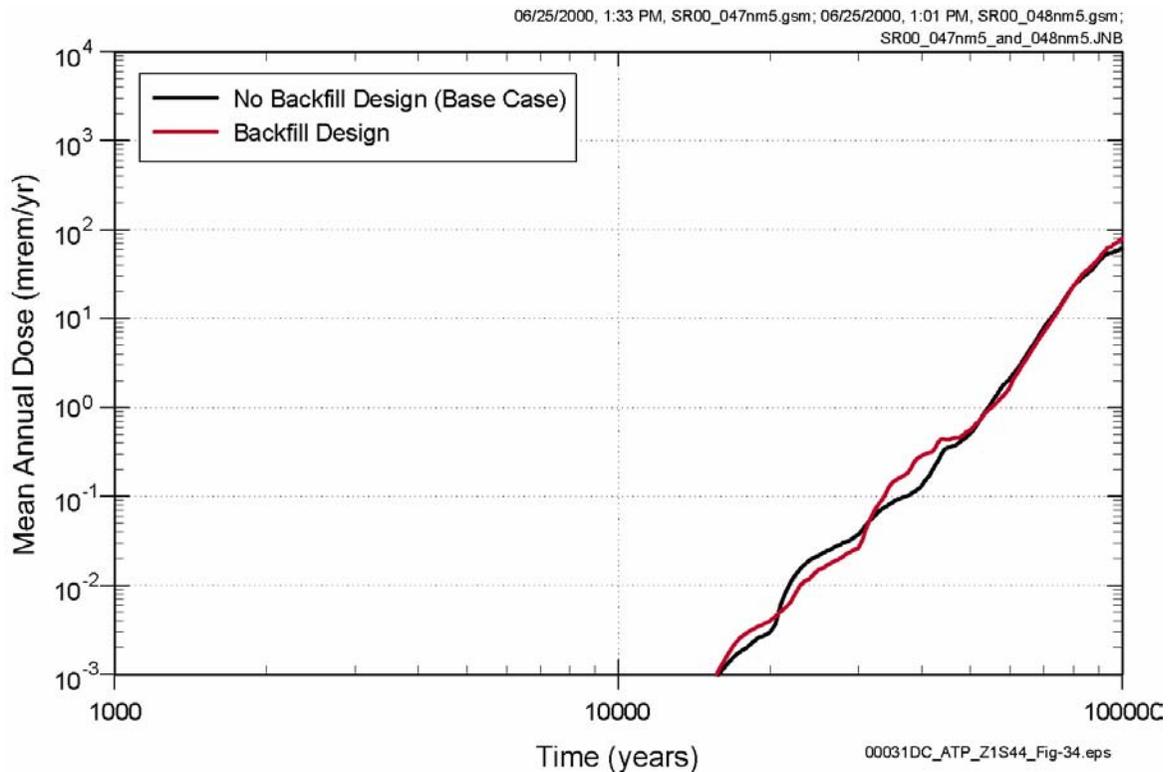
Figure 4-204. Sensitivity of the Mean Annual Dose Calculated by the TSPA-SR Model to Adding Backfill to the Repository Design
Source: CRWMS M&O 2000a, Figure 4.6-5.

ture operating mode, this design would allow boiling to occur several meters into the host rock surrounding the emplacement drifts for tens to hundreds of years after closure, depending on the relative location of the drift (i.e., edge versus center of the potential repository). In this section, the performance of a lower thermal load operating mode based on a reduced thermal loading of 0.90 kW/m and a 100-year ventilated preclosure period is compared to the higher-temperature operating mode. This alternative operating mode would not produce boiling in the host rock. The analysis is summarized in *Total System Performance Assessment for the Site Recommendation* (CRWMS M&O 2000a, Section 4.6.2).

To facilitate the analysis, the following key assumptions were made:

1. It is assumed that a specific line-loaded, two-dimensional, drift-scale, thermal-hydrologic submodel is representative of an average location in the potential repository footprint. This assumption is based on the selected submodel's physical location relative to the geometric center of the potential repository footprint.

2. Spatial variability in potential repository thermal-hydrologic variables does not have a significant effect on engineered barrier system performance. Therefore, thermal-hydrologic output variables from the line-loaded thermal-hydrologic submodel can be applied throughout the potential repository.

3. The reduction of power output from 1.45 kW/m to 0.90 kW/m is accomplished by increasing the waste-package-to-waste-package spacing. This increase in waste package spacing is accounted for in the two-dimensional model by applying a scaling factor to the original design model's thermal power curve.

4. The reduction in linear power output is accomplished by increasing waste-package-to-waste-package spacing in the emplacement drifts. As a result, the poten-

tial repository footprint should also increase accordingly. In the analyses presented here, the effects of an increased footprint on potential repository performance are neglected.

5. The effects and uncertainties associated with coupled thermal-hydrologic-chemical-mechanical processes, such as dissolution and precipitation of minerals and thermally induced fracturing in the host rock, may decrease in magnitude as the potential repository thermal loading decreases. These potential decreases in effects and uncertainties are neglected in the present comparison.

In the lower-temperature operating mode, waste package surface temperatures reach a much lower peak temperature, as expected. In the higher-temperature operating mode, elevated waste package surface temperatures are accompanied by a corresponding decrease in relative humidity around the waste package. This decrease in relative humidity does not occur in the low thermal load case since surface temperatures do not rise significantly.

Curves showing the rate of initial waste package failure (CRWMS M&O 2000a, Section 4.6.2) indicate that there is not a significant difference in the two cases as they are currently modeled. This result illustrates the insensitivity of the waste package corrosion and degradation model to thermal-hydrologic conditions around the waste package. As shown in Figure 4-205, the performance results for the higher-temperature operating modes compared to the lower-temperature modes in both TSPA-SR analyses and supplemental TSPA analyses (CRWMS M&O 2000a; BSC 2001a; BSC 2001b) are similar because neither would expose the engineered barriers (the drip shield and the waste packages) to temperatures or geochemical conditions that would be expected to significantly increase general corrosion or stress corrosion cracking rates, or waste form dissolution rates. The thermal design goals established for the higher-temperature operating mode (see Section 2.3.4.3) were meant to ensure that temperatures or geochemical environments that would promote
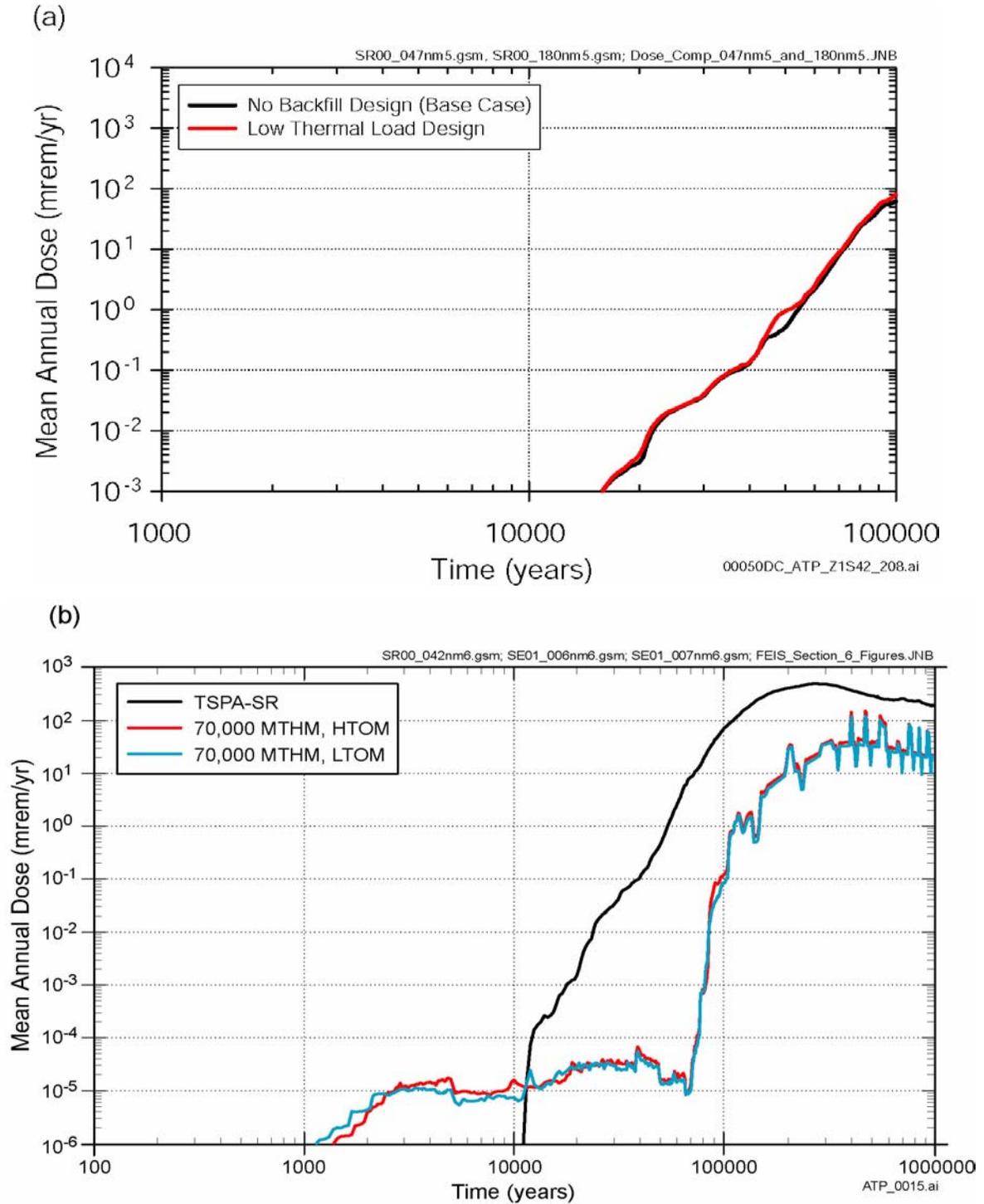
Figure 4-205. Comparison of Doses Projected by the TSPA-SR Model and Revised Supplemental TSPA Model for the Higher- and Lower-Temperature Operating Modes for the Nominal Scenario
(a) Comparison plot of the mean annual dose versus time for the TSPA-SR model for the higher-temperature operating mode and the lower-temperature operating mode for the nominal scenario. (b) Comparison plot of the mean annual dose versus time for the revised supplemental TSPA model for the higher-temperature operating mode (HTOM) and the lower-temperature operating mode (LTOM) for the nominal scenario. Source: CRWMS M&O 2000a, Figure 4.6-10; Williams 2001a, Figure 6-3.

corrosion and stress cracking would not be encountered in the repository. The processes and conditions expected in the natural environment and in the repository emplacement drifts are described in Sections 4.2.2, 4.2.3, and 4.2.5.

In conclusion, although the low thermal load case reduces waste package surface temperatures and increases the relative humidity around waste packages, these effects do not significantly impact waste package performance. In addition, since waste package failure does not occur until after 10,000 years, the thermal-hydrologic conditions for both cases are similar during the period when radionuclides are mobilized. As a result, doses for both cases show very little difference.

4.4.5.1.3 Sensitivity Analyses for Other Lower-Temperature Operating Modes

The effect of heat on the performance of the repository and the associated uncertainties are discussed in *FY01 Supplemental Science and Performance Analyses* (BSC 2001a; BSC 2001b). These studies considered ranges of drift wall temperatures as high as 200°C (392°F) to below the boiling point of water (96°C [205°F]) at the elevation of the emplacement horizon). An objective of the higher-temperature operating mode is to maintain temperatures in a portion of the rock between the emplacement drifts below the boiling point of water. Supplemental TSPA studies include sensitivity analyses that evaluated repository performance limiting all drift wall temperatures below the boiling point of water. Lower-temperature operating modes to reduce uncertainty about corrosion rates associated with waste package performance have also been evaluated in *FY01 Supplemental Science and Performance Analyses* (BSC 2001a; BSC 2001b). These evaluations considered temperatures as low as 85°C (185°F). The result of these studies are reported in Volume 1 of *FY01 Supplemental Science and Performance Analyses* (BSC 2001a). A summary of these studies are found in Section 4.4.5.5 of this report. In general, projected doses for both the higher- and lower-temperature operating modes are similar. This is true for both TSPA-SR model and revised supplemental TSPA model projections (see Figure 4-205).

The performance assessment aspects of the flexible design and ranges of operating modes for a potential repository at Yucca Mountain are related to understanding the impact that a design component or operational performance objective could have on the performance of the site across a range of environmental conditions. The use of TSPA as a tool in the evaluation of the performance characteristics of the proposed repository design over a range of operating conditions is an important step in the evaluation of the design. The evolution of the design and operating mode information is a process that includes (1) refining specific design requirements and performance goals to recognize performance related benefits that could be realized through design and (2) enhancing components of the design to best achieve the performance-related benefits.

Analyses of a range of lower-temperature operating modes was used to support development of further understanding of potential performance benefits that could be realized through specific repository operating modes (BSC 2001a; BSC 2001b). If a design attribute was shown to have a significant impact on the performance of the repository, then the attribute underwent further evaluation to define the positive contribution or limit the negative contribution of this attribute in a manner that could enhance the performance of the repository. If the performance evaluations indicate benefits to be gained by refinement of the basic design or operating mode concept, the evolution of the design will take advantage of those insights.

4.4.5.2 TSPA-SR Model Sensitivity Analyses for Disruptive Scenarios

As Section 4.3.2 describes, igneous disruption is the only disruptive scenario that has been identified as requiring explicit analysis in the TSPA. Section 4.4.3 describes the TSPA results for the igneous disruption scenario. This section presents the results of two sensitivity analyses examining alternatives to the modeling assumptions used in the TSPA-SR model (CRWMS M&O 2000a, Section 5.2.9). These sensitivity analyses have been

performed using 1,000 realizations and a 20,000-year period of simulation. These analyses are presented here to provide insight into the robustness of the TSPA-SR model results for the disruptive scenario performance analyses. The alternative modeling assumptions represented by these analyses are not considered to be realistic, and the mean probability-weighted 50,000-year dose rate described in Section 4.4.3 should be interpreted as the best estimate of future performance for the igneous disruption scenario class.

Figure 4-206 shows a comparison of the probability-weighted 20,000-year mean annual igneous dose rate, as described in Section 4.4.3, with the same dose rate calculated using a fixed annual probability of both eruption and igneous intrusion equal to 10^{-7}, rather than a value for igneous intrusion sampled from a distribution with a mean of 1.6×10^{-8}. For additional conservatism, the conditional probability that an eruptive conduit intersects waste if intrusion occurs is set to 1 in this analysis. This higher probability is the value used

by the NRC in analyses reported in their igneous activity Issue Resolution Status Report (Reamer 1999, p. 11). Because the event probability is used directly in the weighting of probabilistic doses, changes in event probability should result in a linear scaling of the mean annual dose. Figure 4-206 confirms this observation. The mean dose calculated using the fixed higher probability (shown in red) is about 17 times higher during the first 2,000 years than the mean dose calculated using the full distribution of probabilities. At later times, the scaling between the curves varies slightly with time, reflecting both the sampling of the time of intrusion and the influence of individual realizations with varying probabilities on the location of the mean at different times.

Figure 4-207 shows the second of the two one-off sensitivity analyses reported here, which is a comparison of the probability-weighted mean annual dose rate, as described in Section 4.4.3, with the same dose rate calculated using the 95th or 5th percentile values for the number of waste pack-
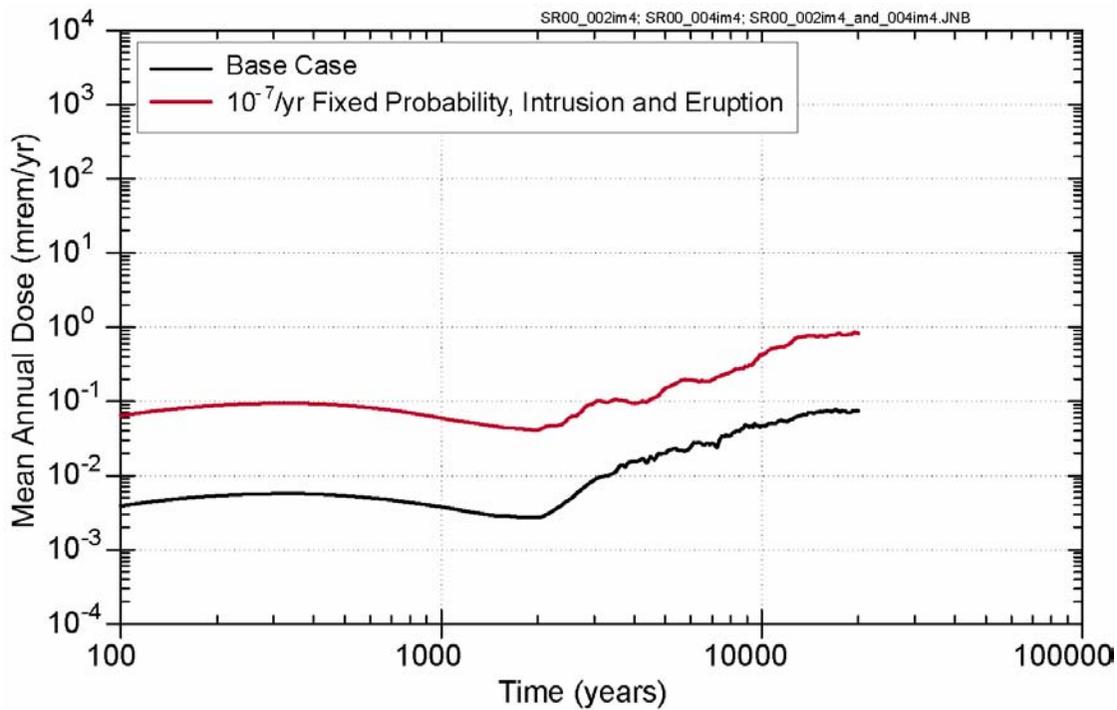
Figure 4-206. Sensitivity of the Mean Annual Dose Calculated by the TSPA-SR Model for the Volcanic Scenario to Uncertainty in Probability of Volcanic Intrusion and Eruption
Source: CRWMS M&O 2000a, Figure 5.2-17.
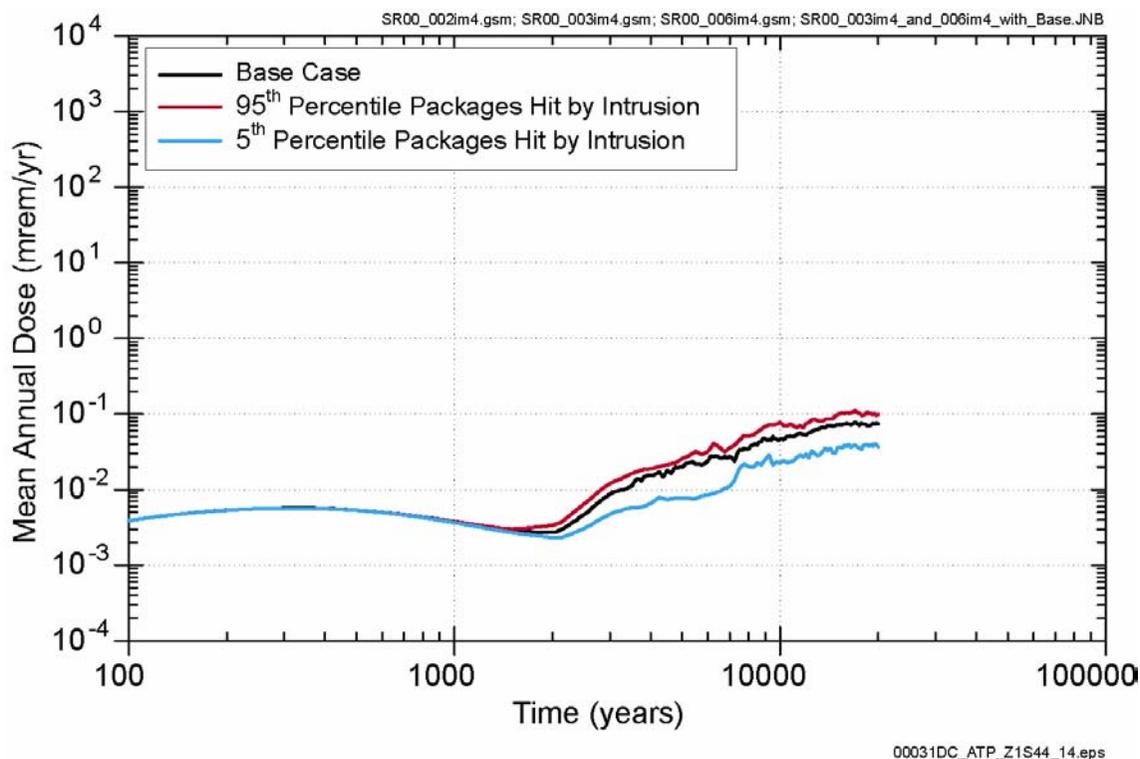
Figure 4-207. Sensitivity of the Mean Annual Dose for the Volcanic Scenario Calculated by the TSPA-SR Model to Uncertainty in the Number and Extent of Waste Packages Damaged by the Volcanic Intrusion

Source: CRWMS M&O 2000a, Figure 5.2-23.

ages damaged by igneous intrusion. This comparison provides insight into the sensitivity of overall performance to uncertainty about the repository's response to igneous intrusion. As Section 4.4.3 describes, packages may be sufficiently damaged by their close proximity to the igneous intrusion that they provide no further protection, or they may be partially damaged due to elevated temperature and pressure in the emplacement drift. Both types of damage are treated as uncertain parameters in the TSPA-SR model. In this sensitivity analysis of 20,000-year performance, these sampled values were replaced with fixed numbers corresponding to the 95th percentiles of the TSPA-SR distributions for the parameters. Specifically, these 95th percentile values are that 219 waste packages are fully damaged by igneous intrusion and that an additional 6,297 packages (more than half those in the repository) are partially damaged. All other parameters have the same values, sampled or fixed, that were used in

the TSPA-SR model. Results of this comparison show that performance is only moderately sensitive to the total number of packages that are damaged by intrusion, with peak dose increasing by less than a factor of 2.

Additional sensitivity analyses were performed by the supplemental TSPA model. These results are presented in Volume 2, Section 3.3 of *FY01 Supplemental Science and Performance Analyses* (BSC 2001b) and Section 4.4.5.3 of this report.

4.4.5.3 TSPA-SR Model Sensitivity Analyses of the Human Intrusion Scenario

Because the 100-year human intrusion dose is largely determined by the stylized nature of the analysis, results are insensitive to uncertainty regarding physical properties and processes related to the intrusion event.

Stochastic sensitivity analyses, as described in Sections 4.4.5 and 4.5, indicate that the mean annual dose rate following a 100-year human intrusion is sensitive to uncertainty in the parameters that affect transport in the saturated zone. Specifically, the parameters controlling advective flux in the saturated zone and the solubility of neptunium-237 show the greatest statistical importance. A one-off sensitivity analysis showed that degradation of the saturated zone flow and transport processes in the TSPA-SR model could result in a moderate increase in the 100-year human intrusion dose rate (CRWMS M&O 2000a, Section 5.3.7). However, the peak mean annual dose rate for the 95th percentile infiltration rate did not exceed 0.02 mrem/yr over the entire 100,000 years and was about 0.01 mrem/yr at 10,000 years after repository closure for the 100-year human intrusion event.

Sensitivity of the human intrusion scenario at 30,000 years to an unlikely igneous event is reported in *Total System Performance Assessment Sensitivity Analyses for Final Nuclear Regulatory Commission Regulations* (Williams 2001b). These results are discussed in Section 4.4.4.2.2 of this report.

4.4.5.4 Summary of TSPA-SR Sensitivity Analyses

The goal of the TSPA-SR sensitivity analyses, and the other analyses documented in *Total System Performance Assessment for the Site Recommendation* (CRWMS M&O 2000a, Section 5), is to provide additional insights into the significant contributors to overall system performance. These significant contributors are defined with respect to how much they modify the mean of the predicted dose response as well as their contribution to the overall uncertainty in the predicted dose response. The focus has been on the significance with respect to the individual dose performance (which includes the nominal performance scenario, the disruptive events performance scenario, and the stylized human intrusion scenario). These sensitivity analyses have been conducted out to 100,000 years to gain insights into the repository system behavior. Additional analyses are presented in Section 4.5 where several factors have been varied simulta-

neously to evaluate the robustness of the repository performance.

4.4.5.5 Supplemental TSPA Sensitivity Analyses For Nominal Performance

This section describes results presented in *FY01 Supplemental Science and Performance Analyses* (BSC 2001a; BSC 2001b) of one-off sensitivity analyses conducted by modifying the models and input parameters used in the TSPA-SR model. Except for the model or parameter being examined, the one-off sensitivity analyses were conducted using the same models and input parameters as those used in the TSPA-SR model base case, and therefore differences in performance measures between these results and those of the TSPA-SR model provide insights into the importance of uncertainty in individual model components. Analyses are presented for each of the major modeling subsystems, and the results are displayed as system-level annual dose histories for nominal performance and as intermediate performance measures, where appropriate. All analyses described in this section use 100 realizations of the TSPA base-case model (as modified for the one-off sensitivity analyses), and the results are compared to those of the TSPA-SR model base case.

Extended Climate Model—A supplemental sensitivity analysis was conducted in which the extended climate model (CRWMS M&O 2000a, Section 3.2.5) was used, but the rest of the model was the same as the TSPA-SR model base case. A comparison of the calculated mean annual dose to the receptor for this analysis with the TSPA-SR model base case is discussed in Volume 2, Section 3.2.1 of *FY01 Supplemental Science and Performance Analyses* (BSC 2001b). Each TSPA simulation is a combination of the low-, medium-, and high-infiltration cases (BSC 2001b, Section 3.2.1.1). The probabilities for the infiltration cases are the same for both simulations. The calculated dose peaks during the glacial climates because of the increased seepage during those periods. Relatively little change in dose is projected during the first glacial climate (at 38,000 years) because the drip shields and waste packages will still be largely intact at that time (CRWMS M&O 2000a, Section 4.1), and they divert most of the seepage water

around the waste packages during that period. The seepage flow rate increases during the glacial climates and decreases during the interglacial climates, as compared to the TSPA-SR base-case model. The interglacial periods occur at 65,000 years, 137,000 years, etc. (CRWMS M&O 2000a, Table 3.2-4). Despite the large increase in infiltration during the glacial periods, the number of waste packages that are subjected to seepage is less than 20 percent higher than the TSPA-SR base-case model.

Updated Seepage Model and Abstraction—Releases from the engineered barrier system are computed for 30 environmental groups that are based on infiltration, waste type, and seepage condition. Each environmental group is associated with one of five infiltration categories. The range for the categories are 0 to 3 mm/yr, 3 to 10 mm/yr, 10 to 20 mm/yr, 20 to 60 mm/yr, and greater than 60 mm/yr. A supplemental sensitivity analysis was conducted in which the revised seepage abstraction was used, but the rest of the model was the same as the TSPA-SR model base case. A comparison between the mean annual dose for the case with the revised seepage abstraction and the TSPA-SR base case is discussed in Volume 2, Section 3.2.2 of *FY01 Supplemental Science and Performance Analyses* (BSC 2001b). The results are essentially the same except near 60,000 years, where the sensitivity case is higher than the TSPA-SR model base case. That difference was traced to one realization in which the seepage flow rate was nearly ten times higher than in the TSPA-SR model base case for some environmental groups, causing the pulse of advective releases from the initial cladding failures in the commercial spent nuclear fuel to occur earlier than in the TSPA-SR model base case (BSC 2001b, Section 3.2.2).

The distributions of seepage flow rate are different in the updated seepage abstraction compared to those in the TSPA-SR model base case, but not greatly different. For example, Volume 2, Section 3.2.2 of *FY01 Supplemental Science and Performance Analyses* (BSC 2001b) discusses a comparison of the mean seepage flow rate for two of the environmental groups. The increase in seepage after 2,000 years is caused by the change from monsoon climate to glacial-transition climate.

The seepage fractions in the updated seepage abstraction are lower because of the inclusion of the lower-lithophysal seepage data; on average, less than half as many waste packages are exposed to seepage in the updated seepage case.

Effects of Flow Focusing on Seepage—The flow focusing factor implied by the new modeling can be bounded by an exponential distribution, with a minimum focusing factor of 1 and a mean focusing factor of 2. This distribution was substituted for the TSPA-SR base-case distribution for a TSPA sensitivity analysis. The comparison of the computed mean annual dose for the supplemental TSPA analysis with the TSPA-SR model base case is discussed in Volume 2, Section 3.2.2 of *FY01 Supplemental Science and Performance Analyses* (BSC 2001b).

The dose comparison shows little difference between the two TSPA simulations even though there is a significant difference in the amount of seepage. Because of the lesser amount of flow focusing in the sensitivity case, the mean seepage flow rate is lower in that case by nearly a factor of 10 (BSC 2001b, Section 3.2.2). By definition, the mean seepage flow rate is the seepage flow rate averaged only over locations that have seepage. With flow focusing, the percolation flux is higher in the locations that have percolation, which then produces higher seep rates in those locations. At the same time, less flow focusing makes the seepage fractions higher in the sensitivity case; approximately 50 percent more waste packages are exposed to seepage in that case than in the TSPA-SR model base case (BSC 2001b, Section 3.2.2.3). The number of waste packages that always receive seepage actually declines, but the number of waste packages that receive seepage only some of the time increases. A high flow-focusing factor increases the chances of seeping all the time, because the focusing enhancement can increase the local percolation flux above the seepage threshold flux even during the dry, present-day climate.

Comparisons of advective releases from the engineered barrier system for technetium-99 and neptunium-237 are discussed in Volume 2, Section 3.2.2 of *FY01 Supplemental Science and Perfor-*

mance Analyses (BSC 2001b). The advective releases are not as different as might be expected from the difference in seepage between the supplemental TSPA model sensitivity case and the TSPA-SR base case. The simulated releases largely are limited by the rate at which the waste inventory is exposed (e.g., by waste-package and cladding failure) and available for transport. In addition, much of the radionuclide release is diffusive rather than advective, especially for technetium-99 (CRWMS M&O 2000a, Section 4.1.2), and diffusive releases are not affected by seepage in the TSPA model. Together, the large amount of diffusive release and the relatively small change in the advective release as the seepage changes lead to the small change in doses (BSC 2001b, Section 3.2.2).

Effects of Episodic Flow on Seepage—A supplemental sensitivity analysis was conducted in which the episodicity distribution was included in the seepage abstraction, but all other parts of the model were the same as the TSPA-SR model base case. A comparison was made between the mean annual dose for that case and the base case in the supplemental TSPA model (BSC 2001b, Section 3.2.2), and the mean annual dose for the sensitivity case is higher than the TSPA-SR model base case after about 40,000 years. The first general-corrosion penetrations of the waste packages occur at about 40,000 years. Before that, no seepage water enters the waste packages in the TSPA-SR model (CRWMS M&O 2000a, Section 4.1.2).

Effects of Drift Degradation and Rock Bolts on Seepage—Recent results show that there is probably no significant increase of seepage because of drift degradation or the presence of rock bolts, but it was also noted that TSPA results are not expected to be sensitive to a change of only 50 percent in the seepage flow rates (BSC 2001a, Section 4.3.4.6). Because there is uncertainty about the effects of drift degradation on seepage, with significant increases in seepage possible in some locations, the 50-percent seepage enhancement is retained for the analyses in this report.

Thermal Effects on Seepage—Several recent supplemental analyses have been conducted to estimate the amount of seepage reduction during the

period when there is a vaporization barrier around the drifts (BSC 2001a, Section 4.3.5). Those analyses found that little, if any, liquid flow reaches the drifts when there is an above-boiling zone around them.

An alternative model is evaluated in which seepage is reduced to zero when the drift wall is above boiling. This change has no effect on doses in the nominal scenario because all waste packages and drip shields remain intact until well past the boiling period in the TSPA-SR model base case (e.g., CRWMS M&O 2000a, Section 4.1). Thus, to determine if there is some effect, this supplemental sensitivity analysis was performed using a case in which there are no drip shields and there is a patch failure in each waste package at 100 years after closure.

Volume 2, Section 3.2.2 of *FY01 Supplemental Science and Performance Analyses* (BSC 2001b) reports on a comparison of the mean annual dose for this supplemental sensitivity case with the case that has neutralized waste packages and drip shields and the TSPA-SR model base-case seepage model. The calculated doses are reduced for approximately the first 500 years because of the reduction in advective releases caused by eliminating seepage while the drifts are above boiling. Diffusive releases also are relatively low during this period (in both cases) because heat from the waste packages reduces the moisture content, and thus the diffusion coefficient, in the invert. Volume 2, Section 3.2.2 of *FY01 Supplemental Science and Performance Analyses* (BSC 2001b) discusses time-histories of drift-wall temperature that were used for the five infiltration bins. Information about the infiltration bins and the thermal hydrologic model can be found in Sections 3.3.2 and 3.3.3 of *Total System Performance Assessment for the Site Recommendation* (CRWMS M&O 2000a). The drift walls are only above boiling temperature (at the repository elevation, the boiling temperature is approximately 96°C [205°F]) for about 300 years or less, depending on the infiltration bin; thus the supplemental seepage model is only changed from the base-case seepage model for about 300 years. The change in seepage for commercial spent nuclear fuel with 20 to 60 mm/yr (0.8 to 2.4 in./yr) infiltration and seepage some of the time is

discussed in Volume 2, Section 3.2.2 of *FY01 Supplemental Science and Performance Analyses* (BSC 2001b). As expected, the mean seepage flow rate is only different from the base case for a little over 300 years.

Combined Effects of Seepage—In this section, results are presented for a supplemental sensitivity analysis in which the changes of the preceding sections are combined. This alternative seepage model includes:

- The updated seepage abstraction (BSC 2001b, Section 3.2.2.2)

- The updated distribution for the flow-focusing factor (BSC 2001b, Section 3.2.2.3)

- The distribution of the episodicity factor (BSC 2001b, Section 3.2.2.4)

- The reduction in seepage by a sampled factor between 0 and 0.2 when the drift wall is above boiling (BSC 2001b, Section 3.2.2.6).

This supplemental sensitivity analysis was performed to see the effect of changes in seepage during the boiling period using the case with neutralized waste packages and drip shields (CRWMS M&O 2001a, Volume 2, Section 3.4.2). The mean annual dose for this supplemental sensitivity case was compared with the case that has neutralized waste packages and drip shields and the TSPA-SR base-case seepage model in Volume 2, Section 3.2.2 of *FY01 Supplemental Science and Performance Analyses* (BSC 2001b). For the modified seepage model, the mean annual dose is about a factor of two higher than the TSPA-SR model at all times. Because the thermal seepage-reduction factor is sampled between 0 and 0.2, there is only one tenth as much seep flow, on average, as in the TSPA-SR model when the drift wall is above boiling. However, the seepage reduction apparently causes no reduction in dose during the boiling period similar to the reduction when seepage was eliminated (BSC 2001b, Section 3.2.2.6). The results show that even a small amount of seepage is enough to provide for release of the highly soluble species (in particular, technetium-99 and iodine-129). The neutralization of waste packages and

drip shields makes this supplemental case more advection-dominated than was the TSPA-SR model, especially at early times (BSC 2001b, Section 3.2.2; CRWMS M&O 2000a, Section 4.1).

Releases from the engineered barrier system are computed for 30 environmental groups that are based on infiltration, waste type, and seepage condition. Each environmental group is associated with one of five infiltration categories. The range for the categories are 0 to 3 mm/yr, 3 to 10 mm/yr, 10 to 20 mm/yr, 20 to 60 mm/yr, and greater than 60 mm/yr.

The change in seepage for commercial spent nuclear fuel with 20 to 60 mm/yr (0.8 to 2.4 in./yr) infiltration and seepage some of the time is discussed in Volume 2, Section 3.2.2 of *FY01 Supplemental Science and Performance Analyses* (BSC 2001b). The mean supplemental seepage flow rate for seepage of 20 to 60 mm/yr for the combined seepage modifications is lower than in the TSPA-SR base-case seepage model by a factor of a little over two at late times and by a factor of ten or more during the boiling period. In these analyses, the mean annual dose increases slightly even though the mean seepage flow rate decreases because the number of waste packages exposed to seepage triples. Over one-third of the waste packages are in locations with seepage in the modified seepage model. The increase in seepage fraction occurs because two changes, lower flow-focusing factors and inclusion of episodicity, tend to increase the seepage fraction (BSC 2001b, Sections 3.2.2.3 and 3.2.2.4), while only one change, inclusion of data from the lower-lithophysal unit in the seepage abstraction, tends to reduce the seepage fraction (BSC 2001b, Section 3.2.2.2).

Analyses of In-Drift Thermal-Hydrologic Conditions—Sensitivity of calculated performance to in-drift temperatures is shown in the comparison of the results for the designs with and without backfill. The results for these two cases (CRWMS M&O 2000a, Section 4.6) suggest that there is little difference between the TSPA-SR model and supplemental TSPA model estimates of system performance (BSC 2001b, Section 3.2.3). However, the use of bounding approximations for

assessing thermal effects limits their usefulness in sensitivity studies. The sensitivity to in-drift thermal-hydrologic conditions is inferred, to some extent, in studies (CRWMS M&O 2000a, Sections 5.2.1 and 5.3.1) that examined the range of flow conditions in the unsaturated zone. Variations in unsaturated zone percolation fluxes due to thermal influences result in variations in drift moisture fluxes (BSC 2001b, Section 3.2.3).

Drift Degradation—Supplemental sensitivity studies of drift degradation are reported in Volume 1, Section 6.3.4 of *FY01 Supplemental Science and Performance Analyses* (BSC 2001a). These studies examine uncertainties in the rock fall model multiplier and in the correction for sub-horizontal fractures, consider a wide range in the size of the fractures to determine the effects on rock fall, and are conducted using a large number of realizations in the Monte Carlo simulations. The results do not show significant increases in the estimate of the size or density of rock fall over that obtained previously. Consequently, TSPA calculations of their effects on the estimate of annual dose have not been conducted.

In-Drift Chemistry—Supplemental work regarding the chemistry of incoming seepage and the evolution of chemistry within the emplacement drift has been evaluated at the subsystem level (BSC 2001b, Section 3.2.4). Results of subsystem sensitivity studies of the thermal-hydrologic model and the precipitates and salts model are reported in Volume 1, Sections 6.3.1, 6.3.3, and 6.4 of *FY01 Supplemental Science and Performance Analyses* (BSC 2001a). These analyses have been incorporated in supplemental evaluations of performance.

Results using the supplemental TSPA model show no significant effect on the estimate of mean annual dose (BSC 2001a, Section 3.2.4). Although the solubilities of radionuclides are affected by these changes and the attendant effects on the in-drift chemistry, residence time in the invert is a sufficiently small fraction of the transport time that this effect apparently is not significant. This result is consistent with previous sensitivity studies (CRWMS M&O 2000a, Section 5.2).

Aging of Alloy 22—To evaluate the potential importance of aging due to phase instability of Alloy 22, an analysis was conducted using a supplemental TSPA model for these effects. In this supplemental TSPA model, the probability of aging enhancement to the corrosion rate was assumed to be 0.0001, and the effect of aging was assumed to enhance the general corrosion rate by a factor of 1,000. These values were used because they are considered conservative.

Supplemental TSPA model results using this analysis are discussed in Volume 2, Section 3.2.5 of *FY01 Supplemental Science and Performance Analyses* (BSC 2001b). In addition to the change in the representation of the aging enhancement, this supplemental TSPA model reflects updates to the TSPA-SR base-case waste package and drip shield model discussed previously.

This supplemental analysis shows that the TSPA-SR model is conservative after 20,000 years. Before this time, the annual dose in the supplemental TSPA model is greater than that in the TSPA-SR base-case analysis; however, the estimated mean annual dose is small (i.e., a peak mean dose of 0.08 mrem/yr over a 10,000-year period), even using the extreme parameters of this model.

Stress Corrosion Cracking—Additional considerations of the sources of uncertainty in the stress corrosion cracking model (BSC 2001a, Section 7.3.3) result in supplements to the stress corrosion cracking model. The effects of these refinements on the estimate of mean annual dose are evaluated in three supplemental calculations that address the expanded range of considerations for the residual stress profile of the closure weld regions, the threshold stress for stress corrosion cracking crack initiation, and the orientation of the weld flaws (BSC 2001b, Section 3.2.5). The models used for these analyses are discussed in Volume 1, Section 7.3.3 of *FY01 Supplemental Science and Performance Analyses* (BSC 2001a), and updates to the TSPA-SR base-case degradation model are discussed in Volume 2, Section 3.2.5 of *FY01 Supplemental Science and Performance Analyses* (BSC 2001b). The effects of waste package degradation on all of these changes are summarized in

Volume 1, Section 7.4.2 of *FY01 Supplemental Science and Performance Analyses* (BSC 2001a).

General Corrosion—The comparison of the TSPA-SR model and supplemental TSPA model results using a probability distribution for general corrosion that reflects uncertainty shows a difference in the estimate of mean annual dose due to different parameter distributions and different conceptual models used. In the TSPA-SR model, conservative assumptions lead to earlier failure by corrosion and shorter waste package lifetimes. The neglect of uncertainty due to variability effectively narrows the temporal failure distributions for the drip shield and waste package associated with general corrosion. This narrowing leads to later initial failures of the drip shields and waste packages. The earliest release is delayed in the supplemental TSPA model compared to the TSPA-SR model because of this later initial failure of these components (BSC 2001b, Section 3.2.5).

A second source of uncertainty in the TSPA-SR model is the temperature dependence of the general corrosion rate. Supplemental analyses of the temperature dependence of the general corrosion rate for Alloy 22 have been conducted (BSC 2001a, Section 7.3.5). The net effect of the temperature dependence is that, while waste package temperatures are greater than 60°C (140°F) (for approximately the first 10,000 years), Alloy 22 general corrosion rates are higher than in the TSPA-SR model. After 10,000 years after closure, the general corrosion rate is lower and the net effect is that, on average, the rate of waste package failure is much lower in the supplemental TSPA model than in the TSPA-SR base-case model.

The results of the estimates of the annual dose using the updated supplemental waste package degradation rate are compared with the results using the TSPA-SR base-case (temperature independent) general corrosion model in Volume 2, Section 3.2.5 of *FY01 Supplemental Science and Performance Analyses* (BSC 2001b). Volume 2, Section 3.2.5.3 of *FY01 Supplemental Science and Performance Analyses* (BSC 2001b) compares the TSPA-SR base-case result to the results in which the temperature dependence of the general corrosion rate is developed from the potentiostatic

polarization test results. Because the rate of waste package failures is much lower in the first 100,000 years in the supplemental TSPA model, the mean annual dose is significantly lower than the TSPA-SR base-case result. The peak mean annual dose during the first 100,000 years is approximately 0.1 mrem/yr. The variance in the estimate of annual dose using the supplemental temperature-dependent model is discussed in Volume 2, Section 3.2.5.3 of *FY01 Supplemental Science and Performance Analyses* (BSC 2001b). Because of the larger variance in the degradation rate due to the treatment of uncertainty, variance in the supplemental estimate of annual dose using the temperature-dependent model is somewhat larger than that for the TSPA-SR base-case general corrosion model.

Early Failure of the Waste Package—In the TSPA-SR model, no releases occur before 10,000 years. In reevaluating the potential of early failure mechanisms and their potential consequences, a more conservative approach resulted in the inclusion of improper heat treatment leading to the possible subsequent failure of a few waste packages in the TSPA supplemental analysis. The nonmechanistic early waste package failure assumes failure of both the inner and outer Alloy 22 lids and the stainless steel inner lid. To ensure that the potential consequence of early waste package failures is treated conservatively, it is included in the nominal scenario, not as a sensitivity analysis. Volume 1, Section 7.3.6 of *FY01 Supplemental Science and Performance Analyses* (BSC 2001a) describes the model developed for the potential consequences of improper heat treatment of a waste package.

Evaporative Reduction of Seepage—Supplemental analyses (BSC 2001a, Section 8.3.1) indicate that, because waste packages remain intact during the period when evaporative reduction of the flow might be important, little effect on radionuclide release is expected. Comparison of supplemental analyses including this effect with the results using the TSPA-SR base-case model confirm this expectation: there is no discernible difference between the results with or without the evaporative reduction (BSC 2001a, Figure 3.2.6.1-1).

Condensation Under the Drip Shield—Supplemental sensitivity analyses using the TSPA-SR base-case model for invert and drip shield temperature indicate condensation under the drip shield throughout the potential repository, even in areas in which no seepage occurs. In this event, there would be advective flow throughout the repository during the early thermal period in spite of the drip shield.

Because the effects of condensation are not significant while the waste packages remain intact, the sensitivity analysis modeled the potential effect of condensation by assuming an early failure of a waste package (BSC 2001b, Section 3.2.6.2). For the supplemental sensitivity analyses, the fraction of water reaching the waste package is sampled from a uniform probability distribution that ranges between zero and one.

In the assumed scenario, the peak mean annual dose rate is increased in the first 10,000 years from about 10^{-2} mrem/yr to slightly less than 10^{-1} mrem/yr. However, the effect would be negligible in nominal scenarios in which waste packages do not experience the early failures. This effect remains screened from TSPA analyses for several reasons (BSC 2001b, Section 1.3).

- Thermal conditions required for water to condense under the drip shield are short-lived, limited only to the first few thousand years after emplacement when the waste packages remain largely unaffected by degradation (BSC 2001b, Section 3.2.6.2; see also Section 4.2.5 of this report).

- The model does not account for bias in the thermal model, which overestimates the potential for condensation to occur (BSC 2001b, Section 3.2.6.2).

- Condensate will tend to flow down the underside of the drip shield rather than falling directly onto the waste package (BSC 2001b, Section 3.2.6.2).

Geometrical Constraint on Flow through the Waste Package—The fraction of water flowing through the waste package may be different from the assumption used in the TSPA-SR model base

case to define the fraction. There are geometrical constraints on this flow if the waste package breaches are not directly under the drip shield breaches. The supplemental analyses in Volume 1, Section 8.3.3 of *FY01 Supplemental Science and Performance Analyses* (BSC 2001a) develop a more realistic representation for this fraction. The difference in the resulting estimate of annual dose is discussed in Volume 2, Section 3.2.6.3 of *FY01 Supplemental Science and Performance Analyses* (BSC 2001b).

Patch breaches do not develop on the drip shield until well after a 10,000-year period. Consequently, the supplemental TSPA model shows no change in the estimate of mean annual dose from that calculated with the TSPA-SR base-case model. After 10,000 years, the geometrical constraint reduces the flux through the waste package, resulting in a reduction in the release of neptunium-237 and other solubility-limited radionuclides. The effect is a modest reduction in the mean annual dose due to this change in the source term (BSC 2001b, Section 3.2.6.3).

Bathtub Effect—Before development of any breach in the bottom of the waste package, water entering a breach in the top of the waste package would accumulate as in a bathtub. After a breach is formed in the bottom, the water could drain. The impact of this accumulation and subsequent drainage is considered in Volume 1, Section 8.3.4 of *FY01 Supplemental Science and Performance Analyses* (BSC 2001a).

The effects on estimate of mean annual dose rate projected by the supplemental TSPA model are analyzed in Volume 2, Section 3.2.6.4 of *FY01 Supplemental Science and Performance Analyses* (BSC 2001b). The effect on the estimate of annual dose is small. First, only a fraction of the waste packages in the potential repository are contacted by water, and only a fraction of these have a sufficient delay of breaching in the bottom (after breaching in the top) to provide a significant bathtub effect. In addition, although accumulations in this small fraction of waste packages can be substantial (on the order of 1 m^3 [35 ft^3] of water for an average waste package in an area with seepage), the accumulated water drains rapidly and

has a short-term effect. Diffusive releases from the engineered barrier system depend only on the concentration of radionuclides in the water and not the additional mass and therefore are not affected. Advective releases from the engineered barrier system are affected but only over a short period, and the net effect averaged over an entire time step of several hundred years is small.

In-Package Chemistry—The TSPA-SR base-case model for in-package chemistry is a simple mixing cell (CRWMS M&O 2000a, Section 3.5.2.1). As indicated in Volume 1, Section 9.3.1 of *FY01 Supplemental Science and Performance Analyses* (BSC 2001a), the TSPA-SR model uses conservatively high dissolution rates. The supplemental TSPA analyses consider a model in which these dissolution rates are represented more realistically. Calculations of total system performance using this supplement in-package chemistry range are compared with the results using the TSPA-SR model in Volume 2, Section 3.2.7 of *FY01 Supplemental Science and Performance Analyses* (BSC 2001b). Section 3.2.7 (BSC 2001b) also discusses the comparison of the mean annual dose curves calculated with the two models (TSPA-SR model and supplemental TSPA model) and the range of realizations calculated using the supplemental TSPA model.

The results show significant effects after about 40,000 years when the contributions from neptunium-237 and other actinides begin to dominate the estimate of mean annual dose (BSC 2001b, Section 3.1.1). The change in chemistry does not have a significant effect on the waste form degradation rate that controls the concentrations of technetium-99 or iodine-129, radionuclides that dominate the annual dose estimate in the first 40,000 years (BSC 2001b, Section 3.1.1). The modified water chemistry, however, affects the solubility limits of neptunium, plutonium, and other actinides; therefore, it affects the annual dose from the associated isotopes with concentrations that are determined by these solubility limits.

Commercial Spent Nuclear Fuel Cladding Degradation—The supplemental TSPA analyses (BSC 2001a, Section 9.3.3) consider information regarding the range of uncertainties in models for cladding degradation processes in addition to that considered in *Total System Performance Assessment for the Site Recommendation* (CRWMS M&O 2000a). In particular, the probability distribution for creep and stress corrosion cracking during dry storage is modified to reflect a more realistic representation of creep failure. The result is a reduction in the estimate of early cladding failures: the mean fraction of early cladding failures is reduced from about 8 percent to about 1 percent. The supplemental analyses (BSC 2001a, Section 9.3.3) also consider the probability distributions for localized corrosion and cladding unzipping. The ranges for these distributions are expanded to take into account additional uncertainty considerations. The effect in this case is greater variance in the distribution of cladding failures. The supplemental analyses also consider perforations due to static loading by fallen rock. These considerations lead to increased degradation of the cladding after sufficient degradation of the waste package and drip shield occurs to permit the rocks to rest directly on the waste form.

The effects of the additional cladding degradation uncertainty on the annual dose estimate are evaluated in Volume 2, Section 3.2.7.2 of *FY01 Supplemental Science and Performance Analyses* (BSC 2001b). The conceptual model for the cladding degradation is summarized in Volume 1, Section 9.4 of *FY01 Supplemental Science and Performance Analyses* (BSC 2001a), and the implementation for these analyses is described in Appendix A. The small reduction in the mean annual dose in the period projected by the supplemental TSPA model arises largely from the reduction in early cladding failure. The other changes to the supplemental cladding degradation model do not result in significant changes to the estimate of mean annual dose in the first 100,000 years (BSC 2001a, Section 3.2.7.2).

In-Package Radionuclide Solubility Limits—Supplemental analyses reported in Volume 1, Section 9.3.2 of *FY01 Supplemental Science and Performance Analyses* (BSC 2001a) consider a wider range for the uncertainty in the effect of the controlling phases for plutonium, neptunium, thorium, and technetium. The effects of the extended range of uncertainty in these concentra-

tion limits, along with the effects on in-package chemistry (e.g., pH), are assessed in Volume 2, Section 3.2.7.3 of *FY01 Supplemental Science and Performance Analyses* (BSC 2001b). Volume 2, Section 3.2.7.3 of *FY01 Supplemental Science and Performance Analyses* (BSC 2001b) compares the mean annual dose taking these supplemental effects into account with the results using the TSPA-SR base-case model. Volume 2, Section 3.2.7.3 of *FY01 Supplemental Science and Performance Analyses* (BSC 2001b) analyzes the contributions of the various radionuclides to the total mean annual dose estimate when these effects are taken into account.

The results of the supplemental analysis (BSC 2001a, Section 3.2.7.3) show significant changes after the waste packages are breached. As indicated previously, neptunium-237 dominates the annual dose estimate in the nominal scenario (BSC 2001b, Section 3.1.1); therefore, changes to the solubility limit of this radionuclide have a large effect on the estimate of total mean annual dose. The estimates for other radionuclides also are reduced by the changes in solubility limits. In particular, the mean annual dose from the plutonium isotopes is reduced by about a factor of three. The overall effect of these supplemental changes is to reduce the estimate of mean annual dose by a factor of more than five.

In-Package Colloid Associated Radionuclide Concentrations—The supplemental TSPA analyses (BSC 2001a, Section 9.3.4) extend the range of uncertainties in these colloid-assisted concentrations and examined sensitivity over this range. The effect of using the colloid concentration and sorption model, considered in Volume 1 of *FY01 Supplemental Science and Performance Analyses* (BSC 2001a), is discussed in Volume 2, Section 3.2.7.4 of *FY01 Supplemental Science and Performance Analyses* (BSC 2001b), which compares the mean annual dose curves for the TSPA-SR base case and the new colloid models and presents the range of the results for the new colloid model. There is little difference between the mean annual doses calculated using these models. In part, the small difference reflects the fact that the mean annual dose is dominated by dissolved radionuclides. However, even the comparison of the results

for the colloids alone would show little change in the mean annual dose because the mean values of the probability distribution in the two models are virtually the same.

Analyses of Radionuclide Transport in the Engineered Barrier System—Supplemental analyses of radionuclide transport in the engineered barrier system are described in Volume 1, Section 10.3 of *FY01 Supplemental Science and Performance Analyses* (BSC 2001a). These analyses include the treatment of diffusion and sorption in the engineered barrier system. The TSPA-SR base-case model does not account for diffusive transport processes within the waste package. Including in-package diffusive transport in the TSPA-SR model results in a modest reduction in dose calculations (BSC 2001b), Section 3.2.8, Figure 3.2.8-1)

One possible reason for the small difference in these two estimates is the diffusion coefficient used for transport within the waste package. Diffusive resistance to radionuclide transport has been shown to be sensitive to the conservative diffusion coefficient used in TSPA calculations, whether applied in the invert or internal to the waste package (BSC 2001b, Section 3.2.8; CRWMS M&O 2000a, Section 5.3.5).

The second consideration is the effect of sorption on radionuclide transport in the engineered barrier system, in particular, the effect of iron corrosion products on reversible and irreversible sorption in the invert and within the waste package. The TSPA-SR base-case model assumes no sorption of dissolved species within the engineered barrier system. However, Volume 1, Section 10.3.4 of *FY01 Supplemental Science and Performance Analyses* (BSC 2001a) considers the conservative nature of this assumption and develops a model for the sorption of radionuclides in the engineered barrier system.

The reduction in mean annual dose after 10,000 years projected by the supplemental TSPA model as compared to the TSPA-SR model derives from two principal effects. The first is the reduction in concentrations in the liquid phase due to the partitioning of the concentrations between the liquid phase and the solid phases not considered in the

TSPA-SR base-case model, the result of which reduces the source term of many of the contributing radionuclides. The second is the effect of sorption on the diffusive transport, which effectively reduces the diffusion coefficient and increases the diffusion resistance of in-package transport. These two effects combine to decrease the source term and the resulting mean annual dose estimate (BSC 2001b, Section 3.2.8, Figure 3.2.8-2).

Effects of the Drift Shadow Zone—In the TSPA-SR base-case model, radionuclide releases from the engineered barrier system are released into the fracture continuum of the unsaturated zone transport model (CRWMS M&O 2000a, Section 3.7.2). This choice is conservative in that fracture transport is faster than matrix transport.

As an initial estimate of the effect of the presence of the drift on unsaturated zone transport, a sensitivity analysis was performed in which advective releases from the potential repository were released into the fracture continuum of the unsaturated zone transport model, as in the TSPA-SR base case, but diffusive releases were released into the matrix continuum of the model instead (BSC 2001a, Section 11.3.1.6.1).

The sensitivity analysis uses the TSPA-SR base-case assumption of a zero-concentration boundary condition at the drift wall for calculating diffusive releases from the engineered barrier system (CRWMS M&O 2000a, Section 3.6.2.2).

The results of this sensitivity analysis are shown in a comparison of the mean annual dose for this case with that of the TSPA-SR model (BSC 2001b, Section 3.2.9.2). The results show a delay of approximately 10,000 years in the mean annual dose for the drift-shadow case as compared to the TSPA-SR model. The effect is as large as it is because a large portion of the radionuclide releases are diffusive, especially for technetium-99 (CRWMS M&O 2000a, Section 4.1) and because transport through the matrix is slower than transport through the fractures.

Unquantified Uncertainties in the Saturated Zone—The saturated zone flow-and-transport

model was evaluated with respect to unquantified uncertainty to determine the parts of the model to change to provide a better representation of the saturated zone. A detailed discussion of the changes made to the saturated zone modeling is presented in Volume 1, Section 12.5.1 and Table 12.5.1-1 of *FY01 Supplemental Science and Performance Analyses* (BSC 2001a).

The impact of the changes made to the saturated zone flow and transport model by the evaluation of unquantified uncertainty is shown in Volume 2, Section 3.2.10 of *FY01 Supplemental Science and Performance Analyses* (BSC 2001b), which compares the mean annual dose for the TSPA-SR base-case model with the mean annual dose calculated using the supplemental saturated zone model. Volume 2, Section 3.2.10 of *FY01 Supplemental Science and Performance Analyses* (BSC 2001b) discusses the results for the multiple realizations of the supplemental saturated zone model. There is virtually no difference between the mean annual doses calculated using the TSPA-SR saturated zone model and the supplemental saturated zone model (BSC 2001b, Section 3.2.10). This uncertainty evaluation provides confidence that the saturated zone modeling used in the TSPA-SR model is a relatively robust description of uncertainty in the saturated zone system and that the uncertainty included in the modeling was adequate for the TSPA-SR nominal case.

No Matrix Diffusion in the Saturated Zone—The mean annual dose calculated in the TSPA-SR model (CRWMS M&O 2000a, Section 4.1) is compared with the mean annual dose calculated without the effects of matrix diffusion in the saturated zone in Volume 2, Section 3.2.10 of *FY01 Supplemental Science and Performance Analyses* (BSC 2001b). This section also discusses the results of the multiple realizations of the TSPA for the saturated transport model without matrix diffusion. The differences between the models with and without matrix diffusion are slight (BSC 2001b, Section 3.2.10.2.2).

Increased Matrix Diffusion in the Saturated Zone—Volume 2, Section 3.2.10 of *FY01 Supplemental Science and Performance Analyses* (BSC 2001b) compares the mean annual dose calculated

in the TSPA-SR model with the mean annual dose calculated with enhanced matrix diffusion in the saturated zone transport model, as described in Volume 1, Section 12.5.2.2 of *FY01 Supplemental Science and Performance Analyses* (BSC 2001a). Volume 2, Section 3.2.10 of *FY01 Supplemental Science and Performance Analyses* (BSC 2001b) presents the results of the multiple realizations of the supplemental TSPA model for the saturated zone transport model with enhanced matrix diffusion. The differences in expected annual dose between the model with matrix diffusion and the model with enhanced matrix diffusion are generally less than 20 percent, and the simulated doses are somewhat lower for the model with enhanced matrix diffusion, as expected (BSC 2001b, Section 3.2.10).

Minimum Flow-Path Length in the Alluvium— The mean annual dose calculated for the TSPA-SR model base case is compared with the mean annual dose calculated with minimal alluvium in the groundwater transport path in Volume 2, Section 3.2.10 of *FY01 Supplemental Science and Performance Analyses* (BSC 2001b). There is only a slight difference (generally less than 10 percent) in results, with the minimal-alluvium case showing slightly higher simulated dose, as expected. The results of the sensitivity analysis examining the minimum flow path length in the alluvium are approximately consistent with the expected behavior of the system, when the impacts of glacial climatic conditions and higher specific discharge are considered.

Increased Uncertainty in the Colloid-Facilitated Transport Models—The results of the colloid sensitivity study for the saturated zone are discussed in Volume 2, Section 3.2.10 of *FY01 Supplemental Science and Performance Analyses* (BSC 2001b). The simulated dose for changes only in the saturated zone flow-and-transport model are presented in Volume 2, Section 3.2.10 of *FY01 Supplemental Science and Performance Analyses* (BSC 2001b). Doses for changes in all relevant components of the supplemental TSPA model (with regard to colloid-facilitated transport) are discussed in Volume 2, Section 3.2.10 of *FY01 Supplemental Science and Performance Analyses* (BSC 2001b). There is virtually no difference in the mean annual dose using the supplemental representation of colloid-facilitated transport with increased uncertainty compared with the base-case colloid model used in the TSPA-SR model. The two radionuclides that comprise greater than approximately 70 percent of the annual dose in the TSPA-SR model (CRWMS M&O 2000a, Section 4.1) are technetium-99 at earlier times and neptunium-237 at later times. Both of these radionuclides are transported as solute and thus are unaffected by the new colloid model. Also, in the new colloid model, the means of the distributions (for colloid concentrations, sorption coefficients for radionuclides onto colloids, and sorption coefficients for radionuclides onto the rock matrix and alluvium) are similar to values used in the TSPA-SR model, and thus the mean behavior is not expected to be significantly different.

Updated Saturated Zone Flow and Transport Model for Supplemental TSPA Model Analyses—Simulated mean annual doses for the TSPA-SR base-case model (CRWMS M&O 2000a) are compared to the results of the supplemental TSPA model using the updated saturated zone flow and transport model in Volume 2, Section 3.2.10 of *FY01 Supplemental Science and Performance Analyses* (BSC 2001b). These results indicate that the changes to the updated saturated zone flow and transport model have little overall impact on the simulated mean annual dose in the supplemental TSPA analyses. The influences of higher values of bulk density in the alluvium and lower sorption coefficients for iodine-129 and technetium-99 on the simulated annual dose tend to counteract one another. In addition, the mean annual dose is influenced by a few of the highest-dose realizations at any particular time in a TSPA simulation. If these highest-dose realizations are the ones in which the importance of the retardation of key radionuclides is diminished (e.g., by low sorption coefficients or short path length in the alluvium), then the impact of the updated values of alluvial bulk density on the mean annual dose would be minimal.

Analyses of the Biosphere—Since the biosphere modeling for the TSPA-SR model, the supporting documentation for the biosphere has been revised, including updates of some parameter values.

The relatively small effect of changes to the biosphere model on the expected annual dose for the nominal scenario is reflected in the TSPA results shown in Volume 2, Section 3.2.11 of *FY01 Supplemental Science and Performance Analyses* (BSC 2001b). The mean annual dose using the supplemental uncertainty distributions for the biosphere dose conversion factors (BSC 2001a, Section 13.4.) is compared to the results calculated in the TSPA-SR model (CRWMS M&O 2000a, Section 4.1). The mean annual dose is slightly lower for the new nominal-scenario biosphere dose conversion factors for all times shown in the plot. The reduction in dose from the previously calculated annual dose (TSPA-SR base-case results) to the new result is less than 10 percent in simulated annual dose for most times and does not constitute a large change.

The results of the supplemental TSPA model using the new volcanic eruption biosphere dose conversion factors are presented in Volume 2, Section 3.2.11 of *FY01 Supplemental Science and Performance Analyses* (BSC 2001b). The mean annual dose using the new uncertainty distributions for the volcanic eruption biosphere dose conversion factors in the supplemental TSPA model is compared to the results calculated in the TSPA-SR model in this figure. These results indicate that, at all times, the expected mean annual dose is approximately 2.5 times greater for the new volcanic biosphere dose conversion factors relative to the previous TSPA-SR igneous model. This represents an increase in the mean dose rate relative to previous results and is primarily due to the increase in the respirable fraction of particulate concentration in air within the model (BSC 2001a, Section 13.3.6.2). However, the higher expected annual dose from direct exposure to contaminated volcanic ash using the new volcanic eruption biosphere dose conversion factors is still lower than the expected annual dose from the igneous groundwater pathway at later times (see *Total System Performance Assessment for the Site Recommendation* [CRWMS M&O 2000a, Section 4.2]).

4.4.5.6   Evaluation of Disruptive Events

In this section, analyses conducted to examine the sensitivity of performance to new information related to disruptive events developed since publication of *Total System Performance Assessment for the Site Recommendation* (CRWMS M&O 2000a) are described. Two potentially disruptive events are addressed: volcanism (i.e., igneous activity) and seismic events.

An uncertainty importance analysis was carried out for the TSPA-SR results (CRWMS M&O 2000a, Section 5.1) using various statistical methods to identify the most important contributors to the spread in the overall model results and to identify contributors to the extreme, or outlier, outcomes in the model results. The analysis showed that the most important parameters affecting the spread in model results are annual frequency of igneous intrusion and wind speed (BSC 2001b, Section 3.3.1).

4.4.5.6.1   Supplemental TSPA Model Igneous Disruptive Results

Igneous Event Wind-Speed Sensitivity—Volume 2, Section 3.3.1.2 of *FY01 Supplemental Science and Performance Analyses* (BSC 2001b) discusses mean probability-weighted annual doses for the supplemental model volcanic eruption case, comparing results from the TSPA-SR model with the mean of a set of 300 realizations that are identical in all regards to the TSPA-SR model except that the alternative distribution for wind speed has been used. Using the Desert Rock Airstrip data as described in Volume 1, Section 14.3.3.5 of *FY01 Supplemental Science and Performance Analyses* (BSC 2001a) increases the probability-weighted annual doses by a factor of approximately 2 from TSPA-SR model.

Igneous Event Waste Particle Size—Volume 2, Section 3.3.1.2 of *FY01 Supplemental Science and Performance Analyses* (BSC 2001b) discusses probability-weighted mean annual doses from the supplemental model eruptive case only, calculated for the seven waste-particle size distributions in Volume 1 of *FY01 Supplemental Science and Performance Analyses* (BSC 2001a, Table

14.3.3.4-1) and the TSPA-SR base-case distribution (CRWMS M&O 2000a, Section 3.10.2.2.2). All other input parameters in each case are identical to those used in the TSPA-SR model (CRWMS M&O 2000a, Sections 3.10.2 through 3.10.4). Calculated annual doses only vary by a factor of approximately 1.3 or less, and performance is relatively insensitive to uncertainty in waste particle diameter within the range considered in these analyses. Consistent with this observation, the distribution used in the supplemental TSPA analyses (BSC 2001b, Section 4) is unchanged from that used in TSPA-SR analyses (CRWMS M&O 2000a, Section 3.10.2.2.2).

Igneous Event Zone 1 and Zone 2 Sensitivity—Volume 2, Section 3.3.1.2 of *FY01 Supplemental Science and Performance Analyses* (BSC 2001b) presents a comparison of the 20,000-year probability-weighted mean annual doses calculated for Zone 1 for the TSPA-SR model distribution and for the supplemental distribution. All other models and input parameters used in these cases are the same as those used in the TSPA-SR model (CRWMS M&O 2000a, Sections 3.10.2.2 through 3.10.2.4). The revised distribution results in an increase in the calculated annual dose at all times, with a maximum change of a factor of approximately 2. Volume 2, Section 3.3.1.2 of *FY01 Supplemental Science and Performance Analyses* (BSC 2001b) presents the set of realizations calculated for Zone 1 with the revised distribution, with the 95th and 50th (median) curves shown with the mean. Note that the 5th percentile curve plots below the lowest value shown on the y-axis. Volume 2, Section 3.3.1.2 of *FY01 Supplemental Science and Performance Analyses* (BSC 2001b) present the same comparison for Zone 2. There is little or no change in the mean annual dose from Zone 2.

Conditional Igneous Events—Conditional mean annual dose histories were calculated for eruptive events at 100, 500, 1,000, and 5,000 years (BSC 2001b, Section 3.3.1.2.4). The mean annual dose history for an event at 100 years is repeated from Volume 2, Section 3.3.1.2.4 of *FY01 Supplemental Science and Performance Analyses* (BSC 2001b), and the mean annual dose histories for events at later times are each derived from 300 realizations analogous to those shown for the 100-year event

(BSC 2001b, Section 3.3.1.2.4). The similarity of the curves is consistent with the use of the same sampling of input parameters, and the differences in the initial annual dose at different times is due entirely to radioactive decay. The conditional mean dose in the first year for an eruptive event at 100 years is approximately 13 rem/yr (1.3×10^4 mrem/yr). The first-year conditional dose decreases to approximately one half this level by 500 years after closure, and is approximately 10 percent of this value after 5,000 years.

The conditional eruptive annual doses described in Volume 2, Section 3.3.1.2.4 of *FY01 Supplemental Science and Performance Analyses* (BSC 2001b) do not include any dose that might be incurred by direct inhalation of the ash cloud during the eruptive event.

Volume 2, Section 3.3.1.2.4 of *FY01 Supplemental Science and Performance Analyses* (BSC 2001b) discusses four annual dose histories discussed previously, with the addition of a conditional mean annual dose history calculated for an eruption occurring at 100 years and with the soil removal rate set to zero. This additional case was calculated to provide graphical confirmation of the relative roles of soil removal and radioactive decay, and it is not intended to represent a realistic estimate of annual doses following a conditional eruption. Soil removal due to agricultural processes is included as part of the set of realistic and reasonable models used in *Total System Performance Assessment for the Site Recommendation* (CRWMS M&O 2000a) and Volume 2, Section 3.3.1.2.4 of *FY01 Supplemental Science and Performance Analyses* (BSC 2001b). This final calculation confirms that the decrease in annual dose in the years following an eruption primarily is due to soil removal. The gradual decrease in annual dose after year 100 in this calculation is due entirely to radioactive decay, and the curve therefore intersects the first-year annual doses calculated for events at later times.

Volume 2, Section 3.3.1.2.4, Figure 3.3.1.2.4-4 of *FY01 Supplemental Science and Performance Analyses* (BSC 2001b) shows 500 out of the 5,000 realizations of 50,000-year igneous intrusion annual dose histories calculated for TSPA-SR model (CRWMS M&O 2000a, Section 4.2).

Results shown in this plot are identical to Figure 3.3.3-1 in Volume 2, Section 3.3.1 of *FY01 Supplemental Science and Performance Analyses* (BSC 2001b), except that the eruptive releases have been removed. Groundwater releases for each realization are shown weighted by the probability of the intrusive event occurring. In Volume 2, Section 3.3.1.2.4 of *FY01 Supplemental Science and Performance Analyses* (BSC 2001b), the same set of realizations are shown without probability-weighting. Peak mean annual dose from the igneous intrusion pathway increases from approximately 0.1 mrem/year in the probability-weighted case to approximately 500 mrem/year, consistent with the overall mean probability of an intrusive igneous event during the 50,000-year simulation of 8×10^{-4}.

Peak conditional annual doses associated with volcanic eruption are significantly higher than those associated with igneous intrusion (BSC 2001b, Section 3.3.1.2.4).

4.4.5.6.2 Supplemental TSPA Model Seismic Activity Analyses

Volume 1, Section 9.3.3 of *FY01 Supplemental Science and Performance Analyses* (BSC 2001a) considers a broad range of events and accounts for additional uncertainty in the magnitude of damage during the vibratory ground motion event. Volume 1 analyses consider the probability distribution shown in Volume 2, Table 3.3.2-1 of *FY01 Supplemental Science and Performance Analyses* (BSC 2001b). The supplemental results using this distribution are compared with the TSPA-SR base-case model results shown in Volume 2, Section 3.2.7.2 of *FY01 Supplemental Science and Performance Analyses* (BSC 2001b, Figure 3.3.2.1-1). The differences between these estimates of mean annual dose are small, and the uncertainty and extended range for the probability distribution for damage due to seismic activity have a negligible effect on the estimate of mean annual dose.

4.4.5.6.3 Supplemental TSPA Model Sensitivity Analyses for the Human Intrusion Scenario

No additional sensitivity analyses were performed on the human intrusion scenario by the supplemental TSPA model because the TSPA-SR model results were considered robust. The possible impact of unlikely igneous activity on human intrusion is analyzed and discussed in *Total System Performance Assessment Sensitivity Analyses for Final Nuclear Regulatory Commission Regulations* (Williams 2001b) and is summarized in Section 4.4.4 of this report.

4.5 MULTIPLE BARRIER ANALYSES

Evaluating the significance of the various natural and engineered barriers requires analyzing their relative importance in containing and isolating radioactive waste from the environment. The objective of such analyses is to evaluate the effectiveness and diversity of the barriers to determine the overall resiliency of the repository system to extreme conditions that are unlikely but within the range of those believed physically possible. These analyses address the nominal performance of the system (i.e., without the occurrence of disruptive events, such as igneous activity) and consist of the following elements:

- Identifying the natural features of the geologic setting and the design features of the engineered barrier system that are considered important to waste isolation

- Describing the capability of each of these barriers and their component features to isolate waste

- Identifying those aspects of each feature that provide assurance of acceptable overall performance of the system even if components of the barrier are degraded, deteriorated, or altered.

The following sections summarize the analyses that describe and evaluate the significance of the multiple barriers in the design of the potential repository at Yucca Mountain. Detailed discussions

and analyses are presented in the *Repository Safety Strategy: Plan to Prepare the Safety Case to Support Yucca Mountain Site Recommendation and Licensing Considerations* (CRWMS M&O 2001a, Volume 2) and *Total System Performance Assessment for the Site Recommendation* (CRWMS M&O 2000a, Section 5.3).

4.5.1 Identification and Description of Barriers

The barriers important to waste isolation at Yucca Mountain may be broadly categorized as natural barriers (associated with the geologic and hydrologic setting) and engineered barriers. The engineered barriers complement the natural barriers by prolonging the containment of radionuclides within the repository and limiting their eventual release. The natural barriers consist of the following:

- Surficial soils and topography, which limit water infiltration

- Unsaturated rock layers above the repository horizon, which limit water flux into repository drifts

- Unsaturated rock layers below the repository horizon, which limit radionuclide transport

- Volcanic tuffs and alluvial deposits below the water table, which limit radionuclide transport in the saturated zone.

The engineered barriers consist of the following:

- A drip shield, which limits the water contacting the waste package and the water available for advective transport through the waste package and invert

- A waste package, which limits the water contacting the waste form

- Cladding, which limits the water contacting the commercial spent nuclear fuel portion of the waste

- A waste form that limits the rate of release of radionuclides to the water that contacts the waste

- A drift invert, which limits the rate of release of radionuclides to the natural barriers.

Directly or indirectly, the identified barriers affect several of the key attributes that influence the ability of the natural and engineered systems to contain and isolate wastes from the biosphere. The key attributes, as detailed in Section 4.2, include: (1) limited water entering emplacement drifts; (2) long-lived waste packages and drip shields; (3) limited release of radionuclides from the engineered barrier system; (4) delay and dilution of radionuclide concentration by the natural barriers; and (5) low mean annual dose considering potentially disruptive events. The potential effects associated with disruptive processes and events are addressed in Section 4.3.2. Section 4.2 also presents the technical basis and uncertainty associated with the projected performance of each barrier and describes the physical and chemical processes that operate on or within each barrier.

Table 4-39 illustrates the correlation between the attributes, barriers, and the processes as described in Section 4.2. The process models indicated in Table 4-39 form the individual component models of the TSPA-SR model. As indicated in Table 4-39, multiple processes must be analyzed to evaluate each barrier's ability to contribute to repository performance. Additional discussion of the model components of the TSPA-SR model are found in Section 4.2 of this report and in Section 3 of the *Total System Performance Assessment for the Site Recommendation* (CRWMS M&O 2000a).

The supplemental and revised supplemental TSPA models have nearly identical component models. Detailed information on the supplemental TSPA model may be found in *FY01 Supplemental Science and Performance Analyses* (BSC 2001a; BSC 2001b), and information on the revised supplemental TSPA model may be found in *Total System Performance Assessment—Analyses for Disposal of Commercial and DOE Waste Inventories at Yucca Mountain—Input to Final*

Table 4-39. **Correlation of Barrier and Barrier Functions to Key Attributes of Yucca Mountain Repository System and Process Models**

Key Attributes of System	Process Model	Barrier	Barrier Function
Limited Water Entering Emplacement Drifts	Climate	Surficial soils and topography	Reduce the amount of water entering the unsaturated zone by surficial processes (e.g., precipitation lost to runoff, evaporation, and plant uptake)
	Net Infiltration		
	Unsaturated Zone Flow	Unsaturated rock layers overlying the repository and host unit	Reduce the amount of water reaching emplacement drifts by subsurface processes (e.g., lateral diversion and flow around emplacement drifts)
	Coupled Effects on Unsaturated Zone Flow		
	Seepage into Emplacement Drifts		
	Coupled Effects on Seepage		
Long-Lived Waste Package and Drip Shield	In-Drift Physical and Chemical Environments	Drip shield around the waste packages	Prevent water contacting the waste package and waste form by diverting water flow around the waste package; therefore limiting advective transport through the invert
	In-Drift Moisture Distribution		
	Drip Shield Degradation and Performance		
	Waste Package Degradation and Performance	Waste package	Prevent water from contacting the waste form
Limited Release of Radionuclides from the Engineered Barriers System	Cladding Degradation and Performance	Spent fuel cladding	Delay and/or limit liquid water contacting spent nuclear fuel after waste packages have degraded
	Radionuclide Inventory	Waste form	Potentially prevent liquid water contacting waste during the period when temperatures in the commercial spent nuclear fuel waste packages are elevated and limit radionuclide release rates as a result low solubilities
	In-Package Environments		
	Commercial Spent Nuclear Fuel Degradation and Performance		
	DOE Spent Nuclear Fuel Degradation and Performance		
	DOE High-Level Radioactive Waste Degradation and Performance		
	Dissolved Radionuclide Concentrations		
	Colloid-Associated Radionuclide Concentrations		
	In-Package Radionuclide Transport		
	Engineered Barrier System (Invert) Degradation and Performance	Drift invert	Limit radionuclide transport out of engineered barrier system
Delay and Dilution of Radionuclide Concentration by the Natural Barriers	Unsaturated Zone Radionuclide Transport (Advective Pathways; Retardation; Dispersion; Dilution)	Unsaturated rock layers below the repository	Delay radionuclide movement to the groundwater aquifer because of water residence time, matrix diffusion, and/or sorption
	Saturated Zone Radionuclide Transport	Volcanic tuff and alluvial deposits below the water table (flow path extending from below the repository to point of compliance)	Delay radionuclide movement to the receptor location by water residence time, matrix diffusion, and/or sorption
	Dilution		
Low Mean Annual Dose Considering Potentially Disruptive Events	Probability of Volcanic Eruption	N/A	N/A: These process and events may affect performance but are not barriers
	Characteristics of Volcanic Eruption		
	Effects of Volcanic Eruption		
	Atmospheric Transport of Volcanic Eruption		
	Biosphere Dose Conversion Factors		
	Probability of Igneous Intrusion		
	Characteristics of Igneous Intrusion		
	Effects of Igneous Intrusion		

NOTE: N/A = not applicable.

Environmental Impact Statement and Site Suitability Evaluation (Williams 2001a).

The following paragraphs summarize the role that the barriers and processes play in the attributes of the Yucca Mountain site.

Barriers and Processes that Contribute to Limit Water Entering Emplacement Drifts—Several barriers combine to limit the amount and distribution of water that may enter emplacement drifts and come into contact with the waste packages. The natural barriers work together to limit water infiltration and seepage flux. Both the amount and distribution of water in the unsaturated rocks at Yucca Mountain are currently controlled by the arid climate regime, which limits annual precipitation in the area, and by the surficial bedrock and soils, which encourage significant loss of water through runoff and evapotranspiration. These processes combine to limit the annual amount of water that infiltrates though the surficial soils. The technical basis and uncertainty associated with the understanding of these processes as they affect performance are described in Section 4.2.1.

The flow characteristics of the welded tuff units at the potential repository horizon limit the amount and distribution of water that can seep into the repository. Much of the limited flux that reaches the repository horizon will be diverted around the drifts by the capillary suction within the fractured rock mass.

Barriers and Processes that Contribute to the Long-Lived Waste Package and Drip Shield—Any water that does seep into the repository drifts will be diverted away from the waste package by the titanium drip shield for as long as the drip shield remains intact. The purpose of this engineered barrier is to protect the waste package from direct contact with water that seeps into the drifts. Another important function of the drip shield is to limit the advective flux of water that can transport waste through the invert materials if waste packages breach earlier than expected during the lifetime of the drip shield. Drip shields also provide a mechanical barrier, protecting waste packages from potential damage from rockfall.

The most important barrier to radionuclide migration is the waste package itself. The characteristics and rates of waste package degradation depend on the environment. Those aspects of the natural environment that affect the performance of the waste package as a barrier consist of the thermal-hydrologic, thermal-chemical, and thermal-mechanical environments.

The waste package lifetime is affected by the degradation modes and rates of the corrosion-resistant Alloy 22 over the surface area of the waste package and at the closure welds. These degradation modes include general and localized corrosion, as well as stress corrosion cracking. The technical basis and uncertainty associated with these degradation modes and their corresponding rates are presented in Section 4.2.4.

In reevaluating the potential of early failure mechanisms and their potential consequences, a more conservative approach resulted in the inclusion of improper heat treatment and subsequent possible failure of a few waste packages in the TSPA supplemental analysis. The nonmechanistic early waste package failure assumes failure of both the inner and outer Alloy 22 lids and the stainless steel inner lid. To ensure that the potential consequence of early waste package failures is treated conservatively, it is included in the nominal scenario, not as a sensitivity analysis. Volume 1, Section 7.3.6 of *FY01 Supplemental Science and Performance Analyses* (BSC 2001a) describes the model developed for the potential consequences of improper heat treatment of a waste package.

Barriers and Processes that Contribute to Limited Release of Radionuclides from the Engineered Barriers—Based on the analyses presented in Section 4.4.2, most waste packages are expected to remain intact for much more than 10,000 years. However, eventually the waste packages will degrade. Once the waste packages have been breached, the possibility exists for water to contact the waste and mobilize radionuclides. Even then, the waste forms (spent fuel or borosilicate glass) will limit the rate of radionuclide release because they are relatively stable solids that will degrade slowly. The thermal-hydrologic-chemical environment inside the waste package affects the

rate and amount of degradation of the waste forms. In addition, in the case of most commercial spent nuclear fuel, a significant mechanism that delays the degradation rate of the waste is Zircaloy cladding.

Once radionuclides are released from the waste package, they must be transported through the invert materials before being released to the natural barriers. During the time when the drip shield is intact, or in instances of insignificant seepage into the drifts, the release of radionuclides through the invert is limited to diffusive processes. Depending on the diffusive characteristics of the invert materials, which depend on the in-drift thermal-hydrologic environment, diffusive processes may be a significant barrier to radionuclide migration.

Barriers and Processes That Contribute to Delay and Dilution of Radionuclide Concentration by the Natural Barriers—Once radionuclides have been released from the waste packages and transported through the engineered invert materials, they must then migrate through the unsaturated rock between the repository and the water table, and then through approximately 18 km (11 mi) of saturated volcanic rocks and alluvial deposits between the repository and the point at which the receptor uses the water. Both the unsaturated and saturated rock units provide natural barriers to the migration of these radionuclides. Their combined effect is to limit the mass breakthrough and, therefore, the concentration of radionuclides in the accessible environment.

Processes That Affect Whether Disruptive Events Will Compromise Repository Performance—Because an igneous intrusion or volcanic eruption could degrade the performance of both the natural and engineered barriers of the site, it is important to evaluate the extent to which these processes would affect performance. Evaluations of volcanic and igneous intrusion scenarios consider both the likelihood and consequences of each type of event, including analyses of potential exposure pathways.

The following section details the approaches taken in evaluating the contribution of the various barriers and the significance of the uncertainty associated with each of the natural and engineered barriers on overall system performance.

4.5.2 Approaches to Evaluation of Multiple Barriers

Three separate approaches were used to evaluate the contribution that different barriers provide to the overall performance of the repository system in the absence of disruptive events. The first approach, documented in Section 4.4.2, details the intermediate performance of the total system as the system evolves over time. This approach describes the results of the system's temporal and spatial evolution and the uncertainty in this evolution. For example, the rate of degradation and the mass release rate for several key radionuclides, as well as the uncertainty associated with this evolution, were identified and analyzed for several discrete spatial locations (the waste package, the edge of the invert, the base of the unsaturated zone, and at the accessible environment approximately 20 km [12 mi] from the repository footprint). Examining the intermediate results both in space and time, as detailed in Section 4.4.2, provides one level of indication of an individual barrier's contribution to the overall performance of the system.

The second approach for evaluating an individual barrier's contribution to the system performance has been termed "barrier-importance analysis." In this approach, the key parameters affecting the performance of each barrier are fixed at the extreme of their uncertainty distribution (either the 5th or 95th percentile, whichever leads to maximizing the dose rate over the time period of interest), and all other parameters and models are sampled stochastically as done in the base case. This partial degradation of the function of the barrier leads to more conservative dose projections. By comparing the TSPA-SR model nominal performance base-case results with the degraded performance results, one can examine the relative contribution of each of the barriers. The results of this approach are presented in Section 5.3 of *Total System Performance Assessment for the Site Recommendation* (CRWMS M&O 2000a).

The third approach for evaluating a barrier's contribution to the system performance has been termed

the "barrier-neutralization analysis." In this approach, the function a particular barrier(s) has in either reducing water contacting waste or reducing the transport of radionuclides is completely removed from the analysis (i.e., the capacity of the barrier(s) to limit the movement of water or radionuclides is set to zero). Neutralization analyses are the extreme of the partially degraded barrier analyses discussed above. They provide insights into the overall system behavior and the importance of the barrier(s) to defense in depth. Further discussion of barrier neutralization analyses are presented in *Repository Safety Strategy: Plan to Prepare the Safety Case to Support Yucca Mountain Site Recommendation and Licensing Considerations* (CRWMS M&O 2001a, Volume 2).

Although the parameter values used in the partially degraded barrier analyses are within the range of values considered reasonably possible, the results should not be interpreted as representing the expected behavior of the system. The expected behavior of the system in the absence of igneous disruption is represented by the mean nominal performance result, and the degraded barrier analyses are presented only to provide insight into the resilience of the repository system to extreme conditions. To ensure a balanced interpretation of the degraded barrier analysis, results are shown paired with comparable analyses using the 5th or 95th percentile values (as appropriate) of the same parameters that result in improved performance. The mean result from the full nominal analysis should be interpreted as the best estimate of future performance, and both the degraded and improved performance analyses should be interpreted as being equally likely (or unlikely) to occur.

The following two sections detail the individual barrier analyses conducted to examine the robustness of the repository system's performance. Section 4.5.3 discusses the effects of the natural barriers on overall performance, and Section 4.5.4 covers the engineered barriers' effects on performance. Table 4-40 lists the figures presented in these two sections. In addition to the partially degraded barrier importance analyses, a representative barrier neutralization analysis is presented in Section 4.5.4. Additional details on these analyses and additional analyses are presented in the *Total*

System Performance Assessment for the Site Recommendation (CRWMS M&O 2000a, Section 5.3) and *Repository Safety Strategy: Plan to Prepare the Safety Case to Support Yucca Mountain Site Recommendation and Licensing Considerations* (CRWMS M&O 2001a, Volume 2), as well as *FY01 Supplemental Science and Performance Analyses* (BSC 2001a; BSC 2001b).

4.5.3 Evaluation of Natural Barrier Components

There are two natural barriers above the repository that contribute to the long-term performance of the repository system: (1) the surficial soils and topography, which limit the amount of water that infiltrates into the rock; and (2) the unsaturated rocks, which limit the amount of water that seeps into the repository. Barrier-importance analyses have been conducted for each of these barriers.

The net surficial infiltration flux into Yucca Mountain is affected by uncertainty about future climate states and surficial processes. As explained in Section 4.2, the TSPA-SR analyses considered a range of infiltration rates. In partially degrading the surficial barrier, the assumption applied was that the maximum possible infiltration rate corresponding to the maximum anticipated climate state (the glacial-transition climate) prevailed throughout the duration of the 100,000-year simulated time period. To evaluate the consequences of a more positively performing surficial barrier, a separate scenario was analyzed, extrapolating the present-day climate's minimum infiltration rate throughout the entire duration of the simulated time period. The effects of these partial degradations of the surficial barrier are illustrated in Figure 4-208, which shows that the surficial infiltration rate over the range of likely conditions does not significantly affect the long-term performance of the repository system.

The net seepage into the repository drifts is affected by the percolation flux through the host rock and the rock properties around the emplacement drifts. To investigate the significance of seepage to system performance, a scenario was constructed that fixed (1) the infiltration rate at the maximum value of the three potential distributions,

Table 4-40. Partially Degraded Barrier Importance Analyses Figures

Key Attributes of System	Process Model Factor	Barrier	Figure
Limited Water Entering Emplacement Drifts	Climate	Surficial soils and topography	4-208
	Net Infiltration		
	Unsaturated Zone Flow	Unsaturated rock layers overlying the repository and host unit	4-209 and 4-211
	Coupled Effects on Unsaturated Zone Flow		
	Seepage into Emplacement Drifts		
	Coupled Effects on Seepage		
Long-Lived Waste Package and Drip Shield	In-Drift Physical and Chemical Environments	Drip shield above the waste packages	4-213
	In-Drift Moisture Distribution		
	Drip Shield Degradation and Performance		
	Waste Package Degradation and Performance	Waste package	4-214 and 4-218
Limited Release of Radionuclides from the Engineered Barriers	Cladding Degradation and Performance	Spent fuel cladding	4-215 and 4-218
	Radionuclide Inventory	N/A	
	In-Package Environments		
	Commercial Spent Nuclear Fuel Degradation and Performance	Waste form	4-216
	DOE Spent Nuclear Fuel Degradation and Performance		
	DOE High-Level Radioactive Waste Degradation and Performance		
	Dissolved Radionuclide Concentrations		
	Colloid-Associated Radionuclide Concentrations		
	In-Package Radionuclide Transport		
	Engineered Barrier System (Invert) Degradation and Performance	Drift Invert	4-217
Delay and Dilution of Radionuclide Concentration by the Natural Barriers	Unsaturated Zone Radionuclide Transport (Advective Pathways; Retardation; Dispersion; Dilution)	Unsaturated rock layers below the repository	4-210 and 4-211
	Saturated Zone Radionuclide Transport	Volcanic tuff and alluvial deposits below the water table (flow path extending from below the repository to point of compliance)	4-212
	Wellhead Dilution		
Low Mean Annual Dose Considering Potentially Disruptive Events	Probability of Volcanic Eruption	N/A	
	Characteristics of Volcanic Eruption		
	Effects of Volcanic Eruption		
	Atmospheric Transport of Volcanic Eruption		
	Biosphere Dose Conversion Factors		
	Probability of Igneous Intrusion		
	Characteristics of Igneous Intrusion		
	Effects of Igneous Intrusion		

NOTE: N/A = not applicable.

06/25/2000, 1:33 PM, SR00_047nm5.gsm; 06/28/2000, 1:40 AM, SR00_062nm5.gsm;
06/28/2000, 5:18 AM, SR00_063nm5.gsm; SR00_062nm5_and_063nm5.JNB

00075DC_ATP_Z1S45_Fig-09.eps

Figure 4-208. Sensitivity of the Mean Dose Rate Projected by the TSPA-SR Base-Case Model Assuming a Degraded and an Enhanced Infiltration Barrier
The receptor is assumed to be 20 km (12 mi) from the repository footprint. Annual water demand was assumed to be approximately 2,000 acre-ft. Source: CRWMS M&O 2000a, Figure 5.2-1.

(2) the flow-focusing factor at its maximum to allow a greater fraction of the total percolation to come into contact with the repository drifts, (3) the seepage fraction at its maximum value, and (4) the seepage flow rate at its maximum value. All of these changes tend to force a greater fraction of the total percolation flux to seep into the repository emplacement drifts. To evaluate the consequences of a more positively performing seepage barrier, the above values were also fixed at their minimum values from the distributions presented in Section 4.2.

The effects of this partial degradation of the seepage barrier are illustrated in Figure 4-209. This figure shows that, for the first 40,000 years, the degradation (or improvement) of this barrier has little net consequence. This is because the waste packages are intact for most of this period, and even when waste packages are breached, the drip shield remains intact for a portion of this time. Even if both these barriers are breached, the domi-

nant radionuclide contributing to dose is the mobile technetium-99, which can diffuse through surface water films relatively rapidly (even in the absence of significant advective flux) because of its extremely high solubility. Because the solubility-limited radionuclides like neptunium-237 are the radionuclides most affected by seepage, the significance of seepage to overall performance does not become pronounced until this radionuclide becomes the dominant dose contributor, at about 40,000 years.

There are two additional natural barriers below the repository block: the unsaturated zone rock units and the saturated zone rock units. Both affect the transport of both dissolved and colloidal radionuclides from the engineered barriers to the point where such radionuclides could be extracted with the groundwater.

The significance of the unsaturated zone transport barrier was evaluated by fixing the transport
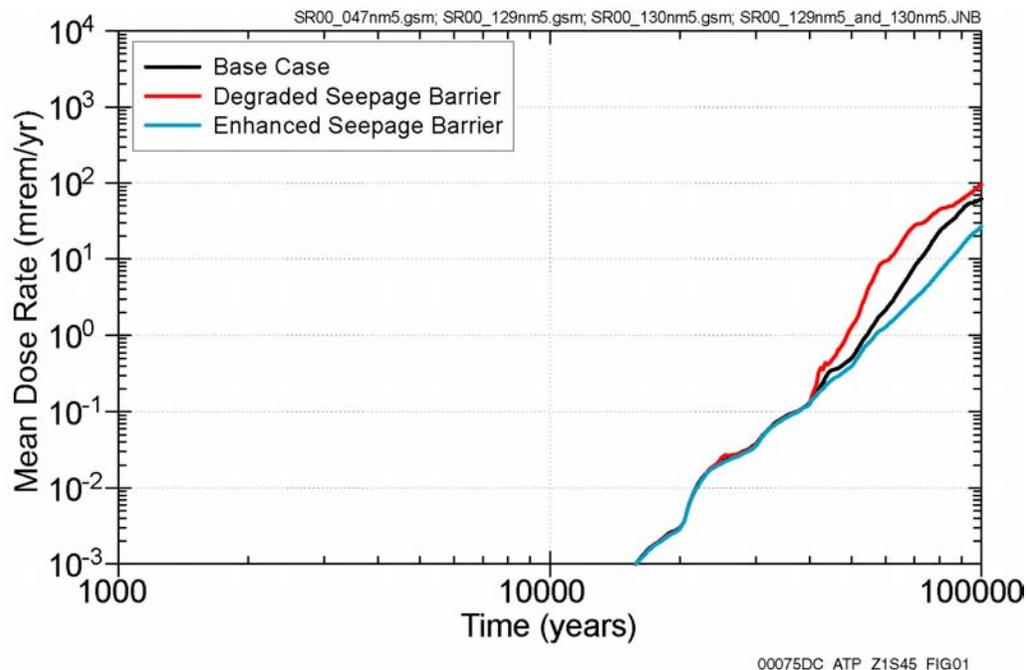
Figure 4-209. Sensitivity of the Mean Dose Rate Projected by the TSPA-SR Base-Case Model Assuming a Degraded and an Enhanced Seepage Barrier
The receptor is assumed to be 20 km (12 mi) from the repository footprint. Annual water demand was assumed to be approximately 2,000 acre-ft. Source: CRWMS M&O 2000a, Figure 5.3-1.

parameters within the transport model to minimize retention in the unsaturated zone. This was accomplished by using the 5th percentile on sorption parameters for aqueous and colloid-borne radionuclides (K_d and K_c, respectively), the 95th percentiles on fracture apertures, and the 5th percentile on the matrix diffusion coefficient. To investigate the more optimistic end of the range of uncertainty, a similar analysis was conducted with the distributions at the opposite extremes. The results of this analysis are illustrated in Figure 4-210. Degrading the unsaturated zone transport barrier decreases the transport time of neptunium-237 through the geologic media and, therefore, increases the dose rate at a point 20 km (12 mi) from the repository footprint for a period from 20,000 to 40,000 years.

To evaluate the combined effect of the two unsaturated zone barriers (seepage in unsaturated rock layers overlying the repository and transport in unsaturated rock layers below the repository), a combined degradation analysis was performed. Figure 4-211 presents the results of this analysis; they illustrate that the combined effect of both

barriers is approximately additive. This indicates that the contributions of the two unsaturated zone barriers are independent.

The significance of the saturated zone transport barrier is affected by several flow and transport parameters. In addition to the transport parameters described previously for unsaturated zone transport, the saturated zone flow fields are also uncertain, as are the possible flow path lengths through the alluvium and the alluvium transport characteristics. To investigate the significance of the saturated zone transport barrier, all realizations used the 95th percentile breakthrough curve (i.e., that distribution of mass flux that for a given release rate to the water table causes the 95th percentile mass flux at a location 20 km [12 mi] from the repository footprint). The results of this analysis are illustrated in Figure 4-212. These results indicate that the saturated zone barrier has minimal significance when it is degraded, since the mean dose response correlates closely to the more conservative portion of the saturated zone transport characteristics. However, the enhanced barrier
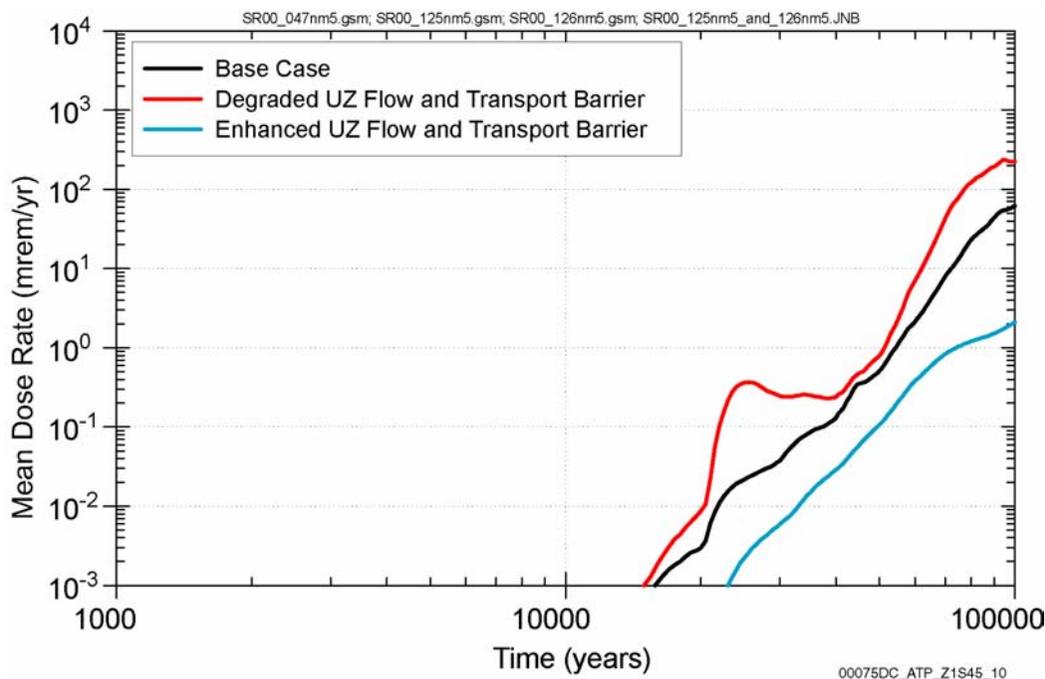
Figure 4-210. Sensitivity of the Mean Dose Rate Projected by the TSPA-SR Base-Case Model Assuming a Degraded and an Enhanced Unsaturated Zone Transport Barrier

The receptor is assumed to be 20 km (12 mi) from the repository footprint. Annual water demand was assumed to be approximately 2,000 acre-ft. UZ = unsaturated zone. Source: CRWMS M&O 2000a, Figure 5.3-11.
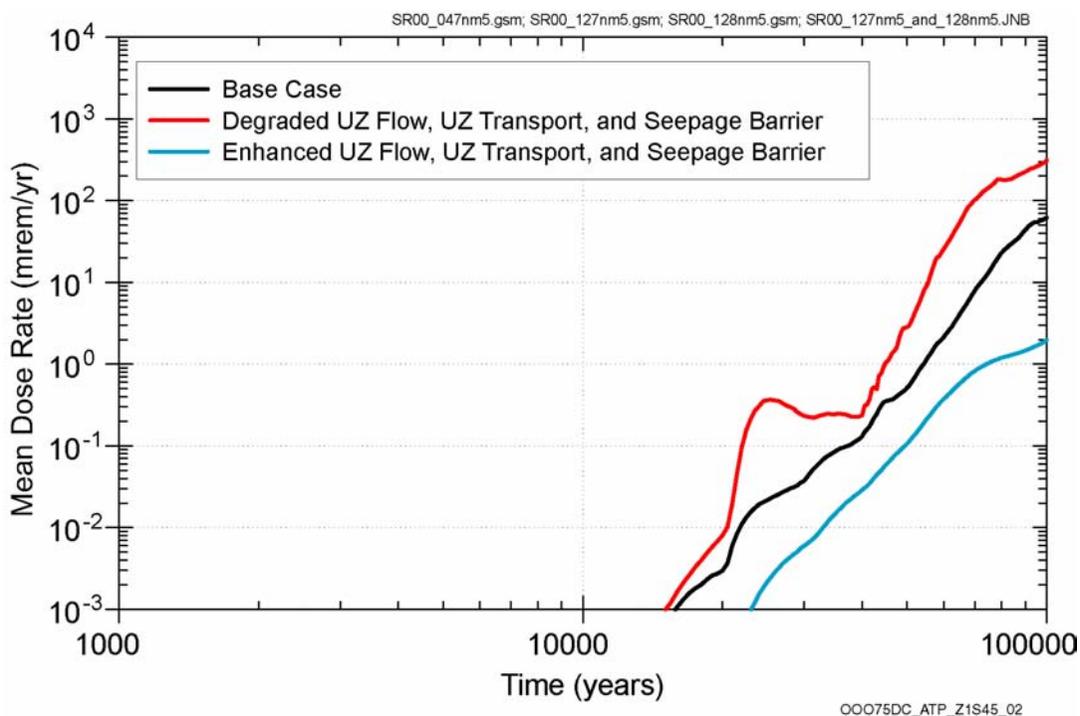
Figure 4-211. Sensitivity of the Mean Dose Rate Projected by the TSPA-SR Base-Case Model Assuming a Degraded and an Enhanced Unsaturated Zone Flow, Unsaturated Zone Transport, and Seepage Barrier

The receptor is assumed to be 20 km (12 mi) from the repository footprint. Annual water demand was assumed to be approximately 2,000 acre-ft. UZ = unsaturated zone. Source: CRWMS M&O 2000a, Figure 5.3-12.

06/25/2000, 1:33 PM, SR00_047nm5.gsm; 07/07/2000, 1:49 AM, SR00_084nm5.gsm;
07/07/2000, 4:09 AM, SR00_087nm5.gsm; SR00_084nm5_and_087nm5.JNB

00075DC_ATP_Z1S45_Fig-03.eps
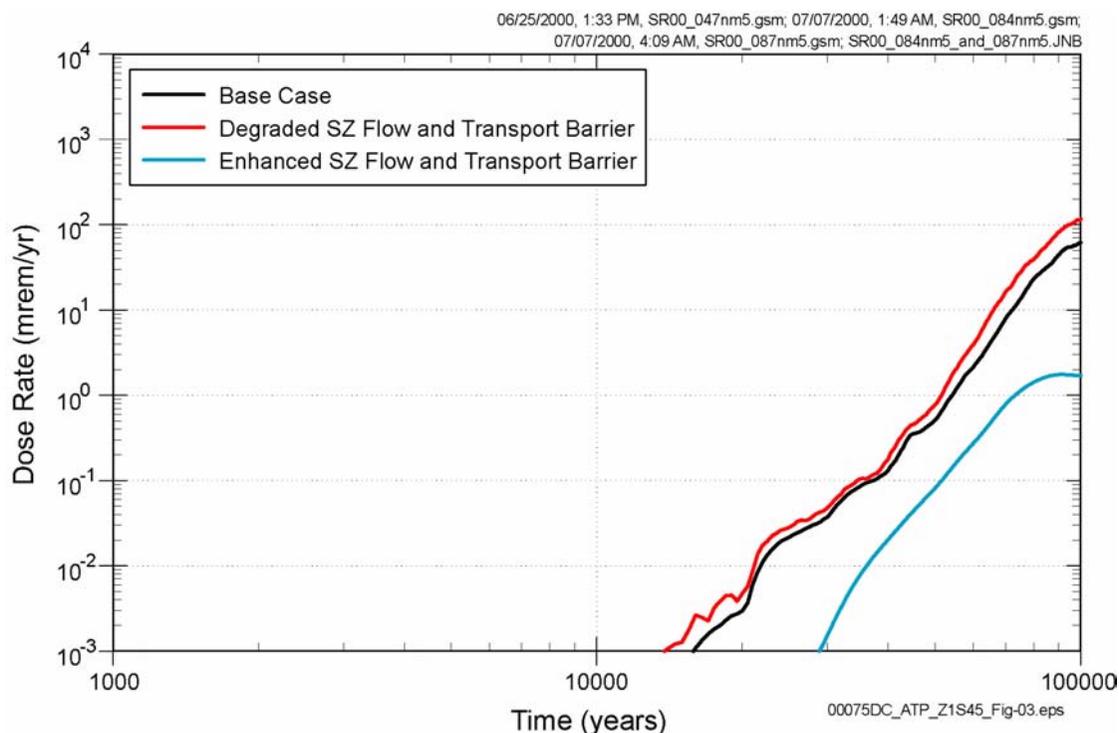
Figure 4-212. Sensitivity of the Mean Dose Rate Projected by the TSPA-SR Base-Case Model Assuming a Degraded and an Enhanced Saturated Zone Flow and Transport Barrier

The receptor is assumed to be 20 km (12 mi) from the repository footprint. Annual water demand was assumed to be approximately 2,000 acre-ft. SZ = saturated zone. Source: CRWMS M&O 2000a, Figure 5.3-13.

performance of the saturated zone (which includes parameter assessments that are believed to be more realistic than the base case) is found to significantly delay the transport of neptunium-237 and therefore lower the expected dose.

4.5.4 Evaluation of Engineered Barrier Components

As shown in Table 4-39, the engineered barrier components consist of the drip shield, the waste package, cladding, the waste form, and the drift invert. The principal function of these engineered barriers is to contain the radionuclides as long as possible and, once the containment has been breached, to slow the release of radionuclides to the natural barriers. This section discusses the significance of each of the engineered barriers.

The significance of the drip shield barrier has been examined by fixing the corrosion rate of titanium at

the 95th percentile of the distribution. This tends to decrease the lifetime of the drip shield from about 20,000 years to less than 10,000 years. The effect of this change on the calculated dose, however, is minimal (Figure 4-213). This minimal impact is a result of the degradation characteristics of the waste package and the form of the radionuclide release from degraded waste packages.

The titanium drip shield emplaced over the waste package has a modeled lifetime of about 20,000 to 40,000 years (see the results presented in Section 4.4.2 using the models and analyses summarized in Section 4.2). The waste package has a modeled lifetime of about 12,000 to over 100,000 years. As noted in Section 4.4.2, when the waste packages initially are breached, the more mobile radionuclide constituents (notably technetium-99 and iodine-129) can diffuse through the waste package and the invert materials and are not significantly affected by seepage through the degraded drip
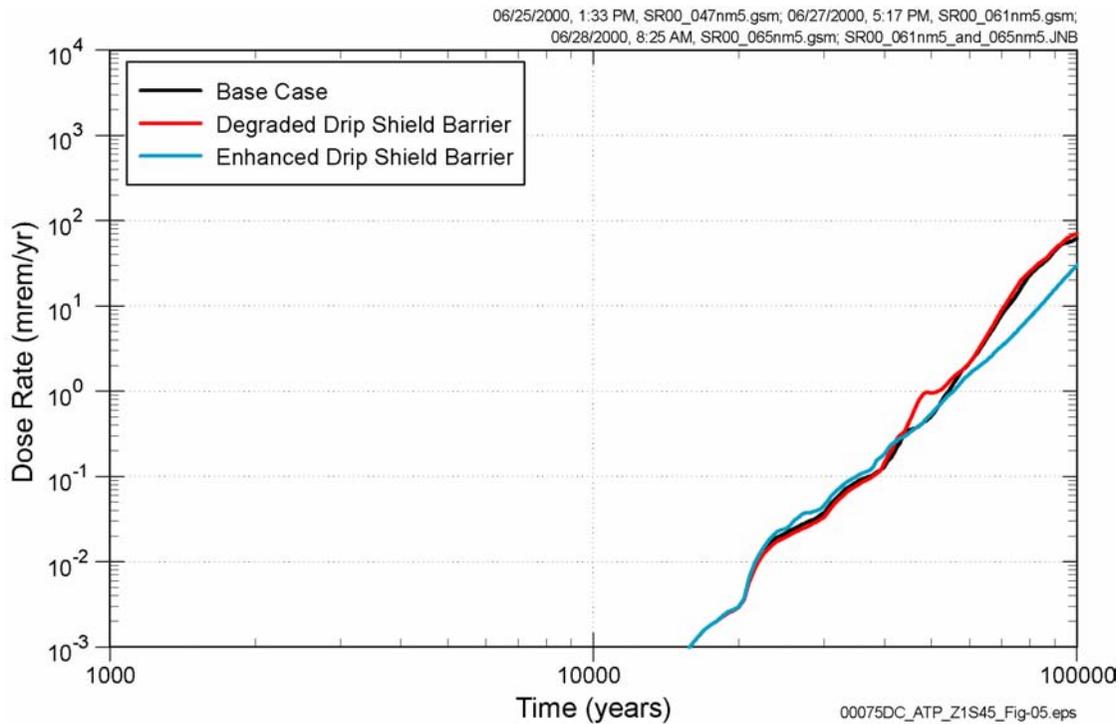
Figure 4-213. Sensitivity of the Mean Dose Rate Projected by the TSPA-SR Base-Case Model Assuming a Degraded and an Enhanced Drip Shield Barrier

The receptor is assumed to be 20 km (12 mi) from the repository footprint. Annual water demand was assumed to be approximately 2,000 acre-ft. Source: CRWMS M&O 2000a, Figure 5.3-3.

shields. Once their degradation starts, the drip shields degrade over about a 20,000-year time frame, which minimizes the function they play once the waste packages are breached. As a result, the significance of the drip shield barrier is primarily as a defense-in-depth barrier in that it provides additional assurance in the unlikely event that waste packages may be prematurely breached by some unanticipated process or event as described in *Repository Safety Strategy: Plan to Prepare the Safety Case to Support Yucca Mountain Site Recommendation and Licensing Considerations* (CRWMS M&O 2001a, Volume 2, Section 3.4.2).

Uncertainty analysis has determined that the waste package degradation parameters that most significantly affect degradation time are:

- Stress state at the stress-relieved closure welds

- Yield strength of the base metal at the closure welds

- Corrosion rate of Alloy 22, especially at the heat-affected zone associated with the outer and middle lid closure welds

- Accelerated corrosion rates associated with aging and microbially influenced corrosion, especially at the closure welds

- Size and frequency of defect flaws at the closure welds.

A degraded waste package barrier importance analysis was conducted in which each of these parameters was fixed at its 95th percentile value (except for yield strength, where the 5th percentile value leads to more conservative early waste package breaches). The results of this analysis are illustrated in Figure 4-214. The analysis illustrates
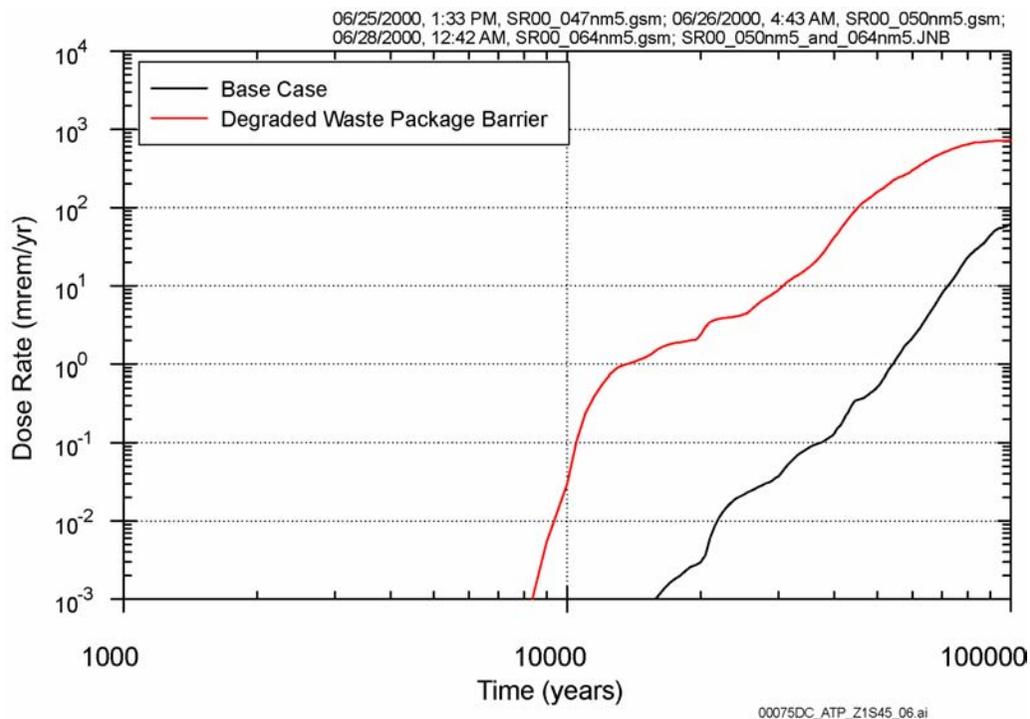
Figure 4-214. Sensitivity of the Mean Dose Rate Projected by the TSPA-SR Base-Case Model Assuming a Degraded and an Enhanced Waste Package Barrier
The receptor is assumed to be 20 km (12 mi) from the repository footprint. Annual water demand was assumed to be approximately 2,000 acre-ft. The enhanced waste package barrier resulted in no dose during the first 100,000 years. Source: CRWMS M&O 2000a, Figure 5.3-5.

that earlier breaches of the waste package lead to earlier doses at the point of water extraction and, ultimately, to higher doses. Even the degraded waste package performance analysis, however, calculated doses that are small compared to the standards, due to the performance of the other natural and engineered barriers.

Once the waste packages are breached, the waste form may be exposed to moisture (in the form of humid air if there is no seepage or the drip shield is intact or liquid seepage if the waste is sufficiently cool and liquid water seeps into the waste package). In the case of commercial spent nuclear fuel, Zircaloy cladding provides another barrier, delaying the time at which moisture may directly contact the spent fuel. The degradation rate of the cladding, however, is uncertain. To evaluate the importance of this barrier, a scenario was constructed in which all fuel rods were assumed to be perforated at the time the waste package was breached, and the unzipping rate was set at the

maximum value. The results of this analysis are illustrated in Figure 4-215.

Once the waste packages and cladding have been breached, the waste forms themselves must be altered, and the radionuclides must transition to a mobile phase before they can be transported out of the engineered barriers. The mobility of each radionuclide is a function of the geochemical environment and the sorption/desorption characteristics of that radionuclide on any mobile colloidal material (e.g., iron oxide, degraded fuel, silicon, or clay). The significance of this geochemical barrier was evaluated by using near-maximum solubilities in the waste package and invert materials and maximizing the sorption of radionuclides onto colloids. The results of this barrier analysis are shown in Figure 4-216. This figure shows, again, that prior to about 40,000 years, the dominant radionuclides are not controlled by the solubility or colloid concentrations. After 40,000 years, the soluble neptunium-237 and colloidal pluto-

06/25/2000, 1:33 PM, SR00_047nm5.gsm; 06/28/2000, 9:18 PM, SR00_066nm5.gsm;
06/28/2000, 7:52 PM, SR00_067nm5.gsm; SR00_066nm5_and_067nm5.JNB

00075DC_ATP_Z1S45_Fig-07.eps
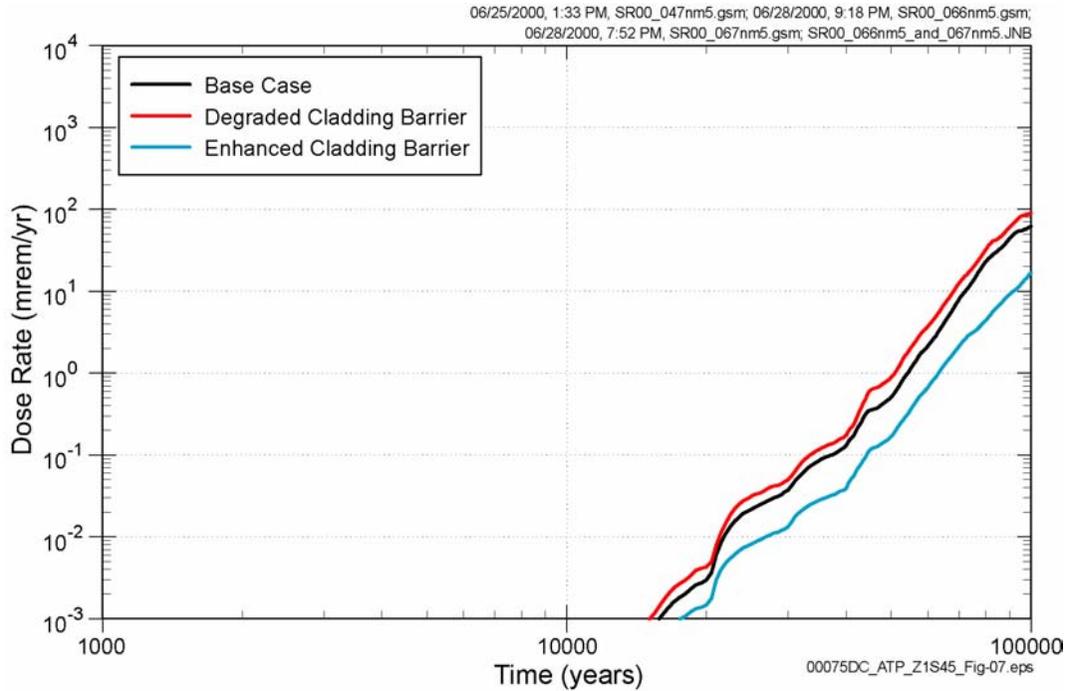
Figure 4-215. Sensitivity of the Mean Dose Rate Projected by the TSPA-SR Base-Case Model Assuming a Degraded and an Enhanced Cladding Barrier

The receptor is assumed to be 20 km (12 mi) from the repository footprint. Annual water demand was assumed to be approximately 2,000 acre-ft. Source: CRWMS M&O 2000a, Figure 5.3-7.

SR00_047nm5; SR00_093nm5; SR00_094nm5; SR00_093nm5_and_SR00_094nm5.JNB

00075DC_ATP_Z1S45_11.eps
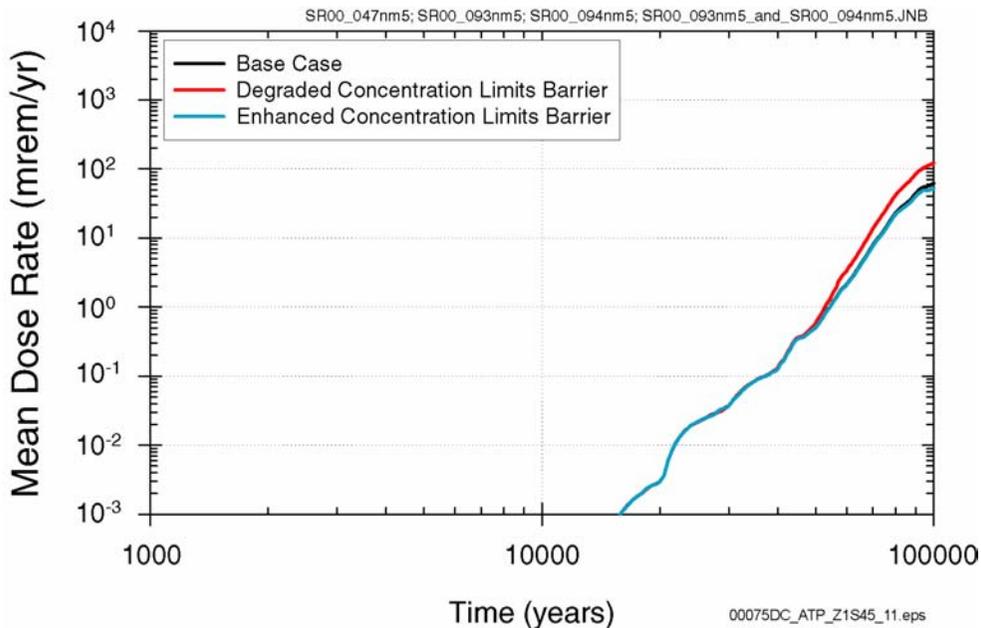
**Figure 4-216. Sensitivity of the Mean Dose Rate Projected by the TSPA-SR Base-Case Model Assuming a Degraded and an Enhanced Concentration Limits Barrier**

The receptor is assumed to be 20 km (12 mi) from the repository footprint. Annual water demand was assumed to be approximately 2,000 acre-ft. Source: CRWMS M&O 2000a, Figure 5.3-8.

nium-239 are important, but degrading this barrier did not have an appreciable effect on overall performance.

In addition to the effect of the waste form and the mobility of different radionuclides, the drift invert materials themselves can significantly affect the release of radionuclides. Figure 4-217 illustrates the combined effect of modifying the in-drift chemistry and colloidal fraction with different diffusion coefficients through the invert. Increasing the diffusion coefficient (i.e., degraded engineered barrier system transport barrier) has the effect of allowing greater diffusive releases through the engineered barrier system, even during the time period that the drip shields are intact (i.e., prior to about 30,000 years). Decreasing the diffusion coefficient (i.e., enhanced engineered barrier system transport barrier) has the effect of allowing essentially no diffusive releases. In this later case, there are essentially no releases from the engineered barrier system at all, until such time as the drip shields have degraded sufficiently to allow advective water into the waste package.

In addition to the partial degradation analyses described previously, a range of barrier neutralization analyses have been conducted to gain additional insight into the defense in depth of the various natural and engineered barriers. An example neutralization analysis is to assume that a waste package has been inadvertently breached at the time it was emplaced. This nonmechanistic early failure of a waste package is outside of the expected degradation modes considered plausible. However, it does provide a useful "what-if" analysis for examining the robustness of the overall system behavior.

The results of the nonmechanistic early failure scenario are illustrated in Figure 4-218. This figure shows the effect of the nonmechanistic early failure waste package, assuming either the nominal cladding degradation model or the degraded cladding degradation model (the same as the model used to generate Figure 4-215). It illustrates that the time to achieve the initial peak dose is about 2,500 years, indicating the advective transport time through the unsaturated and saturated zone. The

dominant radionuclide in this analysis is neptunium-237. The second peak of the dose at about 40,000 years occurs after the drip shields have been sufficiently degraded to have an effect on the advective release from the waste package. This peak is dominated by neptunium-237 and plutonium-239 releases.

4.5.5   Summary of Barrier-Importance Analyses

This section has presented a range of different barrier-importance analyses to evaluate the robustness of the repository performance even under extreme sets of assumptions. Although none of these combinations is expected to occur, they illustrate the behavior of the system over time periods beyond a 10,000-year period. These analyses give insights into the system behavior and are useful in evaluating the overall system response and in evaluating the contribution of the different natural and engineered barriers to the postclosure performance. As in Section 4.4.5, these analyses focused on the nominal performance scenario and the degradation of the barriers during the regulatory time period. Analyses beyond 10,000 years were performed as an indicator of long-term performance.

The analyses indicate that the various natural and engineered barriers contribute to the ability of the system to isolate waste. The total system results appear to be most sensitive to the performance of the waste package barrier. However, even degraded waste packages do not appear likely to result in doses higher than applicable standards because of the performance of other natural and engineered barriers.

Additional barrier-importance analyses are presented in the *Total System Performance Assessment for the Site Recommendation* (CRWMS M&O 2000a, Section 5.3) and *Repository Safety Strategy: Plan to Prepare the Safety Case to Support Yucca Mountain Site Recommendation and Licensing Considerations* (CRWMS M&O 2001a, Volume 2), as well as in Volume 2, Section 3 of *FY01 Supplemental Science and Performance Analyses* (BSC 2001b).
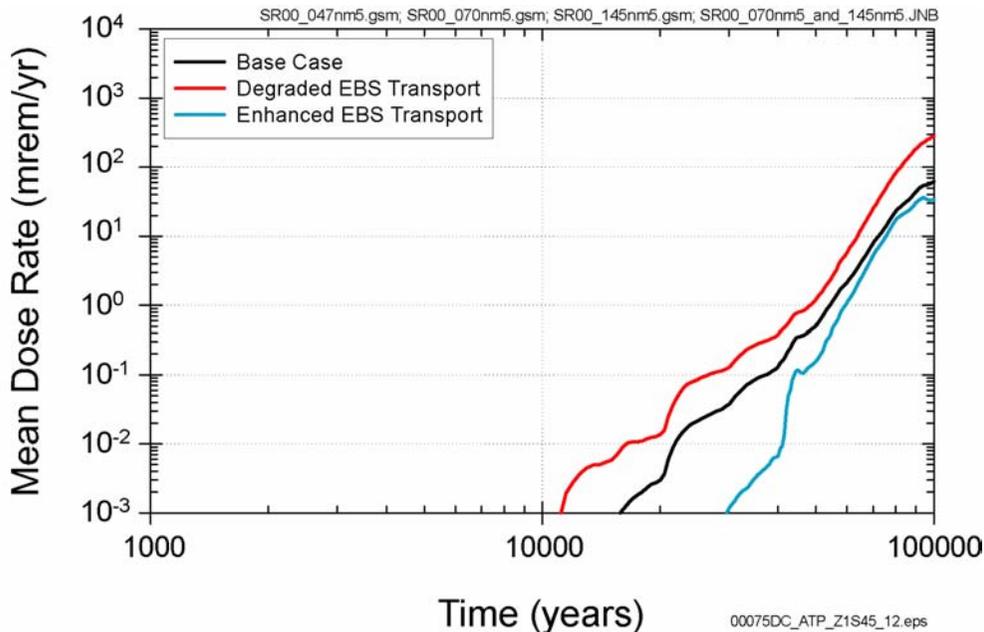
Figure 4-217. Sensitivity of the Mean Dose Rate Projected by the TSPA-SR Base-Case Model Assuming a Degraded and an Enhanced Engineered Barrier System Transport Barrier

The receptor is assumed to be 20 km (12 mi) from the repository footprint. Annual water demand was assumed to be approximately 2,000 acre-ft. EBS = engineered barrier system. Source: Modified from CRWMS M&O 2000a, Figure 5.2-13.
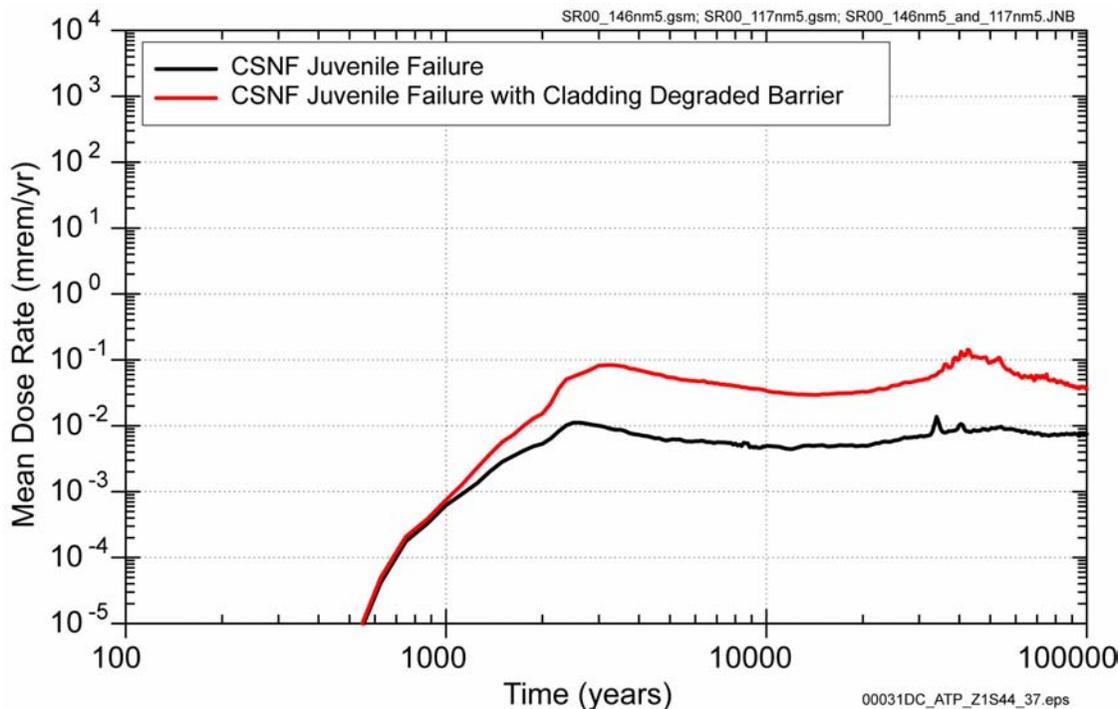
Figure 4-218. Sensitivity of the Mean Dose Rate Projected by the TSPA-SR Base-Case Model Assuming a Juvenile Waste Package Failure with a Degraded Cladding Barrier

The receptor is assumed to be 20 km (12 mi) from the repository footprint. Annual water demand was assumed to be approximately 2,000 acre-ft. CSNF = commercial spent nuclear fuel waste package. Source: Modified from CRWMS M&O 2001a, Figure 3-19.

4.6 PERFORMANCE CONFIRMATION, POSTCLOSURE MONITORING, AND SITE STEWARDSHIP

The quantitative and qualitative analyses of repository performance presented in previous sections are the basis for the DOE's forecast of repository performance. The DOE's confidence in the robustness of these analyses is enhanced by the safety margin and the defense in depth provided by the multiple natural and engineered barriers at Yucca Mountain. Nevertheless, the EPA, NRC, and DOE have all recognized that some uncertainty about repository performance cannot be eliminated. Furthermore, the DOE understands that ensuring public safety requires continued stewardship, including a program for evaluating new information obtained during the construction and operation of the potential repository. Therefore, the final component of the postclosure safety case is a performance confirmation, monitoring, and site stewardship program that accomplishes multiple goals related to the DOE's obligation to protect public health and safety and the environment. Specifically, these programs will include long-term monitoring of the site, maintaining the integrity and security of the repository, and maintaining the ability to retrieve spent nuclear fuel and high-level radioactive waste in the event that new information indicates a need to do so.

The postclosure monitoring and stewardship programs are derived from a variety of sources, including NRC licensing-related regulations and DOE policies. All parts of the program will contribute to the DOE's overall goal of building a repository that will provide for the containment and isolation of waste.

This section briefly describes the key elements of performance confirmation, postclosure monitoring, and site stewardship. These elements include a performance confirmation program to assess the performance of the repository both during operation and before closure. Other activities will include postclosure monitoring, maintenance of institutional control, site stewardship, and safeguards and security.

The objectives of the programs can be summarized as follows:

- Confirm that the repository is performing as expected or take any corrective action necessary, including retrieval of the waste, if warranted

- Provide a sound scientific basis for future generations to decide when to close the repository

- Institute safeguards and security provisions consistent with licensing-related NRC regulations

- Prevent deliberate or inadvertent human intrusion that could adversely affect the performance of the repository.

The components of the programs can be broadly grouped into two categories:

- Performance Confirmation and Monitoring (Section 4.6.1)

- Safeguards and Security (Section 4.6.2).

The following sections describe the activities which will continue or are currently planned or envisioned to be undertaken by the DOE under each of these categories. Data collection, experiments, and testing have been ongoing during site characterization and will continue consistent with NRC regulations.

4.6.1 Performance Monitoring

Performance monitoring will continue and will be conducted under the umbrella of an integrated test and evaluation program (see also Section 5.4) and will take place during all phases of construction and operation of the monitored geologic repository prior to closure. The *Monitored Geologic Repository Test & Evaluation Plan* (CRWMS M&O 2000fj) describes the program designed to ensure that systems are performing as expected to achieve the safety goals of this facility. Performance monitoring is subdivided into the following three

categories, which stem from regulatory requirements:

- Preclosure safety monitoring
- Performance confirmation
- Post-permanent closure monitoring.

Preclosure safety monitoring is conducted to provide a safe working environment for onsite personnel and visitors during the preclosure period, which includes the site characterization, construction, operation, and monitoring phases of the program. Preclosure safety monitoring also provides for a variety of safety measures, such as fire sensors and alarms, in surface facilities, as well as radon gas measurement in the subsurface. Section 5.4 describes preclosure monitoring activities in more detail.

Performance confirmation is the set of testing, monitoring, and analysis activities initiated during site characterization and continue until repository closure. The focus of this monitoring is to gather and analyze data on conditions and systems that will affect the performance of the facility after closure and to evaluate their impacts on postclosure performance. These data will be used to confirm both that subsurface conditions are consistent with the assumptions used in performance analyses and that barrier systems and components operate within the bounds expected. The performance confirmation program will test, monitor, and analyze various systems of the monitored geologic repository. The program will include geologic mapping of subsurface conditions, monitoring of the conditions in and around emplacement drifts, monitoring of other factors important to postclosure safety, and assessment of postclosure implications. The program is described in more detail in Section 4.6.1.1.

A post-permanent closure monitoring program will include the monitoring activities that will be conducted around the repository after the facility has been closed and sealed. A license amendment will be submitted for permanent closure of the repository. This amendment will provide an update of the assessment of the repository's performance for the period after permanent closure, as well as a description of the program for post-permanent

closure monitoring. The details of this program will be defined during processing of the license amendment for permanent closure. Permanent closure of the repository will include closing the subsurface facilities, decontaminating and decommissioning the surface facilities, reclaiming the site, and establishing institutional barriers. As part of the institutional barriers, provisions may be added for post-permanent closure monitoring, which will be described in the license amendment to obtain authorization to close the facility in the future. Deferring the definition of this program to the closure period will allow for identification of appropriate technology, including technology that may not be currently available.

The *Performance Confirmation Plan* (CRWMS M&O 2000ag) is a subtier document to the *Monitored Geologic Repository Test & Evaluation Plan* (CRWMS M&O 2000fj). The objective of the Monitored Geologic Repository Test and Evaluation Program is to define, design, and conduct testing for the repository to, among other things: (1) support system design and development, (2) evaluate operational suitability and effective-ness of the system, and (3) support the implementation of quality controls. Additional information about this program is provided in Section 5.4. The test and evaluation, performance confirmation, and postclosure monitoring programs will each have specific goals and objectives. However, they will also be designed to be sufficiently flexible to allow the DOE to respond to new information acquired as the repository system is observed both during and after construction and operation. If any unanticipated conditions are encountered or observed, the monitoring programs will provide a means for assessing their impact, if any, on long-term performance. As new insights are gained, existing tests may be modified or new tests defined to ensure that the DOE has a sound basis for future decisions affecting the repository.

4.6.1.1 Performance Confirmation Program

The performance confirmation program is an important part of the strategy for the development of the postclosure safety case for the potential repository (CRWMS M&O 2001a, Volume 2,

Section 7.5). It consists of tests, experiments, and analyses that will be implemented in a manner that ensures that the ability of the repository to perform will not be compromised. The performance confirmation program will be periodically updated, for example, to conform to changes in repository design evolving from any licensing process.

In more detail, the aims of the program are to:

- Provide data to verify that subsurface conditions and any changes during construction and waste emplacement will fall within the limits assumed in the license application

- Provide data to verify natural and engineered barrier systems and components required for repository operations and important to postclosure performance (or designed or assumed to operate as barriers after permanent closure) are functioning as intended and anticipated

- Provide consistency with NRC licensing-related requirements for performance confirmation

- Provide information to support the authorization of permanent closure.

These objectives will be pursued in a manner that does not adversely affect the ability of the natural and engineered barrier systems to meet the performance objectives, as demonstrated in site performance protection analyses.

The description of the performance confirmation program will be formally documented in the *Performance Confirmation Plan*; a preliminary version of the plan has been developed (CRWMS M&O 2000ag) based on the repository design and higher-temperature operating mode. As the repository design matures and the thermal operating mode nears selection, the plan will be revised to support the license application and to provide additional details and specifics of performance confirmation activities.

Performance Confirmation Approach—The performance confirmation program will obtain data

indicative of the repository's postclosure performance. Information relevant to the program has been developed during site characterization. Performance confirmation will extend until the beginning of repository closure operations. Key geologic, hydrologic, geomechanical, and other physical processes or factors (and related parameters) will be monitored and tested throughout construction, emplacement, and operation to detect any significant changes from baseline conditions.

Briefly, the overall approach to performance confirmation can be divided into eight steps:

1. Identify key performance confirmation processes (factors) and parameters

2. Establish the performance confirmation baseline database and predict the performance of the key factors and parameters

3. Establish tolerances and bounds for the key factors and parameters

4. Establish the completion criteria (which define when there is no longer a need for a test) and guidelines for corrective actions to be used when data exceed tolerances or bounds

5. Plan and set up the performance confirmation test and monitoring program

6. Monitor, test, and collect data

7. Analyze, evaluate, and assess data

8. Recommend corrective actions and implement changes to the performance confirmation program, as required.

The first four steps of the process define the performance confirmation baseline. The baseline includes the data obtained during site characterization and from test startup and initialization, together with parameter predictions and the definition of tolerances and bounds for these data. These four steps establish the basis on which to evaluate whether the data indicate that the related processes are performing as expected.

After this baseline has been established, related testing, monitoring, and analysis activities can be initiated. Testing and monitoring activities include the physical recovery and laboratory testing of representative repository materials and collection of environmental data. Examples of testing and monitoring activities include geologic mapping, subsurface sampling, coupon recovery, dummy waste package testing, and ventilation monitoring. This information is combined and analyzed to provide a comprehensive performance confirmation program.

Sensors in the emplacement and support drifts obtain raw electronic data that are reduced, processed, and stored. During this process, the raw data are converted into engineering numbers, which are transmitted as performance data to be evaluated during the performance confirmation process by comparing the data to predicted bounds for confirmation. Figure 4-219 illustrates this process schematically. The bounds or tolerances vary with time to reflect the effects of construction

and operation of the repository, together with effects of waste emplacement.

Identifying Performance Confirmation Factors—An essential step in conducting performance confirmation and establishing the baseline is identifying the parameters to be monitored. Factors to be addressed by the performance confirmation program arise from four sources:

1. **Processes important to repository safety**—To correctly focus resources, the performance confirmation program concentrates on the processes (and related parameters) most important to repository postclosure safety. Identification of these processes (termed "performance confirmation factors") considers available performance assessment analyses and the *Repository Safety Strategy: Plan to Prepare the Postclosure Safety Case to Support Yucca Mountain Site Recommen-*
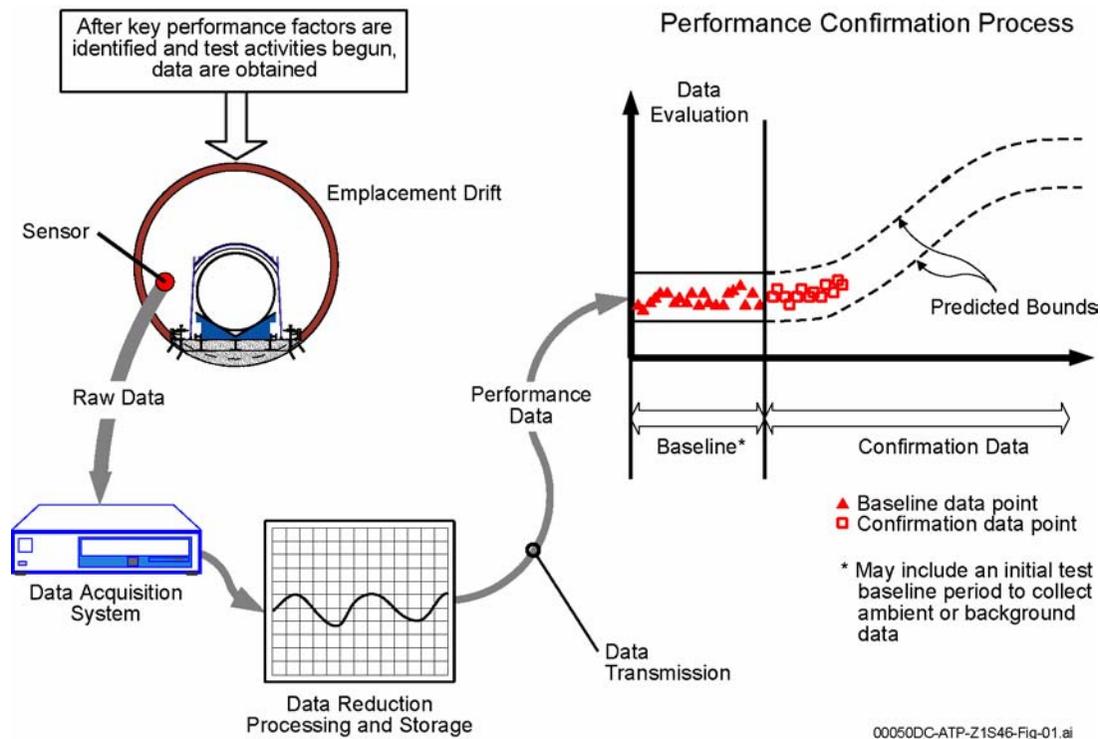
Figure 4-219. Performance Confirmation Process, From Testing to Data Evaluation
Data collected by in situ instrumentation is transmitted, reduced, and processed for analysis. Data observations are compared to predicted values to determine trends and potential deviations from expected performance.

dation and Licensing Considerations (CRWMS M&O 2000fk, pp. 3-7 to 3-10).

2. **Applicable requirements**—The program also must address applicable regulatory and system requirements as part of the licensing process. These requirements identify (or prescribe) particular factors or tests to be included in the performance confirmation program.

3. **Licensing conditions**—As part of the licensing process, requirements or issues that need additional testing may be identified by the NRC or the DOE and may be included in the license as a licensing condition or directive. Testing to address these conditions would be included as part of the performance confirmation program if the issues were important to postclosure safety or were so indicated in the directive.

4. **Data and validation needs of the analysis and process models**—After the completion of the site characterization phase, some additional data related to items that are recognized to have potential postclosure sensitivity may still be required to support the license application. These data needs will be identified in the application with associated test plans to be conducted as part of performance confirmation in accordance with regulatory guidance.

Based on these four sources, analyses have been conducted to identify the key performance confirmation factors to be tested or monitored. Table 4-41 lists the key performance confirmation factors identified in considering the processes important to repository postclosure safety. Table 4-42 shows additional factors that have been identified from evaluations of applicable system requirements and regulations (CRWMS M&O 2000ag, Table 3-7 and Appendix E). Table 4-43 shows the added key performance confirmation factors that have been identified in considering potential data needs in support of process model development. No factors have been identified to date based on licensing conditions. Specific tests that address these factors are discussed in the following section.

Testing Program—Performance confirmation activities will be conducted as part of the repository's overall test and evaluation program. They will be performed under several different test categories of the program. The preliminary list of test activities (and associated test categories) is presented in Table 4-44, and each performance confirmation activity is described briefly in the following sections (CRWMS M&O 2000ag). It is important to note that the performance confirmation program will continue to evolve consistently with the postclosure safety case, applicable licensing-related regulations, and applicable licensing requirements. Any or all of these may change and necessitate revisions to the plan, either before or after license application submittal.

Table 4-41. Performance Confirmation Factors Based on Processes Important to Safety

Performance Confirmation Key Factors	Type of Testing Indicated
Ambient flow through the repository horizon and seepage into unventilated drifts	In situ testing during construction and operation
Failure rate of drip shields	Laboratory testing of drip shield materials over a range of expected repository conditions combined with process modeling of drip shield failure
Amount and chemistry of water contacting waste packages	Process modeling and drift-scale testing to validate process model results
Corrosion rate of waste package materials and failure rate of waste packages	Laboratory testing of waste package materials over a range of expected repository conditions and process modeling of waste package failure
Potential factor of cladding degradation	Potential long-term laboratory testing of Zircaloy failure rate
Potential factor of solubility of actinides	Potential laboratory testing of solubility of actinides

Source: CRWMS M&O 2000ag, Table 3-5.

Table 4-42.   Performance Confirmation Factors Consistent with Potential Licensing Requirement

Performance Confirmation Key Factors	Type of Testing Indicated
Waste package surface temperature to assess cladding condition	Monitoring waste package surface
Emplacement drift air temperatures to assess heat removal	Monitoring temperatures of both incoming and exhaust air of emplacement drifts
pH of water within emplacement drift (seepage) to confirm waste package environment	Monitoring the pH of water (as observed) within emplacement drifts and special test alcoves
Emplacement drift air temperatures to confirm waste package environment	Monitoring temperature within emplacement drifts
Emplacement drift humidity to confirm waste package environment	Monitoring humidity within emplacement drifts
Colloid content of water within emplacement drift to define waste package environment	Monitoring colloid content of water (as observed) within emplacement drifts
Drainage of invert to confirm free-draining conditions	Visually monitoring water accumulations within emplacement drifts
Amount of seepage to confirm expected waste package environment	Monitoring seepage in special test alcoves
Observation of the encountered subsurface (geologic) conditions of the repository horizon	Geologic observation, mapping, and index laboratory testing
In situ rock mass response due to repository construction and waste emplacement	Rock mass monitoring (temperature and displacement) near emplacement drifts
Performance and constructibility of borehole, ramp, and shaft seals	Field testing of borehole, ramp, and shaft seals
Engineered barrier system interaction response of waste packages, backfill (if used), rock, and groundwater	Field testing of engineered barrier system postclosure configuration
In situ waste package monitoring	Remotely monitoring waste package in emplacement drifts
Laboratory investigations of internal waste package material testing	Laboratory materials testing
Groundwater quality measurements	Well monitoring both downgradient (at accessible environment) and upgradient
Potential for disruptive events	Precise leveling surveys over repository Subsurface seismic monitoring Monitoring groundwater temperature and level

Source: Modified from CRWMS M&O 2000ag, Table 3-7 and Appendix E.

Table 4-43. Performance Confirmation Factors Based on Potential Data Needs

Performance Confirmation Key Factors	Type of Testing Indicated
Sorptive properties of the Calico Hills nonwelded hydrogeologic unit immediately below the repository	Sampling and laboratory testing of sorptive properties of the Calico Hills nonwelded hydrogeologic unit
Unsaturated flow and transport within the Calico Hills nonwelded hydrogeologic unit formation to validate conceptual models	Sampling and laboratory and field testing
Rock mass response to cooling	Monitoring rock mass thermal-hydrologic-mechanical response as in cooling of Drift Scale Test
Coupled thermal-mechanical-hydrologic-chemical processes	Field testing around heated test drift
Geochemical interactions as part of coupled processes	Laboratory testing
Stress corrosion cracking of barrier materials: Alloy 22; Titanium Grade 7; and Stainless Steel Type 316NG Long-term phase stability of Alloy 22 and Stainless Steel Type 316NG Long-term stability of passive film on barrier materials	Laboratory materials testing
Dissolved radionuclide concentration limits Colloidal radionuclide concentration and transportation limits Clad performance In-package chemistry Spent nuclear fuel degradation and high-level radioactive waste glass degradation	Laboratory materials testing

Source: Modified from CRWMS M&O 2000ag, Table 3-6.

Table 4-44. Identified Performance Confirmation Testing and Monitoring Activities

Test Category	Performance Confirmation Activity
Core Performance Confirmation	Seepage Monitoring
	In Situ Waste Package Monitoring
	Long-Term Materials Testing
	Ventilation Monitoring
	Rock Mass Monitoring
	In-Drift Monitoring
	Introduced Materials Monitoring
	Recovered Material Coupon Testing
	Dummy Waste Package Testing
	Recovered Waste Package Testing
	Postclosure Simulation Testing
Development Testing	Geologic Observations and Mapping
	Subsurface Sampling and Index Testing
	Baseline Analyses and Evaluations[a]
	Unsaturated Zone Testing
	Near-Field Environment Testing
	Waste Form Testing
	Waste Package Testing
Prototype Testing	Borehole Seal Testing
	Ramp and Shaft Seal Testing
Technical Specifications and Monitoring	Groundwater Quality Monitoring
	Groundwater Level and Temperature Monitoring
	Surface Uplift Monitoring
	Subsurface Seismic Monitoring

NOTES: [a]This activity supports all other performance confirmation activities and is included for completeness.
Source: CRWMS M&O 2000ag, Table G-1.

4.6.1.1.1 Core Performance Confirmation

Core performance confirmation activities, as defined in the *Performance Confirmation Plan* (CRWMS M&O 2000ag), are the monitoring and testing activities focused solely on the postclosure performance of the repository. These core activities generally begin with the start of waste emplacement. Conceptually, activities under this test category include the testing and monitoring activities discussed in the following paragraphs.

Seepage Monitoring—This monitoring evaluates the ambient flow of water into excavations (i.e., seepage). Hydrologic testing and monitoring will be performed in closed alcoves along access or monitoring drifts. The location of the alcoves will be determined by applying such criteria as areas of relatively high and low infiltration; overlying bedrock/alluvium contact; faults and fracture zones; geographic variation (north to south in the Exploratory Studies Facility); and presence of extreme (high or low) lithophysal cavity densities and welded or nonwelded rock units. This activity will also include confirmation testing of the seepage threshold concept arising from the capillary barrier mechanism.

In Situ Waste Package Monitoring—Remote inspection technology will be employed to conduct inspections of the waste packages in the emplacement drifts. In particular, remotely operated inspection gantries that can conduct remote visual, thermal, and radiological inspection of the waste packages, as well as collect and place material samples or coupons, will be used. These vehicles will be remotely operated from a control center and will periodically inspect each emplacement drift and all accessible waste packages. They will be able to inspect the upper and lower surfaces of the waste packages and will operate within the high-temperature and high-radiation environment of the emplacement drifts. A conceptual view of a remotely operated inspection gantry is shown in Figure 4-220.

Long-Term Materials Testing—Long-term laboratory studies of the waste form, waste package, and drip shield materials have been and continue to be conducted to obtain data on various degradation phenomena. Laboratory testing employs a range of environmental conditions that bound and simulate repository conditions at future times. Key parameters affecting drip shield and waste package container performance have been and will continue to be investigated, including parameters associated with oxidation and aqueous corrosion.

Ventilation Monitoring—The emplacement drift environment will also be monitored by sampling the ventilation air that goes into and comes out of each emplacement drift. Conceptually, monitoring instruments can be installed within the air regulator at the isolation door and within the exhaust mains or raises. Some parameters that can be measured as part of ventilation monitoring include wet and dry
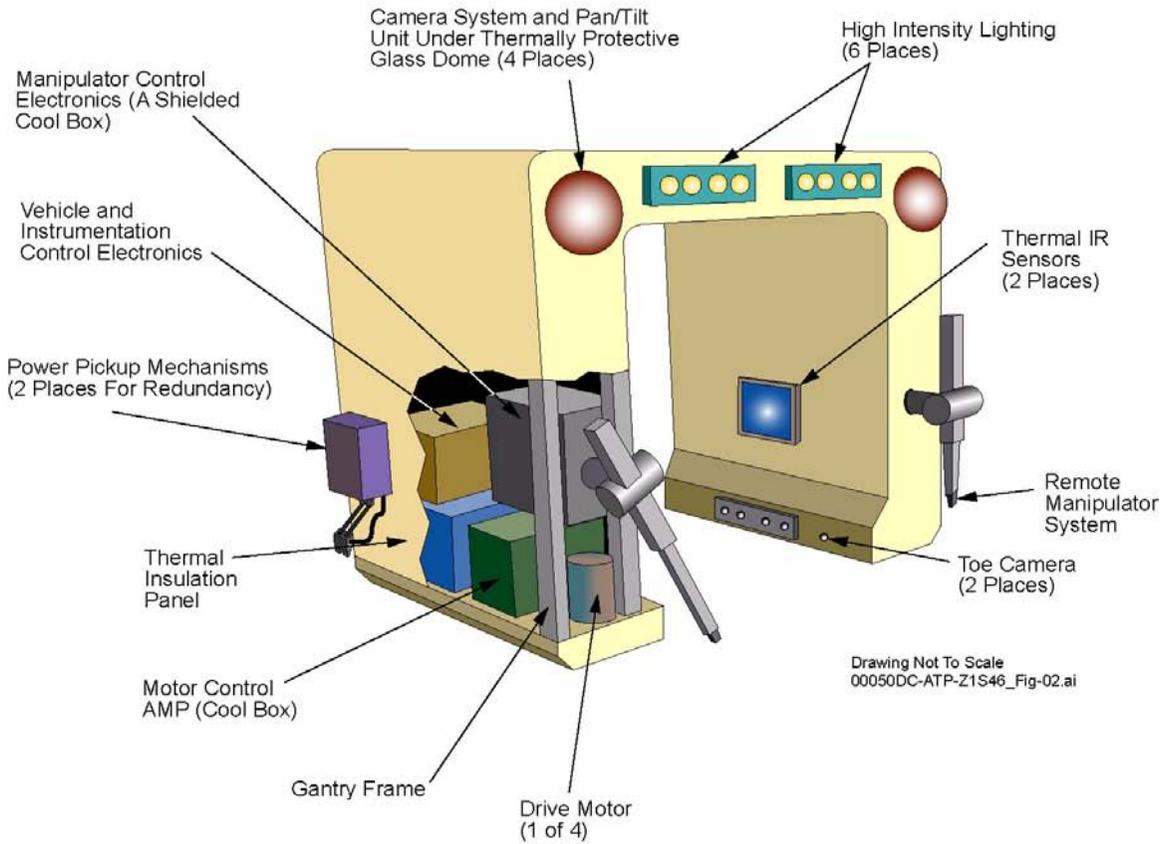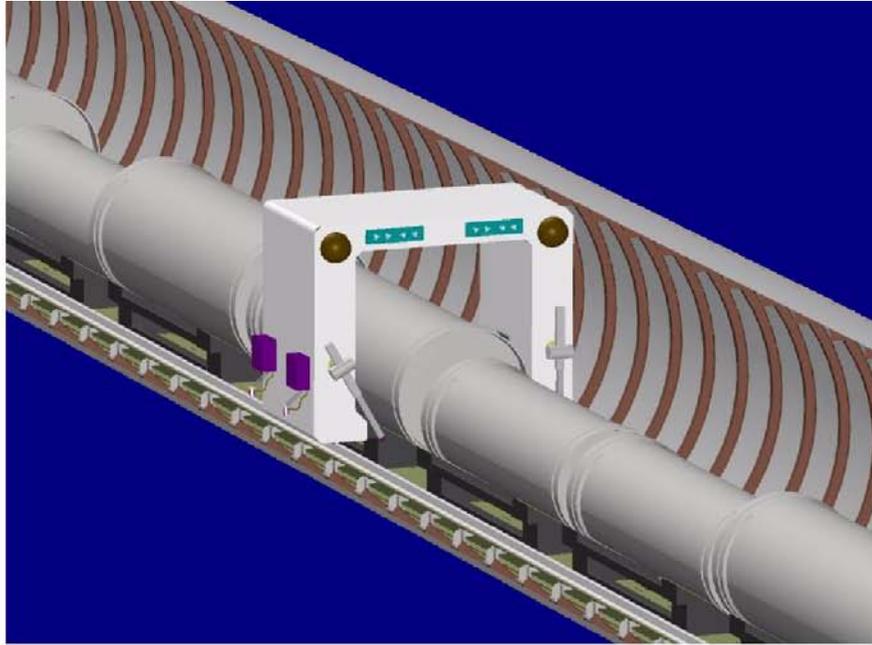
Figure 4-220. Conceptual Illustration of a Performance Confirmation Inspection Gantry
The inspection gantry will have onboard monitoring equipment capable of inspecting waste packages, emplacement drift structures, and environmental conditions. Source: CRWMS M&O 2000ag, Figure 5-1.

bulb temperatures; relative humidity; radioactive gas content (e.g., tritium, krypton-85, and radon); air pressure; percentage of oxygen and carbon dioxide; and dust content.

Rock Mass Monitoring—The coupled thermal-hydrologic-mechanical response of the rock mass around emplacement drifts will be monitored through the performance confirmation period to confirm the conceptual understandings and numerical simulations of coupled processes considered in performance assessments. This monitoring will be conducted at appropriate locations or areas to provide sufficient coverage of the emplacement horizon. Conceptually, this could entail measurement at three locations across the upper block of the potential repository horizon (i.e., at the northern, central, and southern reaches of the horizon). Each test area will monitor approximately 150 m (500 ft) of emplacement drift.

In-Drift Monitoring—To continually monitor the conditions within emplacement drifts, a limited number of in-drift instrument areas will be installed in the drifts. These instruments will provide continual readings at specific locations, at times between the monitoring of the drifts by the inspection gantry, and as a supplement to the indirect monitoring of the drifts (e.g., through ventilation monitoring). The sensors would be similar to those used for the inspection gantry. Several stations would be located along the emplacement drift axis of each test area to provide an estimate of the change in values with distance along the drift. Conceptually, to provide access to these instruments, boreholes from adjacent observation drifts or cross-block drifts could be extended into the emplacement drifts.

Introduced Materials Monitoring—To monitor and analyze changes from the baseline condition of parameters that could affect the performance of a geologic repository, it will be necessary to monitor fluids and other materials introduced into the repository horizon as a result of construction and operations. This monitoring will be done to evaluate the impact that introduced materials (e.g., water from construction activities, fire suppression and ground support materials, hydrocarbons, concrete, steel, and railcars) could have on the

postclosure performance of the repository if they remained after closure.

Recovered Material Coupon Testing—This testing involves the placing of nonradioactive waste package material specimens at different locations in the emplacement drifts to expose them to different environmental conditions. After a defined period, the inspection gantry will retrieve the specimens for laboratory examination at surface or offsite facilities. Specimens will be placed in a variety of exposure locations that will cover a reasonable range of the geological and geochemical variations expected to occur in the repository. Testing with some specimens, including welds, will be focused on container and cladding materials.

Dummy Waste Package Testing—This activity entails the construction of dummy waste packages that have the same external materials, dimensions, and configuration as a real waste package, but do not contain any radioactive waste. Instead of waste, each dummy package will house an electrical heater and will be used in test drifts under simulated postclosure conditions.

Recovered Waste Package Testing—If a waste package must be recovered for remediation, activities will be defined on a contingency basis to examine and test it for any potential surface or weld degradation. However, an active program of waste package recovery and inspection for performance confirmation purposes alone is not proposed in the program.

Postclosure Simulation Testing—Postclosure simulation testing will confirm whether the measured conditions within a simulated postclosure drift are within ranges consistent with those assumed in the license application. The testing would be conducted after the start of waste emplacement and would allow for the use of actual waste in addition to dummy waste packages equipped with heaters. A single test drift will be separated into test sections, allowing for the simulation of several different test cases within the drift. The postclosure configuration will be constructed in the section with either dummy or actual waste packages, a drip shield, and backfill (if employed)

and will employ expected postclosure technology and equipment. The test sections will be monitored for decades, then deconstructed to evaluate barrier response.

4.6.1.1.2   Development and Licensing Testing

Performance confirmation activities under this test category include baseline testing through completion of subsurface construction. Preemplacement testing to support the license application submittal, licensing interactions, and preemplacement licensing conditions, will also be performed under this category.

The performance confirmation testing and monitoring activities under development and licensing testing are described in the paragraphs below.

Geologic Observations and Mapping—Geologic mapping of repository excavations will be conducted during construction to provide information to confirm and document the geologic structure (stratigraphy) of the emplacement horizon and the characteristics of major fracture sets and faults. This mapping will be conducted in accordance with applicable standard engineering practices and procedures. Conceptually, mapping will be performed for all excavations using a combined approach of stereoscopic imaging and digital mapping to obtain a digital record of the excavation surface. This recording will be supplemented with localized, detailed, full-periphery geologic mapping and the collection of discontinuity statistics in selected areas.

Subsurface Sampling and Index Testing—A sampling and laboratory index test program will be implemented to support seepage testing, together with thermal testing and monitoring activities. Rock samples will be collected at sites corresponding to testing and instrumentation locations, including alcoves and observation drifts. Parameters to be tested in the laboratory will include rock chemistry, hydrologic properties, and mechanical and thermal properties. The data will be incorporated into the performance confirmation baseline and performance predictions and are also expected to provide a basis for evaluating the areal variability of properties across the repository horizon.

Baseline Analyses and Evaluations—The activities for baseline development include developing the performance confirmation database and predicting performance for all key parameters, establishing tolerances and bounds for the parameters, and identifying completion criteria and guidelines for corrective actions.

Unsaturated Zone Testing—Based on a preliminary assessment of data needs, additional testing may be conducted to obtain data on the effects of construction on ambient moisture and seepage, as well as on the sorptive and the unsaturated flow and transport properties of the Calico Hills nonwelded hydrogeologic unit.

Near-Field Environment Testing—Based on a preliminary assessment of data needs, additional testing may be conducted to obtain both data on the coupled thermal-mechanical-hydrologic-chemical response of the rock mass due to cooling and additional field and laboratory testing data from ongoing heater tests to investigate coupled processes necessary to confirm the near-field environment.

Waste Form Testing—Based on a preliminary assessment of data needs for the waste form, additional testing may be conducted to obtain data on dissolved radionuclide concentrations, colloidal concentration and transportation limits of waste form materials, and cladding performance data over the range of expected in situ conditions. Laboratory testing has been identified to obtain additional data on in-package chemistry and its effects on cladding performance and on colloidal and dissolved radionuclide concentrations.

Waste Package Testing—Based on a preliminary assessment of data needs for the waste package, additional testing may be conducted to obtain data on barrier materials (such as Alloy 22, Titanium Grade 7, and Stainless Steel Type 316NG), stress corrosion cracking, material phase stability, and the phase stability of passive films that can form on the surface of waste package materials.

4.6.1.1.3   Prototype Testing

Performance confirmation testing activities will also be conducted to examine the performance of full-scale prototypes to demonstrate constructibility and the effectiveness of systems considered important to safety. These activities are described in the following paragraphs.

Borehole Seal Testing—Prototype testing of borehole seals will be performed in surface boreholes, using appropriate drilling technology to install and test the seals. This testing will involve seals emplaced in shallow boreholes to allow for seal recovery and will include hydraulic conductivity and nondestructive testing of the seal. After testing, the seals will be removed from the site for additional materials testing in the laboratory.

Ramp and Shaft Seal Testing—Prototype ramp and shaft seal tests will be conducted to examine seal performance and to resolve design issues associated with large-scale construction not previously addressed by laboratory or small-scale in situ testing. These tests will be performed within representative geologic units and will use construction techniques similar to those identified for repository closure.

4.6.1.1.4   Technical Specifications and Monitoring

Performance confirmation testing, and other testing and evaluation activities, will be conducted within the Geologic Repository Operations Area and in the immediate region around the repository, as necessary. Specific environmental testing and monitoring activities related to performance confirmation are described in the following paragraphs.

Groundwater Quality Monitoring—Active monitoring of the uppermost aquifer will be performed using a series of both upgradient and downgradient wells. The wells will be installed and periodically sampled to evaluate the chemistry and radioactivity of groundwater adjacent to the repository. Conceptually, one upgradient and four downgradient wells will be employed for performance confirmation.

Groundwater Level and Temperature Monitoring—In coordination with groundwater quality measurements, the in situ temperature and the elevation of the groundwater in wells will be measured and compared to prior measurements to determine whether there have been hydrogeologic or other changes that could modify groundwater flow patterns.

Surface Uplift Monitoring—Using periodic, precise measurements, uplift monitoring will be conducted for the elevation grid of reference points on the surface above the repository horizon. Elevation changes over time will be used to determine whether significant local surface movement is occurring above the repository.

Subsurface Seismic Monitoring—Subsurface seismic monitoring will be conducted to measure the occurrence and magnitude of seismic events at repository depth. Measurements will be compared to the seismic design bases to confirm that a sufficient safety margin is being maintained.

4.6.2   Safeguards and Security

A repository at Yucca Mountain would be the first permanent geologic repository for the disposal of spent nuclear fuel and high-level radioactive waste, including immobilized plutonium encased in high-level radioactive waste. The DOE will implement appropriate safeguards, security, and reporting measures consistent with 10 CFR 63.102(k) and 10 CFR 63.21(b)(3) (66 FR 55732).

The DOE will establish a system for verifying, tracking, and mapping each item of waste—both civilian and defense—that is accepted, transported, and eventually emplaced in the repository.

After closure, the DOE will also have the responsibility of maintaining institutional control over the repository. The DOE will maintain appropriate institutional controls consistent with plans to be developed to support a license application if the site is designated.

5. DESCRIPTION OF THE PRECLOSURE SAFETY ASSESSMENT

This section describes the analytical methods and summarizes the results of the preclosure safety assessment for a potential repository at Yucca Mountain. Section 5.1 describes how facilities and systems for the potential repository would use established commercial technologies and nuclear industry technologies to reduce the risk of Category 1 and Category 2 event sequences, since these technologies are well understood. Section 5.2 describes the approach used in assessing the preclosure operational safety of a potential repository at Yucca Mountain. It also discusses event identification, event sequence categorization, event sequence consequence analysis, use of features and controls important to radiological safety, and quality assurance classification. Section 5.3 provides a description of events and the results of consequence analyses and evaluations. Section 5.4 describes the testing and evaluation program planned for the potential repository's preclosure period.

5.1 KNOWN TECHNOLOGY AND OPERATING SYSTEMS

A repository at Yucca Mountain would use commercial and nuclear industry technologies for preclosure construction and operations. The methods these technologies use to reduce the risk of event sequences are well understood.

Over the past 50 years, large nuclear facilities have been designed, constructed, and operated by the commercial nuclear industry and the U.S. government. Incorporated into the design of these facilities are features and controls that prevent or reduce the consequences of accidents. The repository design draws upon this extensive experience and is based on proven technology in use at nuclear installations worldwide. For example, high-efficiency particulate air filters have been used for many years to reduce atmospheric emissions from nuclear facilities. Monitoring systems have also been used for many years to measure atmospheric effluents. Computer codes to estimate exposure from effluents have been developed and are widely used. The principles of radiation shielding are well known, and computer codes are available to aid in

shielding design. The principles of time, distance, and shielding are used to keep radiation doses as low as is reasonably achievable (ALARA) (e.g., *Health Physics Manual of Good Practices for Reducing Radiation Exposure to Levels that are As Low As is Reasonably Achievable* [Munson et al. 1988]).

Spent nuclear fuel transportation casks are routinely loaded and unloaded in the United States. Heavy loads are routinely moved by bridge cranes at nuclear facilities, as they would be at a repository at Yucca Mountain. Across the United States, commercial nuclear power reactors currently operate spent nuclear fuel pools. At all operating nuclear plants, handling spent nuclear fuel is a routine activity. For example, from 1968 to 1994, about 105,000 spent nuclear fuel assemblies were discharged from commercial nuclear power reactors (DOE 1996b, Table 5). The lessons learned from these experiences would be incorporated into the design and concept of operations for any repository.

5.2 BASIC SAFETY ASSESSMENT METHOD

The two basic elements of any safety assessment are event identification and consequence analysis. The first element involves performing a systematic review of relevant site and facility features and processes in order to define the types of events that can occur. Events identified include the full range of probable events, from normal operational events that might occur to very low-probability events. Events are identified by first evaluating potential hazards applicable to the site and facility design, then developing a detailed site- and design-specific event scenario in which event sequences are defined and the anticipated frequency of occurrence of events is established. Based on the frequency of occurrence, events are categorized as Category 1 or Category 2 event sequences. Event sequences with lower frequencies of occurrence are considered beyond Category 1 and Category 2 event sequences and were not analyzed further. The second element of the safety assessment involves estimating the consequences of the event

sequences that are identified as a Category 1 or Category 2 event sequences in the first process.

The safety assessment performs an important role in the design process. It plays a key role in the identification of facility design features and controls important to safety and is a primary input to the quality assurance classification process. In some cases, alternative design approaches or additional design features may be identified based on safety assessment results, which are then considered as part of an iterative design process. Based on the insights and results obtained from the safety assessment, the acceptability of the design can be established.

5.2.1   Event Identification Process

Events are identified based on a review of repository site characteristics, facility design features, and operational processes to be performed. An analysis of the internal and external hazards associated with preclosure operations is performed. Internal hazards are presented by the operation of the facility and associated processes. External hazards involve natural phenomena and outside man-made hazards, such as those posed by aircraft and nearby government or industrial facilities. The methodology used in the event identification analysis provides a systematic means to identify facility hazards and associated events that may result in radiological consequences to the public and workers during the repository preclosure period.

The first step in the hazard identification process is to develop a list of generic internal and external events that could result in radiological consequences to the public or workers. This generic list is not facility-specific and attempts to identify potentially hazardous events by providing a comprehensive list of possible events. The generic lists developed for the internal and external hazard analyses are based on established hazard evaluation techniques (Stephans and Talso 1997; American Institute of Chemical Engineers 1992). Tables 5-1 and 5-2 list these generic internal and external events.

Table 5-1. Generic Internal Events

Internal Event
Collision/Crushing
Chemical Contamination/Flooding
Explosion/Implosion
Fire
Radiation/Magnetic/Electrical/Fissile
Thermal

Source: BSC 2001f, Table 5-1.

Once the site characteristics, facility design, and operational processes are defined, they are evaluated against specified criteria to determine the credibility of generic hazard events that could result in radiological consequences. Event applicability criteria are developed for the generic events to support the applicability determination. If the criteria are satisfied, the generic event has the potential for a radiological consequence and is added to a list of specific initiating events to be considered in the design and safety analysis.

The criteria used to determine the applicability of internal hazards as initiators of event sequences are listed below for each event category. Applicability to a functional area of design is determined by a positive response to all questions within a hazard category or subcategory, as appropriate:

A.   Collision/Crushing

1.   Is kinetic or potential energy present?

2.   Can the kinetic or potential energy be released in an unplanned way?

3.   Can the release of kinetic or potential energy interact with the waste form?

B.   Chemical Contamination/Flooding

1.   Reactions

a.   Are corrosive/reactive chemicals or materials present?

b.   Can these chemicals or materials be released?

c.   Can the chemicals or materials interact with the waste form?

Table 5-2. Generic External Events

External Events		
Aircraft crash	High river stage	Seismic activity, uplifting (tectonic)
Avalanche	Hurricane	Seismic activity, earthquake
Coastal erosion	Inadvertent future intrusions (man-made)	Seismic activity, surface fault displacement
Dam failure	Industrial activity-induced accident	Seismic activity, subsurface fault displacement
Debris avalanching	Intentional future intrusions (man-made)	Static fracturing
Denudation	Landslides	Stream erosion
Dissolution	Lightning	Subsidence
Epeirogenic displacement	Loss of offsite/onsite power	Tornado
Erosion	Low lake level	Tsunami
Extreme wind	Low river level	Undetected past intrusions (man-made)
Extreme weather fluctuations	Meteorite impact	Undetected geologic features
Range fire	Military activity-induced accident	Undetected geologic processes
Flooding (storm, river diversion)	Orogenic diastrophism	Volcanic eruption
Fungus, bacteria, and algae	Pipeline accident	Volcanism, intrusive magmatic activity
Glacial erosion	Rainstorm	Volcanism, ashflow (extrusive magmatic activity)
Glaciation	Sandstorm	Volcanism, ashfall
High lake level	Sedimentation	Waves (aquatic)
High tide	Seiche	

Source: BSC 2001f, Table 5-2.

2. Off-Gassing

    a. Are volatile/condensable materials present?

    b. Can these materials be released?

    c. Can these materials interact with the waste form?

3. Venting

    a. Is there a potential for venting materials in the area?

    b. Can the materials interact with the waste form?

4. Debris/Leaks

    a. Is there a potential for debris or leaks in the area?

    b. Can the debris or fluids interact with the waste form?

5. Flooding

    a. Are sources of water present in the area?

    b. Is there a potential to release the water?

    c. Can the released water interact with the waste form with the potential for criticality?

C. Explosion/Implosion

1. Are pressure and electrical, chemical, or mechanical energy present?

2. Can an event occur that results in an explosion or implosion energy release?

3. Can the released energy impact the waste form directly?

D. Fire

1. Are fuel, oxidizers, and ignition sources present?

2. Is there sufficient fuel and oxidizer to sustain fire?

3. Can fire interact with the waste form?

E. Radiation/Magnetic/Electrical/Fissile

1. Are radiation/magnetic/electrical energy sources present external to the waste form? Is fissile material present?

2. Is a mechanism present to release radioactive/magnetic/electrical energy?

3. Can the release of radiation/magnetic/electrical energy interact with the waste form? Can fissile material be arranged, through operational processes, in a way that will result in criticality?

F. Thermal

1. Are external heat energy sources present?

2. Can heat energy be released?

3. Can the heat energy affect the waste form?

The criteria used to determine the applicability of external events as initiators of event sequences are listed below. The external event is considered a potential initiator of an event sequence if all of the following are determined to be true:

A. The potential exists and is applicable to the Yucca Mountain site.

B. The rate of the process is sufficient to affect the 100-year operational period. (Example: Is erosion expected to occur at the repository during the 100-year operational phase?)

C. The consequence of the process is significant enough to affect the 100-year operational period. (Example: Can the consequences of erosion lead to a radiological release at the repository during the 100-year operational phase?)

D. The event frequency is greater than or equal to 0.000001 events per year. (Example: Is any event associated with erosion expected to occur at a rate greater than or equal to once in a million years?)

If all the above statements are true for any external event, then the event is considered applicable. If any one of the above statements is false for any external event, the event is not considered applicable. If any statement is indeterminate (i.e., its validity cannot be determined at this time), the statement is treated as true and cannot be screened out at this point.

To evaluate the design and operations for the preclosure period, the period to be evaluated must be defined. The process described above used a 100-year operational phase for the higher-temperature operating mode, but the same process is valid for lower-temperature operating modes that have longer preclosure operational phases. Depending on the thermal operating mode, the preclosure period could be longer (see Section 2.1.5.2, Table 2-2) (BSC 2001f). An operational period of 100 years was selected as the duration to be used in the evaluation since it bounds the emplacement period for the range of thermal operating modes. The handling of waste in the surface and subsurface facilities is expected to last a minimum of 24 years (see Section 2.3.4.5). A 100-year preclosure period bounds surface and subsurface facilities operations and is conservative for classifying events as Category 1 and Category 2 event sequences. For example, using a 24-year period would result in a Category 1 cutoff at 4.2×10^{-2} per year and potentially allow more event sequences to be compared with the less restrictive Category 2 dose limits. After the operational phase, when the waste has been emplaced in the subsurface facility, the potential for internal and external events is still possible. Assuming a preclosure period of 325 years would lower the Category 1 cutoff to 3.1×10^{-3} per year

and lower the Category 2 cutoff to 3.1×10^{-7} per year. However, it was determined that with a 325-year preclosure period, no new events would be included (BSC 2001f, Section 4.4.1.2.1). Note that *Preliminary Preclosure Safety Assessment for Monitored Geologic Repository Site Recommendation* (BSC 2001f) describes Category 1 and Category 2 design basis events. There is no difference between Category 1 and Category 2 design basis events and Category 1 and Category 2 event sequences.

5.2.2 Event Sequence Categorization Process

The result of the event sequence identification process is a list of event sequences with a corresponding frequency of occurrence. The frequency of occurrence for each event sequence is determined using fault tree analysis or data from historical events. The frequency of occurrence is usually expressed in terms of the chance of the particular event sequence occurring during facility operations, for example, "3 chances in 100 of occurring before permanent closure of the repository." In this example, if the repository operates for 100 years and the event sequence frequency is uniform over the entire period, it can be expressed as 0.0003 per year or 3.0×10^{-4} per year. Initially, when postulating the event sequence, no credit is given to design features that could prevent or mitigate the event (i.e., the most severe consequences are evaluated). If the radiation dose consequences of an event sequence are unacceptable, design features are added to prevent or mitigate the event.

Based on frequency of occurrence, event sequences are categorized as a Category 1 or Category 2 event sequence or beyond Category 1 and Category 2 event sequences, consistent with 10 CFR 63.2 (66 FR 55732). Category 1 event sequences are expected to occur one or more times before permanent closure. This is about equal to an annual frequency of one chance in one hundred (0.01 per year)[1], based on a 100-year preclosure operational period (BSC 2001f, Section 4.4.1.2.1). Category 2 event sequences are other event sequences that have at least 1 chance in 10,000 of occurring before permanent closure. This is about

equal to an annual frequency of one chance in one million (0.000001 per year), based on a 100-year preclosure operational period (BSC 2001f, Section 4.4.1.2.1). Event sequences that have less than 1 chance in 10,000 of occurring before permanent closure of the repository are considered beyond Category 1 and Category 2 event sequences. The consequences of some of these types of events are presented in *Final Environmental Impact Statement for a Geologic Repository for the Disposal of Spent Nuclear Fuel and High-Level Radioactive Waste at Yucca Mountain, Nye County, Nevada* (DOE 2002, Tables H-6 and H-7).

Event sequences are developed using event trees, which are diagrams that depict the chronological sequence of events. Figure 5-1 shows an example of a typical event tree used to define event sequences and quantify frequency of occurrence. In this example, Event Sequence 1 begins with an unsealed disposal container drop as the initiating event. The second event represents a breach of the spent nuclear fuel assembly. The last event in this branch represents a fully functional ventilation system and associated high-efficiency particulate air filtration. This event sequence has a frequency of 0.0084 per year, classifying it as a Category 2 event sequence. Event Sequence 2 represents a release scenario in which the ventilation system and the high-efficiency particulate air filtration system are nonfunctional. This event sequence has a frequency of 1.4×10^{-9} per year, which is considered to be a beyond Category 1 and Category 2 event sequence; this would be the case even if the probability of the high-efficiency particulate air filtration system not functioning were increased a hundredfold. Event Sequence 3, with zero probability, represents an unsealed disposal container drop that does not breach the enclosed spent nuclear fuel assemblies and does not result in a release.

As illustrated in Figure 5-1, the scenario development process involves the analysis of all facility features or controls that can affect the progression of an event sequence, including the effects of successful operation or failure of the heating, ventilation, and air conditioning systems with

---

[1] All event sequence frequencies are assumed to be constant over the 100-year preclosure operating period.
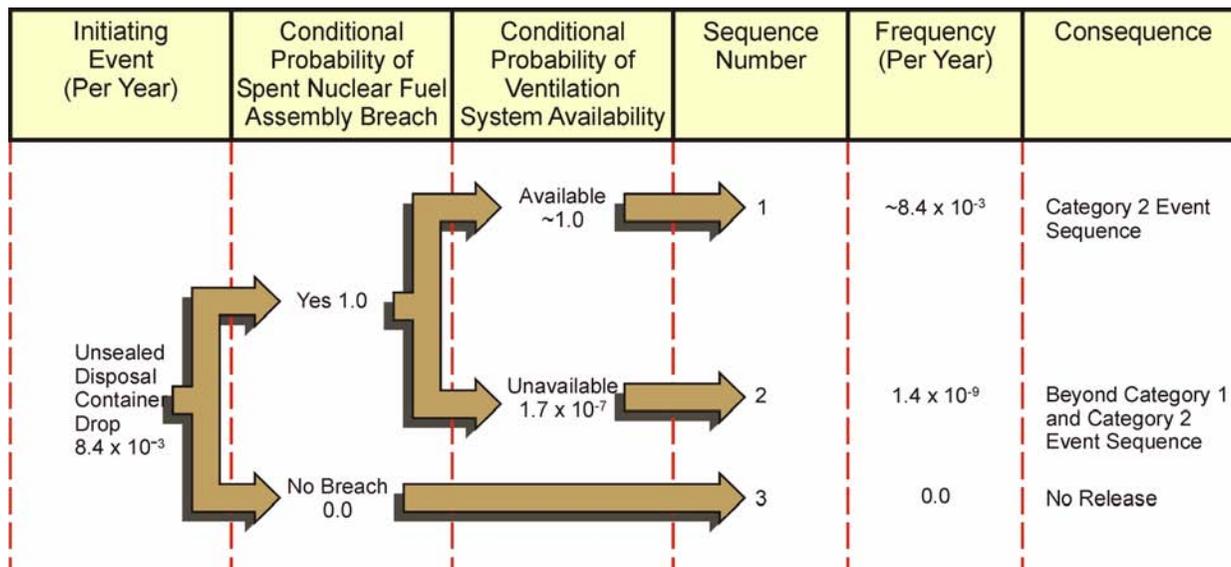
00033DC_ATP_Z1S50_04c.cdr

Figure 5-1.   Sample Event Tree
An event tree depicts the progression of an event sequence, starting at an initiating event and including successful operation or failure of facility features or controls. In this example, the initiating event is an unsealed disposal container drop and the facility feature or control is the ventilation system. The probability of breaching the spent nuclear fuel assembly in this example, given an unsealed disposal container drop, is 100 percent.

high-efficiency particulate air filters, where appropriate. Insights gained from evaluating the frequency and consequences of such failure sequences are especially useful as inputs to the design and quality assurance classification processes.

5.2.3   Event Sequence Consequence Analysis Process

Category 1 Event Sequences—Three sources are expected to contribute to the annual radiation dose to the public or repository workers from Category 1 event sequences during the facility's preclosure operational lifetime: (1) operational effluents from the Waste Handling Building, (2) operational effluents from the subsurface areas of the repository, and (3) event sequences anticipated to occur at a frequency of 0.01 per year or higher. Section 5.3.5.4.1 in *Preliminary Preclosure Safety Assessment for the Monitored Geologic Repository Site Recommendation* (BSC 2001f) describes the

models used to estimate the radiation doses from Category 1 event sequences. Appendix A of *Preliminary Preclosure Safety Assessment for the Monitored Geologic Repository Site Recommendation* (BSC 2001f) considers the influence of flexible thermal operating modes with preclosure periods of up to 325 years on Category 1 event sequence selection.

Category 2 Event Sequences—The radiation doses from Category 2 event sequences come from event sequences anticipated to occur with frequencies between 0.01 and 0.000001 per year. This frequency range assumes a 100-year preclosure period that is associated with the higher-temperature repository operating mode. The Category 2 event sequences all involve drops or collisions while handling fuel assemblies, disposal containers, and transportation casks. Section 5.3.5.4.2 in *Preliminary Preclosure Safety Assessment for the Monitored Geologic Repository Site Recommendation* (BSC 2001f) describes the

models used to estimate the radiation doses from Category 2 event sequences. The influence on the selection of Category 2 event sequences of the flexible thermal operating modes with preclosure periods of up to 325 years is discussed in Appendix A of *Preliminary Preclosure Safety Assessment for the Monitored Geologic Repository Site Recommendation* (BSC 2001f).

Several dosimetric quantities were calculated for Category 1 and Category 2 event sequences: (1) the total effective dose equivalent; (2) the radiation dose for various organs and tissues, such as the thyroid, lungs, and bone marrow; and (3) the radiation dose for the skin. Consistent with *Standard Review Plan for Spent Fuel Dry Storage Facilities* (NRC 2000a, Section 9.5.2.2), the sum of the skin dose equivalent and the total effective dose equivalent was used to indicate the lens of the eye dose.

5.2.4   Use of Features and Controls Important to Radiological Safety

The repository design incorporates a combination of prevention and mitigation features and operational controls. Prevention is the use of design features to reduce the frequency of events that result in radiological release. Mitigation involves the use of design features to reduce the consequences of a postulated radiological release event sequences, and includes those features intended to reduce releases from routine operations that are included in the Category 1 event sequences annual dose summation. The safety assessment is used to identify preventive and mitigative features.

The repository design emphasizes prevention features because prevention provides design and operational benefits. From an operations perspective, surveillance and maintenance of active safety features have been demonstrated to add to the operational complexity of existing nuclear facilities. Prevention features are incorporated in the design by performing the safety assessment as an integral part of the design process in a manner consistent with a performance-based, risk-informed philosophy. A risk-informed approach uses risk insights, engineering analysis and judgment, and equipment performance history to focus attention on the most

important facility activities and to establish design criteria and management controls based upon these risk insights. This approach ensures that design features and operational controls important to radiological safety are selected in a manner that ensures safety while minimizing operational complexity through the use of proven technology.

The repository would be designed, constructed, and operated to withstand external events and natural phenomena for Category 1 and Category 2 event sequences. For example, Section 2.2.4.2.2 of this report discusses requirements for designing the surface facilities to withstand the vibratory motion associated with earthquakes. As an example, in the assembly transfer system and canister transfer system, overhead cranes and assembly transfer machines would be designed so that they would not become dislodged from their rails during a Category 1 or Category 2 event sequence earthquake. Section 2.2.5 also discusses the design processes used to keep radiation doses to workers ALARA.

For accidents involving internal events, the analysis in *Design Basis Event Frequency and Dose Calculation for Site Recommendation* (BSC 2001u, Table 9) shows that drops of a spent nuclear fuel assembly or canister were important contributors to event sequences. To prevent these types of accidents, the assembly transfer system would be designed, constructed, and operated so that the probability of the dry assembly transfer machine dropping an assembly is low (CRWMS M&O 2000v, Section 1.2.2.1.1). In addition, to reduce the probability that the assembly or canister would be breached because of a drop, the lift heights for fuel assemblies and canisters would be limited, as is standard practice in nuclear facility design and operations.

The analyses in *Design Basis Event Frequency and Dose Calculation for Site Recommendation* (BSC 2001u, Section 5.2.5) show that the availability of the Waste Handling Building heating, ventilation, and air conditioning system with high-efficiency particulate air filters plays a large role in mitigating the consequences of accidents. Therefore, the ventilation system would be designed to be highly reliable. For example, it would be designed to withstand earthquakes, impacts from flying debris

(referred to as missiles), fires, or loss of offsite electrical power and still perform its intended safety functions.

The key prevention and mitigation methods rely on the use of:

- Designs that accommodate potential natural phenomena (e.g., fault avoidance, placement, layout, design basis to withstand seismic events, backup power)

- Designs that incorporate safety features for normal operations and Category 1 and Category 2 event sequences (e.g., limits of lift heights, air filtration and confinement systems, redundant systems, limit switches)

- Administration controls (e.g., trained and certified personnel, approved procedures).

5.2.5 Quality Assurance Classification Process

The safety assessment provides valuable input to the quality assurance classification process. Repository features credited as event prevention or mitigation features in the safety assessment are "important to safety," and the safety assessment is useful in determining an item's functional role as part of the repository preclosure safety strategy. Classification is performed in a separate analysis, in accordance with formal quality assurance classification procedures. Structures, systems, and components important to safety are classified in a graded fashion to ensure quality assurance controls are implemented over the facility life cycle commensurate with an item's importance to safety.

The classification process consists of establishing the configuration and function of structures, systems, and components and their effect on repository radiological safety. It is limited to structures, systems, and components procured as a part of the repository system (e.g., transportation casks are not included). This information is then evaluated against criteria provided in the classification procedure to determine the quality assurance classification of the particular item. The following classification categories are specified by Section

3.1.3 of QAP-2-3, *Classification of Permanent Items,* consistent with Section 2 of *Quality Assurance Requirements and Description* (DOE 2000a).

Quality Level (QL)-1—Structures, systems, and components whose failure could directly result in a condition adversely affecting public safety are classified as QL-1. These items have a high safety or waste isolation significance.

QL-1 structures, systems, and components include those items, which:

- Maintain containment and criticality control for spent nuclear fuel and high-level radioactive waste

- Prevent or mitigate a Category 1 or Category 2 event sequence.

QL-1 structures, systems, and components are listed in Table 5-3 with a brief summary of their functions that are important to safety.

QL-2—Structures, systems, and components whose failure or malfunction could indirectly result in a condition adversely affecting public safety, or whose failure would result in doses in excess of normal operational limits, are classified as QL-2. These items have a lower safety or waste isolation significance.

QL-2 structures, systems, and components include those items, which:

- Provide control and management of site-generated radioactive waste

- Provide fire protection/suppression to protect the function of a QL-1 structure, system, or component important to safety

- Maintain structure, system, or component integrity so that a QL-1 structure, system, or component is not prevented from performing its intended function if an event sequence occurs

- Prevent or mitigate a Category 1 event sequence

Table 5-3. QL-1 Structures, Systems, and Components

Structure, System, or Component	Monitored Geologic Repository System	Function Important to Safety
Assembly transfer baskets	Assembly transfer system	Provide criticality control for spent nuclear fuel assemblies
Basket staging racks	Assembly transfer system	Provide criticality control for spent nuclear fuel assemblies
Control and tracking system	Waste emplacement/ retrieval system	Provide operational information to the operations, monitoring, and control system; minimize the likelihood of uncontrolled descent of the waste package transporter and the possible impact of a waste package with the subsurface facility structure or other facility equipment resulting in radiological release
Disposal containers	Waste package designs	Provide containment and criticality control for waste
Drip shield	Emplacement drift system	Provide containment, waste package protection, and heat transfer
Locomotives	Waste emplacement/ retrieval system	Minimize the likelihood of uncontrolled descent of the waste package transporter and the possible impact of a waste package with the subsurface facility structure or other facility equipment, resulting in a radiological release
Modified waste package transporter	Waste emplacement/ retrieval system	Minimize the likelihood of uncontrolled descent of the waste package transporter and the possible impact of a waste package with the subsurface facility structure or other facility equipment resulting in radiological release
Small canister staging racks	Canister transfer system	Provide criticality control for DOE high-level waste canisters
Waste package transporter	Waste emplacement/ retrieval system	Minimize the likelihood of uncontrolled descent of the waste package transporter and the possible impact of a waste package with subsurface facility structure or other facility equipment, resulting in a radiological release
Waste Handling Building structure	Waste Handling Building system	Provide containment of radioactive materials, radiation shielding, and protection of equipment from internal and external hazards

Source: BSC 2001f, Table 4-1.

- In conjunction with an additional item or administrative control, prevent or mitigate a Category 2 event sequence.

QL-2 structures, systems, and components are listed in Table 5-4 with a brief summary of their functions that are important to safety.

QL-3—Structures, systems, and components whose failure or malfunction would not significantly impact public or worker safety, including those defense-in-depth design features intended to keep radiation doses ALARA, are classified as QL-3. These items have a minor impact on public and worker safety and on waste isolation.

QL-3 structures, systems, and components include those items, which:

- Warn of significant increases in radiation levels or concentrations of radioactive materials

- Monitor variables to verify that operating conditions are within technical specification limits

- Support repository emergency response actions

- Assess radionuclide release or dispersion following an event sequence

- Maintain levels of radioactive effluents

- Limit worker doses from normal operations and Category 1 event sequences.

Examples of structures, systems, and components classified as QL-3 include the meteorological monitoring system, area radiation monitoring system, and exhaust stack radiation monitors (BSC 2001f, Table 4-3).

Table 5-4. QL-2 Structures, Systems, and Components

Structure, System, or Component	Monitored Geologic Repository System	Function Important to Safety
Assembly drying system	Assembly transfer system	Collect and manage site-generated radioactive waste produced in the assembly drying process
Backfill emplacement system	Backfill emplacement system	Maintain structural integrity
Bridge cranes	Assembly transfer system Carrier/cask handling system Canister transfer system Disposal container handling system Waste package remediation system	Maintain structural integrity Prevent interactions with QL-1 structures, systems, and components
Control and tracking system	Assembly transfer system	Minimize the likelihood of drop of assembly transfer basket during transfer of spent nuclear fuel assemblies
Control and tracking system	Carrier/cask handling system	Provide operations support necessary for waste handling safety by controlling crane movement during handling of transportation casks
Control and tracking system	Canister transfer system Disposal container handling system Waste package remediation system	Support site-generated radiological waste collection and management functions
Cooling system	Assembly transfer system	Collect and manage the site-generated radioactive waste generated in the spent nuclear fuel container cooling process
Covered shuttlecars	Waste emplacement/retrieval system	Provide for radioactive particulate confinement
Disposal container inerting system	Disposal container handling system	Collect and manage the site-generated radioactive waste generated in the disposal container inerting process
Disposal container loading port mating device	Assembly transfer system	Maintain structural integrity
Disposal container weld station jib crane	Disposal container handling system	Maintain structural integrity
Decontamination systems	Assembly transfer system Canister transfer system Disposal container handling system Waste Handling Building system Waste package remediation system Waste emplacement/retrieval system	Collect and manage the site-generated radioactive waste generated in the process of facility and equipment decontamination
Dry assembly transfer machine	Assembly transfer system	Maintain structural integrity Prevent drop of assembly transfer basket during transfer of spent nuclear fuel assemblies
Dual-purpose canister lid severing tool	Assembly transfer system	Collect and manage radiologically contaminated metal chips generated during dual-purpose canister lid removal operations
Emergency power source and distribution system	Waste Handling Building electrical system	Support the Waste Handling Building primary ventilation system in mitigating the consequences of an event sequence
Emplacement drift ground control	Ground control system	Minimize the likelihood of breach of waste package in emplacement drift due to rockfall
Fire detection systems	Waste Handling Building fire protection system	Protect QL-1 structures, systems, and components from the effects of fire
Fire suppression systems	Waste Handling Building fire protection system	Protect QL-1 structures, systems, and components from the effects of fire
Invert	Emplacement drift system	Provide support for mobile equipment in the drifts and for the drip shield and waste package/pallet combination
Lifting fixtures, cask and dual-purpose canister preparation system Lifting fixtures, disposal container handling system	Assembly transfer system Disposal container handling system	Maintain structural integrity

Table 5-4. QL-2 Structures, Systems, and Components (Continued)

Structure, System, or Component	Monitored Geologic Repository System	Function Important to Safety
Lifting fixtures, dry assembly handling system	Assembly transfer system	Minimize the likelihood of drop of assembly transfer basket during transfer of spent nuclear fuel assemblies
Liquid low-level waste system	Site-generated radiological waste handling system	Collect and manage site-generated radioactive waste generated in the operation of monitored geologic repository facilities
Mixed low-level waste system	Site-generated radiological waste handling system	Collect and manage site-generated mixed waste generated in the operation of monitored geologic repository facilities
Monitored geologic repository operations monitoring and control system	Monitored geologic repository operations monitoring and control system	Mitigate the consequences of an event sequence
Multipurpose hauler	Waste emplacement/retrieval system	Provide for radioactive particulate confinement for breached waste packages
Pool water treatment	Pool water treatment and cooling system	Collect and manage site-generated radioactive waste generated in the process of pool water treatment
Site fire protection system	Site fire protection system	Protect QL-1 structures, systems, and components from the effects of fire
Solid low-level waste system	Site-generated radiological waste handling system	Collect and manage site-generated radioactive waste generated in the operation of monitored geologic repository facilities
Waste Handling Building primary, secondary, and tertiary confinement area ventilation system	Waste Handling Building ventilation system	Mitigate the consequences of an event sequence
Waste package/disposal container weld preparation and opening system	Waste package remediation system	Collect and manage radiologically contaminated metal chips generated during lid removal operations
Waste package horizontal lifting system	Disposal container handling system	Maintain structural integrity
Waste package emplacement pallet	Emplacement drift system	Prevent the waste package from shifting and impacting the drip shield
Waste Treatment Building confinement area ventilation system	Waste Treatment Building ventilation system	Collect and manage site-generated radioactive waste generated in the operation of monitored geologic repository facilities
Waste Treatment Building system	Waste Treatment Building system	Collect and manage site-generated radioactive waste generated in the operation of monitored geologic repository facilities
Wet assembly transfer machine	Assembly transfer system	Maintain structural integrity

Source: BSC 2001f, Table 4-2.

Conventional Quality (CQ)—Those structures, systems, and components not meeting any of the criteria for QL-1, QL-2, or QL-3. Examples of structures, systems, and components classified as CQ include materials for balance-of-plant buildings, utilities, and commercial off-the-shelf materials and equipment.

This classification process is implemented in an iterative fashion, where each analysis iteration is considered for that phase of design. Classifications of repository structures, systems, and components will, therefore, be reevaluated as the design is developed. This approach is consistent with *Technical Position on Items and Activities in the High-Level Waste Geologic Repository Program Subject to Quality Assurance Requirements* (Duncan et al. 1988, Section 4.2(a)), which allows engineering judgment and conservative bounding assumptions to be used in cases where data are limited.

5.3 PRELIMINARY DESCRIPTION OF POTENTIAL HAZARDS, EVENT SEQUENCES, AND CONSEQUENCES

This section presents the preliminary description of potential hazards, event sequences, and consequences of event sequences. Section 5.3.1 identifies the external events and natural phenomena that are the initiating events that could lead to a radiological release. Section 5.3.2 describes internal initiating events, including those that could result in a potential radiological release, no release, or a beyond Category 1 and Category 2 event sequence. Section 5.3.3 presents the consequence evaluations for Category 1 and Category 2 event sequences.

5.3.1 Preliminary Description of External Events

The general strategy for managing external initiating events is to design those structures, systems, and components important to safety to withstand the initiating events so that no release scenarios are initiated and no loss of isolation of radioactive material results. Table 5-5 lists the external events and natural phenomena initiating events considered in this evaluation. The events in Table 5-5 are appropriate for preclosure period of 100 years as well as 325 years (BSC 2001f, Appendix A).

Loss of Offsite Power—This event results in the total loss of external alternating current power to the potential repository for any period of time. It is postulated to occur as a result of an external event (e.g., lightning or downed power line) or an internal event (e.g., fire or random equipment failure). Loss of offsite power would, at a minimum, temporarily halt the transfer of waste. Loss of offsite power at the potential repository is assumed to occur one or more times during preclosure operations; therefore, it is a Category 1 event sequence.

The strategy for this event is to prevent Category 1 or Category 2 release scenarios by providing reliable power through redundant standby power sources (onsite), uninterruptible power, redundant emergency equipment where needed, redundant distribution systems, and mechanical backup controls for components important to safety. Structures, systems, and components important to safety are designed to prevent load drops during a loss of offsite power. Onsite backup power sources with staged loading controls and potential redundant offsite power lines and sources may be used to ensure continuous power is supplied to structures, systems, and components important to safety. The potential repository design would also include such features as external lightning rods to protect against a lightning-initiated loss of offsite power.

Earthquake—Vibratory Ground Motion—An earthquake is the result of sudden relative motions, or slip, between two adjacent rock surfaces in the earth's crust. The sudden slip results in the release of seismic energy, in the form of vibratory ground motion, that propagates from the location of the

Table 5-5. External Initiating Events and Natural Phenomena

Initiating Event/Natural Phenomenon	Location	Frequency (per year)	Initiating Event Frequency Category[a]
Loss of offsite power	Surface and subsurface facilities	<1	1
Earthquake—vibratory ground motion	Surface and subsurface facilities	0.001 0.0001	1 2
Earthquake—fault displacement	Surface and subsurface facilities	0.0001 0.00001	1 2
Probable maximum flood	Surface and subsurface facilities	<<0.01	2
Tornado missiles	Surface facilities	<<0.01	2
Tornado wind	Surface facilities	<<0.01	2

NOTES: [a]For external events, the initiating event (e.g., earthquake) frequency is considered instead of the event sequence.

Source: BSC 2001f, Table 5-4

earthquake to the earth's surface. This ground motion can impact structures, systems, and components in the surface and subsurface facilities and lead to a radiological release. The possible consequences of an earthquake include a collapse of structures, concrete cracking, loss of offsite power, ground displacement, and subsurface rockfall.

The U.S. Department of Energy (DOE) would use proven engineering techniques to design structures to withstand potential earthquakes in the site area. The repository surface facilities, where waste would be received, prepared for emplacement, and moved into the repository, would be subject to stronger earthquake ground shaking than subsurface facilities, where waste would be emplaced.

Preclosure Seismic Design Methodology for a Geologic Repository at Yucca Mountain (YMP 1997, Section 3.1) establishes seismic hazard probability reference values to be used in determining two levels of design basis vibratory ground motion. The two reference values correspond to Category 1 and Category 2 event sequences and are defined as mean annual exceedance probabilities of 10^{-3} and 10^{-4}, respectively. The mean annual probabilities were used in the disaggregation of probabilistic seismic hazard estimates (CRWMS M&O 2000fd, Section 6.5.3) to identify those earthquakes that control the seismic hazard at the reference probabilities.

Ground motion inputs used for preclosure design analyses are described in Section 4.3.2.2.3 (Figure 4-165). These inputs are based on a mean annual exceedance probability of 10^{-4} and were developed for generic locations at the repository elevation (i.e., a depth of 300 m [1,000 ft]) and at a hard-rock outcrop directly above the potential repository.

The safety strategy for the surface facilities is to design the structures, systems, and components important to safety to withstand the effects of a design basis earthquake. The design and construction attributes necessary to ensure that structures and systems are not compromised during a seismic event are well understood and would be applied to the repository facilities.

The following NRC documents related to design basis seismic events were among the sources considered in the repository design process:

- Regulatory Guide 1.29, *Seismic Design Classification*

- Regulatory Guide 1.32, *Criteria for Safety-Related Electric Power Systems for Nuclear Power Plants*

- Regulatory Guide 1.60, *Design Response Spectra for Seismic Design of Nuclear Power Plants*

- Regulatory Guide 1.61, *Damping Values for Seismic Design of Nuclear Power Plants*

- Regulatory Guide 1.92, *Combining Modal Responses and Spatial Components in Seismic Response Analysis*

- Regulatory Guide 1.122, *Development of Floor Design Response Spectra for Seismic Design of Floor-Supported Equipment or Components*

- Regulatory Guide 1.165, *Identification and Characterization of Seismic Sources and Determination of Safe Shutdown Earthquake Ground Motion.*

Earthquake—Fault Displacement—A fault is a fracture or zone of weakness in the earth's crust along which there is the potential for relative motion of rocks on opposing sides of the fracture. Scientists have used the data from site characterization studies to assess the potential for fault rupture related to earthquakes.

Preclosure Seismic Design Methodology for a Geologic Repository at Yucca Mountain (YMP 1997) establishes the probabilistic criteria for fault displacement initiating events appropriate for structures, systems, and components important to safety. Specifically, the mean annual exceedance probabilities of 10^{-4} and 10^{-5} are used for Category 1 and Category 2 initiating event fault displacements, respectively. These values are a factor of 10 lower than the exceedance probabilities of the

corresponding Category 1 and Category 2 initiating event vibratory ground motion, reflecting the more limited experience with engineering designs for facilities that are subject to fault displacement and with assessments of fault displacement hazard.

An evaluation of the fault displacement hazard at nine locations in the Yucca Mountain vicinity was part of the probabilistic seismic hazard analyses (CRWMS M&O 2000fd, Section 6.6.3). The nine locations span the range of known faulting conditions in the area, which include recognized faults, small fractures, and unfaulted (intact) rock. Results of the hazard assessment indicate that mean displacements on the block-bounding Bow Ridge and Solitario Canyon faults are 7.8 cm (3.1 in.) and 32 cm (12.6 in.), respectively, at the 10^{-5} annual exceedance probability level. In contrast, in areas where waste would be emplaced, displacements of 0.1 cm (0.04 in.) have less than one chance in 100,000 of being exceeded each year during the preclosure period.

Unlike vibratory ground motion hazard, fault displacement hazard is concentrated at the location of faults. Consequently, the exposure of structures, systems, and components to fault displacement hazard can be limited by avoiding locations near faults that have a significant potential for fault displacement. Fault avoidance is the DOE's preferred approach to mitigating fault displacement hazards.

The NRC's *Staff Technical Position on Consideration of Fault Displacement Hazards in Geologic Repository Design* (McConnell and Lee 1994) was considered in the repository design process.

Flood—An external flood may be initiated by intense precipitation, runoff, or a landslide. As defined by Section 2 of ANSI/ANS-2.8-1992, *American National Standard for Determining Design Basis Flooding at Power Reactor Sites*, the probable maximum flood is the hypothetical flood (peak discharge, volume, and hydrograph shape) considered to be the most severe reasonably possible flood, based on a probable maximum precipitation and other hydrologic factors favorable for maximum flood runoff, such as sequential storms and snowmelt. A 100-year flood is defined

as the magnitude of peak discharge at any point on a river or drainage channel that can be expected to occur or be exceeded, on average, once in 100 years. Since the Yucca Mountain area is located inland and has no significant surface-water bodies or water-control structures near the site, there is no potential for such events as surges, seiches, tsunamis, dam failures, or ice jams that could affect the site nor is there any potential for future dam development. No evidence for past flooding induced by landslides in the vicinity of the site has been reported. However, floods can produce heavy loads on structures and equipment. The consequences of a flood initiating event are expected to bound the rainstorm, landslide, and debris avalanche events (BSC 2001f, Section 5.2.1.4).

The primary safety strategy for the flood event is to locate facilities outside of flood-prone areas and provide diversion channels to divert runoff away from structures. Taking into account the effects of sediment and debris transported during flood events, a series of worst-case flood studies was completed. The North Portal site is adjacent to the Midway Valley Wash. The maximum depth of water in this wash was estimated to be about 3 to 4 m (9 to 12 ft) during a probable maximum flood, with consideration given to the presence of sediment and debris. Although it was determined that a portion of the North Portal pad is in the flood-prone area, the flood waters would stop at or flow around the boundary of the pad because the pad would be higher than the maximum flood levels. Since water would rise in response to flow restrictions caused by the pad, the Waste Handling Building and Waste Treatment Building would be set approximately 0.5 m (1.5 ft) above the maximum flood elevation. The pad for the balance-of-plant area would be set about 1 m (3 ft) below the floor elevation of the Waste Handling Building to account for its dock height at the southeast corner. The drainage of the Radiologically Controlled Area would protect this pad from a probable maximum flood. An underground storm drainage collection system would contain the runoff from this area and prevent spillage into the balance-of-plant area, protecting the pad from the flood. Two open channels constructed for the Exploratory Studies Facility would protect the

North Portal from the probable maximum flood (BSC 2001f, Section 5.2.1.4).

The Waste Handling Building, Waste Treatment Building, and Carrier Preparation Building are all designed to withstand the probable maximum flood. Other surface facilities are designed to withstand the 100-year flood, based on standard industrial practice (BSC 2001f, Section 5.2.1.4).

For defense in depth, the following additional surface facility characteristics or design features may also be used for flood protection:

- Hardened foundations and structures
- Sandbags, flood doors, and bulkheads
- Waste Handling Building cells located within an interior wall
- Administrative controls during severe weather conditions.

Regulatory Guide 1.59, *Design Basis Floods for Nuclear Power Plants*, was among the sources considered in the repository design process.

Tornado Missiles—This event involves the impact of a tornado-generated missile (flying debris). The tornado initiating event is classified as a Category 2 event sequence (BSC 2001f, Section 5.2.1.5).

The primary safety strategy is to preclude a radiological release by designing structures, systems, and components important to safety that could be vulnerable to a tornado missile to withstand the design basis tornado.

Structures, systems, and components that are vulnerable to tornado missile impacts are either protected from the missiles, designed to withstand a missile impact, or shown to not interact with a missile by a probabilistic analysis. The waste package transporter is designed to prevent any penetration that could breach a waste package as a result of the impact of a tornado missile, the surface facility foundations and structures would be designed to protect the waste forms inside from a tornado missile initiating event, and the Waste Handling Building ventilation system would be designed to continue functioning after a tornado missile initiating event impact.

Sections 3.5.1.4 and 3.5.2 of *Standard Review Plan for the Review of Safety Analysis Reports for Nuclear Power Plants* (NRC 1987) provide NRC guidance on missiles generated by natural phenomena and externally generated missiles, respectively. Additional defense-in-depth safety features may include administrative controls in the event of a tornado warning or extreme weather conditions, hardened buildings, and the installation of underground utilities.

Tornado Wind—This event is associated with the effects produced by high winds during a tornado (i.e., pressure drop and wind loading). The consequences of this event are pressure loads on the surface facilities, waste package transporter, and transportation cask surfaces. The design basis tornado wind is classified as a Category 2 event sequence (BSC 2001f, Section 5.2.1.6).

Structures, systems, and components that are important to safety and potentially vulnerable to a tornado would be designed to withstand the static loading and pressure drops associated with the design basis tornado. This strategy includes designing the Waste Handling Building foundations and structures to withstand the design basis tornado and designing the Waste Handling Building ventilation system to confine and filter particulates following a design basis tornado.

The following NRC documents related to design basis tornadoes were among the sources considered in the repository design process:

- Regulatory Guide 1.76, *Design Basis Tornado for Nuclear Power Plants*

- Regulatory Guide 1.117, *Tornado Design Classification*

- Sections 2.3.1 (Regional Climatology), 3.3.1 (Wind Loadings), and 3.3.2 (Tornado Loadings) of *Standard Review Plan for the Review of Safety Analysis Reports for Nuclear Power Plants* (NRC 1987)

- *Tornado Climatology of the Contiguous United States* (Ramsdell and Andrews 1986).

The design basis tornado wind for the Yucca Mountain region is 304 km/hr (189 mi/hr), with a 0.000001 probability of occurrence and a 90 percent strike probability confidence interval (BSC 2001f, Section 5.2.1.6). This wind speed bounds both the 100-year return period fastest mile wind (100-year, 1-minute gust) referenced in *Standard Review Plan for the Review of Safety Analysis Reports for Nuclear Power Plants* (NRC 1987, Section 2.3.1) and the basic wind (50-year, 3-second gust) calculated from the methodology in Section 6 of ASCE 7-98, *Minimum Design Loads for Buildings and Other Structures*.

As with the tornado-generated missile event, potential defense-in-depth safety features to protect against tornado winds may include administrative controls in the event of a tornado warning or extreme weather conditions, hardened buildings, and the installation of underground utilities.

In summary, the repository structures, systems, and components deemed important to safety would be designed to withstand or to be protected from bounding external events and natural phenomena to prevent the release of radioactive material.

5.3.2 Preliminary Description of Internal Event Sequences

Radiological consequences for the bounding internal event sequences were evaluated. Bounding event sequences include groups of similar event sequences that result in the maximum radiological consequences to a member of the public at the preclosure controlled area boundary or to a worker onsite. Collectively, the bounding event sequences establish constraints on the facility design to ensure that structures, systems, and components important to safety would perform their intended function during an event sequence, and that any radiological releases would remain within established dose limits.

Internal event sequences were screened into one of three groups, based on their frequency of occur-

rence and potential to result in a radiological release:

- Internal event sequences with potential releases
- Internal event sequences with no releases
- Beyond Category 1 and Category 2 event sequences.

5.3.2.1 Internal Event Sequences with Potential Releases

These events could potentially result in a release of radionuclides, and would therefore be mitigated by the facility design. These events have been classified as Category 1 or Category 2 event sequences.

In *Preliminary Preclosure Safety Assessment for Monitored Geologic Repository Site Recommendation* (BSC 2001f, Section 4.4.1.2.1), the impact of preclosure operational periods of up to 325 years on the internal events screening frequency thresholds (see Section 5.2.2) were investigated. For internal events that could impact the surface facility, the conclusion was that the results of using a 100-year preclosure period to screen internal event sequences would be unchanged by extending the period to 325 years since surface fuel handling operations would be completed after approximately 24 years. There would be no waste forms in the surface facility once the waste package subsurface emplacement operations are completed. *Preliminary Preclosure Safety Assessment for Monitored Geologic Repository Site Recommendation* (BSC 2001f, Appendix A2.1) considered the increased number of waste packages for the lower-temperature thermal operating mode with de-rated or smaller waste packages (see Section 2.1.5.2, Table 2-2) and judged that the effect of additional waste package handling could increase the likelihood of some event sequences but would not change the selection of bounding event sequences that result in radionuclide releases. One potential approach to lowering the thermal output of waste packages is to age fuel by placing it into the fuel blending inventory (see Section 2.1.4). *Preliminary Preclosure Safety Assessment for Monitored Geologic Repository Site Recommendation* (BSC 2001f, Appendix A6) judged that the handling and storage of fuel in this scenario is not expected to

change the selection of bounding event sequences that result in radionuclide releases.

For the subsurface facility, extension of preclosure operations to 325 years does impact the screening criteria. However, *Preliminary Preclosure Safety Assessment for Monitored Geologic Repository Site Recommendation* (BSC 2001f) examined the selection of internal event sequences based on an extended preclosure period and found no new internal events that would impact the selection of bounding event sequences. For example, the extended forced circulation ventilation activities in the subsurface facility after emplacement is completed, but before permanent closure, would not be expected to result in a loss of waste package containment.

All the thermal operating modes evaluated periods of forced ventilation (see Section 2.1.5.2, Table 2-2). Forced ventilation system failures are not expected to prevent the waste package from providing containment during the preclosure period. After waste emplacement is completed, it would take about 3 weeks without forced cooling before emplacement drift wall temperature limits are approached. Therefore, temperature goals supporting postclosure performance can be main-

tained by repairing and restarting the forced circulation equipment within about 3 weeks (see Section 2.3.4.3.1.3).

5.3.2.1.1   Category 1 Event Sequences— Internal

The Category 1 event sequences evaluated in *Preliminary Preclosure Safety Assessment for Monitored Geologic Repository Site Recommendation* (BSC 2001f, Section 5.3.2) occurred during the handling of uncanistered commercial spent nuclear fuel assemblies or spent nuclear fuel assembly baskets in the assembly transfer system.

Table 5-6 identifies the Category 1 event sequences that could potentially result in radiological releases.

Sequences Involving Individual Spent Nuclear Fuel Assemblies—Unconfined spent nuclear fuel assemblies (i.e., assemblies not in containers) will be handled remotely, underwater and individually, during transfer from the cask to the assembly transfer system basket staging rack. Then they will be handled in a dry environment during transfer from the assembly transfer system dryer to the disposal container.

Table 5-6. Category 1 Internal Event Sequences

Event Sequence Number	Event Description	Location	Frequency (per year)
1-01	Spent fuel assembly drop onto another spent fuel assembly in cask	Assembly transfer system pool	0.2
1-02	Spent fuel assembly collision	Assembly transfer system pool	0.04
1-03	Spent fuel assembly drop onto empty basket	Assembly transfer system pool	0.04
1-04	Spent fuel assembly drop onto another spent fuel assembly in basket staging rack (lowering into)	Assembly transfer system pool	0.2
1-05	Basket drop onto another basket in basket staging rack (lifting out)	Assembly transfer system pool	0.04
1-06	Basket drop onto another basket in pool (transfer into pool storage)	Assembly transfer system pool	0.04
1-07	Basket drop onto another basket in pool (transfer out of pool storage)	Assembly transfer system pool	0.04
1-08	Basket drop onto transfer cart or pool floor	Assembly transfer system pool	0.04
1-09	Basket drop back into pool	Assembly transfer system pool	0.04
1-10	Basket drop onto assembly transfer system cell floor	Assembly transfer system cell	0.04
1-11	Basket drop onto another basket in dryer	Assembly transfer system cell	0.04
1-12	Spent fuel assembly drop onto another spent fuel assembly in dryer	Assembly transfer system cell	0.2
1-13	Spent fuel assembly drop onto assembly transfer system cell floor	Assembly transfer system cell	0.2
1-14	Spent fuel assembly drop onto another spent fuel assembly in disposal container	Assembly transfer system cell	0.2

Source: BSC 2001f, Table 5-5.

While underwater, spent nuclear fuel assemblies could be dropped or impacted as a result of a mechanical or control system failure of the wet assembly transfer machine, or as a result of operator error. These event sequences would occur in the assembly transfer system pool area, which is a confinement area with high-efficiency particulate air filtration. Individual spent fuel assembly event sequences that occur underwater are identified in Table 5-6 by sequence numbers 1-01 through 1-04.

During transfer from the dryer to the disposal container, individual spent fuel assemblies could be dropped or impacted as a result of a mechanical or control system failure of the dry assembly transfer machine, or operator error. These event sequences would occur in the assembly transfer system cell, which is a confinement area with high-efficiency particulate air filtration. Individual spent fuel assembly event sequences in the cell are identified in Table 5-6 by sequence numbers 1-12, 1-13, and 1-14.

The strategy is to confine particulate releases within the Waste Handling Building and maintain offsite radiological doses ALARA using the high-efficiency particulate air filters in the ventilation system.

Spent Fuel Assembly Basket Event Sequences—Spent nuclear fuel assembly baskets would first be handled underwater, during transfer out of the basket staging rack. From there the assembly baskets, which would contain a maximum of four pressurized water reactor spent nuclear fuel assemblies or eight boiling water reactor spent nuclear fuel assemblies, could be transferred and staged in the pool storage area to facilitate aging and blending or loaded directly into the incline transfer cart. Baskets that are staged in the pool area would have an additional step of movement from the storage pool to the incline transfer cart. Once loaded onto the incline transfer cart, assembly baskets would be transported out of the pool and into the assembly drying stations, where up to six baskets could be loaded into each of the two assembly dryers. The assembly transfer system pool and cell would both be located in confinement areas with high-efficiency particulate air filtration.

Spent nuclear fuel assembly baskets could be dropped or impacted in the pool during lifting out of the basket staging racks, during transport to the pool storage area, or during transport up the inclined transfer canal as a result of mechanical failures, control system failures, or operator error. Event sequences that occur underwater involving spent nuclear fuel assembly baskets are identified in Table 5-6 by sequence numbers 1-05 through 1-09.

The primary safety strategy is to confine radionuclide particulate releases to the assembly transfer system pool water by designing the pool system consistent with ANSI/ANS-57.7-1988, *American National Standard Design Criteria for an Independent Spent Fuel Storage Installation (Water Pool Type)*. The water treatment system will provide the capability to filter radioactive material, purify the water, and remove floating debris from the surfaces of pools. Workers will be able to use vacuums to remove particles from pool walls and floors (see Section 2.2.4.2.9). This same system provides the capability for cleanup of any radionuclide particulate releases into the pool water.

In addition, spent nuclear fuel assembly baskets can be dropped or impacted onto the floor or in one of the assembly dryers as a result of mechanical or control system failure of the dry assembly transfer machine or operator error. Spent nuclear fuel assembly basket sequences that occur in the cell are identified in Table 5-6 by sequence numbers 1-10 and 1-11.

5.3.2.1.2   Category 2 Event Sequences— Internal

The Category 2 event sequences evaluated in the *Preliminary Preclosure Safety Assessment for Monitored Geologic Repository Site Recommendation* (BSC 2001f, Section 5.3.3) would occur as a result of drops or collisions among handling equipment, unsealed disposal containers, or unsealed shipping casks. The bounding Category 2 internal event sequences that are expected to result in radiological releases are identified in Table 5-7.

Spent Nuclear Fuel Assembly Basket Collision During Transfer—A spent nuclear fuel assembly

Table 5-7. Category 2 Internal Event Sequences

Event Sequence Number	Event Description	Location	Frequency (per year)
2-01	Spent fuel assembly basket collision during transfer[a]	Assembly transfer system pool	0.007
2-02	Uncontrolled descent of incline transfer cart	Assembly transfer system pool	0.007
2-03	Handling equipment drop onto spent fuel assembly basket in pool[b]	Assembly transfer system pool	0.002
2-04	Handling equipment drop onto spent fuel assembly basket in cell[b]	Assembly transfer system cell	0.00007
2-05	Unsealed disposal container collision	Disposal container handling cell	0.002
2-06	Unsealed disposal container drop and slapdown	Disposal container handling cell	0.008
2-07	Handling equipment drop onto unsealed disposal container	Disposal container handling cell	0.0001
2-08	Unsealed transportation cask drop into cask preparation pit	Assembly transfer system cask preparation pit	0.009
2-09	Unsealed transportation cask drop into cask unloading pool	Assembly transfer system pool	0.009

NOTES: [a]This event encompasses two individual basket collision events, each with the same frequency and consequence.
[b]Event bounds the consequences of handling equipment drops onto a single spent fuel assembly and of a handling equipment drop onto a spent fuel assembly basket in the assembly transfer system pool.
Source: BSC 2001f, Table 5-6.

basket collides with a wall or other heavy object in the assembly transfer system pool, causing a breach and subsequent release. This event could occur during transfer either from the assembly basket rack to the pool area or from the pool area to the incline transfer cart. The pool water serves as a barrier to particulate release, so only the radioactive gases are released to the Waste Handling Building environment.

The primary safety strategy is to confine particulate releases within the assembly transfer system pool by designing the pool system consistent with ANSI/ANS-57.7-1988.

Uncontrolled Descent of Incline Transfer Cart—A remotely operated incline transfer cart containing a spent fuel assembly basket loses control during ascent up the incline transfer canal, resulting in an uncontrolled descent and impact with the assembly transfer system pool, which causes a breach and subsequent release. The pool water serves as a barrier to particulate release, so only the radioactive gases are released to the Waste Handling Building environment.

The primary safety strategy is to confine particulate releases within the assembly transfer system pool by designing the pool system consistent with ANSI/ANS-57.7-1988.

Handling Equipment Drop onto Spent Fuel Assembly Basket in Pool—A lifting yoke (or other heavy object) is dropped onto an uncanistered spent fuel assembly in the assembly transfer system pool, causing a breach and subsequent release. The pool water serves as a barrier to particulate release, so only the radioactive gases are released to the Waste Handling Building environment.

The primary safety strategy is to confine particulate releases within the assembly transfer system pool by designing the pool system consistent with ANSI/ANS-57.7-1988.

Handling Equipment Drop onto Spent Fuel Assembly Basket in Cell—A lifting yoke (or other heavy object) is dropped onto an uncanistered spent fuel assembly in the assembly transfer system cell, causing a breach and subsequent release.

The strategy is to confine particulate releases within the Waste Handling Building by relying on the high-efficiency particulate air filters in the heating, ventilation, and air conditioning system.

Unsealed Disposal Container Collision—A loaded, unsealed disposal container collides with a wall, shield door, or other heavy object, resulting in the release of a fraction of its radiological contents.

The strategy is (1) to confine particulate releases within the Waste Handling Building and maintain offsite radiological doses ALARA by using the high-efficiency particulate air filters in the heating, ventilation, and air conditioning system and (2) to provide design features (e.g., limit switches, redundant controls, emergency switch) and safe load paths that would minimize the likelihood of a collision that could result in a radiological release.

Unsealed Disposal Container Drop and Slapdown—A loaded, unsealed disposal container is dropped by the disposal container bridge crane onto a welding or staging fixture. After dropping, the unsealed disposal container is presumed to slap down onto the floor and release a fraction of its radiological contents. The drop height for this event is the normal handling height in the disposal container handling cell.

The strategy is (1) to confine particulate releases within the Waste Handling Building and maintain offsite radiological doses ALARA by using the high-efficiency particulate air filters in the heating, ventilation, and air conditioning system and (2) to provide design features (e.g., limit switches for lift height, interlocks, redundant controls, redundant cables, physical restraints) that would minimize unsealed disposal container drops and potential radiological releases.

Handling Equipment Drop onto Unsealed Disposal Container—A lifting yoke (or other heavy object) is dropped onto a loaded, unsealed disposal container, resulting in the release of a fraction of its radiological contents.

The strategy is (1) to confine particulate releases within the Waste Handling Building and maintain offsite radiological doses ALARA by using the high-efficiency particulate air filters in the heating, ventilation, and air conditioning system and (2) to provide design features that would minimize handling equipment drops onto spent nuclear fuel inside a disposal container.

Unsealed Transportation Cask Drop into Cask Preparation Pit—A transportation cask, without impact limiters and with its lid unbolted, is dropped from the normal lift height into the cask preparation pit in the assembly transfer system pool area.

The strategy is (1) to confine particulate releases within the Waste Handling Building and maintain offsite radiological doses ALARA by using the high-efficiency particulate air filters in the heating, ventilation, and air conditioning system and (2) to provide design features that prevent or minimize cask drops (e.g., limit switches, interlocks, redundant control circuitry, cable restraints) or reduce the impact of a drop (e.g., a shock absorber at the base of the pit).

Unsealed Transportation Cask Drop into Cask Unloading Pool—A transportation cask, without impact limiters and with its lid unbolted, is dropped by the cask bridge crane into the assembly transfer system cask unloading pool.

The strategy is to confine particulate releases within the assembly transfer system pool by designing the pool system consistent with ANSI/ANS-57.7-1988. In addition, particulate mitigation in the assembly transfer system pool area is provided by the secondary heating, ventilation, and air conditioning confinement ventilation system.

5.3.2.2 Internal Event Sequence with No Radioactive Material Release

For these event sequences, features of the design either prevent the event sequence from occurring or prevent a radionuclide release if the event occurs. Design features to prevent the event sequence can either physically prevent the event from occurring (e.g., by eliminating, at certain steps, the lifting of transportation casks or canistered waste) or reduce the event sequence frequency below the cutoff frequency of one in one million per year (e.g., by using redundant control features in cranes and control systems). Design features that prevent a release are based on the premise that Category 1 and Category 2 event sequences will occur and that affected structures, systems, and components must be designed to prevent the waste form from releasing radioactivity during such an event sequence. Prime examples of this include the waste package event sequences,

which establish design bases for the waste package to ensure that the waste package will not breach as a result of Category 1 or Category 2 event sequences. Section 3.5 of this report provides waste package event sequence analyses. Table 5-7 of *Preliminary Preclosure Safety Assessment for Monitored Geologic Repository Site Recommendation* (BSC 2001f, Section 5.3.4) identifies these events.

5.3.2.3 Beyond Category 1 and Category 2 Event Sequences

Beyond Category 1 and Category 2 event sequences are event sequences that have less than 1 chance in 10,000 of occurring before permanent closure. This corresponds to an annual frequency of less than 10^{-6} per year, based on an assumed preclosure lifetime of 100 years. Such event sequences are not analyzed further. However, structures, systems, and components reducing event sequences below 10^{-6} per year are considered in the design basis. Appendix A in *Preliminary Preclosure Safety Assessment for Monitored Geologic Repository Site Recommendation* (BSC 2001f) considers the impact of lower-temperature operating modes on the identification of beyond Category 1 and Category 2 event sequences. The frequency of two events were found to be influenced by the thermal operating modes. These events are aircraft crash into the surface facility and rockfall onto a waste package in the subsurface facility. Aircraft hazards are impacted by increases in the surface facility's size, which would accompany an operating mode in which spent nuclear fuel is aged before being emplaced underground. However, Appendix A4.2 of *Preliminary Preclosure Safety Assessment for Monitored Geologic Repository Site Recommendation* (BSC 2001f) considered the influence of the thermal operating modes on the surface facility size and concluded that the aircraft hazards are likely to remain beyond a Category 1 or Category 2 event sequence. Rockfall onto a waste package in the subsurface becomes more likely with increases in the preclosure period, which would accompany an operating mode with extended forced ventilation. However, Appendix A4.1 of *Preliminary Preclosure Safety Assessment for Monitored Geologic Repository Site Recommendation* (BSC 2001f) considered the

possible increase in the preclosure period and changes in the thermal operating modes on the drift temperature and concluded rockfall is likely to remain beyond a Category 1 or Category 2 event sequence with design optimization (e.g., optimized ground support features, waste package emplacement strategy). Table 5-12 of *Preliminary Preclosure Safety Assessment for Monitored Geologic Repository Site Recommendation* (BSC 2001f, Section 5.4) identifies these events.

5.3.3 Consequence Evaluations

5.3.3.1 Category 1 Event Sequence Consequences

Design Basis Event Frequency and Dose Calculation for Site Recommendation (BSC 2001u) evaluated the consequences of Category 1 event sequences. Offsite radiation doses for Category 1 event sequences and normal operational effluents and emissions were based on the following (BSC 2001u, Section 6.1.1):

- Annual radiation doses for the sum of normal operational effluents and emissions, including all Category 1 event sequences

- Inhalation, ingestion, air immersion, and external exposure to radioactive contamination on the ground surface

- Mitigation, by high-efficiency particulate air filters, of particulate emissions from the repository

- For calculating the atmospheric releases from repository surface facilities, the distance to the receptor was 11 km (7 mi), the closest distance from the potential repository surface facilities to the potential site boundary. The ventilation exhaust locations for the subsurface areas of the repository are located about 3 km (2 mi) closer to the potential site boundary than the repository surface facilities. Therefore, for atmospheric emissions from the ventilation exhaust locations for the subsurface areas of the repository, the distance to the receptor is 8 km (5 mi) (BSC 2001u, Section 3.3)

- Annual average ground-level atmospheric dispersion factors (BSC 2001f, Section 5.3.5.3).

The bounding Category 1 event sequences evaluated for the potential repository are internal event sequences that occur during handling of uncanistered commercial spent nuclear fuel assemblies or spent nuclear fuel assembly baskets in the assembly transfer system (Table 5-6). No releases would occur due to external initiating events; therefore, external events have not been included in the dose calculations. No Category 1 event sequences have been identified for the subsurface facilities. All Category 1 event sequences would occur in surface facility confinement areas with high-efficiency particulate air filtration that is functional in the event sequences. The reliability of the heating, ventilation, and air conditioning system, used in event trees to calculate sequence frequencies, is based on the results of *Reliability Assessment of Waste Handling Building HVAC System* (CRWMS M&O 1999r).

The cumulative radiation doses for Category 1 event sequences, including normal operational effluents and emissions, are summarized in Table 5-8. The dose receptor is a member of the public located at the assumed site boundary. The cumulative radiation dose to this hypothetical average member of the public estimated for Category 1 event sequences was 0.06 mrem/yr total effective

dose equivalent (BSC 2001f, Section 5.3.6.1). This very low dose is attributed to several factors, including:

1. The distance between the Waste Handling Building and the nearest unrestricted area of the site boundary (approximately 11 km [7 mi])

2. A maximum allowable radiation dose of 10 mrem/hr at a distance of 2 m (6 ft) from the edge of the transport vehicle

3. Shielding of radiation source within the Waste Handling Building

4. Shielding surrounding the waste package transporter.

All of the Category 1 event sequences occur either in cells, where workers would not be present and would be protected by shield walls, or in pool areas, where particulate radionuclides are retained by the pool water. In addition, the Waste Handling Building ventilation system is designed to control airflow, filter radionuclide particulates, and vent filtered emissions through an elevated stack to the external environment. Therefore, the potential radiation exposure for Category 1 event sequences for workers is calculated at a location outside the Waste Handling Building, at an assumed distance of 100 m (330 ft). These workers are not necessarily the workers that would be involved with

Table 5-8. Summary of Preclosure Category 1 Event Sequence Radiation Doses for the Public and Workers

Case	Dose Type	Radiation Dose
Offsite public, Category 1 event sequences (including normal operational effluents and emissions)	Total effective dose equivalent	0.06 mrem/yr[a]
	External exposure	<< 2 mrem/hr[a]
Workers, Category 1 event sequences (including normal operational effluents and emissions)	Total effective dose equivalent	0.01 rem/yr[b]
	Organ or tissue plus deep dose	0.10 rem/yr[b]
	Skin and extremities	0.13 rem/yr[b]
	Lens of the eye	0.15 rem/yr[b]
Workers, routine occupational exposures	Total effective dose equivalent	0.06 to 0.79 rem/yr[c]

NOTES: [a]BSC 2001f, Section 5.3.6.1—calculated for site boundary.

[b]BSC 2001u, Table 8.

[c]DOE 2002, Tables 4-22, 4-25, 4-28, and 4-31.

waste handling operations and exposed during routine operations; therefore, the radiation doses for workers from Category 1 event sequences are not added to the radiation doses from routine occupational exposures.

The radiation dose to the worker at 100 m (330 ft) from Category 1 event sequences was estimated to be 0.01 rem/yr (BSC 2001u, Table 8). The largest radiation dose to any organ or tissue other than the lens of the eye, plus the deep dose equivalent, was estimated to be 0.10 rem/yr total effective dose equivalent (BSC 2001u, Table 8). The radiation dose to the skin and extremities was estimated to be 0.13 rem/yr total effective dose equivalent (BSC 2001u, Table 8). The radiation dose to the lens of the eye is estimated to be 0.15 rem/yr total effective dose equivalent by summing the total effective dose equivalent and the skin dose (BSC 2001u, Table 8).

The radiation doses for routine occupational exposures for workers are estimated in *Final Environmental Impact Statement for a Geologic Repository for the Disposal of Spent Nuclear Fuel and High-Level Radioactive Waste at Yucca Mountain, Nye County, Nevada* (DOE 2002, Section 4.1.7) and summarized in Table 5-8. Maximum radiation doses ranged from about 0.06 to 0.79 rem/yr total effective dose equivalent, depending on the area of the repository, the phase of operation, and the thermal load alternative (DOE 2002, Tables 4-22, 4-25, 4-28, and 4-31). Section 7 of *Preliminary Preclosure Safety Assessment for Monitored Geologic Repository Site Recommendation* (BSC 2001f) discusses methods that would be used to ensure that occupational radiation doses are ALARA. Worker safety from industrial hazards was also discussed in *Final Environmental Impact Statement for a Geologic Repository for the Disposal of Spent Nuclear Fuel and High-Level Radioactive Waste at Yucca Mountain, Nye County, Nevada* (DOE 2002, Section 4).

5.3.3.2 Category 2 Event Sequence Consequences

Design Basis Event Frequency and Dose Calculation for Site Recommendation (BSC 2001u) evaluated the consequences of Category 2 event sequences. Offsite radiation doses (i.e., in the uncontrolled area) for Category 2 event sequences were based on the following (BSC 2001u, Section 6.1.2):

• Inhalation and air immersion pathways

• Release fractions that take into account the respirable fraction of radionuclide particulates

• Mitigation by high-efficiency particulate air filters of particulate emissions from the surface facilities

• For calculating the atmospheric emissions from repository surface facilities, the distance to the receptor was 11 km (7 mi), the closest distance from the potential repository surface facilities to the assumed site boundary (BSC 2001u, Section 3.3)

• 99.5 percent ground-level atmospheric dispersion factors (BSC 2001f, Section 5.3.5.3).

The radiation doses from bounding Category 2 event sequences were calculated assuming filtration through a high-efficiency particulate air filter. The bounding-consequence Category 2 event sequence is the drop of an unsealed shipping cask.

The highest radiation dose for a member of the public caused by the bounding-consequence Category 2 event sequence was 0.02 rem (BSC 2001f, Section 5.3.6.1). The largest radiation dose to any organ or tissue other than the lens of the eye was estimated to be 0.1 rem total effective dose equivalent (BSC 2001f, Section 5.3.6.1). The radiation dose to the skin and the lens of the eye was estimated to be total effective dose equivalent of 0.04 rem and 0.06 rem, respectively (BSC 2001f, Section 5.3.6.1).

5.4 PRECLOSURE SAFETY: TEST AND EVALUATION PROGRAM

The Monitored Geologic Repository Test and Evaluation Program will include planning, execution, and documentation of the testing, examination, analyses, and demonstrations necessary to verify

safe and efficient operation of the repository. The preclosure components of this comprehensive program address all aspects of verification, from the development of test requirements and acceptance criteria to the performance, recording, and reporting of test procedures. The following discussion of the test and evaluation program is based on *Monitored Geologic Repository Test & Evaluation Plan* (CRWMS M&O 2000fj). The test and evaluation plan will be revised at the time of preparation of any license application for conformance of the plan to more specific design information and any additional performance related testing.

This test and evaluation program would include the following activities and objectives.

- Design and component testing will ensure that structures, systems, and components are designed as specified and perform as required.

- Preoperational testing will ensure that structures, systems, and components operate on an integrated basis and will verify processes and validate procedures for the receipt, preparation, emplacement, and movement (i.e., recovery or retrieval) of waste.

- Operational testing will confirm exposure times and radiation levels during repository operations, and that operational safety has been incorporated into structures, systems, and components.

To achieve these objectives, the test and evaluation program defines, plans, and implements a set of integrated test activities focused on ensuring preclosure safety (CRWMS M&O 2000fj, Section 2). These integrated activities are:

- Development testing
- Prototype testing
  - Proof of concept testing
  - Mockup testing
- Component testing
- Construction and preoperational testing
- Hot startup testing
- Periodic performance testing and surveillance.

A confirmation verification tracking system would identify the tests performed throughout the test program. This tracking system would status the program's performance and would be maintained and updated as a test database that would provide a history of structure, system, and component performance. It would be made available to support the licensing process and the operations, maintenance, system upgrade, and support functions.

5.4.1 Development Testing

Development testing supports design activities by confirming design concepts, evaluating alternative design concepts, and investigating the availability of needed technology. For example, development testing will help evaluate and demonstrate the suitability of ground support systems proposed for the emplacement drifts. Development testing will also help evaluate the suitability, adequacy, and availability of instrumentation, monitoring, and control technologies for use in the subsurface environment.

The repository systems would use microprocessor-based instrumentation and control equipment, including operator control stations, digital data acquisition, data processing, network and communications equipment, borehole instrumentation, air sampling instruments, and infrared cameras. Having a good understanding of the reliability of these systems in a high-temperature and high-radiation repository environment is important to ensure public and worker safety during emplacement activities. Field testing of candidate technologies would investigate how to minimize downtime from failures.

5.4.2 Prototype Testing

Prototype testing includes proof of concept testing and mockup testing.

Proof of Concept Testing—Proof of concept prototype testing is performed for the following cases:

- New technologies or design solutions that have little or no history of use at existing nuclear storage facilities or power plants

- Technologies or design solutions that have not been subjected to a test program and are qualified by the NRC or DOE, as applicable, and from which accepted data were collected or analyzed and documented in a defensible source.

This prototype testing would support the development of structures, systems, and components during construction and preoperation (CRWMS M&O 2000fj, Appendix C).

Mockup Testing—While proof of concept testing supports the design process, mockup testing involves simulation or demonstration with operational realism. Mockup testing follows proof of concept testing and supports preoperational and operational activities.

5.4.3   Component Testing

Component testing, if needed, would be performed as part of the procurement process to establish equipment qualification according to the applicable quality level. Component testing, which includes qualification and acceptance testing, would be used for any unique (not off-the-shelf) equipment. Qualification testing verifies, on a limited sampling basis, the proper operation of the component with respect to extreme bounds (as defined by specifications). Acceptance testing, performed for key parameters, establishes confidence that the manufacturing process is producing the correct product. The component vendor, with quality assurance oversight and concurrence, performs component testing. This testing starts at the beginning of fabrication and is completed before installation.

Compliance with identified safety and radiological requirements would be assessed during component testing to document the appropriate details for test performance. Examples of component testing include shock, vibration, and environmental testing for performance of sensors and alarms that have or support safety functions.

5.4.4   Construction and Preoperational Testing

Construction and preoperational testing would begin during repository construction and end before receipt of waste. This test activity includes the following subactivities:

- Installation and checkout testing
- System integration testing
- Event sequence recovery testing
- Cold startup testing.

5.4.5   Hot Startup Testing

To the extent practicable, the preoperational testing described previously would verify compliance with repository performance requirements, including ALARA considerations. Hot startup testing would verify that operation and maintenance systems work properly and confirm that exposure times and radiation levels fall within acceptable limits during actual repository operations. Hot startup testing would begin after the successful completion of construction and preoperational test activities. It would include the following subactivities:

- Testing and confirming exposure times and radiation dose
- Verifying heat removal features and cooling systems
- Confirming acceptable radiation exposure levels.

5.4.6   Periodic Performance Testing and Surveillance

Periodic performance testing would verify system performance and ensure continued proper functioning of structures, systems, and components important to radiological safety, waste isolation, fire protection, nonnuclear safety, and repository operations. Periodic testing would be performed at the Waste Handling Building and the Waste Treatment Building in the surface facilities and at the emplacement drift panels in the subsurface facilities. This testing would also be performed after maintenance and repair activities.

INTENTIONALLY LEFT BLANK

6. REFERENCES

6.1 DOCUMENTS CITED

Abdel-Salam, A. and Chrysikopoulos, C.V. 1996. "Unsaturated Flow in a Quasi-Three-Dimensional Fractured Medium with Spatially Variable Aperture." *Water Resources Research, 32,* (6), 1531-1540. Washington, D.C.: American Geophysical Union. TIC: 239861.

Ahlers, C.F.; Finsterle, S.; and Bodvarsson, G.S. 1999. "Characterization and Prediction of Subsurface Pneumatic Response at Yucca Mountain, Nevada." *Journal of Contaminant Hydrology, 38,* (1-3), 47-68. New York, New York: Elsevier Science. TIC: 244160.

Albin, A.L.; Singleton, W.L.; Moyer, T.C.; Lee, A.C.; Lung, R.C.; Eatman, G.L.W.; and Barr, D.L. 1997. *Geology of the Main Drift—Station 28+00 to 55+00, Exploratory Studies Facility, Yucca Mountain Project, Yucca Mountain, Nevada.* Milestone SPG42AM3. Denver, Colorado: Bureau of Reclamation and U.S. Geological Survey. ACC: MOL.19970625.0096.

American Institute of Chemical Engineers 1992. *Guidelines for Hazard Evaluation Procedures.* 2nd Edition with Worked Examples. New York, New York: American Institute of Chemical Engineers. TIC: 239050.

Anderson, R.E.; Hanks, T.C.; Reilly, T.E.; Weeks, E.P.; and Winograd, I.J. 1998. *Viability Assessment of a Repository at Yucca Mountain. A Report to the Director, U.S. Geological Survey.* Reston, Virginia: U.S. Geological Survey. ACC: HQO.19990205.0013.

Archambeau, C.B. and Price, N.J. 1991. *An Assessment of J.S. Szymanski's Conceptual Hydro-Tectonic Model and Its Relevance to Hydrologic and Geologic Processes at the Proposed Yucca Mountain Nuclear Waste Repository, Minority Report of the Special DOE Review Panel.* Washington, D.C.: U.S. Department of Energy. ACC: NNA.19911210.0057.

ASME (American Society of Mechanical Engineers) 1995. *1995 ASME Boiler and Pressure Vessel Code.* New York, New York: American Society of Mechanical Engineers. TIC: 245287.

Aydan, O.; Ulusay, R.; Yuzer, E.; and Erdogan, M. 1999. "Man-Made Rock Structures in Cappadocia, Turkey and Their Implications in Rock Mechanics and Rock Engineering." *International Society for Rock Mechanics News Journal, 6,* (1), 63-73. Orebro, Sweden: International Society for Rock Mechanics. TIC: 247253.

Barker, P.; Ellis, C.; and Damadio, S. 2000. "Determination of Cultural Affiliation of Ancient Human Remains from Spirit Cave, Nevada." Reno, Nevada: Bureau of Land Management, Nevada State Office. Accessed October 30, 2000. TIC: 249042. http://www.nv.blm.gov/cultural/spirit_cave_man/SC_final_July26.pdf

Barnard, R.W.; Wilson, M.L.; Dockery, H.A.; Gauthier, J.H.; Kaplan, P.G.; Eaton, R.R.; Bingham, F.W.; and Robey, T.H. 1992. *TSPA 1991: An Initial Total-System Performance Assessment for Yucca Mountain.* SAND91-2795. Albuquerque, New Mexico: Sandia National Laboratories. ACC: NNA.19920630.0033.

Barr, D.L.; Moyer, T.C.; Singleton, W.L.; Albin, A.L.; Lung, R.C.; Lee, A.C.; Beason, S.C.; and Eatman, G.L.W. 1996. *Geology of the North Ramp—Stations 4+00 to 28+00, Exploratory Studies Facility, Yucca Mountain Project, Yucca Mountain, Nevada.* Denver, Colorado: U.S. Geological Survey. ACC: MOL.19970106.0496.

Barton, C.C.; Larsen, E.; and Baechle, P.E. 1985. "Fractal Geometry of Two-Dimensional Planar Sections through Fracture Networks at Yucca Mountain, Southwestern Nevada." *Eos, 66,* (46), 1089. Washington, D.C.: American Geophysical Union. TIC: 223635.

Bassett, R.L.; Neuman, S.P.; Wierenga, P.J.; Chen, G.; Davidson, G.R.; Hardin, E.L.; Illman, W.A.; Murrell, M.T.; Stephens, D.M.; Thomasson, M.J.; Thompson, D.L.; and Woodhouse, E.G. 1997. *Data Collection and Field Experiments at the Apache Leap Research Site, May 1995–1996.* Woodhouse, E.G., ed. NUREG/CR-6497. Washington, D.C.: U.S. Nuclear Regulatory Commission. TIC: 248788.

Bates, J.K.; Bradley, J.P.; Teetsov, A.; Bradley, C.R.; and Buchholtz ten Brink, M. 1992. "Colloid Formation During Waste Form Reaction: Implications for Nuclear Waste Disposal." *Science, 256,* 649-651. Washington, D.C.: American Association for the Advancement of Science. TIC: 239138.

Bear, J. 1988. *Dynamics of Fluids in Porous Media.* New York, New York: Dover Publications. TIC: 217568.

Benson, L.V. and McKinley, P.W. 1985. *Chemical Composition of Ground Water in the Yucca Mountain Area, Nevada, 1971-84.* Open-File Report 85-484. Denver, Colorado: U.S. Geological Survey. ACC: NNA.19900207.0281.

Bidaux, P. and Tsang, C-F. 1991. "Fluid Flow Patterns Around a Well Bore or an Underground Drift with Complex Skin Effects." *Water Resources Research, 27,* (11), 2993-3008. Washington, D.C.: American Geophysical Union. TIC: 247407.

BIOMOVS II (Biospheric Model Validation Study, Phase II) Steering Committee 1994. *An Interim Report on Reference Biospheres for Radioactive Waste Disposal.* Technical Report No. 2. Stockholm, Sweden: Swedish Radiation Protection Institute. TIC: 238733.

BIOMOVS II 1996. *Development of a Reference Biospheres Methodology for Radioactive Waste Disposal, Final Report of the Reference Biospheres Working Group of the BIOMOVS II Study.* Technical Report No. 6. Stockholm, Sweden: Swedish Radiation Protection Institute. TIC: 238329.

Bish, D.L. 1995. "Thermal Behavior of Natural Zeolites." *Natural Zeolites '93: Occurrence, Properties, Use, Proceedings of the 4th International Conference on the Occurrence, Properties, and Utilization of Natural Zeolites, June 20-28, 1993, Boise, Idaho.* Ming, D.W. and Mumpton, F.A., eds. Pages 259-269. Brockport, New York: International Committee on Natural Zeolites. TIC: 243086.

Bish, D.L. and Aronson, J.L. 1993. "Paleogeothermal and Paleohydrologic Conditions in Silicic Tuff from Yucca Mountain, Nevada." *Clays and Clay Minerals, 41,* (2), 148-161. Long Island City, New York: Pergamon Press. TIC: 224613.

Bish, D.L. and Chipera, S.J. 1986. *Mineralogy of Drill Holes J-13, UE-25A#1, and USW G-1 at Yucca Mountain, Nevada.* LA-10764-MS. Los Alamos, New Mexico: Los Alamos National Laboratory. ACC: MOL.19950412.0044.

Bish, D.L. and Vaniman, D.T. 1985. *Mineralogic Summary of Yucca Mountain, Nevada.* LA-10543-MS. Los Alamos, New Mexico: Los Alamos National Laboratory. ACC: MOL.19950412.0041.

Bodvarsson, G.S.; Benson, S.M.; Sigurdsson, O.; Stefansson, V.; and Eliasson, E.T. 1984. "The Krafla Geothermal Field, Iceland, 1. Analysis of Well Test Data." *Water Resources Research, 20,* (11), 1515-1530. Washington, D.C.: American Geophysical Union. TIC: 247406.

Bodvarsson, G.S.; Pruess, K.; Stefansson, V.; Bjornsson, S.; and Ojiambo, S.B. 1987. "East Olkaria Geothermal Field, Kenya, 1. History Match with Production and Pressure Decline Data." *Journal of Geophysical Research, 92,* (B1), 521-539. Washington, D.C.: American Geophysical Union. TIC: 236629.

Bowman, C.D. and Venneri, F. 1996. "Underground Supercriticality from Plutonium and Other Fissile Material." *Science & Global Security, 5,* 279-302. New York, New York: Gordon and Breach Science Publishers. TIC: 238269.

Boyd, P.J.; Martin, R.J., III; and Price, R.H. 1994. *An Experimental Comparison of Laboratory Techniques in Determining Bulk Properties of Tuffaceous Rocks.* SAND92-0119. Albuquerque, New Mexico: Sandia National Laboratories. ACC: NNA.19940315.0003.

Brocoum, S.J. 1997. "Evaluation of Data Provided at U.S. Department of Energy (DOE) and U.S. Nuclear Regulatory Commission (NRC) Igneous Activity Technical Exchange, February 25-26, 1997." Letter from S.J. Brocoum (DOE/YMSCO) to J.T. Greeves (NRC), June 4, 1997, with enclosure.
ACC: MOL.19970722.0276; MOL.19970722.0277.

Brodsky, N.S.; Riggins, M.; Connolly, J.; and Ricci, P. 1997. *Thermal Expansion, Thermal Conductivity, and Heat Capacity Measurements for Boreholes UE25 NRG-4, UE25 NRG-5, USW NRG-6, and USW NRG-7/7A.* SAND95-1955. Albuquerque, New Mexico: Sandia National Laboratories.
ACC: MOL.19980311.0316.

Brookins, D.G. 1986. "Natural Analogues for Radwaste Disposal: Elemental Migration in Igneous Contact Zones." *Chemical Geology, 55,* 337-344. Amsterdam, The Netherlands: Elsevier Science. TIC: 246170.

Brown, S.R. 1987. "Fluid Flow Through Rock Joints: The Effect of Surface Roughness." *Journal of Geophysical Research, 92,* (B2), 1337-1347. Washington, D.C.: American Geophysical Union.
TIC: 222225.

Broxton, D.E.; Chipera, S.J.; Byers, F.M., Jr.; and Rautman, C.A. 1993. *Geologic Evaluation of Six Nonwelded Tuff Sites in the Vicinity of Yucca Mountain, Nevada for a Surface-Based Test Facility for the Yucca Mountain Project.* LA-12542-MS. Los Alamos, New Mexico: Los Alamos National Laboratory. ACC: NNA.19940224.0128.

Bruton, C.J.; Glassley, W.E.; and Bourcier, W.L. 1993. "Testing Geochemical Modeling Codes Using New Zealand Hydrothermal Systems." *Proceedings of the Topical Meeting on Site Characterization and Model Validation, FOCUS '93, September 26-29, 1993, Las Vegas, Nevada.* Pages 240-245. La Grange Park, Illinois: American Nuclear Society. TIC: 102245.

Bruton, C.J.; Glassley, W.E.; and Bourcier, W.L. 1994. *Field-Based Tests of Geochemical Modeling Codes Using New Zealand Hydrothermal Systems.* UCRL-ID-118009. Livermore, California: Lawrence Livermore National Laboratory. TIC: 213717.

BSC (Bechtel SAIC Company) 2001a. *FY01 Supplemental Science and Performance Analyses, Volume 1: Scientific Bases and Analyses.* TDR-MGR-MD-000007 REV 00 ICN 01. Las Vegas, Nevada: Bechtel SAIC Company. ACC: MOL.20010801.0404; MOL.20010712.0062; MOL.20010815.0001.

BSC 2001b. *FY01 Supplemental Science and Performance Analyses, Volume 2: Performance Analyses.* TDR-MGR-PA-000001 REV 00. Las Vegas, Nevada: Bechtel SAIC Company. ACC: MOL.20010724.0110.

BSC 2001c. *Technical Update Impact Letter Report.* MIS-MGR-RL-000001 REV 00 ICN 02. Las Vegas, Nevada: Bechtel SAIC Company. ACC: MOL.20011211.0311.

BSC 2001d. *Site Recommendation Subsurface Layout.* ANL-SFS-MG-000001 REV 00 ICN 02. Las Vegas, Nevada: Bechtel SAIC Company. ACC: MOL.20010411.0131.

BSC 2001e. *Yucca Mountain Groundwater Contour Map.* Input Transmittal 00447.T. Las Vegas, Nevada: Bechtel SAIC Company. ACC: MOL.20010409.0187.

BSC 2001f. *Preliminary Preclosure Safety Assessment for Monitored Geologic Repository Site Recommendation.* TDR-MGR-SE-000009 REV 00 ICN 03. Las Vegas, Nevada: Bechtel SAIC Company. ACC: MOL.20010705.0172.

BSC 2001g. *Lower-Temperature Subsurface Layout and Ventilation Concepts.* ANL-WER-MD-000002 REV 00. Las Vegas, Nevada: Bechtel SAIC Company. ACC: MOL.20010718.0225.

BSC 2001h. *ANSYS Calculations in Support of Natural Ventilation Parametric Study for SR.* CAL-SVS-HV-000003 REV 00 ICN 01. Las Vegas, Nevada: Bechtel SAIC Company. ACC: MOL.20010613.0250.

BSC 2001i. *Thermal Management Analysis for Lower-Temperature Designs.* ANL-SFS-MG-000005 REV 00. Las Vegas, Nevada: Bechtel SAIC Company. ACC: MOL.20010814.0329.

BSC 2001j. *Thermal Hydrology EBS Design Sensitivity Analysis.* CAL-EBS-HS-000003 REV 00 ICN 01. Las Vegas, Nevada: Bechtel SAIC Company. ACC: MOL.20010525.0080.

BSC 2001k. *Temperature-Relative Humidity Time Plot for Operating Mode 50-yrs Forced Ventilation and Indefinite Natural Ventilation.* Input Transmittal 00439.T. Las Vegas, Nevada: Bechtel SAIC Company. ACC: MOL.20010409.0185.

BSC 2001l. *Rock Fall on Drip Shield.* CAL-EDS-ME-000001 REV 01. Las Vegas, Nevada: Bechtel SAIC Company. ACC: MOL.20010713.0043.

BSC 2001m. *Uncanistered Spent Nuclear Fuel Disposal Container System Description Document.* SDD-UDC-SE-000001 REV 01 ICN 01. Las Vegas, Nevada: Bechtel SAIC Company. ACC: MOL.20010927.0070.

BSC 2001n. *Tip-Over of 12-PWR and 24-BWR Waste Packages.* CAL-UDC-ME-000016 REV 00. Las Vegas, Nevada: Bechtel SAIC Company. ACC: MOL.20010425.0023.

BSC 2001o. *Drift-Scale Coupled Processes (DST and THC Seepage) Models.* MDL-NBS-HS-000001 REV 01 ICN 01. Las Vegas, Nevada: Bechtel SAIC Company. ACC: MOL.20010418.0010.

BSC 2001p. *In-Package Chemistry for Waste Forms.* ANL-EBS-MD-000056 REV 00. Las Vegas, Nevada: Bechtel SAIC Company. ACC: MOL.20010322.0490.

BSC 2001q. *Performance Assessment of U.S. Department of Energy Spent Fuels in Support of Site Recommendation.* CAL-WIS-PA-000002 REV 00. Las Vegas, Nevada: Bechtel SAIC Company. ACC: MOL.20010627.0026.

BSC 2001r. *Analysis of Geochemical Data for the Unsaturated Zone.* ANL-NBS-HS-000017 REV 00 ICN 01. Las Vegas, Nevada: Bechtel SAIC Company. ACC: MOL.20010405.0013.

BSC 2001s. *Unsaturated Zone Flow Patterns and Analysis.* MDL-NBS-HS-000012 REV 00. Las Vegas, Nevada: Bechtel SAIC Company. ACC: MOL.20011029.0315.

BSC 2001t. *Evaluation of the Applicability of Biosphere-Related Features, Events, and Processes (FEP).* ANL-MGR-MD-000011 REV 01. Las Vegas, Nevada: Bechtel SAIC Company. ACC: MOL.20010226.0003.

BSC 2001u. *Design Basis Event Frequency and Dose Calculation for Site Recommendation.* CAL-WHS-SE-000001 REV 01 ICN 02. Las Vegas, Nevada: Bechtel SAIC Company. ACC: MOL.20011211.0094.

Buddemeier, R.W. and Hunt, J.R. 1988. "Transport of Colloidal Contaminants in Groundwater: Radionuclide Migration at the Nevada Test Site." *Applied Geochemistry, 3,* 535-548. Oxford, England: Pergamon Press. TIC: 224116.

Budnitz, B.; Ewing, R.C.; Moeller, D.W.; Payer, J.; Whipple, C.; and Witherspoon, P.A. 1999. *Peer Review of the Total System Performance Assessment—Viability Assessment Final Report.* Las Vegas, Nevada: Total System Performance Assessment Peer Review Panel. ACC: MOL.19990317.0328.

Buesch, D.C. and Spengler, R.W. 1998. "Character of the Middle Nonlithophysal Zone of the Topopah Spring Tuff at Yucca Mountain." *High-Level Radioactive Waste Management, Proceedings of the Eighth International Conference, Las Vegas, Nevada, May 11-14, 1998.* Pages 16-23. La Grange Park, Illinois: American Nuclear Society. TIC: 237082.

Buesch, D.C.; Spengler, R.W.; Moyer, T.C.; and Geslin, J.K. 1996. *Proposed Stratigraphic Nomenclature and Macroscopic Identification of Lithostratigraphic Units of the Paintbrush Group Exposed at Yucca Mountain, Nevada.* Open-File Report 94-469. Denver, Colorado: U.S. Geological Survey. ACC: MOL.19970205.0061.

Bureau of the Census 1999. "1990 US Census Data, Database: C90STF3A, Summary Level: State--County--County Subdivision, Amargosa Valley Division: FIPS.STATE=32, FIPS.COUNTY90=023, FIPS.COUSUB=94028." Washington, D.C.: Bureau of the Census. Accessed November 12, 1999. TIC: 245829. http://venus.census.gov/cdrom/lookup

Buscheck, T.A. and Nitao, J.J. 1992. "The Impact of Thermal Loading on Repository Performance at Yucca Mountain." *High Level Radioactive Waste Management, Proceedings of the Third International Conference, Las Vegas, Nevada, April 12-16, 1992. 1,* 1003-1017. La Grange Park, Illinois: American Nuclear Society. TIC: 204231.

Buscheck, T.A. and Nitao, J.J. 1993. "Repository-Heat-Driven Hydrothermal Flow at Yucca Mountain, Part I: Modeling and Analysis." *Nuclear Technology, 104,* (3), 418-448. La Grange Park, Illinois: American Nuclear Society. TIC: 224039.

Buscheck, T.A.; Nitao, J.J.; and Chesnut, D.A. 1992. "The Impact of Episodic Nonequilibrium Fracture–Matrix Flow on Geological Repository Performance." *Proceedings of the Topical Meeting on Nuclear Waste Packaging, FOCUS '91, September 29–October 2, 1991, Las Vegas, Nevada.* Pages 312-323. La Grange Park, Illinois: American Nuclear Society. TIC: 231173.

Canavan, G.H.; Colgate, S.A.; Judd, O.P.; Petschek, A.G.; and Stratton, T.F. 1995. *Comments on "Nuclear Excursions" and "Criticality Issues."* LA-UR: 95 0851. Los Alamos, New Mexico: Los Alamos National Laboratory. ACC: HQO.19950314.0028.

Carey, J.W.; Chipera, S.J.; Vaniman, D.T.; and Bish, D.L. 1997. *Three-Dimensional Mineralogic Model of Yucca Mountain, Nevada, Rev 1.1.* Deliverable SP32B5M4. Draft R0. Los Alamos, New Mexico: Los Alamos National Laboratory. ACC: MOL.19980520.0170.

Carrigan, C.R.; King, G.C.P.; and Barr, G.E. 1990. *A Scoping Study of Water Table Excursions Induced by Seismic Events.* UCRL-ID-105340. Livermore, California: Lawrence Livermore National Laboratory. ACC: NNA.19920504.0125.

Carrigan, C.R.; King, G.C.P.; Barr, G.E.; and Bixler, N.E. 1991. "Potential for Water-Table Excursions Induced by Seismic Events at Yucca Mountain, Nevada." *Geology, 19,* (12), 1157-1160. Boulder, Colorado: Geological Society of America. TIC: 242407.

Carroll, S.A.; Alai, M.; and Copenhaver, S. 1995. *Amorphous Silica Precipitation Kinetics at 100°C and pH 3, 5, & 6.* Letter Report MOL123 OL3ALIW. Livermore, California: Lawrence Livermore National Laboratory. ACC: MOL.19960328.0177.

Castor, S.B.; Garside, L.J.; Tingley, J.V.; La Pointe, D.D.; Desilets, M.O.; Hsu, L-C.; Goldstrand, P.M.; Lugaski, T.P.; and Ross, H.P. 1999. *Assessment of Metallic and Mined Energy Resources in the Yucca Mountain Conceptual Controlled Area, Nye County, Nevada.* Open-File Report 99-13. Reno, Nevada: Nevada Bureau of Mines and Geology. TIC: 245099.

Castor, S.B. and Lock, D.E. 1995. *Assessment of Industrial Minerals and Rocks in the Controlled Area.* Reno, Nevada: Nevada Bureau of Mines and Geology. ACC: MOL.19980717.0139.

Chapman, N.A. and Smellie, J.A.T. 1986. "Introduction and Summary of the Workshop." *Chemical Geology, 55,* 167-173. Amsterdam, The Netherlands: Elsevier Science. TIC: 246750.

Claassen, H.C. 1985. *Sources and Mechanisms of Recharge for Ground Water in the West-Central Amargosa Desert, Nevada—A Geochemical Interpretation.* U.S. Geological Survey Professional Paper 712-F. Washington, D.C.: U.S. Government Printing Office. TIC: 204574.

Codell, R.; Eisenberg, N.; Fehringer, D.; Ford, W.; Margulies, T.; McCartin, T.; Park, J.; and Randall, J. 1992. *Initial Demonstration of the NRC's Capability to Conduct a Performance Assessment for a High-Level Waste Repository.* NUREG-1327. Washington, D.C.: U.S. Nuclear Regulatory Commission. TIC: 204809.

Cohon, J.L. 1998. Nuclear Waste Technical Review Board Review of Reports by Jerry Syzmanski and Harry Swainston. Letter from J.L. Cohon (NWTRB) to L.H. Barrett (DOE/OCRWM), July 24, 1998, with attachment. ACC: MOL.19980814.0396.

Cohon, J.L. 1999. Comments on the Process for Selecting the Repository Design. Letter from J.L. Cohon (U.S. Nuclear Waste Technical Review Board) to L.H. Barrett (DOE/OCRWM), July 9, 1999. ACC: MOL.20000412.0786.

Conca, J.L. and Wright, J. 1992. "Diffusion and Flow in Gravel, Soil, and Whole Rock." *Applied Hydrogeology, 1,* 5-24. Hanover, Germany: Verlag Heinz Heise GmbH. TIC: 224081.

Connor, C.B.; Lane-Magsino, S.; Stamatakos, J.A.; Martin, R.H.; LaFemina, P.C.; Hill, B.E.; and Lieber, S. 1997. "Magnetic Surveys Help Reassess Volcanic Hazards at Yucca Mountain, Nevada." *Eos, 78,* (7), 73, 77 and 78. Washington, D.C.: American Geophysical Union. TIC: 234580.

Costantino, M.S.; Carlson, S.R.; and Blair, S.C. 1998. *Results of a Coupled Fracture-Flow Test at the 0.5-m Scale.* UCRL-ID-131493. Livermore, California: Lawrence Livermore National Laboratory. ACC: MOL.20001002.0156.

Cranwell, R.M.; Guzowski, R.V.; Campbell, J.E.; and Ortiz, N.R. 1990. *Risk Methodology for Geologic Disposal of Radioactive Waste, Scenario Selection Procedure.* NUREG/CR-1667. Washington, D.C.: U.S. Nuclear Regulatory Commission. ACC: NNA.19900611.0073.

Crowe, B.; Perry, F.; Geissman, J.; McFadden, L.; Wells, S.; Murrell, M.; Poths, J.; Valentine, G.A.; Bowker, L.; and Finnegan, K. 1995. *Status of Volcanism Studies for the Yucca Mountain Site Characterization Project.* LA-12908-MS. Los Alamos, New Mexico: Los Alamos National Laboratory. ACC: HQO.19951115.0017.

Crowe, B.; Self, S.; Vaniman, D.; Amos, R.; and Perry, F. 1983. "Aspects of Potential Magmatic Disruption of a High-Level Radioactive Waste Repository in Southern Nevada." *Journal of Geology, 91,* (3), 259-276. Chicago, Illinois: University of Chicago Press. TIC: 216959.

CRWMS M&O (Civilian Radioactive Waste Management System Management and Operating Contractor) 1994. *Total System Performance Assessment—1993: An Evaluation of the Potential Yucca Mountain Repository.* B00000000-01717-2200-00099 REV 01. Las Vegas, Nevada: CRWMS M&O. ACC: NNA.19940406.0158.

CRWMS M&O 1995. *Total System Performance Assessment—1995: An Evaluation of the Potential Yucca Mountain Repository.* B00000000-01717-2200-00136 REV 01. Las Vegas, Nevada: CRWMS M&O. ACC: MOL.19960724.0188.

CRWMS M&O 1996a. *Preliminary MGDS Hazards Analysis.* B00000000-01717-0200-00130 REV 00. Las Vegas, Nevada: CRWMS M&O. ACC: MOL.19961230.0011.

CRWMS M&O 1996b. *Probabilistic Volcanic Hazard Analysis for Yucca Mountain, Nevada.* BA0000000-01717-2200-00082 REV 0. Las Vegas, Nevada: CRWMS M&O. ACC: MOL.19971201.0221.

CRWMS M&O 1996c. *DHLW Glass Waste Package Criticality Analysis.*
BBAC00000-01717-0200-00001 REV 00. Las Vegas, Nevada: CRWMS M&O.
ACC: MOL.19960919.0237.

CRWMS M&O 1996d. *Mined Geologic Disposal System Advanced Conceptual Design Report.*
B00000000-01717-5705-00027 REV 00. Four volumes. Las Vegas, Nevada: CRWMS M&O.
ACC: MOL.19960826.0094; MOL.19960826.0095; MOL.19960826.0096; MOL.19960826.0097.

CRWMS M&O 1996e. *Probabilistic External Criticality Evaluation.* BB0000000-01717-2200-00037
REV 00. Las Vegas, Nevada: CRWMS M&O. ACC: MOL.19961029.0024.

CRWMS M&O 1996f. *Total System Performance Assessment of a Geologic Repository Containing
Plutonium Waste Forms.* A00000000-01717-5705-00011 REV 00. Las Vegas, Nevada: CRWMS M&O.
ACC: MOL.19970109.0229.

CRWMS M&O 1997a. *ISM2.0: A 3D Geologic Framework and Integrated Site Model of Yucca Mountain.*
B00000000-01717-5700-00004 REV 00. Las Vegas, Nevada: CRWMS M&O.
ACC: MOL.19970625.0119.

CRWMS M&O 1997b. *Determination of Waste Package Design Configurations.*
BBAA00000-01717-0200-00017 REV 00. Las Vegas, Nevada: CRWMS M&O.
ACC: MOL.19970805.0310.

CRWMS M&O 1997c. *Waste Package Materials Selection Analysis.* BBA000000-01717-0200-00020
REV 01. Las Vegas, Nevada: CRWMS M&O. ACC: MOL.19980324.0242.

CRWMS M&O 1997d. *Criticality Evaluation of Degraded Internal Configurations for the PWR AUCF
WP Designs.* BBA000000-01717-0200-00056 REV 00. Las Vegas, Nevada: CRWMS M&O.
ACC: MOL.19971231.0251.

CRWMS M&O 1998a. *Parametric Contingency Study of Program Implementation Scenarios for
Constrained Funding.* A00000000-01717-5700-00022 REV 01. Vienna, Virginia: CRWMS M&O. ACC:
MOL.19981124.0297.

CRWMS M&O 1998b. *ECRB Cross Drift Stability Analysis.* BABEE0000-01717-0200-00017 REV 01.
Las Vegas, Nevada: CRWMS M&O. ACC: MOL.19980428.0010.

CRWMS M&O 1998c. *Drift Scale Test As-Built Report.* BAB000000-01717-5700-00003 REV 01. Las
Vegas, Nevada: CRWMS M&O. ACC: MOL.19990107.0223.

CRWMS M&O 1998d. *Drift Ground Support Design Guide.* BCAA00000-01717-2500-00001 REV 01.
Las Vegas, Nevada: CRWMS M&O. ACC: MOL.19990326.0104.

CRWMS M&O 1998e. *Mobile Waste Handling Support Equipment.* BCAF00000-01717-0200-00006
REV 00. Las Vegas, Nevada: CRWMS M&O. ACC: MOL.19980819.0397.

CRWMS M&O 1998f. *Retrievability Strategy Report.* B00000000-01717-5705-00061 REV 01. Las
Vegas, Nevada: CRWMS M&O. ACC: MOL.19980723.0039.

CRWMS M&O 1998g. *Total System Performance Assessment–Viability Assessment (TSPA-VA) Analyses Technical Basis Document.* Las Vegas, Nevada: CRWMS M&O. ACC: MOL.19981008.0001; MOL.19981008.0002; MOL.19981008.0003; MOL.19981008.0004; MOL.19981008.0005; MOL.19981008.0006; MOL.19981008.0007; MOL.19981008.0008; MOL.19981008.0009; MOL.19981008.0010; MOL.19981008.0011.

CRWMS M&O 1998h. *Software Qualification Report (SQR) Addendum to Existing LLNL Document UCRL-MA-110662 PT IV: Implementation of a Solid-Centered Flow-Through Mode for EQ6 Version 7.2B.* CSCI: UCRL-MA-110662 V 7.2b. SCR: LSCR198. Las Vegas, Nevada: CRWMS M&O. ACC: MOL.19990920.0169.

CRWMS M&O 1998i. *Model Prediction of Local Plume Migration from the Cross Drift.* Milestone SP33S3M4, Rev. 1. Las Vegas, Nevada: CRWMS M&O. ACC: MOL.19980702.0075.

CRWMS M&O 1998j. *Saturated Zone Flow and Transport Expert Elicitation Project.* Deliverable SL5X4AM3. Las Vegas, Nevada: CRWMS M&O. ACC: MOL.19980825.0008.

CRWMS M&O 1998k. *Software Qualification Report (SQR) GENII-S 1.485 Environmental Radiation Dosimetry Software System Version 1.485.* CSCI: 30034 V1.4.8.5. DI: 30034-2003, Rev. 0. Las Vegas, Nevada: CRWMS M&O. ACC: MOL.19980715.0029.

CRWMS M&O 1998l. *Seismic Design Basis Inputs for a High-Level Waste Repository at Yucca Mountain, Nevada.* B00000000-01727-5700-00018 REV 0. Las Vegas, Nevada: CRWMS M&O. ACC: MOL.19980806.0711.

CRWMS M&O 1998m. *Report on External Criticality of Plutonium Waste Forms in a Geologic Repository.* BBA000000-01717-5705-00018 REV 01. Las Vegas, Nevada: CRWMS M&O. ACC: MOL.19980318.0412.

CRWMS M&O 1999a. *1999 Design Basis Waste Input Report for Commercial Spent Nuclear Fuel.* B00000000-01717-5700-00041 REV 01. Washington, D.C.: CRWMS M&O. ACC: MOV.19991217.0001.

CRWMS M&O 1999b. *Documentation of Program Change.* B00000000-01717-5700-00021 REV 01. Las Vegas, Nevada: CRWMS M&O. ACC: MOL.19990712.0161.

CRWMS M&O 1999c. *License Application Design Selection Report.* B00000000-01717-4600-00123 REV 01 ICN 01. Las Vegas, Nevada: CRWMS M&O. ACC: MOL.19990908.0319.

CRWMS M&O 1999d. *Enhanced Design Alternative II Report.* B00000000-01717-5705-00131 REV 00. Las Vegas, Nevada: CRWMS M&O. ACC: MOL.19990712.0194.

CRWMS M&O 1999e. *MGR Design Basis Extreme Wind/Tornado Analysis.* ANL-MGR-SE-000001 REV 00. Las Vegas, Nevada: CRWMS M&O. ACC: MOL.19991215.0461.

CRWMS M&O 1999f. *Enhanced Characterization of the Repository Block (ECRB) Cross-Drift Excavation Report.* BCA000000-01717-5700-00001 REV 00. Las Vegas, Nevada: CRWMS M&O. ACC: MOL.19990408.0132.

CRWMS M&O 1999g. *Monitored Geologic Repository Concept of Operations.*
B00000000-01717-4200-00004 REV 03. Las Vegas, Nevada: CRWMS M&O.
ACC: MOL.19990916.0104.

CRWMS M&O 1999h. *TBV-245 Resolution Analysis: Design Basis Block Size Assessment.*
B00000000-01717-5705-00133 REV 00. Las Vegas, Nevada: CRWMS M&O.
ACC: MOL.19991022.0192.

CRWMS M&O 1999i. *Preclosure Criticality Analysis Process Report.* B00000000-01717-5705-00132
REV 00. Las Vegas, Nevada: CRWMS M&O. ACC: MOL.19990930.0102.

CRWMS M&O 1999j. *Evaluation of Codisposal Viability for MOX (FFTF) DOE-Owned Fuel.*
BBA000000-01717-5705-00023 REV 00. Las Vegas, Nevada: CRWMS M&O.
ACC: MOL.19991014.0235.

CRWMS M&O 1999k. *PWR Source Term Generation and Evaluation.* BBAC00000-01717-0210-00010
REV 01. Las Vegas, Nevada: CRWMS M&O. ACC: MOL.20000113.0333.

CRWMS M&O 1999l. *BWR Source Term Generation and Evaluation.* BBAC00000-01717-0210-00006
REV 01. Las Vegas, Nevada: CRWMS M&O. ACC: MOL.20000113.0334.

CRWMS M&O 1999m. *Single Heater Test Final Report.* BAB000000-01717-5700-00005 REV 00 ICN 1.
Las Vegas, Nevada: CRWMS M&O. ACC: MOL.20000103.0634.

CRWMS M&O 1999n. *Addendum to: EQ6 Computer Program for Theoretical Manual, Users Guide, &
Related Documentation.* Software Change Request LSCR198. Las Vegas, Nevada: CRWMS M&O.
ACC: MOL.19990305.0112.

CRWMS M&O 1999o. *Source Terms for HLW Glass Canisters.* CAL-MGR-NU-000002 REV 00. Las
Vegas, Nevada: CRWMS M&O. ACC: MOL.20000124.0244.

CRWMS M&O 1999p. *Waste Package Behavior in Magma.* CAL-EBS-ME-000002 REV 00. Las Vegas,
Nevada: CRWMS M&O. ACC: MOL.19991022.0201.

CRWMS M&O 1999q. *Sensitivity Study of Reactivity Consequences to Waste Package Egress Area.*
CAL-EBS-NU-000001 REV 00. Las Vegas, Nevada: CRWMS M&O. ACC: MOL.19990928.0239.

CRWMS M&O 1999r. *Reliability Assessment of Waste Handling Building HVAC System.*
BCBD00000-01717-0210-00008 REV 00. Las Vegas, Nevada: CRWMS M&O.
ACC: MOL.19990621.0155.

CRWMS M&O 2000a. *Total System Performance Assessment for the Site Recommendation.*
TDR-WIS-PA-000001 REV 00 ICN 01. Las Vegas, Nevada: CRWMS M&O. ACC: MOL.20001220.0045.

CRWMS M&O 2000b. *Yucca Mountain Site Description.* TDR-CRW-GS-000001 REV 01 ICN 01. Las
Vegas, Nevada: CRWMS M&O. ACC: MOL.20001003.0111.

CRWMS M&O 2000c. *Unsaturated Zone Flow and Transport Model Process Model Report.*
TDR-NBS-HS-000002 REV 00 ICN 02. Las Vegas, Nevada: CRWMS M&O.
ACC: MOL.20000831.0280.

CRWMS M&O 2000d. *Determination of Available Repository Siting Volume for the Site Recommendation.* TDR-NBS-GS-000003 REV 00. Las Vegas, Nevada: CRWMS M&O. ACC: MOL.20000705.0054.

CRWMS M&O 2000e. *Drift Degradation Analysis.* ANL-EBS-MD-000027 REV 01. Las Vegas, Nevada: CRWMS M&O. ACC: MOL.20001206.0006.

CRWMS M&O 2000f. *Disruptive Events Process Model Report.* TDR-NBS-MD-000002 REV 00 ICN 02. Las Vegas, Nevada: CRWMS M&O. ACC: MOL.20001220.0047.

CRWMS M&O 2000g. *Data Qualification Report: Water Level Altitude Data for Use on the Yucca Mountain Project.* TDR-NBS-HS-000004 REV 00. Las Vegas, Nevada: CRWMS M&O. ACC: MOL.20000912.0206.

CRWMS M&O 2000h. *Subsurface Facility System Description Document.* SDD-SFS-SE-000001 REV 01. Las Vegas, Nevada: CRWMS M&O. ACC: MOL.20000807.0078.

CRWMS M&O 2000i. *Integrated Site Model Process Model Report.* TDR-NBS-GS-000002 REV 00 ICN 01. Las Vegas, Nevada: CRWMS M&O. ACC: MOL.20000121.0116.

CRWMS M&O 2000j. *FEIS Update to Engineering File—Subsurface Repository.* TDR-EBS-MD-000007 REV 00 ICN 01. Las Vegas, Nevada: CRWMS M&O. ACC: MOL.20000612.0058.

CRWMS M&O 2000k. *Operating a Below-Boiling Repository: Demonstration of Concept.* TDR-WIS-SE-000001 REV 00. Las Vegas, Nevada: CRWMS M&O. ACC: MOL.20001005.0010.

CRWMS M&O 2000l. *Calculation of Potential Natural Ventilation Airflows and Pressure Differential.* CAL-SVS-MG-000001 REV 00. Las Vegas, Nevada: CRWMS M&O. ACC: MOL.20001214.0008.

CRWMS M&O 2000m. *Natural Ventilation Study: Demonstration of Concept.* TDR-SVS-SE-000001 REV 00. Las Vegas, Nevada: CRWMS M&O. ACC: MOL.20001201.0103.

CRWMS M&O 2000n. *Waste Package Degradation Process Model Report.* TDR-WIS-MD-000002 REV 00 ICN 01. Las Vegas, Nevada: CRWMS M&O. ACC: MOL.20000717.0005.

CRWMS M&O 2000o. *Three Lower Temperature Operating Mode Scenarios—Aging, Waste Package Spacing, and Drift Spacing.* Input Transmittal 00395.T. Las Vegas, Nevada: CRWMS M&O. ACC: MOL.20001116.0003.

CRWMS M&O 2000p. *Engineering Files for Site Recommendation.* TDR-WHS-MD-000001 REV 00. Las Vegas, Nevada: CRWMS M&O. ACC: MOL.20000607.0232.

CRWMS M&O 2000q. *WHB/WTB Space Program Analysis for Site Recommendation.* ANL-WHS-AR-000001 REV 00. Las Vegas, Nevada: CRWMS M&O. ACC: MOL.20000808.0408.

CRWMS M&O 2000r. *Repository Surface Facilities Primary System Crane Specifications.* CAL-WHS-ME-000001 REV 00. Las Vegas, Nevada: CRWMS M&O. ACC: MOL.20000922.0006.

CRWMS M&O 2000s. *Waste Handling Building System Description Document.* SDD-HBS-SE-000001 REV 00 ICN 01. Las Vegas, Nevada: CRWMS M&O. ACC: MOL.20000802.0009.

CRWMS M&O 2000t. *Preliminary Dynamic Soil-Structure-Interaction Analysis for the Waste Handling Building.* ANL-WHS-ST-000001 REV 00. Las Vegas, Nevada: CRWMS M&O. ACC: MOL.20000504.0313.

CRWMS M&O 2000u. *Canister Transfer System Description Document.* SDD-CTS-SE-000001 REV 00 ICN 01. Las Vegas, Nevada: CRWMS M&O. ACC: MOL.20000807.0079.

CRWMS M&O 2000v. *Assembly Transfer System Description Document.* SDD-ATS-SE-000001 REV 00 ICN 01. Las Vegas, Nevada: CRWMS M&O. ACC: MOL.20000807.0081.

CRWMS M&O 2000w. *Ground Control for Emplacement Drifts for SR.* ANL-EBS-GE-000002 REV 00. Las Vegas, Nevada: CRWMS M&O. ACC: MOL.20000414.0875.

CRWMS M&O 2000x. *Overall Subsurface Ventilation System.* ANL-SVS-HV-000002 REV 00 ICN 1. Las Vegas, Nevada: CRWMS M&O. ACC: MOL.20000609.0265.

CRWMS M&O 2000y. *Subsurface Transporter Safety Systems Analysis.* ANL-WER-ME-000001 REV 01. Las Vegas, Nevada: CRWMS M&O. ACC: MOL.20000829.0005.

CRWMS M&O 2000z. *Bottom/Side Lift Gantry Conceptual Design.* ANL-WES-ME-000003 REV 01. Las Vegas, Nevada: CRWMS M&O. ACC: MOL.20000420.0399.

CRWMS M&O 2000aa. *Retrieval Equipment and Strategy for WP on Pallet.* ANL-WES-ME-000006 REV 00. Las Vegas, Nevada: CRWMS M&O. ACC: MOL.20001002.0150.

CRWMS M&O 2000ab. *Emplacement Drift System Description Document.* SDD-EDS-SE-000001 REV 01. Las Vegas, Nevada: CRWMS M&O. ACC: MOL.20000803.0348.

CRWMS M&O 2000ac. *Waste Emplacement/Retrieval System Description Document.* SDD-WES-SE-000001 REV 01. Las Vegas, Nevada: CRWMS M&O. ACC: MOL.20000823.0002.

CRWMS M&O 2000ad. *Ground Control System Description Document.* SDD-GCS-SE-000001 REV 01. Las Vegas, Nevada: CRWMS M&O. ACC: MOL.20000803.0355.

CRWMS M&O 2000ae. *Backfill Emplacement System Description Document.* SDD-BES-SE-000001 REV 00. Las Vegas, Nevada: CRWMS M&O. ACC: MOL.20000210.0074.

CRWMS M&O 2000af. *Subsurface Ventilation System Description Document.* SDD-SVS-SE-000001 REV 01. Las Vegas, Nevada: CRWMS M&O. ACC: MOL.20000803.0356.

CRWMS M&O 2000ag. *Performance Confirmation Plan.* TDR-PCS-SE-000001 REV 01 ICN 01. Las Vegas, Nevada: CRWMS M&O. ACC: MOL.20000601.0196.

CRWMS M&O 2000ah. *Instrumentation and Controls for Waste Emplacement.* ANL-WES-CS-000001 REV 00 ICN 01. Las Vegas, Nevada: CRWMS M&O. ACC: MOL.20000825.0004.

CRWMS M&O 2000ai. *Repository Closure and Sealing Approach.* ANL-SCS-MG-000001 REV 00. Las Vegas, Nevada: CRWMS M&O. ACC: MOL.20000714.0553.

CRWMS M&O 2000aj. *Closure Seal Locations and Geologic Environment Study.* TDR-SCS-MG-000002 REV 00. Las Vegas, Nevada: CRWMS M&O. ACC: MOL.20000122.0037.

CRWMS M&O 2000ak. *Closure Seal Materials and Configuration.* TDR-SCS-MG-000001 REV 00. Las Vegas, Nevada: CRWMS M&O. ACC: MOL.20000124.0136.

CRWMS M&O 2000al. *Near Field Environment Process Model Report.* TDR-NBS-MD-000001 REV 00 ICN 03. Las Vegas, Nevada: CRWMS M&O. ACC: MOL.20001121.0041.

CRWMS M&O 2000am. *ESF Ground Support Design Analysis.* BABEE0000-01717-0200-00002 REV 01. Las Vegas, Nevada: CRWMS M&O. ACC: MOL.20000119.0135.

CRWMS M&O 2000an. *Emplacement Ventilation System.* ANL-SVS-HV-000003 REV 00. Las Vegas, Nevada: CRWMS M&O. ACC: MOL.20000413.0688.

CRWMS M&O 2000ao. *Waste Package Transport and Transfer Alternatives.* ANL-WES-ME-000001 REV 00. Las Vegas, Nevada: CRWMS M&O. ACC: MOL.20000317.0261.

CRWMS M&O 2000ap. *Design Analysis for the Ex-Container Components.* ANL-XCS-ME-000001 REV 00. Las Vegas, Nevada: CRWMS M&O. ACC: MOL.20000525.0374.

CRWMS M&O 2000aq. *Invert Configuration and Drip Shield Interface.* TDR-EDS-ST-000001 REV 00. Las Vegas, Nevada: CRWMS M&O. ACC: MOL.20000505.0232.

CRWMS M&O 2000ar. *Drip Shield Emplacement Gantry Concept.* ANL-XCS-ME-000002 REV 00. Las Vegas, Nevada: CRWMS M&O. ACC: MOL.20000418.0817.

CRWMS M&O 2000as. *Engineered Barrier System Degradation, Flow, and Transport Process Model Report.* TDR-EBS-MD-000006 REV 00 ICN 01. Las Vegas, Nevada: CRWMS M&O. ACC: MOL.20000724.0479.

CRWMS M&O 2000at. *Structural Calculations of the Drip Shield Statically Loaded by the Backfill and Loose Rock Mass.* CAL-XCS-ME-000001 REV 00. Las Vegas, Nevada: CRWMS M&O. ACC: MOL.20000216.0098.

CRWMS M&O 2000au. *Uncanistered Spent Nuclear Fuel Disposal Container System Description Document.* SDD-UDC-SE-000001 REV 01. Las Vegas, Nevada: CRWMS M&O. ACC: MOL.20000822.0004.

CRWMS M&O 2000av. *Waste Package Containment Barrier Materials and Drip Shield Selection Report.* B00000000-01717-2200-00225 REV 00. Las Vegas, Nevada: CRWMS M&O. ACC: MOL.20000209.0300.

CRWMS M&O 2000aw. *Defense High Level Waste Disposal Container System Description Document.* SDD-DDC-SE-000001 REV 01. Las Vegas, Nevada: CRWMS M&O. ACC: MOL.20000823.0001.

CRWMS M&O 2000ax. *Naval Spent Nuclear Fuel Disposal Container System Description Document.* SDD-VDC-SE-000001 REV 01. Las Vegas, Nevada: CRWMS M&O. ACC: MOL.20000817.0544.

CRWMS M&O 2000ay. *Preclosure Design Basis Events Related to Waste Packages.*
ANL-MGR-MD-000012 REV 00. Las Vegas, Nevada: CRWMS M&O. ACC: MOL.20000725.0015.

CRWMS M&O 2000az. *Waste Package Design Sensitivity Report.* TDR-EBS-MD-000008 REV 00. Las
Vegas, Nevada: CRWMS M&O. ACC: MOL.20000518.0179.

CRWMS M&O 2000ba. *Waste Package Related Impacts of Plutonium Disposition Waste Forms in a
Geologic Repository.* TDR-EBS-MD-000003 REV 01 ICN 01. Las Vegas, Nevada: CRWMS M&O.
ACC: MOL.20000510.0163.

CRWMS M&O 2000bb. *Waste Packages and Source Terms for the Commercial 1999 Design Basis Waste
Streams.* CAL-MGR-MD-000001 REV 00. Las Vegas, Nevada: CRWMS M&O.
ACC: MOL.20000214.0479.

CRWMS M&O 2000bc. *Update to the EIS Engineering File for the Waste Package in Support of the Final
EIS.* TDR-EBS-MD-000010 REV 00 ICN 01. Las Vegas, Nevada: CRWMS M&O.
ACC: MOL.20000317.0446.

CRWMS M&O 2000bd. *Waste Package Internal Materials Selection Report.*
B00000000-01717-2200-00226 REV 00. Las Vegas, Nevada: CRWMS M&O.
ACC: MOL.20000209.0299.

CRWMS M&O 2000be. *Waste Package Neutron Absorber, Thermal Shunt, and Fill Gas Selection Report.*
B00000000-01717-2200-00227 REV 00. Las Vegas, Nevada: CRWMS M&O.
ACC: MOL.20000209.0301.

CRWMS M&O 2000bf. *Waste Package Operations Fabrication Process Report.* TDR-EBS-ND-000003
REV 00. Las Vegas, Nevada: CRWMS M&O. ACC: MOL.20000217.0244.

CRWMS M&O 2000bg. *21 PWR Waste Package Loading Curve Evaluation.* CAL-UDC-NU-000001
REV 00. Las Vegas, Nevada: CRWMS M&O. ACC: MOL.20000517.0451.

CRWMS M&O 2000bh. *Evaluation of Codisposal Viability for UZrH (TRIGA) DOE-Owned Fuel.*
TDR-EDC-NU-000001 REV 00. Las Vegas, Nevada: CRWMS M&O. ACC: MOL.20000207.0689.

CRWMS M&O 2000bi. *Evaluation of Codisposal Viability for HEU Oxide (Shippingport PWR)
DOE-Owned Fuel.* TDR-EDC-NU-000003 REV 00. Las Vegas, Nevada: CRWMS M&O.
ACC: MOL.20000227.0240.

CRWMS M&O 2000bj. *Evaluation of Codisposal Viability for U-Zr/U-Mo Alloy (Enrico Fermi)
DOE-Owned Fuel.* TDR-EDC-NU-000002 REV 00. Las Vegas, Nevada: CRWMS M&O.
ACC: MOL.20000815.0317.

CRWMS M&O 2000bk. *Evaluation of Codisposal Viability for Th/U Oxide (Shippingport LWBR)
DOE-Owned Fuel.* TDR-EDC-NU-000005 REV 00. Las Vegas, Nevada: CRWMS M&O.
ACC: MOL.20001023.0055.

CRWMS M&O 2000bl. *Design Analysis for UCF Waste Packages.* ANL-UDC-MD-000001 REV 00. Las
Vegas, Nevada: CRWMS M&O. ACC: MOL.20000526.0336.

CRWMS M&O 2000bm. *Waste Form Degradation Process Model Report.* TDR-WIS-MD-000001 REV 00 ICN 01. Las Vegas, Nevada: CRWMS M&O. ACC: MOL.20000713.0362.

CRWMS M&O 2000bn. *Saturated Zone Flow and Transport Process Model Report.* TDR-NBS-HS-000001 REV 00 ICN 01. Las Vegas, Nevada: CRWMS M&O. ACC: MOL.20000821.0359.

CRWMS M&O 2000bo. *Biosphere Process Model Report.* TDR-MGR-MD-000002 REV 00 ICN 01. Las Vegas, Nevada: CRWMS M&O. ACC: MOL.20000620.0341.

CRWMS M&O 2000bp. *Natural Analogs for the Unsaturated Zone.* ANL-NBS-HS-000007 REV 00. Las Vegas, Nevada: CRWMS M&O. ACC: MOL.19990721.0524.

CRWMS M&O 2000bq. *Conceptual and Numerical Models for UZ Flow and Transport.* MDL-NBS-HS-000005 REV 00. Las Vegas, Nevada: CRWMS M&O. ACC: MOL.19990721.0526.

CRWMS M&O 2000br. *Development of Numerical Grids for UZ Flow and Transport Modeling.* ANL-NBS-HS-000015 REV 00. Las Vegas, Nevada: CRWMS M&O. ACC: MOL.19990721.0517.

CRWMS M&O 2000bs. *Geologic Framework Model (GFM3.1).* MDL-NBS-GS-000002 REV 00 ICN 01. Las Vegas, Nevada: CRWMS M&O. ACC: MOL.20000121.0115.

CRWMS M&O 2000bt. *Analysis of Hydrologic Properties Data.* ANL-NBS-HS-000002 REV 00. Las Vegas, Nevada: CRWMS M&O. ACC: MOL.19990721.0519.

CRWMS M&O 2000bu. *In Situ Field Testing of Processes.* ANL-NBS-HS-000005 REV 00. Las Vegas, Nevada: CRWMS M&O. ACC: MOL.20000504.0304.

CRWMS M&O 2000bv. *Analysis of Geochemical Data for the Unsaturated Zone.* ANL-NBS-HS-000017 REV 00. Las Vegas, Nevada: CRWMS M&O. ACC: MOL.20000725.0453.

CRWMS M&O 2000bw. *UZ Flow Models and Submodels.* MDL-NBS-HS-000006 REV 00. Las Vegas, Nevada: CRWMS M&O. ACC: MOL.19990721.0527.

CRWMS M&O 2000bx. *Seepage Model for PA Including Drift Collapse.* MDL-NBS-HS-000002 REV 00. Las Vegas, Nevada: CRWMS M&O. ACC: MOL.19990721.0525.

CRWMS M&O 2000by. *Abstraction of Drift Seepage.* ANL-NBS-MD-000005 REV 00. Las Vegas, Nevada: CRWMS M&O. ACC: MOL.20000322.0671.

CRWMS M&O 2000bz. *Seepage Calibration Model and Seepage Testing Data.* MDL-NBS-HS-000004 REV 00. Las Vegas, Nevada: CRWMS M&O. ACC: MOL.19990721.0521.

CRWMS M&O 2000ca. *Abstraction of Flow Fields for RIP (ID: U0125).* ANL-NBS-HS-000023 REV 00. Las Vegas, Nevada: CRWMS M&O. ACC: MOL.20000127.0089.

CRWMS M&O 2000cb. *Analysis of Base-Case Particle Tracking Results of the Base-Case Flow Fields (ID: U0160).* ANL-NBS-HS-000024 REV 00. Las Vegas, Nevada: CRWMS M&O. ACC: MOL.20000207.0690.

CRWMS M&O 2000cc. *Abstraction of NFE Drift Thermodynamic Environment and Percolation Flux.* ANL-EBS-HS-000003 REV 00 ICN 01. Las Vegas, Nevada: CRWMS M&O. ACC: MOL.20001206.0143.

CRWMS M&O 2000cd. *Ventilation Model.* ANL-EBS-MD-000030 REV 00. Las Vegas, Nevada: CRWMS M&O. ACC: MOL.20000107.0330.

CRWMS M&O 2000ce. *ANSYS Calculation in Support of Thermal Loading Design for SR.* CAL-SFS-MG-000003 REV 00. Las Vegas, Nevada: CRWMS M&O. ACC: MOL.20000608.0003.

CRWMS M&O 2000cf. *Multiscale Thermohydrologic Model.* ANL-EBS-MD-000049 REV 00 ICN 01. Las Vegas, Nevada: CRWMS M&O. ACC: MOL.20001208.0062.

CRWMS M&O 2000cg. *Engineered Barrier System: Physical and Chemical Environment Model.* ANL-EBS-MD-000033 REV 01. Las Vegas, Nevada: CRWMS M&O. ACC: 20001228.0081.

CRWMS M&O 2000ch. *Thermal Tests Thermal-Hydrological Analyses/Model Report.* ANL-NBS-TH-000001 REV 00. Las Vegas, Nevada: CRWMS M&O. ACC: MOL.20000505.0231.

CRWMS M&O 2000ci. *Mountain-Scale Coupled Processes (TH) Models.* MDL-NBS-HS-000007 REV 00. Las Vegas, Nevada: CRWMS M&O. ACC: MOL.19990721.0528.

CRWMS M&O 2000cj. *Calibrated Properties Model.* MDL-NBS-HS-000003 REV 00. Las Vegas, Nevada: CRWMS M&O. ACC: MOL.19990721.0520.

CRWMS M&O 2000ck. *Environment on the Surfaces of the Drip Shield and Waste Package Outer Barrier.* ANL-EBS-MD-000001 REV 00. Las Vegas, Nevada: CRWMS M&O. ACC: MOL.20000328.0590.

CRWMS M&O 2000cl. *In-Drift Precipitates/Salts Analysis.* ANL-EBS-MD-000045 REV 00 ICN 01. Las Vegas, Nevada: CRWMS M&O. ACC: MOL.20001211.0002.

CRWMS M&O 2000cm. *In-Drift Gas Flux and Composition.* ANL-EBS-MD-000040 REV 00. Las Vegas, Nevada: CRWMS M&O. ACC: MOL.20000523.0154.

CRWMS M&O 2000cn. *Waste Form Colloid-Associated Concentrations Limits: Abstraction and Summary.* ANL-WIS-MD-000012 REV 00. Las Vegas, Nevada: CRWMS M&O. ACC: MOL.20000525.0397.

CRWMS M&O 2000co. *In-Drift Colloids and Concentration.* ANL-EBS-MD-000042 REV 00. Las Vegas, Nevada: CRWMS M&O. ACC: MOL.20000509.0242.

CRWMS M&O 2000cp. *In-Drift Microbial Communities.* ANL-EBS-MD-000038 REV 00 ICN 01. Las Vegas, Nevada: CRWMS M&O. ACC: MOL.20001213.0066.

CRWMS M&O 2000cq. *General Corrosion and Localized Corrosion of Waste Package Outer Barrier.* ANL-EBS-MD-000003 REV 00. Las Vegas, Nevada: CRWMS M&O. ACC: MOL.20000202.0172.

CRWMS M&O 2000cr. *General Corrosion and Localized Corrosion of the Drip Shield.* ANL-EBS-MD-000004 REV 00. Las Vegas, Nevada: CRWMS M&O. ACC: MOL.20000329.1185.

CRWMS M&O 2000cs. *Analysis of Mechanisms for Early Waste Package Failure.* ANL-EBS-MD-000023 REV 01. Las Vegas, Nevada: CRWMS M&O. ACC: MOL.20000223.0878.

CRWMS M&O 2000ct. *Aging and Phase Stability of Waste Package Outer Barrier.* ANL-EBS-MD-000002 REV 00. Las Vegas, Nevada: CRWMS M&O. ACC: MOL.20000410.0407.

CRWMS M&O 2000cu. *Stress Corrosion Cracking of the Drip Shield, the Waste Package Outer Barrier, and the Stainless Steel Structural Material.* ANL-EBS-MD-000005 REV 00 ICN 01. Las Vegas, Nevada: CRWMS M&O. ACC: MOL.20001102.0340.

CRWMS M&O 2000cv. *Hydrogen Induced Cracking of Drip Shield.* ANL-EBS-MD-000006 REV 00 ICN 01. Las Vegas, Nevada: CRWMS M&O. ACC: MOL.20001025.0100.

CRWMS M&O 2000cw. *Degradation of Stainless Steel Structural Material.* ANL-EBS-MD-000007 REV 00. Las Vegas, Nevada: CRWMS M&O. ACC: MOL.20000329.1188.

CRWMS M&O 2000cx. *FEPs Screening of Processes and Issues in Drip Shield and Waste Package Degradation.* ANL-EBS-PA-000002 REV 00 ICN 01. Las Vegas, Nevada: CRWMS M&O. ACC: MOL.20001211.0004.

CRWMS M&O 2000cy. *Calculation of Probability and Size of Defect Flaws in Waste Package Closure Welds to Support WAPDEG Analysis.* CAL-EBS-PA-000003 REV 00. Las Vegas, Nevada: CRWMS M&O. ACC: MOL.20000424.0676.

CRWMS M&O 2000cz. *Calculation of General Corrosion Rate of Drip Shield and Waste Package Outer Barrier to Support WAPDEG Analysis.* CAL-EBS-PA-000002 REV 00. Las Vegas, Nevada: CRWMS M&O. ACC: MOL.20000319.0047.

CRWMS M&O 2000da. *Abstraction of Models for Pitting and Crevice Corrosion of Drip Shield and Waste Package Outer Barrier.* ANL-EBS-PA-000003 REV 00. Las Vegas, Nevada: CRWMS M&O. ACC: MOL.20000526.0327.

CRWMS M&O 2000db. *Abstraction of Models of Stress Corrosion Cracking of Drip Shield and Waste Package Outer Barrier and Hydrogen Induced Corrosion of Drip Shield.* ANL-EBS-PA-000004 REV 00 ICN 01. Las Vegas, Nevada: CRWMS M&O. ACC: MOL.20001213.0065.

CRWMS M&O 2000dc. *WAPDEG Analysis of Waste Package and Drip Shield Degradation.* ANL-EBS-PA-000001 REV 00 ICN 01. Las Vegas, Nevada: CRWMS M&O. ACC: MOL.20001208.0063.

CRWMS M&O 2000dd. *EBS Radionuclide Transport Abstraction.* ANL-WIS-PA-000001 REV 00 ICN 02. Las Vegas, Nevada: CRWMS M&O. ACC: MOL.20001204.0029.

CRWMS M&O 2000de. *Initial Cladding Condition.* ANL-EBS-MD-000048 REV 00 ICN 01. Las Vegas, Nevada: CRWMS M&O. ACC: MOL.20001002.0145.

CRWMS M&O 2000df. *Clad Degradation—Local Corrosion of Zirconium and Its Alloys Under Repository Conditions.* ANL-EBS-MD-000012 REV 00. Las Vegas, Nevada: CRWMS M&O. ACC: MOL.20000405.0479.

CRWMS M&O 2000dg. *Hydride-Related Degradation of SNF Cladding Under Repository Conditions.* ANL-EBS-MD-000011 REV 00. Las Vegas, Nevada: CRWMS M&O. ACC: MOL.20000319.0048.

CRWMS M&O 2000dh. *Clad Degradation—Wet Unzipping.* ANL-EBS-MD-000014 REV 00. Las Vegas, Nevada: CRWMS M&O. ACC: MOL.20000502.0398.

CRWMS M&O 2000di. *Clad Degradation—Dry Unzipping.* ANL-EBS-MD-000013 REV 00. Las Vegas, Nevada: CRWMS M&O. ACC: MOL.20000503.0200.

CRWMS M&O 2000dj. *Clad Degradation—Summary and Abstraction.* ANL-WIS-MD-000007 REV 00. Las Vegas, Nevada: CRWMS M&O. ACC: MOL.20000602.0055.

CRWMS M&O 2000dk. *CSNF Waste Form Degradation: Summary Abstraction.* ANL-EBS-MD-000015 REV 00. Las Vegas, Nevada: CRWMS M&O. ACC: MOL.20000121.0161.

CRWMS M&O 2000dl. *Defense High Level Waste Glass Degradation.* ANL-EBS-MD-000016 REV 00. Las Vegas, Nevada: CRWMS M&O. ACC: MOL.20000329.1183.

CRWMS M&O 2000dm. *Summary of In-Package Chemistry for Waste Forms.* ANL-EBS-MD-000050 REV 00. Las Vegas, Nevada: CRWMS M&O. ACC: MOL.20000217.0217.

CRWMS M&O 2000dn. *In-Package Chemistry Abstraction.* ANL-EBS-MD-000037 REV 00. Las Vegas, Nevada: CRWMS M&O. ACC: MOL.20000418.0818.

CRWMS M&O 2000do. *Clad Degradation—FEPs Screening Arguments.* ANL-WIS-MD-000008 REV 00. Las Vegas, Nevada: CRWMS M&O. ACC: MOL.20000525.0378.

CRWMS M&O 2000dp. *Summary of Dissolved Concentration Limits.* ANL-WIS-MD-000010 REV 00. Las Vegas, Nevada: CRWMS M&O. ACC: MOL.20000525.0372.

CRWMS M&O 2000dq. *Pure Phase Solubility Limits—LANL.* ANL-EBS-MD-000017 REV 00. Las Vegas, Nevada: CRWMS M&O. ACC: MOL.20000504.0311.

CRWMS M&O 2000dr. *Secondary Uranium-Phase Paragenesis and Incorporation of Radionuclides into Secondary Phases.* ANL-EBS-MD-000019 REV 00. Las Vegas, Nevada: CRWMS M&O. ACC: MOL.20000414.0644.

CRWMS M&O 2000ds. *Inventory Abstraction.* ANL-WIS-MD-000006 REV 00 ICN 01. Las Vegas, Nevada: CRWMS M&O. ACC: MOL.20001130.0002.

CRWMS M&O 2000dt. *Colloid-Associated Radionuclide Concentration Limits: ANL.* ANL-EBS-MD-000020 REV 00. Las Vegas, Nevada: CRWMS M&O. ACC: MOL.20000329.1187.

CRWMS M&O 2000du. *Per Canister Inventories for DOE SNF for TSPA-SR.* CAL-WIS-MD-000006 REV 00. Las Vegas, Nevada: CRWMS M&O. ACC: MOL.20000510.0155.

CRWMS M&O 2000dv. *Performance Assessment Sensitivity Analyses of Selected U.S. Department of Energy Spent Fuels.* ANL-WIS-MD-000001 REV 00. Las Vegas, Nevada: CRWMS M&O. ACC: MOL.20000710.0530.

CRWMS M&O 2000dw. *Waste Package Radionuclide Inventory Approximations for TSPA-SR.* CAL-WIS-MD-000004 REV 00. Las Vegas, Nevada: CRWMS M&O. ACC: MOL.20000630.0247.

CRWMS M&O 2000dx. *Inventory Abstraction.* ANL-WIS-MD-000006 REV 00. Las Vegas, Nevada: CRWMS M&O. ACC: MOL.20000414.0643.

CRWMS M&O 2000dy. *EBS Radionuclide Transport Model.* ANL-EBS-MD-000034 REV 00 ICN 01. Las Vegas, Nevada: CRWMS M&O. ACC: MOL.20000727.0091.

CRWMS M&O 2000dz. *Invert Diffusion Properties Model.* ANL-EBS-MD-000031 REV 01. Las Vegas, Nevada: CRWMS M&O. ACC: MOL.20000912.0208.

CRWMS M&O 2000ea. *Radionuclide Transport Models Under Ambient Conditions.* MDL-NBS-HS-000008 REV 00. Las Vegas, Nevada: CRWMS M&O. ACC: MOL.19990721.0529.

CRWMS M&O 2000eb. *Unsaturated Zone and Saturated Zone Transport Properties (U0100).* ANL-NBS-HS-000019 REV 00. Las Vegas, Nevada: CRWMS M&O. ACC: MOL.20000829.0006.

CRWMS M&O 2000ec. *UZ Colloid Transport Model.* ANL-NBS-HS-000028 REV 00. Las Vegas, Nevada: CRWMS M&O. ACC: MOL.20000822.0005.

CRWMS M&O 2000ed. *Particle Tracking Model and Abstraction of Transport Processes.* ANL-NBS-HS-000026 REV 00. Las Vegas, Nevada: CRWMS M&O. ACC: MOL.20000502.0237.

CRWMS M&O 2000ee. *Analysis Comparing Advective-Dispersive Transport Solution to Particle Tracking.* ANL-NBS-HS-000001 REV 00. Las Vegas, Nevada: CRWMS M&O. ACC: MOL.19990721.0518.

CRWMS M&O 2000ef. *Features, Events, and Processes in UZ Flow and Transport.* ANL-NBS-MD-000001 REV 00. Las Vegas, Nevada: CRWMS M&O. ACC: MOL.20000502.0240.

CRWMS M&O 2000eg. *Geochemical and Isotopic Constraints on Groundwater Flow Directions, Mixing, and Recharge at Yucca Mountain, Nevada.* ANL-NBS-HS-000021 REV 00. Las Vegas, Nevada: CRWMS M&O. ACC: MOL.20000918.0287.

CRWMS M&O 2000eh. *Saturated Zone Transport Methodology and Transport Component Integration.* MDL-NBS-HS-000010 REV 00. Las Vegas, Nevada: CRWMS M&O. ACC: MOL.20000824.0513.

CRWMS M&O 2000ei. *Saturated Zone Colloid-Facilitated Transport.* ANL-NBS-HS-000031 REV 00. Las Vegas, Nevada: CRWMS M&O. ACC: MOL.20000609.0266.

CRWMS M&O 2000ej. *Calibration of the Site-Scale Saturated Zone Flow Model.* MDL-NBS-HS-000011 REV 00. Las Vegas, Nevada: CRWMS M&O. ACC: MOL.20000825.0122.

CRWMS M&O 2000ek. *Uncertainty Distribution for Stochastic Parameters.* ANL-NBS-MD-000011 REV 00. Las Vegas, Nevada: CRWMS M&O. ACC: MOL.20000526.0328.

CRWMS M&O 2000el. *Input and Results of the Base Case Saturated Zone Flow and Transport Model for TSPA.* ANL-NBS-HS-000030 REV 00. Las Vegas, Nevada: CRWMS M&O. ACC: MOL.20000526.0330.

CRWMS M&O 2000em. *Probability Distribution for Flowing Interval Spacing.* ANL-NBS-MD-000003 REV 00. Las Vegas, Nevada: CRWMS M&O. ACC: MOL.20000602.0052.

CRWMS M&O 2000en. *Modeling Sub Gridlock Scale Dispersion in Three-Dimensional Heterogeneous Fractured Media (S0015).* ANL-NBS-HS-000022 REV 00. Las Vegas, Nevada: CRWMS M&O. ACC: MOL.20000622.0363.

CRWMS M&O 2000eo. *Evaluate Soil/Radionuclide Removal by Erosion and Leaching.* ANL-NBS-MD-000009 REV 00. Las Vegas, Nevada: CRWMS M&O. ACC: MOL.20000310.0057.

CRWMS M&O 2000ep. *Identification of the Critical Group (Consumption of Locally Produced Food and Tap Water).* ANL-MGR-MD-000005 REV 00. Las Vegas, Nevada: CRWMS M&O. ACC: MOL.20000224.0399.

CRWMS M&O 2000eq. *Abstraction of BDCF Distributions for Irrigation Periods.* ANL-NBS-MD-000007 REV 00. Las Vegas, Nevada: CRWMS M&O. ACC: MOL.20000517.0257.

CRWMS M&O 2000er. *Distribution Fitting to the Stochastic BDCF Data.* ANL-NBS-MD-000008 REV 00. Las Vegas, Nevada: CRWMS M&O. ACC: MOL.20000517.0258; MOL.20000601.0753.

CRWMS M&O 2000es. *Non-Disruptive Event Biosphere Dose Conversion Factor Sensitivity Analysis.* ANL-MGR-MD-000010 REV 00. Las Vegas, Nevada: CRWMS M&O. ACC: MOL.20000420.0074.

CRWMS M&O 2000et. *Features, Events, and Processes in Thermal Hydrology and Coupled Processes.* ANL-NBS-MD-000004 REV 00. Las Vegas, Nevada: CRWMS M&O. ACC: MOL.20000602.0053.

CRWMS M&O 2000eu. *Miscellaneous Waste-Form FEPs.* ANL-WIS-MD-000009 REV 00. Las Vegas, Nevada: CRWMS M&O. ACC: MOL.20000526.0339.

CRWMS M&O 2000ev. *Engineered Barrier System Features, Events, and Processes, and Degradation Modes Analysis.* ANL-EBS-MD-000035 REV 00 ICN 01. Las Vegas, Nevada: CRWMS M&O. ACC: MOL.20000727.0092.

CRWMS M&O 2000ew. *Features, Events, and Processes in SZ Flow and Transport.* ANL-NBS-MD-000002 REV 00. Las Vegas, Nevada: CRWMS M&O. ACC: MOL.20000526.0338.

CRWMS M&O 2000ex. *Features, Events, and Processes: Disruptive Events.* ANL-WIS-MD-000005 REV 00 ICN 1. Las Vegas, Nevada: CRWMS M&O. ACC: MOL.20001218.0007.

CRWMS M&O 2000ey. *Total System Performance Assessment–Site Recommendation Methods and Assumptions.* TDR-MGR-MD-000001 REV 00 ICN 02. Las Vegas, Nevada: CRWMS M&O. ACC: MOL.20000307.0384.

CRWMS M&O 2000ez. *Characterize Framework for Igneous Activity at Yucca Mountain, Nevada.* ANL-MGR-GS-000001 REV 00 ICN 01. Las Vegas, Nevada: CRWMS M&O. ACC: MOL.20001221.0001.

CRWMS M&O 2000fa. *Characterize Eruptive Processes at Yucca Mountain, Nevada.* ANL-MGR-GS-000002 REV 00. Las Vegas, Nevada: CRWMS M&O. ACC: MOL.20000517.0259.

CRWMS M&O 2000fb. *Dike Propagation Near Drifts.* ANL-WIS-MD-000015 REV 00 ICN 01. Las Vegas, Nevada: CRWMS M&O. ACC: MOL.20001213.0061.

CRWMS M&O 2000fc. *Igneous Consequence Modeling for the TSPA-SR.* ANL-WIS-MD-000017 REV 00 ICN 01. Las Vegas, Nevada: CRWMS M&O. ACC: MOL.20001204.0022.

CRWMS M&O 2000fd. *Characterize Framework for Seismicity and Structural Deformation at Yucca Mountain, Nevada.* ANL-CRW-GS-000003 REV 00. Las Vegas, Nevada: CRWMS M&O. ACC: MOL.20000510.0175

CRWMS M&O 2000fe. *Effects of Fault Displacement on Emplacement Drifts.* ANL-EBS-GE-000004 REV 00 ICN 01. Las Vegas, Nevada: CRWMS M&O. ACC: MOL.20000504.0297.

CRWMS M&O 2000ff. *Fault Displacement Effects on Transport in the Unsaturated Zone.* ANL-NBS-HS-000020 REV 01. Las Vegas, Nevada: CRWMS M&O. ACC: MOL.20001002.0154.

CRWMS M&O 2000fg. *Water Pooling-Evaporation in a Waste Package.* CAL-EBS-NU-000009 REV 00. Las Vegas, Nevada: CRWMS M&O. ACC: MOL.20000424.0698.

CRWMS M&O 2000fh. *Probability of Criticality Before 10,000 Years.* CAL-EBS-NU-000014 REV 00. Las Vegas, Nevada: CRWMS M&O. ACC: MOL.20001107.0303.

CRWMS M&O 2000fi. *Number of Waste Packages Hit by Igneous Intrusion.* CAL-WIS-PA-000001 REV 00. Las Vegas, Nevada: CRWMS M&O. ACC: MOL.20000602.0054.

CRWMS M&O 2000fj. *Monitored Geologic Repository Test & Evaluation Plan.* TDR-MGR-SE-000010 REV 03. Las Vegas, Nevada: CRWMS M&O. ACC: MOL.20000926.0296.

CRWMS M&O 2000fk. *Repository Safety Strategy: Plan to Prepare the Postclosure Safety Case to Support Yucca Mountain Site Recommendation and Licensing Considerations.* TDR-WIS-RL-000001 REV 03. Las Vegas, Nevada: CRWMS M&O. ACC: MOL.20000119.0189.

CRWMS M&O 2001a. *Repository Safety Strategy: Plan to Prepare the Safety Case to Support Yucca Mountain Site Recommendation and Licensing Considerations.* TDR-WIS-RL-000001 REV 04 ICN 01. Two volumes. Las Vegas, Nevada: CRWMS M&O. ACC: MOL.20010329.0825.

CRWMS M&O 2001b. *Precipitates/Salts Model Results for THC Abstraction.* CAL-EBS-PA-000008 REV 00 ICN 01. Las Vegas, Nevada: CRWMS M&O. ACC: MOL.20010125.0231.

CRWMS M&O 2001c. *Water Distribution and Removal Model.* ANL-EBS-MD-000032 REV 01. Las Vegas, Nevada: CRWMS M&O. ACC: MOL.20010214.0031.

CRWMS M&O 2001d. *Engineered Barrier System Features, Events, and Processes.* ANL-WIS-PA-000002 REV 01. Las Vegas, Nevada: CRWMS M&O. ACC: MOL.20010312.0024.

CRWMS M&O 2001e. *Nominal Performance Biosphere Dose Conversion Factor Analysis.* ANL-MGR-MD-000009 REV 01. Las Vegas, Nevada: CRWMS M&O. ACC: MOL.20010123.0123.

CRWMS M&O 2001f. *Distribution Fitting to the Stochastic BDCF Data.* ANL-NBS-MD-000008 REV 00 ICN 01. Las Vegas, Nevada: CRWMS M&O. ACC: MOL.20010221.0148.

Cullen, A.C. and Frey, H.C. 1999. *Probabilistic Techniques in Exposure Assessment, A Handbook for Dealing with Variability and Uncertainty in Models and Inputs.* New York, New York: Plenum Press. TIC: 242815.

Curry, P.M. 2001. *Monitored Geologic Repository Project Description Document.* TDR-MGR-SE-000004 REV 02 ICN 02. Las Vegas, Nevada: Bechtel SAIC Company. ACC: MOL.20010628.0224.

Czarnecki, J.B. 1984. *Simulated Effects of Increased Recharge on the Ground-Water Flow System of Yucca Mountain and Vicinity, Nevada-California.* Water-Resources Investigations Report 84-4344. Denver, Colorado: U.S. Geological Survey. ACC: HQS.19880517.1750.

D'Agnese, F.A.; Faunt, C.C.; Turner, A.K.; and Hill, M.C. 1997. *Hydrogeologic Evaluation and Numerical Simulation of the Death Valley Regional Ground-Water Flow System, Nevada and California.* Water-Resources Investigations Report 96-4300. Denver, Colorado: U.S. Geological Survey. ACC: MOL.19980306.0253.

D'Agnese, F.A.; O'Brien, G.M.; Faunt, C.C.; and San Juan, C.A. 1999. *Simulated Effects of Climate Change on the Death Valley Regional Ground-Water Flow System, Nevada and California.* Water-Resources Investigations Report 98-4041. Denver, Colorado: U.S. Geological Survey. TIC: 243555.

Danko, J.C. 1987. "Corrosion in the Nuclear Power Industry." In *Corrosion*, Volume 13, pages 928-934 of *Metals Handbook.* 9th Edition. Metals Park, Ohio: ASM International. TIC: 209807.

Davies, J.B. and Archambeau, C.B. 1997a. "Geohydrological Models and Earthquake Effects at Yucca Mountain, Nevada." *Environmental Geology, 32,* (1), 23-35. New York, New York: Springer-Verlag. TIC: 237118.

Davies, J.B. and Archambeau, C.B. 1997b. "Analysis of High-Pressure Fluid Flow in Fractures with Application to Yucca Mountain, Nevada, Slug Test Data." *Tectonophysics, 277,* 83-98. Amsterdam, The Netherlands: Elsevier Science. TIC: 246496.

Davis, O.K. 1990. "Caves as Sources of Biotic Remains in Arid Western North America." *Palaeogeography, Palaeoclimatology, Palaeoecology, 76,* (3/4), 331-348. Amsterdam, The Netherlands: Elsevier Science. TIC: 247413.

Day, W.C.; Dickerson, R.P.; Potter, C.J.; Sweetkind, D.S.; San Juan, C.A.; Drake, R.M., II; and Fridrich, C.J. 1998. *Bedrock Geologic Map of the Yucca Mountain Area, Nye County, Nevada.* Geologic Investigations Series I-2627. Denver, Colorado: U.S. Geological Survey. ACC: MOL.19981014.0301.

Day, W.C.; Potter, C.J.; Sweetkind, D.S.; Dickerson, R.P.; and San Juan, C.A. 1998. *Bedrock Geologic Map of the Central Block Area, Yucca Mountain, Nye County, Nevada.* Miscellaneous Investigations Series Map I-2601. Washington, D.C.: U.S. Geological Survey. ACC: MOL.19980611.0339.

DeLoach, L.; Glassley, W.; Johnson, J.; and Knauss, K. 1997. *Progress Report of Model Results, Account TR3A2FB2, Formation of Flow Barriers Within the Altered Zone.* Milestone SPL2AM4. Livermore, California: Lawrence Livermore National Laboratory. ACC: MOL.19971215.0644.

de Marsily, G.; Ledoux, E.; Barbreau, A.; and Margat, J. 1977. "Nuclear Waste Disposal: Can the Geologist Guarantee Isolation?" *Science, 197,* (4303), 519-527. Washington, D.C.: American Association for the Advancement of Science. TIC: 245104.

Dibble, W.E. and Tiller, W.A. 1981. "Kinetic Model of Zeolite Paragenesis in Tuffaceous Sediments." *Clays and Clay Minerals, 29,* (5), 323-330. Long Island, New York: Pergamon Press. TIC: 221129.

DOE (U.S. Department of Energy) 1980. *Final Environmental Impact Statement Management of Commercially Generated Radioactive Waste.* DOE/EIS-0046F. Three volumes. Washington, D.C.: U.S. Department of Energy, Office of Nuclear Waste Management. ACC: HQZ.19870302.0183; HQZ.19870302.0184; HQZ.19870302.0185.

DOE 1986a. *A Multiattribute Utility Analysis of Sites Nominated for Characterization for the First Radioactive-Waste Repository—A Decision-Aiding Methodology.* DOE/RW-0074. Washington, D.C.: U.S. Department of Energy, Office of Civilian Radioactive Waste Management. ACC: NNA.19870818.0022.

DOE 1986b. *Recommendation by the Secretary of Energy of Candidate Sites for Site Characterization for the First Radioactive-Waste Repository.* DOE/S-0048. Washington, D.C.: U.S. Department of Energy, Office of Civilian Radioactive Waste Management. ACC: MOL.19980701.0391.

DOE 1986c. *Environmental Assessment Yucca Mountain Site, Nevada Research and Development Area, Nevada.* DOE/RW-0073. Three volumes. Washington, D.C.: U.S. Department of Energy, Office of Civilian Radioactive Waste Management. ACC: HQZ.19870302.0332.

DOE 1988. *Site Characterization Plan Yucca Mountain Site, Nevada Research and Development Area, Nevada.* DOE/RW-0199. Nine volumes. Washington, D.C.: U.S. Department of Energy, Office of Civilian Radioactive Waste Management. ACC: HQO.19881201.0002.

DOE 1989. *Review of a Conceptual Model and Evidence for Tectonic Control of the Ground-Water System in the Vicinity of Yucca Mountain, Nevada.* Las Vegas, Nevada: U.S. Department of Energy. ACC: NNA.19890818.0234.

DOE 1996a. *Title 40 CFR Part 191 Compliance Certification Application for the Waste Isolation Pilot Plant.* DOE/CAO-1996-2184. Twenty-one volumes. Carlsbad, New Mexico: U.S. Department of Energy, Carlsbad Area Office. TIC: 240511.

DOE 1996b. *Spent Nuclear Fuel Discharges from U.S. Reactors 1994.* SR/CNEAF/96-01. Washington, D.C.: U.S. Department of Energy. TIC: 232923.

DOE 1997a. *Linking Legacies, Connecting the Cold War Nuclear Weapons Production Processes to Their Environmental Consequences.* DOE/EM-0319. Washington, D.C.: U.S. Department of Energy, Office of Environmental Management. TIC: 232904.

DOE 1997b. *Final Waste Management Programmatic Environmental Impact Statement for Managing Treatment, Storage, and Disposal of Radioactive and Hazardous Waste.* DOE/EIS-0200-F. Summary and five volumes. Washington, D.C.: U.S. Department of Energy, Office of Environmental Management. ACC: MOL.20010727.0150; MOL.20010727.0151; MOL.20010727.0152.

DOE 1997c. *Site Characterization Progress Report: Yucca Mountain, Nevada.* DOE/RW-0498. Number 15. Washington, D.C.: U.S. Department of Energy, Office of Civilian Radioactive Waste Management. ACC: HQO.19970428.0001.

DOE 1997d. *The 1997 "Biosphere" Food Consumption Survey Summary Findings and Technical Documentation.* Washington, D.C.: U.S. Department of Energy, Office of Civilian Radioactive Waste Management. ACC: MOL.19981021.0301.

DOE 1998. *Viability Assessment of a Repository at Yucca Mountain.* DOE/RW-0508. Overview and five volumes. Washington, D.C.: U.S. Department of Energy, Office of Civilian Radioactive Waste Management. ACC: MOL.19981007.0027; MOL.19981007.0028; MOL.19981007.0029; MOL.19981007.0030; MOL.19981007.0031; MOL.19981007.0032.

DOE 1999a. *Draft Environmental Impact Statement for a Geologic Repository for the Disposal of Spent Nuclear Fuel and High-Level Radioactive Waste at Yucca Mountain, Nye County, Nevada.* DOE/EIS-0250D. Summary, Volumes I and II. Washington, D.C.: U.S. Department of Energy, Office of Civilian Radioactive Waste Management. ACC: MOL.19990816.0240.

DOE 1999b. *Site Characterization Progress Report Yucca Mountain, Nevada.* DOE/RW-0512. Number 19. Washington, D.C.: U.S. Department of Energy, Office of Civilian Radioactive Waste Management. ACC: HQO.19990813.0018.

DOE 1999c. *Waste Acceptance System Requirements Document.* DOE/RW-0351, Rev. 03. Washington, D.C.: U.S. Department of Energy, Office of Civilian Radioactive Waste Management. ACC: HQO.19990226.0001.

DOE 1999d. *DOE Spent Nuclear Fuel Information in Support of TSPA-SR.* DOE/SNF/REP-0047, Rev. 0. Washington, D.C.: U.S. Department of Energy, Office of Environmental Management. TIC: 245482.

DOE 2000a. *Quality Assurance Requirements and Description.* DOE/RW-0333P, Rev. 10. Washington, D.C.: U.S. Department of Energy, Office of Civilian Radioactive Waste Management. ACC: MOL.20000427.0422.

DOE 2000b. *Civilian Radioactive Waste Management System Requirements Document.* DOE/RW-0406, Rev. 5, DCN 02. Washington, D.C.: U.S. Department of Energy, Office of Civilian Radioactive Waste Management. ACC: MOL.20010117.0341.

DOE 2000c. *Integrated Safety Management Plan.* DOE/RW-0523, Rev. 0. Washington, D.C.: U.S. Department of Energy, Office of Civilian Radioactive Waste Management. ACC: MOL.20000328.0320.

DOE 2000d. *N Reactor (U-Metal) Fuel Characteristics for Disposal Criticality Analysis.* DOE/SNF/REP-056, Rev. 0. Washington, D.C.: U.S. Department of Energy, Office of Environmental Management. TIC: 247956.

DOE 2001a. *Yucca Mountain Science and Engineering Report.* DOE/RW-0539. Washington, D.C.: U.S. Department of Energy, Office of Civilian Radioactive Waste Management. ACC: MOL.20010524.0272.

DOE 2001b. *Yucca Mountain Preliminary Site Suitability Evaluation.* DOE/RW-0540. Washington, D.C.: U.S. Department of Energy, Office of Civilian Radioactive Waste Management. ACC: MOL.20011101.0082.

DOE 2002. *Final Environmental Impact Statement for a Geologic Repository for the Disposal of Spent Nuclear Fuel and High-Level Radioactive Waste at Yucca Mountain, Nye County, Nevada.* DOE/EIS-0250F. Washington, D.C.: U.S. Department of Energy, Office of Civilian Radioactive Waste Management.

Doughty, C. 1999. "Investigation of Conceptual and Numerical Approaches for Evaluating Moisture, Gas, Chemical, and Heat Transport in Fractured Unsaturated Rock." *Journal of Contaminant Hydrology, 38,* (1-3), 69-106. New York, New York: Elsevier Science. TIC: 244160.

Dublyansky, Y.V. and Reutsky, V.N. 1995. *Preliminary Data on Fluid Inclusions in Epigenetic Minerals from Tunnel Excavated Under Yucca Mountain.* Novosibirsk, Russia: United Institute of Geology, Geophysics and Mineralogy, Russian Academy of Sciences, Siberian Branch. TIC: 247348.

Duderstadt, J.J. and Hamilton, L.J. 1976. *Nuclear Reactor Analysis.* New York, New York: John Wiley & Sons. TIC: 245454.

Duncan, A.B.; Bilhorn, S.G.; and Kennedy, J.E. 1988. *Technical Position on Items and Activities in the High-Level Waste Geologic Repository Program Subject to Quality Assurance Requirements.* NUREG-1318. Washington, D.C.: U.S. Nuclear Regulatory Commission. TIC: 200650.

Dunn, D.S.; Pan, Y-M.; and Cragnolino, G.A. 1999. *Effects of Environmental Factors on the Aqueous Corrosion of High-Level Radioactive Waste Containers—Experimental Results and Models.* CNWRA 99-004. San Antonio, Texas: Center for Nuclear Waste Regulatory Analyses. TIC: 246615.

Dyer, J.R. 2000. "Direction to Prepare Change Request to Delete Backfill from Design Basis for Site Recommendation." Letter from J.R. Dyer (DOE/YMSCO) to D.R. Wilkins (CRWMS M&O), January 24, 2000, OPE:PGH-0559. ACC: MOL.20000128.0238.

Efurd, D.W.; Runde, W.; Banar, J.C.; Janecky, D.R.; Kaszuba, J.P.; Palmer, P.D.; Roensch, F.R.; and Tait, C.D. 1998. "Neptunium and Plutonium Solubilities in a Yucca Mountain Groundwater." *Environmental Science & Technology, 32,* (24), 3893-3900. Easton, Pennsylvania: American Chemical Society. TIC: 243857.

Erickson, J.R. and Waddell, R.K. 1985. *Identification and Characterization of Hydrologic Properties of Fractured Tuff Using Hydraulic and Tracer Tests—Test Well USW H-4, Yucca Mountain, Nye County, Nevada.* Water-Resources Investigations Report 85-4066. Denver, Colorado: U.S. Geological Survey. ACC: NNA.19890713.0211.

Eslinger, P.W.; Doremus, L.A.; Engel, D.W.; Miley, T.B.; Murphy, M.T.; Nichols, W.E.; White, M.D.; Langford, D.W.; and Ouderkirk, S.J. 1993. *Preliminary Total-System Analysis of a Potential High-Level Nuclear Waste Repository at Yucca Mountain.* PNL-8444. Richland, Washington: Pacific Northwest Laboratory. ACC: HQO.19930219.0001.

Evernden, J.F. 1992. *Safety of Proposed Yucca Mountain Nuclear Repository as Regards Geological and Geophysical Factors: Evaluation of Minority Report by Archambeau and Price.* Open-File Report 92-516. Denver, Colorado: U.S. Geological Survey. TIC: 235252.

Fabryka-Martin, J.T.; Wightman, S.J.; Murphy, W.J.; Wickham, M.P.; Caffee, M.W.; Nimz, G.J.; Southon, J.R.; and Sharma, P. 1993. "Distribution of Chlorine-36 in the Unsaturated Zone at Yucca Mountain: An Indicator of Fast Transport Paths." *Proceedings of the Topical Meeting on Site Characterization and Model Validation, FOCUS '93, September 26-29, 1993, Las Vegas, Nevada.* Pages 58-68. La Grange Park, Illinois: American Nuclear Society. TIC: 102245.

Fabryka-Martin, J.T.; Wolfsberg, A.V.; Dixon, P.R.; Levy, S.; Musgrave, J.; and Turin, H.J. 1996. *Summary Report of Chlorine-36 Studies: Sampling, Analysis and Simulation of Chlorine-36 in the Exploratory Studies Facility.* Milestone 3783M. Los Alamos, New Mexico: Los Alamos National Laboratory. ACC: MOL.19970103.0047.

Fabryka-Martin, J.T.; Wolfsberg, A.V.; Levy, S.S.; Roach, J.L.; Winters, S.T.; Wolfsberg, L.E.; Elmore, D.; and Sharma, P. 1998. "Distribution of Fast Hydrologic Paths in the Unsaturated Zone at Yucca Mountain." *High-Level Radioactive Waste Management, Proceedings of the Eighth International Conference, Las Vegas, Nevada, May 11-14, 1998.* Pages 93-96. La Grange Park, Illinois: American Nuclear Society. TIC: 237082.

Faybishenko, B.; Salve, R.; Zawislanski, P.; Doughty, C.; Lee, K.H.; Cook, P.; Freifeld, B.; Jacobsen, J.; Sisson, B.; Hubbell, J.; and Dooley, K. 1998. *Ponded Infiltration Test at the Box Canyon Site, Data Report and Preliminary Analysis.* LBNL Report 40183. Berkeley, California: Lawrence Berkeley National Laboratory. ACC: MOL.19981002.0035.

Ferrill, D.A.; Winterle, J.; Wittmeyer, G.; Sims, D.; Colton, S.; Armstrong, A.; and Morris, A.P. 1999. "Stressed Rock Strains Groundwater at Yucca Mountain, Nevada." *GSA Today, 9,* (5), 1-8. Boulder, Colorado: Geological Society of America. TIC: 246229.

Fetter, C.W. 1993. *Contaminant Hydrogeology.* Upper Saddle River, New Jersey: Prentice Hall. TIC: 240691.

Finsterle, S. 2000. "Using the Continuum Approach to Model Unsaturated Flow in Fractured Rock." *Water Resources Research, 36,* (8), 2055-2066. Washington, D.C.: American Geophysical Union. TIC: 248769.

Flint, A.L.; Hevesi, J.A.; and Flint, L.E. 1996. *Conceptual and Numerical Model of Infiltration for the Yucca Mountain Area, Nevada.* Milestone 3GUI623M. Denver, Colorado: U.S. Geological Survey. ACC: MOL.19970409.0087.

Flint, L.E. 1998. *Characterization of Hydrogeologic Units Using Matrix Properties, Yucca Mountain, Nevada.* Water-Resources Investigations Report 97-4243. Denver, Colorado: U.S. Geological Survey. ACC: MOL.19980429.0512.

Flint, L.E. and Flint, A.L. 1995. *Shallow Infiltration Processes at Yucca Mountain, Nevada—Neutron Logging Data 1984-93.* Water-Resources Investigations Report 95-4035. Denver, Colorado: U.S. Geological Survey. ACC: MOL.19960924.0577.

Flynn, T.; Buchanan, P.; Trexler, D.; Shevenell, L.; and Garside, L. 1996. *Geothermal Resource Assessment of the Yucca Mountain Area, Nye County, Nevada.* BA0000000-03255-5705-00002 REV 0. Las Vegas, Nevada: University and Community College System of Nevada. ACC: MOL.19960903.0027.

Forester, R.M.; Bradbury, J.P.; Carter, C.; Elvidge-Tuma, A.B.; Hemphill, M.L.; Lundstrom, S.C.; Mahan, S.A.; Marshall, B.D.; Neymark, L.A.; Paces, J.B.; Sharpe, S.E.; Whelan, J.F.; and Wigand, P.E. 1999. *The Climatic and Hydrologic History of Southern Nevada During the Late Quaternary.* Open-File Report 98-635. Denver, Colorado: U.S. Geological Survey. TIC: 245717.

Forsyth, P.A. 1989. "A Control Volume Finite Element Method for Local Mesh Refinement." *SPE Symposium on Reservoir Simulation, Houston, Texas, February 6-8, 1989.* SPE 18415. Pages 85-96. Richardson, Texas: Society of Petroleum Engineers. TIC: 247068.

Francis, N.D. 1997. "The Base-Case Thermal Properties for TSPA-VA Modeling." Memorandum from N.D. Francis (SNL) to Distribution, April 16, 1997. ACC: MOL.19980518.0229.

Freeze, G.A.; Brodsky, N.S.; and Swift, P.N. 2001. *The Development of Information Catalogued in REV00 of the YMP FEP Database.* TDR-WIS-MD-000003 REV 00 ICN 01. Las Vegas, Nevada: Bechtel SAIC Company. ACC: MOL.20010301.0237.

French, D.E. 2000. *Hydrocarbon Assessment of the Yucca Mountain Vicinity, Nye County, Nevada.* Open-File Report 2000-2. Reno, Nevada: Nevada Bureau of Mines and Geology. ACC: MOL.20000609.0298.

Fridrich, C.J. 1999. "Tectonic Evolution of the Crater Flat Basin, Yucca Mountain Region, Nevada." Chapter 7 of *Cenozoic Basins of the Death Valley Region.* Wright, L.A. and Troxel, B.W., eds. Special Paper 333. Boulder, Colorado: Geological Society of America. TIC: 248054.

Gdowski, G.E. 1991. *Survey of Degradation Modes of Four Nickel-Chromium-Molybdenum Alloys.* UCRL-ID-108330. Livermore, California: Lawrence Livermore National Laboratory. ACC: NNA.19910521.0010.

Gdowski, G.E. 1997. *Degradation Mode Survey Candidate Titanium-Base Alloys for Yucca Mountain Project Waste Package Materials.* UCRL-ID-121191, Rev. 1. Livermore, California: Lawrence Livermore National Laboratory. ACC: MOL.19980120.0053.

Geldon, A.L.; Umari, A.M.A.; Earle, J.D.; Fahy, M.F.; Gemmell, J.M.; and Darnell, J. 1998. *Analysis of a Multiple-Well Interference Test in Miocene Tuffaceous Rocks at the C-Hole Complex, May-June 1995, Yucca Mountain, Nye County, Nevada.* Water-Resources Investigations Report 97-4166. Denver, Colorado: U.S. Geological Survey. TIC: 236724.

Geldon, A.L.; Umari, A.M.A.; Fahy, M.F.; Earle, J.D.; Gemmell, J.M.; and Darnell, J. 1997. *Results of Hydraulic and Conservative Tracer Tests in Miocene Tuffaceous Rocks at the C-Hole Complex, 1995 to 1997, Yucca Mountain, Nye County, Nevada.* Milestone SP23PM3. Las Vegas, Nevada: U.S. Geological Survey. ACC: MOL.19980122.0412.

Gelhar, L.W.; Welty, C.; and Rehfeldt, K.R. 1992. "A Critical Review of Data on Field-Scale Dispersion in Aquifers." *Water Resources Research, 28,* (7), 1955-1974. Washington, D.C.: American Geophysical Union. TIC: 235780.

Ginn, T.R. and Murphy, E.M. 1997. "A Transient Flux Model for Convective Infiltration: Forward and Inverse Solutions for Chloride Mass Balance Studies." *Water Resources Research, 33,* (9), 2065-2079. Washington, D.C.: American Geophysical Union. TIC: 247422.

Glass, R.J.; Nicholl, M.J.; and Tidwell, V.C. 1996. *Challenging and Improving Conceptual Models for Isothermal Flow in Unsaturated, Fractured Rock Through Exploration of Small-Scale Processes.* SAND95-1824. Albuquerque, New Mexico: Sandia National Laboratories. ACC: MOL.19970520.0082.

Glassley, W.E. and Christenson, B.W. 1992. "Water-Rock Interaction in New Zealand Hydrothermal Systems: Comparison of Some Simulated and Observed Geochemical Processes." *High Level Radioactive Waste Management, Proceedings of the Third International Conference, Las Vegas, Nevada, April 12-16, 1992. 1,* 352-356. La Grange Park, Illinois: American Nuclear Society. TIC: 204231.

Goodman, R.E. and Shi, G-H. 1985. *Block Theory and Its Application to Rock Engineering.* Englewood Cliffs, New Jersey: Prentice-Hall. TIC: 241514.

Griffith, G.W. 2000. "Repository Surface Design Engineering Files Letter Report–MGR Solar Power System (Revised)." Letter from G.W. Griffith (CRWMS M&O) to D. Kane (DOE/YMSCO) and K. Skipper (DOE/YMSCO), November 17, 2000, LV.SFD.GWG.11/00-074, with enclosure. ACC: MOL.20001129.0164.

Guenther, R.J.; Blahnik, D.E.; Campbell, T.K.; Jenquin, U.P.; Mendel, J.E.; Thomas, L.E.; and Thornhill, C.K. 1988. *Characterization of Spent Fuel Approved Testing Material—ATM-103.* PNL-5109-103. Richland, Washington: Pacific Northwest Laboratory. ACC: NNA.19911017.0104.

Guenther, R.J.; Blahnik, D.E.; Campbell, T.K.; Jenquin, U.P.; Mendel, J.E.; Thomas, L.E.; and Thornhill, C.K. 1991. *Characterization of Spent Fuel Approved Testing Material—ATM-105.* PNL-5109-105. Richland, Washington: Pacific Northwest Laboratory. TIC: 203785.

Guenther, R.J.; Blahnik, D.E.; Campbell, T.K.; Jenquin, U.P.; Mendel, J.E.; and Thornhill, C.K. 1988. *Characterization of Spent Fuel Approved Testing Material—ATM-106.* PNL-5109-106. Richland, Washington: Pacific Northwest Laboratory. ACC: NNA.19911017.0105.

Guenther, R.J.; Blahnik, D.E.; Jenquin, U.P.; Mendel, J.E.; Thomas, L.E.; and Thornhill, C.K. 1991. *Characterization of Spent Fuel Approved Testing Material—ATM-104.* PNL-5109-104. Richland, Washington: Pacific Northwest Laboratory. TIC: 203846.

Hardin, E.L. 1998. *Near-Field/Altered-Zone Models Report.* UCRL-ID-129179. Livermore, California: Lawrence Livermore National Laboratory. ACC: MOL.19980630.0560.

Hardin, E.L.; Barton, N.; Lingle, D.; Board, M.; and Voegele, M. 1982. *A Heated Flatjack Test Series to Measure the Thermomechanical and Transport Properties of In Situ Rock Masses ("Heated Block Test").* ONWI-260. Columbus, Ohio: Battelle Project Management Division, Office of Nuclear Waste Isolation. TIC: 232093.

Hardin, E.L. and Chesnut, D.A. 1997. *Synthesis Report on Thermally Driven Coupled Processes.* UCRL-ID-128495. Livermore, California: Lawrence Livermore National Laboratory. TIC: 234838.

Haschke, J.M.; Allen, T.H.; and Morales, L.A. 2000. "Reaction of Plutonium Dioxide with Water: Formation and Properties of PuO_{2+x}." *Science, 287,* 285-287. Washington, D.C: American Association for the Advancement of Science. TIC: 248119.

Helton, J.C.; Anderson, D.R.; Jow, H.-N.; Marietta, M.G.; and Basabilvazo, G. 1999. "Performance Assessment in Support of the 1996 Compliance Certification Application for the Waste Isolation Pilot Plant." *Risk Analysis, 19,* (5), 959-986. New York, New York: Plenum Press. TIC: 247081.

Helton, J.C.; Bean, J.E.; Berglund, J.W.; Davis, F.J.; Economy, K.; Garner, J.W.; Johnson, J.D.; MacKinnon, R.J.; Miller, J.; O'Brien, D.G.; Ramsey, J.L.; Schreiber, J.D.; Shinta, A.; Smith, L.N.; Stoelzel, D.M.; Stockman, C.; and Vaughn, P. 1998. *Uncertainty and Sensitivity Analysis Results Obtained in the 1996 Performance Assessment for the Waste Isolation Pilot Plant.* SAND98-0365. Albuquerque, New Mexico: Sandia National Laboratories. TIC: 238277.

Hevesi, J.A.; Ambos, D.S.; and Flint, A.L. 1994. "A Preliminary Characterization of the Spatial Variability of Precipitation at Yucca Mountain, Nevada." *High Level Radioactive Waste Management, Proceedings of the Fifth Annual International Conference, Las Vegas, Nevada, May 22-26, 1994. 4,* 2520-2529. La Grange Park, Illinois: American Nuclear Society. TIC: 210984.

Hill, C.A.; Dublyansky, Y.V.; Harmon, R.S.; and Schluter, C.M. 1995. "Overview of Calcite/Opal Deposits at or Near the Proposed High-Level Nuclear Waste Site, Yucca Mountain, Nevada, USA: Pedogenic, Hypogene, or Both?" *Environmental Geology, 26,* 69-88. New York, New York: Springer-Verlag. TIC: 222318.

Ho, C.K. 1997a. "Evaporation of Pendant Water Droplets in Fractures." *Water Resources Research, 33,* (12), 2665-2671. Washington, D.C.: American Geophysical Union. TIC: 246969.

Ho, C.K. 1997b. "Models of Fracture–Matrix Interactions During Multiphase Heat and Mass Flow in Unsaturated Fractured Porous Media." *Proceedings of the ASME Fluids Engineering Division, November 16–21, 1997, Dallas, Texas.* FED-Vol. 244. Pages 401-412. New York, New York: American Society of Mechanical Engineers. TIC: 241082.

Howard, C.L.; Finley, R.L.; Johnston, R.L.; Taylor, R.S.; George, J.T.; Lowry, W.E.; and Mason, N.G. 2001. *Engineered Barrier System—Pilot Scale Test #3, Heated Drip Shield Test Results.* TDR-EBS-SE-000001 REV 00. Las Vegas, Nevada: Bechtel SAIC Company. ACC: MOL.20010529.0330.

IAEA (International Atomic Energy Agency) 1998. *Waterside Corrosion of Zirconium Alloys in Nuclear Power Plants.* IAEA-TECDOC-996. Vienna, Austria: International Atomic Energy Agency. TIC: 248234.

Interagency Review Group on Nuclear Waste Management 1979. *Report to the President by the Interagency Review Group on Nuclear Waste Management.* TID-29442. Washington, D.C.: U.S. Department of Energy. ACC: MOL.19980625.0169.

Itkin, I. 2000. Request for a Study on Design and Operational Strategies for Repository Staging. Letter from I. Itkin (DOE/OCRWM) to Dr. B. Alberts (National Research Council), October 19, 2000. ACC: MOL.20001101.0060.

Jackson, C.P.; Hoch, A.R.; and Todman, S. 2000. "Self-Consistency of a Heterogeneous Continuum Porous Medium Representation of a Fractured Medium." *Water Resources Research, 36,* (1), 189-202. Washington, D.C.: American Geophysical Union. TIC: 247466.

Jarzemba, M.S.; LaPlante, P.A.; and Poor, K.J. 1997. *ASHPLUME Version 1.0—A Code for Contaminated Ash Dispersal and Deposition, Technical Description and User's Guide.* CNWRA 97-004, Rev. 1. San Antonio, Texas: Center for Nuclear Waste Regulatory Analyses. ACC: MOL.20010727.0162.

Kastenberg, W.E.; Peterson, P.F.; Ahn, J.; Burch, J.; Casher, G.; Chambre, P.L.; Greenspan, E.; Olander, D.R.; Vujic, J.L.; Bessinger, B.; Cook. N.G.W.; Doyle, F.M.; and Hilbert, L.B., Jr. 1996. "Considerations of Autocatalytic Criticality of Fissile Materials in Geologic Repositories." *Nuclear Technology, 115,* 298-308. Hinsdale, Illinois: American Nuclear Society. TIC: 247504.

Kersting, A.B.; Efurd, D.W.; Finnegan, D.L.; Rokop, D.J.; Smith, D.K.; and Thompson, J.L. 1999. "Migration of Plutonium in Ground Water at the Nevada Test Site." *Nature, 397,* (6714), 56-59. London, England: Macmillan Publishers. TIC: 243597.

Knauss, K.G. 1987. "Zeolitization of Glassy Topopah Spring Tuff Under Hydrothermal Conditions." *Scientific Basis for Nuclear Waste Management X, Symposium held December 1-4, 1986, Boston, Massachusetts.* Bates, J.K. and Seefeldt, W.B., eds. *84,* 737–745. Pittsburgh, Pennsylvania: Materials Research Society. TIC: 203663.

Knauss, K.G. and Beiriger, W.B. 1984. *Report on Static Hydrothermal Alteration Studies of Topopah Spring Tuff Wafers in J-13 Water at 150°C.* UCRL-53576. Livermore, California: Lawrence Livermore National Laboratory. ACC: HQS.19880517.2007.

Knauss, K.G.; Beiriger, W.J.; and Peifer, D.W. 1987. *Hydrothermal Interaction of Solid Wafers of Topopah Spring Tuff with J-13 Water at 90 and 150°C Using Dickson-Type, Gold-Bag Rocking Autoclaves: Long-Term Experiments.* UCRL-53722. Livermore, California: Lawrence Livermore National Laboratory. ACC: NNA.19870713.0081.

Knauss, K.G.; Delany, J.M.; Beiriger, W.J.; and Peifer, D.W. 1985. "Hydrothermal Interaction of Topopah Spring Tuff with J-13 Water as a Function of Temperature." *Scientific Basis for Nuclear Waste Management VIII, Symposium held November 26-29, 1984, Boston, Massachusetts.* Jantzen, C.M.; Stone, J.A.; and Ewing, R.C., eds. *44,* 539-546. Pittsburgh, Pennsylvania: Materials Research Society. TIC: 203665.

Knauss, K.G. and Peifer, D.W. 1986. *Reaction of Vitric Topopah Spring Tuff and J-13 Ground Water Under Hydrothermal Conditions Using Dickson-Type, Gold-Bag Rocking Autoclaves.* UCRL-53795. Livermore, California: Lawrence Livermore National Laboratory. ACC: NNA.19891102.0117.

Knauss, K.G. and Wolery, T.J. 1988. "The Dissolution Kinetics of Quartz as a Function of pH and Time at 70°C." *Geochimica et Cosmochimica Acta, 52,* (1), 43-53. New York, New York: Pergamon Press. TIC: 203242.

Kneafsey, T.J. and Pruess, K. 1997. *Preferential Flow Paths and Heat Pipes: Results from Laboratory Experiments on Heat-Driven Flow in Natural and Artificial Rock Fractures.* LBNL-40467. Berkeley, California: Lawrence Berkeley National Laboratory. ACC: MOL.19971204.0415.

Kneafsey, T.J. and Pruess, K. 1998. "Laboratory Experiments on Heat-Driven Two-Phase Flows in Natural and Artificial Rock Fractures." *Water Resources Research, 34,* (12), 3349-3367. Washington, D.C.: American Geophysical Union. TIC: 247468.

Konikow, L.F. and Ewing, R.C. 1999. "Is a Probabilistic Performance Assessment Enough?" *Ground Water, 37,* (4), 481-482. Worthington, Ohio: Water Well Journal Publishing Company. TIC: 245627.

Kotra, J.P.; Lee, M.P.; Eisenberg, N.A.; and DeWispelare, A.R. 1996. *Branch Technical Position on the Use of Expert Elicitation in the High-Level Radioactive Waste Program.* NUREG-1563. Washington, D.C.: U.S. Nuclear Regulatory Commission. TIC: 226832.

Krumhansl, J.L. and Stockman, H.W. 1988. "Site Selection Criteria and Preliminary Results from the Valles Caldera Natural Analog Study." *Proceedings of Workshop IV on Flow and Transport Through Unsaturated Fractured Rock—Related to High-Level Radioactive Waste Disposal, December 12-15, 1998, Tucson, Arizona.* Pages 249-276. Tucson, Arizona: University of Arizona. TIC: 247519.

Kwicklis, E.M. and Healy, R.W. 1993. "Numerical Investigation of Steady Liquid Water Flow in a Variably Saturated Fracture Network." *Water Resources Research, 29,* (12), 4091-4102. Washington, D.C.: American Geophysical Union. TIC: 226993.

The League of Women Voters 1993. *The Nuclear Waste Primer.* Revised Edition. Washington, D.C.: League of Women Voters Education Fund. TIC: 210697.

LeCain, G.D. 1997. *Air-Injection Testing in Vertical Boreholes in Welded and Nonwelded Tuff, Yucca Mountain, Nevada.* Water-Resources Investigations Report 96-4262. Denver, Colorado: U.S. Geological Survey. ACC: MOL.19980310.0148.

LeCain, G.D. 1998. *Results from Air-Injection and Tracer Testing in the Upper Tiva Canyon, Bow Ridge Fault, and Upper Paintbrush Contact Alcoves of the Exploratory Studies Facility, August 1994 through July 1996, Yucca Mountain, Nevada.* Water-Resources Investigations Report 98-4058. Denver, Colorado: U.S. Geological Survey. ACC: MOL.19980625.0344.

LeCain, G.D.; Anna, L.O.; and Fahy, M.F. 2000. *Results from Geothermal Logging, Air and Core-Water Chemistry Sampling, Air-Injection Testing, and Tracer Testing in the Northern Ghost Dance Fault, Yucca Mountain, Nevada, November 1996 to August 1998.* Water-Resources Investigations Report 99-4210. Denver, Colorado: U.S. Geological Survey. TIC: 247708.

Lee, K.H. and Ueng, T-S. 1991. *Air-Injection Field Tests to Determine the Effect of a Heat Cycle on the Permeability of Welded Tuff.* UCRL-ID-105163. Livermore, California: Lawrence Livermore National Laboratory. ACC: NNA.19910912.0001.

Leigh, C.D.; Thompson, B.M.; Campbell, J.E.; Longsine, D.E.; Kennedy, R.A.; and Napier, B.A. 1993. *User's Guide for GENII-S: A Code for Statistical and Deterministic Simulations of Radiation Doses to Humans from Radionuclides in the Environment.* SAND91-0561. Albuquerque, New Mexico: Sandia National Laboratories. ACC: MOL.20010721.0031.

Leslie, B.W. 1994. *An Annotated Analysis of Logic in the 1992 Report, "The Origin and History of Alteration and Carbonatization of the Yucca Mountain Ignimbrites," by J.S. Szymanski.* San Antonio, Texas: Center for Nuclear Waste Regulatory Analyses. TIC: 247428.

Leverett, M.C. 1941. "Capillary Behavior in Porous Solids." *AIME Transactions, Petroleum Development and Technology, Tulsa Meeting, October 1940. 142,* 152-169. New York, New York: American Institute of Mining and Metallurgical Engineers. TIC: 240680.

Levy, S.S. 1991. "Mineralogic Alteration History and Paleohydrology at Yucca Mountain, Nevada." *High Level Radioactive Waste Management, Proceedings of the Second Annual International Conference, Las Vegas, Nevada, April 28-May 3, 1991. 1,* 477-485. La Grange Park, Illinois: American Nuclear Society. TIC: 204272.

Lichtner, P.C.; Keating, G.; and Carey, B. 1999. *A Natural Analogue for Thermal-Hydrological-Chemical Coupled Processes at the Proposed Nuclear Waste Repository at Yucca Mountain, Nevada.* LA-13610-MS. Los Alamos, New Mexico: Los Alamos National Laboratory. TIC: 246032.

Lide, D.R., ed. 1994. *Handbook of Chemistry and Physics.* 75th Edition. Boca Raton, Florida: CRC Press. TIC: 102972.

Lippmann, M.J. and Bodvarsson, G.S. 1985. "The Heber Geothermal Field, California: Natural State and Exploitation Modeling Studies." *Journal of Geophysical Research, 90,* (B1), 745-758. Washington, D.C.: American Geophysical Union. TIC: 247477.

Liu, H.H.; Doughty, C.; and Bodvarsson, G.S. 1998. "An Active Fracture Model for Unsaturated Flow and Transport in Fractured Rocks." *Water Resources Research, 34,* (10), 2633-2646. Washington, D.C.: American Geophysical Union. TIC: 243012.

Luckey, R.R.; Tucci, P.; Faunt, C.C.; Ervin, E.M.; Steinkampf, W.C.; D'Agnese, F.A.; and Patterson, G.L. 1996. *Status of Understanding of the Saturated-Zone Ground-Water Flow System at Yucca Mountain, Nevada, as of 1995.* Water-Resources Investigations Report 96-4077. Denver, Colorado: U.S. Geological Survey. ACC: MOL.19970513.0209.

Luckner, L.; van Genuchten, M.T.; and Nielsen, D.R. 1989. "A Consistent Set of Parametric Models for the Two-Phase Flow of Immiscible Fluids in the Subsurface." *Water Resources Research, 25,* (10), 2187-2193. Washington, D.C.: American Geophysical Union. TIC: 224845.

Ludwig, K.R.; Peterman, Z.E.; Simmons, K.R.; and Gutentag, E.D. 1993. "$^{234}U/^{238}U$ as a Ground-Water Tracer, SW Nevada–SE California." *High Level Radioactive Waste Management, Proceedings of the Fourth Annual International Conference, Las Vegas, Nevada, April 26-30, 1993. 2,* 1567-1572. La Grange Park, Illinois: American Nuclear Society. TIC: 208542.

Ludwig, K.R.; Simmons, K.R.; Szabo, B.J.; Winograd, I.J.; Landwehr, J.M.; Riggs, A.C.; and Hoffman, R.J. 1992. "Mass-Spectrometric $^{230}Th–^{234}U–^{238}U$ Dating of the Devils Hole Calcite Vein." *Science, 258,* 284-287. Washington, D.C.: American Association for the Advancement of Science. TIC: 237796.

Maloszewski, P. and Zuber, A. 1985. "On the Theory of Tracer Experiments in Fissured Rocks with a Porous Matrix." *Journal of Hydrology, 79,* 333-358. Amsterdam, The Netherlands: Elsevier Science. TIC: 222390.

Mansure, A.J. and Ortiz, T.S. 1984. *Preliminary Evaluation of the Subsurface Area Available for a Potential Nuclear Waste Repository at Yucca Mountain.* SAND84-0175. Albuquerque, New Mexico: Sandia National Laboratories. ACC: NNA.19870407.0047.

Marshall, B.D.; Futa, K.; and Peterman, Z.E. 1998. "Hydrologic Inferences from Strontium Isotopes in Port [Pore] Water from the Unsaturated Zone at Yucca Mountain, Nevada." *Proceedings of FTAM: Field Testing and Associated Modeling of Potential High-Level Nuclear Waste Geologic Disposal Sites, Lawrence Berkeley National Laboratory, December 15-16, 1997.* Bodvarsson, G.S., ed. LBNL-42520. Pages 55-56. Berkeley, California: Lawrence Berkeley National Laboratory. TIC: 243019.

Marshall, B.D.; Neymark, L.A.; Paces, J.B.; Peterman, Z.E.; and Whelan, J.F. 2000. "Seepage Flux Conceptualized from Secondary Calcite in Lithophysal Cavities in the Topopah Spring Tuff, Yucca Mountain, Nevada." *SME Annual Meeting, February 28-March 1, 2000, Salt Lake City, Utah.* Preprint 00-12. Littleton, Colorado: Society for Mining, Metallurgy, and Exploration. TIC: 248608.

Marshall, B.D.; Stuckless, J.S.; Peterman, Z.E.; and Whelan, J.F. 1993. "Isotopic Studies of Cavity Filling and Fracture Coating Minerals as an Aid to Understanding Paleohydrology, Yucca Mountain, Nevada, USA." *Paleohydrogeological Methods and Their Applications, Proceedings of an NEA Workshop, Paris, France, 9-10 November 1992.* Pages 147-159. Paris, France: Organisation for Economic Co-operation and Development. TIC: 225213.

Marshall, B.D. and Whelan, J.F. 2000. "Isotope Geochemistry of Calcite Coatings and the Thermal History of the Unsaturated Zone at Yucca Mountain, Nevada." *Abstracts with Programs—Geological Society of America, 32,* (7), A-259. Boulder, Colorado: Geological Society of America. TIC: 249113.

Marshall, B.D.; Whelan, J.F.; Peterman, Z.E.; Futa, K.; Mahan, S.A.; and Stuckless, J.S. 1992. "Isotopic Studies of Fracture Coatings at Yucca Mountain, Nevada, USA." *Water–Rock Interaction, Proceedings of the 7th International Symposium on Water–Rock Interaction—WRI-7, Park City, Utah, 13-18 July, 1992.* Kharaka, Y.K. and Maest, A.S., eds. *1,* 737-740. Brookfield, Vermont: A.A. Balkema. TIC: 208527.

Martin, R.J., III; Price, R.H.; Boyd, P.J.; and Noel, J.S. 1995. *Creep in Topopah Spring Member Welded Tuff.* SAND94-2585. Albuquerque, New Mexico: Sandia National Laboratories. ACC: MOL.19950502.0006.

Matyskiela, W. 1997. "Silica Redistribution and Hydrologic Changes in Heated Fractured Tuff." *Geology, 25,* (12), 1115-1118. Boulder, Colorado: Geological Society of America. TIC: 236809.

McCarthy, J.F. and Degueldre, C. 1993. "Sampling and Characterization of Colloids and Particles in Groundwater for Studying Their Role in Contaminant Transport." Chapter 6 of *Environmental Particles.* Buffle, J. and van Leeuwen, H.P., eds. Environmental Analytical and Physical Chemistry Series, Volume 2. Boca Raton, Florida: Lewis Publishers. TIC: 245905.

McCarthy, J.F. and Zachara, J.M. 1989. "Subsurface Transport of Contaminants." *Environmental Science & Technology, 23,* (5), 496-502. Easton, Pennsylvania: American Chemical Society. TIC: 224876.

McClure, J.A. and Alsaed, A.A. 2001. *External Criticality Risk of Immobilized Plutonium Waste Form in a Geologic Repository.* TDR-EBS-MD-000019 REV 00. Las Vegas, Nevada: Bechtel SAIC Company. ACC: MOL.20010314.0001.

McConnell, K.I. and Lee, M.P. 1994. *Staff Technical Position on Consideration of Fault Displacement Hazards in Geologic Repository Design.* NUREG-1494. Washington, D.C.: U.S. Nuclear Regulatory Commission. TIC: 212360.

McCright, R.D. 1998. *Corrosion Data and Modeling Update for Viability Assessment.* Volume 3 of *Engineered Materials Characterization Report.* UCRL-ID-119564, Rev. 1.1. Livermore, California: Lawrence Livermore National Laboratory. ACC: MOL.19981222.0137.

McKelvey, V. 1976. Major Assets and Liabilities of the Nevada Test Site as a High-Level Radioactive Waste Repository. Letter from V. McKelvey (USGS) to R.W. Roberts (ERDA), July 9, 1976, with enclosure, "Table 1. Assets and Liabilities of Nevada Test Site as Potential High-Level Radioactive Waste Repository." ACC: MOL.19990119.0314.

Mercer, J.W. and Faust, C.R. 1979. "Geothermal Reservoir Simulation: 3. Application of Liquid- and Vapor-Dominated Hydrothermal Modeling Techniques to Wairakei, New Zealand." *Water Resources Research, 15,* (3), 653-671. Washington, D.C.: American Geophysical Union. TIC: 247493.

Middleman, S. 1995. *Modeling Axisymmetric Flows, Dynamics of Films, Jets, and Drops.* San Diego, California: Academic Press. TIC: 246835.

Monger, H.C. and Adams, H.P. 1996. "Micromorphology of Calcite-Silica Deposits, Yucca Mountain, Nevada." *Soil Science Society of America Journal, 60,* (2), 519-530. Madison, Wisconsin: Soil Science Society of America. TIC: 247738.

Montazer, P. and Wilson, W.E. 1984. *Conceptual Hydrologic Model of Flow in the Unsaturated Zone, Yucca Mountain, Nevada.* Water-Resources Investigations Report 84-4345. Lakewood, Colorado: U.S. Geological Survey. ACC: NNA.19890327.0051.

Moran, J.M.; Morgan, M.D.; and Pauley, P.M. 1997. *Meteorology: The Atmosphere and the Science of Weather.* 5th Edition. Upper Saddle River, New Jersey: Prentice Hall. TIC: 248773.

Morgan, M.G.; Henrion, M.; and Small, M. 1990. "The Propagation and Analysis of Uncertainty." Chapter 8 of *Uncertainty, A Guide to Dealing with Uncertainty in Quantitative Risk and Policy Analysis.* New York, New York: Cambridge University Press. TIC: 247867.

Moridis, G.J. 1999. "Semianalytical Solutions for Parameter Estimation in Diffusion Cell Experiments." *Water Resources Research, 35,* (6), 1729-1740. Washington, D.C.: American Geophysical Union. TIC: 246266.

Mowbray, G.E. 1999. Transmittal of the Naval Nuclear Propulsion Program Addendum to the Yucca Mountain Site Characterization Office "Disposal Criticality Analysis Methodology Topical Report." Letter from G.E. Mowbray (Department of the Navy) to C.W. Reamer (NRC), October 29, 1999. ACC: MOL.20000316.0531.

Mowbray, G.E. 2000. Revised Source Term Data for Naval Spent Nuclear Fuel and Special Case Waste Packages. Letter from G.E. Mowbray (Department of the Navy) to J.R. Dyer (DOE/YMSCO), September 6, 2000, with attachments. ACC: MOL.20000911.0354.

Moyer, T.C.; Geslin, J.K.; and Flint, L.E. 1996. *Stratigraphic Relations and Hydrologic Properties of the Paintbrush Tuff Nonwelded (PTn) Hydrologic Unit, Yucca Mountain, Nevada.* Open-File Report 95-397. Denver, Colorado: U.S. Geological Survey. ACC: MOL.19970204.0216.

Munson, L.H.; Herrington, W.N.; Higby, D.P.; Kathren, R.L.; Merwin, S.E.; Stoetzel, G.A.; and Vallario, E.J. 1988. *Health Physics Manual of Good Practices for Reducing Radiation Exposure to Levels that are as Low as Reasonably Achievable (ALARA)*. PNL-6577. Richland, Washington: Pacific Northwest Laboratory. TIC: 208630.

Murphy, W.M.; Pearcy, E.C.; Green, R.T.; Prikryl, J.D.; Mohanty, S.; Leslie, B.W.; and Nedungadi, A. 1998. "A Test of Long-Term, Predictive, Geochemical Transport Modeling at the Akrotiri Archaeological Site." *Journal of Contaminant Hydrology, 29,* 245-279. Amsterdam, The Netherlands: Elsevier Science. TIC: 247211.

Naples, E.M. 1999. Thermal, Shielding, and Structural Information on the Naval Spent Nuclear Fuel (SNF) Canister. Letter from E.M. Naples (Department of the Navy) to D.C. Haught (DOE/YMSCO), August 6, 1999, with enclosures. ACC: MOL.19991001.0133.

National Academy of Sciences Committee on Waste Disposal 1957. *The Disposal of Radioactive Waste on Land*. Publication 519. Washington, D.C.: National Academy of Sciences, National Research Council. TIC: 221455.

National Research Council 1990. *Rethinking High-Level Radioactive Waste Disposal, A Position Statement of the Board on Radioactive Waste Management*. Washington, D.C.: National Academy Press. TIC: 205153.

National Research Council 1992. *Ground Water at Yucca Mountain: How High Can It Rise? Final Report of the Panel on Coupled Hydrologic/Tectonic/Hydrothermal Systems at Yucca Mountain*. Washington, D.C.: National Academy Press. TIC: 204931.

National Research Council 1995. *Technical Bases for Yucca Mountain Standards*. Washington, D.C.: National Academy Press. TIC: 217588.

National Research Council 1996a. *Nuclear Wastes, Technologies for Separations and Transmutation*. Washington, D.C.: National Academy Press. TIC: 226607.

National Research Council 1996b. *Rock Fractures and Fluid Flow, Contemporary Understanding and Applications*. Washington, D.C.: National Academy Press. TIC: 235913.

Nativ, R.; Adar, E.; Dahan, O.; and Geyh, M. 1995. "Water Recharge and Solute Transport Through the Vadose Zone of Fractured Chalk Under Desert Conditions." *Water Resources Research, 31,* (2), 253-261. Washington, D.C.: American Geophysical Union. TIC: 233563.

NEA (Nuclear Energy Agency) 1991. *The International Probabilistic System Assessment Group, Background and Results, 1990*. Paris, France: Organisation for Economic Co-operation and Development, Nuclear Energy Agency. TIC: 247480.

NEA 1995. *The Environmental and Ethical Basis of Geological Disposal of Long-Lived Radioactive Wastes: A Collective Opinion of the Radioactive Waste Management Committee of the OECD Nuclear Energy Agency*. Paris, France: Organisation for Economic Co-operation and Development, Nuclear Energy Agency. TIC: 225862.

NEA 1999a. *Confidence in the Long-Term Safety of Deep Geological Repositories, Its Development and Communication.* Paris, France: Organisation for Economic Co-operation and Development, Nuclear Energy Agency. TIC: 243970.

NEA 1999b. *An International Database of Features, Events and Processes.* Paris, France: Organisation for Economic Co-operation and Development, Nuclear Energy Agency. TIC: 248820.

Nelson, P.H.; Rachiele, R.; Remer, J.S.; and Carlsson, H. 1981. *Water Inflow into Boreholes During the Stripa Heater Experiments.* LBL-12574. Berkeley, California: Lawrence Berkeley National Laboratory. TIC: 228851.

Neuman, S.P. 1990. "Universal Scaling of Hydraulic Conductivities and Dispersivities in Geologic Media." *Water Resources Research, 26,* (8), 1749-1758. Washington, D.C.: American Geophysical Union. TIC: 237977.

Nevada Bureau of Mines and Geology 1997. *The Nevada Mineral Industry 1996.* Meeuwig, D., ed. Special Publication MI-1996. Reno, Nevada: Nevada Bureau of Mines and Geology. TIC: 240403.

Neymark, L.A.; Amelin, Y.V.; Paces, J.B.; and Peterman, Z.E. 1998. "U-Pb Age Evidence for Long-Term Stability of the Unsaturated Zone at Yucca Mountain." *High-Level Radioactive Waste Management, Proceedings of the Eighth International Conference, Las Vegas, Nevada, May 11-14, 1998.* Pages 85-87. La Grange Park, Illinois: American Nuclear Society. TIC: 237082.

Neymark, L.A. and Paces, J.B. 2000. "Consequences of Slow Growth for ^{230}Th/U Dating of Quaternary Opals, Yucca Mountain, NV, USA." *Chemical Geology, 164,* 143-160. Amsterdam, The Netherlands: Elsevier Science. TIC: 246316.

Nicholl, M.J.; Glass, R.J.; and Wheatcraft, S.W. 1994. "Gravity-Driven Infiltration Instability in Initially Dry Nonhorizontal Fractures." *Water Resources Research, 30,* (9), 2533-2546. Washington, D.C.: American Geophysical Union. TIC: 243493.

Nimick, F.B. and Schwartz, B.M. 1987. *Bulk, Thermal, and Mechanical Properties of the Topopah Spring Member of the Paintbrush Tuff, Yucca Mountain, Nevada.* SAND85-0762. Albuquerque, New Mexico: Sandia National Laboratories. ACC: NNA.19871013.0012.

Nitsche, H. 1991. "Solubility Studies of Transuranium Elements for Nuclear Waste Disposal: Principles and Overview." *Radiochimica Acta, 52/53,* 3-8. München, Germany: R. Oldenbourg Verlag. TIC: 227027.

Nitsche, H.; Gatti, R.C.; Standifer, E.M.; Lee, S.C.; Müller, A.; Prussin, T.; Deinhammer, R.S.; Maurer, H.; Becraft, K.; Leung, S.; and Carpenter, S.A. 1993. *Measured Solubilities and Speciations of Neptunium, Plutonium, and Americium in a Typical Groundwater (J-13) from the Yucca Mountain Region.* LA-12562-MS. Los Alamos, New Mexico: Los Alamos National Laboratory. ACC: NNA.19930507.0136.

NRC (U.S. Nuclear Regulatory Commission) 1987. *Standard Review Plan for the Review of Safety Analysis Reports for Nuclear Power Plants.* NUREG-0800. LWR Edition. Washington, D.C.: U.S. Nuclear Regulatory Commission. TIC: 203894.

NRC 1996. *Human-System Interface Design Review Guideline.* NUREG-0700, Rev. 1. Three volumes. Washington, D.C.: U.S. Nuclear Regulatory Commission. TIC: 246624; 246668; 247803.

NRC 1997. *Standard Review Plan for Dry Cask Storage Systems.* NUREG-1536. Washington, D.C.: U.S. Nuclear Regulatory Commission. ACC: MOL.20010724.0307.

NRC 1999a. *Issue Resolution Status Report Key Technical Issue: Container Life and Source Term.* Rev. 2. Washington, D.C.: U.S. Nuclear Regulatory Commission. TIC: 245538.

NRC 1999b. *Issue Resolution Status Report Key Technical Issue: Unsaturated and Saturated Flow Under Isothermal Conditions.* Rev. 2. Washington, D.C.: U.S. Nuclear Regulatory Commission. ACC: MOL.19990810.0641.

NRC 2000a. *Standard Review Plan for Spent Fuel Dry Storage Facilities.* NUREG-1567. Washington, D.C.: U.S. Nuclear Regulatory Commission. TIC: 247929.

NRC 2000b. "ISG-11—Storage of High Burnup Spent Fuel." Interim Staff Guidance–11. Washington, D.C.: U.S. Nuclear Regulatory Commission. Accessed March 21, 2000. TIC: 247227. http://www.nrc.gov/OPA/reports/isg11.htm

NRC 2000c. *Issue Resolution Status Report Key Technical Issue: Total System Performance Assessment and Integration.* Rev. 3. Washington, D.C.: U.S. Nuclear Regulatory Commission. TIC: 249045.

NWTRB (Nuclear Waste Technical Review Board) 1998. *Report to the U.S. Congress and the U.S. Secretary of Energy, November 1998.* Arlington, Virginia: U.S. Nuclear Waste Technical Review Board. ACC: MOV.19981201.0015.

NWTRB 1999a. *Report to the U.S. Congress and the Secretary of Energy, January to December 1998.* Arlington, Virginia: U.S. Nuclear Waste Technical Review Board. ACC: HQO.19990706.0007.

NWTRB 1999b. *Moving Beyond the Yucca Mountain Viability Assessment, A Report to the U.S. Congress and the Secretary of Energy.* Arlington, Virginia: U.S. Nuclear Waste Technical Review Board. TIC: 243860.

NWTRB 2000. *Report to the U.S. Congress and the Secretary of Energy, January to December 1999.* Arlington, Virginia: U.S. Nuclear Waste Technical Review Board. TIC: 247806.

Olsson, W.A. and Brown, S.R. 1994. *Mechanical Properties of Seven Fractures from Drillholes NRG-4 and NRG-6 at Yucca Mountain, Nevada.* SAND94-1995. Albuquerque, New Mexico: Sandia National Laboratories. ACC: MOL.19941007.0081.

Oversby, V.M. 1984a. *Reaction of the Topopah Spring Tuff with J-13 Water at 120°C.* UCRL-53574. Livermore, California: Lawrence Livermore National Laboratory. ACC: NNA.19890905.0227.

Oversby, V.M. 1984b. *Reaction of the Topopah Spring Tuff with J-13 Well Water at 90°C and 150°C.* UCRL-53552. Livermore, California: Lawrence Livermore National Laboratory. ACC: NNA.19890905.0226.

Oversby, V.M. 1985. *The Reaction of Topopah Spring Tuff with J-13 Water at 150°C—Samples from Drill Cores USW G-1, USW GU-3, USW G-4, and UE-25h#1.* UCRL-53629. Livermore, California: Lawrence Livermore National Laboratory. ACC: NNA.19890905.0229.

Paces, J.B.; Ludwig, K.R.; Peterman, Z.E.; Neymark, L.A.; and Kenneally, J.M. 1998. "Anomalous Ground-Water ^{234}U/^{238}U Beneath Yucca Mountain: Evidence of Local Recharge?" *High-Level Radioactive Waste Management, Proceedings of the Eighth International Conference, Las Vegas, Nevada, May 11-14, 1998.* Pages 185-188. La Grange Park, Illinois: American Nuclear Society. TIC: 237082.

Paces, J.B.; Mahan, S.A.; Ludwig, K.R.; Kwak, L.M.; Neymark, L.A.; Simmons, K.R.; Nealey, L.D.; Marshall, B.D.; and Walker, A. 1995. *Progress Report on Dating Quaternary Surficial Deposits.* Milestone 3GCH510M. Final Draft. Denver, Colorado: U.S. Geological Survey. ACC: MOL.19960611.0220.

Paces, J.B.; Neymark, L.A.; Marshall, B.D.; Whelan, J.F.; and Peterman, Z.E. 1996. *Letter Report: Ages and Origins of Subsurface Secondary Minerals in the Exploratory Studies Facility (ESF).* Milestone 3GQH450M, Results of Sampling and Age Determination. Las Vegas, Nevada: U.S. Geological Survey. ACC: MOL.19970324.0052.

Paces, J.B.; Neymark, L.A.; Marshall, B.D.; Whelan, J.F.; and Peterman, Z.E. 1998. "Inferences for Yucca Mountain Unsaturated-Zone Hydrology from Secondary Minerals." *High-Level Radioactive Waste Management, Proceedings of the Eighth International Conference, Las Vegas, Nevada, May 11-14, 1998.* Pages 36-39. La Grange Park, Illinois: American Nuclear Society. TIC: 237082.

Paces, J.B.; Neymark, L.A.; Persing, H.M.; and Wooden, J.L. 2000. "Demonstrating Slow Growth Rates in Opal from Yucca Mountain, Nevada, Using Microdigestion and Ion-Probe Uranium-Series Dating." *Abstracts with Programs—Geological Society of America, 32,* (7), A-259. Boulder, Colorado: Geological Society of America. TIC: 249113.

Paces, J.B. and Whelan, J.F. 2001. "Water-Table Fluctuations in the Amargosa Desert, Nye County, Nevada." *"Back to the Future—Managing the Back End of the Nuclear Fuel Cycle to Create a More Secure Energy Future," Proceedings of the 9th International High-Level Radioactive Waste Management Conference (IHLRWM), Las Vegas, Nevada, April 29-May 3, 2001.* La Grange Park, Illinois: American Nuclear Society. TIC: 247873.

Paces, J.B.; Whelan, J.F.; Peterman, Z.E.; Marshall, B.D.; and Neymark, L.A. 2000. "Formation of Calcite and Silica from Percolation in a Hydrologically Unsaturated Setting, Yucca Mountain, Nevada." *Abstracts with Programs—Geological Society of America, 32,* (7), A-259. Boulder, Colorado: Geological Society of America. TIC: 249113.

Paperiello, C.J. 1995. "Review of Potential for Underground Autocatalytic Criticality." Letter from C.J. Paperiello (NRC) to L. Barrett (DOE/OCRWM), August 7, 1995, with enclosure. ACC: HQO.19950912.0002.

Paperiello, C.J. 1999. "U.S. Nuclear Regulatory Commission Staff Review of the U.S. Department of Energy Viability Assessment for a High-Level Radioactive Waste Repository at Yucca Mountain, Nevada." Letter from C.J. Paperiello (NRC) to L.H. Barrett (DOE), June 2, 1999, with enclosures, "U.S. Nuclear Regulatory Commission's Staff Evaluation of U.S. Department of Energy's Viability Assessment" and Letter from B.J. Garrick (NRC Advisory Committee on Nuclear Waste) to S.A. Jackson (NRC), dated April 8, 1999. ACC: HQO.19990811.0007; HQO.19990811.0008.

Parks, C.V. 1992. "Overview of ORIGEN2 and ORIGEN-S: Capabilities and Limitations." *High Level Radioactive Waste Management, Proceedings of the Third International Conference, Las Vegas, Nevada, April 12-16, 1992. 1,* 57-64. La Grange Park, Illinois: American Nuclear Society. TIC: 204231.

Parrington, J.R.; Knox, H.D.; Breneman, S.L.; Baum, E.M.; and Feiner, F. 1996. *Nuclides and Isotopes, Chart of the Nuclides.* 15th Edition. San Jose, California: General Electric Company and KAPL, Inc. TIC: 233705.

Peterman, Z.E. and Stuckless, J.S. 1993. "Isotopic Evidence of Complex Ground-Water Flow at Yucca Mountain, Nevada, USA." *High Level Radioactive Waste Management, Proceedings of the Fourth Annual International Conference, Las Vegas, Nevada, April 26-30, 1993. 2,* 1559-1566. La Grange Park, Illinois: American Nuclear Society. TIC: 208542.

Peters, R.R.; Klavetter, E.A.; Hall, I.J.; Blair, S.C.; Heller, P.R.; and Gee, G.W. 1984. *Fracture and Matrix Hydrologic Characteristics of Tuffaceous Materials from Yucca Mountain, Nye County, Nevada.* SAND84-1471. Albuquerque, New Mexico: Sandia National Laboratories. ACC: NNA.19900810.0674.

Philip, J.R.; Knight, J.H.; and Waechter, R.T. 1989. "Unsaturated Seepage and Subterranean Holes: Conspectus, and Exclusion Problem for Circular Cylindrical Cavities." *Water Resources Research, 25,* (1), 16-28. Washington, D.C.: American Geophysical Union. TIC: 239117.

Potter, C.J.; Dickerson, R.P.; and Day, W.C. 1999. *Nature and Continuity of the Sundance Fault.* Open-File Report 98-266. Denver, Colorado: U.S. Geological Survey. TIC: 246609.

Powers, D.W.; Rudnicki, J.W.; and Smith, L. 1991. *External Review Panel Majority Report, A Review of "Conceptual Considerations of the Yucca Mountain Groundwater System with Special Emphasis on the Adequacy of this System to Accommodate a High-Level Nuclear Waste Repository" dated July 26, 1989 by Jerry S. Szymanski.* Washington, D.C.: U.S. Department of Energy. ACC: NNA.19911210.0056.

Pruess, K. 1987. *TOUGH User's Guide.* NUREG/CR-4645. Washington, D.C.: U.S. Nuclear Regulatory Commission. TIC: 217275.

Pruess, K. 1991. *TOUGH2—A General-Purpose Numerical Simulator for Multiphase Fluid and Heat Flow.* LBL-29400. Berkeley, California: Lawrence Berkeley Laboratory. ACC: NNA.19940202.0088.

Pruess, K. 1997. "On Vaporizing Water Flow in Hot Sub-Vertical Rock Fractures." *Transport in Porous Media, 28,* (3), 335-372. Boston, Massachusetts: Kluwer Academic Publishers. TIC: 238922.

Pruess, K.; Tsang, Y.W.; and Wang, J.S.Y. 1984. *Numerical Studies of Fluid and Heat Flow Near High-Level Nuclear Waste Packages Emplaced in Partially Saturated Fractured Tuff.* LBL-18552. Berkeley, California: Lawrence Berkeley Laboratory. TIC: 211033.

Pruess, K.; Wang, J.S.Y.; and Tsang, Y.W. 1990. "On Thermohydrologic Conditions Near High-Level Nuclear Wastes Emplaced in Partially Saturated Fractured Tuffs: 1. Simulation Studies with Explicit Consideration of Fracture Effects." *Water Resources Research, 26,* (6), 1235-1248. Washington, D.C.: American Geophysical Union. TIC: 221923.

Quade, J.; Mifflin, M.D.; Pratt, W.L.; McCoy, W.; and Burckle, L. 1995. "Fossil Spring Deposits in the Southern Great Basin and Their Implications for Changes in Water-Table Levels Near Yucca Mountain, Nevada, During Quaternary Time." *Geological Society of America Bulletin, 107,* (2), 213-230. Boulder, Colorado: Geological Society of America. TIC: 234256.

Quiring, R.F. 1968. *Climatological Data Nevada Test Site and Nuclear Rocket Development Station.* ESSA Research Laboratories Technical Memorandum–ARL 7. Las Vegas, Nevada: U.S. Department of Commerce, Environmental Science Services Administration Research Laboratories. ACC: NNA.19870406.0047.

Ramirez, A.L.; Carlson, R.C.; and Buscheck, T.A. 1991. *In Situ Changes in the Moisture Content of Heated, Welded Tuff Based on Thermal Neutron Measurements.* UCRL-ID-104715. Livermore, California: Lawrence Livermore National Laboratory. ACC: NNA.19910701.0097.

Ramsdell, J.V. and Andrews, G.L. 1986. *Tornado Climatology of the Contiguous United States.* NUREG/CR-4461. Washington, D.C.: U.S. Nuclear Regulatory Commission. ACC: MOL.20010727.0159.

Reamer, C.W. 1999. "Issue Resolution Status Report (Key Technical Issue: Igneous Activity, Revision 2)." Letter from C.W. Reamer (NRC) to S. Brocoum (DOE/YMSCO), July 16, 1999, with enclosure. ACC: MOL.19990810.0639.

Reamer, C.W. 2000. "Safety Evaluation Report for Disposal Criticality Analysis Methodology Topical Report, Revision 0." Letter from C.W. Reamer (NRC) to S.J. Brocoum (DOE/YMSCO), June 26, 2000, with enclosure. ACC: MOL.20000919.0157.

Rechard, R.P. 1999. "Historical Relationship Between Performance Assessment for Radioactive Waste Disposal and Other Types of Risk Assessment." *Risk Analysis, 19,* (5), 763-807. New York, New York: Plenum Press. TIC: 246972.

Reed, M.H. 1982. "Calculation of Multicomponent Chemical Equilibria and Reaction Processes in Systems Involving Minerals, Gases and an Aqueous Phase." *Geochimica et Cosmochimica Acta, 46,* (4), 513-528. New York, New York: Pergamon Press. TIC: 224159.

Reimus, P.W.; Adams, A.; Haga, M.J.; Humphrey, A.; Callahan, T.; Anghel, I.; and Counce, D. 1999. *Results and Interpretation of Hydraulic and Tracer Testing in the Prow Pass Tuff at the C-Holes.* Milestone SP32E7M4. Los Alamos, New Mexico: Los Alamos National Laboratory. TIC: 246377.

Richards, L.A. 1931. "Capillary Conduction of Liquids Through Porous Media." *Physics, 1,* 318-333. New York, New York: American Physical Society. TIC: 225383.

Rimstidt, J.D. and Barnes, H.L. 1980. "The Kinetics of Silica–Water Reactions." *Geochimica et Cosmochimica Acta, 44,* 1683-1699. New York, New York: Pergamon Press. TIC: 219975.

Rojstaczer, S. 1998. Review of "Geohydrological Models and Earthquake Effects at Yucca Mountain, Nevada" and "Analysis of High-Pressure Fluid Flow in Fractures with Application to Yucca Mountain, Nevada, Slug Test Data" by Davies and Archambeau. Letter from S. Rojstaczer (Duke University) to L. Reiter (NWTRB), June 15, 1998, with enclosures. ACC: MOL.19980821.0228.

Rojstaczer, S. 1999. "Stress Dependent Permeability and Its Political Consequences at Yucca Mountain." *Eos, Transactions (Supplement), 80,* (17), S4. Washington, D.C.: American Geophysical Union. TIC: 246513.

Rojstaczer, S. and Wolf, S. 1992. "Permeability Changes Associated with Large Earthquakes: An Example from Loma Prieta, California." *Geology, 20,* (3), 211-214. Boulder, Colorado: Geological Society of America. TIC: 243627.

Roseboom, E.H., Jr. 1983. *Disposal of High-Level Nuclear Waste Above the Water Table in Arid Regions.* Geological Survey Circular 903. Denver, Colorado: U.S. Geological Survey. TIC: 216597.

Ross, B. 1987. *A First Survey of Disruption Scenarios for a High-Level-Waste Repository at Yucca Mountain, Nevada.* SAND85-7117. Albuquerque, New Mexico: Sandia National Laboratories. ACC: MOL.19991116.0414.

Rousseau, J.P.; Kwicklis, E.M.; and Gillies, D.C., eds. 1999. *Hydrogeology of the Unsaturated Zone, North Ramp Area of the Exploratory Studies Facility, Yucca Mountain, Nevada.* Water-Resources Investigations Report 98-4050. Denver, Colorado: U.S. Geological Survey. ACC: MOL.19990419.0335.

Rousseau, J.P.; Loskot, C.L.; Thamir, F.; and Lu, N. 1997. *Results of Borehole Monitoring in the Unsaturated Zone Within the Main Drift Area of the Exploratory Studies Facility, Yucca Mountain, Nevada.* Milestone SPH22M3. Denver, Colorado: U.S. Geological Survey. ACC: MOL.19970626.0351.

Russell, C.E.; Hess, J.W.; and Tyler, S.W. 1987. "Hydrogeologic Investigations of Flow in Fractured Tuffs, Rainier Mesa, Nevada Test Site." *Flow and Transport Through Unsaturated Fractured Rock.* Evans, D.D. and Nicholson, T.J., eds. AGU Geophysical Monograph 42. Pages 43-50. Washington, D.C.: American Geophysical Union. TIC: 247649.

Sammel, E.A.; Ingebritsen, S.E.; and Mariner, R.H. 1988. "The Hydrothermal System at Newberry Volcano, Oregon." *Journal of Geophysical Research, 93,* (B9), 10149-10162. Washington, D.C.: American Geophysical Union. TIC: 247523.

Savino, J.M.; Smith, K.D.; Biasi, G.; Sullivan, T.; and Cline, M. 1999. "Earthquake Ground Motion Effects on Underground Structures/Tunnels." *Eos, Transactions (Supplement), 80,* (17), S10. Washington, D.C.: American Geophysical Union. TIC: 247757.

Sawyer, D.A.; Fleck, R.J.; Lanphere, M.A.; Warren, R.G.; Broxton, D.E.; and Hudson, M.R. 1994. "Episodic Caldera Volcanism in the Miocene Southwestern Nevada Volcanic Field: Revised Stratigraphic Framework, ^{40}Ar/^{39}Ar Geochronology, and Implications for Magmatism and Extension." *Geological Society of America Bulletin, 106,* (10), 1304-1318. Boulder, Colorado: Geological Society of America. TIC: 222523.

Scott, R.B. and Bonk, J. 1984. *Preliminary Geologic Map of Yucca Mountain, Nye County, Nevada, with Geologic Sections.* Open-File Report 84-494. Denver, Colorado: U.S. Geological Survey. ACC: HQS.19880517.1443.

Sharp, J.M., Jr.; Kreisel, I.; Milliken, K.L.; Mace, R.E.; and Robinson, N.I. 1996. "Fracture Skin Properties and Effects on Solute Transport: Geotechnical and Environmental Implications." *Rock Mechanics, Tools and Techniques, Proceedings of the 2nd North American Rock Mechanics Symposium, NARMS '96, A Regional Conference of ISRM, Montreal, Quebec, Canada, 19-21 June 1996.* Aubertin, M.; Hassani, F.; and Mitri, H., eds. *2,* 1329-1335. Brookfield, Vermont: A.A. Balkema. TIC: 239941.

Simmons, A.M. and Bodvarsson, G.S. 1997. *Building Confidence in Thermohydrologic Models of Yucca Mountain Using Geothermal Analogues.* Milestone SPLE1M4. Berkeley, California: Lawrence Berkeley National Laboratory. ACC: MOL.19970710.0328.

Simonds, F.W.; Whitney, J.W.; Fox, K.F.; Ramelli, A.R.; Yount, J.C.; Carr, M.D.; Menges, C.M.; Dickerson, R.P.; and Scott, R.B. 1995. *Map Showing Fault Activity in the Yucca Mountain Area, Nye County, Nevada.* Miscellaneous Investigations Series Map I-2520. Denver, Colorado: U.S. Geological Survey. TIC: 232483.

Slider, H.C. 1976. *Practical Petroleum Reservoir Engineering Methods, An Energy Conservation Science.* Tulsa, Oklahoma: Petroleum Publishing Company. TIC: 247798.

Smellie, J. 1995. "The Fossil Nuclear Reactors of Oklo, Gabon." *Radwaste Magazine, 2,* (2), 18-20, 22-27. La Grange Park, Illinois: American Nuclear Society. TIC: 238322.

SNL (Sandia National Laboratories) 1987. *Site Characterization Plan Conceptual Design Report.* SAND84-2641. Six volumes. Albuquerque, New Mexico: Sandia National Laboratories. ACC: NN1.19880902.0014; NN1.19880902.0015; NN1.19880902.0016; NN1.19880902.0017; NN1.19880902.0018; NN1.19880902.0019.

SNL 1996. *Thermal Properties of Test Specimens from the Single Heater Test Area in the Thermal Testing Facility at Yucca Mountain, Nevada.* Albuquerque, New Mexico: Sandia National Laboratories. ACC: MOL.19961029.0115.

SNL 1998. *Drift Scale Test Status Report #1: Evaluation and Comparative Analysis of the Drift Scale Test Thermal and Thermomechanical Data (Results of 12/3/1997 through 5/31/1998).* Albuquerque, New Mexico: Sandia National Laboratories. ACC: MOL.19980908.0435.

Sonnenthal, E.L. and Bodvarsson, G.S. 1999. "Constraints on the Hydrology of the Unsaturated Zone at Yucca Mountain, NV from Three-Dimensional Models of Chloride and Strontium Geochemistry." *Journal of Contaminant Hydrology, 38,* (1-3), 107-156. New York, New York: Elsevier Science. TIC: 244160.

Spaulding, W.G. 1985. *Vegetation and Climates of the Last 45,000 Years in the Vicinity of the Nevada Test Site, South-Central Nevada.* Professional Paper 1329. Washington, D.C.: U.S. Geological Survey. TIC: 203210.

Spengler, R.W.; Braun, C.A.; Martin, L.G.; and Weisenberg, C.W. 1994. *The Sundance Fault: A Newly Recognized Shear Zone at Yucca Mountain, Nevada.* Open-File Report 94-49. Denver, Colorado: U.S. Geological Survey. ACC: NNA.19940128.0119.

Steefel, C.I. and Lasaga, A.C. 1994. "A Coupled Model for Transport of Multiple Chemical Species and Kinetic Precipitation/Dissolution Reactions with Application to Reactive Flow in Single Phase Hydrothermal Systems." *American Journal of Science, 294,* (5), 529-592. New Haven, Connecticut: Kline Geology Laboratory, Yale University. TIC: 235372.

Steefel, C.I. and Lichtner, P.C. 1998. "Multicomponent Reactive Transport in Discrete Fractures: I. Controls on Reaction Front Geometry." *Journal of Hydrology, 209,* 186-199. New York, New York: Elsevier Science. TIC: 247524.

Stephans, R.A. and Talso, W.W. 1997. *System Safety Analysis Handbook.* 2nd Edition. Albuquerque, New Mexico: System Safety Society. TIC: 236411.

Stewart, A. 1997. "Risk Estimation for Badge-Monitored Radiation Workers." *Environmental Health Perspectives, 105,* (Supplement 6), 1603-1606. Research Triangle Park, North Carolina: National Institute of Environmental Health Sciences. TIC: 248399.

Stockman, H.; Krumhansl, J.; Ho, C.; and McConnell, V. 1994. *The Valles Natural Analogue Project.* NUREG/CR-6221. Washington, D.C.: U.S. Nuclear Regulatory Commission. TIC: 246123.

Stroupe, E.P. 2000. "Approach to Implementing the Site Recommendation Design Baseline." Interoffice correspondence from E.P. Stroupe (CRWMS M&O) to D.R. Wilkins, January 26, 2000, LV.RSO.EPS.1/00-004, with attachment. ACC: MOL.20000214.0480.

Stuckless, J.S. 2000. *Archaeological Analogues for Assessing the Long-Term Performance of a Mined Geologic Repository for High-Level Radioactive Waste.* Open-File Report 00-181. Denver, Colorado: U.S. Geological Survey. ACC: MOL.20000822.0366.

Stuckless, J.S.; Marshall, B.D.; Vaniman, D.T.; Dudley, W.W.; Peterman, Z.E.; Paces, J.B.; Whelan, J.F.; Taylor, E.M.; Forester, R.M.; and O'Leary, D.W. 1998. "Comments on 'Overview of Calcite/Opal Deposits at or Near the Proposed High-Level Nuclear Waste Site, Yucca Mountain, Nevada, USA: Pedogenic, Hypogene, or Both' by C.A. Hill, Y.V. Dublansky, R.S. Harmon, and C.M. Schluter." *Environmental Geology, 34,* (1), 70-78. New York, New York: Springer-Verlag. TIC: 238097.

Stuckless, J.S.; Peterman, Z.E.; Forester, R.M.; Whelan, J.F.; Vaniman, D.T.; Marshall, B.D.; and Taylor, E.M. 1992. "Characterization of Fault-Filling Deposits in the Vicinity of Yucca Mountain, Nevada." *Waste Management '92, "Working Towards a Cleaner Environment," Proceedings of the Symposium on Waste Management at Tucson, Arizona, March 1-5, 1992.* Post, R.G., ed. *1,* 929-935. Tucson, Arizona: University of Arizona. TIC: 205094.

Sudicky, E.A. and Frind, E.O. 1981. "Carbon 14 Dating of Groundwater in Confined Aquifers: Implications of Aquitard Diffusion." *Water Resources Research, 17,* (4), 1060-1064. Washington, D.C.: American Geophysical Union. TIC: 247712.

Suzuki, T. 1983. "A Theoretical Model for Dispersion of Tephra." *Arc Volcanism: Physics and Tectonics, Proceedings of a 1981 IAVCEI Symposium, August-September, 1981, Tokyo and Hakone.* Shimozuru, D. and Yokoyama, I., eds. Pages 95-113. Tokyo, Japan: Terra Scientific Publishing Company. TIC: 238307.

Sweetkind, D.S.; Barr, D.L.; Polacsek, D.K.; and Anna, L.O. 1997. *Administrative Report: Integrated Fracture Data in Support of Process Models, Yucca Mountain, Nevada.* Milestone SPG32M3. Las Vegas, Nevada: U.S. Geological Survey. ACC: MOL.19971017.0726.

Szymanski, J.S. 1987. *Conceptual Considerations of the Death Valley Groundwater System with Special Emphasis on the Adequacy of this System to Accommodate the High-Level Nuclear Waste Repository.* Draft. Las Vegas, Nevada: U.S. Department of Energy, Nevada Operations Office. ACC: NN1.19881122.0086.

Szymanski, J.S. 1989. *Conceptual Considerations of the Yucca Mountain Groundwater System with Special Emphasis on the Adequacy of This System to Accommodate a High-Level Nuclear Waste Repository.* Three volumes. Las Vegas, Nevada: U.S. Department of Energy, Nevada Operations Office. ACC: NNA.19890831.0152.

Taylor, E.M. and Huckins, H.E. 1986. "Carbonate and Opaline Silica Fault-Filling on the Bow Ridge Fault, Yucca Mountain, Nevada—Deposition from Pedogenic Processes or Upwelling Ground Water?" *Abstracts with Programs—Geological Society of America, 18,* (5), 418. Boulder, Colorado: Geological Society of America. TIC: 217522.

Taylor, E.M. and Huckins, H.E. 1995. *Lithology, Fault Displacement, and Origin of Secondary Calcium Carbonate and Opaline Silica at Trenches 14 and 14D on the Bow Ridge Fault at Exile Hill, Nye County, Nevada.* Open-File Report 93-477. Denver, Colorado: U.S. Geological Survey. ACC: MOL.19940906.0001.

Thoma, S.G.; Gallegos, D.P.; and Smith, D.M. 1992. "Impact of Fracture Coatings on Fracture/Matrix Flow Interactions in Unsaturated, Porous Media." *Water Resources Research, 28,* (5), 1357-1367. Washington, D.C.: American Geophysical Union. TIC: 237509.

Thompson, B.G.J. 1999. "The Role of Performance Assessment in the Regulation of Underground Disposal of Radioactive Wastes: An International Perspective." *Risk Analysis, 19,* (5), 809-846. New York, New York: Plenum Press. TIC: 247145.

Thordarson, W. 1965. *Perched Ground Water in Zeolitized-Bedded Tuff, Rainier Mesa and Vicinity, Nevada Test Site, Nevada.* TEI-862. Washington, D.C.: U.S. Geological Survey. ACC: NN1.19881021.0066.

Tombacz, E.; Abraham, I.; Gilde, M.; and Szanto, F. 1990. "The pH-Dependent Colloidal Stability of Aqueous Montmorillonite Suspensions." *Colloids and Surfaces, 49,* 71-80. Amsterdam, The Netherlands: Elsevier Science. TIC: 246046.

Tompson, A.F.B. and Gelhar, L.W. 1990. "Numerical Simulation of Solute Transport in Three-Dimensional, Randomly Heterogeneous Porous Media." *Water Resources Research, 26,* (10), 2541-2562. Washington, D.C.: American Geophysical Union. TIC: 224902.

Trewartha, G.T. and Horn, L.H. 1980. *An Introduction to Climate.* 5th Edition. New York, New York: McGraw-Hill. Readily available.

Triay, I.R.; Degueldre, C.; Wistrom, A.O.; Cotter, C.R.; and Lemons, W.W. 1996. *Progress Report on Colloid-Facilitated Transport at Yucca Mountain.* LA-12959-MS. Los Alamos, New Mexico: Los Alamos National Laboratory. TIC: 225473.

Triay, I.R.; Meijer, A.; Conca, J.L.; Kung, K.S.; Rundberg, R.S.; Strietelmeier, B.A.; and Tait, C.D. 1997. *Summary and Synthesis Report on Radionuclide Retardation for the Yucca Mountain Site Characterization Project.* Eckhardt, R.C., ed. LA-13262-MS. Los Alamos, New Mexico: Los Alamos National Laboratory. ACC: MOL.19971210.0177.

Troeh, F.R.; Hobbs, J.A.; and Donahue, R.L. 1980. *Soil and Water Conservation for Productivity and Environmental Protection.* Englewood Cliffs, New Jersey: Prentice-Hall. TIC: 246612.

Tsang, Y.W. and Birkholzer, J.T. 1999. "Predictions and Observations of the Thermal-Hydrological Conditions in the Single Heater Test." *Journal of Contaminant Hydrology, 38,* (1-3), 385-425. New York, New York: Elsevier Science. TIC: 244160.

Tucci, P. and Burkhardt, D.J. 1995. *Potentiometric-Surface Map, 1993, Yucca Mountain and Vicinity, Nevada.* Water-Resources Investigations Report 95-4149. Denver, Colorado: U.S. Geological Survey. ACC: MOL.19960924.0517.

Turcotte, D.L. and Schubert, G. 1982. *Geodynamics, Applications of Continuum Physics to Geological Problems.* New York, New York: John Wiley & Sons. TIC: 235924.

USGS (U.S. Geological Survey) 2000a. *Future Climate Analysis.* ANL-NBS-GS-000008 REV 00. Denver, Colorado: U.S. Geological Survey. ACC: MOL.20000629.0907.

USGS 2000b. *Simulation of Net Infiltration for Modern and Potential Future Climates.* ANL-NBS-HS-000032 REV 00. Denver, Colorado: U.S. Geological Survey. ACC: MOL.20000801.0004.

USGS 2000c. *Water-Level Data Analysis for the Saturated Zone Site-Scale Flow and Transport Model.* ANL-NBS-HS-000034 REV 00. Denver, Colorado: U.S. Geological Survey. ACC: MOL.20000830.0340.

USGS 2000d. *Hydrogeologic Framework Model for the Saturated-Zone Site-Scale Flow and Transport Model.* ANL-NBS-HS-000033 REV 00. Denver, Colorado: U.S. Geological Survey. ACC: MOL.20000802.0010.

van Genuchten, M.T. 1980. "A Closed-Form Equation for Predicting the Hydraulic Conductivity of Unsaturated Soils." *Soil Science Society of America Journal, 44,* (5), 892-898. Madison, Wisconsin: Soil Science Society of America. TIC: 217327.

Van Kampen, N.G. 1984. *Stochastic Processes in Physics and Chemistry.* New York, New York: North-Holland. TIC: 248058.

Vaniman, D.T.; Bish, D.L.; and Chipera, S. 1988. *A Preliminary Comparison of Mineral Deposits in Faults Near Yucca Mountain, Nevada, with Possible Analogs.* LA-11289-MS. Los Alamos, New Mexico: Los Alamos National Laboratory. ACC: HQS.19880517.3205.

Vaniman, D.T.; Carey, J.W.; Bish, D.L.; and Chipera, S.J. 1999. "Cation Profiles Generated by Downward Transport Into Unsaturated Zeolitic Strata at Yucca Mountain, Nevada." *Eos, Transactions (Supplement), 80,* (17), S5. Washington, D.C.: American Geophysical Union. TIC: 246464.

Vaniman, D.T.; Chipera, S.J.; and Bish, D.L. 1994. "Pedogenesis of Siliceous Calcretes at Yucca Mountain, Nevada." *Geoderma, 63,* 1-17. Amsterdam, The Netherlands: Elsevier Science. TIC: 212060.

Villar, E.; Bonet, A.; Diaz-Caneja, B.; Fernandez, P.L.; Gutierrez, I.; Quindos, L.S.; Solana, J.R.; and Soto, J. 1985. "Natural Evolution of Percolation Water in Altamira Cave." *Cave Science, 12,* (1), 21-24. Bridgwater, United Kingdom: British Cave Research Association. TIC: 247713.

Viswanathan, H.S.; Robinson, B.A.; Valocchi, A.J.; and Triay, I.R. 1998. "A Reactive Transport Model of Neptunium Migration from the Potential Repository at Yucca Mountain." *Journal of Hydrology, 209,* 251-280. Amsterdam, The Netherlands: Elsevier Science. TIC: 243441.

Walker, J.S. 2000. *A Short History of Nuclear Regulation, 1946-1999.* NUREG/BR-0175, Rev. 1. Washington, D.C.: U.S. Nuclear Regulatory Commission. TIC: 246687.

Wang, J.S.Y.; Cook, N.G.W.; Wollenberg, H.A.; Carnahan, C.L.; Javandel, I.; and Tsang, C.F. 1993. "Geohydrologic Data and Models of Rainier Mesa and Their Implications to Yucca Mountain." *High Level Radioactive Waste Management, Proceedings of the Fourth Annual International Conference, Las Vegas, Nevada, April 26-30, 1993. 1,* 675-681. La Grange Park, Illinois: American Nuclear Society. TIC: 208542.

Wang, J.S.Y. and Elsworth, D. 1999. "Permeability Changes Induced by Excavation in Fractured Tuff." *Rock Mechanics for Industry, Proceedings of the 37th U.S. Rock Mechanics Symposium, Vail, Colorado, USA, 6-9 June, 1999.* Amadei, B.; Kranz, R.L.; Scott, G.A.; and Smeallie, P.H., eds. *2,* 751–757. Brookfield, Vermont: A.A. Balkema. TIC: 245246.

Wang, J.S.Y. and Narasimhan, T.N. 1993. "Unsaturated Flow in Fractured Porous Media." Chapter 7 of *Flow and Contaminant Transport in Fractured Rocks.* Bear, J.; Tsang, C-F.; and de Marsily, G., eds. San Diego, California: Academic Press. TIC: 235461.

Wang, J.S.Y.; Trautz, R.C.; Cook, P.J.; Finsterle, S.; James, A.L.; and Birkholzer, J. 1999. "Field Tests and Model Analyses of Seepage into Drift." *Journal of Contaminant Hydrology, 38*, (1-3), 323-347. New York, New York: Elsevier Science. TIC: 244160.

Warburton, P.M. 1981. "Vector Stability Analysis of an Arbitrary Polyhedral Rock Block with Any Number of Free Faces." *International Journal of Rock Mechanics and Mining Sciences & Geomechanics Abstracts, 18*, (5), 415-427. New York, New York: Pergamon Press. TIC: 241134.

Wells, S.G.; McFadden, L.D.; Renault, C.E.; and Crowe, B.M. 1990. "Geomorphic Assessment of Late Quaternary Volcanism in the Yucca Mountain Area, Southern Nevada: Implications for the Proposed High-Level Radioactive Waste Repository." *Geology, 18,* 549-553. Boulder, Colorado: Geological Society of America. TIC: 218564.

Wescott, R.G.; Lee, M.P.; Eisenberg, N.A.; McCartin, T.J.; and Baca, R.G., eds. 1995. *NRC Iterative Performance Assessment Phase 2, Development of Capabilities for Review of a Performance Assessment for a High-Level Waste Repository.* NUREG-1464. Washington, D.C.: U.S. Nuclear Regulatory Commission. ACC: MOL.19960710.0075.

Whelan, J.F. and Moscati, R.J. 1998. "9 M.Y. Record of Southern Nevada Climate from Yucca Mountain Secondary Minerals." *High-Level Radioactive Waste Management, Proceedings of the Eighth International Conference, Las Vegas, Nevada, May 11-14, 1998.* Pages 12-15. La Grange Park, Illinois: American Nuclear Society. TIC: 237082.

Whelan, J.F.; Roedder, E.; and Paces, J.B. 2001. "Evidence for an Unsaturated-Zone Origin of Secondary Minerals in Yucca Mountain, Nevada." *"Back to the Future - Managing the Back End of the Nuclear Fuel Cycle to Create a More Secure Energy Future," Proceedings of the 9th International High-Level Radioactive Waste Management Conference (IHLRWM), Las Vegas, Nevada, April 29-May 3, 2001.* La Grange Park, Illinois: American Nuclear Society. TIC: 247873.

Whelan, J.F.; Roedder, E.W.; Paces, J.B.; Neymark, L.A.; Marshall, B.D.; Peterman, Z.E.; and Moscati, R.J. 2000. "Calcite Fluid Inclusion, Paragenetic, and Oxygen Isotopic Records of Thermal Event(s) at Yucca Mountain Nevada." *Abstracts with Programs—Geological Society of America, 32,* (7), A-259. Boulder, Colorado: Geological Society of America. TIC: 249113.

Wildenschild, D. and Roberts, J. 1999. *Experimental Tests of Enhancement of Vapor Diffusion in Topopah Spring Tuff.* UCRL-JC-134850. Livermore, California: Lawrence Livermore National Laboratory. TIC: 246923.

Wilder, D.G., ed. 1996. *Volume II: Near-Field and Altered-Zone Environment Report.* UCRL-LR-124998. Livermore, California: Lawrence Livermore National Laboratory. ACC: MOL.19961212.0121; MOL.19961212.0122.

Wilder, D.G. and Yow, J.L., Jr. 1987. *Geomechanics of the Spent Fuel Test—Climax.* UCRL-53767. Livermore, California: Lawrence Livermore National Laboratory. ACC: NNA.19900110.0337.

Wilder, D.G.; Lin, W.; Blair, S.C.; Buscheck, T.; Carlson, R.C.; Lee, K.; Meike, A.; Ramirez, A.L.; Wagoner, J.L.; and Wang, J. 1997. *Large Block Test Status Report.* UCRL-ID-128776. Livermore, California: Lawrence Livermore National Laboratory. ACC: MOL.19980508.0727.

Wilkins, D.R. and Heath, C.A. 1999. "Direction to Transition to Enhanced Design Alternative II." Letter from D.R. Wilkins (CRWMS M&O) and C.A. Heath (CRWMS M&O) to Distribution, June 15, 1999, LV.NS.JLY.06/99-026, with enclosures, "Strategy for Baselining EDA II Requirements" and "Guidelines for Implementation of EDA II." ACC: MOL.19990622.0126; MOL.19990622.0127; MOL.19990622.0128.

Williams, N.H. 2001a. "Contract No. DE-AC08-01RW12101—Total System Performance Assessment—Analyses for Disposal of Commercial and DOE Waste Inventories at Yucca Mountain—Input to Final Environmental Impact Statement and Site Suitability Evaluation REV 00 ICN 02." Letter from N.H. Williams (BSC) to J.R. Summerson (DOE/YMSCO), December 11, 2001, RWA:cs-1204010670, with enclosure. ACC: MOL.20011213.0056.

Williams, N.H. 2001b. "Contract No. DE-AC08-01RW12101—Total System Performance Assessment Sensitivity Analyses for Final Nuclear Regulatory Commission Regulations, Rev 00 ICN 01." Letter from N.H. Williams (BSC) to S.J. Brocoum (DOE/YMSCO), December 11, 2001, RWA:cs-1204010669, with enclosure. ACC: MOL.20011213.0057.

Wilson, L. and Head, J.W., III 1981. "Ascent and Eruption of Basaltic Magma on the Earth and Moon." *Journal of Geophysical Research, 86,* (B4), 2971-3001. Washington, D.C.: American Geophysical Union. TIC: 225185.

Wilson, M.L.; Gauthier, J.H.; Barnard, R.W.; Barr, G.E.; Dockery, H.A.; Dunn, E.; Eaton, R.R.; Guerin, D.C.; Lu, N.; Martinez, M.J.; Nilson, R.; Rautman, C.A.; Robey, T.H.; Ross, B.; Ryder, E.E.; Schenker, A.R.; Shannon, S.A.; Skinner, L.H.; Halsey, W.G.; Gansemer, J.D.; Lewis, L.C.; Lamont, A.D.; Triay, I.R.; Meijer, A.; and Morris, D.E. 1994. *Total-System Performance Assessment for Yucca Mountain—SNL Second Iteration (TSPA–1993).* SAND93-2675. Executive Summary and two volumes. Albuquerque, New Mexico: Sandia National Laboratories. ACC: NNA.19940112.0123.

Wilson, N.S.F.; Cline, J.S.; and Amelin, Y.V. 2001. "Fluid Inclusion Microthermometry and U-Pb Dating Constraints to Fluid Movement through the Potential Yucca Mountain Nuclear Waste Repository." Preliminary Programs and Abstracts, Eleventh Annual V.M. Goldschmidt Conference, May 20-24, 2001, Hot Springs, Virginia, USA. Houston, Texas: Lunar and Planetary Institute. Accessed April 3, 2001. TIC: 249671.
http://www.lpi.usra.edu/meetings/gold2001/pdf/3724.pdf

Wilson, N.S.F.; Cline, J.S.; Rotert, J.; and Amelin, Y.V. 2000. "Timing and Temperature of Fluid Movement at Yucca Mountain, NV: Fluid Inclusion Analyses and U-Pb and U-Series Dating." *Abstracts with Programs—Geological Society of America, 32,* (7), A-260. Boulder, Colorado: Geological Society of America. TIC: 249113.

Winograd, I.J. 1981. "Radioactive Waste Disposal in Thick Unsaturated Zones." *Science, 212,* (4502), 1457-1464. Washington, D.C.: American Association for the Advancement of Science. TIC: 217258.

Winograd, I.J. 1986. *Archaeology and Public Perception of a Transscientific Problem—Disposal of Toxic Wastes in the Unsaturated Zone.* Circular 990. Denver, Colorado: U.S. Geological Survey. TIC: 237946.

Winograd, I.J.; Coplen, T.B.; Landwehr, J.M.; Riggs, A.C.; Ludwig, K.R.; Szabo, B.J.; Kolesar, P.T.; and Revesz, K.M. 1992. "Continuous 500,000-Year Climate Record from Vein Calcite in Devils Hole, Nevada." *Science, 258,* 255-260. Washington, D.C.: American Association for the Advancement of Science. TIC: 237563.

Winograd, I.J. and Thordarson, W. 1975. *Hydrogeologic and Hydrochemical Framework, South-Central Great Basin, Nevada–California, with Special Reference to the Nevada Test Site.* Geological Survey Professional Paper 712-C. Washington, [D.C.]: United States Government Printing Office. ACC: NNA.19870406.0201.

Winterle, J.R. and La Femina, P.C. 1999. *Review and Analysis of Hydraulic and Tracer Testing at the C-Holes Complex Near Yucca Mountain, Nevada.* San Antonio, Texas: Center for Nuclear Waste Regulatory Analyses. TIC: 246623.

WoldeGabriel, G.; Keating, G.N.; and Valentine, G.A. 1999. "Effects of Shallow Basaltic Intrusion into Pyroclastic Deposits, Grants Ridge, New Mexico, USA." *Journal of Volcanology and Geothermal Research, 92,* 389-411. New York, New York: Elsevier Science. TIC: 246037.

Wollenberg, H.A. and Flexser, S. 1986. "Contact Zones and Hydrothermal Systems as Analogues to Repository Conditions." *Chemical Geology, 55,* 345-359. Amsterdam, The Netherlands: Elsevier Science. TIC: 246171.

Wong, I.G. and Stepp, C. 1998. *Probabilistic Seismic Hazard Analyses for Fault Displacement and Vibratory Ground Motion at Yucca Mountain, Nevada.* Milestone SP32IM3, September 23, 1998. Three volumes. Oakland, California: U.S. Geological Survey. ACC: MOL.19981207.0393.

Wruck, D.A. and Palmer, C.E.A. 1997. *Status Update on the Analysis of Elevated Temperature Data for Thermodynamic Properties of Selected Radionuclides.* Milestone SPL4B1M4. Livermore, California: Lawrence Livermore National Laboratory. ACC: MOL.19971210.0037.

Yang, I.C. and Peterman, Z.E. 1999. "Chemistry and Isotopic Content of Perched Water." In *Hydrogeology of the Unsaturated Zone, North Ramp Area of the Exploratory Studies Facility, Yucca Mountain, Nevada.* Rousseau, J.P.; Kwicklis, E.M.; and Gillies, D.C., eds. Water-Resources Investigations Report 98-4050. Denver, Colorado: U.S. Geological Survey. ACC: MOL.19990419.0335.

Yang, I.C.; Rattray, G.W.; and Yu, P. 1996. *Interpretation of Chemical and Isotopic Data from Boreholes in the Unsaturated Zone at Yucca Mountain, Nevada.* Water-Resources Investigations Report 96-4058. Denver, Colorado: U.S. Geological Survey. ACC: MOL.19980528.0216.

Yang, I.C.; Yu, P.; Rattray, G.W.; Ferarese, J.S.; and Ryan, J.N. 1998. *Hydrochemical Investigations in Characterizing the Unsaturated Zone at Yucca Mountain, Nevada.* Water-Resources Investigations Report 98-4132. Denver, Colorado: U.S. Geological Survey. ACC: MOL.19981012.0790.

Yau, T.L. and Webster, R.T. 1987. "Corrosion of Zirconium and Hafnium." In *Corrosion,* Volume 13, pages 707-721 of *ASM Handbook.* Formerly 9th Edition, Metals Handbook. Materials Park, Ohio: ASM International. TIC: 240704.

YMP (Yucca Mountain Site Characterization Project) 1997. *Preclosure Seismic Design Methodology for a Geologic Repository at Yucca Mountain.* Topical Report YMP/TR-003-NP, Rev. 2. Las Vegas, Nevada: Yucca Mountain Site Characterization Office. ACC: MOL.19971009.0412.

YMP 1998. *Disposal Criticality Analysis Methodology Topical Report.* YMP/TR-004Q, Rev. 0. Las Vegas, Nevada: Yucca Mountain Site Characterization Office. ACC: MOL.19990210.0236.

YMP 2000a. *Monitored Geologic Repository Requirements Document.* YMP/CM-0025, Rev. 3, DCN 02. Las Vegas, Nevada: Yucca Mountain Site Characterization Office. ACC: MOL.20000720.0540.

YMP 2000b. *Q-List.* YMP/90-55Q, Rev. 6. Las Vegas, Nevada: Yucca Mountain Site Characterization Office. ACC: MOL.20000510.0177.

YMP 2000c. *Disposal Criticality Analysis Methodology Topical Report.* YMP/TR-004Q, Rev. 01. Las Vegas, Nevada: Yucca Mountain Site Characterization Office. ACC: MOL.20001214.0001.

Zimmerman, R.M.; Blanford, M.L.; Holland, J.F.; Schuch, R.L.; and Barrett, W.H. 1986. *Final Report, G-Tunnel Small-Diameter Heater Experiments.* SAND84-2621. Albuquerque, New Mexico: Sandia National Laboratories. ACC: HQS.19880517.2365.

Zimmerman, R.M. and Finley, R.E. 1987. *Summary of Geomechanical Measurements Taken in and Around the G-Tunnel Underground Facility, NTS.* SAND86-1015. Albuquerque, New Mexico: Sandia National Laboratories. ACC: NNA.19870526.0015.

Zyvoloski, G.A.; Robinson, B.A.; Dash, Z.V.; and Trease, L.L. 1997a. *Summary of the Models and Methods for the FEHM Application—A Finite Element Heat- and Mass-Transfer Code.* LA-13307-MS. Los Alamos, New Mexico: Los Alamos National Laboratory. TIC: 235587.

Zyvoloski, G.A.; Robinson, B.A.; Dash, Z.V.; and Trease, L.L. 1997b. *User's Manual for the FEHM Application—A Finite-Element Heat- and Mass-Transfer Code.* LA-13306-M. Los Alamos, New Mexico: Los Alamos National Laboratory. TIC: 235999.

6.2   CODES, STANDARDS, REGULATIONS, AND PROCEDURES

10 CFR 20. Energy: Standards for Protection Against Radiation. Readily available.

10 CFR 71. Energy: Packaging and Transportation of Radioactive Material. Readily available.

10 CFR 73. Energy: Physical Protection of Plants and Materials. Readily available.

10 CFR 835. Energy: Occupational Radiation Protection. Readily available.

10 CFR 960. Energy: General Guidelines for the Recommendation of Sites for Nuclear Waste Repositories. Readily available.

40 CFR 197. Protection of Environment: Public Health and Environmental Radiation Protection Standards for Yucca Mountain, Nevada. Readily available.

49 FR 34658. Waste Confidence Decision, 10 CFR Parts 50 and 51. TIC: 249471

55 FR 38474. Waste Confidence Decision Review, 10 CFR Part 51. TIC: 249472.

64 FR 8640. Disposal of High-Level Radioactive Wastes in a Proposed Geologic Repository at Yucca Mountain, Nevada. Proposed rule 10 CFR Part 63. Readily available.

64 FR 46976. Environmental Radiation Protection Standards for Yucca Mountain, Nevada. Proposed rule 40 CFR Part 197. Readily available.

64 FR 68005. Waste Confidence Decision Review: Status, 10 CFR Part 51. TIC: 249473.

65 FR 1608. Record of Decision for the Surplus Plutonium Disposition Final Environmental Impact Statement. TIC: 248241.

66 FR 32074. 40 CFR Part 197, Public Health and Environmental Radiation Protection Standards for Yucca Mountain, NV; Final Rule. Readily available.

66 FR 55732. Disposal of High-Level Radioactive Wastes in a Proposed Geologic Repository at Yucca Mountain, NV. Final Rule 10 CFR Part 63. Readily available.

ANSI/ANS-2.8-1992. *American National Standard for Determining Design Basis Flooding at Power Reactor Sites.* La Grange Park, Illinois: American Nuclear Society. TIC: 236034.

ANSI/ANS-57.7-1988. *American National Standard Design Criteria for an Independent Spent Fuel Storage Installation (Water Pool Type).* Revision of ANSI/ANS-57.7-1981. La Grange Park, Illinois: American Nuclear Society. TIC: 238870.

ANSI N13.8-1973. *American National Standard Radiation Protection in Uranium Mines.* New York, New York: American National Standards Institute. TIC: 208902.

ASCE 7-98. 2000. *Minimum Design Loads for Buildings and Other Structures.* Revision of ANSI/ASCE 7-95. Reston, Virginia: American Society of Civil Engineers. TIC: 247427.

ASTM A 276-91a. 1991. *Standard Specification for Stainless and Heat-Resisting Steel Bars and Shapes.* Philadelphia, Pennsylvania: American Society for Testing and Materials. TIC: 240022.

ASTM B 575-97. 1998. *Standard Specification for Low-Carbon Nickel-Molybdenum-Chromium, Low-Carbon Nickel-Chromium-Molybdenum, Low-Carbon Nickel-Chromium-Molybdenum-Copper and Low-Carbon Nickel-Chromium-Molybdenum-Tungsten Alloy Plate, Sheet, and Strip.* West Conshohocken, Pennsylvania: American Society for Testing and Materials. TIC: 241816.

ASTM C 1174-97. 1998. *Standard Practice for Prediction of the Long-Term Behavior of Materials, Including Waste Forms, Used in Engineered Barrier Systems (EBS) for Geological Disposal of High-Level Radioactive Waste.* West Conshohocken, Pennsylvania: American Society for Testing and Materials. TIC: 246015.

ASTM C 1220-98. 1998. *Standard Test Method for Static Leaching of Monolithic Waste Forms for Disposal of Radioactive Waste.* West Conshohocken, Pennsylvania: American Society for Testing and Materials. TIC: 247005.

ASTM G 1-90 (Reapproved 1999). 1990. *Standard Practice for Preparing, Cleaning, and Evaluating Corrosion Test Specimens.* West Conshohocken, Pennsylvania: American Society for Testing and Materials. TIC: 238771.

ASTM G 30-94. 1994. *Standard Practice for Making and Using U-Bend Stress-Corrosion Test Specimens.* Philadelphia, Pennsylvania: American Society for Testing and Materials. TIC: 246890.

ASTM G 46-94 (Reapproved 1999). 1994. *Standard Guide for Examination and Evaluation of Pitting Corrosion.* West Conshohocken, Pennsylvania: American Society for Testing and Materials. TIC: 247941.

ASTM G 61-86 (Reapproved 1998). 1987. *Standard Test Method for Conducting Cyclic Potentiodynamic Polarization Measurements for Localized Corrosion Susceptibility of Iron-, Nickel-, or Cobalt-Based Alloys.* West Conshohocken, Pennsylvania: American Society for Testing and Materials. TIC: 246716.

Atomic Energy Act of 1954. 42 U.S.C. 2011 et seq. Readily available.

Department of Energy Organization Act. 42 U.S.C. 7101 et seq. Readily available.

Emergency Planning and Community Right-to-Know Act of 1986. 42 U.S.C. 11001 et seq. Readily available.

Energy Policy Act of 1992. Public Law No. 102-486. 106 Stat. 2776. Readily available.

Energy Reorganization Act of 1974. 42 U.S.C. 5801 et seq. Readily available.

National Environmental Policy Act of 1969. 42 U.S.C. 4321-4347. Readily available.

Nuclear Waste Policy Act of 1982. 42 U.S.C. 10101 et seq. Readily available.

Nuclear Waste Policy Act of 1982. Public Law No. 97-425. 96 Stat. 2201. Readily available.

Nuclear Waste Policy Amendments Act of 1987. Public Law No. 100-203. 101 Stat. 1330. Readily available.

Public Service Co. of Colorado v. Batt, No. 91-0035 (U.S. District Court for the District of Idaho). Filed October 17, 1995. Consent order incorporating settlement agreement. TIC: 240346.

QAP-2-3, Rev. 10. *Classification of Permanent Items.* Las Vegas, Nevada: CRWMS M&O. ACC: MOL.19990316.0006.

Regulatory Guide 1.13, Rev. 1. 1975. *Spent Fuel Storage Facility Design Basis.* Washington, D.C.: U.S. Nuclear Regulatory Commission. Readily available.

Regulatory Guide 1.29, Rev. 3. 1978. *Seismic Design Classification.* Washington, D.C.: U.S. Nuclear Regulatory Commission. Readily available.

Regulatory Guide 1.32, Rev. 2. 1977. *Criteria for Safety-Related Electric Power Systems for Nuclear Power Plants.* Washington, D.C.: U.S. Nuclear Regulatory Commission. Readily available.

Regulatory Guide 1.59, Rev. 2. 1977. *Design Basis Floods for Nuclear Power Plants.* Washington, D.C.: U.S. Nuclear Regulatory Commission. Readily available.

Regulatory Guide 1.60, Rev. 1. 1973. *Design Response Spectra for Seismic Design of Nuclear Power Plants.* Washington, D.C.: U.S. Nuclear Regulatory Commission. TIC: 232770.

Regulatory Guide 1.61. 1973. *Damping Values for Seismic Design of Nuclear Power Plants.* Washington, D.C.: U.S. Nuclear Regulatory Commission. Readily available.

Regulatory Guide 1.76, Rev. 0. 1974. *Design Basis Tornado for Nuclear Power Plants.* Washington, D.C.: U.S. Nuclear Regulatory Commission. TIC: 2717.

Regulatory Guide 1.92, Rev. 1. 1976. *Combining Modal Responses and Spatial Components in Seismic Response Analysis.* Washington, D.C.: U.S. Nuclear Regulatory Commission. TIC: 2775.

Regulatory Guide 1.102, Rev. 1. 1976. *Flood Protection for Nuclear Power Plants.* Washington, D.C.: U.S. Nuclear Regulatory Commission. Readily available.

Regulatory Guide 1.117, Rev. 1. 1978. *Tornado Design Classification.* Washington, D.C.: U.S. Nuclear Regulatory Commission. Readily available.

Regulatory Guide 1.122, Rev. 1. 1978. *Development of Floor Design Response Spectra for Seismic Design of Floor-Supported Equipment or Components.* Washington, D.C.: U.S. Nuclear Regulatory Commission. TIC: 2787.

Regulatory Guide 1.165. 1997. *Identification and Characterization of Seismic Sources and Determination of Safe Shutdown Earthquake Ground Motion.* Washington, D.C.: U.S. Nuclear Regulatory Commission. Readily available.

Regulatory Guide 3.49. 1981. *Design of an Independent Spent Fuel Storage Installation (Water-Basin Type).* Washington, D.C.: U.S. Nuclear Regulatory Commission. Readily available.

Regulatory Guide 8.8, Rev. 3. 1978. *Information Relevant to Ensuring that Occupational Radiation Exposures at Nuclear Power Stations will be as Low as is Reasonably Achievable.* Washington, D.C.: U.S. Nuclear Regulatory Commission. Readily available.

Resource Conservation and Recovery Act of 1976. 42 U.S.C. 6901 et seq. Readily available.

GLOSSARY

3DEC. A heat transfer and distinct element stress-analysis software code used to simulate thermal-mechanical behavior of a rock mass.

ablation. The process of removing by cutting, erosion, melting, evaporation, or vaporization.

abstracted model. Model that reproduces, or bounds, the essential elements of a more detailed process model and captures uncertainty and variability in what is often, but not always, a simplified or idealized form. *See* abstraction.

abstraction. The essential components of a process model that are extracted for use in a total system performance assessment. The abstraction retains the basic intrinsic form of the process model but does not usually require its original complexity.

access main. Horizontal drift that provides access to waste emplacement drifts. *Also*, main drift.

accessible environment. Any point outside of the controlled area, including: (1) the atmosphere (including the atmosphere above the surface area of the controlled area), (2) land surfaces, (3) surface waters, (4) oceans, and (5) the lithosphere.

actinide. Any element of the actinide series, a series of chemically similar, mostly synthetic, radioactive elements with atomic numbers from 89 (actinium) through 103 (lawrencium).

acute dose. The maximum radiation dose that an individual at the site boundary is expected to receive over a relatively short period (e.g., two hours).

adsorb. To collect a gas, liquid, or dissolved substance on a surface.

adsorption. Transfer of solute mass, such as radionuclides, in groundwater to the solid geologic surfaces with which it comes in contact. The term *sorption* is sometimes used interchangeably with this term.

advection. The process in which solutes are transported by groundwater movement.

ALARA (as low as is reasonably achievable). A process that applies a graded approach to reducing dose levels to workers and the public, and releases of radioactive materials to the environment. The goal of this process is not merely to reduce doses to levels specified by regulations, but to reduce them to levels that are as low as reasonably achievable.

alcove. A small excavation (room) off a main drift. Used for scientific study or for installing equipment.

alkaline. (1) Of, relating to, containing, or having the basic chemical properties of an alkali or alkali metal. (2) Having a pH of more than 7. *See* pH.

Alloy 22. A high-nickel alloy used for the outer barrier of the waste package.

alluvium. Sedimentary material (clay, mud, sand, silt, gravel) deposited by a stream or running water.

alpha particle. A positively charged particle ejected spontaneously from the nuclei of some radioactive elements. It is identical to a helium nucleus and has a mass number of 4 and an electrostatic charge of +2. It has low penetrating power and a short range (a few centimeters in air). *See* ionizing radiation.

ambient. Undisturbed, natural conditions such as ambient temperature caused by climate or natural subsurface thermal gradients.

analogue. Natural or man-made systems that include processes similar to those that could occur in a repository system at Yucca Mountain for which information can be obtained to evaluate long-term (e.g., millennia) or large-scale (e.g., kilometers) behavior.

anion. An atom or group of atoms having a negative charge; a negatively charged ion.

anisotropy. The condition in which physical properties vary when measured in different directions or along different axes. For example, in a layered rock section the permeability is often anisotropic in the vertical direction (from layer to layer) but is isotropic in the horizontal direction (within a layer). *See* isotropy.

annealing. Alternately heating and cooling a metal, alloy, or glass to relieve internal stresses in the material.

annual committed effective dose equivalent. A radiation protection term for the effective dose equivalent received by an individual in one year from radiation sources external to the individual plus committed effective dose equivalent.

ANSYS. A finite element code used in thermal and structural dynamic analyses (e.g., ground support design, performance confirmation, engineered barrier components).

aquifer. A subsurface formation or group of formations that is saturated and sufficiently permeable to transmit quantities of water to wells or springs.

areal mass loading. Used in thermal loading calculations, the amount of heavy metal (usually expressed in metric tons of uranium or equivalent) emplaced per unit area in the repository.

arid. Of a climate: very dry; a region in which annual precipitation is less than approximately 250 mm (10 in.). On average, Yucca Mountain receives about 190 mm (7.5 in.) of rain and snow annually.

ash. Fine or very fine pyroclastic particles, less than 4 mm (0.15 in.) in diameter, that are blown out from a volcanic explosion.

ash-fall tuff. Highly-porous volcanic rock that is a result of magma thrown high into the atmosphere, where it cooled and fell back to earth as a blanket of ash.

ash-flow tuff. Dense, nonporous volcanic rock that is a result of magma flowing at ground level where it remained at a high temperature for a long time, welding magma and ash together.

ASHPLUME. A computer software code used to simulate the ash plume that results from an extrusive volcanic event.

asperity. Roughness or irregularity of surface along the boundary between the walls of faults, joints, or fractures.

assembly transfer system. System in the Waste Handling Building to transfer uncanistered spent nuclear fuel assemblies from the shipping casks to disposal containers.

autocatalytic criticality. A transient criticality in which the usual mechanisms that tend to shut down a criticality are delayed until a high fission rate is achieved.

backfill. The general fill that is placed in the excavated areas of the underground facility. If used, the backfill for the repository may be tuff or other material.

background radiation. Radiation arising from natural radioactive material always present in the environment, including solar and cosmic radiation, radon gas, soil and rocks, food, and the human body.

barrier. Any material, structure, or feature that prevents or substantially reduces the rate of movement of water or radionuclides.

base case. The sequence of anticipated conditions expected to occur in and around the potential repository, without the inclusion of unlikely or unanticipated features, events, or processes. The components that contribute to the base case model are intended to encompass this probable behavior of the repository, based on the range of uncertainty for the various parameters and conceptual models used in constructing the base case.

base case. Design that addresses a nuclear waste storage capacity of 70,000 MTHM (63,000 MTHM commercial spent nuclear fuel and 7,000 MTHM DOE high-level radioactive waste). *Also*, statutory case.

binning. (1) A project-specific term that refers to the process of prioritizing systems, structures, and components based on their importance to radiological safety as well as regulatory or design precedent. (2) In computer modeling of a system, a process of averaging relevant variables over a typical subset of the system, while preserving variability. Used in the TSPA; for example, binning provides multiscale model results for waste package temperature, relative humidity at the waste package surface, and the percolation flux in the host rock 5 m (16 ft) above the emplacement drift.

bioaccumulation. Means by which a living organism could ingest, inhale, or otherwise internally accumulate a foreign substance such as a radioactive particle.

biosphere. The ecosystem of the earth and the living organisms inhabiting it.

biosphere dose conversion factor. A multiplier used in converting a radionuclide concentration at the geosphere/biosphere interface into a dose that a human would experience for all pathways considered, with units expressed in terms of annual dose (i.e., the total effective dose equivalent) per unit concentration.

block-bounding fault. A normal fault that divides the crust into structural or fault blocks of different elevations and orientations; typical of the Basin and Range province.

boiling-water reactor. A nuclear power reactor in which water passing as coolant through the core is turned to steam by direct use of fission heat from the uranium oxide fuel; steam for driving the turbogenerator is formed within the reactor vessel itself rather than in an external heat exchanger and, after being condensed, returns as feedwater to the reactor vessel.

bomb-pulse. A detectable increase in radionuclide concentration related to global fallout from above-ground thermonuclear tests.

borehole. A hole drilled for purposes of collecting site characterization data or for supplying water. Sometimes referred to as a drillhole or well bore.

borosilicate glass. A material used to vitrify high-level radioactive waste in which boron takes the place of the lime used in ordinary glass mixtures.

boundary condition. For a model, the establishment of a set condition (set value), often at the geometric edge of the model, for a given variable; for example, using a specified groundwater flux from infiltration as a boundary condition for a flow model.

bounding. For a mathematical model, relating to a set condition (set value) that is considered to reflect the reasonable extreme for that value in the real-world condition being modeled. *See* boundary condition, bounding value.

bounding value. Specific data point that defines the reasonable extreme limit of a variable in an experiment or model.

breakthrough. The time at which the concentration of a substance, usually in groundwater, arrives at a particular point of interest.

breakthrough curve. The curve describing the rate of arrival of radionuclides transmitted through a medium. The breakthrough curve calculation includes the effects of all flow modes, flow in rock matrix, flow in fractures, and retardation and determines the expected proportion of the radionuclide mass transmitted through the medium as a function of time.

bridge crane. A large overhead crane used for material handling that spans across rails on either side of a structure.

Brownian motion. Random movement of small particles suspended in a fluid. Caused by pressure fluctuations over the surfaces of the particles as they interact with the fluid's molecules.

buoyant convection. Fluid movement, typically in the gas phase, in response to a density gradient. An example is the rising of air when it becomes less dense because of heating followed by its subsequent fall when it cools and becomes denser.

burnup. A measure of nuclear-reactor fuel consumption expressed either as the percentage of fuel atoms that have undergone fission or as the amount of energy produced per initial unit weight of fuel.

burnup credit. A factor used in criticality calculations that accounts for the amount of burnup in certain fuel types. As burnup increases, the capability of the nuclear fuel to support criticality decreases. *See* burnup.

caldera. A large basin-shaped volcanic depression, more or less circular, resulting from the collapse of the ground surface following a rapid volcanic eruption. A caldera may be more than 15 km (9 mi) in diameter and more than 1,000 m (3,300 ft) deep.

calibration. (1) In modeling, the process of comparing the conditions, processes, and parameter values used in a model against actual data points or interpolations from measurements at or close to the site to ensure that the model is compatible with "reality" to the extent feasible. (2) For tools used for field or lab measurements, the process of taking instrument readings on standards known to produce a certain response to check the accuracy and precision of the instrument.

canister. The structure surrounding some forms of waste (e.g., high-level radioactive waste immobilized in glass logs or ceramic disks within cans) that facilitates handling, storage, transportation, and/or disposal.

capillary barrier. A contact in the unsaturated zone between a geologic unit containing relatively small-diameter openings and a unit containing relatively large-diameter openings. Water does not flow from the former to the latter due to capillary forces.

capillary force. A phenomenon that results from the force of molecular attraction (adhesion) between a fluid and different solid materials; this force that causes water to rise in small diameter tubes and, in combination with the effects of gravity, is a means of water movement in the unsaturated zone.

capillary pressure. The pressure due to capillary forces; i.e., the pressure of fluids under the influence of surface tension and adhesion.

Carrier Preparation Building. Surface facility where waste transportation casks and their carriers are prepared before they enter the Waste Handling Building.

carrier/cask handling system. System in the Waste Handling Building that unloads the casks from the carriers and transfers the casks to either the assembly transfer system or the canister transfer system. The system also receives empty casks from the assembly and canister transfer systems and nondispos-

able canister overpacks from the assembly transfer system and loads them onto carriers for transfer to the Carrier Preparation Building.

cask. A large, shielded container for shipping or storing spent nuclear fuel and/or high-level radioactive waste that meets all applicable regulatory requirements.

cation. An atom or group of atoms having a positive charge; a positively charged ion.

chronic dose. Of a radiation dose, the annual exposure to an individual living at the site boundary and continuously exposed to an averaged level of exposure over a long period of time.

cinder cone. A conical hill formed by the accumulation of cinders and other pyroclasts around a volcanic vent.

cladding. The metallic outer sheath of a fuel rod element generally made of a zirconium alloy. It is intended to isolate the fuel element from the external environment.

clay. A rock or mineral fragment of any composition that is smaller than very fine silt grains, having a diameter less than 0.00016 in. (1/256 mm). A clay mineral is one of a complex and loosely defined group of finely crystalline hydrous silicates formed mainly by weathering or alteration of primary silicate minerals. They are characterized by small particle size and their ability to adsorb large amounts of water or ions on the surface of the particles.

climate. Weather conditions, including temperature, wind velocity, precipitation, and other factors, that prevail in a region averaged over some period of time.

climate state. Representation of climate conditions. Different climate states are used in performance assessment models to represent changes in climate over the time periods of interest.

closure seal. A generic term for the method(s) that would be used to seal all openings (e.g., access ramps, ventilation shafts, and exploratory boreholes) from the surface to the underground repository facilities once a decision is made to permanently close the repository. If left unsealed, the openings could enhance the movement of moisture from the surface into the waste emplacement area and could also serve as conduits for airborne radioactive material to migrate into the atmosphere.

code (computer). The set of commands used to solve a mathematical model on a computer.

codisposal. A packaging method for disposal of radioactive waste in which more than one type of waste, such as DOE spent nuclear fuel and high-level radioactive waste, are combined in disposal containers. Codisposal takes advantage of otherwise unused space in disposal containers and is more cost-effective than other methods of limiting the reactivity of individual waste packages.

cohesion. (1) In geology, the shear strength of the substance, whether cement or adsorbed water, that separates individual grains of rock at their areas of contact. (2) In physics, the attraction between molecules of a liquid that allows formation of drops or films of that liquid.

colloid. A large molecule or small particle that has at least one dimension with the size range of 10^{-9} to 10^{-6} m, suspended in a liquid such as groundwater. Some radionuclides can bind with colloids (either reversibly or irreversibly) depending on the type of colloid) and travel great distances in groundwater. Colloids may form directly from insoluble radioactive material (intrinsic colloids), may result from degraded spent nuclear fuel or glass waste forms (waste form colloids), or may result from other natural or man-made materials with which radionuclides can bind (pseudocolloids).

colluvium. Any loose, heterogeneous sediment deposited by rainwash, sheetwash, or slow continuous downslope creep, usually at the base of a cliff or slope.

committed effective dose equivalent. A radiation protection term for the effective dose equivalent received over a period of time (as determined by the U.S. Nuclear Regulatory Commission) by an individual from radionuclides internal to the individual following one year intake of these radionuclides.

committed dose equivalent. A radiation protection term for the dose equivalent that is committed to specific organs or tissues that will be received from an intake of radioactive material by an individual during the 50 years following the intake.

complexation capability. The ability of a chemical element to unite with other elements to form a complex compound.

component model. The analysis models that are run separately and then combined into process models for running in the TSPA computer model.

conceptual model. A set of qualitative assumptions used to describe a system or subsystem for a given purpose.

conduction. The flow of thermal energy through a material. Conduction is affected by the amount of heat energy present, the nature of the heat carrier in the material (its thermal conductivity), and the amount of dissipation.

confidence. (1) In statistics, a measure of how close the estimated value of a random variable is to its true value. (2) Degree of assurance that an argument, such as a safety case, is correct.

confidence interval. An interval that is believed, with a preassigned degree of confidence, to include the particular value of the random variable that is estimated.

conservative assumption. (1) An assumption that results in a calculated release of radionuclides exceeding actual or expected releases. (2) An assumption that uses uncertain inputs and does not attempt to include any potentially beneficial effects.

containment. (1) The confinement of radioactive waste within a designated boundary. (2) The use of design features to contain or reduce radioactive releases or radiation doses.

continuum model. A model that represents fluid flow through numerous individual fractures and matrix blocks by approximating them as continuous flow fields.

controlled area. The surface area, identified by passive institutional controls, that encompasses no more than 300 square kilometers. It must not extend farther south than 36º 40' 13.6661" North latitude, in the predominant direction of groundwater flow and must not extend more than five kilometers from the repository footprint in any other direction. It also includes the subsurface underlying the surface area.

convection. (1) The transfer of heat by the circulation of a fluid (at Yucca Mountain, either water or air). (2) The bulk motion of a flowing fluid (gas or liquid) caused by temperature differences that, in turn, cause different areas of the fluid to have different densities (e.g., warmer is less dense).

convective circulation. The transfer of heat from or within a given area by movement of a liquid or gas having a temperature different than the solids over which it flows.

corrosion resistant material. A material that develops a protective film on its surface, creating a high resistance to corrosion. Such a material, the nickel-based alloy, Alloy 22, would be used as the outer barrier of the two-layer waste package.

coupon. A strip of polished metal, of specific weight and size, used in testing to assess the corrosive effects of liquids or gases. Also used to measure the effectiveness of corrosion inhibitors.

creep. A phenomenon in which strain in a solid increases with time when stress producing the strain is held fixed; it may be associated with temperature or mechanical stress.

critical group. The hypothetical group of individuals reasonably expected to receive the greatest exposure to radioactive materials (proposed 10 CFR Part 63). The critical group has been replaced by the reasonably maximally exposed individual in the final NRC regulations (10 CFR 63.2).

criticality. The condition in which nuclear fuel sustains a chain reaction. It occurs when the effective neutron multiplication factor of a system equals one. *See* effective neutron multiplication factor.

Cross-Drift, Enhanced Characterization of the Repository Block (ECRB) Cross-Drift. An excavation above and across the block of the potential repository excavated in a general northeast–southwest direction.

cumulative distribution. For grouped data, a distribution that shows how many of the values are less than or more than specified values. For random variables, this term is synonymous with distribution function.

cumulative probability. The probability that a random variable will have a value equal to or less than some specified value.

curie. A unit of radioactivity equal to 37 billion disintegrations per second, abbreviated Ci.

darcy. A unit of measurement of the permeability of a porous medium. In a cross section of the medium 1 square centimeter by 1 cm in length, 1 darcy equals the passage in 1 second of 1 cm^3 of the fluid when it has 1 centipoise of viscosity under 1 atmosphere of pressure.

Darcy's law. A fundamental law of porous media, discovered by Henri Darcy in 1856, stating that the flow rate Q is proportional to the cross-sectional area A, inversely proportional to the length L of the sand-filter flow path, proportional to the head drop δH, and proportional to the hydraulic conductivity K. Used in hydrology to describe fluid flow in a porous medium.

decommission. The process of removing from service a facility in which nuclear materials are handled. This usually involves decontaminating the facility so that it may be dismantled or dedicated to other purposes.

DECOVALEX. An international software code testing program.

defense in depth. (1) A design strategy based on a system of multiple, independent, and redundant barriers, designed to ensure that failure in any one barrier does not result in failure of the entire system. (2) A system of multiple barriers that mitigate uncertainties in conditions, processes, and events.

deliquescence. The absorption of water vapor from the air by a crystalline solid, leading to dissolution of the solid.

design alternative. (1) A considered alternative to a major design feature that is important to waste isolation. (2) A fundamentally different conceptual repository design, which could stand alone as the License Application repository design concept.

design bases. Information that identifies the specific functions to be performed by a structure, system, or component of a facility and the specific values or ranges of values

chosen for controlling parameters as reference bounds for design. These values may be constraints derived from generally accepted state-of-the-art practices for achieving functional goals or requirements derived from analysis (based on calculation or experiments) of the effects of a postulated event under which a structure, system, or component must meet its functional goals. The values for controlling parameters for external events include: (1) estimates of severe natural events to be used for deriving design bases that will be based on consideration of historical data on the associated parameters, physical data, or analysis of upper limits of the physical processes involved and (2) estimates of severe external human-induced events, to be used for deriving design bases, that will be based on analysis of human activity in the region taking into account the site characteristics and the risks associated with the event.

design basis event. (1) Natural or human-induced events that may occur before permanent closure of the geologic repository's operations area and which are used to assess system safety. (2) A natural or human-induced event that is expected to occur one or more times before permanent closure of the repository (referred to as a *Category 1 Event*) or any other natural or human-induced event that has at least one chance in 10,000 of occurring before permanent closure of the repository (referred to as a *Category 2 Event*).

design margin. Margins of safety in specifications for engineered components to account for uncertainty in the conditions to which the components will be subjected and for variability in the properties of component materials. *See* safety margin.

desorption. A physical or chemical process by which a substance that has been adsorbed or absorbed by a liquid or solid material is removed from the material.

devitrification. The conversion of a glassy substance to a crystalline substance; for example, the alteration of glass in vitrified tuff into zeolites.

diagenetic process. The chemical or physical changes that take place in sediments during and after they are deposited but before they consolidate.

diffusion. (1) A process in which substances move from regions of higher concentrations to regions of lower concentrations. (2) The gradual mixing of the molecules of two or more substances due to random thermal motion.

diffusion coefficient. A material's weight, in grams, as it diffuses in 1 second through 1 square centimeter of a medium of a determined concentration gradient (i.e., a medium having a known variability in the concentration of the substance in solution as it travels over distance).

diffusive transport. Movement of molecules or particles due to their concentration gradient. Occurs when dissolved or suspended radionuclides move from regions of higher or lower concentration.

dike. A tabular body of igneous rock that cuts across the structure of adjacent rocks or cuts massive rocks. Most dikes are caused by the intrusion of magma. Some dikes occur as columnar structures.

dilution. The reduction of a dissolved substance's concentration in a solution caused by an increase in the solvent's proportion of the solution. The solvent frequently is water.

dispersion (hydrodynamic dispersion). (1) The tendency of a solute (substance dissolved in groundwater) to spread out from the path it is expected to follow if only the bulk motion of the flowing fluid moved it. (2) The macroscopic outcome of the actual movement of individual solute particles through a porous medium. Dispersion causes dilution of sol-

utes, including radionuclides, in groundwater and is usually an important mechanism for spreading contaminants in low flow velocity situations.

dispersivity. The degree to which small particles of a solid are distributed throughout either a liquid or another solid.

disposal container. The vessel consisting of the barrier materials and internal components in which the canistered or uncanistered waste form is placed. The disposal container includes the container barriers or shells, spacing structures or baskets, shielding integral to the container, packing contained within the container, and other absorbent materials designed to be placed internal to the container or immediately surrounding the disposal container (i.e., attached to the outer surface of the container). The filled, sealed, and tested disposal container is referred to as the waste package, which is emplaced underground.

disposal container handling system. System in the Waste Handling Building that prepares empty disposal containers for loading, receives full disposal containers from the assembly and canister transfer systems, welds and inspects the containers, and transfers them to the waste emplacement system. The system also receives and handles retrieved waste packages from the subsurface and disposal containers that are defective and routes them to the waste package remediation system.

disruptive processes and events. An unexpected process or event that could affect the performance of the repository, including, for example, human intrusion, volcanic activity, and seismic activity.

disruptive scenario. A well-defined sequence of events and processes that could adversely affect repository performance initiated by a disruptive process or event.

dissolution. The dissolving of a solid or gas in a liquid.

distribution. The overall scatter of values for a set of observed data. A term used synonymously with frequency distribution. Distributions have probability structures that are the probability that a given value occurs in the set.

distribution frequency. A representation of how values of an outcome or variable are distributed over the range of expected values.

distribution function. A function whose values are the probabilities that a random variable assumes a value less than or equal to a specified value. Synonymous with cumulative distribution.

DOE spent nuclear fuel. Radioactive waste created by defense activities. The major contributor to this waste form is the N Reactor fuel currently stored at the Hanford Site. This waste form also includes naval spent nuclear fuel.

dose. The amount of radioactive energy taken into (absorbed by) living tissues.

dose equivalent. The product of the absorbed dose in tissue, quality factor, and all other necessary modifying factors at the location of interest. *See* effective dose equivalent *and* total effective dose equivalent.

downgradient. The direction that water will tend to flow as the result of a difference in pressure, as indicated by the elevation change in the potentiometric surface. Based on current understanding of the hydraulic gradient below Yucca Mountain, downgradient is toward the south to southeast of the potential repository location.

DCPT. Used as a dual continuum particle tracking code for modeling transport in dual media, such as fractures and rock maxtrix.

drift. From mining terminology, a horizontal underground passage. Includes excavations for emplacement (emplacement drifts) and access (main drifts).

drip shield. A corrosion-resistant engineered barrier that is placed above the waste package to prevent seepage water from directly contacting the waste package for thousands of years. The drip shield also offers protection to the waste package from rockfall.

DRKBA. Software used to apply a numerical technique for solving probabilistic key block analysis problems in a rock mass according to probabilistic distributions determined based on tunnel mapping data.

dual permeability conceptual model. A conceptual model of groundwater flow in which fractures and rock matrix are represented as separate, interacting continua, with no assumption of pressure equilibrium between fractures and rock matrix. This concept allows modeling groundwater flow as occurring mostly in the fractures, with less flow in the rock matrix, depending on the degree of connection between the rock matrix and fractures and the capillary pressure gradient. The dual permeability model is one of the conceptual models for groundwater and heat flow for fractured, porous media.

effective dose equivalent. The sum of the products of the dose equivalent received by specified tissues and the appropriate weighting factors applicable to each tissue.

effective neutron multiplication factor (K_{eff}). A measurement of nuclear reactivity or criticality potential. Equal to the number of fissions in one generation divided by the number of fissions in the preceding generation, in a finite medium.

effective porosity. The fraction of a given medium's porosity available for fluid flow and/or solute storage.

Eh. A measure of the state of oxidation of a system. Also known as redox potential or oxidation–reduction potential.

electrical resistivity tomography. A radiograph that shows the electrical resistance of a material within a predetermined plane section.

electrolyte. A substance (e.g., an acid, base, or salt) that, when dissolved in a suitable solvent (e.g., water) or when fused, conducts electric current by the movement of ions instead of electrons

empirical model. A model whose reliability is based on observation and/or experimental evidence and is not necessarily supported by any established theory or law. Validity or applicability of such an empirical model is normally limited to situations that lie within the range of the data that were used to develop the model.

emplacement. The placement and positioning of waste packages in the repository emplacement drifts.

emplacement horizon. The area within the repository block where emplacement drifts would be excavated.

engineered barrier. Any component of the engineered barrier system, such as the drip shield, waste package, or invert. *See* engineered barrier system.

engineered barrier system. The waste packages and the underground facility, including engineered components and systems other than the waste package (e.g., drip shields).

Environmental Impact Statement. A detailed written statement to support a decision to proceed with major Federal actions affecting the quality of the human environment. This is required by the National Environmental Policy Act of 1969. Preparation of an envi-

ronmental impact statement requires a public process that includes public meetings, reviews, and comments, as well as agency responses to the public comments.

eolian deposit. Material deposited by wind, such as sand dunes.

EQ3/6. A computer software code used to estimate equilibrium mineral phases based on thermodynamic equilibrium, thermodynamic disequilibrium, and reaction kinetics.

EQ3NR. Aqueous solution speciation-solubility code component of EQ3/6 that computes thermodynamic state of a solution.

equivalent continuum model. A conceptual model of groundwater and heat flow that is also called a composite porosity model. Key assumptions are that the temperatures and capillary pressures in the rock matrix and fractures are equal. Therefore, the fractures and matrix can be treated as a single composite material, and the hydraulic properties are a combined effect of both fracture and matrix properties.

evapotranspiration. The combined processes of evaporation and plant transpiration that remove water from the soil and return it to the air.

event. (1) An occurrence that has a specific starting time and, usually, a duration shorter than the time being simulated in a model. (2) Uncertain occurrences that take place within a short time relative to the time frame of the model.

event sequence. A series of actions and/or occurrences within the natural and engineered components of a geologic repository operations area that could potentially lead to exposure of individuals to radiation. An event sequence includes one or more initiating events and associated combinations of repository system component failures, including those produced by the action or inaction of operating personnel. Those event sequences that are expected to occur one or more times before permanent closure of the geologic repository operations area are referred to as Category 1 event sequences. Other event sequences that have at least one chance in 10,000 of occurring before permanent closure are referred to as Category 2 event sequences.

event tree. A structurally tree-like diagram that is useful in representing sequences of events and their possible outcomes. Each node, or branching point, represents an event, and each branch from that node represents one of its possible outcomes. Each possible pathway along the tree, from beginning to end of a given line of branching, represents a specific scenario.

expected behavior. (1) The mean value of the probability distribution describing that behavior. (2) The nominal behavior of the repository system and the geologic barrier in the absence of disruptive events.

expected value. A variable's mean, or average, outcome. The weighted average of the number of possible outcomes, with each outcome being weighted by its probability of occurrence. The mean of a probability distribution of a random variable that one would expect to find in a very large, random sample. The sum of the possible values, each weighted by its probability—the center of the random variable's histogram (frequency distribution).

Exploratory Studies Facility. An underground laboratory at Yucca Mountain used for performing site characterization studies. The facility includes a 7.9-km (4.9-mi) main loop (tunnel), the 2.8-km (1.7-mi) Enhanced Characterization of the Repository Block (ECRB) Cross-Drift, and a number of alcoves used for site characterization tests such as the Drift Scale Test.

exposure pathway. The course a chemical or physical agent takes from the source to the exposed organism; describes a unique mechanism by which an individual or population can become exposed to chemical or physical agents at or originating from a release site.

exsolve. To separate or precipitate from a solid crystalline phase.

extrusive event. An igneous (volcanic) event occurring at the surface, i.e., a volcanic eruption. In repository performance analyses, molten material is assumed to intersect waste packages in the repository and cause a release of radionuclides. *Compare* intrusive event.

fault. (1) A fracture in rock along which movement of one side relative to the other has occurred. (2) A fracture or a fracture zone in crustal rocks along which there has been movement of the fracture's two sides relative to one another, so that what were once parts of one continuous rock stratum or vein are now separated.

fault displacement. Rupture along the main plane (or planes) of crustal weakness such that the two sides of a fault move relative to one another.

fault source. Fractures in the earth's crust with characteristics that indicate past movement of one side of the fracture relative to the other side.

FEHM. A finite element heat and mass transport computer software code that is used for saturated zone flow and transport and unsaturated zone transport calculations.

film flow. Movement of water as a thin film along a surface.

fissile material. Material capable of undergoing fission with neutrons of any energy, including thermal, or slow, neutrons. The three primary materials in this category are uranium-233, uranium-235, and plutonium-239.

fission. The splitting of a nucleus into at least two other nuclei resulting in the release of two or three neutrons and a relatively large amount of energy.

fission product. Any nuclide, either radioactive or stable, that arises from fission, including both the primary fission fragments and their radioactive decay products. *Also* daughter product, decay product.

FLAC. A specialized computer code developed to solve soil and rock mechanics problems. It is used in conjunction with TOUGH to form a thermal-hydrologic-mechanical code to analyze those coupled effects.

flow field. A fluid's distribution in and through an area, including its velocity and density, as a function of position and time.

flux. The rate of transfer of fluid, particles, or energy passing through a unit area per unit time.

footwall. The rock beneath a fault, bedded deposit, vein, or mine working.

fracture. A break in rock caused by mechanical stresses. A fracture along which there has been displacement of the sides relative to one another is called a fault. A fracture along which no appreciable movement has occurred is called a joint.

fracture continuum. A continuum that represents fluid flow and transport through numerous individual fractures by approximating them as continuous flow and transport fields.

fracture permeability. The capacity of a rock to transmit fluid through fractures in the rock.

frequency distribution. Data grouped into classes (or ranges of values within the overall set of values, such as 1 to 5, 5 to 10, 10 to 20, etc.), with the classes listed in a table (or other format) showing the number of data points that occur in each class.

fuel assembly. A number of fuel rods held together by plates and separated by spacers, used in a reactor. This assembly is sometimes called a fuel bundle.

fuel blending. The process of loading low heat output waste with high heat output waste in a waste package to balance its total heat output. This process applies only to commercial spent nuclear fuel.

fuel blending inventory. The reserve of commercial spent nuclear fuel that will be inventoried in pools in the Waste Handling Building Annex. The spent nuclear fuel will be inventoried in the pools until selected, according to heat output, for fuel blending.

fuel matrix. The physical form and composition of the substance that holds the fissile material.

fugacity. A parameter that measures the chemical potential of a real gas in the same way that partial pressure measures the free energy of an ideal gas.

galvanic corrosion. Electrochemical corrosion caused by the flow of electricity that occurs when two dissimilar metals with differing electrical potentials are near each other in the presence of a conductor such as water with solutes in it.

gamma radiation. Electromagnetic radiation emitted during the radioactive decay process. The gamma ray is the most penetrating wave of radiant nuclear energy. It does not contain particles and can be stopped by dense materials such as concrete or lead.

gamma radiolysis. The breakdown of molecules through exposure to gamma radiation.

gantry. A hoisting machine that slides along a fixed platform or track, either raised or at ground level.

GENII-S. A quasi-stochastic computer software code used to evaluate the dose from the migration of radionuclides in the biosphere that may affect humans through ingestion, inhalation, and direct radiation. It is used to develop biosphere dose conversion factors.

geologic repository. A system for the disposal of radioactive waste in excavated geologic media. A geologic repository includes the engineered barrier system and the portion of the geologic setting that provides isolation of the radioactive waste.

geologic repository operations area. A high-level radioactive waste facility that is part of a geologic repository, including both surface and subsurface areas, where waste handling activities are conducted.

glacial transition. One of the climate states of the future climate model for Yucca Mountain; others examples include modern and monsoon climates.

GoldSim. A software code used as a probabilistic shell for the TSPA component models that, in combination, simulate potential long-term behavior of the repository.

ground control. Support of rock in the subsurface of the repository (e.g., rock bolts and steel sets).

ground support. The system (rock bolt with wire mesh, steel cast, etc.) used to line the main and emplacement drifts to minimize rock or earth falling into the drifts.

groundwater. Water contained in pores or fractures in either the unsaturated or saturated zones below ground level.

groundwater flux. The rate of groundwater flow through a unit area of the aquifer.

half-life. The time in which half the atoms of a radioactive substance decay to another nuclear form. Half-lives range from millionths of a second to millions of years, depending on the stability of the nuclei.

heat exchanger. A device that transfers heat from one medium or system to another; for example, heat from hot fluid contained in a radiator dissipates when the metal walls of the device come in contact with cold air.

heat pipe. A zone characterized by a continuous process of boiling, vapor transport, condensation, and migration of water back to the heat source.

heterogeneous. Being composed of parts or elements of different kinds, such as a mixture of liquid–vapor or liquid–vapor–solid. A condition in which the value of a parameter, such as porosity of rock, varies over space and time.

high-level radioactive waste. The highly radioactive material resulting from the reprocessing of spent nuclear fuel, including liquid waste produced directly in reprocessing; and any solid material derived from such liquid waste that contains fission products in sufficient concentrations; and other highly radioactive material that the U.S. Nuclear Regulatory Commission determines by rule requires permanent isolation.

high-level radioactive waste glass. The waste form of high-level radioactive waste in which the radioactive waste is mixed with borosilicate glass.

Holocene. The most recent epoch of geologic time that extends from the end of the Pleistocene to the present, or approximately the past 10,000 years; also the series of rocks and deposits formed during that time.

host rock. (1) The rock unit in which the potential repository would be located. For a repository at Yucca Mountain, the host rock would be the middle portion of the of the Topopah Spring Tuff of the Paintbrush Group. (2) The geologic medium in which the waste is emplaced.

human intrusion. Breaching of any portion of the Yucca Mountain disposal system within the repository footprint by any human activity.

human intrusion scenario. A disruptive event assessed in a separate TSPA according to specific characteristics defined by the U.S. Nuclear Regulatory Commission in 10 CFR 63.113(d). According to the U.S. Nuclear Regulatory Commission rule at 10 CFR 63.322, the human intrusion scenario assumes that a drill penetrates the repository and a waste package during exploratory drilling for groundwater resources. The U.S. Nuclear Regulatory Commission rule requires a determination of the earliest time after disposal that the waste package would degrade sufficiently that a human intrusion could occur without recognition by the drillers (10 CFR 63.321).

hydraulic conductivity. A measure of the ability to transmit water through a permeable medium. A number that describes the rate at which water can move through a permeable medium. The hydraulic conductivity depends on the size and arrangement of water-transmitting openings such as pores and fractures, the dynamic characteristics of the water such as density and viscosity, and the driving force.

hydraulic gradient. The difference in the height of water levels with respect to the distance between two locations.

hydraulic head. The pressure in the liquid expressed as equivalent height (head) of the water column.

hydrogen embrittlement. A process resulting in a decrease of fracture toughness or ductility of a metal due to the presence of hydrogen.

hydrogen-induced cracking. Occurs when atomic hydrogen generated at the surface of a metal migrates into the metal and forms hydride phases with the metal components, causing the metal to be more brittle. Hydride phases cause the metal to be more susceptible to cracking, and, thus, to localized corrosion. *Also* hydride cracking.

hydrogeologic nomenclature. A stratigraphic nomenclature system used for the classification of rock at Yucca Mountain based on the hydrogeologic properties that govern the rock's capacity to hold, transmit, and deliver water. *Compare* lithostratigraphic nomenclature *and* thermomechanical nomenclature.

hydrologic properties. Those properties of a rock that govern the capacity to hold, transmit, and deliver water, such as porosity, effective porosity, specific retention, permeability, and the directions of maximum and minimum permeabilities.

hydrostatic pressure. The pressure, measured at a point in a fluid, due solely to the weight of the fluid in the column above the point.

hygroscopic salt. Of a substance, absorbing or attracting moisture from the air; having an affinity for moisture.

hypogene. Of or pertaining to a substance formed by ascending solutions within the earth, e.g., ore or mineral deposits. Occurring or forming within or below the Earth's crust.

hysteresis. The dependence of system behavior on its history; in particular, failure to return to initial conditions following retraction of stimulus.

igneous. (1) A type of rock that has formed from a molten, or partially molten, material. (2) A type of activity related to the formation and movement of molten rock either in subsurface (plutonic) or on the surface (volcanic).

imbibition. The absorption of a fluid, usually water, by porous rock (or other porous material) under the force of capillary attraction and without pressure.

in situ. In its natural position or place. The phrase distinguishes in-place experiments, conducted in the field or underground facility.

indurated. Of a rock, characterized by a solid, hard structure, hardened by pressure, heat, or cementation.

INFIL. A numerical software code used to analyze infiltration of precipitation.

initiating event. A natural or human-induced event that causes an event sequence.

infiltration. The process of water entering the soil at the ground surface and the ensuing movement downward. Infiltration becomes percolation when water has moved below the depth at which it can be removed (to return to the atmosphere) by evaporation or evapotranspiration.

intrablock faults. Faults (i.e., rock fractures having experienced movement along their plane) found within a block of rock; in this case, within the repository block, which is located within the Topopah Spring Tuff formation.

intrusive event. An igneous event occurring at the underground. In repository performance analyses, molten material is assumed to intersect waste packages in the repository and cause a release of radionuclides. *Compare* extrusive event.

inverse modeling. The model calibration process by which values of important model parameters are estimated and optimized to produce the best fit of the model output to the observed data.

invert. (1) The floor of a drift. (2) The structure constructed in a drift to provide the floor of that drift. In an emplacement drift, ballast in the invert serves as a barrier to migration of radionuclides that might escape from breached waste packages.

ion-exchange resins. (1) Any of a number of (usually organic) materials that are capable of exchanging the included ions with ions in a surrounding solution; used for deionizing water or for chromatography of organic molecules. (2) A synthetic resin that can combine or exchange ions with a solution; such a resin produces the exchange of sodium for calcium ions in the softening of hard water.

ionic strength. A measure of the level of electrical force in an electrolytic solution.

ionizing radiation. (1) Alpha particles, beta particles, gamma rays, x-rays, neutrons, high-speed electrons, high-speed protons, and other particles capable of producing ions. (2) Any radiation capable of displacing electrons from an atom or molecule, thereby producing ions.

irreducible uncertainty. Uncertainty that cannot be further reduced, given current best knowledge, expert insights, and calculational abilities.

irreversible colloid. A colloid with permanently attached radionuclides.

isothermal seepage. The flow of water into a drift under ambient conditions with constant temperature.

isotope. (1) Atoms of a chemical element with the same atomic number. (2) One of two or more atomic nuclei with the same number of protons (i.e., the same atomic number) but with a different number of neutrons (i.e., a different atomic weight). For example, uranium-235 and uranium-238 are both isotopes of uranium.

isotropy. The condition wherein all significant physical properties are equal when measured in any direction or along any axes. *See* anisotropy.

J-13 water. Groundwater taken from Well J-13 or water made in a laboratory that has the same chemical composition. The chemical composition of this water is used as the standard for Yucca Mountain ambient groundwater composition for modeling and testing purposes.

joint. A fracture in rock, usually more or less vertical to bedding, along which no appreciable movement has occurred.

joint set. In a rock mass, a group of parallel joints (fractures without displacement).

juvenile failure. (1) Premature failure of a waste package because of material imperfections or damage by rockfall during emplacement. (2) In modeling, a breach in the waste package artificially set to occur early in order to provide insight into system performance. This term is distinguished from mechanistically possible early failures.

key technical issues. Issues important for assessing the long-term safety of a potential Yucca Mountain repository, as defined by the U.S. Nuclear Regulatory Commission (NRC). The issues are (a) Support Revision of the U.S. Environmental Protection Agency Standard/NRC Rule Making; (b) Total System Performance Assessment and Technical Integration; (c) Igneous Activity; (d) Unsaturated and Saturated Flow Under Isothermal Conditions; (e) Thermal Effects on Flow; (f) Container Life and Source Term;

(g) Structural Deformation and Seismicity; (h) Evolution of Near-Field Environment; (i) Radionuclide Transport; (j) Repository Design and Thermal Mechanical Effects.

Large Block Test. A prototype test of thermal-mechanical processes at Yucca Mountain in the middle nonlithophysal zone of the Topopah Spring unit. The test was to develop testing approaches for thermal-hydrologic and other coupled processes.

laser peening. Process of applying laser-generated compressive stresses to the welds of the waste package lids. Hardens the weld and reduces remaining tensile stresses.

Latin hypercube sampling. A sampling technique that divides the cumulative distribution function into intervals of equal probability and then samples from each interval.

Latin square. A method for ordering the observations of an experiment in an $n \times n$ square array of n different symbols, where each symbol appears once in each row and once in each column.

license application. An application to the Nuclear Regulatory Commission (NRC) to construct a geologic repository operations area for the disposal of spent nuclear fuel and high-level radioactive waste. The application would be considered by the U.S. Nuclear Regulatory Commission in any decision whether to grant the U.S. Department of Energy authorization to begin constructing a geologic repository operations area.

line loading. Placing the waste packages at very close distances end-to-end to achieve a more uniform thermal profile along the length of the emplacement drifts. *Compare* point loading; *see* thermal loading.

linear regression. A regression where the relationship between the (conditional) mean of a random variable and one or more independent variables can be expressed by the mathematical equation that describes a line. A relationship between two variables such that the dependence of one variable on the other can be described by (the equation of) a straight line.

linear stepwise regression. An analysis designed to determine variables that have the greatest influence on an output value (e.g., peak dose rate) when there are many variables whose input values go into the calculation. In simple terms, a linear regression is performed for a line in a multidimensional space, and the correlation of the values of different variables to the line are examined by performing the calculation multiple times and varying the value of one variable at a time while holding the others constant. This is a stepwise process in which one variable at a time is examined to determine the impact of its influence on the final outcome (peak dose rate, for instance).

lithologic. Pertaining to rock features such as color, texture, mineral content, and weathering characteristics.

lithophysae. Small, bubble-like holes in the rock caused by volcanic gases trapped in the rock matrix as the ash-flow tuff cooled.

lithophysal. Pertaining to tuff units with lithophysae, voids having concentric shells of finely crystalline alkali feldspar, quartz, and other materials that were formed by entrapped gas that later escaped.

lithostratigraphic nomenclature. A stratigraphic nomenclature system used for the classification of rock at Yucca Mountain based on primary geologic processes (e.g., the depositional character and assemblage of the rock) and secondary geologic processes (e.g., the degree of welding, devitrification, and vapor-phase crystallization). *Compare* hydrogeologic nomenclature *and* thermomechanical nomenclature.

loading curve. A function of the average burnup versus initial enrichment of a fuel assembly, which provides the necessary information on whether a fuel assembly can be loaded, unaltered, into a standard waste package without concern for criticality. *See* burnup.

localized corrosion. A type of corrosion induced by local variations in electrochemical potential on a microscale over small regions. Variations in electrochemical potential may be caused by localized irregularities in the structure and composition of usually protective passive films on metal surfaces and in the electrolyte composition of the solution that contacts the metal.

log normal distribution. A distribution of a random variable *x* such that the natural logarithm of *x* is normally distributed.

logic tree methodology. An analytical approach that involves sequencing the studies in an analysis and then addressing certain attributes in each study

longitudinal dispersion. Dispersion of a solute moving in groundwater in the same direction as the groundwater flow path.

long-term-average climate. The conditions used to represent climate changes through time. Representative of the expected typical climate conditions at Yucca Mountain, with precipitation twice that of the present-day climate.

lookup table. A multidimensional table containing columns of data representing relationships between parameters in the table. A lookup table is a convenient way to represent and implement functional relationships between parameters considered in the model.

low-level radioactive waste. Radioactive waste producing small quantities of ionizing radiation and that is not classified as high-level radioactive waste, transuranic waste, or byproduct tailings containing uranium or thorium from processed ore. Usually generated by hospitals, research laboratories, and certain industries.

main drift. (1) One of four main access tunnels in the potential repository design. *Also* access main. (2) The main north–south trending drift segment in the current Exploratory Studies Facility.

mass spectrometry. A technique for identifying chemical structures in a material. The technique involves sending a beam of ions through a combination of electric and magnetic fields, which deflects ions according to their masses, indicating the atoms and molecules.

matrix. Rock mass between explicitly considered fractures.

matrix diffusion. The process by which molecular or ionic solutes, such as radionuclides in groundwater, move from areas of higher concentration to areas of lower concentration. This movement is through the pore spaces of the rock material as opposed to movement through the fractures.

matrix permeability. The capacity of the matrix to transmit fluid.

matrix porosity. In the solid, but porous, portion of rock, the ratio of openings, or voids, to the total volume of the matrix expressed as a decimal fraction or as a percentage.

mean. For a statistical data set, the sum of the values divided by the number of items in the set. The arithmetic average.

mechanical dispersion. As a process for transport, a type of dispersion by means of physical forces.

median. A value such that half of the observations are less than that value and half are greater than the value.

meniscal flow. Flow of a curved-surface fluid, the curved free surface being due to surface tension and the shape of the solid the fluid flows over.

meteoric water. Groundwater that originates in the atmosphere and percolates to the saturated zone.

metric ton heavy metal (MTHM). A metric ton is a unit of mass equal to 1,000 kg (2,205 lb). Heavy metals are those with atomic masses greater than 230. Examples include thorium, uranium, plutonium, and neptunium. The term usually pertains to heavy metals in spent nuclear fuel and high-level radioactive waste. In this document, MTHM is equal to MTU (metric tons of uranium).

microbially influenced corrosion. Corrosion of the waste package that is induced by the activity of microbes.

microsphere. Spheres of carboxylate-modified latex of varied diameters between 280 to 640 nm (0.000011 to 0.000025 in.), used as colloid tracers in the C-Wells testing.

millirem (mrem). A millirem is one one-thousandth of a rem, which is the unit of equivalent dose. Equivalent dose is a measure of the effect that radiation has on humans. The equivalent dose takes into account the type of radiation and the absorbed dose. *See* rem.

MING. Model code used to estimate impact of microbes on the near-field environment geochemistry.

Miocene Epoch. The fourth of the five geologic epochs of the Tertiary Period, extending from the end of the Oligocene Epoch to the beginning of the Pliocene Epoch.

mitigation. (1) Avoiding an impact by not taking a certain action or parts of an action. (2) Minimizing impacts by limiting the degree or magnitude of the action and its implementation. (3) Rectifying an impact by repairing, rehabilitating, or restoring the affected environment. (4) Reducing or eliminating an impact over time by preservation and maintenance operations during the life of the action. (5) Compensating for an impact by replacing or providing substitute resources or environments.

mixed waste. Waste containing both radioactive hazardous substances and nonradioactive hazardous substances, regardless of whether these types of substances are combined chemically or mixed together.

model. (1) A conceptual description and the associated mathematical representation of a system, subsystem, component, or condition that is used to predict changes from a baseline state as a function of internal and/or external stimuli and as a function of time and space. (2) A depiction of a system, phenomenon, or process including any hypotheses required to describe the system or explain the phenomenon or process.

model validation. A process used to establish confidence that a conceptual model represented in a mathematical model by software or by other analytical means adequately represents the phenomenon, process, or system under consideration.

moderator. Material that contains nuclei that cause energetic neutrons to slow down. In general, the lighter the element, the better it works as a moderator. Hydrogen, the lightest element, is a very efficient moderator; since water contains hydrogen nuclei, it, too, is a very effective moderator.

modern climate. One of the climate states of the future climate model at Yucca Mountain; others include monsoon and glacial transition. Consists of two active components, the tropical and polar air masses, and a more passive component, the westerlies.

molal. Of a solution, containing one mole of solute per one kilogram of solvent. *See* mole.

mole. The fundamental unit used to measure the amount of a substance. Avogadro's number of particles (6.023×10^{23}).

molecular diffusion. The transfer of mass in a fluid by random molecular motion.

monitored geologic repository. A system, requiring licensing by U.S. Nuclear Regulatory Commission, intended or used for the permanent underground disposal of spent nuclear fuel and high-level radioactive waste. A geologic repository includes (a) the geologic repository operations area, and (b) the geologic setting within the controlled area that provides isolation of the radioactive waste.

monsoon climate. One of the climate states of the future climate model at Yucca Mountain; others include modern and glacial transition.

Monte Carlo simulation. An analytical method that uses random sampling of parameter values available for input into numerical models as a means of approximating the uncertainty in the process being modeled. A Monte Carlo simulation comprises many individual runs of the complete calculation using different values for the parameters of interest as sampled from a probability distribution. A different final outcome for each individual calculation and each individual run of the calculation is called a realization. Each realization is equally likely to occur in the Monte Carlo process.

mountain scale. (1) Similar to far-field for processes that are related to the area of the geosphere and biosphere far enough away from the repository that, when numerically modeled, show that releases from the repository are represented as a homogeneous, single source term. The effects of individual, small-scale components such as individual waste packages are not modeled because they are considerably smaller than the scale of the model. (2) A scale of hundreds of meters, or even kilometers, as opposed to tens of meters.

muck. Material excavated from a mine or geologic repository.

MULTIFLO. A computer software code used by the U.S. Nuclear Regulatory Commission to simulate the flow of groundwater and heat in unsaturated porous and fractured media. The code MULTIFLO is similar to TOUGH2.

natural barriers. The physical components of the geologic environment that individually and collectively act to limit the movement of water or radionuclides.

near field. The area and conditions within the repository including the drifts and waste packages and the rock immediately surrounding the drifts. The region around the repository where the natural hydrogeologic system has been significantly impacted by the excavation of the repository and the emplacement of waste.

net infiltration. The water that has infiltrated down from the soil zone or exposed rock surface to a depth below which it cannot be removed by evapotranspiration. Net infiltration is the total infiltration at the surface minus water lost to evaporation and plant transpiration.

neutron absorber. A material (such as boron or gadolinium) that absorbs neutrons. Used in nuclear reactors, transportation casks, and waste packages to control neutron activity.

neutron logging. The analysis of the water content of soil and rocks in a borehole by means of neutron bombardment and the measurement of the reflected radiation.

nominal scenario or nominal case. The performance assessment case, or conceptual model, representing the expected conditions of the disposal system as perturbed only by the presence of the repository, in the absence of disruptive events.

nonstandard fuel. For the purpose of this document, nonstandard fuel is defined as commercial spent nuclear fuel assemblies, single-assembly canisters, and packages that satisfy the following criteria: (1) the maximum nominal physical dimensions are larger than those of intact light-water reactor standard fuel assemblies; (2) assemblies, canisters, or packages that require special handling other than with standard fuel assembly transfer equipment; (3) non-power reactor fuel assemblies that are not packaged in sealed canisters; (4) consolidated fuel rods that require reconfiguration or repackaging; (5) failed fuel assemblies with damaged cladding, structural deformations, or high levels of contamination resulting from released radioactive particulates and activated corrosion products (crud).

NUFT. A nonisothermal unsaturated zone flow and transport software code used for simulation of three-dimensional flow of groundwater, heat, and contaminant transport. It is used for drift-scale thermal-hydrologic calculations.

numerical model. An approximate representation of a mathematical model that is constructed using a numerical description method, such as finite volumes, finite differences, or finite elements. A numerical model is typically represented by a series of program statements that are executed on a computer.

observation drift. A drift near an emplacement drift, from which conditions in the emplacement drifts can be observed without adverse effects from radiation or temperature.

occupational dose. The radiation dose received by an individual in the course of employment in which the individual's assigned duties involve exposure to radiation or to radioactive material from sources of radiation, whether in the possession of the licensee or other person. Occupational dose does not include, for example, dose received from background radiation, from any medical administration the individual has received, from voluntary participation in medical research programs, or as a member of the public.

one-off sensitivity analysis. A method used to examine the effects of each component model or parameter on overall system performance. These analyses are conducted by fixing one important parameter of a particular component model at either its expected value, the median (or 50th percentile value), or at a specified extreme value (the 5th or 95th percentile value). These analyses are used to display the effect of the change on other measures of system or subsystem performance, as well as the effect on the variance of the projected dose history. By fixing a particular parameter that significantly affected the spread of the overall system performance results, it was possible to directly examine the significance of that parameter on the performance outcome.

order of magnitude. A range of numbers extending from some value to 10 times that value.

ORIGEN. Family of software codes that simulate radionuclide decay and estimate buildup and depletion of isotopes in reactor fuel.

overpack. A secondary container used to hold or contain one or more smaller canisters.

oxidation. (1) A chemical reaction, such as the rusting of iron, that increases the oxygen content of a substance. (2) A reaction in which the valence of an element or compound is increased as a result of losing electrons.

paleoclimate. The climate of a past interval of geologic time.

Paleozoic. (1) A geologic era extending from the end of the Precambrian to the beginning of the Mesozoic, dating from about 600 to 230 million years ago. (2) The rock strata formed during this era.

patch. For corrosion modeling, one of two geometries for an opening in a waste package layer created by corrosion (the other geometry is a pit). A patch is generally wider than it is deep.

pedogenic. Of or pertaining to the formation of soil; soil-forming.

perched water. Groundwater of limited lateral extent separated from an underlying body of groundwater by an unsaturated zone.

percolating water. Water passing through a porous substance. In rock or soil it is the movement of water through the interstices and pores under hydrostatic pressure and the influence of gravity. The downward or lateral flow of water that becomes net infiltration in the unsaturated zone.

percolation. The downward or lateral flow of water that becomes net infiltration in the unsaturated zone.

percolation flux. (1) Volumetric percolation rate per unit area. The flux anywhere below the root zone of plants and is no longer susceptible to removal back into the atmosphere by evapotranspiration. (2) Volume of water moving downward or laterally through the unsaturated zone in a given period.

performance assessment. An analysis that forecasts the behavior of a system or system component under a given set of constant and/or transient conditions. Performance assessment includes estimates of the effects of uncertainties in data and modeling. *See* total system performance assessment.

permeability. In general terms, the capacity of a medium (like rock, sediment, or soil) to transmit liquid or gas.

person-rem. A unit used to measure the radiation exposure to an entire group and to compare the effects of different amounts of radiation on groups of people; it is the product of the average dose equivalent (in rem) to a given organ or tissue multiplied by the number of persons in the population of interest.

phase stability. A measure of the ability of matter to remain in a given phase.

phreatic. Of, pertaining to, or deriving from groundwater

phreatophytic plant. A very deep-rooted plant that obtains its water from perched water or from the saturated zone.

pit. For corrosion modeling, one of two geometries for an opening in a waste package layer created by corrosion (the other geometry is a patch). A pit is generally deeper than it is wide.

Pitzer approach. An analytic technique using the Pitzer equation, which estimates the amount of heat produced by the vaporization of organic and simple inorganic compounds.

playa. A nearly level area at the bottom of an undrained desert basin, sometimes temporarily covered with water.

Pliocene. The last of the five geologic epochs of the Tertiary Period, extending from the end of the Miocene to the beginning of the Pleistocene, and the rocks formed during that time.

plume. A measurable discharge of a contaminant, such as radionuclides, from a point of origin. The contaminants are usually moving in groundwater, and the plume may be defined by concentration gradients.

plume of contamination. That volume of groundwater in the predominant direction of groundwater flow that contains radioactive contamination from releases from the Yucca Mountain repository. It does not include releases from any other potential sources on or near the Nevada Test Site.

pluvial. In climatology: relating to former periods of abundant rains, especially in reference to glacial periods. In geology: Said of a geologic episode, change, process, deposit, or feature caused by the action or effects of rain.

point loading. An emplacement drift design in which waste packages are spaced away from each other along the drift. *Compare* line loading; *see* thermal loading.

point of compliance. The place where the DOE must project the amount of radionuclides in the groundwater as defined by proposed 40 CFR 197.

pore water. The water and any material it is carrying that exist in the pore spaces of the rock matrix. *Also* pore fluid.

porosity. The ratio of openings, or voids, to the total volume of soil or rock, expressed as a decimal fraction or as a percentage.

postclosure. The period of time after closure of the geologic repository.

potentiometric. Pertaining to the distribution of groundwater level.

precipitate. A solid particle that has separated from a liquid as a result of physical or chemical changes.

precipitation. (1) The process of substance coming out of solution by the action of gravity or by a chemical reaction. (2) Any form of water particles, such as frozen water in snow or ice crystals, or liquid water in raindrops or drizzle, that falls from clouds in the atmosphere and reaches the earth's surface. (3) An amount of water that has fallen at a given point over a specified period of time, measured by a rain gauge.

preclosure. The period of time before and during closure of the Yucca Mountain disposal system.

preclosure safety evaluation. A preliminary assessment of the adequacy of repository support facilities to prevent or mitigate the effects of postulated initiating event sequences and their consequences and the site, structures, systems, components, equipment, and operator actions that would be relied on for safety.

pressurized water reactor. A type of nuclear power reactor that uses uranium fuel elements cooled and moderated by water under high pressure to keep the water from boiling. The water boiled to generate steam is in an external heat exchanger rather than in the reactor vessel body.

probabilistic analyses. Analyses in which uncertainty in processes and events is represented through probability distributions for the parameters of those processes and events.

probabilistic risk assessment. (1) A systematic process of identifying and quantifying the consequences of scenarios that could cause a release of radioactive materials to the environment. (2) Using predictable behavior to define the performance of natural, geologic, human, and engineered systems for thousands of years into the future using probability distributions.

probability-density function. A frequency distribution such that the bars of a histogram that would represent it are so narrow that their tops would form a smooth curve if connected by a line. This type of distribution can be made if the number of observations of the value of a continuous random variable increases indefinitely, and the width of the range represented by each class (class inter-

val) becomes smaller and smaller. The area under the density function curve between any two points on the curve represents the probability that the value of the random variable will lie between these two values.

process model. A depiction or representation of a process along with any hypotheses required to describe or to explain the process.

pseudocolloid. A colloid from natural or man-made materials, as distinguished from a colloid from insoluble radionuclides (intrinsic colloid) or from altered fragments of spent nuclear fuel or glass waste forms (waste-form colloid). *See* colloid.

pyroclastic. Of or relating to clastic rock material of any size that is formed by volcanic explosion or ejected from a volcanic vent.

Quaternary. The second period of the Cenozoic Era, beginning about 2 million years ago at the end of the Tertiary Period and extending to the present.

rad (radiation absorbed dose). A unit of an absorbed dose of radiation equivalent to 100 ergs per gram

radioactive decay. The process in which one radionuclide spontaneously transforms into one or more different radionuclides called decay products or daughter products.

radioactive waste. High-level radioactive waste and other radioactive materials, including spent nuclear fuel, that are received for emplacement in the geologic repository.

radioactivity. The property possessed by some elements (e.g., uranium) of spontaneously emitting alpha, beta, or gamma rays by the disintegration of atomic nuclei.

Radiologically Controlled Area. An area of the surface repository enclosed by security fences, control gates, lighting, and access detection systems. This area includes the

facilities and transportation systems required to receive and ship rail and truck waste shipments, prepare shipping casks for handling, and load waste forms into disposal containers for underground emplacement. It also includes the facility and systems required to treat and package site-generated, low-level radioactive waste for offsite disposal.

radiolysis. The chemical dissociation of molecules caused by exposure to radiation. For example, under certain circumstances, radiation can cause the hydrogen and oxygen molecules in water to separate.

radiolytic corrosion. The process of dissolving or wearing away gradually caused by chemical changes associated with exposure to radiation (i.e., radiolysis).

radionuclide. A radioactive atom with an unstable nucleus that spontaneously decays, emitting ionizing radiation in the process.

raise. From mining terminology, an upward opening, either vertical or inclined, driven in rock from one level to that above it.

reasonably maximally exposed individual (RMEI). Under the U.S. Nuclear Regulatory Commission rule, a hypothetical person who meets the following criteria: (1) lives in the accessible environment above the highest concentration of radionuclides in the plume of contamination; (2) has a diet and living style representative of the people who now reside in the Town of Amargosa Valley, Nevada (the DOE must use projections based upon surveys of the people residing in the Town of Amargosa Valley, Nevada, to determine their current diets and living styles and use the mean values of these factors in the assessments conducted for 10 CFR 63.311 and 63.321); (3) uses well water with average concentrations of radionuclides based on an annual water demand of 3,000 acre-ft; (4) drinks 2 L (0.53 gal) of water per day from wells drilled into the groundwater

at the location specified in the regulations; and (5) is an adult with metabolic and physiological considerations consistent with present knowledge of adults.

recharge. The movement of water from an unsaturated zone to the saturated zone.

reference biosphere. The description of the environment inhabited by the reasonably maximally exposed individual. The reference biosphere comprises the set of specific biotic and abiotic characteristics of the environment, including but not necessarily limited to climate, topography, soils, flora, fauna, and human activities.

reflux water. Water that is vaporized near waste packages, migrates to cooler areas, condenses, and then flows back toward the waste packages.

regression analysis. The analysis of a paired dependent variable and the independent variable upon which it depends to quantify the relationship.

rem (roentgen equivalent man). The unit of a dose equivalent from ionizing radiation to the human body. It is used to measure the amount of radiation to which a person has been exposed.

repository block. The portion of rock in Yucca Mountain that would house the repository if the site is found suitable.

repository footprint. The outline of the outermost locations of where the waste is emplaced in the Yucca Mountain geologic repository.

retardation. Slowing of radionuclide movement in groundwater by mechanisms that include sorption of radionuclides, diffusion into rock matrix pores and microfractures, and trapping of large colloidal molecules or particles in small pore spaces or dead ends of microfractures.

reversible colloid. A colloid to which radionuclides are reversibly bound.

revised supplemental TSPA model. The model used in supplemental calculations of total system performance assessment as documented in *Total System Performance Assessment—Analyses for Disposal of Commercial and DOE Waste Inventories at Yucca Mountain—Input to Final Environmental Impact Statement and Site Suitability Evaluation.* The model is a modification of the supplemental TSPA model that conforms to the requirements of the final U.S. Environmental Protection Agency rule at 40 CFR Part 197. This model was also used in sensitivity analyses in *Total System Performance Assessment Sensitivity Analyses for Final Nuclear Regulatory Commission Regulations* to address provisions of the final Nuclear Regulatory Commission rule at 10 CFR Part 63. *See* total system performance assessment. *Compare* TSPA-SR model *and* supplemental TSPA model.

rhyolite. A volcanic rock type with a chemical composition similar to granite.

risk. The probability that an undesirable event will occur multiplied by the consequences of the undesirable event.

risk assessment. An evaluation of risks associated with a potential system or action. This assessment focuses on potential impacts on human health or the environment.

roadheader. An underground excavating machine that uses either a transverse or in-line cutter head for excavations.

runoff. Water from rain and snow that flows over land to streams.

run-on. The volume or depth of the routed surface-water flow.

safety case. The set of data and analyses that, collectively, are intended to provide the reasonable assurance that a successful license application would require.

safety margin. The difference between expected performance and the regulatory limit for that performance. *See* design margin.

saturated zone. The region below the water table where rock pores and fractures are completely saturated with water.

scarp. An escarpment, cliff, or steep slope of some extent that is produced by faulting or by differential erosion.

scenario. A well-defined, connected sequence of features, events and processes that can be thought of as an outline of a possible future condition of the repository system. Scenarios can be undisturbed, in which case the performance would be expected, or nominal, behavior for the system. The scenario can also be disturbed if altered by disruptive events, such as human intrusion or natural phenomena such as volcanism.

secular equilibrium. A condition in which a daughter radionuclide has reached a steady-state amount, in terms of radioactive activity, with respect to the amount of its parent radionuclide.

sedimentation. A geologic process in which particles accumulate in water or air and settle in layers of rock.

seepage. (1) The inflow of groundwater moving in fractures or pore spaces of permeable rock to an open space in the rock; the amount of percolation flux that enters the drift in a given time period. (2) Flow of liquid water into an underground opening such as a waste emplacement drift or exploratory tunnel. Does not include water vapor movement into openings or condensation of water vapor within openings.

seepage threshold. A critical percolation flux below which seepage into the openings is unlikely to occur.

seismicity. A seismic event or activity such as an earthquake or vibratory motion.

semiarid. Of a climate: having precipitation, only sufficient for growth of sparse vegetation; a region in which the annual precipitation is about 250 to 500 mm (10 to 20 in.).

sensitivity study. An analytic or numerical technique for examining the effects of varying specified parameters in a computer model. Shows the effects that changes in various parameters have on model outcomes and illustrates which parameters have a greater impact on the predicted behavior of the system being modeled. Also called *sensitivity analysis* because it shows the sensitivity of the consequences (e.g., radionuclide release) to uncertain parameters (e.g., the infiltration rate that results from precipitation).

shotcrete. Cementitious material sprayed onto a surface at high pressure.

site characterization. Activities, whether in the laboratory or in the field, undertaken to establish the geologic and hydrologic conditions and the ranges of the parameters of a candidate site relevant to the location of a repository. These activities include borings, surface excavations, subsurface excavations and borings, and in situ testing needed to evaluate the suitability of a candidate site for the location of a repository but do not include preliminary borings and geophysical testing needed to assess whether site characterization should be undertaken.

sorption. The binding, on a microscopic scale, of one substance to another. A term that includes both adsorption and absorption. The sorption of dissolved radionuclides onto aquifer solids or waste package materials by means of close-range chemical or physical forces is an important process modeled in

this study. Sorption is a function of the chemistry of the radioisotopes, the fluid in which they are carried, and the mineral material they encounter along the flow path.

sorption coefficient (K_d). A factor to calculate sorption of one substance to another (e.g., sorption of a radionuclide to a colloid or sorption of a radionuclide to the rock).

source term. Types and amounts of radionuclides that are the source of a potential release of radioactivity from the repository.

spent nuclear fuel. Fuel and the associated hardware withdrawn from a nuclear reactor following irradiation, the constituent elements of which have not been separated by reprocessing. Spent fuel that has been burned (irradiated) in a reactor to the extent that it no longer makes an efficient contribution to a nuclear chain reaction. This fuel is more radioactive than it was before irradiation, and it is thermally hot.

splay. A branch of a fault or fault zone.

split. The two halves of an emplacement, performance confirmation, or reserve drift, separated by an exhaust raise.

staging area. An area in the Waste Handling Building or a part of the waste-handling process in which spent nuclear fuel or high-level radioactive waste is retained for future loading in a disposal container.

standard deviation. (1) For a set of observations or a frequency distribution, the square root of the average of the squared deviations from the mean divided by n-1 (where n is the sample size). (2) The square root of the variance.

steady-state criticality. An self-sustained nuclear chain reaction where the reaction remains constant, with the effective neutron multiplication factor equal to one. *See* effective neutron multiplication factor.

steady-state modeling. Modeling a system under the assumption that the variables are not changing with time. For example, flow fields can be simulated at a steady state if the boundary conditions, saturations, and fluxes are not changing with time.

steel set. A steel support used in tunnels, drifts, and shafts.

stochastic. Involving a variable (e.g., temperature, porosity) that may take on values of a specified set with a certain probability. Data from a stochastic process is an ordered set of observations, each of which is one item from a probability distribution.

stochastic model. A model whose outputs are predictable only in a statistical sense. A given set of model inputs produces outputs that are not the same, but follow statistical patterns.

stress corrosion cracking. Preferential corrosion initiation in response to high tensile stresses, requiring the simultaneous action of a corrosion mechanism and sustained tensile stress.

stress intensity. The amount of stress at a given point in a structure. Derived from combined totals of both positive (tension) stress and negative (compression) stress.

stylized human intrusion scenario. A disruptive event assessed in a separate TSPA according to specific characteristics defined by the EPA in 40 CFR 197.26 and the NRC in 10 CFR 63.113(d). According to these regulations, the human intrusion scenario assumes that a drill penetrates the repository and a waste package during exploratory drilling for groundwater resources, one hundred years after final closure of the repository.

subsurface facilities. The repository's underground structures and systems. The surface facilities include the main drifts, exhaust mains, turnouts, emplacement drifts, ventila-

tion shafts, mechanical and structural support systems, underground utilities, waste emplacement and retrieval equipment, and surface-based control systems.

supplemental TSPA model. The model used in supplemental calculations of total system performance assessment as documented in Volume 2 of *FY01 Supplemental Science and Performance Analyses*. The model is a modification of the TSPA-SR model that incorporates new component models and input parameter values for some components. The model was based on specifications of proposed U.S. Environmental Protection Agency and U.S. Nuclear Regulatory Commission regulations. *See* total system performance assessment. *Compare* TSPA-SR model *and* revised supplemental TSPA model.

surface complexation. The process that describes the formation of complex molecules between the solute in the aqueous phase and the reactive groups on the solid surface, under specific chemical conditions.

surface facilities. All permanent facilities within the restricted area constructed in support of site characterization activities and repository construction, operation, and closure activities, including surface structures, utility lines, roads, railroads, and similar facilities, but excluding the underground facility.

system model. The analytical tool to examine the future behavior of the potential repository and its component barriers.

system performance. The complete behavior of a geologic repository system at Yucca Mountain in response to the features, events, and processes that may affect it.

SZ_CONVOLUTE. Software used to calculate saturated zone response curves based upon unsaturated zone radionuclide source terms, generic saturated zone response and expected climate scenarios

tectonic. Pertaining to geologic forms or effects created by deformation of the earth's crust.

Tertiary. The first of two geologic periods of the Cenozoic Era extending from the end of the Mesozoic Era to the beginning of the Quarternary Period, covering a time span from about 65 million to about 2 million years ago.

thermal conduction. The flow of thermal energy through a material. This conduction is affected by the amount of heat energy present, the nature of the heat carrier in the material, and the amount of dissipation.

thermal loading. (1) The spatial density at which waste packages are emplaced within the repository as characterized by the areal power density and the areal mass loading. *See* line loading *and* point loading. (2) The application of heat to a system, usually measured in terms of watt density. The thermal loading for a repository is the watts per acre produced by the radioactive waste in the active disposal area.

thermal stress. Stress caused by temperature changes in a material that is physically restricted and unable to expand or contract accordingly.

thermal-mechanical effects. Changes in the geomechanical properties of the repository host rock produced by heating of the rock associated with the emplacement of radioactive waste in the repository. An example might be decreased rock strength related to increased fracturing caused by heating of the rock.

thermogravimetric analysis. A method of analysis that measures the loss or gain of weight by a substance as the temperature of the substance is raised or lowered at a constant rate.

thermomechanical nomenclature. A stratigraphic nomenclature system used for the classification of rock at Yucca Mountain based on the thermal and mechanical properties of the rock. *Compare* lithostratigraphic nomenclature, hydrogeologic nomenclature, *and* lithostratigraphic nomenclature.

three-dimensional model. A three-dimensional representation of physical conditions and/or processes.

total effective dose equivalent. For purposes of assessing doses to workers, the sum of the deep-dose equivalent (for external exposures) and the committed effective dose equivalent (for internal exposures). For purposes of assessing doses to members of the public (including the reasonably maximally exposed individual), total effective dose equivalent means the sum of the effective dose equivalent (for external exposures) and the committed effective dose equivalent (for internal exposures). *See* annual committed effective dose equivalent.

total system performance assessment (TSPA). A risk assessment that quantitatively estimates how the proposed Yucca Mountain disposal system will perform in the future under the influence of specific features, events, and processes, incorporating uncertainty in the models and data.

TOUGH2. A computer software code used to simulate three-dimensional flow of groundwater and heat in unsaturated or saturated porous and fractured media. It is the basis for the unsaturated zone flow process model.

TOUGHREACT. Thermal-hydrologic-chemical software code used to simulate the water composition on the drip shield and waste package.

tracer. A substance or dye used in hydrologic tests to observe the movement of groundwater and sorbing and nonsorbing chemical species. Also applicable to gas injection tests using gaseous tracers to measure the breakthoughs at observation points.

transmissive fracture. A fracture in rock through which groundwater could flow.

transparency. The ease of understanding the process by which a study was carried out, which assumptions drove the results, how they were determined, and the rigor of the analyses that led to the results. Transparency provides a reader or reviewer with a clear picture of what was done in an analysis, what the outcome was, and why.

transpiration. The process by which water absorbed by plants, usually through the roots, is evaporated into the atmosphere from the plants' surfaces. It is an important process for removal of water that has infiltrated below the zone where it could be removed by evaporation.

transport. A process in which substances carried in groundwater move through the subsurface by means of the physical mechanisms of convection, diffusion, and dispersion and the chemical mechanisms of sorption, leaching, precipitation, dissolution, and complexation. Types of transport include advective, diffusive, and colloidal transport.

transportation cask. A heavily shielded container that meets applicable regulatory requirements used to ship spent nuclear fuel or high-level radioactive waste.

transuranic waste. Waste materials (excluding high-level radioactive waste and certain other waste types) contaminated with alpha-emitting radionuclides that are heavier than uranium with half-lives greater than 20 years and that occur in concentrations greater than 100 nanocuries per gram.

Transuranic waste is primarily a result of treating and fabricating plutonium, as well as from research activities at DOE defense installations.

transverse dispersion. The spreading of a solute in groundwater in directions perpendicular to the direction of the groundwater flow path.

travertine. A finely crystalline, massive deposit of calcium carbonate formed by chemical precipitation from solution in surface and groundwaters or in limestone caves, as stalactites, stalagmites, or dripstone.

TSPA-SR model. The model used in the calculations of total system performance assessment as documented in *Total System Performance Assessment for the Site Recommendation*. The model was based on specifications of proposed U.S. Environmental Protection Agency and U.S. Nuclear Regulatory Commission regulations. *See* total system performance assessment. *Compare* supplemental TSPA model *and* revised supplemental TSPA model.

tufa. A chemical sedimentary rock composed of calcium carbonate formed by evaporation around the mouth of a spring, along a stream, or as a thick concretionary deposit in a lake or along its shore.

tuff. Igneous rock formed from compacted volcanic fragments from pyroclastic (explosively ejected) flows with particles generally smaller than 4 mm (0.16 in.) in diameter. The most abundant type of rock at the Yucca Mountain site. Nonwelded tuff results when volcanic ash cools in the air sufficiently that it doesn't melt together, yet later becomes rock through compression. Welded tuff results when the volcanic ash is hot enough to melt together and is further compressed by the weight of overlying materials.

two-dimensional model. (1) A two-dimensional slice through an entity, such as the earth's crust, usually in the horizontal and vertical directions, on which known features are placed and are used to predict likely features that may exist between points of known data. (2) Mathematically, a model that represents physical conditions or processes; this mathematical model is composed of both horizontal rows and vertical columns of grid cells arrayed in L-shaped configurations only one grid cell thick.

UDEC. Distinct element code used to perform underground opening stability analysis.

uncertainty. A measure of how much a calculated or estimated value that is used as a reasonable guess or prediction may vary from the unknown true value.

underground facility. The underground structure, backfill materials, if any, and openings that penetrate the underground structure.

unsaturated zone. The zone of soil or rock below the ground surface and above the water table.

unzipping. The splitting of the cladding on a fuel rod.

uptake. Intake by and exposure of the receptor to a contaminant.

van Genuchten's capillary-strength parameter. A parameter in a functional relationship between saturation (or water content) and potential (a measure of the suction due to capillary forces). *Also* α-parameter.

variability (statistical). A measure of how a quantity varies over time or space.

vitric tuff. Volcanic rock composed of glassy shards of volcanic ash.

vitrified high-level radioactive waste. A type of processed high-level radioactive waste where the waste is mixed with glass-forming chemicals and put through a melting process. The melted mixture is then put into a canister where it becomes a dry, solid "log" of waste in a glassy matrix.

WAPDEG. A computer software code used to analyze drip shield and waste package degradation.

wash. Term used in the southwest for a broad, gravelly, dry bed of an ephemeral stream, generally in the bottom of a canyon.

waste form. A generic term that refers to the different types of radioactive wastes.

Waste Handling Building. In the North Portal Area, a structure designed to support waste handling operations and the loading and staging of waste packages.

waste package. A sealed container containing waste that is ready for emplacement. The waste package includes the waste form and any containers, spacing structures or baskets, and other absorbent materials immediately surrounding an individual waste container placed internally to the container or attached to the outer surface of the disposal container.

waste package remediation system. A repair facility for disposal containers and waste packages that have failed the weld inspection processes, that are defective or abnormal, or that have been selected for retrieval from the repository for performance confirmation examinations.

waste stream. Input of waste into the repository over time.

water table. (1) The upper limit of the portion of the ground wholly saturated with water. (2) The upper surface of a zone of saturation above which the majority of pore spaces and fractures are less than 100 percent saturated with water most of the time (unsaturated zone) and below which the opposite is true (saturated zone).

welded tuff. A tuff that was deposited under conditions where the particles making up the rock were heated sufficiently to cohere. In contrast to nonwelded tuff, welded tuff is considered to be denser, less porous, and more likely to be fractured (which increases permeability).

xerophytic. Plants adapted to low moisture conditions.

Yucca Mountain disposal system. A combination of underground engineered and natural barriers within the controlled area that prevents or substantially reduces releases from the waste.

Young's modulus. The ratio between tensile or compressive stress and elongation of a solid stressed in one direction.

zeolites. A large group of hydrous aluminosilicate minerals that act as molecular "traps" because they can adsorb molecules with which they interact. At Yucca Mountain, they are secondary alteration products in tuff rocks, caused by exposure to groundwater. Zeolites could act to retard the migration of radionuclides.

Zircaloy. A family of alloys of zirconium that may have any of several compositions. These alloys are frequently used as a cladding material.

INTENTIONALLY LEFT BLANK